GEOLOGY OF CALIFORNIA

Allison Jones, Cole Heap, Debra Brooks, Emily Wright, Martha House, Steven Newton & Steven Skinner
Academic Senate of California Community Colleges
Open Education Resources Initiative

LibreTexts™

Geology of California

An Open Educational Resource by Allison D. Jones, Emily V. Wright, Martha A. House, Cole I. Heap, Steven Newton, Debra A. Brooks, and Steven Skinner

This text is disseminated via the Open Education Resource (OER) LibreTexts Project (https://LibreTexts.org) and like the thousands of other texts available within this powerful platform, it is freely available for reading, printing, and "consuming."

The LibreTexts mission is to bring together students, faculty, and scholars in a collaborative effort to provide an accessible, and comprehensive platform that empowers our community to develop, curate, adapt, and adopt openly licensed resources and technologies; through these efforts we can reduce the financial burden borne from traditional educational resource costs, ensuring education is more accessible for students and communities worldwide.

Most, but not all, pages in the library have licenses that may allow individuals to make changes, save, and print this book. Carefully consult the applicable license(s) before pursuing such effects. Instructors can adopt existing LibreTexts texts or Remix them to quickly build course-specific resources to meet the needs of their students. Unlike traditional textbooks, LibreTexts' web based origins allow powerful integration of advanced features and new technologies to support learning.



LibreTexts is the adaptable, user-friendly non-profit open education resource platform that educators trust for creating, customizing, and sharing accessible, interactive textbooks, adaptive homework, and ancillary materials. We collaborate with individuals and organizations to champion open education initiatives, support institutional publishing programs, drive curriculum development projects, and more.

The LibreTexts libraries are Powered by NICE CXone Expert and were supported by the Department of Education Open Textbook Pilot Project, the California Education Learning Lab, the UC Davis Office of the Provost, the UC Davis Library, the California State University Affordable Learning Solutions Program, and Merlot. This material is based upon work supported by the National Science Foundation under Grant No. 1246120, 1525057, and 1413739.

Any opinions, findings, and conclusions or recommendations expressed in this material are those of the author(s) and do not necessarily reflect the views of the National Science Foundation nor the US Department of Education.

Have questions or comments? For information about adoptions or adaptions contact info@LibreTexts.org or visit our main website at https://LibreTexts.org.

The LibreTexts name, logo, and book covers are trademarked by LibreTexts, Inc. (a 501(c)(3) not-for-profit organization) and protected against unauthorized use.

This text was compiled on 10/27/2026

TABLE OF CONTENTS

Licensing

Program Page

Preface

About the Authors

Acknowledgements

Land Acknowledgment

Licensing

Recommended Citations

1: Introduction to the Geology of California

1.1: How to Read California's Geologic Map

1.2: Geologic Map Symbols

1.3: Detailed Figure Descriptions

2: Minerals and Rocks

2.1: Minerals

2.2: Mineral Properties

2.3: The Rock Cycle

2.4: Igneous Rocks

2.5: Sedimentary Rocks

2.6: Metamorphic Rocks

2.7: Chapter Summary

2.8: Detailed Figure Descriptions

3: Plate Tectonics

3.1: Earth's Interior

3.2: Tectonic Plates, Plate Motions, and Plate Boundaries

3.3: Mechanisms for Plate Motion

3.4: California's Plates and Plate Boundaries

3.5: Chapter Summary

3.6: Detailed Figure Descriptions

4: Geologic Structures and Seismology

4.1: Stress and Strain

4.2: Folding

4.3: Jointing and Faulting

4.4: Earthquakes

4.5: Measuring Earthquakes

4.6: Chapter Summary

4.7: Detailed Figure Descriptions

5: Geologic Time

5.1: Relative Dating

5.2: Unconformities

5.3: Dating Rocks Using Fossils

5.4: Absolute Dating of Geologic Materials

5.5: The Geologic Time Scale

5.6: Chapter Summary

5.7: Detailed Figure Descriptions

6: A Brief Geologic History of California

6.1: Developing a Geologic History

6.2: Precambrian California (4.6 Ga – 541 Ma)

6.3: Paleozoic California (541 – 252 Ma)

6.4: Mesozoic California (250 – 66 Ma)- Subduction and Mountain Building

6.5: Cenozoic California (66 Ma – Present)- Faulting, Uplift, and Basin Formation

6.6: Chapter Summary

6.7: Detailed Figure Descriptions

7: Cascade Range and Modoc Plateau

7.1: The Cascadia Subduction Zone and the Cascade Continental Volcanic Arc

7.2: Rock Types of the Cascades

7.3: The Variety of Volcanoes in the Cascades and the Modoc Plateau

7.4: Volcanic Hazards

7.5: Mount Shasta

7.6: Lassen Volcanic National Park

7.7: Medicine Lake Volcano

7.8: Glaciers in the Cascades

7.9: Chapter Summary

7.10: Detailed Figure Descriptions

8: Basin and Range

8.1: Regional Extent and Overview of the Basin and Range

8.2: Rifting in the Basin and Range

8.3: Rift-Related Faulting in Eastern California

8.4: Sedimentary Products of Rifting in the Basin and Range

8.5: Rift-Related Volcanism in Eastern California

8.6: The Oldest Rocks in the Basin and Range

8.7: Chapter Summary

8.8: Detailed Figure Descriptions

9: Sierra Nevada

9.1: The Sierra Nevada Today

9.2: Ancient Seas Form the Oldest Rocks

9.3: The Sierra Nevada Batholith
9.4: Gold of the Sierra Nevada
9.5: Volcanic Features of the Sierra Nevada
9.6: Ice Shapes the Landscape
9.7: Natural Hazards of the Sierra Nevada
9.8: Chapter Summary
9.9: Detailed Figure Descriptions

10: Klamath Mountains

10.1: Assembling a Continent
10.2: The McCloud Limestone- An Ancient Coral Reef
10.3: The Josephine Ophiolite- A Little Slice of the Mantle
10.4: Plutons of the Klamath Mountains
10.5: Uplifting a Mountain Range
10.6: Chapter Summary
10.7: Detailed Figure Descriptions

11: Coast Ranges

11.1: A Complicated Land
11.2: The Coast Range Ophiolite
11.3: The Great Valley Sequence
11.4: The Franciscan Complex
11.5: Cenozoic Events
11.6: Quaternary Events
11.7: Representative Coast Range Rocks
11.8: Chapter Summary
11.9: Detailed Figure Descriptions

12: Great Valley

12.1: Geomorphology and General Overview of the Great Valley Province
12.2: Geology of the Great Valley
12.3: Soil, Streams and Agriculture
12.4: Natural Hazards of the Great Valley Province
12.5: Natural Resources of the Great Valley
12.6: Chapter Summary
12.7: Detailed Figure Descriptions

13: Mojave and Colorado Deserts

13.1: Physiographic Features of the Mojave and Colorado Desert Provinces
13.2: Geologic Overview and Evolution of the Mojave and Colorado Desert Provinces
13.3: Creating the Desert Environment
13.4: Wind Driven Sediment Transport
13.5: Sand Dunes and Dune Fields

13.6: Erosional Desert Land Forms
13.7: Water in the Desert
13.8: Geological Resources of the Desert Provinces
13.9: Geologic Hazards of the Mojave and Colorado Desert Provinces
13.10: Chapter Summary
13.11: Detailed Figure Descriptions

14: Transverse Ranges

14.1: Physiographic Overview of the Transverse Ranges Province
14.2: Bedrock Geology of the Transverse Ranges Province
14.3: Cenozoic Sedimentation and Basin Development
14.4: Tectonic and Structural Evolution of the Transverse Ranges
14.5: Geologic Hazards of the Transverse Ranges Province
14.6: Mineral and Petroleum Resources of the Transverse Ranges Province
14.7: Chapter Summary
14.8: Detailed Figure Descriptions

15: Peninsular Ranges

15.1: Geomorphology of the Peninsular Ranges
15.2: Tectonics and Geologic History of the Peninsular Ranges Province
15.3: Rocks of the Peninsular Ranges
15.4: Geologic Hazards of the Peninsular Ranges
15.5: Natural Resources of the Peninsular Ranges
15.6: Chapter Summary
15.7: Detailed Figure and Video Descriptions

16: California Coastline

16.1: Coastal Processes
16.2: California Coastline Anatomy
16.3: California Coastal Hazards
16.4: Human Alteration and Mitigation
16.5: Coastal Access
16.6: The Edge of California
16.7: Chapter Summary
16.8: Detailed Figure Descriptions

17: California's Climate

17.1: Note on Usage
17.2: The Past
17.3: The Present
17.4: The Future
17.5: Hotter, Drier, Tougher
17.6: Chapter Summary

17.7: Detailed Figure Descriptions

18: California's Water

18.1: The Hydrologic Cycle

18.2: Running Water

18.3: Groundwater

18.4: Water Infrastructure and Management

18.5: Threats to California’s Water

18.6: Understanding California's Water Landscape

18.7: Chapter Summary

18.8: Detailed Figure Descriptions

19: California's Earthquake History and Hazards

00: Front Matter

Table of Contents

19.1: Front Matter

19.1.1: Table of Contents

19.2: The Hazard of Buildings

19.3: The Hazard of Place

19.4: Liquefaction and the Role of Soil Type

19.5: What's Coming

19.6: Beyond the San Andreas - Earthquakes of the North Coast

19.7: Preparing for the Worst

19.8: A State of Danger

19.9: Chapter Summary

19.10: Detailed Figure Descriptions

Index

Glossary

Interactive Geologic Time Scale

Interactive Geologic Map of California

Detailed Licensing

Detailed Licensing

This page titled Geology of California is shared under a CC BY-NC 4.0 license and was authored, remixed, and/or curated by Allison Jones, Cole Heap, Debra Brooks, Emily Wright, Martha House, Steven Newton, & Steven Skinner.

Licensing

A detailed breakdown of this resource's licensing can be found in ***Back Matter/Detailed Licensing***.

This page titled Licensing is shared under a license and was authored, remixed, and/or curated by LibreTexts.

Program Page



An Open Educational Resource Supported by the Academic Senate for California Community Colleges Open Educational Resources Initiative

The Academic Senate for California Community Colleges Open Educational Resources Initiative (OERI) was funded by the California legislature in trailer bill language during the summer of 2018. The OERI's mission is to reduce the cost of educational resources for students by expanding the availability and adoption of high quality Open Educational Resources (OER). The OERI facilitates and coordinates the curation and development of OER texts, ancillaries, and support systems. In addition, the OERI supports local OER implementation efforts through the provision of professional development, technical support, and technical resources.

The information in this resource is intended solely for use by the user who accepts full responsibility for its use. Although the author(s) and ASCCC OERI have made every effort to ensure that the information in this resource is accurate, openly licensed, and accessible at press time, the author(s) and ASCCC OERI do not assume and hereby disclaim any liability to any party for any loss, damage, or disruption caused by errors or omissions, whether such errors or omissions result from negligence, accident, or any other cause.

Please bring all such errors and changes to the attention of Academic Senate of California Community Colleges OER Initiative via e-mail (oeri@asccc.org).

Academic Senate for California Community Colleges
One Capitol Mall, Suite 230
Sacramento, CA 95814

This page titled Program Page is shared under a CC BY-NC 4.0 license and was authored, remixed, and/or curated by Allison Jones.

Preface

About the Book

Welcome to *Geology of California,* an open educational resource (OER) "textbook" designed to support students in their exploration of California's diverse geology. This text is crafted with a student-centered pedagogical approach, incorporating multiple modes of engagement to enhance learning.

This text is also designed to be adapted— instructors should feel empowered to rearrange, remove, and add content to suit the unique needs of their students, whether they have an understanding of foundational geology concepts, need a review of said concepts, or are entirely new to the study of geology. This text is licensed under a Creative Commons Attribution Non-Commercial license, allowing reusers to distribute, remix, adapt, and add to the material in any medium or format so long as:

- Credit is given to the creators
- It is only used for noncommercial purposes

Pedagogical Approach

In this textbook, students will interact with content in a variety of ways to support different learning styles and reinforce key concepts. Each chapter includes:

- Text-based content, providing clear and concise explanations of geological principles.
- Embedded images and videos, illustrating key concepts and real-world geological features.
- Interactive H5P activities, designed as formative assessments to allow students to check their understanding and engage with the material in an interactive way.
- A dynamic glossary, where glossary terms are underlined and popover definitions are provided in the online version of the text, ensuring a dynamic and engaging learning experience.

This multimodal approach helps students develop a deeper understanding of geology by integrating visual, textual, and interactive elements. Additionally, instructors may adapt these materials to align with their course objectives and student needs.

Organization of the Textbook

This textbook is organized into 19 chapters, progressing from fundamental geological concepts to more specialized topics. The first six chapters provide essential background knowledge for students who may not have prior experience with geology. These introductory chapters cover:

1. Introduction to the Geology of California – A broad overview of the text
2. Minerals and Rocks – An introduction to mineral properties, rock types, and the rock cycle.
3. Plate Tectonics – Understanding Earth's dynamic crust, plate boundaries, and the mechanisms driving plate motion.
4. Geologic Structures and Seismology – Exploring folds, faults, earthquakes, and how geologists interpret Earth's structural features.
5. Geologic Time – Examining relative and absolute dating methods, the geologic time scale, and Earth's history.
6. A Brief Geologic History of California – Highlighting major geologic events that have shaped California’s landscapes.

Beyond these foundational chapters, chapters 12-16 delve into California's physiographic provinces:

7. Cascade Range and Modoc Plateau
8. Basin and Range
9. Sierra Nevada
10. Klamath Mountains
11. Coast ranges
12. Great Valley
13. Mojave and Colorado Deserts

14. Transverse Ranges
15. Peninsular Ranges
16. California Coastline

Each chapter follows a structured format, with clearly defined learning objectives and summary sections to reinforce comprehension.

The final three chapters of the book explore major environmental and geologic issues influencing California, its residents, its economy, and its politics, including:

17. California's Climate
18. California's Water
19. California's Earthquake History and Hazards

How to Use This Textbook

We encourage students to actively engage with the material by working through the embedded activities, revisiting key concepts, and utilizing the provided resources. Instructors may adapt or supplement the text as needed to fit their course structure. This flexibility ensures that the textbook can be tailored to different teaching styles and student needs.

We hope that this OER textbook serves as a valuable resource in your studies of California's unparalleled geology and fosters a deeper appreciation for the Earth and its dynamic systems.

Allison Jones (Sierra College), Martha House (Pasadena City College), Emily Wright (College of the Redwoods), Steven Newton (College of Marin), Cole Heap, P.G., Debra Brooks (Santiago Canyon College), Steven Skinner (California State University, Sacramento),
March 2025

References

Creative Commons. (2013). *Attribution-NonCommercial 4.0 International (CC BY-NC 4.0)*.

This page titled Preface is shared under a CC BY-NC 4.0 license and was authored, remixed, and/or curated by Allison Jones.

About the Authors

Allison D. Jones, M.S.

Allison Jones, M.S. is a professor of Earth Science at Sierra College teaching primarily at the campus located in Rocklin, California. A late bloomer to geology, Allison began her higher education journey studying Communication at University of the Pacific. In her senior year she enrolled in a general education course *Geology of California* which inspired her to later make a career shift and return to school to study geoscience. She earned her AS Geology from Diablo Valley College, and an MS Geoscience from the University of Wisconsin-Madison. Allison's interests are wide- (and deep-!) reaching: from finite strain of rocks and discrete fault behavior, to how students best learn geoscience in online and in-person modalities. It is her hope that this text makes California's top-notch geology accessible for all students, and ultimately inspires some like herself to become Earth scientists.



Figure 1: Allison Jones is a professor of Earth Science at Sierra College. This work by Jeff Armstrong is licensed under CC BY.

Emily V. Wright, M.S.

Emily Wright earned her B.A. in Geology from Colorado College and her M.S. from Central Washington University. Originally from Oregon, Emily has a deep love for everything Cascadia. She was attracted to take a position teaching geology at the College of the Redwoods in 2016 because of its proximity to the Mendocino Triple Junction. Emily has traveled extensively in the western United States in pursuit of rock climbing and mountain biking adventures. She has also developed an interest in surfing since moving to the coast, which in turn sparked her interest in studying and teaching oceanography. Before moving to Humboldt, Emily taught geology at Yakima Valley College in Washington and Front Range Community College in Colorado. Emily is passionate about pedagogical innovation and is interested in addressing the challenges of bringing active learning to the online environment.

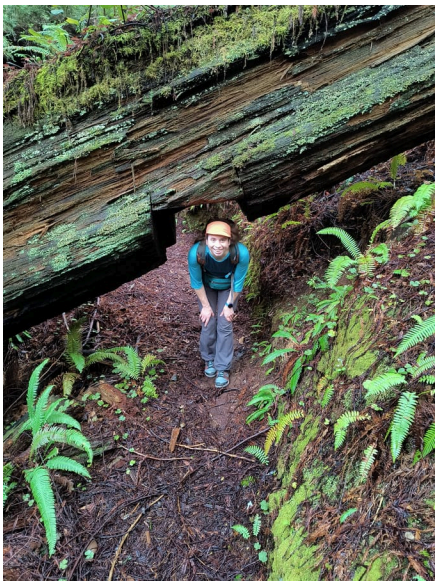


Figure 2: Emily Wright lives in Humboldt County, CA, somewhere among the sword ferns and redwood trees. NEEDS ATTRIBUTION

Martha A. House

Martha earned her B.S. in Geology from University of Michigan and her Ph.D. in Geology from the Massachusetts Institute of Technology. She has post-doctoral experience at the California Institute of Technology and has been an associate professor at St. Louis University. She is currently a Professor of Geology at Pasadena City College, where she also has served as a Division Dean. She fell in love with geology when she realized she could do quantitative science outdoors as well as indoors, and in interesting places. Her choice of career path has not disappointed: she's had the opportunity to work with amazing collaborators on geologic problems in New Zealand, China, Australia, Antarctica, the European Alps, and throughout the western US, including across California. As an instructor at PCC, she is part of an amazing team of educators who work to bring students to field sites across the western US and California. Her priority these days is to continue to support her students (geology majors and those just meeting transfer requirements) in the same way that she was supported by instructors and collaborators over the years: by providing a challenging but welcoming learning environment and helping them identify opportunities that will help them to reach their goals, whatever they are. And she's really happy to be part of the team who has created this book!



Figure 3: Geoscientist and educator Martha House, here shown snowshoeing, enjoys spending time outdoors. "Martha House" by Martha House is licensed under CC BY-NC 4.0.

Cole I. Heap, M.S., P.G.

Cole Heap, P.G., brings over a decade of expertise in the energy sector, specializing in geologic interpretation, well development, and earth modeling. As a licensed Professional Geologist in California and Wyoming, he collaborates with regulatory agencies, IM&T professionals, and consulting firms to achieve exceptional outcomes. Additionally, he serves as adjunct faculty at multiple community colleges, instructing courses in geology, geography, and GIS. With a Bachelor's and Master's degree in Geology, as well as a Master's in Geographic Information Technology and Science, Cole's dedication to continuous learning and knowledge sharing enriches both industry projects and educational endeavors.



Figure 4: Cole Heap is a licensed professional geologist in California and Wyoming. "Cole Heap" by Chong Moua is licensed under CC BY.

Steven Newton

Steven Newton passed after a very long battle with asthma and a very short battle with an angry raccoon. After a storied career as a professional gambler and alpaca farmer--a lifestyle which ended dramatically in an incident known in Peru as the “Night of the Card-Counting Alpaca”--Newton had to flee his Andean compound and change his career to become a professor of Geology at College of Marin, where he proceeded to bore an endless stream of suffering students not only with the wonders of California Geology, Oceanography, and Historical Geology, but also with pedantic pontifications about the differences between early drafts of “The Star Wars” and the final shooting script. True fact: Newton created slides detailing the state of matter known as plasma just as an excuse to ignite his combat-ready LED lightsaber in class. Interesting fact: Steve worked for almost a decade at the National Center for Science Education, a non-profit dedicated to defending the teaching of evolution and climate change in public schools. Fun fact: Steve has met legendary geologic mapper Thomas Dibblee, science educator Bill Nye, and the founder of plate tectonics Alfred Wegener [one of these is not true]. Reports of Newton’s demise may be premature.



Figure 5: Steven Newton [left]. "Two trash pandas" by Steven Newton is licensed under CC BY-NC 4.0

Debra A. Brooks

Back in the Pleistocene, after finishing an AA in Physics from San Bernardino Valley College in California, Debra Brooks transferred to U.C. Riverside and noticed there were all these scruffy people who sat in the back of physics lectures and always seemed to be going on field trips. They were the geophysics majors. Because she liked backpacking, it seemed she might have more in common with the scruffy people who went on field trips than the physics majors who never seemed to leave the building. She did. She completed a B.S. in Geophysics from U.C. Riverside and became a mining geophysicist. Eventually this led to grad school and an M.S. in Geophysics from Texas A&M University and a career change from mining to oil exploration. After many years however California called. She surprised everyone by quitting her job, returning to California, and becoming a geology professor at what is now Santiago Canyon College in Orange, California. In January of 2020, she retired after almost 30 years of teaching. It didn't take long before she went back to work as an adjunct instructor and volunteered for this project. She wishes to thank her co-authors for not laughing too loud as they repeatedly tried to help her join the world of the digital workplace.



Figure 6: Debra Brooks is a professor emerita at Santiago Canyon College. "Cousin Debbie hiking with us." by Deborah Charowsky is licensed under CC BY-NC 4.0.

Steven Skinner

Steven Skinner is a professor of Geology at California State University, Sacramento. Steve is a native Californian and grew up in the Los Angeles basin where he earned his BS and PhD in Geology. Steve's current research interests include unravelling the tectonic history of California, particularly the northern Sierra Nevada. Steve has previously worked on projects studying the subduction zones in Mexico and Peru as well as paleomagnetic studies in Baja California, Antarctica, and the South China Sea. After a short stint teaching geology and geophysics in Wichita Kansas, Steve is happy to be back in the tectonically active landscape of California. At Sac State, Steve teaches a wide variety of courses including physical geology, geophysics, structural geology, field methods, programming, GIS, and the Geology of California. Steve is excited to share this open educational resource with his students.

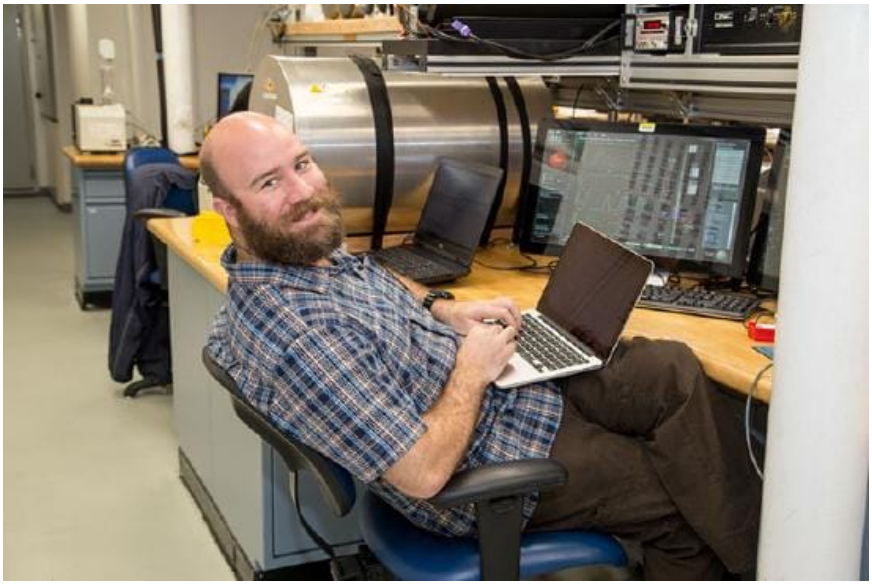


Figure 7: Steve enjoying squiggles on the computer. "Steve enjoying squiggles" by William Crawford, IODP JRSO is licensed under CC BY 4.0.

This page titled About the Authors is shared under a CC BY-NC 4.0 license and was authored, remixed, and/or curated by Allison Jones.

Acknowledgements

This textbook is the result of collaboration among seven geoscience educators, each representing a different California educational institution. This work has benefited from the input of educators, geoscientists, and accessibility specialists. We extend our gratitude to the Academic of California Community Colleges (ASCCC) Open Educational Resources Initiative (OERI) for recognizing the need for and supporting the creation of this resource, our subject matter expert reviewers Randy Reed (Shasta College) and Samuel Raskin (Folsom Lake College) for their invaluable pedagogical and geological feedback, Kim Saccio, and Suzanne Wakim for helping to make this resource accessible for all students, and our project manager Shagun Kaur (De Anza College) for her unwavering support throughout the duration of this project. This resource is infinitely better because of them.

This page titled Acknowledgements is shared under a CC BY-NC 4.0 license and was authored, remixed, and/or curated by Allison Jones.

Land Acknowledgment

We acknowledge that this important textbook was created throughout the unceded territory of California, home to nearly 200 tribal nations, including those whose tribal lands cross colonial state boundaries. We acknowledge and honor the original Peoples and their descendants, past, present, and emerging, of the various regions where we authors now live and work. We support ongoing movements for tribal sovereignty and we stand in solidarity with all Indigenous peoples worldwide. A land acknowledgment is a critical step towards working with Native communities to secure meaningful partnerships in the stewardship and protection of their homelands and cultural resources. In this respect, we are continuously striving to be good relatives.

The image in Figure 1 titled "Native Californian Tribes" by Timara Lotah Link (Chumash Coastal Band) features text that reads "Native People of This Place. In all of North America, California has always been home to the largest number of different Native people and their cultures. Many of the tribal groups on this map speak different languages and have different traditions. Their homelands––established for thousands of years––extend far beyond state boundaries. These Native cultures overlap in ways that this map cannot show, through shared resources, trade, and family relationships." The map shows the tribal areas of eight-five out of the hundreds of California Native nations in their own languages and features a quote by Richard Bugbee (Luiseño, raised by Kumeyaay) that reads, "Language is a reflection of our environment, unique to each area."



Figure 1: Map of present day boundaries of California, locations of native Californian tribes, and their languages. "Native Californian Tribes" by Timara Lotah Link, *Santa Clara University Digital Exhibits*, is available for free online with an undefined license.

Figure 1 includes the names of the tribes in the following list:

- Tolowa
- Yurok
- Chilula
- Wiyot
- Chimariko
- Mattole
- Nongatl
- Sinkyone
- Lassik
- Kenneto
- Cahto
- Coast Yuki
- Huchnom
- Lake Miwok
- Wappo

- Coast Miwok
- Ohlone
  - Awaswas
  - Chochenyo
  - Karkin
  - Ramayutsh
  - Tamyen
  - Chalon
  - Mutsun
  - Rumsen
- Yokut
  - Choinumni
  - Chukchansi
  - Dumna
  - Gashowu
  - Tachi
  - Wukchumni
  - Yowlumni
  - Bankalachi
  - Chowchilla
  - Nutunutu
  - Esselen
- T’epoteha’l
- Chumash
  - yak titʸu titʸu yak tiłhini
  - Amuwu
  - Kuyam
  - S’amala
  - Shmuwich
  - Micqanaqa’n
  - Hul Kuhk;u
  - Kasthik
  - Michumash
- Tongva
- Kumeyaay
- Karuk
- Shasta
- Hupa
- Wintu
- Nomlaki
- Yuki
- Yana
- Kankow
- Patwin
- Nisenan
- Sierra Miwok
- Mono
- Modoc
- Achumawi
- Atusgewi
- Maidu
- Northern Paiute
- Washo
- Numa
- Owens Valley Paiute
- Western Shoshone
- Tubatulabal
- Kawaiiisu

- Southern Paiute
- Kitanemuk
- Tatviam
- Kawaiisu
- Maarangea'yam
- Ivatim
- Chemehuevi
- Mojave
- Hakhidhoma
- Payómkawichum
- Kuupangaxwichem
- Quechan

This land acknowledgement is adapted from the California Indian Culture and Sovereignty Center, CSU San Marcos.

This page titled Land Acknowledgment is shared under a CC BY-NC 4.0 license and was authored, remixed, and/or curated by Allison Jones.

Licensing

A detailed breakdown of this resource's licensing can be found in ***Back Matter/Detailed Licensing***.

This page titled Licensing is shared under a CC BY-NC 4.0 license and was authored, remixed, and/or curated by Allison Jones.

Recommended Citations

Geological Society of America (GSA) Style

Jones, A.D., Wright, E.V., House, M.A., Heap, C.I., Newton, S., Brooks, D.A., and Skinner, S., 2025, Geology of California, Academic Senate of California Community Colleges Open Educational Resource Initiative.

American Geophysical Union (AGU) Style

Jones, A. D., Wright, E. V., House, M. A., Heap, C. I., Newton, S., Brooks, D. A., & Skinner, S. (2025). *Geology of California*. Academic Senate of California Community Colleges Open Educational Resource Initiative.

APA (7th edition)

Jones, A. D., Wright, E. V., House, M. A., Heap, C. I., Newton, S., Brooks, D. A., & Skinner, S. (2025). *Geology of California*. Academic Senate of California Community Colleges Open Educational Resource Initiative.

MLA (9th edition)

Jones, Allison D., et al. *Geology of California*. Academic Senate of California Community Colleges Open Educational Resource Initiative, 2025.

References

The Geological Society of America (n.d.). *Reference Guidelines and Examples*. Retrieved January 13, 2025, from https://www.geosociety.org/GSA/GSA/P...-examples.aspx

American Geophysical Union. (2023). *AGU publications author guide: References*. AGU Journals. https://www.agu.org/Publish-with-AGU...ide-References

American Psychological Association. (2020). *Publication manual of the American Psychological Association* (7th ed.). American Psychological Association.

Modern Language Association. (2021). *MLA handbook* (9th ed.). Modern Language Association of America.

This page titled Recommended Citations is shared under a CC BY-NC 4.0 license and was authored, remixed, and/or curated by Allison Jones.

TABLE OF CONTENTS

Licensing

Program Page

Preface

About the Authors

Acknowledgements

Land Acknowledgment

Licensing

Recommended Citations

1: Introduction to the Geology of California

1.1: How to Read California's Geologic Map

1.2: Geologic Map Symbols

1.3: Detailed Figure Descriptions

2: Minerals and Rocks

2.1: Minerals

2.2: Mineral Properties

2.3: The Rock Cycle

2.4: Igneous Rocks

2.5: Sedimentary Rocks

2.6: Metamorphic Rocks

2.7: Chapter Summary

2.8: Detailed Figure Descriptions

3: Plate Tectonics

3.1: Earth's Interior

3.2: Tectonic Plates, Plate Motions, and Plate Boundaries

3.3: Mechanisms for Plate Motion

3.4: California's Plates and Plate Boundaries

3.5: Chapter Summary

3.6: Detailed Figure Descriptions

4: Geologic Structures and Seismology

4.1: Stress and Strain

4.2: Folding

4.3: Jointing and Faulting

4.4: Earthquakes

4.5: Measuring Earthquakes

4.6: Chapter Summary

4.7: Detailed Figure Descriptions

5: Geologic Time

5.1: Relative Dating

5.2: Unconformities

5.3: Dating Rocks Using Fossils

5.4: Absolute Dating of Geologic Materials

5.5: The Geologic Time Scale

5.6: Chapter Summary

5.7: Detailed Figure Descriptions

6: A Brief Geologic History of California

6.1: Developing a Geologic History

6.2: Precambrian California (4.6 Ga – 541 Ma)

6.3: Paleozoic California (541 – 252 Ma)

6.4: Mesozoic California (250 – 66 Ma)- Subduction and Mountain Building

6.5: Cenozoic California (66 Ma – Present)- Faulting, Uplift, and Basin Formation

6.6: Chapter Summary

6.7: Detailed Figure Descriptions

7: Cascade Range and Modoc Plateau

7.1: The Cascadia Subduction Zone and the Cascade Continental Volcanic Arc

7.2: Rock Types of the Cascades

7.3: The Variety of Volcanoes in the Cascades and the Modoc Plateau

7.4: Volcanic Hazards

7.5: Mount Shasta

7.6: Lassen Volcanic National Park

7.7: Medicine Lake Volcano

7.8: Glaciers in the Cascades

7.9: Chapter Summary

7.10: Detailed Figure Descriptions

8: Basin and Range

8.1: Regional Extent and Overview of the Basin and Range

8.2: Rifting in the Basin and Range

8.3: Rift-Related Faulting in Eastern California

8.4: Sedimentary Products of Rifting in the Basin and Range

8.5: Rift-Related Volcanism in Eastern California

8.6: The Oldest Rocks in the Basin and Range

8.7: Chapter Summary

8.8: Detailed Figure Descriptions

9: Sierra Nevada

9.1: The Sierra Nevada Today

9.2: Ancient Seas Form the Oldest Rocks

9.3: The Sierra Nevada Batholith
9.4: Gold of the Sierra Nevada
9.5: Volcanic Features of the Sierra Nevada
9.6: Ice Shapes the Landscape
9.7: Natural Hazards of the Sierra Nevada
9.8: Chapter Summary
9.9: Detailed Figure Descriptions

10: Klamath Mountains

10.1: Assembling a Continent
10.2: The McCloud Limestone- An Ancient Coral Reef
10.3: The Josephine Ophiolite- A Little Slice of the Mantle
10.4: Plutons of the Klamath Mountains
10.5: Uplifting a Mountain Range
10.6: Chapter Summary
10.7: Detailed Figure Descriptions

11: Coast Ranges

11.1: A Complicated Land
11.2: The Coast Range Ophiolite
11.3: The Great Valley Sequence
11.4: The Franciscan Complex
11.5: Cenozoic Events
11.6: Quaternary Events
11.7: Representative Coast Range Rocks
11.8: Chapter Summary
11.9: Detailed Figure Descriptions

12: Great Valley

12.1: Geomorphology and General Overview of the Great Valley Province
12.2: Geology of the Great Valley
12.3: Soil, Streams and Agriculture
12.4: Natural Hazards of the Great Valley Province
12.5: Natural Resources of the Great Valley
12.6: Chapter Summary
12.7: Detailed Figure Descriptions

13: Mojave and Colorado Deserts

13.1: Physiographic Features of the Mojave and Colorado Desert Provinces
13.2: Geologic Overview and Evolution of the Mojave and Colorado Desert Provinces
13.3: Creating the Desert Environment
13.4: Wind Driven Sediment Transport
13.5: Sand Dunes and Dune Fields

13.6: Erosional Desert Land Forms
13.7: Water in the Desert
13.8: Geological Resources of the Desert Provinces
13.9: Geologic Hazards of the Mojave and Colorado Desert Provinces
13.10: Chapter Summary
13.11: Detailed Figure Descriptions

14: Transverse Ranges

14.1: Physiographic Overview of the Transverse Ranges Province
14.2: Bedrock Geology of the Transverse Ranges Province
14.3: Cenozoic Sedimentation and Basin Development
14.4: Tectonic and Structural Evolution of the Transverse Ranges
14.5: Geologic Hazards of the Transverse Ranges Province
14.6: Mineral and Petroleum Resources of the Transverse Ranges Province
14.7: Chapter Summary
14.8: Detailed Figure Descriptions

15: Peninsular Ranges

15.1: Geomorphology of the Peninsular Ranges
15.2: Tectonics and Geologic History of the Peninsular Ranges Province
15.3: Rocks of the Peninsular Ranges
15.4: Geologic Hazards of the Peninsular Ranges
15.5: Natural Resources of the Peninsular Ranges
15.6: Chapter Summary
15.7: Detailed Figure and Video Descriptions

16: California Coastline

16.1: Coastal Processes
16.2: California Coastline Anatomy
16.3: California Coastal Hazards
16.4: Human Alteration and Mitigation
16.5: Coastal Access
16.6: The Edge of California
16.7: Chapter Summary
16.8: Detailed Figure Descriptions

17: California's Climate

17.1: Note on Usage
17.2: The Past
17.3: The Present
17.4: The Future
17.5: Hotter, Drier, Tougher
17.6: Chapter Summary

17.7: Detailed Figure Descriptions

18: California's Water

18.1: The Hydrologic Cycle

18.2: Running Water

18.3: Groundwater

18.4: Water Infrastructure and Management

18.5: Threats to California’s Water

18.6: Understanding California's Water Landscape

18.7: Chapter Summary

18.8: Detailed Figure Descriptions

19: California's Earthquake History and Hazards

00: Front Matter

Table of Contents

19.1: Front Matter

19.1.1: Table of Contents

19.2: The Hazard of Buildings

19.3: The Hazard of Place

19.4: Liquefaction and the Role of Soil Type

19.5: What's Coming

19.6: Beyond the San Andreas - Earthquakes of the North Coast

19.7: Preparing for the Worst

19.8: A State of Danger

19.9: Chapter Summary

19.10: Detailed Figure Descriptions

Index

Glossary

Interactive Geologic Time Scale

Interactive Geologic Map of California

Detailed Licensing

Detailed Licensing

This page titled Geology of California is shared under a CC BY-NC 4.0 license and was authored, remixed, and/or curated by Allison Jones, Cole Heap, Debra Brooks, Emily Wright, Martha House, Steven Newton, & Steven Skinner.

This page titled 19.1.1: Table of Contents is shared under a license and was authored, remixed, and/or curated by LibreTexts.

1: INTRODUCTION TO THE GEOLOGY OF CALIFORNIA

Why California Geology?

California's geology is so rich, so diverse, so dynamic that one could conceivably see almost every type of rock and mineral, every type of volcano, every type of fault, every type of climate and water system, without leaving the boundaries of the Golden State.

Travel is, of course, a virtue and a necessity for a well-rounded life; as Twain wrote in *Innocents Abroad*, "Travel is fatal to prejudice, bigotry and narrow-mindedness." But to experience virtually everything in geology, California by itself is an open-air textbook of the Earth.

Glacially-carved landscapes with three thousand foot cliffs? Yosemite. Boiling mud lakes reeking of sulfur, heated and supplied from an ancient volcano that blew itself apart? Lassen. Mysterious dolomite boulders moving and plowing through the soil of a vast dry lake bed? Death Valley. Giant lava flows with endless miles of underground lava tubes? Lava Beds National Monument. The fault scarp of a plate boundary extending as far as you can see? The Carrizo Plain in the Great Valley. Fossils from the dawn of animal life? White Mountains. Rugged coastlines with mountains that touch the sea? Big Sur. Glassy domes of obsidian rising out of a vast lake created by accident? Salton Sea. California has all this and much more.

Other states have fascinating geology too. Kick any rock in any stream in Missouri and it probably is chock-full of mollusk fossils from when the whole of the Midwest was under a vast inland ocean. People walk miles along the southern coast of the Big Island of Hawaii to witness yellow-orange lava spilling into the hissing waves of the Pacific.

But California has a unique range of amazing geologic features, concentrated between parched deserts and freezing glaciers, between fault-crushed hills and river-carved canyons, between the highest point in the contiguous United States (Mt. Whitney, Figure 1.1) and the lowest point in the contiguous United States (Badwater, Death Valley).

We write this book because this is a place we love and when you love something, you want to share it with the world.



Figure 1.1: View of the highest peak in the lower 48 states: Mount Whitney, from the Alabama Hills in Lone Pine, California. This location has appeared in movies like Star Wars, Gladiator, and more since the 1950s. "Rocky road" by Mark Gunn via Flickr is licensed under CC BY.

Who It Is For

This textbook was designed to accommodate diverse backgrounds and learning needs among students enrolling in California Geology courses. It caters to both those with prior geology education and those without, allowing instructors to adapt the material to their particular course.

To ensure inclusivity, the book begins with foundational concepts such as minerals, rocks, plate tectonics, geologic structures, and seismology, assuming no prior geology knowledge. This approach facilitates the onboarding of new learners while enabling experienced students to refresh their understanding of core concepts.

Additionally, the book prioritizes accessibility of the material for students. All elements, including text, images, videos, and interactive activities, have been carefully crafted and curated to be compatible with assistive technology such as screen readers. We invite you to read more about our approach to accessibility.

Why This OER Was Written

This book was written to offer geology students and instructors at California Community Colleges and four-year institutions across California a text that was:

- Low cost
- Online
- Accessible and
- Openly licensed

Though excellent traditional textbooks for California Geology courses existed at the time that this book was written (e.g. *California Geology* by Deborah R. Harden, *California's Amazing Geology* by Donald R. Prothero), there were few low-cost (<$60) or online textbook options (e.g. Mira Costa College's online geology books by Phil Stofer). This book is freely available to anyone who wishes to learn from it. Its online format makes it easy to access from any device.

This text meets the accessibility requirements of the Academic Senate of California Community Colleges Open Educational Resource Initiative allowing as many students as possible to perceive the information.

The text is licensed under a Creative Commons Attribution Non-Commercial license (CC BY-NC) meaning it can be shared and adapted so long as it is not used for commercial purposes.

Finally, we wrote this book to be adaptable. In our years of teaching experience we have come to understand the various different approaches instructors might take to teaching a California Geology course. For that reason, the format of this text allows instructors to change the order of chapters, and add or remove content as they see fit, while meeting all of the requirements of C-ID GEOL 200 for Geology of California.

Why Organize by Geomorphic Province?

Like a Pleistocene saber cat trying to devour a whole Columbian mammoth stuck in what would become Los Angeles' La Brea Tar pits, our Golden State is simply too huge to digest all at once and needs to be bitten into smaller pieces. California's size warrants parsing in some meaningful way.

California's geomorphic provinces were first identified by California's Chief Geologist Olaf Jenkins when he first published the Geomorphic Map of California in 1938. The 11 provinces that Jenkins identified then have gone mostly unchanged since that time. We follow this same organization, although two chapters combine multiple provinces for the purposes of brevity; These are the Cascade Range and Modoc Plateau, and the Colorado and Mojave deserts.

Accessibility of the Geosciences

There are many aspects of the geology discipline that are inherently inaccessible. Complex maps, detailed figures, and rock and mineral samples are difficult to describe fully to those who cannot perceive them. Geology students must keenly distinguish very similar colors when studying minerals and rocks, and this is a real problem for those with color blindness. Field locations are difficult to access for those with mobility limitations; in fact, the traditional capstone undergraduate course for geology majors, Field Camp, has historically required not only full mobility, but also a high level of aerobic fitness and tolerance of sometimes extreme elevation and temperature conditions, and is therefore not accessible to many students, in the same way that playing on college football teams is not accessible to all students.*

We would like a different, more open approach to the variety of college students who can engage with California's geology – a book for everyone.

Future Work and a Call to Action

While new geology OER are being produced, there is still more we as a community of scientists and educators can do to increase the accessibility of the geoscience disciplines:

1. Field trips are often a core component of an undergraduate degree in geology. The authors of this book look forward to contributing a collection of openly licensed field guides to lower the barrier to teaching and learning geology in the field.
2. There is a great need for openly licensed ancillary materials such as figures, maps, and homework problems. Here are some recommendations for sharing your creative and scientific work using Creative Commons licensing so that it can be included in projects like this one and enhance student learning.
3. The recent move toward Open Access scientific journals allows that work to be accessed by anyone and shared under a Creative Commons license. It also allows figures from these works to be included in OER like this one. We fully support the movement toward Open Access scientific literature.

We will also continue to expand this repository of ancillary materials for educators.

Learning Objectives

By the end of this chapter, you should be able to:

- Describe why California is considered one of the most geologically diverse regions in the world and identify several types of geologic environments represented within the state.
- Explain the purpose of organizing California's geology by geomorphic province and summarize how this framework helps geologists interpret the state's complex geologic history.
- Interpret the basic features of a geologic map, including the role of the map key/legend, color conventions, and the meaning of common geologic symbols.

1.1: How to Read California's Geologic Map

1.2: Geologic Map Symbols

1.3: Detailed Figure Descriptions

* We do wish to acknowledge the enormous efforts within the geoscience community to make these field experiences more inclusive. Notably, the GeoSPACE Project and the International Association for Geoscience Diversity (IAGD).

This page titled 1: Introduction to the Geology of California is shared under a CC BY-NC 4.0 license and was authored, remixed, and/or curated by Allison Jones & Steven Newton.

1.1: How to Read California's Geologic Map

Geologic Maps

(Figure 1.1.1) is a geologic map shows the geological features of a region. A rock unit is color-coded and identified in the map legend. Faults and folds are also shown on geologic maps (Back Matter). The geology is superimposed on a topographic map to give a more complete view of the geology of the region.

The geologic data, in layer fashion, are typically printed upon a base map. The base map may show the topography, roads, rivers, or other cultural or natural features in the map area. Modern maps are in digital form, extending their usefulness in decision-making by allowing geologic information to be combined with other data, such as demographics or infrastructure. Explanatory text on the maps provides information on the geologic age of the materials as well as their physical properties.

A segment of a typical geologic map is shown in Figure 1.1.1. On the map the geologist has recorded the locations, types, and ages of the rock units and surficial materials by using various standard colors, symbols, and patterns overlain on a topographic base map. The basic rock units shown on the map are called formations. For example, on the map the green area labeled "Kp" shows the aerial extent of the Panoche Formation which is of Cretaceous age (symbolized by K). Similarly, the red portion of the map labeled "Mvqa" represents the aerial extent of an unnamed formation composed of a volcanic rock of Miocene age (symbolized by M). A formation is usually named after a geographic feature (mountain, canyon, or town) near the area where the rock unit was first identified. The geologically most recent deposits on the map are the landslides ("Qls") depicted in yellow with arrows showing the direction of movement or "flow". Using special symbols, the geologist has recorded other significant observations on the map such as faults (bold black lines), folds (pink arrows), contacts between rock units (thin black lines), and the strike and dip of formations (respectively, the direction of a horizontal line within a unit and the angle that the unit slopes in outcrop).

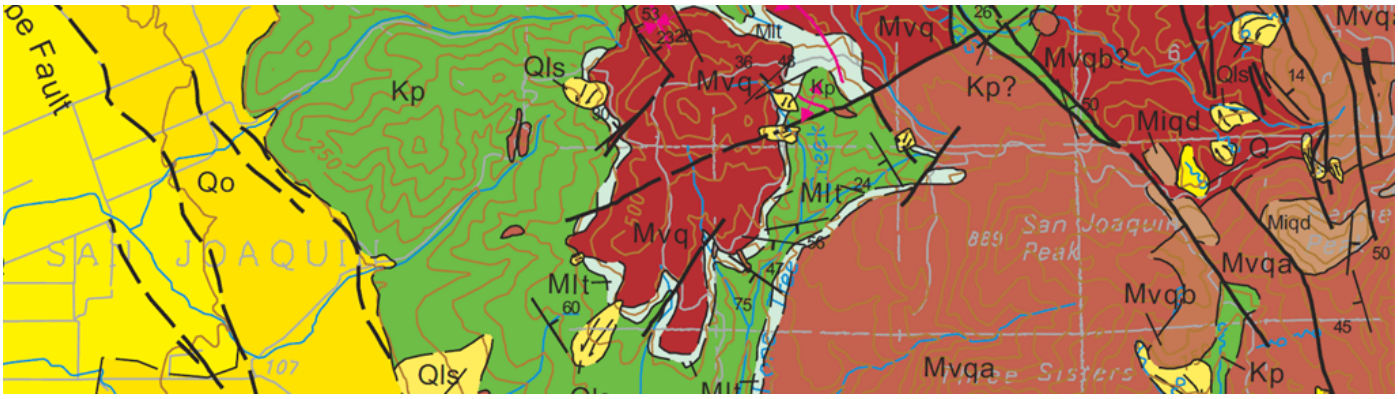


Figure 1.1.1: An excerpt from a geologic map of San Joaquin county, California. Various colors and symbols indicate differing rock and sediment types visible at the surface. Those color polygons are overlain on top of a topographic map which indicates the elevation of the land above sea level. Heavy solid dark lines indicate known fault traces, dashed lines indicate approximate or suspected fault locations. "Geologic map example" by the California Geological Survey is in the public domain. Access a detailed description

Geologic maps are important for two reasons. First, as geologists create geologic maps, explanatory text, and cross-sections, they develop a theoretical understanding of the geology and geologic history of a given area. Second, geologic maps are essential tools for practical applications such as zoning, civil engineering, and hazard assessment. Geologic maps are also vital in finding and developing geological resources, such as gravel to help build the road you drive on, oil to power the car you travel in, or aluminum to build the more fuel-efficient engine in your next vehicle. Another resource that is developed on the basis of geologic maps is groundwater, which many cities, farms, and factories rely on for the water they use.

Essential Components of Geologic Maps

A complete geologic map has at least two features:

- the map itself

- the map legend that explains all the symbols on the map.

Professional geologic maps usually have two other components as well:

- an accompanying explanation of the rock or sediment units
- geologic cross-sections of the map area.

The legend to a geologic map is usually printed on the same page as the map and follows a customary format. The symbol for each rock or sediment unit is shown in a box next to its name and brief description. These symbols are stacked in age sequence from oldest at the bottom to youngest at the top. The geologic era, or period, or epoch–the geologic age–is listed for each rock unit in the key (see Geologic Time). By stacking the rock units in age sequence from youngest at the top to oldest at the bottom, and identifying which interval of geologic time each unit belongs to, the map reader can quickly see the age of each rock or sediment unit. The map key also contains a listing and explanation of the symbols shown on the map, such as the symbols for different types of faults and folds. See the Tables of Geologic Map Symbols for pictures and an overview of the map symbols, including strikes and dips, faults, folds, and an overview.

Generalized Geologic Map of California

Let's now take a look at California's generalized geologic map (Figure 1.1.2). At first glance, you will likely notice some interesting patterns: Perhaps the light tan swath in the center of the state stands out, or the pink and red units along the eastern border catch your eye. These patterns are not random: they are the result of tectonic plates converging and diverging over many millennia (see Plate Tectonics and A Brief Geologic History).

California's geology is particularly complex compared to some of the flatter states of the Midwest where the geology can be described as "layer cake" geology–simple undisturbed layers of strata stacked on top of one another. By contrast, California is the only state in the U.S. with all three types of plate boundaries, and it is the only state that straddles two tectonic plates. We will revisit the generalized geologic map of California throughout this text.

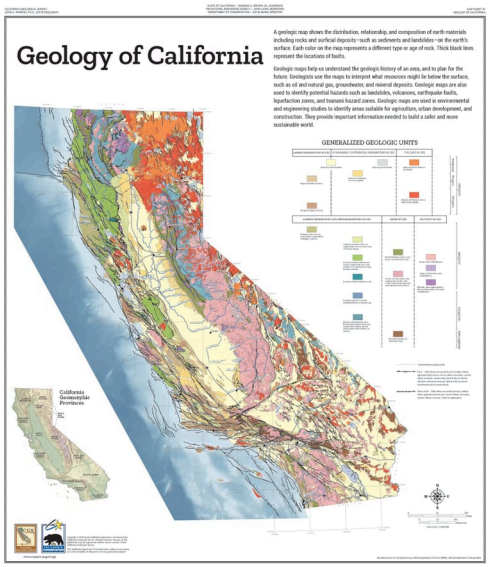


Figure 1.1.2: Generalized geologic map of California. Generalized geologic units are indicated by different colors, fault traces are indicated with black lines. Read the explanatory pamphlet that accompanies this map. "MS_057-2018-Geology-of-California" by the California Geological Survey is in the public domain. Access a detailed description.

The California Geological Survey has also made available an interactive geologic map of California which can be navigated by panning and zooming in and out. As you zoom in, more detailed geology appears. The data of this interactive map can also be downloaded for use with geographical information systems (GIS) software such as ESRI ArcGIS or open-source program QGIS.

References

1. California Geological Survey. (2018). *Geology of California* (Map Sheet No. 57). California Department of Conservation. https://www.conservation.ca.gov/cgs/Documents/Publications/Map-Sheets/MS_057-2018-Geology-of-California.pdf

This page titled 1.1: How to Read California's Geologic Map is shared under a CC BY-NC 4.0 license and was authored, remixed, and/or curated by Allison Jones.

1.2: Geologic Map Symbols

Tables of Common Geologic Map Symbols

Jump to:

- Strike and Dip Symbols
- Fault Symbols
- Fold Symbols

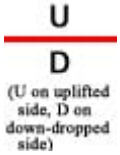
Strike and Dip Symbols

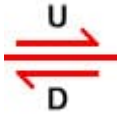
Table 1: Strike and Dip Symbols

Map Symbol	Definition	Explanation of Symbol
	Strike and dip of beds other than horizontal or vertical	• strike (longer line) is horizontal line on bedding plane • strike parallels nearby contacts between stratified rocks • dip shows which way beds run downhill • dip angle, number at end of dip symbol, is how much beds tilt down from horizontal
	Horizontal beds	• because the bed is horizontal it strikes in all directions • because the bed is horizontal, the dip is 0 degrees
	Strike and dip of vertical beds	• strike (longer line) is horizontal line on bedding plane • because the bed dips vertically (has a 90° dip), it dips equally in either direction at right angles to strike, so the dip line is shown extending in both directions

Fault Symbols

Table 2: Fault Symbols

Map Symbol	Definition	Explanation of Symbol
	Unknown dip-slip fault (could be normal or reverse)	• Down-dropped side is marked with "D" • Up-thrown side is marked with "U"
	Normal	• Rectangles are on the hanging wall side

Map Symbol	Definition	Explanation of Symbol
	Thrust or reverse	• Triangles are on the hanging wall side
	Strike-slip (right-lateral or left-lateral)	• Arrows indicate relative sense of motion
	Oblique-slip fault (components of both dip-slip and strike-slip)	• Arrows indicate relative sense of motion • Down-dropped side is marked with "D" • Up-thrown side is marked with "U"

Fold Symbols

Table 3: Fold Symbols

Map Symbol	Definition	Explanation of Symbol
	Anticline	• Convex up (arch-shaped) fold
	Syncline	• Convex down (U-shaped) fold
	Plunging anticline	• Convex up (arch-shaped) fold • Plunging down in the direction of the long arrow
	Plunging syncline	• Convex down (U-shaped) fold • Plunging down in the direction of the long arrow

References

1. Compton
2. Lumen learning

This page titled 1.2: Geologic Map Symbols is shared under a CC BY-NC 4.0 license and was authored, remixed, and/or curated by Steven Newton.

1.3: Detailed Figure Descriptions

Geologic map of San Joaquin County, California

The image is a geologic map showing a region divided into multiple irregularly shaped areas representing different rock units. This map demonstrates how geologists use spatial distribution, labeling, and structural features, such as faults, to interpret the geologic history of a region, including rock formation, deformation, and erosion.

Each unit is identified by a short label (such as “Qls,” “Kp,” “Mvq,” and “Qo”) placed within its boundary. These labels correspond to specific geologic formations or time periods. The map uses multiple colors to distinguish rock units, including yellow, green, red, tan, and brown. Because color alone can be difficult to interpret, each unit is also clearly separated by solid boundary lines and labeled directly within the region. The boundaries between units are uneven and follow natural geologic patterns rather than straight lines.

Several black lines cross the map diagonally and horizontally. These represent fault lines. Some faults are thicker and more prominent, indicating major structural features. In a few places, fault lines intersect or branch, suggesting a complex tectonic setting. Thin blue lines run across the map and represent rivers or streams. These lines follow winding paths and often cut across multiple rock units, indicating erosion and surface water flow. Contour lines appear in some areas as thin, closely spaced curved lines, indicating changes in elevation. These lines are most visible in the green and red regions, and help show the topography of the landscape. Place names and geographic references, such as “San Joaquin” and “San Joaquin Peak,” are printed in light text across the map, providing regional context. The left side of the map is dominated by a large yellow region labeled “Qo,” while the central and right portions contain a more complex mix of smaller, interlocking units in green, red, and tan. The density of labels and boundaries increases toward the center and right, indicating more geologic complexity in those areas.

Unit Abbreviations (decoded)

- Qls: Quaternary landslide deposits
- Qo: Quaternary older alluvium
- Kp: Cretaceous plutonic rocks
- Mvq (and variants): Miocene volcanic rocks

Geological Map of California

This image is a poster titled “Geology of California.” Across the top are institutional credits: California Geological Survey; John G. Parrish, Ph.D., State Geologist; State of California – Edmund G. Brown Jr., Governor; The Natural Resources Agency – John Laird, Secretary; Department of Conservation – David Bunn, Director; and “Map Sheet 57, Geology of California.”

To the right of the title are two explanatory paragraphs. The first explains that a geologic map shows the distribution, relationships, and composition of Earth materials, including rocks and surface deposits such as sediments and landslides. It states that each color represents a different rock type or age, and that thick black lines represent faults. The second paragraph explains that geologic maps are used to understand geologic history and to plan for the future. They help identify resources such as oil, natural gas, groundwater, and mineral deposits, as well as hazards including landslides, volcanoes, earthquake faults, liquefaction zones, and tsunami hazard zones. They are also used in environmental and engineering studies to identify areas suitable for agriculture, urban development, and construction, thereby supporting safer, more sustainable decisions.

The central portion of the image is a detailed geologic map of California. The state is divided into many irregularly shaped regions representing different geologic units. Each region is distinguished by both color and clearly defined boundary lines. Colors include greens, reds, yellows, browns, purples, and blues, but meaning is not dependent on color alone because units are separated by boundaries and referenced through the legend.

The map includes numerous labels for geographic locations, including “San Joaquin” and “San Joaquin Peak.” The Pacific Ocean is shown along the western edge in blue, and rivers are depicted as thin blue lines crossing multiple geologic units. A large, light-colored region extending north to south through the center represents the Central Valley, while surrounding areas show more complex patterns of smaller, interlocking units. Black lines across the map represent faults. These lines vary in thickness and style

to indicate different levels of certainty. Solid lines represent well-located faults, while dashed or dotted lines indicate approximate or concealed faults. Some faults intersect or branch, indicating complex tectonic relationships. Thrust faults are indicated with symbols showing the direction of movement.

To the right of the map is a legend titled “Generalized Geologic Units.” This section organizes rock types into categories, including:

- Marine sedimentary rocks
- Nonmarine (continental) sedimentary rocks
- Volcanic rocks
- Marine sedimentary and metasedimentary rocks
- Mixed rocks
- Plutonic rocks

Each category includes colored boxes paired with text descriptions of rock types, such as sandstone, shale, volcanic flows and deposits, granitic rocks, and metamorphic rocks. These categories are arranged vertically to align with geologic time divisions labeled Cenozoic, Mesozoic, and Paleozoic, allowing connections between rock types and ages.

Below the legend is a key explaining map symbols. It identifies:

- Contacts between geologic units (boundaries)
- Faults, with line styles indicating whether their location is well known, approximate, or concealed
- Thrust faults, marked with directional indicators showing relative motion

In the lower left corner, an inset map titled “California Geomorphic Provinces” shows major physical regions of the state, providing additional context for landscape organization. At the bottom right, a compass rose indicates cardinal directions (north, south, east, west), and a scale bar provides distance in both miles and kilometers. The map scale is approximately 1:750,000. At the bottom of the poster are logos for the California Geological Survey and California Conservation, along with a copyright statement indicating that the map was compiled by the California Department of Conservation and that no warranty is made regarding its use.

This page titled 1.3: Detailed Figure Descriptions is shared under a license and was authored, remixed, and/or curated by LibreTexts.

2: MINERALS AND ROCKS

Introduction to Minerals and Rocks

Before we can begin to discuss rocks and the rock materials that make up the state of California, we must address the building blocks of rocks: minerals; and the components that make up minerals: atoms and elements.

Minerals are all around us: the graphite in your pencil, the salt on your table, the plaster on your walls, and the trace amounts of gold (Figure 2.1) in your computer. Minerals can be found in a wide variety of consumer products including paper, medicine, processed foods, cosmetics, electronic devices, and many more. Everything made of metal is also derived from minerals.

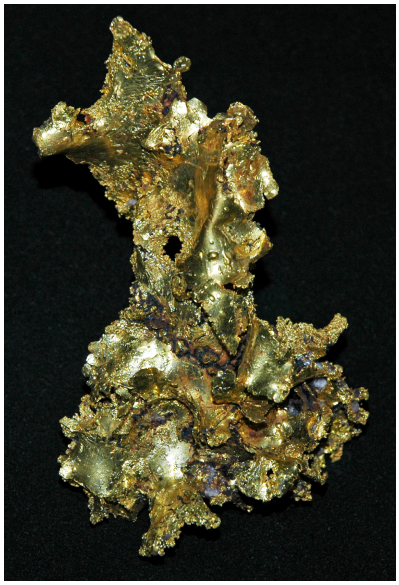


Figure 2.1: California's State Mineral, gold, from a gold-quartz hydrothermal vein in the "motherlode" of California, USA. (public display, Carnegie Museum of Natural History, Pittsburgh, Pennsylvania, USA). "Gold from quartz-gold hydrothermal vein (California, USA) 1" by James St. John via Flickr is licensed under CC BY 2.0.

A rock is a consolidated aggregate of minerals. By consolidated, we mean hard and strong. A mixture of minerals implies the presence of more than one mineral grain, but not necessarily more than one type of mineral. A rock can be composed of only one type of mineral (e.g., limestone is commonly made up of only calcite), but most rocks are composed of several different minerals. A rock can also include non-minerals, such as fossils or the organic matter within a coal bed.

Rocks are grouped into three main categories based on how they form:

- Igneous: formed from the cooling of magma (molten rock)
- Sedimentary: formed when weathered fragments of other rocks are buried, compressed, and cemented together, or when minerals precipitate directly from solution
- Metamorphic: formed by alteration (due to heat, pressure, and/or chemical action) of a pre-existing rock

This chapter wraps up with a discussion of the distribution of rocks in the state of California, using the Geologic Map of California as our guide.

Learning Objectives

By the end of this chapter, you should be able to:

- Explain how atoms bond to form compounds, including the chemical structures that create minerals.

- Differentiate between minerals and rocks by analyzing their composition and formation.
- Identify and compare the three major rock types, explain how each forms, and illustrate how they are interconnected through the rock cycle.
- Describe and interpret the general distribution of rock types across California, connecting patterns to geologic processes.

2.1: Minerals
2.2: Mineral Properties
2.3: The Rock Cycle
2.4: Igneous Rocks
2.5: Sedimentary Rocks
2.6: Metamorphic Rocks
2.7: Chapter Summary
2.8: Detailed Figure Descriptions

This page titled 2: Minerals and Rocks is shared under a CC BY-NC 4.0 license and was authored, remixed, and/or curated by Allison Jones.

2.1: Minerals

Defining "Mineral"

A mineral is a naturally occurring inorganic element or compound that is solid at room temperature (25° C), has a regular internal structure, and has a defined chemical composition. Let's break down the five aspects of this definition:

"Naturally occurring" implies that minerals are not artificially made. Many minerals (e.g., diamond) can be made in laboratories, but if they can also occur naturally, they still qualify as minerals.

Organic chemicals are made of the element carbon (C), so generally minerals are not composed of carbon. There are a handful of important minerals that include carbon so the term "organic" in this case means compounds of carbon, oxygen, and hydrogen. Sugar crystals, therefore, are not minerals. "Inorganic" with respect to minerals means not consisting of or deriving from living matter.

At 25° C minerals must be in the solid state. There are a few exceptions to this rule made for substances defined as minerals before 1959 when strict procedures were established for defining what a mineral is. For example, water ice is considered a mineral which is only solid at or below 0° C. Mercury is also considered a mineral even though it is only solid below -39° C. When found in rocks above -39° C, mercury forms silvery liquid blobs (Figure 2.1.1).



Figure 2.1.1: Drops of native mercury (pure mercury, Hg), also known as quicksilver, from California, USA. This sample is on public display at the Carnegie Museum of Natural History, Pittsburgh, Pennsylvania, USA. "Mercury (California, USA) 1" by James St. John via Flickr is shared under CC BY.

A mineral has a specific "repeating three-dimensional structure" or "lattice," which is the way in which the atoms are arranged. The elements sodium (Na) and chlorine (Cl) atoms bond in a regular repeating pattern to form the mineral halite (Figure 2.1.2). That happens to be about the simplest mineral lattice of all; most mineral lattices are much more complicated.

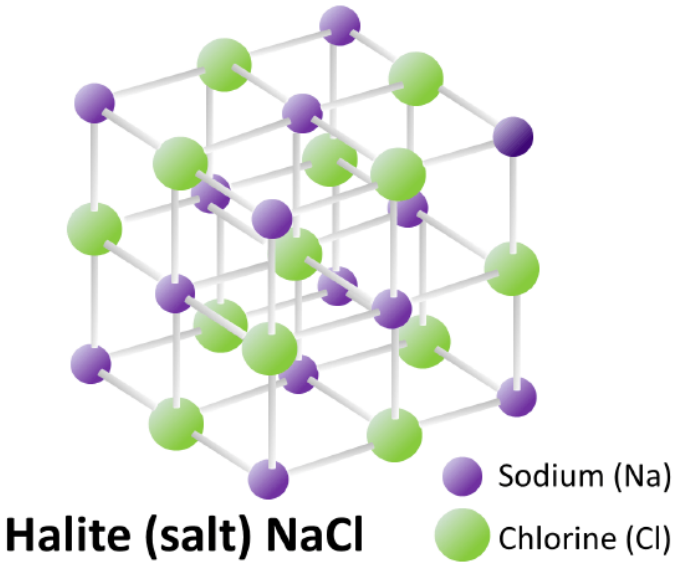


Figure 2.1.2: Halite crystal lattice model, with atoms at each corner and along the edges and faces, forming a repeating unit cell in three dimensions. The smaller purple spheres, located each corner of the cube and at the center of each face, represent the cation sodium (Na^+) and the larger green spheres, located in the center of each edge, represent the anion chlorine (Cl^-). Bars between atoms represent ionic bonds. Each sodium ion is surrounded by six chlorine ions, and each chlorine ion is surrounded by six sodium ions. "Halite Crystal Lattice" by Steven Earle is licensed under CC BY 4.0.

Some substances that we think of as minerals are actually not minerals by definition because they lack this repeating three-dimensional structure. Volcanic glass is an example, as are pearl, and opal. Figure 2.1.3 illustrates how the Si and O atoms in quartz are arranged in a regular repeated pattern. Compare that to Figure 2.1.4 which illustrates the irregular arrangement of these same atoms in silica glass. While some bonds exist, they are not consistent throughout the material.

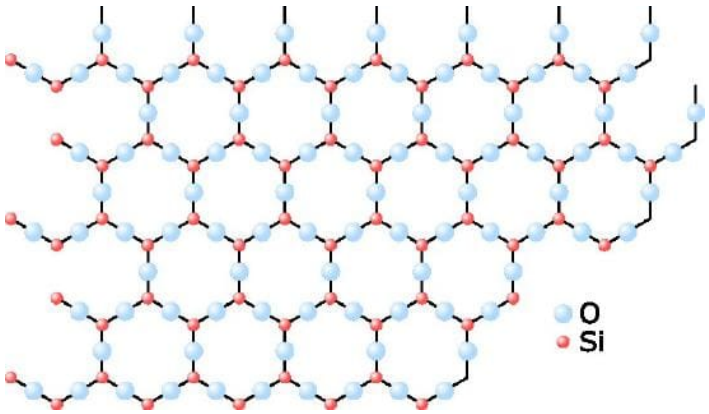


Figure 2.1.3: The regular internal crystalline structure of SiO_2 in two dimensions. Smaller red spheres represent silicon atoms which are bonded in a regular repeating pattern with oxygen, represented by larger blue spheres. This mesh-like view is a slice through the crystal lattice of quartz wherein each silicon atom is actually bonded to four oxygen atoms. The fourth oxygen atom is not visible in this plane of view. "SiO2 Quartz" by Wimmel via Wikimedia Commons is in the public domain. Access a detailed description.

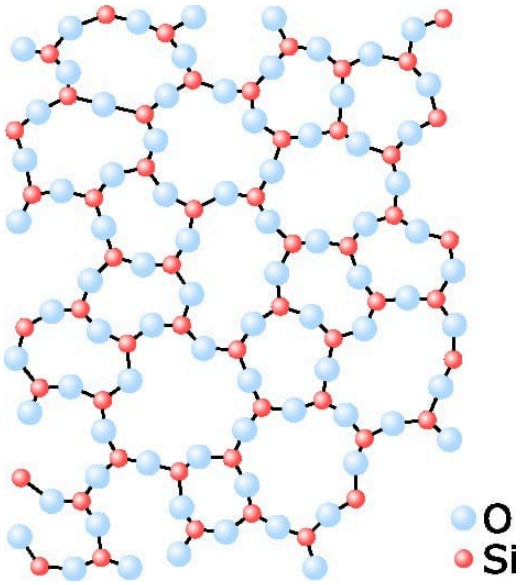


Figure 2.1.4: The random network structure of silica glass in two dimensions, seen as a network of irregular shapes. As in the crystal, each silicon atom is bonded to four oxygen atoms, where the fourth oxygen atom is obscured from view in this plane. "Silica.jpg" by Jdrewitt via Wikimedia Commons, a derivative of the original work, is in the public domain.

"Defined chemical composition" means that most minerals have a specific chemical formula or composition. The mineral pyrite, for example, is FeS_2 (two atoms of sulfur for each atom of iron), and any significant departure from that would make it a different mineral. But many minerals can have variable compositions within a specific range. The mineral olivine, for example, can range from Fe_2SiO_4 to $FeMgSiO_4$ to Mg_2SiO_4. Intervening compositions are written as $(Fe,Mg)_2SiO_4$ meaning that Fe and Mg can be present in any proportion, and that there are two of them for each Si present. This type of substitution is known as a solid solution. Other common minerals such as plagioclase feldspar also occur in solid solution.

Query 2.1.1

This interactive element is not available in this format. Visit the link or scan the QR code to access it online.

View this Interactive Content online

Atoms

Minerals are made up of atoms, and all atoms are made up of three main subatomic particles known as protons, neutrons and electrons. As summarized in Table 2.1.1, protons are positively charged, neutrons are uncharged, and electrons are negatively charged. The negative charge of one electron balances the positive charge of one proton. Both protons and neutrons have a mass of 1 amu, while electrons have almost no mass.

Table 2.1.1: Charges and masses of atomic particles

Particle	Charge	Mass (amu)
Electron	-1	~0
Proton	1	1
Neutron	0	1

The simplest atom is that of hydrogen (atomic number 1) which has one proton and one electron. The proton forms the nucleus, while the electron spins around it. All other elements have neutrons as well as protons in their nucleus, such as helium (atomic number 2). The positively-charged protons tend to repel each other, and the neutrons help to hold the nucleus together.

The atomic number is the number of protons. The mass number is equal to the total number of protons and neutrons in an atom. Hydrogen (H) for example, has an atomic number of 1 because it has 1 proton. Helium (He) has an atomic number of 2 because it has 2 protons. Figure 2.1.5 provides a simplified view of the elements up to number 36.

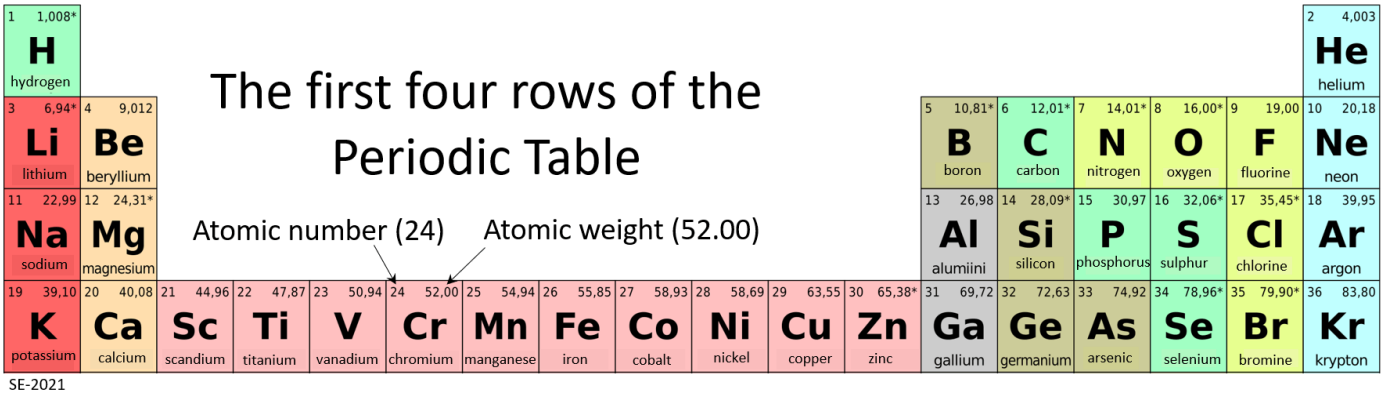


Figure 2.1.5: The first four rows of the Periodic Table Showing Element Symbols (e.g., Cr), Names (e.g., chromium), Atomic Numbers (upper left of each element symbol) and Atomic Weights (upper right of each element symbol). "First four rows of the periodic table" by Steven Earle, a derivative of the original, is licensed under CC BY. Access a detailed description.

Electron orbits around the nucleus of an atom are arranged in what we call shells—also known as energy levels. The first shell can hold only two electrons, while the next shell will hold up to eight electrons. Subsequent shells can hold more electrons, but the outermost shell of an atom will hold no more than eight electrons. These outermost shells are important in bonding between atoms, and bonding takes place between atoms that do not have full outer shells.

Isotopes

Isotopes are atoms that have the same atomic number (number of protons), but different mass numbers due to a difference in the number of neutrons.

The atomic mass (or atomic weight) of an element is a weighted average of all naturally occurring isotopes of that atom. Let's consider oxygen. There are three naturally occurring stable isotopes of oxygen on Earth: oxygen-16 (denoted ^{16}O), oxygen-17 (^{17}O), and oxygen-18 (^{18}O). Table 2.1.2 summarizes the characteristics of these three stable isotopes. Oxygen's atomic mass (Figure 2.1.5) is ~15.999 amu, illustrating that oxygen-16 is more abundant than oxygen's other two stable isotopes.

Table 2.1.2: Stable oxygen isotopes

Nuclide	Protons (Z)	Neutrons (N)	Natural abundance
^{16}O	8	8	99.738%
^{17}O	8	9	0.0367%
^{18}O	8	10	0.187%

This is an example of a stable isotope, an isotope which does not decay (or change) over time. Oxygen-18, which is noted in the table above and is referred to as one of the environmental isotopes. It is important in paleoclimatology, the study of past climates, for example, because we can use the ratio between Oxygen-18 and Oxygen-16 in ice cores to determine the temperature of precipitation over time.

Radioactive, or unstable, isotopes are essential for dating minerals and rocks. For more on how isotopes are used to study the ages of Earth materials, see Geologic Time.

Bonding and Lattices

An atom seeks to have a full outer shell (i.e. 8 electrons for most elements, or 2 electrons for hydrogen, helium, lithium, and beryllium) to be atomically stable and thus, nonreactive. This is accomplished by lending, borrowing, or sharing electrons with other atoms. The noble gasses, such as helium, neon, argon etc., already have completed outer orbits so they don't need to lose or gain any electrons.

Sodium has 11 electrons, 2 in the first shell, 8 in the second, and 1 in the third (Figure 2.1.6). Sodium readily gives up this third shell electron, and when it does it loses one negative charge and becomes positively charged. Chlorine, on the other hand, has 17 electrons, 2 in the first shell, 8 in the second, and 7 in the third. Chlorine readily accepts an eighth electron for its third shell, and therefore becomes negatively charged. In changing their number of electrons these atoms become ions—the sodium a positive ion or cation, the chlorine a negative ion or anion. The resulting electric attraction between these ions is known as an ionic bond. Electrons can be thought of as being transferred from one atom to another in an ionic bond.

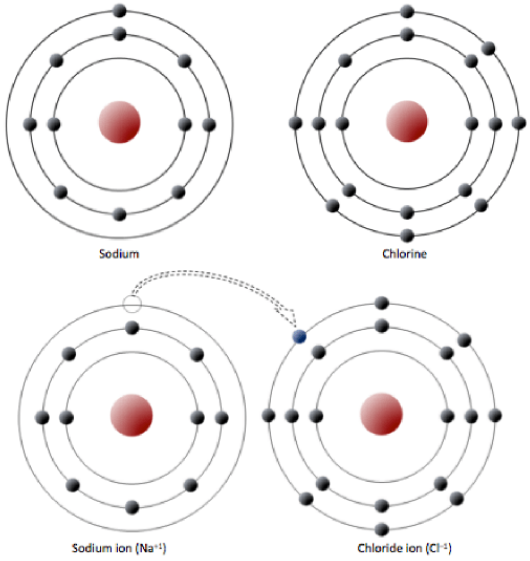


Figure 2.1.6: Electron configuration of sodium and chlorine atoms. Sodium gives up an electron to become a cation and chlorine accepts an electron to become an anion. "NaCl" by Steven Earle is licensed under CC BY 4.0. Access a detailed description.

Common table salt (NaCl) is a mineral composed of chlorine and sodium linked together with ionic bonds that are depicted as grey lines in (Figure 2.1.2). The mineral name for NaCl is halite and its structure is cubic, meaning that all of the bonds are at right angles to each other. This is why halite grows as cubic crystals (Figure 2.1.7), and it is also why it breaks along three planes at right angles to each other (see Mineral Properties).



Figure 2.1.7: The mineral halite is composed of sodium and chlorine bonded together with ionic bonds. It has a cubic crystal lattice, which is why it breaks into cubic crystals. "Halite" by Hans-Joachim Engelhardt is licensed under CC BY-SA 4.0.

Video 2.1.1: How Atoms Bond

The following video illustrates these different ways in which atoms bond to one another:

This interactive element is not available in this format. Visit the link or scan the QR code to access it online.

View this YouTube Video online

The elements silicon and oxygen are the most abundant elements in Earth's crust and mantle and are present in the minerals that make up most rocks. Silicon and oxygen bond together to create a four-sided pyramid shape with an oxygen at each corner and a silicon in the middle, known as a silicon-oxygen tetrahedron (Figure 2.1.8). This is the building block of the many important silicate minerals. The bonds in a silicon-oxygen tetrahedron have some of the properties of covalent bonds and some of the properties of ionic bonds. As a result of the ionic character, silicon becomes a cation (with a charge of +4) and oxygen becomes an anion (with a charge of -2). The net charge of a silicon-oxygen tetrahedron (SiO_4) is -4. As we will see later, silicon-oxygen tetrahedra are linked together in a variety of ways to form most of the common minerals of the crust.

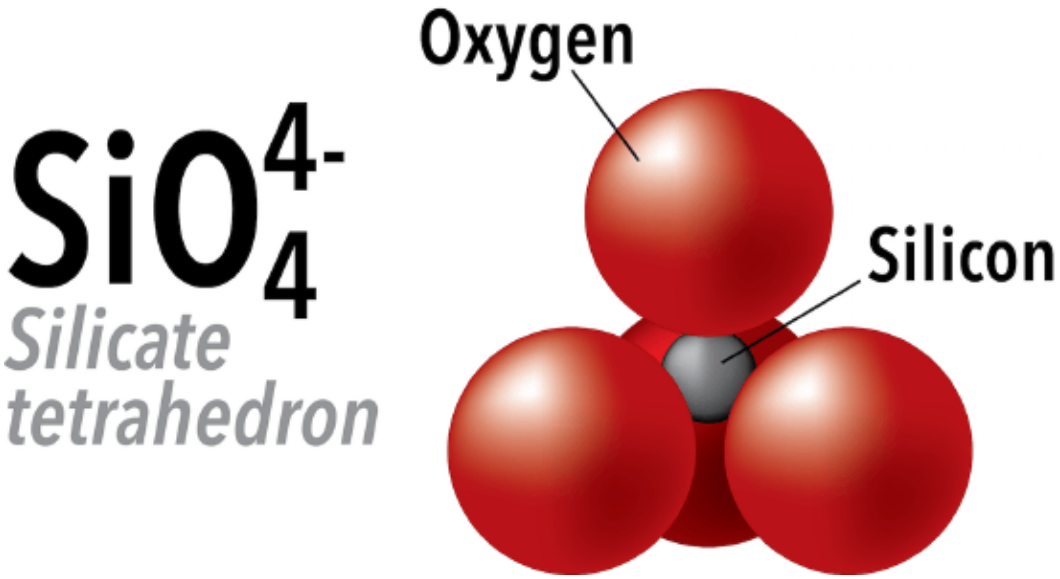


Figure 2.1.8: The silicon-oxygen tetrahedron, made of four oxygens bonded to one silicon (represented as the small gray sphere in the center), is the building block of all silicate minerals. "SiO4 4- Silicate tetrahedron" by Karla Panchuk, a derivative of the original work, is licensed under CC BY-SA 3.0.

3D Model of Silicon-Oxygen Tetrahedron

The following 3D model illustrates the silicon oxygen tetrahedron in three dimensions:

This interactive element is not available in this format. Visit the link or scan the QR code to access it online.

View this Interactive Content online

SiO_4 tetrahedron by **Earth Sciences, University of Newcastle** on **Sketchfab**

Box 2.1.1: Silicon (Si)

The element silicon (Si) is one of the most important geological elements and is the second-most abundant element in Earth's crust (after oxygen). Silicon bonds readily with oxygen to form a silica tetrahedron (Figure 2.1.8). Pure silicon crystals are used to make semi-conductive media in electronic devices called silicon wafers. A silicate mineral is one in which silicon and oxygen are present as silica tetrahedra (plural of tetrahedron). Silica also refers to a chemical component of a rock, and is expressed as % SiO_2. The mineral quartz is made up entirely of silica tetrahedra, and some forms of quartz are known as silica. Silicone is a synthetic product (e.g., silicone rubber, resin, or caulking) made from silicon-oxygen chains and various organic molecules.

The following video provides an overview of the ways we use the abundant element silicon:

This interactive element is not available in this format. Visit the link or scan the QR code to access it online.

View this YouTube Video online

Mineral Groups

Minerals are most often organized into groups according to their chemical composition, particularly their anion or anionic group (the negatively charged end of the chemical formula).

Elements bonded together in various configurations form minerals. A mineral is a naturally occurring, solid compound with a specific composition and a regular repeating lattice structure (like the halite in Figure 2.1.3). Most minerals are made up of a cation (a positively charged ion) or several cations, and an anion (a negatively charged ion) or an anion group. For example, in the mineral hematite (Fe_2O_3) the cation is Fe (iron – Fe^{3+}) and the anion is O (oxygen O^{2-}). (The two +3 iron ions contribute 6 positive charges and the three -2 oxygen ions contribute 6 negative charges, so the charge is balanced, which is a requirement of all minerals.) We group minerals into classes on the basis of their predominant anion or anion group. These include oxides, sulfides, carbonates and silicates, and others. Silicates are by far the predominant group in terms of their abundance within the crust and mantle, and they will be discussed in the next section. Some examples of minerals from the different mineral groups are given in Table 2.1.2.

Table 2.1.2: The primary mineral groups, their anions, and examples of minerals for each group

Group	Anion	Example Minerals
Oxides	O-	Hematite (iron-oxide – Fe_2O_3), corundum (aluminum-oxide Al_2O_3), water ice (H_2O)
Sulfides	S-	Galena (lead-sulfide – PbS), pyrite (iron-sulfide – FeS_2), chalcopyrite (copper-iron-sulfide – $CuFeS_2$)
Carbonates	CO_3^{2-}	Calcite (calcium-carbonate – $CaCO_3$), dolomite (calcium-magnesium-carbonate – $(Ca,Mg)CO_3$
Phosphates	PO_4^{4-}	Apatite ($Ca_5(PO_4)_3(OH)$), monazite (Ce, La, Y, Th)PO_4, turquoise $CuAl_6(PO_4)_4(OH)_8{\cdot}4H_2O$
Silicates	SiO	Quartz (SiO_2), feldspar (sodium-aluminum-silicate – $NaAlSi_3O_8$), olivine (iron or magnesium-silicate – $(Mg,Fe)SiO_4$) Note that in quartz the anion is oxygen, and while it could be argued, therefore, that quartz is an oxide, it is always classed as a silicate.
Halides	Halogen element	Fluorite (calcium-fluoride – CaF_2), halite (sodium-chloride – NaCl) Halide minerals have halogen elements as their anion – the minerals in the second last column on the right side of the Periodic Table, such as F, Cl, Br etc. (see **Figure 2.1.5**)
Sulfates	SO_4^{-2}	Gypsum (calcium-sulfate – $CaSO_4{\cdot}2H_2O$), barite (barium-sulfate – $BaSO_4$) Note that *sulfates* are different from *sulfides*. Sulfates have the SO_4^{-2} ion while sulfides have the S^{-2} ion)
Native elements	Single element	Gold (Au), diamond (C), graphite (C), sulfur (S), copper (Cu)

Oxide minerals have oxygen as their anion, but they exclude those with oxygen complexes such as carbonate (CO_3^{2-}), sulfate (SO_4^{2-}), or silicate (SiO_4^{4-}). If the oxygen is also combined with hydrogen to form the hydroxyl anion (OH–) the mineral is known as a hydroxide. Some important hydroxides are limonite (FeO(OH)) and gibbsite ($Al(OH)_3$), which are common within ores of iron and aluminum.

Sulfides are minerals with the S^{2-} anion, and they include galena (PbS), sphalerite (ZnS), chalcopyrite ($CuFeS_2$) and molybdenite (MoS_2), which are the most important ores of lead, zinc, copper and molybdenum respectively. Another important sulfide mineral is pyrite (FeS_2).

The **carbonates** include minerals in which the anion is the CO_3^{2-} complex. The carbonate combines with +2 cations to form minerals such as calcite ($CaCO_3$), magnesite ($MgCO_3$), dolomite ($(Ca,Mg)CO_3$) and siderite ($FeCO_3$). The copper minerals malachite and azurite are also carbonates.

In **phosphate** minerals the anion is PO_4^{4-}. An important phosphate mineral is apatite ($Ca_5(PO_4)_3(OH)$), which is what your teeth are made of.

The **silicate** minerals include the elements silicon and oxygen in varying proportions ranging from SiO_2 to SiO_4. These are discussed in more detail in the next section.

The **halides** are so named because the anions include the halogen elements chlorine, fluorine, bromine etc. Examples are halite (NaCl) and fluorite (CaF_2).

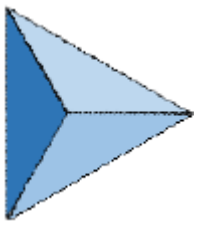
Sulfates are minerals with the SO_4^{-2} anion, and these include anhydrite ($CaSO_4$ and its cousin gypsum $CaSO_4 \cdot 2H_2O$) and the sulfates of barium and strontium: barite ($BaSO_4$) and celestite ($SrSO_4$). In all of these cases the cation has a +2 charge which balances the -2 charge on the sulfate ion.

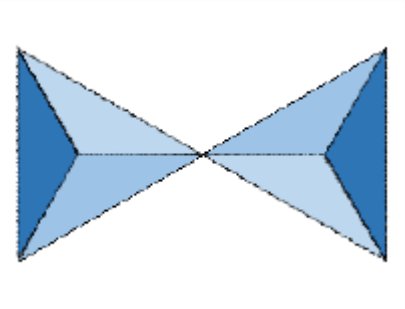
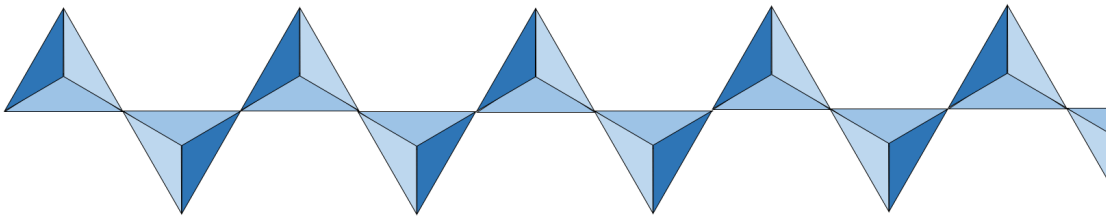
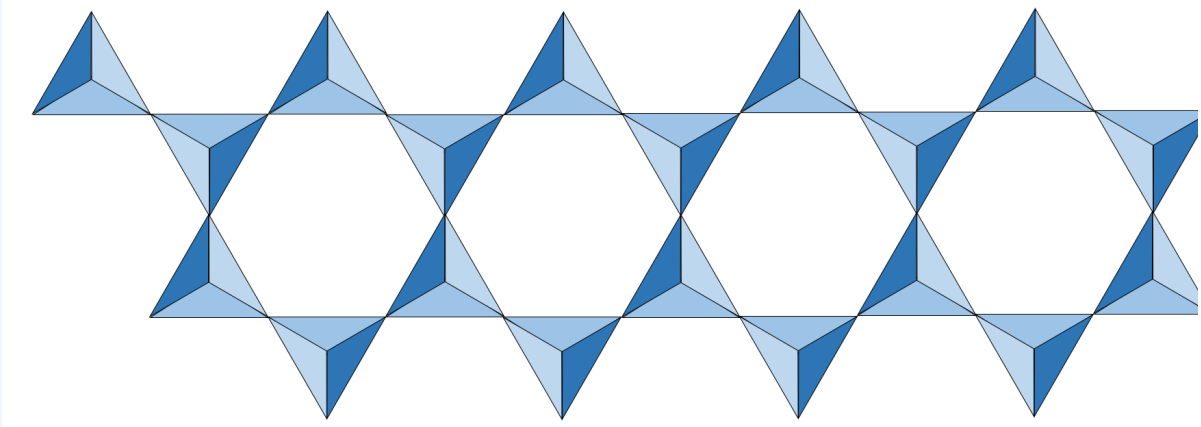
Native minerals include only one element (bonded to itself), such as gold, copper, sulfur, or carbon (which could be graphite or diamond).

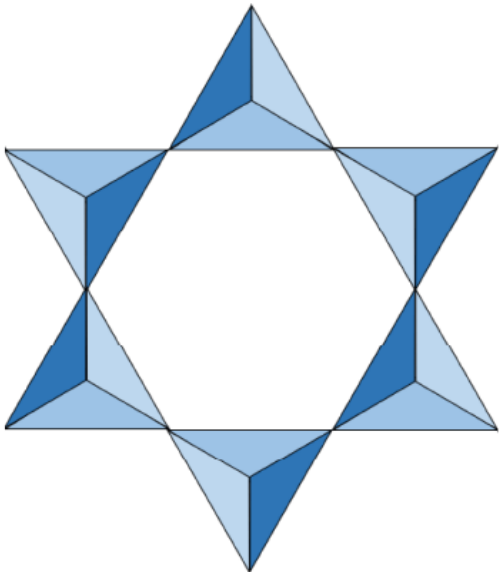
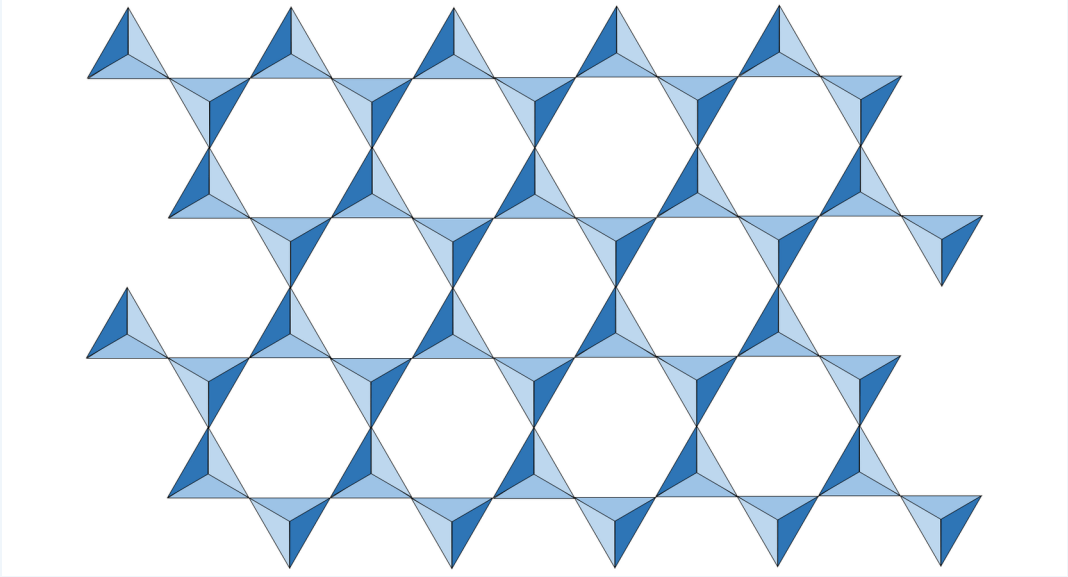
Silicate Minerals

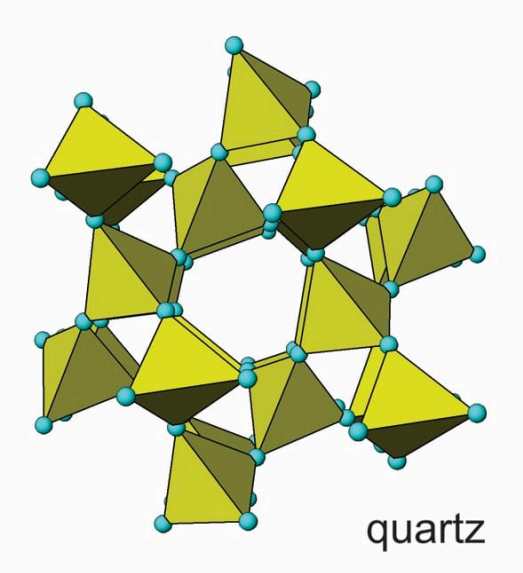
The vast majority of the minerals that make up the rocks of Earth's crust are silicate minerals. These include minerals such as quartz, feldspar, mica, amphibole, pyroxene, olivine, and a great variety of clay minerals. The building block of all of these minerals is the **silica tetrahedron**,. As discussed in the section on bonding and lattices, it is a combination of four oxygen atoms and one silicon atom. In silicate minerals these tetrahedra are arranged and linked together by sharing oxygen atoms in a variety of ways, from single units to complex frameworks (**Table** 2.1.2). The simplest silicate structure, that of the mineral olivine, is composed of isolated tetrahedra bonded to iron and/or magnesium ions. In olivine the -4 charge of each silica tetrahedron is balanced by the addition of two divalent (i.e., +2) iron or magnesium cations. Olivine can be either Mg_2SiO_4 or Fe_2SiO_4, or some combination of the two, which is written like this: $(Mg,Fe)_2SiO_4$, meaning that any proportions of Mg and Fe are possible.

Table 2.1.3: Silicate Mineral Subgroups

Silicate Subgroup	Tetrahedral Arrangement
Isolated tetrahedra (nesosilicates)	 "Nesosilicate structure" by Allison Jones, a derivative of the original, is licensed under CC BY-NC-SA 4.0.

Silicate Subgroup	Tetrahedral Arrangement
Sorosilicates	 "Sorosilicate structure" by Allison Jones, a derivative of the original, is licensed under CC BY-NC-SA 4.0.
Single chain (inosilicates)	 A single chain of silica tetrahedra; each tetrahedron is connected to two other tetrahedra. "Inosilicate structure R. Hendricks is licensed under CC BY-NC-SA 4.0.
Double chain (inosilicates)	 A double chain of silica tetrahedra. Note that every other silica tetrahedron shares a corner oxygen with the pa This work by Jonathan R. Hendricks is licensed under CC BY-NC-SA 4.0.

Silicate Subgroup	Tetrahedral Arrangement
Cyclosilicates	 "Cyclosilicate structure" by Allison Jones, a derivative of the original, is licensed under CC BY-NC-SA 4.0.
Sheet (phyllosilicates)	 A sheet of silica tetrahedra. Note that each silica tetrahedron shares a corner oxygen with three other tetrahed "Phyllosilicate structure" by Jonathan R. Hendricks is licensed under CC BY-NC-SA 4.0.

Silicate Subgroup	Tetrahedral Arrangement
Framework (tectosilicates)	 Three-dimensional framework (tectosilicate) atomic structure. This is the simplest example: quartz. "Tectosilica Allison Jones, a derivative of the original, is licensed under CC BY-NC-SA 4.0. View a 3D model of quartz, a tectosilicate.

References

1. "Atomic Weight of Oxygen | Commission on Isotopic Abundances and Atomic Weights". *ciaaw.org*. Retrieved 2022-03-15.
2. • 1. Earle, S. (2019). *Physical Geology – 2nd Edition*. Victoria, B.C.: BCcampus. Retrieved from https://opentextbc.ca/physicalgeology2ed March 2024
3. Klein, C., and C. S. Hurlbut, Jr. 1999. *Manual of Mineralogy*, after J.D. Dana. John Wiley & Sons, Inc., New York, 681 pp.
4. Press, F., and R. Siever. 1994. *Understanding Earth*. W. H. Freeman and Company, New York, 593 pp.

This page titled 2.1: Minerals is shared under a CC BY-NC 4.0 license and was authored, remixed, and/or curated by Allison Jones.

2.2: Mineral Properties

Identifying Minerals

The properties of minerals are dependent upon their chemistry and crystalline structure. Often referred to as “physical properties” they are used to identify minerals and to determine the usefulness of individual minerals in society.

Color

While some minerals have particularly distinctive colors that make good diagnostic properties, many do not, and for many, color is simply unreliable. The mineral sulfur (S) is always a distinctive and unique yellow. Hematite, on the other hand, is an example of a mineral for which color is not diagnostic. In some forms, hematite is deep dull red, but in others it is black and shiny metallic. Many other minerals can have a wide range of colors (e.g., quartz, feldspar, amphibole, fluorite, and calcite). In most cases, the variations in colors are a result of varying proportions of trace elements within the mineral. In the case of quartz, for example (Figure 2.2.1), yellow quartz (citrine) has trace amounts of ferric iron (Fe3+), rose quartz has trace amounts of manganese (Mn), purple quartz (amethyst) has trace amounts of iron (Fe), milky quartz, which is very common, has millions of fluid inclusions (tiny cavities, each filled with water), and smoky quartz occurs when trace amounts of aluminum create structural defects that are activated by natural radiation in the surrounding rock.



Figure 2.2.1: The many colors of quartz. Quartz can be clear and colorless (top left), opaque whitish (milky quartz, top middle), a grayish color (smoky quartz, top right), purple (amethyst, bottom left), yellow (citrine, bottom middle), and pink (rose quartz, bottom right). The many colors of Quarts by Karla Panchuk is shared under a CC BY-NC-SA 4.0 license.

Streak

In the context of minerals, “color” is what you see when light reflects off the surface of the sample. One reason that color can be so variable is that the type of surface is variable. It may be a crystal face or a fracture surface or a cleavage plane, and the crystals may be large or small depending on the nature of the rock. If we grind a small amount of the sample to a powder we get a much better indication of its actual color. This can easily be done by scraping a sample of the mineral across a **streak plate** (a piece of unglazed porcelain) to make a **streak**. The result is that some of the mineral gets ground to a powder and we can get a better impression of its “true” color (Figure 2.2.2).



Figure 2.2.2: Hematite leaves a distinctive reddish-brown streak whether the sample is gray and metallic (left) or earthy deep red (right). Hermatite leaves by Karla Panchuk is licensed under CC BY 4.0.

Luster

Luster is the way light reflects off the surface of a mineral, and the degree to which it penetrates into the interior. The key distinction is between metallic and non-metallic lusters. Light does not pass through metals, and that is the main reason they appear "metallic." Even a thin sheet of metal—such as aluminum foil—will not allow light to pass through it. Many non-metallic minerals may look as if light will not pass through them, but if you take a closer look at a thin edge of the mineral you can see that it does. If a non-metallic mineral has a shiny, reflective surface, then it is called "vitreous" (from the Latin word for glass). If it is dull and non-reflective, it is considered "earthy." Other types of non-metallic lusters are "silky," "pearly," and "resinous." Luster is a good diagnostic property since most minerals will always appear either metallic or non-metallic. There are a few exceptions to this (e.g., hematite in Figure 2.2.2).

Terms that describe luster:

- Nonmetallic
  - Vitreous (glassy)
  - Silky
  - Pearly
  - Resinous
  - Earthy (dull)
  - Greasy (oily)
  - Waxy
- Metallic
- Submetallic

Query 2.2.1

This interactive element is not available in this format. Visit the link or scan the QR code to access it online.

View this Interactive Content online

Hardness

One of the most important diagnostic properties of a mineral is its hardness. In 1812 German mineralogist Friedrich Mohs came up with a list of 10 common minerals that had a wide range of hardnesses. These minerals are listed in Figure 2.2.3, with the Mohs scale of hardness along the bottom axis and Table 2.2.1. In fact, while each mineral on the list is harder than the one before it, the

relative measured hardnesses (vertical axis) are not linear. Apatite is about three times harder than fluorite and diamond is three times harder than corundum. Some commonly available reference materials are also shown on this diagram, including a natural fingernail (2.5), a piece of copper (3.0), a knife blade (5.5), a piece of window glass (5-5.5), a hardened steel file (6.5), and an unglazed porcelain streak plate (7). These are tools that a geologist can use to measure the hardness of unknown minerals. For example, if you have a mineral that you can't scratch with your fingernail, but you can scratch with a copper wire, then its hardness is between 2.5 and 3.5. And of course the minerals themselves can be used to test other minerals.

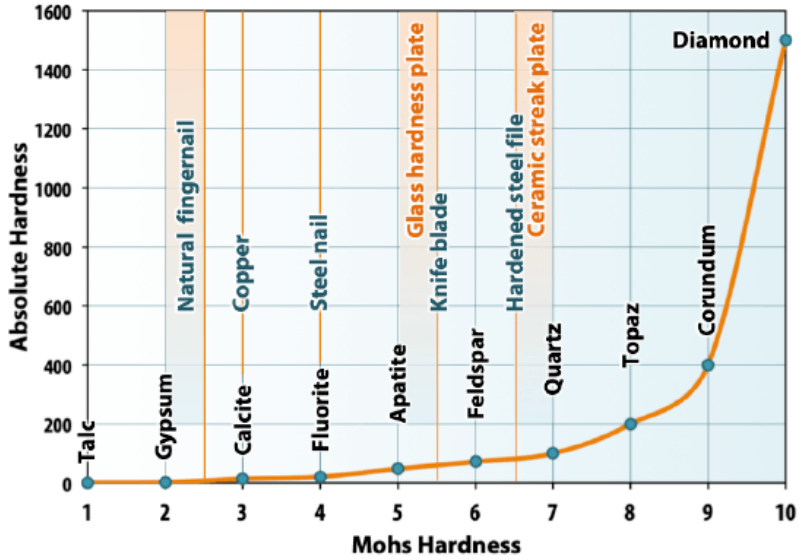


Figure 2.2.3: Mohs Hardness Scale of minerals from hardness of 1 (talc) to hardness of 10 (diamond); notice that the scale is not linear. Described in Table 2.2.1. Mohs scale of hardness by Karla Panchuk is licensed under CC BY 4.0.

Table 2.2.1: Mohs hardness scale

Mohs Hardness	Mineral	Common Reference Materials
1	Talc (softest)	
2	Gypsum	2.5 - Natural fingernail
3	Calcite	3.5 - Copper coin
4	Fluorite	
5	Apatite	5.5 - Glass plate, knife blade
6	Orthoclase Feldspar	6.5 - Hardened steel file, unglazed porcelain plate
7	Quartz	
8	Topaz	
9	Corundum	
10	Diamond (hardest)	

Query 2.2.2

This interactive element is not available in this format. Visit the link or scan the QR code to access it online.

View this Interactive Content online

Crystal Habit (Form)

When minerals form within rocks, there is a possibility that they will form in distinctive crystal shapes if they formed slowly and if they are not crowded out by other pre-existing minerals. Every mineral has one or more distinctive crystal habits, but it is not that common, in ordinary rocks, for the shapes to be obvious. Quartz, for example, will form six-sided prisms with pointed ends (Figure 2.2.4 left), but this typically happens only when it crystallizes from a hot water solution within a cavity in an existing rock. Pyrite can form cubic crystals (Figure 2.2.4 center), but can also form crystals with 12 faces, known as dodecahedra ("dodeca" means 12). The mineral garnet also forms dodecahedral crystals (Figure 2.2.4 right).

Because well-formed crystals are rare in ordinary rocks, habit isn't as useful a diagnostic feature as one might think. However, there are several minerals for which it is important. One is garnet, which is common in some metamorphic rocks and typically displays the dodecahedral shape. Another is amphibole group minerals, such as hornblende, which form long thin crystals, and are common in igneous rocks like granite.

Mineral habit is often related to the regular arrangement of the molecules that make up the mineral. Some of the terms that are used to describe habit include bladed, botryoidal (grape-like), dendritic (branched), drusy (an encrustation of minerals), equant (similar in all dimensions), fibrous, platy, prismatic (long and thin), and stubby.



Figure 2.2.4: The crystal habits of common minerals. Quartz (left) forms six-sided prisms with pointed ends. Pyrite (center) forms cubic crystals as well as dodecahedral crystals (not pictured). Garnet (right) forms dodecahedral (12-sided) crystals. Quartz, Pyrite and Garnet by Karla Panchuk is licensed under CC BY-NC-SA 4.0. Photos by R. Weller/ Cochise College.

Cleavage and Fracture

Crystal **habit** is a reflection of how a mineral grows, while **cleavage** and **fracture** describe how it breaks. Cleavage and fracture are the most important diagnostic features of many minerals, and often the most difficult to understand and identify. Cleavage is what we see when a mineral breaks along a specific plane or planes, while fracture is an irregular break. Some minerals tend to cleave along planes at various fixed orientations, some do not cleave at all (they only fracture). Minerals that have cleavage can also fracture along surfaces that are not parallel to their cleavage planes.

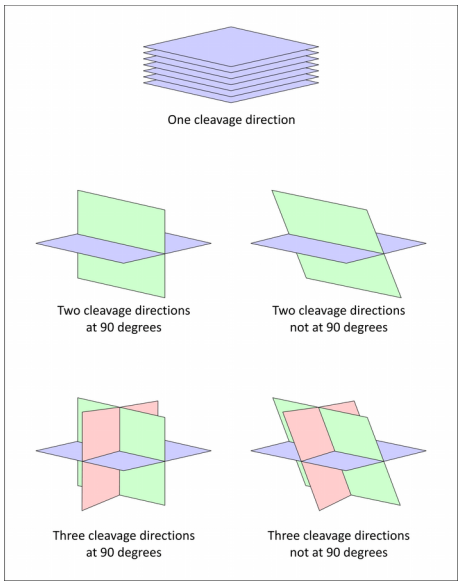


Figure 2.2.5: Five common types of mineral cleavage: One direction of cleavage (also known as “basal” cleavage). Two cleavage directions at 90 degrees to one another. Two cleavage directions not at 90 degrees. Three cleavage directions at 90 degrees. Three cleavage directions not at 90 degrees.
Mineral Cleavage by Rygel, M.C. via Wikimedia Commons is licensed under CC BY-SA 3.0.

The way that minerals break is determined by their atomic arrangement and specifically by the orientation of weaknesses within the lattice. Graphite and the micas, for example, have one direction of cleavage parallel to their sheets, and halite has three cleavage planes at 90° to one another and parallel to the lattice directions. Calcite has three cleavage planes that are not at 90° to one another as illustrated in video 2.2.2.

Video 2.2.1: Mineral Cleavage A - Breakage Test

The following video illustrates the breakage test which can help determine a mineral's cleavage. In the video, a translucent white mineral crystal is gently and repeatedly struck with a hammer. It breaks into smaller pieces along its cleavage planes. This particular mineral breaks along planes that are at right angles (90°) to one another. There are three distinct directions of cleavage resulting in each piece having roughly six sides.

This interactive element is not available in this format. Visit the link or scan the QR code to access it online.

View this YouTube Video online

Quartz has no cleavage because it has equally strong Si–O bonds in all directions, yet feldspar, a different framework silicate mineral, has two cleavages at 90° to each other.

One of the main difficulties with recognizing and describing cleavage is that it is visible only in individual crystals. Most rocks have small crystals and it is very difficult to see the cleavage within those crystals.

It is important to recognize the difference between cleavage planes and crystal surfaces. As already noted, crystal surfaces are related to how a mineral grows while cleavage planes are related to how it breaks. In most minerals cleavage planes and crystal surfaces do not align with one-another. An exception is halite, which grows in cubic crystals and has cleavage along those same planes. This isn’t true for most minerals. Quartz has crystal surfaces but no cleavage at all. Fluorite forms cubic crystals like those of halite, but it cleaves along planes that differ in orientation from the crystal surfaces.

Query 2.2.4

This interactive element is not available in this format. Visit the link or scan the QR code to access it online.

View this Interactive Content online

Density

Density is a measure of the mass of a mineral per unit volume, and it is a useful diagnostic tool in some cases. Most common minerals, such as quartz, feldspar, calcite, amphibole, and mica, have what we call "average density" (2.6 to 3.0 grams per cubic centimeter (g/cm^3)), and it would be difficult to tell them apart on the basis of their density. However, many of the metallic minerals, such as pyrite, hematite, and magnetite, have densities over 5 g/cm^3. They can easily be distinguished from the lighter minerals on the basis of density, but not necessarily from each other. A limitation of using density as a diagnostic tool is that one cannot assess it in minerals that are a small part of a rock that is mostly made up of other minerals.

Density of a mineral is often expressed as Specific Gravity (SG) which is a ratio of the density of the mineral you are measuring compared to the density of the same volume of water (Table 2.2.2).

$$\text{S.G.} = \frac{\text{density of mineral}}{\text{density of water}} \tag{2.2.1}$$

***Table** 2.2.2**:** Specific gravities of common minerals*

Mineral	Specific Gravity
Borax	1.7
Ulexite	1.9
Kernite	1.95
Gypsum	2.3-2.4
Bauxite	2.4-2.6
Quartz	2.65
Calcite	2.7
Fluorite	3.0-3.2
Barite	4.2-4.6
Stibnite	4.6
Zircon	4.6-4.7
Pyrite	4.9-5.2
Hematite	4.9-5.3
Galena	7.4-7.6
Cinnabar	8.0-8.2
Native Copper	8.9
Native Gold	19.32

Other Properties

Several other properties are also useful for identification of some minerals:

- Calcite is soluble in dilute acid and will give off bubbles of carbon dioxide (Video 2.2.3).
- Some minerals, like magnetite, are magnetic. A few other minerals are weakly magnetic.
- Sphalerite ((Zn,Fe)S) gives off a smell of sulfur when drawn across a streak plate.
- Halite tastes salty.
- Talc feels soapy to the touch.
- Plagioclase feldspar has striations (parallel razor-thin lines on the surface of cleavage planes caused by the way the crystal grows internally).
- Some minerals will also exhibit photoluminescence: they will glow when exposed to certain wavelengths of light.

Video 2.2.3: How to identify rocks & minerals using HCl acid

This video explains how dilute hydrochloric acid can be helpful for identifying certain minerals like calcite.

This interactive element is not available in this format. Visit the link or scan the QR code to access it online.

View this YouTube Video online

Video 2.2.4: Identifying Minerals

The following video provides an overview of the different mineral properties.

This interactive element is not available in this format. Visit the link or scan the QR code to access it online.

View this YouTube Video online

References

1. Earle, S. (2019). *Physical Geology – 2nd Edition*. Victoria, B.C.: BCcampus. Retrieved from https://opentextbc.ca/ March 2024
2. Krause, B. (1996). *Mineral Collector's Handbook*, Sterling Publishing Co, Inc.

This page titled 2.2: Mineral Properties is shared under a CC BY-NC 4.0 license and was authored, remixed, and/or curated by Allison Jones.

2.3: The Rock Cycle

What Are Rocks, Exactly?

There three main types of rocks: igneous, sedimentary, and metamorphic. These different types form in different ways and they have specific properties that help us to distinguish them. Through geological processes the rocks on Earth can be transformed from one type to another. These relationships and processes are illustrated using the rock cycle (Figure 2.3.1). The three types of rock and some of the intermediate forms of rocky materials (magma, outcrop, and loose sediments) are depicted in the rock cycle, along with the processes that are important in their transformations (indicated as arrows). Those processes include:

- Uplift (such as mountain formation) that results in rock that was present at depth in the crust being brought to surface and exposed to weathering
- Erosion and transportation of weathered products (e.g., sand, clay, and ions in solution) and then deposition as sediments (e.g., within rivers or the ocean)
- Burial of those sediments beneath other sediments, followed by compaction (squeezing) and cementation to make sedimentary rock
- Further burial which results in heating and more squeezing and then mineral transformations to form metamorphic rock
- Further heating or other changes in conditions that result in melting to form magma
- Movement of magma towards Earth's surface where cooling forms igneous rock. It can cool slowly to make intrusive igneous (plutonic) rock, or it can cool quickly to make extrusive igneous (volcanic) rock.

The rock cycle can be disrupted at any point by a change in conditions brought about by uplift, or burial, or in rare cases by the nearby presence of magma. Table 2.3.1 summarizes some key processes that are included in the rock cycle.

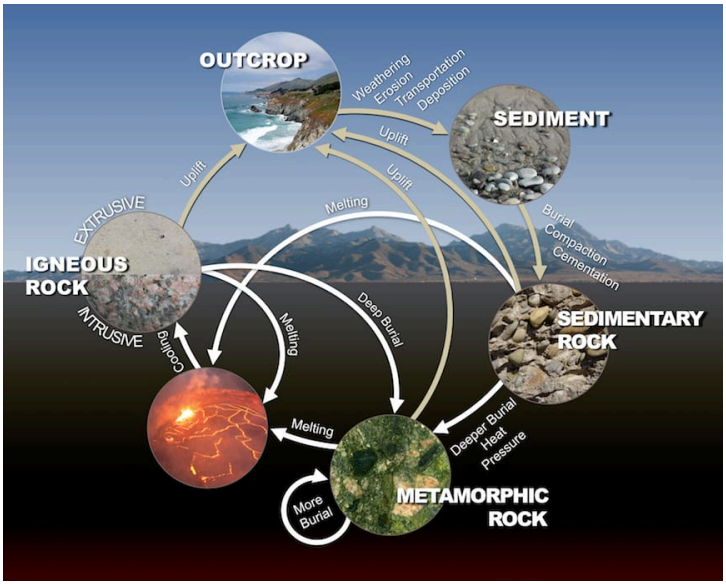


Figure 2.3.1: A schematic view of the rock cycle. The rock cycle takes place both above and below the Earth's surface. The rock deepest beneath the earth's surface, and under extreme heat and pressure, is metamorphic rock. This metamorphic rock can melt and become magma. When magma cools below the earth's surface, it becomes "intrusive igneous rock." If magma cools above the earth's surface, it is "extrusive igneous rock" and becomes part of the outcrop. The outcrop is subject to weathering and erosion, and can be moved and redeposited around the earth by forces such as water and wind. As the outcrop is eroded, it becomes sediment which can be buried, compacted, and cemented beneath the Earth's surface to become sedimentary rock. As sedimentary rock gets buried deeper and comes under increased heat and pressure, it returns to its original state as metamorphic rock. Rocks in the rock cycle do not always make a complete loop. It is possible for sedimentary rock to be uplifted back above the Earth's surface and for intrusive and extrusive igneous rock to be reburied and become metamorphic rock. "Rock cycle" by Karla Panchuk is licensed under CC BY-SA 4.0.

Table 2.3.1: Common geologic processes that take place on Earth.

Process	Description
Burial	The process by which more sediments are deposited onto existing sediments.
Compaction	The process whereby sediment is converted to consolidated rock.
Cementation	The process by which clastic sediments become lithified or consolidated into hard, compact rocks, usually through deposition or precipitation of minerals in the spaces between the individual grains of sediment; may occur simultaneously with sedimentation or at a later time.
Metamorphism	The mineralogical, chemical, and structural changes that transform solid rock into other types of solid rock, generally imposed at depth below the surface zones of weathering and cementation.
Melting	The change of a material from solid to liquid. In the case of rocks, the change from solid rock to liquid magma.
Cooling/ Crystallizing	The process of liquid rock freezing into solid rock.
Uplift	An increase in the vertical elevation of Earth's surface in response to natural causes.
Weathering	The chemical breakdown or physical breakup of rock.
Erosion	The general process or group of processes that loosen, dissolve, wear away, and simultaneously move from one place to another, the materials of Earth's crust; includes weathering, solution, abrasive actions, and transportation, but usually excludes slope movements.
Transportation	The movement of material across Earth's surface by water, wind, ice, or gravity.
Deposition	The process by which sediments, soil, and rocks are added to a landform or landmass. Or, what happens when transportation stops.

Query 2.3.1

This interactive element is not available in this format. Visit the link or scan the QR code to access it online.

View this Interactive Content online



References

1. Bates, R. L., and J. A. Jackson, editors. 1984. Dictionary of geological terms. Third edition. American Geological Institute, Alexandria, Virginia.
2. Earle, S. (2019). *Physical Geology – 2nd Edition*. Victoria, B.C.: BCcampus. Retrieved from https://opentextbc.ca/ March 2024
3. Neuendorf, K. K. E., J. P. Mehl Jr., and J. A. Jackson. 2005. *Glossary of geology*. Fifth edition. American Geological Institute, Alexandria, Virginia. https://www.nps.gov/subjects/geology/gri-glossary-of-geologic-terms.htm

This page titled 2.3: The Rock Cycle is shared under a CC BY-NC 4.0 license and was authored, remixed, and/or curated by Allison Jones.

2.4: Igneous Rocks

How Igneous Rocks Form

Igneous rocks form from the cooling of magma (molten rock), either slowly at depth within the crust, or quickly at or near the surface. In general, the longer the cooling process takes (up to millions of years), the larger the crystals in the rock. Volcanic (extrusive) rock, rock that cooled at or near Earth's surface, typically has mineral crystals that are less than 0.1 mm across (because they cooled within seconds or minutes), while intrusive (plutonic) igneous rock has crystals that are typically larger than 1 mm across.

Magma, the molten rock from which igneous rock forms, does not all cool and crystallize in an instant as soon as it reaches a certain temperature. Magma is chemically homogeneous and thus its various chemical constituents cool at different temperatures.

Order of Crystallization: Bowen's Reaction Series

The minerals that make up igneous rocks crystallize at a range of different temperatures. This explains why a cooling magma can have some solid crystals within it and yet remain predominantly liquid. The sequence in which minerals crystallize from a magma is known as Bowen's reaction series (Figure 2.4.1).

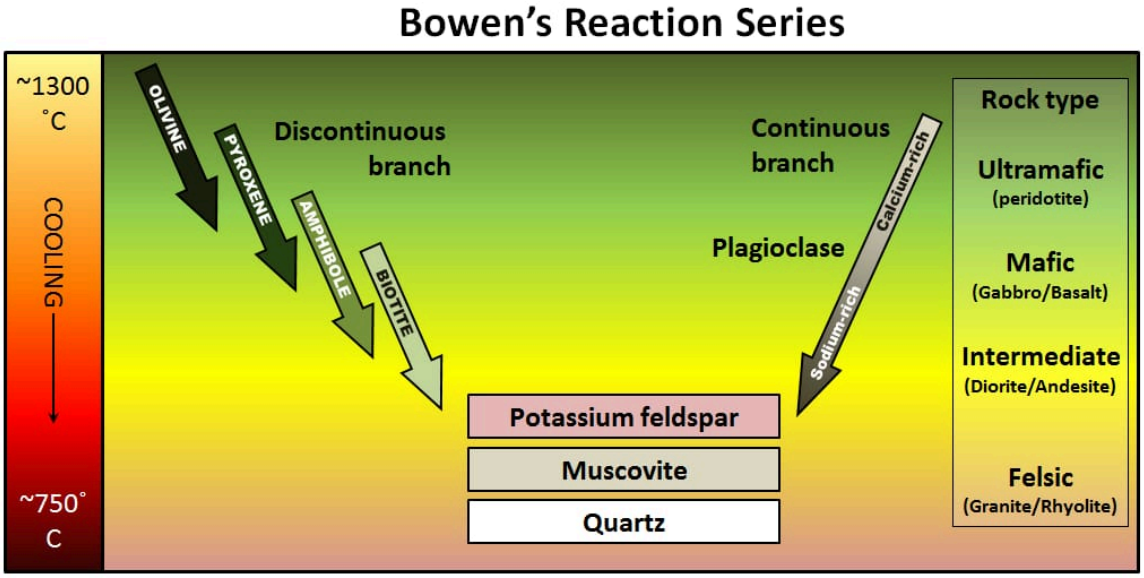


Figure 2.4.1: Bowen's reaction series describes the order in which minerals crystallize from a melt (magma or lava). "Bowen's reaction series" by Steven Earle is licensed under CC BY. Access a detailed description.

Bowen's reaction series has two pathways for minerals to form as magma cools: the discontinuous series (left side of Figure 2.4.1) and the continuous series (right side of Figure 2.4.1).

Discontinuous Series

On the discontinuous series, olivine normally crystallizes first, between 1200° and 1300°C. As the temperature drops, and assuming that some silica remains in the magma, the olivine crystals will react (combine) with some of the silica in the magma to form pyroxene. As long as there is silica remaining and the rate of cooling is slow, this process continues down the discontinuous branch: olivine to pyroxene, pyroxene to amphibole, and (under the right conditions) amphibole to biotite.

$$Mg_2SiO_4 + SiO_2 \rightarrow 2MgSiO_3$$

olivine + silica → pyroxene

Finally, if the magma is quite silica-rich to begin with, there will still be some silica left at around 750° to 800°C, and from this last remnants of the magma, potassium feldspar, quartz, and maybe muscovite mica will form.

Continuous Series

On the continuous series, at about the point where pyroxene begins to crystallize, plagioclase feldspar also begins to crystallize. At that temperature, the plagioclase is calcium-rich (a variety of plagioclase feldspar called anorthite). As the temperature drops, and providing that there is sodium left in the magma, the plagioclase that forms is a more sodium-rich variety (albite).

Magma Composition Influences Which Minerals Form

The composition of the original magma is critical to magma crystallization because it determines how far the reaction process can continue before all of the silica is used up. The compositions of typical mafic, intermediate, and felsic magmas are shown in Figure 2.4.2. Note that these compositions are expressed in terms of “oxides” (e.g., Al2O3 rather than just Al). There are two reasons for this: one is that in the early analytical procedures, the results were always expressed that way, and the other is that all of these elements combine readily with oxygen to form oxides.

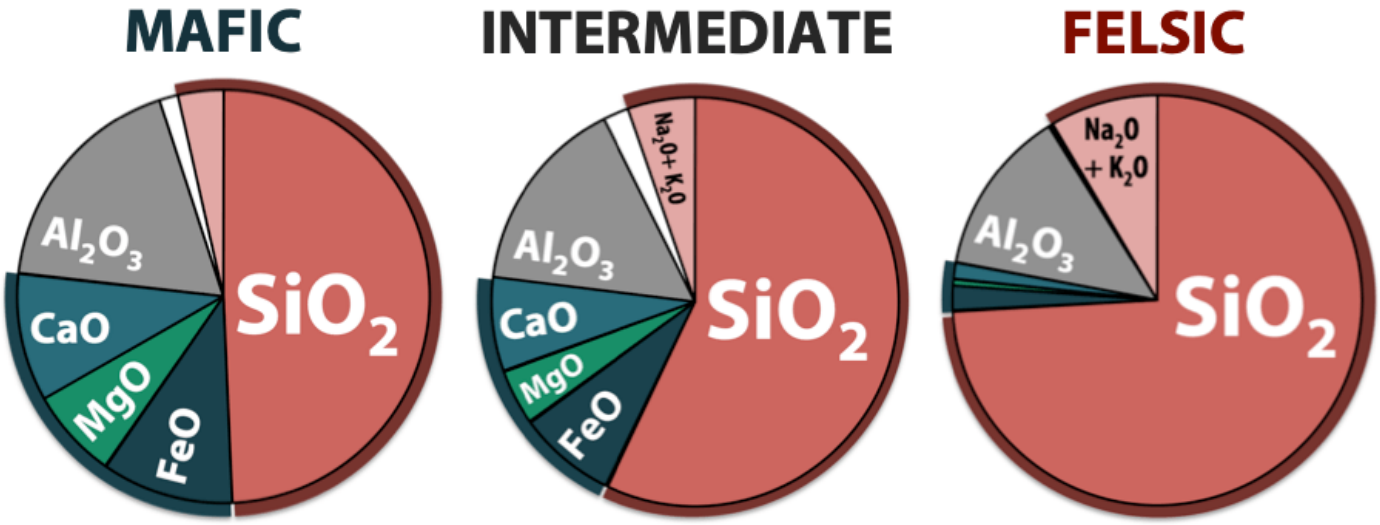


Figure 2.4.2: Chemical compositions of typical mafic, intermediate, and felsic magmas. See Table 2.4.1 for the oxide proportions described by these three pie charts. "Compositions" by Karla Panchuk, a derivative of the original, is licensed under CC BY 4.0.

Table 2.4.1: Proportions of oxides for the main chemical components in mafic, intermediate, and felsic magma.

Oxide	Felsic Magma	Intermediate Magma	Mafic Magma
SiO_2	65% to 75%	55% to 65%	45% to 55%
Al_2O_3	12% to 16%	14% to 18%	14% to 18%
FeO	2% to 4%	4% to 8%	8% to 12%
CaO	1% to 4%	4% to 7%	7% to 11%
MgO	0% to 3%	2% to 6%	5% to 9%
Na_2O	2% to 6%	3% to 7%	1% to 3%
K_2O	3% to 5%	2% to 4%	0.5% to 3%

Mafic magmas have 45% to 55% SiO_2, about 25% total of FeO and MgO plus CaO, and about 5% Na_2O + K_2O. Felsic magmas, on the other hand, have much more SiO_2 (65% to 75%) and Na_2O + K_2O (around 10%) and much less FeO and MgO plus CaO (about 5%).

As a mafic magma starts to cool, some of the silica combines with iron and magnesium to make olivine. As it cools further, much of the remaining silica goes into calcium-rich plagioclase, and any silica left may be used to convert some of the olivine to pyroxene. Soon after that, all of the magma is used up and no further changes take place. The minerals present will be olivine, pyroxene, and calcium-rich plagioclase. If the magma cools slowly underground, the product will be gabbro; if it cools quickly at the surface, the product will be basalt (Figure 2.4.3).

Felsic magmas tend to be cooler than mafic magmas when crystallization begins (because they don't have to be as hot to remain liquid), and so they may start out crystallizing pyroxene (not olivine) and plagioclase. As cooling continues, the various reactions on the discontinuous branch will proceed because silica is abundant, the plagioclase will become increasingly sodium-rich, and eventually potassium feldspar and quartz will form. Commonly even very felsic rocks will not have biotite or muscovite because they may not have enough aluminum or enough hydrogen to make the OH complexes that are necessary for mica minerals. Typical felsic rocks are granite and rhyolite (Figure 2.4.3).

The cooling behavior of intermediate magmas lie somewhere between those of mafic and felsic magmas. Typical mafic rocks are gabbro (intrusive) and basalt (extrusive). Typical intermediate rocks are diorite and andesite. Typical felsic rocks are granite and rhyolite (Figure 2.4.3).

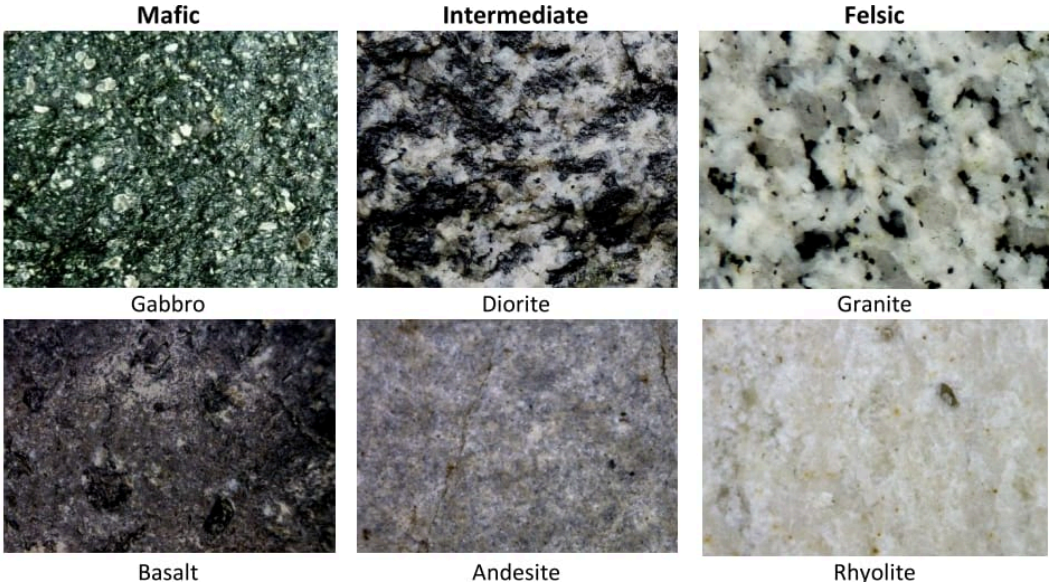


Figure 2.4.3: Examples of the igneous rocks that form from mafic, intermediate, and felsic magmas. "Common igneous rocks" by Steven Earle is licensed under CC BY. Access a detailed description.

Query 2.4.1

This interactive element is not available in this format. Visit the link or scan the QR code to access it online.

View this Interactive Content online

Igneous Rock Compositions

Classification of igneous rock is based mainly on the rock composition and texture, which is illustrated in Figure 2.4.4.

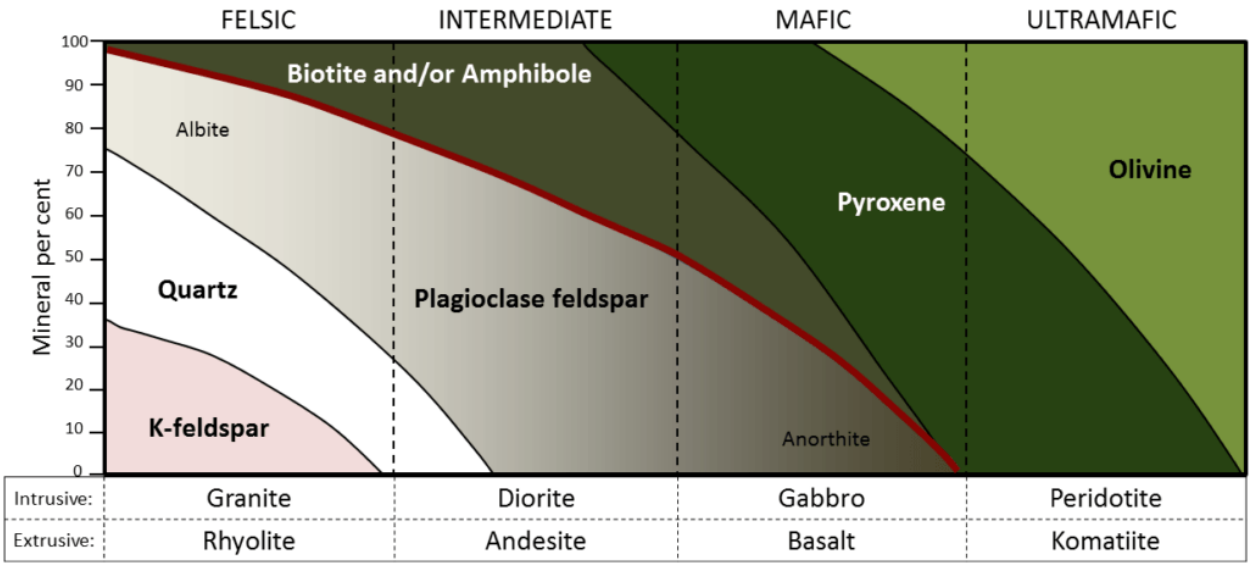


Figure 2.4.4: A simplified classification diagram for igneous rocks based on their mineral compositions. "Igneous rock classification by mineral composition" by Steven Earle is licensed under CC BY 4.0. Access a detailed description.

Four broad compositional classes of igneous rocks are shown, namely felsic, intermediate and mafic, and ultramafic. These are determined by the proportions of the dark silicate minerals (biotite, amphibole, pyroxene and olivine). Felsic rocks are light colored, often close to white, with less than 20% dark minerals. Intermediate rocks are medium-dark (typically gray) with 20 to 50% dark minerals, and mafic rocks are close to black (with more than 50% dark minerals). The three main types of intrusive igneous rocks are granite, diorite and gabbro. The equivalent volcanic (extrusive) rocks—which are fine grained—are rhyolite, andesite and basalt. Igneous rocks with close to 100% dark minerals are known as ultramafic, such as peridotite; these are rare on the Earth's surface, but common in the mantle. While komatiite is the name given to an ultramafic, extrusive rock, these rocks are very rare and almost never occur.

Mafic igneous rocks (e.g., basalt or gabbro) are denser than felsic igneous rocks. Basalt has a specific gravity of about 3 g/cm^3, while for granite the value is about 2.7 g/cm^3. This small difference becomes very important in the context of plate tectonics. In comparison, the ultramafic rock of the mantle has a density of about 3.3 g/cm^3.

Igneous Rock Textures

The second part of classifying igneous rocks is identifying the texture of the igneous rock. Remember, the cooling rate of the magma determines how large crystals grow. Therefore intrusive (plutonic) igneous rock and extrusive (volcanic) igneous rock are differentiated by crystal size. Rocks with crystals large enough to be easily seen with the unaided eye are plutonic and their texture is called phaneritic (from the Greek root, "phaneros" meaning visible). Rocks with crystals difficult to be seen with the unaided eye are volcanic and their texture is called aphanitic (or "not" visible). Variations occur depending upon the circumstances of the igneous rock's formation. Common variations include:

Pegmatitic

Igneous rocks with pegmatitic texture have exceptionally large crystals, usually only found in felsic and intermediate compositions (Figure 2.4.5). Their basic texture will be phaneritic, not aphanitic. These rocks are therefore given the adjective "pegmatitic" before their names, such as a pegmatitic granite or a pegmatitic diorite. Or, they are referred to as either a "granite pegmatite" or a "diorite pegmatite."



Figure 2.4.5: Pegmatite containing lepidolite, tourmaline, and quartz from the White Elephant Mine in the Black Hills, South Dakota. "Wepegmatite" by Jstuby via Wikimedia Commons is in the public domain.

Porphyritic

the crystals are of mixed-sized, with noticeably larger crystals, or "phenocrysts", surrounded by smaller crystals, or "groundmass." These rocks are usually felsic, intermediate, or mafic, and are seldom ultramafic. They can also be either plutonic or volcanic in their basic texture. They are therefore given the adjective “porphyritic” before their names or are referred to by their compositional name followed by the term "porphyry." For example a porphyritic rock with an intermediate composition might be a diorite porphyry or a porphyritic diorite, or it might be an andesite porphyry or a porphyritic andesite. Figure 2.4.6 shows a sample of rock with porphyritic texture.



Figure 2.4.6: This is an example of a rock with porphyritic texture with a camera lens cap for scale. The white crystals are large and visible without aid whereas the darker groundmass is made of crystals too small to identify. This rock originated from the 1915 eruption of Lassen Peak (see: Cascade Range and Modoc Plateau). "Black porphyritic dacite (upper Holocene, 14 May 1915; Devastated Area, Lassen Volcano National Park, California, USA) 4" by James St. John via Flickr is licensed under CC BY.

There are three additional textural terms commonly used for igneous rock - glassy, vesicular, and pyroclastic. All of these terms are used with volcanic rock and not plutonic rock. They reflect different conditions that can occur during volcanic eruptions.

Glassy

A rock can develop a glassy texture when lava cools so fast that crystals do not have time to form. Commonly glassy rocks are of felsic composition and are called obsidian. Note that because it does not have crystals, the commonly used color conventions for identifying whether its composition would be felsic, intermediate, or mafic don't apply. Obsidian is almost always black, even though its composition is almost always felsic (Figure 2.4.7).

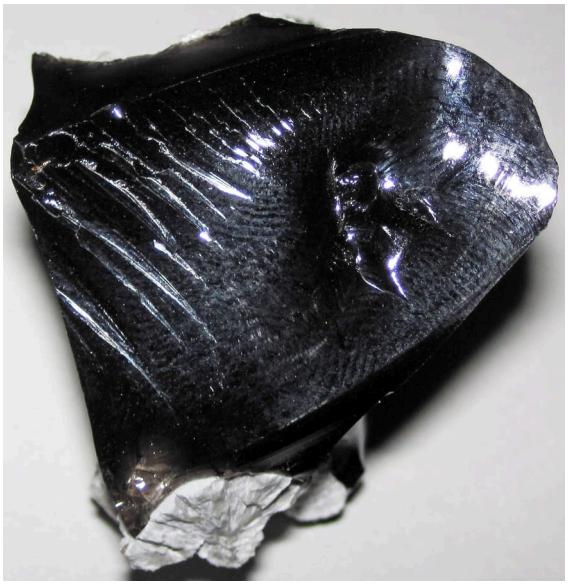


Figure 2.4.7: A sample of obsidian, a glassy textured rock. This sample is from the Medicine Lake Volcano (see Cascade Range and Modoc Plateau). "Spherulitic obsidian (Medicine Lake Highlands, California, USA) 2" by James St. John via Flickr is licensed under CC BY.

Vesicular (Porous)

When a volcano erupts and there is an abundance of gas in the lava, holes from the escaping gasses can be preserved as the crystals form. Such rocks have a porous texture and are given the adjective, vesicular, before their name, for example, vesicular basalt (Figure 2.4.8). One special example of a porous rock occurs when the rock is both glassy and porous. Essentially such a rock is "rock foam" like the foamy head on a glass of root beer or beer and is given the name, pumice, from the Latin word "pumex" meaning foam.



Figure 2.4.8: Weathered vesicular basalt from Amboy Crater, Mojave Desert, CA. "Vesicular basalt (Upper Pleistocene, ~79 ka; lava flow from Amboy Crater, Mojave Desert, California, USA) 1" by James St. John via Flickr is licensed under CC BY.

Pyroclastic

The last of these textural terms relating to volcanic eruptions is pyroclastic or fragmental. This texture occurs when the volcano explodes. The hot explosion debris, when it falls back to Earth's surface, compacts and cements into rock that may contain rock fragments, crystals, and glass (Figure 2.4.9). Such rocks are commonly referred to as tuff and usually have either a felsic or intermediate composition. Their composition may be used as an adjective, for example, rhyolitic tuff or andesitic tuff.



Figure 2.4.9: Sample of tuff with a pyroclastic texture. This rock is from Hole in the Wall in the Mojave National Preserve, CA (see: Mojave and Colorado Deserts). "HoleInTheWallTuff" by Wilson44691 via Wikimedia Commons is in the public domain.

Using Composition and Texture to Classify Igneous Rocks

Once the composition and texture of an igneous rock have been determined, rocks can be classified using Table 2.4.2.

Table 2.4.2: Classification of igneous rocks according to composition (first row) and texture (first column).

	Felsic	Intermediate	Mafic	Ultramafic
Pegmatite	Granite pegmatite	Diorite Pegmatite	Gabbro Pegmatite	Rare
Phaneritic	Granite	Diorite	Gabbro	Peridotite
Porphyritic - phanerititc	Granite Porphyry	Diorite Porphyry	Gabbro Porphyry	Rare
Porphyritic - aphanitic	Rhyolite Porphyry	Andesite Porphyry	Basalt Porphyry	Rare
Aphanitic	Rhyolite	Andesite	Basalt	Komatiite
Glassy	Obsidian	Obsidian	Obsidian	Rare
Vesicular (porous)	Pumice	Pumice/Scoria	Scoria	Rare

	Felsic	Intermediate	Mafic	Ultramafic
Pyroclastic (fragmental)	Rhyolite tuff	Andesite tuff	Rare	Rare

References

1. Earle, S. (2019). *Physical Geology – 2nd Edition*. Victoria, B.C.: BCcampus. Retrieved from https://opentextbc.ca/physicalgeology2ed March 2024

This page titled 2.4: Igneous Rocks is shared under a CC BY-NC 4.0 license and was authored, remixed, and/or curated by Allison Jones.

2.5: Sedimentary Rocks

Clastic (Detrital) Sedimentary Rocks

Sedimentary rock forms near Earth's surface following the accumulation of fragments of rocks and minerals that have been weathered and eroded from outcrops, transported by gravity, rivers, waves, wind, or glacial ice, and then deposited as sediment (Figure 2.5.1). The fragments of rock and minerals, or detritus, are also known as clasts, and the resulting sedimentary rocks are called clastic sedimentary rocks or detrital sedimentary rocks if they are composed mostly of such grains.



Figure 2.5.1: Coarse sand composed primarily of quartz, chert, igneous rock fragments, and shell fragments from Pismo Beach, CA. "Pismo Beach Sand" by Mark A. Wilson via Wikimedia Commons is in the public domain.

Sediment Size

The size of clasts is related to sediment transport. In general, the longer and/or farther the clast has been transported, the smaller its size. Clasts can range in size from tiny (invisible) clay fragments to boulders the size of buildings (Table 2.5.1) and we classify clastic sedimentary rock on the basis of clast size. There is no upper or lower limitation on the size of clasts. The key piece of information to remember is that anything sand-sized or larger can be seen with the unaided eye. Sand grains range in size from 1/16th mm to 2 mm. Very fine sand will feel gritty (not slippery) between your fingertips.

Clasts smaller than sand or 1/16th mm are classified as silt and clay. Clasts larger than 2 mm are granules, pebbles, cobbles, and boulders (in order of increasing size). Granules and larger fragments can typically only be transported and deposited by fast-flowing water, and so they are commonly deposited in high-energy parts of streams. Sand grains can be transported by rivers with medium flow, by strong winds, and by waves, and so sand deposits tend to accumulate in rivers, deltas, deserts, and on beaches. Silt and clay can be transported in similar environments, but they tend not to be deposited unless the transport medium slows significantly, so they will usually be deposited in water moving more slowly such as in lakes and the deep ocean basins. Any of these sediments must then become buried beneath other layers of sediment, compressed and cemented before they can become sedimentary rock.

Table 2.5.1: Udden-Wentworth grain-size scale for classifying sediment sizes.

Type	Description	Size range (millimeters)	Size range (microns)
Boulder	large	1024 and up	N/A
	medium	512 to 1024	N/A

Type	Description	Size range (millimeters)	Size range (microns)
	small	256 to 512	N/A
Cobble	large	128 to 256	N/A
	small	64 to 128	N/A
Pebble (Granule)	very coarse	32 to 64	N/A
	coarse	16 to 32	N/A
	medium	8 to 16	N/A
	fine	4 to 8	N/A
	very fine	2 to 4	N/A
Sand	very coarse	1 to 2	1000 to 2000
	coarse	0.5 to 1	500 to 1000
	medium	0.25 to 0.5 (1/4 to 1/2 mm)	250 to 500
	fine	0.125 to 0.25 (1/8th to 1/4 mm)	125 to 250
	very fine	0.063 to 0.125 (or 1/16th to 1/8th mm)	63 to 125
Silt	very coarse	N/A	32 to 63
	coarse	N/A	16 to 32
	medium	N/A	8 to 16
	fine	N/A	4 to 8
	very fine	N/A	2 to 4
Clay	clay	N/A	0 to 2

Other Sediment Characteristics

While size is the main characteristic used to classify sediment, other observed characteristics are also important to the description of clasts and analysis of sedimentary environments. Roundness or angularity of the clasts is another important observed characteristic. Roundness is a measure of the smoothness of the clasts. When clasts are well-rounded, they are very smooth. In contrast, when clasts are angular they are not at all smooth and have a jagged, rough shape (Figure 2.5.2). As with size, the longer/farther the transport, generally the more rounded the clasts.

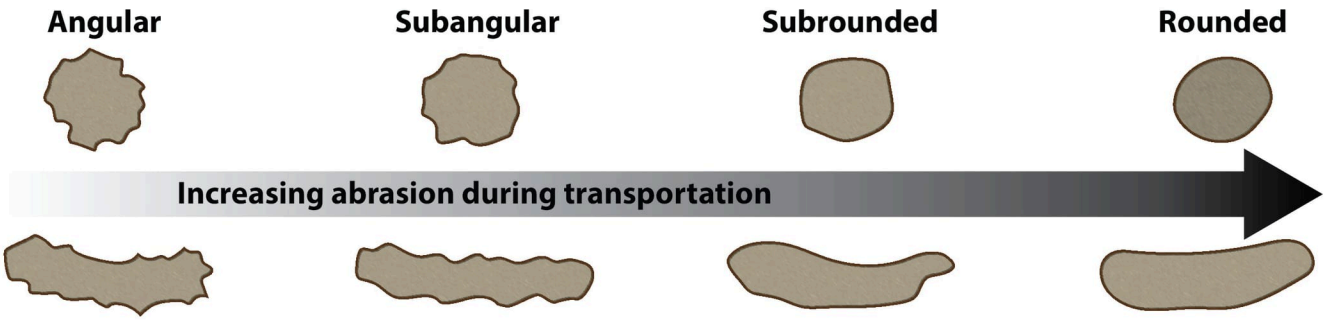


Figure 2.5.2: A visual reference for descriptions of roundness of sediments and grains in clastic sedimentary rocks. Note that rounded grains are not necessarily spherical in shape! Grain shapes are controlled by both the extent of transportation (and abrasion) and by the physical properties of the grain. "Sediment roundness" by Allison Jones, a derivative of sorting roundness, is licensed under CC BY 4.0. Access a detailed description.

The other major characteristic of sediment is sorting. Sorting is a measure of the range of clast size within the sediment or

the sedimentary rock. Well sorted sediment is mostly the same size and the more variation in size the more poorly sorted the sediment (Figure 2.5.3). As with size and roundness, the longer/farther the transport, the better sorted the sediment. The sediment in Figure 2.5.1 is an example of moderate sorting.



Figure 2.5.3: A visual reference for descriptions of sorting of sediments and grains in clastic sedimentary rocks. Very poorly sorted sediments contain clasts of a wide range of sizes whereas very well sorted sediments contain clasts of the same size. "Sediment sorting" by Allison Jones, a derivative of sorting roundness, is licensed under CC BY 4.0. Access a detailed description.

Clastic Sediment to Sedimentary Rock

Clastic sedimentary rocks are primarily named by the size of the largest clasts present in the rock (Table 2.5.2). Rocks with clasts smaller than sand-sized are subdivided by the presence or absence of bedding, or fine layering within the rock (Figure 2.5.4). Rocks with sand-sized clasts are subdivided by the composition of the clasts (e.g. quartz, rock/lithic fragments; Figure 2.5.5). Rock with clasts larger than sand-sized are subdivided by the angularity/roundness of the clasts (e.g. conglomerate and breccia; Figure 2.5.6).

Table 2.5.2: The main types of clastic sedimentary rocks and their characteristics.

Group	Examples	Characteristics
Mudrock	mudstone	Greater than 75% silt and clay, not bedded
	shale	Greater than 75% silt and clay, finely bedded (laminations)
Sandstone	quartz sandstone	Dominated by sand, greater than 90% quartz
	arkose	Dominated by sand, greater than 10% feldspar
	lithic wacke (aka "graywacke")	Dominated by sand, greater than 10% rock fragments, greater than 15% silt and clay
Conglomerate	N/A	Dominated by rounded clasts, granule size and larger
Breccia	N/A	Dominated by angular clasts, granule size and larger



Figure 2.5.4: Sample of shale. Laminations are in the plane of the photo and not visible. Gray Shale by James St. John via Flickr is licensed under CC BY.



Figure 2.5.5: Sample of quartz arenite sandstone. This sample contains more than 90% quartz sand grains. Sandstone by James St. John via Flickr is licensed under CC BY.



Figure 2.5.6: A sample of conglomerate from the Amargosa Valley Formation in the Funeral Mountains, Inyo County, CA in the Basin and Range. Conglomerate by James St. John via Flickr is licensed under CC BY.

Chemical and Biochemical Sedimentary Rock

Sedimentary rock can also form from the crystallization of ions that are dissolved in water. These rocks are known as chemical sedimentary rocks because they form by a chemical process. For example, when minerals crystallize from the evaporation of water in an inland sea or lake, layers of rock salt (halite) or rock gypsum can form.

When chemical processes are assisted by biological organisms, the rocks that form are called biochemical sedimentary rocks. For example, marine organisms extract bicarbonate and calcium ions (HCO^{3-} and Ca^{2+}) from ocean-water to make calcite shells ($CaCO_3$) which then accumulate on the seafloor (typically in tropical areas around reefs) to form calcite mud and sand that later gets buried and becomes limestone. Some organisms make their shells out of silica, and those can accumulate on the seafloor to make the rock chert. Chemical and biochemical sedimentary rocks are classified and named according to their composition.

Carbonate Rocks

Carbonate rocks are usually formed from the carbonate minerals calcite, aragonite, or dolomite. The most common carbonate rocks are limestones and dolostones.

Limestone is usually formed from the mineral calcite, $CaCO_3$, or may be formed by its polymorph, aragonite. Limestone is also one of the few sedimentary rocks that can form as either a clastic, chemical, or biochemical sedimentary rock. Frequently limestone is formed from marine organisms, but limestones form in many different ways and often have names based on their formation. For example, fossiliferous limestone is formed from the fossilized remains of organisms (Figure 2.5.7), tufa forms at springs (2.5.8), and travertine can form in caves or at hot springs (Figure 2.5.9). Limestone is of economic importance because it is a raw material used in the formation of concrete and also used in steel production.



Figure 2.5.7: A fossiliferous layer of the Delmar Formation at Torrey Pines Beach, San Diego County, CA in the Peninsular Ranges. This rock contains abundant oyster fossils from an ancient oyster reef. "Torrey Pines Delmar Formation" by Allison Jones is licensed under CC BY-NC.



Figure 2.5.8: Tufa towers precipitating ion-rich fluids transported along faults beneath Mono Lake, Mono County California. Mono Lake is located in the Basin and Range. "Mono Lake Tufa" by Fred Moore via Flicker is licensed under CC BY-NC.



Figure 2.5.9: Travertine forming from the walls and ceilings of the Shasta Caverns, Shasta County, CA located in the Cascade Range. This type of travertine is sometimes called flowstone. "Shasta Cavern travertine" by Allison Jones is licensed under CC BY.

Dolostone is the carbonate rock made of the mineral dolomite ($CaMg(CO_3)_2$). Dolostone is common in some parts of the world, for example there is a whole Italian mountain range named after it (the Dolomite Mountains). This is surprising because marine organisms do not directly precipitate dolomite. Dolomite forms through dolomitization, a process involving chemical reactions between magnesium-rich water percolating through rocks, and sediments containing calcite.

Calcite and dolomite can be distinguished from one another by applying a drop of weak acid to the rock; calcite will react with weak acid, whereas dolomite will not. Also, when dolomite weathers, it tends to turn buff (tan) in color, whereas calcite tends to turn either gray or white.

Chert

Chert is made of silica (SiO_2). It has the same chemical formula as quartz, but is cryptocrystalline, meaning that the quartz crystals comprising chert are so small that it is difficult to see them even under a microscope. Chert can be a chemical sedimentary rock, often forming as beds within limestone, or as irregular lenses or blobs (nodules).

Chert can also be biochemical. Some tiny marine organisms, such as diatoms and radiolaria, make their tests from silica. When they die their tiny shells settle slowly to the bottom of the lake or ocean, where they accumulate and are transformed into chert (Figure 2.5.10).

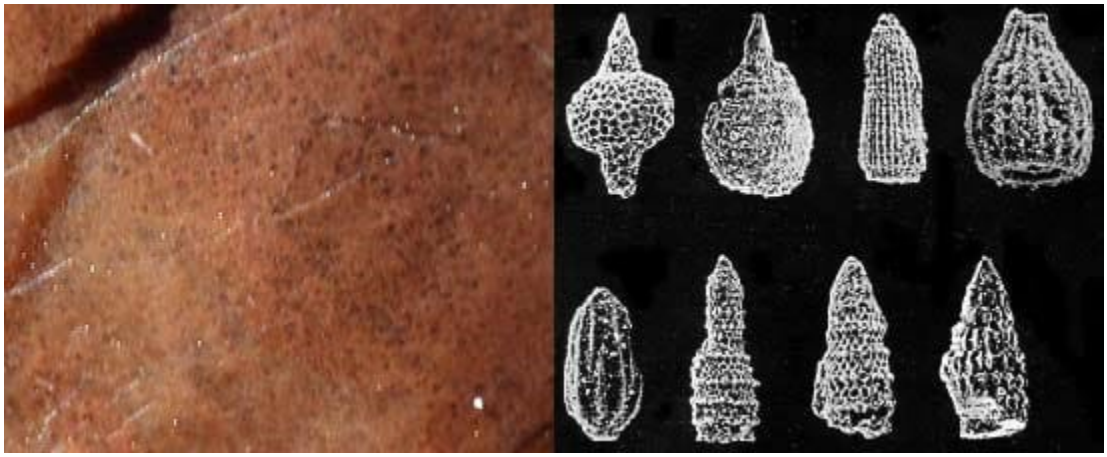


Figure 2.5.10: A magnified piece of chert shows radiolaria as small dark spheres about the size of a pencil point (left), and a scanning electron microscope image of extracted radiolaria (right). "Chert-rads" by the National Park Service is in the public domain.

Evaporites

In arid regions, lakes and inland seas typically have no stream outlet, and the water that flows into them is removed only by evaporation. Under these conditions, the water becomes increasingly concentrated with dissolved salts, and eventually some of these salts may reach saturation levels and start to crystallize (Figure 2.5.11).

Although all evaporite deposits are unique because of differences in the chemistry of the water, in most cases minor amounts of carbonates start to precipitate when the solution is reduced to about 50% of its original volume. The mineral gypsum ($CaSO_4 \cdot 2H_2O$) precipitates at about 20% of the original volume, and halite (NaCl) precipitates at 10%. Other important evaporite minerals include sylvite (KCl) and borax ($Na_2B_4O_7 \cdot 10H_2O$). In California, sylvite occurs in dry lake beds in Inyo and Imperial Counties.



Figure 2.5.11: Rock salt, an evaporite chemical sedimentary rock made of the mineral halite, forms at Badwater Basin in Death Valley National Park in the Basin and Range. "Salt at Badwater Basin" by Allison Jones is licensed under CC BY.

Depositional Environments

Sedimentary rocks and sediments reflect the environments in which they are deposited. This makes them incredibly useful when trying to determine the geologic history of an area. They are classified by their distinctive physical and chemical indicators caused by whether they are on land (terrestrial), transitional between the land and the sea (coastal), or marine. The physical and chemical indicators in terrestrial environments in particular are useful for helping to determine the paleoclimate of areas over time.

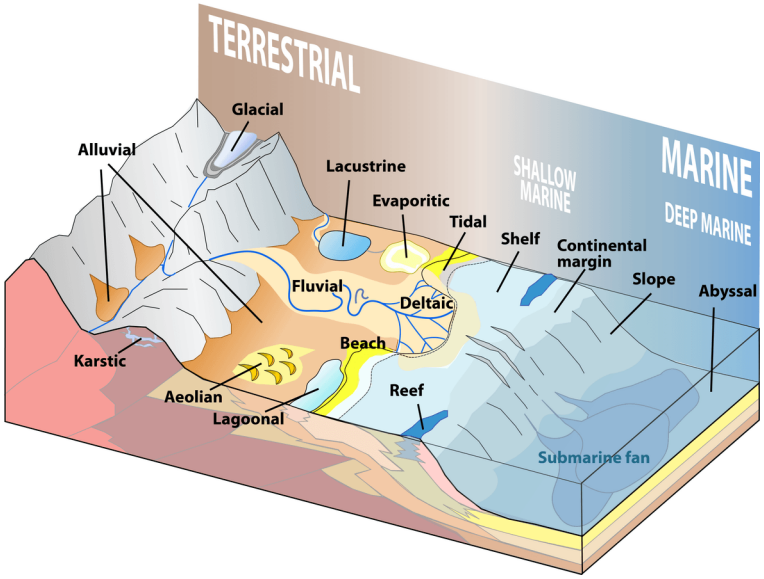


Figure 2.5.12: Some of the important depositional environments for sediments and sedimentary rocks. These environments are further described in Tables 2.5.3 and 2.5.4. "Main depositional environments v1" by Karla Panchuk, a derivative of the original, is licensed under CC BY-SA 3.0.

Table 2.5.3: Terrestrial depositional environments and their sediments.

Environment	Key Transport Process(es)	Depositional Setting(s)	Typical Sediments
Glacial	Gravity, moving ice, moving water	Valleys, plains, streams, lakes	Glacial till, gravel, sand, silt, clay
Alluvial	Gravity, moving water	Where steep-sided valleys meet plains	Coarse angular fragments
Fluvial	Moving water	Streams	Gravel, sand, silt, organic matter
Aeolian	Wind	Deserts and coastal regions	Sand, silt
Lacustrine	Moving Water	Lakes	Sand, silt, clay, organic matter
Evaporite	Still water	Lakes in arid regions	Salts, clay

Table 2.5.4 Marine and transitional depositional environments.

Environment	Key Transport Process(es)	Depositional Setting(s)	Typical Sediments
Deltaic	Moving water	Deltas	Sand, silt, clay, organic matter
Beach	Waves, long-shore currents	Beaches, spits, sand bars	gravel, sand
Tidal	Tidal currents	Tidal flats	Fine-grained sand, silt, clay
Reef	Waves, tidal currents	Reefs and adjacent basins	Carbonates
Shallow marine	Waves, tidal currents	Shelves, slopes, lagoons	Carbonates in tropical climates; sand/silt/clay elsewhere.
Lagoonal	Little transportation	Lagoon bottom	Carbonates in tropical climates, silt, clay
Submarine fan	Underwater gravity flows (turbitity currents)	Continental slopes, abyssal plains	Gravel, sand, silt, clay
Deep water	Ocean currents	Deep-ocean abyssal plains	Clay, carbonate mud, silica mud

References

1. Earle, S. (2019). *Physical Geology – 2nd Edition*. Victoria, B.C.: BCcampus. Retrieved from https://opentextbc.ca/ March 2024

This page titled 2.5: Sedimentary Rocks is shared under a CC BY-NC 4.0 license and was authored, remixed, and/or curated by Allison Jones.

2.6: Metamorphic Rocks

Metamorphism

Metamorphism is the change that takes place within a body of rock as a result of it being subjected to conditions that are different from those in which it formed. In most cases, but not all, this involves the rock being deeply buried beneath other rocks, where it is subjected to higher temperatures and pressures than those under which it formed. Metamorphic rocks typically have different mineral assemblages and different textures from their parent rocks, but they may have the same overall composition.

Controls on Metamorphism

The main factors that control metamorphic processes are:

- the mineral composition of the parent rock,
- the temperature at which metamorphism takes place,
- the amount and type of pressure during metamorphism,
- the types of fluids (mostly water) that are present during metamorphism, and
- the amount of time available for metamorphism.

Parent Rock

The parent rock is the rock that exists before metamorphism starts. Sedimentary or igneous rocks can be considered the parent rocks for metamorphic rocks. Although an existing metamorphic rock can be further metamorphosed or re-metamorphosed, metamorphic rock doesn't normally qualify as a "parent rock". For example, if a mudstone is metamorphosed to slate and then buried deeper where it is metamorphosed to schist, the parent rock of the schist is mudstone, not slate. The critical feature of the parent rock is its mineral composition because it is the stability of minerals that counts when metamorphism takes place. In other words, when a rock is subjected to increased temperatures, certain minerals may become unstable and start to recrystallize into new minerals.

Temperature

The temperature that the rock is subjected to is a key variable in controlling the type of metamorphism that takes place. As we learned in the context of igneous rocks, mineral stability is a function of temperature, pressure, and the presence of fluids (especially water). All minerals are stable over a specific range of temperatures. For example, quartz is stable from surface temperatures all the way up to about 1800°C. If the pressure is higher, that upper limit will be even higher. If there is water present, it will be lower. On the other hand, most clay minerals are only stable up to about 150° or 200°C; above that, they transform into micas. Most feldspars are stable up to between 1000°C and 1200°C. Most other common minerals have upper limits between 150°C and 1000°C.

Some minerals will crystallize into different polymorphs (same composition, but different crystalline structure) depending on the temperature and pressure. The minerals kyanite, andalusite, and sillimanite are polymorphs with the composition Al_2SiO_5. They are stable at different pressures and temperatures, and, as we will see later, they are important indicators of the pressures and temperatures that existed during the formation of metamorphic rocks (Figure 7.1.1).

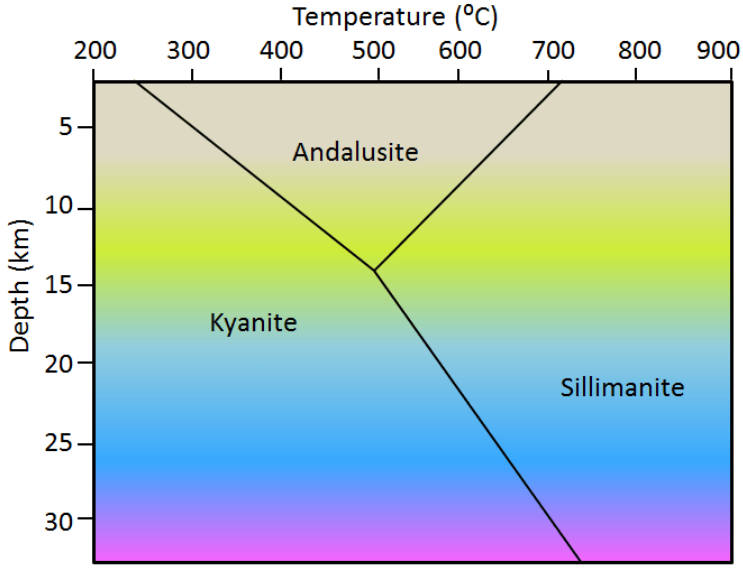


Figure 2.6.1: The temperature and pressure stability fields of the three polymorphs of Al_2SiO_5. Depth here approximates pressure. Kyanite is stable at low to moderate temperatures and low to high pressures, andalusite at moderate temperatures and low pressures, and sillimanite at higher temperatures. Detailed information available in Table 2.6.1. "Aluminosilicate polymorphs" by Steven Earle is licensed under CC BY.

Table 2.6.1: The temperature ranges that polymorphs of Al_2SiO_5 are stable at at various depths.

Depth (kilometers)	Kyanite	Andalusite	Sillimanite
5	Less than 300°C	300 to 650°C	Greater than 670°C
10	Less than 400°C	410 to 580°C	Greater than 590°C
15	Less than 500°C	Not stable	Greater than 500°C
20	Less than 570°C	Not stable	Greater than 590°C
25	Less than 640°C	Not stable	Greater than 620°C
30	Less than 700°C	Not stable	Greater than 700°C

Pressure

Pressure is important in metamorphic processes for two main reasons. First, it has implications for mineral stability (Figure 7.1.1). Second, it has implications for the texture of metamorphic rocks. Rocks that are subjected to very high confining pressures are typically denser than others because the mineral grains are squeezed together (Figure 7.1.2 a), and also because they may contain minerals that have greater density because the atoms are more closely packed.

Because of plate tectonics, pressures within the crust are typically not applied equally in all directions. In areas of plate convergence, for example, the pressure in one direction (perpendicular to the direction of convergence) is typically greater than in the other directions (Figure 7.1.2 b). In situations where different blocks of the crust are being pushed in different directions, the rocks will likely be subjected to sheer stress (Figure 7.1.2 c).

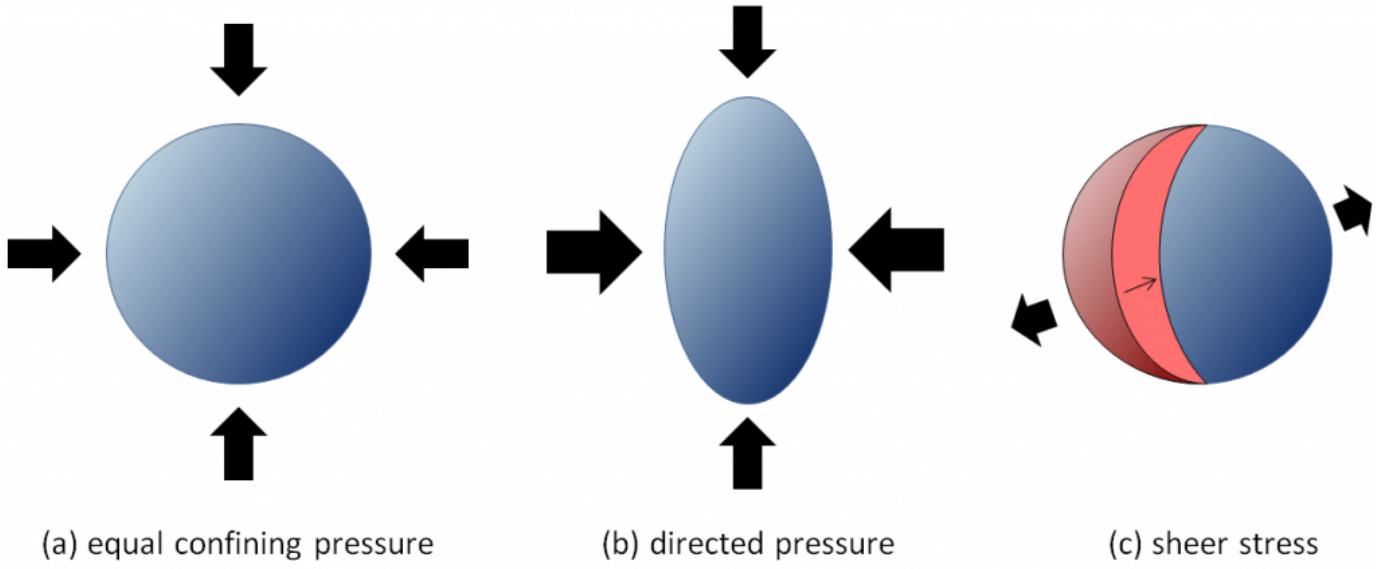


Figure 2.6.2: An illustration of different types of pressure on rocks. (a) confining pressure, where the pressure is essentially equal in all directions, (b) directed pressure, where the pressure from the sides is greater than that from the top and bottom, and (c) shear stress caused by different blocks of rock being pushed in different directions. In a and b there is also pressure in and out. "Pressure" by Steven Earle is licensed under CC BY.

One of the results of directed pressure and shear stress is that rocks become foliated—meaning that they'll have a directional fabric. Foliation a very important aspect of metamorphic rocks, and is described in more detail in the next section.

Fluids

Water is the main fluid present within rocks of the crust, and the only one that we'll consider here. The presence of water is important for two main reasons. First, water facilitates the transfer of ions between minerals and within minerals, and therefore increases the rates at which metamorphic reactions take place. So, while the water doesn't necessarily change the outcome of a metamorphic process, it speeds the process up so metamorphism might take place over a shorter time period, or metamorphic processes that might not otherwise have had time to be completed are completed.

Secondly, water, especially hot water, can have elevated concentrations of dissolved elements (ions), and therefore it is an important medium for moving certain elements around within the crust. So not only does water facilitate metamorphic reactions on a grain-to-grain basis, it also allows for the transportation of elements from one place to another. This is very important in hydrothermal processes, which are discussed toward the end of this chapter, and in the formation of mineral deposits.

Time

Most metamorphic reactions take place at very slow rates. For example, the growth of new minerals within a rock during metamorphism has been estimated to be about 1 millimeter per million years. For this reason, it is very difficult to study metamorphic processes in a lab.

While the rate of metamorphism is slow, the tectonic processes that lead to metamorphism are also very slow, so in most cases, the chance for metamorphic reactions to be completed is high. For example, one important metamorphic setting is many kilometers deep within the roots of mountain ranges. A mountain range takes tens of millions of years to form, and tens of millions of years more to be eroded to the extent that we can see the rocks that were metamorphosed deep beneath it.

Classification of Metamorphic Rocks

There are two main types of metamorphic rocks: those that are foliated because they have formed in an environment with either directed pressure or shear stress, and those that are not foliated because they have formed in an environment without directed pressure or relatively near the surface with very little pressure at all. Some types of metamorphic rocks, such as quartzite and marble, which can form whether there is directed-pressure or not, do not typically exhibit foliation because their minerals (quartz

and calcite respectively) do not tend to show alignment.

When a rock is squeezed under directed pressure during metamorphism it is likely to be deformed, and this can result in a textural change such that the minerals appear elongated in the direction perpendicular to the main stress (Figure 7.2.1). This contributes to the formation of foliation.

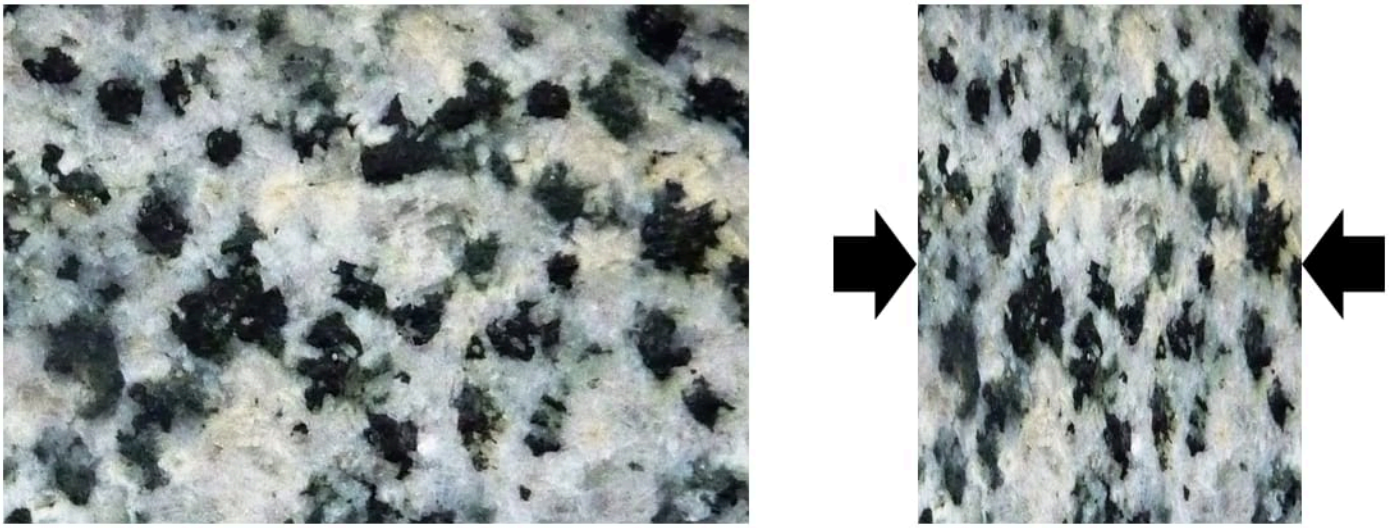


Figure 2.6.1: Foliation develops when a rock is put under differential stress. Minerals within the rock deform by lengthening in the direction perpendicular to the greatest stress (indicated by black arrows). Left: randomly oriented minerals before squeezing. Right: minerals move into alignment after squeezing. "Foliated" by Steven Earle is licensed under CC BY.

When a rock is both heated and squeezed during metamorphism, and the temperature change is enough for new minerals to form from existing ones, there is a strong tendency for new minerals to grow with their long axes perpendicular to the direction of squeezing.

Table 2.6.2 provides a nice summary of the types of metamorphic rocks the form for various protoliths at different temperatures.

Table 2.6.1: A generalized guide to the types of metamorphic rocks that form from different protoliths at different grades of regional metamorphism.

	Very Low Grade (150-300°C)	Low grade (300-450°C)	Medium Grade (450-550°C)	High Grade (Above 550°C)
Shale, mudstone	Slate	Phyllite	Schist	Gneiss
Ultramafic igneous rocks	Serpentinite	Serpentinite	Serpentinite	Serpentinite
Granite	No change	No change	Almost no change	Granite gneiss
Quartz sandstone	No change	Little change	Quartzite	Quartzite
Limestone	Little change	Marble	Marble	Marble

Foliated Metamorphic Rocks

The various types of foliated metamorphic rocks, listed in order of the grade or intensity of metamorphism and the type of foliation are: slate, phyllite, schist, and gneiss (Figures $2.6.2-5$). Slate is formed from the low-grade metamorphism of shale, and has microscopic clay and mica crystals that have grown perpendicular to the stress. Slate tends to break into flat sheets. Phyllite is similar to slate, but has typically been heated to a higher temperature; the micas have grown larger and are visible as a sheen on the surface. Where slate is typically planar, phyllite can form in wavy layers. In the formation of schist, the temperature has been hot enough so that individual mica crystals are big enough to be visible, and other mineral crystals, such as quartz, feldspar, or garnet may also be visible. In gneiss, the minerals may have separated into bands of different colors. In the example shown in

Figure 2.6.5, the dark bands are largely amphibole while the light-colored bands are feldspar and quartz. Most gneiss has little or no mica because it forms at temperatures higher than those under which micas are stable. Unlike slate and phyllite, which typically only form from mudstone, schist, and especially gneiss, can form from a variety of parent rocks, including mudstone, sandstone, conglomerate, and a range of both volcanic and intrusive igneous rocks.

Schist and gneiss can be named on the basis of important minerals that are present. For example a schist derived from basalt is typically rich in the mineral chlorite, so we call it chlorite schist. One derived from shale may be a muscovite-biotite schist, or just a mica schist, or if there are garnets present it might be mica-garnet schist. Similarly, a gneiss that originated as basalt and is dominated by amphibole, is an amphibole gneiss or, more accurately, an amphibolite.



Figure 2.6.2: Slate – A low-grade metamorphic rock formed from shale. It exhibits slaty cleavage, breaking into flat, sheet-like layers due to aligned microscopic minerals. "Gray slate (Martinsburg Formation, Ordovician; near Bangor, Slate Belt, Pennsylvania, USA) 1" by James St. John via Flickr is licensed under CC BY.



Figure 2.6.3: Phyllite – A metamorphic rock that forms from slate under higher temperature and pressure. It has a slightly wavy foliation and a silky luster from fine-grained micas. "Phyllite (French Slate, Paleoproterozoic; Snowy Range Road roadcut, Medicine Bow Mountains, Wyoming, USA) 6" by James St. John via Flickr is licensed under CC BY.



Figure 2.6.4: Schist – A medium-high-grade metamorphic rock with prominent foliation and visible mineral grains. Commonly contains mica and accessory minerals like garnet. "Garnet-chlorite schist (Lake Martin, Alabama, USA) 2" by James St. John via Flickr is licensed under CC BY.



Figure 2.6.5: Gneiss – A high-grade metamorphic rock with distinct compositional banding. Forms under intense heat and pressure from pre-existing rocks like granite or schist. "Gneiss 1" by James St. John via Flickr is licensed under CC BY.

Nonfoliated Metamorphic Rocks

Metamorphic rocks that form under either low-pressure conditions or just confining pressure do not become foliated. In most cases, this is because they are not buried deeply, and the heat for the metamorphism comes from a body of magma that has moved into the upper part of the crust. This is contact metamorphism. Some examples of non-foliated metamorphic rocks are marble, quartzite, and hornfels.

Marble

Marble is metamorphosed limestone. When it forms, the calcite crystals tend to grow larger, and any sedimentary textures and fossils that might have been present are destroyed. If the original limestone was pure calcite, then the marble will likely be white (Figure 2.6.6), but if it had impurities such as clay, silica, or magnesium, the marble could be “marbled” in appearance. Marble that forms during regional metamorphism (most marble) may or may not develop a foliated texture, but foliation is typically not

easy to see in marble.



Figure 2.6.6: A sample of fairly pure marble. "Marble (Murphy Marble, Ordovician; quarry near Tate, Georgia, USA) 1" by James St. John via Flickr is licensed under CC BY.

Quartzite

Quartzite is metamorphosed sandstone (Figure 2.6.7). It is dominated by quartz, and in many cases, the original quartz grains of the sandstone are welded together with additional silica. Most sandstone contains some clay minerals and may also include other minerals such as feldspar or fragments of rock, so most quartzite has some impurities with the quartz.



Figure 2.6.7: A sample of quartzite, a nonfoliated metamorphic rock formed from sandstone. "Quartzite 4" by James St. John via Flickr is licensed under CC BY.

Hornfels

Hornfels is another non-foliated metamorphic rock that normally forms during contact metamorphism of fine-grained rocks like mudstone or volcanic rock (Figure 2.6.8). In some cases, hornfels has visible crystals of minerals like biotite or andalusite. If the hornfels formed in a situation without directed pressure, then these minerals would be randomly orientated, not aligned with one-another, as they would be if formed with directed pressure.



Figure 2.6.8: Hornfels, a generally nondescript dark-colored rock often confused with basalt. This sample is from Genesse Valley, CA (see: Sierra Nevada). "Hornfels (Genesse Valley, California, USA)" by James St. John via Flickr is licensed under CC BY.

Serpentinite: California's State Rock

All 50 states have an official state rock, and California's state rock is serpentinite, a metamorphic rock common in the Coast Ranges, Klamath Mountains, and the Sierra Nevada foothills of California. Serpentinite is a rock composed of the minerals of the serpentine group. The serpentine minerals are named for their smooth, but scaly appearance. The name is derived from the Latin *serpentinus* meaning "serpent rock". The serpentine group has over 20 varieties of silicate minerals containing abundant magnesium and iron.

Chrysotile is one polymorph of serpentine mineral. It has a fibrous crystal habit, and importantly, is one of the asbestos minerals. "Asbestos" is a generic commercial term for a group of naturally occurring silicate minerals that form in a particular fibrous crystal habit (this group also includes actinolite, amosite, anthophyllite, crocidolite, and tremolite - all amphibole minerals). Asbestos fibers make it an excellent fire retardant and thus it was used widely in construction (insulation in buildings and ships), the automotive industry (for brake shoes and clutch fittings), and in fabric treatment (clothing, kitchen linens). Over the first half of the 20th century, growing evidence indicated a link between inhalation of asbestos mineral fibers and lung disease (asbestosis) and what is now known as mesothelioma cancer. In the 1970s, The United States Environmental Protection Agency (EPA) enacted the Clean Air Act in 1970. The act classified asbestos as a hazardous air pollutant.

Not all serpentine minerals exhibit asbestos crystal habit. Other polymorphs have a platy (non-asbestos forming) crystal habit. Antigorite (Figure 2.6.9 center) and lizardite (Figure 2.6.9 right) are examples of non asbestos serpentine.



Figure 2.6.9: Left: A sample of chrysotile serpentine, which exhibits a fibrous crystal habit and is considered an asbestos mineral. Center: Antigorite serpentine, which exhibits a platy habit rather than a fibrous one. Right: Lizardite, a smooth serpentine mineral that is not asbestos forming. "Chrysotile" by USGS is in the public domain. "Antigorite" by James St. John via Flickr is licensed under CC BY. "Lizardite" by James St. John via Flickr is licensed under CC BY.

Serpentine minerals form from the metamorphism of mafic and ultramafic igneous rocks such as those derived from the ocean crust (basalt) and the upper mantle (peridotite). Serpentine minerals tend to form where hydrothermal alteration of ultramafic rocks is possible such as the hydration of olivine rich rocks at low temperatures 0°-60° Celsius.

Serpentinite is most common in the Coast Ranges, the Klamath Mountains, and the Sierra Nevada foothills (Figure 2.6.10. Interestingly, the soils derived from serpentine bedrock are toxic to many plants. The flora that grow from such soil is thus very distinctive. These areas are called serpentine barrens because they often consist of grassland or savannas where the climate would normally lead to the growth of forests. Grass Valley, California is one of these serpentine barrens. Just as many plants fail to grow in serpentine soils, some are uniquely evolved to thrive there. *Calamagrostis ophitidis* is an endemic species of grass more commonly known as Serpentine Reedgrass (Figure 2.6.12). Similarly, the Tiburon Mariposa Lily (*Calochortus tiburonensis*) grows only in challenging serpentine soils, and is known in only one location just north of San Francisco, Ring Mountain (Figure 2.6.13).

Officially, the state rock of California is listed as "serpentine." Technically, this is incorrect as serpent*ine* is the mineral that makes up the rock serpentin*ite*.

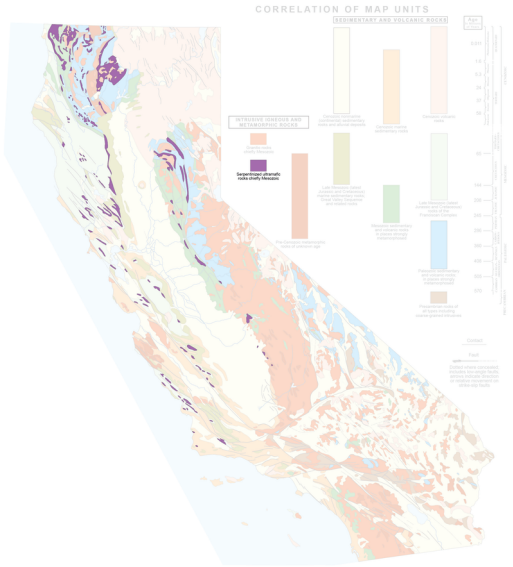


Figure 2.6.10: Locations of serpentinite outcrops in California (shown in purple). Serpentinite is most abundant in the Coast Ranges, the Klamath Mountains, and the Sierra Nevada foothills. "Serpentinite outcrops" by Steven Skinner, a derivative of the simplified geologic map of California, is licensed under CC BY-NC. Access a detailed description.



Figure 2.6.11: Calamagrostis ophitidis — serpentine reedgrass. Endemic to serpentine slopes in the northern San Francisco Bay Area. Specimen in the University of California Botanical Garden, Berkeley, California, U.S. "*Calamagrostis ophitidis*" by Daderot via Wikimedia commons is in the public domain.



Figure 2.6.12: The endemic Tiburon Mariposa Lily thrives in serpentine soils and is known to grow in just one locale: Ring Mountain north of San Francisco. "Tiburon Mariposa Lily" by Tom Hilton via Flickr is licensed under CC BY.

Serpentine Mineral Quick Facts

The following are some key characteristics of the mineral serpentine:

- Composition: $Mg_6Si_4O_{10}(OH)_8$
- Crystal system: Monoclinic (antigorite has a hexagonal polymorph, chrysotile two orthorhombic polymorphs).
- Habit: Crystals unknown: the serpentine minerals usually occur in structureless masses, except when asbestiform.
- Cleavage: None observable
- Hardness: 4-6
- Density: 2.5-2.6
- Color: Usually green, also yellow, brown, reddish brown and gray.
- Streak: White
- Luster: Waxy or greasy in massive varieties, silky in fibrous material.

- Occurrence: Serpentine is formed by the alteration of olivine and enstatite under conditions of low-and medium-grade metamorphism. It sometimes occurs as large rock masses. Massive serpentinite is sometimes cut and polished as an ornamental stone.

Plate Tectonics and Metamorphism

References

1. Earle, S. (2019). *Physical Geology – 2nd Edition*. Victoria, B.C.: BCcampus. Retrieved from https://opentextbc.ca/ March 2024

This page titled 2.6: Metamorphic Rocks is shared under a CC BY-NC 4.0 license and was authored, remixed, and/or curated by Allison Jones.

2.7: Chapter Summary

2.1 Minerals

- A mineral is a naturally occurring crystalline solid with a distinct chemical formula.
- An atom is made up of protons and neutrons in the nucleus, and electrons arranged in energy shells around the nucleus.
- The main types of bonding in minerals are ionic bonding (electrons transferred) and covalent bonding (electrons shared).
- Minerals are grouped according to the anion part of their formula.
- Silicate minerals are the most common minerals in Earth's crust and mantle. They all have silica tetrahedra (four oxygens surrounding a single silicon atom) arranged in different structures (chains, sheets, etc).

2.2 Mineral Properties

- Minerals can be identified using their properties such as hardness, cleavage/fracture, density, luster, color, and streak color.
- Hardness describes the ability or inability of a mineral to be scratched. Mohs hardness scale from 1-10 is used for assigning hardness values.
- A mineral exhibits cleavage when it breaks along regular planes as a result of its internal structure. If a mineral does not exhibit cleavage, it will simply fracture randomly or conchoidally.
- Luster is the quality of light reflected off of a mineral's surface. Minerals can generally be categorized as metallic or nonmetallic (though there are other terms that can describe luster).
- Color is not often useful for identifying minerals. However, streak, or the color of the powdered mineral is more useful.
- Other properties such as density or reaction with acid can be useful for identify particular minerals.

2.3 The Rock Cycle

- Rocks are consolidated aggregates of minerals and other materials. There are three main types: igneous, sedimentary, and metamorphic.
- The rock cycle relates different rock types (igneous, metamorphic, and sedimentary) and intermediate materials (magma, sediment) to the different processes they experience on Earth.
- Rocks may undergo various processes such as weathering, melting, and crystallization.

2.4 Igneous Rocks

- Igneous rock forms from molten rock (magma or lava) that has cooled and crystallized.
- There is a predictable order in which minerals will crystallize from a melt so long as the chemical constituents are present. This sequence is known as Bowen's reaction series.
- Igneous rocks can be identified using their texture (crystal size) and their composition (the minerals present).
- There are a number of textural terms that are useful for describing igneous rocks that can also help identify whether the rock cooled at the surface as extrusive igneous rock, or below the surface as intrusive igneous rock.
- The composition of an igneous rock depends on the composition of the melt from which it crystallized.

2.5 Sediments and Sedimentary Rocks

- Sedimentary rocks form from the accumulation and lithification of sediments derived from pre-existing rocks, biological material, or chemical precipitation.
- There are three main types: clastic, chemical, and biochemical sedimentary rocks.
- Common clastic rocks include conglomerate, sandstone, and shale, classified by grain size.
- Chemical sedimentary rocks form from dissolved minerals precipitating out of solution, like limestone and evaporites.
- California has extensive sedimentary rock formations, including marine deposits and river sediments.

2.6 Metamorphic Rocks

- Metamorphic rocks form when pre-existing rocks undergo heat, pressure, and chemical changes without melting.
- Foliated metamorphic rocks, like schist and gneiss, have a layered or banded appearance due to differential stress.
- Non-foliated metamorphic rocks, such as marble and quartzite, do not have layering and form under different conditions.
- Metamorphic grade indicates the intensity of metamorphism, ranging from low to high grade.
- California's state rock Serpentinite is a metamorphic rock that is common in the Coast Ranges, Klamath Mountains, and Sierra Nevada foothills.

This page titled 2.7: Chapter Summary is shared under a CC BY-NC 4.0 license and was authored, remixed, and/or curated by Allison Jones.

2.8: Detailed Figure Descriptions

Figure 2.1.3 SiO_2 Quartz

This image illustrates the regular repeating atomic structure of a silicate mineral in two dimensions. The structure is represented at the atomic level.

Visual Elements:

- Small red spheres represent silicon (Si) atoms.
- Larger blue spheres represent oxygen (O) atoms.
- The atoms are connected by lines indicating covalent bonds.

Structural Arrangement:

- The silicon and oxygen atoms form tetrahedral units, where one silicon atom is bonded to four oxygen atoms.
- These tetrahedra are arranged in a hexagonal pattern, sharing three of their oxygen atoms with adjacent tetrahedra.

Figure 2.1.5 First Four Rows of the Periodic Table

This diagram presents the first four periods (rows) of the periodic table, including elements with atomic numbers 1–36. Elements are arranged left to right by increasing atomic number. Color coding visually differentiates element types, such as the following.

- Noble gases in the last column on the right (light blue): helium neon, argon, krypton
- Alkali metals in the first column on the left (red): lithium, sodium, potassium.
- Nonmetals on the right side of the table (green/yellow): carbon, phosphorus, sulphur, selenium, nitrogen, oxygen, flourine, chlorine, bromine.

Each element is shown in a square containing:

- The element symbol (e.g., H for hydrogen)
- The element name (e.g., hydrogen)
- The atomic number (top left)
- The atomic weight (bottom)

Figure 2.1.6 Electron configuration of sodium and chlorine atoms

The top two diagrams show the electron configuration of sodium and chlorine.

- Sodium atoms have 11 electrons: 2 in the first shell, 8 in the second, and 1 in the outermost (third) shell
- Chlorine atoms have 17 electrons: 2 in the first shell, 8 in the second, and 7 in the outermost (third) shell.

The bottom two diagrams show a sodium ion giving up one electron (from its outmost shell) to become a cation, while the chlorine ion accepts the electron into its outermost shell - becoming chloride, which is an anion.

Figure 2.4.1 Bowen's Reaction Series

This diagram illustrates Bowen’s Reaction Series, a conceptual model showing how different silicate minerals crystallize from magma as it cools from around 1300°C to 750°C. The series splits into two branches—discontinuous and continuous—with corresponding mineral types and associated igneous rock classifications.

Layout Description:

- Vertical temperature gradient:
  - A color gradient bar from yellow(top, ~1300°C) to deep red (bottom, ~750°C) represents the cooling of magma.
  - An arrow labeled “Cooling” points downward, indicating decreasing temperature.
- Discontinuous branch:
  - Minerals form in sequence as temperature decreases:
    - Olivine
    - Pyroxene
    - Amphibole
    - Biotite
  - Each mineral forms, then reacts with the melt to form the next.
- Continuous branch:
  - Involves plagioclase feldspar, which evolves from
    - Calcium-rich at high temperatures to
    - Sodium-rich at lower temperatures
- Final minerals (bottom center), which crystallize at the lowest temperatures and are common in felsic rocks:
  - Potassium feldspar
  - Muscovite
  - Quartz
- Rock types, listed on the far right:
  - Classification of igneous rocks by their dominant minerals:
    - Ultramafic (e.g., peridotite)
    - Mafic (e.g., gabbro, basalt)
    - Intermediate (e.g., diorite, andesite)
    - Felsic (e.g., granite, rhyolite)

Figure 2.4.3 Common Igneous Rocks

This image presents a side-by-side comparison of six igneous rock samples, arranged by both composition (mafic, intermediate, felsic) and type (intrusive vs. extrusive). Each sample shows a close-up of the rock's texture, helping students visually identify mineral composition and grain size.

Category	Intrusive Rock (Top Row)	Extrusive Rock (Bottom Row)
Mafic	Gabbro	Basalt
Intermediate	Diorite	Andesite
Felsic	Granite	Rhyolite

Top Row (Intrusive Rocks):

- Gabbro (Mafic): Dark greenish-black with coarse grains of light-colored minerals.
- Diorite (Intermediate): Salt-and-pepper texture with nearly equal light and dark minerals.
- Granite (Felsic): Light-colored with large visible crystals of quartz and feldspar.

Bottom Row (Extrusive Rocks):

- Basalt (Mafic): Very dark gray to black with fine-grained texture.
- Andesite (Intermediate): Grayish, intermediate texture with subtle mineral contrast.
- Rhyolite (Felsic): Light pink to white, fine-grained and uniform.

Figure 2.4.4 Igneous Rock Classification by Mineral Composition

This diagram shows the relative mineral composition of igneous rocks across the spectrum from felsic to ultramafic. The vertical axis represents mineral percent (0–100%), while the horizontal axis categorizes rocks by composition and texture (intrusive vs. extrusive).

Horizontal Rock Categories from left to right:

- Felsic: Granite / Rhyolite
- Intermediate: Diorite / Andesite
- Mafic: Gabbro / Basalt
- Ultramafic: Peridotite / Komatiite

Vertical (Y) axis is labeled “Mineral percent” from 0% (bottom) to 100% (top). The following table summarizes the four major compositions of igneous rocks (felsic, intermediate, mafic, ultramafic) and the proportions of common minerals in each. The names for both intrusive and extrusive rock names are summarized at the bottom of the table.

Igneous compositions by mineral proportion and their corresponding intrusive and extrusive rock names.

	Felsic	Intermediate	Mafic	Ultramafic
K-feldspar	0 to 35%	0%	0%	0%
Quartz	25 to 35%	0 to 25%	0%	0%
Plagioclase feldspar	25 to 50%	50 to 70%	0 to 50%	0%
Biotite and/or amphibole	0 to 20%	20 to 40%	0 to 30%	0%
Pyroxene	0%	0 to 20%	20 to 75%	0% to 75%
Olivine	0%	0%	0 to 25 %	25% to 100%
Intrusive rock name	Granite	Diorite	Gabbro	Peridotite
Extrusive rock name	Rhyolite	Andesite	Basalt	Komatiite

Figure 2.5.2 Sediment Roundness

This diagram illustrates how the shape of sediment particles changes due to abrasion during transportation. The process is key in sedimentology and helps geologists interpret the transport history and depositional environment of sedimentary rocks.

The image is organized left to right, showing a progression of particle shapes:

- Angular
- Subangular
- Subrounded
- Rounded

A horizontal gradient arrow runs beneath the images labeled "Increasing abrasion during transportation" from left (white) to right (black), indicating progressive rounding over time and distance.

Description of Each Shape Category:

- Angular:
  - Sharp corners and irregular edges.
  - Indicates minimal transport from source.
- Subangular:
  - Still has corners but less pronounced.
  - Suggests short transport or limited abrasion.
- Subrounded:
  - More smoothed edges, rounded but not fully.
  - Implies moderate transport distance or time.
- Rounded:
  - Smooth and curved, no sharp corners.
  - Represents long-distance or prolonged transport.

Figure 2.5.3 Sediment Sorting

- Very poorly sorted: Example shows very large clasts among tiny specks and moderately sized clasts.
- Poorly sorted: Example shows moderately sized clasts among many smaller clasts.
- Moderately sorted: Example shows moderately sized clasts with a few smaller clasts and tiny specks.
- Well sorted: Example shows clasts with little variation in size.
- Very well sorted: Example shows clasts of close to identical sizes.

Figure 2.6.10 Serpentinite Outcrops

This geologic map of California emphasizes the spatial distribution of serpentinite, California's state rock. The entire state is shown with clear coastal boundaries and fault traces. The serpentinite outcrops (~245–65 Ma) appear as small purple patches. They are especially concentrated along the Coast Ranges, Klamath Mountains, and parts of the Sierra Nevada foothills.

The figure place the Precambrian rocks in the context of California's overall geologic framework.

- Cenozoic (0–65 Ma)
  - Cenozoic nonmarine (continental) sedimentary rocks and alluvial deposits (~0.011–65 Ma). These rocks are shown mainly in large lowland areas, especially the Central Valley and other broad interior basins. They also appear in smaller patches along major river valleys and coastal lowlands.
  - Cenozoic marine sedimentary rocks (~1.6–65 Ma). These rocks occur primarily along the coastal regions of California. They form discontinuous belts near the shoreline and adjacent offshore-margin areas.
  - Cenozoic volcanic rocks (~1.6–65 Ma). These rocks are concentrated in northeastern California and parts of eastern California. Smaller volcanic areas also appear scattered in the Coast Ranges and southern California.
- Mezozoic (65–245 Ma)
  - Late Mesozoic (latest Jurassic and Cretaceous) marine sedimentary rocks; Great Valley Sequence and related rocks (~145–65 Ma). These rocks form a long, continuous band along the western side of the Central Valley. They are positioned between the Coast Ranges and the Sierra Nevada.
  - Mesozoic sedimentary and volcanic rocks in places strongly metamorphosed (~245–65 Ma). These rocks occur mainly in the Sierra Nevada foothills and parts of the Klamath Mountains. They appear as elongated belts adjacent to large areas of granitic rocks.
  - Late Mesozoic (latest Jurassic and Cretaceous) Franciscan Complex (~145–65 Ma). This unit is widely distributed throughout the Coast Ranges of California. It forms a broad, irregular belt parallel to the coastline.
  - Granitic rocks chiefly Mesozoic (~245–65 Ma). These rocks dominate the Sierra Nevada and form a large, continuous region there. Smaller granitic bodies also appear in southern California and parts of the Coast Ranges.
  - Serpentinized ultramafic rocks chiefly Mesozoic . These rocks occur as narrow, scattered bodies primarily within the Coast Ranges and the Klamath Mountains. They are also present in small patches along major fault zones.
- Paleozoic (245–570 Ma)
  - Paleozoic sedimentary and volcanic rocks; in places strongly metamorphosed (~570–245 Ma). These rocks are found in eastern California and in parts of the Klamath Mountains. They also appear in smaller, isolated areas within mountain ranges.
- Precambian (older than 570 Ma)
  - Precambrian rocks of all types including coarse-grained intrusives (>570 Ma). These rocks are restricted mainly to southeastern California. They appear as isolated patches within desert mountain ranges.
- Pre-Cenozoic (>65 Ma)
  - Pre-Cenozoic metamorphic rocks of unknown age (>65 Ma). These rocks are shown in scattered areas within mountain belts across the state. They commonly occur adjacent to granitic rocks in the Sierra Nevada and southern California.

This page titled 2.8: Detailed Figure Descriptions is shared under a CC BY-NC 4.0 license and was authored, remixed, and/or curated by Allison Jones.

3: PLATE TECTONICS

Introduction to Plate Tectonics

Plate tectonics is a theory that best explains all available observations concerning the Earth's geological features and their changes over time. As a theory it is constantly being evaluated and refined. More specifically, it is a model that explains the origins of continents and oceans, folded rocks and mountain ranges, igneous and metamorphic rocks, earthquakes and volcanoes, and the movements of the continents. Plate tectonics was first proposed in 1915, but did not become an accepted part of geology until 1965. It took 50 years for this theory to be accepted for a few reasons.

First, plate tectonics was a paradigm shift in thinking about Earth and it was difficult for many established geologists to accept. While observations made by Alfred Wegener concerning the movement of continents were complete and his hypothesis of 'drifting continents' was very astute, he could not explain a driving mechanism that would account for the perceived motion of the continents through time. Many geoscientists would not accept his ideas without an explanation of a plausible driving mechanism.

Second, many of Wegener's observations were from studies of rocks, fossils and landforms in the southern hemisphere and most geologists of the time were in the northern hemisphere (Europe and North America). These Northern Hemisphere geologists were unfamiliar with the rocks and structures in the southern hemisphere. It was difficult for them to independently verify Wegener's observations and therefore easier to discount them.

Third, the technology necessary to collect the data to develop the concept of plate tectonics simply did not exist until the middle of the 20th century. Though not covered in depth in this resource, we recommend exploring the development of Plate Tectonics theory in *Physical Geology – H5P Edition*.

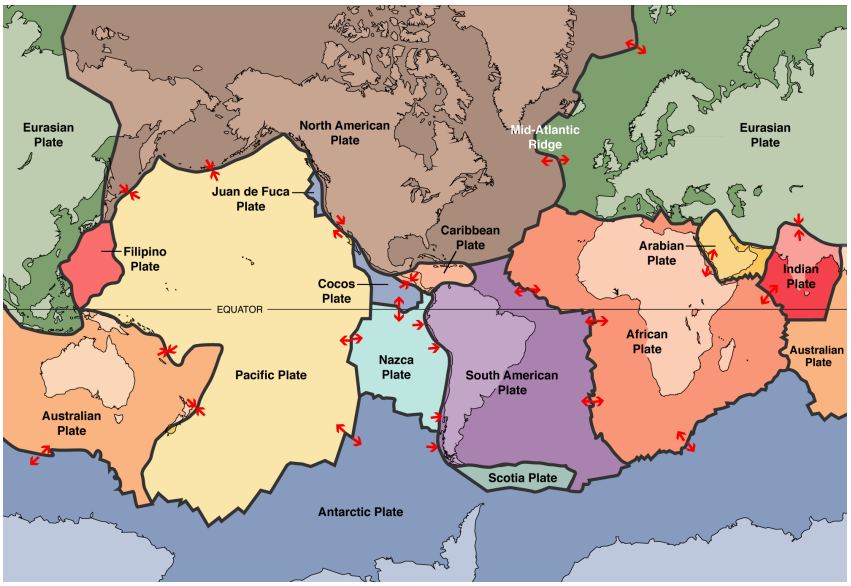


Figure 3.1: World map showing the boundaries of the tectonic plates. California lies along the transform boundary between the Pacific Plate and the North American Plate, accounting for its frequent earthquake activity. The Juan de Fuca Plate subducting beneath the North American Plate contributes to volcanic activity in the Pacific Northwest. The North American Continent takes up only part of the North American plate (brown). The Mid-Atlantic Ridge, a spreading center (in other words, a place where plates are moving away from one another) is also labeled. The arrows indicate the directions of plate movement. Convergent boundaries are indicated by arrows pointing toward each other, divergent boundaries are indicated by arrows pointing away from each other, and transform boundaries are indicated by arrows pointed in opposite directions parallel to the plate margin. "Global Plate Boundaries and Plate Motion" by Earth@Home, a derivative of the original work, is in the public domain. Access a detailed description.

Learning Objectives

By the end of this chapter, you should be able to:

- Describe the geological processes that take place at divergent, convergent, and transform plate boundaries.
- Describe the physical mechanisms that drive plate movement.
- Locate and describe California's major plate boundaries.

3.1: Earth's Interior
3.2: Tectonic Plates, Plate Motions, and Plate Boundaries
3.3: Mechanisms for Plate Motion
3.4: California's Plates and Plate Boundaries
3.5: Chapter Summary
3.6: Detailed Figure Descriptions

This page titled 3: Plate Tectonics is shared under a CC BY-NC 4.0 license and was authored, remixed, and/or curated by Allison Jones.

3.1: Earth's Interior

What's Below the Surface

In order to understand the details of plate tectonic theory, it is essential to first understand the layers that make up Earth's interior. Firsthand information about what is below the surface is very limited; most of what we know is inferred from data of Earth's gravitational and magnetic fields, the movement of seismic waves through Earth, the geothermal heat measured at Earth's surface, and inferences from the composition of meteorites. There are two ways in which we divide Earth into layers: by chemical composition and by physical properties (Figure 3.1.1).

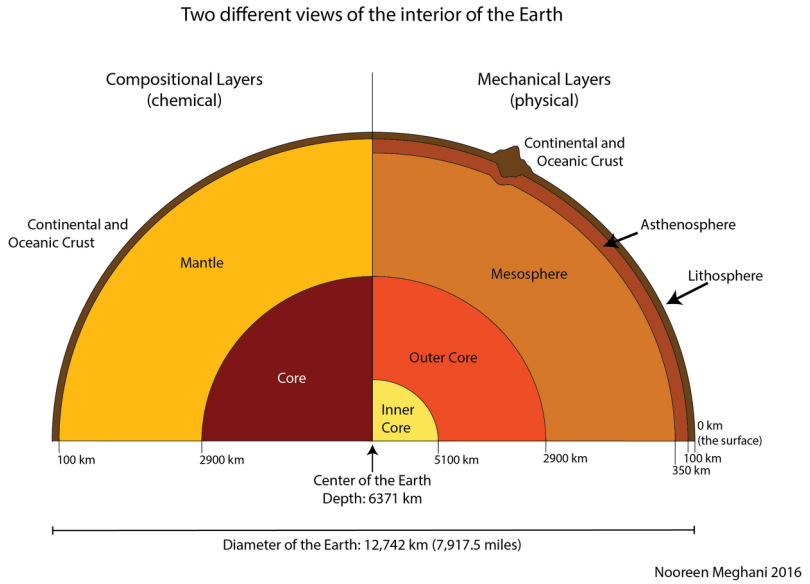


Figure 3.1.1: The two ways in which Earth's layers can be defined. Left: Earth's compositional layers include the crust, mantle, and core. Right: Earth's mechanical layers include the lithosphere, mesosphere, outer core, and inner core. "Compositional and Mechanical Layers of Earth's Interior" by Nooreen Meghani is licensed under CC BY-NC-SA. Access a detailed description.

Layers Defined by Chemical Composition

The Earth is not made up of a single, uniform chemical composition. As the planet formed and continued to evolve, it differentiated into layers based on compositional and density differences, with its heavier elements sinking to its center and lighter elements remaining near its surface. This process resulted in the Earth developing roughly concentric layers with varying compositions, creating its crust, mantle, and core (Figure 3.1.1).

The Crust

The outermost chemical layer of the Earth is the crust Figure 3.1.2. There are two types of crust: continental and oceanic.

The continental crust has a relatively low density because it has an average composition that is felsic. Although there are a range of different rock types that make up the continental crust, geologists generally refer to it as "granitic" in average composition (granite is a common example of a felsic rock and it has an average density of 2.7 g/cm^3). The average thickness of continental crust is 25 to 70 km (16 to 43 mi), and its average elevation is 840 m (2,750 ft) above sea level.

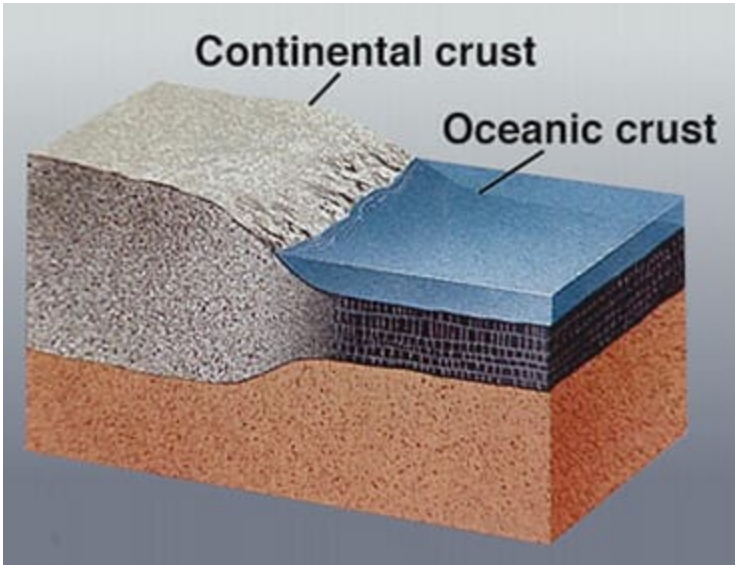


Figure 3.1.2: Differences between continental and oceanic crust. Continental crust is thicker and less dense compared to the thinner and more dense oceanic crust. The continental crust and oceanic crust are supported by the asthenosphere. "Crust" by USGS Earthquakes Hazards Program is in the public domain.

The oceanic crust has a higher density, reflecting the fact that it is primarily made of the mafic rock “basalt”. The density of basalt is ~3.0 g/cm^3. Oceanic crust is also much thinner than continental crust, ranging from 7 to 10 km (4.3 to 6.2 mi), and because it is denser, it is generally found below sea level. Mafic is a chemical term for rock that is lower in silica and has a greater amount of iron and magnesium. The density of oceanic crust also increases as it gets older and colder.

Box 3.1.1: Why are Mountains Tall?

What holds up a mountain? Have you ever wondered why mountains are tall? Most people would say that rock is strong; strong enough to hold itself up, which is sometimes true, but not always. It depends on the size of the mountain or the mountain range. The strength of the rock is only a small part of the story. Mountains are supported in part by the strength of the rock, but mostly by the buoyancy of the rock below them.

First consider the strength of the rock, not the buoyancy of the rock below. As an analogy, consider the cover on a swimming pool to be like the strength of the rock and a house cat to be like a small mountain. As the cat walks across the pool cover it flexes, but continues to support the cat. This holds true for a small mountain. The rock in the lithosphere may slightly flex, but it supports the small mountain. Most mountains or mountain ranges, though, are not small, so the strength of the rock alone is not enough to hold the mountain up.

Then why do mountains even exist? The surface of Earth is anything but uniform in elevation, there are lots of mountains and basins and continents and oceans. These changes in elevation at the surface of Earth are all expressions of the relationship of the rocks in the lithosphere and the asthenosphere trying to achieve gravitational or isostatic equilibrium, a balance between the force of gravity pulling downwards on the rock, the buoyancy of the rock at depth, and the strength of the rock.

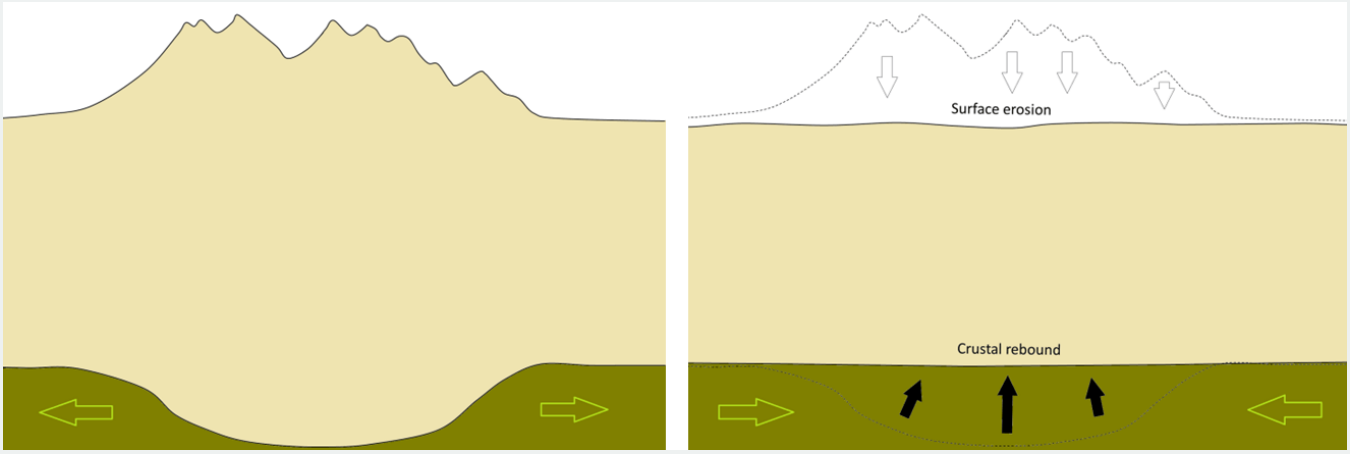
The rocks of the lithosphere vary in thickness and density - think of continental crust and oceanic crust as a broad example. The rocks of the continental crust are generally thicker and less dense, while the rocks of the oceanic crust are thinner and denser. Thin or thick, less or more dense, the rocks of the lithosphere actually float on the asthenosphere. The relative height (or lack of height) occurs as a balancing act.



Box Figure 3.1.1.1: Iceberg with submerged portion visible. The submerged portion is larger (more voluminous) that the exposed portion. "Iceberg in the Arctic with its underside exposed" by AWeith via Wikimedia Commons is licensed under CC BY-SA.

The first and the most important part of the balancing act is to consider how an ice cube floats in a glass of lemonade, or an iceberg floats in the ocean (Box Figure 3.1.1.1). It is the ice below the surface of the ocean that is important for the iceberg to float. Gravity is trying to pull the iceberg down, but because the ice is less dense than the surrounding seawater, its buoyancy is making it rise. If it were to snow, the iceberg would become heavier and sink a bit more but would still be supported by the ice below the water level because that part of the iceberg is surrounded by denser seawater. On the other hand, if it were warmer, some of the ice might melt and flow into the sea. There would be less ice to support, so the iceberg would rise a little. Either way there is a balance, and isostatic or gravitational equilibrium is eventually achieved.

Now consider rocks. A mountain in the lithosphere floats like an iceberg (Box Figure 3.1.1.2). It is made of rock rather than ice, and the asthenosphere is also made of rock. But just like ice and seawater, the rock in the lithosphere is less dense than the rock in the asthenosphere. However, unlike seawater, the asthenosphere is solid, but it's a ductile solid that behaves like an extremely viscous liquid. Think of it as more like peanut butter than water. Peanut butter flows very slowly. If you tip over a jar of peanut butter, it will take hours for peanut butter to flow out of the jar. The rock of the asthenosphere by comparison would take thousands of years. However, because it can flow, even if the flow is very slow, it behaves like a very viscous fluid and the lithosphere can therefore float on the asthenosphere.



Box Figure 3.1.1.2: The isostatic relationship between the crust and the mantle. Left: The weight of a mountain bears down on the asthenosphere below the crust (lithosphere), causing the asthenosphere to flow away from that area. Right: As the mountain erodes away and the weight decreases, the lithosphere rebounds and the asthenosphere flows back into the area. "Isostatic Relationships" by Steven Earle is licensed under CC BY 4.0.

Now a mountain or a mountain range stands tall, which makes it easy to erode. As the mountain erodes, and material is removed, the land may rise because the rock supporting it from below is adjusting to the removal of the eroded material. But as the land rises, the mountain also rises, so erosion continues, until perhaps there no longer is a mountain to erode. The opposite can also occur. Consider the sediment that eroded from the mountain. If it piles up somewhere else, the mass of sediment may cause the land surface to subside, as the rock below adjusts to the additional weight, and a basin may form. The Sierra Nevada and the Great Valley are California examples.

One last consideration, the isostatic equilibrium of an area is always slowly changing. This is because of the changes occurring to the rock at or near Earth's surface and because the lithosphere is not exactly like a pool cover. Unlike a pool cover, its strength varies with temperature and depth. To complicate matters, the asthenosphere and lower mantle below are also constantly in motion because of mantle convection.

The Mantle

The mantle is the largest compositional layer by volume, extending from the base of the crust to a depth of about 2,900 km (1,802 mi). Most of what we know about the mantle is inferred from seismic wave analysis and the study of rocky meteorites. Ophiolites and xenoliths are also used to study conditions within the mantle and mantle composition. Ophiolites are pieces of oceanic lithosphere that have been uplifted and exposed at Earth's surface (Figure 3.1.3). In California, ophiolites are preserved in the Coast Ranges, the Klamath Mountains, and the foothills of the Sierra Nevada. The changes these rocks undergo provide information on the pressure and temperatures within the mantle. Mantle xenoliths are rocks from depth brought to the surface of Earth by volcanic eruptions. As magma moves upward through the mantle, it can break off pieces of the mantle it is rising through, and those pieces can be preserved as inclusions within the rock that forms as the lava from the volcanic eruption cools. Most xenoliths are made of peridotite, an ultramafic class of igneous rock (see Igneous Rocks). Because of this, geoscientists hypothesize that portions of the mantle are made of peridotite.

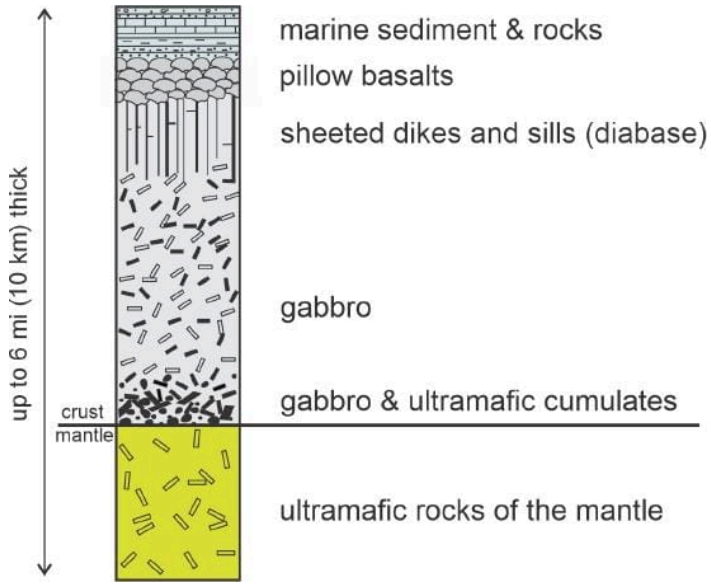


Figure 3.1.3: Idealized ophiolite sequence, from the mantle through the crust. Ultramafic rocks of the mantle are overlaid by gabbro and ultramafic cumulates. Moving up, successive layers are gabbro, sheeted dikes and sills (diabase), pillow basalts, and marine sediments and rocks. These sequences are typically around 10 km (6 mi) thick. "ophiolite-cross-section.jpg" by Dexter Perkins is licensed under CC BY-NC-SA 4.0.

Mantle Xenolith 3D Model

The following 3D model is of a mantle xenolith preserved in a five-sided sample of basalt. As the basalt made its way to the surface, pieces of the mantle became entrained in the rock. This material appears as irregular green blotches with a crystalline structure that is clearly visible against the porous gray surface of the basalt.

This interactive element is not available in this format. Visit the link or scan the QR code to access it online.

View this Interactive Content online

This model by Ryan Hollister via Sketchfab is licensed under CC BY.

The boundary between the crust and the mantle is identified by a seismic discontinuity called the Mohorovičić Discontinuity (or Moho for short; Figure 3.1.4). The discontinuity refers to the change in seismic wave velocities, which increase dramatically as seismic waves travel from the crust into the denser mantle. The change in wave direction and speed is caused by significant mineralogical differences between the crust and mantle. Underneath the oceans, the Moho is roughly 5 km (3 mi) below the ocean floor. Under the continents, it is about 30-40 km (18.5-25 miles) below the surface. Near large mountain-building events, or orogenies, the continental Moho depth can be more than double that depth.

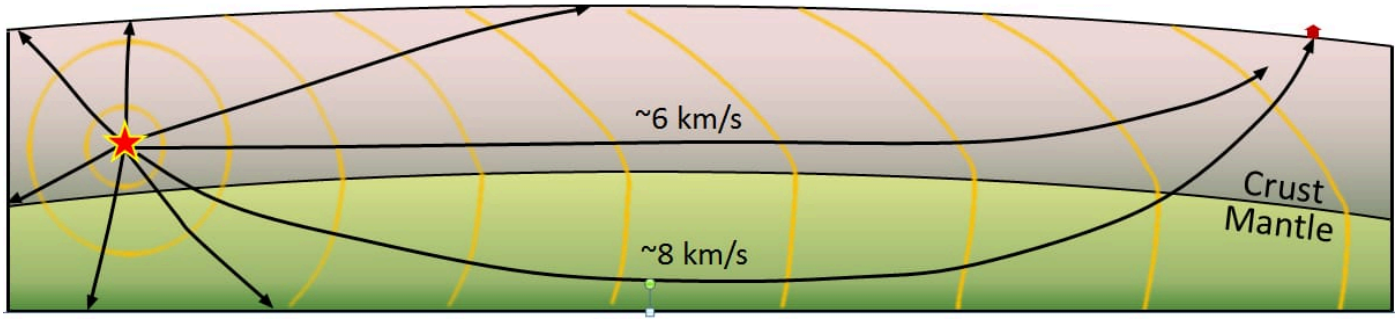


Figure 3.1.4: Depiction of seismic waves emanating from an earthquake (shown here as a red star). The boundary between the crust and mantle represents the Mohorovičić discontinuity (Moho). Some waves travel through the crust to the seismic station indicated at the top right (at ~6 km/s), while others go down into the mantle (where they travel at ~8 km/s) and are bent upward toward the surface, reaching the station before the ones that traveled only through the crust. The image demonstrates Snell's Law in action—seismic waves bend toward the slower medium and away from the faster one. "Seismic Wave Propagation in the Crust an Mantle" by Steven Earle is licensed under CC BY 4.0. Access a detailed description.

The Core

While there is no direct evidence about the composition of the core, the relative prevalence of chemical elements in our Solar System among other observations suggest the core to be made primarily of iron (Fe) and nickle (Ni) alloy.

Box 3.1.2: Discovering Earth's Internal Layers

Ancient cultures have long imagined caves and volcanoes provided openings into a mysterious and marvelous underworld filled with chasms, rivers, and fantastic beasts. In more recent times, writers like Jules Verne tapped into this natural understanding with his adventure novel, *Journey to the Center of the Earth*. But even before Verne's time, observations of Earth's gravitational and magnetic fields began to reveal an Earth with a very different interior. The scientific effort to understand Earth's interior is an interesting history of using observations made at Earth's surface to infer the properties of its interior.

In 1687, Isaac Newton outlined a procedure for determining the density of Earth. Density, or mass per unit volume of a material, is what determines the gravitational potential of an object, such as a planet. Astronomers were interested in determining the density of Earth to improve their understanding of the Solar System and planetary motion. It wasn't until 1738 that Pierre Bouguer and Charles-Marie de La Condamine attempted to use Newton's procedure at Mount Chimborazo in Ecuador to calculate the density of Earth and were able to prove that Earth is not hollow. This experiment was refined and repeated in 1774 by Charles Hutton, who was able to calculate that Earth's interior must consist of material with a higher

density than the average density of Earth's surface rock. Then, in 1798, Henry Cavendish performed the first experiment specifically designed to calculate the average density of Earth. He found it to be 5.48 g/cm^3, which closely approximates the current established value of 5.51 g/cm^3. So by 1798, the description of Earth as a planet had changed from that of a hollow Earth to that of a solid Earth filled with material more dense than the density of surface rock.

Stepping away from gravity measurements to magnetic measurements is the next step towards understanding Earth as a planet. Earth's magnetic field was first measured by Charles Friedrich Gauss in 1832. He discovered that the magnetism of surface rocks was insufficient to account for Earth's strong magnetic field and therefore he inferred that the interior of Earth must contain more iron than Earth's surface rock. Iron is very dense compared to most rock, so more iron inside the Earth could also help account for the discrepancy between the density of surface rock and the higher density needed inside Earth to produce Earth's gravitational field.

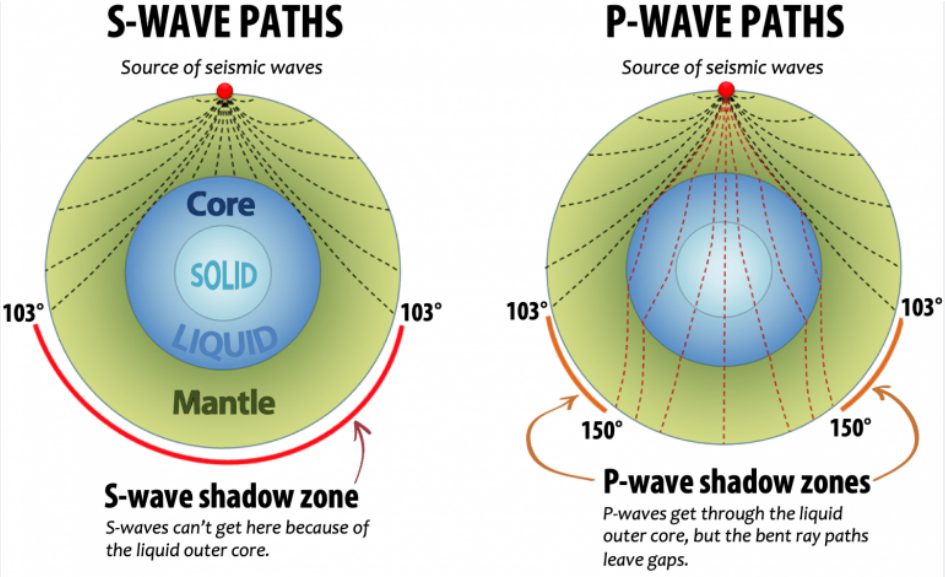
Geologists, planetary astronomers, and physicists therefore postulated that Earth must have an internal core containing significant amounts of iron. Without more information, there was however no technique that would allow them to calculate the distribution of iron within Earth, other than it must be near the center. All of this changed with the invention of the modern seismometer in 1880 by John Milne. This is because seismic waves can be used to infer physical properties of materials, like rocks, and they can also infer the location of changes in those physical properties within rock (see Earthquakes for a description of seismic waves).

In order for seismic waves to infer the physical properties of rock, knowledge about how temperature, pressure, and composition affect the physical properties of rock is also needed. Changes in temperature and pressure can cause rock recrystallization or a partial melting of the rock, either of which changes the physical properties of the rock (see Igneous Rocks and Metamorphic Rocks). In general, as pressure increases, rock becomes stiffer, and seismic wave velocities increase. But, as temperature increases, rock becomes weaker, and seismic wave velocities decrease. Therefore, the interplay of composition, pressure, and temperature determines the seismic wave velocity at any location within Earth. Melting or partial melting decreases P-wave velocities, while partial melting attenuates the strength of S-waves; if the material melts, S-waves are stopped. With the invention of the modern seismometer however seismic waves and changes in seismic waves could be recorded for analysis.

Continuous recordings of earthquake waves from the 1897 Assam, India earthquake allowed Richard Dixon Oldham in 1906 to identify the arrival of different types of seismic waves. Using a network of seismometers in Europe, and analyzing the waves recorded on seismograms from different locations, Oldham was able to show that Earth must have a core based upon how P-waves and S-waves had moved through Earth. He was also the first to try and estimate the size of Earth's core. This supported the work of Emil Wiechert, who in 1897 tried to synthesize the information known about Earth from gravity, magnetic, and seismic data and had postulated that Earth must have an iron core, surrounded by a rocky shell or mantle (Mantle is an old English word for covering). Therefore by 1906, scientists had determined that not only was the Earth solid rather than hollow, but that it also has a layered internal structure.

Other geoscientists were also using seismic wave interpretation techniques and in 1909 Andrija Mohorovičić (pronounced mo-ho-ro-vee-cheech; audio pronunciation) studying seismograms from a local earthquake in Croatia identified a boundary between what is now known as the crust and the mantle, which was named the Mohorovičić Discontinuity in his honor. This important boundary is commonly referred to as the Moho. Discontinuity is a term used for a location where the physical properties of a material change across a short distance. A discontinuity may either be a distinct surface or a transition zone. The Moho is defined by an increase in P-wave velocity from approximately 6 km/s to 8 km/s (Figure 3.1.4), which occurs as P-waves move through crustal rock into mantle rock of a different composition.

By 1914, Beno Gutenberg was able to use changes in seismic wave velocities to map the interior of Earth as three layers, an outermost crust, a mantle, and a core (Figure 3.1.1). The core-mantle boundary, abbreviated CMB, is also called the Gutenberg Discontinuity. At the CMB, P-wave velocity decreases and P-waves are refracted, whereas S-waves are stopped. This creates shadow zones where direct arrivals of P-waves and S-waves are not recorded (Box Figure 3.1.2).



Box Figure 3.1.2: Patterns of seismic waves travel through Earth's mantle and core. Left: S-waves cannot travel through the liquid outer core, so they leave a 103-degree shadow in the mantle on Earth's far side. This is designated as the "S-wave shadow zone." Right: P-waves do travel through both the liquid outer core and solid inner core, but the bent ray paths leave gaps as P-wave refraction bends seismic waves away from P-wave shadow zones. This leaves 150-degree P-wave shadow zones in the mantle opposite the source. "Seismic Shadow Zones with Explanation" by Karla Panchuk (2021), a derivative of "Seismic Shadow Zones", is licensed under CC BY 4.0.

Because S-waves are stopped at the CMB, the core of Earth was inferred to be liquid. The importance of finding a liquid core was that it could also explain the Earth's magnetic field, not because of the total amount of iron in the core, but because of the motion of the iron in the core. Moving liquid iron in the core creates the geodynamo that generates Earth's magnetic field, as was proposed in the late 1940s by Walter Elsasser and Edward Bullard.

This concept of a simple liquid core changed in 1936 when, Inge Lehmann, analyzing P-wave data recorded in Europe from the 1929 Murchison earthquake in New Zealand, found a solid inner core inside the liquid outer core, as shown by the different shadow zones for P-waves and S-waves (Box Figure 3.1.2). The boundary between the solid inner core and the liquid outer core is called the Lehmann Discontinuity.

Seismologists continue to map the interior of Earth based on variations of seismic wave velocities, and this information became part of both the framework of the development of the theory of plate tectonics and a more complete model for the structure within Earth. Figure 3.1.1 therefore illustrates how a system of layers based on the behavior of materials, or rocks, was delineated by the work of numerous seismologists and geophysicists since the 1930s.

In the 1970s, with both the advent of digital seismic recording systems and supercomputing power becoming common, the technique of seismic tomography has allowed geodynamicists to create 3-D images of the relatively subtle lateral variations in seismic velocity within the mantle, using methods like those used in medical CT scans. This has further delineated velocity differences within the mantle which lead to the development and refinement of an alternative system to describe Earth based upon physical properties and the layers – lithosphere, asthenosphere, and lower mantle.

Layers Defined by Physical Properties

The Earth can also be divided into five physical layers based on how each layer responds to stress. While there is some overlap in the chemical and physical designations of layers, specifically the core-mantle boundary, there are significant differences between the two systems. (Figure 3.1.1)

Lithosphere

Lithos is Greek for "stone", and the lithosphere is the outermost physical layer of Earth; in fact, the "plates" of plate tectonics are actually lithospheric plates.

The lithosphere consists of all of the crust and the uppermost part of Earth's mantle. This layer is defined by the brittle behavior of rock under stress. The lithosphere is grouped into two types: oceanic and continental. The oceanic lithosphere is thinner and relatively rigid. It ranges in thickness from nearly zero at mid-ocean ridges, to as much as 120 km (75 mi) away from them. The continental lithosphere is generally thicker ranging from 40 to 280 km (25 to 174 mi).

The lithosphere is not continuous. It is broken into segments called tectonic plates. A plate boundary is where two plates meet and move relative to each other. Plate boundaries are where we see plate tectonics in action—mountain building, ocean basin formation, earthquakes, and volcanic activity.

Asthenosphere

The asthenosphere is the layer below the lithosphere. Astheno- means *lacking strength*, and the most distinctive property of the asthenosphere is movement. Unlike the rigid lithosphere, this layer, which is made of rock that in places can be partially melted, moves and flows. Unlike the lithosphere which consists of multiple plates, the asthenosphere is relatively unbroken. Seismologists determined this by analyzing seismic waves that pass through this layer. The depth to the asthenosphere is temperature dependent and generally extends to depths no more than 200 km (124 mi). The asthenosphere is closer to Earth's surface in areas where lateral forces are pulling Earth's surface apart, such as mid-ocean ridges and continental rifts. It is much deeper underneath mountains and the centers of lithospheric plates.

Lower Mantle (Mesosphere)

The lower mantle, while still ductile, is less mobile than the asthenosphere. The top of the lower mantle is located at a depth of approximately 660 km (410 mi) below Earth's surface. The lower mantle is subjected to very high pressures and temperatures, which is why it is considerably less mobile than the asthenosphere.

Box 3.1.3: Mantle Minerals

The extreme conditions within the mantle create a transition zone in the uppermost part of the lower mantle where minerals continuously change into various forms or pseudomorphs. Scientists identify this zone by changes in seismic velocity (the speed of seismic waves) and occasional physical barriers to movement. Below this upper transitional zone, the lower mantle is relatively uniform until it reaches the core.

Perovskite silicates (e.g. Bridgmanite, $(Mg, Fe)SiO_3$) are thought to be the main component of the lower mantle, making them the most common minerals in or on Earth.

The following video describes the abundant mineral perovskite:

This interactive element is not available in this format. Visit the link or scan the QR code to access it online.

View this YouTube Video online

Inner and Outer Core

The deepest two layers within Earth are the outer core and inner core. While they have the same composition, they behave in distinctly different ways. The outer core is the only entirely liquid layer within Earth and the inner core is a rigid solid layer. The outer core starts at a depth of 2,900 km (1,800 mi) and extends to 5,100 km (3,200 mi), making it ~2,200 km (1,400 mi) thick. The solid inner core's radius is ~1,200 km (750 mi). The combined radius of the inner and outer cores is 3,400 km (2,100 mi), which makes it larger than Earth's moon.

Earth's liquid outer core is critically important in maintaining a breathable atmosphere and other environmental conditions favorable for life at or near Earth's surface. The motion of the liquid outer core is what creates Earth's strong magnetic field. If circulation in the outer core were to stop, Earth's magnetic field would weaken and Earth's atmosphere would be destroyed by

the solar wind**.** Ions from the sun's corona, the solar wind, can energize and strip away gas molecules from the atmosphere. In fact, this was the premise of the 2003 fictional film "The Core". Should Earth's liquid core stop circulating, its surface would cool and more solar radiation would reach the planet's surface making conditions for life more difficult. This is what happened, and continues to happen, on Mars.

It may seem like a contradiction that the deepest and hottest part of Earth is solid because at such high temperatures metals such as iron and nickel should be molten. However this area within Earth not only has the highest temperature, it also has the highest pressure. The high pressure forces these metals to remain solid in spite of the high temperatures. From the center of Earth outward, both the pressure and the temperature decrease. Eventually you reach a pressure that is no longer high enough to force the metals in the core into the solid state, while the temperature is still more than enough for them to melt. Therefore, they melt and you transition from a solid inner core to a liquid outer core.

Video: Layers of the Earth - What are they? How were they found? (Educational)

The following video provides a nice summary of this section on Earth's interior.

This interactive element is not available in this format. Visit the link or scan the QR code to access it online.

View this YouTube Video online

References

1. Danson, Edwin (2006). Weighing the World. Oxford University Press.
2. *Geomagnetism Frequently Asked Questions*. (2022, March 9). National Centers for Environmental Information (NCEI). https://www.ncei.noaa.gov/products/geomagnetism-frequently-asked-questions
3. *Historical Geology – A free online textbook for Historical Geology courses*. (2020, January 17). https://opengeology.org/historicalgeology/
4. Pasyanos, M. E. (15 May 2008). "Lithospheric Thickness Modeled from Long Period Surface Wave Dispersion" (PDF). Retrieved 2014-04-25.
5. Stacey, F. D. (1977). Physics of the Earth, 2nd ed., John Wiley and Sons.
6. Turcotte, D. L. & Schubert, G. (2014). Geodynamics, 3rd ed., Cambridge University Press.

This page titled 3.1: Earth's Interior is shared under a CC BY-NC 4.0 license and was authored, remixed, and/or curated by Allison Jones.

3.2: Tectonic Plates, Plate Motions, and Plate Boundaries

Earth's Tectonic Plates

Earth is covered with eight major tectonic plates: Eurasia, Pacific, India, Australia, North America, South America, Africa, and Antarctica. There are also numerous small plates (e.g., Juan de Fuca, Cocos, Nazca, Scotia, Philippine, Caribbean), and many very small plates or sub-plates. For example the Juan de Fuca Plate is actually three separate plates (Gorda, Juan de Fuca, and Explorer) that all move in the same general direction but at slightly different rates.

Plates can include continental crust, oceanic crust, or both; their boundaries do not necessarily coincide with the edges of continents or ocean basins. For example, the North American Plate includes most of North America, plus half of the northern Atlantic Ocean. Similarly the South American Plate extends across the western part of the southern Atlantic Ocean, while the European and African plates each include part of the eastern Atlantic Ocean. The Pacific Plate is almost entirely oceanic, but it does include the part of California that is west of the San Andreas Fault.

A plate boundary exists anywhere where two plates meet and move in opposing directions. Boundaries between the plates are of three types: divergent (i.e., plates move apart or away from one another), convergent (i.e., plates move toward one another), and transform (plates move side by side, parallel to the boundary).

Query 3.2.1

This interactive element is not available in this format. Visit the link or scan the QR code to access it online.

View this Interactive Content online

Divergent Boundaries

Divergent boundaries are locations where two plates move away from one another. These are areas of tension and normal faulting, as well as crustal thinning.

As the plates move away from one another, new oceanic plate material is formed, derived from partial melting of the mantle below the boundary. The cause of melting here is decompression as hot mantle rock from depth is moved toward the surface (Figure 3.2.1). Because new oceanic lithosphere is created at these boundaries, and plates are moved away from them, they are also referred to as spreading centers.

Most divergent boundaries are located at oceanic ridges (although some continue into continents), and the crustal material created at a spreading boundary is always oceanic in character; in other words, it is mafic igneous rock (e.g., basalt or gabbro, rich in ferromagnesian minerals). The rate at which new plate material is created (spreading rates) varies considerably, from 2 cm/year to 6 cm/year (~1 inch/year to 2 inches/year) in the Atlantic, to between 12 cm/year and 20 cm/year (~5 inches/year to 8 inches/year) in the Pacific. (Note that spreading rates are typically double the velocities of the two plates moving away from a ridge.)

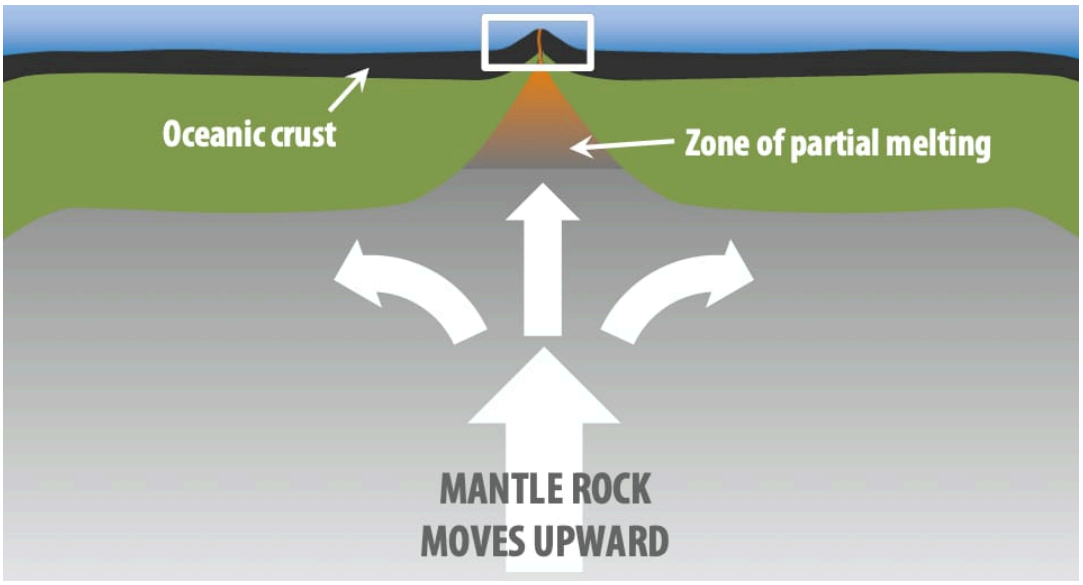


Figure 3.2.1: Mantle upwelling taking place along an oceanic divergent plate margin. Here, the spreading of ocean crust creates space for mantle rock to move upward. This mantle rock experiences partial melting as it nears the oceanic crust and is eventually erupted at the surface on the seafloor. "Mantle Upwelling" by Karla Panchuk, a derivative of the original, is licensed under CC BY-NC-SA.

Some of the processes that take place in a divergent boundary setting (Figure 3.2.2) include:

- Magma from the mantle pushes up to fill the voids left by divergence of the two plates
- Pillow lavas form where magma is pushed out into seawater
- Vertical sheeted dikes intrude into cracks that developed from the spreading
- Magma cools more slowly in the lower part of the new crust and forms gabbroic bodies

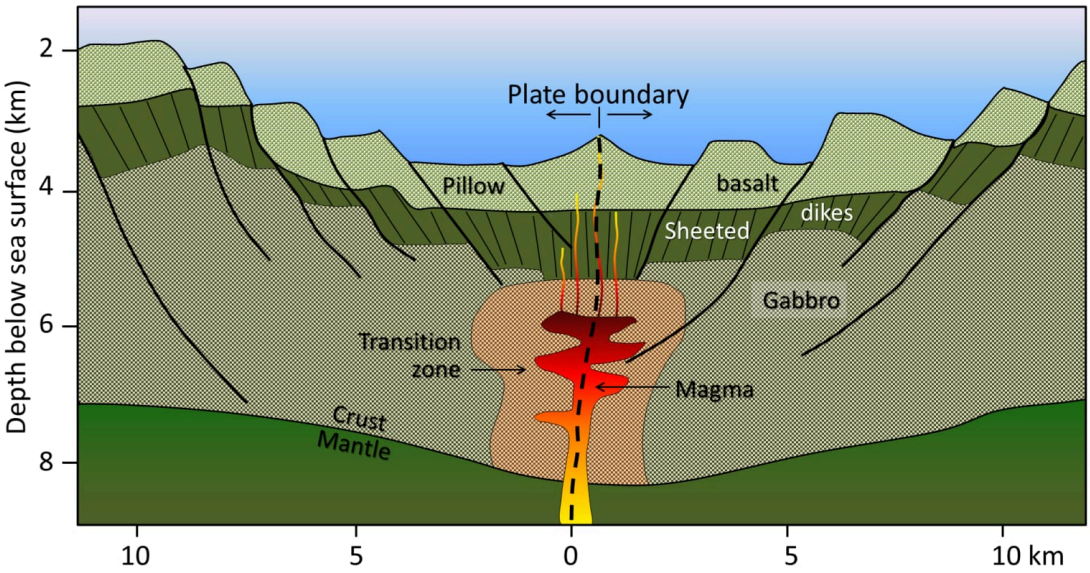


Figure 3.2.2: At spreading centers, the crust is actively pulling apart. This creates tension and results in normal faulting near the plate boundary. A predictable sequence of rocks occurs at these locations: Gabbro, overlain by sheeted dikes, overlain by pillow basalts. "Spreading Center" by Steven Earle is licensed under CC BY 4.0. Access a detailed description.

Creating a Divergent Boundary

The formation of a divergent boundary is hypothesized to start within a continental area with up-warping or doming related to an underlying mantle plume or series of mantle plumes. The buoyancy of the mantle plume material creates a dome within the crust, causing it to fracture in a radial pattern, with three arms spaced at approximately 120° (Figure 3.2.3).

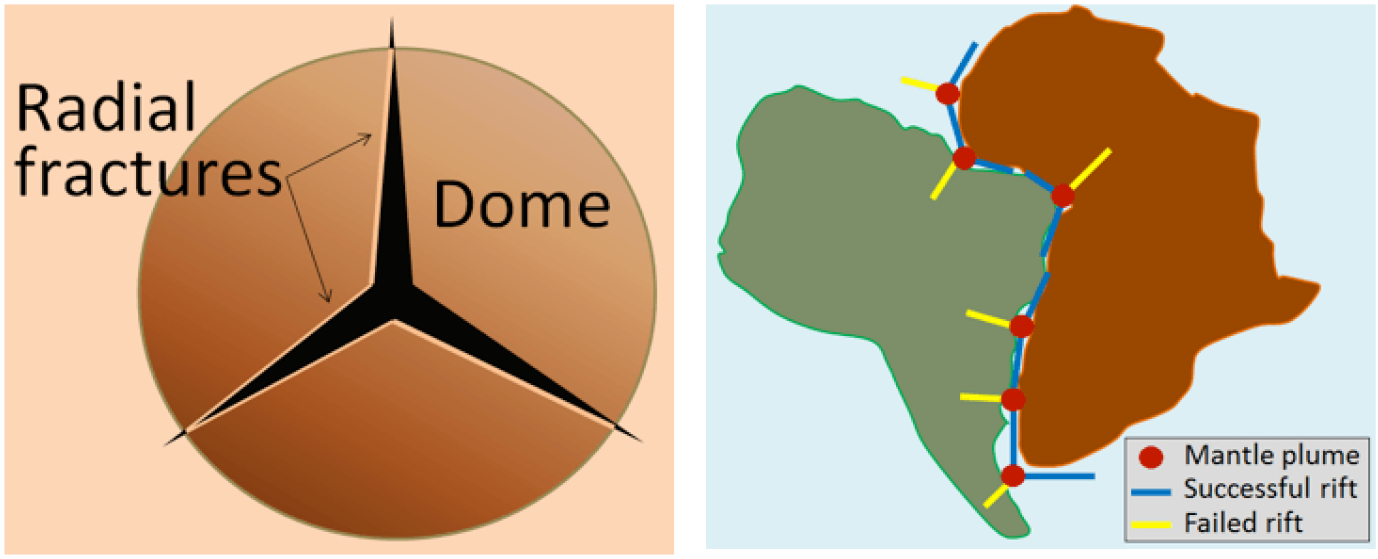


Figure 3.2.3: Dome and three-part rift formation (left) and continental rifting (right) between the African and South American parts of Pangea at around 200 Ma. "Rift Formation" by Steven Earle is licensed under CC BY 4.0. Access a detailed description.

When a series of mantle plumes exists beneath a large continent, the resulting rifts may align and lead to the formation of a rift valley (such as the present-day Great Rift Valley in eastern Africa). It is suggested that this type of valley eventually develops into a linear sea (such as the present-day Red Sea, or the Gulf of California between Baja California and mainland Mexico), and finally into an ocean (such as the Atlantic). It is likely that as many as 20 mantle plumes, many of which still exist, were responsible for the initiation of the rifting of Pangea along what is now the mid-Atlantic ridge.

Convergent Boundaries

There are three possible combinations of tectonic plates that can move toward each other at a convergent boundary, depending on the type of lithosphere at the boundary. The combinations are ocean-ocean, ocean-continent, and continent-continent. All of these boundaries are associated with compression, crustal thickening, and thrust or reverse faulting.

Ocean-Ocean Convergence

At an ocean-ocean convergent boundary, one of the plates (oceanic crust and lithospheric mantle) is pushed, or subducted, under another plate of oceanic lithosphere because older rock is colder and therefore more dense than younger, warmer rock, it is the older and colder plate that is denser and subducts beneath the younger and hotter plate. An oceanic trench forms along the subduction boundary due to the bending of the downgoing plate.

The subducted plate and its overlying oceanic sediments contain a significant volume of water and other fluids within their minerals. These fluids are released as the subducted plate is heated. These fluids rise and mix with the overlying mantle rock, lowering the mantle rock's melting point and leading to the formation of magma. This process is termed flux melting (Figure 3.2.4).

The magma is more buoyant than the surrounding mantle material. It rises through the mantle and the overlying oceanic crust to the ocean floor where it creates a chain of volcanic islands parallel to the subduction boundary known as a volcanic island arc. A mature island arc develops into a chain of relatively large islands (such as modern Japan or Indonesia) as more and more volcanic material is extruded and sedimentary rock accumulates around the islands.

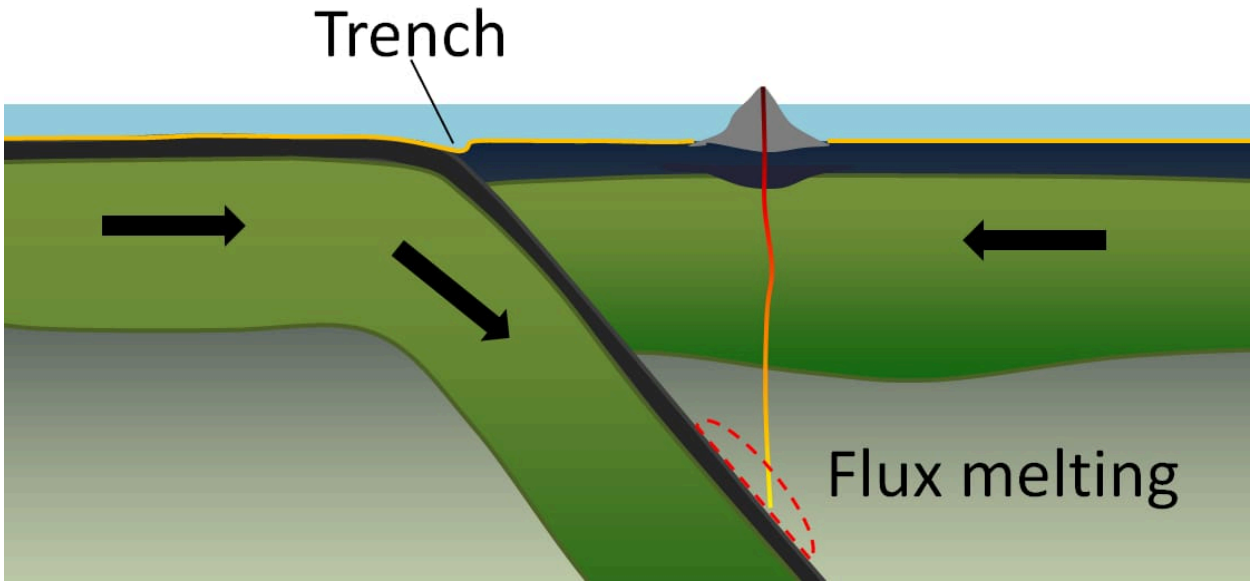


Figure 3.2.4: Configuration and processes of an ocean-ocean convergent boundary. As a plate of oceanic lithosphere subducts beneath another, a trench develops. Flux melting is generated along the subducting slab, causing buoyant magma to rise through the overlying plate. "Ocean-Ocean Convergence" by Steven Earle is licensed under CC BY 4.0.

Examples of ocean-ocean convergent zones are subduction of the Pacific Plate beneath the North America Plate south of Alaska (Aleutian Island Arc) and beneath the Philippine Plate west of the Philippines, subduction of the India Plate beneath the Eurasian Plate south of Indonesia, and subduction of the Atlantic Plate beneath the Caribbean Plate.

Ocean-Continent Convergence

At an ocean-continent convergent boundary, the oceanic plate is subducted under the continental plate in the same manner as at an ocean-ocean boundary. Some of the sediment that has accumulated on the downgoing oceanic plate, along with sediment that has accumulated on the continental slope, is thrust up into an accretionary wedge. Compressional forces associated with convergence leads to thrust faulting within the overriding continental plate (Figure 3.2.5).

As with the ocean-ocean boundary, flux melting of mantle rocks creates a mafic magma. This magma rises to the base of the continental crust and leads to partial melting of the overlying crustal rock. The resulting magma ascends through the crust, producing a mountain chain with many volcanoes called a volcanic arc. Examples of ocean-continent convergent boundaries are found where the oceanic Nazca Plate subducts under western South America (which has created the volcanic arc of the Andes Range) and subduction of the Juan de Fuca Plate under western North America (creating the Cascade Range, which includes Mt. Shasta and Mt. Lassen in California).

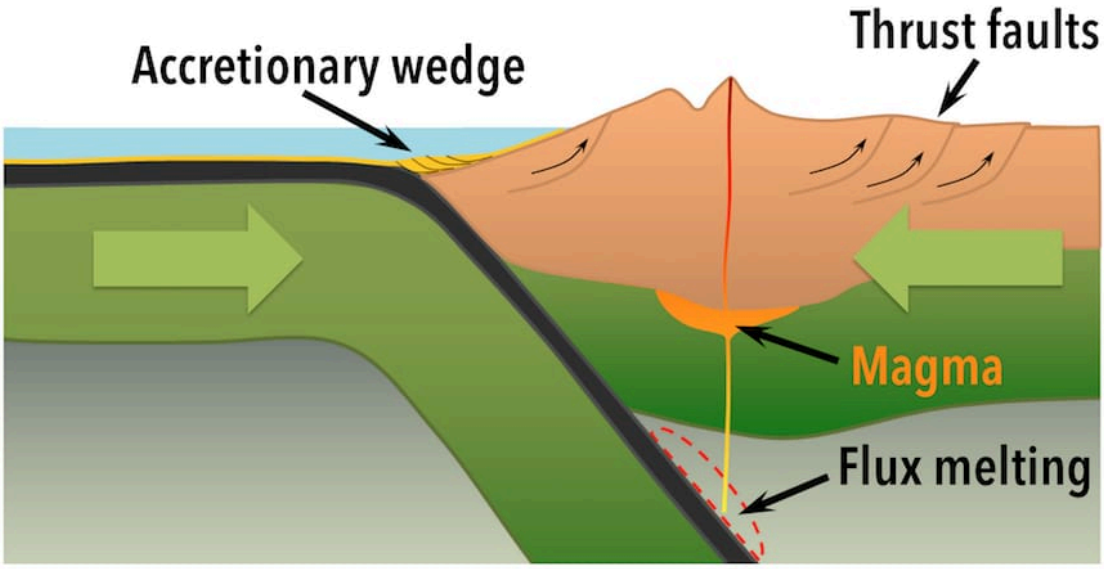


Figure 3.2.5: Cross section of an ocean-continent convergent boundary. As oceanic lithosphere subducts beneath continental lithosphere, an accretionary wedge of seafloor sediment develops near the trench, generating thrust faults at the surface. Flux melting is generated above the subducting slab, causing buoyant magma to rise through the overlying plate. "Ocean-Continent Convergence Illustrating Magma Formation" by Karla Panchuk, a derivative of the original, is licensed under CC BY 4.0.

Continent-Continent Convergence

Continent-continent convergence (or collision) occurs when a continent or large island collides with another continent (Figure 3.2.6). In this case, the colliding continental material will not be subducted because it is too buoyant (i.e., because it is composed largely of less dense, more felsic, and more buoyant continental rocks) and much thicker than oceanic crust.

At this type of plate boundary, tremendous deformation of the pre-existing continental rocks dramatically thickens the crust and builds high-standing mountain ranges consisting of any sediments that had accumulated along the shores of both continental masses, and commonly also some ocean crust and upper mantle material. These large mountain ranges consist of fold-and-thrust belts, as well as a suture zone, which marks the boundary between the original plates. The oceanic lithosphere (slab) subducted before this collision is believed to founder beneath these zones as it is recycled into the mantle.

The formation of this type of plate boundary is how oceans are destroyed and how supercontinents, such as Pangea, are formed. Examples of continent-continent convergent boundaries are found where the India Plate meets the Eurasian Plate and creates the Himalayan Mountains, and where the African Plate meets the Eurasian Plate, creating the series of ranges extending from the Alps in Europe to the Zagros Mountains in Iran.

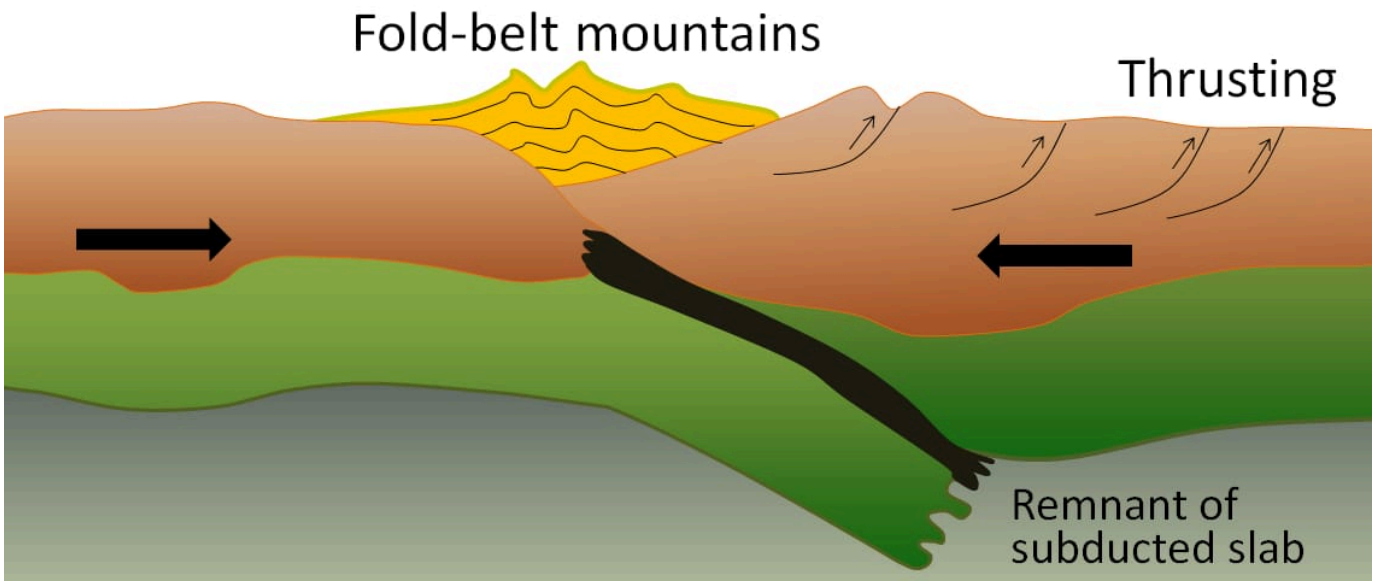


Figure 3.2.6: Configuration and processes of a continent-continent convergent boundary. Here tectonic plates are moving toward each other and whatever ocean existed between continents has now closed. The remnant of a subducted slab exerts thrrusting force on the surface. As those continents continue to collide, fold-belt mountains form. "Continent-Continent Convergence" by Steven Earle is licensed under CC BY 4.0

Query 3.2.1

This interactive element is not available in this format. Visit the link or scan the QR code to access it online.

View this Interactive Content online

Transform Boundaries

Transform boundaries are named for the fact that they "transform" the motion at one plate boundary into the motion at another, forming the connections between areas of convergence and areas of divergence, or areas that are diverging or converging at different rates. Plate motion at transform boundaries occurs along very large strike-slip fault systems that are parallel to the boundary: one plate slides past another without the production or destruction of crustal material. While small transform faults occur at divergent plate boundaries, where they connect spreading segments of mid-ocean ridges, actual transform plate boundaries, such as the San Andreas fault system, are much larger. The San Andreas fault system (Figure 3.2.7), for example, connects the convergence on the Cascadia trench offshore of the Pacific Northwest with the divergence at the East Pacific Rise, where it enters the Gulf of California.

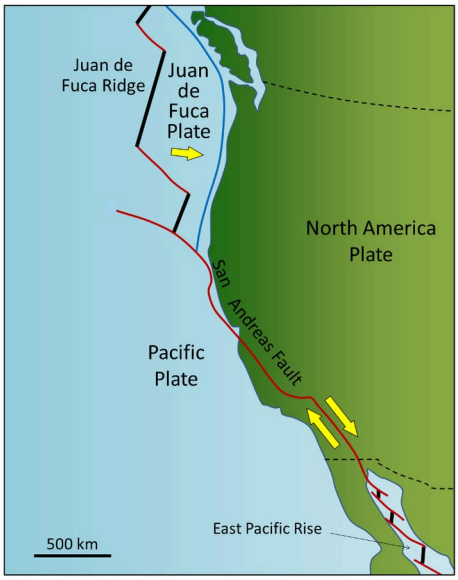


Figure 3.2.7: The San Andreas Fault, a transform boundary, extends from the north end of the East Pacific Rise in the Gulf of California to the southern end of the Juan de Fuca Ridge (adjacent to the Juan de Fuca Plate) in northern California. In the Gulf of California transform faults (red lines) connect segments of divergence (black lines). "Example of a Transform Plate Boundary - The San Andreas Fault of California" by Steven Earle is licensed under CC BY 4.0.

Query 3.2.1

This interactive element is not available in this format. Visit the link or scan the QR code to access it online.

View this Interactive Content online

Plate Tectonics and Supercontinent Cycles

Length: 1 minute 30 seconds

Description: As originally described by Alfred Wegener in 1915, the present continents were once all part of a supercontinent, which he termed Pangea (meaning “all land”). More recent studies of continental matchups and the magnetic ages of ocean-floor rocks have enabled us to reconstruct the history of the break-up of Pangea.

Pangea began to rift apart along a line between Africa and Asia and between North America and South America at around 200 Ma. During the same period, the Atlantic Ocean began to open up between northern Africa and North America, and India broke away from Antarctica. Between 200 and 150 Ma, rifting started between South America and Africa and between North America and Europe, and India moved north toward Asia. By 80 Ma, Africa had separated from South America, most of Europe had separated from North America, and India had separated from Antarctica. By 50 Ma, Australia had separated from Antarctica, and shortly after that, India collided with Asia.

The following silent video demonstrates how continents have moved from the time of Pangea to present day:

This interactive element is not available in this format. Visit the link or scan the QR code to access it online.

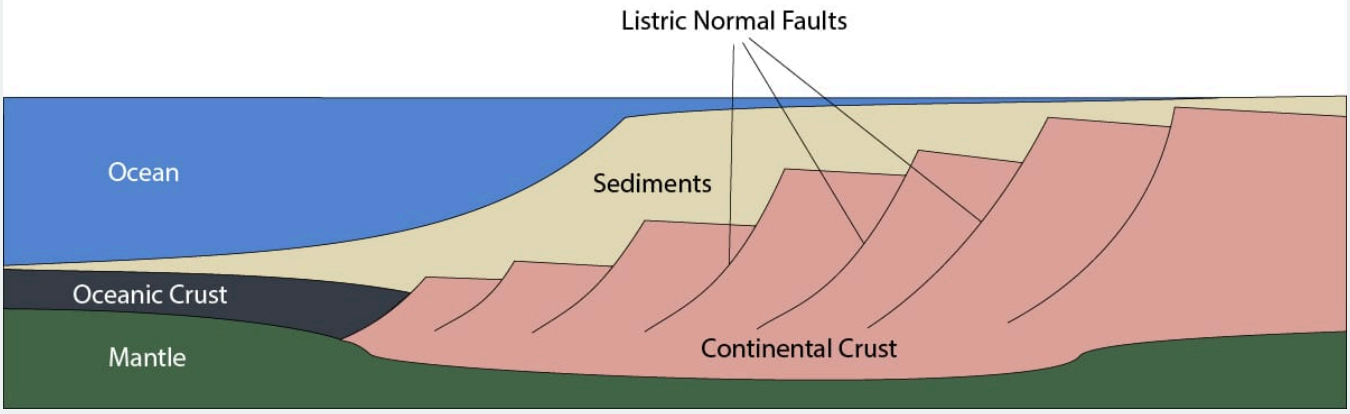
View this YouTube Video online

Within the past few million years, rifting has taken place in the Gulf of Aden and the Red Sea, and also within the Gulf of California. Incipient rifting has begun along the Great Rift Valley of eastern Africa, extending from Ethiopia and Djibouti on the Gulf of Aden (Red Sea) all the way south to Malawi.

Over the next 50 million years, it is likely that there will be full development of the east African rift and creation of new ocean floor. Eventually Africa will split apart. There will also be continued northerly movement of Australia and Indonesia. The western part of California (including Los Angeles and part of San Francisco) will split away from the rest of North America, and eventually sail right by the west coast of Vancouver Island, en route to Alaska. Because the oceanic crust formed by spreading on the mid-Atlantic ridge is not currently being subducted (except in the Caribbean), the Atlantic Ocean is slowly getting bigger, and the Pacific Ocean is getting smaller. If this continues without changing for another couple hundred million years, we will be back to where we started, with one supercontinent.

Pangea, which existed from about 350 to 200 Ma, was not the first supercontinent. It was preceded by Pannotia (600 to 540 Ma), by Rodinia (1,100 to 750 Ma), and by others before that.

In 1966, Tuzo Wilson proposed that there has been a continuous series of cycles of continental rifting and collision; that is, break-up of supercontinents, drifting, collision, and formation of other supercontinents. At present, North and South America, Europe, and Africa are moving with their respective portions of the Atlantic Ocean. The eastern margins of North and South America and the western margins of Europe and Africa are, at present, passive margins because there is no subduction taking place along them, or any other types of plate boundary nearby.



Box Figure 3.2.1: A diagrammatic passive margin resembling what western North America looked like. Continental crust that has been rifted is broken up by west-dipping listric normal faults. It is overlain by thick ocean sediments. Note that this diagram is vertically exaggerated to emphasize the different features. "Passive Margin" by Allison Jones, is in the public domain. Access a detailed description.

This situation may not continue for too much longer, however. As the Atlantic Ocean floor gets weighed down around its margins by great thickness of continental sediments, it will be pushed farther and farther into the mantle, and eventually the oceanic lithosphere may break away from the continental lithosphere (Box Figure 3.2.1). A subduction zone will develop, and the oceanic plate will begin to descend under the continent. Once this happens, the continents will no longer continue to move apart because the spreading at the mid-Atlantic ridge will be taken up by subduction. If spreading along the mid-Atlantic ridge continues to be slower than spreading within the Pacific Ocean, the Atlantic Ocean will start to close up, and eventually (in a 100 million years or more) North and South America will collide with Europe and Africa. These cycles of collision and rifting proposed by Wilson are called Wilson cycles. The following video illustrates a single Wilson cycle from continental rifting to continental collision:

YouTube Video

This interactive element is not available in this format. Visit the link or scan the QR code to access it online.

View this YouTube Video online

References

1. Sinton, J. M., and Detrick, R. S. (1992). Mid-Ocean Ridge Magma Chambers. Journal of Geophysical Research 97(B1), 197-216.
2. J. Tuzo Wilson (1966), “Did the Atlantic Close and then Re-Open?” Nature 211, 676–681. https://doi.org/10.1038/211676a0

This page titled 3.2: Tectonic Plates, Plate Motions, and Plate Boundaries is shared under a CC BY-NC 4.0 license and was authored, remixed, and/or curated by Allison Jones.

3.3: Mechanisms for Plate Motion

The Current Interpretation

While there is still debate about the exact mechanisms for plate motion, the current interpretation calls for three factors: mantle convection, ridge push, and slab pull. Convection of the mantle, not unlike convection in a pot of water on the stove, circulates mantle material. Traction between the convecting mantle allows the overlying lithospheric plates to move.

Ridge push and slab pull are likely also key factors in plate motion: Ridge-push refers to gravity causing the lithosphere to slide down and away from the elevated mid-ocean ridges. Slab-pull also refers to gravity as the weight of the subducting slab drags the rest of the plate down into the mantle. (Figure 3.3.1)

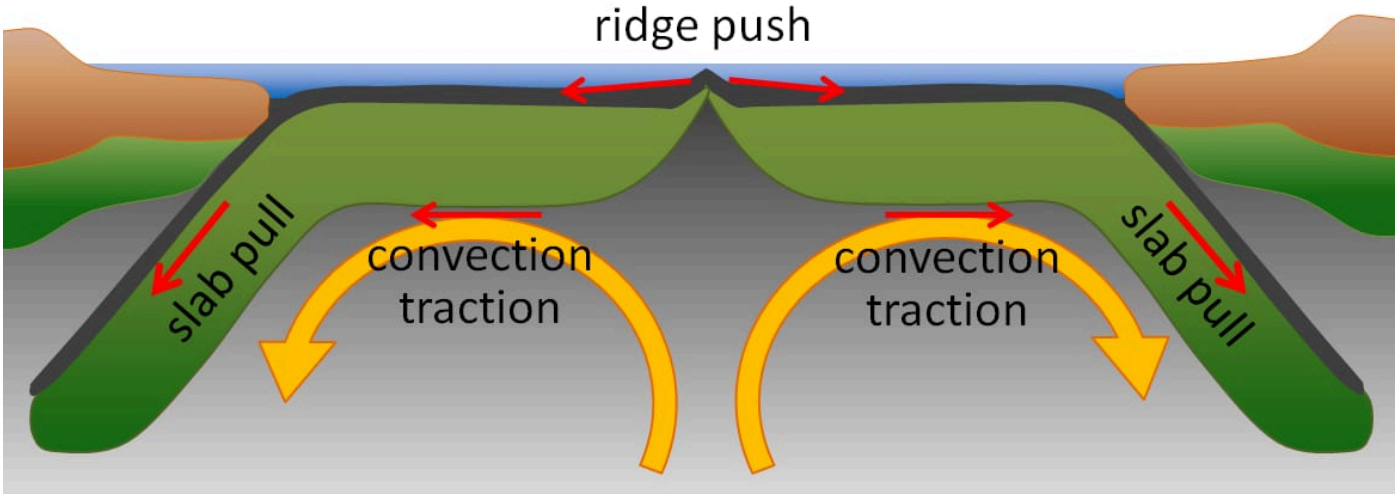


Figure 3.3.1: In this model, there are three forces working to move the plates. Ridge-push forces cause two plates to pull apart on the surface. Slab-pull forces pull the plates down. This movement of out and down is also encouraged by convection traction, or clockwise and counterclockwise currents that are present beneath the plates. Ridge-push by Steven Earle is licensed under CC BY 4.0.

Video 3.3.1: Plate Tectonics - What Drives the Plates? Overview of processes (educational)

Watch the following video to learn more about what drives plate motion:

This interactive element is not available in this format. Visit the link or scan the QR code to access it online.

View this YouTube Video online

Although ridge-push/slab-pull is the widely favored mechanism for plate motion, it's important not to underestimate the role of mantle convection. Without convection, there would be no ridges to push from because upward convection brings hot buoyant rock to the surface.

References

1. Kearey, P., & Vine, F. (1996). Global Tectonics (2nd E.). Oxford: Blackwell Science Ltd.

This page titled 3.3: Mechanisms for Plate Motion is shared under a CC BY-NC 4.0 license and was authored, remixed, and/or curated by Allison Jones.

3.4: California's Plates and Plate Boundaries

Where Plates Collide

The result of multiple moving lithospheric plates, California is home to not one, not two, but all three plate boundary types (Figure 3.4.1). The North American Plate which makes up the North American continent is moving to the southeast relative to its neighboring plates. The Pacific Plate which makes up the coastal regions of California and the Pacific Ocean is moving relatively northwestward. The Juan de Fuca and Gorda plates are small lithospheric plates west of the Cascadia subduction zone that are both moving eastward toward the North American Plate (see Klamath Mountains, Cascade Range, and Coast Ranges).

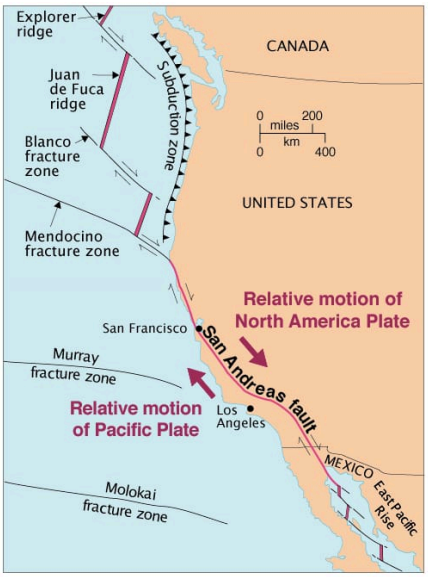


Figure 3.4.1: The Pacific Plate-North American Plate-Juan de Fuca plate boundaries. "San Andreas Fault and Plate Boundary Features of the U.S. West Coast" by the USGS is in the public domain. Access a detailed description.

California's Transform Boundaries: San Andreas and the Mendocino Fracture Zone

From the Mendocino Triple Junction to the Salton Trough exists one of the most famous plate boundaries on Earth: the San Andreas fault system. The San Andreas fault system is a transform plate boundary where the Pacific Plate is moving northwest relative to the North American plate (Figure 3.4.1). The motion within the system is right-lateral strike-slip faulting. Average slip rates along the entire fault system range from 20 to 35 mm per year (~8 to 14 inches/year).

The San Andreas fault system begins offshore of Cape Mendocino, at the Mendocino Triple junction, where the Juan de Fuca, North American, and Pacific plates meet. The northern segment of the system parallels the California coast from the Mendocino Triple Junction off Cape Mendocino southwest to Daly City, California. It then moves onshore through the Santa Cruz Mountains until it reaches Hollister, California.

The central segment of the San Andreas runs from Hollister to Parkfield, California. Unlike the northern and southern segments of the system, the central segment seldom has earthquakes and the motion on the system is mostly aseismic creep, or continuous slip.

The southern segment starts at Parkfield, runs through the Carrizo Plain on the west side of the Great Valley, and starts to curve near the San Gabriel Mountains from a northwest-southeast orientation to a west-northwest to east-southeast orientation. This area where the fault system changes its orientation is known as the “Big Bend” and is related to divergent plate motion occurring to the south as the East Pacific Rise moves onshore in the Salton Trough. This “Big Bend Region" is one of transpression, where both strike-slip motion and reverse faulting occur (Figure 3.4.2).

South of the “Big Bend,” the fault runs along the northern boundary of the San Gabriel Mountains, through Cajon Pass, along the southern boundary of the San Bernardino Mountains and the fault then ends near Bombay Beach, California. This is a transtensional area where the plate boundary is both transform and divergent (Figure 3.4.2). A system of faults continues south, moving offshore at the northern end of the Gulf of California, where it eventually meets the Rivera Triple junction, at the northern end of the East Pacific Rise.

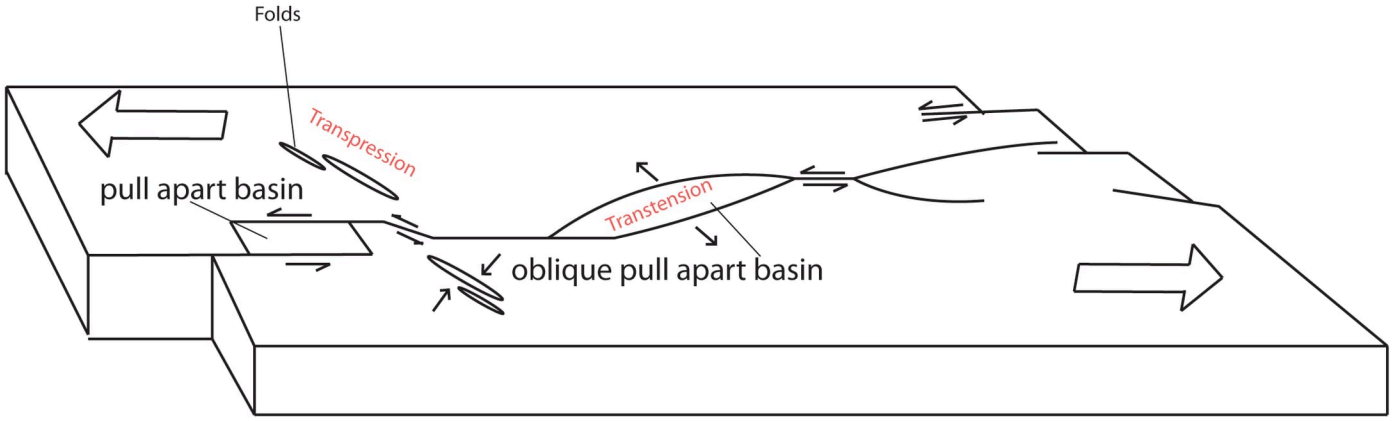


Figure 3.4.2: Transtension and transpression are both the result of bends in a fault. Transtension occurs where a bend creates an area of extension as well as transform. Transpression occurs where a bend creates an area of compression and transform. "Pull apart basin" by Wtbarron via Wikimedia Commons is licensed under CC BY-SA 3.0. Access a detailed description.

Geologically, the San Andreas fault system is relatively young and has only existed for approximately 30 Ma. For most of California today, the plate boundary is the San Andreas transform fault system between the Pacific plate and the North American plate. Prior to 30 Ma, the plate boundary was a subduction zone, where the Farallon plate was being subducted beneath the North American plate. On the other side of the Farallon plate, was a spreading ridge between the Farallon Plate and the Pacific plate. The eastern side of the Farallon plate was subducting under North America faster than new oceanic crust was being created at the spreading ridge with the Pacific plate. Eventually, the spreading ridge reached the subduction zone at an oblique angle (Figure 3.4.3 below). The relative motion between the Farallon plate and the North American plate was different from the relative motion between the Pacific plate and the North American plate. Thus, when the spreading ridge intersected western North America, a new relative motion and style of deformation formed and the San Andreas Fault system began.

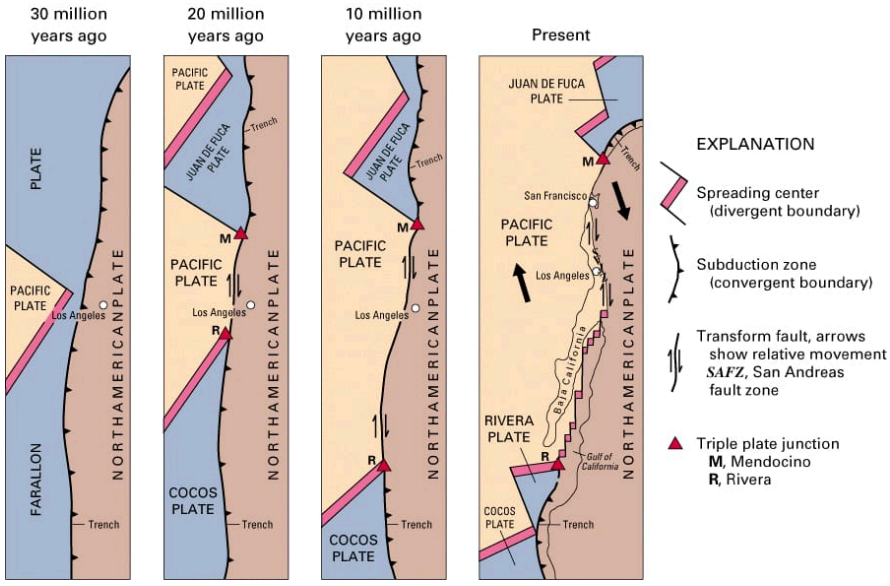


Figure 3.4.3: These four diagrams illustrate the shrinking of the formerly very large Farallon Plate, as it was consumed beneath the North American and Caribbean Plates. Present day, only the Juan de Fuca, Rivera, and Cocos plates remain (remnants of the Farallon Plate). Large solid arrows show the present-day sense of relative movement between the Pacific and North American Plates. "Tectonic Evolution of the West Coast Plate Boundary: 30 Million Years Ago to Present" by the USGS is in the public domain. Access a detailed description.

The San Andreas fault system has continued to lengthen over time. Remnants of the Farallon plate, now called the Juan de Fuca,

Rivera, and Cocos plates, are continuing to subduct north and south of the San Andreas.

Another Large Transform Boundary: The Mendocino Transform

The San Andreas Fault System is a well-known transform plate boundary in California, but it is not the only one impacting the state. The Mendocino Transform (sometimes called the Mendocino Fracture zone as in Figure 3.4.1) is another plate boundary offshore California that is capable of producing large earthquakes (such as a magnitude 7.2 earthquake in April of 1992). The Mendocino Transform is the fault segment which connects the offshore Juan de Fuca Ridge to the Mendocino Triple Junction. The Mendocino Triple Junction is therefore the intersection of two transform fault systems with a subduction zone. Even though this fault system is offshore of California, medium or large earthquakes occurring on it potentially could have as great an effect on northern California as earthquakes on the San Andreas system can have on central and southern California.

California's Convergent Boundary: Cascadia Subduction Zone

The Cascadia subduction zone, which is offshore of northern California, Oregon and Washington, is created by the subduction of the tiny Juan de Fuca Plate beneath North America (Figure 3.4.4). This ocean-continent convergent boundary is what creates the volcanoes of the Cascade Range. Notable volcanoes in this range include Mt. Rainier and Mt. Saint Helens in Washington (the latter of which, in 1980, famously produced the largest volcanic eruption in the contiguous United States of modern times), Mt Hood in Oregon, and Medicine Lake, Mount Shasta and Lassen Peak in California. Lassen Peak is famous for its 1915 eruption, which prior to 1980 was the only volcano to erupt in the contiguous United States since the formation of the United States.

Compared to the earthquake activity of the neighboring transform boundaries, and other subduction zones in the world, the Cascadia Subduction Zone has been relatively quiet; the most recent major Cascadia Subduction Zone earthquake was in 1700 A.D. That is not to say that it is not associated with significant earthquake risk. All the largest earthquakes in history are associated with subduction zones. Examples include the 2011 earthquake and associated tsunami in Japan in 2011 and the 2004 Indonesian earthquake and tsunami in the Indian Ocean. The Cascadia Subduction Zone has the potential for similar earthquakes and tsunamis.

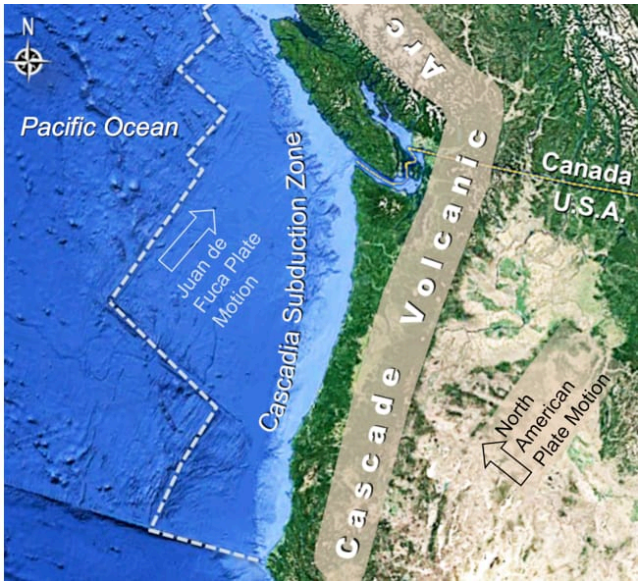


Figure 3.4.4: Cascade volcanic arc, a continental volcanic arc formed by the Juan de Fuca plate subducting beneath the North American plate. The North American plate is moving to the northwest while the Juan de Fuca plate moves to the northeast. The relative plate motion is convergent. "Cascade Volcanic Arc" by Karla Panchuk is licensed under CC BY-NC-SA. Access a detailed description.

California's Divergent Boundary: Salton Trough and Gulf of California

Between Baja California and mainland Mexico is the Gulf of California, which is the northern extension of the spreading ridge of the East Pacific Rise (Figure 3.4.5). This spreading ridge extends onshore through Mexico and into the Salton Trough of southern California, where the tectonic motion then transfers from extension to transform motion, transtension, on the San Andreas fault

system. This is different from the northern terminus of the San Andreas fault system which ends at the Mendocino triple junction.

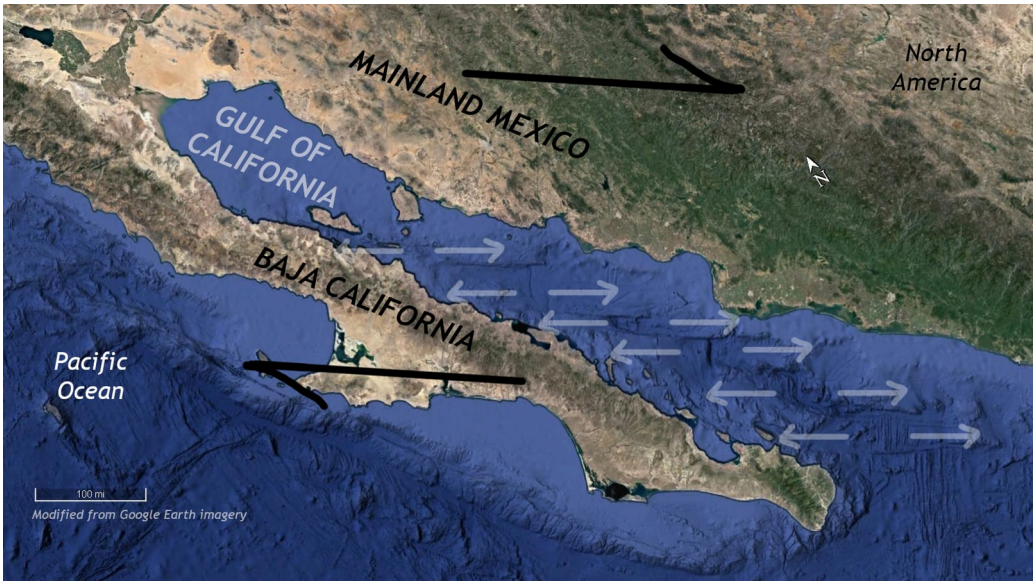


Figure 3.4.5: An aerial view of the Gulf of California with Baja California to the west and mainland Mexico to the east. The Gulf of California as well as the Salton Trough to the north are all an extension of the East Pacific Rise, a divergent boundary. "Divergence in the Gulf of California" by Callan Bentley is licensed under CC BY 4.0. Access a detailed description.

Video 3.4.1: Plate Tectonics and California Geology

For a concise summary of California's modern plate boundaries and their development, check out the following video:

This interactive element is not available in this format. Visit the link or scan the QR code to access it online.

View this YouTube Video online

Query 3.4.1

This interactive element is not available in this format. Visit the link or scan the QR code to access it online.

View this Interactive Content online

This page titled 3.4: California's Plates and Plate Boundaries is shared under a CC BY-NC 4.0 license and was authored, remixed, and/or curated by Allison Jones.

3.5: Chapter Summary

3.1 Earth's Interior

- Earth's interior can be described both by its composition and its physical properties.
- Earth's compositional layers include the crust (both continental and oceanic), the mantle, and the core.
- Continental crust is, on average, granitic in composition; oceanic crust is, on average, basaltic.
- Earth's mantle is made of ultramafic minerals.
- The core, though it has not been observed directly, is believed to be made of iron and nickle alloys.
- Mechanically, Earth can be divided into the rigid lithosphere, the flowing asthenosphere, the lower mantle (or mesosphere), the liquid outer core, and the solid inner core.

3.2 Tectonic Plates, Plate Motion, and Plate Boundaries

- The Earth's surface is made up of tectonic plates that are constantly moving. There are three types of plate boundaries: divergent, convergent, and transform.
- Divergent boundaries are where plates move apart. This creates new crust as magma rises from the mantle.
- Convergent boundaries are where plates move together. This can cause subduction, where one plate is pushed under the other, or collision, where the plates grind together.
- Transform boundaries are where plates slide past each other.
- The movement of tectonic plates is responsible for many of the Earth's features, such as mountains, oceans, volcanoes, and earthquakes. It is also thought to be responsible for the formation of supercontinents.

3.3 Mechanisms for Plate Motion

- While convection is believed to be part of reason for tectonic plate motion on Earth, it is driven by two other processes: ridge push and slab pull.
- Ridge push is the process by which boyant new crust forming at mid-ocean ridges apply a force on neighboring lithosphere.
- Slab pull is the result of old, cold oceanic crust subducting and pulling on the lithsphere behind it.

3.4 California's Plate Boundaries

- California is home to all three types of plate boundary types.
- Most famously is California's San Andreas fault system, which is a transform boundary between the North American plate and the Pacific plate.
- Lesser known, but more likely to produce large earthquakes is the Mendocino transform fault off the coast of California where the Pacific and Juan de Fuca/Gorda plates are sliding past one another.
- North of the Mendocino triple junction, convergence in the form of subduction is taking place. The Juan de Fuca/Gorda plate is subducting beneath the North American plate.
- In the Gulf of California, Baja California is actively rifting away from mainland Mexico, forming our very own divergent boundary.

This page titled 3.5: Chapter Summary is shared under a CC BY-NC 4.0 license and was authored, remixed, and/or curated by Allison Jones.

3.6: Detailed Figure Descriptions

Figure 3.1 Global Plate Boundaries and Plate Motion

This is a global map showing the major tectonic plates of Earth's lithosphere. This image is relevant in the context of California geology because the Pacific Plate and North American Plate boundary explains California's tectonic activity.

Major Tectonic Plates

- North American Plate – Covers most of North America, part of the Atlantic Ocean.
- Pacific Plate – Lies beneath the Pacific Ocean and borders the western edge of North America.
- Eurasian Plate – Encompasses Europe and much of Asia.
- African Plate – Covers the African continent and parts of the surrounding ocean floor.
- South American Plate – Includes South America and part of the Atlantic seafloor.
- Antarctic Plate – Includes and surrounds Antarctica.
- Indo-Australian Plates – Includes the Indian Plate and Australian Plate.
- Nazca Plate – Located west of South America.
- Cocos Plate – Located southwest of Central America.
- Juan de Fuca Plate – A small plate off the Pacific Northwest of North America.
- Caribbean Plate, Scotia Plate, Arabian Plate, and Filipino Plate are also shown.

Plate Boundaries and Movements

Arrows along the plate boundaries indicate the relative direction of plate motion to identify divergent, convergent, and transform plate boundaries, as listed here.

Divergent boundaries (arrows pointing away from each other) are shown between the following plates:

- North American and Eurasian plates, at the Mid-Atlantic Ridge, indicating seafloor spreading
- Antarctic and Australian plates
- Antarctic and Pacific plates
- Antarctic and African plates
- Nazca and Pacific plates
- Nazca and Cocos plates
- South American and African plates
- African and Arabian plates
- African and Indian plates

Convergent boundaries (arrows pointing toward each other) are shown between the following plates:

- Pacific and Australian plates
- Pacific and North American plates
- Nazca and South American plates
- Cocos and Caribbean plates
- Indian and Eurasian plates

Transform boundaries (arrows sliding past each other) are shown between the Pacific and North American plates (San Andreas Fault)

Figure 3.1.1 Compositional and Mechanical Layers of Earth's Interior

This diagram is a labeled cross-section of Earth's interior, showing two complementary ways of dividing Earth's internal structure:

- The left half represents the compositional (chemical) layers, based on chemical makeup.
- The right half illustrates the mechanical (physical) layers, based on physical properties and behavior.

Each section is color-coded and labeled, with boundary depths noted in kilometers. The Earth's full diameter is labeled as 12,742 km (7,917.5 miles), and the center is noted at 6,371 km depth.

Compositional Layers (Chemical) – Left Side

- Continental and Oceanic Crust: Thin, outermost layer; 100 km deep.
- Mantle: Thick layer beneath the crust composed of silicate minerals rich in iron and magnesium; extending from 100 to 2,900 km deep.
- Core: Deepest layer, composed primarily of iron and nickel, and extending from 2,900 km to the center (6,371 km).

Mechanical Layers (Physical) – Right Side

- Lithosphere: Rigid outer shell made up of the crust and the uppermost mantle. Extends to 100 km depth.
- Asthenosphere: Ductile, partially molten upper mantle layer beneath the lithosphere (100–350 km).
- Mesosphere: Strong, solid lower mantle extending from 350 km to 2,900 km deep.
- Outer Core: Liquid layer of molten iron and nickel, extending from 2,900 to 5,100 km.
- Inner Core: Solid central sphere composed mostly of iron, extending from 5,100 km to the center (6,371 km).

Figure 3.1.4 Seismic Wave Propagation in the Crust and Mantle

This diagram illustrates the paths and velocities of seismic waves generated by an earthquake, showing how they move through the crust and mantle of Earth's outer layers. A cross-sectional slice of Earth's outer shell is shown, with color gradients and labeled layers to show how wave speed and direction change at different depths. This visual information is described here.

Seismic Wave Source and Paths

- Seismic rays emanate from an earthquake epicenter in several directions, traveling upward directly through the crust, refracting at the crust-mantle boundary, and bending downward into the mantle, then curving back upward toward the surface.
- Two wave velocity paths are identified:
  - ~6 km/s in the crust (slower, upper path).
  - ~8 km/s in the mantle (faster, deeper path).

Wave Behavior

- Wave paths curve due to refraction, bending as seismic velocity increases with depth.
- The deeper path allows seismic waves to arrive at distant locations more quickly despite traveling farther.

Figure 3.2.2 Spreading Center

This geologic cross-section illustrates how new oceanic crust forms at a mid-ocean ridge. It depicts the layers of crust and mantle beneath the seafloor, the upward movement of magma, and the structure of the oceanic lithosphere. The image shows depth from the seafloor down to about 9 kilometers and a horizontal distance of about 20 kilometers across the ridge axis. (A tactile graphic, Mid Ocean Ridge, is available from the Geological Tactile Image Repository.)

Key Features (Top to Bottom)

- Seafloor Topography
  - A rift valley sits at the center, labeled "Plate boundary," where the seafloor is pulled apart.
  - On either side of the rift, layers of oceanic crust are shown, dipping away from the ridge axis.
- Oceanic Crust Layers
  - Pillow basalts: Green, lumpy structures near the seafloor, representing lava erupted underwater.

    - Sheeted dikes: Vertical dark bands that ferd lava to the surface.
    - Gabbro: Coarse-grained intrusive rock at deeper levels of the crust, crystallized from slowly cooling magma.
- Transition Zone between the crust and the underlying mantle
- Magma Chamber
    - Magma sits beneath the rift, feeding material into the crust above.
    - Wavy lines indicate the upward flow of magma toward the surface.
- Mantle
    - Beneath the crust and transition zone lies the mantle, which serves as the source of magma.

Scale and Orientation

- The vertical axis is labeled “Depth below sea surface (km)” and ranges from 0 to 9 km.
- The horizontal axis is labeled in kilometers, spanning from -10 to +10 km, centered on the ridge axis.
- The central black dashed line marks the plate boundary, with diverging arrows at the plate boundary indicating seafloor spreading.

Figure 3.2.3 Doming and Three-Part Rifts

A top-down view of a dome shows radial fractures that divide the dome into three sections. This represents how doming associated with formation of a mantle plume creates three-part rifts. A schematic showing the supercontinent Pangea breaking into the continents of Africa and South America shows conjoined successful rifts between the two new continents, created by mantle plumes. Noting that these plumes indicate three-part rifts, a single yellow lines radiates from each mantle plume to show a third, failed rift.

Box Figure 3.2.1.1 A Diagrammatic Passive Margin

This simplified diagram shows a passive margin along the western North American continent. From left to right we see the ocean depicted above a thin layer of sediment, which rests on a thicker oceanic crust above a still thicker mantle region. The middle of the diagram shows the sediments quickly increasing in thickness as the ocean layer thins. The oceanic crust gives way as the continental crust thrust upward, pushing the mantle downward. When we reach the right side of the diagram the ocean has receded and the continental crust takes up most of the vertical space. The continental crust exhibits a series of listric normal faults, shown as diagonal lines slanted in the general direction of the thrust. A very thin layer of sediment overlays the continental crust, and the mantle has thickened below it.

Figure 3.4.1 San Andreas Fault and Plate Boundary Features of the U.S. West Coast

This map displays tectonic features along the western edge of North America, from southern Canada through the United States and into northern Mexico. The focus is on transform and divergent plate boundaries and the relative motion between the Pacific Plate and the North American Plate.

Major Plate Boundaries

- The San Andreas Fault stretches through California, along the Mendocino fracture zone. This fracture zone is shown moving through the Pacific Ocean and along the California coast just above San Francisco, then moving inland at the San Francisco Bay. It then continues southward and inland from Los Angeles, moving through Mexico and into the Gulf of California.
- In Mexico, the East Pacific Rise runs north to south along the eastern shore of the Gulf of California.
- A subduction zone is shown north of the Mendocino fracture zone, moving through Oregon and Washington in the United States and terminating in the northern area of Vancouver Island in British Columbia (Canada).
- Further out to sea and running roughly parallel to the subduction zone, from north to south, we see Explorer Ridge, then Juan de Fuca Ridge, and finally the Blanco fracture zone (all north of the Mendocino fracture zone).

Plate Motion

- The North American Plate moves southeast in a relative motion
- The Pacific Plate moves northwest in a relative motion.
- Transform motion occurs along the San Andreas Fault, where the Pacific Plate slides past the North American Plate.

Several east-west trending fracture zones and north-south trending ridges are visible offshore, including (from north to south):

- Explorer Ridge
- Juan de Fuca Ridge
- Blanco Fracture Zone
- Mendocino Fracture Zone
- Murray Fracture Zone
- Molokai Fracture Zone

Figure 3.4.2 Transtension and transpression

A diagram showing plate boundaries along the San Andreas Fault is used illustrate the concepts of transpression and transtension. At the top of the diagram the plate motion is indicated as moving westward, while the plate motion at the bottom of the diagram moves eastward. At the left of the diagram we see a pull-apart basin indicated as a gap between the plates. Beginning just above this basin and then moving southeast across the fault line we see ovals indicating folds. Above the fault line the folds are labeled "transpression." Below of the fault line we see arrows indicating force moving against the the folds from two sides. Directly to the right of this region, we see an area on the fault when forces are pulling the plates apart. This is identified as an "oblique pull-apart basin," and is labeled "transtension."

Figure 3.4.3 Tectonic Evolution of the West Coast Plate Boundary: 30 Million Years Ago to Present

This four-panel image illustrates the tectonic evolution of the Pacific–North American plate boundary over time, from 30 million years ago to the present. It shows how the subduction of the Farallon Plate has been replaced by a transform boundary (the San Andreas Fault Zone) as new plates formed and spreading centers shifted.

30 Million Years Ago

- The Farallon Plate is subducting beneath the North American Plate at a long, continuous trench.
- The Pacific Plate is to the west of the Farallon Plate.
- A spreading center (divergent boundary) is shown along the southeast edge of the Pacific Plate.
- The San Andreas Fault has not yet formed.

20 Million Years Ago

- Two sections of the Pacific Plate come into view. The southmost section begins to subduct beneath the North American Plate in roughly the area where Los Angeles is located today. As it moves, it bisects the Farallon Plate, which becomes the Juan de Fuca Plate in the north and Cocos Plate in the south.
- Long trenches remain where the North American Plate abuts the Juan De Fuca and Cocos plates.
- Spreading centers (divergent boundaries) are shown along the southeast edges of the Pacific Plate where it meets the Juan De Fuca Plate in the north and the Cocos Plate in the south.
- Triple junctions are indicated where the Pacific Plate meets the North American Plate:
    - In the north, the Mendocino Triple Junction is where the Juan De Fuca, Pacific, and North American plates meet.
    - In the south, the Rivera Triple Junction is where the Cocos, Pacific, and North American plates meet.
    - A transform fault (early San Andreas Fault) has begun forming between the Pacific and North American plates, as the Pacific Plate moves in a northward direction and the North American Plate moves southward.

10 Million Years Ago

- As the Pacific Plate (moving northward) continues to subduct beneath the North American Plate (moving southward), the transform fault becomes longer. It stretches from roughly what is now Central California in the north to what is now Baja California in the south; accordingly, the distance between the Mendocino and Rivera triple junctions has increased dramatically.
- Trenches remain where the North American Plate abuts the Juan De Fuca and Cocos plates.
- Spreading centers (divergent boundaries) are shown along the southeast edges of the Pacific Plate where it meets the Juan De Fuca Plate in the north and the Cocos Plate in the south.

Present

- As the Pacific Plate slides northwest past the North American Plate, the San Andreas Fault is a dominant boundary feature. It now extends from the Mendocino Triple Junction north of San Francisco to the Rivera Triple Junction in the Gulf of California.
- The Juan de Fuca Plate is shown in the north, bordered by a trench along its south edge where it meets the North American Plate.
- The Rivera Plate now appears along the coast of Mexico, bounded on the east by the trench along the North American Plate. It is shown as a rough triangle with the Rivera Triple Junction as one of its points.
- The Cocos Plate still appears in the south, at the bottom of the map, bounded on the east by the trench along the North American Plate.
- Spreading centers (divergent boundaries) are still shown along the southeast edges of the Pacific Plate where it meets the Juan De Fuca Plate in the north, and where it meets the Rivera and Cocos plates in the south. However, additional divergent boundaries now appear along the San Andreas Fault from roughly its midpoint and moving south.

Figure 3.4.4 Cascade Volcanic Arc

This is a shaded-relief satellite map depicting the Pacific Northwest region of the United States and southwestern Canada. The map illustrates the tectonic setting responsible for the Cascade Volcanic Arc, emphasizing the Cascadia Subduction Zone off the coast of northern California and British Columbia, as well as the northeastern movement of the Juan de Fuca Plate and the dominant northwestern movement of the North American Plate.

- The rough texture in the Pacific Ocean represents oceanic crust.
- Cascadia Subduction Zone is where the Juan de Fuca Plate is subducting beneath the North American Plate. This is an irregularly shaped area bounded on the west by ridges that run along the ocean floor.
- The Cascade Volcanic Arc runs roughly north–south along the inland side of the subduction zone through Washington, Oregon, and northern California.

Figure 3.4.5 Divergence in the Gulf of California

This satellite-based map highlights tectonic motion in the Gulf of California region, illustrating how Baja California is moving northwestward relative to mainland Mexico. The map focuses on the rifting process that is forming an ocean basin between these landmasses.

Key Points:

- Mainland Mexico and North America are moving generally northeast.
- The Baja California peninsula is moving northwest, away from the mainland.
- Divergent motion is occurring beneath the Gulf of California, resulting in seafloor spreading and the extension of the crust between the two landmasses.
- These arrows alternate direction on either side of the central rift structures, highlighting the relative motion of crustal blocks.

This page titled 3.6: Detailed Figure Descriptions is shared under a CC BY-NC 4.0 license and was authored, remixed, and/or curated by Allison Jones.

4: GEOLOGIC STRUCTURES AND SEISMOLOGY

Introduction to Geologic Structures and Seismology

Since the arrival of Europeans, California has been a land famous for many things - moderate climate, good land for farming and ranching, giant trees along beautiful rugged coasts, gold and the hope of riches, home for movies and theme parks, great beaches and surfing, and of course, earthquakes. To the rest of the United States, the 1906 San Francisco Earthquake set the state apart, because most of the conterminous United States is not tectonically active and earthquakes rarely occur. Fires, floods, tornadoes and hurricanes were disasters that most Americans understood, but having the ground move and destroy a city was almost beyond comprehension.

Today, most Californians are awaiting some version of “The Big One,” the large earthquake that will someday either destroy Los Angeles, maybe San Francisco, or occur off the Northern California coast and sweep towns away in a giant tsunami. Such is daily existence in a tectonically active state where faulting and earthquakes are part of the background of life.

California is the only state with examples of all three types of plate boundaries: divergent, convergent, and transform. As a result, it has numerous active fault zones and the earthquakes associated with their movements. To understand the geology of California, it is necessary to understand the basics of faulting and earthquakes. The many hazards associated with earthquakes vary within the state and are addressed in Chapter 19.

Even though California may be known for its earthquakes, they are not the only type of deformation (any change in size, shape, or volume of the crust) that exist. Folds, with all their different types, also are evidence of how Earth’s surface can be deformed. So why sometimes do folds occur instead of faults? What is happening within Earth to cause deformation? That requires examination of the forces that can occur and learning which ones cause faults and which ones cause folds.

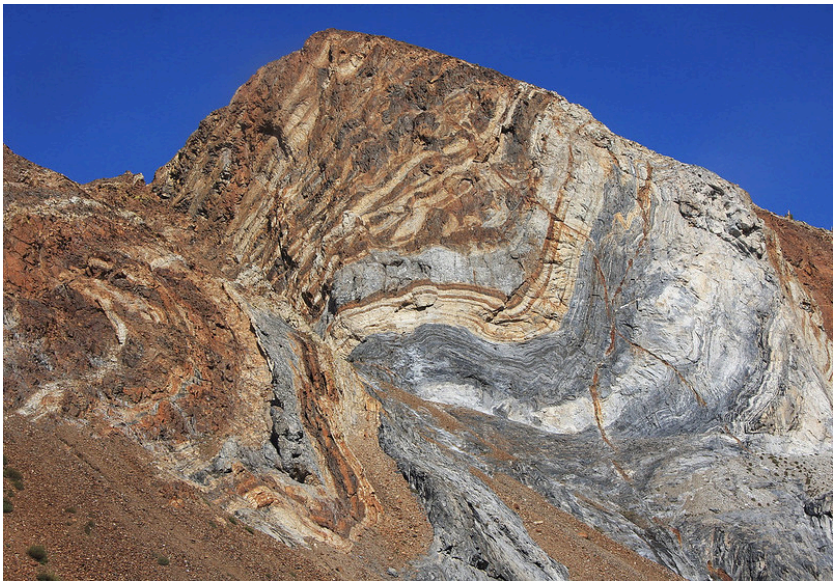


Figure 4.1: Folded rocks of Sevehah Cliff, looking north from the trail up Convict Canyon. John Muir Wilderness, Sierra Nevada, California. These rocks have experienced forces that caused them to buckle. "Sevehah Cliff" by Jane S. Richardson is licensed under CC BY.

Learning Objectives

By the end of this chapter, you should be able to:

- Differentiate between stress and strain.
- Illustrate how stresses in the crust lead to deformation in the forms of joints, faults, and folds.
- Define faulting, earthquakes, and the relationship between them.

- Describe the types of faults, the forces responsible for each, and the motion for each.
- Explain the relationship between epicenter and hypocenter.
- Describe the main types of seismic waves and their effects.
- Distinguish between earthquake intensity and magnitude.
- Explain why adapting to earthquakes is better than trying to predict them.

4.1: Stress and Strain
4.2: Folding
4.3: Jointing and Faulting
4.4: Earthquakes
4.5: Measuring Earthquakes
4.6: Chapter Summary
4.7: Detailed Figure Descriptions

This page titled 4: Geologic Structures and Seismology is shared under a CC BY-NC 4.0 license and was authored, remixed, and/or curated by Allison Jones.

4.1: Stress and Strain

Forces and Stress

Stress is a force distributed over an area. Rocks are subject to stress—mostly related to plate tectonics but also to the weight of overlying rock.

Stress can fall into two categories: normal stress, which acts at right angles to a surface, and shear stress, which acts parallel to a surface. Normal stress can be subdivided into compression, in which rock is squeezed, and tension, where rocks are being pulled apart. Where plates collide, rocks experience compression, and where plates diverge, rocks experience tension. Shear stress is common at transform plate boundaries where plates move side by side.

We can describe the stress applied to a rock by breaking it down into three dimensions—all at right angles to one-another (Figure 4.1.1). If the rock is subject only to the pressure of burial (the lithostatic stress), the stresses in all three directions will likely be the same. If it is subject to both burial and tectonic forces, the pressures will be different in different directions.

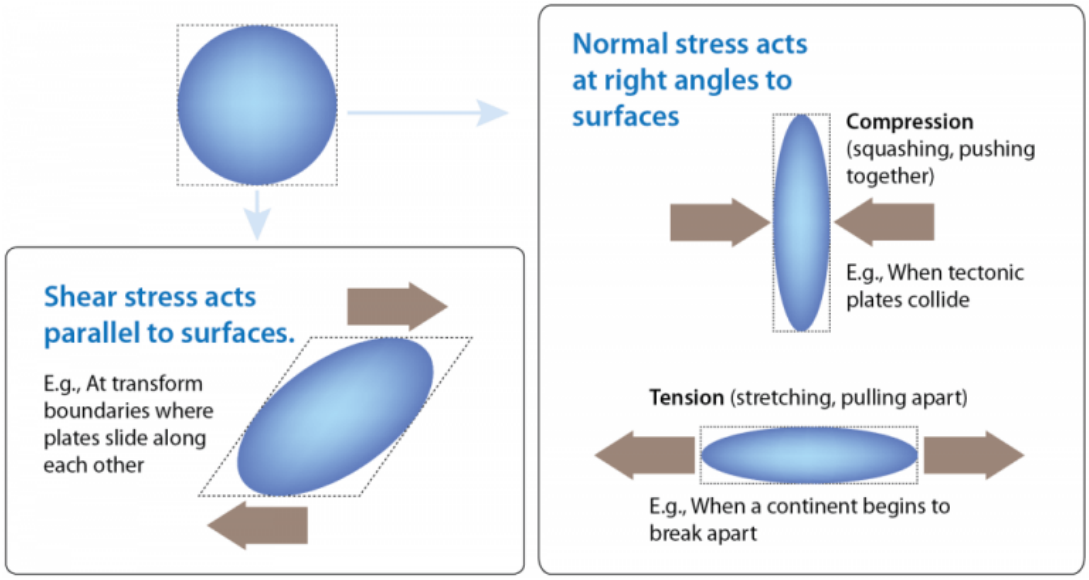


Figure 4.1.1: Shear stress acts parallel to surfaces, common at transform boundaries where plates slide past each other. Normal stresses act at right angles to surfaces and include compression, which occurs at convergent boundaries, and tension, which occurs in rifts and areas under extension. "Illustrations of Stress" by Karla Panchuk is licensed under CC BY 4.0. Access a detailed description.

Strain and Deformation

Rock's response to stress is called strain (deformation), but not all stress results in strain. Several factors influence how rocks respond to stress, including composition, physical properties, temperature, the amount and duration of stress, and the rate at which stress is applied.

Rock can respond to stress in three ways: it can deform elastically, deform plastically, or break (fracture) Figure 4.1.2. Elastic strain is reversible; if the stress is removed, the rock will return to its original shape, just like a rubber band that is stretched and released. However, plastic strain is not reversible. As already noted, different rocks at different temperatures will respond in different ways to stress. Higher temperatures generally lead to more plastic behavior. Some rocks or sediments respond more plastically when they are wet. Another factor is the rate at which the stress is applied. If the stress is applied quickly (for example, because of an extraterrestrial impact or an earthquake), rocks are more likely to fracture.

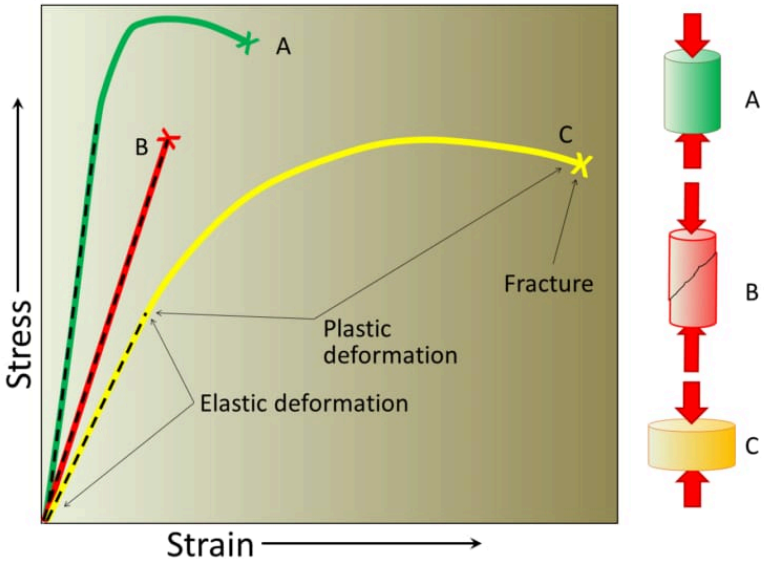


Figure 4.1.2: Responses of geological materials to stress. Dashed lines show elastic strain, curved lines show plastic strain, and X marks the fracture point. A deforms little and fractures at high stress. B is brittle, with no plastic deformation and fractures after minimal elastic strain. C deforms the most, fracturing after significant elastic and plastic strain. Diagrams on the right show A and C before breaking, and B after breaking. "Responses of Geological Materials" by Steven Earle is licensed under CC BY 4.0. Access a detailed description.

The response from placing rock under stress is highly variable. The rock might fracture or break without significant movement of either side of the rock. Fracturing is particularly common in volcanic rock, which shrinks as it cools. Sometimes there is significant movement and faulting can occur (Figure 4.1.3).



Figure 4.1.3: This fence at Point Reyes National Seashore was laterally offset during the 1906 San Francisco earthquake. The original fence has been replaced but in the same location. "1906 Earthquake - Offset Fence" by Dave Schumaker via Flickr is licensed under CC BY-NC-ND.

Rocks are sometimes stretched or squeezed, tilted, or even folded (Figure 4.1.4). The varieties of deformation that can occur when a rock is under stress can be truly amazing.



Figure 4.1.4: A syncline in California's Mojave Desert. Synclines are folds where the limbs dip inward toward the center of the fold. Here, the youngest rocks are near the top and center of the fold. "Barstow Syncline" by Allison Jones is licensed under CC BY 4.0.

Measuring Deformation

Much like crime scene investigation, unraveling deformation in rocks helps us understand the geological history of a region. For this reason, it is important for geologists to quantify deformation by measuring the orientations of geological features. One of the key features to measure is the orientation of bedding. Sedimentary beds are deposited in horizontal layers, so if the layers are no longer horizontal, then we can infer that they have been affected by tectonic forces and have become either tilted, or folded. The orientation of a bed (or any other planar feature) can be expressed with two measurements: first, the compass orientation of a horizontal line on the surface—the strike—and second, the angle at which the surface dips below a horizontal plane —the dip (Figure 4.1.5). Dip is measured in a plane perpendicular or at a right angle to the strike.

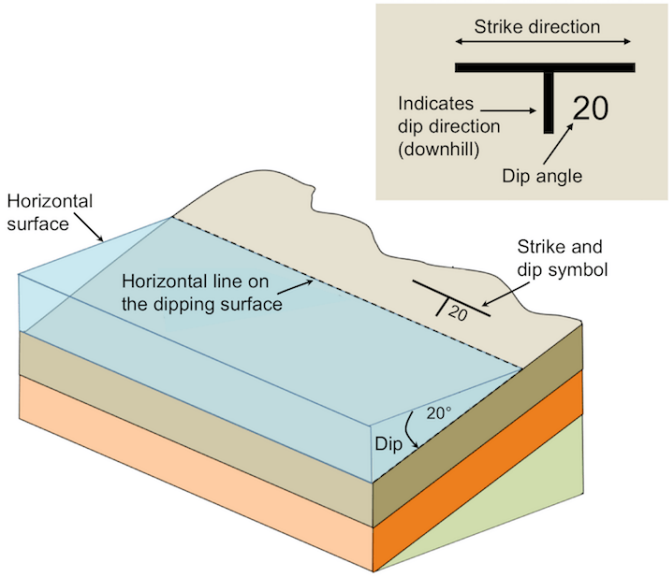


Figure 4.1.5: Strike and dip for tilted sedimentary beds. Water provides a horizontal surface. The strike and dip symbol is a T with the long horizontal bar representing the strike direction, and the small tick mark indicating the dip direction. The dip angle is written next to the tick mark. "Strike and Dip Map Symbols" by Karla Panchuk, a derivative of "Strike and Dip", is licensed under CC BY 4.0. Access a detailed description.

To better understand strike and dip, it may help to imagine a vertical surface, such as a wall in your house. The strike is the compass orientation of the wall and the dip is 90° from horizontal. If you could push the wall so that it is leaning over, but still

attached to the floor, the strike direction would be the same, but the dip angle would be less than 90°. If you pushed the wall over completely so it was lying on the floor, it would no longer have a strike direction and its dip would be 0°. When describing the dip it is important to include the direction. In other words. if the strike is 0° (i.e., north) and the dip is 30°, it would be necessary to say “to the west” or “to the east.” Similarly if the strike is 45° (i.e., northeast) and the dip is 60°, it would be necessary to say “to the northwest” or “to the southeast.”

Strike and dip are also used to describe any other planar geological features, including joints (fractures without displacement) and faults (fractures with displacement; see Jointing and Faulting). Strike and dip are just two of the many measurements geologists record on maps to show structural relationships. You can find more information on strike and dip and other features and measurements that appear on geologic maps in the Appendix. Figure 4.1.6 shows an example of how to depict the beds that make up an antiform fold on a map.

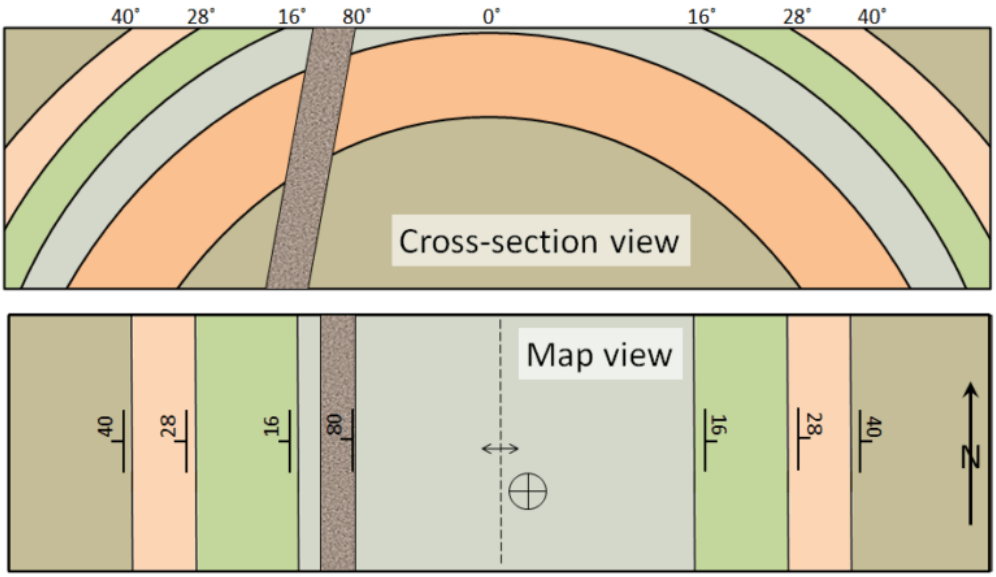


Figure 4.1.6: Cross section (top) and map (bottom) showing rock layers folded into an anticline (convex up fold). North is at the top of the map, with strike and dip symbols indicated. An igneous dike dips 80 degrees to the west. See text for detailed descriptions of the cross-section and map. "Cross-section to Map" by Steven Earle is licensed under CC BY 4.0.

The beds on the west (left) side of the map are dipping at various angles to the west. The beds on the east side are dipping to the east. The middle bed (light gray) is horizontal; this is denoted by a cross within a circle. The igneous intrusion is dipping at 80° to the west.

Query 4.1.1

This interactive element is not available in this format. Visit the link or scan the QR code to access it online.

View this Interactive Content online

This page titled 4.1: Stress and Strain is shared under a CC BY-NC 4.0 license and was authored, remixed, and/or curated by Allison Jones.

4.2: Folding

Anticlines, Synclines, and Monoclines

When a body of rock, especially sedimentary rock, is squeezed from the sides by tectonic forces, it may either bend or break. If the rock is cold and brittle, it is more likely to fracture and form joints or faults. If it is warm enough to behave plastically, it may fold.

An anticline is a fold that is convex upward, whose core contains relatively older rock (Figure 4.2.1). If the ages of the folded rocks are unknown, then the fold is called an antiform. A syncline is a fold that is convex downward, whose core contains relatively younger rock (Figure 4.2.2). If the ages of the folded rocks are unknown, then the fold is called a synform.

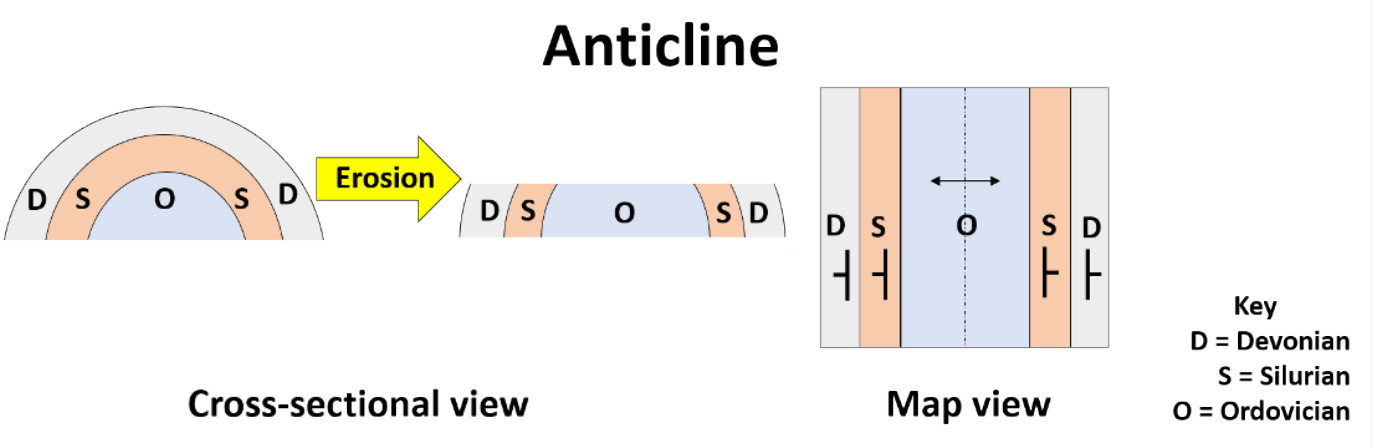


Figure 4.2.1: An anticline in cross-sectional view (left) and map view (right). The beds are convex upward. O = Ordovician, S = Silurian, D = Devonian. The youngest rocks are in the center of the fold. "Anticline" by Chloe Branciforte is licensed under CC BY 4.0. Access a detailed description.

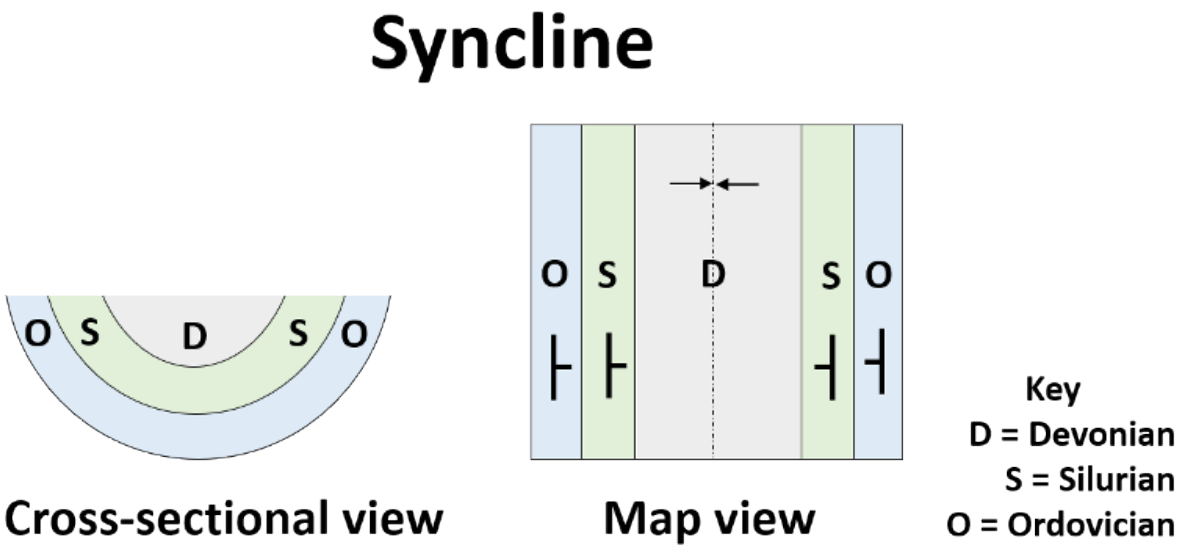


Figure 4.2.2: A syncline in cross-sectional view (left) and map view (right). The beds are convex downward in a "U" shape. O = Ordovician, S = Silurian, D = Devonian. The youngest rocks are in the center of the fold. "Syncline" by Chloe Branciforte is licensed under CC BY 4.0. Access a detailed description.

It is common to find a series of antiforms and synforms, although some sequences of rocks are folded into a single antiform or synform. A plane drawn through the crest of a fold in a series of beds is called the axial plane or axial surface of the fold (Figure

4.2.3). The sloping beds on either side of an axial plane are limbs. An antiform or synform is described as symmetrical if the angles between each limb and the axial plane are generally similar, and asymmetrical if they are not. If the axial plane is sufficiently tilted that the beds on one side have been tilted past vertical, the fold is known as an overturned antiform or synform.

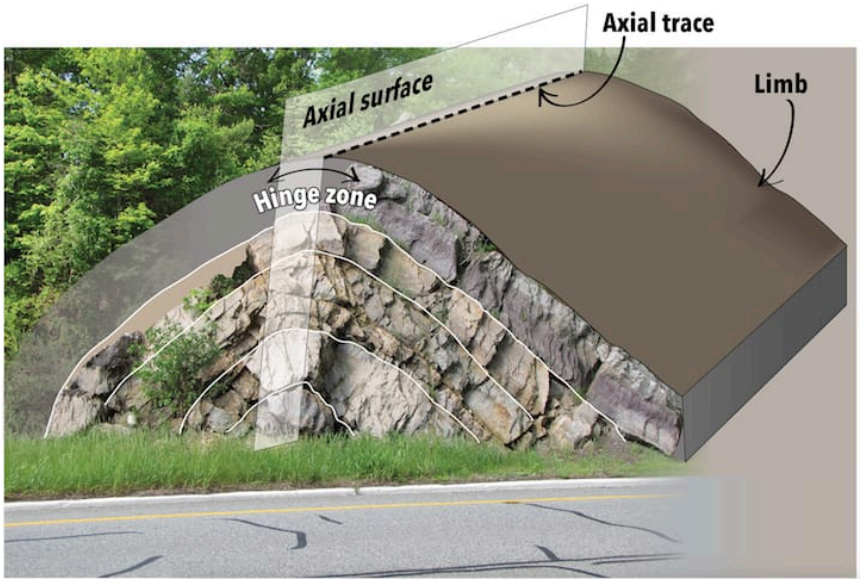


Figure 4.2.3: A fold consists of limbs that meet at the hinge zone. An axial surface bisects the fold along the hinge zone. The axial trace is where the axial surface intersects another surface, called a limb. "Labeled Antiform" by Karla Panchuk is licensed under CC BY-NC-SA 4.0.

A monocline is a step-like fold in rock strata, where horizontal or gently dipping layers transition to a zone of steeper dip (Figure 4.2.4). Monoclines are often caused by deformation from the movement on a fault beneath the folded layers.

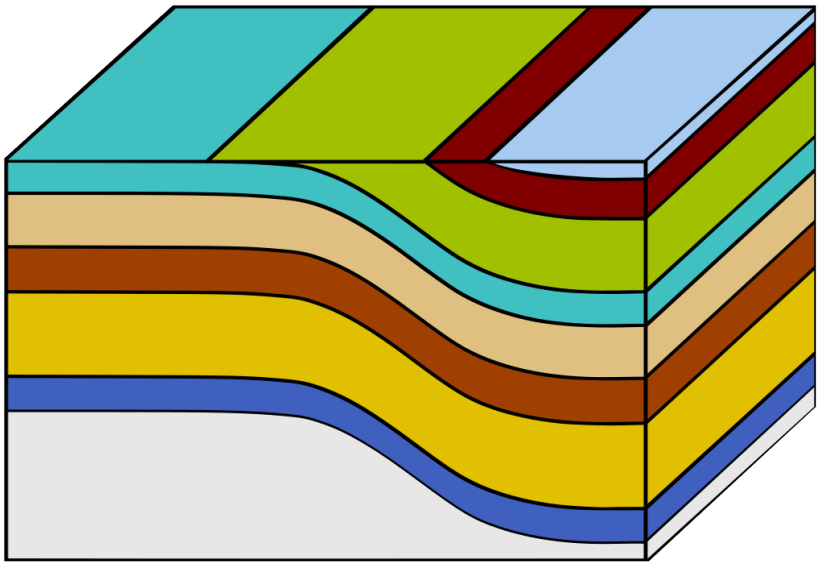


Figure 4.2.4: A block diagram of a monocline fold with horizontal or near-horizontal beds and a region of more steeply dipping beds in the center. "Monocline01.svg" by Kilom691 via Wikimedia Commons is licensed under CC BY-SA 3.0.

Describing Simple Folds

The tightness, or angle between the limbs of a fold (known as the interlimb angle), can range from gentle, with a large angle between limbs, to parallel or nearly parallel (Figure 4.2.5). This very tight fold is called an isoclinal fold.

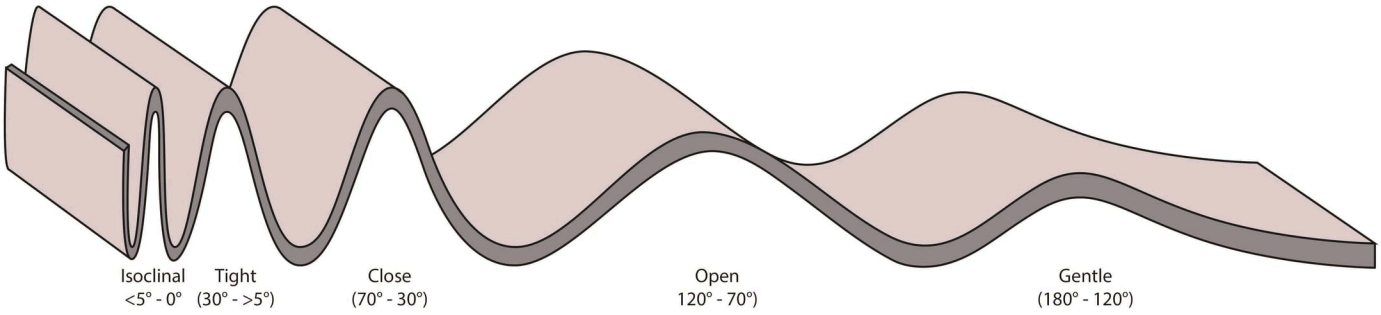


Figure 4.2.5: The angle between the limbs of the fold can be described as isoclinal (<5°), tight (5°-30°), close (30°-70°), open (70°-120°), or gentle (120°-180°). "Interlimb angles.jpg" by Alejandro Guevara Alday is licensed under CC BY-SA 4.0.

The orientation of a fold's axial plane can also vary. An upright fold is one which has a vertical axial plane. If that axial plane is horizontal, we call the fold recumbent. Any angle in between is considered inclined.

You can also describe the orientation of the fold hinge, or line of maximum curvature. If this line is horizontal then again, you have an upright fold. However, if that hinge line is in an orientation other than horizontal, the fold is considered "plunging". Plunging folds create map patterns that look like the letter V (Figure 4.2.6). In a plunging anticline, the oldest strata can be found at the center of the V, and the V points in the direction of the plunge of the fold axis. In a plunging syncline, the youngest strata are found at the center of the V, and the V points in the opposite direction of the plunge of the fold axis.

Folds can be of any size, and it is very common to have smaller folds within larger folds. Large folds can have wavelengths of tens of kilometers, and very small ones might be visible only under a microscope.

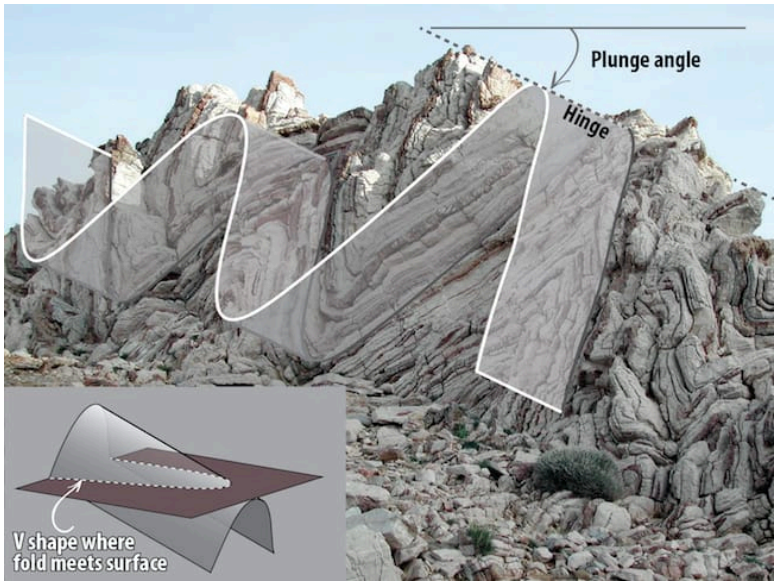


Figure 4.2.6: Plunging folds have hinges that are not horizontal, described by the plunge angle—the angle the hinge makes with a horizontal line. When a plunging fold intersects Earth's surface, it creates a V-shaped pattern. "Plunging Folds" by Karla Panchuk is licensed under CC BY-SA 4.0.

Domes and Basins

A dome is a symmetrical or semi-symmetrical upwarping of rock layers, shaped like an inverted bowl, similar to an architectural dome on a building.

A basin is the inverse of a dome, a bowl-shaped depression in rock strata. Some structural basins are also sedimentary basins,collecting large quantities of sediment over time. While sedimentary basins can form from folding, they are more commonly created during mountain building, forming between mountain blocks or through faulting. As the basin subsides, it can accumulate more sediment, with the added weight causing further subsidence in a positive feedback loop.

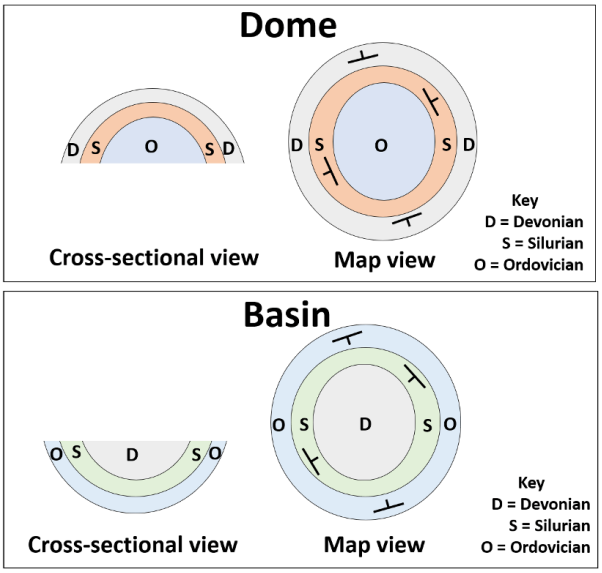


Figure 4.2.7: O = Ordovician, S = Silurian, D = Devonian. A dome (top) has the oldest units at the center. Beds dip out and away from the center in all directions. A structural basin (bottom) has the oldest units on the outside. Beds dip in toward the center. "Complex Folds" by Chloe Branciforte is licensed under CC BY 4.0. Access a detailed description.

Query 4.2.1

This interactive element is not available in this format. Visit the link or scan the QR code to access it online.

View this Interactive Content online

Economical Significance of Antiforms and Domes

Antiforms and domes (described below) are particularly favorable locations for oil and natural gas to collect. It is estimated that about 80 percent of the world's petroleum is found in these anticlinal traps, and California is no different Because of the low density of petroleum, oil migrates upward out of the source rock until it becomes trapped by an impermeable surface.

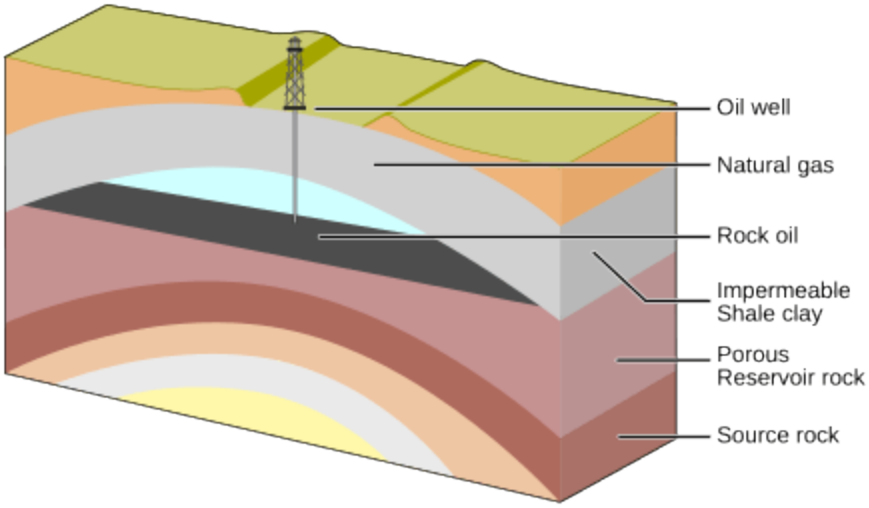


Figure 4.2.8: Antiforms make excellent petroleum traps. Buoyant oil and natural gas make their way upward until they reach an impermeable layer and become trapped. "Anticline trap.svg" by MagentaGreen via Wikimedia Commons is licensed under CC BY-SA 3.0. Access a detailed description.

References

1. Riva, Joseph P. "Accumulation in reservoir beds". *Encyclopædia Britannica*. Retrieved December 10, 2015.
2. Branciforte, Haddad. GEOS: A Physical Geology Lab Manual for California Community Colleges.

This page titled 4.2: Folding is shared under a CC BY-NC 4.0 license and was authored, remixed, and/or curated by Allison Jones.

4.3: Jointing and Faulting

Brittle Deformation

A body of rock that is brittle—either because it is cold or because of its composition, or both— is likely to break rather than fold when subjected to stress, and the result is jointing or faulting.

Jointing

A joint is a fracture in a rock in which no displacement or side-to-side movement has occurred. Most joints form where a body of rock is expanding because of reduced pressure, which is the case of Half Dome in Yosemite National Park (Figure 4.3.1). Joints can also form where the rock itself is contracting but the body of rock remains the same size (the cooling volcanic rock in (Figure 4.3.2). In all of these cases, the pressure regime is one of tension as opposed to compression.



Figure 4.3.1: Exfoliation joints, sometimes called “sheeting”, on Half Dome in Yosemite National Park. “Half dome Yosemite” by Saibo via Wikimedia Commons is licensed under CC BY-SA 3.0.



Figure 4.3.2: Polygonal fractures at Devil's Postpile in the eastern Sierra Nevada. This jointing pattern formed during the cooling and shrinking of the lava. "Devil's Postpile" by Jared Sneed via Flickr is licensed under CC BY-NC.

Joints can also develop when rock is under compression as shown on Figure 4.3.3, where there is differential stress on the rock, and joint sets develop at angles to the compression directions.

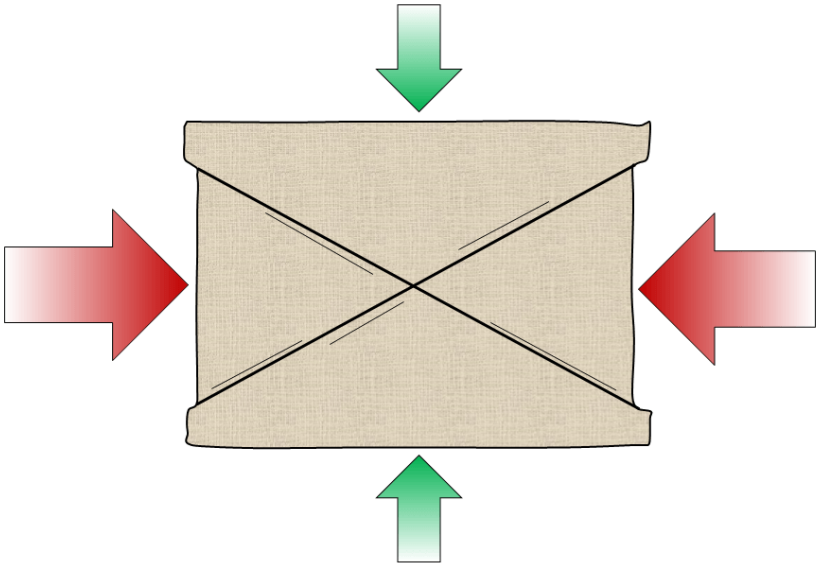


Figure 4.3.3: Joints developed in a rock under compressive stresses. "Joints developed in a rock" by Steven Earle is licensed under CC BY 4.0.

Faulting

A fault is a boundary between two bodies of rock along which there has been relative motion. An earthquake occurs when one body of rock slides past another. Earthquakes don't always happen on existing faults, but once an earthquake occurs, a fault will form at that location. Some large faults, like the San Andreas Fault in California, show evidence of hundreds of kilometers of movement, while others show less than a millimeter. In order to estimate the amount of motion on a fault, we need to find some geological feature that shows up on both sides and has been offset (Figure 4.3.4).



Figure 4.3.4: The San Andreas Fault exposed in the Carrizo Plain. Streams which once flowed uninterrupted straight across the fault are now displaced by the fault, taking a step to the right, illustrating the right-lateral movement the fault has experienced. "2018_01_23_sba-188-sba_107" by Doc Searls via Flickr is licensed under CC BY 2.0.

There are several kinds of faults and they develop under different stress conditions. The terms hanging wall and footwall apply to situations where the fault is not vertical. The body of rock above the fault is called the hanging wall, and the body of rock below it is called the footwall (Figure 4.3.5). When a fault is vertical, there is no obvious hanging wall or footwall. Hanging wall and footwall are mining terminology. Many mines are in fault zones. When a miner is walking within an adit, or horizontal tunnel within the Earth, their feet are on one side of the fault, the footwall, and their head could bump on the other side of the fault, the hanging wall.

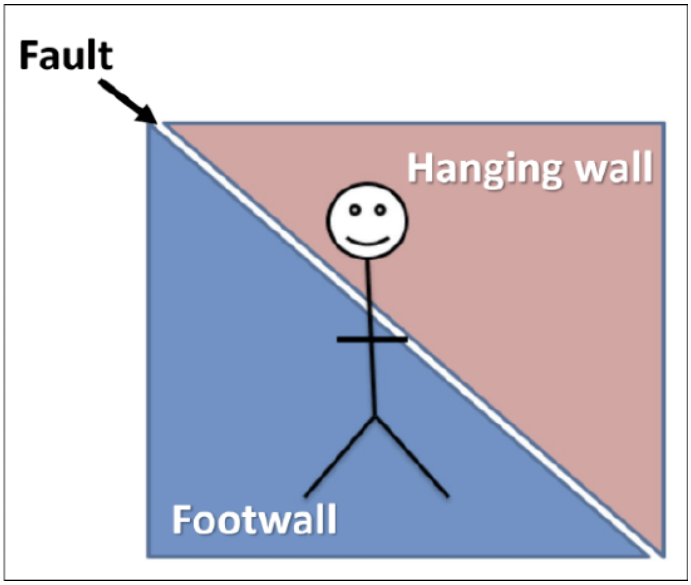


Figure 4.3.5: A cross section of a dip slip fault. The hanging wall is the upper block and the footwall is the lower block. "Dip-Slip Faults" by Chloe Branciforte, a derivative of "Footwall/Hanging Wall", is licensed under CC BY-SA 3.0.

Dip-Slip Faults

A dip-slip fault is a fault which moves in the dip direction of the fault plane. In other words, the hanging wall is moving up or down relative to the footwall.

Normal faults are dip slip faults in which the hanging wall moves down relative to the footwall. Normal faults are created by

extension of the crust and commonly occur at divergent plate boundaries, where the crust is being stretched.

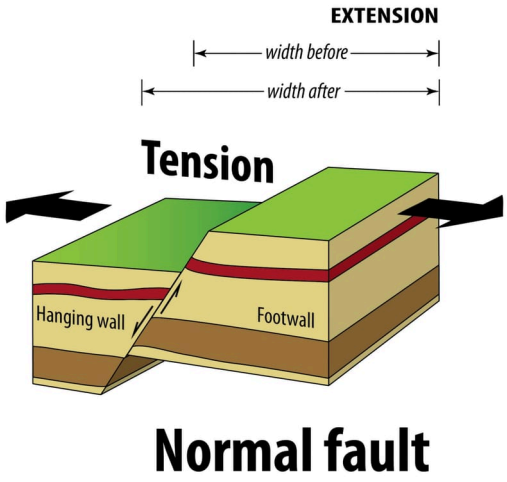


Figure 4.3.6: A normal fault forms where the hanging wall has dropped down relative to the footwall. The lateral tension caused by a normal fault results in extension and overall thinning of the crust. "Normal Fault" by Allison Jones, a derivative of "What Causes Dip-slip Faults?", is licensed under CC BY-SA 4.0.

3D Model of a Normal Fault

The following 3D model is of a normal fault. As shown in this model, the hanging wall moves downward as the footwall moves upward. The area of the hanging wall that is left exposed is called the "scarp."

This interactive element is not available in this format. Visit the link or scan the QR code to access it online.

View this Interactive Content online

"Normal fault" by paulinkenbrandt via Sketchfab is licensed under CC BY 4.0.

Video 4.3.1: Normal fault

The following video illustrates the formation of a normal fault. There is no audio, but the the animation shows the process that has been described in the text. In a normal fault, the block above the fault (the hanging wall) moves down relative to the block below the fault (the foot wall), exposing the fault plane. This fault motion (earthquake) is caused by extensional forces and results in lengthening.

This interactive element is not available in this format. Visit the link or scan the QR code to access it online.

View this YouTube Video online

Normal faults are very common in both the Basin and Range and Mojave Desert provinces of California where the crust is

undergoing extension. In these locations, the crust is being pulled apart, which can result in down dropped blocks known as grabens and raised blocks called horsts.

Reverse and thrust faults are created by compressional forces within the crust. In both reverse and thrust faults the hanging wall moves up relative to the footwall. Thrust faults are a particular type of reverse fault that is dipping at a very low angle (<30°). Often, thrust faults underlie other structural features like anticlines (Figure 4.3.7).

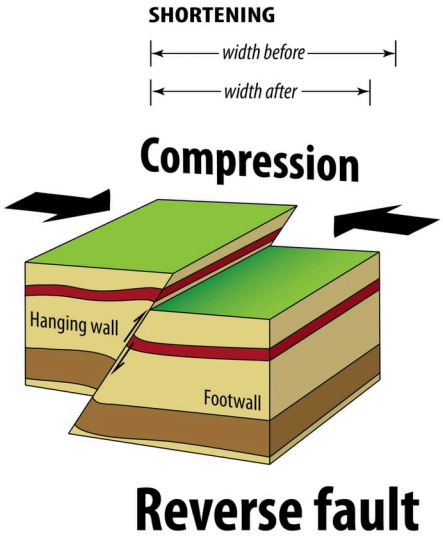


Figure 4.3.7: Reverse faults form when the hanging wall has moved up relative to the footwall, due to compression forces. They result in shortening and thickening of the crust. "Reverse Fault" by Allison Jones, a derivative of "What Causes Dip-slip Faults?", is licensed under CC BY-SA 4.0.

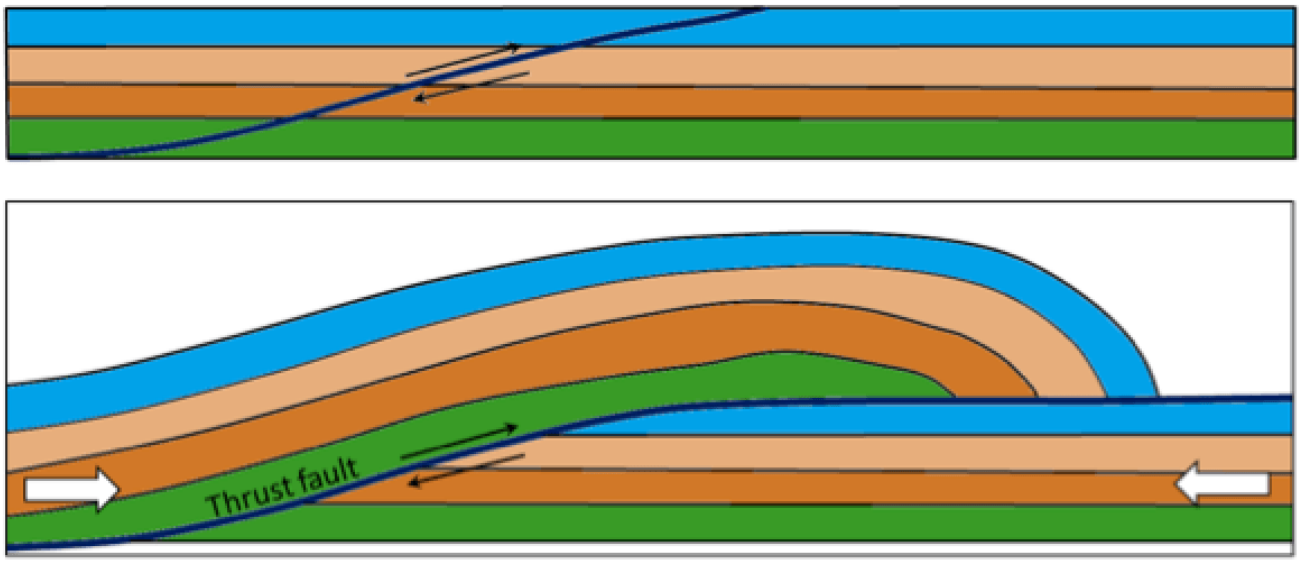


Figure 4.3.8: A thrust fault. Top: Before faulting, strata are continuous. Bottom: After faulting and significant offset, strata are thrust up and over each other, creating a repeating sequence. "Thrust Fault Deformation" by Steven Earle is licensed under CC BY 4.0.

Reverse faults, thrust faults, and compressional forces commonly occur at convergent plate boundaries, where the crust is either overlapping at subduction zones or colliding at continent-continent collisions. Reverse and thrust faults are common in the Transverse Ranges and parts of the Coast Range provinces of California where the crust is actively experiencing compression.

3D Model of a Reverse Fault

The following 3D model is of a reverse fault that shows how the hanging wall has moved up relative to the footwall. The exposed area of the hanging wall is called the "scarp."

This interactive element is not available in this format. Visit the link or scan the QR code to access it online.

View this Interactive Content online

"Reverse Fault" by paulinkenbrandt via Sketchfab is licensed under CC BY.

3D Model of a Thrust Fault

The following 3D model is of a thrust fault. Like a reverse fault, the hanging wall has moved up relative to the footwall, however the fault is dipping at a much shallower angle.

This interactive element is not available in this format. Visit the link or scan the QR code to access it online.

View this Interactive Content online

"Thrust Fault" by paulinkenbrandt via Sketchfab is licensed under CC BY.

Video 4.3.2: Reverse fault

The following video illustrates the formation of a reverse fault. There is no audio, but the the animation shows the process that has been described in the text. In a reverse fault, the block above the fault (the hanging wall) moves up relative to the block below the fault (the foot wall). This fault motion (earthquake) is caused by compressional forces and results in shortening. A reverse fault is called a *thrust fault* if the dip of the fault plane is small.

This interactive element is not available in this format. Visit the link or scan the QR code to access it online.

View this YouTube Video online

Strike-Slip Faults

Strike-slip faults (Figure 4.3.9) are created by shear stresses within the crust. They commonly occur at transform plate boundaries: the San Andreas fault zone of California is a transform plate boundary between the Pacific and the North American plates that consists of a system of strike-slip faults.

Strike-slip faulting is common in the Peninsular Ranges province of southern California and the Coast Ranges province of central California, where many faults are parallel to the orientation of the San Andreas fault zone. Strike-slip faults move with mostly

horizontal motion and typically are vertical or near vertical and thus do not have hanging walls or footwalls. These faults are named strike-slip because the direction of motion or slip is along the line of their strike.

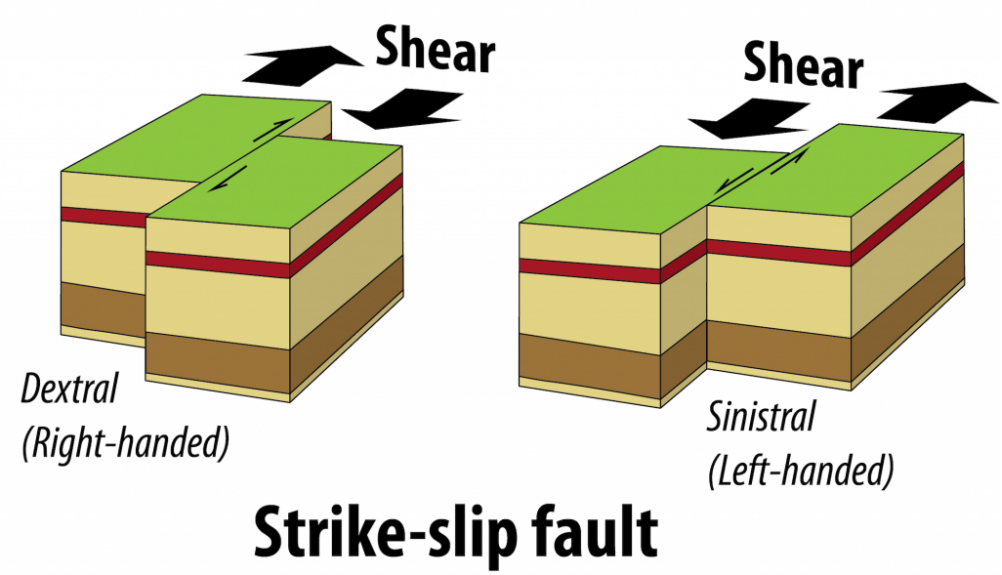


Figure 4.3.9: Strike-slip faults. Rocks on either side of the fault move parallel to the fault. In dextral (right-lateral) strike-slip faults the far side moves to the right of the observer. In sinistral (left-lateral) strike-slip faults the far side moves to the left of the observer. "Types of Strike-slip Faults" by Karla Panchuk is licensed under CC BY 4.0.

3D Model of a Strike Slip Fault

The following 3D model is of a strike-slip fault where the two fault blocks are moving past one another. In this example, the far side has moved to the right of the observer, indicating that it is a right-lateral strike-slip fault.

This interactive element is not available in this format. Visit the link or scan the QR code to access it online.

View this Interactive Content online

"Strike Slip" by paulinkenbrandt via Sketchfab is licensed under CC BY.

Video 4.3.3: Strike-slip fault

The following video illustrates the formation of a strike-slip fault. There is no audio, but the the animation shows the process that has been described in the text. In a strike-slip fault, the movement of blocks along a fault is horizontal. If the block on the far side of the fault moves to the left, as shown in this animation, the fault is called left-lateral. If the block on the far side moves to the right, the fault is called right-lateral. The fault motion (earthquake) of a strike-slip fault is caused by shearing forces.

This interactive element is not available in this format. Visit the link or scan the QR code to access it online.

View this YouTube Video online

Oblique Slip Faults

It is not uncommon for faults to have components of both strike-slip and dip slip. If that is the case, the fault is said to have oblique slip. The Corona Heights fault in San Francisco has experienced both strike-slip and dip-slip motion. We can tell because the fault is covered in slickenside surfaces, surfaces that indicate the direction of slip on the fault either with slickenlines, grooves in the surface of the fault, or slickenfibers, mineral fibers that have grown in the direction of fault slip. The slickenlines here indicate that the block to the left has moved relatively up and away from where the photographer is standing in Figure 4.3.10.



Figure 4.3.10: Slickenside covered Corona Heights fault in San Francisco. The hanging wall is the block to the left and the footwall is the ground on which the photographer is standing. "Corona Heights Fault" by Allison Jones is licensed under CC BY 4.0.

Interactive Content

This interactive element is not available in this format. Visit the link or scan the QR code to access it online.

View this Interactive Content online

References

1. Earle, S. (2019). *Physical Geology – 2nd Edition*. Victoria, B.C.: BCcampus. Retrieved from https://opentextbc.ca/physicalgeology2ed March 2024

This page titled 4.3: Jointing and Faulting is shared under a CC BY-NC 4.0 license and was authored, remixed, and/or curated by Allison Jones.

4.4: Earthquakes

What Was That? Was That an Earthquake?

“What was that?” is one of the questions heard most often when a small earthquake occurs; the other is “Was that an earthquake?” Fortunately, most people live their lives without ever experiencing the ground becoming mobile beneath them, but not in California. California is one of the most seismically active areas on Earth because the entire length of the state is relatively near, if not actually on some type of plate boundary. Plate boundaries are basically just large fault zones that allow two plates to move by one another (see Tectonic Plates, Plate Motions, and Plate Boundaries).

Earthquakes can occur anywhere the Earth is deforming, but most medium to large earthquakes happen at or near plate boundaries. As shown in Figure 4.4.1, the largest earthquakes, with magnitudes greater than 9, occur at subduction zones. An example of a subduction zone in California is the Cascadia Subduction Zone in northern California.

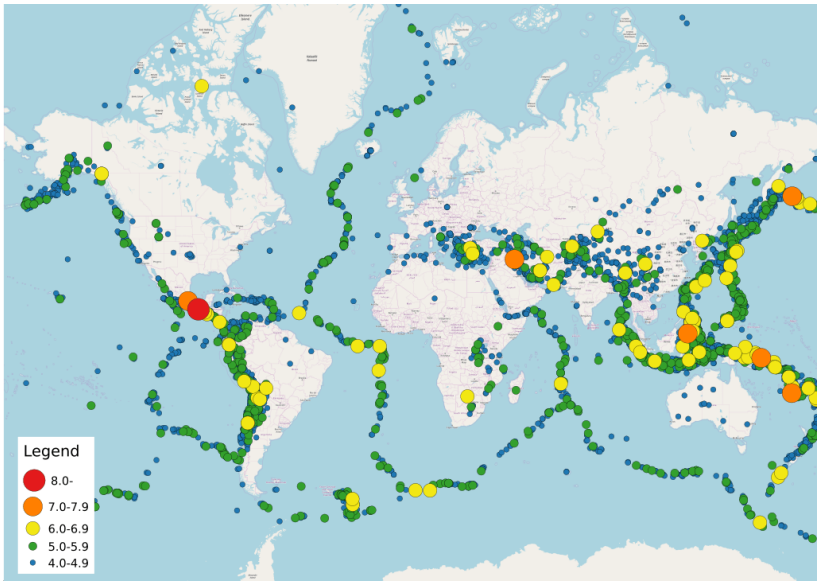


Figure 4.4.1: World map of earthquakes larger than magnitude 6.0 from 1900 to 2017. Earthquakes greater than 9.0 occur in subduction zones. Earthquakes from 8.0 up to 9.0 occur in subduction zones, collision zones, and occasionally on transform plate boundaries. Earthquakes between 6.0 and 8.0 occur at any type of plate boundary. Also note, earthquakes larger than 6.0 rarely occur away from a plate boundary. "Map of Earthquakes" by Phoenix7777 via Wikimedia Commons, is licensed under CC BY-SA 4.0. Access a detailed description.

As for the next smallest earthquakes, of a magnitude between 8 and 9, they can also occur on large and long faults. An example in California would be the San Andreas fault system. Therefore, the potential for big earthquakes exists in California. For a Californian, knowing about earthquakes and being prepared for them should also be part of daily life (Figure 4.4.2).



Figure 4.4.2: USGS Mobile Laser Scanning Truck collecting data near the zone of maximum surface displacement for the magnitude 7.1 Searles Valley earthquake of July 6, 2019. This is the top of a rupture that extends 45 km (28 miles) in length and 8 km (5 miles) in depth. "Near Zone of Maximum Surface Rupture" by Ben Brooks, USGS, is in the public domain.

What is an Earthquake?

Earthquakes occur when an area is experiencing a force or stress that builds up over time until a fault finally breaks, and each side of the fault moves past the other side. The energy released then propagates as waves through Earth and is what is called an earthquake. Elastic deformation is the basic mechanism used to describe Earth's response when stress is applied. Elastic is like a rubber band, if the stress were removed, the rock would return to its original shape. However, just like pulling on a rubber band, if the stress is too great, or continues for too long, a break, or fault, can occur. The rocks on either side of the fault return to their previous unstressed condition, just in a new location. Figure 4.4.3 illustrates rock in a pre-stressed state (left), stressed rock experiencing elastic deformation (center), and rock that is unstressed after a rupture (right).

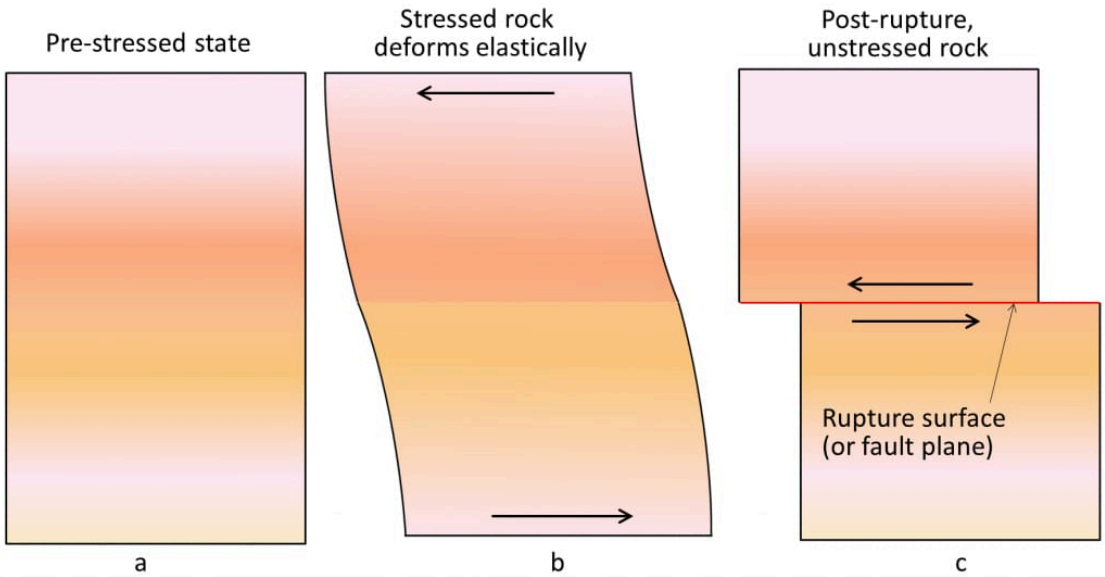


Figure 4.4.3: Three figures showing the progression of elastic deformation to rupture. (a) Pre-stressed state of undeformed rock. (b) Stressed rock deforms elastically as the top moves to the right and the bottom moves to the left. If stress is removed, the rock returns to its pre-stressed state and there is no permanent record. (c) Stress exceeds the fault's strength, causing rupture at the fault plane (rupture surface). Stress is released, resulting in two sections of post-rupture, unstressed rock. "Elastic deformation and Rupture" by Steven Earle is licensed under CC BY 4.0.

This is called elastic rebound and was first hypothesized as the mechanism for the 1906 magnitude 7.9 San Francisco earthquake. The 1906 earthquake changed the way Americans perceived earthquakes because up until then, no major U.S. city had ever been destroyed by one.

A commission was formed to look at the observable aspects of what had happened and why. One of the members of the Commission, Harry Fielding Reid, studied geodetic survey records for the 50 years before the earthquake and found evidence that the ground had deformed by more than 3m (10 ft) during those 50 years. He hypothesized that the ground deformation before the earthquake was from the buildup of elastic deformation of the rock. This deformation increased the stress on the fault, and when the build up of stress became larger than the strength of the fault, it broke. The 1906 San Francisco earthquake was the result. Modern seismic studies of earthquake waves and ground motion before and after earthquakes using GPS data support his observations and hypothesis.

It's also important to recognize that an earthquake is not just a point inside Earth. While the earthquake starts at a single point, it actually ruptures an area on a fault inside Earth within a matter of seconds.The rupture doesn't spread equally in all directions. Rock properties, stress buildup, and the amount of stress influence the direction and size of the rupture. Also, when an earthquake occurs and stress is relieved in one area, it can increase the stress in surrounding areas. This transfer of stress from a fault to surrounding rocks can help trigger another earthquake.

Earthquakes therefore may have foreshocks, aftershocks, or both. A foreshock is a smaller earthquake that occurs in a fault zone or related fault zone before a larger earthquake. An aftershock is a smaller earthquake that occurs in a fault zone or a related fault zone after a larger earthquake. Not all earthquakes have foreshocks and not all earthquakes have aftershocks.

Video 4.4.1: Foreshocks - Mainshock - Aftershocks

A series of earthquakes in the Alaska Range are used to illustrate how foreshocks and aftershocks are related to an earthquake.

This interactive element is not available in this format. Visit the link or scan the QR code to access it online.

View this YouTube Video online

A California example of both foreshocks, a mainshock, and aftershocks is the 2019 Ridgecrest Earthquake Sequence (Inset Box 4.4.1.)

Box 4.4.1: The 2019 Ridgecrest Earthquake Sequence

The 2019 Ridgecrest earthquake sequence began in the California desert on July 4, 2019 and was widely felt in central and southern California and Nevada.

Based on statistics derived from prior California earthquakes, there was a 6% estimated probability that this earthquake was a foreshock for another larger earthquake within the next 3 days, and that is what happened. Two days after the initial magnitude 6.4 earthquake, a magnitude 7.1 earthquake occurred. The basic statistics and the weekly predictions for three weeks after the earthquake sequence began are summarized in Box Figure 4.4.1. Note that there are many smaller aftershock earthquakes.

The following information is adapted from infographic "2019 Ridgecrest Earthquake Sequence" by USGS Earthquake Hazards Program is in the public domain:

2019 Ridgecrest Earthquake Sequence

July 4, 2019 – July 16, 2019
Prepared by the U.S. Geological Survey (USGS)

Overview

- **3,557 earthquakes** recorded since **July 4, 2019**, above magnitude 2.
- This sequence included:
  - **M6.4 earthquake** on **July 4, 2019** at **17:33:49 UTC**
    - Epicenter: 12 km west of Searles Valley, CA
    - **51,000+ "Did You Feel It?" responses**
  - **M7.1 earthquake** on **July 6, 2019** at **03:19:53 UTC**
    - Epicenter: 18 km west of Searles Valley, CA
    - **42,000+ "Did You Feel It?" responses**

Impact Summary

- **631** earthquakes of magnitude **M3+** (strong enough to be felt)
- **5** earthquakes of magnitude **M5+** (strong enough to cause damage)

Aftershock Forecast

Be prepared for more earthquakes. Probabilities for additional quakes by **July 22, 2019**:

Magnitude Range	Probability	Description
M3+	>99%	23–52 such earthquakes expected
M5+	30%	0–3 such earthquakes possible
M6+	4%	Low probability
M7+	<1%	About 1 in 300 chance

Note: Forecast was issued on July 15, 2019, at 16:31:15 UTC and was valid through July 22, 2019.

Science in Action

Photos depict USGS and academic researchers in the field:

- Collecting data from surface rupture sites
- Deploying instruments for aftershock monitoring
- Working near Ridgecrest and Trona, California

Background Image Description

- Aerial view of Highway 178 southwest of Trona showing a surface rupture from the July 4, 2019 M6.4 earthquake.
- Background graphic includes stylized seismograph trace and location map of Ridgecrest region

Box Video 4.4.1: A Tear in the Mojave

Watch how the data from the earthquakes were compiled and analyzed. Of special note is notice how the foreshocks and aftershocks are part of a sequence that occurred on 2 faults at right angles to each other.

This interactive element is not available in this format. Visit the link or scan the QR code to access it online.

View this YouTube Video online

One of the interesting results of the research done on this earthquake sequence is that it may have increased the possibility of a major earthquake on the nearby Garlock fault.

Query 4.4.1

This interactive element is not available in this format. Visit the link or scan the QR code to access it online.

View this Interactive Content online

Not all earthquakes are the same. Sometimes stress can be released within a fault zone by processes other than earthquakes. One of these processes is episodic tremors and slip (ETS) that occur on both subduction zones and parts of the San Andreas fault zone (Inset Box 4.4.2).

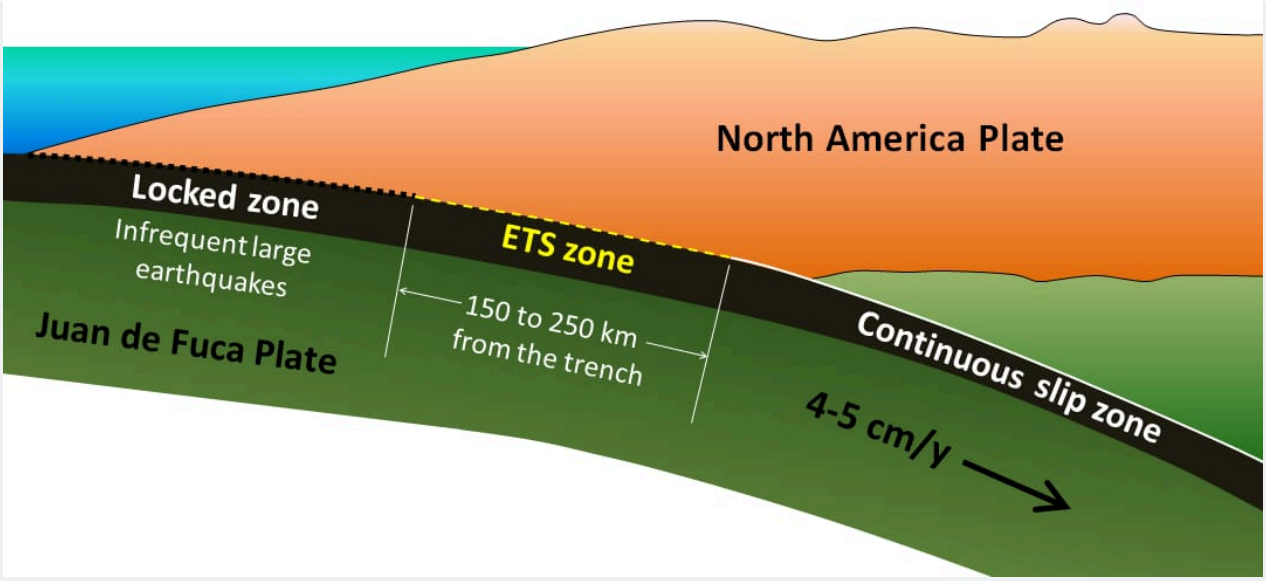
Box 4.4.2: Episodic Tremor and Slip (ETS): When an Earthquake is Not Really an Earthquake

Episodic Tremor and Slip (ETS) is a seismic phenomenon observed in many subduction zones. This is nearly imperceptible seismic rumbling, known as tremor, and slow slip along the plate interface. ETS events are imperceptible to humans, but not to seismometers, and do not cause damage.

So, why do we care?

Scientists are interested in studying ETS because it may provide insight into how stress is transferred within the crust, and how larger more destructive megathrust earthquakes are generated.

In the Cascadia subduction zone, where the Juan de Fuca Plate is subducting beneath the North American Plate, the cold upper part of the fault within the subduction zone is considered “locked” because of friction between the plates (Inset Box Figure 4.4.2). When slip occurs here, it generates very large earthquakes. In the warm, lower part of the fault, sliding is continuous because of how warm and weak the rock is. Between the two zones is the ETS zone, where rocks are not cold enough to be stuck long term but aren’t warm enough to slide continuously. Rather, this part of the boundary slips episodically on average every 14 months for a duration of about 2 weeks, moving a few centimeters at a time. These episodes are known as slow slip events.



Box Figure 4.4.2: Episodic tremor and slip along the Cascadia subduction zone. The Juan de Fuca plate is locked to the North American plate at the top of the subduction zone, causing infrequent large earthquakes. Lower down in the intermediate (ETS) zone, the plate alternately sticks and slips on a regular schedule it is slipping continuously. At the lowest level, in the continuous slip zone, movement occurs at a rate of 4 to 5 centimeters per year. "Episodic tremor and slip" by Steven Earle is licensed under CC BY 4.0.

These episodes are detected using geodetic measurements, such as GPS. GPS markers above the locked zone of the Cascadia subduction zone are steadily moving to the east, because the Juan de Fuca Plate is frictionally locked with the North American plate and dragging it eastward. GPS markers above the continuous slip zone are not moving, indicating that there is no friction between the plates here. Above the ETS zone, the North American plate generally moves eastward, then every 14 months or so, it reverses course for about two weeks and then it returns to its previous eastward motion.

Box Video 4.4.2: Subduction Zone - Deformation Zones (educational)

The following video illustrates how geodesy, the science of measuring Earth's shape, position, and movement, is used to detect Episodic Tremor and Slip (ETS).

This interactive element is not available in this format. Visit the link or scan the QR code to access it online.

View this YouTube Video online

It might seem like this periodic slip would help release stress buildup, thus reducing the risk of larger, more destructive earthquakes. However, the movement along the ETS zone actually appears to transfer stress to the adjacent locked zone, increasing the chance of a large earthquake.

ETS has been observed in a number of subduction zones including the Cascadia, Hikurangi, Mexican, and Nankai subduction zones. In addition to subduction zones, ETS has also been detected in transform faults like the San Andreas. Tremors have been observed along the Parkfield segment of the San Andreas which is considered the transition between the southern locked segment and the northern creeping section.

The Role of Fluids

Tremor is often associated with the movement of underground magmatic or hydrothermal fluids. In the case of the San Andreas fault zone and the subduction zones previously mentioned, hydrothermal fluids, not magma, are believed to be the cause of the tremor. Geoscientists have suggested that minerals undergoing metamorphic dehydration reactions could be a

source of these non-magmatic fluids. As minerals are buried deeper, they experience increased temperatures and become unstable. Some minerals undergo metamorphic reactions that may include the release of water resulting in increased pore fluid pressure.

Interestingly, one mineral that might be the culprit of fluid induced tremor along parts of the San Andreas fault zone may actually be serpentine, the mineral that makes up California's state rock serpentinite. Serpentine will undergo dehydration to olivine, talc, and water at increased temperatures. The ancient subduction zone that preceded the transform San Andreas fault zone (see A Brief Geologic History) is known to have produced significant quantities of serpentinized rock and those rocks may still be undergoing dehydration and producing water. These increased pore-fluid pressures may be responsible for lowering the frictional stress and generating tremor along parts of the San Andreas fault zone.

Seismic Waves

Waves occur frequently in nature and in many different situations. What makes a wave a wave? Consider a wave in the ocean or a ripple in a pond. The wave moves forward, but the water doesn't go with the wave. If you watch a cork floating on the water, it moves up and down as the wave moves the water under it, but it ends up where it started. When an earthquake occurs, the fault slips, and seismic waves are created and propagate away from the fault rupture in all directions. Like a water wave, the seismic wave propagates onward, but the particles of rock just oscillate and end up where they started. There are two major types of seismic waves - body waves and surface waves. Body waves move through materials; surface waves move along surfaces.

Body waves are P-waves and S-waves. The difference between them has to do with how the particles of the material move or vibrate as the wave passes through. The following two videos illustrate P-wave motion and S-wave motion. Neither video has audio, but both will be discussed in the text afterwards.

Video 4.4.2: P-Waves

The following animation uses a mass of small cubes to represent an imaginary rock. The cubes are compressed and extended as the p-waves move through it. This video contains no audio, but the process is described in the text.

This interactive element is not available in this format. Visit the link or scan the QR code to access it online.

View this YouTube Video online

Video 4.4.3: S-Waves

The following animation again uses a mass of small cubes to represent an imaginary rock. Watch as the cubes move up and down as the S-waves move through it. This video contains no audio, but the process is described in the text.

This interactive element is not available in this format. Visit the link or scan the QR code to access it online.

View this YouTube Video online

The imaginary rock in both Videos 4.4.2 and 4.4.3 has the shape of a brick, which has been divided into small cubes. The wave in both videos propagates from one end of the brick to the other. The movement of the small cubes within the brick shows the particle motion. And the difference between P-waves and S-waves is the difference in the movement of the small cubes.

With the P-wave, the small cubes compress and then expand with motion in the same direction as the wave motion. Notice that

they do not move side to side, or up and down. With the S-wave, the small cubes do not compress or expand. Instead they move up and down as the wave moves through the brick. This is like people doing the wave in a sports stadium, where the “wave” moves through the crowd as people raise their arms while standing up and then sitting down. The people in the sports stadium, and the little cubes in the brick start and end in the same place.

P-waves are compressional waves. The particle motion of a P-wave is in the same direction as the wave motion. P-waves can propagate through solids, liquids, and gases. When you hear someone speak, you are listening to a P-wave. P-waves are also called primary waves because they propagate the fastest, and on seismograms, arrive before S-waves. Seismograms are the recordings made of the arrival of earthquake waves. Now imagine that the brick in the P-wave video was rotated vertically and you were standing on its end. When a P-wave arrives, the motion you experience would be up and down because of the compression and expansion of the little cubes beneath your feet.

S-waves are shear waves. The particle motion of an S-wave is perpendicular, or at right angles, to the wave motion. The motion of the little cubes in the video is vertical, but an S-wave could also move horizontally, like the motion of a snake. Unlike P-waves, S-waves can only propagate through solids. They cannot propagate through liquids or gasses. S-waves are also called secondary waves because they are slower and come in second on a seismogram, after the P-waves. Now imagine the brick in the S-wave video rotating to vertical like you imagined the rotation of the brick in the P-wave video. Both the vertical and the horizontal versions of an S-wave in this orientation would cause side-to-side shaking.

Query 4.4.2

This interactive element is not available in this format. Visit the link or scan the QR code to access it online.

View this Interactive Content online

When a P-wave or S-wave arrives at the surface of Earth, most of the wave reflects back into the Earth. However, some of the wave energy becomes trapped near the surface of the Earth making new waves, surface waves.

There are two types of surface waves, Rayleigh waves and Love waves (Figure 4.4.4). They move slower and have larger amplitudes than P-waves or S-waves; therefore, they cause much of the damage that occurs during earthquakes. Love waves are just trapped S-waves and are experienced as strong side to side shaking. Rayleigh waves are generally experienced as a rolling motion like that of an ocean wave; their motion along the surface is actually elliptical as is indicated in Figure 4.4.4.

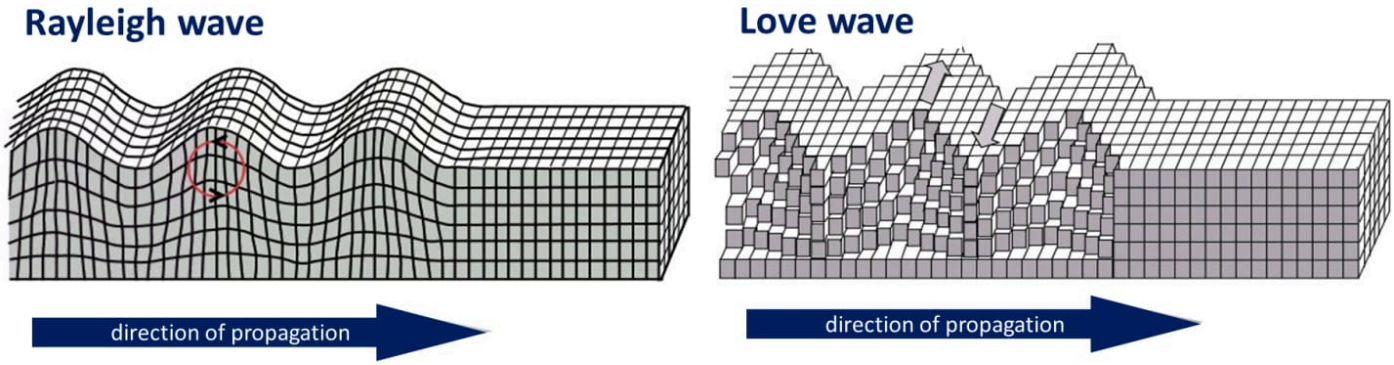


Figure 4.4.4: Block models showing the motion of surface waves: Rayleigh waves roll in the direction of propagation, while Love waves move side to side. Both are confined to the near-surface and weaken with depth. "Surface Waves" by Steven Earle is licensed under CC BY 4.0.

When an earthquake occurs the P-waves arrive first, then S-waves, and finally surface waves. Figure 4.4.5 is a record of the arrival of seismic waves, a seismogram. Notice also that the seismogram records the time of the arrival of the different seismic waves.

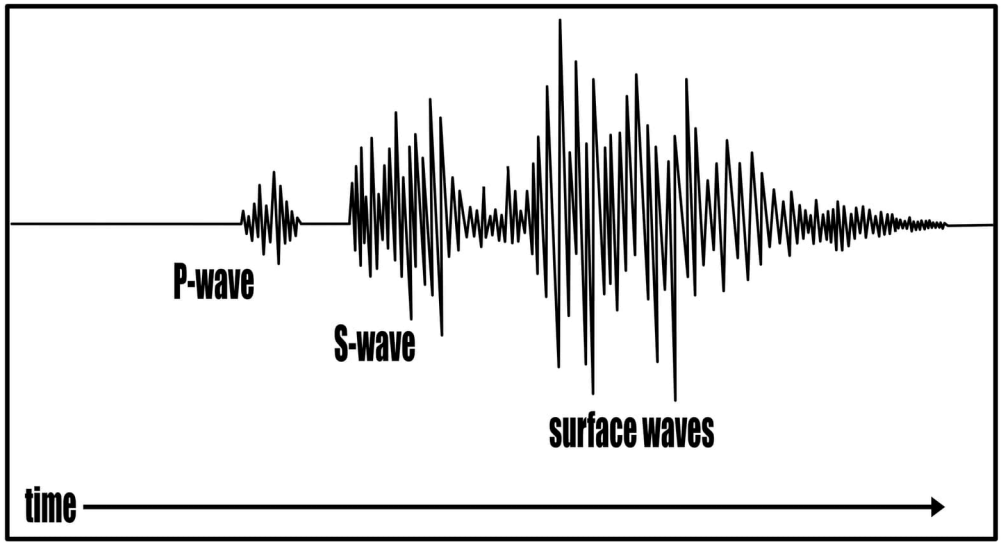


Figure 4.4.5: Simplified seismogram showing the ground motion of P-waves, S-waves, and surface waves over time. The P-wave comes first, moving to peak intensity and then quickly tapering back down to baseline for a short time. This is followed by the S-wave, which is characterized by a rapid onset and quick buildup to greater intensity, for a longer time period, than a P-wave. There is a sudden dropoff, then lower intensity waves that transition into surface waves. These are longest in duration and variable, but reach greater intensities before tapering back to baseline. "First Arrivals of Seismic Waves" by Steven Newton is licensed under CC BY-NC 4.0.

Video 4.4.4: Seismic Waves from an Earthquake

The following animation describes the arrival of seismic waves.

This interactive element is not available in this format. Visit the link or scan the QR code to access it online.

View this YouTube Video online

Query 4.4.3

This interactive element is not available in this format. Visit the link or scan the QR code to access it online.

View this Interactive Content online

Query 4.4.4

This interactive element is not available in this format. Visit the link or scan the QR code to access it online.

View this Interactive Content online

Epicenter and Hypocenter

When an earthquake occurs another question that is immediately asked is “Where’s the epicenter?” While the epicenter is related to the earthquake, it’s not where the earthquake occurs. The epicenter is the location on Earth’s surface directly above where the earthquake begins; the hypocenter, or focus, is on the fault inside the Earth (Figure 4.4.6). The hypocenter is where the earthquake begins and the fault propagates away from there. For a medium to large earthquake, magnitude 6 or greater, the fault will typically propagate 10s of kilometers from its starting point at the hypocenter. The epicenter is a useful location to refer to on a map that is commonly used for the earthquake’s location.

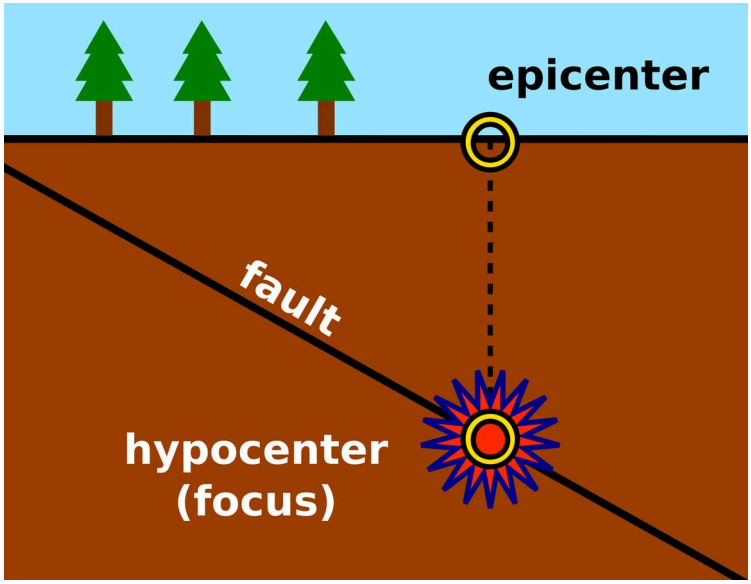


Figure 4.4.6: Cross-section within the Earth showing a fault with the hypocenter (or focus) of an earthquake along the faultline. The epicenter is at the surface directly above the hypocenter. "Epicenter-Hypocenter" by Ansate via Wikimedia Commons is licensed under CC BY-SA 1.0.

Historically, large or notable earthquakes are given names based on where the maximum damage from the earthquake occurred. This is because there was no way to calculate the actual location of the hypocenter of an earthquake until 1880 when modern seismometers, machines to measure seismic waves, were invented. With the invention of the seismometer, it became possible to locate the hypocenter of an earthquake and find its epicenter, but referring to an earthquake by the location of maximum damage was still common. An example would be the 1933 magnitude 6.4 Long Beach earthquake. This earthquake is the second most deadly earthquake in modern times in California, 120 people died and Long Beach suffered massive damage, but the hypocenter and its associated epicenter were actually to the south 20 kilometers (12.5 miles) near Huntington Beach.

As global seismic networks became more common, calculations of hypocenters improved, and epicenters are now reported by latitude and longitude with major or notable earthquakes named by the city, town, or geographic feature closest to the geographic location of the epicenter. For example, the 1989 magnitude 6.9 Loma Prieta earthquake, is named after Loma Prieta Peak in the Santa Cruz mountains, even though extensive damage happened in the cities of Santa Cruz and San Francisco.

Query 4.4.5

This interactive element is not available in this format. Visit the link or scan the QR code to access it online.

View this Interactive Content online

Locating an Earthquake

Finding where an earthquake is located can be complicated and several methods that can be used. Automated systems can

calculate an estimate of its hypocenter (and epicenter) very fast, but not necessarily with the high level of accuracy needed to study the earthquake. But people want to know about the earthquake, now! They don't want to wait for the results of intensive analysis that might take hours, days, or even longer.

Therefore, a compromise occurs, a fast automated estimate of the earthquake's location is usually reported almost immediately, and then the information is updated and improved as more data are analyzed. This does not mean that a mistake is being corrected because the location changes; it means that the first report was done using methods that are quick, computerized, with an emphasis on speed and good enough to help people responding to the earthquake, but the emphasis is on fast and useful, not on highest level of accuracy possible. This initial automated estimate of an earthquake's location will be within a few kilometers of the actual location (and the estimated magnitude will be within a few tenths).

Commonly the automated estimate is updated within an hour, after the initial estimate was reported. It may then be updated again within a few days. Eventually when all of the data recorded are analyzed a "final" hypocenter is found and it is listed in databases and reported in scientific papers, but in some cases this can take a year or more. While the epicenter may slightly change, it's usually very close to the original quick estimation of the automated systems from when it occurred. The 1994 magnitude 6.7 Northridge earthquake is however an example of what can happen.

Originally the epicenter was reported in Northridge, California. More than a year later, once all the data were analyzed, it turned out the epicenter was actually 1.6 km (1 mile) to the south-southwest in Reseda, California. Even though the epicenter is now known to be in Reseda, it's still however referred to as the Northridge earthquake. As Earth models are improved, and the physics of earthquakes and faulting is better understood, new methods are developed to study seismic waves and sometimes decades later the hypocenter of an earthquake may be recalculated yet again (see Inset Box 4.4.3).

One common way to locate an earthquake, starts with reading seismograms (Figure 4.4.7). It begins by finding the arrival times for the first P-wave and first S-wave. These waves travel the nearly same path within Earth, and subtracting the arrival time for the P-wave from the arrival time for the S-waves finds the time difference between their arrivals. Because the P-waves travel faster than the S-waves, the further apart they are on a seismogram, the farther the distance to the earthquake (Figure 4.4.7).

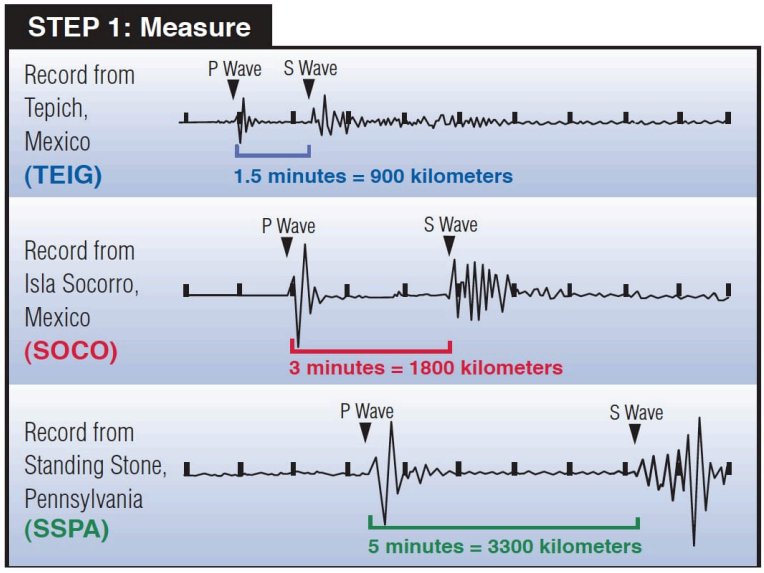


Figure 4.4.7: Simplified seismograms for an earthquake recorded by three different seismometers at different locations with the P-wave and S-wave first arrivals indicated. The time difference is given in minutes along with a distance in km. "Measuring Seismograms" by IRIS is licensed under CC BY 4.0. Accessible version of these data.

The time difference can then be used to estimate the distance to the earthquake using a travel-time curve. Travel-time curves are graphs of distance versus time for different seismic waves (Figure 4.4.8). Their construction is described in Video 4.4.5.

Video 4.4.5: Travel-Time Curves

This video explains how travel-time curves are constructed.

This interactive element is not available in this format. Visit the link or scan the QR code to access it online.

View this YouTube Video online

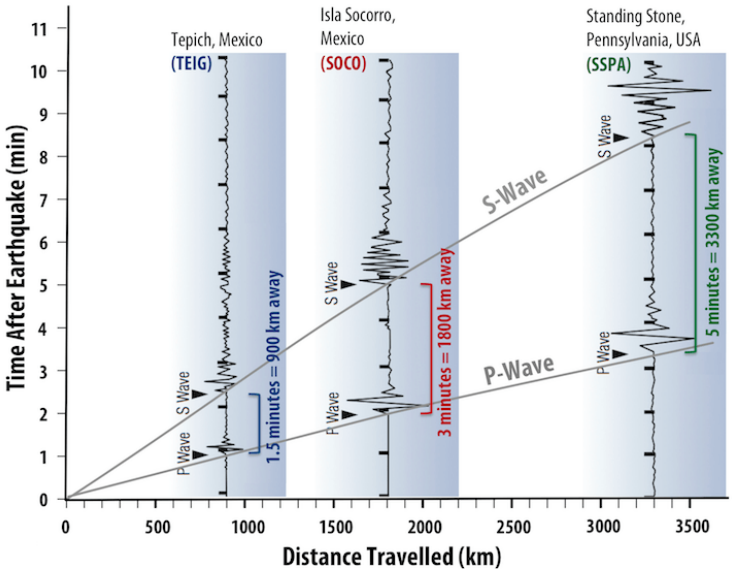


Figure 4.4.8: Seismograms overlaid on a travel-time curve to show how earthquake distance is determined. The seismogram is rotated to align time on the vertical axis, while matching the P-wave and S-wave time time difference with the travel-time graph. "Distance Traveled" by Karla Panchuck is licensed under CC BY-NC-SA 4.0. Access key data in accessible form.

Query 4.4.6

This interactive element is not available in this format. Visit the link or scan the QR code to access it online.

View this Interactive Content online

Each seismogram provides the distance to the earthquake from that seismometer but tells nothing about the direction to the earthquake. To actually find the location of an earthquake, requires data from at least three seismometers using a method called triangulation. On a map, draw a circle around each seismometer with a radius equal to the distance to the earthquake, and where they intersect is the epicenter of the earthquake (Figure 4.4.9).

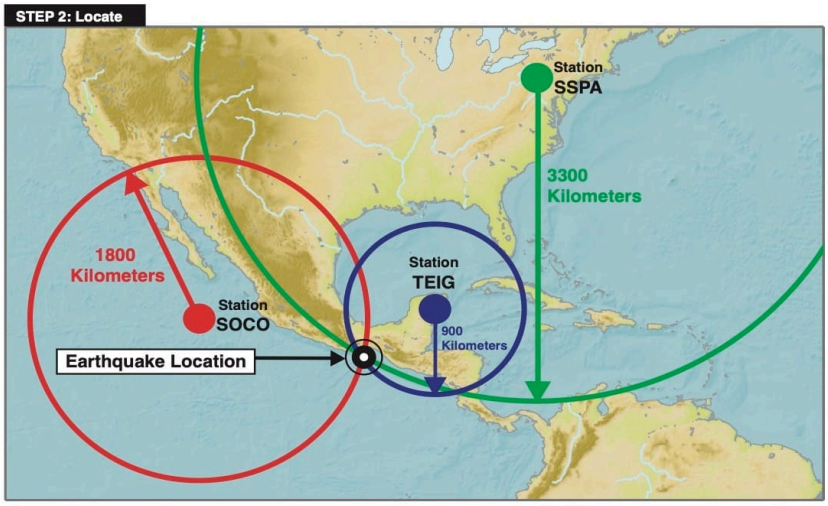


Figure 4.4.9: Triangulating data from three seismic stations to locate the earthquake's epicenter. The distance to the earthquake is determined by the method shown in Figure 4.4.8. The epicenter is located where the circles intersect. "Locate" by IRIS is licensed under CC BY 4.0. Access an accessible description.

Query 4.4.7

This interactive element is not available in this format. Visit the link or scan the QR code to access it online.

View this Interactive Content online

Box 4.4.3: When Earthquake Locations Change

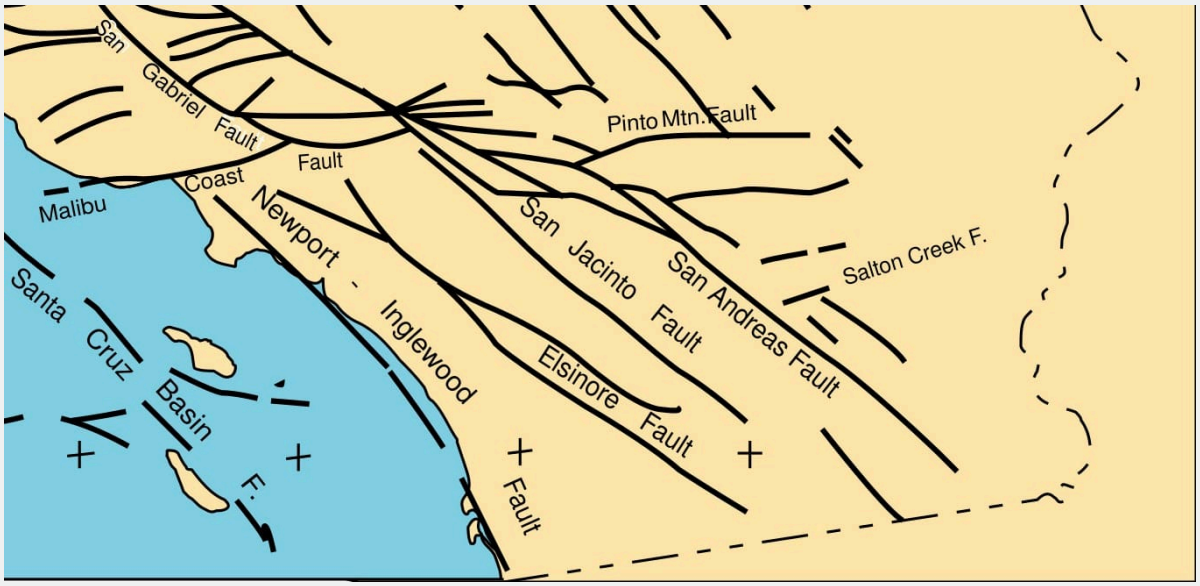
An extreme example of how the location of an earthquake can change over time, as either new information becomes available, or as understanding of the physics of earthquakes changes, or new analysis methods are discovered is what used to be called the 1812 San Juan Capistrano earthquake.

It was large, did massive damage throughout the missions of Alta California, but the worst damage was at San Juan Capistrano and the missions to the north. At San Juan Capistrano the “Great Stone Church” was destroyed and 40 people died. The earthquake occurred before seismometers were invented, so there are no seismograms to read. It was originally assumed to be an earthquake on the Newport-Inglewood fault zone (Box Figure 4.4.3), because that fault was reasonably close and has a historical record of large earthquakes which includes the 1933 magnitude 6.4 Long Beach earthquake.

Later when computer modeling became common and as Earth models for the geology of southern California were improved the damage patterns for older earthquakes were being reassessed. Everything that could be discovered about the damage done at the time, and how the buildings were constructed, and the geology of the area was put into models to determine where and how big the earthquake must have been. A better match to the damage was if the earthquake were located on the San Jacinto fault zone to the east.

But it did not end there, new research on how fault zones can interact with each other has again changed the understanding of where this earthquake may have begun and how large it might have been. Now the earthquake is believed to have started on the San Andreas fault zone.

It seems that the epicenter of the earthquake was on the San Andreas fault near Wrightwood, California and the rupture jumped fault zones. The San Jacinto fault zone is part of the greater San Andreas fault system and near Cajon Pass it jumped from the San Andreas fault zone to the San Jacinto fault zone based on patterns mapped in the faults and subsequent paleoseismic evidence from tree ring analysis. By transitioning between the San Andreas and San Jacinto faults, the rupture surface expanded, leading to a greater release of energy. The earthquake today is estimated to be a magnitude 7.5 starting on the San Andreas fault zone and then transferring to the San Jacinto fault zone, and it is now called the 1812 Wrightwood earthquake.



Box Figure 4.4.3: Simplified fault map of southernmost California “Faults of Southern California” by Debra Brooks, a derivative of "Southern California Faults" by BrucePL is licensed under CC BY-NC 4.0. Access a detailed description.

References

1. Berkeley Seismological Lab. (2004). *Where Can I Learn More About the 1906 San Francisco Earthquake?* https://web.archive.org/web/20080327145305/http://seismo.berkeley.edu/faq/1906_0.html
2. Bolt, B. A. (1999). *Earthquakes*. (4th ed.). W. H. Freeman and Company.
3. Brumbaugh, D. S. (1999). *Earthquakes - Science and Society*. Prentice Hall.
4. Earle, S. (2019). *Physical Geology*. (2nd ed.). PressBooks. https://opentextbc.ca/geology/
5. Earthquakes Hazards Program. (n.d.). *1906 Marked the Dawn of the Scientific Revolution*. U.S. Geological Survey. https://earthquake.usgs.gov/earthquakes/events/1906calif/18april/revolution.php
6. Hough, S. E., & Graves, R. W. (2020). The 1933 Long Beach Earthquake (California, USA): Ground Motions and Rupture Scenario. *Scientific Reports*. 10(10017). https://doi.org/10.1038/s41598-020-66299-w
7. Lemelson - MIT. (n.d.). *John Milne Seismograph*. Massachusetts Institute of Technology. https://lemelson.mit.edu/resources/john-milne
8. Panchuck, K. (2021). *Physical Geology* (H5P ed.). BCcampus. https://opentextbc.ca/physicalgeologyh5p/
9. Reid, H. F. (1910). Permanent Displacements of the Ground. In A. C. Lawson (Chairman), *The California Earthquake of April 18, 1906 - Report of the State Earthquake Investigation Commission. Vol. II The Mechanics of the Earthquake*. (pp. 16-28). The Carnegie Institution of Washington.
10. SAGE-IRIS Consortium. (n.d.). Education & Outreach Series No. 6: *How are Earthquakes Located?* EarthScope Consortium. https://www.iris.edu/hq/inclass/fact-sheet/how_are_earthquakes_located
11. Seismological Society of America. (2023, June 28). *What Are the Characteristics of Foreshocks for Large Earthquakes?* https://www.seismosoc.org/news/what-are-the-characteristics-of-foreshocks-for-large-earthquakes/
12. Southern California Earthquake Data Center (2013). *Earthquake Information* [data set]. Caltech. DOI:10.7909/C3WD3xH1
13. U.S. Geological Survey. (n.d.). *How do Seismologists Locate an Earthquake?* https://www.usgs.gov/faqs/how-do-seismologists-locate-earthquake
14. Wald, L. (n.d.). Earthquakes Hazards Program: *The Science of Earthquakes*. U.S. Geological Survey. https://www.usgs.gov/programs/earthquake-hazards/science-earthquakes

Inset Box 4.4.1 References

1. Barnhart, W. D., Hayes, G. P., & Gold R. D. (2019, October 15). The July 2019 Ridgecrest, California, Earthquake Sequence: Kinematics of Slip and Stressing in Cross-Fault Ruptures. *Geophysical Research Letters*, 46(21) 11859-11867. https://doi.org/10.1029/2019GL084741
2. California Institute of Technology Division of Geological and Planetary Sciences (2024). *Earthquake Information: Earthquake Probabilities*. Southern California Earthquake Data Center. https://scedc.caltech.edu/earthquake/probabilities.html
3. Lozos, J. C., & Harris, R. A. (2020, March 12). Dynamic Rupture Simulations of the M6.4 and M7.1 July 2019 Ridgecrest, California Earthquakes. *Geophysical Research Letters*, 47(7) https://doi.org/10.1029/2019GL086020

Inset Box 4.4.2 References

1. Beroza, G. C., & Ide, S. (2011). Slow Earthquakes and Nonvolcanic Tremor. *Annual Review of Earth and Planetary Sciences*, *39*(1) 271–296. https://doi.org/10.1146/annurev-earth-040809-152531
2. Kirby, S. H., Wang, K., & Brocher, T. M. (2014). A large mantle water source for the northern San Andreas fault system: A ghost of subduction past. *Earth, Planets and Space, 66*(1), 67. https://doi.org/10.1186/1880-5981-66-67
3. Rogers, G. & Dragert, H., 2003, Episodic tremor and slip on the Cascadia subduction zone: the chatter of silent slip, *Science,* 300(5627) 1942-1943. DOI: 10.1126/science.10847

Index Box 4.4.3 References

1. Rodriguez Padilla, A. M., Oskin, M. E., Rockwell, T. K., Delusina, I., & Singleton, D. M. (2021). Joint earthquake ruptures of the San Andreas and San Jacinto faults, California, USA. *Geology*, 50(4) 387-391. https://doi.org/10.1130/G49415.1
2. Southern California Earthquake Data Center (2013). *Earthquake Information – Chronological Earthquake Index* [data set]. Caltech. https://scedc.caltech.edu/earthquake/wrightwood1812.html

This page titled 4.4: Earthquakes is shared under a CC BY-NC 4.0 license and was authored, remixed, and/or curated by Allison Jones & Debra Brooks.

4.5: Measuring Earthquakes

Seismometers

Machines to measure earthquakes are seismometers. But, confusion exists between what a seismometer and a seismograph are because, before computers, there needed to be both a sensor to measure the seismic waves and a recording device. The sensor is the seismometer and it was usually buried, and out-of-sight, while the recording device, the seismograph was visible. It was a drum with paper and either a stylus or a pen that marked the paper as the drum turned, recording the seismic waves (Figure 4.5.1). The data record is a seismogram, the sensor measuring the seismic waves is the seismometer, and the recording device is the seismograph. Because people saw the seismograph, and seldom actually saw the seismometer, it became common to refer to the seismograph as if it were actually the seismometer.

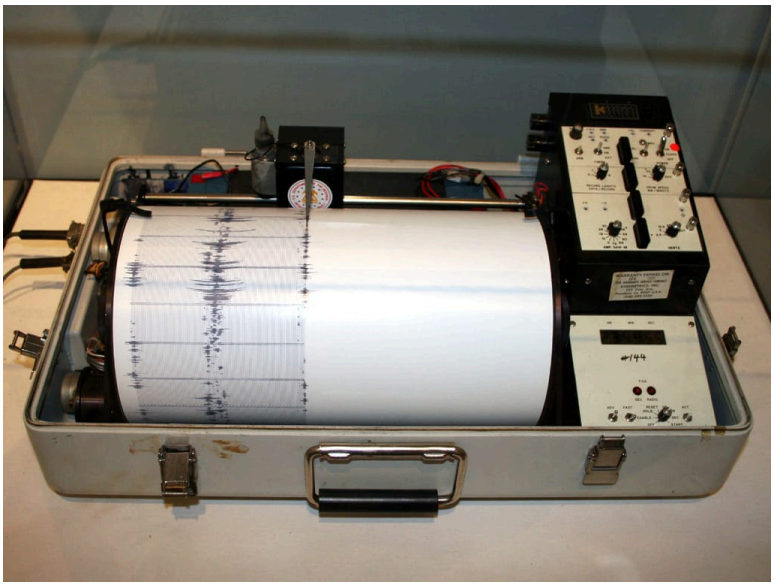


Figure 4.5.1: Portable seismic pack from the 1970s showing a seismogram being recorded on a seismograph. The seismometer, or sensor used to measure the seismic wave arrivals is not pictured. "Kinemetrics Seismograph" by Yamaguchi先生 via Wikimedia Commons is licensed under CC BY-SA 3.0.

Fast forward to today, and the situation has changed dramatically. Seismographs are seldom used, the signal measured by the seismometer is sent directly to a computer and stored digitally. Also, seismometers have greatly improved. Older seismometers could measure one direction of motion, so to record the movement of the Earth in 3-dimensions required 3 seismometers, each positioned along a different axis - one vertical, one horizontal and oriented north-south, and a second one horizontal, but oriented east-west (Figure 4.5.2). Now all three seismometers are packaged into one container.

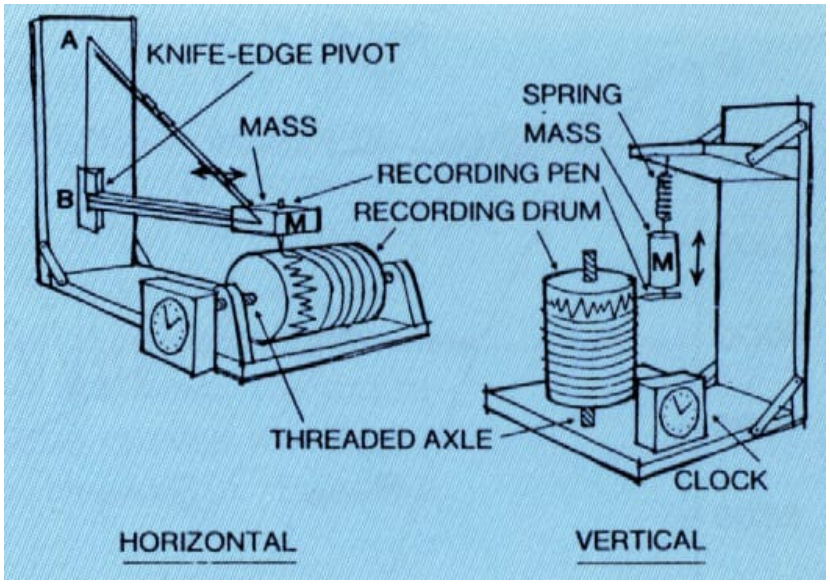


Figure 4.5.2: Diagrams of old-style, early 1900s pendulum seismometers that each measure only one component of motion and their associated seismographs. At a seismic station three seismometers would be required, two horizontal - one oriented east-west and the other north-south, and a vertical seismometer. "Seismographs" by the USGS is in the public domain. Access a detailed description.

Pendulum seismometers were some of the earliest designs and are based on the inertia of the suspended mass. They were generally replaced by electromagnetic seismometers by the mid 1900s. These still use a mass, but instead of being suspended by a wire, the mass is attached to a spring. The motion of the mass is measured by an electromagnet. A practical difference is the seismometer is now small enough to be portable whereas pendulum seismometers are large, permanent installations. Portable seismometers are valuable for detecting earthquakes in new locations or when previously quiet areas, such as volcanoes preparing to erupt, become seismically active. They are also useful for investigating the geology of relatively unexplored regions to detect local earthquake activity too small to be recorded globally.

A critical difference among electromagnetic seismometers is they can be designed to measure different frequencies. Local earthquakes have higher frequency data than distant earthquakes. These teleseismic events have mostly lower frequency data because the higher frequency information attenuates or weakens with distance. Therefore, measuring an earthquake that occurred at a great distance and not being able to record the high frequency information means that the energy from the earthquake will be underestimated, as will its magnitude.

Seismometers therefore are often referred to as short period for local earthquakes, long period for measuring distant earthquakes, or broadband when they record a broad band of frequencies and can be used to study either local or distant earthquakes. They can also be deployed either on land (usually in the ground; Figure 4.5.3) or on the sea bottom (Figure 4.5.4).



Figure 4.5.3: A modern seismometer being buried at a seismic station KOSM on the Southwest Rift Zone of Kīlauea Volcano in Hawai'i Volcanoes National Park, Hawai'i. "New Seismometer" by USGS is in the public domain.

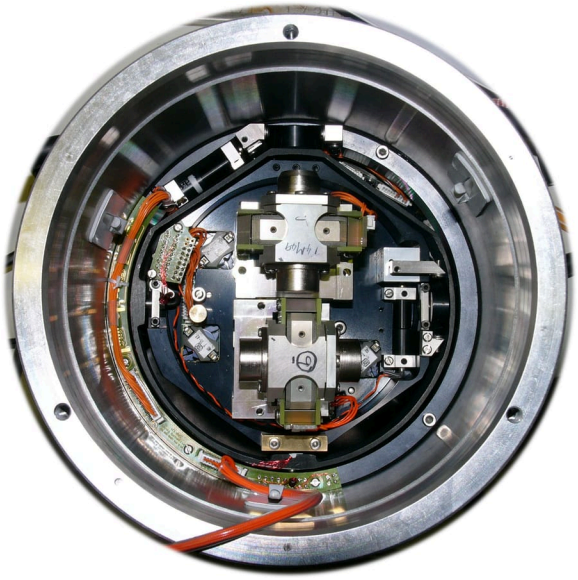


Figure 4.5.4: Three compact seismometers and electronics inside a marine, three-component seismometer. The diameter of the casing is approximately 15 cm (6 inches). "Seismometer" by Hannes Grobe via Wikimedia Commons is licensed under CC BY-SA 2.5.

Query 4.5.1

This interactive element is not available in this format. Visit the link or scan the QR code to access it online.

View this Interactive Content online

Other differences between modern and older seismology is that paper seismographs are for the most part no longer used. Data are now digital, not analog. The data are either recorded on a digital recording device which is periodically retrieved, or sent by telemetry to an offsite computer. This has changed the processing and interpretation of seismic data dramatically. It's much easier to compare data on different earthquakes digitally. Also analog/paper records (or their digital equivalent, webicorder records) can have the problem of the signals from multiple earthquakes overlapping each other and making them hard to

interpret. A digital signal however doesn't have to be viewed like a paper record or a webicorder display. It can be viewed over time, removing the overlap problem. This problem is illustrated in Video 4.5.1 on webicorder displays.

Reading Seismograms

The following video explains how to read seismograms.

This interactive element is not available in this format. Visit the link or scan the QR code to access it online.

View this YouTube Video online

Today most analog records are more for public display rather than earthquake research. Data are recorded digitally, transmitted back to a university or research center for use on a computer. They may be displayed as webicorder records, but are usually interpreted digitally. A video of a museum display in Canberra, Australia, summarizes how seismic data are collected and used.

Earthquake Monitoring

A visit to a museum in Canberra, Australia, reviews how earthquake data are collected and how they are used.

This interactive element is not available in this format. Visit the link or scan the QR code to access it online.

View this YouTube Video online

California Seismic Networks

If the information from one seismometer is useful, imagine how much more useful the information from multiple seismometers might be. One example that has already been discussed is finding the epicenter of an earthquake, which takes a minimum of three stations. The data recorded by seismic networks present opportunities for finding out much more about Earth than data from a single station (Figure 4.5.5).



Figure 4.5.5: Typical seismic station with a buried seismometer and a box for processing and transmitting data. It is powered by a solar panel. A GPS station lies at its base along with a transmitter for data transfer.. "GPS Receiver and Seismometer" by USGS is in the public domain.

Networks for data collection are important. The more stations in the network, the more data collected and the better the understanding of the earthquake and the surrounding geology. The way the network is designed is important. If the seismic stations in the network are widely dispersed, information can be gathered on smaller earthquakes everywhere within the network. The closer the stations, the smaller the earthquakes that can be recorded on multiple seismometers. The magnitude of completeness (Mc), or the smallest magnitude earthquake that can be confidently recorded by a network, is determined by the station density. If an "earthquake" is recorded on only a single seismometer, it may be wind, or traffic or other noise, or it's too small to be substantiated.

An important advantage of having a network of seismic stations is that it makes it possible to develop early warning systems that inform people that an earthquake has started.

Box 4.5.1: ShakeAlert

One of the results of having strong seismic networks has been the creation of an earthquake early warning system. It's called ShakeAlert and extends along the west coast from British Columbia in Canada to Mexico. ShakeAlert does not predict earthquakes. Data being transmitted from a seismic station to a processing center are automatically analyzed and screened to see if an earthquake has occurred. If a possible earthquake is detected, the data from nearby stations are queried to see if they are also recording an earthquake. If that appears so, the automated system quickly calculates a first approximation for the location and size of the quake (see Locating an Earthquake). The U.S. Geological Survey then sends the information out to organizations and agencies that have it distributed as an alert to mobile phones in the areas where shaking is most likely to occur.

The following video offers a more detailed look at the West Coast's earthquake warning system.

This interactive element is not available in this format. Visit the link or scan the QR code to access it online.

View this YouTube Video online

It works because computers can do all of this analysis very quickly, and electromagnetic waves, such as radio waves, move at the speed of light (approximately 300,000 km/s), whereas the seismic waves move much slower (5 to 8 km/s, depending upon the rock). Once an earthquake is detected, it's possible to warn people that an earthquake is happening, and the

farther away, the more warning time. It does however take time for an automated system to make its predictions, so the system is not perfect and people closest to the earthquake may experience shaking before they get a warning. The farther the location is from the earthquake, the more advanced the warning. For more information about the ShakeAlert system see Earthquake History and Hazards. Also, the ShakeAlert Website has information on how to sign up for and use the ShakeAlert system.California has three main seismic management networks - CGS, NCSN, and SCSN. They are organized under the Advanced National Seismic System (ANSS) operated by the U.S. Geological Survey. There are more than 15 seismic networks within the state that share data and report to the three main management networks.

The California Geological Survey (CGS) operates a network of over 900 accelerometers. Accelerometers are a type of seismometer that collects data on the acceleration of the ground motion. Most seismometers collect information on the velocity of the ground motion. Acceleration information is especially important to engineers designing structures because it measures how fast changes in velocity occur. If a structure cannot respond well to standing still, then suddenly being in motion, it is likely to fail (Figure 4.5.6).



Figure 4.5.6: Collapsed section of the I-5 in Gavin Canyon, Los Angeles, CA caused by the Northridge earthquake. "Collapsed Freeway" by FEMA via Wikimedia Commons is in the public domain.

Established in 1967, the Northern California Seismic Network (NCSN) is managed jointly by the U.S. Geological Survey and the University of California, Berkeley and operates 580 stations in northern and central California, along with incorporating 159 stations from the Southern California Seismic Network, and networks maintained by California state agencies, the University of Nevada, Reno, and public utility companies. It also includes additional seismic stations in the Pacific Northwest and Nevada because of its affiliation with the U.S. Geological Survey's California Volcano Observatory. A more detailed description of the network, including a current map of station locations can be found at the USGS Northern California Seismic Network.

Approximately 60% of the network is digital and most of the stations are short-period, vertical-component seismometers. The magnitude of completeness (Mc) varies from Mc 1.0 in the central Coast Ranges to Mc 2.6 in the Klamath Mountains. Data from the network are distributed by the Northern California Earthquake Data Center and by EarthScope Data Center (IRISMC).

The Southern California Seismic Network (SCSN) is the oldest seismic network in California. It was established in 1926, and it has been jointly managed by the California Institute of Technology (Caltech) and the U.S. Geological Survey since 1970. As of 2008, it has more than 400 stations and extends south from a line between San Luis Osbipo to Big Pine, California then continues south to Mexico. It has an approximate Mc 1.8. A detailed description of the network, including a current map of station locations can be found at Southern California Seismic Network. Data from the network are distributed by the Southern California Earthquake Data Center and by EarthScope Data Center (IRISMC).

Query 4.5.2

This interactive element is not available in this format. Visit the link or scan the QR code to access it online.

View this Interactive Content online

Earthquake Intensity and ShakeMaps

Intensity is the scale that has been historically used to measure earthquakes. It is based on the damage done by earthquakes and intensity values are reported using Roman numerals (Table 4.5.1). People experienced earthquakes long before instrumentation was invented to measure earthquakes, and therefore what could be measured was the effect earthquakes had on structures and the landscape. There are, however, problems with any intensity scale. Building materials and construction methods vary around the world, therefore intensity scales are modified and not the same world-wide. The intensity scale used in the United States is the Modified Mercalli Scale (Table 4.5.1), which is the 1931 modification of a scale originally developed by the Italian volcanologist Giuseppe Mercalli.

Table 4.5.1: Modified Mercalli Intensity Scale

Intensity	Shaking	Description/damage
I	Not felt	Not felt except by a very few under especially favorable conditions.
II	Weak	Felt only by a few persons at rest, especially on upper floors of buildings.
III	Weak	Felt quite noticeably by persons indoors, especially on upper floors of buildings. Many people do not recognize it as an earthquake. Standing motor cars may rock slightly. Vibrations similar to the passing of a truck. Duration estimated.
IV	Light	Felt indoors by many, outdoors by few during the day. At night, some awakened. Dishes, windows, doors disturbed; walls make cracking sound. Sensation like heavy truck striking building. Standing motor cars rocked noticeably.
V	Moderate	Felt by nearly everyone; many awakened. Some dishes, windows broken. Unstable objects overturned. Pendulum clocks may stop.
VI	Strong	Felt by all, many frightened. Some heavy furniture moved; a few instances of fallen plaster. Damage slight.
VII	Very strong	Damage negligible in buildings of good design and construction; slight to moderate in well-built ordinary structures; considerable damage in poorly built or badly designed structures; some chimneys broken.
VIII	Severe	Damage slight in specially designed structures; considerable damage in ordinary substantial buildings with partial collapse. Damage great in poorly built structures. Fall of chimneys, factory stacks, columns, monuments, walls. Heavy furniture overturned.
IX	Violent	Damage considerable in specially designed structures; well-designed frame structures thrown out of plumb. Damage great in substantial buildings, with partial collapse. Buildings shifted off foundations.
X	Extreme	Some well-built wooden structures destroyed; most masonry and frame structures destroyed with foundations. Rails bent.

Another concern is that an intensity scale cannot be used to compare one earthquake with another earthquake. For example, if a building is damaged by an earthquake, and then a second earthquake occurs a few days later and the building now collapses,

does this mean the second earthquake was larger? Or does it mean that the first earthquake damaged the building such that it could collapse if a smaller earthquake occurred? Also the damage caused by earthquakes is dependent upon the distance to the earthquake. If damage caused by two earthquakes is different, might it be because one earthquake was closer rather than bigger? Questions such as these led seismologists to find another way to measure earthquakes, such that one earthquake could be compared with another. Even though intensity is not a good way to compare one earthquake with another, it's a great way to compare the earthquake with itself. Sometimes, a video can do a better job of describing motion than words.

Video : Earthquake Intensity

In the following video, light bulbs are used to explain the concept of intensity and how intensity is used to describe earthquakes.

This interactive element is not available in this format. Visit the link or scan the QR code to access it online.

View this YouTube Video online

Intensity depends on multiple factors:

- how big the earthquake was
- how far away the earthquake was
- the local geology
- duration of shaking
- construction of buildings

The bigger the earthquake the larger the energy release. The farther from the earthquake, the more earthquake energy will attenuate or weaken. The local geology depends upon many factors. If the shaking lasts longer, the potential for damage is greater, and usually more damage occurs (Figure 4.5.7). If a building or structure is not constructed to withstand motion, it is more likely to experience damage (see California's Earthquake History and Hazards).



Figure 4.5.7: Damage to apartment buildings in the San Fernando Valley of Los Angeles, California from the 1994 M_W 6.7 Northridge earthquake. "Building Damage and Squashed Cars" by USGS is in the public domain.

Box 4.5.2: The Effect of Geology on Earthquake Intensity

Pretend an earthquake occurs. You and a friend are in different locations, but are equally distant from the earthquake. One of you is on campus, in class and in a well constructed building built on strong igneous rock. The other one has no classes that day and is at the beach. Who will experience the most shaking and probably see the most building damage?

Interestingly enough, because of the local geology, the person at the beach will probably experience more shaking and is more likely to see more damage to structures. The strong rock will most likely move as a unit and that minimizes the shaking and the shearing that can happen to structures. The loose beach sediments have no internal connections to give them strength and can move every which way, which will also cause seismic waves to slow down. Therefore, when the seismic waves encounter a material such as beach sands, the amplitude of the waves increases which will magnify the shaking. Often in areas of loose, wet sediment or weak, water-saturated sedimentary rock, liquefaction can occur (see Liquefaction and the Role of Soil Type). Many people have the misconception that the loose beach sands will act more like “packing peanuts” and somehow protect structures. Packing peanuts protect the contents of packages because they are packed in a box very tightly and have no room to move. Sand on the beach has no such constraints.

Intensity is usually mapped as an isoseismal map or ShakeMap. Sometimes the information is displayed by drawing isoseismal lines, or contour lines of equal intensity, as in the Interactive Isoseismal Map for the 1994 Northridge Earthquake or as colors on a gradational scale (Figure 4.5.8) with warm colors (reds, in this example) for the areas of highest intensity to cool colors (blues, in this example) for areas of lowest intensity. The pattern of gradational color changes or of contour lines draws attention to the areas of damage. This information can then be compared with other information such as geology maps or maps of local building zones to help determine why these areas experienced damage and to determine if measures such as new building codes or zoning restrictions could help prevent future damage.

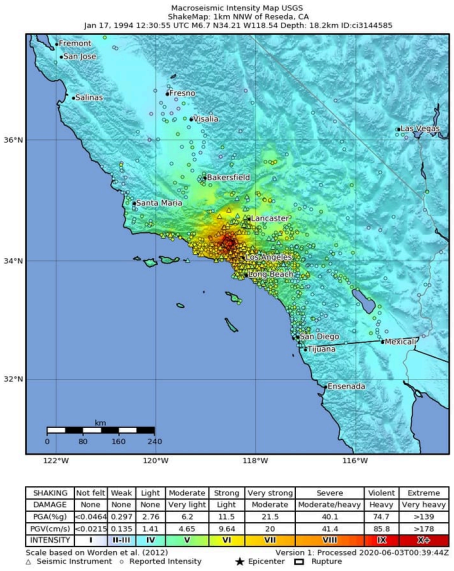


Figure 4.5.8: Intensity Map for the 1994 M_W 6.7 Northridge earthquake. "Intensity or ShakeMap for the 1994 M6.7 Northridge, CA Earthquake" by USGS is in the public domain. Access a detailed description (includes data shown).

For earthquakes in the United States or large earthquakes globally the U.S. The U.S. Geological Survey’s Earthquake Hazards Program maintains a website, Latest Earthquakes, where data on historical and recent earthquakes are available, including ShakeMaps, and also includes an opportunity for people to contribute to earthquake intensity data by reporting their experience during an earthquake - Did You Feel It?

Query 4.5.3

This interactive element is not available in this format. Visit the link or scan the QR code to access it online.

View this Interactive Content online

Earthquake Magnitude

Earthquake magnitude was designed as a way of measuring earthquake strength using properties of the earthquake as measured on seismometers, rather than on damage done by the earthquake. While there are multiple scales used to measure magnitude, most news media refer to any magnitude scale as the Richter Scale because Charles Richter's original scale was widely used and accepted for decades.

In 1935, American seismologist Charles Richter developed the first scale to measure what is now referred to as local magnitude or M_L. This measurement is based upon the amplitude of seismic waves as recorded on seismometers with corrections applied for distance to the origin of the earthquake. A problem eventually became apparent with this scale. Very large earthquakes occur when there is a long length of fault that ruptures. This energy is long period, and long period data are not part of the calculations used in determining a Richter magnitude. This means the original Richter magnitude scale underestimates the size of large earthquakes and the larger the earthquake, the larger the underestimation.

The moment magnitude scale or M_W was developed in 1979 and measures earthquakes based upon what is called the seismic moment in addition to the ground motion as measured on seismograms used to calculate the Richter or local magnitude M_L. The seismic moment is also incorporating information from the geometry and motion of the fault and properties of the rock.

Both scales are logarithmic with respect to ground motion, and every whole number increase represents an increase of 10 times greater ground motion than the previous number. For smaller earthquakes, magnitude 5 or less, the magnitude is approximately the same on either scale. However as earthquakes get larger than a magnitude 5, the moment magnitude gets progressively larger much more quickly than the Richter magnitude does. Therefore, the larger the earthquake, the greater the difference between the two magnitude scales and the greater the underestimation of the magnitude when using the Richter scale. Because of this, the moment magnitude scale has become the standard for reporting large earthquakes and has replaced the Richter and other magnitude scales.

Video 4.5.4: Earthquake Magnitudes and Why They Can Change

The following video provides a more detailed explanation of how earthquake magnitudes vary and why some are better than others for trying to estimate the energy released during an earthquake.

This interactive element is not available in this format. Visit the link or scan the QR code to access it online.

View this YouTube Video online

The moment magnitude scale was designed to better understand the energy released during earthquakes. One unit of magnitude is 10 times more ground motion and this increase in ground motion is from 32 times more energy being released. Therefore a magnitude 6 earthquake requires 32 times more energy than a magnitude 5 earthquake. An example of this can be illustrated using dry spaghetti noodles (Video 4.5.5).

Video 4.5.5: Moment Magnitude

A detailed example of how moment-magnitudes are calculated and why it takes 32 times the energy release to create 10 times the movement when an earthquake occurs.

This interactive element is not available in this format. Visit the link or scan the QR code to access it online.

View this YouTube Video online

When the Richter scale was being developed, Richter was using the best available equipment available. However, seismometers have greatly improved since the 1920s and 1930s. Therefore a "0" on the Richter scale back then meant no motion measured. Richter understood that there could be earthquakes that small, but they could not be reliably measured on the equipment used then. Today seismometers are much more sensitive and magnitude "0" earthquakes can easily be measured, in fact, magnitude -1 and -2 can be measured and detection levels are approaching -3 earthquakes. Humans are lousy earthquake detectors, the smallest earthquakes most humans can experience are magnitude 2. Therefore, today's seismometers can measure earthquakes 10,000 times smaller than a human can experience.

Query 4.5.4

This interactive element is not available in this format. Visit the link or scan the QR code to access it online.

View this Interactive Content online

Query 4.5.5

This interactive element is not available in this format. Visit the link or scan the QR code to access it online.

View this Interactive Content online

Earthquake Risk

If you can measure an earthquake, why can't you predict them? It's complicated. Earthquakes have been rarely predicted, but not consistently. They have also been mis-predicted. The problem is understanding just when a bit of fault will break, where this will be, and then how will the rupture propagate? The challenge is illustrated by two earthquakes that occurred in China during the 1970s. The M7.3 Haicheng earthquake of February 4, 1975 was successfully predicted; the M_W7.6 Tangshan earthquake of July 28, 1976 was not predicted and approximately 240,000 people died. Two earthquakes, less than two years apart, in the same country, so the protocols and technology are comparable. Why wasn't the second one predicted?

The easiest way to approach that question is to look at why the first one was. It had a foreshock sequence that was recognized as such, the second earthquake did not have a foreshock sequence. If seismicity were the same before all earthquakes, prediction would be much easier, but it's not. Earthquakes vary in tectonic setting and geology and no one-size approach works.

In the 1970s, the fact that a major earthquake had been predicted made more scientific organizations acknowledge that it was

possible under the right conditions; the fact that the next major earthquake was not predicted, made these same agencies more cautious and steered earthquake awareness in a different direction - increasing the emphasis on earthquake preparedness.

Video 4.5.6: Why Earthquakes Are So Hard to Predict

This video provides more detailed explanation of how earthquake magnitudes vary and why some are better than others for trying to estimate the energy released during an earthquake.

This interactive element is not available in this format. Visit the link or scan the QR code to access it online.

View this YouTube Video online

Video 4.5.6 illustrates some of the problems with earthquake prediction, a major one being that while many things are known about what can happen before an earthquake, why do they happen sometimes and not happen other times? Today, many seismologists believe that predicting earthquakes will never be entirely successful. Therefore, while research continues to try and learn more, the questions become - What is known? And what can be done to make the best use of that information?

What is known? Where earthquakes occur, how large an earthquake is possible, and what amount of ground shaking will occur, but not when an earthquake will happen or how large it will be (Figure 4.5.9). Therefore, the approach that is being taken by both the state and the federal government is to try and prepare for earthquakes in areas where there is a risk of major earthquakes and to continue to try and learn more about earthquakes in the hope that one day earthquake prediction can become a reality. For more about the hazards presented by earthquakes and how to prepare for an earthquake see California's Earthquake History and Hazards.

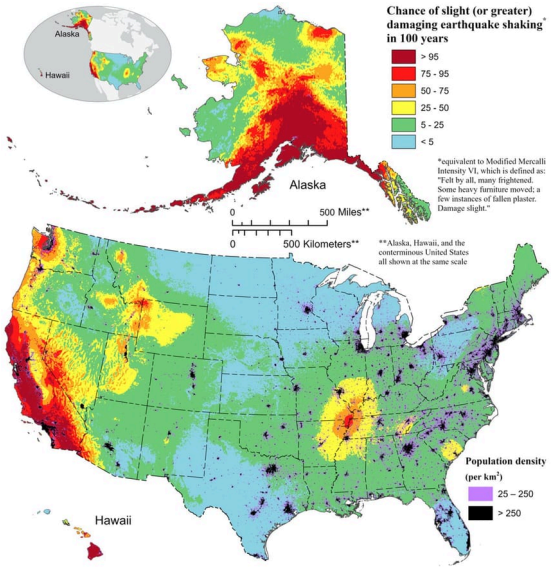


Figure 4.5.9: National Seismic Hazard Map (2023) of the US showing the possibility of shaking at Modified Mercalli Intensity VI or higher occurring within the next 100 years by USGS Earthquake Hazards Program is in the public domain. Notice that the only state in the United States with a greater risk than California is Alaska. Access a detailed description.

References

1. Adams, R. D. (1976). The Haicheng, China, Earthquake of 4 February, 1975; The First Successfully Predicted Major Earthquake. *Bulletin of the New Zealand National Society for Earthquake Engineering*. 9(1) 32-42. https://www.earthquakeprediction.gr/HAICHENG-EARTHQUAKE-1975.pdf
2. Bolt, B. A. (1999). *Earthquakes*. (4th ed.). W. H. Freeman and Company.

3. Brumbaugh, D. S. (1999). *Earthquakes - Science and Society*. Prentice Hall.
4. California Institute of Technology & U. S. Geological Survey Pasadena (1926): *Southern California Seismic Network* [data set]. International Federation of Digital Seismograph Networks. https://www.fdsn.org/networks/detail/CI/
5. Cooper, J. D., Fiedland, I. M., Buckle, I. G., Nimin, R. B., & MuMullin Bobb, N. (1994). The Northridge Earthquake: Progress Made, Lessons Learned in Seismic-Resistant Bridge Design. *Public Roads*, 58(1). https://highways.dot.gov/public-roads/summer-1994/northridge-earthquake-progress-made-lessons-learned-seismic-resistant
6. Earthquake Hazards Program. (n.d.). *Repeating Earthquakes*. U.S. Geological Survey. https://earthquake.usgs.gov/learn/parkfield/eq_predict.php
7. Natural Hazards FAQ. (n.d.). *Can You Predict Earthquakes?* U.S. Geological Survey. https://www.usgs.gov/faqs/can-you-predict-earthquakes
8. Hanks, T. C., & Kanimori, H. (1979). A moment magnitude scale. *Journal of Geophysical Research Solid Earth*, 84(B5) 2348-2350.
9. Hauksson, E. (2012). California Integrated Seismic Network (CISN). In Bormann, P. (Ed.), *New manual of Seismological Observatory Practice - 2 (NMSOP-2)*. Deutsches GeoForschungsZentrum GFZ, 1-5. https://gfzpublic.gfz-potsdam.de/rest/items/item_43343/component/file_56124/content
10. Hutton, K., Woessner, J., & Hauksson, E. (2010). Earthquake Monitoring in Southern California for Seventy-Seven Years (1932-2008). *Bulletin of the Seismological Society of America*, 100(2) 423-446. https://doi.org/10.1785/0120090130
11. Kwiatek, G., & Ben-Zion, Y. (2016). Theoretical limits on detection and analysis of small earthquakes. *Journal of Geophysical Research Solid Earth*, 121(8) 5898-5916. https://doi.org/10.1002/2016JB012908
12. Lukasik, L. (2021, July 28). The Great Tangshan Earthquake: One of the worst earthquakes in modern history destroys Chinese city. *Building Safety Journal*. International Code Council. https://www.iccsafe.org/building-safety-journal/bsj-dives/the-great-tangshan-earthquake-one-of-the-worst-earthquakes-in-modern-history-destroys-chinese-city/
13. Natural Resources Canada. (2012, April 6). *How we record Earthquakes*. Government of Canada. https://www.earthquakescanada.nrcan.gc.ca/info-gen/smeters-smetres/seismograph-en.php
14. Peterson, M. D., Shumway, A. M., Powers, P. M., Field, E. H., Moschetti, M. P., Jaiswal, K. S., Milner, K. R., Rezaeian, S., Frankel, A. D., Llenos, A. L., Michael, A. J., Altekruse, J. M., Ahdi, S. K., Withers, K. B., Mueller, C. S., Zeng, Y., Chase, R. E., Salditch, L. M., Luco, N., ... Witter, R. C., (2024). The 2023 US 50-State National Seismic Hazard Model: Overview and implications. *Earthquake Spectra*, 40 (1) 5–88. https://doi.org/10.1177/87552930231215428
15. Richter, C. F. (1935). An Instrumental Earthquake Magnitude Scale. *Bulletin of the Seismological Society of America,* 25(1) 1-32.
16. Richter, C. F. (1958). *Elementary Seismology*. Freeman.
17. SAGE-IRIS Consortium. (n.d.). Education & Outreach Series No.7: *How Does a Seismometer Work?* EarthScope Consortium. https://www.iris.edu/hq/inclass/fact-sheet/how_does_a_seismometer_work?zoombox=0
18. U.S. Geological Survey. (2021, November 5). General Interest Publications: *The Severity of an Earthquake*. https://pubs.usgs.gov/gip/earthq4/severitygip.html
19. USGS Menlo Park. (1966). *USGS Northern California Seismic Network* [Data set]. International Federation of Digital Seismograph Networks. https://doi.org/10.7914/SN/NC
20. Wald, D. J., Quitoriano, V., Worden, C. B., Hopper, M., & Dewey, J. W. (2012). USGS “Did You Feel It?” Internet-based Macroseismic Intensity Maps. In R. Bossu & P. S. Earle (Eds.), *On the Use of the Internet to collect earthquake information*. Annals of Geophysics 54(6) 688-707. DOI:https://doi.org/10.4401/ag-5354

This page titled 4.5: Measuring Earthquakes is shared under a CC BY-NC 4.0 license and was authored, remixed, and/or curated by Debra Brooks.

4.6: Chapter Summary

4.1 Stress and Strain

- Stress is a force distributed over an area. Rocks can experience compression, tension, and shear stresses.
- Strain is a rock's response to stress. A rock can either deform elastically, plastically, or it can fracture (brittle deformation). Generally, higher temperatures yield more plastic behavior and rocks are generally more plastic when they are wet. If stress is applied quickly, rocks are more likely to break.
- Deformation can be measured using strike and dip. Strike is a compass direction that is parallel to the plane being measured and a horizontal surface. Dip is an angle between 0 (horizontal) and 90 (vertical), measured perpendicular to strike. These measurements are taken using a special compass with an inclinometer.

4.2 Folding

- When rocks deform in a ductile fashion, typically at higher temperatures deep in the crust, they may form folds.
- Anticlines are A-shaped folds with oldest rocks at the center, Synclines are U-shaped folds with the youngest rocks at the center. If the ages of the rocks are unknown, then they are called antiforms and synforms respectively.
- Anticlines and synclines can have a variety of orientations: being upright, recumbent, or plunging (or anywhere in between!). They can also have a variety of interlimb angles from isoclinal (parallel or near parallel) to gentle.
- Domes are folds that resemble and upside down bowl, with their limbs dipping away in all directions. Basins are bowl-shaped folds.

4.3 Jointing and Faulting

- Joints are fractures in rocks that have not been displaced. In other words, the two sides of the fracture have not moved relative to one another. Exfoliation joints and columnar joints frequently form in igneous rocks.
- Joints are often formed in tension, but they can also be formed in compression.
- Faults are any fractures that have been displaced. There are dip-slip, strike-slip, and oblique-slip faults.
- Dip-slip faults include normal faults, wherein the hanging wall moves down relative to the footwall; reverse faults wherein the hanging wall moves up relative to the footwall, and thrust faults which are low-angle (<30 degree) reverse faults. Typically, normal faults form where the crust is experiencing extension, and thrust and reverse faults form where the crust is undergoing shortening.
- Strike slip faults are faults which move parallel to their strike. They can be right-lateral (dextral) or left-lateral (sinistral).
- Faults can also have components of both dip-slip and strike-slip. We call these oblique-slip faults.

4.4 Earthquakes

- Earthquakes are the energy released when a fault ruptures.
- Stress is stored within the Earth and is released during an earthquake.
- Foreshocks are smaller earthquakes that precede a larger earthquake, and aftershocks are smaller earthquakes that follow a larger earthquake.
- Body waves move through the Earth. P-waves occur when the particle motion of a wave is in the same direction as the wave motion. S-waves are when the particle motion is perpendicular to the wave motion. P-waves cause up-and-down motion, while S-waves cause side-to-side motion.
- Surface waves move on surfaces or interfaces and include Love and Rayleigh waves. Love waves travel side-to-side on an interface or surface and cause side-to-side motion. Rayleigh waves travel with circular motion like an ocean wave and are experienced as a rolling motion.
- A seismogram is the record of the arrival of earthquake waves. Seismic waves arrive in an order - P-waves, S-waves, and then surface waves.
- Earthquakes begin at a hypocenter inside Earth. The epicenter is the point at the surface of Earth directly above the hypocenter.
- Earthquakes are located by the triangulation of the distances from 3 or more seismic stations.

4.5 Measuring Earthquakes

- Seismometers are machines or sensors that measure earthquake waves. Seismographs are recording devices that have largely been replaced by computers.
- The record of the arrival of seismic waves is a seismogram.
- Seismic networks are arrays of seismometers within an area. The density or magnitude of completeness of a network determines how small of an earthquake can be reliably recorded.
- Intensity is a measure of the damage done by an earthquake. The most commonly used intensity scale is the Mercalli Scale.
- Magnitude measures the energy released by an earthquake. Earthquakes have one magnitude, but magnitudes can be calculated many different ways and not all magnitude scales calculate the same values. Magnitude scales are based on the ground motion of an earthquake as measured on a seismogram rather than on damage.
- The most common magnitude scale reported and used today is moment-magnitude (M_W). Historically, Richter magnitude (M_L) was used and reported. M_L and M_W are the same for earthquakes less than M5. For earthquakes greater than M5, M_W is more accurate.
- Magnitude scales are logarithmic. Each increase of 1-unit means 10 times more ground motion and 32 times more energy.
- Essentially all of California is likely to experience an earthquake with an intensity level of Mercalli VI within the next 100 years.
- ShakeAlert is the earthquake early warning system on the west coast of the United States.

This page titled 4.6: Chapter Summary is shared under a CC BY-NC 4.0 license and was authored, remixed, and/or curated by Allison Jones.

4.7: Detailed Figure Descriptions

Figure 4.1.1 Illustrations of Stress

This diagram explains how different types of stress—shear, compression, and tension—act on materials in the Earth's crust. Each type of stress is shown deforming a circular shape, along with labeled arrows and real-world geologic examples.

Shear stress acts parallel to surfaces. Under shear stress, the circle is now an oval, slanted to the right as it is affected forces moving to the right at the top and to the left at the bottom. Example: transform boundaries where plates slide along each other.

Normal stress acts at right angles to surfaces. There are two types of normal stress: compression and tension.

Compression stress is shown as a circle squeezed into a vertical ellipse by opposing forces on either side. Example: when tectonic plate collide.

Tension is shown by a circle that is stretched into a thin horizontal ellipse, pulled by opposing forces on either side. Example: when a continent begins to break apart.

Figure 4.1.2 Responses of Geological Materials

This diagram illustrates how materials respond to increasing stress by showing three distinct stress–strain curves for materials A, B, and C. It helps explain the mechanical behavior of materials—how they deform and eventually fail under stress—and is commonly used in geology, engineering, and materials science.

Stress (force per unit area) is plotted along the Y-axis, while strain (deformation) is plotted on the X-axis.

The curve for Material A shows mostly elastic deformation with a quick return to original shape after stress is removed; however, it fractures under high stress. This is typical of strong, ductile materials.

The curve for Material B exhibits a steep elastic region, followed by brittle fracture with minimal plastic deformation. It breaks or cracks shortly after reaching its elastic limit, which is typical of brittle materials like glass or some rocks.

The curve for Material C displays both elastic and plastic deformation before it fractures. It has a long, flat curve indicating ductile behavior, meaning that it flows or bends without breaking easily. However, it does fracture after undergoing significant strain.

Definitions:

- Elastic deformation: The linear part of each curve, where materials return to their original shape when stress is removed.
- Plastic deformation: The curved portion beyond the elastic limit, where permanent deformation occurs.
- Fracture point: The endpoint, where materials fail or break.

Figure 4.1.5 Strike and Dip

This diagram illustrates how strike and dip are measured on an inclined surface. Here, a water line intersects tilted sedimentary beds. This is the orientation of strike. Dip is perpendicular to the strike line and points downslope. Strike and dip are indicated by a “T” shaped symbol where the top of the T indicates strike and the stem of the T indicates dip. The dip angle is written next to the strike and dip symbol. In this example, the dip is 20 degrees so a 20 is written next to the symbol.

Figure 4.2.1 Anticline

The cross-sectional view shows an anticline before and after erosion. Three layers are visible. Before erosion the anticline is curved upward, like a dome, with only the Devonian layer exposed. After erosion the dome is worn away to expose all three layers. The outermost is labeled Devonian; the middle is Silurian; and the core is Ordovician.

The map view shows the three layers side by side - moving from outward to core, then core to outward. The core layer is doubled, with arrows showing forces moving from the center outward.

There are sideways T-shaped elements under the S and D units in the right panel indicating faults, specifically showing dip direction and relative motion on faults in map view. The vertical line of each “T” marks the trace of a fault cutting across the rock layers. The short horizontal bar attached to the fault line indicates the down-dropped side of the fault (the direction of dip), which is a standard geologic map symbol for a normal fault or a fault with vertical displacement. Their placement beneath the S and D rock units shows that those units are offset by faults, rather than being continuous across the map.

Figure 4.2.2 Syncline

The cross-sectional view shows a syncline, with three layers visible in a nested U shape. The outermost layer is labeled Ordovician; the middle is Silurian; and the core is Devonian.

The map view shows the three layers side by side - moving from outward to core, then core to outward. The core layer is doubled, with arrows showing forces moving from the outside in.

There are sideways T-shaped elements under the S and D units in the right panel indicating faults, specifically showing dip direction and relative motion on faults in map view. The vertical line of each “T” marks the trace of a fault cutting across the rock layers. The short horizontal bar attached to the fault line indicates the down-dropped side of the fault (the direction of dip), which is a standard geologic map symbol for a normal fault or a fault with vertical displacement. Their placement beneath the S and D rock units shows that those units are offset by faults, rather than being continuous across the map.

Figure 4.2.7 Domes and Basins

The dome is represented with three layers, the outermost labeled Devonian; the middle, Silurian; and the core, Ordovician. The map view shows a circle version of the dome, with the central core surrounded by the two outer layers.

The basin is represented as a bowl, or the bottom half of a circle, with three layers. The outermost layer is labeled Ordovician; the middle is Silurian; and the core is Devonian. The map shows a circle version, with the central core surrounded by the two outer layers.

There are sideways T-shaped elements in the S and D units in the right panel indicating faults, specifically showing dip direction and relative motion on faults in map view. The vertical line of each “T” marks the trace of a fault cutting across the rock layers. The short horizontal bar attached to the fault line indicates the down-dropped side of the fault (the direction of dip), which is a standard geologic map symbol for a normal fault or a fault with vertical displacement. Their placement beneath the S and D rock units shows that those units are offset by faults, rather than being continuous across the map.

Figure 4.2.8 Petroleum Traps

This cross-section of a landscape shows the layers of rock and other materials that lie underneath an oil well.

At the base we see an antiform (dome-shaped layers of rock), labeled Source Rock. Above that is a layer of porous reservoir rock. Above that is a dome-shaped layer labeled impermeable shale clay - and trapped between the porous reservoir rock and the top of the dome is a layer of rock oil, overlaid by natural gas. Above the impermeable shale layer we see topsoil and sod. The oil well shaft breaks through the impermeable shale clay to reach the rock oil.

Figure 4.4.1: World Map of Earthquakes

This world map shows the global distribution of earthquakes, with earthquakes represented by colored circles whose size and color indicate magnitude. The earthquakes form long, narrow belts that outline tectonic plate boundaries, including mid-ocean ridges, subduction zones, and major transform faults, while the interiors of most continents show relatively few events.

The largest circles (reds and oranges) are concentrated mainly along subduction zones around the Pacific Ocean, forming the well-known Ring of Fire, as well as parts of southern Asia and the eastern Mediterranean region. Smaller circles (greens and blues) are more widespread and appear not only along plate boundaries but also along mid-ocean ridges and some continental

fault zones.

Earthquake magnitudes and where they are generally found

- Magnitude 8.0+ earthquakes are found almost exclusively at major subduction zones, such as along the western coasts of the Americas, Japan, Indonesia, and the southwest Pacific. They occur where one tectonic plate is being forced beneath another.
- Magnitude 7.0–7.9 earthquakes also cluster along subduction zones, but are more widespread than magnitude 8+ events. They occur around the Pacific Rim and in collision zones such as the Himalayan region.
- Magnitude 6.0–6.9 earthquakes are common along plate boundaries of all types, including subduction zones, transform faults, and some continental collision zones. They appear both along ocean margins and within active continental belts.
- Magnitude 5.0–5.9 earthquakes are widely distributed along mid-ocean ridges, transform faults, and subduction margins. They form continuous chains along oceanic spreading centers and linear belts on land.
- Magnitude 4.0–4.9 earthquakes are the most widespread and numerous, appearing along nearly all plate boundaries and some intraplate regions. They outline plate margins very clearly, especially along mid-ocean ridges and diffuse fault zones.

Figure 4.4.7 Simplified Seismograms

Data from Simplified Sonograms

Location of Record	Time Lag Between P Wave and S Wave	Distance Between P Wave and S Wave
Tepich, Mexico	1.5 minutes	900 kilometers
Isla Socorro, Mexico	3 minutes	1,800 kilometers
Standing Stone, Pennsylvania, US	5 minutes	3,300 kilometers

Figure 4.4.8 Seismograms on a Time-Travel Curve

This shows how seismic waves from the same earthquake are recorded at three different seismic stations located at increasing distances from the source. The figure combines waveform records (seismograms) with a time–distance graph to illustrate how P-waves and S-waves arrive at different times depending on distance.

The horizontal axis is labeled “Distance Travelled (km)” and increases from left to right, reaching a little over 3,500 km. The vertical axis on the left is labeled “Time After Earthquake (min)” and increases upward from 0 to about 11 minutes. Diagonals line extends from the lower left corner upward to the right, representing increasing S–P arrival time difference with distance.

- On the left side is a vertical seismogram labeled “Tepich, Mexico (TEIG)”. The waveform shows a small, early arrival labeled “P Wave”, followed shortly by a larger-amplitude arrival labeled “S Wave.” This station’s distance iss “1.5 minutes = 900 km away,” showing that the station is relatively close to the earthquake source.
- The middle seismogram is labeled “Isla Socorro, Mexico (SOCO)” in red text. Here, the P wave arrives earlier on the time axis than the S wave, but the gap between them is larger than at TEIG. This station is “3 minutes = 1800 km away,”; it is about twice as far from the earthquake as the first one.
- The rightmost seismogram is labeled “Standing Stone, Pennsylvania, USA (SSPA)” in green text. The P wave arrival occurs much earlier than the S wave, and the separation between them is the largest of the three stations. This station is “5 minutes = 3300 km away,”; it is the farthest from the earthquake source.

Across all three stations, P waves arrive first and have smaller amplitudes, while S waves arrive later and show larger oscillations. The increasing time gap between P and S waves from left to right visually demonstrates how seismologists use S–P time differences to calculate distance to an earthquake.

Figure 4.4.9 Triangulating Seismic Data

This image is a map-based diagram illustrating how an earthquake’s epicenter is located using triangulation from three seismic stations. The background is a shaded relief map showing North America, Central America, the Caribbean, and part of South America.

Three seismic stations are marked:

- Station TEIG is shown with a dot located near southern Mexico or Central America. A circle centered on TEIG is labeled “900 Kilometers.”
- Station SOCO is shown with a dot located offshore to the west, near Isla Socorro in the eastern Pacific Ocean. A circle centered on SOCO is labeled “1800 Kilometers.”
- Station SSPA is shown with a green dot in the eastern United States, near Pennsylvania. A arc extending from SSPA is labeled “3300 Kilometers.”

Each station serves as a reference point for distance measurements to the earthquake. Near southern Mexico, where the distance circles overlap, there is a target symbol marking the Earthquake Location. A black arrow and label point directly to this intersection, emphasizing that the epicenter is found where all three distance measurements coincide.

Box Figure 4.4.3 Simplified Fault Map of Southern California

This map lists some of the faults in Southern California, focusing on the southernmost region roughly between Los Angeles and the Mexican border. The faults shown are listed here in order of appearance on the map from left to right.

1. Santa Cruz Basin Fault runs between the Channel Islands
2. Newport - Inglewood fault runs along the coast, extending roughly from the Newport Beach area to south San Diego County
3. Malibu Coast Fault runs perpendicular to the coast, extending from an area just off the shore of Malibu inland to meet the San Gabriel Fault
4. San Gabriel Fault is a curving fault system extending northwest to northeast through the San Gabriel Valley
5. Elsinore Fault is inland from the Newport - Inglewood fault, running in roughly the sane northwest to northeast direction.
6. San Jacinto Fault sits roughly between the Elsinore Fault and the massive San Andreas Fault
7. San Andreas Fault is a complex system with many branches, one of which is labeled Pinto Mountain Fault
8. Salton Creek Fault is a small fault just inland of the San Andreas Fault and oriented roughly perpendicular to it

Figure 4.5.2 Diagrams of 1900s Seismometers

Two pendulum seismometers are shown, one in a horizontal orientation and the other in a vertical orientation. These sensors work by having a mass suspended on either a lever arm (horizontal) or from a spring (vertical). The mass is attached to a stylus or a pen, which scribes a line across paper on a rotating drum. The drum is on a threaded axle that is attached to a clock drive. This drive controls the drum's rotation.

Figure 4.5.8 Intensity map for the 1994 Northridge Earthquake

This map of California and Baja California shows the area from Fremont (in the San Francisco Bay Area) down to Ensenada (in Baja California). A small area of Nevada is also shown, with Las Vegas being the eastmost city identified. The epicenter lies beneath the San Fernando Valley, in Reseda, which is located approximately 20 miles NNW of Los Angeles.

The following information is provided at the top of the map.

- Macroseismic Intensity Map USGS
- Shake Map: 1 km NNW of Reseda, CA on January 17, 1994 at 12:30:55 UTC (Greenwich Mean Time)
- Coordinates: M6.7 N34.21 W118.54
- Depth: 18.2 km
- ID: ci3144585

Earthquake intensities are indicated by colored circles and shading, with details provided in a data table. The table here includes those data, plus the cities that experienced the intensities noted on the map.

Northridge Earthquake Intensity at Key Locations in California

Shaking	Damage	PGA (%g)	PGV (CM/S)	Intensity	Location
Not felt	None	<0.0464	<0.0215	I (1)	No unaffected areas
Weak	None	0.297	0.135	II-III (2 to 3)	Fresno, Las Vegas
Light	None	2.76	1.41	IV (4)	Fremont, San Jose, Salinas, Tijuana, Mexicali, Ensenada
Moderate	Very light	6.2	4.65	V (5)	San Diego, Santa Maria, Bakersfield
Strong	Light	11.5	9.64	VI (6)	Long Beach, Lancaster
Very Strong	Moderate	21.5	20	VII (7)	Los Angeles
Severe	Moderate/heavy	40.1	41.4	VIII (8)	San Fernando Valley
Violent	Heavy	74.7	85.8	IX (9)	San Fernando Valley, areas closest to epicenter
Extreme	Very Heavy	>139	>178	X+ (10+)	Reseda (epicenter)

Figure 4.5.9 National Seismic Hazard Map of the US

This 2023 map predicts the chance of shaking equivalent to Modified Mercalli Intensity VI or more from an earthquake during the next 100 years. The intensity scale in the legend is color coded from >95% to <5%. The areas with a greater than 95% chance include almost all of California east of the Sierras, most of south-central Alaska and the Aleutian Islands, and the Big Island of Hawaii.

Areas of a 75 to 95% chance include most of the rest of California with the exception of the Sierras, the Cascades, and the Modoc Plateau. Areas outside of California are western Nevada, the greater Seattle metropolitan area; the tri-state area where Missouri, Arkansas, and Tennessee meet; the Yellowstone area of Wyoming, Nevada, and Idaho; central Maui in Hawaii; the North Slope, and most of the rest of southern Alaska.

Areas of a 50 to 75% chance include the California Owens Valley and areas east of the Sierras, and the Cascades; the Oregon coast; the Washington Olympic Peninsula; the greater Port Clarence area and the Fort Yukon area of Alaska; Utah's Wasatch front; central Idaho; and the midcontinent area surrounding the junction of the tri-state area where Missouri, Arkansas, and Tennessee meet; and the rest of Maui, and the islands of Kahoolawe, Lanai, and western Molokai in Hawaii.

The rest of the United States has less than a 50% chance of experiencing such shaking.

Major population centers are also included on the map. Of note, the greater Seattle metropolitan area; the San Francisco Bay Area; and much of Los Angeles, Orange, and San Diego counties lie within high-risk areas (greater than 95% chance).

This page titled 4.7: Detailed Figure Descriptions is shared under a CC BY-NC 4.0 license and was authored, remixed, and/or curated by Allison Jones.

5: GEOLOGIC TIME

Introduction to Geologic Time

At the heart of geology is the story of Earth's past. Part of telling a good story is placing events in a sequential order. Geologists have almost always focused on reconstructing the order of geologic events based on relationships in the rocks and between rock units. This approach, when combined with a study of the relative relationships of units with fossil sequences, is the basis for the geologic time scale. This time scale can be considered like a calendar in which the largest subdivisions of time (Eons) are subdivided into Eras, which in turn are subdivided into Periods and Epochs. Epochs are then subdivided into early, late and middle sections and approximate ages in Ma are labeled. With the discovery of radioactivity around the turn of the 20th century, the relative order of events could be placed in a specific timeline, and rates of processes could be quantified. The determination of numerical (or absolute) ages for these minerals and the rocks in which they were found added an additional level of detail to our ability to reconstruct the geologic history of different terranes and the earth as a whole.

Before starting, consider the units of geologic time. Geologists measure events in Earth's history in years before the present date. They use certain conventions for abbreviating intervals of time. One thousand years is represented by the abbreviation "ka," which means "kilo-annum." The prefix "kilo-" means "thousand". A kilogram equals one thousand grams and a kilometer equals one thousand meters. "Annum" means "year." Similarly, one million years is represented by "Ma," meaning "mega annum." One billion years is abbreviated as "Ga" for "giga annum." As an example: dinosaur species went extinct at approximately 66 Ma. The process of assigning actual ages – in years before the present date – is referred to as numerical (absolute) dating.



Figure 5.1: Only once the concepts of relative and absolute ages are understood can landscapes like that of Yosemite Valley be fully appreciated. "Yosemite Valley" by rabesphoto is licensed under CC BY.

Learning Objectives

By the end of this chapter, you should be able to:

- Explain the difference between relative and absolute (numeric) dating.
- Describe major relative time Principles of Superposition, Original Horizontality, Lateral continuity, Cross-cutting Relations, Included Fragments, and Faunal Succession.
- Compare and contrast three major Unconformities (Angular Unconformities, Disconformities, and Nonconformities).
- Describe how radioisotopic dating is accomplished and the commonly used isotopic systems.
- List the Eons, Eras, and Periods of the geologic time scale and explain the basis behind the divisions.

5.1: Relative Dating
5.2: Unconformities
5.3: Dating Rocks Using Fossils
5.4: Absolute Dating of Geologic Materials
5.5: The Geologic Time Scale
5.6: Chapter Summary
5.7: Detailed Figure Descriptions

This page titled 5: Geologic Time is shared under a CC BY-NC 4.0 license and was authored, remixed, and/or curated by Martha House.

5.1: Relative Dating

Placing Events in Geologic Order Using Principles of Relative Dating

Relative dating is the process of determining whether one rock or geologic event is older or younger than another rather than determining a specific age. The fundamental principles of relative time were developed from the mid-1600's to the early 1800's by key players, including Nicolas Steno (1638-1686), James Hutton (1726-1797), and Charles Lyell (1797-1875), among many others. Once geologists realized that many geologic processes are slow, the concept that "the present is the key to the past" provided a basis for interpreting rocks of the Earth using scientific principles.

An important concept is the fact that strata (layers of rock) equate to events.

Stratigraphic Cross Sections: Interpreting the Geologic History

This video describes the way in which concepts of geologic time can be applied to the interpretation of a geologic region.

This interactive element is not available in this format. Visit the link or scan the QR code to access it online.

View this YouTube Video online

The following section reviews concepts that are applied to resolve the relative order of geologic events in the field. The key thing to remember here is that events = time (in other words, sequences of events take time, so an event can be equated to a period of time).

Relative Dating Principles

The following relative dating principles are useful in studying layered sedimentary rocks and volcanic units that are deposited at the Earth's surface.

Principle of Superposition

In an otherwise undisturbed sequence of sedimentary strata, or rock layers, the layers on the bottom are the oldest and layers above them are younger. In Figure 5.1.1, the horizontal layers of thick sedimentary rocks have been uplifted (in this case via the nearby Garlock fault) and eroded, but there is no indication of any other events affecting their position.



Figure 5.1.1: Layered sedimentary units of the Ricardo Group at Red Rock Canyon State Park in California. The oldest are on the bottom and the youngest are on the top. "Redrock Canyon" by Martha House, is licensed under CC BY-SA-NC.

Principle of Original Horizontality

Layers of rocks deposited from above, such as sediments and lava flows, are originally laid down horizontally. The exception to this principle is at the margins of basins, where the strata can slope slightly downward into the basin. The lower to middle Pliocene, lacustrine rocks of the Anaverde Formation in Figure 5.1.2, for example, were originally deposited in a horizontal fashion, but have contorted due to interactions with the nearby San Andreas and Little Lake Faults. Relative dating cannot determine the exact age or duration of the contortion, but we know it took time.



Figure 5.1.2: Folded Late Cenozoic sedimentary units are exposed on the northeast side of Highway 14 in Palmdale, CA. These rocks have been tilted due to their proximity to the San Andreas Fault. "Palmdale Roadcut" by Jens Bludau is licensed under CC BY-SA 4.0.

Principle of Lateral Continuity

Within the depositional basin, strata are continuous in all directions until they thin out at the edge of that basin. Of course, all strata eventually end, either by hitting a geographic barrier, such as a ridge, or when the depositional process extends too far from its source, either a sediment source or a volcano. Strata that are cut by a canyon later remain continuous on either side of

the canyon. The Grand Canyon strata in Figure 5.1.3, for example, can be seen to continue on the far side of the canyon.



Figure 5.1.3: Kaibab Fm., Mather Point, Grand Canyon National Park. Light units in the foreground are correlative with light units in the background, even though they are separated by the canyon. "Mather Point at Grand Canyon National Park in October 2015" by Tim Adams, is licensed under CC BY 3.0.

Not all geologic materials are deposited horizontally at the Earth's surface. For example, plutonic rocks and dikes do not form horizontal layers; they intrude into the rocks around them. And faults cut across older units. In order to recognize these events and the time they take, additional concepts are needed:

Principle of Cross-cutting Relationships

Deformation events like folds, faults and igneous intrusions that cut across rocks are younger than the rocks they cut across. Younger things cut older things. Figure 5.1.4 shows normal faults that cut the older Noonday Dolomite in Death Valley National Park. The faults are younger than all units they cut through.



Figure 5.1.4: Normal faults in Noonday Dolomite, Death Valley National Park. The dark layers in the center are truncated by the two inward dipping normal faults that drop the large tan block of Noonday Dolomite downward. The faults post-date the sedimentary units. "Normal faults in Noonday Dolomite, Death Valley National Park" by Marli Miller, by permission.

Principle of Inclusions

Inclusions are pieces of an older rock that are contained within a younger rock. These are often found in sedimentary rocks, but can also be found when igneous rocks intrude pre-existing rocks surrounding them (pieces of the country rock might be found within the intrusive rock. In general, the younger unit contains or envelops the older unit. The large glacial dropstone in Figure 5.1.5, for example, is from an original rock that is older than the Kingston Peak Fm. and is distinct from the surrounding rocks in that it is larger, more irregular in shape, and deforms the layers around it.



Figure 5.1.5: Glacial dropstone in Proterozoic diamictite of Kingston Peak Formation, SE California. "Glacial dropstone in Proterozoic diamictite of Kingston Peak Formation, SE California" by Marli Miller, by permission.

In addition to these concepts which apply to relative ordering of rock units, fossil remnants preserved in sedimentary rocks provide a means to link chronostratigraphic (time-correlative) units across large, sometimes global, distances.

Principle of Faunal Succession

Assemblages of fossils contained in strata are unique to the time they lived, and can be used to correlate rocks of the same age across a wide geographic distribution. Assemblages of fossils refers to groups of several unique fossils occurring together. When assemblages are found in short sequences, the overlap of portions of the sequences from place to place can be used to extend relative time constraints. For example, in (Figure 5.1.6), a sequence of geologic strata contains a particular sequence of fossil organisms. Another sequence of fossiliferous units is similar and can be correlated to the first set of units on the basis of the fossil succession, even though a unit might be missing from one of the sequences.

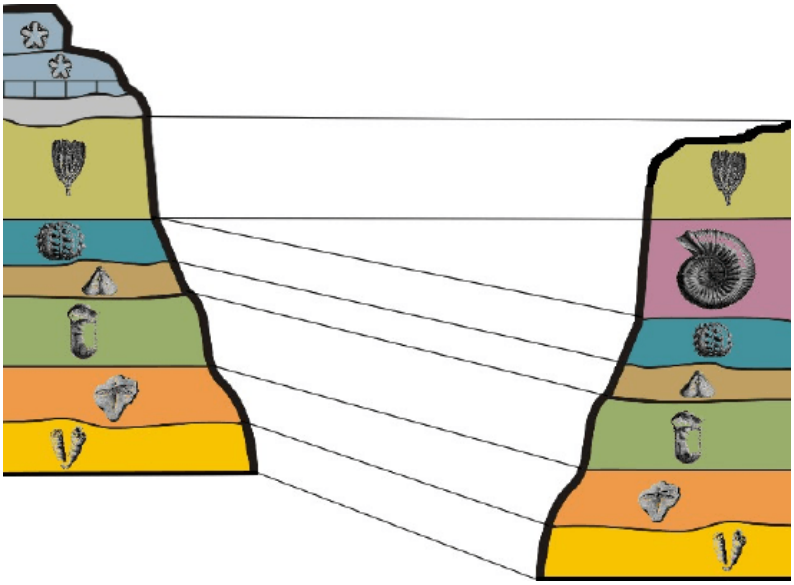


Figure 5.1.6: Fossil succession in two outcrops that are exposed on either side of a canyon. In each exposure of layered rocks, a distinctive sequence of fossils can be used for comparison of the outcrop sequences. The correlation of the units in the two areas can be done by comparing these sequences and noticing where a layer might be missing (based on the lack of a specific fossil). "Faunal Succession" by Paul Webb is licensed under CC BY-NC-SA. Access a detailed description.

Principle of Chilled Margins

When an igneous intrusion cools and crystallizes in the Earth, the portion that is on the edges, adjacent cold surrounding rock will form smaller crystals than the portion of the intrusion that cooled more slowly deeper in the intrusion. Sometimes, the smaller crystals appear darker in color than larger crystals, so a chilled margin appears as a darkening of the intrusive rock towards the surrounding rock. This principle can be used to distinguish between an igneous sill, which will have a chilled margin at top and bottom, and a lava flow, which will have a chilled margin only at the bottom.

Principle of Baked Contacts

Rocks that surround igneous intrusions are affected by the heat of these intrusions. As a result, rocks surrounding the intrusions, sometimes called the country rock or host rock, may be metamorphosed. The presence of a metamorphic aureole (zone) or “baked contact” indicates the intrusion is younger than the rocks around it. In contrast, if an intrusive igneous rock is exposed via erosion, then later buried by sediments, the surrounding rocks will not be baked, as the intrusion was already cold at the time of sediment deposition.

Query 5.1.1

This interactive element is not available in this format. Visit the link or scan the QR code to access it online.

View this Interactive Content online

Query 5.1.2

This interactive element is not available in this format. Visit the link or scan the QR code to access it online.

View this Interactive Content online

References

1. Bentley, C. (2020, January 17). *Historical Geology – A free online textbook for Historical Geology courses*. OpenGeology. Retrieved June 20, 2023, from https://opengeology.org/historicalgeology/
2. Deline, B., Harris, R., & Tefend, K. (2016). *Laboratory Manual for Introductory Geology*. University of North Georgia.
3. Earle, S. (2019). *Physical Geology*. BCcampus, BC Open Textbook Project.Johnson, C. (n.d.). *An Introduction to Geology – Free Textbook for College-Level Introductory Geology Courses*. OpenGeology. Retrieved June 20, 2023, from https://opengeology.org/textbook/
4. Johnson, C., Affolter, M. D., Inkenbrandt, P., & Mosher, C. (2019). *An Introduction to Geology*. Salt Lake Community College. https://slcc.pressbooks.pub/introgeology/
5. Kessell, L. (n.d.). *Palmdale road cut*. Strike Slip Faults. Retrieved June 16, 2023, from https://strike-slip.geol.ucsb.edu/KESSEL/palmdaleroadcut.html
6. Mathis, A., & Bowman, C. (2018, April 25). *Telling Time at Grand Canyon National Park (U.S*. National Park Service. Retrieved June 20, 2023, from https://www.nps.gov/articles/age-of-rocks-in-grand-canyon.htm
7. *Panchuk, K. (2023). Physical Geology – H5P Edition V1.1. University of Saskatchewan*. https://pressbooks.bccampus.ca/physicalgeologyh5p/
8. *Sedimentary – Geology Pics*. (n.d.). Geology Pics. Retrieved June 20, 2023, from https://geologypics.com/geological-item/sedimentary/

This page titled 5.1: Relative Dating is shared under a CC BY-NC 4.0 license and was authored, remixed, and/or curated by Martha House.

5.2: Unconformities

Types of Unconformities

There are three types of unconformities: nonconformity, disconformity, and angular unconformity.

A nonconformity occurs when sedimentary rock or volcanic lavas are deposited directly on top of crystalline intrusive igneous rocks or metamorphic rocks. In order for this situation to arise, considerable erosion must have occurred in order to bring the metamorphic or igneous intrusive rocks to the surface. The stages in the formation of a nonconformity are shown in Figure 5.2.1 , the formation of a nonconformity is demonstrated in three panels. At Time 1, a magma has intruded the lower layers of a group of horizontal sedimentary rocks. At Time 2, uplift and erosion at a later time have removed the horizontal sediments from above the (now) crystalline rock and exposed it's surface to the atmosphere. Finally, at Time 3, subsidence has led to deposition of new horizontally layered sedimentary rocks above the original crystalline igneous rock. The nonconformity is the boundary between the older igneous rock and the newly deposited sedimentary layers above it.

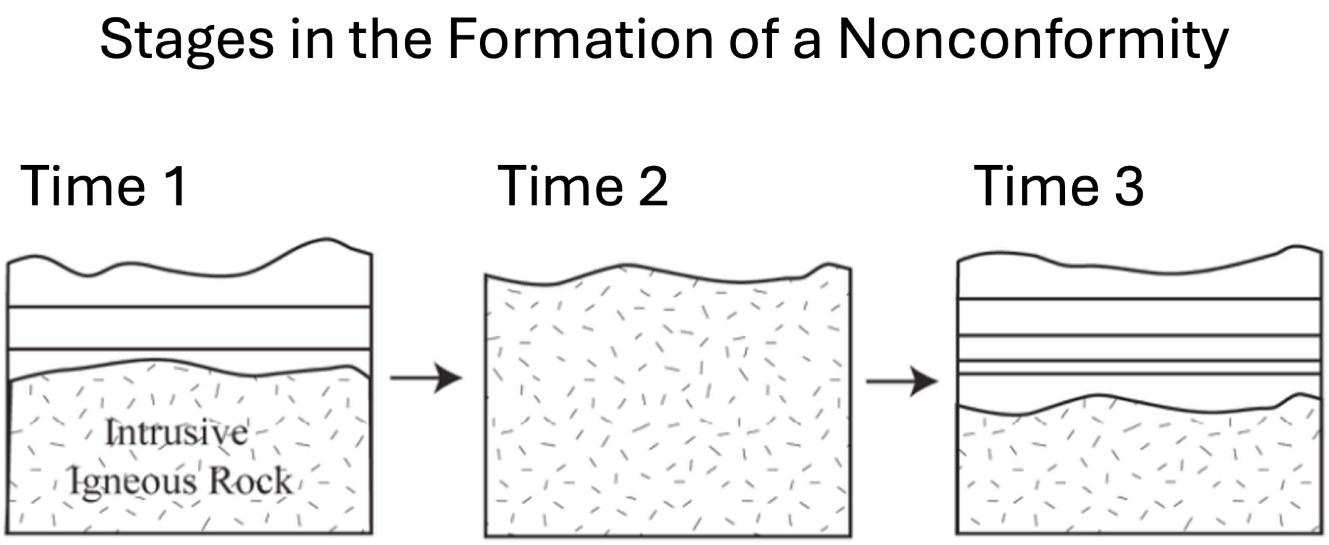


Figure 5.2.1: Stages in the formation of a nonconformity, which is created when an intrusive igneous rock or metamorphic rock is eroded and then new layers are deposited atop. The nonconformity separates the older eroded crystalline rocks from the younger horizontal strata above. "Stages in the Formation of a Nonconformity" by Martha House, a derivative of nonconformity, is licensed under CC BY-SA. Access a detailed description.

An angular unconformity can be recognized where horizontal sedimentary strata or volcanic lavas are deposited on a terrain of deformed sedimentary or volcanic strata that have been tilted, folded, and/or faulted so that they are no longer horizontal. The stages in the formation of an angular unconformity is depicted in Figure 5.2.2. At Time 1, layered horizontal sedimentary (or volcanic) rocks have been deposited. At Time 2, uplift, tilting and erosion at a later time have produced a sequence of tilted layers that outcrop at the surface. At Time 3, subsidence has led to the deposition of new horizontally layered sedimentary rocks above the older tilted strata. The angular unconformity is the boundary that separates the tilted layers from the horizontal sedimentary layers above.

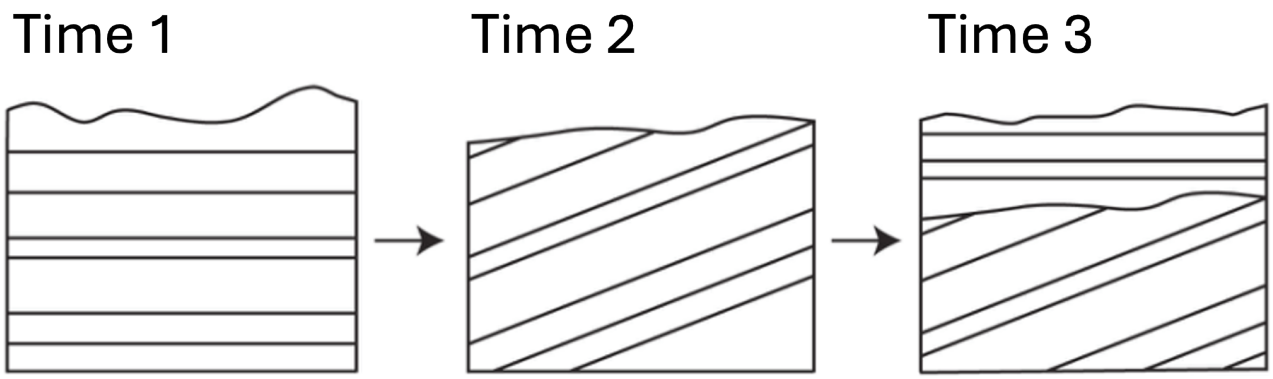


Figure 5.2.2: Stages in the formation of an angular unconformity, which is created when layered sedimentary rocks or volcanics are tilted and eroded and new horizontal sedimentary or volcanic layers are deposited atop; the angular unconformity separates the tilts strata from the younger horizontal strata above. "Stages in the Formation of an Angular Unconformity" by Martha House, a derivative of unconformity, is licensed under CC BY-SA. Access a detailed description.

A disconformity is created when either non-deposition or erosion took place. In other words, layers of rock that could have been present, are absent. The time that could have been represented by such layers is instead represented by the disconformity. A disconformity is an unconformity that occurs between parallel layers of strata indicating either a period of no deposition or a period of erosion. They can be recognized by subparallel surfaces and sometimes layers of distinctive sediments above and/or below the disconformity. The stages in the formation of a disconformity are depicted in Figure 5.2.3. At Time 1, layered horizontal sedimentary (or volcanic) rocks have been deposited. At Time 2, a sequence of horizontal layers that outcrop at the surface. Finally, at Time 3, subsidence has led to the deposition of new horizontally layered sedimentary rocks above the older horizontal strata. The disconformity is the subparallel line that separates the older horizontal layers from the horizontal sedimentary layers above.

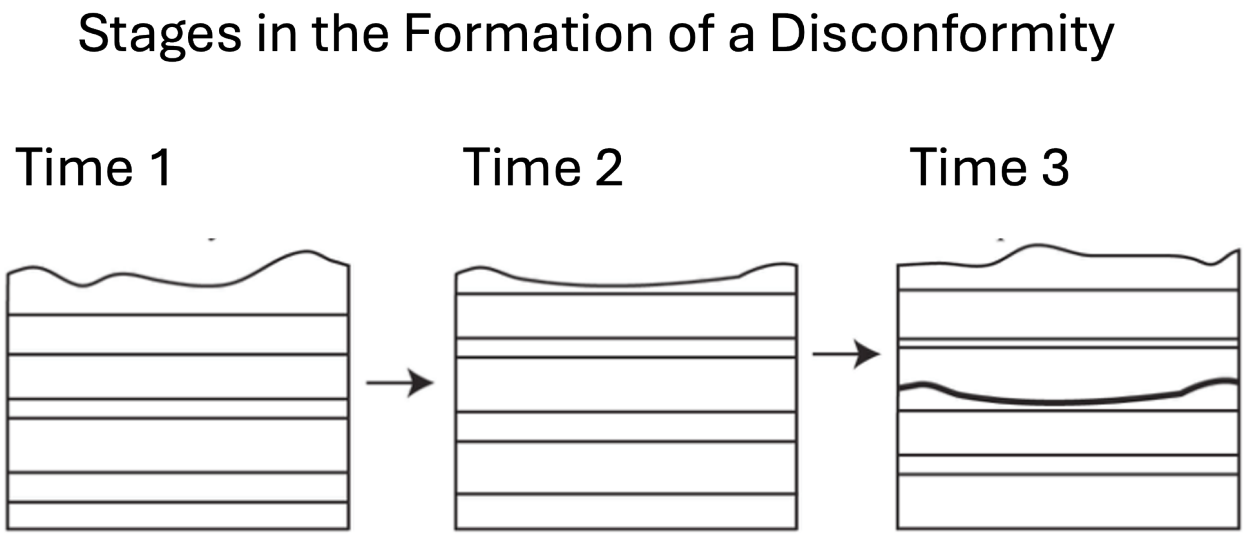


Figure 5.2.3: Stages in the formation of a disconformity, which is created when layered sedimentary rocks or volcanics are uplifted and eroded and new horizontal sedimentary or volcanic layers are deposited atop; the disconformity is subparallel to the horizontal layers above and below. "Stages in the Formation of a Disconformity" by Martha House, a derivative of disconformity, is licensed under CC BY-SA. Access a detailed description.

Query 5.2.1

This interactive element is not available in this format. Visit the link or scan the QR code to access it online.

View this Interactive Content online

The Grand Canyon

The Grand Canyon in Arizona is a natural geologic laboratory that can illustrate the major Principles of Cross-cutting Relationships, Superposition, and Original Horizontality, as well as the importance of recognizing unconformities in the study of a geologic region. Figure 5.2.4 shows a simplified cross-section of the rocks exposed on the walls of the Grand Canyon. These units are summarized in the table as well. Numbers in the images correspond to numbered units in the table and the text that follows.

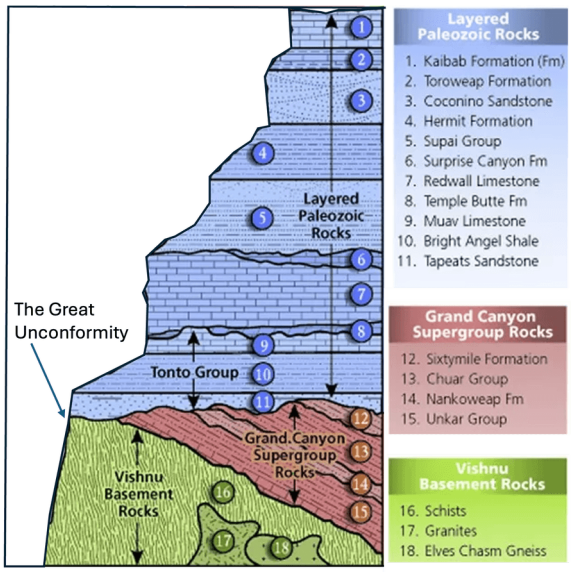


Figure 5.2.4: Cross section of Grand Canyon geologic units. A schematic cross-section of the strata exposed in the Grand Canyon illustrating very general geological relationships between the Precambrian Basement Rocks, the Precambrian Grand Canyon Supergroup rocks, and the overlying horizontal Paleozoic rocks of the Grand Canyon. This image is modified from "Grand Canyons three sets of rocks" by US Park Service, is licensed under public domain. Access a detailed description.

Simplified summary of strata and geologic relationships for the Grand Canyon as shown in Figure 5.2.4.

Unit Number in Figure 5.2.4	Geologic Unit/ Formation and Unconformity with approximate age gap	Description	Layer thickness in feet	Approximate Age in millions of years (Ma)
1	Kaibab Formation	Cliff forming, dominantly limestone that is Permian in age.	350	270
2	Toroweap Formation	Easily eroded, interbedded shale and limestone unit that is Permian in age.	250	273
3	Coconino Sandstone	Cliff forming cross-bedded sandstone, Permian in age.	300	275
4	Hermit Formation	Slope forming shale and siltstone unit that is Permian in age.	300	280
5	Supai Group	Slope forming shales and siltstones of Pennsylvanian age capped by ridge forming sandstone that is Permian in age. A 5-35 Ma disconformity separates it from the unit below.	1000	285-315

Unit Number in Figure 5.2.4	Geologic Unit/ Formation and Unconformity with approximate age gap	Description	Layer thickness in feet	Approximate Age in millions of years (Ma)
6	Surprise Canyon Formation	Limestone that is Mississippian in age. A 20 Ma disconformity separates it form the unit below.	0-75	320
7	Redwall Limestone	Cliff forming limestone that is Mississippian in age; a 45 Ma disconformity separates it from the unit below.	500	340
8	Temple Butte Formation	Dolomitic unit that is separated from unit below by a 120 Ma disconformity.	0-50	385
9	Muave Limestone	Cliff forming limestone that is the upper part of the Cambrian Tonto Group.	450	505
10	Bright Angel Shale	Slope forming shale unit.	350	515
11	Tapeats Sandstone	Basal cliff forming sandstone of the Tonto Group; unconformable with all units of the Grand Canyon Supergroup across a 215 Ma angular unconformity (the Great Unconformity)	0-200	575
12	Sixtymile Formation	Tilted upper shale unit of the Proterozoic Grand Canyon Supergroup. Separated form the underlying unit by a >30 Ma disconformity.	200	<740
13	Tilted Chuar Group	Tilted shale unit of the Proterozoic Grand Canyon Supergroup; disconformable with the underlying unit. The disconformity is 130-160 Ma.	5200	740-770
14	Nankoweap Formation	Tilted shale unit of the Proterozoic Grand Canyon Supergroup; disconformable with underlying unit. The disconformity is 200-300 Ma.	370	900
15	Unkar Group	Tilted shale and basal limestone unit of the Proterozoic Grand Canyon Supergroup; nonconformable with underlying basement rocks. The disconformity is 380-470 Ma.	6800	1100-1200
16, 17, 18	Vishnu Basement	Schists (#16), Gneisses (#17) and younger granites (#18); schists are in nonconformable contact with overlying Grand Canyon Supergroup rocks.	Unknown Thickness	1680-1840

In the lowest parts of the Grand Canyon, deformed Proterozoic igneous and metamorphic crystalline rocks form the "basement". The principle of cross-cutting relationships reveals the sequence of events in the basement rocks: the metamorphic schist (#16) is the oldest rock formation and the cross-cutting granite intrusion (#17) is younger. The Elves Chasm gneiss (#18) is intermediate to these units because it cuts the older schist and is intruded by the younger granite.

These ancient crystalline basement rocks (1680-1840 Ma in age) are unconformably overlain by the tilted Grand Canyon Supergroup (a series of layered sediments), which is roughly 1200-740 Ma in age. The nonconformity separating these groups of rocks could represent as much as 480 Ma of Earth's history! We know that the basement rock were brought to the surface by erosion and/or faulting, but we don't know much else from this section alone!

The overlying Grand Canyon Supergroup is a tilted sequence of limestones, shales and siltstones that is approximately 12570 ft thick. These units, which are all parallel to one another, are broken by three disconformities: the oldest separates the Unkar Group (#15) from the Nankoweap Formation (#14) and accounts for 200-300 Ma; the next is a gap of approximately 130-160 Ma between the Nakoweap and the overlying Chuar Group (#13); a final discontinuity is a gap of at least 30 Ma separating the Chuar Group from the overlying Sixtymile Formation (#12). Each of these disconformities could represent a period of non-deposition or deposition, followed by erosion. It's impossible to know without further study and it's impressive to keep in mind that we are in the dark about as much as 490 Ma of geologic time during the late Precambrian in this area!

The entire package of Precambrian Grand Canyon Supergroup Rocks and basement rocks in the lower part of the Grand Canyon

are unconformably overlain by a thick sequence of horizontal Paleozoic rocks which make up much of the Grand Canyon. Where these rocks rest on the tilted Grand Canyon Supergroup units, this "Great Unconformity" defines an angular unconformity representing a gap of approximately 215 Ma Figure 5.2.5.



Figure 5.2.5: The great angular unconformity in the Grand Canyon, Arizona. Horizontal Paleozoic sedimentary rocks rest atop tilted Proterozoic layers below. The tilted rocks at the bottom are part of the Proterozoic Grand Canyon Group (aged 825 to 1,250 Ma). The flat-lying rocks at the top are Paleozoic (540 to 250 Ma). The boundary between the two represents a time gap of hundreds of millions of years. "Great Angular Unconformity" by Steven Earl is licensed under CC-BY.

In some areas, horizontal Paleozoic rocks rest directly upon the basement units, forming a nonconformity, which can be seen between the Vishnu Schist (basement) and the overlying Tapeats Sandstone Figure 5.2.6.

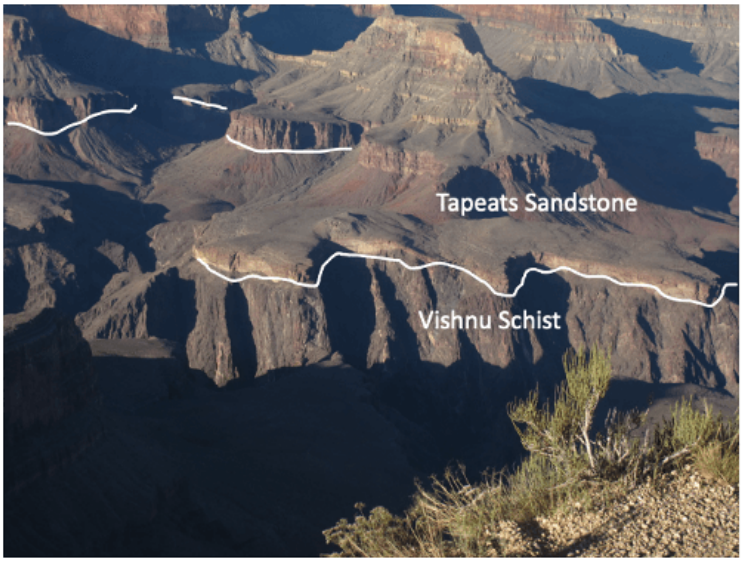


Figure 5.2.6: View from Hopi Point of the Great Unconformity. The Cambrian Tapeats sandstone rests atop the steeply foliated and veined late Paleoproterozoic to early Mesoproterozoic Vishnu Basement Rocks. A nonconformity separates the Vishnu basement and Tapeats Sandstone. "View from Hopi Point" by Martha House, a derivative from the Tapeats Sandstone, is licensed under CC BY-SA 4.0.

The Paleozoic rocks of the Grand Canyon are horizontal limestones, shales, siltstones, sandstones and some dolomites with an overall thickness of roughly 3500-3825 ft. and spanning approximately 300 Ma. In the figure and table, the other layers on the walls of the Grand Canyon are numbered with #1 (the Permian Kaibab Formation) being the youngest and the last to form, and #11 (the Cambrian Tapeats Sandstone) the earliest of this group. This sequence illustrates the Principle of Superposition. The

Colorado River carves through the Colorado Plateau, exposing the horizontal strata. The layers can be followed from one side of the canyon to the other, illustrating the Principle of Lateral Continuity. These rock strata have been barely disturbed from their original deposition, except by a broad regional uplift.

Most of these rocks are conformable with one another except for units immediately above and below the cliff-forming Red Wall Limestone. This prominent unit (approx. 500 ft thick) is bound by disconformities above it and below, and the relatively thin unit above (the 320 Ma Surprise Canyon Formation) and below (the 385 Ma Temple Butte Formation) are, in turn, separated from older and younger units by disconformities. Together, these four disconformities (two that bound the Surprise Canyon Formation and two that bound the Temple Butte Formation) account for as much as 225 Ma of geologic time (160 Ma below the Red Wall Limestone and as much as 65 Ma above it). This is a significant fraction of the entire period of the entire 300 Ma represented by the Paleozoic rocks of the Grand Canyon!

A closeup of a younger disconformity in New Mexico gives an idea of what these features look like in the field. Notice the parallel layers of sedimentary rocks and the slightly angled boundary between the Chinle Group (lower) and the Entrada Sandstone above (Figure 5.2.7). Close examination of surfaces like this sometimes reveals pebble layers or evidence of surface exposure (oxidation, for example).

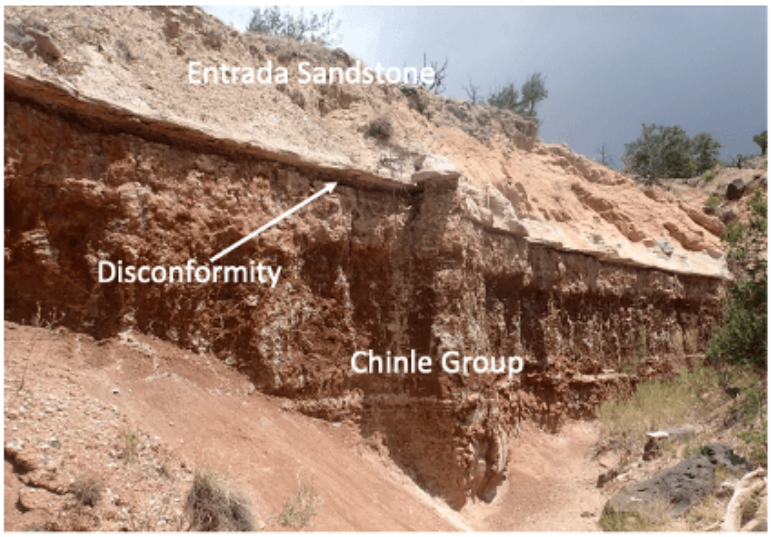


Figure 5.2.7: This image shows an exposure of Rock Point Formation of the Chinle Group capped by Entrada Formation sandstone in which an erosional disconformity separates the horizontal sedimentary layers. The Entrada Sandstone is a Jurassic formation, separated from the lower unit by the regional J-2 disconformity, a gap of about 45 million years in the geologic record. "Rock Point Formation" by Martha House,a derivative from the Rock point formation, is licensed under CC0.

Video 5.2.2: When a Billion Years Disappeared

This video dives into the discovery of the Great Unconformity and discusses the significance of the missing time it represents.

This interactive element is not available in this format. Visit the link or scan the QR code to access it online.

View this YouTube Video online

Query 5.2.2

This interactive element is not available in this format. Visit the link or scan the QR code to access it online.

View this Interactive Content online

Query 5.2.3

This interactive element is not available in this format. Visit the link or scan the QR code to access it online.

View this Interactive Content online

References

1. Bentley, C. (2020, January 17). *Historical Geology – A free online textbook for Historical Geology courses*. OpenGeology. Retrieved June 20, 2023, from https://opengeology.org/historicalgeology/
2. Deline, B., Harris, R., & Tefend, K. (2016). *Laboratory Manual for Introductory Geology*. University of North Georgia.
3. Earle, S. (2019). *Physical Geology*. BCcampus, BC Open Textbook Project.Johnson, C. (n.d.). *An Introduction to Geology – Free Textbook for College-Level Introductory Geology Courses*. OpenGeology. Retrieved June 20, 2023, from https://opengeology.org/textbook/
4. Johnson, C., Affolter, M. D., Inkenbrandt, P., & Mosher, C. (2019). *An Introduction to Geology*. Salt Lake Community College. https://slcc.pressbooks.pub/introgeology/
5. Mathis, A., & Bowman, C. (2018, April 25). *Telling Time at Grand Canyon National Park (U.S.* National Park Service. Retrieved June 20, 2023, from https://www.nps.gov/articles/age-of-rocks-in-grand-canyon.htm
6. *Panchuk, K. (2023). Physical Geology – H5P Edition V1.1. University of Saskatchewan.* https://pressbooks.bccampus.ca/physicalgeologyh5p/
7. *Sedimentary – Geology Pics*. (n.d.). Geology Pics. Retrieved June 20, 2023, from https://geologypics.com/geological-item/sedimentary/

This page titled 5.2: Unconformities is shared under a CC BY-NC 4.0 license and was authored, remixed, and/or curated by Martha House.

5.3: Dating Rocks Using Fossils

Geologic Range and Faunal Succession

The oldest undisputed fossils on Earth are from rocks dated around 3.5 Ga. Although fossils this old are tiny, typically poorly preserved, and often not useful for dating rocks, they can still provide important information about conditions at the time they were buried. The oldest well-understood fossils are from rocks dating back to around 600 Ma, and the sedimentary record from that time forward is rich with fossil remains that provide a detailed record of the history and evolution of life on Earth.

Fossils alone cannot provide us with numerical ages of rocks, but over the past century geologists have acquired enough isotopic dates from rocks associated with fossil-bearing rocks (such as igneous dikes cutting through sedimentary layers, or volcanic layers between sedimentary layers) to be able to put specific age limits on most fossils.

If we understand the sequence of evolution on Earth, we can apply that knowledge to determining the relative ages of rocks. This is what the Principle of Faunal (Fossil) Succession is built upon.

If we can identify a fossil to the species level, or at least to the genus level, and we know the time period in which the organism lived, we can assign a range of time to the rock. That range might be several million years because some organisms survived for a very long time. If the rock we are studying has several types of fossils in it, and we can assign time ranges to several of them, we might be able to narrow the time range for the age of the rock considerably.

Some organisms survived for a very long time, and are not particularly useful for dating rocks. Sharks, for example, have been around for over 400 million years. This is not a useful range: if you find a shark fossil in a sedimentary layer, it only tells you, “This layer is 400 million years old, or younger.” However, the great white shark has a range of 16 million years, so far, which is a much shorter amount of time. Organisms that lived for relatively short time periods are particularly useful for dating rocks, especially if they were distributed over a wide geographic area, and so can be used to compare rocks from different regions. These are known as index fossils. There is no specific limit on how short the time span has to be to qualify as an index fossil. Some lived for millions of years, and others for much less than a million years.

A geoscientist can also date rocks using the geologic ranges of a fossil assemblage from a single sedimentary layer. A fossil assemblage (or faunal assemblage) is a group of organisms that are all found fossilized together in that layer. This application involves the bracketing of overlapping ranges to constrain the age of a rock based on several fossils (Figure 5.3.1). Imagine that four species of fossils (A, B, C, D) were collected from one stratum. Imagine that fossil species A lived between 14-7 Ma, fossil species B lived between 12-4.5 Ma, fossil species C lived between 9.5-1 Ma, and fossil species D lived between 8.3-3 Ma. If these geologic ranges for each species are plotted side by side in a geologic range chart where each range is depicted as a bar, the overlap of the species can be determined. Comparison of these geologic ranges shows only a short time interval (from 8.3-7 Ma) when all four species overlap. Therefore, we can narrow down the likely age of the rock to just 700,000 years during which all four species coexisted.

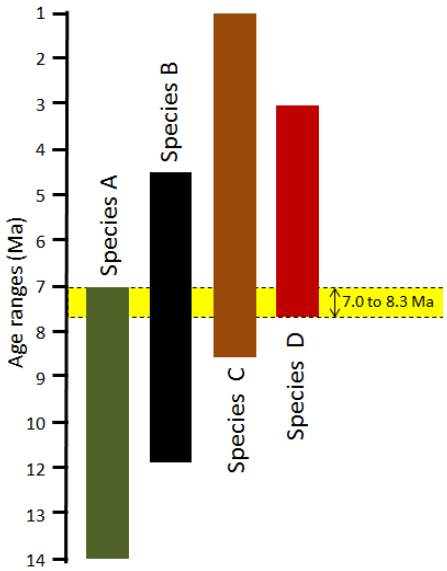


Figure 5.3.1: Geologic Range Chart. The application of bracketing to constrain the age of a rock based on several fossils. In this diagram, the colored bars represent the time range during which each of the four species (A, B, C, D) existed on Earth. Although each species lived for several million years, we can narrow down the likely age of the rock to just 700,000 years during which all four species coexisted. "Geologic Range Chart" by Steven Earle vs licensed under CC BY. Access a detailed description.

Smilodon californicus: California's State Fossil

The "saber-toothed cat," *Smilodon*, is the California State Fossil and the second most common fossil mammal found in the La Brea tar pits (see the Transverse Ranges Province for more information on the La Brea tar pits). Hundreds of thousands of *Smilodon* bones have been found at La Brea since they were first identified in 1932. These finds have permitted remarkably detailed reconstructions of how *Smilodon* lived. We now know *Smilodon* was about a foot shorter than living lions but was nearly twice as heavy. Also, unlike cheetahs and lions (which have long tails that help provide balance when the animals run) *Smilodon* had a bobtail. These suggest that *Smilodon* did not chase down prey animals over long distances as lions, leopards, and cheetahs do. Instead, it probably charged from ambush, waiting for its prey to come close before attacking.

Smilodon is a relatively recent sabertooth, from the Late Pleistocene. It went extinct about 10,000 years ago. Fossils have been found all over North America and Europe. *Smilodon* fossils from the La Brea tar pits include bones that show evidence of serious crushing or fracture injuries, or crippling arthritis and other degenerative diseases. Such problems would have been debilitating for the wounded animals. Yet many of these bones show extensive healing and regrowth indicating that even crippled animals survived for some time after their injuries. How did they survive? It seems most likely that they were cared for, or at least allowed to feed, by other saber-toothed cats. Solitary hunters with crippling injuries would not be expected to live long enough for the bones to heal. *Smilodon* appears to have lived in packs and had a social structure like modern lions. They were unlike tigers and all other living cats, which are solitary hunters. Occasional finds of sabertooth-sized holes in *Smilodon* bones suggest the social life of *Smilodon* was not always peaceful. The cats may have fought over food or mates as lions do today. Such fights were probably accompanied by loud roaring. From the structure of the hyoid bones in the throat of *Smilodon*, we know it could roar.



Figure 5.3.2: Smilodon californicus, a saber-tooth cat fossil extracted from and on display at the La Brea Tar Pits in Los Angeles, California. This work by Allison Jones is licensed under CC BY 4.0.

Biozones

Some well-studied groups of organisms qualify as biozone fossils (a stratigraphic interval that can be defined on the basis of a specific fossil) because, although the genera and families lived over a long time, each species lived for a relatively short time and can be easily distinguished from others on the basis of specific features. For example, ammonoids have a distinctive feature known as a suture line—where the internal shell layers (septae) that separate the individual chambers meet the outer shell wall. These suture lines are sufficiently variable to identify species and can be used to estimate the age of ammonite fossils, and thus the rocks in which they are found. Generally, the more complex the suture pattern, the younger the fossil. Figure 5.3.2 and the following table demonstrate how these features appear in different specimens and how they are correlated to periods of geologic time. This figure compares three different ammonites: Goniatites, Ceretites and the youngest one, Ammonites. These ammonites have distinctive septae patterns that can be used to identify them and they are known to have lived at distinctive time periods such that they can be used as indicators of time.

Table 5.3.1: Ammonite ages and suture patterns used to bracket ages as shown in Figure 5.3.2.

Fossil Name	Fossil patterns	Fossil age Range
Ammonites	Alternating saddles and lobes that are complex with sub-saddles and sub-lobes superimposed upon them.	Middle Triassic through Upper Cretaceous
Ceretites	Alternative smooth and rounded saddles and lobes that are more regular in shape than those of Goniatites.	Early Permian through Latest Triassic
Goniatites	Simple but irregularly shaped saddles separated by lower lobes.	Early Devonian through latest Permian

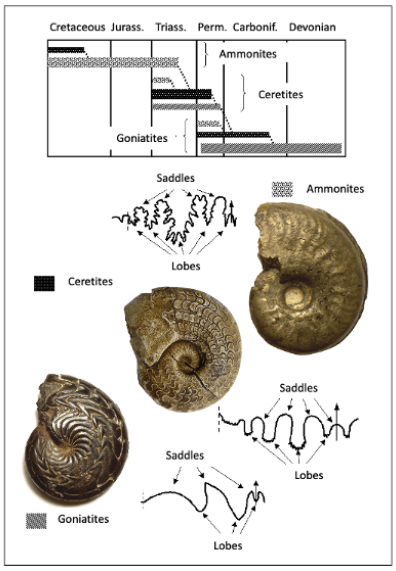


Figure 5.3.3: The main sutural patterns of Ammonoidea (ammonites), and relative distribution in time and within the principal taxonomic groups. Line drawings next to each image depict the suture patterns of that organism. This work by Martha House, a derivative from the Ammonites main sutural pattern, is in the public domain. Access a detailed description.

Query 5.3.1

This interactive element is not available in this format. Visit the link or scan the QR code to access it online.

View this Interactive Content online

References

1. Bentley, C. (2020, January 17). *Historical Geology – A free online textbook for Historical Geology courses*. OpenGeology. Retrieved June 20, 2023, from https://opengeology.org/historicalgeology/
2. Carroll, R.L. 1988. *Vertebrate Paleontology and Evolution*. W.H. Freeman & Co., New York.
3. Deline, B., Harris, R., & Tefend, K. (2016). *Laboratory Manual for Introductory Geology*. University of North Georgia.
4. Earle, S. (2019). *Physical Geology*. BCcampus, BC Open Textbook Project.Johnson, C. (n.d.). *An Introduction to Geology – Free Textbook for College-Level Introductory Geology Courses*. OpenGeology. Retrieved June 20, 2023, from https://opengeology.org/textbook/
5. Johnson, C., Affolter, M. D., Inkenbrandt, P., & Mosher, C. (2019). *An Introduction to Geology*. Salt Lake Community College. https://slcc.pressbooks.pub/introgeology/
6. Mestel, R. 1993. Saber-toothed tales. *Discover*, April, pp. 50-59.
7. Radinsky, L., and S. Emerson. 1982. The late, great sabertooths. *Natural History* 91(4).

This page titled 5.3: Dating Rocks Using Fossils is shared under a CC BY-NC 4.0 license and was authored, remixed, and/or curated by Martha House.

5.4: Absolute Dating of Geologic Materials

Numerical Ages

Numerical (also known as absolute) dating deals with assigning actual dates (in years before the present) to geological events. Contrast this with relative dating, which instead is concerned with determining the order of events in Earth's past. The science of absolute age dating is known as geochronology and the fundamental method of geochronology is radiometric dating (also known as isotopic dating).

Absolute ages of rocks are determined from rates of radioactive decay of some isotopes of elements that occur naturally in rocks. These absolute ages might correspond to the crystallization age of a rock, the metamorphic age of a rock, or the time that has elapsed since a once-living organism died. There are a range of tools for these studies which will be discussed after a brief review of the chemistry associated with them.

Elements and Isotopes

An element is a particular kind of atom that is defined by the number of protons that it has in its nucleus. The number of protons equals the element's atomic number. Have a look at the periodic table of the elements below. Carbon's (C) atomic number is 6 because it has six protons in its nucleus; gold's (Au) atomic number is 79 because it has 79 protons in its nucleus (Figure 5.4.1).

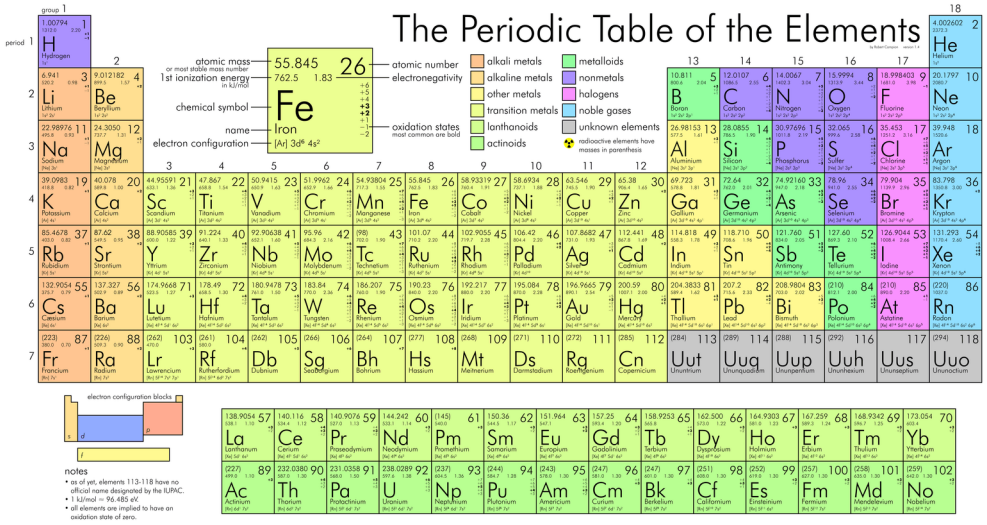


Figure 5.4.1: The periodic table of the elements of the world, showing element names, oxidation states, electron negativities, first ionization energies, and electron configurations. Periodic table large" by 2012rc, is licensed under public domain. A fully accessible version is also available.

Even though individual elements always have the same number of protons, the number of neutrons in their nuclei sometimes varies. These variations are called isotopes. Isotopes of individual elements are defined by their mass number, which is simply the number of protons plus the number of neutrons.

Consider, for example, the following three different isotopes of carbon as a demonstration of this concept:

- Carbon-12 (^{12}C): 6 protons, 6 neutrons
- Carbon-13 (^{13}C): 6 protons, 7 neutrons
- Carbon-14 (^{14}C): 6 protons, 8 neutrons

Figure 5.4.2 illustrates the arrangement of protons, neutrons and electrons in these carbon isotopes.

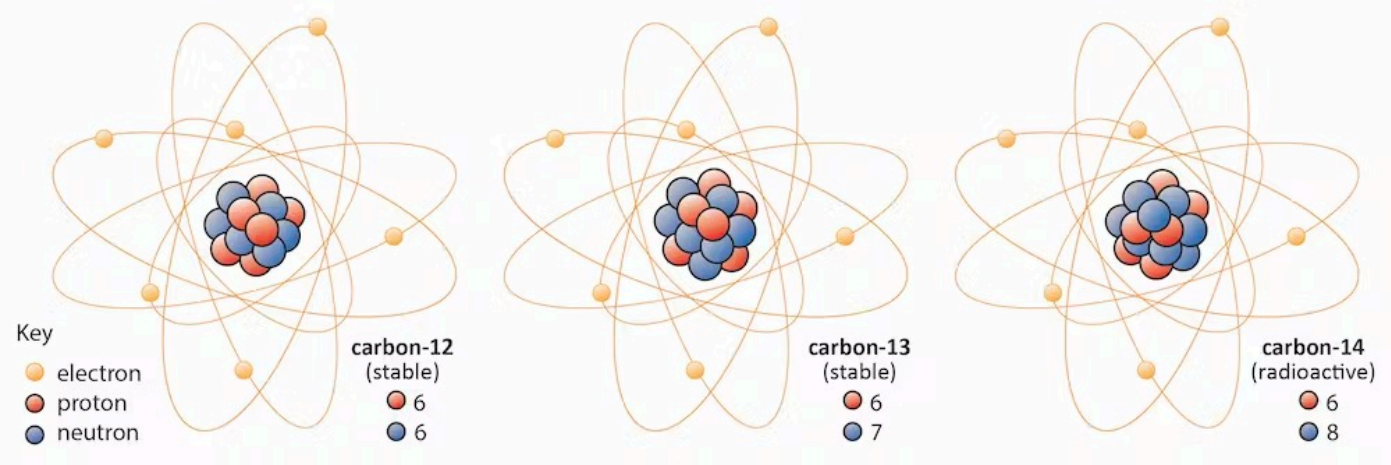


Figure 5.4.2: Three isotopes of carbon each have the same number of electrons (6) which orbit the nucleus within schematic electron shells. Each nucleus consists of 6 protons, but each isotope has a different number of neutrons as described in the text. Both Carbon-12 and Carbon-13 are stable, but Carbon-14 is radioactive. "The three isotopes of carbon" by Tessa Koumoundouros, is licensed under CC-ND 2.0. Access a detailed description.

Radioactive Decay

While many common isotopes are stable, meaning that they do not change, or decay, over time, some isotopes are unstable and undergo radical change through the process of radioactive decay. When these isotopes, called “radioisotopes”, decay, they shed energy in the form of radiation and subatomic particles which causes changes to their numbers of protons and neutrons. Once the number of protons changes, the isotope is no longer the same element. Ultimately, radioisotopes will decay to form a different, stable element. The atomic nucleus that undergoes radioactive decay is known as the parent and the resulting stable element, the daughter product (or, decay product).

One cannot predict the radioactive decay of any individual atom, however because rock samples contain trillions of atoms, the overall pattern becomes statistically predictable. For example, in a hand sample of uranium ore, you don't know which individual uranium atom will decay next, but when you put a Geiger counter next to a sample you hear a continuous stream of radioactivity.

However, some rock specimens have an enormous number of radioactive isotopes, perhaps trillions of atoms, and this large group of radioactive isotopes does have a predictable pattern of radioactive decay. The radioactive decay of half of the radioactive isotopes in this group takes a specific amount of time. The time it takes for half of the atoms in a substance to decay is called the half-life. In other words, the half-life of an isotope is the amount of time it takes for half of a group of unstable isotopes to decay to a stable isotope. The half-life is constant and measurable for a given radioactive isotope, so it can be used to calculate the age of a rock.

Returning to the carbon example in the previous section, consider that there are 15 total isotopes of carbon. Most naturally occurring carbon is stable ^{12}C (98.9%) or ^{13}C (1.09%). The remainder of naturally occurring carbon, including ^{14}C, is unstable and decays to form new elements. For example, carbon-14 (^{14}C) decays to nitrogen-14 (^{14}N); the half life of this decay is 5,730 years.

The principles behind numerical dating of geologic materials require three key assumptions.

1. The mineral grains containing the isotope formed at the same time as the rock, such as minerals in an igneous rock that crystallized from magma.
2. The mineral crystals remain a closed system, meaning they are not subsequently altered by elements moving in or out of them after they crystallize.
3. The only daughter isotopes present in the mineral crystal are created by radioactive decay of the parent (or there is a means to determine the original amount present).

These requirements place some constraints on the kinds of rock suitable for this type of dating, with igneous rock being the best. For example, igneous pyroclastic layers and lava flows within a sedimentary sequence can be used to date the sequence. Cross-cutting igneous rocks such as sills can be used to bracket the ages of affected, older sedimentary rocks. Igneous pyroclastic layers and lava flows within a sedimentary sequence can be used to date the sequence.

Metamorphic rocks are crystalline, but the processes of metamorphism may reset the clock and derived ages may represent a smear of different metamorphic events rather than the age of original crystallization.

Detrital sedimentary rocks are made from the pieces of older rocks and sometimes those pieces can be radiometrically dated; however, if we do that, then we learn the age of those pieces rather than when they came together into the sedimentary rock. In fact, the resistant mineral zircon, found as clasts in many ancient sedimentary rocks, has been successfully used for establishing very old dates, including the age of Earth's oldest known rocks. Knowing that zircon minerals in metamorphosed sediments came from older rocks that are no longer available for study, scientists can date zircon to establish the age of the pre-metamorphic source rocks.

Radioactive Decay

This short video reviews the concept of Radioactive Decay.

This interactive element is not available in this format. Visit the link or scan the QR code to access it online.

View this YouTube Video online

Types of Radioactive Decay

There are several ways radioactive atoms decay; three that are most relevant for geologic applications are discussed below.

Alpha decay occurs when an alpha particle, which consists of two protons and two neutrons, is emitted from the nucleus of an atom (Figure 5.4.3). This also happens to be the nucleus of a helium atom; helium gas may get trapped in the crystal lattice of a mineral in which alpha decay has taken place. When an atom loses two protons from its nucleus, lowering its atomic number, it is transformed into an element that is two atomic numbers lower on the Periodic Table of the Elements.

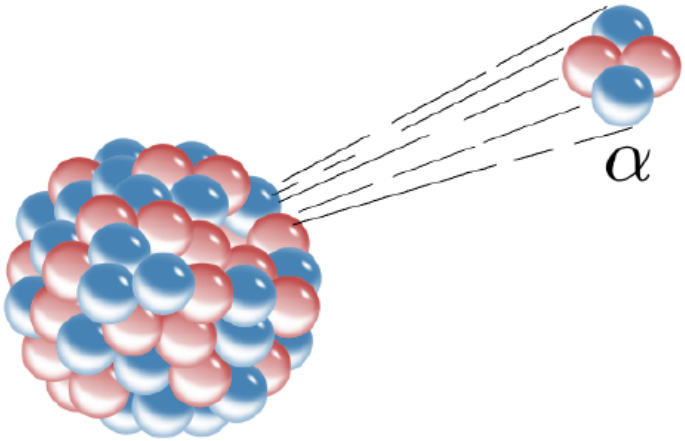


Figure 5.4.3: A diagram showing an alpha particle (α), consisting of two protons (red) and two neutrons (blue) being ejected from the nucleus of an atom, which consists of a mixture of protons and neutrons. "Alpha Decay" by Inductiveload, is licensed under public domain. Access a detailed description.

The loss of four particles, in this case two neutrons and two protons, also lowers the mass of the atom by four. For example alpha decay takes place in the unstable isotope ^{238}U, which has an atomic number of 92 (92 protons) and mass number of 238 (total

of all protons and neutrons). When ^{238}U spontaneously emits an alpha particle, it becomes thorium-234 (^{234}Th). The radioactive decay product of an element is called its daughter isotope and the original element is called the parent isotope. In this case, ^{238}U is the parent isotope and ^{234}Th is the daughter isotope. The half-life of ^{238}U is 4.5 billion years, i.e., the time it takes for half of the parent isotope atoms to decay into the daughter isotope. This isotope of uranium, ^{238}U, can be used for absolute dating the oldest materials found on Earth, and even meteorites and materials from the earliest events in our solar system.

Beta decay occurs when a neutron in its nucleus splits into an electron and a proton. The electron is emitted from the nucleus as a beta ray. The new proton increases the element's atomic number by one, forming a new element with the same atomic mass as the parent isotope. For example, ^{234}Th is unstable and undergoes beta decay to form protactinium-234 (^{234}Pa), which also undergoes beta decay to form uranium-234 (^{234}U). Notice these are all isotopes of different elements but they have the same atomic mass of 234. The decay process of radioactive elements like uranium keeps producing radioactive parents and daughters until a stable, or non-radioactive, daughter is formed. Such a series is called a decay chain. The decay chain of the radioactive parent isotope ^{238}U is extensive and progresses through a series fourteen different decay steps that include both alpha and beta decays and produce a range of different elements (some of which are extremely short-lived), until it forms the stable daughter isotope, lead-206 (^{206}Pb).

Electron capture is when a proton in the nucleus captures an electron from one of the electron shells and becomes a neutron. This produces one of two different effects: 1) an electron jumps in to fill the missing spot of the departed electron and emits an X-ray, or 2) another electron is released and changes the atom into an ion. The atomic number is reduced by one and mass number remains the same. An example of an element that decays by electron capture is potassium-40 (^{40}K). Radioactive 40K makes up a tiny percentage (0.012%) of naturally occurring potassium, most of which are not radioactive. Potassium-40 decays to argon-40 (^{40}Ar) with a half-life of 1.25 billion years, so it is very useful for dating geological events. Below is a table of some of the more commonly-used radioactive dating isotopes and their half-lives.

Table of common radioisotopes and their half lives.

Elements	Parent symbol	Daughter symbol	Half-life
Potassium-40/Argon-40*	^{40}K	^{40}Ar	1.25 billion years
Uranium-238/Lead-206	^{238}U	^{206}Pb	4.5 billion years
Rubidium-87/Strontium-87	^{87}Rb	^{87}Sr	48.8 billion years
Carbon-14/Nitrogen-14	^{14}C	^{14}N	5,730 years
Uranium-235/Lead-207	^{235}U	^{207}Pb	704 million years

*$^{40}Ar/^{40}K$ is closely related to $^{40}Ar/^{39}Ar$ dating; both are in use today.

Radio-isotope Dating

For a given sample of rock the dating procedure begins with the chemical extraction of the parent and daughter isotopes from a mineral. Then the isotopes are measured; in the case of uranium, ^{238}U and ^{235}U isotopes are separated out together, as are the ^{206}Pb and ^{207}Pb with an instrument called a mass spectrometer.

Once the parent and daughter are measured, the age is calculated. The process of measuring the amount of parent and daughter and calculating an age can be quite complex and there are different considerations for each of the different systems listed on the table above.

For our purposes, we'll consider a simple example in which one parent decays to form one daughter isotope. When the mineral initially forms, it consists of 0% daughter and 100% parent isotope, so the daughter-to-parent ratio (D/P) is 0. After one half-life, half the parent has decayed so there is 50% daughter and 50% parent, a 50/50 ratio, with D/P = 1. After two half-lives, there is 75% daughter and 25% parent (75/25 ratio) and D/P = 3. (Figure 5.4.4).

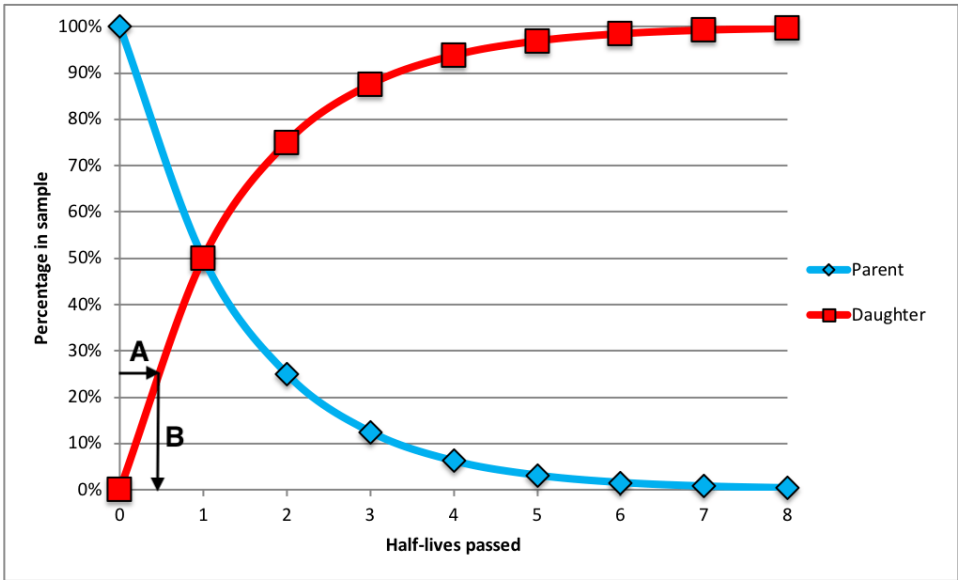


Figure 5.4.4: Percentage of parent and daughter remaining as a function of half-life. When 0.5 half-lives have passed, the sample contains approximately 25% daughter and 75% parent; the D/P ratio is ⅓. "Radioactive Decay Curve Diagram" by Callan Bentley, is licensed under CC BY-NC 4.0. Access a detailed description.

Modern applications of this method have achieved remarkable accuracies of plus or minus two million years in 2.5 billion years (that's ± 0.055%). Applying the uranium/lead technique in any given sample analysis provides two separate clocks running at the same time, ^{238}U and ^{235}U. The existence of these two clocks in the same sample gives a cross-check between the two. Many geological samples contain multiple parent/daughter pairs, so cross-checking the clocks confirms that radioisotopic dating is highly reliable.

Another radioisotopic dating method involves carbon and is useful for dating archeologically important samples containing organic substances like wood or bone. Radiocarbon dating, also called carbon dating, uses the unstable isotope carbon-14 (^{14}C) and the stable isotope carbon-12 (^{12}C). Carbon-14 is constantly being created in the atmosphere by the interaction of cosmic particles with atmospheric nitrogen-14 (^{14}N). Cosmic particles such as neutrons strike the nitrogen nucleus, kicking out a proton but leaving the neutron in the nucleus. The collision reduces the atomic number by one, changing it from seven to six, changing the nitrogen into carbon with the same mass number of 14. The ^{14}C quickly bonds with oxygen (O) in the atmosphere to form carbon dioxide ($^{14}CO_2$) that mixes with other atmospheric carbon dioxide ($^{12}CO_2$) and this mix of gasses is incorporated into living matter. While an organism is alive, the ratio of $^{14}C/^{12}C$ in its body is in equilibrium with respect to the ratio in the environment because CO_2 is constantly exchanged with the atmosphere. However, when the organism dies, the organism is no longer taking in carbon and excreting carbon, and the $^{14}C/^{12}C$ in its body gradually changes as the ^{14}C decays back to ^{14}N by beta decay. This process is the basis of this "clock", which has a half-life of 5,730 years.

The radiocarbon dating technique relies upon the world's most sensitive weighing scale, the mass spectrometer, which can distinguish the mass of a single neutron. However, even a mass spectrometer has limits, and as time goes on, the radioactive parent isotopes diminish so much that there may be so little still remaining that we cannot meaningfully distinguish an experiment result from "background noise." Beyond about ten half lives--which for carbon dating is just over fifty thousand years--the remaining sample is too small to analyze. (Happily, for archeological investigations, fifty thousand years is perfectly in the range for dating human artifacts, but for the longer timescales of geology is not as useful.)

Query 5.4.1

This interactive element is not available in this format. Visit the link or scan the QR code to access it online.

View this Interactive Content online

References

1. *Accessible Periodic Table of Elements*. (n.d.). American Chemical Society. Retrieved August 14, 2023, from https://www.acs.org/education/students/highschool/olympiad/prepare-for-exams/accessible-periodic-table.html
2. Bentley, C. (2020, January 17). *Historical Geology – A free online textbook for Historical Geology courses*. OpenGeology. Retrieved June 20, 2023, from https://opengeology.org/historicalgeology/
3. Deline, B., Harris, R., & Tefend, K. (2016). *Laboratory Manual for Introductory Geology*. University of North Georgia.
4. Earle, S. (2019). *Physical Geology*. BCcampus, BC Open Textbook Project.
5. Johnson, C., Affolter, M. D., Inkenbrandt, P., & Mosher, C. (2019). *An Introduction to Geology*. Salt Lake Community College. https://slcc.pressbooks.pub/introgeology/
6. Williams, E. (2013, January 10). *Explainer: what is an isotope?* The Conversation. Retrieved June 19, 2023, from https://theconversation.com/explainer-what-is-an-isotope-10688

This page titled 5.4: Absolute Dating of Geologic Materials is shared under a CC BY-NC 4.0 license and was authored, remixed, and/or curated by Martha House.

5.5: The Geologic Time Scale

Making Sense of So Much Time

The geological time scale is one of the crowning achievements of science, and geology in particular. It is a reference and communication system for comparing rocks and fossils from throughout the world and is geology's equivalent of the periodic table of the elements.

The geological time scale is currently maintained by the International Commission on Stratigraphy (ICS), which is part of the International Union of Geological Sciences. The time scale is continuously being updated as geoscientists learn more about the timing and nature of past geological events. You can view the ICS time scale online.

The geological time scale provides a global summary of countless small-scale temporal correlations of rock layers made at local and regional scales. It is based almost entirely upon careful observations of the distributions of fossils both geographically and stratigraphically. The dates were added much later following the advent of numerical dating techniques giving us the ability to bracket the ages of different organisms in relation to numerical dates provided by associated igneous activity. The simple Principle of Superposition and Principle of Faunal Succession have provided geologists with the ability to reconstruct the geological history of Earth by correlating rocks and fossils from different places. This is critically important because no single place on Earth preserves a complete geological history, or even a small fraction of it. We only get a sense of the full story if we look everywhere, using multiple locations to piece together the puzzle of snapshots of the Earth through time.

Organization of the Time Scale

Because geologic time is so very long, the time scale has been subdivided into sections, much like we subdivide the yearly calendar into months, weeks and days or our day into hours, minutes and seconds. In the case of the geologic time scale, the component parts from largest to smallest are Eons, Eras, Periods, and Epochs (Figure 5.5.1). The details of the geologic time scale are listed here; more details and descriptions follow in this section.

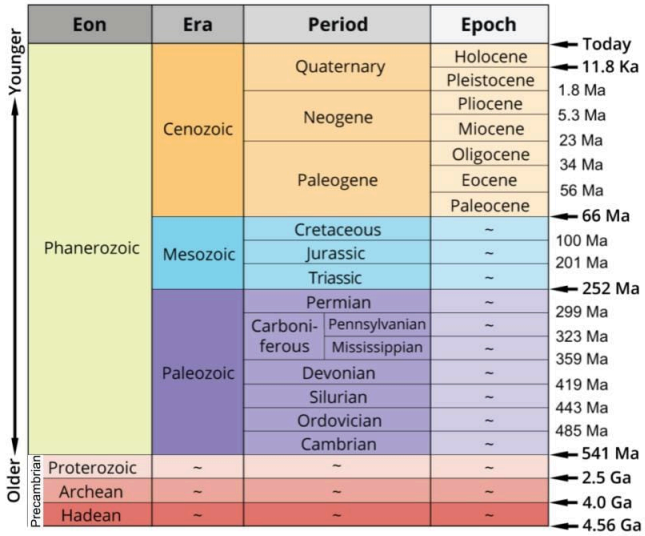


Figure 5.5.1: The geologic time scale organizes Earth's nearly 4.6 billion years of history. "The geological time scale" by Jonathan R. Hendricks is licensed under CC BY-SA 4.0.

A Simplified Geologic Time Scale

Earth's Geologic Time 4.56 Ga to present:

1. Phanerozoic Eon 541 Ma to present
    1. Cenozoic Era 66 Ma to present
        1. Quaternary Period 1.8 Ma to present
            1. Holocene Epoch 11.8 Ka to present
            2. Pleistocene Epoch 1.8 Ma to 11.8 Ka
        2. Neogene Period 23 to 1.8 Ma
            1. Pliocene Epoch 5.3 to 1.8 Ma
            2. Miocene Epoch 23 to 5.3 Ma
        3. Paleogene Period 66 to 23 Ma
            1. Oligocene Epoch 34 to 23 Ma
            2. Eocene Epoch 56 to 34 Ma
            3. Paleocene Epoch 66 to 56 Ma
    2. Mesozoic Era 252 to 66 Ma
        1. Cretaceous Period 100 to 66 Ma
        2. Jurassic Period 201 to 100 Ma
        3. Triassic Period 252 to 201 Ma
    3. Paleozoic Era 541 to 252 Ma
        1. Permian Period 299 to 252 Ma
        2. Carboniferous Period 359 to 299 Ma
            1. Pennsylvanian Period 323 to 299 Ma
            2. Mississippian Period 359 to 323 Ma
        3. Devonian 419 to 359 Ma
        4. Silurian 443 to 419 Ma
        5. Ordovician 485 to 443 Ma
        6. Cambrian 541 to 485 Ma
2. Precambrian (Group of Eons) 4.56 Ga to 541 Ma
    1. Proterozoic Eon 2.5 Ga to 541 Ma
    2. Archean Eon 4.0 Ga to 2.5 Ga
    3. Hadean Eon 4.56 Ga to 4.0 Ga

Eons

The Eon is the broadest category of geological time. Earth's history is characterized by four Eons; in order from oldest to youngest, these are the Hadean (4.65-4.0 Ga; 13% of Earth's total history), Archean (4.0-2.5 Ga, 33% of Earth's total history), Proterozoic (2.5-0.541 Ga, 42% of Earth's total history), and Phanerozoic (541 Ma to present, 12% of Earth's total history) (Figure 5.5.2). Collectively, the Hadean, Archean, and Proterozoic are sometimes informally referred to as the "Precambrian." The Cambrian Period defines the beginning of the Phanerozoic Eon; so, all rocks older than the Cambrian are Precambrian in age.

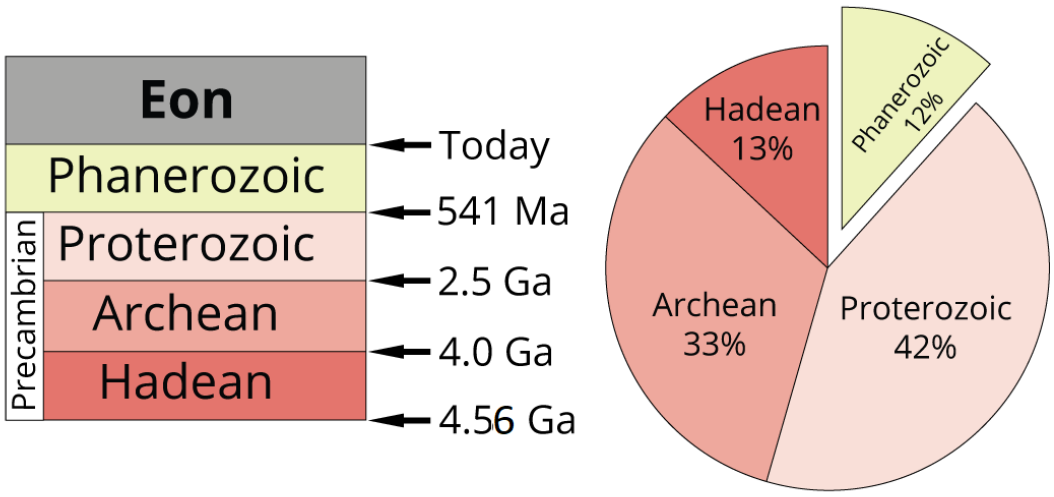


Figure 5.5.2: The four eons of geological time. "GeologicalTimeScale-Eons2" by Jonathan R. Hendricks, is licensed under CC BY-SA 4.0.

We live during the Phanerozoic, which means “visible life.” This is the interval of geological time characterized by abundant, complex fossilized remains. Being the youngest Eon of time, it is also very well represented by rock at Earth’s surface (because of the Principle of Superposition). Because of these two factors, most paleontologists and geologists study fossils and rocks from the Phanerozoic Eon.

Consider that Earth is roughly 4.56 billion years old. This age is based on the analysis of some of the oldest geological materials found so far. The Phanerozoic Eon began 541 million years ago (or, 0.541 billion years ago). Thus, the Phanerozoic Eon represents a paltry 12% of Earth’s history! Instead, most of Earth’s history is represented by the three Precambrian Eons. These older Eons tell the story of Earth’s beginning, life’s origin, and the rise of complex life.

Video 5.5.1: A Brief History of Geologic Time

This video is a good quick summary of the immensity of geologic time.

This interactive element is not available in this format. Visit the link or scan the QR code to access it online.

View this YouTube Video online

Eras

Eons of geologic time are subdivided into Eras, which are the second-longest units of geological time. The Phanerozoic Eon is divided into three Eras: the Paleozoic, or "Old Life" Era (541-252 Ma), the Mesozoic, or "Middle Life" Era (252-66 Ma), and Cenozoic, or "New Life" Era (66 Ma to present) (Figure 5.5.3).

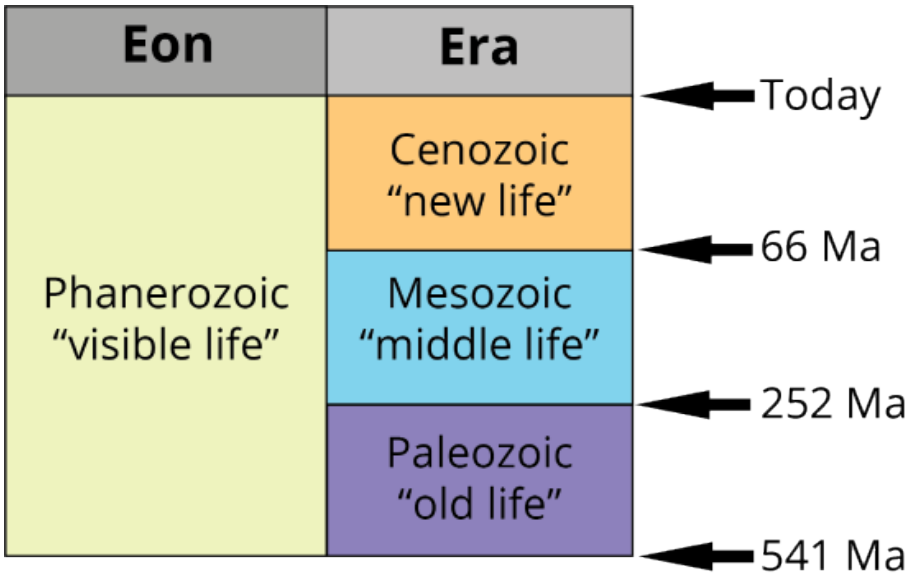


Figure 5.5.3: "The three eras of the Phanerozoic eon" by Jonathan R. Hendricks, is licensed under CC BY-SA 4.0.

Most of our knowledge of the fossil record comes from the three eras of the Phanerozoic Eon. The Paleozoic (“old life”) Era is characterized by trilobites, the first four-limbed vertebrates, and the origin of land plants. The Mesozoic (“middle life”) Era represents the “age of dinosaurs,” though also is noteworthy for the first appearances of mammals and flowering plants. Finally, the Cenozoic (“new life”) Era is sometimes called the “age of mammals” and is the Era during which we live today.

As temporal points of reference, it is worth memorizing the ages of the boundaries that separate the three eras of the Phanerozoic Eon. Long before geologists knew these absolute age dates, they realized that the boundaries represent important events in the history of life: mass extinctions. For example, many fossils that are commonly found in the youngest Paleozoic rocks are

not found in overlying Mesozoic rocks. Similarly, dinosaur fossils found in the youngest Mesozoic rocks are never again found in the overlying Cenozoic rocks. Paleontologists and geologists used these mass extinction events to define these (and other) boundaries within the Phanerozoic portion of the geological time scale. It is therefore no coincidence that some of the major boundaries coincide with mass extinction events!

The older Archean and Proterozoic Eons are similarly divided into several eras. For example, the youngest Era of the Proterozoic Eon is called the Neoproterozoic. For the sake of simplicity, these older eras are not included on the time scale shown at the top of this page; they do, however, exist!

Periods

Just as Eons are subdivided into eras, eras are subdivided into units of time called periods.

The Paleozoic Era (541-252 Ma) is divided into six periods (Figure 5.5.4). From oldest to youngest, these are the Cambrian, Ordovician, Silurian, Devonian, Carboniferous, and Permian. Note that in the United States, the Carboniferous is divided into two separate periods: the Mississippian and the Pennsylvanian.

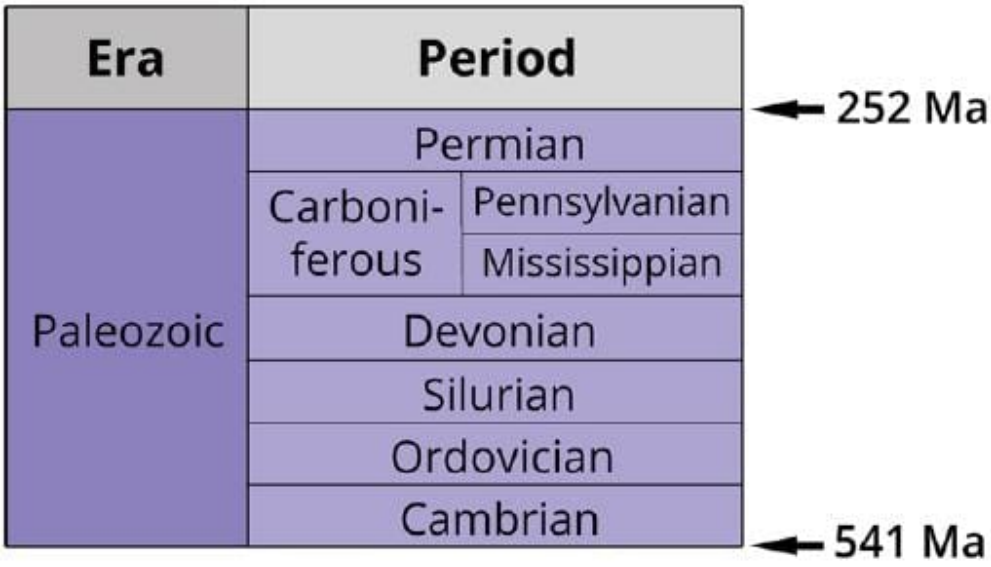


Figure 5.5.4: "The seven periods of the Paleozoic era" by Jonathan R. Hendricks, is licensed under CC BY-SA 4.0.

The Mesozoic Era (252-66 Ma) is divided into the Triassic, Jurassic, and Cretaceous periods (Figure 5.5.5).

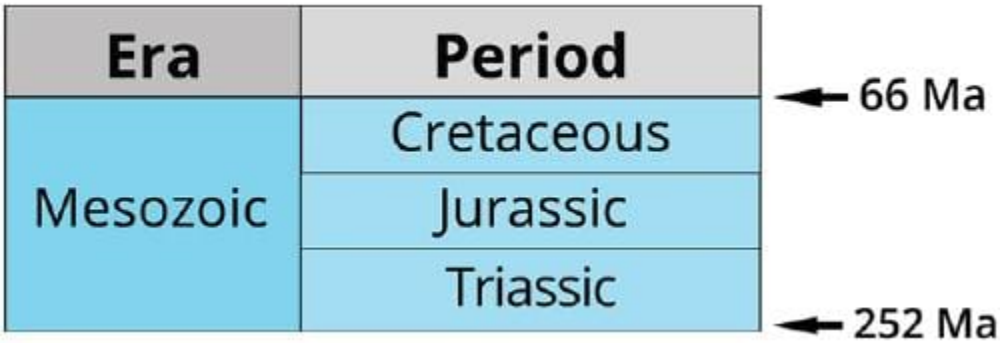


Figure 5.5.5: "The three periods of the Mesozoic era" by Jonathan R. Hendricks, is licensed under CC BY-SA 4.0.

Finally, the Cenozoic Era (66 Ma to present) is divided into three periods: the Paleogene, Neogene, and Quaternary (Figure 5.5.6).

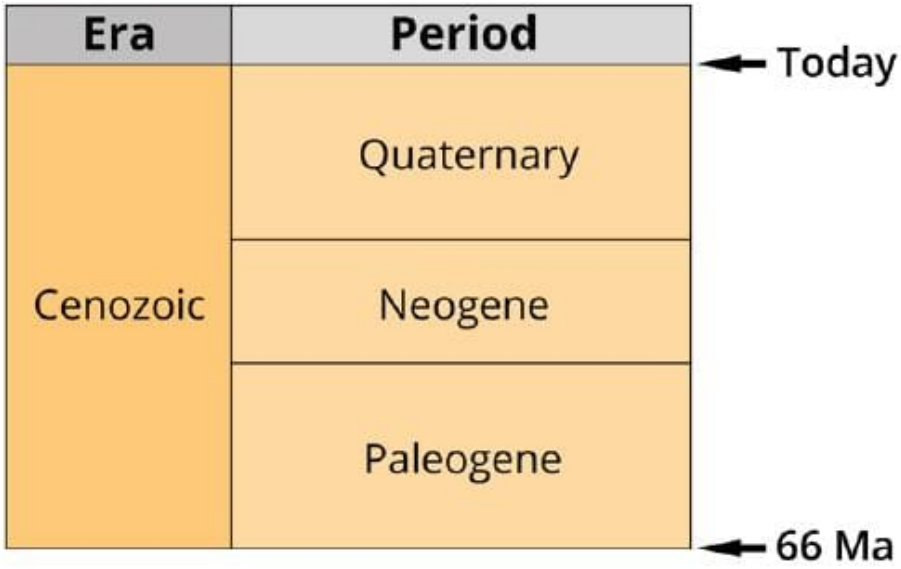


Figure 5.5.6: "The three periods of the Cenozoic era" by Jonathan R. Hendricks, is licensed under CC BY-SA 4.0.

Epochs and Ages

Periods of geological time are subdivided into epochs (Figure 5.5.7). In turn, Epochs are divided into even narrower units of time called ages. For the sake of simplicity, only the Epochs of the Paleogene, Neogene, and Quaternary periods (66 Ma-present) are considered in this text. The Palegene Period consists of the Paleocene, Eocen and Oligocene Epochs (from oldest to youngest). The Neogene Period begins with the Miocene Epoch and concludes with the Pliocene. The Quaternary Period begins with the Pleistocene Epoch, and the Holocene (beginning at 11.8 Ka). It is important to note, however, that all of the periods of the Phanerozoic Era are subdivided into the Epochs and ages.

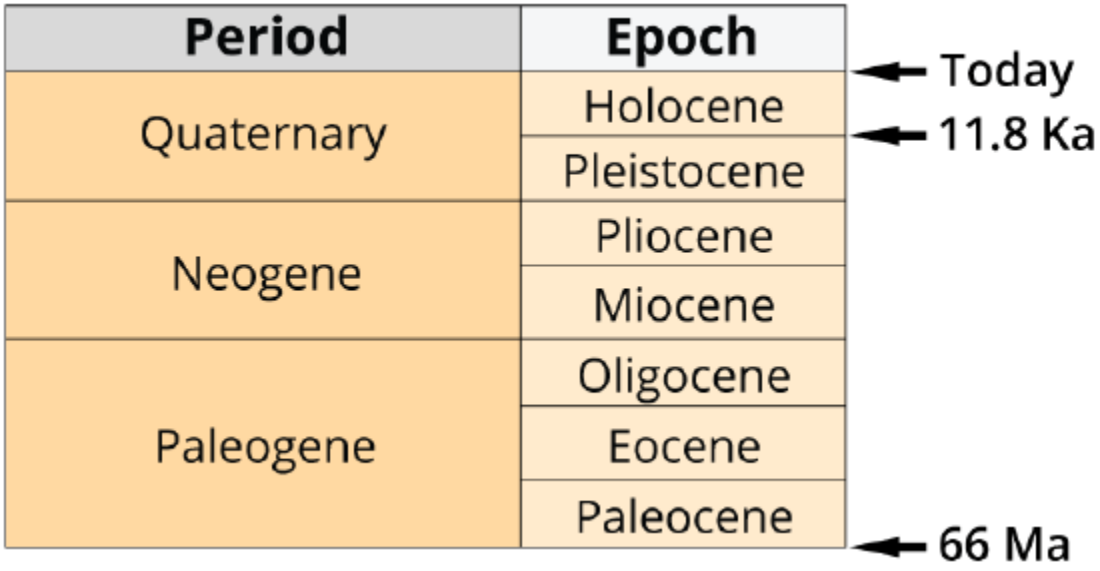


Figure 5.5.7: The Paleogene Period is divided into–from oldest to youngest–the Paleocene, Eocene, and Oligocene epochs. The Neogene is divided into the Miocene and Pliocene epochs. Finally, the Quaternary is divided into the Pleistocene and Holocene epochs. Some geologists now think that–since humans are having such a notable impact on the Earth and its life–a new, youngest Epoch should be added to the Quaternary: the Anthropocene. "Epochs of the Paleogene, Neogene, and Quaternary periods" by Jonathan R. Hendricks, is licensed under CC BY-SA 4.0.

Query 5.5.1

This interactive element is not available in this format. Visit the link or scan the QR code to access it online.

View this Interactive Content online

References

1. Bentley, C. (2020, January 17). *Historical Geology – A free online textbook for Historical Geology courses*. OpenGeology. Retrieved June 20, 2023, from https://opengeology.org/historicalgeology/
2. Earle, S. (2019). *Physical Geology*. BCcampus, BC Open Textbook Project.
3. *Hendricks, J. R. (n.d.). 3. Geological time scale. Digital Atlas of Ancient Life*. Retrieved August 4, 2023, from https://www.digitalatlasofancientlife.org/learn/geological-time/geological-time-scale/
4. *ics-chart*. (n.d.). International Commission on Stratigraphy. Retrieved June 20, 2023, from https://stratigraphy.org/timescale/
5. Johnson, C., Affolter, M. D., Inkenbrandt, P., & Mosher, C. (2019). *An Introduction to Geology*. Salt Lake Community College. https://slcc.pressbooks.pub/introgeology/

This page titled 5.5: The Geologic Time Scale is shared under a CC BY-NC 4.0 license and was authored, remixed, and/or curated by Martha House.

5.6: Chapter Summary

5.1 Relative Dating

- Relative dating techniques provide a way to place geologic events in sequential order, but do not indicate the amount of time each event took.
- Units deposited in horizontal layers at the earth's surface can be organized according to the Principles of Original Horizontality, Superposition, and Lateral Continuity.
- Units that are not emplaced as layers, such as igneous intrusive rocks, dikes or metamorphic rocks can be placed in a relative order using the Principle of Cross-cutting Relationships and Principle of Inclusions. The Principles of Baked Contacts and Chilled Margins are variations on the Principles of Cross-Cutting Relationships and Inclusions.
- The Principle of Faunal Succession relies on fossil assemblages to correlate units across large distances. .
- The Grand Canyon is a good example of all of these concepts in one place.

5.2 Unconformities: Missing Time

- Unconformities are indicators of missing time due to erosion or nondeposition.
- Three different types of unconformity can be recognized based on geological relationships around them.
- An angular unconformity is indicated when tilted sedimentary layers or volcanic flows are truncated by overlying horizontal sedimentary layers or volcanic flows.
- A disconformity is apparent when horizontal sedimentary or volcanic layers are separated by horizontal or subhorizontal erosional surfaces.
- A nonconformity is developed when crystalline rocks (igneous intrusive or metamorphic rocks) are capped by horizontal or subhorizontal volcanic flows or sedimentary layers.

5.3 Dating Rocks Using Fossils

- Fossil assemblages represent distinct periods in earth history.
- Index fossils are organisms that lived for relatively short time periods; if they were distributed over a wide geographic area, they can be used to compare the relative ages of rocks from different regions.
- Biozone fossils are groups of organisms that contain genera and families that lived over a long time, and species that lived for a relatively short time. They can be easily distinguished from others on the basis of specific features.
- Fossil studies must be combined with numerical dating to provide absolute ages for rock units.

5.4 Absolute Dating of Geologic Materials

- Numerical or absolute ages for rocks and minerals in them can be determined using radioactive decay of elements contained in them.
- Radio-isotopes are elements that are unstable and decay to form stable daughter isotopes. The rate of day decay is called the "half-life".
- Dating requires determining the ratio of parent and daughter isotopes in target minerals.
- The age that's obtained for a particular rock or mineral has different significance depending on the isotope system and material being analyzed.
- Isotopic systems with a range of half lives can be used to learn different things about geological materials including their crystallization ages, metamorphic ages, and time of death (for organic materials).

5.5 The Geologic Time Scale

- The geologic time scale was initially constructed based on correlations of units across the globe, based on fossil assemblages.
- Absolute ages were subsequently added to the time scale as they were obtained.

- The time scale is structured based on Eons, Eras, Periods and Epochs, which are identified on the basis of extinctions.

This page titled 5.6: Chapter Summary is shared under a CC BY-NC 4.0 license and was authored, remixed, and/or curated by Martha House.

5.7: Detailed Figure Descriptions

Figure 5.1.6: Fossil Succession

This image shows two separated rock columns with layered strata and fossils, illustrating how geologists correlate rock layers across distance using fossil evidence to match equivalent layers. It shows how fossil correlation is used to identify equivalent rock layers across different locations and reconstruct geologic history.Lines drawn between the columns indicate correlations. On the left and right sides are vertical stacks of horizontal rock layers. Each layer is shown as a distinct band, separated by clear boundaries. The two columns are separated by a gap, representing missing or eroded rock between locations. Within each layer are fossil illustrations. These fossils vary in shape and type and are used as identifying markers for each layer. Matching fossils appear in corresponding layers on both sides.

Several diagonal lines extend across the gap from layers on the left column to layers on the right column. These lines connect layers that contain the same fossil types, showing how they are correlated even though they are physically separated. The layers are distinguished by position, fossil content, and boundaries rather than color alone. The fossils provide the key evidence for matching layers.

Figure 5.2.1: Stages in the Formation of a Non-Conformity

This diagram shows a three-step sequence of geologic change over time, read from left to right using arrows between panels. It shows intrusive igneous rock forms forming first below the surface, which are later covered by younger sedimentary layers.

In the first panel, several flat, horizontal sedimentary layers sit above a lower rock unit. Inside that lower unit, the text “Intrusive Igneous Rock” is written. This unit also features a repeated short-line texture, while the layers above are smooth, parallel bands. The boundary between them is uneven, showing the igneous rock formed beneath earlier material.

An arrow points to the second panel. The arrows indicate the sequence of events. In the second panel, the entire block is composed of the same textured rock, with no sedimentary layers present and no additional text shown. Another arrow points to the third panel.In the third panel, horizontal sedimentary layers appear again above the same textured rock unit. The boundary between them remains uneven, and the layered bands are clearly distinct from the textured rock below.

Figure 5.2.2: Stages in the Formation of an Angular Unconformity

This image shows a three-step sequence of geologic change over time, read from left to right using arrows, illustrating how rock layers are first deposited horizontally, then tilted by geologic forces, and later covered by younger, flat-lying layers.

Across all panels, layers are distinguished by line orientation and position rather than color, and arrows indicate the sequence of events over time. In the first panel, multiple horizontal rock layers are depicted as flat, parallel bands stacked on top of one another. The top surface is uneven, representing the land surface. An arrow points to the second panel. In the second panel, those same layers are no longer horizontal. Instead, they are tilted diagonally from lower left to upper right. The layers remain parallel to each other, but their orientation has changed. The top surface is still uneven. Another arrow points to the third panel. In the third panel, a new set of horizontal layers appears at the top. These newer layers are flat and parallel, clearly oriented differently from the tilted layers below. The boundary between the tilted layers and the horizontal layers is uneven, indicating a break in deposition. The tilted layers remain visible beneath the newer horizontal layers.

Figure 5.2.3: Stages in the Formation of a Disconformity

This image shows a three-step sequence of geologic change over time, read from left to right using arrows, illustrating how originally flat sedimentary layers can be disturbed and later preserved as a buried, uneven layer within otherwise horizontal strata. Arrows between the panels indicate the sequence of events.

In the first panel, several horizontal rock layers are shown as flat, parallel bands stacked on top of each other. The top surface is uneven, representing land surface. In the second panel, the same horizontal layers remain, still flat and parallel, with no visible

disturbance. In the third panel, a middle layer becomes uneven and wavy, forming a distinct boundary that contrasts with the flat, parallel layers above and below. The surrounding layers remain horizontal, clearly distinguishing the irregular shape of this layer.

Figure 5.2.4: Cross-section of Grand Canyon geologic units

This image is a vertical diagram of Grand Canyon rock layers, showing their names, order, and relative ages from top to bottom and shows how geologists interpret rock order, deformation, and unconformities to identify gaps in Earth's geologic history. A labeled boundary called "The Great Unconformity" marks a gap in the geologic record. Arrows indicate vertical relationships between layers. At the top are Layered Paleozoic Rocks, shown as flat, horizontal layers. A numbered list identifies:

1. Kaibab Formation (Fm)
2. Toroweap Formation
3. Coconino Sandstone
4. Hermit Formation
5. Supai Group
6. Surprise Canyon Fm
7. Redwall Limestone
8. Temple Butte Fm
9. Muav Limestone
10. Bright Angel Shale
11. Tapeats Sandstone

The lower part of this section includes the Tonto Group (units 9–11), with arrows reinforcing layer order. Below this is an uneven, wavy boundary labeled "The Great Unconformity," indicating erosion or missing time. Under this boundary are Grand Canyon Supergroup Rocks, shown as tilted layers. A list identifies:

12. Sixtymile Formation
13. Chuar Group
14. Nankoweap Fm
15. Unkar Group

At the bottom are Vishnu Basement Rocks, labeled:

16. Schists
17. Granites
18. Elves Chasm Gneiss

Figure 5.3.1: Geologic Range Chart

This image is a vertical bar chart showing the age ranges of four fossil species labeled Species A, Species B, Species C, and Species D showing how overlapping fossil ranges are used to correlate rock layers and determine their relative ages. A vertical axis on the left is labeled "Age ranges (Ma)", meaning millions of years ago, with values from about 1 at the top to 14 at the bottom. The scale increases downward, so lower positions represent older ages. Each species is shown as a vertical bar spanning its age range:

- **Species A** extends from about 7 to 14 million years ago.
- **Species B** extends from about 5 to 12 million years ago.
- **Species C** extends from about 1 to about 9 million years ago.
- **Species D** extends from about 3 to about 8 million years ago.

A horizontal highlighted band across the chart is labeled "7.0 to 8.3 Ma." This band marks the time interval where multiple species overlap. Within this highlighted range, all four species are present, indicating a shared time period.

Figure 5.3.3: The main sutural patterns of ammonites

The image combines a timeline and fossil diagrams to compare three ammonoid groups—Goniatites, Ceratites, and

Ammonites—showing how their age ranges and shell features help scientists identify fossils and understand evolutionary changes over geologic time. Arrows, labels, and patterns provide multiple ways to interpret the information.

At the top is a timeline labeled Cretaceous, Jurassic, Triassic, Permian, Carboniferous, and Devonian. Horizontal bars show when each group existed:

- Goniatites occur mainly from the Devonian through the Permian.
- Ceratites occur mainly in the Triassic.
- Ammonites extend from the Triassic through the Cretaceous.

The bars overlap, indicating periods when groups coexisted. Below the timeline are fossil images labeled Ammonites, Ceratites, and Goniatites, each showing a coiled shell. Next to the fossils are line diagrams labeled “Saddles” and “Lobes.” Arrows point to these features along the shell suture lines:

- Goniatites show simple, smooth curves.
- Ceratites show more complex patterns, with jagged lobes and smoother saddles.
- Ammonites show highly complex, detailed patterns in both lobes and saddles.

Figure 5.4.2: Protons, neutrons, and electrons in carbon isotopes

This illustration compares three carbon isotopes: carbon-12 (stable), carbon-13 (stable), and carbon-14 (radioactive), showing how differences in neutrons help explain stability and radioactive decay. A labeled key identifies particles, and each atom diagram uses position, labels, and counts rather than color alone. A key on the left labels three particle types:

- electron
- proton
- neutron

Each of the three diagrams shows an atom with a central nucleus and electrons moving in circular orbits around it. In all three atoms, the nucleus contains 6 protons, and this is labeled beneath each diagram. This confirms all three are carbon. The differences are in the number of neutrons:

- carbon-12 (stable) shows 6 protons and 6 neutrons
- carbon-13 (stable) shows 6 protons and 7 neutrons
- carbon-14 (radioactive) shows 6 protons and 8 neutrons

Electrons are shown orbiting each nucleus, with the same number in each diagram, indicating that electron count does not change between isotopes. Each isotope is labeled directly below its diagram with its name and whether it is stable or radioactive. This image illustrates that isotopes of the same element have the same number of protons but different numbers of neutrons, and that these differences affect whether the atom is stable or radioactive.

Figure 5.4.3: Alpha Particle

This image shows alpha decay, where an atomic nucleus emits a small particle, illustrating how radioactive decay changes an atom over time. In alpha decay, a nucleus loses 2 protons and 2 neutrons, changing into a different element.Lines indicate motion from left to right. On the left is a large atomic nucleus made up of many small spheres grouped together. These spheres represent protons and neutrons, forming a dense cluster. To the right of the nucleus is a smaller cluster of four spheres moving away. This smaller group is labeled with the Greek letter “α” (alpha). It represents an alpha particle, which consists of 2 protons and 2 neutrons. Thin lines between the large nucleus and the smaller cluster indicate the direction of movement, showing that the alpha particle is being emitted from the nucleus.

Figure 5.4.4: Radioactive Decay Curve

This graph of radioactive decay over time, showing how a parent isotope decreases and a daughter isotope increases across half-lives, helping explain how scientists use predictable decay patterns to determine the age of rocks and fossils. Across the graph, the relationship between the two curves shows that each half-life reduces the parent isotope by half while increasing the daughter isotope by the same proportion. Axes, labels, symbols, and markers provide multiple ways to interpret the data, and

arrows highlight key changes early in the process.

The horizontal axis is labeled “Half-lives passed” and runs from 0 to 8. The vertical axis is labeled “Percentage in sample” and runs from 0% to 100%. Two curves are shown:

- The Parent curve starts at 100% at 0 half-lives and steadily decreases: about 50% at 1 half-life, 25% at 2, about 12% at 3, and approaching 0% by 8 half-lives.
- The Daughter curve starts at 0% at 0 half-lives and increases: about 50% at 1 half-life, about 75% at 2, about 88–90% at 3, and approaching 100% by 8 half-lives.

A legend on the right labels the two curves as “Parent” and “Daughter.” Data points along each curve mark values at each half-life. Near the first half-life, two arrows are labeled:

- “A” points horizontally toward the midpoint, emphasizing the increase in daughter material.
- “B” points downward, emphasizing the decrease in parent material.

This page titled 5.7: Detailed Figure Descriptions is shared under a license and was authored, remixed, and/or curated by LibreTexts.

6: A BRIEF GEOLOGIC HISTORY OF CALIFORNIA

Introduction to the Geologic History of California

Geologists are historians who have a story to tell that is incredibly broad in both space and time. Geologists are also detectives who must search for the evidence and clues to the tectonic past. Often, subsequent geologic events obscure the evidence we are looking for in many ways: rocks are buried and no longer exposed at the surface, rocks are metamorphosed and may no longer look like the original rocks or have the same chemistry, tectonic processes can transport rocks great distances so they are no longer in the same place where they formed, subduction zones can return entire ocean basins to the mantle well beyond our view. While these physical and chemical changes obscure the original properties of the rocks, they are part of the story of how the rocks came to be where we see them today. Geologists are trained to identify these changes to rocks and what they mean about the environment in which the rock was formed. Geologists then put these environments and events in chronological order based on cross-cutting relationships or absolute ages.

The geologic history of California explains the origins of the state's diverse landscapes, natural resources, and geologic hazards. Processes such as rifting, subduction, terrane accretion, mountain building, and later transform faulting have shaped the physiography of California over hundreds of millions of years. This chapter provides the temporal framework necessary to understand the geologic provinces discussed in later chapters.

In this chapter we will look at a broad overview of how the tectonic plates interacting along the western margin of North America have changed through time. We will also look at time slices of the geologic map of California to see how the geologic environment has changed through time and understand the evidence used to unravel the geologic past.

Table 6.1 summarizes the major geologic events that shaped California into what we see today. Like many geologic timescales, this table is organized with the oldest events at the bottom and youngest events at the top. This chapter presents a chronologic account of these major geologic events with each of the following pages detailing a different geologic era. This chapter acts as the temporal link between the various geological provinces presented in the following chapters. For more detailed information on the geology of a specific region, consult the relevant geomorphic province chapter.

Table 6.1: Geologic time scale and major geologic events in California*

Era	Period	Epoch	Major Geologic Events in California
Cenozoic (66 Ma to present)	Quaternary (3 Ma to present)	Holocene (12 ka to present)	
		Pleistocene (3 Ma to 12 ka)	Ice age glaciers carve the Sierra Nevada and Klamath Mountains. Lakes flood the valleys in Modoc Plateau and Basin and Range. High Cascades volcanoes erupt.
	Neogene (23 to 3 Ma)	Pliocene (5 to 3 Ma)	Sutter Buttes volcanoes erupt. Sediments eroded from the Sierra Nevada and Coast Range are deposited into the Great Valley.
		Miocene (23 to 5 Ma)	Flood basalts cover the Modoc Plateau. Basin and Range extension begins.

Era	Period	Epoch	Major Geologic Events in California
	Paleogene (66 to 23 Ma)	Oligocene (34 to 23 Ma)	Spreading center is subducted and the San Andreas Fault begins to develop.
		Eocene (56 to 34 Ma)	Laramide Orogeny ends.
		Paleocene (66 to 56 Ma)	
Mesozoic (251 to 66 Ma)	Cretaceous (143 to 66 Ma)		Sierra Nevada sediments begin to fill Great Valley Klamath terrane accretes onto N. America Laramide Orogeny begins
	Jurassic (201 to 143 Ma)		Sevier Orogeny Nevadan Orogeny Supercontinent Pangaea begins to rift apart Sonoma Orogeny
	Triassic (252 to 201 Ma)		Subduction of the Farallon plate begins.
Paleozoic (539 to 251 Ma)	Permian (299 to 252 Ma)		Calaveras complex rocks are deposited on the ocean floor.
	Pennsylvanian (323 to 299 Ma)		
	Mississippian (359 to 323 Ma)		Antler Orogeny deforms accreted rocks into tightly folded Shoo Fly complex.
	Devonian (420 to 359 Ma)		
	Silurian (443 to 485 Ma)		
	Ordovician (487 to 443 Ma)		Trinity ophiolite forms.
	Cambrian (539 to 487 Ma)		
Proterozoic (2,500 to 539 Ma)	Neoproterozoic (1,000 to 539 Ma)		Supercontinent Rodinia begins to rift apart. Beginning of passive margin.
	Mesoproterozoic (1,600 to 1,000 Ma)		Abundant carbonate rocks form off the coast.
	Paleoproterozoic (2,500 to 1,600 Ma)		Oldest rocks in California form.
Archean (4.0 to 2.5 Ga)			Ancient North American continent craton formed east of California.

The dates on the table above are based on v2023/09 of the International Chronostratigraphic Chart from the International Commission on Stratigraphy. The latest version can be found on the ICS website.

Learning Objectives

By the end of this chapter, you should be able to:

- Describe the evidence used to recreate the past tectonic environments in California.
- Describe the tectonic setting of the Precambrian, Paleozoic, Mesozoic, and Cenozoic stages of development of California geology.
- Identify modern tectonic settings that we can use as analogs to understand the processes that created the geology of California.

6.1: Developing a Geologic History

6.2: Precambrian California (4.6 Ga – 541 Ma)

6.3: Paleozoic California (541 – 252 Ma)

6.4: Mesozoic California (250 – 66 Ma)- Subduction and Mountain Building

6.5: Cenozoic California (66 Ma – Present)- Faulting, Uplift, and Basin Formation

6.6: Chapter Summary

6.7: Detailed Figure Descriptions

References

1. Cohen, K.M., Harper, D.A.T., Gibbard, P.L. 2024. ICS International Chronostratigraphic Chart 2023/09. International Commission on Stratigraphy, IUGS. www.stratigraphy.org (visited: 2024/10/18)
2. *California's Amazing Geology*, 2nd, by Donald Prothero, 1032294906.
3. *Roadside Geology of Northern California*, by David Alt and Donald Hyndman, 0878426701.
4. *Roadside Geology of Southern California*, by Arthur Sylvester and Elizabeth Gans, 0878426531.

This page titled 6: A Brief Geologic History of California is shared under a CC BY-NC 4.0 license and was authored, remixed, and/or curated by Allison Jones & Steven Skinner.

6.1: Developing a Geologic History

How Do Geologists Develop a Geologic and Tectonic History?

We can determine a very general and broad history of an area based on what we know about the global distribution of tectonic plates and how they have moved through time. We can track the motion of tectonic plates quantitatively using the magnetic anomalies and fracture zones on the seafloor. The information that we gather from these types of studies has low spatial and temporal resolution but gives us a framework to start with of our understanding of the tectonic development of a specific area, such as California.

To flesh out and tell a more detailed tectonic history of an area we need to look at the rocks. Rocks record information about the environment in which they formed. From sedimentary rocks we can determine if the environment was marine or non-marine, and the depth of water. We can determine flow directions of wind and water transported sediments. Igneous rocks will have a chemistry that is determined by the processes through which that melt formed and subsequently cooled. Metamorphic rocks will hold information about the original parent rock and the pressure and temperature conditions that it experienced during metamorphism. By learning to read the rocks we can determine the environment that existed when that rock formed.

Another important clue that we can glean from rocks is *when* they formed or when they were metamorphosed (see Geologic Time). If we can determine ages for rocks, we can put them in a sequential order and see how the geologic environments have changed through space and time.

Earth is a tectonically active planet that continues writing its geologic history. Recent tectonic events often overprint or even erase the evidence for earlier events. Additionally, not all periods of geologic time are equally represented or accessible in certain regions leading to gaps in geologic histories. Geologists interrogate the rocks with various laboratory and field techniques in order to unwrap these overprints and interpolate across space and time to tell the geologic history of an area.

Video 6.1.1: A Quantitative Plate Reconstruction of Western North America and the Eastern Pacific Basin [no audio]

This animation shows the tectonic evolution of western North America and the eastern Pacific Ocean over the past 170 million years, from the Jurassic Period to the present. The reconstruction is based on a combination of geological evidence at Earth's surface and seismic imaging of subducted plates deep within the mantle.

This interactive element is not available in this format. Visit the link or scan the QR code to access it online.

View this YouTube Video online

Overview

The video illustrates the western margin of North America forming through a complex sequence of interactions involving multiple oceanic plates, island arcs, and microcontinents. Rather than a single oceanic plate subducting beneath the continent, the region was characterized by a broad offshore system of subduction zones and volcanic arcs. North America (dark blue) gradually moved westward into this system, overriding and accreting these terranes over time.

Key ideas shown in the animation:

- Multiple oceanic plates, including the Farallon plate (green) and later the Kula plate (pink), exist between the Pacific Ocean and North America. Subduction occurs in more than one direction at the same time.

- Terranes comprised of island arcs and microcontinents—Angayucham (red), Intermontane (purple), Insular (dark orange), Western Jurassic (orange), and Guerrero (yellow)—form offshore before being added to the continent.
- North America (dark blue) moves westward and overrides this system

Early configuration (Jurassic, ~170–147 million years ago)

At the beginning of the animation, North America (dark blue) is positioned farther east than it is today. To the west lies a large ocean basin which is subdivided by divergent plate boundaries (red lines), convergent plate boundaries (blue lines with triangular teeth on the overriding plate), transform plate boundaries (green lines).

Subduction is active within this ocean basin. Oceanic plates descend into the mantle beneath island arcs, and subduction occurs in multiple directions, including both westward- and eastward-dipping zones. These processes form a broad archipelago of volcanic arcs and microcontinents, including the Angayucham arcs (red), Insular superterrane (dark orange), Intermontane superterrane (purple), Guerrero superterrane (yellow), and the Western Jurassic belt (orange), located offshore of North America (dark blue). The Farallon plate (green) is already present and subducting beneath parts of this offshore system rather than directly beneath the continent.

Important features at this time:

- North America (dark blue) is not yet at a subduction boundary.
- Offshore regions contain multiple plates and volcanic arcs.
- Subduction zones dip in different directions.
- The Farallon plate (green) subducts beneath offshore terranes rather than the continent.
- The Angayucham arcs (red) and Mezcalera-related systems are separated from North America by ocean basins

Evolution of the offshore arc system (~147–115 million years ago)

As the animation progresses, the offshore plate system becomes more complex. Multiple small plates and island arcs evolve within the eastern Pacific basin. The Farallon plate (green) continues to subduct beneath offshore plates and arcs, including those associated with the Insular superterrane (dark orange), Guerrero superterrane (yellow), and Western Jurassic belt (orange). Subduction zones reorganize, and new plate boundaries form.

At the same time, North America (dark blue) continues to drift westward toward this system of arcs and microcontinents.

Collision and accretion along the continental margin (~115–83 million years ago)

North America (dark blue) begins to interact directly with the offshore archipelago. Island arcs and microcontinents, including the Insular superterrane (dark orange), Intermontane superterrane (purple), Guerrero superterrane (yellow), and Western Jurassic belt (orange), are progressively accreted to the western edge of the continent. The Angayucham terranes (red) are also involved in complex interactions and deformation, particularly in northern regions.

This accretion occurs at different times along the margin, and some terranes are transported long distances before final attachment.

As the continent overrides these subduction zones, the geometry of subduction changes. In some locations, the direction of subduction reverses, and subduction begins beneath the continental margin, similar to modern Andean-type systems. During this time, the Farallon plate (green) increasingly subducts beneath North America.

Continued plate reorganization (~83–55 million years ago)

The Kula plate (pink) forms and begins interacting with the Farallon plate (green) and other plates. Terranes continue to move along the continental margin, including continued translation of the Insular (dark orange) and Intermontane (purple) terranes.

Subduction beneath the continent continues and is associated with widespread magmatism. By this time, much of the previously offshore archipelago has been accreted onto North America (dark blue).

Development of the modern plate boundary (~55 million years ago to present)

In the final portion of the animation, most terranes—including the Insular (dark orange), Intermontane (purple), Guerrero (yellow), Western Jurassic (orange), and Angayucham-related terranes (red)—have been accreted to North America (dark blue). Subduction is concentrated along the continental margin, including the Cascadia region, where remnants of the Farallon plate (green) continue to subduct.

As plate boundaries reorganize, parts of the margin transition from subduction to transform motion, leading to the development of the San Andreas Fault system. The influence of the Kula plate (pink) diminishes as plate configurations evolve.

The present-day configuration of western North America is established during this time.

Download the paper or on ResearchGate and download the plate model

Clennett, E. J., Sigloch, K., Mihalynuk, M. G., Seton, M., Henderson, M. A., Hosseini, K., et al., 2020, A quantitative tomotectonic plate reconstruction of western North America and the eastern Pacific basin. Geochemistry, Geophysics, Geosystems, 20, e2020GC009117. https://doi.org/ 10.1029/2020GC009117.

This page titled 6.1: Developing a Geologic History is shared under a CC BY-NC 4.0 license and was authored, remixed, and/or curated by Allison Jones & Steven Skinner.

6.2: Precambrian California (4.6 Ga – 541 Ma)

Formation of the North American Craton

While the Earth is 4.5 billion years old, there are no rocks exposed anywhere that are that old, let alone in California, so we will skip over the first 3 billion years of Earth history and start in the Proterozoic Eon with the supercontinent Rodinia, which existed before the most recent supercontinent, Pangea. Geologists have used multiple lines of evidence to reconstruct the position of the continents in the past, one possible reconstruction of Rodinia places the portion of Laurentia that will eventually be California, adjacent to Australia or Antarctica (Figure 6.2.1).

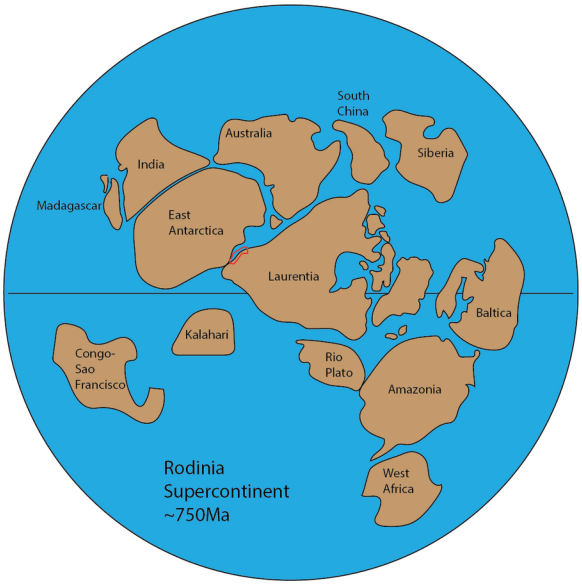


Figure 6.2.1: One proposed reconstruction of the supercontinent Rodina at 750 Ma. Outline of California in red superimposed to orient the viewer; note that this lies along the top edge of the "arrowhead" shape of Laurentia, bisected laterally by the coastline. ("Rodinia" by Steven Skinner, a derivative from the Rodinia map, is licensed under CC BY-NC 4.0. Access a detailed description.

Forming the Oldest Rocks in California

At approximately 750 Ma, the supercontinent Rodinia began to break apart. A continental rift developed that began to separate Laurentia from East Antarctica and Australia.

Until about 250 Ma, California was a passive margin during which time little to no tectonic activity was taking place. Instead, thick sequences of sediments were accumulating in the ocean basins that developed from rifting (Figure 6.2.2. Over time these thick sediments would eventually compact, become lithified into sedimentary rock, and undergo metamorphism. They would ultimately become California's oldest exposed rocks and the continental basement. (Figure 6.2.3).

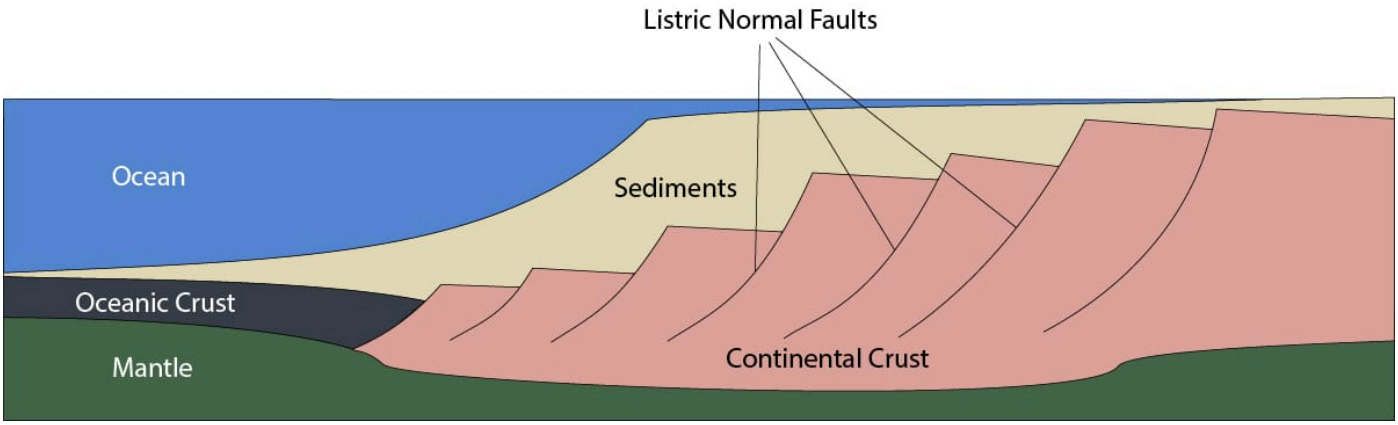


Figure 6.2.2: A diagrammatic passive margin resembling what western North America looked like. Continental crust that has been rifted is broken up by west-dipping listric normal faults. It is overlain by thick ocean sediments. Note that this diagram is very vertically exaggerated to emphasize these different features. "Passive Margin" by Allison Jones, a derivative of passive margin, is in the public domain. Access a detailed description.

If we look at the geologic map of California, we can see that Precambrian rocks are only exposed in the south and eastern parts of the state (Figure 6.2.3). This limited exposure of the oldest rocks is due to the fact that most of California's geology is made of rocks that are much younger and were added to the North American Plate in the Phanerozoic Eon. The Precambrian rocks in the southeast corner of the state are plutonic and high-grade metamorphic rocks that formed kilometers deep in the Earth. They are the continental basement rocks that were part of the Rodinian supercontinent.

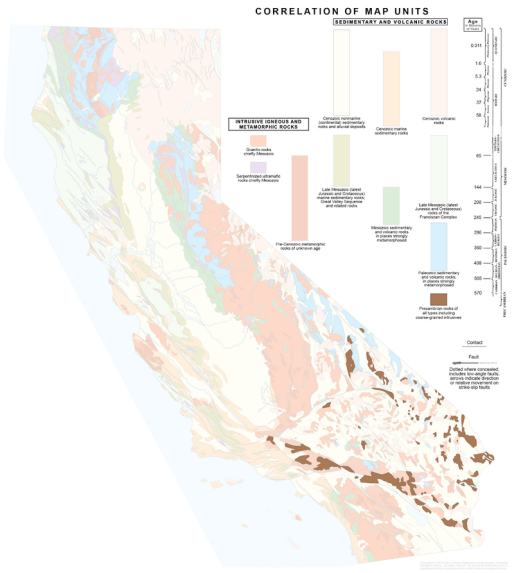


Figure 6.2.3: Simplified Geologic map of California highlighting the distribution of Precambrian rocks. "Precambrian Rocks" by Steven Skinner, a derivative of the Geology of California, is licensed under CC BY-NC 4.0. Access a detailed description.

There are also Precambrian rocks exposed in the ranges to the east of the Sierra Nevada. The White-Inyo Mountains as well as the ranges around Death Valley contain a thick sequence of metamorphic rocks, however, the level of metamorphism is relatively low grade such that the original lithology can be identified through the metamorphic overprint. Before metamorphism, these rocks formed a thick and laterally expansive package of sediments. Around 750 million years ago, as the supercontinent Rodina started to break apart, Australia and Antarctica were where California exists now. As rifting progressed and pulled Antarctica away from Laurentia, a sedimentary basin developed. The early stages of this rifting process would look something like modern-day East Africa (Figure 6.2.4). The process of rifting will create fault bounded basins that accumulate coarse clastic sediments as well as volcanic deposits. As the rift developed further extension and subsidence would lead to a marine incursion, or spreading of the sea over a land area (6.2.5).

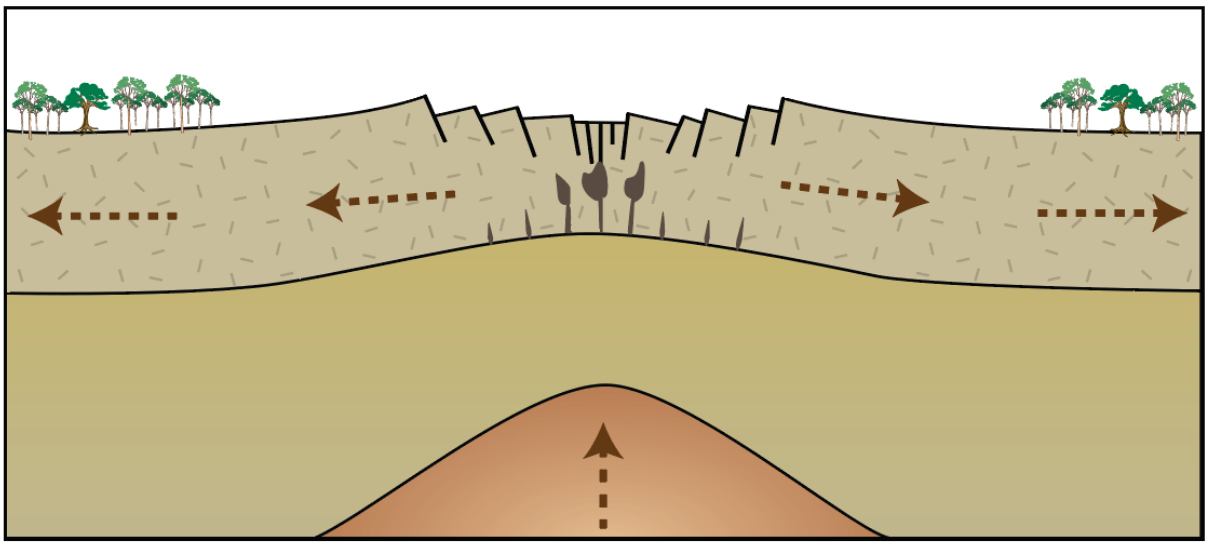


Figure 6.2.4: Rifting of a continental plate with upwelling. Stretching of the continental lithosphere results in faulting of the upper crust and thinning of the lower crust that allows for upwelling of the asthenosphere. Continental Rifting by MIT OpenCourseWare is licensed under CC BY-NC-SA 4.0

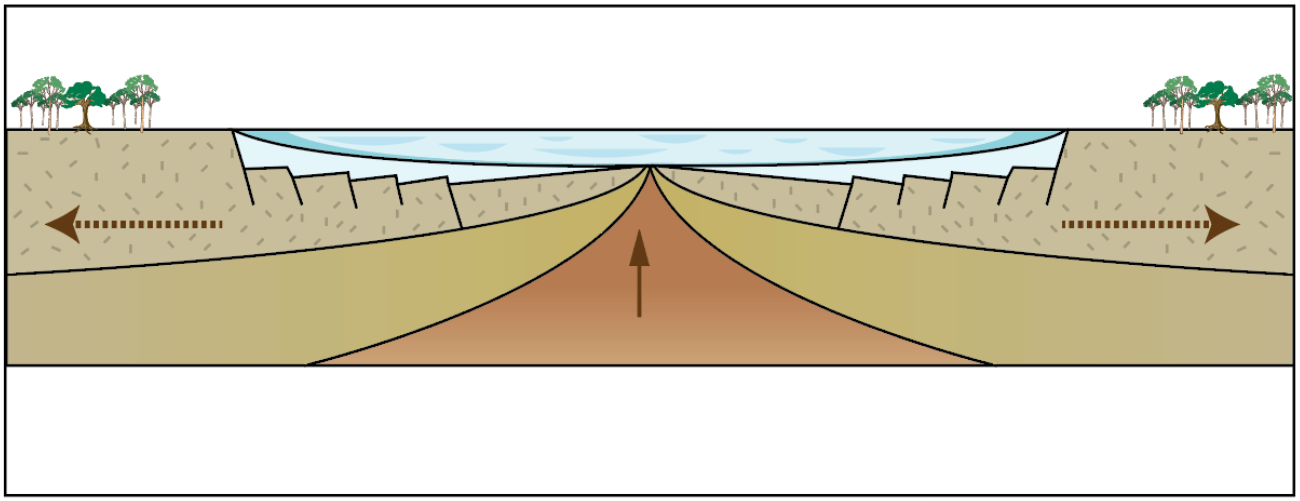


Figure 6.2.5: Rifting of a continental plate with ocean incursion. As the rift develops, opposing forces cause thinning of the continental lithosphere. This results in low elevations that allow sea water to cover the continent. Seafloor Spreading Center by MIT OpenCourseWare is licensed under CC BY-NC-SA 4.0

As the continental rift continued to evolve, the plate boundary shifted from faulting and stretching of continental crust to the creation of new oceanic crust through decompression melting. This margin would have resembled the present-day gulf of California, a narrow sea bounded by continental blocks on either side and a central spreading ridge producing basaltic ocean floor (Figure 6.2.6). As the ocean basin continued to expand, the margin would have looked like the present-day East Coast of the United States: that is a passive margin where no tectonic deformation is occurring. Upon this rifted margin, a great thickness of Precambrian marine sediments were deposited. Measured stratigraphic columns of eastern California show the sandstones, shales, and carbonate rocks that were deposited in this marine basin and how the thickness of these deposits changes from the shelf in the east to the deeper basin in the west. The deposition of these marine sediments continued into the Paleozoic era. This thick sequence of sedimentary deposits on a passive margin is sometimes referred to as a miogeocline.

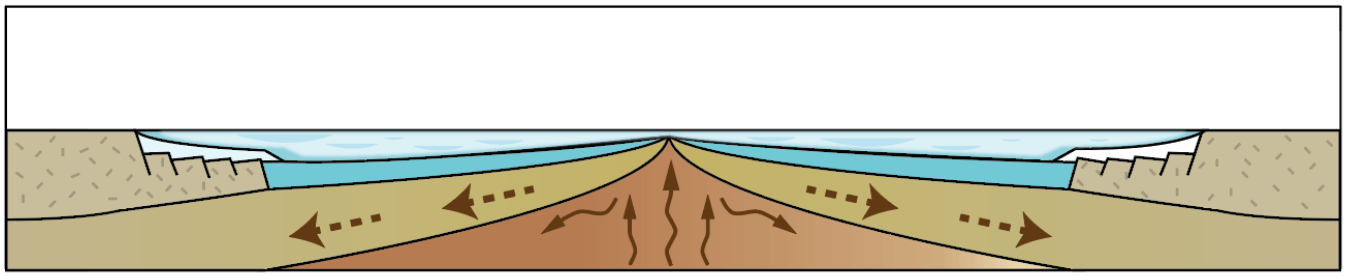


Figure 6.2.6: Rifting of a continental plate that eventually results in the formation of new oceanic crust. Widening Ocean Basin by MIT OpenCourseWare is licensed under CC BY-NC-SA 4.0. Access a detailed description.

You can read more about this stage of California's geologic past in the chapters on the Basin and Range Province and the Mojave Desert Province where these oldest rocks are still preserved today.

References

1. Burchfiel, B. C., & Davis, G. (1975). Nature and controls of Cordilleran orogenesis, western United States: Extensions of an earlier synthesis. American Journal of Science, 275(A).
2. Dickinson, W. R. (2004). Evolution of the North American Cordillera. Annual Review of Earth and Planetary Sciences, 32(1), 13-45. https://doi.org/10.1146/annurev.eart....101802.120257
3. Li, Z. X., Bogdanova, S. V., Collins, A. S., Davidson, A., De Waele, B., Ernst, R. E., . . . Vernikovsky, V. (2008). Assembly, configuration, and break-up history of Rodinia: A synthesis. Precambrian Research, 160(1-2), 179-210. https://doi.org/10.1016/j.precamres.2007.04.021
4. Lund, K. (2008). Geometry of the Neoproterozoic and Paleozoic rift margin of western Laurentia: Implications for mineral deposit settings. Geosphere, 4(2). https://doi.org/10.1130/ges00121.1
5. Tikoff, B., Kelso, P., Fayon, A. K., Gaschnig, R., Russo, R. M., Vervoort, J., . . . Kahn, M. J. (2023). The jagged western edge of Laurentia: The role of inherited rifted lithospheric structure in subsequent tectonism in the Pacific Northwest. In Laurentia: Turning Points in the Evolution of a Continent (pp. 425-455). https://doi.org/10.1130/2022.1220(22)
6. Whitmeyer, S., & Karlstrom, K. E. (2007). Tectonic model for the Proterozoic growth of North America. Geosphere, 3(4). https://doi.org/10.1130/ges00055.1

This page titled 6.2: Precambrian California (4.6 Ga – 541 Ma) is shared under a CC BY-NC 4.0 license and was authored, remixed, and/or curated by Allison Jones & Steven Skinner.

6.3: Paleozoic California (541 – 252 Ma)

California as Part of a Passive Continental Margin

The Paleozoic rocks in California continue the record of passive margin sedimentation. The thick deposits of shallow marine clastic and chemical sedimentary rocks continued to accumulate in the early Paleozoic as the region continued to slowly sink below sea level in response to rifting.

Early Accretion and the First Signs of Tectonic Activity

Early in the Paleozoic, the western side of North America was a relatively quiet passive margin. However, things began to change in the Devonian to early Mississippian. In the region that is now northern Nevada, thrust sheets were emplaced over the passive margin sediments. This event, known as the Antler Orogeny, marks a change from a tectonically quiet passive margin to an active margin with volcanic rocks and oceanic sediments that are thrust onto the continent. The Antler Orogeny involved multiple episodes of thrust faulting and basin development rather than a single collision event. These pulses resulted in repeated stacking of allochthonous rocks above the former passive margin and the deposition of deep marine sediments in associated basins. The package of rocks that was emplaced onto the continent is referred to as the Roberts Mountains allochthon or the Roberts Mountain Thrust. An allochthon (Figure 6.3.1) is a package of older rocks that have been thrust above younger rocks. It may seem like these events recorded in Nevada are beyond the scope of a tectonic history of California, but political boundaries did not exist when these rocks formed, and geologic processes pay little attention to the lines we draw on maps.

The rocks displaced along the Roberts Mountains Thrust signal a change at the plate boundary: the western boundary of North America had gone from an active rift, to a passive margin accumulating marine sediments, and was now experiencing compression. Emplacement of the Roberts Mountains allochthon required a compressive force, most likely generated by a convergent margin somewhere offshore to the west.

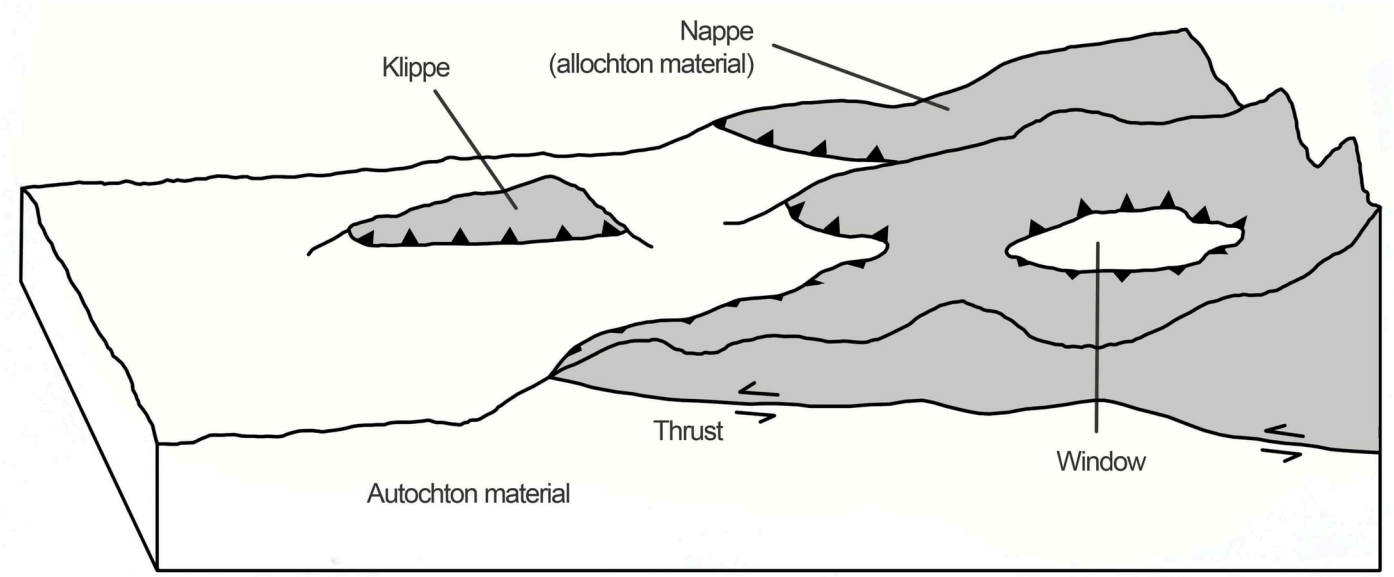


Figure 6.3.1: Illustration of a thrust system.Glacial landscape featur include cirque, tarn, arête, and horn. Arrows indicate an ice sheet, with varying elevations and labeled landforms. Allochthonous crust is indicated in dark gray and has been thrust overtop of autochton material. These units are out of sequence. "Thrust system en.jpg" by Woudloper via Wikimedia Commons is in the public domain. Access a detailed description.

Sonoma Orogeny

Following the Antler orogenic event, another compressional event, the Sonoma orogeny, added a package of exotic rocks, the

Golconda allochthon, to North America. The rocks of the Golconda allochthon represent the sediments that were once on the floor of an ocean that has since disappeared. The Paleozoic rocks of the marine Golconda Allochthon suggest that not only was compression occurring, but subduction was also happening to the west. There are multiple instances of these types of marine sedimentary rocks, originating both nearby and far traveled, that were added to North America at this time. The exact geometries of the Sonoma orogeny are even less well understood than those of the Nevadan.

When imagining what this paleoenvironment looked like, geologists use the western Pacific as a modern analog. The western Pacific is characterized by numerous subduction zones with associated volcanic island arcs as well as marine basins that are collecting sediment from a continental source in one direction and volcanic island arcs in the other (Figure 6.3.2). If we could wind the tectonic clock forward and watch these ocean basins close, the resulting geology would resemble what geologists have mapped out as the Paleozoic geology in the western US.

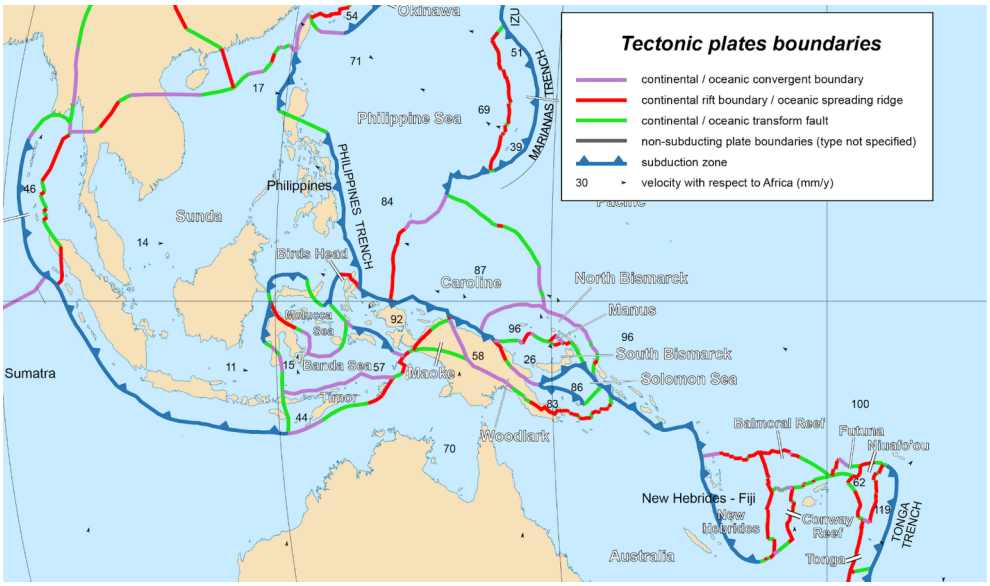


Figure 6.3.2: Tectonic map of the western pacific. "Tectonic plates boundaries" by Eric Gaba is licensed under CC BY-SA 2.5. Access a detailed description.

If we look at the reconstructed trend of the Paleozoic coastline of western North America, there is a striking feature, namely that the rocks indicating the location of the coastline do not continue very far into California. This truncation of the miogeoclinal passive margin sediments and the accreted terranes is an important feature for the next chapter in the tectonic history of California. Geologists hypothesize a left-lateral fault, the California-Coahuila transform, displaced these rocks and truncated the Laurentian shoreline (Figure 6.3.3).

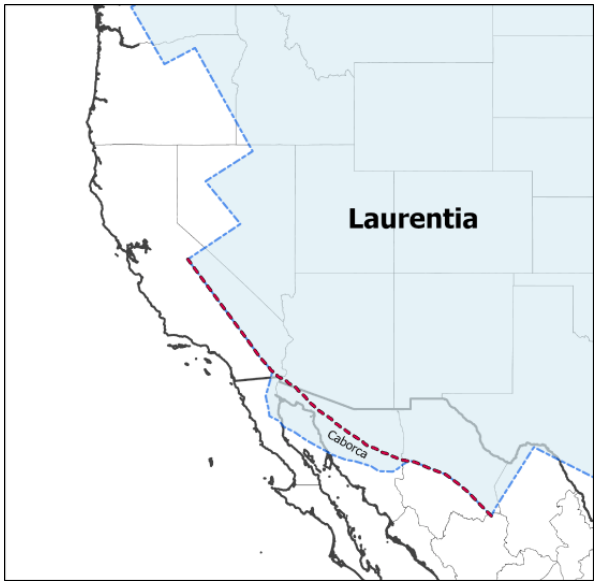


Figure 6.3.3: Truncation of the passive margin and the offset Caborca Block by the California-Coahuila transform (red line). "Passive Margin Truncated by the California-Coahuila Transform" by Skinner is licensed under CC BY-NC 4.0. Access a detailed description.

References

1. Burchfiel, B. C., & Davis, G. (1975). Nature and controls of Cordilleran orogenesis, western United States: Extensions of an earlier synthesis. American Journal of Science, 275(A).
2. Dickinson, W. R. (2004). Evolution of the North American Cordillera. Annual Review of Earth and Planetary Sciences, 32(1), 13-45. https://doi.org/10.1146/annurev.eart....101802.120257
3. Saleeby, J. (2011). Geochemical mapping of the Kings-Kaweah ophiolite belt, California—Evidence for progressive mélange formation in a large offset transform-subduction initiation environment. GSA Special Papers, 480, 31-73. https://doi.org/10.1130/2011.2480(02)
4. Winn, R. D., & Chilingarian, G. V. (1978). Deep-sea fan turbidites of the Great Valley sequence. *AAPG Bulletin*, 62(7), 1329–1349.

This page titled 6.3: Paleozoic California (541 – 252 Ma) is shared under a CC BY-NC 4.0 license and was authored, remixed, and/or curated by Allison Jones & Steven Skinner.

6.4: Mesozoic California (250 – 66 Ma)- Subduction and Mountain Building

The Shift from Passive to Active Margin

The Mesozoic is when most of the rocks that make up California are added onto North America. These Mesozoic rocks are dominantly subduction related: igneous intrusions, forearc sediments, arc volcanics, and accreted terranes. The exact geometry, orientation, and even number of subduction zones that created the features we see today is an area of active research and debate among geologists. There is resounding agreement, however, that the Mesozoic margin was shaped by long lived subduction processes.

A Magmatic Arc Forms

The Sierra Nevada, the Peninsular Ranges, as well as numerous smaller ranges throughout eastern California are made of predominantly felsic plutonic rocks that were generated through flux melting associated with this subduction (Figure 6.4.1). These plutons essentially stitch together the North American continent, accreted island arcs, and sediments from the ocean basins that once separated them.

Magmatism related to this subduction did not occur at a constant rate. Instead, it happened in episodic pulses. During these intervals, magma production increased significantly, generating large volumes of felsic plutonic rocks that now form the core of the Sierra Nevada and other Mesozoic batholiths in California. These flare-ups were separated by quieter periods with comparatively little magmatic activity. This episodic pattern is a hallmark of continental arc systems and reflects changes in subduction rate, mantle heat flow, and crustal thickness through time.

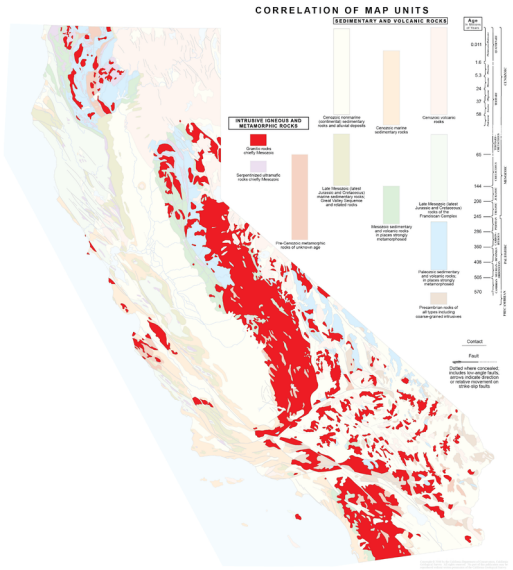


Figure 6.4.1: Simplified Geologic map of California highlighting the distribution of Mesozoic granitoids. "Mesozoic granites" by Skinner, a derivative of the Geology of California, is licensed under CC BY-NC 4.0. Access a detailed description.

Accretion of Exotic Terranes and the Franciscan Complex

Along the coast of California are widespread exposures of the Franciscan Complex, a suite of rocks formed through repeated cycles of subduction, metamorphism, and accretion. Rather than being a randomly mixed deposit, the mélange textures and diverse rock blocks reflect systematic tectonic processes associated with the growth of an accretionary wedge above a subduction zone (Figure 6.4.2). Sediments, oceanic crust, and seamounts were progressively scraped from the descending

Farallon Plate and incorporated into the continental margin. Some materials were carried to great depths, where they experienced high-pressure, low-temperature metamorphism, before being uplifted and exposed again at the surface. These processes produced the characteristic juxtapositions of blueschist, greywacke, chert, basalt, and serpentinite that define the Franciscan Complex.

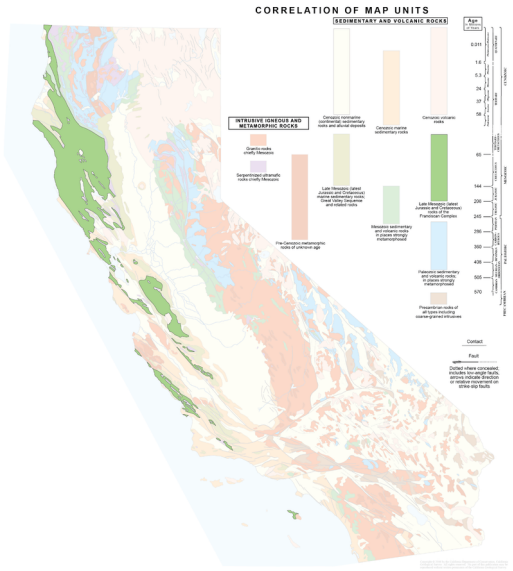


Figure 6.4.2: Simplified Geologic map of California highlighting the distribution of Mesozoic Franciscan Complex. "Mesozoic Franciscan" by Skinner, a derivative of the Geology of California, is licensed under CC BY-NC 4.0 Access a detailed description.

Great Valley Forearc Basin and Its Sedimentary Record

The Cretaceous sediments are not all a tumble jumble, though. In the Coast Range, the Great Valley Group is also preserved (Figure 6.4.3). This unit represents the sedimentary fill of a forearc basin that developed between the continental volcanic arc and the subduction zone. Rivers draining the rising Sierra Nevada and adjacent highlands transported sand and mud westward, where they were deposited in the deep-marine basin as submarine fan systems. These deposits consist primarily of alternating sandstone and shale formed by turbidity currents, recording the long-lived interaction between arc uplift, erosion, and marine sedimentation during the Mesozoic.

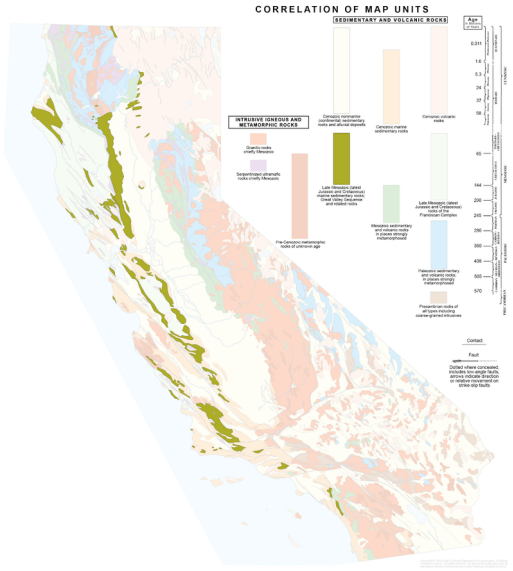


Figure 6.4.3: Geologic map of California highlighting the distribution of Mesozoic Great Valley group. "Mesozoic Great Valley" by Skinner, a derivative of Geology of California, is licensed under CC BY-NC 4.0. Access a detailed description.

Orogenies and their Impact on California's Landscape

Three Mesozoic mountain-building episodes were particularly important in the formation of the western United States and ultimately California. The Nevadan, Sevier, and Laramide orogenies took place one after another (with some overlap) from the Jurassic to the Paleogene, between about 180 and 50 million years ago. These orogenies were caused by the subduction of the Farallon Plate under the North American Plate.

During these events, subduction was occurring along the western margin of California. The topography and geology of the state thus reflect the features of a subduction zone. The California Coast Ranges formed as an accretionary wedge. In some places, mafic rocks (rocks rich in iron and magnesium) can be found in the Coast Ranges; these rocks came from ocean crust or the Earth's mantle. They were scraped off the subducting Farallon Plate and accreted to the edge of the overriding North American Plate, forming ophiolites. Serpentinite, the state rock of California, is a type of rock formed when ophiolite is metamorphosed.

Nevadan Orogeny

The first major orogenic event in the Mesozoic of North America was the Nevadan orogeny. This occurred on the other side of North America from the breakup of Pangaea and started later, in the mid-Jurassic. At some point prior to the Nevadan deformation, an active margin had developed with a volcanic arc along the west coast. These volcanic rocks and related sediments were deformed with the accretion of numerous terranes from the ancient Pacific Ocean, brought eastward as the Farallon Plate (along with the Kula plate) subducted beneath the North American Plate. The Farallon Plate used to exist between the Pacific Plate and the North American Plate.

The Farrallon's western boundary with the Pacific Plate was divergent: it was a spreading center (an oceanic ridge). The Farallon's eastern boundary adjacent to the North American Plate was convergent: a subduction zone. There, the Farallon was recycled into the mantle. Any island arcs, microcontinents, or oceanic plateaus it was carrying were too thick, buoyant, or protruding too much to subduct. When they reached the subduction zone, these terranes were scraped off and pushed onto the North American continent, adding to its volume. As they were pushed eastward, they acted like a bulldozer, scraping and shoving the volcanic and sedimentary rocks that were layered atop the continental crust. The deformation of the Nevadan orogeny is most easily seen in the Sierra Nevada mountains of California and the Klamath mountains along the coast of California and Oregon.

Sevier Orogeny

The next orogeny to occur in western North America was the Sevier orogeny. While terranes still played a factor in the deformation, the Sevier orogeny occurred much further inland and was more widespread than the Nevadan orogeny. The earliest events associated with the Sevier orogeny are as early as 160 Ma (even before the Nevadan) and the latest deformation was 50 million years ago. However, the majority of this deformation occurred between 120 and 80 million years ago. Subduction at this time changed due to the fact that the Farallon plate was hot and young, causing a Chilean-style subduction zone.

This means the resistance to subduction caused extra convergent forces in the overriding plate, mainly in the form of a fold-and-thrust belt, which extended inland. Much like the modern Andes, this created a two-ridged mountain chain, with the volcanic arc positioned closer to the trench, and a back-arc mountain range formed from compressional, low-angle thrust faulting. Between these two ridges today is a high plain, called the Altiplano in the Andes. While the exact geography of the mountains during Sevier time is unknown, it can be assumed that it was similar. Igneous rocks, closer to the Sierra Nevada, and shoved stacks of sedimentary rocks far from their original positions deep in the crust and further to the west back up this assertion. These displaced layers of rock arched upward and broke, with the slabs of older rock traveling along thrust faults up on top of younger rocks.

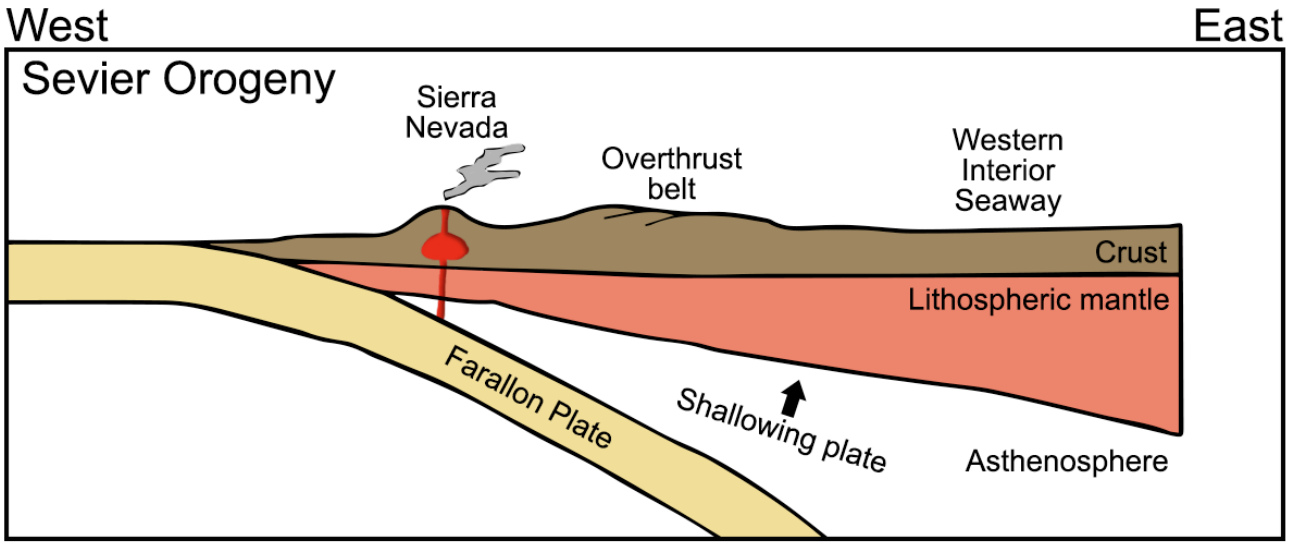


Figure 6.4.4: Diagram of the subduction of the Farallon plate during the Cretaceous Sevier Orogeny. The Wester Interior Seaway formed when the continental crust was downwarped in the central region of the North American continent. To the west, underground magma formed and the Sierra Nevada experienced volcanism. An overthrust belt occurred between the Sierra Nevada and the Western Interior Seaway. "Sevier Orogeny diagram" by Earth@Home, a derivative of Geologic History, is licensed under CC BY-NC-SA 4.0. Access a detailed description.

Laramide Orogeny

Near the end of the Mesozoic, the long-lived subduction related volcanic arc was disrupted by the tectonic forces that led to the Laramide Orogeny. The Laramide Orogeny, named for a range in Wyoming, might seem like an odd subject to cover under the title of California Geology, however, the forces that enabled the deformation well into the interior of North America were exerted along the California subduction zone. There are multiple models for transmitting compression deep into the continent. One model calls upon the collision of a series of island arcs and microcontinents, that are then translated north along transform faults and by oblique convergence at the subduction zone. Another model for the Laramide deformation is a change in the geometry of the subducting slab. A flat slab geometry, where the downgoing plate rides just beneath the overriding plate, rather than immediately descending into the mantle, allows for deformation in the interior of the continent because the area where the two plates are in contact extends well into the interior as the continent rides over the shallow dipping subducted slab. The flat slab model has been used to explain the progressive northward shutoff of magmatism in the Mesozoic arc, the removal of mantle lithosphere beneath southern California, as well as the exhumation of the southern Sierra Nevada.

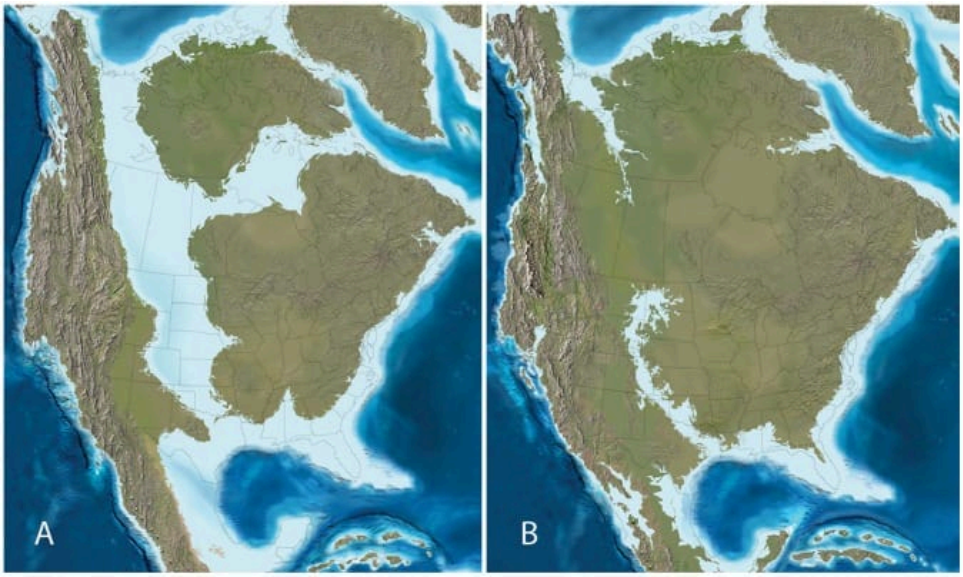


Figure 6.4.5: Paleogeographic maps illustrate the deformation taking place during the Sevier Orogeny (left, A) at ~75 Ma and the Laramide Orogeny (right, B) at ~65 Ma. The inland sea that had been present during the Sevier disappeared as the interior of North America was uplifted. "Sevier and Laramide Orogeny Paleogeogeographic Maps" by Gates, et al., a derivative of paleographic maps, are licensed under CC BY 4.0. Access a detailed description.

The third mountain-building event that took place in the western US during the late Mesozoic and early Cenozoic, overlapping with but distinct from the Sevier orogeny, is the Laramide orogeny. Ultimately, the Laramide, too, was caused by the subduction of the Farallon Plate. Compared to the Sevier, however, Laramide orogeny deformation:

- was typically more recent
- took place further east
- was deeper in the crust, involving the crystalline basement

These three characteristics allow the two orogenies to be distinguished.

The Laramide Orogeny was driven from beneath. Continuing the trend from the Sevier orogeny, the subducting plate was even younger and hotter, causing the subduction angle to become more shallow over time, eventually getting so small that the slab was dragging along the base of the overriding plate. This is known as flat-slab subduction. This subducting but dragging slab is believed to put pressure on the overriding plate, causing warps in the crust to develop. The lack of a mantle wedge below the overriding plate and above the subducting plate also meant that no magmatism occurred during the Laramide orogeny, or at least none related to subduction as it had occurred in the previous orogenies. The onset of Laramide mountain-building was in the late Cretaceous, 80 to 70 Ma, with the activity wrapping up in the window of 55 to 35 Ma. So the two orogenies overlapped in time, but the Sevier began and ended first.

Laramide Deformation Style

The Laramide orogeny's style of deformation is thick-skinned, which is a way of noting that the crystalline rocks deep in the crust are very much involved. Laramide deformation is characterized by very large anticlines and synclines that involve basement rock. The anticlines generated highlands and mountain ranges, which were weathered and eroded. The synclines were so significant that they warped the surface of the Earth, generating lowlands. These sedimentary basins that were filled with huge amounts of cast-off sedimentary detritus from the eroding mountains nearby, making new Cenozoic-aged sedimentary deposits that filled the depressions. In some cases, these young sedimentary layers reach thicknesses of 5000 meters! The economically important coal and natural gas deposits of Wyoming formed in Laramide basins, as did the fossil-rich lake deposits of the Green River Formation.

Laramide deformation does not geographically overlap Sevier deformation. Generally, Laramide deformation is further east. The Black Hills of South Dakota, the Bighorn Mountains of Wyoming, and the Colorado Front Range are all examples of basement-cored Laramide deformation. In contrast, the Sevier fold and thrust belt is further west, in a sinuous arc that runs from the Alberta/British Columbia border through western Montana, Wyoming, Utah, and Nevada, and all the way to Mexico. The Sevier orogen

is a much longer feature, too, running twice as long from Canada through the U.S. to Mexico, while the Laramide uplifts are all clustered in the mountain west of the United States alone.

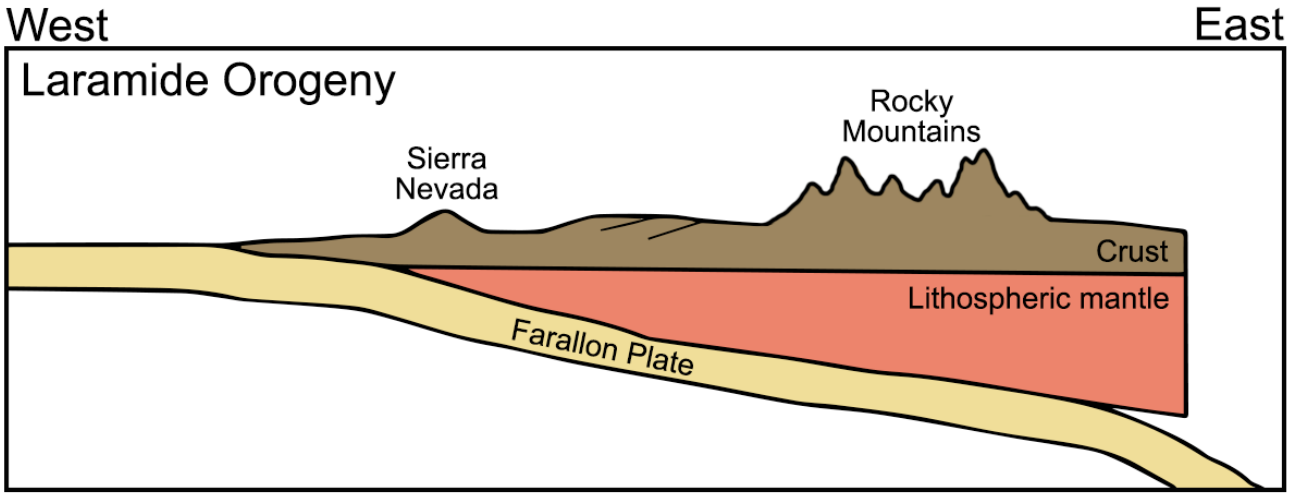


Figure 6.4.6: Subduction of the Farallon plate during the Late Cretaceous to Paleogene in what is known as the Laramide Orogeny. During this orogeny, the Western Interior Seaway closed and the Rocky Mountains were uplifted. The Sierra Nevada was no longer volcanically active. "Laramide Orogeny diagram" by Earth@Home, a derivative of Farallon Plate, is licensed under CC BY-NC-SA 4.0. Access a detailed description.

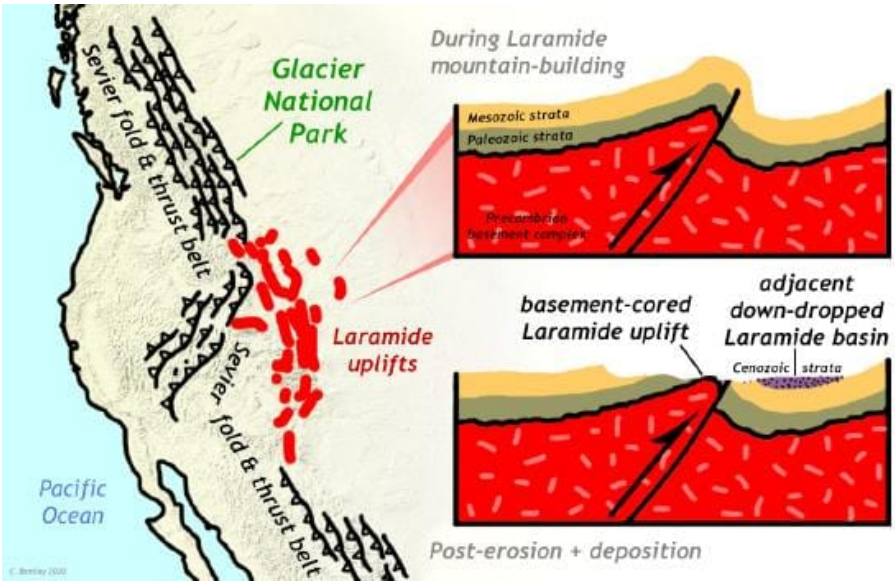


Figure 6.4.7: The Sevier fold and thrust belt is exposed in part of the western U.S. and Canada including Glacier National Park. The Laramide uplifts are present further east. Sevier fold by Bentley, et al. is licensed CC BY-NC Access a detailed description.

References

1. Bentley, C. (2020). *Historical Geology*. https://opengeology.org/historicalgeology/
2. Bird, P. (1984). Laramide crustal thickening event in the Rocky Mountain Foreland and Great Plains. Tectonics, 3(7), 741-758. https://doi.org/10.1029/TC003i007p00741
3. Burchfiel, B. C., & Davis, G. (1975). Nature and controls of Cordilleran orogenesis, western United States: Extensions of an earlier synthesis. American Journal of Science, 275(A).
4. Chapman, A., Saleeby, J., Wood, D. J., Piasecki, A., Kidder, S. B., Ducea, M. N., & Farley, K. A. (2012). Late Cretaceous gravitational collapse of the southern Sierra Nevada batholith, California. Geosphere, 8(2), 314. https://doi.org/10.1130/ges00740.1
5. Clennett, E. J., Sigloch, K., Mihalynuk, M. G., Seton, M., Henderson, M. A., Hosseini, K., . . . Müller, R. D. (2020). A Quantitative Tomotectonic Plate Reconstruction of Western North America and the Eastern Pacific Basin. Geochemistry, Geophysics, Geosystems, 21(8). https://doi.org/10.1029/2020gc009117

6. DeCelles, P. G. (2004). Late Jurassic to Eocene evolution of the Cordilleran thrust belt and foreland basin system, western U.S.A. American Journal of Science, 304(2), 105-168. https://doi.org/10.2475/ajs.304.2.105
7. Dickinson, W. R. (2004). Evolution of the North American Cordillera. Annual Review of Earth and Planetary Sciences, 32(1), 13-45. https://doi.org/10.1146/annurev.eart....101802.120257
8. Liu, L., Gurnis, M., Seton, M., Saleeby, J., Müller, R. D., & Jackson, J. M. (2010). The role of oceanic plateau subduction in the Laramide orogeny. Nature Geoscience, 3(5), 353-357. https://doi.org/10.1038/ngeo829
9. Moores, E. M. (1998). Ophiolites, the Sierra Nevada, "Cordilleria," and Orogeny along the Pacific and Caribbean Margins of North and South America. International Geology Review, 40(1), 40-54. https://doi.org/10.1080/00206819809465197
10. Quinn, D. P., Saleeby, J. B., Ducea, M. N., Luffi, P., & Asimow, P. D. (2018). Late Cretaceous Construction of the Mantle Lithosphere Beneath the Central California Coast Revealed by Crystal Knob Xenoliths. Geochemistry, Geophysics, Geosystems, 19(9), 3302-3346. https://doi.org/10.1029/2017gc007260
11. Saleeby, J. (2011). Geochemical mapping of the Kings-Kaweah ophiolite belt, California—Evidence for progressive mélange formation in a large offset transform-subduction initiation environment. GSA Special Papers, 480, 31-73. https://doi.org/10.1130/2011.2480(02)
12. Saleeby, J. B. (1999). On some aspects of the geology of the Sierra Nevada. 338, 173-184. https://doi.org/10.1130/0-8137-2338-8.173
13. Sigloch, K., & Mihalynuk, M. G. (2017). Mantle and geological evidence for a Late Jurassic–Cretaceous suture spanning North America. GSA Bulletin. https://doi.org/10.1130/b31529.1
14. Tikoff, B., Housen, B. A., Maxson, J. A., Nelson, E. M., Trevino, S., & Shipley, T. F. (2023). Hit-and-run model for Cretaceous–Paleogene tectonism along the western margin of Laurentia. In Laurentia: Turning Points in the Evolution of a Continent (pp. 659-705). https://doi.org/10.1130/2022.1220(32)
15. Wakabayashi, J., 1999, Subduction and the rock record: Concepts developed in the Franciscan Complex, California, *in* Moores, E. M., Sloan, D., and Stout, D. L., eds., Classic Cordilleran Concepts: A View from California: Boulder, Colorado, Geological Society of America Special Paper 338. https://doi.org/10.1130/0-8137-2338-8.123

This page titled 6.4: Mesozoic California (250 – 66 Ma)- Subduction and Mountain Building is shared under a CC BY-NC 4.0 license and was authored, remixed, and/or curated by Allison Jones & Steven Skinner.

6.5: Cenozoic California (66 Ma – Present)- Faulting, Uplift, and Basin Formation

Constant Change

Thought it might be hard for residents of present day California to be believe it, by about 50 million years, the ancestral Sierra Nevada that had been uplifted in the Mesozoic had eroded down to relatively low-lying hills. Large rivers flowed from Nevada and gravels laden with gold (placer gold). This continued until around 40 million years ago when once again things began to change.

End of Subduction and the Birth of the San Andreas Fault

Throughout the Mesozoic Era, the interactions between the subducting Farallon Plate and the North American Plate shaped the tectonic evolution of western North America. As the Farallon Plate continued to subduct beneath the continent, the spreading ridge between the Farallon and Pacific plates—known as the East Pacific Rise—gradually approached the subduction zone (Figure 6.5.1).

Around 30 million years ago, the East Pacific Rise reached the margin and disrupted the subduction system. This event marked a significant tectonic shift, leading to the formation of a new plate boundary: the Proto-San Andreas Fault. As a result of this change, the Farallon Plate was split into the Nazca Plate to the south and the remaining Farallon Plate to the north. The Pacific Plate was now in direct contact with the North American Plate, initiating a transform plate boundary where the plates slide past one another, rather than converge.

This newly formed boundary gave rise to two migrating triple junctions—points where three tectonic plates meet. The Mendocino Triple Junction moved northward, while the Rivera Triple Junction moved southward. As the Mendocino Triple Junction progressed north, the margin transformed from a subduction zone to a transform fault system. The Pacific Plate, which was not being subducted, left a slab window—a gap where the subducting plate had been. This gap allowed asthenospheric mantle to rise and triggered a northward-migrating pulse of magmatism, which can be traced today by a series of volcanic rocks along California's coast.

This tectonic reorganization also caused crustal rotation in Southern California. Several blocks, including the Transverse Ranges and California Borderland, rotated clockwise as a response to the new stress regime, a unique feature among North American mountain ranges.

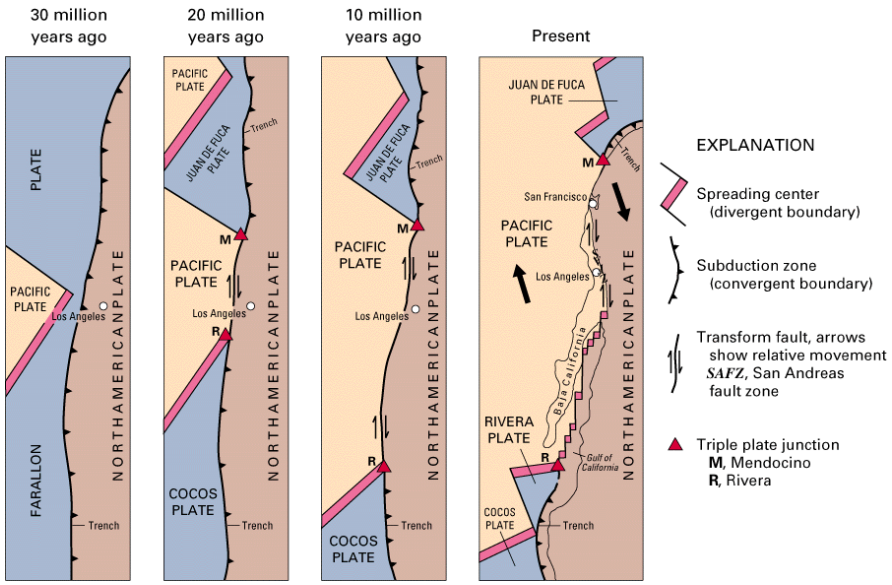


Figure 6.5.1: Evolution of the tectonic boundary from a subduction zone to a transform margin. "Evolution of the San Andreas Fault" by USGS is in the public domain. Access a detailed description.

Video 6.5.1: Cenozoic Plate Boundary Evolution

This silent video animation presents a model showing how the plate boundary evolved over time and extended inland. A detailed text description is available on YouTube. As you watch, pay close attention to the changes in eastern California as the Basin and Range province begins to form.

This interactive element is not available in this format. Visit the link or scan the QR code to access it online.

View this YouTube Video online

Cascade Volcanism

In far northern California, the Cascade Range represents a continuation of active subduction-related volcanism. While most of California transitioned to a transform boundary with the development of the San Andreas Fault, a portion of the former Farallon Plate—the Gorda Plate—continues to subduct beneath the North American Plate offshore of northern California and southern Oregon.

This active subduction drives melting in the mantle above the subducting slab, generating the Cascade Volcanic Arc. Although the Cascade Range extends from British Columbia to Northern California, only two major Cascade volcanoes lie within California's borders: Mount Shasta and Lassen Peak.

Subduction of the Gorda Plate continues today, making northern California volcanically active. However, seismic and geologic data suggest that the rate of subduction is slowing. If this trend continues, magmatism in the Cascades may diminish and eventually cease in the geologic future.

Basin and Range Extension and Crustal Thinning

The change from compressional subduction to lateral transform motion also altered the stress regime far into the continental interior. During subduction, crustal shortening had thickened the lithosphere, forming high-elevation regions. When subduction ceased, this thickened crust lost its tectonic support and began to collapse under its own weight, a process called gravitational

collapse.

This collapse produced widespread extensional faulting across a broad swath of the western U.S., creating the Basin and Range Province. This geologic province, extending from eastern California through Nevada and into Utah, is characterized by alternating mountain ranges and valleys formed by normal faults. These faults accommodate the east-west extension and crustal thinning that is still ongoing today. Additionally, right-lateral strike-slip faulting—related to the San Andreas system—also contributes to the complex deformation patterns in this region.

Video 6.5.2: Changing Plates: The Tectonic Story (85 to 20 million years ago)

This animation highlights the tectonic evolution of California from the Late Cretaceous through the early Cenozoic, emphasizing the transition from subduction to transform faulting around 20 million years ago.

This interactive element is not available in this format. Visit the link or scan the QR code to access it online.

View this YouTube Video online

Changes to the Great Valley and Coast Ranges

In the Cenozoic, especially after the onset of transform motion along the coast, the Great Valley gradually shifted from a primarily marine environment to a terrestrial one. As subduction slowed and eventually ceased in central California, the Sierra Nevada began to uplift more dramatically, increasing the rate of erosion and sediment delivery to the valley. Simultaneously, the Coast Ranges also rose, isolating the valley and enhancing its role as a sediment trap.

References

1. Atwater, T., & Stock, J. (2010). Pacific-North America Plate Tectonics of the Neogene Southwestern United States: An Update. International Geology Review, 40(5), 375-402. https://doi.org/10.1080/00206819809465216
2. Dickinson, W. R. (2004). Evolution of the North American Cordillera. Annual Review of Earth and Planetary Sciences, 32(1), 13-45. https://doi.org/10.1146/annurev.eart....101802.120257
3. Furlong, K. P., & Schwartz, S. Y. (2004). Influence of the Mendocino Triple Junction on the tectonics of coastal California. *Annual Review of Earth and Planetary Sciences*, 32, 403–433. https://doi.org/10.1146/annurev.earth.32.101802.120252
4. Luyendyk, B. P., Kamerling, M. J., & Terres, R. (1980). Geometric model for Neogene crustal rotations in southern California. Geological Society of America Bulletin, 91(4). https://doi.org/10.1130/0016-7606(1980)91<211:Gmfncr>2.0.Co;2
5. McQuarrie, N., & Wernicke, B. P. (2005). An animated tectonic reconstruction of southwestern North America since 36 Ma. Geosphere, 1(3), 147-172. https://doi.org/10.1130/GES00016.1

This page titled 6.5: Cenozoic California (66 Ma – Present)- Faulting, Uplift, and Basin Formation is shared under a CC BY-NC 4.0 license and was authored, remixed, and/or curated by Allison Jones & Steven Skinner.

6.6: Chapter Summary

6.1 Developing a Geologic History

- Quantitative global plate tectonic reconstructions can provide a starting point for understanding the geologic development of a region.
- Detailed studies of rock units and their relationships can provide more information about how a region has changed through time.
- Sedimentary rocks can be used to reconstruct the surface conditions at the time they were deposited.
- Metamorphic and igneous rocks can be used to reconstruct processes that occur beneath the surface of the Earth.

6.2 Proterozoic Eon (2500–540 Ma)

- Initial stages of rifting of the supercontinent Rodinia creates basins that fill with sediment along the western margin of Laurentia.
- Continued rifting results in the creation of a oceanic spreading center and new oceanic lithosphere.
- As the rifted margin cools, thermal subsidence creates additional space for sediment accumulation
- Thick deposits of marine sedimentary rocks accumulate along the passive margin.

6.3 Paleozoic Era (540–250 Ma)

- Marine sedimentary rocks continue to accumulate across the passive margin.
- A subduction zone initiates offshore and creates a compressional environment.
- Large packages of rock are displaced from where they formed and thrust onto the continent.

6.4 Mesozoic Era (250–66 Ma)

- An ocean-continent subduction zone forms with the Farallon plate going beneath the North American plate.
- Flux melting above the subducting plate produces magmas that intrude into the earlier sedimentary sequences.
- The Sierra Nevada represents the intrusive component of the Mesozoic arc while the extrusive component has mostly eroded away into great valley sediments.
- The subducting plate brings with it island arcs that get added to North America.

6.5 Cenozoic Era (66 Ma–Present)

- The Pacific-Farallon spreading ridge intersects the subduction trench and creates a new tectonic boundary between the Pacific and North American plates.
- The new Pacific and North American plate boundary has a right-lateral transform sense of motion.
- The zone of contact between the Pacific and North American plates grows as the Mendocino triple junction migrates north.
- Migration of the triple junction is accompanied by a slab window that creates a migrating pulse of volcanism along the coast.
- A wide zone of extension, the Basin and Range province, also develops in response to the changes at the plate boundary.

This page titled 6.6: Chapter Summary is shared under a CC BY-NC 4.0 license and was authored, remixed, and/or curated by Allison Jones & Steven Skinner.

6.7: Detailed Figure Descriptions

Figure 6.2.1 Rodinia

This circular paleogeographic reconstruction shows the Rodinia supercontinent as it may have appeared about 750 million years ago (Ma), during the Neoproterozoic era. The supercontinent is composed of multiple continental blocks labeled with their modern names. These include:

- Laurentia at the center
- East Antarctica, Australia, South China, Siberia, India, and Madagascar to the west and north
- Baltica, Amazonia, West Africa, Rio Plata, and Kalahari surrounding Laurentia on the south and east
- Congo–São Francisco in the southwestern sector

All landmasses are shown in brown against a blue ocean background. The map provides a simplified visualization of tectonic reconstructions used in geology to understand ancient plate configurations and supercontinent cycles.

Figure 6.2.2 A Diagrammatic Passive Margin

This simplified diagram shows a passive margin along the western North American continent. From left to right we see the ocean depicted above a thin layer of sediment, which rests on a thicker oceanic crust above a still thicker mantle region. The middle of the diagram shows the sediments quickly increasing in thickness as the ocean layer thins. The oceanic crust gives way as the continental crust thrust upward, pushing the mantle downward. When we reach the right side of the diagram the ocean has receded and the continental crust takes up most of the vertical space. A very thin layer of sediment overlays the continental crust, and the mantle has thickened below it.

Figure 6.2.3 Distribution of Precambrian Rocks

This detailed diagram from the California Geological Survey displays a statewide geologic map with a corresponding correlation chart of map units based on age and rock type.

Highlighed are precambian Rocks (older than 541 million years). These are some of the oldest rocks in California, representing the ancient continental basement that formed long before most tectonic accretion events that built the rest of the state's geology. Precambrian rocks are not widespread across California. They are restricted to specific regions, mainly: Southeastern California, Eastern California, east of the Sierra Nevada.

- Precambrian plutonic rocks . These rocks are shown in the southeastern part of California, concentrated in the southeastern corner of the state. They appear as isolated exposures surrounded by younger rock units. The map indicates that these rocks are older than 541 million years and are limited in geographic extent.
- Precambrian metamorphic rocks. These rocks are shown in eastern California, primarily east of the Sierra Nevada, including ranges near Death Valley and the White–Inyo Mountains. They occur in narrow belts and blocks rather than continuous statewide coverage.
- Precambrian metasedimentary rocks. These rocks are also shown in eastern California, commonly associated with the same regions where Precambrian metamorphic rocks are mapped. They appear in elongate outcrop areas within mountain ranges east of the Sierra Nevada.

The figure place the Precambrian rocks in the context of California's overall geologic framework.

- Cenozoic (0–65 Ma)
  - Cenozoic nonmarine (continental) sedimentary rocks and alluvial deposits (~0.011–65 Ma). These rocks are shown mainly in large lowland areas, especially the Central Valley and other broad interior basins. They also appear in smaller patches along major river valleys and coastal lowlands.
  - Cenozoic marine sedimentary rocks (~1.6–65 Ma). These rocks occur primarily along the coastal regions of California. They form discontinuous belts near the shoreline and adjacent offshore-margin areas.
  - Cenozoic volcanic rocks (~1.6–65 Ma). These rocks are concentrated in northeastern California and parts of eastern

California. Smaller volcanic areas also appear scattered in the Coast Ranges and southern California.

- Mezozoic (65–245 Ma)
  - Late Mesozoic (latest Jurassic and Cretaceous) marine sedimentary rocks; Great Valley Sequence and related rocks (~145–65 Ma). These rocks form a long, continuous band along the western side of the Central Valley. They are positioned between the Coast Ranges and the Sierra Nevada.
  - Mesozoic sedimentary and volcanic rocks in places strongly metamorphosed (~245–65 Ma). These rocks occur mainly in the Sierra Nevada foothills and parts of the Klamath Mountains. They appear as elongated belts adjacent to large areas of granitic rocks.
  - Late Mesozoic (latest Jurassic and Cretaceous) Franciscan Complex (~145–65 Ma). This unit is widely distributed throughout the Coast Ranges of California. It forms a broad, irregular belt parallel to the coastline.
  - Granitic rocks chiefly Mesozoic (~245–65 Ma). These rocks dominate the Sierra Nevada and form a large, continuous region there. Smaller granitic bodies also appear in southern California and parts of the Coast Ranges.
  - Serpentinized ultramafic rocks chiefly Mesozoic (~245–65 Ma). These rocks occur as narrow, scattered bodies primarily within the Coast Ranges and the Klamath Mountains. They are also present in small patches along major fault zones.
- Paleozoic (245–570 Ma)
  - Paleozoic sedimentary and volcanic rocks; in places strongly metamorphosed (~570–245 Ma). These rocks are found in eastern California and in parts of the Klamath Mountains. They also appear in smaller, isolated areas within mountain ranges.
- Pre-Cenozoic (>65 Ma)
  - Pre-Cenozoic metamorphic rocks of unknown age (>65 Ma). These rocks are shown in scattered areas within mountain belts across the state. They commonly occur adjacent to granitic rocks in the Sierra Nevada and southern California.

Figure 6.2.6 Rifting of a Continental Plate

This diagram illustrates how a continental landmass begins to split apart and eventually forms new oceanic crust. The figure shows stretching and thinning of the continental lithosphere, which leads to the development of deep basins and the upwelling of hot mantle material from below. As rifting progresses, surface rocks fracture along large normal faults, and the crust becomes increasingly thin. Continued extension allows molten rock to rise and form new basaltic crust in the center of the rift. This process marks the transition from a continent-breaking-apart environment to the formation of a young ocean basin. The diagram represents the early stages of what would eventually become the passive margin along the ancient western edge of North America.

Figure 6.3.1 Thrust System and Allochthonous Rocks

This figure depicts a simplified model of a thrust fault system in which older rocks are pushed above younger rocks due to compressional forces. The upper block of rock, which has been transported from elsewhere, is called an allochthon. It rests above the lower block, known as the autochthon, which remains in its original position. This type of deformation results from horizontal compression associated with convergent plate boundaries.

The figure also includes a klippe: an isolated remnant of the thrust sheet (the allochthon) that has been left behind after erosion removes most of the surrounding overlying rock. Also included is a window which occurs erosion cuts through the overlying thrust sheet, creating an opening that exposes the underlying autochthonous rocks beneath.

Figure 6.3.2 Western Pacific as an Analog for Paleozoic Tectonics

This is a map of the modern western Pacific region that is used as an analogy for the Paleozoic tectonic environment of western North America. It includes multiple subduction zones, volcanic island arcs, ocean basins, and microcontinents. The purpose of the figure is to show that during the Paleozoic, the margin of Laurentia was not a simple passive margin but included oceanic plates and island arcs separated by narrow basins, much like the western Pacific today. The image emphasizes that material from different tectonic environments can later become accreted to a continental margin as convergence continues.

Locations of each tectonic plate boundary:

- Continental / oceanic convergent boundary. This boundary type appears along the margins of island chains and continental edges. It is found near labeled locations such as the Aleutian Arc, Kuril Arc, Japan Arc, Ryukyu Arc, Izu-Bonin Arc, and Mariana Arc, and along boundaries adjacent to the Philippines and New Hebrides – Fiji regions.
- Continental rift boundary / oceanic spreading ridge. This boundary type appears in open ocean areas where boundary

lines pass through water between landmasses. It is found in regions labeled Banda Sea, Woodlark, Manus, and near South Bismarck and North Bismarck.
- Continental / oceanic transform fault. This boundary type appears as straight or gently curving boundary segments that run alongside other boundaries. It is found near labeled regions such as Timor, Birds Head, Solomon Sea, and along boundary segments near New Guinea and surrounding islands.
- Non-subducting plate boundaries (type not specified). These boundaries appear as simple boundary lines without additional symbols. They are found between labeled regions such as Caroline, Manus, North Bismarck, and South Bismarck, and in several ocean areas without trench labels.
- Subduction zone. This boundary type appears as curved boundary lines adjacent to trench labels. It is found at locations labeled Marianas Trench, Philippines Trench, Tonga Trench, and along curved boundaries near Sumatra, Timor, and New Hebrides – Fiji.

The map uses arrows with numbers to show plate velocities relative to Africa. Africa is the reference frame, so other plates have arrows indicating both direction of motion and speed compared to Africa.

- The Pacific Plate has long arrows pointing generally westward or northwestward, with larger numerical values, indicating faster motion relative to Africa.
- Plates closer to Africa, such as the Eurasian Plate and Indian Plate, have shorter arrows with smaller numbers, indicating slower motion relative to Africa.
- Southern plates such as the Australian Plate and Antarctic Plate have arrows pointing generally northward or northeastward, each labeled with a specific cm/yr value.
- Plates in the Americas, such as the North American Plate, show arrows pointing generally westward, with moderate numerical values.

Figure 6.3.3 Truncated Passive Margin by the California-Coahuila Transform

This figure illustrates how part of the Paleozoic passive margin and its sedimentary deposits were displaced along a large-scale transform fault known as the California–Coahuila transform. The diagram shows that a block of continental crust referred to as the Caborca Block was shifted relative to the remainder of the margin. This motion displaced the original alignment of shelf sediments and accreted terranes, explaining why these rocks are not continuous across the present-day region.

Figure 6.4.1 Distribution of Mesozoic Granitoids in California

This map highlights the areas in California underlain by large bodies of granitoid rock that formed during Mesozoic subduction (~245–65 Ma). The plutonic rocks, which cooled slowly from magma deep within the crust, form the core of mountain ranges such as the Sierra Nevada and the Peninsular Ranges. The spatial pattern of these rocks outlines the location of a former magmatic arc generated above a subduction zone. The figure provides evidence that subduction-related magmatism was widespread and long-lasting during the Mesozoic.

The figure place the Precambrian rocks in the context of California's overall geologic framework.

- Cenozoic (0–65 Ma)
  - Cenozoic nonmarine (continental) sedimentary rocks and alluvial deposits (~0.011–65 Ma). These rocks are shown mainly in large lowland areas, especially the Central Valley and other broad interior basins. They also appear in smaller patches along major river valleys and coastal lowlands.
  - Cenozoic marine sedimentary rocks (~1.6–65 Ma). These rocks occur primarily along the coastal regions of California. They form discontinuous belts near the shoreline and adjacent offshore-margin areas.
  - Cenozoic volcanic rocks (~1.6–65 Ma). These rocks are concentrated in northeastern California and parts of eastern California. Smaller volcanic areas also appear scattered in the Coast Ranges and southern California.
- Mezozoic (65–245 Ma)
  - Late Mesozoic (latest Jurassic and Cretaceous) marine sedimentary rocks; Great Valley Sequence and related rocks (~145–65 Ma). These rocks form a long, continuous band along the western side of the Central Valley. They are positioned between the Coast Ranges and the Sierra Nevada.
  - Mesozoic sedimentary and volcanic rocks in places strongly metamorphosed (~245–65 Ma). These rocks occur mainly in the Sierra Nevada foothills and parts of the Klamath Mountains. They appear as elongated belts adjacent to large areas

of granitic rocks.
    - Late Mesozoic (latest Jurassic and Cretaceous) Franciscan Complex (~145–65 Ma). This unit is widely distributed throughout the Coast Ranges of California. It forms a broad, irregular belt parallel to the coastline.
    - Serpentinized ultramafic rocks chiefly Mesozoic (~245–65 Ma). These rocks occur as narrow, scattered bodies primarily within the Coast Ranges and the Klamath Mountains. They are also present in small patches along major fault zones.
- Paleozoic (245–570 Ma)
    - Paleozoic sedimentary and volcanic rocks; in places strongly metamorphosed (~570–245 Ma). These rocks are found in eastern California and in parts of the Klamath Mountains. They also appear in smaller, isolated areas within mountain ranges.
- Precambrian (older than 570 Ma)
    - Precambrian rocks of all types including coarse-grained intrusives (>570 Ma). These rocks are restricted mainly to southeastern California. They appear as isolated patches within desert mountain ranges.
- Pre-Cenozoic (>65 Ma)
    - Pre-Cenozoic metamorphic rocks of unknown age (>65 Ma). These rocks are shown in scattered areas within mountain belts across the state. They commonly occur adjacent to granitic rocks in the Sierra Nevada and southern California.

Figure 6.4.2 Distribution of Mesozoic Franciscan Complex

This map shows the geographic extent of the Franciscan Complex along the California Coast Ranges. The Franciscan Complex (~145–65 Ma) is composed of highly deformed sedimentary and volcanic rocks that were scraped off the downgoing oceanic plate in a subduction zone. These rocks were transported to great depth, metamorphosed under high pressure, and then returned to the surface. The irregular distribution of rock types reflects the chaotic nature of subduction and accretion processes.

The figure place the Precambrian rocks in the context of California's overall geologic framework.

- Cenozoic (0–65 Ma)
    - Cenozoic nonmarine (continental) sedimentary rocks and alluvial deposits (~0.011–65 Ma). These rocks are shown mainly in large lowland areas, especially the Central Valley and other broad interior basins. They also appear in smaller patches along major river valleys and coastal lowlands.
    - Cenozoic marine sedimentary rocks (~1.6–65 Ma). These rocks occur primarily along the coastal regions of California. They form discontinuous belts near the shoreline and adjacent offshore-margin areas.
    - Cenozoic volcanic rocks (~1.6–65 Ma). These rocks are concentrated in northeastern California and parts of eastern California. Smaller volcanic areas also appear scattered in the Coast Ranges and southern California.
- Mezozoic (65–245 Ma)
    - Late Mesozoic (latest Jurassic and Cretaceous) marine sedimentary rocks; Great Valley Sequence and related rocks (~145–65 Ma). These rocks form a long, continuous band along the western side of the Central Valley. They are positioned between the Coast Ranges and the Sierra Nevada.
    - Mesozoic sedimentary and volcanic rocks in places strongly metamorphosed (~245–65 Ma). These rocks occur mainly in the Sierra Nevada foothills and parts of the Klamath Mountains. They appear as elongated belts adjacent to large areas of granitic rocks.
    - Granitic rocks chiefly Mesozoic (~245–65 Ma). These rocks dominate the Sierra Nevada and form a large, continuous region there. Smaller granitic bodies also appear in southern California and parts of the Coast Ranges.
    - Serpentinized ultramafic rocks chiefly Mesozoic (~245–65 Ma). These rocks occur as narrow, scattered bodies primarily within the Coast Ranges and the Klamath Mountains. They are also present in small patches along major fault zones.
- Paleozoic (245–570 Ma)
    - Paleozoic sedimentary and volcanic rocks; in places strongly metamorphosed (~570–245 Ma). These rocks are found in eastern California and in parts of the Klamath Mountains. They also appear in smaller, isolated areas within mountain ranges.
- Precambrian (older than 570 Ma)
    - Precambrian rocks of all types including coarse-grained intrusives (>570 Ma). These rocks are restricted mainly to southeastern California. They appear as isolated patches within desert mountain ranges.
- Pre-Cenozoic (>65 Ma)
    - Pre-Cenozoic metamorphic rocks of unknown age (>65 Ma). These rocks are shown in scattered areas within mountain belts across the state. They commonly occur adjacent to granitic rocks in the Sierra Nevada and southern California.

Figure 6.4.3 Distribution of Mesozoic Great Valley Group Sedimentary Rocks

This map illustrates the location of sedimentary rocks of the Great Valley Group, which formed in a forearc basin between the Mesozoic volcanic arc and the subduction zone (~145–65 Ma). These rocks accumulated as thick layers of sand and mud transported by rivers draining the rising Sierra Nevada. The sediments formed deep marine submarine fan systems that filled the basin. The distribution of these rocks records the position of the forearc basin and helps reconstruct the geometry of the late Mesozoic continental margin.

The figure place the Precambrian rocks in the context of California's overall geologic framework.

- Cenozoic (0–65 Ma)
  - Cenozoic nonmarine (continental) sedimentary rocks and alluvial deposits (~0.011–65 Ma). These rocks are shown mainly in large lowland areas, especially the Central Valley and other broad interior basins. They also appear in smaller patches along major river valleys and coastal lowlands.
  - Cenozoic marine sedimentary rocks (~1.6–65 Ma). These rocks occur primarily along the coastal regions of California. They form discontinuous belts near the shoreline and adjacent offshore-margin areas.
  - Cenozoic volcanic rocks (~1.6–65 Ma). These rocks are concentrated in northeastern California and parts of eastern California. Smaller volcanic areas also appear scattered in the Coast Ranges and southern California.
- Mezozoic (65–245 Ma)
  - Mesozoic sedimentary and volcanic rocks in places strongly metamorphosed (~245–65 Ma). These rocks occur mainly in the Sierra Nevada foothills and parts of the Klamath Mountains. They appear as elongated belts adjacent to large areas of granitic rocks.
  - Late Mesozoic (latest Jurassic and Cretaceous) Franciscan Complex (~145–65 Ma). This unit is widely distributed throughout the Coast Ranges of California. It forms a broad, irregular belt parallel to the coastline.
  - Granitic rocks chiefly Mesozoic (~245–65 Ma). These rocks dominate the Sierra Nevada and form a large, continuous region there. Smaller granitic bodies also appear in southern California and parts of the Coast Ranges.
  - Serpentinized ultramafic rocks chiefly Mesozoic (~245–65 Ma). These rocks occur as narrow, scattered bodies primarily within the Coast Ranges and the Klamath Mountains. They are also present in small patches along major fault zones.
- Paleozoic (245–570 Ma)
  - Paleozoic sedimentary and volcanic rocks; in places strongly metamorphosed (~570–245 Ma). These rocks are found in eastern California and in parts of the Klamath Mountains. They also appear in smaller, isolated areas within mountain ranges.
- Precambrian (older than 570 Ma)
  - Precambrian rocks of all types including coarse-grained intrusives (>570 Ma). These rocks are restricted mainly to southeastern California. They appear as isolated patches within desert mountain ranges.
- Pre-Cenozoic (>65 Ma)
  - Pre-Cenozoic metamorphic rocks of unknown age (>65 Ma). These rocks are shown in scattered areas within mountain belts across the state. They commonly occur adjacent to granitic rocks in the Sierra Nevada and southern California.

Figure 6.4.4 Sevier Orogeny Cross Section

This is a cross-sectional diagram illustrating the tectonic processes during the Sevier Orogeny, which was a mountain-building event that affected western North America during the Late Cretaceous. The diagram presents a simplified west-to-east slice through the region, showing the geological features and tectonic interactions at the time.

On the left (west) side of the diagram, the Sierra Nevada mountain range is depicted, with an active volcano shown. A magma reservoir is shown within the crust, but the volcano shaft extends down through the lithospheric mantel and the asthenosphere to the Farallon Plate, which is subducting beneath the North American Plate at a steep angle.

Beneath the North American Plate lies the lithospheric mantle, and below that is the asthenosphere, a layer of the Earth's mantle that is involved in the tectonic movement. The angle of the subducting Farallon Plate becomes becoming less steep as it subducts. This is indicated on the diagram as the shallowing plate.

Moving to the right (east) side, the diagram shows the overthrust belt, where rock layers have been pushed over one another due to compression, which is a key feature of the Sevier Orogeny. The Western Interior Seaway is a body of water extending to the east of the mountain range.

Figure 6.4.5 Paleogeographic Maps

During the Sevier Orogeny, at ~75 Ma, much of North America was submerged. Most of modern-day Mexico was under water, with only a strip of land along its western flank visible. Much of what is now Texas, Louisiana, North and South Carolina, Florida, and coastal states along the Eastern Seaboard were submerged. An inland sea is shown in a rough Y shape. The western leg is shown extending from what is now the Yukon and Alberta in Canada through a swath including what is now Montana, Wyoming, and Colorado to empty into the sea in what is now eastern Texas; the eastern leg splits off (approximately) where Minnesota is now and extends northeast through Quebec, Canada, where it meets the wider ocean.

By the time of the Laramide Orogeny, at ~65 Ma, most of the inland sea has disappeared and the North American coastline is closer to what we would recognize today. Much of the area that is now Mexico has uplifted, as has much of Texas and the gulf states (although the Texas panhandle is still submerged). A remnant of the inland sea remains as a curved arc entering along what is now eastern Texas and moving up through modern-day Oklahoma, Colorado, Wyoming, and South Dakota.

Figure 6.4.6 Laramide Orogeny Cross Section

This image is a cross-sectional diagram depicting the tectonic setting during the Laramide Orogeny, showing a west-to-east slice through the western United States. On the west side, the Sierra Nevada mountain range a relatively low, rounded highland. Beneath it, the Farallon Plate is a broad, gently dipping slab moving eastward beneath the North American continent. Toward the east, the Rocky Mountains a series of high, rugged peaks. The crust beneath them rests above the lithospheric mantle.

The Farallon Plate extends beneath the entire section, subducting at a shallow angle beneath the North American Plate, and descending at a much lower angle than typical subduction zones.

Figure 6.4.7 Features Associated with the Laramide Orogeny

The Laramide Orogeny was a mountain-building event that affected western North America during the Late Cretaceous to early Paleogene.

The main portion of the image is a simplified map of the western United States, showing major structural features of the Laramide and Sevier Orogenies. The Sevier fold and thrust belt is depicted as a series of parallel, wavy lines running from the southwestern U.S. toward the northwest. To the east of the Sevier belt, the Laramide uplifts are marked, representing block uplifts of Precambrian basement rock that formed during the Laramide Orogeny.

Glacier National Park is labeled near the northernmost extent of the Sevier fold and thrust belt. The Pacific Ocean is labeled to indicate the western boundary of the region.

Two cross-sectional diagrams on the right illustrate the geological processes occurring during and after the Laramide Orogeny.

During Laramide Mountain-Building

- This diagram represents an uplifted region during the Laramide Orogeny.
- A deep-seated fault cuts through the Precambrian basement complex, forcing it upward and tilting overlying Paleozoic and Mesozoic sedimentary layers.
- The faulting causes the formation of a Laramide uplift (a block of rock pushed upward) adjacent to a down-dropped basin.

Post-Erosion and Deposition

- This diagram shows the landscape after erosion and sediment deposition.
- The uplifted block remains structurally elevated but has been subjected to erosion, reducing its topographic relief.
- In the adjacent down-dropped basin, younger Cenozoic strata have accumulated, burying parts of the faulted sedimentary layers.

Figure 6.5.1 Tectonic Evolution of the West Coast Plate Boundary: 30 Million Years Ago to Present

This four-panel image illustrates the tectonic evolution of the Pacific–North American plate boundary over time, from 30 million years ago to the present. It shows how the subduction of the Farallon Plate has been replaced by a transform boundary (the San Andreas Fault Zone) as new plates formed and spreading centers shifted.

30 Million Years Ago

- The Farallon Plate is subducting beneath the North American Plate at a long, continuous trench.
- The Pacific Plate is to the west of the Farallon Plate.
- A spreading center (divergent boundary) is shown along the southeast edge of the Pacific Plate.
- The San Andreas Fault has not yet formed.

20 Million Years Ago

- Two sections of the Pacific Plate come into view. The southmost section begins to subduct beneath the North American Plate in roughly the area where Los Angeles is located today. As it moves, it bisects the Farallon Plate, which becomes the Juan de Fuca Plate in the north and Cocos Plate in the south.
- Long trenches remain where the North American Plate abuts the Juan De Fuca and Cocos plates.
- Spreading centers (divergent boundaries) are shown along the southeast edges of the Pacific Plate where it meets the Juan De Fuca Plate in the north and the Cocos Plate in the south.
- Triple junctions are indicated where the Pacific Plate meets the North American Plate:
  - In the north, the Mendocino Triple Junction is where the Juan De Fuca, Pacific, and North American plates meet.
  - In the south, the Rivera Triple Junction is where the Cocos, Pacific, and North American plates meet.
  - A transform fault (early San Andreas Fault) has begun forming between the Pacific and North American plates, as the Pacific Plate moves in a northward direction and the North American Plate moves southward.

10 Million Years Ago

- As the Pacific Plate (moving northward) continues to subduct beneath the North American Plate (moving southward), the transform fault becomes longer. It stretches from roughly what is now Central California in the north to what is now Baja California in the south; accordingly, the distance between the Mendocino and Rivera triple junctions has increased dramatically.
- Trenches remain where the North American Plate abuts the Juan De Fuca and Cocos plates.
- Spreading centers (divergent boundaries) are shown along the southeast edges of the Pacific Plate where it meets the Juan De Fuca Plate in the north and the Cocos Plate in the south.

Present

- As the Pacific Plate slides northwest past the North American Plate, the San Andreas Fault is a dominant boundary feature. It now extends from the Mendocino Triple Junction north of San Francisco to the Rivera Triple Junction in the Gulf of California.
- The Juan de Fuca Plate is shown in the north, bordered by a trench along its south edge where it meets the North American Plate.
- The Rivera Plate now appears along the coast of Mexico, bounded on the east by the trench along the North American Plate. It is shown as a rough triangle with the Rivera Triple Junction as one of its points.
- The Cocos Plate still appears in the south, at the bottom of the map, bounded on the east by the trench along the North American Plate.
- Spreading centers (divergent boundaries) are still shown along the southeast edges of the Pacific Plate where it meets the Juan De Fuca Plate in the north, and where it meets the Rivera and Cocos plates in the south. However, additional divergent boundaries now appear along the San Andreas Fault from roughly its midpoint and moving south.

This page titled 6.7: Detailed Figure Descriptions is shared under a CC BY-NC 4.0 license and was authored, remixed, and/or curated by Allison Jones & Steven Skinner.

7: CASCADE RANGE AND MODOC PLATEAU

Introduction to the Cascade Range and Modoc Plateau

The Cascade Range geomorphic province of California represents the southern end of the larger, North American Cascade Mountain Range, which extends north into Oregon, Washington and British Columbia and is the result of subduction at the Cascadia subduction zone. This narrow province is bounded by the Klamath Mountains to the west, the Modoc Plateau to the east, and the Sierra Nevada to the south (Figure 7.1). It is characterized by high mountainous terrain of volcanic origin.

The Modoc Plateau lies to the East of the Cascades and west of the Basin and Range and can be thought of as the transition between the two (Figure 7.1). The geology is influenced by the tectonics of Cascadia subduction as well as Basin and Range extension. As the name 'Plateau' implies, this geologic province is high in elevation and relatively flat. The volcanic features here differ from the iconic snow-covered peaks of the Cascade Range and consist mainly of smaller volcanoes and lava flows. In the rain shadow of the Cascades, the climate of the Modoc Plateau is dry. This same rain shadow effect exists throughout the Cascade Range and creates a dramatic change in climate from the rainy cities of Portland and Seattle to the deserts of eastern Oregon and Washington. The rain shadow effect is described in Regional Extent and Overview of the Basin and Range in the context of the Sierra Nevada Mountain Range.

While both the Cascades and the Modoc Plateau contain varied geology, this chapter is focused primarily on the volcanoes and volcanic processes in the two provinces. We first introduce the conceptual framework for understanding volcanoes and their tectonic origins, then dive into three important case study areas, Mount Shasta, Lassen Volcanic National Park and the Medicine Lake Volcano (including Lava Beds National Monument). There is considerable overlap between the geology of the Klamath Mountains, Cascade Range, Modoc Plateau and Basin Range provinces. Many of the non-volcanic rocks in the western part of the Cascade Range are described in Chapter 10: Klamath Mountains (for example, The McCloud Limestone- An Ancient Coral Reef), and the nature of faulting within the southeastern Modoc Plateau is comparable to that of the Basin and Range province (see Rift-Related Faulting in Eastern California).



Figure 7.1: "Cascade Range and Modoc Plateau Provinces of California" by Emily Wright, is licensed under CC-BY-NC / a derivative from the Geology of California. Access a detailed description.

Learning Objectives

By the end of this chapter, you should be able to:

- Explain how magma is produced and how volcanic arcs are formed at subduction zones.

- Classify volcanoes based on shape, size, and composition.
- Explain the relationship between magma viscosity and volcano type.
- Recognize common volcanic features.
- Describe the process of formation of hydrothermal systems in volcanic environments.
- Identify the major volcanic hazards associated with Cascade Volcanoes.
- Recognize evidence of past glaciation in a volcanic setting.
- Locate the Cascade Range and Modoc Plateau on a map of California.
- Explain how the Cascade Range and Modoc Plateau fit into the broader context of the tectonic and geologic history of California.

7.1: The Cascadia Subduction Zone and the Cascade Continental Volcanic Arc

7.2: Rock Types of the Cascades

7.3: The Variety of Volcanoes in the Cascades and the Modoc Plateau

7.4: Volcanic Hazards

7.5: Mount Shasta

7.6: Lassen Volcanic National Park

7.7: Medicine Lake Volcano

7.8: Glaciers in the Cascades

7.9: Chapter Summary

7.10: Detailed Figure Descriptions

This page titled 7: Cascade Range and Modoc Plateau is shared under a CC BY-NC 4.0 license and was authored, remixed, and/or curated by Emily Wright.

7.1: The Cascadia Subduction Zone and the Cascade Continental Volcanic Arc

Tectonic Setting of the Cascade Range

The Cascade Range Province of California is located in the northern portion of the state and composes part of a larger, regional province, which extends from Northern California through Oregon and Washington into British Columbia (Figure 7.1.1). The Cascade Range (sometimes simply referred to as “the Cascades”) is known for its classic composite volcanoes (also referred to as stratovolcanoes or composite cones), including Mount Rainier (Tahoma), Mount Saint Helens (Loowit, Louwala-Clough), Mount Hood (Wy’east), and Mount Shasta (Waka-nunee-Tuki-wuki). However, the Cascade Range also includes many other volcanoes and volcanic features as well as non-volcanic, tectonically uplifted mountains. The Cascade Range is the volcanic arc mountain range produced by the subduction of the Juan de Fuca plate beneath the North American plate at the Cascadia subduction zone and also makes up part of the Ring of Fire, a series of such volcanic ranges that surround the Pacific Ocean (Figure 7.1.2). The Modoc Plateau is also part of the Cascadia subduction system. This province lies to the east of the main Cascade volcanic arc and is confined to California, although similar plateau provinces can also be found east of the Cascades in Oregon, including the High Lava Plateau and Columbia Plateau.

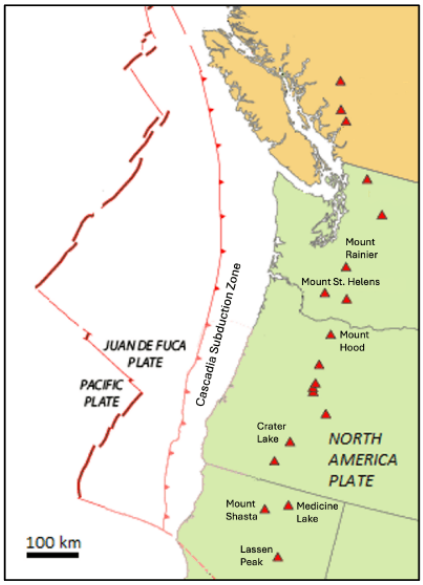


Figure 7.1.1: Location of the major volcanoes of the Cascades (red triangles) in relation to the Cascadia subduction zone. The Juan de Fuca plate is forming along the Juan de Fuca ridge, which separates it from the Pacific plate, and is then subducted beneath the North American plate along the Cascadia subduction zone, indicated by the red line with teeth on it. This map was modified from the original "Volcanoes and Subduction" by Steven Earle, Physical Geology – 2nd Edition is licensed under CC BY 4.0. Access a detailed description.

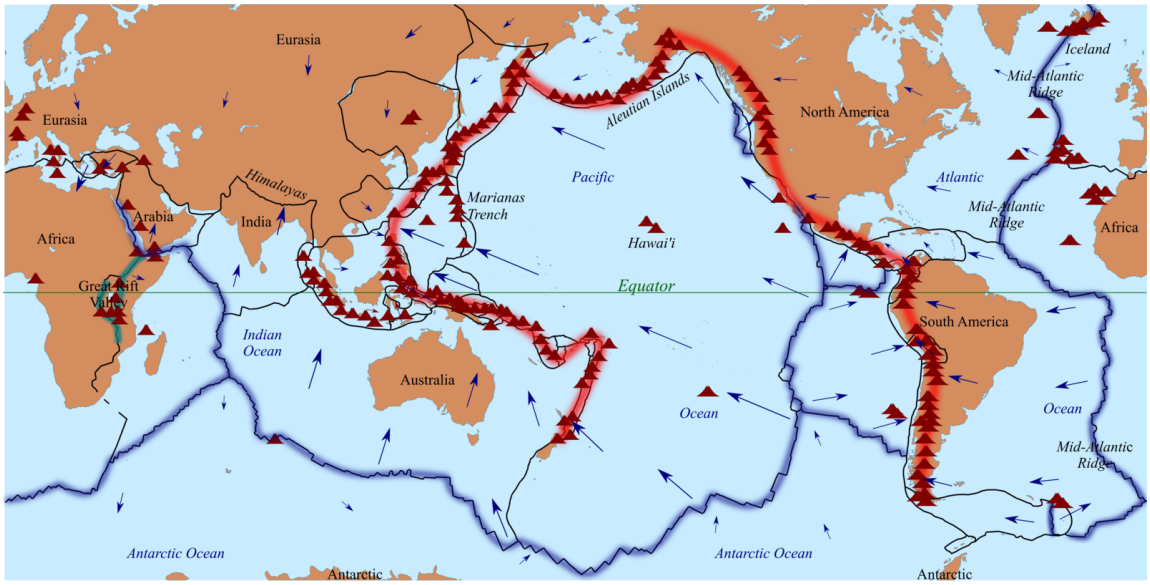


Figure 7.1.2: Map of the global distribution of major volcanoes. Dark red triangles indicate the locations of volcanoes, dark blue shading highlights mid ocean ridges and red shading connects the volcanoes of the Ring of Fire, including the Cascade Volcanoes on the west coast of North America. "Tectonic plates and ring of fire" by Astroskiandhike is licensed under CC BY-SA 4.0. Access a detailed description.

How and Why Magma is Produced in the Cascadia Subduction Zone

North of the Mendocino Triple Junction, off the coast of California, the Juan de Fuca plate subducts beneath the North American plate. Some geologists divide the Juan de Fuca plate into two plates: the larger Juan de Fuca plate to the north and a smaller plate known as the Gorda plate to the south. For the sake of simplicity we will holistically refer to them as the Juan de Fuca plate. Before it is subducted, the Juan de Fuca plate begins its journey at the Juan de Fuca and Gorda ridges. The Gorda ridge is located 250 km (or about 150 miles) off the coast of Northern California (Figure 7.1.3). Upwelling under the mid ocean ridge results in mid ocean ridge spreading, and new oceanic lithosphere is created. Near the mid ocean ridge, water from the ocean above becomes incorporated into the rock through the process of hydrothermal metamorphism.

The lithosphere that makes up the Juan de Fuca plate then travels eastward, away from the Juan de Fuca (and Gorda) ridge, until it reaches the edge of the continental slope, about 60 km (or 40 miles) off the coast of northern California, where it plunges beneath the overriding North American plate at the Cascadia Subduction Zone. From there, the subducting slab continues to sink downwards, at an angle, into the mantle beneath North America. Approximately 250 km (150 miles) inland from the point where it first begins to descend, the plate reaches the depth in the mantle where conditions are right for mantle melting.

At this depth, the water and other fluids that were incorporated into the crust through hydrothermal metamorphism are released through a different type of metamorphism, which occurs under high-pressure conditions deep in the mantle. This fluid is forced out of the subducting slab into the mantle above, where it acts as a flux. A flux is a chemical compound that lowers the melting temperature of a solid. In this case, the water and other fluids lower the melting temperature of the mantle. At depths of over 100 km, the mantle rock is just below its melting temperature and therefore because of the addition of water and other flux fluids, it can melt. This is called flux melting. Back-arc upwelling occurs at the leading edge of the subducting plate.

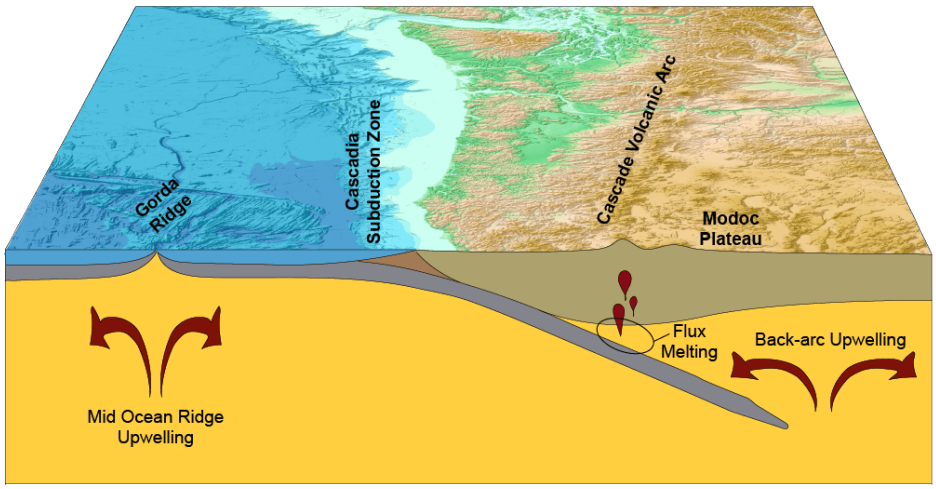


Figure 7.1.3: Block diagram showing production of new crust at the Gorda Ridge, subduction of the oceanic lithosphere along the Cascadia trench, and associated flux melting and back-arc upwelling. Some learners may benefit from the tactile graphic, "Continental Subduction Zone," which can be found in the Geological Tactile Image Repository. The descriptions within this chapter will help students relate the generalized labels in the tactile graphic to the specifics of the Cascadia subduction zone. "Cascades and Modoc Plateau Block Diagram" by Emily Wright is is licensed under CC BY 4.0.

There is a common misconception that many people develop about why volcanoes occur near subduction zones. Be sure that you don't have this misconception by completing the activity, "melting and subduction zones".

Query 7.1.1

This interactive element is not available in this format. Visit the link or scan the QR code to access it online.

View this Interactive Content online

Video 7.1.1: Flux Melting Demonstration with Ice and Salt

Flux melting in the context of subduction zones seem like a strange concept at first, but there are other cases where flux melting is more familiar. One example occurs in cold climates; local highway maintenance departments sometimes salt bridges and roads to prevent ice from forming. In this case, the salt acts as the flux, not the water. The video, "Flux Melting Demonstration with Ice and Salt" demonstrates an example of flux melting that can be used as an analogy to better understand the process at subduction zones. The video includes narration but can also stand on its own with the sound off.

This interactive element is not available in this format. Visit the link or scan the QR code to access it online.

View this YouTube Video online

Magma Generation Beneath the Modoc Plateau

Magma generation beneath the Modoc Plateau has a different cause. The chemistry of the volcanic rock suggests that there was no flux involved in the original melting of the magma. Here, melting is a result of back-arc upwelling (Figure 7.1.3) and other similar processes. The motion of the downgoing Juan de Fuca slab results in the upward flow of mantle material into the space above the subducting slab (known as the mantle wedge). This convection brings relatively hot mantle material upward and also decreases the pressure. Because solid rock is denser than liquid magma, high-pressure conditions keep mantle rock solid even though it is very hot. A decrease in these high-pressure conditions can therefore result in melting. Even within the Cascade Range province, rock chemistry suggests that some magma originates from this mantle flow around the subducting slab, while other rocks are sourced from flux melting.

Whatever the cause of melting, once magma is produced in the mantle, volcanoes are likely to occur. Since liquid magma is less dense than the surrounding mantle, the magma produced by this melting rises upwards through the mantle, much like cooking oil added to water. Some of this magma may cool again before reaching the surface forming intrusive igneous rock, but some will reach the surface, erupt as lava, and form volcanoes.

Magma Evolution During the Rise to the Surface

The Cascade Range and the Modoc Plateau are host to many different types of volcanoes and a variety of volcanic rocks. The variety found in the Cascade Range is a result of the processes that occur as magma undergoes its journey from the mantle to the surface.

Because the mantle is composed of many different minerals, it does not melt uniformly. As minerals with lower melting points turn into liquid magma, those with higher melting points remain as solid crystals. Each mineral has a unique melting and crystallization temperature. Mafic minerals (those high in iron and magnesium) have higher melting temperatures, so they are usually the last minerals to melt and the first to crystallize as magma cools. Since most rocks are made of many different minerals, when they start to melt, some minerals begin melting sooner than others. This is known as partial melting and it is one part of a process called magmatic differentiation, which describes the physical and chemical changes that take place as magma slowly rises and cools into solid rock.

The most important example of partial melting occurs as magma is generated from mantle rock. The chemistry of mantle rock (peridotite) is ultramafic, low in silica, and high in iron and magnesium. When peridotite begins to melt, the silica-rich portions melt first due to their lower melting point (see Igneous Rocks). As this continues, an increasingly silica-rich magma forms, and the ultramafic mantle rock produces a mafic magma.

Liquid magma is less dense than the surrounding solid rock, so it rises through the mantle and crust. As magma begins to cool and crystallize, further magmatic differentiation changes the chemistry of the resultant rock into a more felsic composition. This happens two ways through both assimilation and fractionation. During assimilation, pieces of country rock with a different, often more felsic, composition are added to the magma. These solid pieces may melt, which further changes the composition of the magma.

Fractionation or fractional crystallization is another process that increases the silica content, making a magma more felsic. As a magma diapir rises through the crust, the temperature drops and some minerals will crystallize and settle to the bottom of the magma chamber, leaving the remaining melt depleted of ions in those minerals. For example, olivine is a mafic mineral with a high melting point, making it one of the first minerals to crystallize in cooling magma (Figure 7.1.4a). The solid olivine crystals are denser than the surrounding liquid magma, so they will settle to the bottom of the magma chamber (Figure 7.1.4b). Because olivine contains more iron and magnesium and less silica than other common igneous minerals, the settling olivine removes a significant amount of iron and magnesium from the magma but does not remove much silica. This means the remaining melt becomes more silica-rich and felsic (Figure 7.1.4c). As the mafic magma further cools, and other mafic minerals crystallize, which remove even more low-silica components from the magma, it becomes even more felsic. This process of separating magmas into differing compositions can occur multiple times as the magma moves upward from one magma chamber to the next.

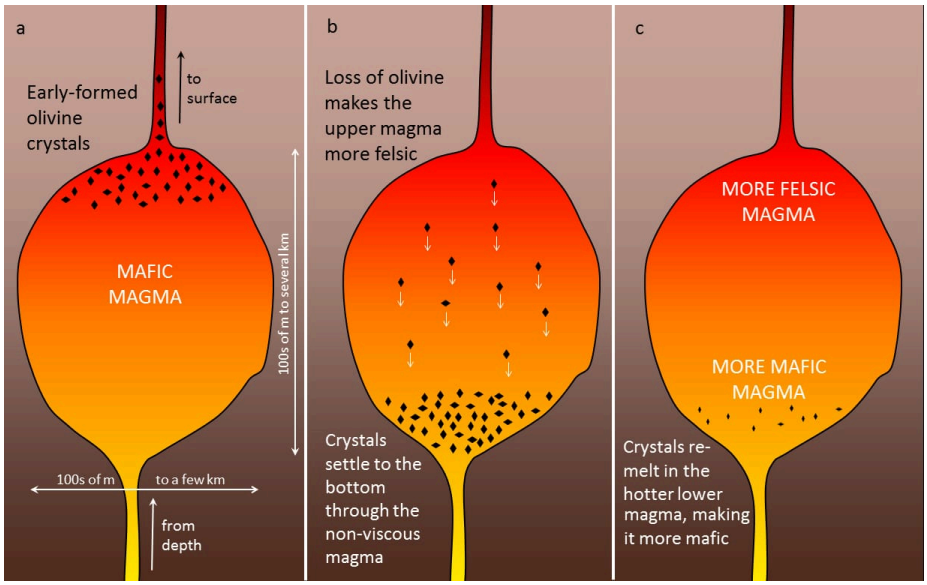


Figure 7.1.4: An example of crystal settling and the formation of a zoned magma chamber. Olivine minerals form (a), then settle to the bottom (b), leaving more felsic magma behind at the top of the magma chamber (c). "Crystal Settling" by Steven Earle is licensed under CC BY 4.0. Access a detailed description.

When mafic magma rises through the thick continental crust of the North American plate, the journey is much longer than when magma rises through thin oceanic crust. This gives the magma more time to react with the surrounding country rock and to undergo fractionation. Much of the continental lithosphere is felsic (i.e. granitic), therefore the process of assimilation can now also occur. Thus the mafic magma tends to assimilate felsic rock, becoming more silica-rich as it migrates through the lithosphere and changing into intermediate or felsic magma by the time it reaches the surface.

Video 7.1.2: Partial Melting of Igneous Rocks

The video “Partial Melting of Igneous Rocks” describes the process of partial melting and describes how different types of magma form in association with different types of plate settings. Pay attention to the descriptions of magma associated with subduction zones and use this information to predict which types of rocks are common in the California Cascades.

This interactive element is not available in this format. Visit the link or scan the QR code to access it online.

View this YouTube Video online

Each magma diapir travels its own unique journey originating in the mantle (Figure 7.1.5). Not all diapirs make it to the surface (see Basement Geology of the Sierra Nevada: The Core of an Ancient Volcanic Arc and Peninsular Ranges), but volcanoes are formed by those that do. Some of these diapirs change significantly and erupt as felsic lava, while some change less and erupt as mafic or intermediate lava. The result is that the volcanic rocks of the Cascade Range include a variety of compositions and contribute to a variety of volcano shapes and sizes.

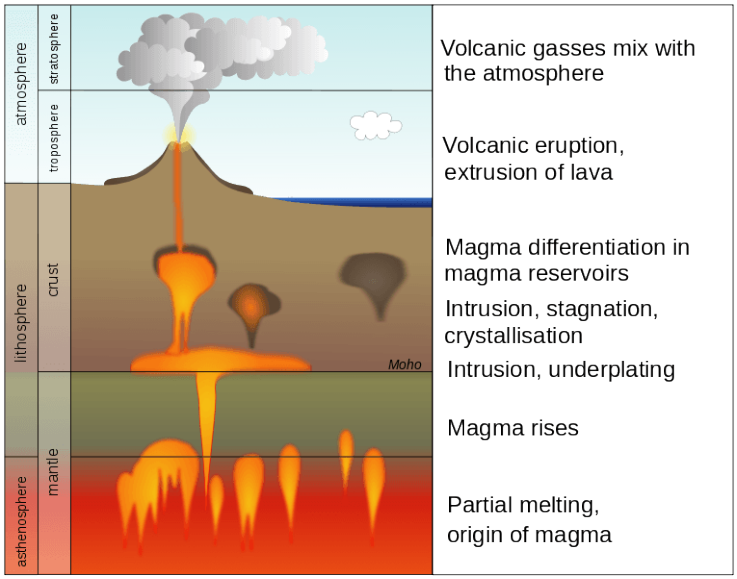


Figure 7.1.5: Rising magma diapirs in mantle and crust. Fractional crystallization and assimilation occur as diapirs rise through the crust. The thickness of the Earth and atmospheric layers is not to scale. "Magmatism and Volcanism" by An Introduction to Geology is licensed under CC BY 4.0. Access a detailed description.

Query 7.1.2

This interactive element is not available in this format. Visit the link or scan the QR code to access it online.

View this Interactive Content online

Acknowledgments

Parts of the text on this page were taken with some editing from existing Open Educational Resources by Earl (2019) and Johnson et al. (2017). Links to the original text can be found in the reference section on this page.

References

1. Earle, S. (2019). Chapter 4 Volcanism. In *Physical Geology* (2nd ed.). BCcampus. https://opentextbc.ca/physicalgeology2ed/part/chapter-4-volcanism/
2. Gao, H., & Long, M. D. (2022). Tectonics and Geodynamics of the Cascadia subduction zone. *Elements*, *18*(4), 226–231. https://doi.org/10.2138/gselements.18.4.226
3. Humphreys, E. D., & Grunder, A. L. (2022). Tectonic controls on the origin and segmentation of the Cascade Arc, USA. *Bulletin of Volcanology*, *84*(12), 102. https://doi.org/10.1007/s00445-022-01611-2
4. Johnson, C., Affolter, M. D., Inkenbrandt, P., & Mosher, C. (2017). Chapter 4: Igneous Processes and Volcanoes. In *An Introduction to Geology*. https://slcc.pressbooks.pub/introgeology/chapter/4-igneous-processes-and-volcanoes/
5. Paguican, E. M. R., & Bursik, M. I. (2016). Tectonic Geomorphology and Volcano-Tectonic Interaction in the Eastern Boundary of the Southern Cascades (Hat Creek Graben Region), California, USA. *Frontiers in Earth Science*, *4*. https://doi.org/10.3389/feart.2016.00076
6. Till, C. B., Grove, T. L., Carlson, R. W., Donnelly-Nolan, J. M., Fouch, M. J., Wagner, L. S., & Hart, W. K. (2013). Depths and temperatures of <10.5 Ma mantle melting and the lithosphere-asthenosphere boundary below southern Oregon and northern California. *Geochemistry, Geophysics, Geosystems*, *14*(4), 864–879. https://doi.org/10.1002/ggge.20070

This page titled 7.1: The Cascadia Subduction Zone and the Cascade Continental Volcanic Arc is shared under a CC BY-NC 4.0 license and was authored, remixed, and/or curated by Emily Wright.

7.2: Rock Types of the Cascades

Rocks Classified by Composition

In section 2.4: Igneous Rocks, you learned that igneous rocks are usually classified mainly by two attributes: first by texture, whether they are intrusive (plutonic) or extrusive (volcanic), then by composition. This chapter focuses primarily on extrusive or volcanic rocks. For more discussion of intrusive igneous rocks, see 9.2: Basement Geology of the Sierra Nevada: The Core of an Ancient Volcanic Arc. The major types of volcanic rocks, therefore, are distinguished and identified from one another based on composition. In truth, volcanic rock composition varies continuously along a spectrum, from mafic to felsic, yet to classify these rocks and give them names, we must separate them into distinct categories. Typically, an introductory geology student learns to divide volcanic rocks into three such categories: basalt (mafic), andesite (intermediate), and rhyolite (felsic). However, if you travel in the Cascades and read interpretive signs and visit visitor centers, you will likely encounter a fourth volcanic rock named 'dacite'. Dacite describes a volcanic rock with a composition that falls between intermediate and felsic.

The overall composition of an igneous rock can be determined by identifying the minerals that make up the rock (see 2.4: Igneous Rocks). However, in volcanic rock, the texture is usually aphanitic, meaning that many of the mineral crystals are too small to be seen (and definitely too small to be identified) with the naked eye. Geologists who study volcanic rocks often use microscopes to look at thin sections of rocks. Thin sections are slabs of rock ground thin enough for light to pass through them. This makes identifying the minerals using a microscope easier. Unfortunately, it is oftentimes difficult to have a microscope in the field, which makes classifying rocks by "hand sample" useful. When information about the mineral composition is not directly available, the overall color or tone of the rock can provide useful information. Felsic minerals tend to be lighter in color and the common felsic mineral, potassium feldspar often appears pink. Therefore, the overall tone of rhyolite, a felsic rock, is usually light and it can have a pinkish tint. By contrast, unweathered basalt (mafic) is black or very dark gray. Dacite and andesite fall somewhere in between (Figure 7.2.1).



Figure 7.2.1: Color Comparison of Rhyolite Andesite and Basalt. This figure by Emily Wright is licensed under CC BY-NC 4.0. Original photos: "Rhyolite (Tertiary; Castle Rock, Colorado, USA) 2", "Andesite (Tertiary; Yellowstone, Wyoming, USA) 1", and "Olivine basalt (Cedar Canyon, Iron County, Utah, USA) 13" by James St. John are licensed under CC BY 2.0.

When using color to identify the composition of a rock, it is important to keep two things in mind. First, color is most useful as an identifying characteristic on unweathered surfaces. Freshly broken surfaces are least likely to be weathered, and this is one of the reasons that geologists carry rock hammers. The second thing to keep in mind is that composition is not defined by color; rather, color is merely a useful tool for approximating mineral composition when minerals can't be seen. Nature does not always follow perfect rules and sometimes the color of rocks can be misleading.

In some cases, minerals can be identified in volcanic rocks. Although the texture of volcanic rocks is usually aphanitic, sometimes it is also porphyritic, meaning that there are larger phenocrysts, surrounded by an aphanitic groundmass. Phenocrysts can often be large enough to be identified in hand samples by the naked eye. Magmas which are closer to the felsic end of the composition spectrum have had more time to evolve. Therefore, they have also had more opportunity for growth of phenocrysts. Basalt generally has few phenocrysts, and the most common is olivine, the first mineral to cool according to Bowen's Reaction Series (see 2.4: Igneous Rocks). Andesite has more phenocrysts, usually composed of plagioclase feldspar or hornblende, two common intermediate minerals. Rhyolite often has many phenocrysts, composed of a variety of minerals. In particular, quartz phenocrysts can be useful for identifying rhyolite, as quartz is one of the last minerals to cool. Practice identifying a volcanic rock using both color and identification of phenocrysts in the activity, "Rock Identification: Chaos Jumbles".

Query 7.2.1

This interactive element is not available in this format. Visit the link or scan the QR code to access it online.

View this Interactive Content online

Accessibility guidance for this activity

Rocks Classified by a Special Volcanic Texture

There are a few notable volcanic rocks that are not named using the standard igneous rock naming scheme, but instead are named for their special volcanic textures. Aphanitic texture forms when rocks cool quickly at the surface of the earth and the resulting mineral crystals are too small to be seen. In some cases, lava can cool in a way that no crystals form at all. The resulting material is volcanic glass. Obsidian is a rock consisting of volcanic glass. Obsidian has excellent conchoidal fracture, similar to the mineral quartz (see 2.2: Mineral Properties). Obsidian is, however, a rock with a color that can be misleading. Obsidian is usually felsic in composition but almost always appears dark in color (Figure 7.2.2). However, a thin shard of obsidian can often appear translucent. Like manufactured glass, obsidian is mostly clear, but obsidian often has enough dark impurities to make the translucent material appear dark.



Figure 7.2.2: Obsidian from Glass Mountain, part of the Medicine Lake Volcano in the California Cascades. The white to gray pumice in the background is similar in composition, but very different in color and texture from the glassy obsidian. "Glass Mountain in northern California in summer 2012 (15)" by Chmee2 is licensed under CC BY-SA 3.0.

Pumice is another rock made of volcanic glass, but it is usually white, gray, or otherwise light colored. Pumice forms when escaping gas bubbles become trapped in the solidifying lava to create a vesicular texture, with holes called vesicles (Figure 7.2.3) present throughout the rock. The abundance of vesicles in the translucent glass make it appear white, much like the white water in a raging river or broken ocean wave, or the white color of meringue made from whipped egg whites. Vesicular texture is also the defining feature of the rock scoria. Scoria is a mafic rock with more than 50% vesicle by volume. Rocks that are vesicular, but are more rock than vesicle are described by their standard igneous rock name, preceded by the term 'vesicular', such as 'vesicular basalt'. Scoria and vesicular basalt are contrasted in figure 7.2.4.



Figure 7.2.3: Airfall pumice from the 1065 A.D. eruption of Medicine Lake Volcano's Glass Mountain eruptive center. "Airfall Pumice" by James St. John is licensed under CC BY 2.0.

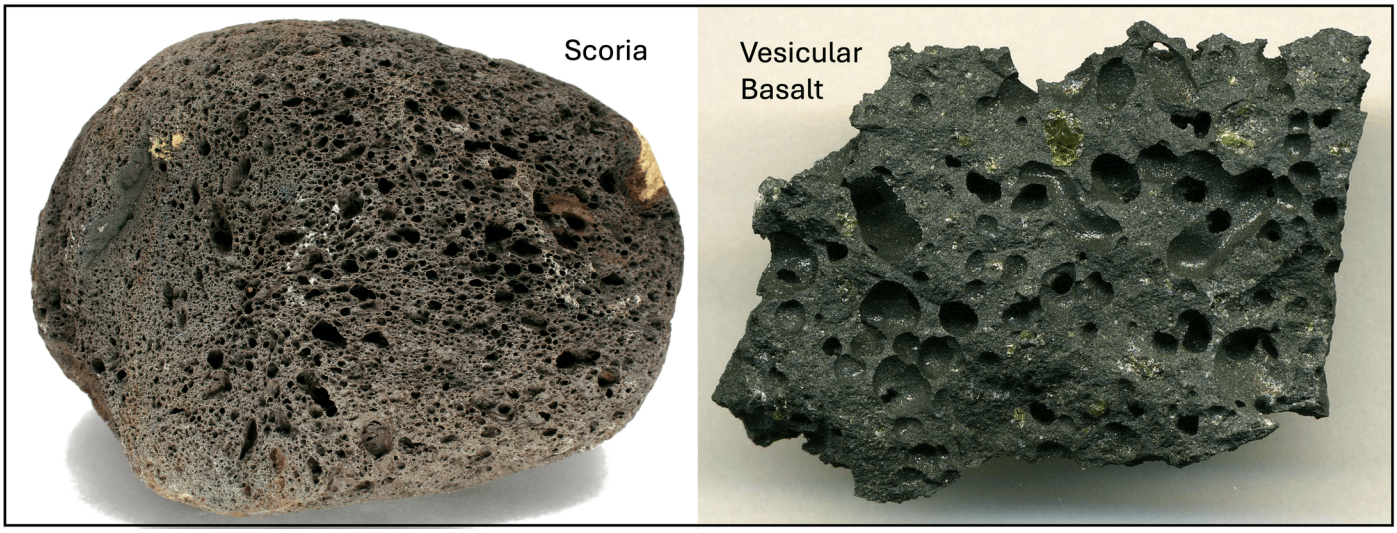


Figure 7.2.4: Scoria and vesicular basalt. Scoria is a mafic rock containing vesicles, in which half or more of the volume is air (filling the vesicles). Vesicular basalt is similar to scoria, but there is more rock than vesicle."Scoria Macro" by Jonathan Zander (Digon3) is licensed under CC BY-SA 3.0. "Vesicular porphyritic olivine basalt" by James St. John is licensed under CC BY 2.0.

When volcanoes erupt explosively, vast amounts of lava, rock, ash, and gasses are thrown into the atmosphere. The solid parts, called tephra, settle back to earth and cool into rocks with pyroclastic textures. 'Pyro', meaning fire, refers to the igneous source of the tephra and clastic refers to the rock fragments. Tephra fragments are named based on size—ash (<2 mm), lapilli (2-64 mm), and bombs or blocks (>64 mm). Pyroclastic texture is usually recognized by the chaotic mix of crystals, angular glass shards, and rock fragments. Rock formed from large deposits of tephra fragments is called tuff (Figure 7.2.5). If the fragments accumulate while still hot, the heat may deform the crystals and weld the mass together, forming a welded tuff.



Figure 7.2.5: A sample of volcanic tuff contains fragments of pumice, volcanic glass and other rocks. Red scale bar is 2.0 cm. "Welded tuff" from An Introduction to Geology is licensed under CC BY-NC-SA 4.0.

Box 7.2.1: Fantastic Lava Beds



Figure Box 7.2.1.1: Basalt from the Fantastic Lava Beds with quartz xenocrysts. "Quartz basalt" by James St. John is licensed under CC BY 2.0.

Any good student of Bowen's Reaction Series (see 2.4: Igneous Rocks) knows that visible quartz crystals in a basalt should never exist. Quartz is one of the last minerals to cool; thus, when mafic lava cools, the whole rock will crystallize into mafic minerals before the lava cools to the crystallization temperature of quartz. Yet this very phenomenon can be found in the Fantastic Lava Beds, which erupted from Cinder Cone in Lassen National Park. Clear, white quartz crystals sparkle within a dark basalt rock (Figure 7.2.6) . How can this be?

In fact, the quartz crystals in the Fantastic Lava Beds are not phenocrysts, which crystalize as the magma cools, but instead are xenocrysts, mineral crystals that were incorporated into the magma from the surrounding country rock and never melted in the first place. You may be familiar with the term xenolith; a xenolith is formed similarly to a xenocryst, but xenocrysts consist of individual mineral crystals, rather than large pieces of country rock.

Acknowledgments

Parts of the text on this page were taken with some editing from existing Open Educational Resources by Earl (2019) and Johnson et al. (2017). Links to the original text can be found in the reference section on this page.

References

1. Clynne, M. A. (2011). *Stratigraphy and compositional evolution of Cinder Cone, a composite monogenetic cone in Lassen Volcanic National Park, California*. *2011*, V13C-2621.
2. Clynne, M., & Muffler, L. (2010). *Geologic Map of Lassen Volcanic National Park and Vicinity, California: U.S. Geological Survey Scientific Investigations Map 2899* [Map]. https://pubs.usgs.gov/sim/2899/
3. Earle, S. (2019). Chapter 4 Volcanism. In *Physical Geology* (2nd ed.). BCcampus. https://opentextbc.ca/physicalgeology2ed/part/chapter-4-volcanism/
4. Johnson, C., Affolter, M. D., Inkenbrandt, P., & Mosher, C. (2017). Chapter 4: Igneous Processes and Volcanoes. In *An Introduction to Geology*. https://slcc.pressbooks.pub/introgeology/chapter/4-igneous-processes-and-volcanoes/
5. Szymanski, M. E., & Teasdale, R. (2015). Groundmass Crystallinities of Proximal and Distal Lavas from Cinder Cone, Lassen Volcanic Field. *AGU Fall Meeting Abstracts*, *2015*, V23B-3106. https://ui.adsabs.harvard.edu/abs/2015AGUFM.V23B3106S/abstract

This page titled 7.2: Rock Types of the Cascades is shared under a CC BY-NC 4.0 license and was authored, remixed, and/or curated by Emily Wright.

7.3: The Variety of Volcanoes in the Cascades and the Modoc Plateau

Magma Viscosity, Eruptive Style and Volcano Type

Volcanoes come in many different shapes and sizes. The shape of a volcano and the way it will behave when it erupts are largely due to a property of magma called viscosity. Viscosity is the resistance to flow. Highly viscous fluids flow slowly, whereas fluids that flow easily are said to have lower viscosity. For example, honey has higher viscosity than water. When low-viscosity magmas erupt at the surface of the earth as lava, they quickly flow away from the vent, creating a broad, flat volcano. More viscous lava, on the other hand, travels less far and thus accumulates near the vent, often building a relatively steep cone.

Viscosity is also a major player in determining the explosivity of an eruption. When magma is deep in the earth, it has gasses dissolved within it. The gasses remain dissolved due to the high pressure at great depth. However, as the magma rises upwards and the pressure decreases, the gasses come out of solution, forming bubbles. A similar process can be seen in a bottle of soda. Soda is bottled under pressure, with gas dissolved in the liquid. Opening the cap releases the pressure, causing the gasses to come out of solution. In low-viscosity lavas, the lava flows easily out of the way of the expanding bubbles, and the gasses easily escape the lava. In high-viscosity lavas, the lava can't flow as easily around the expanding bubbles; instead, the expanding gasses rip the lava apart into fragments, creating violent, explosive eruptions.

Felsic lavas tend to be more viscous than mafic lavas and thus tend to form steeper volcanoes that exhibit more explosive eruptions. Mafic lavas tend to form broad, flat volcanoes with effusive eruptions. An effusive eruption is where lava pours from a vent in the form of a lava flow, with little explosion of material into the air. Viscosity is not the factor that determines explosivity. The temperature of the lava, dissolved gas content of the lava, and the rate of eruption also contribute to eruption style. Even highly viscous felsic lava can erupt in an effusive lava flow if the eruption is slow enough.

Because subduction zones produce a variety of magma compositions, they also produce a variety of volcano shapes and sizes. Subduction zones are known for their iconic composite volcanoes (sometimes called composite cones or stratovolcanoes), and indeed composite volcanoes are known to form only at subduction zones, but subduction zones also produce a variety of other volcano types.

Classifying Cascade Volcanoes

Before you learn about the specific types of volcanoes, complete the activity, "anatomy of a volcano" to learn the names for some basic features present in most volcanoes. Place the terms in the correct box. Start with the terms that you are most confident about, then for the rest, make your best educated guess. Attempt the activity as many times as you need to learn the terminology.

Query 7.3.1

This interactive element is not available in this format. Visit the link or scan the QR code to access it online.

View this Interactive Content online

Accessibility guidance for this activity

Volcanoes generally are classified by their size and shape. The two types of large, mountain-forming volcanoes found in the Cascades are shield volcanoes and composite volcanoes. Shield volcanoes are broad and flat, in contrast to composite volcanoes, which have a distinctive steep triangular profile. Two types of smaller volcanoes found in the Cascades and Modoc Plateau are cinder cones and lava domes.

Composite Volcanoes

Composite volcanoes can be the most picturesque of all volcanoes. A classic composite volcano is conical with a concave shape that is steeper near the top. These mountains commonly have snow-covered peaks standing high above the surrounding mountainous terrain. Composite volcanoes are also sometimes called stratovolcanoes or composite cones. Many of the iconic volcanoes of the Cascade Range are composite volcanoes, including Mount Shasta in California (see 7.5: Mount Shasta) as well as numerous Pacific Northwest volcanoes, such as Mount Rainier, Mount St. Helens and Mount Hood.

Composite volcanoes are large volcanoes (many thousands of feet or meters tall) and are probably the most complex type of volcanic edifice as they experience multiple eruptions, erupt lavas with a range of compositions, and experience many different types of eruptions. This variety of compositions and eruption styles leads to a variety of materials. Composite volcanoes are composed of a mixture of volcanic materials, including lava flows, pyroclastic deposits, and lava domes. Although composite volcanoes can erupt a range of compositions from basalt to rhyolite, intermediate (andesitic) and dacitic magmas are most common.

Composite volcanoes may have multiple vents, but most have a main vent at the summit. Accumulation of materials around this vent during successive eruptions gives these volcanoes their distinctive shape, but eruptions can also destroy large areas of their summits, such as the May 1980 explosion and landslide at Mount St. Helens. Composite volcanoes are active over long periods (tens to hundreds of thousands of years) and can experience multiple stages of growth and destruction over many eruptions in that time. Figure 7.3.1 shows the many different hazards associated with eruptions of composite volcanoes, which build and shape the volcanic edifice.

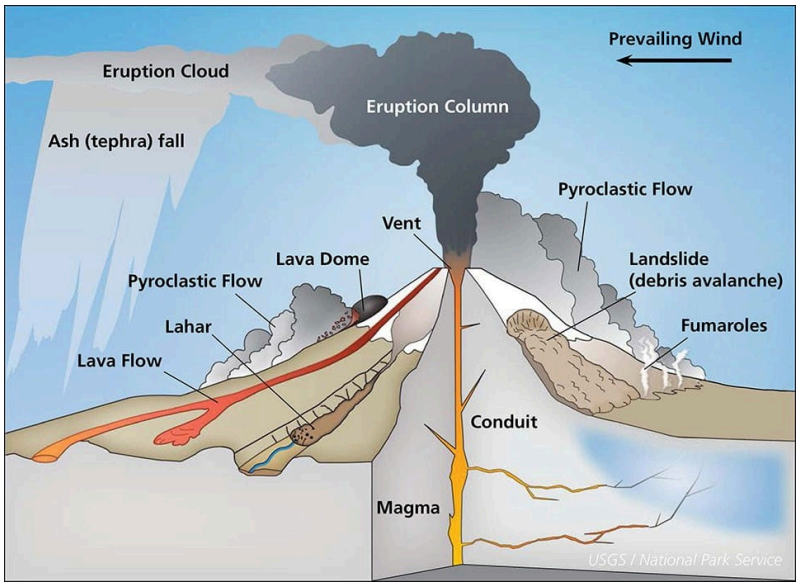


Figure 7.3.1: Composite volcanoes erupt a variety of volcanic materials and produce a variety of volcanic hazards, which build and alter the shape of the volcano. The features pictured in the diagram do not all occur simultaneously. For example, lava flows are a product of an effusive eruption, whereas pyroclastic flows usually require an explosive eruption. Composite Volcanoes by the USGS is in the public domain. Access a detailed description.

Shield Volcanoes

Although shield volcanoes are the largest volcanoes on Earth, they do not form soaring mountains with conical peaks like composite volcanoes. Instead, they are broad volcanoes with gentle slopes and are shaped somewhat like a warrior's shield lying flat on the Earth. In contrast to the concave shape typical of composite volcanoes, shield volcanoes have a convex shape as they are flatter near the summit. While the most famous shield volcanoes are found in Hawaii, there are also shield volcanoes in California (see 7.6: Lassen Volcanic National Park and 7.7: Medicine Lake Volcano).

Like composite volcanoes, shield volcanoes are built by repeated eruptions that occur intermittently over vast periods of time (up to a million years or longer). However, shield volcanoes are more consistent in their style of eruption. They are usually constructed almost entirely of basaltic and/or andesitic lava flows which are very fluid when erupted. When erupted at high rates, this low-viscosity lava travels fast and can cover large areas, giving a shield volcano its broad, flat shape. Figure 7.3.2 shows the features

of a typical shield volcano.

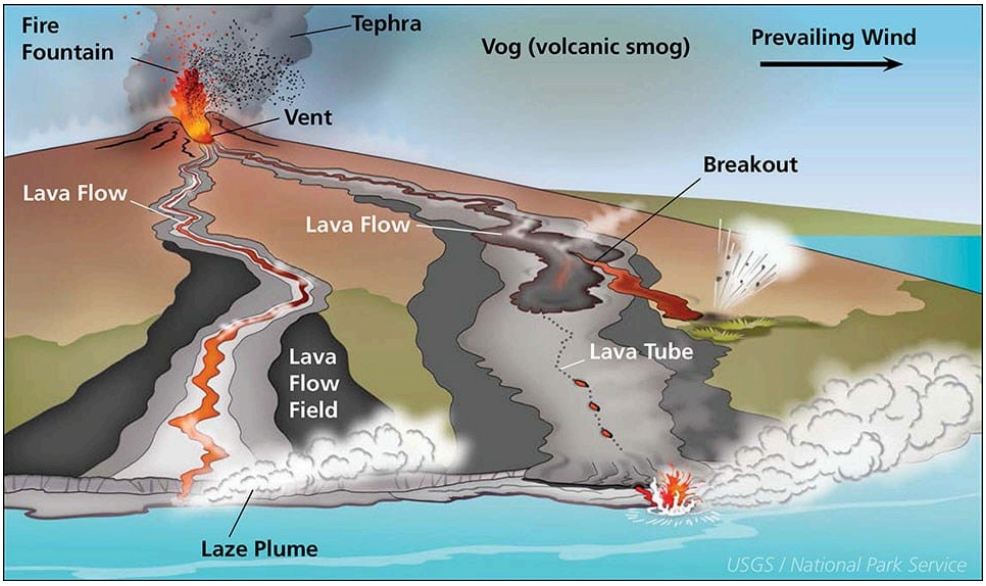


Figure 7.3.2: Shield volcanoes erupt mostly lava flows. In some cases these lava flows are fed by fire fountains. Other volcanic hazards include vog (volcanic smog) and laze, which is formed when hot lava interacts with ocean water. Shield Volcanoes by the USGS is in the public domain. Access a detailed description.

Cinder Cones

Cinder cones are the most common type of volcano in the world. They may look like an idealized depiction of a volcano as they are steep, conical hills that usually have a prominent crater at the top. There are many cinder cones in both the California Cascades and the Modoc Plateau, including one creatively named Cinder Cone, in Lassen Volcanic National Park (see 7.6: Lassen Volcanic National Park).

Cinder cones are more technically known as scoria cones. Scoria forms when blobs of gas charged lava are thrown into the air during an eruption and cool in flight, falling as dark volcanic rock containing cavities created by trapped gas bubbles. Cinder is a more colloquial term that is widely used in the United States for pieces of scoria that are roughly nut- to fist-size.

Most cinder cones are basaltic to basaltic andesite in composition, but they may be andesitic (intermediate). This low-viscosity mafic lava results in eruptions that are usually mildly to moderately explosive. A fountain of scoria erupts from a central vent and accumulates in a ring around the vent. Unlike shield and composite volcanoes, cinder cones usually form in a single eruptive episode. Cinder cone eruptions usually have a short duration. Half of all historic cinder cone eruptions have lasted less than 30 days; and 95% have lasted less than 1 year. Most cinder cones are a few hundred feet tall (100 to 150 m), and rarely are larger than 600 to 900 feet (200 to 300 m) in height.

While sometimes they are nearly perfect cones, cinder cones frequently have an asymmetric shape. Cinder cones that form over a linear fissure vent are elongated, and ones that form in areas with strong prevailing winds may be much taller on the downwind side. Elongated cinder cones may also form when the location of the vent shifts during the eruption. They may also be breached when lava flows erupting from near the base of the cone carry away a part of the flank. Because cinder cones are usually mafic in composition, they are also often associated with lava flows. Much like an uncapped bottle of shaken soda, volcanic eruptions can often begin as mildly explosive eruptions, then transition to effusive eruptions as the gas content decreases.

Cinder cones commonly occur in association with other volcanoes. They may occur within calderas, near volcanic domes, and as satellite cones on the flanks of composite and shield volcanoes. Cinder cones frequently occur in volcanic fields with as many as hundreds of other cinder cones. Figure 7.3.3 shows a schematic diagram of a cinder cone.

Cinder cones can also be relatively ephemeral. Sometimes a cinder cone starts an eruptive sequence and what begins as a cinder cone may eventually develop into a larger shield volcano or composite volcano.

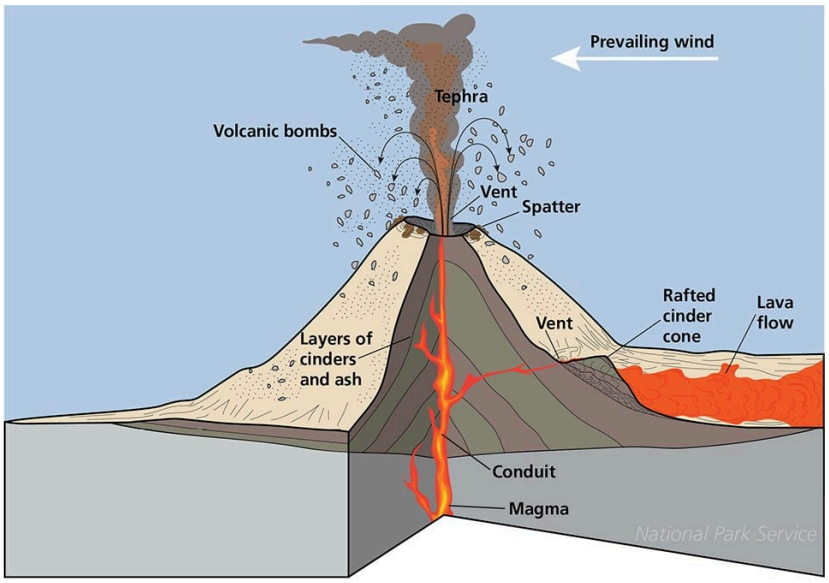


Figure 7.3.3: Cinder cones are formed from the eruption of tephra from a single vent. They are also often associated with lava flows that emerge from vents near the base of the cone. Cinder Cones by Trista Thornberry-Ehrlich, Colorado State University for the National Park Service is in the public domain. Access a detailed description.

Lava Domes

Lava domes form from the slow extrusion of highly viscous felsic lava. The low gas content and slow rate of eruption keep these eruptions effusive despite the high viscosity of the lava. However, these lavas are too thick to spread out into a lava flow. Most lava domes are small and many do not have a crater. Some dome-forming eruptions start with highly explosive eruptions that wane into dome-building ones as the gas content in the magma decreases. Other dome-building eruptions begin effusively until the growing dome explodes or collapses to produce pyroclastic flows. Lava domes can collapse because they may become over-pressured from gasses trapped inside or become over-steepened.

Lava domes can form volcanic edifices in their own right but also occur in clusters. Lava domes may be extruded in the summit craters of composite volcanoes or within calderas as part of a post-caldera eruptive phase. Like many terms for volcano types, there are several synonym variations of ‘lava dome’. These include ‘volcanic dome’, ‘plug dome’, or sometimes, just ‘dome’.

Because they are made of viscous lava, domes are usually steep-sided. They typically have rough brecciated surfaces, and sometimes they have glassy rinds due to quenching of the hot lava once it has erupted onto the surface. Most domes are relatively small volcanoes with limited volume. Like cinder cones, lava domes usually grow in a single eruptive episode, which frequently last days to months. The features of a lava dome are shown in figure 7.3.4.

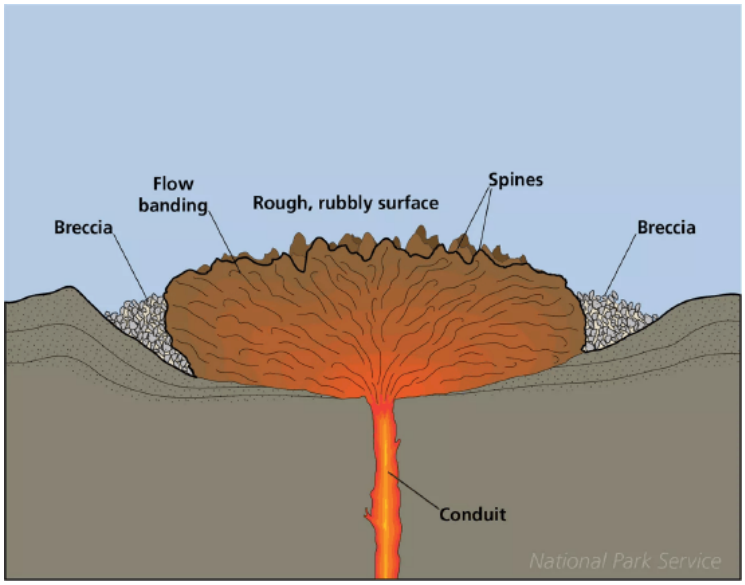


Figure 7.3.4: Lava domes form close to the eruption vent, often within a crater formed by an earlier eruptive phase. domes by Trista Thornberry-Ehrlich, Colorado State University for the National Park Service is in the public domain. Access a detailed description.

Practice Classifying Volcanoes

Video 7.3.1: How to Classify Volcanoes

For further review of volcano classification and to practice visually identifying volcano types, please watch the video, "How to Classify Volcanoes."

This interactive element is not available in this format. Visit the link or scan the QR code to access it online.

View this YouTube Video online

Accessibility guidance for this video

Apply your knowledge of volcano classification to the California Cascades in the activity "Classifying California Cascade Volcanoes".

Query 7.3.2

This interactive element is not available in this format. Visit the link or scan the QR code to access it online.

View this Interactive Content online

Accessibility guidance for this activity

Volcanoes of the California Cascades

Most of the major Cascade volcanoes are located in Oregon and Washington, but most lists of major Cascade volcanoes will include three in California: Mount Shasta, Lassen Peak, and Medicine Lake Volcano. Mount Shasta, an iconic composite volcano, is the second-highest peak in the whole Cascade range and although it is the fifth-highest peak in California, it is the only peak in the top five that is a volcano. Lassen Peak, a lava dome, is known for its 1915 eruption and for being the site of a National Park. For most of the 20th Century, until the 1980 eruption of Mount Saint Helens, the Lassen Peak eruption was the most well-known volcanic eruption in the United States. Medicine Lake Volcano is one of the largest volcanoes in the Cascade Range by volume, at around 600 km^3 (143 mi^3). It is usually described as a shield volcano, but studies of older rocks at the core of the volcano suggest that its classification may not be that straightforward.

Though most maps of Cascade volcanoes show only the large, young composite and shield volcanoes, there are countless other smaller cinder cones, domes, and eroded volcano remnants throughout the Cascades, including the California Cascades. In the eastern part of the range, the Cascades transition to the Modoc Plateau, which is characterized by smaller volcanoes and lava flows rather than large, prominent composite volcanoes.

In the Cascades and Modoc Plateau, smaller volcanoes tend to occur in clusters. Some of these clusters form lines, with a north-northwest trend. This trend is consistent with the strike of faults in the area. Faults in this area are normal faults associated with Basin and Range extension. The linear clusters of cinder cones and other small volcanoes are thought to have resulted from the interaction of Cascadia and Basin and Range tectonics. Cascadia subduction is mainly responsible for the generation of magma, but as the magma moves toward the surface, it exploits pre existing weaknesses in the crust created by Basin and Range faulting.

Acknowledgments

The descriptions of volcano types are slightly modified from text provided by the National Park Service, which is in the public domain. Links to the original text can be found in the reference section on this page.

References

1. Earle, S. (2019). Chapter 4 Volcanism. In *Physical Geology* (2nd ed.). BCcampus. https://opentextbc.ca/physicalgeology2ed/part/chapter-4-volcanism/
2. Johnson, C., Affolter, M. D., Inkenbrandt, P., & Mosher, C. (2017). Chapter 4: Igneous Processes and Volcanoes. In *An Introduction to Geology*. https://slcc.pressbooks.pub/introgeology/chapter/4-igneous-processes-and-volcanoes/
3. U.S. National Park Service. (n.d.-a). *Cinder Cones*. Retrieved March 13, 2024, from https://www.nps.gov/articles/000/cinder-cones.htm
4. U.S. National Park Service. (n.d.-b). *Composite Volcanoes (Stratovolcanoes)*. Retrieved May 24, 2024, from https://www.nps.gov/articles/000/composite-volcanoes.htm
5. U.S. National Park Service. (n.d.-c). *Shield Volcanoes*. Retrieved May 24, 2024, from https://www.nps.gov/articles/000/shield-volcanoes.htm
6. U.S. National Park Service. (n.d.-d). *Volcanic Domes*. Retrieved May 24, 2024, from https://www.nps.gov/articles/000/domes.htm

This page titled 7.3: The Variety of Volcanoes in the Cascades and the Modoc Plateau is shared under a CC BY-NC 4.0 license and was authored, remixed, and/or curated by Emily Wright.

7.4: Volcanic Hazards

Active Volcanoes in California

In the 2018 update to the USGS national volcanic threat assessment, three California volcanoes were placed in the "very high threat" category. Two of these are located in the Cascades; Mount Shasta is considered the fifth most threatening volcano in the US and Lassen volcanic center is ranked 11th. The third California volcano in this category is the Long Valley Caldera, located in the Basin and Range Province (see 8.5: Rift-Related Volcanism in Eastern California). The variety of lava compositions and volcano types in the Cascades lead to a variety of hazards associated with a potential volcanic eruption. The sections below describe the various hazards that might occur during the eruption of one of the California Cascade volcanoes.

Lava Flows

While news of lava flowing through neighborhoods and destroying houses is more likely to come from Hawaii than California, the presences of lava flows throughout the Cascade Range and Modoc Plateau imply that lava flows certainly can occur in California as well. Lava flows are streams of molten rock that pour or ooze from an erupting vent. Lava is erupted during either non-explosive activity or explosive lava fountains. The speed at which lava moves across the ground depends on several factors, including the type of lava erupted and its viscosity, the steepness of the ground over which it travels, and the rate of lava production at the vent. Basalt, which is mafic and low-viscosity, can flow tens of kilometers from an erupting vent. These flows are commonly associated with shield volcanoes like Medicine Lake Volcano or Lava field, such as those that exist throughout the eastern Cascades and Modoc Plateau. More viscous andesite flows are more commonly associated with composite volcanoes like Mount Shasta. These flows move only a few kilometers per hour (a couple of feet per second) and rarely extend more than 8 km (5 mi) from their vents. Dacite and rhyolite, which are also commonly found on composite cones, often form steep-sided lava domes, rather than spread-out lava flows.

Pyroclastic Flows

Lava flows and pyroclastic flows are often grouped together for the purposes of volcano hazard mapping because the two hazards encompass a similar area surrounding the volcano. However, these two hazards are very different in style and origin and do not usually occur simultaneously. A single eruption may progress from explosive to effusive, but cannot be both at once. While lava flows consist of lava, pyroclastic flows contain a mixture of materials, including hot lava blocks, pumice, ash, and volcanic gas. They move at very high speed down volcanic slopes, typically following valleys.

Pyroclastic flows form in a variety of ways. During a highly explosive eruption, a column of volcanic material is ejected upwards into the atmosphere. Once the gas in the column cools, the column can become too dense to maintain upward momentum, and can collapse in a pyroclastic flow (Figure 7.4.1). Small pyroclastic flows of this nature occurred during the May 22, 1915 eruption of Lassen Peak. In some cases, a pyroclastic flow can form in an explosive eruption without first forming a column. Pyroclastic flows can also form from the collapse of lava domes or flows. The fronts of lava flows or domes can become so steep that they collapse due to gravitational force.

Once formed, pyroclastic flows destroy nearly everything in their path. With rock fragments ranging in size from ash to boulders that travel across the ground at speeds typically greater than 80 km per hour (50 mph), pyroclastic flows knock down, shatter, bury, or carry away nearly all objects and structures in their path. The extreme temperatures of rocks and gas inside pyroclastic flows, generally between 200°C and 700°C (390-1300°F), can ignite fires and melt snow and ice. Despite common depictions in movies and literature, most people who directly die from volcanic eruptions, die from pyroclastic flows, not from lava flows.



Figure 7.4.1: A collapsing eruptive column forms pyroclastic flows that surge down the flanks of Mayan Volcano, Philippines during the 1984 eruption. "Pyroclastic flows at Mayon Volcano" by C.G. Newhall, USGS is in the public domain.

Volcanic Ash and Tephra

All explosive volcanic eruptions generate tephra, fragments of rock that are produced when magma or rock is explosively ejected. The largest fragments, blocks and bombs (>64 mm, 2.5 inches diameter), can be expelled with great force but are deposited near the eruptive vent. Lapilli-sized material (6-64 mm, 0.24-2.5 inches diameter) can be carried upward within a volcanic plume and downwind in a volcanic cloud, but fall to the ground as the eruption cloud cools. The smallest material, volcanic ash (<2 mm diameter) is both easily convected upward within the plume and carried downwind for very long distances (Figure 7.4.2; as it falls out of suspension it can potentially affect communities and farmland across hundreds, or even thousands, of square kilometers (Figure 7.4.2.



Figure 7.4.2: Ash buries cars and buildings after the 1984 eruption of Rabaul, Papua New Guinea. "Ash buries cars" by the USGS is in the public domain.

The activity, “Volcanic Ash Comparison” will help you apply lessons learned from a past Cascade volcanic eruption to understand future hazards.

Query 7.4.1

This interactive element is not available in this format. Visit the link or scan the QR code to access it online.

View this Interactive Content online

Access a detailed description of the image in this activity

Lahars

'Lahar' is an Indonesian term that describes a hot or cold mixture of water, volcanic ash, rock fragments, and other debris that flows down the slopes of a volcano and typically enters a river valley. The main fluid medium for a lahar is water, which makes it distinctly different from a pyroclastic flow, in which the fluid medium is gas. Lahars are one of the most concerning volcanic hazards in the Cascades for two main reasons. One is that they can flow further from the volcano than lava flows or pyroclastic flows and the other is that they can occur without an eruption. Lahars occurred during several of the eruptions in the 1914-1917 eruption sequence of Lassen Peak and have occurred on Mount Shasta both with and without an eruption.

To make a lahar, all that is necessary is a large volume of water combined with a large volume of loose volcanic material. Even after thousands of years of quiet slumber, composite volcanoes still have abundant loose volcanic material covering their slopes. Therefore, all that's needed to produce a lahar is a rapid input of water. Eruptions may trigger lahars by ejecting water from a crater lake melting snow and ice. Many of the composite volcanoes of the Cascades, including Mount Shasta, have year-round ice in the form of glaciers and snow fields, and also have significant snowpack throughout much of the winter and spring. On May 18, 1980, nearly all of the spring snowpack and glaciers of Mount St. Helens melted nearly instantaneously, producing large lahars (Figure 7.4.3).



Figure 7.4.3: Bridge destroyed by lahar in North Fork Toutle River during eruption of Mount St. Helens, May 18,1980. "Mount St Helens Lahar" by Richard Waitt, USGS is in the public domain.

Lahars can also form when heavy rainfall or rapid snow melt occurs without an eruption. On steep slopes, rainwater or meltwater can easily erode and transport fine-grained, loose volcanic sediment and form a slurry, especially if vegetation has not had time to grow back on recent volcanic deposits. Ice-clad volcanoes are common locations for the initiation of small seasonal lahars, more often referred to as 'debris flows' or 'mudflows'. As Cascade glaciers melt in a warming climate, there is increasing concern over the potential for larger and more frequent non-eruptive debris flows at many Cascade volcanoes, including at Mount Shasta.

Acknowledgments

Parts of the descriptions of volcanic hazards are taken with minimal editing from sources provided by the USGS Volcano Hazards Program, which are in the public domain. Links to the original text can be found in the reference section on this page.

References

1. Ewert, J. W., Diefenbach, A. K., & Ramsey, D. W. (2018). *2018 update to the US Geological Survey national volcanic threat assessment*. US Geological Survey. https://pubs.usgs.gov/publication/sir20185140
2. Mangan, M., Ball, J., Wood, N., Jones, J. L., Peters, J., Abdollahian, N., Dinitz, L., Blankenheim, S., Fenton, J., & Pridmore, C. (2019). California's exposure to volcanic hazards. In *Scientific Investigations Report* (2018–5159). U.S. Geological Survey. https://doi.org/10.3133/sir20185159
3. U.S. Geological Survey. (n.d.-a). *Ashfall is the most widespread and frequent volcanic hazard*. Volcano Hazards Program. Retrieved May 29, 2024, from https://www.usgs.gov/programs/VHP/ashfall-most-widespread-and-frequent-volcanic-hazard
4. U.S. Geological Survey. (n.d.-b). *Lahars move rapidly down valleys like rivers of concrete*. Volcano Hazards Program. Retrieved May 29, 2024, from https://www.usgs.gov/programs/VHP/lahars-move-rapidly-down-valleys-rivers-concrete
5. U.S. Geological Survey. (n.d.-c). *Lava flows destroy everything in their path*. Volcano Hazards Program. Retrieved May 29, 2024, from https://www.usgs.gov/programs/VHP/lava-flows-destroy-everything-their-path
6. U.S. Geological Survey. (n.d.-d). *Pyroclastic flows move fast and destroy everything in their path*. Volcano Hazards Program. Retrieved May 29, 2024, from https://www.usgs.gov/programs/VHP/pyroclastic-flows-move-fast-and-destroy-everything-their-path

This page titled 7.4: Volcanic Hazards is shared under a CC BY-NC 4.0 license and was authored, remixed, and/or curated by Emily Wright.

7.5: Mount Shasta

Mount Shasta, California's Iconic Volcano

American poet and novelist, Joaquin Miller wrote, "As lone as God, and white as a winter moon, Mount Shasta starts up sudden and solitary from the heart of the great black forests of Northern California." At an elevation of 4,317 m (14,163 ft), the composite volcano of Mount Shasta towers over the surrounding landscape (Figure 7.5.1). With nearly 10,000 ft (3,000 m) of local prominence, Mount Shasta has been a source of fascination and inspiration for as long as humans have lived in the region. Mount Shasta is located at the ancestral territorial boundary of the Shasta, Modoc, Ajumawi/Atsuwegi, and Wintu peoples. It can also be seen from the ancestral lands of the Karuk and Klamath, making the mountain a unique and important traditional landmark. As such an important and prominent landmark, Mount Shasta has had many different names in many languages. Wakanunee-Tuki-wuki is a name that was used by the Shasta people, but neighboring tribes like the Ajumawi, Karuk, and Wintu also have names for it, such as Ako-Yet, Uytaahkoo, and Bohem Puyuik, respectively.



Figure 7.5.1: Mount Shasta in winter. "Mount Shasta" by Harold Litwiler is licensed under CC BY-NC 2.0.

Although Mount Shasta has not had a volcanic eruption in historic times, within the last 4,000 years, it has been one of the more active among the Cascade volcanoes. The U.S. Geologic Survey has ranked Mount Shasta fifth in the list of volcanic threats in the United States, a list that takes into account not only the likelihood of an eruption but also the severity of damage if an eruption were to occur. Within the Cascade volcanoes, it ranks only behind Mount Saint Helens and Mount Rainier, both in Washington. The USGS monitors Mount Shasta (and other volcanoes throughout California) for signs of unrest, and issues an alert level of 'normal', 'advisory', 'watch, or 'warning'. The current alert level is published on the California Volcano Observatory (CalVO) website.

Eruption History

Before the Mount Shasta that we know today began to form, a similar volcano was built in the same place, beginning 590,000 years ago. Around 300,000 years ago, this ancestral composite cone collapsed, destroying the edifice of the volcano and spawning one of the largest landslides known on Earth, covering more than 440 km2 (170 mi2) of Shasta Valley to the northeast. The hummocky terrain of this landslide deposit remained a mystery to geologists for many decades (Figure 7.5.2). Eruptions that caused edifice collapse had not often been observed in action and so little was known about the processes leading up to and during such an eruption. Then, on May 18, 1980, geologists witnessed an edifice-collapsing eruption at Mount Saint Helens, a volcano in the Washington Cascades. The influx of magma swelled the volcano, oversteepening its northern flank. This resulted in a large landslide, which in turn triggered the explosive eruption. When the dust settled, geologists found hummocky terrain, similar to that of Shasta Valley. True to the mantra, "the present is the key to the past," this new development allowed geologists to re-interpret the hummocky terrain in Shasta Valley and conclude that it was produced in a similar, though much larger, volcanic

eruption that included a landslide.



Figure 7.5.2: Small hills NNW of Mt. Shasta are hummocks created during a massive landslide. This view is from the top of Gregory Mountain, located about 40 km from the summit of the volcano. The prominent cone on the right skyline is Black Butte. "Small hills NNW of Mt. Shasta" by Brantley, S. R., USGS is in the public domain.

Video 7.5.1: Mystery Mounds at Mt Shasta

If you would like to learn more about this hummocky terrain in the Shasta Valley, and to see a variety of images, watch "Mystery Mounds at Mt Shasta; A Landslide that Traveled 30 Miles".

This interactive element is not available in this format. Visit the link or scan the QR code to access it online.

View this YouTube Video online

The modern edifice of Mount Shasta was primarily constructed during four major cone-building episodes that were centered on separate vents, shown in Figure 7.5.3. The eruptions that formed these cones probably lasted for only a few hundred or a few thousand years, during which numerous lavas erupted, mainly from each cone's central vent. The final major eruptions from each of the central craters produced dacitic domes and dense-fragment pyroclastic flows. After each episode of rapid cone building, the volcano underwent significant erosion while less frequent central- and flank-vent eruptions occurred. The Sargents Ridge cone, the oldest of the four, is younger than approximately 250,000 years, has undergone two major glaciations, and is exposed mainly on the south side of Mount Shasta. The next younger Misery Hill cone is younger than approximately 130,000 years, has been sculpted in one major glaciation, and forms much of the upper part of the mountain.

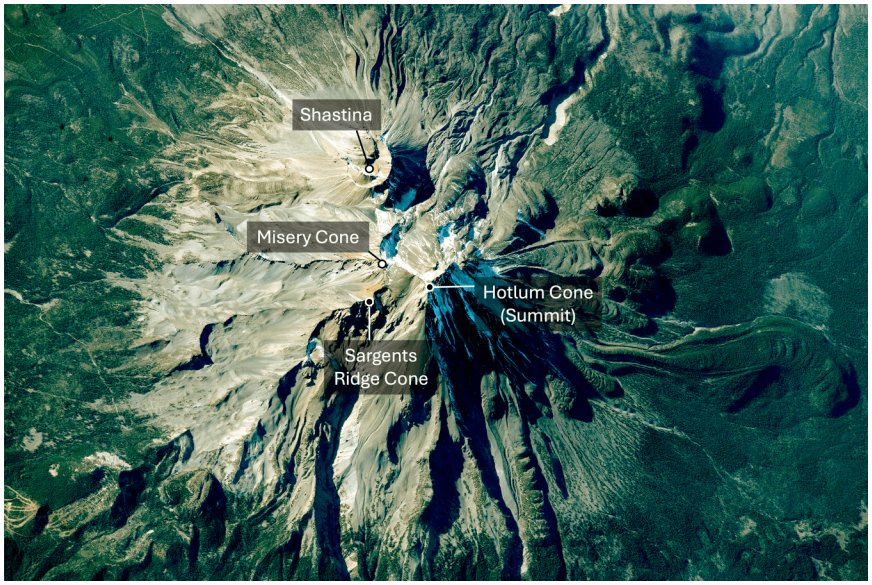


Figure 7.5.3: The four cones of Mount Shasta labeled on an image photographed by a crew member during the International Space Station's 68th expedition, in October 2022. "Shasta's Four Cones" by Emily Wright is licensed under CC BY-NC 4.0 / A derivative from the original work. Access a detailed description.

Two of the main eruptive centers at Mount Shasta, Shastina (3,758 m 12,303 ft), and Hotlum cones were constructed during Holocene time, which includes about the last 10,000 years. Holocene eruptions also occurred at Black Butte, a group of overlapping dacite domes about 13 km (8 mi) west of Mount Shasta (Figure 7.5.2). Evidence of geologically recent eruptions at these two main vents and at flank vents forms the chief basis for assessing the most likely kinds of future eruptive activity and associated potential hazards.

The youngest, well-documented eruption of Mount Shasta was about 3,000 years ago. Small, short-lived blasts of steam and ash may have occurred more recently, perhaps as recently as 1,800 to 200 years ago, but these events need additional field verification. Hot springs and volcanic gasses seep from the summit indicating a relatively young and still-hot system. The record of eruptions over the last 10,000 years suggests that, on average, at least one eruption occurs every 800 to 600 years at Mt Shasta, which is one of the reasons for its fifth place ranking in the USGS National Volcanic Threat Assessment.

Review your rock identification skills (7.2: Rock Types of the Cascades) and apply them in the activity, “Rock Identification: Mount Shasta” to learn more about Mount Shasta.

Query 7.5.1

This interactive element is not available in this format. Visit the link or scan the QR code to access it online.

View this Interactive Content online

Accessibility guidance for this activity

Volcano Hazard Map

Figure 7.5.4 shows the USGS Volcano Hazards Zones map for Mount Shasta and the surrounding region. The towns of Weed, Mount Shasta and McCloud all lie within the Near-volcano hazard zone, which is susceptible to lava flows, pyroclastic flows, tephra fall and lahars during an eruption. Lahars are also likely to affect river valleys downstream of the volcano and ash fall may affect a very large region downwind (not pictured on the hazard map). The hazard map also shows an area susceptible to regional lava

flows. Flows originating from the cones that make up Mount Shasta would not reach this area. Rather, the area is susceptible to lava flows from smaller volcanic vents.

In an explosive eruption of Mount Shasta, ash fall would affect a large region surrounding the volcano. Ash fall is not pictured on the volcano hazard map (Figure 7.5.4), in part because the area likely to be affected is larger than that of other hazards and in part because the precise patterns of ash fall are difficult to predict. The thickness and area of ash distribution depend not only on the eruption itself but also on the wind conditions at the time of the eruption. In general, the prevailing wind direction at Mount Shasta is from the west, and therefore the region most likely to be affected by ashfall is the region to the east of the volcano.

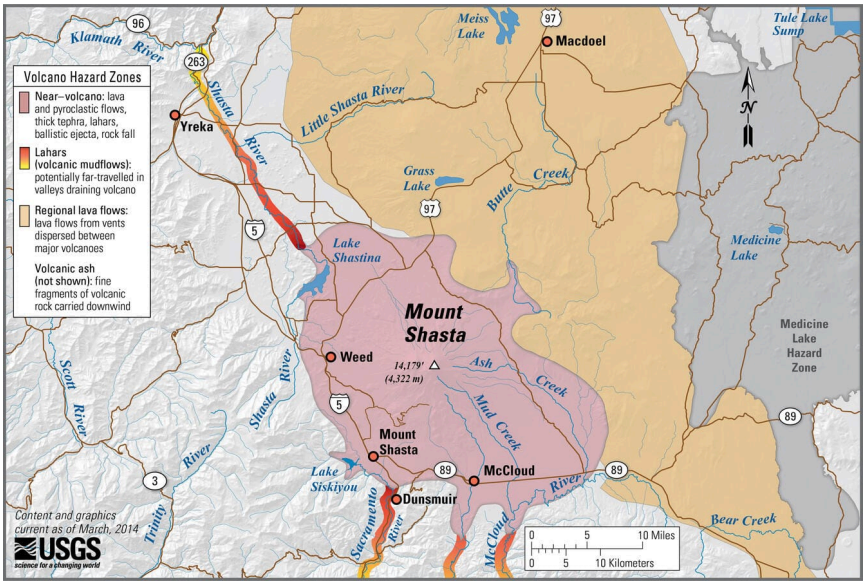


Figure 7.5.4: Mount Shasta, California simplified hazards map showing potential impact area for ground-based hazards during a volcanic event. "Mount Shasta, CA simplified hazards map" by Lisa Faust, USGS is in the public domain. Access a detailed description.

Although Mount Shasta has less snow and ice than its sister volcanoes further north, there is enough to create the potential for significant lahars during an eruption. Eruptions at the Hotlum and Shastina vents, about 10,000 years ago, produced many lahars, about 20 percent of which reached more than 20 km from the summit of Mount Shasta, and spread out on fans around the base of the volcano. The largest lahars and floods extended beyond the base of the volcano and entered the McCloud and Sacramento Rivers. If they occur in the future, lahars may cover valley floors and other low areas as much as several tens of kilometers from the volcano. They will also impact the systems of rivers that flow from Mount Shasta. A primary concern in this category is the Sacramento River.

There is also a history of non-eruptive lahars at Mount Shasta. These events typically occur after the snowpack has diminished during mid-to-late summer. In the last 1,000 years, more than 70 such mudflows and debris flows have inundated stream channels surrounding Mount Shasta.

Aptly named Mud Creek is the longest and deepest drainage on Mount Shasta and is the site of the most frequent non-eruptive lahars. Between 1924 and 1931, the Konwakiton glacier at the head of the Mud Creek drainage broke apart, causing a series of debris flows that threatened the town of McCloud. Though none of these flows inundated the town itself, roads were closed, railways washed out and the town's main water supply cut off. One of these mudflows, in 1924, sent a pulse of mud into the Sacramento River, which was detected as far away as San Francisco Bay.

The community of McLoud remains vulnerable to lahars. Figure 7.5.5 shows a roadway buried by a mudflow along Mud Creek Canyon in Sept. 2014. As recently as 2021, nearby roads were closed and the water supply was once again threatened by debris flows. As the climate warms, there is concern over the increased potential for non-eruptive mudflows. In a warmer climate, there is greater potential for rapid snowmelt and heavy rain events. Additionally, as glaciers recede, they leave behind loose material that can easily be eroded by meltwater or rainwater.



Figure 7.5.5: Mud covering a highway after a September, 2014 mudflow along Mud Creek Canyon. "Mud Creek after Debris Flow event" by USFS, shared by the Associated Press, is in the public domain.

Acknowledgments

Parts of the text on this page were taken with minimal editing from sources provided by the USGS, which are in the public domain. Links to the original text can be found in the reference section on this page.

References

1. *2 roads, bridge remain closed due to Mt. Shasta mudslide triggered by melting glacier | Fox News*. (n.d.). Retrieved May 28, 2024, from https://www.foxnews.com/us/2-roads-bridge-remain-closed-due-to-mt-shasta-mudslide-triggered-by-melting-glacier
2. Blodgett, J. C., Poeschel, K. R., & Osterkamp, W. R. (1996). *Characteristics of debris flows of noneruptive origin on Mount Shasta, northern California* (Open-File Report 96–144). US Geological Survey. https://books.google.com/books?hl=en&lr=&id=7WBRAQAAIAAJ&oi=fnd&pg=PA1&dq=Characteristics+of+Debris+Flows+of+Noneruptive+Origin+on+
3. bubbasuess. (n.d.). *The 4 Eruption Cones Of Mount Shasta*. Hike Mt. Shasta. Retrieved May 24, 2024, from https://hikemtshasta.com/2018/01/12/the-4-eruption-cones-of-mount-shasta/
4. Chapman, M. (n.d.). *Mudflow near flank of Mt. Shasta covers road northeast of McCloud*. Record Searchlight. Retrieved March 17, 2024, from https://www.redding.com/story/news/2021/07/10/mudflow-near-flank-mt-shasta-covers-road-east-mccloud/7926982002/
5. College of the Siskiyous Library. (2005). *Mount Shasta Fact Sheet*. https://www.siskiyous.edu/library/shasta/documents/MS_Fact_Sheet_20050617_4pp.pdf
6. Ewert, J. W., Diefenbach, A. K., & Ramsey, D. W. (2018). *2018 update to the US Geological Survey national volcanic threat assessment*. US Geological Survey. https://pubs.usgs.gov/publication/sir20185140
7. Mangan, M., Ball, J., Wood, N., Jones, J. L., Peters, J., Abdollahian, N., Dinitz, L., Blankenheim, S., Fenton, J., & Pridmore, C. (2019). California's exposure to volcanic hazards. In *Scientific Investigations Report* (2018–5159). U.S. Geological Survey. https://doi.org/10.3133/sir20185159
8. McClung, S. C. (2005). *Lahar hazard mapping of Mount Shasta, California: A GIS-based delineation of potential inundation zones in Mud and Whitney Creek basins* [Master's Thesis, Oregon State University]. https://ir.library.oregonstate.edu/concern/graduate_thesis_or_dissertations/1c18dk67z?locale=en
9. Miesse, W. C. (1993). *Mount Shasta: An annotated bibliography*. College of the Siskiyous.
10. Sahagún, L. (2021, September 8). *First the snow vanished, then the mudslides began: Mt. Shasta's summer of pain*. Los Angeles Times. https://www.latimes.com/environment/story/2021-09-08/mt-shasta-snow-vanished-replaced-by-mudflows
11. U.S. Geological Survey. (n.d.-a). *Geology and History of Mount Shasta*. Retrieved March 13, 2024, from https://www.usgs.gov/volcanoes/mount-shasta/science/geology-and-history-mount-shasta
12. U.S. Geological Survey. (n.d.-b). *Lahars at Mount Shasta*. Retrieved March 17, 2024, from https://www.usgs.gov/volcanoes/mount-shasta/science/lahars-mount-shasta

This page titled 7.5: Mount Shasta is shared under a CC BY-NC 4.0 license and was authored, remixed, and/or curated by Emily Wright.

7.6: Lassen Volcanic National Park

A Natural Volcanology Classroom

Lassen Volcanic National Park (Figure 7.6.1) began as two separate national monuments designated by President Theodore Roosevelt in 1907: Cinder Cone National Monument and Lassen Peak National Monument. Beginning in 1914, Lassen Peak gained the interest of the nation during a series of volcanic eruptions, and the National Park was established on August 9, 1916. While Lassen Volcanic Lassen National Park remains one of the least visited U.S. National Parks visited annually, it remains one of the most geologically and historically interesting parks in the National Park System.



Figure 7.6.1: Map of Lassen area showing hydrothermal features (red dots) and volcanic features or remnants (yellow cones). Also shown is the outline of Brokeoff Volcano. "Lassen VNP Map" by Emily Wright is licensed under CC BY-NC-SA 4.0 and is a derivative of Lassen VNP map by the USGS, which is in the public domain. Access a detailed description.

Long before its designation as a National Park, at least four Native American Indian groups used the Lassen area as a meeting point. The area was not conducive to year-round living due to snow conditions, high elevation, and migrating deer populations, but the Atsugewi, Yana, Yahi, and Mountain Maidu people camped, hunted, and gathered there during the warmer months.

Lassen Volcanic National park is unique in that it includes examples of four types of volcanoes: shield, composite volcano, cinder cone, and lava dome (see 7.3: The Variety of Volcanoes in the Cascades and the Modoc Plateau-Figure 7.6.2). Lassen peak is one of the world's largest lava dome volcanoes, but the 3,187 m (10,457 ft) tall volcano sits on the north-east flank of the remains of Mount Tehama, a composite volcano. Numerous other lava domes surround Lassen Peak and many cinder cones dot the landscape in the eastern part of the park, including the creatively named Cinder Cone. There are four shield volcanoes in the park; Mount Harkness (southwest corner of the park), Red Mountain (at south-central boundary), Prospect Peak (in northeast corner) (Figure 7.6.3), and Raker Peak (north of Lassen Peak). They range in elevation from 2,133–2,560 meters (7,000–8,400 feet) above sea level and each is topped by a cinder cone volcano.

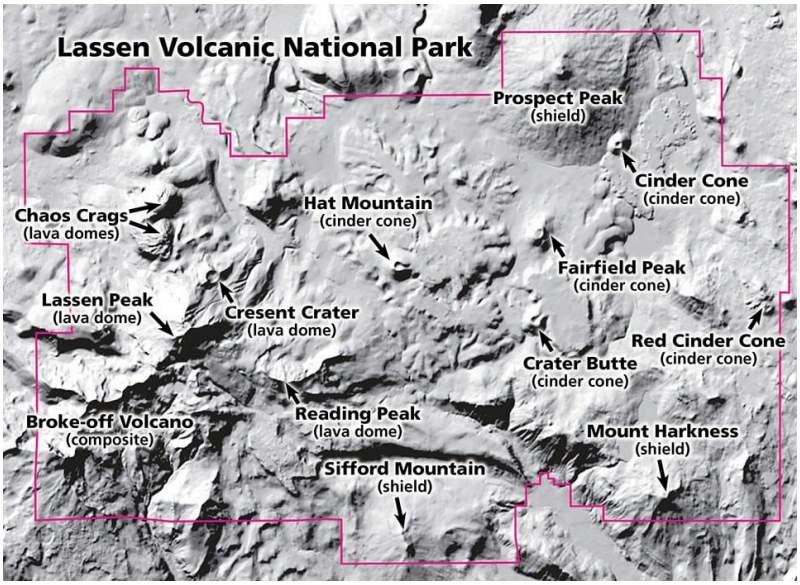


Figure 7.6.2: Shaded Relief Map of Lassen Volcanic National Park labeled with the name and type of volcanoes. "Map view with feature labels" by the National Park Service is in the public domain. Access a detailed description.

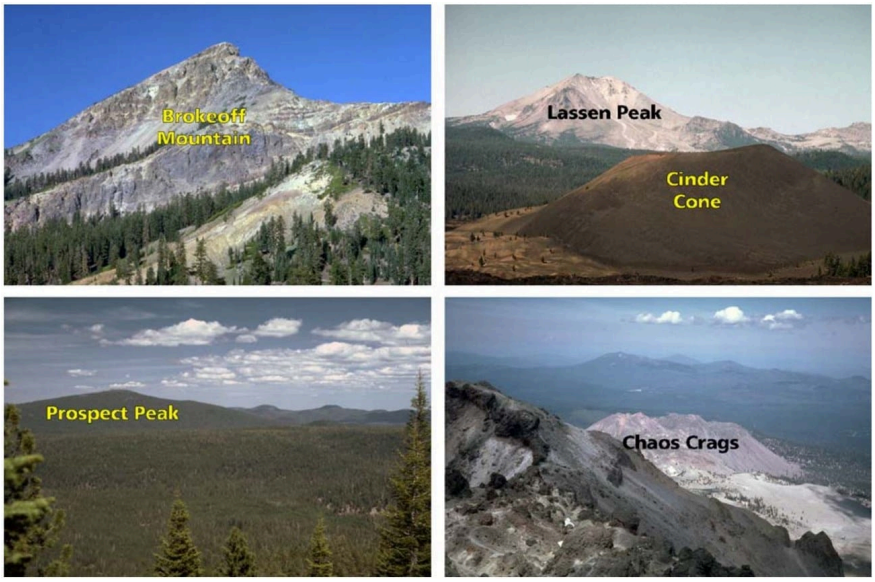


Figure 7.6.3: Four primary types of volcanoes occur within the park: composite volcano (upper left; Brokeoff Mountain, which is a remnant of Brokeoff Volcano), cinder cone (upper right, a brown hill with Lassen Peak lava dome in the background), shield volcano (lower left; Prospect Peak), and lava dome (lower right; the domes of Chaos Crags). Photographs by Michael A. Clynne (upper and lower left) and Patrick Muffler (upper and lower right). "Four Types of Volcanoes" by USGS is in the public domain.

In earlier activities in this chapter, you identified both the type of rock and the type of volcano at Chaos Crags in Lassen Volcanic National Park. Now, put these concepts together and review what you learned about magma viscosity in section 7.3: The Variety of Volcanoes in the Cascades and the Modoc Plateau in the activity “Chaos Crags: Putting it all Together”.

Query 7.6.1

This interactive element is not available in this format. Visit the link or scan the QR code to access it online.

View this Interactive Content online

The Missing Volcano: Mount Tehama

When students learn to recognize composite volcanoes, they are taught to picture iconic summits, like Mount Fuji in Japan or Mounts Shasta and Rainier in the Cascade Range. Unlike the other three general types of volcanoes (cinder cones, shield volcanoes, and lava domes), a representative of this type of volcano is not currently easily recognizable in Lassen Volcanic National Park. Once upon a time, however, an impressive composite volcano, Mount Tehama, also known as Brokeoff Volcano existed. It consisted of lava domes, lava flows, and pyroclastic deposits that are between 590,000 and 385,000 years old. In its heyday, Mount Tehama would have been around 300 meters (a thousand feet) higher than Lassen Peak is today, and was 20 km (12 miles) wide at its base. This volcano was eroded, primarily by glaciers, so that only remnants remain. The surviving portions of the central rim include Brokeoff Mountain, Mount Diller, Mount Conrad, and Pilot Pinnacle. Figure 7.6.4 shows an outline of the projected original shape of Mount Tehama (Brokeoff Volcano) with Lassen Peak in the background for comparison.

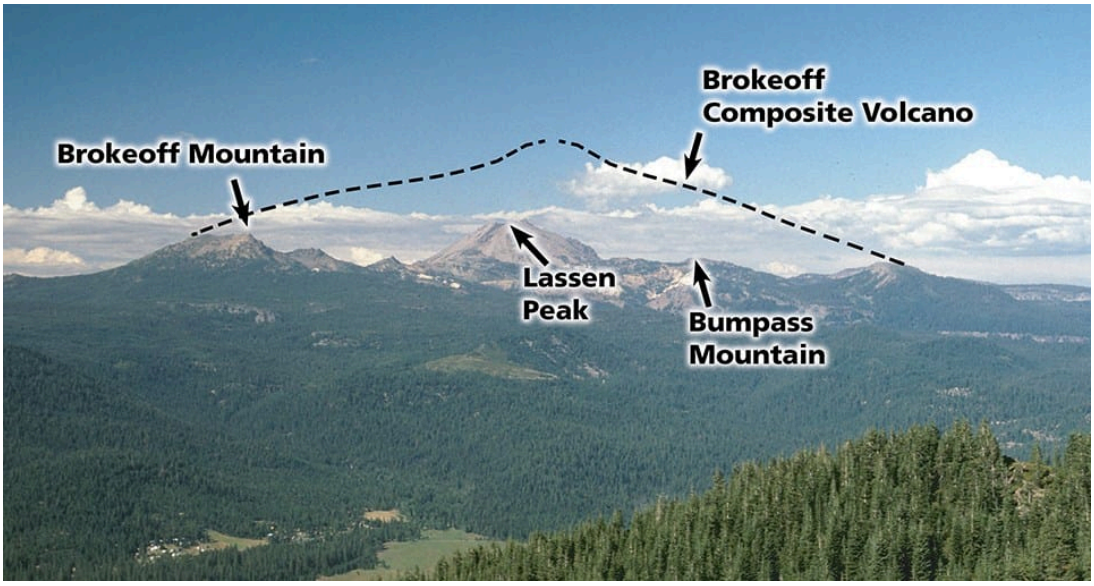


Figure 7.6.4: Projected profile of Brokeoff Volcano which would have risen to an elevation of 11,000 ft (3300, m). Lassen Peak is visible behind the area where Brokeoff Volcano once existed. "Projected profile" by Michael A. Clynne, USGS is in the public domain. Access a detailed description.

The 1914-1917 Eruption of Lassen Peak

On May 22, 1915, a large explosive eruption at the summit of Lassen Peak, California devastated nearby areas and rained volcanic ash as far away as 280 miles to the east. This explosion was the most powerful in a series of eruptions during 1914–17 that were the last to occur in the Cascade Range before the 1980 eruption of Mount St. Helens, Washington.

The 1914–17 eruptions of Lassen Peak were among the first volcanic events to occur after photography became readily available to amateurs. Thus, they were documented and popularized by the northern California media, primarily the San Francisco Chronicle, and subsequently by the popular scientific media. The photographs of amateur photographers, particularly those of Benjamin Franklin Loomis (1857–1935) proved crucial to understanding the chronology and processes of the May 1915 eruptions. Some eruptive events were even caught on film by Red Bluff resident J.J. Hammer.

Video 7.6.1: Mt Lassen 1915

"Mt Lassen 1915" shows the film by J.J. Hammer. The original film was silent and the YouTube version includes only added film reel sound effects, but no relevant audio. Access a text description.

This interactive element is not available in this format. Visit the link or scan the QR code to access it online.

View this YouTube Video online

Initial Rumblings

On May 30, 1914, Lassen Peak awoke from a 27,000-year-long slumber when it was shaken by a steam explosion. Such steam blasts occur when molten rock (magma) rises toward the surface of a volcano and heats shallow groundwater. The hot water then rises under pressure through cracks and, on nearing the surface, vaporizes and may vent explosively. That first explosion created a small crater at the summit of Lassen Peak, and each of more than 180 subsequent steam explosions enlarged it (Figure 7.6.5). Over more than 11 months, these steam explosions blasted out a crater 1,000 feet (300 m) long.

In mid-May 1915, the character of the eruption changed dramatically. On the evening of May 14, 1915, incandescent blocks of lava could be seen bouncing down the flanks of Lassen Peak from as far away as Manton, 20 miles (32 km) to the west. By the next morning, a growing dome of dacitic lava had welled up and filled the crater at the summit of Lassen Peak.



Figure 7.6.5: A steam-explosion eruption at Lassen Peak on June 14, 1914. Such steam-blast eruptions ranged from a few minutes to several hours in duration and often sent plumes thousands of feet above the volcano. Photograph taken by B.F. Loomis from a point west of Manzanita Lake, about 6 miles (10 km) from Lassen Peak. Steam Explosion, made available by the National Park Service, is in the public domain.

Events of May 19–20, 1915

On the evening of May 19, a large explosion shattered the still-hot lava dome that had filled Lassen's summit crater during the previous week, blasting out a new crater at the volcano's summit and creating an avalanche of hot lava blocks, volcanic debris, and snow. As the snow melted, a huge lahar rushed 18 km (11 miles) down Lost Creek, releasing huge volumes of water and flooding lower Hat Creek Valley. The avalanche, lahars, and floods produced by this explosion uprooted and carried away trees 30 m (100 feet) tall with ease and damaged several ranch houses. During that night (May 19–20), lava welled up into the crater created by the explosion, overflowed the summit depression, and fed two lobes that flowed about 300 m (1,000 feet) down the northeast and west flanks of the mountain.

Climactic Event of May 22, 1915

On May 22, Lassen Peak exploded again in a powerful climactic eruption that blasted rock fragments and pumice high into the

air, creating the larger and deeper of the two craters seen at the summit of the volcano today and generating a vertical eruption column that rose to 10,000 m (30,000 feet; Figure 7.6.6). Partial collapse of the eruption column generated a pyroclastic flow that swept down the northeast side of the volcano. Trees still standing after the May 19 eruption were now blown down. The pyroclastic flow rapidly melted snow in its path, creating a lahar that followed the path of the lahar two days earlier and rushed down Lost and Hat Creeks to Old Station, releasing water that again flooded lower Hat Creek Valley.



Figure 7.6.6: Lassen Peak in northern California produced a series of eruptions during 1914–17. The largest of those eruptions, on May 22, 1915, blasted rock fragments and pumice high into the air and rained fine volcanic ash as far away as Elko, Nevada, 280 miles (450 km) to the east. This photograph, taken from the town of Red Bluff, 40 miles (65 km) west of the volcano, shows the huge eruption column of ash and gas, which rose to a height of more than 30,000 feet (9,000 m). Lassen Peak by R.E. Stinson, has been made available by the National Park Service and is in the public domain.

Continued Volcanic Activity and Future Eruptions

For several years after the eruption of May 22, 1915, snowmelt percolating down into Lassen Peak, especially in the spring, triggered steam explosions, indicating that rocks beneath the volcano's surface remained hot. Particularly vigorous steam explosions in May 1917 blasted out the northern of the two craters now seen at the volcano's summit. Steam vents could still be found in these craters into the 1950s, but they gradually weakened and are difficult to locate today.

Figure 7.6.7 shows the extent of the deposits from the May 1915 eruptions of Lassen Peak. The total volume of the 1915 eruptions was approximately 0.03 km3 (0.007 cubic mile)—tiny compared to a major eruption like that of Mount St. Helens in 1980 (1 km3 or 0.24 cubic mile). The deposits from the Lassen Peak eruptions are rapidly becoming obscured by vegetation and erosion (Figure 7.6.8), and the small size and unconsolidated nature of the thin deposits make the 1915 eruptions unlikely to be preserved in the long-term geologic record. Today, Lassen Peak sleeps again, but active steam vents, hot springs, and bubbling mud pots are still found elsewhere in Lassen Volcanic National Park. No one can say when, but it is almost certain that the Lassen area will experience volcanic eruptions again. The USGS California Volcano Observatory operates a sophisticated sensor network to detect any increase in seismicity, ground deformation, or gas emissions that could indicate magma rising toward the surface in preparation for the next Lassen eruption. Early detection of such eruption precursors is essential to effective hazard mitigation and forecasting.

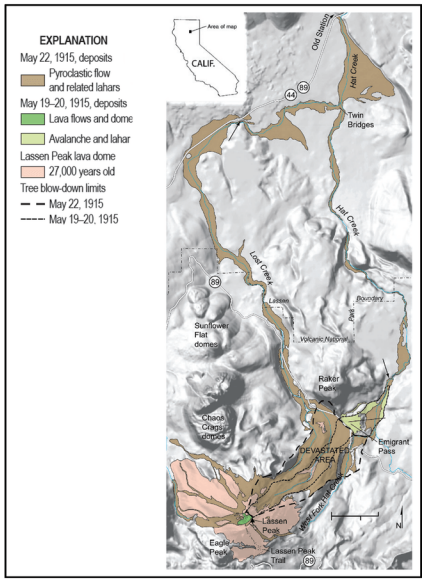


Figure 7.6.7: This generalized geologic map shows Lassen Peak and the deposits from its May 1915 eruptions. The 27,000-year-old Lassen Peak Lava Dome (pale peach) erupted multiple times in May 1915. Those eruptions destroyed an area of 3 square miles (7.7 square kilometers) on the northeast flank of the volcano, now called the Devastated Area. Deposits from the May 19-20 eruptions can be found near the summit (darker green lava flows and dome), near Emigrant Pass (lighter green avalanche and lahar), and near the location of “Hot Rock” on the northeast flank of the mountain (see Figure 7.6.8). Deposits from the pyroclastic flow and related lahars (light brown) of May 22, 1915 are located mainly in the Lost Creek and Hat Creek drainages. "Deposits from Lassen Peak’s May 1915 Eruptions" by USGS is in the public domain. Access a detailed description.



Figure 7.6.8: Sequence of photographs taken before and after the cataclysmic eruptions of Lassen Peak in May 1915. **The first image** in the sequence shows a view of the northeast flank of Lassen Peak taken before 1914. Mature conifer forest covers the lower slopes. **The next photo** was taken at noon on May 22, 1915, showing the destruction from the avalanche and lahar of May 19–20. Trees 30 m (100 feet) tall were uprooted and carried away with ease. The large rock in the foreground, labeled “hot rock” by Loomis, is a piece of the lava dome that filled the crater during the previous week that was carried down by the avalanche. Note the remaining tree-covered slopes at the left and right margins of the avalanche path and the dark gray tongue of new dacite lava below the volcano’s summit that erupted on the night of May 19–20. **The third image** is a view of Lassen Peak’s northeast flank taken in June 1915, showing the full devastation caused by the cataclysmic explosive eruption of May 22. Trees still standing on the morning of that day were blown down or snapped off and their trunks left lying on the ground, pointing away from Lassen Peak. The lava flow below the summit is gone, and the May 22 mudflows have smoothed the surface of the May 19 avalanche and lahar deposit. The “hot rock” remains—and can still be seen today on the Devastated Area Interpretive Trail, as seen in the **fourth image** taken in 2023. The appearance of the Devastated Area changed little for 50 years as seedlings struggled to gain a foothold. Today, however, young vigorously growing trees are obscuring the devastation and reclaiming the area as forest. The first three photos by B.F. Loomis, published by the USGS, are in the public domain. The final photo was taken by Emily Wright, who also compiled this figure, which is licensed under CC BY-NC-SA 4.0.

Hydrothermal Activity in Lassen National Park

Today, the active volcanism at Lassen Volcanic National Park still produces remarkable hydrothermal features, including fumaroles, mud pots, boiling pools, and thermal ground. These are very active most of the time, emitting hydrogen sulfide (H2S) and coating rocks with yellow sulfur deposits.

Water enters the Lassen hydrothermal system at high elevations, when water from rain and snow percolates into the subsurface and is heated by hot rock surrounding a magma chamber 8-10 km (5-6 mi) below the surface. The water penetrates the rock surrounding the heat source and is heated by conduction. Hydrochloric acid, sulfurous gasses, and other volatiles emitted by the

body of magma or the hot rock dissolve in the water as it is heated. Because it is less dense than cold water, the heated water rises by convection. As the water rises, acids react with surrounding rock, enriching the water in dissolved silica (SiO_2) and metals. Hot water eventually reaches low enough pressures to boil in the vapor-dominated zone. Steam and gasses are released to surface fumaroles and acidic hot springs. Residual thermal water flows down gradient and emerges as hot springs and geysers south of the park. Figure 7.6.9). In active hydrothermal areas, hot water enriched in dissolved metals and other chemicals evaporates. This leaves behind colorful sulfate minerals like the yellow copiapite (hydrous iron sulfate) and black or brassy pyrite (iron sulfide or fool's gold). Algal and bacterial mats also contribute to the colorful display of the hot springs.

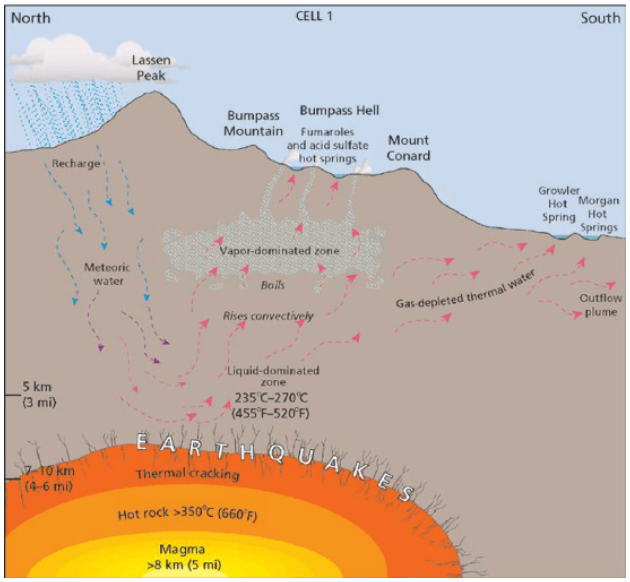


Figure 7.6.9: Recharge of the Lassen hydrothermal system begins at high elevations. Water from rain and snow percolates into the subsurface and is heated by hot rock surrounding a magma chamber 8-10 km (5-6 mi) below the surface. Hot water rises via convection. Hot water eventually reaches low enough pressures to boil in the vapor-dominated zone. Steam and gasses are released to surface fumaroles and acidic hot springs. Residual thermal water flows down gradient and emerges as hot springs and geysers south of the park. This Graphic by Trista Thornberry-Ehrlich, Colorado State University, is published by the USGS and is in the public domain. Access a detailed description.

Perhaps the most famous of these hydrothermal areas is Bumpass Hell (Figure 7.6.10), which marks the principal area of upflow and steam discharge from the Lassen hydrothermal system. The area was named for a miner Kendall Vanhook Bumpass who was the first European settler to visit in the 1860s. On his second trip to the boiling mud pots, he broke through the thin crust and scalded his leg so badly it required amputation. Hydrothermal features like Bumpas Hell are indicators of the ongoing potential for future volcanic eruptions in the Lassen volcanic center.



Figure 7.6.10: "Bumpass Hell" by Don DeBold via Flickr is licensed under CC BY 2.0.

Video 7.6.2: Hiking Bumpass Hell

If you are interested in learning more about Bumpass Hell, watch this video field guide by the National Park Service.

This interactive element is not available in this format. Visit the link or scan the QR code to access it online.

View this YouTube Video online

Cinder Cone and the Fantastic Lava Beds

Many small cinder cones throughout the southeastern Cascades and Modoc Plateau are unnamed. Others have unoriginal names like Black Butte or Red Cinder Cone (not to be confused with the distinctly more cone-shaped Red Cinder about a half-mile to the east). Perhaps the least originally named of all is Cinder Cone in Lassen National Park (Figure 7.6.11). This classically shaped, relatively young cinder cone in a National Park makes an excellent case study of a typical Cascade cinder cone.



Figure 7.6.11: Author Emily Wright prepares to ascend Cinder Cone. Early in the hike, exhaustion has not yet set in. Photo by Micah Wright is licensed under CC BY-NC-SA 4.0.

The hike up Cinder Cone (258 m or 846 ft) starts with a broad path skirting the edge of the Fantastic Lava Beds (see the Box: Fantastic Lava Beds). The pumice-y soil makes walking a bit strenuous despite the gentle slope in this early part of the trail. The contrast between the mature forest on the right and the very young-looking lava flow on the left is striking. The youthful appearance of the lava flow deceived early explorers of Lassen. In 1875, H.W. Harkness described Cinder Cone as probably being no more than 25 years old. Geologists now know that Cinder Cone erupted in 1666, so it would have then been around 200 years old when Harkness described it. Geologically speaking, that's still very young!

There is a distinct change in character of the trail as you start up the Cinder Cone itself. The steep angle of the trail in the loose scoria makes the climb to the summit quite arduous, but the views are well worth the effort. At the summit, the double rimmed crater is visible (Figure 7.6.12). The double rim was probably created by fluctuating eruptive activity late in the formation of the cone. There are also good views of the several blocky lava flows associated with Cinder Cone. To the casual observer and even to some of the first geologists to study Cinder Cone, there appear to be multiple ages of lava flow. The soft, sand-dune-like appearance of the Painted Dunes Lava Flow makes it seem much more weathered than the sharp, dark, Fantastic Lava Beds (Figure 7.6.13). However, geologists have now shown that the entire eruptive sequence at Cinder Cone represents a single continuous event that probably spanned no more than a few months. During this event, the composition of the molten rock (magma) feeding the eruption changed from basaltic andesite to andesite and then back to basaltic andesite, but with a higher

titanium content. Two cones erupted over the course of this event. The remnants of a nearly completely buried earlier cone can be seen on the larger cone's south side. Much of the earlier cone was probably destroyed by lava flows erupting from its base. The weathered look of the Painted Dunes flow is actually the result of ash falling onto still-hot lava from an earlier phase of the eruption. The ash is brightly oxidized because it fell on the lava flows when they were still hot, giving the dunes their "painted" look.



Figure 7.6.12: Double rim of Cinder Cone. Photo by Emily Wright is licensed under CC BY-NC-SA 4.0.



Figure 7.6.13: View of the Painted Dunes and Fantastic Lava Flow from the summit of Cinder Cone. "Painted Dunes as seen from Cinder Cone" by Ilja Klutman is licensed under CC BY-NC-SA 2.0.

Video 7.6.3: Lassen Volcanic National Park | Cinder Cone Trail | the Best View of Mt. Lassen in California

For video footage of the hike described in the previous paragraphs, complete with summit views, watch the video. There is no audio narration for this video, only music.

This interactive element is not available in this format. Visit the link or scan the QR code to access it online.

View this YouTube Video online

Acknowledgments

Parts of the text on this page were taken with minimal editing from sources provided by the USGS and the National Park Service, which are in the public domain. Links to the original text can be found in the reference section on this page.

References

1. Clynne, M. A. (2011). *Stratigraphy and compositional evolution of Cinder Cone, a composite monogenetic cone in Lassen Volcanic National Park, California. 2011*, V13C-2621.
2. Clynne, M. A., Champion, D. E., Trimble, D. A., Hendley II, J. W., & Stauffer, P. H. (2000). *How Old is "Cinder Cone"?—Solving a Mystery in Lassen Volcanic Park, California* [Fact Sheet 023-00]. US Geological Survey. https://pubs.usgs.gov/publication/fs02300
3. Clynne, M. A., Christiansen, R. L., Stauffer, P. H., Hendley II, J. W., & Bleick, H. A. (2014). *A sight" fearfully grand": Eruptions of Lassen Peak, California, 1914 to 1917*. US Geological Survey. https://pubs.usgs.gov/publication/fs20143119
4. Clynne, M. A., Janik, C. J., & Muffler, L. J. P. (2003). *"Hot Water" in Lassen Volcanic National Park—Fumaroles, Steaming Ground, and Boiling Mudpots* (Fact Sheet 101-02). US Geological Survey. https://pubs.er.usgs.gov/publication/fs10102
5. Clynne, M., & Muffler, L. (2010). *Geologic Map of Lassen Volcanic National Park and Vicinity, California: U.S. Geological Survey Scientific Investigations Map 2899* [Map]. https://pubs.usgs.gov/sim/2899/
6. KellerLynn, K. (2014). *Lassen Volcanic National Park: Geologic Resources Inventory Report* (NPS/NRSS/GRD/NRR—2014/755). US National Park Service. https://irma.nps.gov/DataStore/DownloadFile/489001
7. Klemetti, E. (2016, February 17). Watch One of the First Volcanic Eruptions Ever Filmed. *Wired*. https://www.wired.com/2016/02/watch-one-of-the-first-volcanic-eruptions-ever-filmed/
8. Loomis, B. F. (1926). *Pictorial History of the Lassen Volcano*. California Press.
9. Szymanski, M. E., & Teasdale, R. (2015). Groundmass Crystallinities of Proximal and Distal Lavas from Cinder Cone, Lassen Volcanic Field. *AGU Fall Meeting Abstracts*, *2015*, V23B-3106. https://ui.adsabs.harvard.edu/abs/2015AGUFM.V23B3106S/abstract
10. U.S. National Park Service. (2023, April 17). *Volcanic Resources Summary—Lassen Volcanic National Park*. https://www.nps.gov/articles/000/volcanic-resources-summary-lassen-volcanic-national-park.htm

This page titled 7.6: Lassen Volcanic National Park is shared under a CC BY-NC 4.0 license and was authored, remixed, and/or curated by Emily Wright.

7.7: Medicine Lake Volcano

Not Your Grandmother's Shield Volcano

When viewed from a distance, Medicine Lake Volcano has the apparent classic shape of a shield volcano, though one covered with a pox of cinder cones (Figure 7.7.1). However, as one approaches the volcano more closely, the rocks tell a somewhat different story than the overall shape might lead one to believe. The most iconic shield volcanoes, such as Mauna Loa and Mauna Kea in Hawaii, are generally uniform in lava composition, with only slight variations in chemistry over their eruptive history. They are composed of only basalt. By contrast, outcrops exposed on the flanks of the Medicine Lake Volcano range from basaltic to andesitic and even rhyolitic at high elevations. Drill cores indicate that rhyolites are also found at depth. This extreme range of volcanic rock compositions indicates that the degree of crustal contamination is highly variable over the life of this volcano. At times, very little magmatic assimilation produced basaltic lavas, and at other times, extensive assimilation produced rhyolitic tuffs and obsidian flows. The range of composition might more reasonably classify Medicine Lake Volcano as a composite volcano, but it has erupted more low-viscosity basalt flows than a typical composite cone, giving it a shield, rather than cone, shape.



Figure 7.7.1: Medicine Lake Volcano is a broad shield volcano. This view is from Captain Jack's Stronghold in Lava Beds National Monument. "Medicine Lake Volcano from Captain Jack's Stronghold in Lava Beds NM" by Daniel Mayer is licensed under CC BY-SA 3.0.

Medicine Lake Volcano began forming around 500,000 years ago, with the most recent eruption at Glass Mountain occurring about 950 years ago. Near the center of the shield-shaped edifice, there is an enclosed basin or caldera, 12.1 km (7.5 miles) long by 6.9 km (4.3 miles) wide, which is partially flooded by the namesake 2 km-long (1.2 mile-long) Medicine Lake (Figure 7.7.2). The caldera formed when the center block began to collapse along fractured lines between 180,000 and 100,000 years ago, although no single large eruption was responsible for the caldera formation. Lava erupted after the caldera formed and lava was squeezed up the fracture lines forming rim volcanoes. The volcanoes discharged lava onto the caldera floor and down the outer edges of the original volcano edifice.

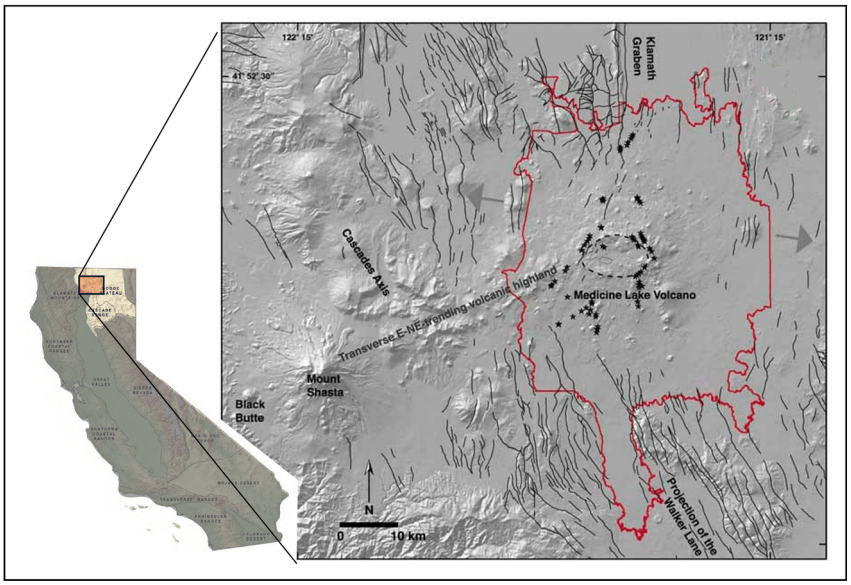


Figure 7.7.2: Shaded relief map of Medicine Lake volcano. The red outline indicates the extent of lava flows originating from the Medicine Lake Volcano. Volcanic vents are marked by stars and the caldera rim is a dashed black ellipse. Faults are indicated by thin black lines and are the result of regional Basin and Range extension. Gray arrows at east and west sides indicate approximate direction of extension across the volcano. "Shaded relief map shows locations of Medicine Lake volcano" by Donnelly-Nolan et. al. 2008, USGS is in the public domain. Location map (Figure 7.1) added by Emily Wright. Access a detailed description.

Lava Beds National Monument

Lava Beds National Monument on the north slope of Medicine Lake shield volcano contains the highest concentration of lava tube caves in North America. There are up to 500 known lava tube caves within the boundaries of Lava Beds National Monument (Figure 7.7.3).



Figure 7.7.3: Cave formed from a lava tube in Lava Beds National Monument. The horizontal traces near the floor of the cave wall are remnants of high stands of lava as it drained away during the final stages of lava-flow activity within the tube. The drip structures from the ceiling were formed as the top of the cave remelted and dripped downward due to the high temperatures within the tube system. "Lava Tube Cave" by Volcano Hazards Program, USGS is in the public domain.

Much of the north and south flanks of the Medicine Lake shield were built from molten lava transmitted through lava tubes. These tubes formed beneath the congealing surface of basalt flows in somewhat the same way that a stream may continue to flow beneath a cover of its own winter ice. As molten lava emerges from a vent and flows down slope, congealing lava from the top and

sides of the central channel often forms a bridge over the lava flow. The sticking together of bits of lava spatter and fragile lava crusts strengthens the bridge in the same way that thin crusts of floating ice raft together to cover a stream during early stages of a winter freeze. Because the viscosity of the lava depends on temperature, and the roof of the lava tube insulates it, lava can flow much further from the vent in the insulated lava tube compared to being exposed at Earth's surface. The leading edges of basalt flows at Earth's surface can travel as fast as 10 km/h (6 mph) on steep slopes but they typically advance less than 1 km/h (0.27 m/s or about 1 ft/s) on gentle slopes. When basalt lava flows are confined within an insulating channel or lava tube on a steep slope, the main body of the flow can reach velocities greater than 30 km/h (19 mph).

Eruption of basaltic lava is a much more violent and spasmodic process than the steady gathering of tributaries that feed a stream. If lava stops rising from its source deep within Earth, the still-molten lava moving within a lava tube will continue to drain downhill and may ultimately leave an open tube-shaped cave -- often large enough for people to walk through. Even before the top and walls of a lava flow have time to cool from one eruption, a new eruption of lava may refill the open tube, overflow its upper end, and spread a new lava flow beside or on top of the first flow. Even if the original tube is large enough to contain the renewed supply of lava, this tube can then deliver the new lava beyond the end of its original flow and thus the lava field extends farther and farther down slope. If the gradient of flow flattens, the tube may subdivide into a number of smaller distributaries, which spread laterally over the more gently sloping ground.

Within Lava Beds National Monument, most lava tubes are found within the basalt of Mammoth Crater. Complicated lava-tube systems originating from Mammoth Crater and other vents have built a broad fan of complexly interfingering lava flows that form the lower northeast flank of the Medicine Lake Volcano. Some tubes conveyed lava underground 25-30 km (about 15-20 miles) from their sources. Nevertheless, today it is hard to walk for a distance of even 6 km (4 miles) within any one lava tube. Large parts of the roofs of most lava tubes have fallen in, hiding the floor under huge piles of angular broken rock, often stacked so tightly that access to both upstream and downstream portions of the tube is closed. In some places, however, collapse of the tube's roof has provided a large entrance into the lava tube through which one can walk with ease. Multiple collapses have created the hundreds of caves within the dozen or so lava tubes that distributed lava over two thirds of the monument.

Box 7.7.1: The Modoc War

The winter of 1872-1873 was a troubled one in the Lava Beds, where a small band of Modoc Indians was besieged by a US Army force outnumbering them as much as ten to one. The conflict arose after the United States government relocated the Modoc people to the Klamath Reservation, north of present-day Klamath Falls, along with the Klamaths and members of the Yahooskin band of Paiutes. A group of several hundred Modocs left the Klamath Reservation and returned to their homeland, demanding their own separate reservation within their ancestral territory. The resulting conflict was one of the most costly wars in U.S. history. According to some estimates it cost $10,000 (about $300,000 today) per warrior to subdue the Modocs in battle. The Modoc warriors totaled between 50 and 60, while there were as many as 1000 U.S. troops at the height of the conflict. The war lasted six months, from November 29, 1872 to June 1, 1873, although tensions leading to the conflict began much earlier.

Much of the war was centered around Captain Jack's Stronghold, a natural lava fortress characterized by lava tubes, small caves, and deep clefts within the lava flows (Figure 7.7.4). The deep clefts provided excellent cover for snipers and the network of clefts and lava tube caves provided hidden, protected pathways for the Modoc to maneuver through during skirmishes with the US Army. The Stronghold was named for the Modocs' war leader Keintpoos, or Captain Jack as he was known to the settlers. Some 150 Modoc men, women,and children lived in the Stronghold for five months of the war, including the harsh winter months. By the war's end, the fatalities included 53 U.S. soldiers, 17 civilians, 2 Warm Springs Scouts, 5 Modoc women and children, and 15 Modoc warriors, five of which were killed in battle; many were executed for "crimes against the United States" after their surrender and the survivors were eventually transported to a reservation in Oklahoma.

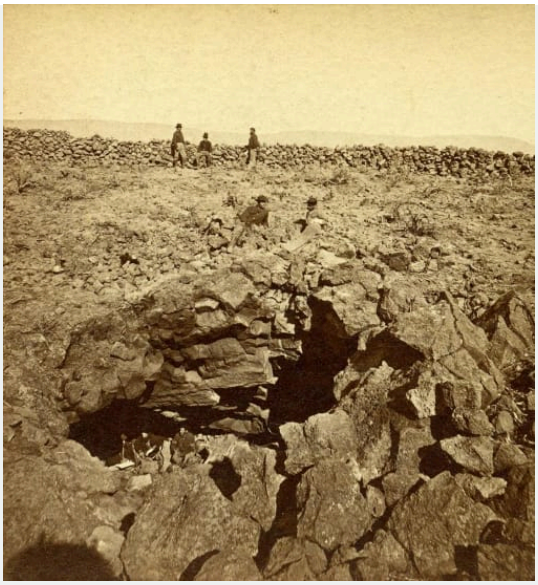


Figure Box 7.7.1.1: U.S. soldiers inspect Captain Jack's cave in the Lava Beds in 1873. "Captain Jack's Stronghold, Lava Beds" from the National Archives is in the public domain.

Although the Modoc people did not prevail in the end, their ability to hold off the U.S. troops for as long as they did was due in large part to their knowledge and skill in using the local terrain, especially the network of lava tubes, to their advantage. The rugged landscape formed by the lava flows and collapsed lava tubes provided natural military fortifications and hidden pathways for travel for the Modoc people.

Obsidian Domes

In addition to the many cinder cones scattered throughout the Cascades and Modoc Plateau, there are also many lava domes. Two of the most iconic lava domes are Glass Mountain and Little Glass mountain, located on the Medicine Lake Volcano. These formed when silica-rich (rhyolitic) magma erupted effusively at the surface. In order for rhyolitic lava to erupt effusively, it must have a very low gas content. This usually occurs when the gasses have already escaped the magma before it erupts at the surface. Because of the high viscosity of rhyolitic lava, it does not flow long distances, as basaltic lava does, and instead builds a dome (Figure 7.7.5). The relatively rapid cooling that occurs at the surface of Earth, combined with the high viscosity of rhyolitic lava, impedes the growth of mineral crystals. Instead, the lava cools into volcanic glass, or obsidian, which is solid, but with no crystalline structure.



Figure 7.7.5: Glass Mountain, one of the smaller volcanoes surrounding the Medicine Lake caldera rim, northern California. "Glass Mountain" by Julie Donnelly-Nolan, USGS is in the public domain.

The lack of crystalline structure in obsidian causes conchoidal fracture. Through a technique called 'knapping', conchoidal fracture can be controlled to produce very sharp tools, such as arrowheads and knives. This made obsidian incredibly valuable to the people of North America before Europeans introduced metal alloy technology. Not only does obsidian remain culturally important today, but it is also still used in some cutting applications, such as certain surgeries because it can produce a sharper edge than steel. Local tribes, including the Modoc and Pit River peoples collected, used, and widely traded the high-quality obsidian from sources like Glass Mountain and Lassen Creek in the Warner Mountains. Obsidian was a popular trade item to other tribes from as far away as 100 miles.

Today, collecting obsidian anywhere in the Medicine Lake Highlands is prohibited by law. The Modoc National Forest has four obsidian mines in the Warner Mountains near Davis Creek, Calif. on the east side of the forest where it is legal to collect obsidian with a free permit.

Acknowledgments

Parts of the text on this page were taken with minimal editing from sources provided by the USGS and the National Park Service, which are in the public domain. Links to the original text can be found in the reference section on this page.

References

1. Alt, D., Hyndman, D. W., & Baylor, K. J. (2016). *Roadside Geology of Northern and Central California* (2nd edition). Mountain Press.
2. Donnelly-Nolan, J. M. (1987). *Medicine Lake Volcano and Lava Beds National Monument, California*. https://pubs.geoscienceworld.org/gsa/books/book/786/chapter/4880695/Medicine-Lake-Volcano-and-Lava-Beds-National
3. Horton, K. (2023, October 3). 150 years ago, the US military executed Modoc war leaders in Fort Klamath, Oregon. *Oregon Public Broadcasting*. https://www.opb.org/article/2023/10/03/modoc-war-captain-jack-execution-fort-klamath-oregon/
4. U.S. Geological Survey. (n.d.). *Eruption History of Medicine Lake Volcano*. Retrieved March 24, 2024, from https://www.usgs.gov/volcanoes/medicine-lake/science/eruption-history-medicine-lake-volcano
5. U.S. Geological Survey. (2023a, October 7). *The Modoc War*. https://www.usgs.gov/volcanoes/medicine-lake/science/modoc-war
6. U.S. Geological Survey. (2023b, October 31). *Lava tubes at Lava Beds National Monument*. https://www.usgs.gov/volcanoes/medicine-lake/science/lava-tubes-lava-beds-national-monument
7. U.S. Geological Survey. (2023c, November 3). *Geology and History of Medicine Lake*. https://www.usgs.gov/volcanoes/medicine-lake/science/geology-and-history-medicine-lake
8. U.S. National Park Service. (n.d.). *Geology—Lava Beds National Monument*. Retrieved March 20, 2024, from https://www.nps.gov/labe/learn/nature/geology.htm

9. U.S. National Park Service. (2023, December 10). *Modoc War—Lava Beds National Monument*. https://www.nps.gov/labe/learn/historyculture/modoc-war.htm
10. U.S. National Park Service. (2024, April 4). *History & Culture—Lava Beds National Monument*. https://www.nps.gov/labe/learn/historyculture/index.htm

This page titled 7.7: Medicine Lake Volcano is shared under a CC BY-NC 4.0 license and was authored, remixed, and/or curated by Emily Wright.

7.8: Glaciers in the Cascades

Evidence of Pleistocene Glaciers

Although the Cascades are noted primarily for their volcanic terrain and associated hydrothermal features, volcanism and glaciation have gone hand in hand in the creation of the landscape. Today, glaciers in the California Cascades are rather limited compared with the large ice caps that covered the mountainous terrain several times during ice ages of the recent geologic past. Glaciers advanced at least five times during the ice ages of the Pleistocene Epoch, creating landforms such as moraines and outwash deposits that “overprint” much of the volcanic foundation. The alteration of volcanic rocks by hydrothermal processes facilitated glacial erosion, and glacially eroded features such as U-shaped valleys, cirques, and arêtes occur throughout the province.

At higher elevations, the main effects of Pleistocene glaciation were erosional. Glaciers deepened major valleys, removed bedrock from large parts of the landscape, and created or enlarged hundreds of lake basins. Glaciers also polished and scratched striations and grooves on bedrock surfaces (Figure 7.8.1).



Figure 7.8.1: Left: Glaciers carved striations into the volcanic rock on the trail to Bumpass Hell. Right: This boulder, called a glacial erratic, was carried to this location and deposited by a glacier. "Glacial Features of Lassen VNP" by Emily Wright is licensed under CC BY-NC-SA 4.0.

Glacial deposition also helped to shape the landscape of the Cascades. Glaciers and widely distributed till (a mixture of clay, silt, sand, gravel, and boulders), developed moraines, and deposited erratics (Figure 7.8.1). Glacial meltwater also deposited outwash (sand and gravel) beyond the margins of glacial ice.

Modern Glaciers and Climate Change

The story of glaciation in the California Cascades is mostly a story of the geologic past. However, Mount Shasta still hosts seven glaciers: Whitney, Bolam, Hotlum, Konwakiton, Watkins, Mud Creek, and Wintun. Although there are more glaciers in the Sierra Nevada, the Cascades can claim both California’s largest glacier by volume (Hotlum Glacier) and its longest (Whitney Glacier).

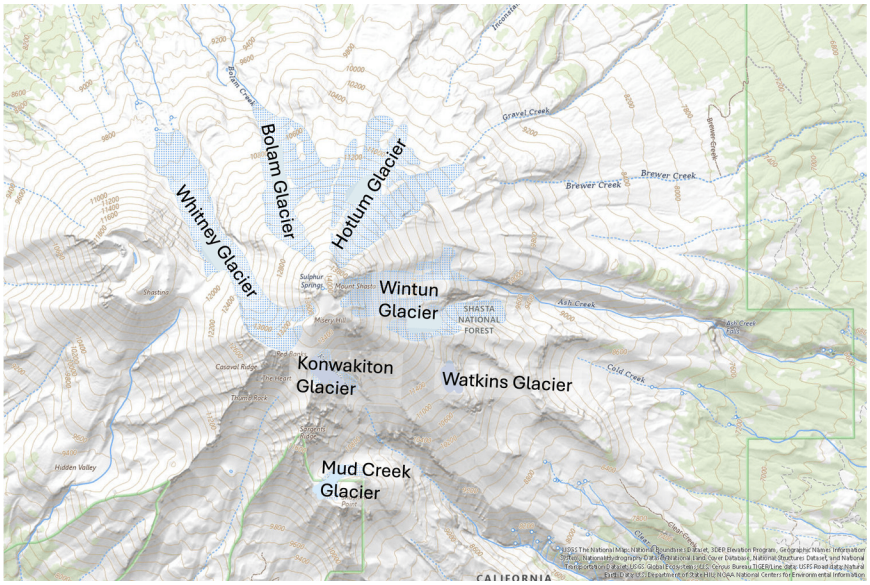


Figure 7.8.2: "Glaciers of Mount Shasta" by Emily Wright using topoBuilder from the USGS is in the public domain. Access a detailed description.

By the early 2000s, a pattern of glacial retreat was evident throughout the American West and the world. However, researchers found that this pattern did not hold true for the glaciers of Mt. Shasta. Both Whitney and Hotlum Glaciers were, at the time, actually growing. Whether a glacier grows or shrinks depends primarily on two climatic factors, temperature and precipitation. The researchers reasoned that, although the climate surrounding Mt. Shasta was getting warmer each year, the winters were also getting wetter during the same period. The increased snowpack in the winter was making up for the increase in melting during the summer months. They also hypothesized, in 2006, that this trend was not likely to hold in the future. In the subsequent decades this prediction has been shown to be correct. California was struck with a prolonged drought from 2012 to 2016, and the warming trend continued, with spikes of record breaking summer heat in the early 2020's. Between 2020 and 2022, Whitney Glacier lost over a quarter of its volume. By the end of the 21st Century, it's unlikely that any glaciers will remain in the California Cascades.

Acknowledgments

Parts of the text on this page were taken with minimal editing from sources provided by the USGS and the National Park Service, which are in the public domain. Links to the original text can be found in the reference section on this page.

References

1. Arthur, D. (n.d.). *California's weather hasn't been kind to Mt. Shasta's glaciers. Can they survive?* Record Searchlight. Retrieved May 21, 2024, from https://www.redding.com/story/news/local/2024/04/22/mt-shasta-glaciers-shrinking-as-climate-change-intensifies/73261591007/
2. Garwood, J., Fountain, A., Lindke, K., Hattem, M., & Basagic, H. (2020). 20th Century Retreat and Recent Drought Accelerated Extinction of Mountain Glaciers and Perennial Snowfields in the Trinity Alps, California. *Northwest Science*, *94*, 44. https://doi.org/10.3955/046.094.0104
3. Howat, I. M., Tulaczyk, S., Rhodes, P., Israel, K., & Snyder, M. (2007). A precipitation-dominated, mid-latitude glacier system: Mount Shasta, California. *Climate Dynamics*, *28*(1), 85–98. https://doi.org/10.1007/s00382-006-0178-9
4. U.S. National Park Service. (2022, February 10). *NPS Geodiversity Atlas—Lassen Volcanic National Park, California*. https://www.nps.gov/articles/nps-geodiversity-atlas-lassen-volcanic-national-park-california.htm

This page titled 7.8: Glaciers in the Cascades is shared under a CC BY-NC 4.0 license and was authored, remixed, and/or curated by Emily Wright.

7.9: Chapter Summary

7.1: The Cascadia Subduction Zone and the Cascade Continental Volcanic Arc

- The Cascade Volcanoes are produced by the subduction of the Juan de Fuca plate beneath the North American plate.
- Water released from the subducted Juan de Fuca slab causes flux melting in the mantle beneath the North American plate.
- The Cascades are a continental volcanic arc mountain range
- The Cascade Range extends from Northern California, through Oregon and Washington, and into British Columbia.

7.2: Rock Types of the Cascades

- The California Cascades include a variety of volcanic rocks.
- As magma diapirs rise from the mantle, some have more time to evolve into more felsic compositions, while others are less changed from the ultramafic mantle.
- Rock types include basalt, andesite, dacite and rhyolite, which are all named based on their composition.
- Other rocks such as obsidian, pumice and volcanic tuff are named for their unique textures and appearance.

7.3: The Variety of Volcanoes in the Cascades and the Modoc Plateau

- Subduction zones are often associated with composite volcanoes, but other types of volcanoes are present as well.
- Composite volcanoes and shield volcanoes are regional volcanoes and both are present in the California Cascades.
- Mount Shasta is a classic example of a composite volcano.
- Medicine Lake Volcano is sometimes classed as a shield volcano based on its shape, but its composition is atypical of a shield volcano.
- Cinder Cones and Lava Domes are examples of individual vent volcanoes and can be found throughout the California Cascades, both as part of larger regional volcanoes and on their own.

7.4: Volcanic Hazards

- Lava flows form when molten rock reaches the surface of the earth and flows across the ground or down the slopes of a volcano.
- Pyroclastic flows are a mixture of gas, ash and other debris that flows along the ground surface.
- Lahars are water-based mudflows composed of volcanic material.
- Lahars can form with or without a volcanic eruption.
- Lahars travel in river valleys and can reach distances further from the volcano than is typical for lava flows or pyroclastic flows.
- Ash and tephra are ejected in the air and can rain down far from the volcano. Ash in particular can travel hundreds of kilometers from the eruption.

7.5: Mount Shasta

- Mount Shasta is California's iconic composite volcano.
- The modern edifice has been built over the past 250,000 years, through four cone-building episodes.
- Mount Shasta is ranked fifth in the U.S. Geological Survey's National Volcanic Threat Assessment, meaning that there is a significant potential for a future eruption.
- Lahars and debris flows occur without eruptions, as hot summer temperatures result in rapid melting of glaciers.

7.6: Lassen Volcanic National Park

- The 1915 Lassen Peak eruption is one of the most famous volcanic eruptions in US History.
- Volcanic domes, cinder cones and shield volcanoes can all be found in the park.
- Mount Tehama, or Brokeoff Volcano, is the eroded remnant of a composite volcano.
- Hot springs and geysers are the result of hydrothermal heating from the magma chamber at depth.

7.7: Medicine Lake Volcano

- Medicine Lake Volcano is shaped much like a classic shield volcano, but while most shield volcanoes are made of exclusively basalt, Medicine Lake volcano consists of felsic rocks as well.
- Glass Mountain is an example of an obsidian dome.
- Lava Beds National Monument, known for its caves formed by lava tubes, is located on the flank of Medicine Lake Volcano where there are many basalt lava flows.

7.8: Glaciers in the Cascades

- During the Pleistocene ice ages, glaciers were extensive.
- Volcanic rock is often easily eroded by glaciers, and thus these glaciers significantly shaped the landscape of the Cascades.
- The only glaciers that remain in the California Cascades today are on Mount Shasta, but these too are threatened as the climate continues to warm.

This page titled 7.9: Chapter Summary is shared under a CC BY-NC 4.0 license and was authored, remixed, and/or curated by Emily Wright.

7.10: Detailed Figure Descriptions

Figure 7.1 Province Map

The Cascade Range topography is characterized by several conical peaks in a narrow band between the Klamath Mountains and the Modoc Plateau. The Cascade Range extends into Oregon, but the California province stops at the Oregon border. It is bounded by the Sierra Nevada and Great Valley to the South. The Modoc Plateau is located directly east of the Cascade Range province and is bounded by the Basin and Range to the east and south. The Modoc Plateau province also reaches the Oregon border. It is characterized by relatively flat topography compared to the surrounding provinces.

Figure 7.1.1 Volcanoes and Subduction

This map depicts the relationships between the major volcanoes of the Cascade Mountains and the tectonic setting of the Pacific Northwest where the Pacific plate, Juan de Fuca plate and North American plate meet. The Pacific plate and Juan de Fuca plate are separated by the spreading center (bold red lines) of the Juan de Fuca ridge. The Juan de Fuca plate and the North American plate are separated by the Cascadia subduction zone (thin red line with teeth). The major Cascade Volcanoes (red triangles) are located approximately 200 to 300 km inland from the Cascadia subduction zone. Only the major volcanoes are pictured, including Mount Shasta, Lassen Peak and Medicine Lake Volcano in California. Volcanoes in other states and provinces include: eight volcanoes in Oregon, with Crater Lake and Mount Hood labeled; five volcanoes in Washington, with Mount St. Helens and Mount Rainier labeled; and three volcanoes in British Columbia.

Figure 7.1.2 Ring of Fire

This figure is included here to show the location of the Cascade Range in the broader context of global plate tectonics. Many of Earth's volcanoes occur at suduction zones and many of these subduction zones surround the Pacific Ocean, creating a ring of volcanoes known as the Ring of Fire. The Ring of Fire is produced by the subduction of the westward moving Pacific Plate along its western margin as well as some smaller eastern moving oceanic plates subducting beneath the west coasts of the Americas. The Juan de Fuca Plate is one of these smaller eastward moving plates, and the Cascade volcanoes are shown as part of the Ring of Fire, although neither is labeled. It is worth noting that not all volcanoes are located in the Ring of Fire. Some of the volcanoes outside the Ring of Fire are not formed by subduction, but there is also subduction related volcanism elsewhere in the world. One example is the Sunda Arc of the Indian Ocean, which is very near the Ring of Fire, but is not shown as part of it in this figure. This figure also depicts the arrangement of continents, oceans, tectonic plate boundaries and plate motions for the whole earth with labels for the continents, oceans and other features. Global Plate Tectonics and global geography are not specific learning outcomes of this chapter, but if a review of this material is desired, helpful tactile graphics can be found in the Geological Tactile Image Repository.

Figure 7.1.4 Crystal Settling

A magma chamber is depicted in all three stages of crystal settling and the formation of a zoned magma. The magma chamber may be 100s of meters to several kilometers in diameter. Magma generally moves from depth to the surface, entering the magma chamber from a conduit at the bottom and leaving from a conduit at the top. In the first stage, early formed olivine crystals begin to form near the top of the chamber of mafic magma. In the second stage, these denser crystals settle to the bottom through the non-viscous magma. The loss of olivine to the bottom of the magma chamber makes the upper magma more felsic. In the third stage, the crystals re-melt in the hotter, lower magma, making it more mafic. This leaves a zoned magma chamber with more felsic magma at the top and more mafic magma at the bottom.

Figure 7.1.5 Rising Magma Diapirs

The origin of magma is partial melting of the mantle, near the top of the asthenosphere. Some magma then rises as diapirs through the lithospheric mantle into the crust, forming intrusions. Intrusion at the base of the crust is called “underplating.” Stagnation and crystallization of the diapirs form plutons of intrusive igneous rocks in the crust. Magma differentiation and

assimilation in magma reservoirs also occurs in the crust. Some magma continues rising through the crust causing volcanic eruptions and extrusion of lava. Volcanic gasses mix with the atmosphere in both the troposphere and the stratosphere above.

Query 7.2.1 Rock Identification: Chaos Jumbles

This activity requires interpretation of visual information, including the recognition of color. It may not be appropriate for all learners.

Query 7.3.1 Anatomy of a Volcano

Although this activity can be completed with a screen reader, some learners may achieve a better conceptual framework with addition of the tactile graphic, Magmatic Environments in the Geological Tactile Image Repository.

Figure 7.3.1 Composite Volcano Cut-Away

A composite volcano may erupt in different ways over time, forming features described here. A cut-away of the volcano interior shows magma rising through a conduit and intruding into cracks. At the main summit vent, an eruption column rises into the atmosphere and an eruption cloud has formed downwind in the prevailing wind direction. Ash (tephra) is shown falling from the eruption cloud. Pyroclastic flows appear as clouds that hug the flank of the volcano. One of these is associated with a lava dome part-way up the volcano flank. A landslide (debris avalanche) is also shown on the flank of the volcano. Near this there are gas clouds indicating fumaroles. An active, molten lava flow reaches from the summit to the base of the volcano. A lahar (volcanic mudflow) is shown surging down a river valley.

Figure 7.3.2 Shield Volcano Cut-Away

At the summit of the shield volcano a fire fountain emerges from the main vent. A small amount of tephra forms a cloud above the fire fountain and haze of vog (volcanic smog) has collected downwind in the prevailing wind direction. Multiple lava flows issue from the fire fountain and flow down the volcano's flanks. Active flows are surrounded by cooled lava flow fields. Some lava flows through a lava tube, which is covered by dark, hardened lava except in a few places. In one place a lava flow emerges from a tube at a breakout. Laze plumes emanate from locations where lava flows enter the ocean.

Figure 7.3.3 Cinder Cone Cut-Away

Magma rises through a conduit and intrudes into cracks. One intrusion emerges from the volcano at a vent on the lower flank, above a rafted cinder cone. A red lava flow also originates from this smaller flank vent. From the main summit vent, a plume of tephra and volcanic bombs emerges. The plume shape is slightly extended downwind in the direction of the prevailing winds. Spatter has accumulated around the crater rim and layers of cinders and ash have accumulated to form the edifice of the cone.

Figure 7.3.4 Lava Dome Cut-Away

Magma rises through a conduit and forms a lava dome within an existing crater. The dome is surrounded by rubbly breccia. The dome exhibits flow banding within and a rough, rubbly surface with spines.

Video 7.3.1: How to Classify Volcanoes

Portions of this video require viewers to practice visual identification of images, which may not be appropriate for all learners. Some learners may benefit from the Volcano Types tactile graphic available in the Geological Tactile Image Repository.

Query 7.3.2 Classifying California Cascade Volcanoes

This activity requires interpretation of images and may not be appropriate for all learners. Some learners may benefit from the Volcano Types tactile graphic available in the Geological Tactile Image Repository.

Query 7.4.1 Volcanic Ash Comparison

Areas that received 2 inches to 5 inches of ash during the May 18, 1980 eruption of Mount St. Helens (red) are limited to the area surrounding the volcano and a small patch near Ritzville, in eastern Washington. The area that received between a half inch and 2 inches (orange) is an elongated oval extending to the east of Mount St. Helens as far as the Idaho/Montana border. The area that received trace amounts less than a half inch (yellow) is much larger, extending east from the volcano and fanning outwards. Trace ash traveled as far as Minnesota, New Mexico and presumably into Canada (though Canada is not shown). A small isolated patch of trace ash also exists in Oklahoma.

Mount Shasta is in Northern California. Eureka, CA, which is west of Mount Shasta on the coast, is the closest of the three cities listed in the question to Mount Shasta. Sacramento, CA is further and is nearly directly due south. Boise, ID is the furthest of the three cities and is located to the east and slightly north of Mount Shasta.

Figure 7.5.3 The Cones of Mount Shasta

The four cones of Mount Shasta are Shastina, Misery Cone, Hotlum Cone, and Sargents Ridge Cone. Shastina is the northernmost cone, with Misery Cone due south (and slightly east), roughly at the center of Mount Shasta. Sargents Ridge Cone is southwest of Misery Cone. Hotlum Cone is the summit of Mount Shasta, located to the east of Misery and Sargents Ridge, lying roughly between them as the right corner of a triangle.

Query 7.5.1 Rock Identification: Mount Shasta

This activity requires interpretation of visual information, including the recognition of color. It may not be appropriate for all learners.

Figure 7.5.4 Mount Shasta Hazard Map

The near-volcano hazard zone includes lava and pyroclastic flows, thick tephra, lahars, ballistic ejecta and rock fall. This area surrounds Mount Shasta, which has an elevation of 14,179 feet (4,322 meters), to a distance of around 15 to 25 km (about 10 to 17 miles). The near-volcano zone includes the parts of Interstate 5 as well as Highways 89 and 97. The towns, Weed, Mount Shasta and McCloud are all in this zone.

An additional Lahar (volcanic mudflows) hazard zone includes river valleys outside the near-volcano hazard zone to show that lahars can be potentially far-traveled in valleys draining the volcano. These valleys include the Sacramento River Valley and two tributaries of the McCloud River to the South of Mount Shasta and the Shasta River Valley to the northwest.

A zone of Regional lava flows lies to the east of Mount Shasta, between the near-volcano hazard zone of Mount Shasta and the Medicine Lake Hazard Zone. This zone is susceptible to lava flows from vents dispersed between major volcanoes.

Volcanic Ash is not shown on the map, but is a hazard associated with a potential eruption. Fine fragments of volcanic rock are carried downwind.

Figure 7.6.1 Map of Lassen Volcanic National Park

Lassen Volcanic National Park is approximately 25 km across east to west and 20 km north to south. Highway 89 weaves its way north-south through the west side of the park, while the eastern part of the park has fewer major roads. A road with a separate park entrance goes to Butte Lake near Cinder Cone. There are several lakes in the eastern part of the park, including Snag Lake, Juniper Lake and Horseshoe Lake. Manzanita Lake is in the northwest part of the park. Mount Diller, Brokeoff Mountain and Mount Conard are all remnants of Brokeoff Volcano, which is located in the southwest corner of the park. Lassen Peak lies to the North of Brokeoff Volcano and Chaos Crags is further north. Red Cinder is located at the far eastern edge of the park. Most of the hydrothermal features are in the southern part of the park, including Bumpass Hell, which is related to Brokeoff Volcano. Growler Hot Springs and Morgan Hot Springs are south of the park boundary.

Figure 7.6.2 Lassen Volcano Map

Volcanic features labeled as lava domes include: Chaos Crags, Lassen Peak, Crescent Center, and Reading Peak, all in the western part of the park. Broke-off Volcano, a composite volcano, is in the southwest. The cinder cones are Hat Mountain, Crater Butte, Red Cinder Cone, Fairfield Peak, and Cinder Cone. These are all in the central or eastern part of the park. Two shield volcanoes, Sifford Mountain and Mount Harkness, are near the southern park boundary and one, Prospect Peak is near the northern park boundary.

Figure 7.6.4 Projected Profile of Brokeoff Volcano

This landscape shows the jagged remains of what was once the Brokeoff Composite Volcano, which is indicated by a dotted line tracing the outline of a volcano that appears above the landscape elements listed here. To the left we see Brokeoff Mountain; roughly in the center of where the volcano would have been, below its peak, is Lassen Peak, and Bumpass Mountain appears at the left.

Video 7.6.1 Mount Lassen 1915

The silent begins with a placard reading "Mt. Lassen Volcano: America's Greatest Natural Scenic Wonder. Photographed and copyrighted by J. J. Hammer, Red Bluff, California."

Scene 1 placard, "Mt. Lassen in Repose." The camera looks across a calm lake to a stand of evergreen trees, with a snow-clad mountain in the left of the frame. It pans left and then cuts to a view of the same mountain with white clouds of smoke billowing from the its peak, apparently from a location along the right of the peak.

Scene 2 placard, "The crater." The camera seems to have been placed on the ground or perhaps on a low bolder. We see a ridge of jagged, ash-covered ground and rocks with smoke billowing in the near distance.

Scene 3 placard, "Mt. Lassen in action." We are back to the same view of the mountain in Scene 1, but this time the smoke clouds have developed into explosive bursts of black smoke shooting up, with white/gray smoke or ash shooting to the right. As we watch the black smoke shoots upward still higher as the lighter smoke/ash cloud on the right grows larger. The camera pans up to capture the roiling black smoke plume as it grows and expands. We can clearly see the plume being ejected upward from the peak of the volcano.

Scene 4 placard, "Watch the smoke cloud form 'Vulcans face'." We watch as the black smoke is ejected forcefully up from the peak and the smoke and ash clouds expands to the right of the volcano. The black smoke rises up and to the right; the white/gray smoke or ash cloud rolls down the right flank of the volcano. By now the volcano is dwarfed by the huge clouds of smoke and ash that roil from it.

Figure 7.6.7 Generalized Geologic Map of Lassen Peak

Lassen Peak lies in the southeast portion of the irregularly shaped Lassen Peak Lava Dome. The May 1915 eruptions from this dome destroyed a large region on the northeast flank of the volcano, now called the Devastated Area. This area extends as far as Emigrant Pass to the east and Raker Peak to the north. Deposits from the May 19-20 eruptions can be found near the summit of Lassen Peak, near Emigrant Pass to the northeast of Lassen Peak, and on the northeast flank of the mountain. Deposits from the pyroclastic flow and related lahars of May 22, 1915 are located mainly in the Lost Creek and Hat Creek drainages far to the north of Lassen Peak, and beyond the national park boundary. These deposits continue northward, reaching multiple tens of kilometers from the volcano.

Figure 7.6.9 Lassen Hydrothermal System

Precipitation falls mostly to the north of Lassen Peak, where it enters the ground as groundwater recharge. This meteoric water percolates to depths of about 5 kilometers (or 3 miles) where it is heated by the magma chamber. The actual magma is deeper, at depths of more than 8 kilometers (or 5 miles), but the solid rock surrounding the magma is also hot. It is more than 350 degrees Celsius (or 660 degrees Fahrenheit). This heat also causes thermal cracking, which can induce earthquakes. When the water is heated to 235 to 270 degrees Celsius (or 455 to 520 degrees Fahrenheit), it rises convectively first through the liquid

dominated zone. When the water moves up into low enough pressure, some of the water boils, creating a vapor-dominated zone. This vapor rises and emerges at the surface as fumeroles in places like Bumpass Hell, located between Bumpass Mountain and Mount Conard. Hot water also produces acid sulfate hot springs in this area. Some of the gas depleted thermal water that did not boil flows southward underground as an outflow plume, emerging at the Growler and Morgan Hot Springs.

Figure 7.7.2 Shaded Relief Map of Medicine Lake Volcano

Medicine Lake Volcano is northeast of Mount Shasta, at the upper end of a transverse ast-northeast trending volcanic highland. The ovoid caldera at its center is longer along its east-west axis and is surrounded by eruptive vents. Lava flows extend from the volcano in largely a north-south orientation, abutting Klamath Graben at the north and the Walker Lane at the south. There are few regional faults within the lava flow area, but many in the surrounding regions. These faults have a general southeast-northwest strike, accommodating east-west extension.

Figure 7.8.2 Glaciers of Mount Shasta

This map of Mount Shasta shows the locations of its seven glaciers. Radiating from the summit and following vertical depressions in the side of the mountain we see long, narrow, Whitney Glacier extending along a southeast to northwest path. To the north of Whitney, Bolam Glacier is shorter and wider, extending along a south-southeast to north-northwest path. To the east and almost abutting Bolam is Hotlum Glacier, which is shaped like an arrowhead with its apex near the peak of Mount Shasta and its widest portions extending north and northeast.To the south of Hotlum we see Wintun Glacier, which extends from the peak of Mount Shasta along an eastern route that encompasses Shasta National Forest. Three smaller glaciers are located in the southeast flank of Mount Shasta: Konwakiton Glacier is closest to the peak, with Mud Creek Glacier to the south and slightly east. Directly to the east of Konwakiton is Watkins Glacier.

This page titled 7.10: Detailed Figure Descriptions is shared under a CC BY-NC 4.0 license and was authored, remixed, and/or curated by Emily Wright.

8: BASIN AND RANGE

Introduction to the Basin and Range

The Basin and Range Province is situated in easternmost California (Figure 8.1) and is probably one of the most important natural geologic laboratories in the world. Because of its lack of vegetation and the long span of geologic time that is represented in this region, scientists from all over the world have used this area to formulate and test their geologic hypotheses. Important studies emerging from this region have produced tectonic reconstructions of the western U.S., proposals of an ancient “snowball earth,” and a new understanding of the ways Earth’s crust behaves during mountain building! This region is also the home of Death Valley National Park and the focal point of water rights and land use controversies that have been evolving for centuries.

The geologic story of the Basin and Range is a long one, going back to the Middle Proterozoic Eon. Its most recent history, however, is one of continental rifting, which has produced the distinctive “basin and range” structures for which this region is named, along with volcanism caused by crustal thinning. Widespread normal faulting caused by this rifting has exposed old rocks (including some of the oldest found in California) in uplifted footwall blocks, making it possible to study the earlier history of this region. Geologic activity also continues today: ongoing seismic and magmatic activity present not only serious hazards in the region, but also important geothermal resources and create a dynamic landscape with a lot to interest geologists.

There is plenty of geology to discuss in this region and it would be impossible to complete this study in a one-semester course. This chapter will, instead, aim to provide an introduction to a few key aspects of the region and lay the groundwork for future study and examination as your interests guide you. In particular, our focus will be on the concept of continental rifting, illustrated with examples from the Death Valley and Owens Valley regions, including some of the hazards and benefits resulting from this rift environment. The chapter will conclude with a discussion of some of the bedrock geology that was exposed by this rifting and the insights it provides about the geologic past.



Figure 8.1: Location of the Basin and Range Province of California. The Basin and Range Province of California is in easternmost California. This region is bounded by the Nevada border on the east, the Garlock fault on the south and the Sierra Nevada Mountains on the west. "The Basin and Range Province of California" by Emily Wright, is licensed under CC-BY-NC / a derivative from the Geology of California. Access a detailed description.

Learning Objectives

By the end of this chapter, you should be able to:

- Locate the Basin and Range Province on a map of California.

- Describe the primary geomorphic features in the Basin and Range Province.
- Recall the major geologic units in this province as presented on a simplified map of California.
- Explain the origin of the “basin and range” structures in this geomorphic province.
- Outline the evidence for ongoing seismic hazard in this geomorphic province.
- Summarize the geologic evidence for continental rifting in the Basin and Range Province.
- Explain the origin of rift-related volcanic features found in this region and their associated hazards and benefits.
- Summarize the evidence for Late Proterozoic rifting and glaciation in this region.

8.1: Regional Extent and Overview of the Basin and Range
8.2: Rifting in the Basin and Range
8.3: Rift-Related Faulting in Eastern California
8.4: Sedimentary Products of Rifting in the Basin and Range
8.5: Rift-Related Volcanism in Eastern California
8.6: The Oldest Rocks in the Basin and Range
8.7: Chapter Summary
8.8: Detailed Figure Descriptions

This page titled 8: Basin and Range is shared under a CC BY-NC 4.0 license and was authored, remixed, and/or curated by Martha House.

8.1: Regional Extent and Overview of the Basin and Range

The Basin and Range of the Western United States

The Basin and Range Province of California is the westernmost expression of the much larger Basin and Range Province of the southwest U.S. and western Mexico (Figure 8.1.1). This region extends southward from the Columbia Plateau into central and western Mexico, and westward from the Wasatch Range of Utah and the Colorado Plateau, through eastern California. Throughout this broad continental rift zone, some 400 north-trending normal-fault bounded ranges are separated by adjacent low-lying linear basins (Figure 8.1.2).



Figure 8.1.1: Map of the Basin and Range Province including boundaries and landmarks. "Basin and Range Province Boundaries and Landmarks" by Kathleen Smith is licensed under CC BY 3.0. Access a detailed description.



Figure 8.1.2: The Basin and Range landscape of the Basin and Range Province in Central Nevada viewed from space is a series of northwest trending mountain ranges separated by narrow basins in an arid desert region. "Basin and Range Province" by NASA is in the public domain.

Geomorphology and Climate

The Basin and Range Province of California occupies the extreme eastern limits of the state with its largest expanse found in southern California to the north of the Garlock fault and bounded on the west by the Sierra Nevada Range (Figure 8.1.1). Across this region of the state, mountain ranges with elevations of more than 4,000 meters (13,000 ft.) are juxtaposed against low-elevation valleys roughly 1,000 m (3,000 ft.) above sea level. Notably, the most extreme range in relief is entirely in California. Here, the highest point in the lower 48 states, Mt. Whitney at 4,341 m (14,242 ft.), is only 85 km (53 miles) west of Death Valley's Badwater Basin, which is situated 86 m (282 ft.) below sea level (Figure 8.1.3 and Figure 8.1.4)!



Figure 8.1.3: The high peaks of the Sierra Nevada Mountains, including Mt. Whitney, the highest peak in the lower 48 US states, loom above and to the west of the rounded granite outcrops of the lower-elevation Alabama Hills near Lone Pine, CA. Mt. Whitney has an elevation of 4,341 m above sea level. Mt. Whitney by Martha House is licensed under CC BY-NC.

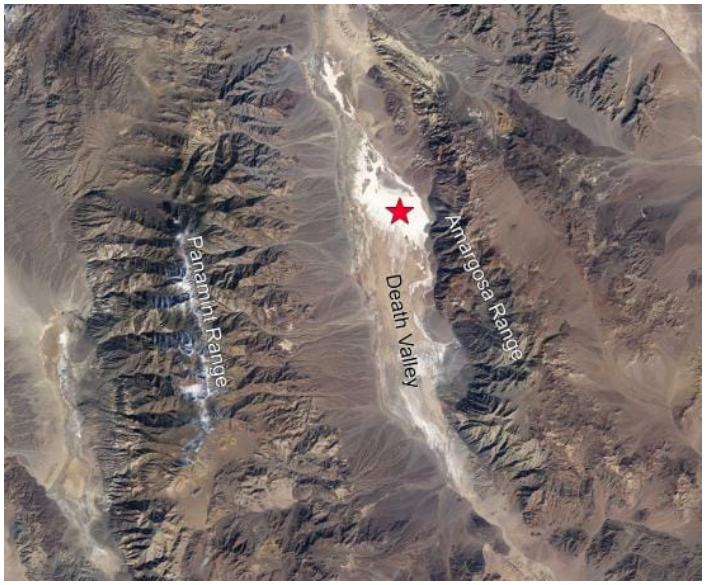


Figure 8.1.4: Satellite image of Death Valley in the Basin and Range province, eastern California. Death Valley is bounded by the Panamint Range to the west and the Amargosa Range to the East. At the center of valley lies Badwater Basin (marked with a red star). At 86 meters (282 feet) below sea level, this basin is at the lowest elevation in North America. Photo by Robert Simmons, based on Landsat data from the USGS Global Visualization Viewer (NASA Earth Observatory, used following NASA's image use policy). This work by Paleontological Research Institution for the Earth@Home project is licensed under CC BY-NC-SA 4.0.



Figure 8.1.5: A sign posted at a viewpoint in Death Valley National Park tells the visitor that Badwater Basin is 282 feet (or 86 meters) below sea level. The extent of the salt flat that occupies the basin extends in the background. "Badwater Elevation Sign" by Ivan, is licensed under CC BY-SA 3.0.

This region is a desert climate due to its location in the rain shadow of the Sierra Nevada Range to the west (Figure 8.1.6). At these latitudes, the dominant weather systems move from west to east. Orographic uplift occurs as eastward traveling winds are forced over the high peaks of the Sierra Nevada Range. As they rise in altitude and cool at elevation, their ability to hold water diminishes, and most of their moisture falls as rain on the windward (western) side of the range, leaving little for the region to the east (Figure 8.1.7). As a result, the landscape of eastern California is dry and landforms such as alluvial fans, dune fields), and dry lake beds occur throughout the region.



Figure 8.1.6: The dry Owens Valley basin is in the rain shadow of the Sierra Nevada Range to the west. The valley sits between the high snow covered peaks of the Sierra Nevada range to the west and the Inyo Range-White Mountains to the east. Separated from the Sierras by a fault escarpment, the valley contains ephemeral lakes that fill during rainy season. "Sierra Escarpment CA" by G. Thomas is in the public domain.

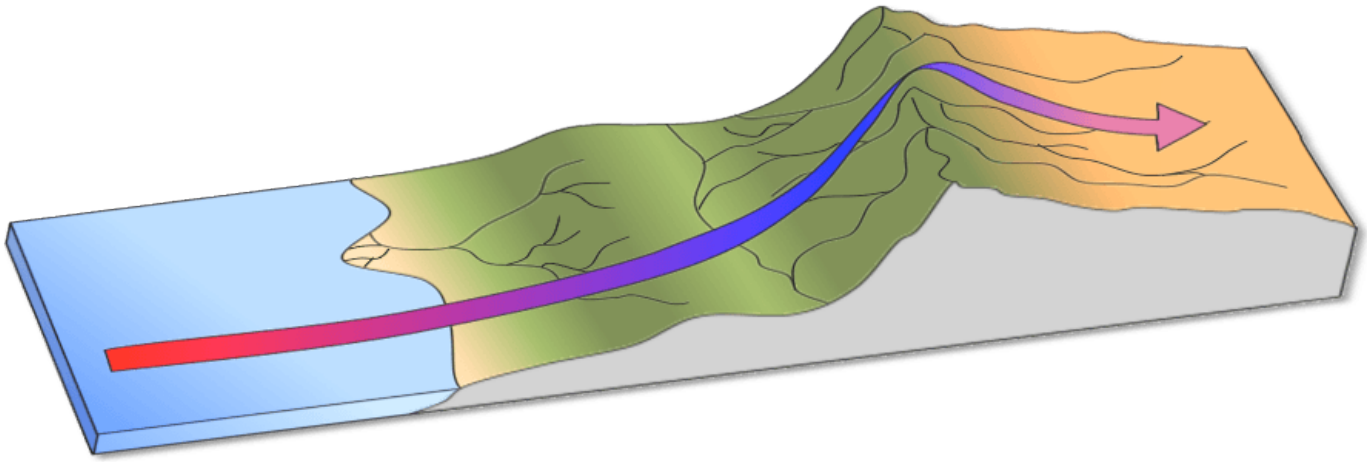


Figure 8.1.7: As an air mass reaches the continent after flowing from an ocean (or other large body of water), the air mass is forced into the upper atmosphere by topographic barriers such as mountains in a process known as orographic lift. The side of the topographic barrier that forces the air mass upward is vegetated due to precipitation that is dropped by the rising air mass. The side of the barrier beyond the topographic high point is the rain shadow region with little to no precipitation and a resulting lack of vegetation. "Rain shadow effect caused by orographic lift" by Thebiologyprimer, is licensed under CC0.

Query 8.1.1

This interactive element is not available in this format. Visit the link or scan the QR code to access it online.

View this Interactive Content online

Bedrock Geology Overview

Due to the lack of moisture in this region, there is sparse vegetation and almost total exposure of bedrock geology, which has contributed to the popularity of this region among geologists. Geology students from all over California and elsewhere travel to the Basin and Range to hone their skills.

California's Basin and Range Province bedrock geology encompasses a broad range of geologic time and environments. The simplified geological relationships in this region can be described as North-South trending exposures of uplifted basement rocks in the footwalls of North-South trending normal faults separated by elongate, narrow basins of non-marine sedimentary rocks (Figure 8.1.8). The rocks mapped in the elongate ranges include Precambrian rocks, Paleozoic sedimentary and metamorphic rocks, and Mesozoic igneous rocks. The ranges alternate with elongate basins filled with unlithified or weakly lithified units that include alluvial fans and seasonal (dry) lake beds. These basin sediments are Quaternary and Neogene non-marine units and surficial deposits which are found in the hanging-walls of the normal faults. Throughout this province, outcrops of younger (Late Cenozoic) volcanic rocks (cones, domes, flows and tuff) overlap and are cut by the normal faults.

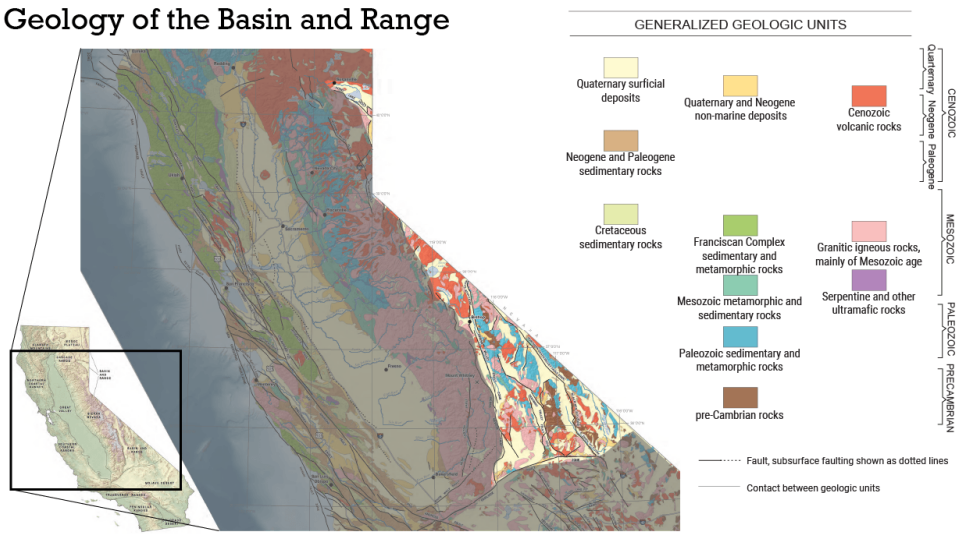


Figure 8.1.8: Excerpt from the Geologic Map of California with the Basin and Range Province highlighted. “Excerpt from the Geologic Map of California” by Emily Wright, is licensed under CC-BY-NC / a derivative from the Geology of California.

Box 8.1.1 Death Valley National Park

Death Valley National Park straddles the California–Nevada border, east of the Sierra Nevada. The park is one of extremes: it is not only the largest national park in the contiguous United States, but it’s also the hottest, driest, and lowest of all the national parks in the United States. The oldest part of the park started out as a National Monument that was established in 1933 in response to growing tourism interest in the region. UNESCO included Death Valley as the principal feature of its Mojave and Colorado Deserts Biosphere Reserve in 1984. In 1994, the region was expanded and designated a national park.

The region has been inhabited by humans since around 10,000 years ago, and the modern indigenous community of the Timbisha Shoshone, who call themselves Nümü Tümpisattsi ("Death Valley People"; literally: "People from the place of red ochre face paint), has been in the region for around 1,000 years. In 1849, European gold seekers moved through the area, spurred by the gold rush. Not only were these folks the source for the name “Death Valley," but they were also the first in a steady stream of ranchers, miners, and homesteaders who migrated to Death Valley, gradually taking control of the region’s water resources and establishing gold, silver and borax mines.

Despite the fact that tribal members continued to live within monument boundaries throughout the early 20th century, they were seriously limited in their activities and faced ongoing challenges to their right to be there. During the 1950s National Park Service officials began efforts to evict the Shoshones from the region and prohibited them from using sacred places in the park to conduct traditional sacred ceremonies as well. It wasn’t until 1982 that the Timbisha Shoshone Tribe was recognized by the US government and a small reservation of land was established. After much tribal effort, federal politics, and mutual compromise, the Timbisha Shoshone Homeland Act of 2000 finally returned 7,500 acres (30 km^2) of ancestral homelands to the Timbisha Shoshone tribe.

References

1. Burchfiel, B. C., Cowan, D. S., & Davis, G. A. (1992). Tectonic overview of the Cordilleran orogen in the western United States. In The Cordilleran Orogen: Conterminous U.S. (Vol. G-3, pp. 407-479). Geological Society of America.
2. Burchfiel, B. C., & Davis, G. A. (1981). Mojave desert and environs. In The geotectonic development of California (Vol. 1, pp. 218-252). Prentice-Hall, Inc.
3. Burnham, A. (n.d.). Timbisha. Wikipedia. Retrieved July 17, 2023, from https://en.Wikipedia.org/wiki/Timbisha
4. Death Valley National Park. (n.d.). Wikipedia. Retrieved July 17, 2023, from https://en.Wikipedia.org/wiki/Death_Valley_National_Park
5. Hall, C. A. (Ed.). (1991). Natural History of the White-Inyo Range, Eastern California. University of California Press.
6. Johnson, C., Affolter, M. D., Inkenbrandt, P., & Mosher, C. (2017). An Introduction to Geology. https://slcc.pressbooks.pub/

introgeology/
7. Lynch, D. (2010). Geology of California. San Andreas Fault. Retrieved July 1, 2023, from http://www.sanandreasfault.org/CaGeo.html
8. Nelson, C. A. (1981). Basin and Range Province. In The geotectonic development of California (Vol. 1, pp. 203-216). Prentice-Hall, Inc.
9. Our Dynamic Desert. (2009, December 18). Our Dynamic Desert. Retrieved June 28, 2023, from https://pubs.usgs.gov/of/2004/1007/geologic.html
10. Owens Valley Geology. (n.d.). Owens Valley Committee. Retrieved June 28, 2023, from https://owensvalley.org/geology/
11. Stock, G. M., & Glazner, A. F. (2010). Geology Underfoot in Yosemite National Park. Mountain Press Pub.
12. National Park Service. (n.d.). National Park Service. Retrieved July 17, 2023, from https://www.nps.gov/museum/exhibits/death_valley/timbisha.html

This page titled 8.1: Regional Extent and Overview of the Basin and Range is shared under a CC BY-NC 4.0 license and was authored, remixed, and/or curated by Martha House.

8.2: Rifting in the Basin and Range

Continental Rifting and Associated Features

Continental rifting (in fact all rifting) occurs when a tectonic plate is subjected to tensional stress, leading to extension and thinning. This process is an important part of the Wilson Cycle, a concept that describes the origin and breakup of supercontinents, such as Pangea and Rodinia, throughout geologic time. This cycle is directly correlated to the development of plate boundaries (see Plate Tectonics).

Figure 8.2.1 is a simplified summary of the stages involved in the Wilson Cycle. In this image, the first stage of the cycle is continental break up (part A of Figure 8.2.1, which begins with a series of interconnected fault zones and fracture zones that link regions impacted by mantle plumes. As the cycle progresses (in part B), rifting has progressed to the point that two regions on either side of the rift are now separated by a narrow sea. Fracture zones called "failed rifts" extend away from the sea, and volcanic centers related to the original plume locations persist. With progressive changes in plate motion, extension and tension are converted to convergence and compression (part C). This phase results in the buildup of fold-belt mountains in the region that was once the narrow sea. With continued geologic change, the cycle of rifting begins again (part D), resulting in re-separation.

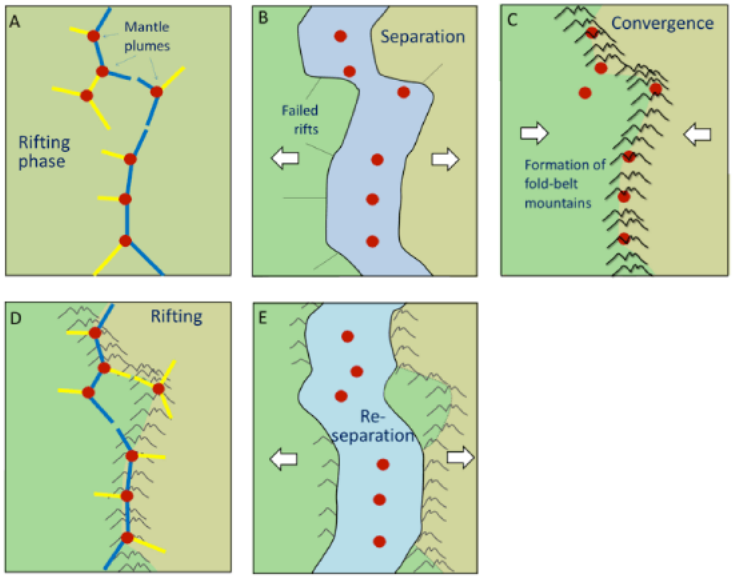


Figure 8.2.1: A summary of the the Wilson cycle of rifting and collision. (A) Continental rifting initiates. As rifting progressed and sea floor spreading initiated, the passive continental margin developed (B). Sediments of the Paleozoic were deposited in this setting. (C) Continents re-converge some time later, forming a fold-belt mountain chain. (D) Separation repeats. "Wilson Cycle" by Steven Earle, is licensed under CC BY.

When the continental crust experiences rifting, distinctive geological relationships result (Figure 8.2.2). As the crust is stretched, normal faults thin and extend the crust. In the upper levels of the crust, this thinning produces sub-parallel belts of uplifted ranges and down-dropped rift valleys, or basins. Lava flows and other volcanic materials are deposited in these basins, along with river and lake sediments as they fill with sedimentary rocks and volcanic layers. Earthquakes occur within the seismic zones of the range bounding faults. At the same time, the lower crust stretches and thins in a ductile manner (see Earthquake Mechanics). As rifting progresses, rocks in the footwalls of normal faults are uplifted and rotated, exposing older geologic features at the surface fault escarpment that might otherwise not be seen. As basins in the hanging walls of normal faults drop down, sediment eroded from the uplifted footwalls fills them, preserving a record of uplift and erosion, as well as extension. The thinning allows mantle rocks to move closer to the surface, resulting in decompression melting and volcanism throughout the region as magma reaching the surface erupts from volcanoes and fissures along the normal faults.

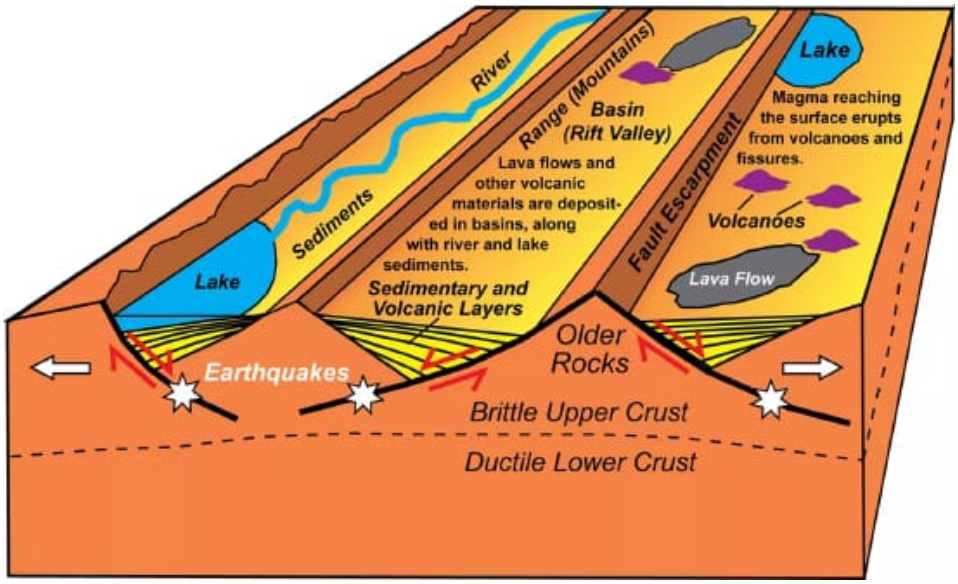


Figure 8.2.2: Major features of continental rift zones. Continental rift zones reveal long mountain ranges separated by deep valleys (basins) that are partially filled with sedimentary and volcanic material. Earthquakes (white stars) occur when the fault lines separating the basins and ranges suddenly let go. "Continental Rift Block Diagram" by NPS is in the public domain. Access a detailed description.

There is definitely a lot to interest geologists, ranging from outcrops of older rocks in uplifted footwall ranges, to sedimentary units in the down-dropped basins, as well as rift-controlled volcanism and even earthquakes!

Query 8.2.1

This interactive element is not available in this format. Visit the link or scan the QR code to access it online.

View this Interactive Content online

Rifting in the Basin and Range

The continental rifting that is occurring in the Basin and Range Province is somewhat different from the style of rifting discussed in the context of the Wilson Cycle or the development of divergent plate boundaries (see Plate Tectonics). Rather than developing a single valley, rifting in the Basin and Range is widely distributed over many kilometers and has not yet organized into a single oceanic spreading center.

In the Basin and Range region, it is likely that interactions between two tectonic plates led to the formation of this broad rift zone. Geological work has shown that during the Late Cenozoic, changing plate motions led to the development of a transform boundary to the west of this region which eventually evolved into our modern San Andreas Fault System (see A Brief Geologic History of California). As this happened, much of western North America began to feel the effects of this changing motion as tension, resulting in widespread faulting and crustal thinning which produced the distinctive topographic basins and ranges of this region (Figure 8.2.2). Although the age of the onset of extension is variable across the entire Basin and Range, within California, it initiated at roughly 17 Ma, with most activity occurring between 11 - 7 Ma.

Video 8.2.1: Tectonic Evolution of the Western United States

The video animation that follows presents a model for how this region has extended as the plate boundary to the west developed. There is no narration for this video, but a detailed text description is available.

This interactive element is not available in this format. Visit the link or scan the QR code to access it online.

View this YouTube Video online

Based on studies of faults across the entire Basin and Range Province (not just that in California), east-west extension is estimated to have roughly doubled the distance across this region at the latitude of Las Vegas, NV. Geodetic data and geologic studies of recent earthquakes indicate that extension continues today.

Video 8.2.2: Basin and Range-Measuring Extension

This video illustrates the way GPS has been used to measure ongoing extension in this region. The video contains no audio; a cartoon animation of two GPS stations move apart as heat rises from the mantle toward the surface. At the same time as it is pushed upward by the heat below it, the tectonic plate stretches and thins and the crust fractures as normal faults form in response to the tension.

This interactive element is not available in this format. Visit the link or scan the QR code to access it online.

View this YouTube Video online

References

1. Affolter, M., Bentley, C., Jaye, S., Kohrs, R., Layou, K., & Ricketts, B. (2020). Historical Geology. https://opengeology.org/historicalgeology/
2. Burchfiel, B. C., Cowan, D. S., & Davis, G. A. (1992). Tectonic overview of the Cordilleran orogen in the western United States. In The Cordilleran Orogen: Conterminous U.S. (Vol. G-3, pp. 407-479). Geological Society of America.
3. Earle, S. (2019). Physical Geology. BCCampus Open Education. https://opentextbc.ca/physicalgeology2ed/
4. Johnson, C., Affolter, M. D., Inkenbrandt, P., & Mosher, C. (2017). An Introduction to Geology. Salt Lake Community College. https://slcc.pressbooks.pub/introgeology/
5. Nelson, C. A. (1981). Basin and Range Province. In The geotectonic development of California (Vol. 1, pp. 203-216). Prentice-Hall, Inc.
6. Our Dynamic Desert. (2009, December 18). Our Dynamic Desert. Retrieved June 28, 2023, from https://pubs.usgs.gov/of/2004/1007/geologic.html

This page titled 8.2: Rifting in the Basin and Range is shared under a CC BY-NC 4.0 license and was authored, remixed, and/or curated by Martha House.

8.3: Rift-Related Faulting in Eastern California

Normal Fault Structures in the Basin and Range

Throughout the Basin and Range, extension related to rifting happens via normal faults of two styles: horst-and-grabens and half-grabens/tilt block faults. These features form in response to tension and are usually oriented perpendicular to the tension direction.

In horst-graben structures (Figure 8.3.1), two normal faults face one another such that the region between them is the hanging wall for each. As crustal tension begins, pulling the faults away from each other, tension cracks start to propagate downward into the brittle part of the crust, as illustrated in the first part of the figure. With continued tension, these cracks evolve into normal faults that dip steeply toward one another, sharing the same hanging walls (the graben). As extension progresses, shown in the second part of the figure, the grabens between them drop downward to create symmetric valleys bordered by fault scarps. The footwalls of each (the horsts) move upward, creating topographically higher ranges. As shown in the third part of the figure, graben valleys often contain broad, shallow closed basin lakes as run-off from the uplifted ranges is trapped in them. Slope deposits and alluvial fans cover fault traces and begin to fill in the basin along the fault scarps; heavy erosion along the fault also occurrs. As extension progresses, these zones of horst-graben structures are repeated, forming a broad region of down dropped valleys separated by uplifted ranges. As they age, fault scarps are progressively covered by erosional debris shed from the uplifted ranges.

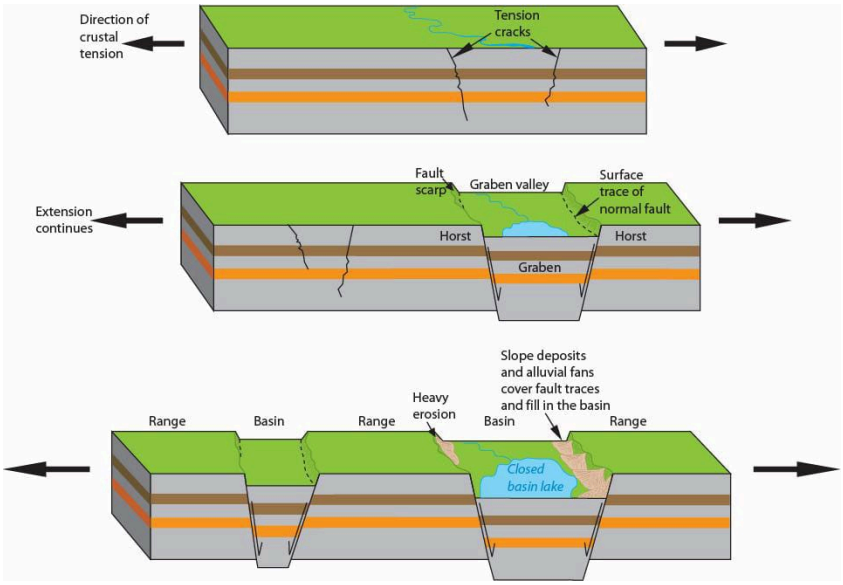


Figure 8.3.1: Basin and Range topography formed by repeated horsts and grabens. Such repetition and relief is caused by ongoing extension and crustal thinning. "Basin and Range topography" by NPS/Trista L. Thornberry-Ehrlich is in the public domain.

Half-grabens are a one-sided version of a horst and graben where a series of parallel normal faults develop, as shown in Figure 8.3.2, Diagrams A and B. Diagram A shows the unextended faults, while B shows the developing normal faults with extensional basins. As opposing forces pull the faults apart and extension progresses, these faults thin the crust and the hanging-walls drop downward to form asymmetric valleys separated from asymmetric ranges that are tilted by a normal fault on one side, creating an asymmetrical valley-mountain arrangement. Diagram C shows the upper crust fault block rotation that occurs as the process continueds. When these basins are down dropped, they fill with sediments that are shed off of the adjacent uplifted ranges.

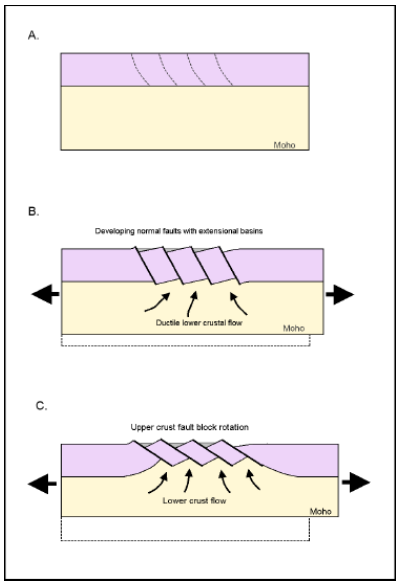


Figure 8.3.2: The evolution of tilted fault blocks in response to crustal thinning, as discussed in the text. Here, normal faults tilt in the same direction and rotate hanging walls as the crust thins (Diagram A). Some researchers propose that the ductal lower crust flows upward to support these newly thinned basins, as in Diagrams B and C. "Tilted Blocks" by Aturn4000, is licensed under CC BY-SA 3.0.

In either case, the normal faults that develop are brittle and generally tilted at a high angle relative to the surface of the Earth, dipping at approximately 30°-60°. There is some discussion about what happens to them at depth, however, as pressures and temperatures of the middle and lower crust are more likely to produce ductile deformation, rather than brittle deformation. For this reason, many people consider that normal faults are “rooted” in ductile shear zones, and some have proposed that the lower crust flows upward in response to the thinning of the upper crust.

Video 8.3.1: Basin and Range Structures

This video explains the way the features in the Basin and Range are related to rifting processes. The video includes useful narrated animations that further illustrate the origin of the “basin and range” structures in this geomorphic province.

This interactive element is not available in this format. Visit the link or scan the QR code to access it online.

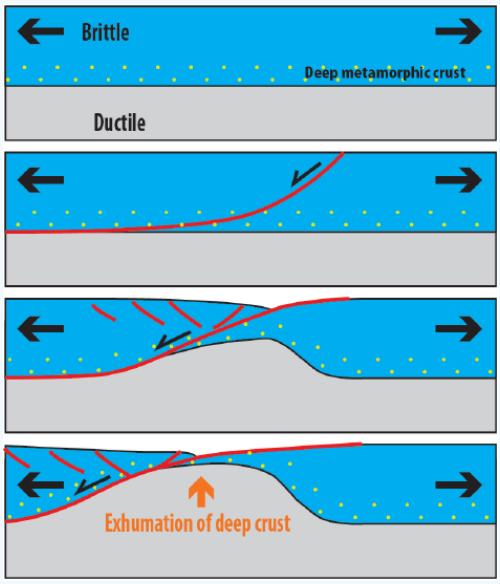
View this YouTube Video online

Box 8.3.1: Metamorphic Core Complexes

Rocks in the uplifted footwalls of Basin and Range normal faults give geologists a way to study geologic processes that occur at deeper levels in the crust and quantify the temperatures and pressures under which these processes occur. Exposures of rocks that were deformed and metamorphosed at deeper crustal levels provided an opportunity to advance our understanding of normal faulting! The two important and related features that were recognized in this region are the detachment fault and the metamorphic core complex.

In the Death Valley region, geologists first noted that regions of uplifted metamorphic rocks seemed to have gently sloped, somewhat rounded surfaces; these features were called “turtlebacks” after their sloping, somewhat rounded appearances. As geologists working throughout the West began to compile their findings, they realized that these metamorphic “cores” were often found in the footwalls of gently dipping mylonitic fault zones; the term “metamorphic core complex” came into use to describe these features. Inset Figure 8.3.2 illustrates the stages in the formation of these structures using simple diagrams. The development of a metamorphic core complex starts with crustal thinning that stretches the deep metamorphic

crust and creates faults in the brittle upper crust. The ductile lower crust then balloons toward the surface along a developing detachment surface. As the detachment surface evolves and extension progresses, upward movement of the ductile lower crust progresses, causing an exhumation of deep crust and bringing deep crustal rocks closer to the surface.



Inset Box Figure 8.3.2: Stages in the formation of a metamorphic core complex. "Core Complex" by ManuRoquette, is licensed under CC BY-SA 4.0

Mylonite is a sheared metamorphic rock. It forms by intense ductile deformation of rocks in and along fault zones deep in the crust, and is commonly associated with metamorphic core complexes. The features of mylonite are used to infer the sense of motion on detachments and can also indicate the temperature and pressure conditions of movement (Inset Figure 8.3.2).



Inset Figure 8.3.3: A sample of myolite from Virginia, USA. This is a cross-section view of the layered mylonitic foliation on a wet, cut surface. This rock is oriented such that the sense of shear is parallel to the top and bottom of the image. The top of the sample is being sheared to the right and the bottom is sheared toward the left; alternating bands of light mineral material contain asymmetrically rotated clasts that stand out amid the darker intervening layers of mica. "Mylonite (Rockbridge County, Virginia, USA" by James St. John, is licensed under CC BY 2.0.

The gently dipping mylonitic shear zones (called *detachment faults* or *low-angle normal faults*) were very controversial when they were first described. Most normal faulting occurs at high angles, more than 30° from horizontal, typically around 60°. Detachment faults, however, are shallowly dipping structures. Scientists believed they either started as faults with steep dips and rotated to lower angles with extension, or they formed at initially low angles, which pushed the known limits of rock mechanics at the time. Geologists simply couldn't understand how these low-angle structures could be active! Over the years, however, geologists realized that there are many of these structures throughout the West, and they are also found in other mountain ranges around the world (such as the Himalayan Mountains), as well as on the ocean floor. Notable examples of metamorphic core complexes with detachment faults are found in the Funeral Mountains and the Black Mountains near Death Valley, and also in regions of the Mojave Province that are impacted by Basin and Range extension (the Whipple Mountains).

Pull-Apart Basins and Oblique Normal Faults

Although east-west tension is the dominant tectonic stress in the Basin and Range region, it is not the only stress: the San Andreas transform boundary to the west generates shear stress as well. The combination of these forces creates a type of basin called a "pull-apart basin"; Death Valley is a perfect example in which half-graben structures can be observed. Death Valley is situated between the Panamint Mountains to the west and the Black Mountains to the east; the Amargosa Range is to the north-northeast. Panamint Valley is to the west of the Panamint Range.

As shown in Figure 8.3.3, a right lateral strike-slip fault to the south of Death Valley transitions to a normal fault that separates the Panamint Range from Panamint Valley on the west, with the Panamint Range in the footwall. To the northeast, a right lateral strike slip fault transitions to a normal fault to the south, separating Death Valley from the Black Mountains to the west. Together the system of normal faults and right lateral strike slip faults create an overall tension that is oriented northwest-southeast, and act together to pull the ranges apart from one another, thereby downdropping the Death Valley and Panamint Valley grabens and uplifting the adjacent Panamint and Black Ranges as east-ward tilted range blocks.

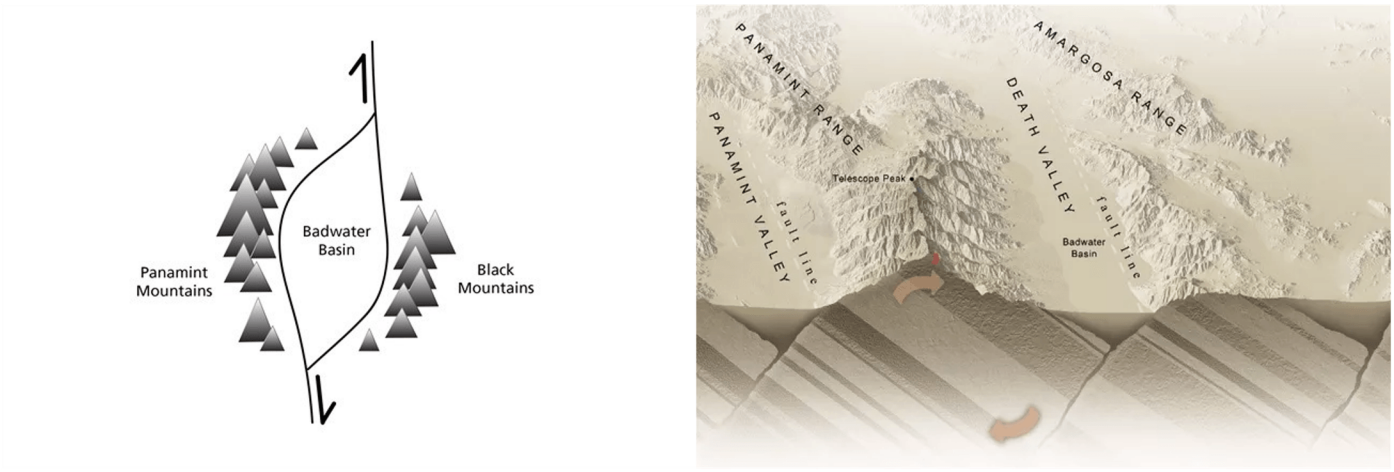


Figure 8.3.3: Death Valley's pull-apart basin formed between the Panamint Mountains and the Black Mountains. The ranges are half-graben tilt blocks as described in the text. "Death Valley's pull-apart basin" by NPS/Christian Poutre & J. Jurado, is in the public domain.

In other areas of the Basin and Range Province, normal faults are actually oblique faults (Figure 8.3.4), which move partly along dip directions (normal motion) and partly along strike directions (strike-slip motion). This combination is formed when faults are not completely perpendicular to the tension or shearing direction.

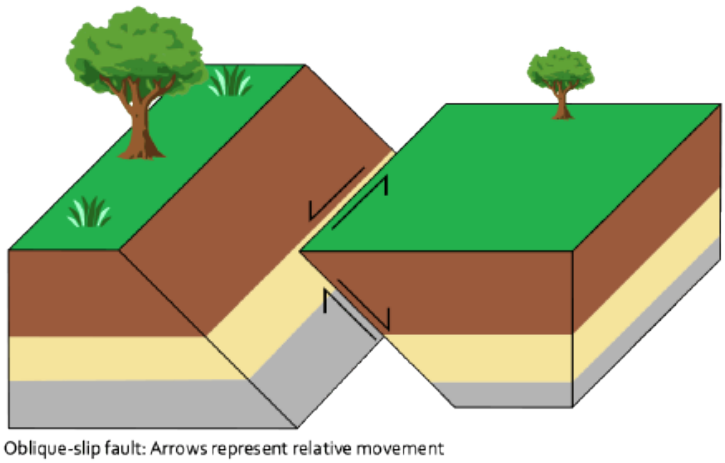


Figure 8.3.4: An oblique slip fault combines normal and shear (strike-slip) motion. In the block diagram, a fault plane cuts horizontal strata and tilts downward to the right. The offset is a result of normal motion and left lateral strike slip motion; the hanging wall on the right is dropped downward and also slides to the left relative to the footwall block "Oblique Slip Fault" by NAishik Rehman is licensed under CC BY-SA 4.0.

Ongoing Faulting and Seismicity in the Basin and Range

The Basin and Range Province in California remains seismically active at present. While most of the current relative plate motion between the North American and the Pacific plates is accommodated by the San Andreas fault, approximately 15-25% of the total motion is also taken up by the right-lateral oblique normal faults of California's Basin and Range Province and others to the north in western Nevada. These zones of active faulting form a seismic belt called the "Walker Lane," which may represent an incipient major transform fault zone which could replace the San Andreas as the plate boundary in the future!

Most of the faults within the Death Valley area have been active in the Holocene epoch, and some are active at present. A good example of the seismic risk in the Basin and Range Province is the Ridgecrest region south of the Panamint Range and just north of the east-west trending, left-lateral Garlock fault.

As shown in Figure 8.3.5, throughout this region, normal faults and right lateral strike-slip faults tend to be oriented north-northwest and separate uplifted ranges in their footwalls (such as the Sierra Nevada Mountains, the Inyo Mountains, the Panamint Range, and the Black Mountains) from down dropped basins (such as the Owens Valley, Panamint Valley and Death Valley). Fresh fault scarps and active seismicity throughout this region (which has been the site of many moderately sized historical earthquakes extending as far back as 1946) attest to ongoing tectonism. The most recent was a series of shallow strike-slip events south of the Panamint Range that culminated in an M_w 7.1 earthquake that produced 2.5 m of right lateral offset occurred in 2019.

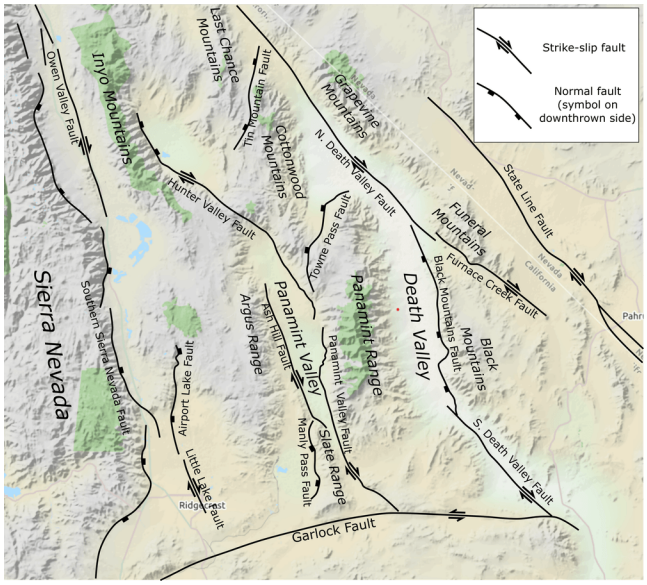


Figure 8.3.5: Map of NNW-SSE trending normal and strike-slip faults in the Death Valley area that have been active during the Quaternary period. Faults separate the ranges of the Death Valley region from the adjacent valley floors. The Garlock fault trends east-west to the south of Death Valley. The epicenter of the Ridgecrest Earthquake is south of the Panamint range, east of the Panamint Valley fault and north of the Garlock fault. "Death Valley Area Faults" by Mikenorton is licensed under CC BY-SA 4.0.

Video 8.3.2: Basin and Range Earthquakes

This video demonstrates the way in which earthquake hazard is monitored in this region. The silent animation shows that the build up of stress along a normal fault leads to rupture, which creates earthquakes. Seismic waves travel away from the epicenters and reach monitoring stations.

This interactive element is not available in this format. Visit the link or scan the QR code to access it online.

View this YouTube Video online

An important historical example of the Walker Lane risk is the 1872 Owens Valley earthquake (also known as the Lone Pine earthquake), which struck on March 26, 1872 in the Owens Valley. The epicenter was near the town of Lone Pine. Its magnitude has been estimated at M_w 7.4 to 7.9, with a maximum Mercalli Intensity Scale rating of X (Extreme). This earthquake was one of the largest earthquakes to hit California in recorded history and was similar in size to the 1906 San Francisco earthquake. Twenty-seven people were killed and 56 were injured. The earthquake resulted from sudden vertical movement of 4.6 - 6.1 m (15 - 20 ft.) and right-lateral movement of 11 - 12 m (36-39 ft.) on the Lone Pine Fault and part of the Owens Valley Fault; the scarp can still be visited and studied today. The scarp for a segment of this fault is shown in Figure 8.3.6. The scarp is developed in poorly sorted alluvial fan deposits and is approximately 4.6 - 6.1 m (15 - 20 ft.) high.



Figure 8.3.6: The Lone Pine Fault Scarp cuts across the alluvium. The person is standing on the down-dropped hanging wall and the boulder covered slope behind is the upthrown footwall. "Lone Pine fault scarp 1200px" by Mav is licensed under CC BY-SA 1.0.

The Lone Pine earthquake of 1872 was so intense that naturalist John Muir famously wrote about experiencing shaking in Yosemite Valley over 180 km (115 miles) away (Muir, 1901):

> "...one morning about two o'clock I was aroused by an earthquake; and though I had never before enjoyed a storm of this sort, the strange, wild thrilling motion and rumbling could not be mistaken, and I ran out of my cabin, both glad and frightened, shouting, "A noble earthquake!" feeling sure I was going to learn something. The shocks were so violent and varied, and succeeded one another so closely, one had to balance in walking as if on the deck of a ship among the waves...
>
> Then, suddenly, out of the strange silence and strange motion there came a tremendous roar. ... and I saw ... falling ... thousands of ... great boulders ...pouring to the valley floor in a free curve luminous from friction, making a terribly sublime and beautiful spectacle-an arc of fire fifteen hundred feet span, as true in form and as steady as a rainbow, in the midst of the stupendous roaring rock-storm. It seemed to me that if all the thunder I ever heard were condensed into one roar it would not equal this rock roar at the birth of a mountain talus."

References

1. Affolter, M., Bentley, C., Jaye, S., Kohrs, R., Layou, K., & Ricketts, B. (2020). Historical Geology. https://opengeology.org/historicalgeology/
2. Burchfiel, B. C., Cowan, D. S., & Davis, G. A. (1992). Tectonic overview of the Cordilleran orogen in the western United States. In The Cordilleran Orogen: Conterminous U.S. (Vol. G-3, pp. 407-479). Geological Society of America.
3. Burchfiel, B. C., & Davis, G. A. (1981). Mojave desert and environs. In The geotectonic development of California (Vol. 1, pp. 218-252). Prentice-Hall, Inc.
4. Burchfiel, B. C., & Stewart, J. H. (1966). Pull-Apart Origin of the Central Segment of Death Valley, California. Geological Society of America Bulletin, 77(4), 439-442.
5. Cassidy, E. (2023, March 31). A Surge of Floodwater For Owens Lake. NASA Earth Observatory. Retrieved June 22, 2023, from https://earthobservatory.nasa.gov/images/151157/a-surge-of-floodwater-for-owens-lake
6. Earle, S. (2019). Physical Geology. BCCampus Open Education. https://opentextbc.ca/physicalgeology2ed/
7. 1872 Owens Valley earthquake. (n.d.). Wikipedia. Retrieved June 13, 2023, from https://en.Wikipedia.org/wiki/1872_Owens_Valley_earthquake
8. Hall, C. A. (Ed.). (1991). Natural History of the White-Inyo Range, Eastern California. University of California Press.
9. Johnson, C., Affolter, M. D., Inkenbrandt, P., & Mosher, C. (2017). An Introduction to Geology. Salt Lake Community College. https://slcc.pressbooks.pub/introgeology/
10. Lynch, D. (2010). Geology of California. San Andreas Fault. Retrieved July 1, 2023, from http://www.sanandreasfault.org/CaGeo.html
11. Muir, J. (1901). Our National Parks. Houghton, Mifflin and Company. https://vault.sierraclub.org/john_muir_exhibit/writings/our_national_parks/

12. Nelson, C. A. (1981). Basin and Range Province. In The geotectonic development of California (Vol. 1, pp. 203-216). Prentice-Hall, Inc.
13. Our Dynamic Desert. (2009, December 18). Our Dynamic Desert. Retrieved June 28, 2023, from https://pubs.usgs.gov/of/2004/1007/geologic.html
14. Owens Valley Geology. (n.d.). Owens Valley Committee. Retrieved June 28, 2023, from https://owensvalley.org/geology/
15. Stock, G. M., & Glazner, A. F. (2010). Geology Underfoot in Yosemite National Park. Mountain Press Pub.
16. Walker Lane. (n.d.). Wikipedia. Retrieved June 13, 2023, from https://en.Wikipedia.org/wiki/Walker_Lane
17. Wernicke, B. (1992). Cenozoic extensional tectonics of the U.S. Cordillera. In The Cordilleran Orogen: Conterminous U.S. (Vol. G-3, pp. 553-581). Geological Society of America.

This page titled 8.3: Rift-Related Faulting in Eastern California is shared under a CC BY-NC 4.0 license and was authored, remixed, and/or curated by Martha House.

8.4: Sedimentary Products of Rifting in the Basin and Range

Sediments in Rift Basins

As continental rifting progresses, uplifted footwall blocks are eroded, and clastic debris is shed into adjacent valleys. This debris can be used to reconstruct the history of extension and basin formation. Depending on how far it travels into the rift basin, this sediment will be poorly sorted or well-sorted.

Video 8.4.1: Basin and Range: Extension, Erosion, Sedimentation

This silent animation illustrates the way the way that sediment fill basins develop under basin and range extension, showing how the tectonic processes described earlier in this chapter interact with erosional processes to form sequences of sedimentary deposits. Take note of where the sedimentary sequences are thickest and be sure you can explain why. Access a detailed description.

This interactive element is not available in this format. Visit the link or scan the QR code to access it online.

View this YouTube Video online

Sediment that does not travel far, or for very long, tends to be compositionally and texturally immature. Alluvial fans are examples of structures built of immature sediment; they are built of poorly sorted gravel and flank the uplifted regions, smoothing out the highest relief areas. These fan deposits emerge from the canyons of uplifted ranges and either stand alone as distinct alluvial fans at the base of mountains (Figure 8.4.1 or merge along range fronts.



Figure 8.4.1: Alluvial fans, viewed from the air, are built up at the foot of the Black Mountains. Within each fan, material spills out onto Badwater Basin, forming a perfect fan shape with a radial drainage pattern on the surface. Alluvial fans like this form at the mouths of every canyon in Death Valley. Generally, the coarsest sizes lie near the canyon mouth and the finest lie at the distal edges of the fan. "Badwater Fans" by USGS, is in the public domain.

Finer grained sediment gets carried further into valleys and create deposits of arkosic sand (a poorly sorted sand that contains rock fragments, feldspars and other easily weathered minerals). These deposits accumulate great thicknesses as a basin

continues to drop down. If the basin is part of a horst and graben, the sediment thicknesses are symmetric,, as isrepresented in Figure 8.4.2 where two sets of inwardly dipping normal faults bound a down-dropped basin. Within the basin, the sediment that is shed from the ranges is coarse in grain size near the faults, but becomes finer toward the center of the basin. If the basin is created by a half-graben, the sediment thickness is greater adjacent to the primary normal faults. The Owens Valley, for example, is a half-graben basin that contains roughly 3219 m (2 miles) of sediment in its western half, closest to the major normal fault.

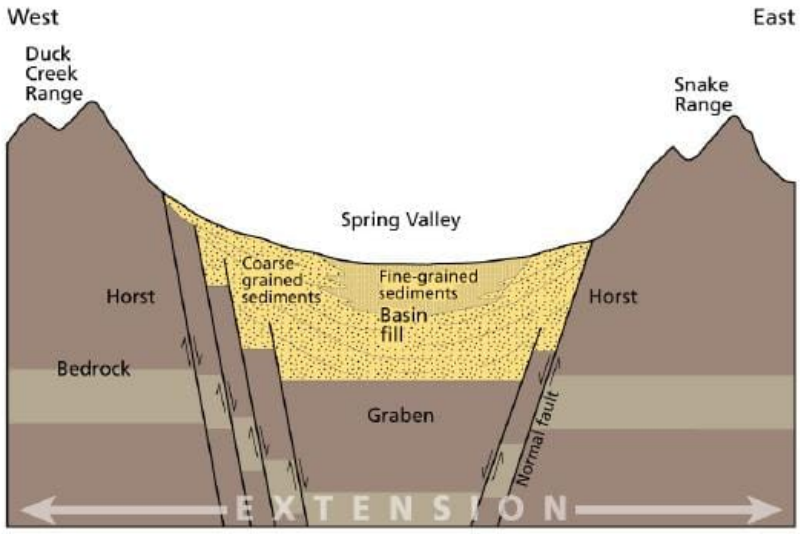


Figure 8.4.2: A cross-section of the sediment filling a horst and graben valley. Coarse-grained sediment lies adjacent to horsts and finer sediments appear toward the valley center (in the basin fill area). Crustal extension along normal faults caused the Basin and Range Province to rift, creating horsts, such as Duck Creek Range on the left and Snake Range on the right, with grabens such as Spring Valley between them. Grabens are filled with sediment eroded from the adjacent horsts. Similar structures have developed in California. "Spring Valley" by NPS/Trista L. Thornberry-Ehrlich, is in the public domain.

Lakes often form in the lowest regions of these basins, towards their centers and furthest from the rift escarpment. When they are situated in dry areas, like the Basin and Range Province, these lakes grow salty as they evaporate and are important sources of evaporite minerals (refer to Chapter 13 to learn more about these types of deposits).

Dry Lakes of the Basin and Range Province

The climate of the Basin and Range region has not always been as dry and warm as it is today. During the last glacial stage, which peaked at around 20,000 years ago, there was an extensive interconnected lake system (refer to Chapter 13 to learn more about this ancient system of lakes). For example, the dry lake in Badwater Basin is the last remnant of the much larger Pleistocene Lake Manly, which had depths as great as 600 ft. This is quite a change, since Badwater today is mostly dry.

Both Mono Lake and Owens Dry Lake have experienced the same climate impacts as those that changed Lake Manly into Badwater. These lakes faced additional depletion and reduction due to the diversion of their tributaries by the city of Los Angeles. This diversion began in 1913 and has been the subject of political turmoil and angst ever since. Motivated by the development of Los Angeles, representatives of the Los Angeles Department of Water and Power purchased land and water rights throughout the valleys east of the Sierra Nevada Range. Diversion of water to feed Los Angeles has greatly changed the environment of these valleys and impacted the surrounding communities. California's Water discusses this situation in more detail.

Mono Lake, which once drained to other lakes in the region, is now a closed lake with no outlets and an average depth of 48 m (149 ft). Changes in lake level can be tracked by “strandlines,” or ancient shorelines. These features are like rings in a bathtub, providing evidence of the ancient water levels and the reduction in water depth in this area. These "bathtub rings" can be seen easily from the air, appearing like thin lines parallel to the lake shores like those shown in Figure 8.4.3 around Mono Lake. Because today’s Mono Lake occupies an arid climate and has no outlet streams, evaporation has produced very high salinity and alkalinity (pH = 10). A series of calcium-rich freshwater springs around the perimeter of the lake interact with these alkaline waters, causing the precipitation of tufa, a freshwater form of limestone. The calcium carbonate towers created by this process are also a marker of past lake levels, since they can only form in the water. The tufa towers that today rise above the water were formed when the lake levels were higher (Figure 8.4.4).



Figure 8.4.3: Mono Lake strand lines marking ancient lake levels parallel the perimeter of the lake. "Mono Lake and the Sierra Nevada at the western edge of the Basin and Range" by Marli Miller, used with permission.



Figure 8.4.4: These tufa towers mark the past highest levels of Mono Lake and are now “dead”. "Tufa towers of the Mono Lake" by CatalpaSpirit is licensed under CC BY-SA 4.0.

Video 8.4.2: The Geologic Oddity in California; Mono Lake Tufas

If you would like to learn more about Mono Lake's tufa towers, this video provides further detail about their formation and shows additional views of the towers.

This interactive element is not available in this format. Visit the link or scan the QR code to access it online.

View this YouTube Video online

Another example of the impact of water diversion is found in Owens Lake, which was originally a perennial lake that held water

continuously and periodically overflowed to the south over the past 800,000 years. During the late 1800s and early 1900s the lake was as deep as 15 m (49 ft.); steamboats hauled ore across the lake from mines in the Inyo Range. The city of Los Angeles began diverting water in 1913, and by 1926 Owens Lake was dry.

Due to the diversion, large areas of very fine lake bed sediments were exposed to winds of the Owens Valley; when these winds whip up, large clouds of dust develop, obscuring the view at lake levels and higher (Figure 8.4.5). Residents tolerated this development, calling the clouds “Keeler Fog,” after the town of Keeler on the east of the lake, which was strongly impacted by the dust. However, by the latter half of the 20th century, the impact became more severe and the dust cloud was found to be the largest single source of PM10 dust (aerosol particles smaller than 10 microns in aerodynamic diameter) in the United States. As a result of legal action taken by the residents of the region, Los Angeles is now required to contain and prevent dust emissions through actions such as shallow flooding, managed vegetation, gravel, and tillage.

Additional legal action taken by valley residents has forced the city of Los Angeles to partially restore these lakes and to limit diversion. Nature has helped mitigate the problem as well: in March 2023, climate change-induced atmospheric rivers brought an unusually large amount of precipitation to California (5-13 inches), breaching the Los Angeles Department of Water and Power’s aqueduct and filling Owens Lake.



Figure 8.4.5: Dry lake deposits are whipped up by winds and create white clouds of alkali dust above Owens Lake. "Blowing alkali dust Owens Lake" by Eeekster (Richard Ellis) is licensed under CC BY 3.0.

Query 8.4.1

This interactive element is not available in this format. Visit the link or scan the QR code to access it online.

View this Interactive Content online

References

1. Burchfiel, B. C., Cowan, D. S., & Davis, G. A. (1992). Tectonic overview of the Cordilleran orogen in the western United States. In The Cordilleran Orogen: Conterminous U.S. (Vol. G-3, pp. 407-479). Geological Society of America.
2. Burchfiel, B. C., & Davis, G. A. (1981). Mojave desert and environs. In The geotectonic development of California (Vol. 1, pp. 218-252). Prentice-Hall, Inc.
3. Burchfiel, B. C., & Stewart, J. H. (1966). Pull-Apart Origin of the Central Segment of Death Valley, California. Geological Society of America Bulletin, 77(4), 439-442.

4. Cassidy, E. (2023, March 31). A Surge of Floodwater For Owens Lake. NASA Earth Observatory. Retrieved June 22, 2023, from https://earthobservatory.nasa.gov/images/151157/a-surge-of-floodwater-for-owens-lake
5. Earle, S. (2019). Physical Geology. BCCampus Open Education. https://opentextbc.ca/physicalgeology2ed/
6. Geology - Mono Lake. (n.d.). Mono Lake Committee. Retrieved June 28, 2023, from https://www.monolake.org/learn/aboutmonolake/naturalhistory/geology/
7. Hall, C. A. (Ed.). (1991). Natural History of the White-Inyo Range, Eastern California. University of California Press.
8. Harmony Borax Works - Death Valley National Park U.S. (2022, November 30). National Park Service. Retrieved June 14, 2023, from https://www.nps.gov/deva/learn/historyculture/harmony.htm
9. Johnson, C., Affolter, M. D., Inkenbrandt, P., & Mosher, C. (2017). An Introduction to Geology. Salt Lake Community College. https://opengeology.org/textbook/
10. Lake Badwater, Death Valley. (2009, March 16). NASA Earth Observatory. Retrieved June 28, 2023, from https://earthobservatory.nasa.gov/images/37536/lake-badwater-death-valley
11. Lynch, D. (2010). Geology of California. San Andreas Fault. Retrieved July 1, 2023, from http://www.sanandreasfault.org/CaGeo.html
12. Nelson, C. A. (1981). Basin and Range Province. In The geotectonic development of California (Vol. 1, pp. 203-216). Prentice-Hall, Inc.
13. Our Dynamic Desert. (2009, December 18). Our Dynamic Desert. Retrieved June 28, 2023, from https://pubs.usgs.gov/of/2004/1007/geologic.html
14. Owens Valley Geology. (n.d.). Owens Valley Committee. Retrieved June 28, 2023, from https://owensvalley.org/geology/
15. Reheis, M. C. (2016, December 9). Owens (Dry) Lake, California: A Human-Induced Dust Problem. Retrieved June 14, 2023, from https://geochange.er.usgs.gov/sw/impacts/geology/owens/
16. Stock, G. M., & Glazner, A. F. (2010). Geology Underfoot in Yosemite National Park. Mountain Press Pub.

This page titled 8.4: Sedimentary Products of Rifting in the Basin and Range is shared under a CC BY-NC 4.0 license and was authored, remixed, and/or curated by Martha House.

8.5: Rift-Related Volcanism in Eastern California

Crustal Thinning and Volcanism

As normal faulting thinned the crust throughout the Basin and Range continental rift, asthenospheric mantle was brought closer to the surface. As this material rose closer to the surface, pressure was reduced and the material underwent decompression-induced partial melting. Such partial melting of the ultramafic peridotite of the mantle produces a magma that is basaltic in composition. This magma is less dense than the surrounding rock and continues to rise through the crust to the surface. If the path to the surface is direct and there is little interaction with the crust, then it will erupt as basaltic lava, producing flood basalts, cinder cones, and basaltic lava flows. Alternatively, if there is a lot of crustal interaction, the lava that erupts will be more felsic. Examples of both are found in eastern California.

Video 8.5.1: Basin and Range Volcanic Processes

The following video provides further explanation of how melting and magma generation occurs in the Basin and Range; some of these processes are discussed in Chapter 2, Rocks and Minerals, and Chapter 9, Sierra Nevada.

This interactive element is not available in this format. Visit the link or scan the QR code to access it online.

View this YouTube Video online

Volcanism began in the southern Owens Valley approximately 6 million years ago, just after the most intense period of extension in the Basin and Range, and continued until 1.1 - 0.04 Ma. Notable examples of young volcanic features are in Death Valley (Ubehebe Crater; Figure 8.5.1) and all along the Owens Valley (e.g. Red Hill near Coso Junction; Figure 8.5.2). These volcanic structures are typically located along normal faults, which serve as conduits or paths for magma.



Figure 8.5.1: The Ubehebe Crater, Death Valley National Park. This is a cinder cone with a large depression in the center. "Ubehebe Crater, Death Valley, California" by Daniel Mayer, is licensed under CC-SA 3.0.



Figure 8.5.2: A view from the south of Red Hill, a small volcanic cinder cone located in the Southern Owens Valley. Little Lake is in the foreground, and the high Sierra Nevada Range in is located to the west. "Red Hill" by Martha House, is licensed under CC-BY-NC.

Video 8.5.2: Fossil Falls California

This video explores an area in southern Owens valley called “Fossil Falls”. This area was a path through which Pleistocene lakes drained and contains interesting sculpted shapes as a result of the water that flowed over it. The video will explain the landscape of the area, and will also give an overview of the power of water to erode rock

This interactive element is not available in this format. Visit the link or scan the QR code to access it online.

View this YouTube Video online

To the north, in Long Valley, dramatic examples of extension-related volcanism abound. An important feature is the Bishop Tuff, a widespread deposit that was produced by the eruption of the Long Valley Caldera 760,000 years ago.

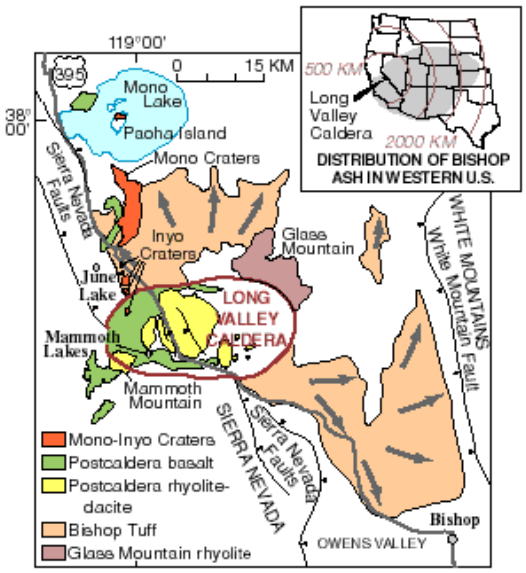


Figure 8.5.3: Simplified map of the geology of the Long Valley Caldera. Outcrops of the Bishop tuff are on the north and southeast, and related volcanic features are on the perimeter of the caldera. "Geologic Map of Long Valley and Mono Basin region" by USGS, is in the public domain. Access a detailed description.

As described in Figure 8.5.3, this pyroclastic eruption produced ash fall that is preserved to the north and southeast of the caldera. Other volcanic features associated with this volcanic system include Mammoth Mountain to the west, Glass Mountain to the northeast, and the Inyo-Mono craters to the north. Scientists estimate that the eruption of this caldera produced the Bishop Tuff and also created more than 100 km^3 (24 mi^3) of tephra that was dispersed widely as ashfall. Evidence suggests that more than 200 km^3 (48 mi^3) of pyroclastic flows were deposited outside the caldera, and approximately 350 km^3 (85 mi^3) ponded and welded together within the caldera. Outside the caldera, these pyroclastic flows swept over an area of more than 2,200 km^2 and buried the pre-existing ground to depths of nearly 200 m (660 ft.) just south of the caldera. The tuff blankets a large area of the northern Owens Valley, and fragments associated with the eruption of this caldera were detected as far east as Nebraska (Figure 8.5.3). The appearance of this tuff is highly variable. In some places, it's very ashy and unconsolidated (the lower part of Figure 8.5.4), while in others it's welded into a rock solid enough to support rock climbers (the upper part of Figure 8.5.4.



Figure 8.5.4: Two different examples of the Bishop Tuff. In the upper image, dark colored welded tuff contains petroglyphs carved through the dark coating (Sky Rock Petroglyphs near Bishop, CA). Bishop Tuff by Ryan James (dangerismycat via Flickr), is licensed under CC BY-NC-ND 2.0.In the lower image, an example of the air fall pumice and pyroclastic layer of the tuff shows rills from water erosion and has a light-colored appearance. "Bishop Tuff" by USGS, is in the public domain.

A large caldera complex is the southernmost expression of a chain of explosion pits, volcanic domes and lava flows of the Inyo-Mono craters, which extends as far north as Mono Lake (Figure 8.5.5).

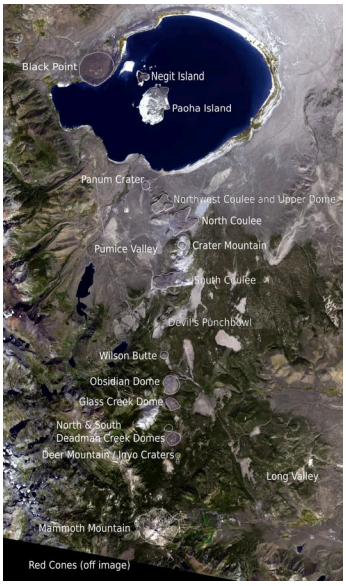


Figure 8.5.5: The Inyo-Mono Craters chain of volcanic domes and craters extends southward from Mono Lake to Mammoth Mountain in the south. Pahoa Island is in the center of the lake. Long Valley is shown in the lower left (SE) corner of the image. "Mono-Inyo Craters satellite image-annotated" by NASA, is in the public domain. Access a detailed description.

The well-known ski area, Mammoth Mountain, sits on the edge of a large caldera; skiers who ride the gondola can see active steam vents on the side of this young dacite dome. This chain of volcanic features, which includes dacite domes such as Mammoth Mountain, rhyolite and obsidian domes, and explosion craters (Figure 8.5.6) is thought to be linked via large dike structures that are fault controlled; their location along the major normal faults indicates that fault features may have served as conduits for magma.



Figure 8.5.6: Three different examples of volcanic features found in the Inyo-Mono Craters chain. Top Image: Mammoth Mountain forms a large sloped volcanic features with the Ritter Range to the west in the background and Lake Mary in the foreground. "Ritter Range and Mammoth Mountain" by Hike395, is licensed under CC BY 3.0. In the middle image, the rough surface of the rhyolitic Panum Crater is viewed from the air and is surrounded by a tephra apron. i"Panum Crater" work by USGS, is in the public domain. In the bottom image, the Inyo Craters and South Deadman Dome are viewed from the south. The rough surfaces of the dome emerge from above the surrounding forest, while the explosion pits of the craters to the south sink below "Inyo Craters" by USGS, is in the public domain.

While the volcanism that produced this chain of features began approximately 50,000 yrs ago, the most recent eruptions occurred during the Holocene. For example, volcanic Paoha Island in Mono Lake is only about 300 years old.

Query 8.5.1

This interactive element is not available in this format. Visit the link or scan the QR code to access it online.

View this Interactive Content online

Volcanic Hazards

The Long Valley region, as well as other sites within the Basin and Range Province, present significant volcanic hazard potentials. Particular threats from the Long Valley Caldera region include fast-moving pyroclastic flows and surges. The current hazard zone associated with this caldera is based on explosive eruptions from vents located along the Inyo-Mono chain in the past 10,000 years that are known to have ejected magma and generated pyroclastic flows or surges. The hazard zone shown in Figure 8.5.7 , is centered along the south moat of the caldera, which is the location of epicenters of many swarms of earthquakes since 1980 and the area of most intense ground movement. It has been mapped to extend northward from the Long Valley Caldera to Conway Summit, and along the eastern edge of the Sierra Nevada Range and the western limits of the northern White Mountains. Scientists suggest that future eruptions might occur from this restless zone, and pyroclastic flows and surges could travel as far as 15 km from a new vent. The South Moat, which is located to the south of the town of Mammoth Lakes, is a potentially hazardous volcanic vent that could produce a large pyroclastic flow that would extend as far north as Conway Summit on the north side of Mono Lake.

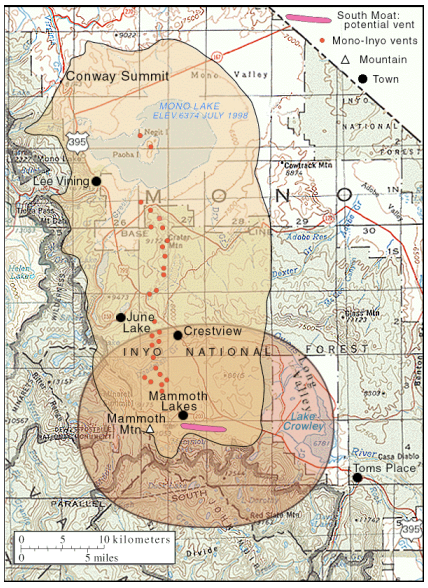


Figure 8.5.7: A map of the hazard zone for pyroclastic flows and surges around existing explosive vents along the Mono-Inyo Craters volcanic chain and from potential vents located in Long Valley's south moat. The hazard zone extends approximately 60 km (~35 miles) northward from the Long Valley Caldera to Conway Summit, and along the eastern edge of the Sierra Nevada Range and the western limits of the northern White Mountains. Hazards Summary for Mono-Inyo Craters by USGS/C.D. Miller, is in the public domain.

Video 8.5.3: Volcanology and the Long Valley Caldera

This video discusses the last large eruption at Long Valley Caldera.

This interactive element is not available in this format. Visit the link or scan the QR code to access it online.

View this YouTube Video online

Volcanic eruptions are not the only hazard in this area: gas emissions have produced high concentrations of carbon dioxide (CO_2) that can accumulate in the winter in tree wells, around buildings, and immediately below the snow surface. For example, high CO_2 levels have built up in soil and are killing trees on the flanks of Mammoth Mountain. First noted in 1990, the areas of tree kill total about 170 acres in six general areas, including the most visually impressive tree-kill area adjacent to Horseshoe Lake on the south side of Mammoth Mountain. The soil gas in the tree-kill areas is composed of 20 - 90% CO_2. Note that there is less than 1% CO_2 in soils outside the tree-kill areas.

The ultimate source of much of the CO_2 is magma beneath Mammoth Mountain. The onset of CO_2 emissions is closely linked to a major seismic swarm beneath the mountain in 1989. Scientific studies indicate that there may be a large reservoir of gas deep below the mountain.

Geothermal Activity (Coso and Round Valley)

Once the crust has thinned, the mantle can rise up and replace it, bringing heat close to the surface. This is shown in very high heat flows in the Basin and Range area. In 2023, 98% of the geothermal electricity in the United States was produced in Basin and Range states, and volcanic areas in California and Nevada were the most productive. The Casa Diablo hydrothermal plant, for example, takes advantage of the heating power of the magma below the Long Valley Caldera. Here, the hydrothermal system is recharged with water primarily from snow-melt in the Sierra Nevada highlands along the western rim of the caldera. This water infiltrates to depths of a few kilometers where it is heated to at least 220 °C (428 °F) by hot rock near geologically young intrusions of magma. The thermal water rises along fractures to depths of 1-2 km in the western part of the caldera, just north of the town of Mammoth Lakes, and then flows eastward within permeable rock layers to discharge points along Hot Creek and around Crowley Lake in the eastern half of the caldera. This process creates many natural hot springs in the region.

Query 8.5.1

This interactive element is not available in this format. Visit the link or scan the QR code to access it online.

View this Interactive Content online

References

1. Affolter, M., Bentley, C., Jaye, S., Kohrs, R., Layou, K., & Ricketts, B. (2020). Historical Geology. https://opengeology.org/historicalgeology/
2. Bacon, C. R. (1982, December 31). Geology and History | U.S. Geological Survey. USGS.gov. Retrieved June 9, 2023, from https://www.usgs.gov/volcanoes/coso-...gy-and-history
3. Bailey, R. A. (1989). Geologic map of the Long Valley caldera, Mono-Inyo Craters volcanic chain, and vicinity, eastern California (Issue IMAP 1933) [Report]. USGS. https://doi.org/10.3133/i1933
4. Burchfiel, B. C., Cowan, D. S., & Davis, G. A. (1992). Tectonic overview of the Cordilleran orogen in the western United States. In The Cordilleran Orogen: Conterminous U.S. (Vol. G-3, pp. 407-479). Geological Society of America.
5. Burchfiel, B. C., & Davis, G. A. (1981). Mojave desert and environs. In The geotectonic development of California (Vol. 1, pp. 218-252). Prentice-Hall, Inc.
6. Hydrothermal Monitoring at Long Valley Caldera | U.S. Geological Survey. (n.d.). USGS.gov. Retrieved June 9, 2023, from https://www.usgs.gov/volcanoes/long-...valley-caldera

7. Johnson, C., Affolter, M. D., Inkenbrandt, P., & Mosher, C. (2017). An Introduction to Geology. Salt Lake Community College. https://opengeology.org/textbook/
8. Mammoth Mountain | U.S. Geological Survey. (n.d.). USGS.gov. Retrieved June 9, 2023, from https://www.usgs.gov/volcanoes/mammoth-mountain
9. Mono-Inyo Craters | U.S. Geological Survey. (n.d.). USGS.gov. Retrieved June 9, 2023, from https://www.usgs.gov/volcanoes/mono-inyo-craters
10. Nelson, C. A. (1981). Basin and Range Province. In The geotectonic development of California (Vol. 1, pp. 203-216). Prentice-Hall, Inc.
11. Our Dynamic Desert. (2009, December 18). Our Dynamic Desert. Retrieved June 28, 2023, from https://pubs.usgs.gov/of/2004/1007/geologic.html
12. Owens Valley Geology. (n.d.). Owens Valley Committee. Retrieved June 28, 2023, from https://owensvalley.org/geology/
13. Stock, G. M., & Glazner, A. F. (2010). Geology Underfoot in Yosemite National Park. Mountain Press Pub.

This page titled 8.5: Rift-Related Volcanism in Eastern California is shared under a CC BY-NC 4.0 license and was authored, remixed, and/or curated by Martha House.

8.6: The Oldest Rocks in the Basin and Range

Before Rifting

The uplift of older rocks in the footwalls of normal faults in the Basin and Range Province provide a peek into the geologic environment during the Late Proterozoic-Early Paleozoic period when most of what is now California did not yet exist. Well before the onset of extension leading to the formation of the basins and ranges of this region, what is now the Basin and Range Province of eastern California was part of the ancient, or passive continental margin that developed following the rifting of the supercontinent Rodinia.

Passive Margin Basics

A passive continental margin is formed where the edge of a continent meets oceanic crust within a tectonic plate. An example of a modern passive continental margin is found along the east coast of the United States, where a broad continental shelf extends beyond the current coastline. This continental shelf preserves the geologic record of changes to this region following the rifting of Pangea.

These margins are “passive” because they lack the tectonic activity seen at active continental margins, such as subduction zones or continental collision zones. A key feature found at a passive margin is a broad continental shelf, which is the submarine continuation of the continent (Figure 8.6.1). This shelf has a shallow slope and is the site of continuous sedimentation and subsidence dating back to the time of rifting (and before). They are typically covered by a mix of terrestrially derived sediments and marine sediments. The specific types of sediments can vary depending on factors such as the geological history of the region, the climate, the proximity to tectonic boundaries, and the input of sediment from nearby rivers and other sources. Sediment types may include terrestrially derived gravel, sand and mud, or marine muds and limestones (including shell matter and reef material), as well as layers of evaporite deposits. These sediments may drape over faulted basement rocks whose structures originate with the initial rifting of the continent.

Because the continental shelf is generally less than 200 m deep, it can also preserve the history of global sea level change: these regions may be extensively flooded during times of sea level rise and partially exposed during glacial periods. Each of these situations brings a sedimentary signature with it. For example, as sea level lowers, these regions may preserve intertidal mud flats and sandy beach deposits, as well as shallow water evaporite minerals. As sea level rises, these near-shore deposits may be “drowned” and covered with deeper water deposits (mud and clay).

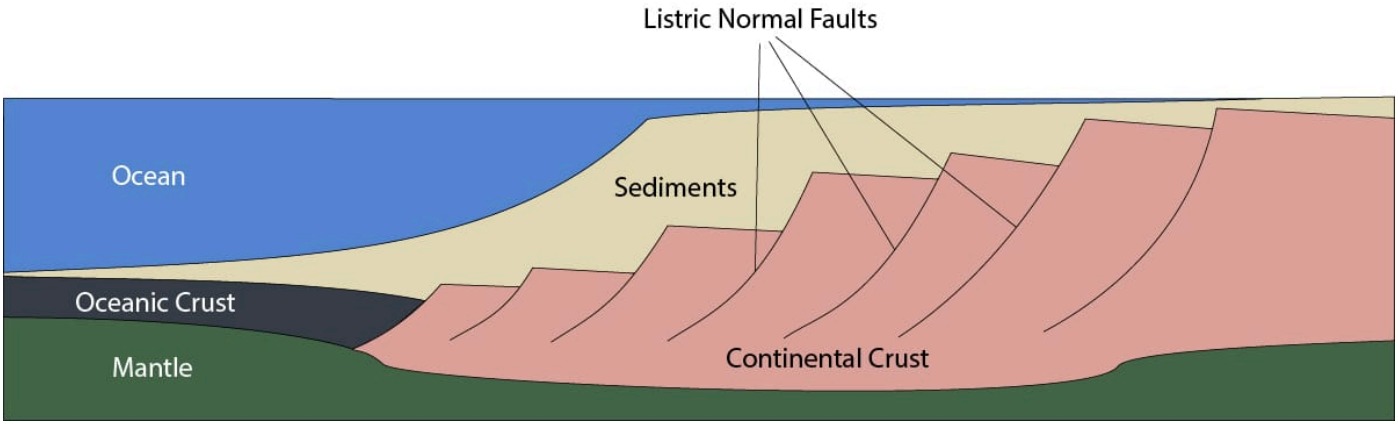


Figure 8.6.1: A diagrammatic passive margin resembling what western North America looked like. Continental crust that has been rifted is broken up by west-dipping listric normal faults. It is overlain by thick ocean sediments. Note that this diagram is very vertically exaggerated to emphasize these different features. This work by Allison Jones, a derivative of the original, is in the public domain. Access a detailed description.

The Paleozoic Passive Margin of the Western US

Geologists have determined that the Paleozoic rocks of the Basin and Range represent an ancient passive margin along an ancient coastline of a stable craton that resided close to sea level at low latitudes. In these areas, sedimentary rocks that are marine in origin (such as siltstones, limestones, dolomites, and quartzites) are common. Geologists have been able to demonstrate that the distinctive units in one area can be correlated with units in other areas; as a result, they have been able to reconstruct the geometry of the ancient continental shelf. They've even been able to determine the direction that sediment was transported and have been able to estimate the depth of water in these areas; in some areas, fossils and sedimentary structures suggest that water was only a few meters deep (Figure 8.6.2).

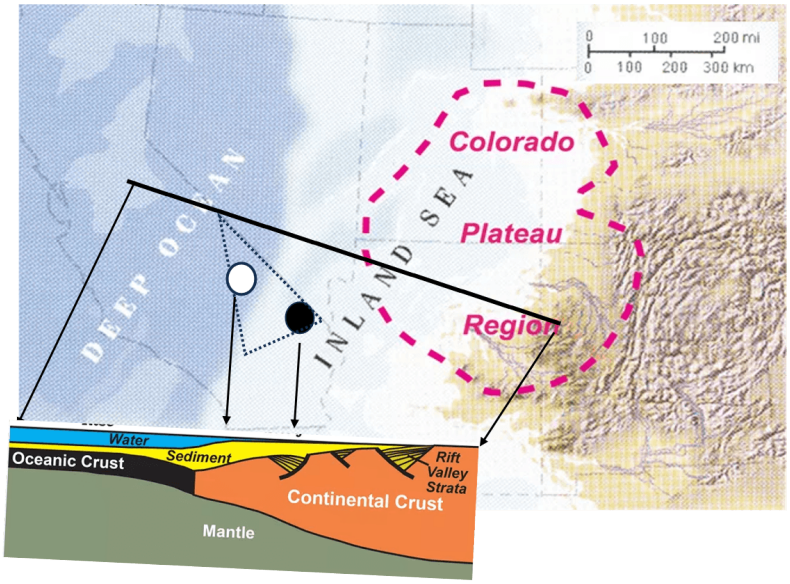


Figure 8.6.2: Paleogeography of the Basin and Range of California at the beginning of the Paleozoic era. This work by Martha House, is licensed under public domain /derivative of original work by NPS. Access a detailed description.

An example of this correlation is shown between the Late Proterozoic-Cambrian rock layers in the White-Inyo Mountains, on the east side of the Owens Valley and those of the Death Valley region to the east (Figure 8.6.3). The rocks of the Death Valley region are thought to have been deposited closer to the craton because they contain more debris that is shed from the continent (such as sand), so the stratigraphic column in the figure is shown above this region of a schematic cross section of a passive margin. On the other hand, the sedimentary units in the White Mountains region appear to be thicker and to have more deep-water features, such as more shale and mudstone, therefore, the stratigraphic column illustrating these units is shown above the deep-water portion of the passive margin cross section. Correlations between these units are shown in the diagram as well. These correlations are described below starting with the White Mountains units:

- Middle Cambrian Units
  - Bonanza King Dolomite (is found in both areas)
  - Monola Formation (corresponds to upper Carrara Formation in Death Valley area)
- Lower Cambrian Units
  - Mule Springs Limestone (corresponds to middle Carrara Formation in Death Valley)
  - Saline Valley Formation (corresponds to Zabriskie Quartzite in Death Valley area)
  - Harkless Formation (corresponds to upper Wood Canyon Formation in Death Valley)
  - Poleta Formation (corresponds to middle Wood Canyon Formation in Death Valley)
  - Campito Formation ((corresponds to lower Wood Canyon Formation and Upper Stirling Quartzite in Death Valley)
  - Deep Spring Formation and Upper Reed Dolomite (corresponds to middle Stirling Quartzite in Death Valley)
- Upper Proterozoic (Late Proterozoic)
  - middle and lower Reed Dolomite (corresponds to middle Stirling Quartzite in Death Valley)
  - Wyman formation, base is not exposed (corresponds to lower Sirling Quartzite, entire Johnnie Formation, Noonday Dolormite and possibly underlying Pahrump group in Death valley)

Reconstructions of these units creates a sketch of the pattern of sediments above the continental shelf at the time of deposition.

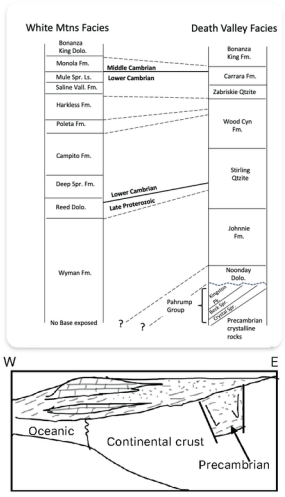


Figure 8.6.3: Simplified stratigraphic columns for Early Paleozoic stratigraphy in the White Mountains and Death Valley region, as described in the text. The upper panel shows suggested correlations between the regions after Nelson (1981) and Hall (1991). Abbreviations are as follows: Fm = formation; Ls = limestone; dolo = dolomite; Quartzite = quartzite; Spr = Spring; Pk = Peak. Lower panel shows the approximate location of these columns relative to a developing passive margin. White Mountains facies are more distal shelf units, while Death Valley facies represent proximal shelf sequences and rift deposits. This work after Nelson (1981) & Hall (1991) by Martha House, is licensed under CC-BY-SA-NC.

Query 8.6.1

This interactive element is not available in this format. Visit the link or scan the QR code to access it online.

View this Interactive Content online

Continental Rifting and a Snowball Earth

An interesting feature of these very old units is found at the base of the Death Valley sequence, where the sedimentary rocks unconformably overlie very old basement rocks that have been dated at 1.7 billion years. The rocks directly above them are called the Pahrump group. This tilted group of weakly metamorphosed sedimentary rocks contains the sedimentary record for rifting of the ancient Rodinia supercontinent, as well as the likely evidence for ancient “snowball earth” glaciations in which low-latitude regions all around the Earth were fully glaciated.

The “Snowball Earth” glaciations were a series of ice ages during the Neoproterozoic era. These ice ages were thought to have been so profound that perhaps the entire surface of the planet froze over, all the way from the poles to the equator. At roughly the same time, the supercontinent Rodinia was rifting apart. The region that would become eastern California was part of the rifted zone that would become the passive margin discussed earlier. As the edge of the rifted continent is faulted and subsides, fault-bounded basin fill with seawater. Poorly sorted sediments shed from the rift flanks, as well as from marine mass movements called continental shelf are deposited in these areas(see the discussion in the Coast Ranges chapter).

So how did geologists come to the conclusion that rifting was happening at this time, in this place? And what is the evidence for the glaciation here? A key unit that is part of this story is found in the Pahrump Group. A unit called the Kingston Peak Formation, which has been dated at approximately 700 -750 Ma, contains mafic volcanic rocks of the type that form in rift environments, along with diamictite units (a diamictite is a type of poorly sorted sedimentary rock containing terrigenous sediments; Figure 8.6.3). This unit is similar to others of the same age that are found throughout the west, and the mapped geometries of these units indicate that they were deposited in narrow bays or rift zones along the developing passive margin.

So what about the glacial evidence? In this region, the dominant evidence is, interestingly, also the diamictite, which contains features called “dropstones”, which are fine-grained, thin-bedded or laminated deep water deposits of clay and silt, into which drop much larger particles, such as pebbles, cobbles, or boulders (Figure 8.6.4).



Figure 8.6.4: A dropstone in Proterozoic diamictite of Kingston Peak Formation, SE California. A dropstone cobble is surrounded by layered mudstones and sandstones of the Kingston Peak formation. The layers below are deformed slightly suggesting this rock dropped into soft sediment. Layers above drape over it. "Glacial Dropstone" by Marli Miller is used with permission.

Dropstones pierce into the soft pre-existing sedimentary layers, disrupting their continuity. The layers of clay and silt indicate that the depositional environment was low energy, so it is somewhat strange to see cobbles and boulders, which require high energy to be transported. Geologists believe that that these dropstones in the Kingston Peak Formation are glacial in origin. The idea is that when outlet glaciers from the Snowball Earth ice sheets reached the sea, they calved off icebergs full of gravel, sand, cobbles, and silt. These icebergs floated out to deep water, melted, and let their load of sediment fall through the water below.

Query 8.6.2

This interactive element is not available in this format. Visit the link or scan the QR code to access it online.

View this Interactive Content online

References

1. Affolter, M., Bentley, C., Jaye, S., Kohrs, R., Layou, K., & Ricketts, B. (2020). Historical Geology. https://opengeology.org/historicalgeology/
2. Burchfiel, B. C., & Davis, G. A. (1981). Mojave desert and environs. In The geotectonic development of California (Vol. 1, pp. 218-252). Prentice-Hall, Inc.
3. Corsetti, F. A., Awramik, S. M., & Pierce, D. (2003). A complex microbiota from snowball Earth times: Microfossils from the Neoproterozoic Kingston Peak Formation, Death Valley, USA. Proceedings of the National Academy of Sciences, 100(8), 4399-4404. https://doi.org/10.1073/pnas.0730560100
4. Dickinson, W. R. (1981). Plate tectonics and the continental margin of California. In The geotectonic development of California (Vol. 1, pp. 1-28). Prentice-Hall, Inc.
5. Earle, S. (2019). Physical Geology. BCCampus Open Education. https://opentextbc.ca/physicalgeology2ed/
6. Hall, C. A. (Ed.). (1991). Natural History of the White-Inyo Range, Eastern California. University of California Press.
7. Johnson, C., Affolter, M. D., Inkenbrandt, P., & Mosher, C. (2017). An Introduction to Geology. Salt Lake Community College.

https://opengeology.org/textbook/
8. Kirschvink, J. L. (1992). Late Proterozoic Low-Latitude Global Glaciations: the Snowball Earth. In The Proterozoic biosphere; a multidisciplinary study (pp. 51-51). Cambridge University Press.
9. Lillie, R. J. (1999). *Whole earth geophysics: an introductory textbook for geologists and geophysicists*. Prentice Hall.
10. Mahon, R. C., Dehler, C. M., Link, P. K., Karlstrom, K. E., & Gehrels, G. E. (2014). Geochronologic and stratigraphic constraints on the Mesoproterozoic and Neoproterozoic Pahrump Group, Death Valley, California: A record of the assembly, stability, and breakup of Rodinia. GSA Bulletin, 126(5/6), 652-664. 10.1130/B30956.1
11. Miller, E. L., Miller, M. M., Stevens, C. H., Wright, J. E., & Madrid, R. (1992). Late Paleozoic paleogeographic and tectonic evolution of the western U.S. Cordillera. In The Cordilleran Orogen: Conterminous U.S. (Vol. G-3, pp. 57-106). Geological Society of America.
12. Nelson, C. A. (1981). Basin and Range Province. In The geotectonic development of California (Vol. 1, pp. 203-216). Prentice-Hall, Inc.
13. Our Dynamic Desert. (2009, December 18). Our Dynamic Desert. Retrieved June 28, 2023, from https://pubs.usgs.gov/of/2004/1007/geologic.html
14. Poole, F. G., Stewart, J. H., Palmer, A. R., & Sandberg, C. A. (1992). Latest Precambrian to latest Devonian time; Development of a continental margin. In The Cordilleran Orogen: Conterminous U.S. (Vol. G-3, pp. 9-106). Geological Society of America.
15. Stock, G. M., & Glazner, A. F. (2010). Geology Underfoot in Yosemite National Park. Mountain Press Pub.

This page titled 8.6: The Oldest Rocks in the Basin and Range is shared under a CC BY-NC 4.0 license and was authored, remixed, and/or curated by Martha House.

8.7: Chapter Summary

8.1 Regional Extent and Overview of the Basin and Range

- The Basin and Range of California is part of a much larger physiographic province that extends to Utah and south to Mexico.
- The region is known for its linear fault bounded ranges and basins.
- This arid region lies in the rain-shadow of the Sierra Nevada mountains to the west.
- The Basin and Range Province is a large continental rift zone.

8.2 Rifting in the Basin and Range

- Continental rifting can be caused by heat buildup beneath the continent or by changes in plate boundary configurations.
- The onset of rifting in the Basin and Range Province was approximately 17 Ma.
- Extension associated with the Basin and Range Province doubled the width of the crust!
- Development of this continental rift zone is associated with plate boundary changes to the west.
- Continental rifts are associated with distinctive patterns of sedimentation, faulting and volcanism.

8.3 Rift-Related Faulting in Eastern California

- Normal fault structures found in this region are horst-graben or half-grabens.
- Brittle normal faults are steeply dipping.
- Ongoing seismic activity associated with the Walker Lane is responsible for earthquakes as large as M_w 7.1 that are felt throughout southern California.
- Pull-apart basins form in some areas, produced by a combination of strike-slip and normal faulting.
- Metamorphic core complexes exposed in footwall rocks record evidence of earlier crustal extension.

8.4 Sedimentary Products of Rifting in the Basin and Range

- Erosion of uplifted fault blocks forms large alluvial fans along range fronts.
- Finer sediments fill the centers of rift basins.
- Sediment thicknesses can be quite large in the basins.
- Shallow seasonal lakes occupy the centers of many rift basins.
- The modern system of basin lakes are dry lakes that were once much larger, but have been reduced due to climate change and diversion by the City of Los Angeles.
- Tufa towers and strand lines record the maximum heights of ancient basin lakes.
- Desiccation of the Owens Lake in the southern Owens Valley is a major source of air pollution in the region.

8.5 Rift-Related Volcanism in Eastern California

- Crustal thinning leads to decompression melting of mantle rocks.
- Volcanic activity produced by decompression melting produces a range of volcanic products (domes, cinder cones, lava flows and pyroclastic flows) and compositions.
- Volcanism in the Basin and Range Province is young, generally co-eval with faulting.
- The Bishop Tuff was produced by a large pyroclastic eruption of the Long Valley Caldera less than 1 m.y. ago.
- The Long Valley Caldera is part of a chain of young (<1 m.y.) volcanic features that extends to Mono lake
- Continued volcanic activity in the Basin and Range Province presents a risk of seismic activity, volcanic flows, pyroclastic eruptions and gas emissions.
- Geothermal activity associated with current volcanic heating is an important source of energy.

8.6 The Oldest Rocks in the Basin and Range

- The oldest rocks in the Basin and Range Province are exposed in ranges bounded by normal faults.
- The oldest rocks date back to 1.7 billion years ago, and record the rifting of Rodinia, as well as evidence for the “snowball earth”.
- Most of the Paleozoic rocks in the region are associated with the development of a passive margin following rifting.
- The Snowball Earth refers to global glaciation during the Neoproterozoic era.
- Evidence for rifting and glaciation are found in the oldest sedimentary rocks of this region.

This page titled 8.7: Chapter Summary is shared under a CC BY-NC 4.0 license and was authored, remixed, and/or curated by Martha House.

8.8: Detailed Figure Descriptions

Figure 8.1 Location of the Basin and Range Province of California

A physiographic map of California highlights the area that corresponds to the Basin and Range Geomorphic Province. The region is situated in eastern California, to the north of the Garlock Fault, and to the west of the Sierra Nevada Range. The regions' alternating basins and uplifted range extend into Nevada.

Figure 8.1.1 Basin and Range Province

The province is in the western U.S. and northern Mexico. It extends along the Gulf of Mexico on the Baja California to the Bajia de Los Angeles and also continuing along the east side of the gulf and along the Pacific coastline to the Trans-Mexican Volcanic Belt. In the U.S., the province is bounded by the Sierra Nevada Mountains on the west, and it extends to the east as far as the Wasatch Range of Utah and the Rio Grande Rift of New Mexico. Reno, Nevada, sits close to the northwest edge of the province; Salt Lake City, Utah, is at the northeast edge. The province curves west just south of Salt Lake City. Near Flagstaff, Arizona, the province curves west along the Colorado Plateau before moving north and then dipping back down south-west into Mexico. The northern boundary of this region is the Columbia Plateau of Oregon and it extends southward into Mexico, bordering the Sierra Madre Occidental.

Video 8.2.1 Tectonic Evolution of the Western United States

1. Present (last frame of movie). At Present the Pacific Plate fills most of the northeast Pacific Ocean basin with only the small Juan de Fuca and Cocos plates remaining from the previous configuration. The Pacific plate is moving northwest past North America. It has captured some slivers of the continental edge and is carrying them northwestward toward Alaska. Thus, the present Pacific-North America plate boundary lies within the continent, along the San Andreas fault system. It is connected to other plate boundaries at three-plate triple junctions, the so-called Mendocino and Rivera triple junctions; the locations and motions of these triple junctions help determine the on-shore geology in each time and place.
2. Early Cenozoic, 38 million years ago (first frame of movie). In the early Cenozoic, 40 Million Years Ago, other oceanic plates lay between the Pacific and North American plates. They were spreading away from the Pacific plate and subducting beneath the rim of the continent.
3. East Pacific Rise Migration. Coming forward in time, the eastern edge of the Pacific plate moved steadily northeastward as new seafloor was accreted by sea floor spreading. Eventually, the spreading center itself reached the subduction zone and the intervening plate was destroyed. The Pacific plate began to break off pieces of North America and carry them along the coast, creating the San Andreas-Gulf of California plate boundary inside the continent. Triple Junction Evolution. The Mendocino triple junction migrated steadily up the coast, attached to the Mendocino fracture zone on the Pacific plate. The Rivera triple junction hovered near the southern California borderland then, about 12 million years ago, when sea-floor spreading and subduction ceased off Baja California, it jumped to its modern position at the mouth of the Gulf of California.
4. San Andreas System Evolution. The past evolution of the San Andreas fault system occurred in two stage process. First the Salinian and borderland pieces of the continent were gradually transferred to the Pacific plate, later Baja California was transferred.
5. A third stage has begun: the Sierra Nevada/Great Valley block is in the early stages of being transferred and carried away. Pacific Plate Motion. It continually moved off to the northwest.
6. Basin and Range Expansion. In the early Cenozoic, western North America was much narrower. During the late Cenozoic it expanded, forming the Basin and Range province. This occurred during the time that the Pacific plate was pulling the rim of the continent away to the northwest, perhaps causing the expansion or, more likely, just making room for it. (It was already elevated, hot and weak, ready to fall apart given the chance.)

Video 8.4.1 Basin and Range: Extension, Erosion, Sedimentation

The silent animation is labeled "Extension, deformation, and sedimentation in a basin-and-range province"

The animation begins with a simplified diagram of a section of land with a few trees on it; bands of color indicate five layers of

earth. On the left and right sides of the block, arrows are shown pointing away from each other. The arrows are labeled "Extension direction." The following text is also shown:

Typical rift features include:

1. Down-dropped faults and uplifted escarpments
2. Sediment-filled valleys from erosion and streams

The arrows move away from each other and the words "Extension direction" begin to stretch on a horizontal axis. Diagonal lines begin to appear on the surface of the land and extend underneath it; the text "Extension causes fractures and faults" appears.

The lines become more defined and each one is now labeled "fault." Now cut into sections, the land begins to move. Arrows point to areas on the surface where land has risen as the sections of earth tilt; these are labeled "deformation forms escarpments."

As expansion continues, the escarpments increase in height. Wavy lines to indicate streams appear under the shear walls; areas of sediment are indicated with yellow. The words "Mountains erode; streams carry sediment" appear on screen.

As the lateral movement continues, now the blocks of land are clearly set at an angle. Valleys have formed at the base of each escarpment and lakes begin to appear. The yellow sediment is clearly thickest in the deepest part of the valleys.

This text appears on screen: "Valleys fill with sediment. Lakes form on the valley floor."

The final scene shows a series of uplifted ranges (escarpments) and basins (valleys).

This text is repeated on screen:

1. Down-dropped faults and uplifted escarpments
2. Sediment-filled valleys from erosion and streams

Figure 8.5.3 Simplified map of the geology of the Long Valley caldera

This geologic map highlights the geological units, fault lines, and other significant geologic features in eastern California, primarily focused on Long Valley and Mono Basin. The region is bounded on the west by the Sierra Nevada Range, and on the east by the White Mountains. The Long Valley Caldera is an oval depression that is approximately 30 by 15 km in dimension. The town of Mammoth Lakes is on the western rim of the Caldera, and Mammoth Mountain is on the southwestern rim.

The Sierra Nevada Fault trends north-northwest, and cuts through the western portion of the caldera. The White Mountain fault is to the east of the complex.

Different geological formations on this map include:

1. Glass Mountain Rhyolite, which is found along the northeast border of the Long Valley caldera.
2. Bishop tuff occurs in large deposits to the north and southeast of the caldera.
3. Younger rhyolites and basalts occur in the western portion of the caldera and along it's perimeter, toward Mammoth Lakes.
4. The Mono-Inyo Craters occur in a chain that extends between the Long Valley Caldera and Mono Lake approximately 25 km to the north.

An inset map indicates that deposits of Bishop ash (tuff) can be found in most of the western US, including Nevada, Utah, Arizona, New Mexico, Colorado, and Wyoming, as well as portions of Nebraska, Kansas, Texas and the panhandle of Oklahoma, as well as a portion of southeast Idaho.

Figure 8.5.5 The Inyo-Mono Craters chain

This satellite photograph shows a chain of volcanic domes and craters extending from Mono Lake south to Mammoth Mountain. Panum Crater lies in Pumice Valley, close to Mono Lake. Southeast we see Northwest Courlee and Upper Dome, with North Coulee southeast from that area. Due south from North Coulee is Crater Mountain, where we leave the valley floor. South from Crater Mountain we see an area that extends due east labeled South Coulee. The Devil's Punchbowl is south and slightly east from that area. Due south from the Devil's Punchbowl we see a string of features that are close together and arrayed in a rough line

that moves south and slightly east along the mountain range: Wilson Butte, Obsidian Dome, Glass Creek Dome, North and South Deadman Creek Domes, Deer Mountain Crater, and Inyo Crater. Long Valley lies due east from this region. The southmost feature pictured is Mammoth Mountain, but the map indicates that Red Cones is southwest from Mammoth Mountain (off image).

Figure 8.6.1 A Diagrammatic Passive Margin

This simplified diagram shows a passive margin along the western North American continent. From left to right we see the ocean depicted above a thin layer of sediment, which rests on a thicker oceanic crust above a still thicker mantle region. The middle of the diagram shows the sediments quickly increasing in thickness as the ocean layer thins. The oceanic crust gives way as the continental crust thrust upward, pushing the mantle downward. When we reach the right side of the diagram the ocean has receded and the continental crust takes up most of the vertical space. The continental crust exhibits a series of listric normal faults, shown as diagonal lines slanted in the general direction of the thrust. A very thin layer of sediment overlays the continental crust, and the mantle has thickened below it.

Figure 8.6.2 Paleogeography of the Basin and Range of California

During the Paleozoic era what is now the Western US was in the deep ocean. The Colorado Plateau region was mostly covered by the shallower Inland Sea, with the easternmost regions of land exposed (this region is indicated with red dashed lines on the map). The zone that corresponds to the Basin and Range is due West of the Colarado Plateau Region, located offshore at the edge of the continental shelf transition to deeper water. It is indicated on the map by a black-dashed triangle oriented with its longest side along what is now the California-Nevada border and its shortest side beginning in what is now Death Valley and moving southwest to the approximate center of the current state. A black circle on the map in the southeast corner of the triangle indicates Death Valley, the approximate location of Paleozoic continental shelf rocks that are now exposed. The third side of the triangle runs almost due North-South. To the northwest of Death Valley and within the triangle, a white circle indicates the approximate location of the deep water sedimentary facies represented by Paleozoic rocks in the White-Inyo Range, east of the Sierra Nevada. The region that will become the future Colorado Plateau lies to the east of this area, straddling a shallow inland sea to the west and a coastal area to the east.

Inserted into the map is a cross-sectional diagram of a generic passive margin representing a geological cross-section that is shown by a solid black line. This line projects due east from what is now the San Francisco Bay Area and moves southeast to a mountainous area in the southern Colorado Plateau Region. In this diagram, from left to right, we see water above a thin layer of sediment, which rests on a thicker oceanic crust above the mantle. The middle of the diagram shows the sediments increasing in thickness as the oceanic crust subducts and thins. It gives way to the continental crust, at roughly the point where the water recedes. The sediment layer and mantle both thin as the continental crust expands. Rift valley strata are shown along the right third of the diagram. Arrows show the approximate location of the White-Inyo and Death Valley facies. This is discussed in the chapter text..

This page titled 8.8: Detailed Figure Descriptions is shared under a CC BY-NC 4.0 license and was authored, remixed, and/or curated by Martha House.

9: SIERRA NEVADA

Introduction to the Sierra Nevada

The Sierra Nevada province is a 644 km-long (400 mile) 80 km-wide (50 mile) region trending north-northwest and located primarily in central and eastern California. A small spur of the province called the Carson Range is just over the border in Nevada. It is bounded by the Cascade province to the north, the Basin and Range province to the east, and the Great Valley province to the west. The Garlock fault forms the southern boundary of of the Sierra Nevada province, separating it from the Mojave province (Figure 9.1)



Figure 9.1: The Sierra Nevada province is located in eastern California, extending into Nevada around Lake Tahoe. The Sierra Nevada province is bounded by the Cascade Range to the north, the Great Valley to the west, and the Basin and Range province to the east. This work by Emily Wright is licensed under CC BY 4.0 a derivative from the Geology of California. Access a detailed description.

The most prominent feature of the Sierra Nevada province is its mountain range of the same name which boasts notable features such as the highest peak in the contiguous United States, Mount Whitney at 4,421 m (14,505 ft); Yosemite Valley and National Park; and Lake Tahoe, the largest alpine lake in North America.

The Sierra Nevada range of California has a complex geologic history that spans 210 million years. While the majority of what would become the Sierra Nevada Province started forming during the Mesozoic Era, what we see today did not exist and is very different from the Sierra Nevada of that time.

The Sierra Nevada Mountains began to form when a series of intrusive plutonic events began to formed much of the range's granitic rock, including iconic features like Half Dome and El Capitan in Yosemite National Park. Over time, erosion and crustal extension gradually revealed plutonic granite formations at Earth's surface. Tectonic forces continued to uplift the emerging Sierra Nevada range, shaping it into the distinctive landscape we observe today.

During the Cenozoic Era, tectonic forces continued to uplift the Sierra Nevada, and the mountains were sculpted by glaciers during the Pleistocene, giving rise to the dramatic landscapes seen today.

This chapter explores the history of this region, including the emplacement, exhumation, and erosion of batholiths - magma chambers that fed a once extensive volcanic arc, the accumulation of gold deposits that would make the Sierra Nevada famous in recent times, and glacial evidence attesting to a changing climate in this region.

Learning Objectives

By the end of this chapter, you should be able to:

- Describe the Sierra Nevada province in terms of rock types, age, and tectonic development.
- Assess the geologic hazards and risks associated with the Sierra Nevada province.
- Describe the geologic processes involved the formation and preservation of gold.

9.1: The Sierra Nevada Today

9.2: Ancient Seas Form the Oldest Rocks

9.3: The Sierra Nevada Batholith

9.4: Gold of the Sierra Nevada

9.5: Volcanic Features of the Sierra Nevada

9.6: Ice Shapes the Landscape

9.7: Natural Hazards of the Sierra Nevada

9.8: Chapter Summary

9.9: Detailed Figure Descriptions

This page titled 9: Sierra Nevada is shared under a CC BY-NC 4.0 license and was authored, remixed, and/or curated by Cole Heap.

9.1: The Sierra Nevada Today

Physiographic Proprieties and Characteristics of the Sierra Nevada

The Sierra Nevada Province is a prominent geological and physiographic region extending approximately 400 miles (644 km) in a north-northwest direction. It is bounded by the Cascade Province to the north, the Basin and Range Province to the east, and the Great Valley Province to the west, with the Garlock Fault forming its southern boundary and separating it from the Mojave Province. This extensive mountain range is characterized by a diverse landscape that includes a mix of rugged peaks, expansive valleys, and dramatic geological features shaped by a long history of tectonic activity.

The Sierra Nevada is primarily composed of intrusive and metamorphic rocks, but it also hosts significant volcanic features that speak to the region's dynamic volcanic past. From ancient lava flows that now form resistant tablelands to striking examples of columnar jointing, the range showcases the results of both ancient and relatively recent volcanic activity. Volcanic domes, remnants of past eruptions, can be found throughout the range, along with deposits from volcanic mudflows, or lahars, which have left their mark on the landscape. The Sierra Nevada's complex geology, diverse topography, and striking natural features make it a key area of interest for understanding the geological history and ongoing processes that have shaped the western United States. This chapter will explore these aspects in detail, highlighting the province's key physiographic properties and characteristics.

Snow and Rain

The Sierra Nevada's climate is profoundly shaped by California's Mediterranean climate, which features wet winters and dry summers. During the fall, winter, and spring months, the range experiences significant precipitation, varying from 510 to 2,030 millimeters (20 to 80 inches), with the majority falling as snow at elevations above 1,800 meters (6,000 feet). This snowfall is a critical component of California's water supply, as the snowpack accumulates during the winter and melts in the spring and summer, feeding rivers and reservoirs that supply water to millions of people in the state. The highest levels of precipitation occur on the central and northern portions of the western slope, particularly between 1,500 and 2,400 meters (5,000 and 8,000 feet) in elevation (see Figure 9.1.1). This phenomenon is driven by orographic lift, where moist air masses are forced upward by the Sierra's towering peaks, cooling and condensing to produce precipitation. However, above 2,400 meters (8,000 feet), precipitation levels diminish as much of the moisture has already been released at lower elevations. This creates a gradient where the western slopes are lush and verdant, while the eastern slopes, lying in the rain shadow of the Sierra crest, are much drier, receiving less than 635 millimeters (25 inches) of precipitation annually.

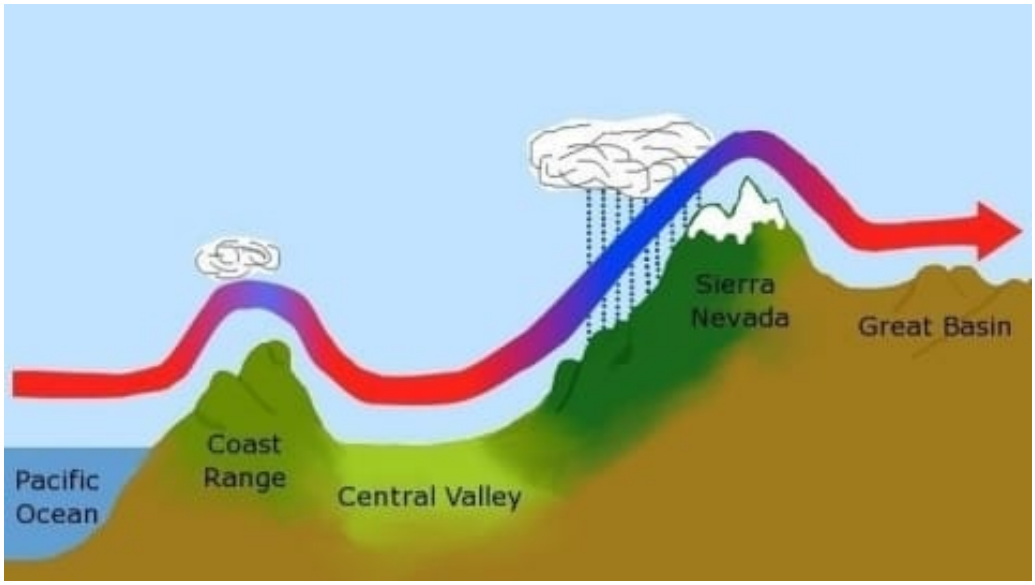


Figure 9.1.1: As air rises up the windward/western side of the Sierra Nevada mountains, it condenses has its moisture squeezed out. When the air begins to descend the leeward/eastern side of the mountains, it expands and is dry. As shown here, the topography of California influences weather patterns, particularly the distribution of precipitation, which is critical for understanding the region's climate and ecosystems. Temperature Change by UC Merced is in the public domain. Access a detailed description.

The summer climate in the Sierra Nevada contrasts sharply with the wetter seasons. Most summer days are marked by dry and warm conditions, typical of the Mediterranean climate. However, the region is not entirely devoid of summer precipitation. Afternoon thunderstorms are relatively common, particularly during the North American Monsoon, which typically occurs in mid to late summer. These storms can be intense, sometimes delivering over an inch of rain in a short period, leading to flash flooding and contributing to the fire risk in the region due to lightning strikes. The Sierra's highest elevations, which boast an alpine climate, experience cooler temperatures year-round and retain snow cover well into the summer months. These alpine zones are characterized by short, cool summers and long, harsh winters, where the snowpack can reach significant depths. The combination of heavy winter snowfall and summer thunderstorms creates a dynamic and varied climate across the Sierra Nevada, influencing the region's ecosystems, hydrology, and fire regimes.

Mountains

The Sierra Nevada Mountains, the most prominent geological feature of the Sierra Nevada Province, are renowned for their dramatic topography and significant elevation changes. This majestic range is predominantly underlain by felsic to intermediate plutonic and metamorphic rocks, which have been exposed and uplifted over millions of years through tectonic processes. The Sierra Nevada is distinguished by its asymmetrical profile (Figure 9.1.2): it gently slopes westward towards California's Great Valley while its eastern side rises sharply from the floor of the Great Basin, a contrast accentuated by the Sierra Nevada fault system. This fault system marks a significant tectonic boundary that has played a crucial role in shaping the range's steep eastern escarpment.

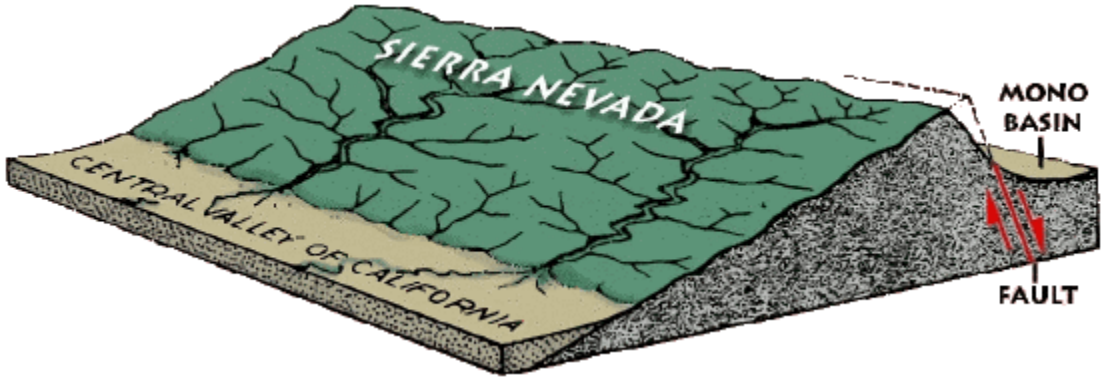


Figure 9.1.2: The Sierra Nevada mountain range is asymmetric with a shallowly sloped western side and a notably steeper eastern side. Sierra Fault by the USGS is in the public domain. Access a detailed description.

Elevations within the Sierra Nevada range from approximately 2,700 to 4,300 meters (9,000 to 14,000 feet), with the highest peaks located in the southern part of the range. The most notable of these is Mount Whitney, the tallest peak in the contiguous United States, standing at an elevation of 14,496 feet (4,418 meters). Mount Whitney towers more than 3,048 meters (10,000 feet) above the Owens Valley to the east, creating a striking contrast between the mountain's summit and the valley floor. The southern Sierra Nevada is particularly rugged and elevated, featuring a series of high peaks and steep canyons. This part of the range also exhibits a noticeable westward bend just north of the Garlock Fault, a major geological feature that marks the boundary between the Sierra Nevada and Mojave Desert provinces.

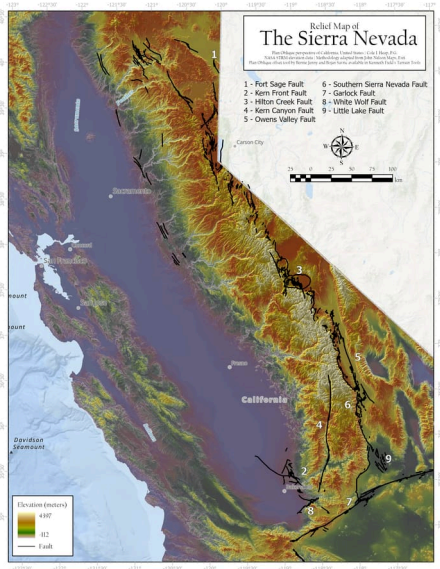


Figure 9.1.3: "Relief Map of the Sierra Nevada" by Cole Heap is licensed under CC BY-NC 4.0 Constructed in a GIS using data from California Open Data Portal. Access a detailed description.

To the north, the Sierra Nevada gradually decreases in elevation, with peaks becoming less prominent as the range extends towards the Cascade Province (Figure 9.1.3). This gradual reduction in height is accompanied by a change in landscape, with the northern Sierra displaying more gentle topography compared to the rugged terrain of the southern Sierra. The varied elevations and distinct topographical features of the Sierra Nevada not only define its landscape but also influence the region's climate, hydrology, and ecology, making it a critical area for geological and environmental studies.

Streams and Canyons

The Sierra Nevada Province's asymmetric topography significantly influences its river systems. On the western side of the range, the gentler slope allows for the development of a series of regularly spaced river drainages that flow toward the Pacific Ocean. These rivers, which cut through the mountainous terrain, have carved deep valleys and gorges over millions of years. From north to south, the major rivers include the Feather, Yuba, American, Cosumnes, Mokelumne, Stanislaus, Tuolumne, San Joaquin, Kings, Tule, and Kern. These rivers play a crucial role in the hydrology of California, providing water for agriculture, cities, and ecosystems throughout the Central Valley and beyond.

In contrast, the eastern slope of the Sierra Nevada is much steeper, leading to rivers with high gradients that rapidly descend into the adjacent Owens Valley and other low-lying areas. The stark difference in elevation between the crest of the Sierra and the valley floor creates some of the most dramatic landscapes in the region. The rivers on this side of the range, though fewer in number and shorter in length, are characterized by their fast flow and the deep canyons they have carved into the eastern escarpment. These eastern rivers are critical for the arid regions they drain into, providing essential water resources in an otherwise dry landscape.

The accompanying map (Figure 9.1.4) illustrates the major river systems in California, highlighting the westward-flowing rivers of the Sierra Nevada Province and their contribution to the state's overall water system. The image serves as a visual guide to understanding the distribution and flow patterns of these rivers, emphasizing the importance of the Sierra Nevada's topography in shaping California's hydrology.



Figure 9.1.4: Most of California's rivers originate in the Sierra Nevada province and flow westward feeding into either the Sacramento or San Joaquin rivers. They ultimately flow into the Pacific Ocean through San Francisco Bay. California Rivers by Shannon1 via Wikimedia Commons is in the public domain. Access a detailed description.

References

1. Argus, D.F. and Gordon, R.G. (1991). *Current Sierra Nevada-North America motion from very long base-line interferometry: implications for the kinematics of the western United States*. Geology, v. 19, p. 1085-1088.
2. Bateman, P.C. (1992). *Plutonism in the central part of the Sierra Nevada batholith, California*. U.S. Geological Survey Professional Paper, v. 1483.
3. Figueroa, A.M. and Knott, J.R. (2010). *Tectonic geomorphology of the southern Sierra Nevada mountains (California): evidence for uplift and basin formation*. Geomorphology, v.123.
4. Miller, J. R., & Dunne, T. (1977). *Topographic influence on the regional groundwater flow systems of the Sierra Nevada*. Journal of Hydrology, 35(1-2), 35-49.
5. Storer, T. I., & Usinger, R. L. (1963). *Sierra Nevada Natural History: An Illustrated Handbook*. University of California Press.

This page titled 9.1: The Sierra Nevada Today is shared under a CC BY-NC 4.0 license and was authored, remixed, and/or curated by Cole Heap.

9.2: Ancient Seas Form the Oldest Rocks

What We Know From the Oldest Rocks

The Sierra Nevada's geological history is rich and complex, with the oldest rocks exposed in the range dating back to around 540 million years ago, during the Cambrian period. These ancient rocks provide a glimpse into the early stages of the Sierra Nevada's formation. However, even older rocks that offer more insights into the region's deep geological past are found in the nearby White and Inyo Mountains, located just to the east (see Basin and Range). These areas are part of the Basin and Range Province and contain rocks that predate the Sierra Nevada's exposed formations, helping geologists piece together the broader tectonic and sedimentary history of the western United States.

Geologists categorize the ancient rocks of the Sierra Nevada into two primary groups based on their ages: the Paleozoic rocks, which are older than 250 million years, and the Mesozoic rocks, which are older than 65 million years. The Paleozoic rocks predominantly consist of sedimentary sequences that were deposited in ancient marine environments, including limestone, shale, and sandstone. These rocks record a time when the region was submerged under a shallow sea, hosting diverse marine life. In contrast, the Mesozoic rocks are primarily igneous and metamorphic, formed during a period of significant tectonic activity associated with the subduction of the Farallon Plate beneath the North American Plate. This tectonic activity led to the formation of large magmatic bodies, regional metamorphism, and the accretion of various terranes, shaping the Sierra Nevada into its current form.

Sediments Accumulate in Ancient Seas

During the Paleozoic Era, more than 400 million years ago, the western margin of North America was a passive margin that ran from present day southeastern Idaho, through central Nevada, and into Southern California (see A Brief Geologic History of California). Offshore, where what is now the Sierra Nevada was under water, thick layers of sediments accumulated: 1 km (0.6 mi) in the south to 10 m (6 mi) in the north indicating that the ocean basin was deeper to the south.

For more than 500 million years, these sediments accumulated, creating a record of what the environment was like during that time. Most of these sediments are marine in origin indicating they formed in a shallow sea. The types of rocks and the few recognizable fossils that remain (most have been obliterated by metamorphism and deformation) indicate that the eastern side of the sierra was closer to shore.

Seaward, beyond the continent, were "island arcs" not unlike the Aleutian island arc that exists today (Figure 9.2.1), an offshore omen of what would later become California and the Sierra Nevada.

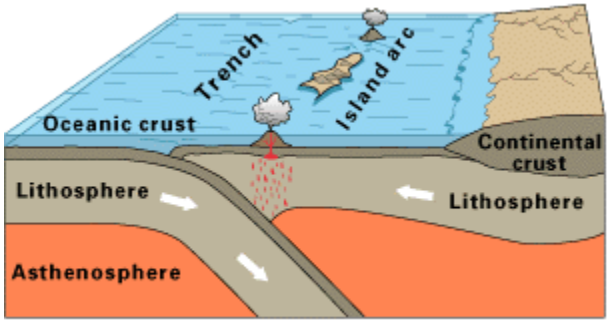


Figure 9.2.1: An illustration of what western North America may have looked like during the Paleozoic era. The western edge was a passive margin where ocean sediments were depositing. Out at sea, subduction of oceanic crust beneath other oceanic crust was forming island arcs. Ocean by the USGS is in the public domain. Access a detailed description.

How these ancient seafloor sediments and offshore island arcs wound up metamorphosed and accreted onto the western margin of North America is an interesting and complex story and continues to be an area of active research for geologists.

Query 9.2.1

This interactive element is not available in this format. Visit the link or scan the QR code to access it online.

View this Interactive Content online

Metamorphic Roof Pendants

Today, the oldest rocks of the Sierra Nevada no longer resemble ancient seafloor sediments. They have been metamorphosed by the intrusion of the Sierra Nevada batholith. Since the intrusion, weathering and erosion have exposed the batholith to the surface, leaving small remnants of the metasedimentary rocks interspersed throughout as "roof pendants". The name comes from the fact that the country rock is literally hanging down from the roof of the magma chamber like a pendant (Figure 9.2.2).

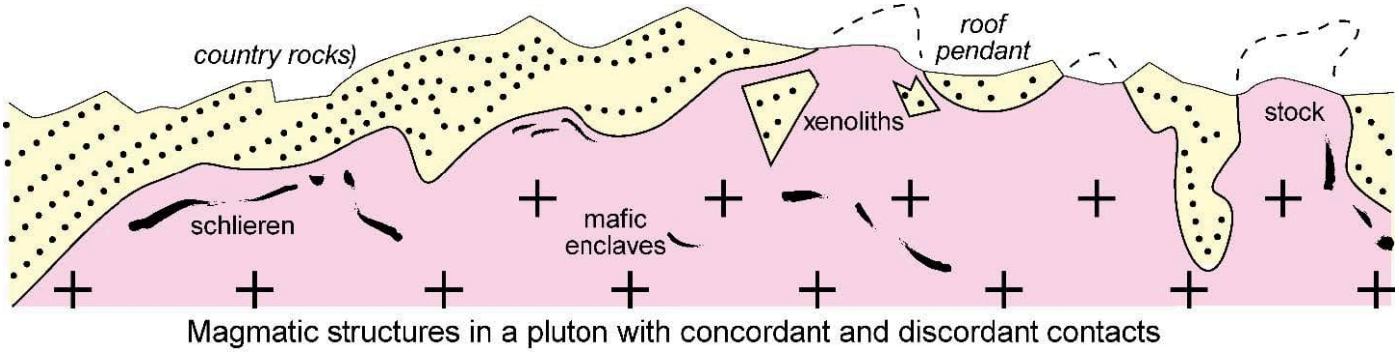


Figure 9.2.2: Features formed by the intrusion of plutonic igneous rock into preexisting country rock. Upon erosion, roof pendants form resembling "islands" of country rock surrounded by plutonic rock. Pluton by Jean-Pierre Berg is licensed under CC BY-NC 4.0. Access a detailed description.

More than one hundred of these roof pendants speckle the otherwise intrusive igneous rocks of the Sierra Nevada, concentrated in the central and southern parts of the province. The largest of these roof pendants include the Mt. Tom pendant, the Mt. Morrison pendant (Figure 9.2.3), and the Saddlebag Lake pendant.

These "roof pendants" record moderate to high amounts of ductile deformation, resembling stretched taffy in some locations.



Figure 9.2.3: Mt. Morrison roof pendant visible from Convict Lake on the eastern side of the Sierra Nevada range. Dark-colored metamorphic country rock is in contact with the lighter colored plutonic rock. Boulders by Ralph Earlandson is licensed under CC BY 2.0. Access a detailed description.

Accreted Terranes

While roof pendants contain the oldest rocks of the Sierra Nevada, a majority of the metamorphic rocks are preserved as roughly north-south trending metamorphic belts. Sediments stopped being deposited around 180 to 160 Ma. During this time, subduction of the Farallon plate beneath the North American plate initiated, slowly shoving the oceanic crust beneath the continental crust. As oceanic crust continued to subduct, it brought along with it slivers of volcanic arcs and microcontinents which were too buoyant to subduct and were thus accreted or attached to the western edge of North America. The earliest known of these orogenic or accretion events in western North America is known as the Antler Orogeny.

These sequential accretions are known as terranes or exotic terranes because they are pieces of crust that were transported from elsewhere. Today, each terrane is comprised of numerous identifiable rock units and each terrane has a distinct geologic history. What separates these terranes are faults and shear zones, sometimes called sutures or suture zones. Not coincidentally, major gold deposits were discovered along these suture zones.

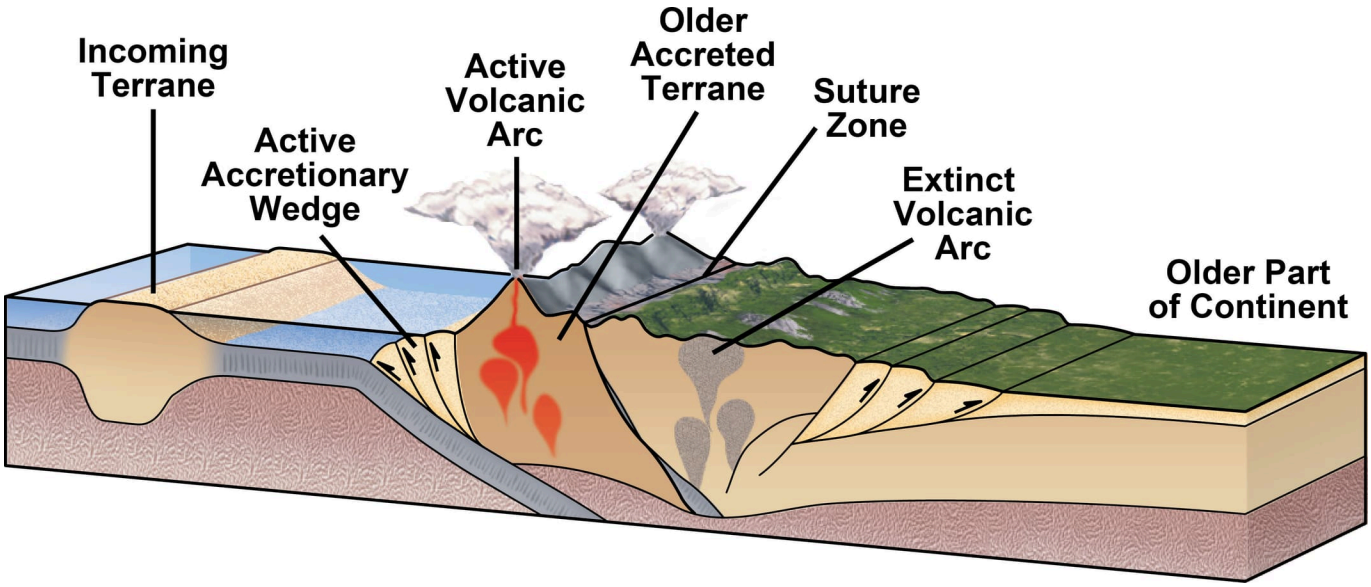


Figure 9.2.4: An exotic terrane attached to subducting oceanic crust approaching the continent. Beneath the continent, flux melting is taking place, forming a continental volcanic arc within older accreted terrane. Terrane Accretion by the National Park Service is in the public domain. Access a detailed description.

The Sierra Nevada terranes resemble a series of books that have fallen down on their book shelf: dipping down toward the east, with rocks within each terrane getting younger toward the east. The foothills terranes are incredibly complex and difficult to parse, thus the exact number of terranes remains an area of active research and debate among geologists. Most recent observations suggest that there are five distinct exotic terranes: the Northern Sierra terrane, Feather River terrane, Calaveras Complex, Jura-Triassic arc belt, and Middle—Late Jurassic arc sequence (Figure 9.2.5).

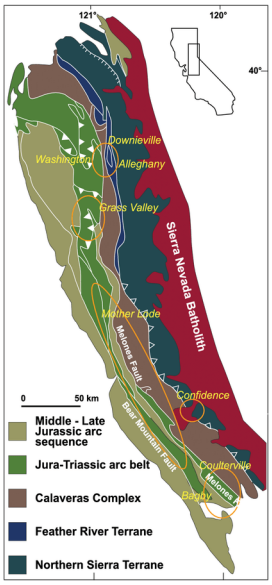


Figure 9.2.5: Major exotic terranes of the northern Sierra Nevada province. The five terranes: Northern Sierra Terrane (dark gray), Feather River (dark blue), Calaveras Complex (brown), Jura-Tirassic arc belt (green), and Middle-late Jurassic Arc Sequence (tan) are separated by faults and shear zones (white lines). The Melones Fault and Bear Mountain Fault are two major boundaries. "Terrane map of the western Sierra Nevada Foothills metamorphic belt with location of gold districts" by Arizona Geological Society in the public domain. Access a detailed description.

Northern Sierra Terrane

The Northern Sierra Terrane (Figure 9.2.5 indicated by dark gray) is the easternmost of the five terranes in the Sierra Nevada. More of the terrane is exposed in the north than in the south. It contains a number of different rock units, but its most notable unit is the Shoo Fly Complex. The Shoo Fly Complex consists primarily of:

- Mylonitic gneisses
- Schist and calcareous rocks
- Rare amphibolite
- Phyllite
- Metabasite and metaultramafic blocks

The protolithic sediments of the Northern Sierra terrane were initially deposited during the early Paleozoic, before the Antler orogeny. They were accreted to western North America during the Antler orogeny.

Shoo Fly Complex

The Shoo Fly Complex is a vital component of the Northern Sierra Terrane, comprising Paleozoic metasedimentary and metavolcanic rocks that have undergone extensive deformation and metamorphism. This complex provides critical insights into the tectonic processes that shaped the Sierra Nevada. Its primary rock types include mylonitic gneisses, schist, calcareous rocks, rare amphibolite, phyllite, and blocks of metabasite and metaultramafic rocks. These varied rock types reflect the diverse depositional environments and tectonic settings during the early Paleozoic era. Mylonitic gneisses, characterized by their foliated texture, formed under intense shear stress conditions, indicating significant deformation typically associated with major fault zones. Schist (Figure 9.2.6), known for its pronounced foliation and abundant mica minerals, and calcareous rocks, including marble and calc-silicate rocks, suggest ancient carbonate sediment presence. Rare amphibolite, formed from basaltic rock metamorphism and rich in hornblende, indicates volcanic activity and high-pressure metamorphism. Phyllite, a low- to medium-grade metamorphic rock with a foliated texture finer than schist but coarser than slate, forms from the metamorphism of mudstones and shales. Metabasite and metaultramafic blocks, remnants of ancient oceanic crust and mantle materials, suggest the incorporation of oceanic lithosphere into the continental margin during subduction.



Figure 9.2.6: Chlorite schist like that found in the Shoo Fly Complex. Chlorite Schist by by Siim is licensed under CC BY-SA 3.0. Access a detailed description.

The Shoo Fly Complex records a complex tectonic history beginning in the early Paleozoic, prior to the Antler Orogeny. Initially deposited in a marine environment, the protolithic sediments of the Shoo Fly Complex were accreted onto the western margin of North America during the Devonian period due to the Antler Orogeny. This significant tectonic event involved the collision and accretion of island arcs and other terranes onto the North American continent, causing extensive deformation and metamorphism in the Shoo Fly Complex, evidenced by mylonitic textures and high-grade metamorphic minerals. The subsequent subduction of the Farallon Plate during the Mesozoic further influenced the complex, leading to additional metamorphic and deformational events.

Structural features of the Shoo Fly Complex include numerous folds, faults, and shear zones that record the intense tectonic forces shaping the region. Major faults, such as the Melones Fault Zone, define the boundaries of the Shoo Fly Complex and its juxtaposition with adjacent terranes. The complex's folds are typically tight and asymmetrical, reflecting compressional tectonic regimes, while prevalent shear zones, characterized by mylonitic fabrics, indicate significant ductile deformation. These structural

features are crucial for understanding the tectonic evolution of the Northern Sierra Terrane and the broader Sierra Nevada region.

Feather River Terrane

The Feather River Terrane (Figure 9.2.5 indicated in dark blue) is a geologically significant and distinct component of the Northern Sierra Nevada, primarily exposed in the northern region of the range. This terrane, indicated by dark blue on geological maps, is a narrow zone dominated by Devonian-age ultramafic rocks, particularly serpentinized peridotite. These rocks are remnants of ancient oceanic crust and upper mantle that were accreted to the North American continental margin during the late Paleozoic to early Mesozoic periods. The Feather River Terrane is especially notable for including the Permian Devil's Gate ophiolite, which likely formed atop the older peridotite. This ophiolite complex, composed of gabbro, sheeted dikes, and basaltic pillow lavas, represents a well-preserved slice of oceanic lithosphere that has undergone varying degrees of metamorphism since its emplacement.

Structurally, the Feather River Terrane is bounded by major fault zones that delineate its relationships with neighboring geological units. To the east, it is separated from the Northern Sierra Terrane by the Downieville Fault, while to the west, it is bordered by the Calaveras Complex, with the Goodyears Creek and Rich Bar faults marking this boundary. These faults are part of the larger Melones Fault Zone, a critical structural feature that played a central role in the accretion and deformation processes affecting the Feather River Terrane. The absence of the Feather River Terrane south of Interstate 80, where the Shoo Fly Complex of the Northern Sierra Terrane comes into direct contact with the Calaveras Complex, underscores the localized nature of this terrane and its unique tectonic history.

The Feather River Terrane provides valuable insights into the tectonic evolution of the Sierra Nevada, particularly in understanding the processes of subduction and accretion that shaped the region. The complex interplay between these ultramafic rocks, their overlying ophiolitic sequences, and the surrounding fault systems reveals a dynamic geological past, marked by significant crustal movements and metamorphism.

In the southern Sierra Nevada, south of Interstate 80, the Feather River Terrane is not present and the Shoo Fly complex of the Northern Sierra Terrane is in direct contact with the Calaveras Complex.

Calaveras Complex

The Calaveras Complex, a significant geological unit within the Northern Sierra Nevada Terrane, is characterized by its complex and challenging assemblage of rocks. Following the Antler Orogeny, additional sedimentary rocks accumulated along the newly formed continental margin. As the North American plate converged with the subducting Farallon plate, these sediments were progressively shoved into the accretionary wedge. This tectonic activity metamorphosed the sediments into a variety of metamorphic rocks, including slates, phyllites, and serpentinite, creating the intricate and diverse rock assemblages seen in the Calaveras Complex today.

The ongoing subduction and associated flux melting resulted in the intrusion of granitic magma into these metamorphosed sediments. These granitic intrusions further complicated the geological interpretation of the Calaveras Complex, making it a challenging area for even experienced geologists to decipher. The region south of Interstate 80 highlights the complexity of this terrane, where the Shoo Fly Complex of the Northern Sierra Terrane comes into direct contact with the Calaveras Complex along a significant thrust fault. This contact zone provides valuable insights into the tectonic processes that have shaped the Northern Sierra Nevada, reflecting the dynamic interactions between sedimentary deposition, subduction, metamorphism, and magmatic intrusion.

As previously mentioned, south of Interstate 80, the Shoo Fly Complex of the Northern Sierra Terrane and the Calaveras Complex are in direct contact. This particular contact is a thrust fault.

Jurassic-Triassic Arc Belt (Central Belt)

The Jurassic-Triassic Arc Belt, also know as the Central Belt, is the next terrane to the west. Like the Calaveras Complex, it is a complicated mess of rocks. At its most basic, the Jurassic-Triassic Arc Belt is Paleozoic ocean crust, overlain by a volcanic arc that existed approximately 200 to 150 million years ago. The Central Belt is composed of a diverse assemblage of metamorphosed volcanic and sedimentary rocks, including basaltic flows, volcanic breccias, tuffs, cherts, and argillites. These rocks were originally deposited in a marine environment, forming part of a volcanic island arc that developed above a subduction zone where oceanic crust was being consumed beneath the North American continental margin.

The tectonic history of the Jurassic-Triassic Arc Belt is marked by intense deformation and metamorphism, reflecting the dynamic processes at play during its formation. The rocks within the Central Belt have been significantly folded, faulted, and sheared, indicating multiple phases of tectonic activity. This deformation is closely associated with the accretion of the arc complex onto the western edge of North America, as well as subsequent tectonic events that shaped the Sierra Nevada. The Central Belt is also intruded by granitic plutons of the Sierra Nevada Batholith, particularly during the Late Jurassic to Early Cretaceous periods, which further influenced the structural and metamorphic characteristics of the belt. The interaction between these intrusions and the arc rocks has led to contact metamorphism, creating complex mineral assemblages and adding to the geological diversity of the region. The Jurassic-Triassic Arc Belt is essential for understanding the tectonic and magmatic evolution of the Sierra Nevada and provides a window into the processes that operated along the western margin of North America during the Mesozoic era.

Middle-Late Jurassic Arc Sequence/Jurassic Foothills Belt

The Middle-Late Jurassic Arc Sequence, often referred to as the Jurassic Foothills Belt, is a prominent geological feature within the Northern Sierra Nevada Terrane. This sequence represents the remnants of a volcanic arc that was active approximately 160 to 150 million years ago during the Jurassic period. The Jurassic Foothills Belt is composed of a complex assemblage of metavolcanic and metasedimentary rocks, including volcanic flows, tuffs, graywackes, and shales, all of which have been subjected to varying degrees of metamorphism. These rocks were originally deposited in a marine environment, likely as part of a volcanic island arc system associated with the subduction of oceanic crust beneath the western margin of North America.

The tectonic history of the Middle-Late Jurassic Arc Sequence is marked by significant deformation events, which have imparted complex structural features to the belt. The rocks within the Jurassic Foothills Belt exhibit folding, faulting, and shearing, indicative of the intense tectonic forces that shaped the region during the Jurassic period. These structural complexities are often associated with the emplacement of granitic plutons from the Sierra Nevada Batholith, which intruded into the arc sequence during the Late Jurassic to Early Cretaceous periods. The interaction between these plutons and the surrounding metamorphic rocks has resulted in contact metamorphism, further altering the original characteristics of the arc sequence. The Jurassic Foothills Belt is a key component in understanding the evolution of the Sierra Nevada and the broader tectonic framework of the western United States during the Mesozoic era.

Due to its nature and formation, yet another ophiolite appears here in the Middle-Late Jurassic Arc Sequence: the Smartville Complex ophiolite.

Smartville Complex Ophiolite

The Smartville Complex is composed of a range of ultramafic and mafic rocks, including serpentinized peridotite, gabbro, sheeted dikes, and basaltic pillow lavas, which collectively represent the different layers of oceanic lithosphere. These rocks were originally formed at a mid-ocean ridge or back-arc basin and were later thrust onto the North American Plate as the Farallon Plate subducted beneath it. The accretion of the Smartville Complex provides critical insights into the processes of subduction, obduction, and the assembly of the Sierra Nevada terranes during the Jurassic. This ophiolite is also significant for its association with gold-bearing quartz veins, making it an area of historical mining interest, much like many of the terranes found in the Northern Sierra Terranes (Figure 9.2.7).

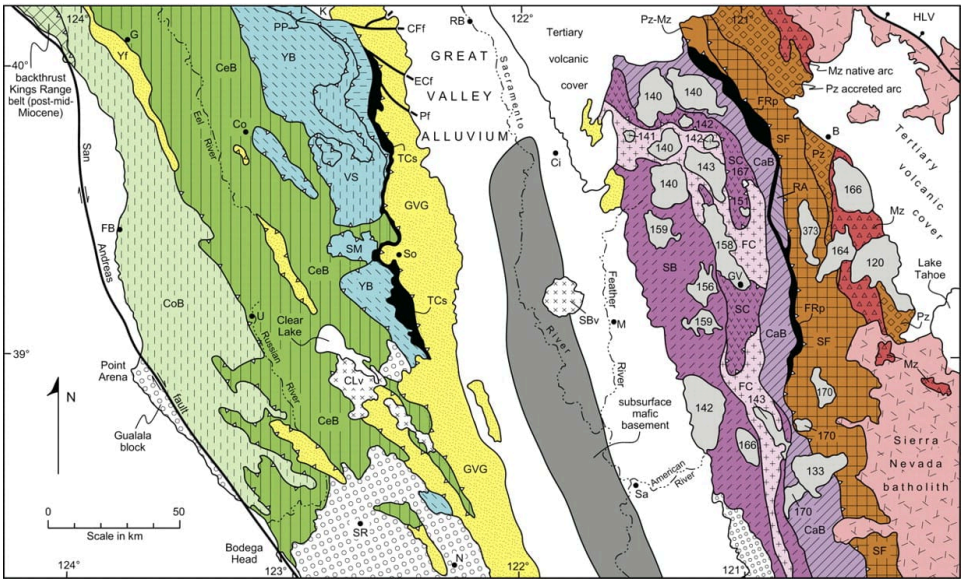


Figure 9.2.7: Map showing plutons and accreted terranes of the Sierra Nevada, California by the USGS is in the public domain. Access a detailed description.

Some of the oceanic crust, rather than being subducted, was instead obducted up onto the continent where it has been preserved for geologists to study. This process of obduction is further described in the Klamaths and Coast Ranges chapters.

Southern Sierra Terrane

The Sonoma Orogeny brought additional terranes to the North American continent including the Kings River and Kaweah Terranes in the Southern Sierra Nevada. The Southern Sierra Nevada region is characterized by a series of metamorphic terranes that provide key insights into the tectonic history and geological evolution of the area. These terranes, which include the Kings River, Mineral King, and Kaweah terranes, represent ancient volcanic and sedimentary sequences that have been significantly altered by metamorphism and deformation. Each terrane has a unique geological history and composition, contributing to the overall complexity of the Southern Sierra Nevada.

Kings River Terrane

The Kings River Terrane is a significant metamorphic terrane in the southern Sierra Nevada, primarily composed of Paleozoic and Mesozoic rocks. This terrane is characterized by a complex assemblage of metamorphic rocks, including schist, gneiss, quartzite, and marble. These rocks were originally sedimentary and volcanic in origin but have undergone extensive metamorphism due to tectonic processes, such as subduction and continental collision.

The Kings River Terrane is notable for its high-grade metamorphic rocks, which indicate deep burial and high-temperature conditions during metamorphism. This terrane is also associated with several significant faults and shear zones, which have played a crucial role in its geological evolution. The presence of these structural features suggests that the Kings River Terrane has experienced multiple episodes of deformation, contributing to its complex geological history.

Kings River Ophiolite

The Kings River ophiolite, located in the southwestern Sierra Nevada foothills of California, is a significant geological formation that offers insights into the region's complex tectonic history. This ophiolite sequence represents remnants of ancient oceanic crust and upper mantle that were thrust onto the continental margin during the Late Paleozoic to early Mesozoic era. The Kings River ophiolite is composed of a variety of rock types, including serpentinized peridotite, gabbro, basalt, and chert, which collectively provide a snapshot of oceanic lithosphere and the processes associated with its formation and emplacement. The presence of these rocks in the Sierra Nevada foothills (Figure 9.2.8) indicates a history of subduction and accretion, where pieces of oceanic crust were scraped off and added to the edge of the North American plate.

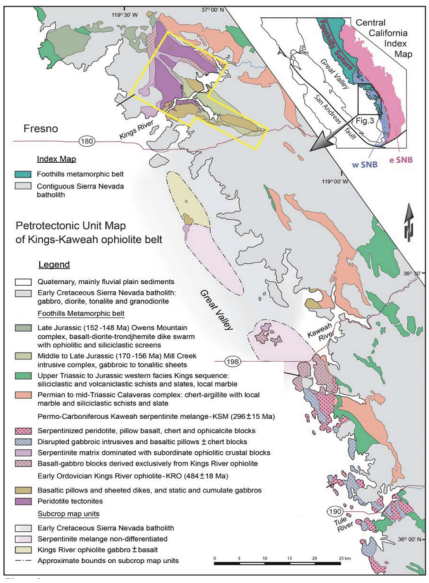


Figure 9.2.8: Generalized map showing the Kings River ophiolite, Kaweah serpentinite melange, and metasedimentary rock pedants along the eastern margin of the ophiolite belt by J. Saleeby and Caltech Tectonics Observatory is licensed under CC BY 2.0. Access a detailed description.

The structural complexity of the Kings River ophiolite is evident in its faulted and folded nature, reflecting the intense tectonic forces that have acted upon it. This ophiolite is crucial for understanding the tectonic evolution of the southwestern Sierra Nevada, as it marks the location of a former subduction zone where oceanic and continental plates interacted. Studies of the Kings River ophiolite have revealed valuable information about the processes of subduction, accretion, and the dynamics of ancient oceanic crust (Figure 9.2.9). The ophiolite also hosts various mineral deposits, including chromite and asbestos, which have been of economic interest in the past. Ongoing research continues to unravel the complex geological history recorded in this portion of the Sierra Nevada.

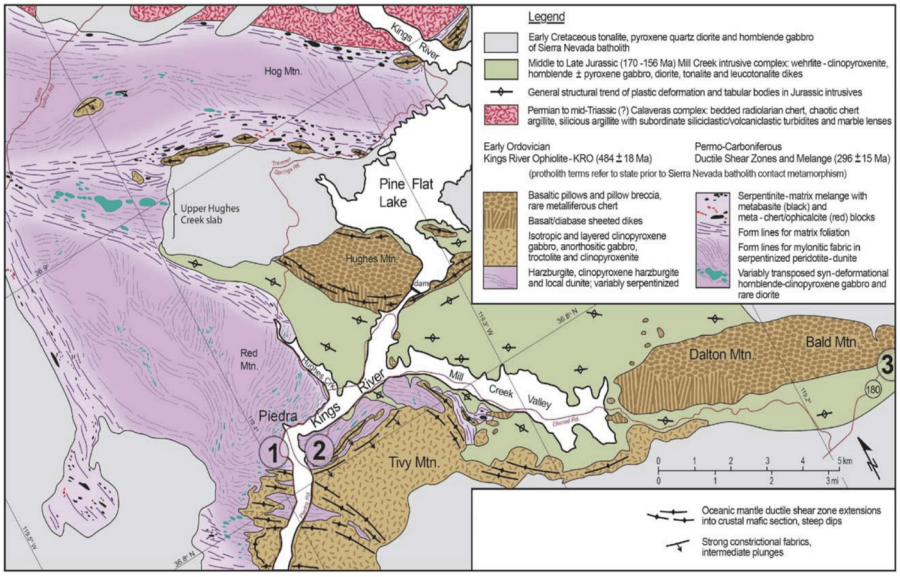


Figure 9.2.9: A zoomed in and generalized map showing the Kings River ophiolite by J. Saleeby and Caltech Tectonics Observatory is licensed under CC BY 2.0. Access a detailed description.

Mineral King Terrane

The Mineral King Terrane is another important metamorphic terrane in the southern Sierra Nevada, known for its diverse rock types and significant mineralization. This terrane primarily consists of metavolcanic and metasedimentary rocks, including amphibolite, schist, and phyllite. The Mineral King Terrane is also characterized by the presence of serpentinized ultramafic rocks,

which are remnants of ancient oceanic crust that have been metamorphosed and altered by tectonic processes.

Metamorphism in the Mineral King Terrane occurred under conditions of medium to high pressure and temperature, resulting in the formation of distinctive mineral assemblages. The terrane is also notable for its mineral deposits, particularly those containing copper, zinc, and silver. These mineral deposits are associated with hydrothermal activity along fault zones and shear zones, which provided pathways for mineral-rich fluids to circulate and precipitate ore minerals.

Kaweah Terrane

The Kaweah Terrane is a key metamorphic terrane in the southern Sierra Nevada, characterized by its complex lithology and tectonic history. This terrane includes a wide variety of metamorphic rocks, such as schist, gneiss, quartzite, and amphibolite. The Kaweah Terrane also contains significant amounts of metavolcanic and metasedimentary rocks, which were originally part of an ancient volcanic arc and associated sedimentary basin.

Metamorphism in the Kaweah Terrane occurred under a range of pressure and temperature conditions, leading to the development of diverse mineral assemblages and metamorphic textures. This terrane is also associated with major fault zones, such as the Kern Canyon Fault, which have played a significant role in its tectonic evolution. The presence of these fault zones indicates that the Kaweah Terrane has undergone significant deformation, contributing to its complex geological structure.

The Kaweah Terrane is also notable for its mineral deposits, particularly those containing gold and other precious metals. These deposits are often found in association with quartz veins and shear zones, which provided conduits for hydrothermal fluids to circulate and precipitate ore minerals. The economic importance of these mineral deposits has historically made the Kaweah Terrane a focus of mining activity in the southern Sierra Nevada.

References

1. Bateman, P. C. (1992). *Plutonism in the central part of the Sierra Nevada Batholith, California*. U.S. Geological Survey Professional Paper 1483.
2. Beard, J. S., & Day, H. W. (1987). The Smartville Complex: Jurassic oceanic lithosphere and its bearing on the tectonics of western Nevada. *Geological Society of America Bulletin*, 99(3), 417-427.
3. Bogen, N. L., Schweickert, R. A., & Cowan, D. S. (1997). Tectonics of the Shoo Fly Complex, Sierra Nevada, California: A Paleozoic subduction complex. *Geological Society of America Bulletin*, 109(6), 777-794.
4. Coleman, R. G. (1977). *Ophiolites: Ancient Oceanic Lithosphere?*. Springer-Verlag.
5. Ducea, M. N. (2001). The California arc: Thick granitic batholiths, eclogite residues, lithospheric-scale thrusting, and magmatic flare-ups. *GSA Today*, 11(11), 4-10.
6. Glazner, A. F., & Stock, J. M. (1999). Geology of the Sierra Nevada. *University of California Press*.
7. Harwood, D. S. (1992). Stratigraphy and structure of the Shoo Fly Complex, northern Sierra Nevada, California. *U.S. Geological Survey Professional Paper 1529*.
8. Harwood, D. S., & Helley, E. J. (1987). Late Triassic and Jurassic geology of the northern Sierra Nevada, California. *U.S. Geological Survey Professional Paper 1225*.
9. Saleeby, J. B. (1981). Oceanic crustal sections in the central Sierra Nevada and foothills, California. *Geological Society of America Bulletin*, 92(9), 663-678.
10. Saleeby, J. B., & Busby, C. J. (1993). Paleogeographic and tectonic setting of the Jurassic volcanic arc in the southern Sierra Nevada, California. *Geological Society of America Bulletin*, 105(11), 1650-1670.
11. Saleeby, J. B. (1982). Polyphase tectonics in the eastern Sierra Nevada Shoo Fly Complex. *Geological Society of America Bulletin*, 93(3), 264-273.
12. Saleeby, J. B. (2003). Segmentation of the Laramide slab: Evidence from the southern Sierra Nevada region. *Geological Society of America Bulletin*, 115(6), 655-668.
13. Schweickert, R. A., & Snyder, W. S. (1981). Paleozoic plate tectonics of the western U.S.: Implications for the Shoo Fly Complex of the northern Sierra Nevada, California. *Journal of Geophysical Research: Solid Earth*, 86(B1), 664-674.
14. Sharp, W. D. (1988). Pre-Cretaceous crustal evolution in the Sierra Nevada region, California. *Tectonics*, 7(4), 887-904.
15. Wakabayashi, J., & Sawyer, T. L. (2001). Stream incision, tectonics, uplift, and evolution of topography of the Sierra Nevada, California. *Journal of Geology*, 109(5), 539-562.
16. Wood, D. J., & Saleeby, J. B. (1998). Late Cretaceous-Paleocene extensional collapse and disaggregation of the southernmost Sierra Nevada batholith. *International Geology Review*, 40(8), 706-743.

This page titled 9.2: Ancient Seas Form the Oldest Rocks is shared under a CC BY-NC 4.0 license and was authored, remixed, and/or curated by Cole Heap.

9.3: The Sierra Nevada Batholith

How Plutonic Rock Forms

Plutonic rocks, or intrusive igneous rocks, form from the cooling and solidification of magma beneath the Earth's surface. This process differs significantly from the formation of volcanic or extrusive rocks, which cool rapidly at or near the surface. The formation of plutonic rocks involves the slow crystallization of magma, allowing for the development of large, visible crystals. This slow cooling occurs because the magma is insulated by the overlying rock, resulting in coarse-grained textures typical of plutonic rocks. Plutonic rocks typically form large bodies known as plutons, which can range in size from a few cubic meters to hundreds of cubic kilometers.

The origin of the magma that forms plutonic rocks can be traced to several geological processes, including partial melting of the mantle or crust due to subduction, rifting, or mantle plumes. In subduction zones, for example, oceanic crust is pushed beneath continental crust, leading to melting and magma formation. This magma can then rise through the crust, cooling slowly to form plutonic rocks. This process can take thousands to millions of years, during which the magma can interact with surrounding rock, further influencing its composition and texture.

One of the critical aspects of plutonic rock formation is the nucleation process. Nucleation is the initial stage of crystal formation where small clusters of atoms or molecules begin to arrange into a crystal lattice. In a cooling magma body, nucleation occurs when the temperature drops below the temperature at which crystals begin to form from the melt. The rate of nucleation depends on several factors, including the degree of undercooling, the presence of nucleation sites, and the composition of the magma.

As the temperature continues to decrease, these small clusters grow into larger crystals through a process known as crystal growth. The balance between nucleation and crystal growth determines the final texture of the plutonic rock. In slowly cooling magmas, crystal growth dominates, leading to the formation of large, well-developed crystals. Conversely, in rapidly cooling magmas, nucleation may dominate, resulting in many small crystals. This balance is critical in developing the coarse-grained texture characteristic of plutonic rocks. (For more information please see Minerals and Rocks).

The formation of plutonic rocks is a fundamental geological process that contributes to the growth of continental crust and the creation of various mineral deposits. The slow cooling and crystallization processes allow for the development of diverse mineral assemblages, making plutonic rocks important sources of valuable minerals and providing essential insights into the Earth's geological history.

Query 9.3.1

Interactive Content

This interactive element is not available in this format. Visit the link or scan the QR code to access it online.

View this Interactive Content online

Query 9.3.2

This interactive element is not available in this format. Visit the link or scan the QR code to access it online.

View this Interactive Content online

Sierran Granodiorite

The Sierra Nevada Batholith is predominantly composed of granodiorite, a coarse-grained plutonic rock. Granodiorite is a significant and widespread component of the Sierra Nevada range, playing a crucial role in its geological and geomorphological character. The rock is characterized by its intermediate composition between granite and diorite, containing a higher proportion of plagioclase feldspar relative to potassium feldspar, with abundant quartz and biotite. This mineralogical composition gives granodiorite its distinctive appearance, with a speckled texture of light and dark minerals. For comparison of visual differences between granite and diorite, please see the 3D models below.

3D Model - Granite

This interactive element is not available in this format. Visit the link or scan the QR code to access it online.

View this Interactive Content online

Granite 3D model by Paleontological Research Institute is licensed under public domain.

3D Model - Diorite

This interactive element is not available in this format. Visit the link or scan the QR code to access it online.

View this Interactive Content online

Diorite 3D model by Paleontological Research Institute is licensed under public domain.

In terms of its extent, Sierran granodiorite is pervasive throughout the Sierra Nevada, forming the core of many of its highest peaks and most recognizable landscapes. Notable exposures of granodiorite can be seen in Yosemite National Park, where it forms the iconic El Capitan and Half Dome. The widespread distribution of granodiorite across the range is a testament to the extensive magmatic activity that occurred during the formation of the Sierra Nevada Batholith.

Variations in the mineralogy and texture of granodiorite can be observed across different regions of the Sierra Nevada. These variations are a result of differences in the conditions of crystallization and subsequent geological processes that have affected the rock. For example, granodiorite in the northern Sierra Nevada may display different textural and compositional characteristics compared to that in the southern Sierra Nevada. Understanding these variations provides important insights into the geological history and processes that have shaped the Sierra Nevada range, including magma mixing, assimilation, and cooling rates.

How the Sierra Nevada Batholith Formed

The Sierra Nevada Batholith is a massive geological structure that formed over a period of approximately 100 million years, from the Late Triassic to the Late Cretaceous period. Its formation is closely linked to the tectonic processes associated with the subduction of the Farallon Plate beneath the North American Plate. This subduction zone, located along the western margin of North America, was a site of intense magmatic activity, leading to the generation of large volumes of magma.

The emplacement of the Sierra Nevada Batholith occurred in multiple stages, involving the intrusion of numerous plutons into the Earth's crust. The formation of volcanic arcs, or chains of volcanoes formed at convergent plate boundaries, is one piece of surface evidence of larage plutons (see Plate Tectonics). The subduction of oceanic crust beneath continental crust generates intense heat and pressure, leading to the melting of the descending crust and the overlying mantle. Magma generated by this process is buoyant and rises towards the surface. As it ascends, it may intrude into the overlying crust, where it cools and solidifies to form plutonic rocks. In the case of the Sierra Nevada, the region was once situated along the western margin of North America, adjacent to a subduction zone where the Farallon Plate was being subducted beneath the North American Plate (see A Brief Geologic History of California). Such tectonic actions are illustrated in Figure 9.3.1.

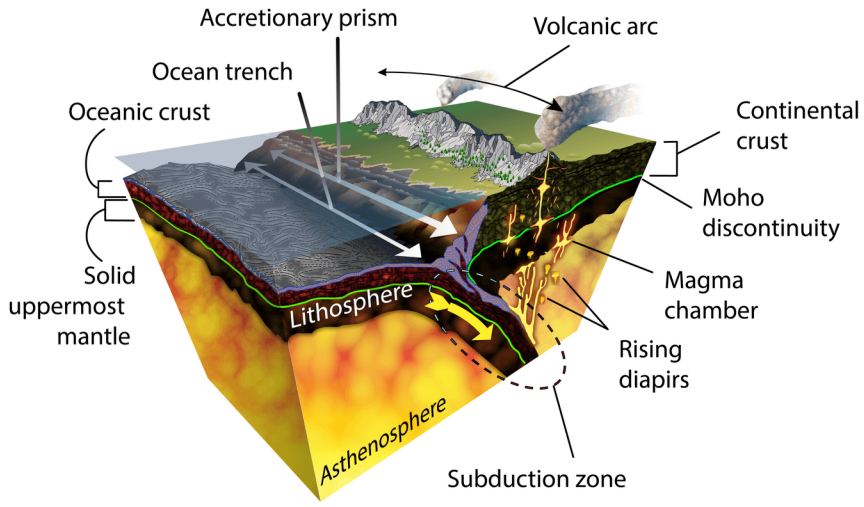


Figure 9.3.1: Subduction and Volcanic Arc by K. D. Schroeder is licensed under CC BY-SA 4.0. Access a detailed description.

These plutons, which are now exposed at the surface, represent successive pulses of magmatic activity. Each pulse contributed to the growth of the batholith, with older plutons being intruded by younger ones. This complex history of emplacement is recorded in the geological relationships between different plutonic bodies and the surrounding rock.

The tectonic environment during the formation of the Sierra Nevada Batholith was dynamic and complex. The subduction of the Farallon Plate caused significant deformation of the overlying continental crust, leading to the development of mountain ranges and deep crustal roots. The heat generated by the subduction process facilitated the partial melting of the mantle and lower crust, producing the magmas that formed the batholith. Additionally, the interaction between the rising magmas and the surrounding rock further influenced the composition and texture of the plutonic rocks.

The history of the Sierra Nevada Batholith is also marked by episodes of regional metamorphism and deformation, which have modified the original characteristics of the plutonic rocks. These processes have resulted in the formation of metamorphic aureoles around the plutons and the development of various structural features, such as folds and faults. Understanding the formation and evolution of the Sierra Nevada Batholith provides important insights into the geological processes that shape continental crust and the development of large magmatic systems.

Tuolemne Intrusive Suite

The Tuolumne Intrusive Suite is one of the most well-studied and significant components of the Sierra Nevada Batholith. Located in the central Sierra Nevada, this intrusive suite is renowned for its geological complexity and the insights it provides into the processes of pluton emplacement and magmatic differentiation. The Tuolumne Intrusive Suite consists of multiple intrusive

phases, each representing a distinct episode of magmatic activity.

The formation of the Tuolumne Intrusive Suite began with the intrusion of early, more mafic magmas, which formed the older phases of the suite. These early intrusions were followed by successive pulses of more felsic magmas, leading to the emplacement of younger phases. This sequence of intrusive events is recorded in the varying compositions and textures of the rocks within the suite. The presence of chilled margins and cross-cutting relationships between different intrusive phases provides evidence for multiple intrusive events.

One of the key features of the Tuolumne Intrusive Suite is the presence of compositional zoning, where the outermost rocks are more mafic and the innermost rocks are more felsic. This zoning is interpreted as a result of magmatic differentiation, where the composition of the magma evolves as it cools and crystallizes. The outer, more mafic phases crystallized first, followed by the intrusion of more felsic magmas into the core of the suite. This process of magmatic differentiation is crucial for understanding the evolution of large intrusive bodies and the generation of diverse rock types within a single intrusive complex.

The Tuolumne Intrusive Suite also provides valuable insights into the dynamics of magma chamber processes and the interaction between different magmas. Field studies and geochemical analyses have revealed the presence of hybrid rocks, which form from the mixing of different magmas. These hybrid rocks provide evidence for the physical and chemical interactions that occur within magma chambers, contributing to the complexity and diversity of plutonic rocks.

Jointing and Sheeting of Igneous Rocks

Jointing is a common feature of igneous rocks, including those of the Sierra Nevada Batholith. Joints are fractures in the rock along which there has been no significant movement. They form as a result of various geological processes, such as cooling and contraction of the rock, tectonic stresses, and unloading due to erosion of overlying material. In the Sierra Nevada, jointing is a prominent feature of many of the granitic rocks, influencing their weathering and erosion patterns.

One of the most distinctive types of jointing in the Sierra Nevada is exfoliation jointing, also known as sheeting. Exfoliation jointing occurs when rock breaks into thin, curved sheets that peel away from the surface, similar to the layers of an onion. This type of jointing is particularly common in granitic rocks and is believed to result from the release of pressure as overlying rock is removed by erosion. The reduction in pressure allows the rock to expand and fracture along curved surfaces parallel to the rock's surface as shown in Figure 9.3.2.



Figure 9.3.2: Exfoliation jointing, or sheeting, on Half Dome in Yosemite National Park by Ronnie Macdonald is licensed under CC BY 2.0. Access a detailed description.

Exfoliation jointing is prominently displayed in several locations within the Sierra Nevada, including Yosemite National Park. Iconic features such as Half Dome and El Capitan exhibit well-developed exfoliation joints, contributing to their distinctive shapes and steep, smooth surfaces. Video 9.3.1 is a virtual flight over Half Dome using enhanced Google Earth imagery. This video shows the stunning exfoliation jointing, or sheeting, that shapes the iconic granite face of Half Dome. The development of exfoliation joints

is influenced by several factors, including the mineral composition of the rock, the presence of pre-existing fractures, and the rate of erosion.

Video 9.3.1: Half Dome Flyover

This video highlights the exfoliation jointing, or sheeting, on the surface of Half Dome. There is no audio, but you may access a detailed description.

This interactive element is not available in this format. Visit the link or scan the QR code to access it online.

View this YouTube Video online

Video 9.3.1: "Half Dome Flyover" by Cole Heap is licensed under CC BY-NC 4.0

Understanding the processes that lead to jointing and sheeting in igneous rocks is important for interpreting the geological history of the Sierra Nevada and for practical considerations such as rock stability and erosion. Jointing can influence the behavior of rock masses in response to weathering and tectonic forces, affecting landscape development and the potential for rockfalls and landslides.

References

1. Barton, M. D., & Hanson, R. B. (1989). Magmatism and the development of low-pressure metamorphic belts: Implications from the western United States and thermal modeling. *Geological Society of America Bulletin*, 101(8), 1051-1065.
2. Bateman, P. C. (1992). *Plutonism in the central part of the Sierra Nevada Batholith, California*. U.S. Geological Survey Professional Paper 1483.
3. Ducea, M. N. (2001). The California arc: Thick granitic batholiths, eclogite residues, lithospheric-scale thrusting, and magmatic flare-ups. *GSA Today*, 11(11), 4-10.
4. Glazner, A. F., Bartley, J. M., Coleman, D. S., Gray, W., & Taylor, R. Z. (2004). Are plutons assembled over millions of years by amalgamation from small magma chambers? *Geological Society of America Today*, 14(4/5), 4-11.
5. Hanson, R. B., & Glazner, A. F. (1995). Thermal requirements for extensional emplacement of granitoids. *Geology*, 23(3), 213-216.
6. Nadin, E. S., & Saleeby, J. B. (2010). Origin of high-Mg andesites and the continental crustal growth rate: Constraints from the Sierra Nevada Batholith. *Geological Society of America Bulletin*, 122(3/4), 323-335.
7. Saleeby, J. B. (2003). Segmentation of the Laramide slab: Evidence from the southern Sierra Nevada region. *Geological Society of America Bulletin*, 115(6), 655-668.

This page titled 9.3: The Sierra Nevada Batholith is shared under a CC BY-NC 4.0 license and was authored, remixed, and/or curated by Cole Heap.

9.4: Gold of the Sierra Nevada

How Gold Forms

A mineral deposit is a place in Earth's crust where geologic processes have concentrated one or more minerals at greater abundance than in the average crust. An ore deposit is a mineral deposit that can be produced to make a profit. Thus, all ore deposits are mineral deposits, but not all mineral deposits are ore deposits.

Ores and ore minerals vary greatly in quality. Ideal ores contain 100% ore minerals. Such ores do not exist, but some come close. Ideal *ore minerals* contain 100% of the commodity of interest. Native copper, for example, is an ideal copper ore mineral. Ideal ore minerals are, however, uncommon. The most commonly mined ores are not ideal. Instead they are rich in ore minerals that can be processed relatively inexpensively to isolate desired components.

Gold is a unique ore in that it comes in two forms: as native gold (like the gold nugget in Figure 9.4.1), and as the mineral calaverite ($AuTe_2$) (Figure 9.4.2). The name "calaverite" originates from its discovery in Calaveras County, California. The foremost is a large natural nugget from a placer deposit in California. The discovery of gold nuggets in rivers and streams of California's Sierra Nevada foothills triggered the famous "Gold Rush" of 1848 and 1849. The gold is ultimately derived from quartz-gold hydrothermal veins in the bedrock of the Sierra Nevada Mountains of eastern California--but more on that in a moment.



BFigure 9.4.1: Large gold nugget (placer gold) from California on display in the Carnegie Museum of Natural History, Pittsburgh, Pennsylvania, USA. Gold Nugget By James St. John and licensed under CC BY 2.0. Access a detailed description.

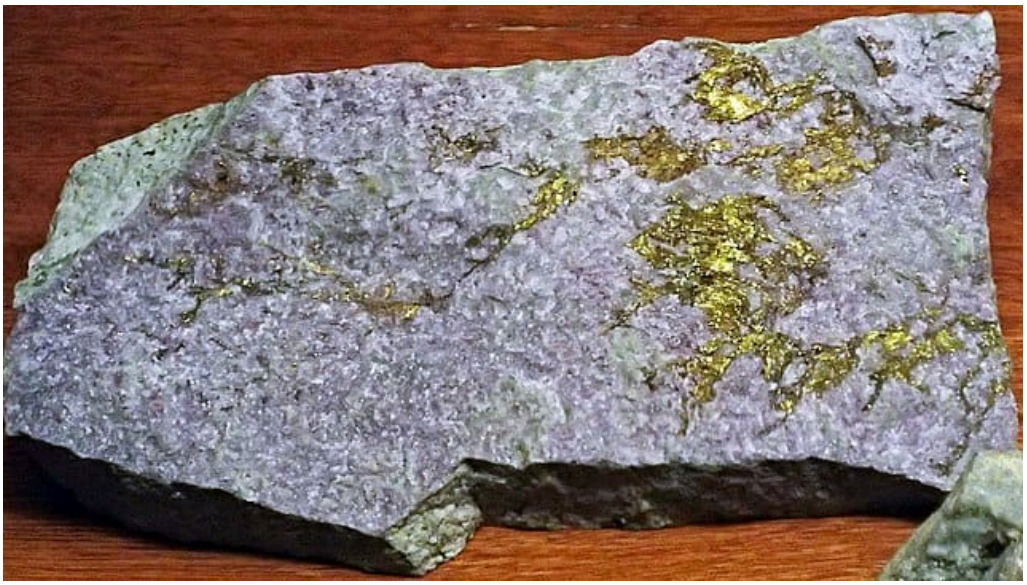


Figure 9.4.2: Calaverite-fluorite vein from the Oligocene of Colorado, USA. On display in the Denver Museum of Nature and Science, Denver, Colorado, USA) Gold-colored mineral = calaverite (AuTe2); Purplish areas = fluorite (CaF2). Calaverite-fluorite vein by James St. John is licensed under CC BY 2.0. Access a detailed description.

Gold, commonly mined as nuggets, flakes, wires, or scales, is often found in quartz-rich hydrothermal veins, typically alongside silver. While large, visible gold specimens, like those shown in Figure 9.4.3, are rare, most gold occurs in very fine grains, often microscopic. These precious metals are usually embedded within the quartz, forming part of intricate mineral veins.Within these veins, concentrated pockets of gold, known as ore shoots, can form large, vertical bodies rich in gold and silver.



Figure 9.4.3: Placer gold flakes from the Drava River, Murakeresztúr, Hungary. Placer gold is commonly found in alluvial deposits, where gold particles accumulate after being eroded from larger veins. Placer Gold Flakes by James St. John is licensed under CC BY 2.0. Access a detailed description.

In the western Sierra Nevada foothills, gold is predominantly found in these quartz veins, rather than being alloyed with other elements to form gold-bearing minerals. These veins can range from 30 cm to 30 meters (~12 inches to 98 feet) in thickness and often include other minerals like calcite and pyrite, also known as "fool's gold."

Lode Deposits

Sometimes geological processes concentrate ore minerals in vein deposits consisting of veins that are centimeters to meters

thick. If ore is distributed in many small veins, geologists call a lode deposit. Vein deposits account for most of the world's gold and silver mines, and also some copper and lead-zinc mines. Figure 9.4.4 shows a gold bearing quartz veins from the Mother Lode, California. In still other kinds of igneous deposits, ore minerals become concentrated in layers.



Figure 9.4.4: Gold-bearing quartz from the Mother Lode, CA by United States Geological Survey is licensed under public domain. Access a detailed description.

Lode deposits represent one of the primary forms of gold mineralization in the Sierra Nevada. These deposits typically occur within quartz veins, faults, and shear zones, reflecting the legacy of tectonic forces that have shaped the region. As hot fluids rich in dissolved minerals migrate through fractures in the earth's crust, they encounter favorable conditions for gold deposition. Upon cooling, these fluids precipitate gold along with other minerals, forming veins of economic significance.

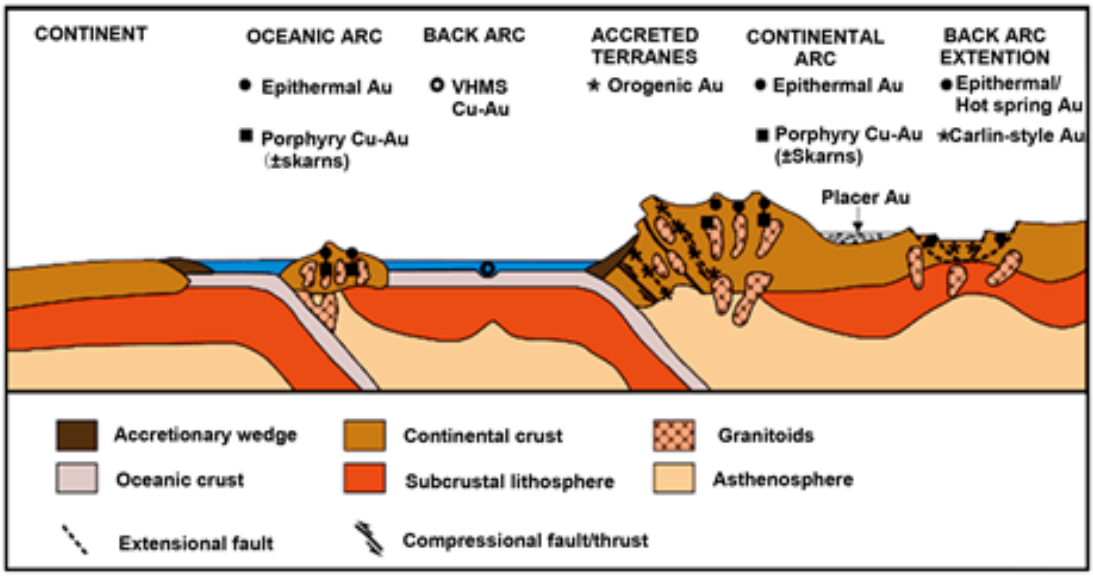


Figure 9.4.5: Tectonic Setting of Most Common Gold Deposits by Nguimatsia et al. is licensed under CC BY 4.0 DEED. Access a detailed description.

As Figure 9.4.5 shows, granitic intrusions buoy up through the crust carrying hot, mineral saturated fluids. The granitoids in Figure 9.4.2.1A would be a portion of these hot fluids. The black dots and squares that are located in the continental arc would be the lode deposits that are injected into place along the Sierra Nevada.

The formation of lode deposits in the Sierra Nevada is intricately linked to the region's geological history. During periods of mountain building and tectonic activity, such as the Sierra Nevada's uplift during the Cenozoic era, fractures and faults provided

conduits for mineral-rich fluids to migrate upwards from deep within the earth. Over time, the deposition of gold within these structures resulted in the formation of economically viable ore bodies.

Lode deposits in California are primarily found in the western foothills of the Sierra Nevada, often associated with regions of active or past tectonic activity. These deposits occur in a variety of geological settings, including fault zones, shear zones, and igneous intrusions. The gold mineralization in lode deposits is thought to be primarily of hydrothermal origin, with gold-bearing fluids migrating through fractures and faults in the surrounding rocks. Over time, the deposition of gold within these structures forms economically viable ore bodies, which have been extensively mined throughout California's history.

Lode Deposits and California's Gold Rush

The Mother Lode, an uninterrupted expanse of gold-bearing quartz veins and gold-enriched rock, extends for approximately 200 kilometers along the Melones fault zone. Journeying along California's historic Highway 49, which traverses Gold Rush towns and mines, also means traveling along the boundary, or suture, between accreted oceanic terranes. Numerous mines were developed to trace the quartz veins within this 1.5-kilometer-wide belt. Given the inclined nature of most veins, the lode deposits have the potential to extend to depths reaching thousands of meters beneath the Earth's surface.

While the initial discoveries of gold in California were in the form of nuggets within stream gravels, early miners quickly realized that the origin of the stream sediments lay in gold-bearing quartz veins. These veins were found to be predominantly situated in the metamorphic rocks of the western foothills. Subsequently, geologists established a connection between lode deposits and submarine volcanic rocks originating from accreted terranes, which had been intruded by more recent granitic rocks.

Geologists theorize that the gold in the Sierra Nevada region was initially deposited within rocks from accreted oceanic terranes. The migration of fluids enriched with gold likely occurred in the vicinity of submarine volcanic vents, leading to the creation of mineralized zones akin to those observed in contemporary submarine spreading centers, known as "black smokers." Following the accretion of these rocks to North America, the intrusion of the Sierra Nevada Batholith generated heat that mobilized and concentrated the gold in the veins observed today. As previously mentioned, Figure $9.4.4$ exhibits gold bearing quartz from the Mother Lode of California.

Box: Hydrothermal Vents - "Black Smokers"

Hydrothermal vents, known colloquially as black smokers, are captivating geological phenomena discovered in the depths of the ocean. Formed by the dynamic interplay between seawater and the intense heat of subterranean magma, these vents release jets of superheated water laden with minerals and gases. The moniker "black smokers" originates from the appearance of these vents, which emit dark plumes resembling smoke as they disperse into the surrounding oceanic depths (Figure $9.4.6$).

While predominantly situated along mid-ocean ridges, where tectonic plates diverge, hydrothermal vents are also found in unexpected locales, such as subduction boundaries. Here, the process of plate subduction creates conditions conducive to the formation of these remarkable features. These vents, whether nestled in the seafloor trenches or dotted along volcanic arcs, serve as vital ecosystems, harboring a plethora of life uniquely adapted to thrive in the extreme conditions they offer.

These ecosystems are home to an astonishing array of life, from resilient extremophiles like thermophiles to complex organisms such as giant tube worms and deep-sea crabs. The high temperatures and chemical composition of the vent fluids provide the necessary energy and nutrients to sustain this diverse community, which forms intricate food webs. The study of hydrothermal vents not only deepens our understanding of geological processes shaping our planet but also broadens our perspective on the potential for life in harsh environments, both here on Earth and beyond.

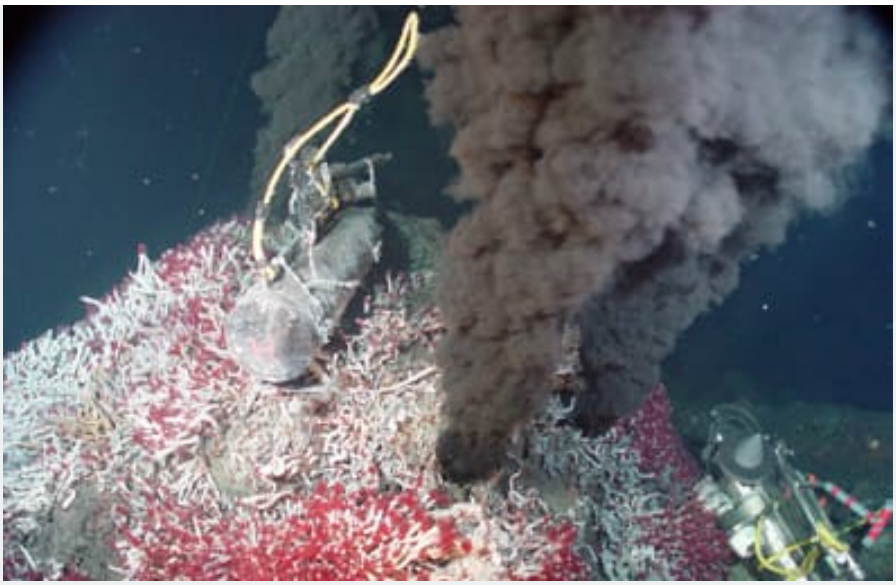


Figure 9.4.6: Venting black smoker emits jets of particle-laden fluids by NOAA is licensed under public domain. Access a detailed description.

These gold-bearing veins traverse Mesozoic metamorphic rocks and some plutonic rocks, indicating that the gold mineralization occurred subsequent to the formation of these rocks. Through the dating of rocks predating and succeeding the gold-bearing veins, geologists estimate that the emplacement of the gold veins took place approximately between 140 and 160 million years ago.

Placer Deposits

In addition to hard-rock deposits, gold is also found in placer deposits, or simply, placers: accumulations in river, stream, or other kinds of sediments.

Placer deposits develop when heavy minerals, weathered from igneous, sedimentary, or metamorphic rocks, are transported by streams. Eventually, the water slows enough for those dense minerals to be deposited, usually along point boars, in braided streams, or in alluvial fans. Placer deposits form when one or more minerals concentrate in this way to become an ore deposit. The word *placer* is Spanish for *alluvial sand*. Figure 9.4.7 shows the general origin of placer gold deposits originating from "Mother Lode" deposits as they erode into streambeds and are carried down slope.

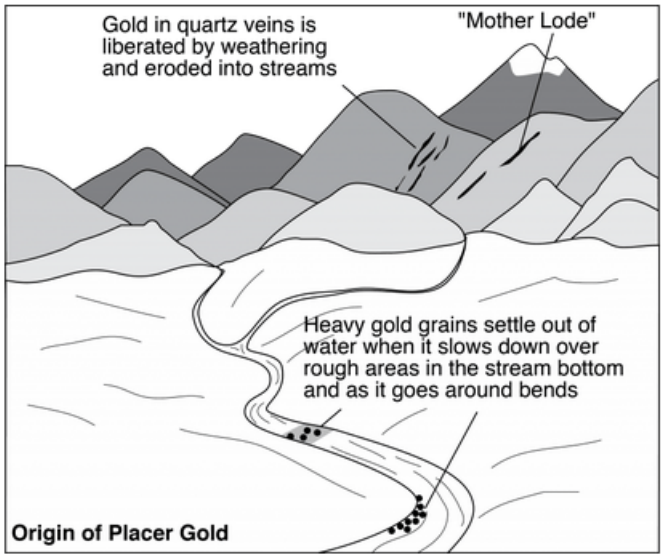


Figure 9.4.7: The origin of placer gold deposits. Gold in these veins is liberated by weathering and erosion into streams. Gold is dense and naturally settles out of water when it slows down. This work by Dexter Perkins is licensed under CC BY-SA. Access a detailed description.

Placer gold set off the historically important California Gold Rush of 1849. The original sources of minerals in placers are often difficult to determine but, in California, the source has been identified. The California gold weathered from extensive vein deposits, called the mother lode, in the Sierra Nevada Mountains. The lode is in a zone east of Sacramento and San Francisco that is 1 to 6 km (0.62 to ~3.7 miles) wide and extends almost 200 km (~124 miles) north-south. Mother Lode gold is in quartz veins up to 20 meters (~66 ft) thick and thousands of meters long.

The California gold rush resulted in California being admitted to the United States in 1850 and later provided a name for a San Francisco football team (the 49ers). Although once one of the most productive gold-producing districts in the United States, the Mother Lode is presently mostly a tourist destination and the home of wineries.

Placer minerals must be both dense and durable to be deposited and remain in place without decomposing. Native metals such as copper or gold, sulfide minerals such as pyrite or pyrrhotite, and oxide minerals such as magnetite or ilmenite are all dense and likely to be found in placers. Metal oxides, especially magnetite (iron oxide), are common and especially dense and durable, and often dominate such deposits. And gold is dense and extremely resistant to any kind of weathering and so can accumulate in stream and river sediments. Gold in placer deposits is found as nuggets that range from microscopic size to basketball size.

Box: Timeline of the 1849 Gold Rush

The discovery of gold at Sutter's Mill in January 1848 triggered the California Gold Rush, leading to a massive influx of prospectors and settlers seeking fortune in the Sierra Nevada foothills. By the end of 1848, news of the discovery had spread across the United States and internationally, sparking "gold fever" and prompting thousands to embark on the perilous journey to California. In 1849, known as the peak of the Gold Rush, approximately 80,000 "49ers" arrived, transforming San Francisco from a small town into a booming city.

Throughout 1849, mining camps sprang up along the Sierra Nevada's rivers and streams, where prospectors used pans and simple tools to extract gold from placer deposits. The rapid population growth and intense mining activity led to significant environmental changes, with rivers being diverted, forests cleared, and hillsides stripped bare. By the end of the year, California had become a bustling hub of economic activity, leading to its admission as the 31st state in 1850. The Gold Rush era left a lasting legacy on California's development and the cultural and physical landscape of the Sierra Nevada.



Figure 9.4.8: 1852 miners in California work their "long tom" to separate gold from gravel by the National Park Service is in the public domain. Access a detailed description.

Gold Recovery

One of the simplest and enduring methods for separating gold from sediments was through panning, a technique that remains popular among hobbyists today. California miners employed either a flat-bottomed pan crafted from iron, tin, or a wooden bowl. The process involved filling the pan with sediment and water, extracting larger gravel, and then submerging the pan into a stream or pool at a slight tilt while swirling the sediment. Lighter materials were carried away, leaving behind the heavier grains or "pay dirt," which often included heavy minerals like magnetite and pyrite, along with the desired gold flakes or nuggets. The miner would be optimistic upon seeing a glint in the pan, but there were occasions when the sediment did not yield the desired results.

Panning, although a simple and cost-effective method of placer mining, is limited in its ability to handle large volumes of sediment. In response, miners developed more efficient methods for processing substantial amounts of material. One such innovation was the rocker or cradle, employed as early as 1848. The rocker, resembling a long box mounted on rockers akin to a baby's cradle, operated on a slope with one end positioned downhill and the other uphill. At the top end of the cradle, there was a hopper equipped with a sieve at its base.

To facilitate the process, water was continuously poured onto the hopper, generating a current. Gold, being heavier, tended to settle in the rocker box behind cleats, effectively trapping it. The cradle's design allowed three or more individuals to collaborate in washing a substantial volume of sediment. Many of California's most lucrative and easily accessible placer deposits were worked using a combination of panning and the cradle.

In the latter part of 1849, miners initiated the extensive movement of sediment by diverting rivers to access the gold concealed within the stream beds. Figure 9.4.9 displays a map published by the USGS in 1968 and shows a shaded focused area along the Yuba River of placer deposits in Nevada County, CA.

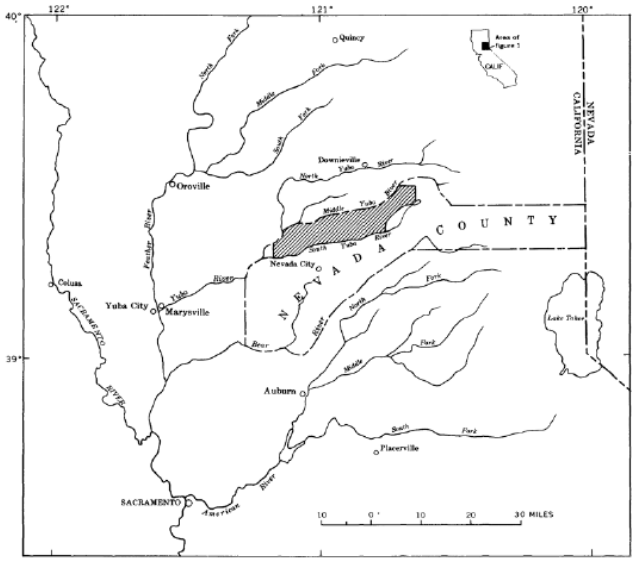


Figure 9.4.9: Index map of part of Northern California showing location of 1968 Placer Deposits in Nevada County, CA by the USGS is in the public domain. Access a detailed description.

Environmental Impacts of Lode Extraction

The extraction of lode gold deposits in the Sierra Nevada has historically had significant environmental impacts, many of which continue to affect the region today. Lode mining involves the excavation of hard rock to access veins of gold embedded within the bedrock. This process often requires extensive tunneling and the removal of large volumes of rock, leading to substantial landscape alteration and habitat disruption.

One of the primary environmental concerns associated with lode mining is the generation of mine tailings, which are the waste materials left after the gold has been extracted from the ore. These tailings, often containing heavy metals and other toxic substances, are typically stored in tailings ponds or heaps. Over time, these storage sites can leak or fail, releasing harmful contaminants into nearby soil and water bodies, referred to by geologists as acid mine drainage. The leaching of heavy metals such as mercury, arsenic, and lead from mine tailings into streams and rivers poses a significant threat to aquatic ecosystems and human health.

While not directly related to lode extraction, the Spring Creek acid mine drainage event has been an ongoing issue since the mid-20th century, with the most significant impacts occurring in the 1960s and 1970s and is an example of potenital environmental impacts from mining (Figure 9.4.10). The problem originated from the Iron Mountain Mine, where extensive mining activities exposed sulfide-rich ore bodies (e.g. copper, zinc, and pyrite), leading to severe acid mine drainage. The peak of the environmental impact occurred during heavy rainfall events, which exacerbated the flow of acidic water into Spring Creek and subsequently the Sacramento River. The situation was particularly dire in the late 1960s, prompting environmental cleanup efforts that have continued to this day.



Figure 9.4.10: Acid mine drainage into Spring Creek (1970s), in Shasta County by NOAA is in the public domain. Access a detailed description.

Water usage in lode mining is another critical issue. The processing of ore to extract gold requires large quantities of water, which can deplete local water resources and affect downstream water availability. Additionally, the diversion of rivers and streams to facilitate mining operations can alter natural water courses, impacting aquatic habitats and the organisms that depend on them. The historical practice of diverting rivers, as mentioned in the preceding text, often led to increased sedimentation and erosion, further degrading water quality and riparian environments.

Acid mine drainage (AMD) is a particularly severe environmental impact associated with lode mining. When sulfide minerals in the excavated rock are exposed to air and water, they can oxidize, producing sulfuric acid. This acid can then leach heavy metals from the surrounding rock, creating highly acidic runoff that can contaminate nearby water bodies. AMD can persist for decades or even centuries after mining operations have ceased, making it a long-term environmental challenge.

The physical alteration of landscapes due to lode mining, including the creation of open pits, waste rock piles, and mine shafts, can lead to habitat destruction and fragmentation. These changes can have profound effects on local wildlife, disrupting migration patterns, breeding grounds, and food sources. In the Sierra Nevada, where biodiversity is rich and includes numerous endemic species, the loss of habitat due to mining activities has had lasting ecological consequences.

In response to these environmental challenges, regulations and remediation efforts have been implemented to mitigate the impacts of lode mining. The U.S. Geological Survey (USGS) and other agencies have conducted studies to assess the extent of contamination and to develop strategies for restoring affected areas. Remediation efforts often involve the stabilization of tailings, treatment of contaminated water, and rehabilitation of disturbed landscapes. However, the legacy of historical mining activities continues to pose environmental risks, highlighting the need for ongoing monitoring and management.

Overall, while lode mining has played a crucial role in the economic development of the Sierra Nevada region, it has also left a complex legacy of environmental degradation. Addressing these impacts requires a comprehensive understanding of the historical and current practices of mining, as well as a commitment to sustainable and responsible resource management.

Environmental Impacts of Placer Extraction

In the early 1850s, a significant portion of the easily accessible placer gold had been extracted from the riverbeds in the Western Foothills. The entire beds of most stream channels had been extensively worked, with some areas being overturned more than once. The rivers underwent substantial modifications, including diversions and damming, to access the placer gold. Even in the present day, remnants of this intensive mining activity are evident throughout the foothills, where piles of sediment persist, resembling the excavations of numerous large-scale prospectors.

Following the depletion of easily accessible placer deposits, miners shifted their focus to older placer formations created by streams flowing westward from a previous Sierra Nevada range. Cornish miners were among the first to explore these older, buried gravel deposits, which geologists referred to as Tertiary gravels. Due to the uplift of the Sierra Nevada, these Tertiary gravels are

now situated above contemporary river channels. Consequently, miners needed a method to wash these gravels effectively to access the gold concentrated near the bottom layers of sediment.

In certain regions, miners took to tunneling beneath the Table Mountain volcanic flows to reach the ancient gravels beneath. The Omega Mine near Jamestown stands as an example of successful tunneling efforts in this pursuit.

In 1853, resourceful miners conceived the idea of affixing a nozzle to a hose and using forceful water jets to wash sediment down from the hillsides, giving rise to hydraulic mining. This method, which drastically altered the landscape from the Sierra Nevada foothills to San Francisco Bay, represented a significant departure from the slower processes of earlier mining practices. Instead of being limited to washing 1 cubic yard of sediment in a day, or 4 cubic yards with a sluice, a miner employing hydraulic systems alongside a sluice could wash 50 to 100 cubic yards per day. Movement of such materials is exhibited in Figure 9.4.11.

However, the widespread use of hydraulic mining had unintended consequences. The massive influx of sediment into the streams of the Sacramento Valley and the San Francisco-San Joaquin Delta began to impact navigation and irrigation. In response to these issues, the Sawyer Decision of 1884 prohibited the dumping of mining-related sediment into the Sacramento and San Joaquin Rivers and their tributaries. Even today, the effects of sedimentation from hydraulic mining in the late 1800s are still evident in the eastern part of the San Francisco Bay, more than a century after the mining activities took place.



Figure 9.4.11: Hydraulic Mining, California, 1870s by United States Geological Survey is licensed under public domain. Access a detailed description.

Gold Production Since the Mid 1800s

California boasts notable instances of substantial gold finds, such as the 195-pound mass uncovered at Carson Hill in 1854 and a 54-pound pure gold nugget discovered at Magalia in the same year, albeit the latter was melted down shortly after its revelation. However, such large masses are exceptional. Most of the gold extracted in the Sierra Nevada region has originated from deposits containing between 1/4 and 1/2 ounce of gold per ton of ore.

In geological terms, ore refers to any accumulation of a specific element, including metals like gold, silver, or mercury, that has been adequately concentrated to be economically viable for mining. It is evident from this definition that economic factors, accessibility, and technological advancements play crucial roles in determining what qualifies as ore. Materials discarded as waste rock during one period may become profitable to mine in later years, influenced by fluctuations in commodity prices or the introduction of new mining methods and technologies.

California's gold production has experienced fluctuations driven by changes in economic conditions, accessibility, and technological advancements. Ventures and investments in precious metals, like gold, are inherently financially risky due to the intricacies of market conditions and the geological uncertainties associated with ore deposits.

In the 1980s, a surge in the price of gold, coupled with the adoption of a novel extraction method, triggered a renewed interest

in mining operations at previously abandoned sites in the Sierra Nevada. Today, mining companies are employing a chemical process known as heap leaching to extract gold from deposits that were previously considered unprofitable. Heap leaching, which utilizes cyanide to dissolve gold from quartz veins, has significantly enhanced gold recovery, surpassing other methods for lode deposit mining by a factor of 100. This method is presently in use at various mines in California and Nevada. As of 2023, there were 15 active and/or newly permitted gold mines in California. Figure 9.4.12 shows the locations of active and close gold mines from 1995 to the start of 2023.

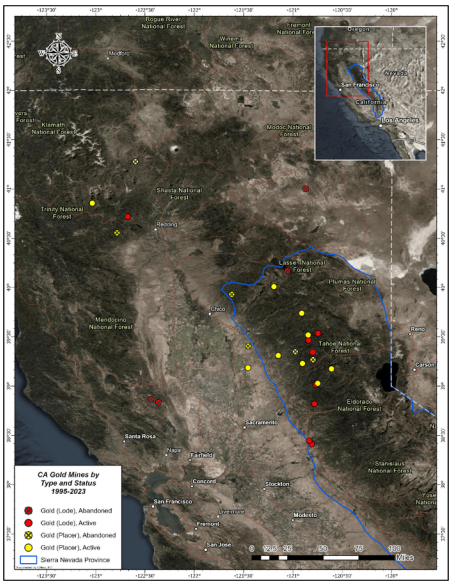


Figure 9.4.12: CA Gold Mines by Type and Status 1995-2023 by Cole Heap (2023) is licensed under CC BY-NC 4.0. Constructed in a GIS using data from data.ca.gov. Access a detailed description.

References

1. Brereton, R. (1976). *Mining Techniques in the California Goldfields During the 1850*s. Pacific Historian 20 no. 3: 286-302.
2. Britannica, T. Editors of Encyclopedia (2010, December 15). placer deposit. Encyclopedia Britannica. https://www.britannica.com/science/placer-deposit
3. Limbaugh, R. H. and Fuller, W.P.H. (2004). *Calaveras Gold: The Impact of Mining on a Mother Lode County*. University of Nevada Press, Reno.
4. Logan, C.A. (1981). *History of Mining and Milling Methods in California*. California Geology, September: 194.
5. Nguimatsia, F. , Bolarinwa, A. , Yongue, R. , Ndikumana, J. , Olajide-Kayode, J. , Olisa, O. , Abdu-Salam, M. , Kamga, M. and Djou, E. (2017) Diversity of Gold Deposits, Geodynamics and Conditions of Formation: A Perspective View. Open Journal of Geology, 7, 1690-1709. doi: 10.4236/ojg.2017.711113(opens in new window).
6. Paul, Rodman W. (1965). *California Gold: The Beginning of Mining in the Far West*. University of Nebraska Press, Lincoln NB.

This page titled 9.4: Gold of the Sierra Nevada is shared under a CC BY-NC 4.0 license and was authored, remixed, and/or curated by Cole Heap.

9.5: Volcanic Features of the Sierra Nevada

Young Volcanics

Although the Sierra Nevada is largely defined by its ancient geological formations, the region also hosts a series of younger volcanic features that have formed within the last few million years. These young volcanics are a result of relatively recent tectonic and volcanic activity, which is often associated with the extensional processes occurring in the adjacent Basin and Range Province. This ongoing tectonic activity has caused the Earth's crust to stretch and thin, leading to the formation of faults and the upwelling of magma. The Mono-Inyo Craters volcanic chain, located near the eastern edge of the Sierra Nevada, is one of the most notable examples of this young volcanic activity. This chain consists of a series of rhyolitic domes, craters, and lava flows that have erupted over the past few thousand years, with the most recent eruptions occurring approximately 600 years ago.

The Mono-Inyo Craters are particularly significant because they provide a clear record of volcanic activity in the region during the Holocene epoch. The rhyolitic domes, such as Panum Crater, are composed of highly viscous lava that erupted explosively, forming steep-sided volcanic features. These eruptions were accompanied by pyroclastic flows and the deposition of tephra, which blanketed the surrounding area. The region remains geologically active, with ongoing seismic activity suggesting that magma continues to move beneath the surface, indicating the potential for future eruptions. In addition to the Mono-Inyo Craters, the Long Valley Caldera, just south of Mono Lake, is another prominent feature associated with young volcanism but does not reside within the Sierra Nevada Province.



Figure 9.5.1: South Inyo Crater Lake near Mammoth, CA by Cole Heap is licensed under CC BY-NC 4.0. Access a detailed description.

The Inyo Craters, located near the eastern edge of the Sierra Nevada (the southernmost Inyo Crater is shown in Figure 9.5.1) are a series of three volcanic craters formed during explosive eruptions approximately 600 years ago. These craters, part of the larger Mono-Inyo Craters volcanic chain, were created when magma interacted with groundwater, resulting in steam-driven explosions that blasted through the surface. The largest of the Inyo Craters, South Inyo Crater, measures about 600 feet in diameter and 200 feet deep. The craters are surrounded by deposits of pumice and ash, remnants of the eruptions that shaped them. The Inyo Craters serve as a vivid reminder of the relatively recent volcanic activity in the Sierra Nevada and remain a point of interest for both geologists and visitors exploring the region's dynamic volcanic landscape.

Additionally, Obsidian Dome, located near the Inyo Craters, is a prominent volcanic feature formed during an eruption approximately 600 years ago. This dome is composed primarily of obsidian, a naturally occurring volcanic glass, and rhyolite, which were extruded during a series of explosive eruptions (Figure 9.5.2). The eruptions forced viscous lava to the surface, where it cooled and solidified into a steep-sided dome. Obsidian Dome rises about 300 feet above the surrounding landscape and spans roughly a mile in diameter. Its rugged surface is marked by large blocks of obsidian and pumice, creating a striking contrast with the surrounding forested terrain. Obsidian Dome is an excellent example of the type of volcanic activity that has shaped the

Mono-Inyo Craters region and remains a popular destination for visitors interested in the geological history of the Sierra Nevada.



Figure 9.5.2: Obsidian Dome near Inyo Craters by Cole Heap is licensed under CC BY-NC 4.0. Access a detailed description.

Figure 9.5.3 exhibits a hand-sized sample of snowflake obsidian, which is a unique variety of volcanic glass that forms when molten lava cools rapidly, preventing the formation of a crystalline structure. What sets snowflake obsidian apart are the white or grayish "snowflake" patterns, which are actually clusters of cristobalite, a type of quartz. These patterns form when the obsidian slowly begins to crystallize over time, allowing small crystals of cristobalite to develop within the glassy matrix. As the obsidian cools, the cristobalite crystals grow and spread, creating the distinctive snowflake-like inclusions. The contrast between the deep black of the obsidian and the light-colored cristobalite makes snowflake obsidian a striking and sought-after material for both collectors and jewelers. This process of slow crystallization within the volcanic glass typically occurs after the initial formation of the obsidian, as the lava continues to cool and stabilize.



Figure 9.5.3: Snowflake obsidian from Obsidian Dome by Cole Heap is licensed under CC BY-NC 4.0. Access a detailed description.

Beyond the Mono-Inyo Craters, another noteworthy example of young volcanism within the Sierra Nevada is the volcanic activity in the area surrounding Mammoth Mountain. Although Mammoth Mountain itself is part of the Long Valley volcanic field, its formation is distinctly tied to the volcanic processes that have influenced the eastern Sierra Nevada. Mammoth Mountain, a large dacitic dome complex, began forming around 110,000 years ago and has seen multiple eruptions over its history. While not erupting in recent history, Mammoth Mountain continues to exhibit volcanic unrest, including earthquake swarms, ground deformation, and the release of volcanic gases, indicating that the area remains a site of potential future volcanic activity.

These young volcanic features illustrate the ongoing tectonic and volcanic processes that continue to shape the Sierra Nevada, highlighting the region's dynamic geological evolution and potential for future volcanic events.

Table Mountains and Inverted Topography

Inverted topography is a fascinating geomorphological phenomenon common in the American West, and the Sierra Nevada is home to several striking examples. This process occurs when volcanic deposits, such as lava flows or ash-flow tuffs, descend into river valleys and other topographic lows, filling them with resistant volcanic rock. Over time, the surrounding softer materials, like sedimentary rocks that once formed the valley sides, erode more quickly than the harder volcanic rock. This differential erosion causes the former valleys, now capped with erosion-resistant volcanic material, to stand elevated as mesas or ridges, effectively reversing the original topography. As a result, areas that were once topographic highs become valleys, while former valleys are transformed into elevated features (Figure 9.5.4).

The Table Mountains in the Sierra Nevada, particularly those near Sonora in Tuolumne County, provide some of the most striking examples of inverted topography. During the Miocene epoch, approximately 10 million years ago, volcanic eruptions filled ancient river valleys with thick layers of basaltic lava. As the lava solidified into hard rock, it resisted erosion far better than the surrounding sedimentary materials. Over millions of years, erosional processes removed the softer surrounding rocks, leaving behind the distinctive flat-topped ridges we see today. The Stanislaus Table Mountain is a classic example of this process, where the ancient Stanislaus River was buried by a lava flow that now forms a prominent ridge, shaping the course of modern rivers and streams in the area.

Inverted topography in the Sierra Nevada is not only a geological curiosity but also offers important insights into the region's volcanic and erosional history. The preservation of these lava-capped ridges allows geologists to reconstruct the ancient landscapes of the Sierra Nevada, providing clues about the climate, tectonics, and volcanic activity that occurred millions of years ago. These features serve as natural laboratories for studying the processes of erosion, weathering, and landscape evolution. The Table Mountains and other examples of inverted topography in the Sierra Nevada illustrate the long-lasting impact of volcanic activity on the landscape and the intricate interplay between tectonic forces and surface processes.

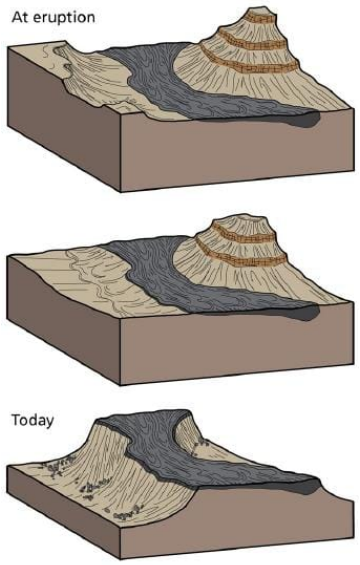


Figure 9.5.4: Schematic illustrations of the formation of inverted topography. Lava is represented by black bands. At eruption, the terrain is covered by loose volcanic ash or tephra. By the National Park Service is in the public domain. Access a detailed description.

There are a number of examples of this inverted topography in the Sierra Nevada providing yet more evidence of an ancestral Sierra Nevada mountain range that predates the one we see today.

Big Table Mountain and Kennedy Table Mountain in Madera County are prominent examples of inverted topography in the Sierra Nevada, illustrating the dramatic effects of volcanic activity and erosion on the landscape. These table mountains were formed during the Miocene epoch when basaltic lava flows filled ancient river valleys of the San Joaquin River and its tributaries. Over millions of years, the surrounding softer sedimentary rocks eroded away, leaving the resistant basalt-capped ridges elevated above the current landscape. Big Table Mountain, located near the city of Auberry, and Kennedy Table Mountain, situated closer

to the San Joaquin River, both exhibit the flat-topped, steep-sided morphology typical of inverted topography. Figure 9.5.5 shows Big Table Mountain on the horizon, with the board flat top, and the San Joaquin River just below. This image was taken from Pincushion Peak and is looking to the southeast. Figure 9.5.6 shows an aerial view of Big Table Mountain (highlighted in yellow). One might note the sinuous shape that these table mountains take on further demonstrating lava flow direction and the ancient San Joaquin River channel.



Figure 9.5.5: Looking southeast from Pincushion Peak towards Big Table Mountain, Madera County, CA by Cole Heap is licensed under CC BY-NC 4.0. Access a detailed description.

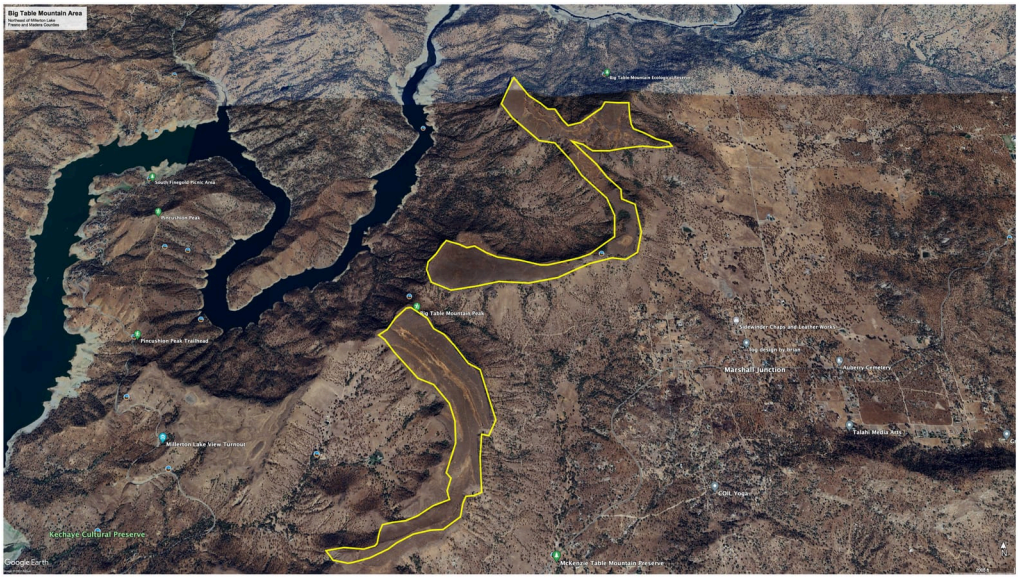


Figure 9.5.6: Aerial imagery showing Big Table Mountain in Fresno and Madera Counties, CA. Its flat-topped mesas are outlined in yellow. Created in Google Earth Pro by Cole Heap is licensed under CC BY-NC 4.0. Access a detailed description.

The connection of these table mountains to the San Joaquin River highlights the powerful interplay between volcanic activity and fluvial processes in shaping the Sierra Nevada's landscape. As the San Joaquin River carved its course through the Sierra Nevada, volcanic eruptions periodically filled its valleys with lava, which later became the high-standing table mountains after extensive erosion of the surrounding terrain. These features not only offer striking visual evidence of the region's geological history but also provide insights into the ancient river systems and the volcanic events that shaped them. Together with other examples like the Stanislaus Table Mountain, Big Table Mountain and Kennedy Table Mountain underscore the significance of inverted topography in understanding the Sierra Nevada's complex volcanic and erosional history.

Late Cenozoic Uplift of the Sierra Nevada

The Late Cenozoic uplift of the Sierra Nevada, beginning around 5 million years ago, has played a critical role in shaping the region's current landscape and volcanic features. This uplift, driven by tectonic forces related to the subduction of the Farallon Plate and the extension of the Basin and Range Province, has elevated the Sierra Nevada to its present height, dramatically increasing the relief of the range. The uplift has caused the Sierra Nevada to tilt westward, resulting in the gentle western slope and the steep eastern escarpment that characterizes the range today. This tilting has also influenced the drainage patterns of the region's rivers, with many rivers cutting deep, steep-sided canyons into the western slope as they flow toward the Central Valley.

The uplift of the Sierra Nevada has also had significant implications for the region's volcanic history. As the mountains rose, they altered the stress patterns in the Earth's crust, creating conditions that favored volcanic activity along the eastern margin of the range. This activity is particularly evident in the formation of the Long Valley Caldera, one of the largest and most active volcanic systems in the western United States. The caldera was formed by a massive eruption approximately 760,000 years ago, which released an estimated 600 cubic kilometers of ash and debris, blanketing large parts of what is now the western United States. The uplift of the Sierra Nevada has also contributed to the preservation of volcanic features such as the Mono-Inyo Craters and the various lava-capped Table Mountains, which were protected from erosion as the landscape around them was uplifted and dissected.

The Late Cenozoic uplift of the Sierra Nevada is also closely linked to the region's ongoing tectonic activity. The uplift has created a series of normal faults along the eastern edge of the range, which have accommodated the extension of the Basin and Range Province and contributed to the formation of the steep eastern escarpment. These faults are still active today, as evidenced by the numerous earthquakes that occur along the eastern Sierra Nevada, including the historic Lone Pine earthquake of 1872. The combination of uplift, volcanic activity, and tectonic deformation in the Sierra Nevada makes this region a key area for studying the interplay between tectonic processes and surface features. The ongoing uplift and deformation of the Sierra Nevada continue to shape the landscape, providing a dynamic environment where the forces of nature are on full display.

Devils Postpile

Devils Postpile, a striking geological formation located in the Sierra Nevada, is renowned for its impressive basalt columns and the nearby Rainbow Falls. Though not designated as a full national park, Devils Postpile National Monument is a protected area that showcases one of the finest examples of columnar jointing in the world. Columnar joints are captivating geological formations arising from the cooling and contraction of volcanic or igneous rock, most commonly basalt. These distinct hexagonal or pentagonal structures are a testament to the intricate interplay of geology and physics. It all begins with the eruption of molten rock rich in minerals like silica and iron. As the lava flows and spreads, it gradually loses heat to the surrounding environment, causing it to cool and solidify. During this cooling process, the lava contracts, creating internal stress that leads to the formation of cracks. These cracks develop perpendicular to the cooling surface, resulting in a polygonal pattern that eventually forms the characteristic hexagonal or pentagonal columns. The geometry of these columns is a consequence of the efficient packing of polygons, minimizing gaps and maximizing stability. The size and regularity of these columns are influenced by the cooling rate and the composition of the rock. Slower cooling rates yield larger columns, while faster cooling rates produce smaller ones. Basalt, with its particular mineral composition, is a common rock type associated with these formations. Columnar joints are a testament to the beauty of nature's artistic expressions in rock, born from the gradual cooling and solidification of molten material.

Devils Postpile's columns tower up to 60 feet and display a striking symmetry. However, this was not the case an estimated 80,000 to 100,000 years ago a lava vent began spewing hot basaltic lava into the Reds Meadow Valley near present-day Upper Soda Springs, a few miles north of the Monument. Basalt lava is rich in iron and magnesium and is typically much hotter than other types of lava. Because of these traits, basaltic lava tends to have a lower viscosity and will flow more quickly than other lava types. The lava flowed down the valley like a river until it was blocked by a natural dam, probably a glacial moraine left down-valley by a receding glacier during a previous ice age. The lava began filling the valley behind this dam, creating a lava lake 400 ft. deep in some areas. Such depth is uncommon among lava flows and plays a crucial role in the formation of the long columns we see today and that are exhibited in Figure 9.4.7.



Figure 9.5.7: Devils Postpile by Cole Heap is licensed under CC BY-NC 4.0. Access a detailed description.

As the lava flow ceased, the molten rock began cooling into solid rock. Shallow parts of the lava flow would have solidified first, with deeper parts of the lava lake requiring much more time to release the massive amount of stored thermal energy. As the lava lake cooled and solidified from a molten soup to solid rock it began to contract. Contraction stresses developed because the cool solid form of basalt has a lesser volume than the hot liquid form. Cracks, also called joints by geologists, began to form. Jointing releases internal stress created by the cooling and associated contraction. In some locations, such as at the Devils Postpile, the jointing formed columns. Jointing would have begun at the top and bottom, as well as all around the edges of the lava lake, where the lava made direct contact with a cooler surface. The cracks would have extended inwards over time as the more insulated locations within the lava lake finally released enough thermal energy to change from a liquid to a solid state. Figure 9.5.8 is a schematic of this described process of columnar joint formation.

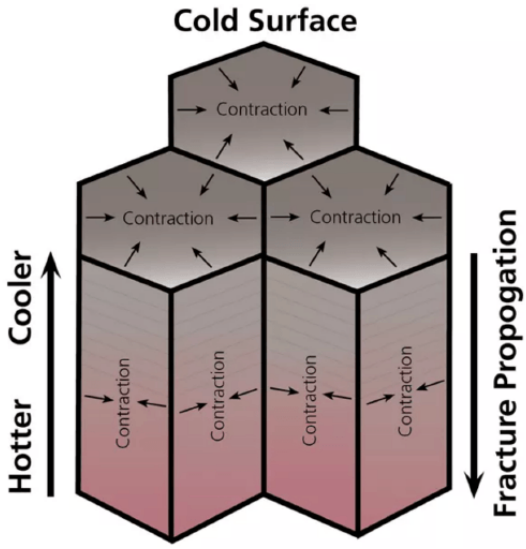


Figure 9.5.8: Diagram showing the formation of columnar jointing, which occurs in cooling lava or magma. By the National Park Service is in the public domain. Access a detailed description.

The Devils Postpile used to be much taller than what we see today. Powerful erosive forces have been at work during the last 80,000 to 100,000 years carving, shaping and demolishing remnants of the lava flow. Freeze-thaw cycles help break apart the columns. Earthquakes knock columns down into the talus slope below. The river slowly eats away at pieces that fall into the water. But no force has left a greater footprint on the Postpile than that of glaciers. In fact, the beautifully straight hexagonal columns hidden within the depths of the lava flow would not been seen had glaciers not excavated the formation. Figure 9.5.9 exhibits these hexagons from on top of Devils Postpile. Several distinct glacial periods have occurred since the Postpile was formed and

each has dug deeper and deeper into the dense, heavy rock known officially as basaltic trachyandesite. The last major glacial period ended about 18,000 years ago. Glacial polish and striations evident on top of the Postpile are from this last glaciation.



Figure 9.5.9: On top of Devils Postpile by Cole Heap (2023) is licensed under CC BY-NC 4.0. Access a detailed description.

Volcanic Legacy and Geomorphic Evolution of the Sierra Nevada

This section explored the more recent volcanic legacy and related geomorphic evolution of the Sierra Nevada, focusing on the dynamic interplay between volcanic activity and tectonic processes that shaped the region's landscape. Key features such as the Mono-Inyo Craters, Obsidian Dome, and Devils Postpile highlighted the relatively recent volcanic activity that left a lasting imprint on the eastern Sierra Nevada. Additionally, the concept of inverted topography, exemplified by the Table Mountains, illustrated how volcanic deposits transformed ancient river valleys into elevated ridges over millions of years.

The section also delved into the Late Cenozoic uplift of the Sierra Nevada, which intensified erosion and exposed these volcanic features, contributing to the region's dramatic topography. From the towering basalt columns of Devils Postpile to the unique snowflake obsidian found near Obsidian Dome, each aspect of young volcanism provided a comprehensive overview of how volcanic and tectonic forces combined to create the unique, varied, and young portions of the Sierra Nevada landscape.

References

1. Bateman, P. C. (1992). *Plutonism in the central part of the Sierra Nevada Batholith, California*. U.S. Geological Survey Professional Paper 1483.
2. Bateman, P. C. (1992). *Plutonism in the central part of the Sierra Nevada Batholith, California*. U.S. Geological Survey Professional Paper 1483.
3. Hildreth, W., & Fierstein, J. (2016). *Eruptive history of Mammoth Mountain and its mafic periphery, California*. U.S. Geological Survey Professional Paper 1812.
4. Huber, N. K. (1981). *Amount and timing of Late Cenozoic uplift and tilt of the central Sierra Nevada, California—evidence from the upper San Joaquin River basin*. U.S. Geological Survey Professional Paper 1197.
5. Lindgren, W. (1911). *The Tertiary Gravels of the Sierra Nevada of California*. U.S. Geological Survey Professional Paper 73.
6. Slemmons, D. B., & Brock, V. E. (1975). *Late Cenozoic volcanism and tectonism in the western Great Basin*. Geological Society of America Bulletin, 86(11), 1485-1492.

This page titled 9.5: Volcanic Features of the Sierra Nevada is shared under a CC BY-NC 4.0 license and was authored, remixed, and/or curated by Cole Heap.

9.6: Ice Shapes the Landscape

How Glaciers Form

Glaciers form in regions where the accumulation of snow exceeds its melting over long periods, allowing snow to build up and compact into ice. In the Sierra Nevada, this process began during the Pleistocene Epoch, when colder global temperatures enabled snow to persist year-round at higher elevations. As snow accumulates, it compacts under its own weight, causing the individual snowflakes to recrystallize into firn, a granular type of ice. Over time, the firn becomes increasingly dense as the air trapped within it is squeezed out, eventually forming solid glacial ice. This ice, under the pressure of its own weight, begins to deform and flow.

The Sierra Nevada's climate and topography were ideal for glacier formation during the Pleistocene. High elevations provided cold temperatures necessary for sustaining snow and ice, while the steep topography encouraged snow to accumulate in mountain valleys and basins. This process was especially evident in areas like Yosemite National Park, where glaciers formed in high alpine valleys and carved out many of the park’s iconic features, such as the deep U-shaped Yosemite Valley and the steep cliffs of Half Dome and El Capitan. The Kings Canyon region also saw significant glacier formation, with glaciers carving out the park’s deep canyons and rugged peaks.

As glaciers advanced and retreated with fluctuations in climate, they left behind a record of their activity in the form of glacial deposits, including till and outwash. These deposits, made up of unsorted material ranging from fine silt to large boulders, provide geologists with clues about the extent and movement of ancient glaciers. In the Sierra Nevada, these deposits are found throughout the range, marking the boundaries of former glaciers and helping to reconstruct the region's glacial history.

How Glaciers Move

Glaciers move under their own weight, a process that is driven by gravity and facilitated by the unique physical properties of glacial ice. The movement of a glacier occurs through two main mechanisms: internal deformation and basal sliding. Internal deformation happens when the ice within the glacier flows plastically, meaning it deforms without fracturing. This flow is driven by the immense pressure exerted by the overlying ice, which causes the ice crystals to rearrange and slide past each other, allowing the glacier to move slowly downhill. This process is particularly important in cold, dry climates where the base of the glacier remains frozen to the bedrock.

Basal sliding, on the other hand, involves the entire glacier sliding over the bedrock beneath it, facilitated by a layer of meltwater that acts as a lubricant. This meltwater is produced by pressure melting at the base of the glacier or by geothermal heat. In temperate glaciers, such as those that once covered much of the Sierra Nevada, basal sliding is a significant contributor to glacier movement as exhibited in Figure 9.6.1. The presence of meltwater not only speeds up the glacier’s movement but also enhances its ability to erode the landscape, carving deep valleys and fjords.

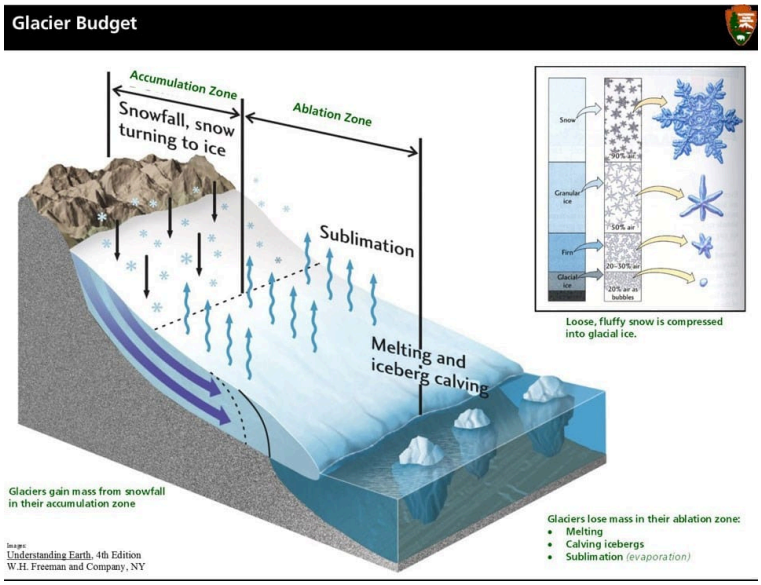


Figure 9.6.1: Anatomy of a glacier. This diagram explains the concept of the glacier budget, which is the balance between the accumulation and ablation of ice within a glacier. If accumulation exceeds ablation, the glacier will advance; if ablation exceeds accumulation, the glacier will retreat. By the National Park Service and licensed under public domain. Access a detailed description.

The glaciers that once covered Yosemite and Kings Canyon National Parks moved in much the same way. For example, the Maclure Glacier in Yosemite, still active today, moves primarily through internal deformation, though it also exhibits some basal sliding during warmer months when meltwater is present. This movement, while slow, is powerful enough to have carved the deep valleys and polished granite domes that are hallmarks of Yosemite's landscape. Similarly, the glaciers that once filled Kings Canyon were responsible for shaping its steep-walled valleys and creating features such as hanging valleys and cirques.

Erosional and Depositional Features of Glaciers

Glaciers are powerful agents of erosion and deposition, capable of reshaping entire landscapes as they move. The process of glacial erosion involves two primary mechanisms: plucking and abrasion. Plucking occurs when a glacier moves over fractured bedrock, causing pieces of rock to break off and become embedded in the ice. As the glacier continues to move, these rocks are transported along with the ice, grinding against the bedrock and deepening valleys. This grinding action, known as abrasion, polishes the bedrock surface and creates striations—linear grooves that indicate the direction of the glacier's movement (Figure 9.6.2). Observing these striations helps geologists understand the dynamics of glacier flow and reconstruct the history of glaciation in a given area.



Figure 9.6.2: Glacial striations and polish near Lambert Dome, Tuolumne Meadows by Daniel Mayer licensed under CC BY-NC 4.0. Access a detailed description.

In the Sierra Nevada, the erosional power of glaciers is evident in the many U-shaped valleys, cirques, and arêtes that characterize the region (Figure 9.6.3). Yosemite Valley is perhaps the most famous example of a U-shaped valley (Figure 9.6.4), formed as glaciers carved through the softer rock, leaving behind steep walls and a flat valley floor. Similarly, cirques—amphitheater-like hollows found at the head of glacial valleys—are common throughout the Sierra Nevada. These features, along with the sharp, knife-like ridges known as arêtes, are remnants of the glaciers that once dominated the region during the Pleistocene.



Figure 9.6.3: Geologic history and formation of Yosemite National Park by National Park Service and Eric Knight is licensed under public domain. Access a detailed description.



Figure 9.6.4: Yosemite from Tunnel View. This view is particularly famous for its ability to capture the essence of Yosemite's grandeur, often inspiring artists, photographers, and nature enthusiasts alike. The combination of geological wonders and natural beauty encapsulates the timeless allure of Yosemite National Park. By Cole Heap is licensed under CC BY-NC 4.0. Access a detailed description.

Glacial deposition, on the other hand, occurs when glaciers lose their ability to carry debris, often due to melting as they retreat. As the ice melts, it deposits the material it has transported, creating a variety of landforms. Moraines, which are accumulations of debris deposited at the edges of glaciers, are common in the Sierra Nevada. Terminal moraines mark the furthest advance of a glacier, while lateral moraines form along the sides. In Kings Canyon National Park, for example, the El Capitan Moraine is a prominent feature that illustrates the extent of glaciation during the Tioga glaciation. Additionally, glacial outwash plains—flat areas formed by sediments carried away from the glacier by meltwater—are found throughout the region, further shaping the landscape.

Query 9.6.1

This interactive element is not available in this format. Visit the link or scan the QR code to access it online.

View this Interactive Content online

Video 9.6.1: Glaciation and Hanging Valley Formation

This video shows how hanging valleys are formed over a long period of glacial history.

This interactive element is not available in this format. Visit the link or scan the QR code to access it online.

View this YouTube Video online

Video 9.6.1: Animation showing glaciers and how hanging valleys form by InterAct Consortium. Used with permission. Access a detailed description.

Sierra Nevada Glaciations

The Sierra Nevada has experienced multiple glaciations, particularly during the Quaternary Period, with each glaciation leaving a distinct mark on the landscape. The Tahoe, Tenaya, and Tioga glaciations are the most notable, with the Tioga glaciation being the most recent and best-preserved. The Tahoe glaciation, which occurred around 70,000 years ago, was the most extensive, covering large portions of the Sierra Nevada with thick ice sheets. These glaciers carved deep valleys, shaped mountains, and left behind a landscape that was dramatically altered by the power of ice.

Following the Tahoe glaciation, the Tenaya and Tioga glaciations occurred, with the Tioga glaciation reaching its maximum extent around 20,000 years ago. The Tioga glaciation, though less extensive than the Tahoe, was responsible for many of the glacial features we see today in Yosemite and Kings Canyon National Parks. During this time, glaciers extended far down the valleys, carving the iconic U-shaped valleys, hanging valleys, and cirques that are now synonymous with the Sierra Nevada's glacial landscape. The retreat of these glaciers left behind a wealth of moraines, erratics, and other depositional features that continue to shape the region's topography. Figure 9.6.5 shows the extent of late glaciation and direction of ice flow in Yosemite National Park and further emphasizes the vast geomorpological features created by glacial movement.

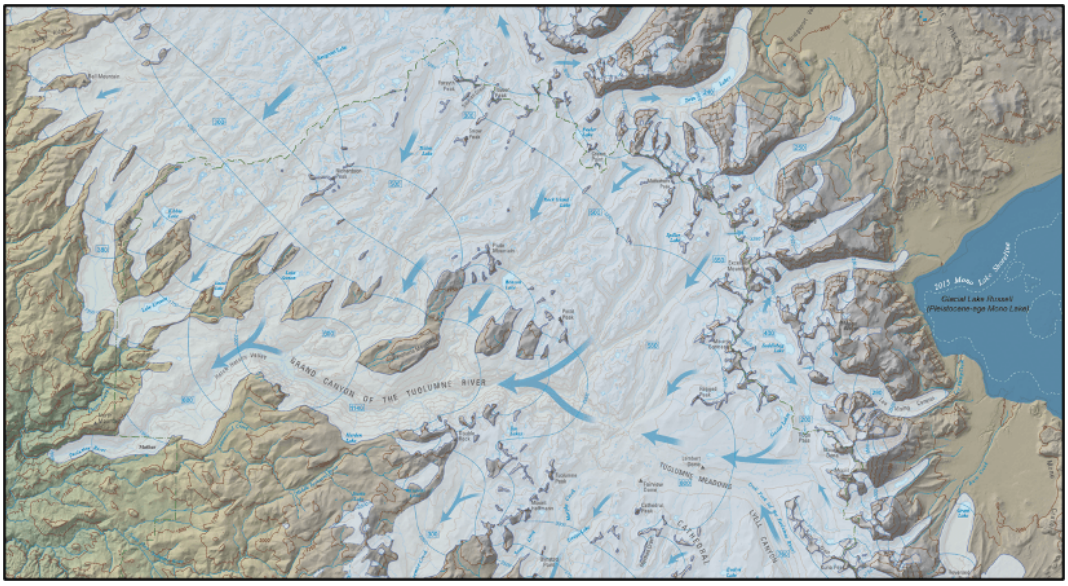


Figure 9.6.5: Glacial extent and direction of ice flow in Yosemite National Park by National Park Service is licensed under public domain. Access a detailed description.

The study of these glaciations provides valuable insights into the climatic conditions of the past and the processes that have shaped the Sierra Nevada. By analyzing glacial deposits and the geomorphology of the landscape, geologists can reconstruct the extent and timing of these glaciations, offering a window into the region's dynamic geological history. The glacial history of the Sierra Nevada also has implications for understanding the potential impacts of future climate change, as the region's glaciers continue to retreat in response to warming temperatures

Query 9.6.2

This interactive element is not available in this format. Visit the link or scan the QR code to access it online.

View this Interactive Content online

Query 9.6.3

This interactive element is not available in this format. Visit the link or scan the QR code to access it online.

View this Interactive Content online

Glaciers Today

Today, the glaciers of the Sierra Nevada are mere remnants of their former selves, a testament to the region's cooler, glacial past. The most notable of these remnants are the Lyell and Maclure Glaciers in Yosemite National Park, the southernmost glaciers in North America. These glaciers, although significantly smaller than they were during the Pleistocene, continue to provide important insights into the processes of glacial movement and climate change. The Maclure Glacier, for example, still exhibits some movement, albeit much slower than in the past, while the Lyell Glacier has ceased moving altogether, indicating that it may no longer be considered an active glacier.

The retreat of these glaciers is indicative of broader trends in global climate change. As temperatures rise, glaciers worldwide are shrinking, and the Sierra Nevada is no exception. The reduction in glacial ice has implications not only for the landscape but also for water resources in the region, as glaciers contribute to streamflow during the dry summer months. The loss of these glaciers would mark the end of an era in the Sierra Nevada's geological history, but they continue to be closely monitored by scientists studying the impacts of climate change.

Video 9.6.2: Retreat of Lyell and Maclure Glaciers

This video shows the retreat of the Maclure and Lyell glaciers from 1883 to 2016. It is silent, and an accessible description is available.

This interactive element is not available in this format. Visit the link or scan the QR code to access it online.

View this Interactive Content online

Video 9.6.2: Animation by the United States Geological Survey and National Park Service is licensed under public domain.

Despite their retreat, the glaciers of the Sierra Nevada remain a critical part of the region's natural heritage. They are not only key indicators of environmental change but also serve as living laboratories where scientists can study the ongoing interactions between climate, ice, and the landscape. As the climate continues to warm, these glaciers offer a poignant reminder of the powerful forces that have shaped, and continue to shape, the Sierra Nevada.

Query 9.6.4

This interactive element is not available in this format. Visit the link or scan the QR code to access it online.

View this Interactive Content online

References

1. Bateman, P. C. (1992). *Plutonism in the central part of the Sierra Nevada Batholith, California*. U.S. Geological Survey Professional Paper 1483.
2. Calkins, F.C. (1930). *The granitic rocks of the Yosemite Region*, in Matthes, F.E. *Geologic history of the Yosemite Valley*. U.S. Geological Survey Professional Paper 160, 120-129. Kessler, M.A., Anderson, R.S., and Stock, G.M. (2006). *Modeling topographic and climatic control of east-west asymmetry in Sierra Nevada glacier length during the Last Glacial Maximum*. Journal of Geophysical Research – Earth Surface, v. 111, F02002.
3. Hildreth, W., & Fierstein, J. (2016). *Eruptive history of Mammoth Mountain and its mafic periphery, California*. U.S. Geological Survey Professional Paper 1812.
4. Huber, N. K. (1981). *Amount and timing of Late Cenozoic uplift and tilt of the central Sierra Nevada, California—evidence from the upper San Joaquin River basin*. U.S. Geological Survey Professional Paper 1197.
5. Lindgren, W. (1911). *The Tertiary Gravels of the Sierra Nevada of California*. U.S. Geological Survey Professional Paper 73.
6. Moore, J.G. and Mack, G.S. (2008). *Map showing limits of Tahoe Glaciation in Sequoia and Kings Canyon National Parks*. Scientific Investigations Map 2945, https:pubs.usgs.gov/sim/2945/
7. Slemmons, D. B., & Brock, V. E. (1975). *Late Ceno
8. Wakabayshi, J. and Sawyer, T. L. (2001). *Stream incision, tectonics, uplift, and evolution of topography of the Sierra Nevada California*. Journal of Geology, v. 109, 539-562.

This page titled 9.6: Ice Shapes the Landscape is shared under a CC BY-NC 4.0 license and was authored, remixed, and/or curated by Cole Heap.

9.7: Natural Hazards of the Sierra Nevada

Introduction to Hazards

In exploring the Sierra Nevada region, it becomes evident that its breathtaking beauty is accompanied by a complex array of geologic hazards. From the rumblings of seismic activity to the cascading threat of landslides, this majestic landscape harbors a myriad of natural dangers. Nestled within its rugged terrain, earthquakes, landslides, rock falls, flooding, and volcanic activity intertwine, each presenting its own unique challenge to those who call this region home.

The Sierra Nevada's geological makeup, characterized by steep slopes and an intricate network of fault lines, sets the stage for a delicate dance of peril. Heavy precipitation, whether in the form of torrential rains or the sudden release of snow melt, serves as the catalyst for landslides, posing a significant threat to communities, vital infrastructure, and the very fabric of the landscape itself.

While the forces of nature shape this region in profound ways, it's important not to overlook the role of wildfires, though not geologic in origin, as they too wield considerable influence. Together, these hazards paint a comprehensive portrait of the challenges inherent in navigating and inhabiting the Sierra Nevada, reminding us of the delicate balance between its breathtaking allure and the ever-present specter of natural disaster.

Landslides and Mass Wasting

Mass wasting, also known as slope movement or landsliding, is the process by which soil, rock, and other debris move down a slope under the influence of gravity. This movement can vary in speed, ranging from very slow creep to rapid landslides, and is a critical geological process that reshapes landscapes over time. The key factors that contribute to mass wasting include gravity, slope steepness, water content, and the strength of the material making up the slope. When the gravitational force acting on a slope exceeds the strength of the material, mass wasting occurs.

There are several different types of mass wasting, each characterized by the material involved and the type of movement. Rockfalls occur when individual rocks or a mass of rocks suddenly break free from a steep slope or cliff and tumble down. This type of mass wasting is common in mountainous areas, particularly in places with steep, exposed rock faces. Rockslides, similar to rockfalls, involve the movement of a large mass of rock down a slope but typically occur along a defined plane of weakness, such as a bedding plane or fault line. These events can be rapid and devastating, moving large volumes of rock in a short period.

Mudslides or debris flows are another type of mass wasting where a mixture of water-saturated soil, rock, and organic material flows down a slope. These flows can be triggered by heavy rainfall, rapid snowmelt, or volcanic activity, and they can move quickly, carrying large amounts of debris over long distances. Mudslides often occur in areas with loose, unconsolidated material and steep slopes, making them common in regions with significant seasonal rainfall. Slumps are a slower form of mass wasting where a block of earth material moves down a curved surface, often creating a stepped or terraced appearance on the slope. This type of movement is typically slower than other forms of mass wasting and can be triggered by factors such as the gradual weakening of the slope material or the addition of water, which reduces the cohesion of the soil or rock. Examples of each of these mass wasting events are exhibited in Figure 9.7.1.

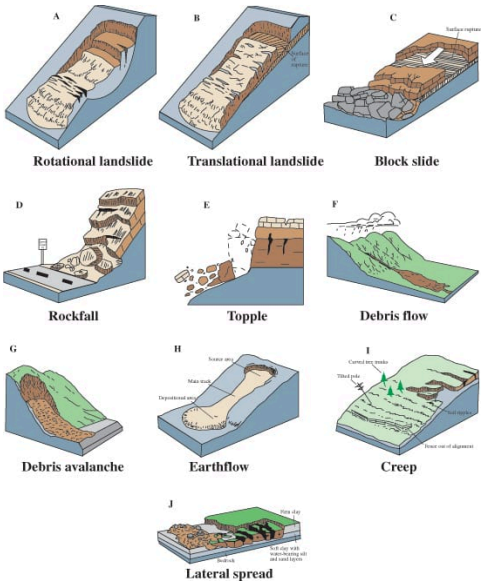


Figure 9.7.1: Examples of some types of mass wasting: rotational landslide (A), translational landslide (B), block slide (C), rockfall (D), topple (E), debris flow (F), debris avalanche (G), earthflow (H), creep (I), and lateral spread (J). By the USGS is in the public domain. Access a detailed description.

The causes of mass wasting are varied but generally include natural processes such as weathering, erosion, and tectonic activity, as well as human activities like deforestation, mining, and construction, which can destabilize slopes. Water plays a crucial role in mass wasting by reducing the friction between particles, adding weight to a slope, and acting as a lubricant that can trigger or accelerate slope failure. The interaction of these factors determines the type, speed, and impact of the mass wasting event. Video 9.7.1 further expounds upon landslide hazards.

Video 9.7.1: Landslide Hazards

In this 6-minute video from the USGS experts discuss a few types of landslides and describe the damage that they can do.

This interactive element is not available in this format. Visit the link or scan the QR code to access it online.

View this YouTube Video online

Mass Wasting of the Sierra Nevada

Steep topography and elevations between 2,438 and 4,267 meters (8,000 and 14,000 feet) combine to create several different natural hazards in the Sierras. These include rockfalls, rockslides and mudslides, floods as well as droughts, avalanches and of course, earthquakes.

The steep topography and elevations of the Sierra Nevada are the result of thousands of years of earthquakes, most occurring along the eastern Sierra Nevada Fault zone, which roughly follows highway 395, running north-south along the eastern edge of the mountain range. This is a predominantly vertical normal fault where the mountain range is the footwall and the desert plateau is the headwall. The entire mountain range has lifted up along its eastern margin, creating a steep ramp of granite and volcanic rock that dips to the west. The fault zone is made of several active faults that are capable of generating large earthquakes like the Lone Pine Earthquake of 1872 which is estimated to have a moment magnitude between 7.4 and 7.9.

The high elevations of the mountains create orographic lift of the atmosphere, which causes rainfall along the western slope of the range. Over time, the rainfall has eroded the rock and carved numerous river canyons into the western slope. In the northern portion are the Pitt, Feather and American Rivers and in the south are the Mokulumne, Stanislaus, Tuolumne, Merced and Kings,

among others. During the recent Ice Ages, glaciers formed in the mountains and flowed downslope, carving many of the river canyons into deep, U-shaped valleys. Along these canyons, both glaciated and not, rockfalls, rockslides and mudflows occur. Rockfalls and rockslides are created as erosion over steepens slopes and rocks give way to gravity, aided by lubrication of rain water and frost wedging from ice that forms in cracks on cold nights. Rockfalls in Yosemite Valley, such as the 1996 Happy Isles Rockfall that fell from Glacier Point receive a lot of news, however there are numerous rockfalls throughout the mountain range. Some impact roads, like the Ferguson Slide on Highway 140 (see Case Study – Ferguson Slide in this section), and some will never be observed in person, except by backpackers.

Query 9.7.1

This interactive element is not available in this format. Visit the link or scan the QR code to access it online.

View this Interactive Content online

Case Study - Ferguson Slide

Introduction

In April of 2006, after two years of heavy rain in the Sierra, approximately 800,000 cubic meters of slate and phyllite slid downslope in the Merced River Canyon, burying Highway 140, between mile posts 103 and 104, and temporarily blocking the Merced River. Highway 140 was closed for 92 days and when it finally re-opened traffic was diverted around the slide and across a temporary bridge to the other side of the river. The slide was not a surprise as the rock layers tilted down toward the highway between 38 and 45 degrees and had been slipping for some time before this event.



Figure 9.7.2: Looking northwest of the east-facing Ferguson Rockslide, Merced River, with the talus covering Highway 140 by United States Geological Survey is licensed under public domain. Access a detailed description.

Background

The Ferguson Slide is situated in Mariposa County, California, within the rugged terrain of the Sierra Nevada Mountain range. This section of Highway 140 traverses through steep canyons and rocky slopes, making it particularly susceptible to geological hazards such as landslides. Because Highway 40 is one of the main roads into Yosemite National Park and used by many park employees to come to work, the road is exceptionally important regionally.

Event Timeline

The Ferguson Slide gained notoriety in April 2006 when heavy rainfall triggered the initial movement of the slope, causing portions of the highway to buckle and crack. Subsequent years saw intermittent periods of activity, with the slide exhibiting ongoing movement and posing challenges to road maintenance crews. In January 2019, a significant movement of the Ferguson Slide occurred, resulting in the complete closure of Highway 140 for an extended period.

Geological Factors

The geological factors contributing to the Ferguson Slide are multifaceted. They include the predominant presence of fractured and weathered metamorphic rock, prone to erosion and instability under certain conditions. The steep terrain and narrow canyon through which Highway 140 passes exacerbate the risk of landslides, as gravity acts upon loose materials. Additionally, heavy rainfall, snowmelt, and freeze-thaw cycles play pivotal roles in triggering slope movements, especially during the wetter months of the year.

Impacts and Mitigation

The closure of Highway 140 due to the Ferguson Slide has had significant ramifications for commuters, tourists, and local businesses, necessitating lengthy detours and impacting regional economies. Mitigating the impacts of the Ferguson Slide has presented substantial engineering challenges, requiring innovative solutions to stabilize the slope and ensure the long-term safety of the highway.

Because Highway 40 is one of the main roads into Yosemite National Park and used by many park employees to come to work, the road is exceptionally important regionally. In 2021, the California Department of Transportation (Caltrans) began developing a mitigation structure that many have come to know as “The Rock Shed”, which will allow the rocks to continue to move downslope but will protect the roadway underneath. As of 2023 they have stabilized much of the slide and will begin to build the rock shed structure in 2024.

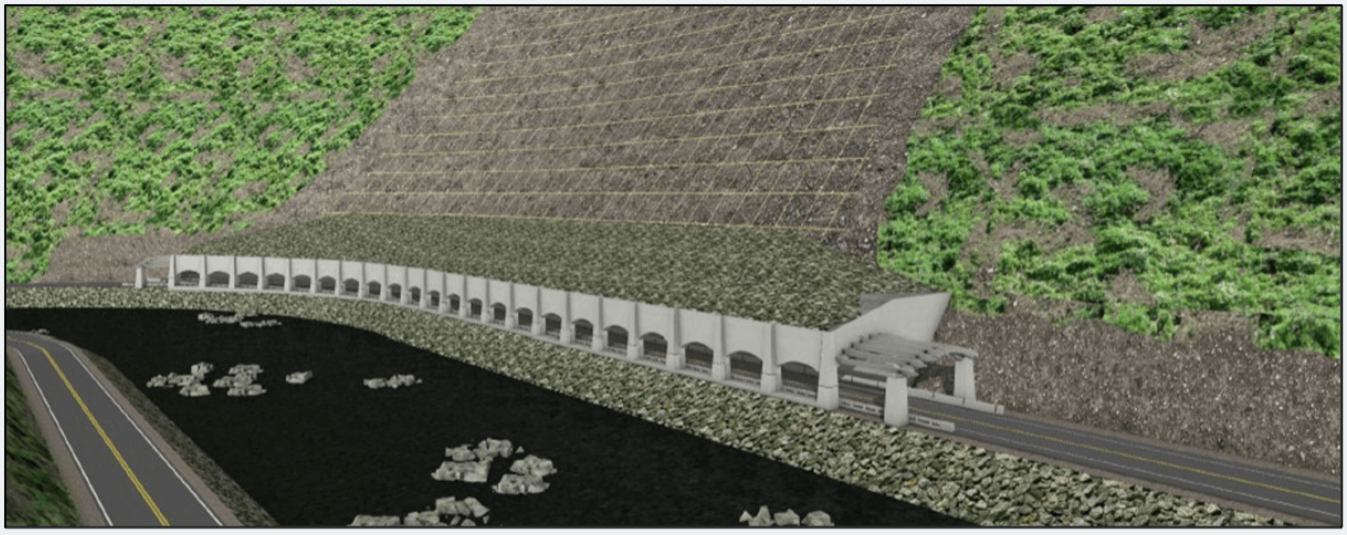


Figure 9.7.3: 3D model of a rock shed built to mitigate mass wasting effects in the Merced River Canyon over Highway 140. The tunnel-like pass built over the road allows rock material to fall on and over the structure, protecting the road. By Caltrans, licensed under public domain. Access a detailed description.

The Ferguson Slide serves as a stark reminder of the intricate interplay between geological processes and human infrastructure. As California continues to grapple with the effects of climate change and natural hazards, understanding and managing geological risks such as landslides will remain paramount for safeguarding lives and livelihoods in the region.

Avalanches

Some years the Sierra Nevada receives incredible amounts of snow during the winter. It was extreme snowfall in the winter of 1846 that trapped the Donner Party near present day Truckee and sealed their fate. Multiple snow events produce variations in the layers of snow, where some layers are light and fluffy, and others are dense and wet. It is this variation in the layers that produce avalanches when one layer slides loose on top of the layer below, sending snow crashing down a slope. Avalanches are powerful

erosional agents that carry trees and rocks down slope with them, steepening the chutes they form and depositing debris where they land. Like rockfalls and slides, most avalanches occur in the back country regions of the mountains, however they do occur frequently near ski resorts and are often marked for back county skiers. Avalanches are also one of the reasons several of the tran-Sierra highways close during the winter. It is simply not worth the risk to try to keep the roads open to traffic in the winter.

Flooding

The Sierra Nevada receives substantial snowfall in the winter, which can lead to spring snowmelt and increased runoff. This runoff can cause flooding in downstream areas, particularly during warm periods when snowmelt is rapid.

The Sierra's river canyons are also prone to floods. When atmospheric conditions are right, the western slope of the mountains are inundated with atmospheric rivers, narrow bands of subtropical moisture that are focused on western North America, generating focused and copious rainfall. The rainfall can be so intense that the water cannot soak into the ground fast enough and flows into creeks and streams and eventually the larger rivers. So much water rushes downslope that the system cannot move it fast enough, and rivers overtop their banks and flood. This process further erodes canyons, causing the slopes to steepen once again, leading to additional rockslides. In the lower elevations of the range, when moisture from rain does soak into and saturate soils, mudslides occur. Mudslides can be observed along roads and highways throughout the foothills and help to shape the topography of the region.

Drought and Wildfires

The western portion of North America is prone to prolonged droughts. A reduction in winter snowfall as well as summer rain, decreases soil moisture which stresses and kills vegetation. The dry and dead vegetation easily catches fire, and so if lighting occurs or if human activities cause a fire, the forests can burn. As climate change warms the atmosphere and creates more erratic weather patterns, droughts are more common, and consequently so are wildfires. The aftermath of wildfires cause debris flows and flooding. This is due to the loss of root structures that hold soil in place. When rain returns, the loose soil and rock are easily washed downslope across roads and into streams and rivers where they can produce local flooding.

While wildfires are not directly geological hazards, they are often exacerbated by the region's geology. The dry climate, coupled with the presence of flammable vegetation, can lead to destructive wildfires. Additionally, post-fire debris flows and erosion can follow wildfires, posing further hazards.

Seismic Hazards

The Sierra Nevada foothills are traversed by a complex network of faults that present significant seismic hazards to the region. Among the most notable of these is the Melones Fault Zone, a major fault system that runs along the western edge of the Sierra Nevada. The Melones Fault is part of a larger system of faults associated with the tectonic activity that has shaped the Sierra Nevada over millions of years. This fault zone, which extends for hundreds of kilometers, marks the boundary between the Sierra Nevada block and the Great Valley block to the west. The movement along the Melones Fault and its associated faults has contributed to the uplift of the Sierra Nevada and the deformation of the surrounding rocks. The seismic activity along this fault zone can generate earthquakes that pose risks to nearby communities, infrastructure, and natural landscapes. While Figure 9.7.4 was first seen in section 9.1 of this chapter, it is placed here to reemphasize the Sierra Nevada elevation changes influenced by faulting. Some of the major and deemed "active" faults (that is, movement having been shown in the last 11,000 years) are present.



Figure 9.7.4: "Relief Map of the Sierra Nevada" by Cole Heap is licensed under CC BY-NC 4.0 Constructed in a GIS using data from California Open Data Portal. Access a detailed description.

In addition to the Melones Fault Zone, the Sierra Nevada foothills are home to several other significant faults, such as the Bear Mountain Fault Zone and the Foothills Fault System. These faults are remnants of ancient tectonic boundaries and continue to exhibit tectonic activity. For instance, the Foothills Fault System, which includes a series of parallel faults extending from the northern to the southern Sierra Nevada foothills, has been the site of numerous small to moderate earthquakes. Although these earthquakes are generally not as powerful as those along the more famous San Andreas Fault, they still represent a serious hazard due to the potential for ground shaking, landslides, and other secondary effects.

Seismic hazards in the Sierra Nevada foothills are further complicated by the region's geology, which includes a mix of brittle metamorphic rocks and younger, more deformable sedimentary rocks. The interplay between these different rock types can amplify seismic waves, leading to more intense ground shaking during an earthquake. This makes the region particularly vulnerable to seismic hazards, even from relatively moderate-sized earthquakes. Understanding the behavior of these fault zones and the potential impacts of seismic activity is crucial for mitigating risks and protecting the communities and ecosystems within the Sierra Nevada foothills.

The risk associated with seismic hazards in the Sierra Nevada depends on factors such as the proximity to active fault lines, the geology of the area, and the vulnerability of infrastructure and communities. While the risk may be lower compared to other parts of California, it is still important for residents, businesses, and policymakers in the Sierra Nevada region to be aware of and prepared for potential seismic events.

Box 9.7.1: Tsunami! In Lake Tahoe?

A seismic event beneath Lake Tahoe, renowned for its pristine beauty nestled in the Sierra Nevada mountains, has sparked discussions among scientists about the potential for a tsunami. Recent research suggests that a massive collapse of the lake's western bank, triggered by seismic activity, could generate waves towering over 9 meters (30 feet), threatening the surrounding communities. And in some cases, it could be as simple as a landslide occurring and debris moving into the lake!

Geologists, utilizing advanced imaging techniques, have uncovered evidence of past tsunamis in the lake's geological history, indicating that such events are not unprecedented. In fact, the USGS has publications showing that landslide events may even have lowered the lake by ~10 meters (~32 feet) during one episode of slope movement! These findings have prompted calls for improved monitoring and preparedness measures to mitigate the potential impact of a future tsunami on the densely populated regions surrounding Lake Tahoe.

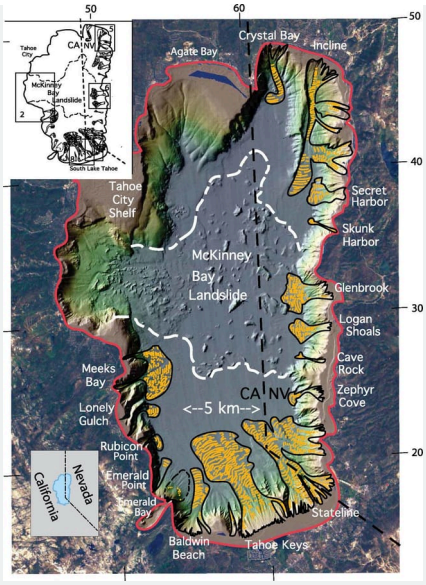


Figure 9.7.5: Lake Tahoe bathymetry showing distribution of giant blocks of McKinney Bay Landslide by United States Geological Survey is licensed under public domain. Access a detailed description.

Hazards experts emphasize the importance of public awareness and education regarding tsunami risks, urging residents and visitors alike to familiarize themselves with evacuation procedures and warning signs. Additionally, ongoing research endeavors aim to refine predictive models and enhance early warning systems, providing vital seconds or minutes for authorities to issue alerts in the event of an impending tsunami.

While the likelihood of a catastrophic tsunami striking Lake Tahoe remains relatively low, the potential consequences underscore the imperative for proactive measures to safeguard vulnerable communities and infrastructure from such geohazards. Through collaborative efforts between scientists, policymakers, and the public, steps can be taken to mitigate risks and ensure the safety and resilience of the region in the face of potential natural disasters.

9.5.7 Mitigation and Looking Towards the Future

To mitigate these hazards, local authorities and geologists monitor seismic activity, assess landslide-prone areas, and implement measures to reduce wildfire risk. Additionally, public education and preparedness are crucial for residents and visitors to the Sierra Nevada to stay safe in the face of these geologic hazards.

Like all geohazards, they are simply part of the natural processes of uplift, erosion and weather in the Sierra Nevada. These hazards are only considered a problem if and when they impact infrastructure and human lives. As more people move to the foothills of the Sierra, and as more people use the mountains for recreation, the need to understand, plan for, and educate the public about the various geohazards of the Sierra will increase.

References

1. California, S. of. (2023). Ferguson Rock Shed Project. Ferguson Rock Shed Project | Caltrans. https://dot.ca.gov/caltrans-near-me/district-10/district-10-current-projects/ferguson-slide-project
2. Harp, E.L., Reid, M.E., Godt, J.W., DeGraff, J.V., and Gallegos, A.J. (2008). *Freguson rock slide buries California state highway near Yosemite National Park*. Landslides, v.5, 331-337.
3. Hutchinson, J. N. (1988). General Report: Morphological and geotechnical parameters of landslides in relation to geology and hydrology. *Proceedings of the 5th International Symposium on Landslide*s, Lausanne, Switzerland.
4. Keller, E. A., & DeVecchio, D. E. (2016). *Natural Hazards: Earth's Processes as Hazards, Disasters, and Catastrophes* (4th ed.). Pearson Education.
5. Montgomery, D. R. (1994). *Slope Movements and Processes*. In *Environmental Geology* (pp. 77-99). John Wiley & Sons.
6. Moore, J.G., Schweickert, R.A., and Kitts, C.A. (2014). *Tsunami-generated sediment wave channels at Lake Tahoe, California-Nevada, USA.* Geosphere (2014) 10(4): 757-768.

7. Moores, E. M., & Twiss, R. J. (1995). *Tectonics*. W.H. Freeman and Company.
8. Page, W. D., & Sawyer, T. L. (2002). *Assessment of active faulting in the Sierra Nevada foothills, California*. U.S. Geological Survey Professional Paper 1646.
9. Selby, M. J. (1993). *Hillslope Materials and Processes* (2nd ed.). Oxford University Press.
10. Stock, G.M. and Uhrhammer, R.W. (2010). *Catastrophic rock avalanche 3600 years BP from El Capitan, Yosemite Valley. California*. Earth Surface Processes and Landforms, v. 35. 941-951.
11. Unruh, J. R., & Moores, E. M. (1992). Quaternary blind thrusting in the southwestern Sierra Nevada, California. *Geology*, 20(3), 251-254.

This page titled 9.7: Natural Hazards of the Sierra Nevada is shared under a CC BY-NC 4.0 license and was authored, remixed, and/or curated by Cole Heap.

9.8: Chapter Summary

9.1 The Sierra Nevada Today

- The Sierra Nevada Province is a 400-mile-long mountain range bordered by the Cascade Range (north), Basin and Range Province (east), and Great Valley Province (west).
- Elevations range from 400 feet to Mount Whitney at 14,496 feet, the highest point in the contiguous U.S.
- The Sierra features diverse glacial formations, such as U-shaped valleys, cirques, and hanging valleys, particularly in Yosemite National Park.
- California's Mediterranean climate brings wet winters and dry summers, with snowpack feeding major rivers into the Great Valley.
- The range's asymmetric profile slopes gently westward, while the eastern side rises sharply, shaped by the Sierra Nevada fault system.

9.2 Ancient Seas Form the Oldest Rocks

- Paleozoic and Mesozoic rocks in the Sierra record over 500 million years of geological history, including marine sediment deposition in ancient seas.
- Roof pendants of metamorphosed sediments, such as the Shoo Fly Complex, represent remnants of ancient oceanic crust and island arcs.
- Sequential accretions of terranes, like the Feather River and Calaveras Complex, reveal complex tectonic processes during the Antler Orogeny.
- Exotic terranes with distinct compositions, such as the Jurassic-Triassic Arc Belt, formed through subduction and collision events.

9.3 The Sierra Nevada Batholith

- The Sierra Nevada Batholith, primarily composed of granodiorite, formed from magmatic pulses during the subduction of the Farallon Plate.
- Plutons intruded over 100 million years, creating the batholith's complex structure, seen in features like Half Dome and El Capitan.
- Jointing and sheeting, such as exfoliation jointing at Yosemite, influenced erosion and shaped iconic landscapes.
- The Tuolumne Intrusive Suite exemplifies magmatic differentiation, with outer mafic zones and inner felsic zones.

9.4 Gold of the Sierra Nevada

- Gold deposits in the Sierra include placer, lode, and disseminated types, typically associated with quartz veins and hydrothermal activity.
- Hydraulic mining during the Gold Rush caused extensive sedimentation, leading to environmental restrictions like the Sawyer Decision.
- Modern mining methods, such as heap leaching, have renewed interest in Sierra deposits.

9.5 Volcanic Features of the Sierra Nevada

- The Sierra Nevada hosts young volcanic features, formed over the last few million years due to extensional processes associated with the adjacent Basin and Range Province.
- The Mono-Inyo Craters volcanic chain, including rhyolitic domes like Panum Crater, erupted explosively within the last 600 years, depositing tephra and pyroclastic flows.
- The Inyo Craters, formed by steam-driven explosions, include South Inyo Crater, measuring 600 feet in diameter and 200 feet deep, surrounded by pumice and ash deposits.
- Obsidian Dome, composed of volcanic glass and rhyolite, formed 600 years ago during explosive eruptions, creating a steep-

sided dome spanning a mile in diameter.
- Mammoth Mountain, a dacitic dome complex near the Sierra's eastern edge, has exhibited volcanic unrest, including earthquake swarms and gas emissions, despite no recent eruptions.
- Devils Postpile showcases columnar jointing in basalt, formed by contraction during cooling of a lava lake 80,000–100,000 years ago, later exposed by glacial erosion.
- Table Mountains demonstrate inverted topography, where Miocene lava flows filled ancient river valleys and erosion of surrounding sedimentary rocks left elevated basalt-capped ridges.
- The Late Cenozoic uplift of the Sierra Nevada reshaped the landscape, preserving volcanic features and influencing tectonic activity along its eastern boundary.

9.6 Ice Shapes the Landscape

- Glaciers in the Sierra Nevada formed during the Pleistocene Epoch, where colder temperatures allowed snow accumulation and compression into ice at higher elevations.
- Glacier movement occurs through internal deformation and basal sliding, carving features such as U-shaped valleys, cirques, and arêtes, evident in Yosemite and Kings Canyon National Parks.
- Erosional processes like plucking and abrasion created iconic features like Yosemite Valley, while depositional processes left moraines and outwash plains.
- Major glaciations (Tahoe, Tenaya, Tioga) reshaped the landscape, with the Tioga glaciation (20,000 years ago) being the most recent and best-preserved.
- Today, remnants like the Lyell and Maclure Glaciers are shrinking, providing key insights into glacial movement and the effects of climate change.
- The retreat of glaciers in the Sierra Nevada has implications for water resources and serves as a marker of global warming's impact on natural landscapes.

9.7 Natural Hazards of the Sierra Nevada

- The Sierra Nevada is prone to natural hazards such as earthquakes, landslides, avalanches, flooding, and wildfires, exacerbated by steep terrain, fault systems, and climate conditions.
- Landslides and mass wasting, including events like the Ferguson Slide, are triggered by rainfall, frost wedging, and erosion, impacting infrastructure and safety.
- Avalanches, common in winter, reshape slopes and disrupt travel in backcountry and trans-Sierra highways.
- Flooding from spring snowmelt and atmospheric rivers erodes canyons and triggers mudslides, while drought and wildfires lead to post-fire debris flows and increased hazards.
- Seismic risks stem from active fault zones, like the Melones and Foothills Fault Systems, posing threats to communities and infrastructure.

This page titled 9.8: Chapter Summary is shared under a CC BY-NC 4.0 license and was authored, remixed, and/or curated by Cole Heap.

9.9: Detailed Figure Descriptions

Figure 9.1 Geomorphic Provinces of California

California is divided into distinct geomorphic provinces, each characterized by unique geological features and landscapes. These provinces include the Klamath Mountains in the northwest, known for their rugged terrain and ancient rocks, and the Modoc Plateau in the northeast, which is a volcanic highland area. The Cascade Range, found to the north of the state, is part of a major volcanic arc in North America.

Moving southward, the Northern and Southern Coastal Ranges run parallel to the Pacific coast, featuring a mix of mountain ranges and valleys. The Great Valley, located in the central part of the state, is a large and fertile agricultural region. The Sierra Nevada, one of the most prominent mountain ranges in California, runs north to south along the eastern edge of the Great Valley and is known for its dramatic peaks and alpine scenery.

To the east of the Sierra Nevada lies the Basin and Range province, characterized by a series of alternating basins and mountain ranges. The Mojave Desert, located in the southeastern part of the state, is a vast arid region with a unique desert landscape. The Transverse Ranges, located in southern California, run east to west, which is unusual compared to the general north-south orientation of most California mountain ranges.

Further south, the Peninsular Ranges extend into Baja California, featuring coastal mountains and valleys. Lastly, the Colorado Desert, situated in the southeastern corner of the state, is part of the larger Sonoran Desert and is known for its extremely arid conditions and distinctive desert features. Each of these geomorphic provinces contributes to the rich geological diversity of California, shaping its natural environment and influencing human activities within the state.

Figure 9.1.1 Air Rises Up the Windward/Western Side of the Sierra Nevada Mountains

This simplified cross-sectional diagram illustrates the process of orographic lift, which affects weather patterns across California's diverse landscapes. Starting from the left, moist air from the Pacific Ocean moves towards land.

As the moist air reaches the Coast Range, a small mountain range, it begins to rise due to the topography. This rising air cools as it ascends. As the air cools, it can hold less moisture, leading to cloud formation and potential precipitation over the Coast Range.

The air then descends into the Central Valley, a flat area between the Coast Range and the Sierra Nevada mountains, warming up as it descends. This reduces the likelihood of precipitation in the valley.

Next, the air encounters the Sierra Nevada mountains, a larger and more prominent range. As the air is forced to rise sharply over these higher elevations, it cools rapidly, leading to significant cloud formation and precipitation as rain or snow on the windward side of the mountains.

Finally, the air descends into the Great Basin. As it moves down the leeward side of the Sierra Nevada, it warms up and dries out. This results in a rain shadow effect, where the Great Basin and other areas east of the Sierra Nevada receive much less precipitation, leading to a more arid climate.

Figure 9.1.2 The Sierra Nevada Mountain Range

This diagram illustrates the geological structure of the Sierra Nevada mountain range in California, showing the relationship between that mountain range, the Central Valley of California, and the Mono Basin.

Starting on the left side, the Central Valley of California is a flat, tan-colored area representing the large, fertile basin located west of the Sierra Nevada. This valley is known for its extensive agriculture, benefiting from the fertile soils and relatively gentle topography.

Moving to the right, the Sierra Nevada mountains are illustrated in green, highlighting the rugged and elevated terrain that characterizes this mountain range. The diagram shows the complex network of rivers and streams (depicted as black lines) that drain from the higher elevations towards the Central Valley. These waterways originate in the high peaks and carve through the landscape, contributing to the dramatic topography of the region.

On the right side of the diagram, the eastern slope of the Sierra Nevada drops sharply towards the Mono Basin. The Mono Basin lies in a tectonically active region, with faults contributing to the uplift of the Sierra Nevada and the subsidence of the basin. Arrows shown along the fault lines emphasize the geological forces at play, particularly the extension (pulling apart) occurring in the region as the Mono Basin area moves downward while the Sierra Nevada moves upward.

Figure 9.1.3 Relief and fault map of the Sierra Nevada

The relief map of the Sierra Nevada region illustrates the diverse topography and significant geological features, including various fault lines that shape the landscape. Most of the faultlines appear along the eastern side of the Sierras, at high elevations, with a few faults along the western slopes at lower elevations. Elevation is color-coded, with green indicating lower elevations along the western flanks of the mountain range and brown to white representing higher elevations along the central core of the range running northwest to southeast. Several major faults are shown:

1. Fort Sage, running north to southeast roughly miles northeast of Sacramento and northwest of Carson City, Nevada
2. Kern Front, running northwest to southeast roughly 5 miles northeast of Bakersfield at the base of the Sierras
3. Hilton Creek, running north to southeast roughly 100 miles northeast of Fresno (almost parallel to San Jose)
4. Kern Canyon, running north to southwest roughly 60 miles due east of Salinas
5. Owens Valley, running north to southeast roughly 90 miles due east of Fresno
6. Southern Sierra Nevada, running north to southeast roughly between the Kern Canyon and Owens Valley faults
7. Garlock, running north to southwest along the southern edge of the Sierras
8. White Wolf, running northeast to southwest roughly 20 miles southeast of Bakersfield
9. Little Lake, the easternmost fault, running north to southeast roughly 90 miles northeast of Bakersfield at a low elevation

Figure 9.1.4 The major river systems in California

This map show the major rivers of California. The map is oriented with north at the top and highlights the extensive network of rivers and water bodies across the state.

California's rivers are depicted in blue, with the most prominent ones labeled, including the Sacramento River, San Joaquin River, Kern River, and the Colorado River. The rivers meander across various regions of the state, flowing from the mountainous areas toward lower elevations, eventually draining into the Pacific Ocean or inland basins.

The map also shows major lakes and reservoirs in light blue, such as Lake Tahoe, Clear Lake, and the Salton Sea. Dry lakes, indicated by dashed lines, are visible in areas like the Mojave Desert, highlighting the state's diverse hydrological features.

The terrain's topography is subtly represented, showing the Sierra Nevada mountain range along the state's eastern edge, the Central Valley through which many of the rivers flow, and the coastal ranges to the west. The map provides a comprehensive overview of California's water system, emphasizing the importance of rivers in the state's geography and ecology.

Overall, this map serves as a vital tool for understanding the distribution and flow of water across California, showcasing the intricate connections between its rivers, lakes, and the surrounding landscape.

Figure 9.2.1 What western North America may have looked like during the Paleozoic era

This cross-sectional diagram illustrates the process of ocean-to-oceanic convergence. The diagram shows two tectonic plates, the oceanic crust, and the continental crust, converging at a subduction zone.

On the left side, the oceanic crust is descending beneath another section of oceanic crust into the Earth's mantle, forming a deep oceanic trench at the boundary. This process is known as subduction. As the oceanic plate descends, it melts due to the high temperatures and pressures within the mantle, leading to the formation of magma.

The magma rises through the overlying plate, eventually reaching the surface, where it forms volcanic islands known as an island arc. These islands are typically located parallel to the trench on the oceanic plate that is not subducting. The diagram also shows the lithosphere and asthenosphere, with the lithosphere being the rigid outer layer of the Earth and the asthenosphere being the more fluid, underlying layer that the lithospheric plates move on.

This image provides a clear representation of how ocean-to-oceanic plate convergence leads to the creation of trenches and volcanic island arcs, key features in understanding plate tectonics and the dynamic processes that shape the Earth's surface.

Figure 9.2.2 Features formed by the intrusion of plutonic igneous rock into preexisting country rock

This cross-sectional diagram of a pluton showcases the magmatic structures within it, with both concordant and discordant contacts. At the top, the diagram shows "country rocks," which are the surrounding older rocks into which the pluton has intruded. The boundary between the country rocks and the pluton is irregular, reflecting the complex interactions between the intruding magma and the existing rocks.

The pluton itself is depicted in pink, with several notable features. "Xenoliths," or fragments of country rock that have been incorporated into the magma, are scattered throughout the pluton. These xenoliths represent pieces of the surrounding rock that were not completely melted by the intruding magma.

Also present are "mafic enclaves," which are darker, denser portions of the pluton, possibly representing earlier or more mafic (rich in magnesium and iron) magmas that were mingled with the main body of the pluton.

"Schlieren," shown as dark streaks or lines within the pluton, represent elongated, lens-shaped concentrations of minerals that form due to the movement and flow of magma. These schlieren often indicate the direction of magma flow and can provide clues about the dynamics of the magma chamber.

Above the pluton, a "roof pendant" is depicted, which is a portion of the overlying country rock that has been left suspended within the magma chamber as the surrounding magma solidified.

Finally, a "stock" is shown on the right side of the diagram, representing a smaller, cylindrical body of intrusive rock that has been fed by the main pluton.

This diagram highlights the complexity of magmatic processes and the variety of features that can form within a pluton as it interacts with the surrounding country rocks.

Figure 9.2.3 Mt. Morrison roof pendant visible from Convict Lake

A serene mountain landscape at sunset, with a calm lake in the foreground that perfectly reflects the surrounding scenery. The water is still, mirroring the rocky shoreline composed of large boulders that extend into the water, creating a natural barrier. The mountains in the background rise steeply, with rugged, angular peaks that are bathed in a soft, pinkish-purple light from the setting sun. The cliffs of the mountains show a mix of gray, brown, and white tones, highlighting the geological layers and textures. Sparse vegetation can be seen on the slopes, and a few trees are visible along the shoreline, adding subtle green and yellow hues to the otherwise rocky landscape. The sky above is clear, with a subtle gradient from the light of the sunset, creating a tranquil and almost ethereal atmosphere. The reflection in the lake captures the entire scene, doubling the beauty of the rugged mountain backdrop.

Figure 9.2.4 An exotic terrane attached to subducting oceanic crust approaching the continent

This diagram illustrates the geological process of terrane accretion, where fragments of the Earth's crust are added to a tectonic plate at a convergent boundary. On the left side of the diagram, an "Incoming Terrane" is approaching the boundary. This terrane is part of the oceanic crust, moving towards the continent. As it approaches, it encounters an "Active Accretionary Wedge," which is a mass of sediment that has accumulated and is being scraped off the oceanic plate as it subducts beneath the continental plate.

To the right of the accretionary wedge, an "Active Volcanic Arc" is shown. This volcanic arc forms as a result of the subduction process, where the oceanic plate is forced down into the mantle, causing melting and the rise of magma, leading to volcanic activity. The volcanic arc is depicted with active volcanism, including an erupting volcano.

Moving further to the right, the diagram shows an "Older Accreted Terrane," which is a previously accreted fragment that has become part of the continental crust. This terrane is shown as more stable, with vegetation growing on it, indicating that it is no longer tectonically active.

Next, a "Suture Zone" is depicted, representing the boundary where the older accreted terrane has joined the "Older Part of the Continent." This zone marks the location of the collision and welding of the terrane to the continental margin.

To the right of the suture zone, the "Extinct Volcanic Arc" is illustrated, representing an older volcanic arc that formed during a previous subduction event. This arc is no longer active, and its remnants have become part of the continental crust, covered with layers of sediment and vegetation.

Finally, the diagram ends with the "Older Part of the Continent," which is a stable, long-established portion of the continental crust, showing little to no tectonic activity and covered with a thick layer of soil and vegetation. The diagram as a whole demonstrates the dynamic process of terrane accretion, where pieces of the Earth's crust are gradually added to continents over geological time scales.

Figure 9.2.5 Major exotic terranes of the northern Sierra Nevada province

This geological map of a section of the Sierra Nevada region illustrates the distribution of various geological formations and terranes. The map labels specific geological units and features:

- Middle to Late Jurassic Arc Sequence, which consists of rocks formed during the Middle to Late Jurassic period, associated with volcanic and sedimentary processes of that era. This sequence is primarily found in the western portion of the map.
- Jura-Triassic Arc Belt, composed of rocks formed during the Jurassic and Triassic periods, also associated with volcanic activity. This belt lies adjacent to the Middle to Late Jurassic Arc Sequence.
- Calaveras Complex, consisting of a mix of volcanic, sedimentary, and metamorphic rocks. It is positioned further east and is a significant geological feature in the Sierra Nevada region. The navy blue color represents the Feather River Terrane, characterized by metamorphic rocks and forming part of the larger Sierra Nevada geological structure. This terrane occupies the northeastern part of the map.
- Northern Sierra Terrane, another distinct geological unit within the Sierra Nevada, consisting of older metamorphic and igneous rocks. It occupies the northeastern part of the map. The maroon or red color represents the Sierra Nevada Batholith, a large, intrusive body of igneous rock that underlies much of the Sierra Nevada. This batholith forms the core of the Sierra Nevada mountains and is a prominent feature on the map.

Key locations identified such as Downieville, Alleghany, Grass Valley, and Confidence are marked on the map, along with the Mother Lode, Melones Fault, and Bear Mountain Fault. These faults and terranes are crucial to understanding the complex geological history and structure of the Sierra Nevada region. The map provides a visual representation of the different geological components that make up this area, illustrating the relationship between various terranes and fault lines.

Figure 9.2.6 Chlorite schist like that found in the Shoo Fly Complex

A sample of chlorite schist from the Shoo Fly Complex. Chlorite schist is a type of metamorphic rock that is characterized by its foliated texture, meaning the minerals are aligned in layers or bands, giving the rock a distinct layered appearance. The rock sample in the image exhibits a range of greenish hues, typical of chlorite minerals, which are a major component of this rock type. The surface of the rock shows the fine-grained, sheet-like layers that are a hallmark of schist, with some areas appearing more coarse or rugged due to the presence of larger mineral grains or inclusions. The texture and color variations on the rock's surface reflect the complex geological processes that have acted upon the original material, transforming it into the metamorphic chlorite schist seen here. The label attached to the rock, marked with the number "150," indicates its identification within a collection, possibly for educational or research purposes. This chlorite schist is part of the Shoo Fly Complex, a geologically significant formation within the Sierra Nevada region, known for its diverse and complex rock types, which have undergone extensive metamorphism and deformation over geological time.

Figure 9.2.7 Map showing plutons and accreted terranes of the Sierra Nevada, California

This geological map of a region in Northern California shows various geologic units and structures with different colors and patterns to represent different rock types and ages. The map is oriented with north at the top and includes a scale bar in kilometers for reference.

On the left side of the map, the Great Valley Alluvium is shown as a broad band stretching from the north to the south of the map. This region is depicted in light gray, representing the unconsolidated sedimentary deposits that fill the Central Valley. To the west of this alluvium, the Coast Ranges are illustrated with various shades of green and yellow. These colors indicate different geological units, such as the Franciscan Complex, a highly deformed and metamorphosed suite of rocks that are part of an accretionary wedge. The San Andreas Fault is prominently marked with a thick black line running through the Coast Ranges, separating different blocks of geological formations.

To the east of the Great Valley Alluvium, the Sierra Nevada foothills and mountains are represented by a range of colors, including purples, browns, and reds, indicating a variety of rock types, including metavolcanic, metasedimentary, and granitic rocks. These colors correspond to different geological terranes, such as the Sierra Nevada Batholith, the Smartville Complex, and the Shoo Fly Complex. The map also shows several major fault lines, including the Melones Fault, which runs parallel to the eastern edge of the map.

The map provides a detailed view of the complex geology of this region, highlighting the interactions between different geological terranes, fault systems, and the processes that have shaped the landscape over millions of years.

Map Features and Units

The map shows a series of geologic units and structures distributed roughly north–south, with the Sierra Nevada Batholith and associated terranes toward the eastern side and older accreted units toward the west. The units include:

- Sierra Nevada Batholith and Plutonic Rocks
  - Large, contiguous areas representing plutonic igneous rocks associated with the Sierra Nevada Batholith.
  - These appear as regions of crystalline intrusive rock bodies with labels indicating rock types such as gabbro, diorite, tonalite, granodiorite, etc.
  - Plutons are often shown as solid bodies with irregular outlines representing the deep-seated intrusive masses.
- Foothills Metamorphic Belt
  - Regional belts of metamorphic rocks occur mainly in the foothills.
  - These belts are separated by faults or significant structural boundaries.
  - Within these belts, smaller subdivisions represent specific complexes such as the Owens Mountain complex, Mill Creek intrusive complex, and others.
  - These metamorphic belts represent accreted terranes and oceanic remnants that were added to the continental margin during tectonic events.
- Ophiolitic and Mélange Units
  - Specific bodies of ophiolite sequences such as the Kings River ophiolite and Smartville-type complexes are labeled and located within the foothills.
  - Serpentinite mélange zones like the Kaweah serpentinite mélange are shown as structurally chaotic assemblages, often next to ophiolitic units.
  - These represent ancient oceanic lithosphere that was thrust onto the continent during subduction and accretion.
- Major Faults and Structural Boundaries
  - The map includes solid and dashed lines showing major faults and shear zones that separate different geologic units.
  - These structural features are labeled with names (e.g., regional fault names) and often mark the boundary between distinct terranes or lithologic units.
  - The orientation of faults is generally north–south with minor curving or jogs indicating complex deformation history.

Spatial Relationships and Interpretation

- Plutonic rocks of the Sierra Nevada Batholith are generally shown east of the metamorphic and ophiolitic units, indicating their position beneath the high crest of the Sierra Nevada range.

- Accreted terranes and metamorphic belts wrap around or lie adjacent to the batholith, reflecting a tectonic assemblage history where oceanic fragments and island arc pieces were added to the continent.
- Oceanic crust remnants preserved as ophiolite bodies and serpentinite mélange are interspersed among the foothill metamorphic units, illustrating a richly tectonically modified ancient margin.

Figure 9.2.8 Petrotectonic Unit Map of Kings-Kaweah Ophiolite Belt

This detailed petrotectonic unit map of the Kings-Kaweah ophiolite belt in central California depicts various geological formations and structures. The map includes a legend that explains the colors and patterns used to represent different rock types and ages, as well as tectonic features.

The map is oriented with north at the top and covers a region that includes Fresno and the surrounding areas, particularly focusing on the Kings River and Kaweah River regions. The map is divided into various geological units, each represented by different colors and patterns.

The legend indicates that the light gray color represents the Early Cretaceous Sierra Nevada batholith, which includes rocks such as gabbro, diorite, tonalite, and granodiorite. The green areas on the map represent the Foothills Metamorphic Belt, which includes several different formations such as the Late Jurassic Owens Mountain complex (depicted in dark green) and the Middle to Late Jurassic Mill Creek intrusive complex (shown in a lighter green).

Other significant units include the Permo-Carboniferous Kaweah serpentinite mélange, represented by a dotted pink pattern, and the Early Ordovician Kings River ophiolite, depicted in a pink color. These formations are associated with complex tectonic processes, including the accretion of oceanic crust onto the continental margin and subsequent deformation and metamorphism.

The map also includes the locations of major rivers, such as the Kings and Kaweah Rivers, and major roads, including Highways 180 and 198. Additionally, there is an inset map in the upper right corner showing the regional context within central California, including the location of the map area relative to the Sierra Nevada Batholith (SNB) and the San Andreas Fault.

Overall, the map provides a comprehensive view of the geological history and structure of the Kings-Kaweah ophiolite belt, highlighting the diverse rock types and tectonic features that have shaped this region over hundreds of millions of years.

Figure 9.2.9 Generalized map showing the Kings River ophiolite

This geological map depicts the area surrounding Pine Flat Lake, Kings River, and nearby mountain ranges such as Dalton Mountain and Bald Mountain, covering a region that includes Pine Flat Lake, Hughes Mountain, and the Mill Creek Valley.

The area includes several significant geological formations.

- Sierra Nevada Batholith (Early Cretaceous intrusive rocks): deep-seated plutonic rocks including tonalite, pyroxene-quartz diorite, and hornblende gabbro that crystallized from magma related to subduction along the western margin of North America. These intrusive rocks form the core and highest structural backdrop in the region, occupying broad exposures in the eastern and central parts of the map area and underlying much of the surrounding topography.
- Mill Creek Intrusive Complex (Middle to Late Jurassic intrusive and metamorphosed volcanic rocks): a complex assemblage of diorite, gabbro, leucotonalite dikes, volcaniclastic sediments, and fragmented metamorphic rocks that record older arc-related magmatic and volcanic activity. This unit appears as elongate bodies and blocks in the western and central sectors of the map, particularly around the Mill Creek Valley and adjacent slopes, structurally between the batholith and older accreted terranes.
- Calaveras Complex (Permian to mid-Triassic deep-marine and mélange rocks): a tectonically mixed suite of bedded radiolarian chert, siliceous argillite, chaotic chert-argillite mélange, siliciclastic and volcaniclastic turbidites, and lenses of marble—remnants of ancient deep-sea sedimentation and deformation. These rocks are exposed in discontinuous belts and blocks in the western and southwestern portions of the map, commonly along fault or shear zone margins adjacent to ophiolitic and intrusive units.
- Kings River Ophiolite (Early Ordovician oceanic lithosphere remnants): a slice of ancient oceanic crust and upper mantle that was tectonically emplaced onto the continental margin. Rock types include pillow basalts, sheeted dike sequences, layered clinopyroxenite, troctolite, and rare chert, representing progressively deeper levels of oceanic lithosphere. This ophiolitic sequence forms a fault-bounded belt in the central and southern areas of the map, especially along the corridor of the Kings River and near Pine Flat Lake, marking where oceanic crust was accreted during ancient subduction events.

- Ductile Shear Zones and Mélange (Permo-Carboniferous tectonic mélange): highly deformed zones containing blocks of metabasite, meta-chert, and metaperidotite within a serpentinite matrix, recording intense tectonic shearing and mixing during Paleozoic to early Mesozoic accretion. These shear and mélange zones commonly appear along the boundaries between the Kings River ophiolite and surrounding units, cutting across the map in linear trends that highlight areas of major structural deformation.

The map also highlights several key structural features, such as oceanic mantle ductile shear zone extensions, strong constrictional fabrics, and steeply dipping crustal sections. These features are important in understanding the tectonic evolution of the region and the processes that have shaped the Sierra Nevada and surrounding areas. Overall, the map provides a detailed and informative view of the complex geological history of this part of California, illustrating the relationships between different rock units and the tectonic forces that have influenced the region over hundreds of millions of years.

Figure 9.3.1 Subduction and Volcanic Arc

This is a detailed cross-sectional view of a subduction zone, where an oceanic plate is being forced beneath a continental plate. The oceanic crust, shown on the left, moves towards the continent and descends into the Earth's mantle at an ocean trench, marked by a deep groove in the seafloor. As the oceanic crust is subducted, it enters the lithosphere, the rigid outer part of the Earth, which includes the crust and upper mantle. The subducting slab pushes into the asthenosphere, a more ductile layer of the mantle below the lithosphere, where it begins to melt due to the increasing pressure and temperature.

The diagram also highlights the creation of an accretionary prism, which forms from sediments scraped off the subducting plate and accreted onto the edge of the overriding continental plate. Above this zone, a volcanic arc is shown forming on the surface of the continental crust, fed by magma generated from the melting of the subducting slab. The magma rises through the lithosphere, accumulating in magma chambers, and eventually reaching the surface to form volcanoes.

The Moho discontinuity, which marks the boundary between the Earth's crust and the mantle, is also illustrated. This boundary is crucial for understanding the difference in material properties and seismic behavior between the crust and the underlying mantle. Additionally, the image depicts rising diapirs, blobs of less dense material that ascend through the lithosphere from the mantle, contributing to the complex processes within the subduction zone. Overall, this cross-section provides a comprehensive view of the dynamic and interconnected processes occurring at a convergent plate boundary.

Figure 9.3.2 Exfoliation jointing, or sheeting, on Half Dome in Yosemite National Park

The iconic Half Dome in Yosemite National Park, California, a massive granite rock formation known for its distinct shape, resembling a giant dome that appears to have been cleaved in half. The smooth, rounded side is contrasted by the steep, vertical face on the opposite side, which towers above the valley floor. The rock surface is a light gray, characteristic of the granite that forms much of the Sierra Nevada mountains.

A significant geological feature visible in the image is the process known as exfoliation jointing or sheeting. This process involves the peeling away of outer layers of rock, much like the layers of an onion, due to the reduction of pressure as overlying material is eroded away. In the case of Half Dome, these exfoliation joints are evident in the form of parallel, curved cracks and fractures that follow the contours of the dome. These joints create the appearance of horizontal layers, which can be seen clearly near the summit and along the steep faces of the formation. The sheeting results in large, slab-like sections of granite that eventually break off and fall, contributing to the smooth, rounded shape of the dome over time.

Visible in the image are the cables used by hikers to ascend the final steep section of the dome, a popular but challenging route. The cables are affixed along a narrow, steep path that climbs toward the summit, illustrating the scale and difficulty of the ascent. In the foreground, a few resilient pine trees cling to the rocky surface, adding a touch of greenery against the stark, towering rock. The bright blue sky overhead provides a clear and vibrant backdrop, emphasizing the sheer height and majesty of Half Dome as it rises dramatically from the surrounding landscape.

This scene captures not only the awe-inspiring natural beauty and the geological grandeur that make Half Dome a symbol of Yosemite but also the dynamic geological processes like exfoliation that continue to shape this iconic formation, making it a destination for adventurers and nature lovers alike.

Video 9.3.1 Half Dome Flyover

The video provides a dynamic flyover of Half Dome, an iconic granite formation located in Yosemite National Park. The camera starts from the northwest, gradually approaching Half Dome, showcasing its imposing height and the smooth, curved face that has been sculpted by geological processes over millennia. As the perspective shifts, the viewer is taken around the southeast side of the dome, offering a sweeping view of the dramatic drop-offs and the surrounding landscape.

As the flyover continues, the video highlights the exfoliation jointing, or sheeting, on the surface of Half Dome. This geological feature is characterized by large, curved slabs of rock peeling away from the main granite body, much like layers of an onion. These layers are a result of the release of pressure from overlying rock, causing the granite to expand and fracture in a series of concentric sheets. The video captures these joints in detail, emphasizing the rounded, stair-like appearance they give to the surface of Half Dome, which is particularly visible as the camera loops around the formation, providing a close-up view of the intricate patterns formed by the exfoliation process. The video concludes by pulling back to reveal the full majesty of Half Dome in its natural setting, framed by the surrounding wilderness of Yosemite.

Figure 9.4.1 Large Gold Nugget (Placer Gold) From California

A large, naturally formed gold nugget against a black background. The nugget has a rough, irregular surface with a slightly flattened shape, showcasing the distinctive luster and bright yellow color characteristic of pure gold. The surface appears uneven with various indentations, which are typical of gold nuggets as they are shaped by natural processes such as erosion and weathering over time. This nugget likely formed over millions of years as gold-rich water deposited tiny particles of the metal into a larger mass. The image effectively highlights the texture and brilliance of the gold, making the nugget a striking example of native gold in its natural form.

Figure 9.4.2 Calaverite Sample

Rock with visible gold veins running through it. The rock is primarily composed of a pale purple to lavender-colored fluorite, which serves as the host for the bright yellow gold that appears in irregular, branching patterns across its surface. The contrast between the dull, opaque fluorite and the shiny, metallic gold makes the veins stand out prominently. The gold appears to be embedded within the fluorite, indicating it was deposited within the rock during the mineralization process. This type of specimen is typical of fluorite veins where gold is often found in hard rock mining environments. The rock is placed against a wooden background, which provides a neutral contrast to the vivid colors of the fluorite and gold.

Figure 9.4.3 Placer Gold Flakes

Irregular gold flakes, with a bright yellow color typical of pure gold. These flakes vary in size but are generally small, with some almost appearing as dust while others are slightly larger. The overall texture of the pile gives the impression of a shimmering mass due to the reflective properties of the gold, which catches the light and highlights the individual flakes' glossy surfaces. The light background enhances the brightness of the gold, making the pile stand out prominently.

Figure 9.4.4 Gold Bearing Quartz from the Mother Lode, CA

A specimen of gold-bearing quartz from the Mother Lode region. The quartz, which appears as a white, translucent mineral, is the host rock that contains visible streaks and patches of gold. The gold is seen as bright yellow metallic flecks and veins interspersed throughout the quartz, contrasting with the white background. Additionally, areas of the specimen have dark, almost black mineralization, which could be associated sulfide minerals that are commonly found alongside gold in quartz veins. The overall appearance highlights the rich, natural occurrence of gold within its host quartz matrix, a characteristic feature of the Mother Lode gold deposits.

Figure 9.4.5 Tectonic Setting of Most Common Gold Deposits

This geological cross-section diagram illustrates the formation of various mineral deposits in different tectonic settings. Oceanic crust subducts beneath continental crust. Along the edges of the subduction are igneous plumes that are buoying upwards, intruding into the surrounding country rock and leaving ore (gold) deposits.

On the left side of the diagram is the continental crust. This region includes Epithermal Au (gold) deposits. Adjacent to the continent is the accretionary wedge, an accumulation of sediments and oceanic crust. Next to that we see the oceanic arc, which represents a volcanic arc formed by subduction. It shows deposits of Epithermal Au, VHMS (Volcanogenic Massive Sulfide) Cu-Au, and Porphyry Cu-Au (skarns).

Positioned behind the volcanic arc is the back arc area, characterized by extensional tectonics and containing VHMS Cu-Au and Porphyry Cu-Au (skarns) deposits. The back arc gives way to accreted terranes, which represent terrains that have been accreted to the continent, featuring Orogenic Au deposits. Further inland, the continental arc shows Epithermal Au and Porphyry Cu-Au (skarns) deposits..

At the far right, the back arc extension region indicates extensional tectonics behind the arc, featuring Epithermal/Hot Spring Au and Carlin-style Au deposits.

Figure 9.4.6 Venting Black Smoker

A hydrothermal vent located on the ocean floor. In the center of the image, there is a venting chimney emitting dark, smoky plumes of mineral-rich fluids. These fluids are released into the surrounding water, creating a dense cloud of black smoke due to the high concentrations of sulfide minerals.

Surrounding the vent, the ocean floor is covered with vibrant red and white tube worms, indicating a thriving biological community. These tube worms rely on the chemicals released by the vent for their energy source, forming a symbiotic relationship with chemosynthetic bacteria.

In the upper part of the image, equipment and cables are visible, indicating the presence of scientific instruments used to study the hydrothermal vent. On the right side, a diver or remotely operated vehicle (ROV) can be seen, providing a sense of scale and highlighting the efforts to explore and understand these unique underwater ecosystems. The overall scene captures the dynamic interaction between geological activity and biological life at hydrothermal vent sites.

Figure 9.4.7 The Origin of Placer Gold Deposits

The geological process through which gold becomes concentrated in streambeds. Gold deposits in quartz veins indicated along mountain slopes are labeled "Mother Load."

Over time, the gold is liberated through weathering and erosion, eventually being carried down into streams. As a stream flows downhill, heavy gold grains settle out of the water when it slows down, particularly around rough areas in the streambed and as the water flows around bends. This settling of gold particles in the streambed leads to the formation of placer gold deposits.

Figure 9.4.8 1852 miners in California work their "long tom" to separate gold from gravel

A black-and-white photograph from 1852, depicting miners in California working at a mining site. The focus is on a group of four miners engaged in using a "long tom" to separate gold from gravel. In the foreground, two miners are actively working, one holding a shovel and the other standing near the long tom, a trough-like structure used in gold mining. The long tom is filled with gravel, which is being washed by water to separate out the gold. Behind them, a third miner is sitting on a wooden cart pulled by a horse, which is waiting nearby. The scene is set in a rural, hilly area with some trees and vegetation in the background, capturing a moment from the Gold Rush era, highlighting the labor-intensive process of gold mining during that time.

Figure 9.4.9 Index Map of 1968 Placer Deposits in Nevada County, CA

A map of Nevada County in California, highlighting its river systems and neighboring areas. This region is located in northeast California, along the Nevada border, and includes the North, Middle, and South Forks of the Yuba River, which converge near Nevada City.

The 1968 placer deposits are shown along the north edge of Nevada County, between the Middle Yuba River and the South Yuba River.

Key locations outside of Nevada County include the following:

- Feather River, to the west of the county and running roughly North-South. Cities on the river, from north to south, include Oroville, Yuba City, and Maryville.
- Sacramento River, to the west of the Feather River. Cities on the river, from north to south, include Colusa and Sacramento (which is about 60 miles southwest of Nevada City).
- American River, which joins the Sacramento River at Sacramento and runs northeast from there, splitting into the North Fork and South Fork after approximately 20 miles. The city of Auburn is shown along the North Fork, located near the location of another split in the river (the Middle Fork). Placerville is just south of the South Fork, about 60 miles east from Sacramento.
- Lake Tahoe spans the state line and is about 100 miles east of Sacramento.

Figure 9.4.10 Acid mine drainage into Spring Creek, in Shasta County

An aerial view of a site where acid mine drainage is flowing into Spring Creek, California. The landscape appears dry and rugged, with a mix of sparse vegetation and exposed earth. A narrow stream, heavily stained with orange and yellow hues from the acidic water and iron deposits, runs through the center of the image. The vibrant colors are a result of the chemical reactions between the acidic water and minerals, which are common in areas affected by mining activities. The surrounding area includes steep, eroded slopes, indicating the impact of both natural and human activities on the landscape. The road at the top left of the image suggests that the site is near a developed area, but the environmental damage from the acid mine drainage is evident, highlighting the ecological challenges posed by abandoned or improperly managed mining sites.

Figure 9.4.11 Hydraulic Mining, CA, 1870s

Hydraulic mining was a method used during the California Gold Rush. Water is shot through a nozzle at high pressure onto the face of a cliff, thereby washing away tons of boulders, gravel, dirt, and, in the hopes of the miners, gold would be washed out of the gravel. The image shows powerful jets of water being directed at a mountainside to dislodge large volumes of earth and rock. These water jets, emerging from several high-pressure hoses, arc through the air, creating a misty spray.

In the foreground, a wooden structure resembling a flume or sluice can be seen, which was used to channel water and washed material. Several men are standing on the rocky ground, indicating the scale of the operation. The background reveals a steep, eroded cliff face, highlighting the significant environmental impact of hydraulic mining.

The overall scene illustrates the intensity and scale of hydraulic mining operations, where large amounts of water were used to extract gold from sediment. The method involved washing away entire hillsides to access gold deposits, which caused substantial changes to the landscape and had long-term environmental consequences.

Figure 9.4.12 CA Gold Mines by Type and Status, 1995-2023

Map of gold mine locations between 1995 and 2023 in California, most of which are shown in the northern portion of the Sierra Nevada Province.

This map illustrates the locations and statuses of gold mines in California from 1995 to 2023. It features a satellite image of Northern California, overlaid with symbols indicating the type and status of gold mines.

The map highlights several clusters of gold mines, particularly in the regions of the Sierra Nevada and Northern California. Significant concentrations of active and abandoned mines are visible around Shasta National Forest, Lassen National Forest, and Tahoe National Forest. The inset in the upper right corner offers a broader view of the map's coverage area within California, indicating the Sierra Nevada Province's location relative to major cities such as San Francisco and Los Angeles.

This visual representation helps to understand the distribution and historical activity of gold mining within the state, showcasing both the enduring legacy of the Gold Rush era and the ongoing exploration and extraction efforts.

Figure 9.5.1 South Inyo Crater Lake near Mammoth, CA

The crater is a circular depression with steep, rocky walls composed of volcanic material. The slopes leading down to the lake

are strewn with loose rocks and boulders, indicating the volcanic origin of the crater. The lake itself is a serene, turquoise body of water that fills the bottom of the crater, contrasting vividly with the darker, rugged terrain surrounding it. Dense forests of coniferous trees surround the crater, with tall pine trees dominating the landscape. In the background, the peaks of the Sierra Nevada mountains are visible, partially obscured by a hazy sky. The scene captures the natural beauty and geological significance of the area, with the crater being a remnant of past volcanic activity in the region.

Figure 9.5.2 Obsidian Dome near Inyo Craters

Rugged terrain in the foreground is filled with loose, angular boulders and rocks that are dark in color, likely volcanic in origin. The steep slope leads up to a jagged ridge of volcanic rock. The sun is positioned just above the ridge, casting bright rays of light and creating a lens flare effect across the image. The intense sunlight highlights the rough texture of the rock formations, adding depth and contrast to the scene. The sky is clear, with a deep blue hue that emphasizes the harsh, exposed nature of the landscape. The overall atmosphere is one of stark beauty and raw geological power, characteristic of the volcanic features in this region.

Figure 9.5.3 Snowflake Obsidian Sample from Obsidian Dome

A piece of snowflake obsidian, a type of volcanic glass, being held in someone's hand. The obsidian is dark black with a glossy, glass-like texture, characteristic of this material. Scattered across the surface of the obsidian are small, white, snowflake-like patterns, which give this particular variety of obsidian its name. These snowflake patterns are formed by the crystallization of the mineral cristobalite within the volcanic glass as it cools. The hand holding the obsidian is positioned in such a way that the viewer can see the texture and detail of the rock clearly, with sunlight highlighting the contrast between the black obsidian and the white snowflakes. The background suggests an outdoor setting, likely at the site where the obsidian was found, such as Obsidian Dome in California. The surrounding environment, partially visible in the background, includes vehicle components, suggesting that this piece of obsidian was collected or observed during fieldwork or a visit to the volcanic site.

Figure 9.5.4 Schematic Illustrations of the Formation of Inverted Topography

Three diagrams illustrate the process of inverted topography formation over time. The first diagram, labeled "At Eruption," shows a volcanic landscape immediately after an eruption. A lava flow extending from the base of a volcano and down a slope. This lava flow has solidified and sits atop the surrounding volcanic ash or tephra. The landscape at this stage has a typical volcanic profile, with the lava flow lying lower in the landscape compared to the surrounding, higher areas.

The middle diagram represents an intermediate stage in the formation of inverted topography. Over time, the softer surrounding materials, such as ash and tephra, begin to erode away due to weathering and other natural processes. As a result, the lava flow, which is more resistant to erosion, starts to stand out more prominently as the surrounding landscape is worn down. The previously lower-lying lava flow is now becoming more elevated relative to the eroding landscape around it.

The final diagram, labeled "Today," depicts the present-day landscape after significant erosion has taken place. The formerly low-lying lava flow has now become a raised, flat-topped ridge or mesa, while the surrounding softer materials have been almost entirely eroded away. This results in what is known as inverted topography, where the once lower-lying lava flow is now a prominent elevated feature in the landscape, and the former higher terrain is now at a lower elevation. The diagrams effectively show the transition from a typical volcanic landscape to one where the more resistant lava flow becomes an elevated ridge due to the differential erosion of the surrounding softer materials, illustrating the concept of inverted topography.

Figure 9.5.5 Looking Southeast from Pincushion Peak towards Big Table Mountain

This landscape is characterized by rolling hills covered in lush green vegetation, indicative of a typical springtime scene in the region. In the foreground, scattered rocks and a few trees, some of which appear to be affected by fire or disease, dot the grassy terrain. The middle ground reveals a calm body of water, likely a reservoir or small lake, nestled between the hills. The water level is visibly lower, with a distinct lighter-colored band of exposed shoreline encircling it, suggesting a recent drop in water levels.

In the background, Big Table Mountain stands out as a prominent, flat-topped mesa, a result of the area's unique geologic history involving volcanic activity. The steep cliffs of the mesa are partially covered with trees, and the overall landscape is framed by a sky with light, wispy clouds. The scene captures the serene beauty of the Sierra Nevada foothills, where natural features like mesas and valleys are sculpted by the forces of erosion and volcanic activity.

Figure 9.5.6 Aerial Imagery Showing Big Table Mountain in Fresno and Madera Counties, CA

This aerial view captures the distinct topography of the region, highlighting the rugged, undulating terrain. The image is dominated by the presence of Millerton Lake, whose deep blue waters contrast sharply with the surrounding dry, brown hills. The lake's irregular shape forms several inlets and peninsulas, including the prominent Pincushion Peak area, which juts out into the water.

Big Table Mountain is characterized by its long, flat-topped mesas, which stand out against the surrounding landscape. These mesas are remnants of ancient lava flows that have resisted erosion, leaving behind these prominent features. The mesas are primarily covered in sparse vegetation, with some areas more densely forested, particularly along the northern edges.

To the southeast, near Marshall Junction, the terrain becomes less rugged, transitioning into more developed areas with visible roads, structures, and agricultural lands. The image also shows various points of interest, such as trailheads and ecological reserves, indicating the area's significance for recreation and conservation.

The overall view provides a comprehensive look at the geological and topographical features of Big Table Mountain, showcasing its unique formation and the way it dominates the landscape in this part of California.

Figure 9.5.7 Devils Postpile

This striking geological formation, characterized by vertical, columnar basalt structures known as columnar jointing. These columns appear as tall, hexagonal pillars of rock, rising vertically from the ground. The formation is prominently featured on a hillside, with the columns creating a ribbed effect along the slope.

In the foreground, there is a field of large, angular rocks and boulders, likely fragments that have broken off from the main basalt columns over time. The rocky ground gradually ascends towards the middle ground, where the columns begin.

Above the columns, the landscape transitions into a more vegetated area. The top of the hill is dotted with tall pine trees, adding a contrasting element of greenery to the gray and black tones of the basalt columns. These trees are scattered, some standing alone while others form small clusters.

The sky above is clear and blue, with no visible clouds, indicating a sunny day. The overall scene combines the ruggedness of the basalt columns with the natural beauty of the pine trees, showcasing a unique intersection of geological and botanical elements.

Figure 9.5.8 Diagram Showing the Formation of Columnar Jointing

Three hexagonally shaped columns that represent the jointing pattern typical of this geological phenomenon. The top of the columns is labeled as a "Cold Surface," indicating that this is where cooling begins.

As the surface cools, it contracts, causing the rock to fracture. The fractures propagate downward as the cooling and contraction continue, eventually forming the characteristic hexagonal columns seen in columnar jointing.

The left side of the image is labeled with "Hotter" at the bottom and "Cooler" at the top, highlighting the temperature gradient from the hot, cooling lava or magma below to the cooler surface above. The right side of the image indicates "Fracture Propagation" with an arrow pointing downwards, showing how the fractures deepen as the cooling process advances.

Overall, the diagram effectively demonstrates how the contraction of cooling lava or magma leads to the formation of these distinct hexagonal columns, a process commonly observed in places like the Giant's Causeway in Northern Ireland and Devil's Postpile in California.

Figure 9.5.9 On Top of Devils Postpile

This basaltic formation has a distinct hexagonal pattern, characteristic of columnar jointing. The hexagonal basalt columns are arranged in a tightly packed pattern, creating a tiled appearance on the ground's surface. The columns are slightly raised and uneven, with some sections appearing more weathered than others, resulting in a textured surface.

In the background, the image transitions into a wooded area with tall pine trees. These trees are scattered and cast shadows over the basaltic formation, adding depth to the scene. Beyond the immediate area of the columns, a forested valley is visible, showcasing a variety of vegetation and rugged terrain. The distant cliffs and rock faces add to the dramatic natural landscape.

The overall scene combines the unique geological structure of the basalt columns with the lush greenery of the pine forest, illustrating the interplay between geological formations and the surrounding natural environment.

Figure 9.6.1 Anatomy of a Glacier

This diagram is divided into two primary zones: the Accumulation Zone and the Ablation Zone. A glacier is shown along the side of a rocky mountain, with the Accumulation Zone near the top of the mountain and the Ablation Zone about halfway down its slope.

Snowfall and ice formation occur in the Accumulation Zone. Glaciers gain mass as snowfall accumulates and compresses over time, transforming into glacial ice. An inset diagram provides a detailed explanation of this process, showing the transition from loose, fluffy snow (containing about 90% air) to granular ice (with 50% air), then to firn (with 20% to 30% air), and finally into dense glacial ice with about 20% air as bubbles. As the glacier moves down the mountainside, it reaches the Ablation Zone. Glaciers lose mass in their ablation zone, due to sublimation (or evaporation), the direct transformation of ice into water vapor; melting as the glacier meets the ocean; and the calving of icebergs, where chunks of the glacier break off into the ocean.

Figure 9.6.2 Glacial striations and polish near Lambert Dome

Glacial striations are formed when a glacier moves over a bedrock surface, dragging along rocks and debris embedded in the ice. The resulting linear grooves are indicative of the direction of the glacier's movement and can provide important information about past glacial activity.

In this image, the striations are clearly visible as linear features cutting across the bedrock surface. The patterns are parallel to each other and vary in depth and width, depending on the size of the debris and the force exerted by the moving glacier. The smooth, polished appearance of the rock surface alongside the striations further highlights the erosive power of glacial ice as it shapes the landscape.

Figure 9.6.3 Geologic History and Formation of Yosemite National Park

The series of images illustrates the formation of Yosemite Valley over geological time, depicting the transformation of the landscape through various stages of glacial activity.

The first image shows Yosemite Valley before significant glaciation, with steep granite walls and a deep, V-shaped valley typical of river erosion. Vegetation covers much of the valley floor and the surrounding mountains.

In the second image, the onset of glaciation is evident as glaciers begin to flow into the valley. The glaciers carve out the granite, deepening and widening the valley into a U-shape. The movement of the ice is marked by striations and moraines, indicating the powerful erosive forces at work.

The third image depicts the peak of glaciation, with the valley entirely filled with thick glacial ice. The glaciers continue to sculpt the granite, polishing and rounding the valley walls. This stage shows the maximum extent of glaciation, with ice flowing through the valley and over the surrounding highlands.

In the fourth image, the glaciers begin to recede, leaving behind glacial lakes and deepened valleys. The retreating ice reveals the U-shaped valley, now filled with glacial meltwater. The newly formed lakes are bounded by moraines and other glacial deposits, creating a dramatic landscape of water and rock.

The fifth image shows the post-glacial landscape of Yosemite Valley. The glaciers have fully retreated, leaving behind a wide, flat valley floor with remnants of glacial lakes and polished granite cliffs. The iconic features of Yosemite, such as Half Dome and El Capitan, stand prominently in the landscape, sculpted by the glacial activity. Vegetation begins to recolonize the valley, adding green to the stark granite and blue waters.

This sequence visually captures the dynamic processes of glaciation and deglaciation, highlighting the profound impact glaciers have had on shaping Yosemite Valley through time. The transformation from a river-carved valley to a glacially sculpted U-shaped valley showcases the power of natural forces in creating the dramatic and iconic landscapes we see today.

Figure 9.6.4 Yosemite from Tunnel View

The iconic Tunnel View overlook in Yosemite National Park, providing one of the most famous and breathtaking vistas in the park. From this vantage point, you can see a panoramic view of Yosemite Valley, framed by towering granite cliffs and lush forests. On the left side of the image, El Capitan dominates the scene with its sheer vertical face, a favorite among rock climbers worldwide.

To the right, you can see Bridalveil Fall, known for its ethereal beauty as the water cascades down a 620-foot drop, often creating a delicate mist that resembles a bridal veil. In the distance, Half Dome rises majestically, its distinctive silhouette marking one of Yosemite's most recognizable landmarks. The valley floor below is covered with a dense forest of conifers, and during different seasons, the colors and lighting can dramatically change, enhancing the natural beauty of the landscape.

Video 9.6.1: Glaciation and Hanging Valleys Formation

This Interact educational resource describes how hanging valleys are formed through a long period of glacial history. It is an educational resource produced by Tom State University for Interact, Wicked Weather Watch, University Arctic and EduArctic. During the last ice age, which ended about 10,000 years ago, much of the north was covered in ice sheets, such as that that can be seen in the distance.

These ice sheets had outlets in glaciers that flowed under the force of gravity down through the mountain valleys, many into the sea. In this case, we are stood above the glacier looking to the ice sheet which accumulates snow, and behind us the mouth of the glacier reaches much further behind us. It's snowing to denote that this is a cold period, but of course it snows every year in the north.

As well as the accumulation of ice and snow in the glacier and the ice sheet in the valleys, we have small ice caps and areas of snow on the mountain tops. Some mountain tops, however, are clear of snow and ice and these are called nunnitacks. These nunnitacks were important habitats in previous cold periods for the survival of plants.

During a warm period, such as 10,000 years ago or now, the snow accumulation decreases and the glacier and ice sheet start to lose volume and the glacier starts to retreat along the valley from behind us until it's in front of us and we can see the snout of the glacier retreating into the background. At the same time, the mountain glacier on the right-hand side starts to lose volume and disconnects with the glacier in the valley below. At the tops of the mountains, frost works on rocks to shatter them, producing small materials and these are washed down the mountain slopes in gullies in the rocks and accumulate at the foot of the mountain slopes as alluvial fans.

During the past 10,000 years there have been many climate fluctuations with warm and cold periods. Here we see a cold period denoted by snow, although remember that the snow falls every year. During these cold periods the ice sheets accumulate more snow and ice and the glaciers flow again towards us and down the valleys and the connection between the hanging glacier on the right at the top of the mountain and the glacier at the bottom is established again.

In a renewed period of warming, the glacier of course starts to retreat again as we saw earlier on. This time you can see a moraine being left behind as the glacier retreats. This moraine marks a point at which the glacier terminated following the last advance.

These moraines are formed when materials, rocks sliding down the mountains, fall on the glacier and also from materials being pushed from the valley floor in front of the glacier and of course they're most visible when the glacier retreats and leaves them behind. During the warming process the hanging glacier or the mountain glacier has been disconnected from the glacier and the valley and now there is a hanging valley with a small lake in it and a waterfall down to the valley floor below. As the climate continues to warm the snow and ice disappear leaving the hanging valley with its lake and waterfall to the valley floor below.

Also vegetation starts to move in. Initially the grasses and herbs are established but later trees become established also and of course the land which has been without snow and ice for the longest have the most advanced vegetation of the forest. The sequence you have seen represents what has happened since the last ice age in an area for example like Scotland or the English Lake District or the Swedish Subarctic but of course we have only shown one advance and two retreats.

In practice there may have been very many in the 10,000 years that have been depicted in just a few moments. The finishing frame is what we see today but of course the sequence we've shown could depict what happens now and from now onwards to the high arctic area which is now glaciated much as the north of Britain would have been 10,000 years ago. So we have provided two scenarios.

One an animation of what we have seen over the past 10,000 years for areas which now look like this frame you are looking at but also areas of the high arctic which are now covered in ice and snow which could in some hundreds of years look like the frame we're looking at now. This has been an interact educational resource. The animation was developed by Vyacheslav Rudchenko of Tomsk State University and it was designed by Professor Terry Callaghan on behalf of Interact, the University of Arctic, Wicked Weather Watch and Eduarctic.

It had valuable input from Professor Perlmund of Stockholm University and Dr Kristi Jönsson of Uppsala University.

Figure 9.6.5 Glacial Extent and Direction of Ice Flow in Yosemite National Park

This map of ice and glacier flow within Yosemite National Park focuses on the Tuolumne River region. The intricate patterns of glacial movement are depicted with arrows, indicating the direction and flow of the ice across the landscape. This map highlights the extensive glaciation that shaped Yosemite's topography over thousands of years.

You can see the vast ice fields and the paths they carved through the valleys and over the ridges. The Tuolumne River canyon, prominently featured in the center, is shown to have been heavily influenced by glacial activity, with the ice flows converging and diverging as they moved through the terrain. The arrows indicate the dominant flow directions, demonstrating how the ice would have moved from downhill from the high Sierra crest, primarily toward the west, with local variations to the northwest or southwest depending on valley orientation, sculpting the granite and creating the dramatic landscape Yosemite is famous for today.

The map also includes elevation markers, providing a sense of the scale and vertical relief within the park. The detail of the glacial flows offers insight into the dynamic processes that have contributed to Yosemite's formation, illustrating the powerful forces of nature that continue to shape the park's environment. This visual representation of ice and glacier movement is a testament to the geological history of Yosemite, showing the enduring impact of glaciation on its stunning landscapes.

Video 9.6.2 Retreat of Lyell and Maclure Glaciers

This silent animation shows how two major glaciers lose volume over a span of 132 years.

1883: Maclure Glacier is located in the northwest of the region shown and has an area of 0.4 square kilometers. To the southeast, the much larger Lyell Glacier - actually two connected glaciers, Lyell Glacier West and Lyell Glacier East - has an area of approximately 1.2 square kilometers.

1903: Macclure Glacier is now approximately 0.35 square kilometers in size, while Lyell Glacier has shrunk more dramatically to approximately 1.5 square kilometers. Shrinkage is occurring along the northern borders of both glaciers.

1931: Maclure Glacier is now at approximately 0.3 square kilometers in size, while Lyell Glacier has shrunk at a greater rate down to approximately 0.9 square kilometers. Both glaciers continue to retreat along their northern borders. The Macclure Glacier is also retreating along its western flank, while the Lyell retreats along its western and eastern flanks.

1944: Macclure Glacier has a flatter slope of retreat, and is now just over 0.2 square kilometers, while Lyell Glacier has shrunk to less than 0.8 square kilometers in size. Both glaciers continue the same pattern of retreat. The Lyell Glacier is now in two sections that meet only in one small area.

1955: Macclure Glacier has shrunk to just above 0.2 square kilometers in size, while Lyell Glacier haas dropped dramatically to about 0.6 square kilometers. Both glaciers are now retreating along their western, northern, and eastern flanks.

1972: Macclure Glacier is now about 0.2 square kilometers in size, while Lyell Glacier has dipped below 0.6 square kilometers. The pattern of retreat continues, but now Lyelle Glacier East has begun retreating along its southern border as well.

1993: Macclure Glacier is just under 0.2 square kilometers in size, while Lyell Glacier is approximately 0.5 square kilometers. For both glaciers, the rate of retreat has slowed over the previous 20 years. The same pattern of retreat continues, and now Lyelle Glacier West is now retreating along its southern border too.

2003: Macclure Glacier has stabilized at 0.2 square kilometers, but Lyelle Glacier has dropped to just above 0.4 square kilometers in size. The patterns of retreat continue.

2012: There is little change in Macclure Glacier, but Lyelle Glacier has dropped to approximately 0.4 square kilometers in size. Lyelle Glacier is now in three separate sections, with Lyelle Glacier East in two small areas - a band along its west and south flank, and a much smaller area to the northeast.

2013: Both glaciers suddenly retreat, with Macclure Glacier now at approximately 0.15 square kilometers and Lyelle Glacier just below 0.4 square kilometers. The patterns of retreat continue.

2014: Macclure Glacier is at approximately 0.1 square kilometers, with Lyelle Glacier at approximately 0.3 square kilometers in size. Both sections of Lyelle Glacier East are dramatically smaller than Lyelle Glacier West.

2015: There is little change in Macclure Glacier, but Lyelle Glacier is now below 0.3 square kilometers in size.

Figure 9.7.1 Examples of Some Types of Mass Wasting

Types of mass movements and landslides are classified based on their movement mechanisms and the materials involved.

Figure A depicts a rotational landslide, which occurs when a mass of earth or rock moves down a slope along a curved surface, causing the sliding mass to rotate backward. This type of landslide often leaves a concave scar on the slope.

Figure B shows a translational landslide, where the sliding material moves down a slope along a relatively planar or flat surface. Unlike rotational landslides, translational landslides typically involve less rotation of the sliding mass.

Figure C illustrates a block slide, a type of translational landslide where the moving mass consists of a large, intact block of rock or soil that slides down along a surface of rupture.

Figure D displays a rockfall, where rock fragments break off from a steep or vertical cliff and fall freely or bounce down the slope. Rockfalls are common in mountainous regions and can be triggered by weathering, earthquakes, or other factors.

Figure E portrays a topple, a type of mass movement where a rock or earth mass tilts forward and falls due to the gravitational pull, often occurring on slopes where the base of the mass is weaker or eroded.

Figure F shows a debris flow, which involves the rapid downslope movement of loose soil, rocks, and organic material mixed with water. Debris flows are highly fluid and can travel long distances, often following river valleys.

Figure G depicts a debris avalanche, a fast-moving, turbulent flow of debris that can travel at high speeds, carrying large volumes of material downslope. Debris avalanches are typically triggered by earthquakes, volcanic activity, or heavy rainfall.

Figure H represents an earthflow, where fine-grained materials, such as clay or silt, flow downslope in a viscous manner. Earthflows typically move slowly and are common in humid environments.

Figure I illustrates creep, a slow and gradual downslope movement of soil or rock, often imperceptible over short time periods. Creep is usually indicated by curved tree trunks or tilting fences and other structures on the slope.

Figure J shows a lateral spread, which occurs when a layer of soil or rock spreads laterally due to liquefaction or the failure of underlying layers. Lateral spreads are commonly associated with earthquakes and can cause significant ground deformation.

Figure 9.7.2 Ferguson Rockslide

An aerial view of a steep, rocky hillside with a distinct slope and exposed rock formation. The terrain is densely vegetated with green shrubs and trees on both sides, highlighting the rugged and natural landscape. At the base of the slope, a river flows, bordered by additional vegetation, indicating a typical riverine environment.

The rock formation appears to be a result of geological processes, with visible layers and a clear demarcation between the rocky slope and the surrounding vegetation. The slope seems to have experienced some erosion, evidenced by the debris and exposed rock at its base.

This landscape exemplifies the natural beauty and geological diversity of the region, providing insight into the area's geomorphological history and the ongoing natural processes shaping it.

Figure 9.7.3 3D Model of Rock Shed Used to Mitigate Mass Wasting Effects in Merced River Canyon

A digitally rendered model of a slope stabilization and road protection structure. A steep hillside, covered in a combination of greenery and exposed rock, looms in the background. The slope has a grid pattern of reinforcement to prevent erosion and landslides.

In the foreground, a multi-arched concrete structure runs parallel to the base of the hillside. This structure likely serves as a protective barrier for the roadway running adjacent to it, shielding it from potential rockfalls and debris. The road, which is well-paved and marked with yellow lines, is seen to the left of the protective barrier.

The barrier design includes a series of evenly spaced arches, providing structural integrity and potentially allowing for drainage and maintenance access. The overall scene reflects engineering efforts to ensure road safety in areas prone to natural hazards such as rockfalls and landslides, highlighting the integration of civil engineering and environmental considerations.

Figure 9.7.5 Lake Tahoe Bathymetry

The bottom of Lake Tahoe is strewn with rubble from the McKinney Bay Landslide, which appears in an irregular band across the middle of the oval lake, from the Tahoe City Shelf area in the west across to Glenbrook, Logan Shoals, Cave Rock, and Zephyr Cove along the eastern shore. The lake is 5 kilometers across at its narrowest point, just below the landslide area. Note that Tahoe City is at the northwest edge of the Tahoe City Shelf.

Points of interest along the lake shore are listed as follows:

- Western shore, below the landslide area: Meeks Bay, Lonely Gulch, Rubicon Point, Emerald Point, and Emerald Bay
- Northern shore: Agate Bay, Crystal Bay, and Incline
- Eastern shore, above the landslide area: Secret Harbor and Skunk Harbor
- Southern shore: Baldwin Beach and Tahoe Keys

This page titled 9.9: Detailed Figure Descriptions is shared under a CC BY-NC 4.0 license and was authored, remixed, and/or curated by Cole Heap.

10: KLAMATH MOUNTAINS

Introduction to the Klamath Mountains

In the far northwest corner of California, just inland from the fog belt and its towering old growth redwood trees, the Klamath Mountains province is one of the most remote places in the state. Wild and scenic rivers cut deep valleys into steep hillsides covered in impenetrable brush, which give way to rocky peaks and alpine lakes at higher elevations. There are eleven designated wilderness areas in the Klamath Mountains, including the Trinity Alps, Marble Mountain and Siskiyou Wilderness areas.

The Klamath Mountains extend into southeast Oregon, with a little over half of the province existing on the California side and half on the Oregon side; geology doesn't care about arbitrary state borders. The province is bounded by the Coast Ranges to the west, the Cascade Range to the east, and the Great Valley to the southeast (Figure 10.1). The bedrock geology is also closely related to the geology of the Sierra Nevada, though the two provinces are not immediately adjacent.

In their current configuration, the Klamath Mountains comprise part of the forearc mountain range at the southern end of the Cascadia subduction system. "Forearc" meaning that they lie between the subduction zone trench and the associated volcanic arc mountain range (in this case, the Cascade Range). The Klamath Mountains are considerably higher in elevation above sea level and relief compared to the Oregon Coast Range, which is the forearc range to the north. The Klamath Mountains produce a rain shadow effect (see California's Climate). The western part of the range is the one of the wettest regions of the state, with over 150 inches of average annual precipitation in some areas.

Because forearc deformation and uplift processes are typically not associated with volcanism, forearc ranges such as the Klamath Mountains can provide a window into the geology that makes up the foundation of the continent. To the east, this basement rock is covered by younger volcanic and sedimentary rocks, but uplift without volcanism strips away the younger cover. In the 1960s and 1970s, coincident with the development of the modern Theory of Plate Tectonics, geologic mapping of the Klamath Mountains laid the foundations for our current understanding of how continents form and grow. The bedrock geology consists mainly of accreted terranes. Each terrane was once an island arc that developed offshore and was later added to the North American continent at the subduction zone. Each island arc was thrust up against and partially beneath an older, previously accreted terrane forming a sequence of terranes that get progressively younger to the west, separated by large eastward dipping thrust faults. Later, arc related volcanism intruded into these accreted terranes, leaving plutons that stitch together the quilt of terranes. These plutons have allowed geologists to use cross cutting relationships to determine the age of accretion related faulting.

The Klamath Mountains province was also important in the development of geologists' understanding of oceanic crust and the processes that form at mid-ocean ridges. In the process of accretion, sometimes bits of oceanic crust get caught up into the accreted terrane and part of the continental plate, forming ophiolites. There are several ophiolites of a variety of different ages within the Klamath Mountains, but in this chapter we have chosen to focus on one case-study example; the Josephine Ophiolite, one of the best exposed and most intact ophiolites in North America.

Although the general concept of terrane accretion is now fully accepted, geologists are still working to understand the details. Questions remain about where the terranes came from and why and when they accreted. Geologists are currently working to better comprehend exactly why the Klamath Mountains have anomalously higher modern elevations, compared to other forearc ranges. These questions and others continue to drive geologists into the Klamath Mountains, as this province remains key to understanding how our planet works.



Figure 10.1: Location of the Klamath Mountains of California. This province is bounded by the Nevada border on the east, the Garlock fault on the south and the Sierra Nevada Mountains on the west. "The Klamath Mountains of California" by Emily Wright, is licensed under CC-BY-NC / a derivative from the original work. Access a detailed description.

Learning Objectives

By the end of this chapter, you should be able to:

- Explain the process of terrane accretion and describe how it has led to the sequence of rocks present in the Klamath Province.
- Compare and contrast Andean vs Mariana type subduction.
- Locate the forearc and back-arc on a map of cross section sketch of a subduction zone.
- List the sequences of rocks and structures in the ophiolite sequence and explain how each forms.
- Distinguish between obduction and subduction.
- Apply the principle of cross cutting to interpret the relative ages of plutons and country rock.
- Recognize the relative timing of geologic events experienced by a particular location including: formation of bedrock, accretion to the continent and uplift of a mountain range.

10.1: Assembling a Continent
10.2: The McCloud Limestone- An Ancient Coral Reef
10.3: The Josephine Ophiolite- A Little Slice of the Mantle
10.4: Plutons of the Klamath Mountains
10.5: Uplifting a Mountain Range
10.6: Chapter Summary
10.7: Detailed Figure Descriptions

This page titled 10: Klamath Mountains is shared under a CC BY-NC 4.0 license and was authored, remixed, and/or curated by Emily Wright.

10.1: Assembling a Continent

Klamath Clues to the Geologic Puzzle

In 1969, geologist Warren Hamilton of the U.S. Geological Survey laid out a bold new idea in his paper titled, “Mesozoic California and the Underflow of Pacific Mantle”. This new idea for how California came to be part of North America was largely based on work in the Klamath Mountains. For decades prior, geologists like Hamilton’s USGS colleague, William Porter Irwin, had been roaming the steep, loose hills of the Klamath range, forging through old-growth poison oak and a variety of other nasty underbrush, to uncover the secrets of the Klamath Mountains. At first geologists were in search of valuable resources, like gold (see 10.5: Uplifting a Mountain Range), copper, and chromium (see 10.3: The Josephine Ophiolite: A Little Slice of the Mantle), but later work sought to put together a bigger picture of Earth’s geologic history. Early geologists were puzzled by some things about the Klamath Mountains, such as the common presence of ultramafic rocks, typically formed in the mantle, in an alpine environment, but in the 1960’s a new idea called, “plate tectonics,” was taking hold in geology and reframing how geologists looked at just about everything. The idea that Hamiliton and Irwin described for the Klamath Mountains and other parts of California, would later come to be called, “terrane accretion.” This concept would eventually revolutionize how geologists thought about not only California, but all of western North America, as well as other mountain belts around the world. Today, this idea is the foundation of our understanding of how continents came to be in the first place, and how they have grown over time.

The word ‘terrane’ (not to be confused with the homonym, ‘terrain’), refers to a block of crust that has unique characteristics that are geologically distinct from the surrounding area. The terrane is interpreted as having formed elsewhere, and then moved to its current location by later tectonic processes. Terranes can include multiple stratigraphic units, but these units formed in the same geologic or tectonic context. For example, a single terrane might include volcanic rocks associated with an island arc, as well as sedimentary rocks associated with the coral reef that at one time surrounded the volcanic islands. Terranes can be transported by multiple tectonic processes, including transform plate boundaries like the San Andreas Fault zone (see 11.3: Evolution of the Coast Ranges). However, the term accreted terrane usually refers to terranes emplaced through the process of subduction.

Query 10.1.1

This interactive element is not available in this format. Visit the link or scan the QR code to access it online.

View this Interactive Content online

Access accessibility guidance for this activity.

In general terms, accretion is a process by which an object grows larger through the gradual addition of material. At subduction zones, accretion usually occurs when any part of the subducting plate ends up in or on the overriding plate, rather than sinking into the mantle. In addition to terrane accretion, the word ‘accretion’ is also used to describe the process that occurs within an accretionary wedge. Both processes involve the accretion of material from the subducting plate to the overriding plate, but there are important distinctions between the two. In an accretionary wedge, material is removed from the top of the subducting plate and is highly altered and jumbled in the process. The resulting material is referred to as a mélange, a word of French origin, meaning “mixture”. This type of mélange contains a significant amount of serpentinite, a metamorphic rock formed in the deeper part of the accretionary wedge (see 2.6: Metamorphic Rocks). Terrane accretion differs from accretion in an accretionary wedge in that an entire block of lithosphere, not just the top of the plate, is accreted to the continent. Figure 10.1.1 illustrates both processes. The accretionary wedge is shown in purple and the accreted terrane is shown in green. Compared with a mélange, the original geologic structures in an accreted terrane remain relatively intact. Although, as one can imagine, the process of terrane accretion still results in quite a bit of folding, faulting and metamorphism.

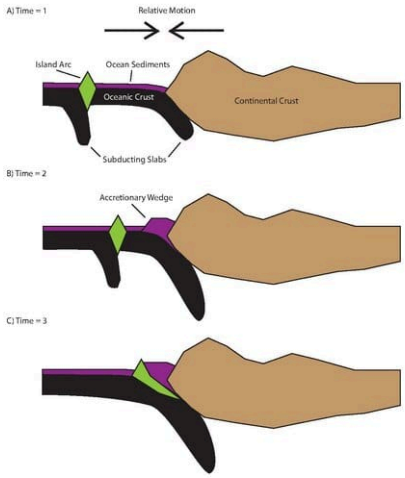


Figure 10.1.1: The process of accretion at a subduction zone. "Plate accretion stages through time" by BZenith is licensed under CC BY-SA 4.0. Access a detailed description.

Figure 10.1.1 shows an example of an island arc being accreted onto a continent. Notice that by time 3 (Figure 10.1.1 C), both the mélange formed in the accretionary wedge (purple) and the former island arc (green) have become part of the continent. The purple mélange has been thrust above the former island arc along a fault that dips inland (toward the continent). If we were to continue the cartoon beyond time 3, a new accretionary wedge would form on the seaward side of the island arc (left side in Figure 10.1.1, and perhaps, another island arc might come along in time and it too would be accreted to the continent. The resulting pattern would be an alternating sequence of mélange and terranes, with each terrane getting progressively older moving inland, and separated from its neighbor by large thrust faults that dip towards the continent. This simplified description generally represents the geology of the Klamath Mountains province (Figure 10.1.2).

Since the idea of terrane accretion was first invoked in the 1970s, geologists have sought to refine their understanding of exactly where these terranes came from. A healthy scientific debate has developed over whether the terranes were “exotic” island arcs, formed far from the continent, or whether they were home-grown arcs, that formed just offshore and remained close to the continent until finally accreting. Such home-grown island arcs are common elsewhere in the world today, particularly in the West Pacific (for example, the Japanese Islands) and Indian Ocean (for example, the Andaman Islands).

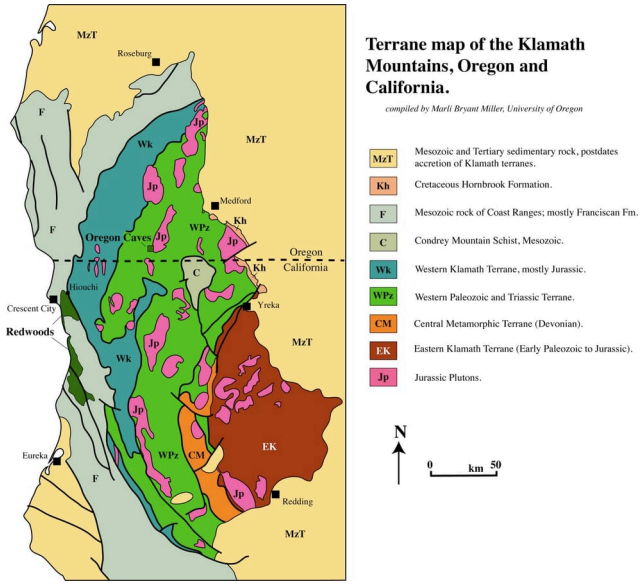


Figure 10.1.2: Terrane map of the Klamath Mountains showing terranes in Oregon and California, by Marli Bryant Miller, University of Oregon. Access a detailed description.

The Klamath Core

During the later part of the Paleozoic Era, Earth's continents were all merged together into the supercontinent, Pangea, surrounded by the Panthalassa Ocean. What is now northeastern California and northern Nevada was the coastline of Pangea (see 6.3: Paleozoic Era (540 – 250 Ma)). Somewhere off the coast, in the Panthalassa Ocean, there was an ocean island arc, which would later become the Eastern Klamath Terrane. As island arcs go, this one must have been around for a long time, because the Eastern Klamath Terrane contains a long record of sedimentary rocks, from Silurian-Devonian time through the Jurassic.

The Eastern Klamath Terrane was already an accretionary backstop before it docked with the mainland of Pangea. The Central Metamorphic Terrane accreted to the Eastern Klamath Terrane before both accreted to Pangea during the Late Permian - Early Triassic.

The Eastern Klamath Terrane is the oldest of the Klamath terranes and consists of the Redding, Trinity, and Yreka subterranes (smaller terranes within a larger terrane group). The Eastern Klamath Terrane includes volcanic rocks, plutonic rocks, and sedimentary rocks that would be expected in an island arc setting, some of which have been metamorphosed. It also includes the Trinity Ophiolite, which is a little piece of the Panthalassan oceanic crust. Some of the sedimentary rocks have remained intact and unmetamorphosed enough to preserve fossils (see 10.2: The McCloud Limestone: An Ancient Coral Reef).

Mesozoic Expansion

After the docking of the Eastern Klamath and Central Metamorphic terranes, the rate of growth of the Klamath province slowed for a period of time. Then, in the late Triassic through the Jurassic, North America (which was then splitting away from the rest of Pangea), grew rapidly, with the addition of several terranes.

A mountain building event called the Siskiyou orogeny took place during the Jurassic Period and involved sequential accretion of three additional terranes, which had been forming offshore during the Late Paleozoic and Early Mesozoic. These are lumped together into the Western Paleozoic and Triassic Terrane in Figure 10.1.2. The first and most easterly is the Sawyers Bar terrane, which represents a Permian oceanic arc, associated sedimentary rocks from marine and coastal environments, plus some mélange from an accretionary wedge. Accretion of the Sawyers Bar terrane was followed by the accretion of two other terranes. The Western Hayfork terrane is composed of a younger oceanic arc (formed around 177–167 Ma). The Rattlesnake Creek terrane was, at one time, the oceanic crust on which the Sawyers Bar island arc formed, and thus contains mafic and ultramafic rocks, though they are mostly no longer neatly organized in the expected ophiolite sequence and many have been metamorphosed to serpentinite.

Following the accretion of the Rattlesnake Creek terrane, a back-arc basin, called the Josephine Basin opened, once again separating the island arc from the main continent. It was during this time that the Western Klamath terrane (Figure 10.1.2 formed. The Josephine Ophiolite, which will be further discussed later in this chapter (see 10.3: The Josephine Ophiolite: A Little Slice of the Mantle), was the oceanic crust that formed in the back-arc spreading ridge, while the Galice Formation is composed of the sedimentary rocks that were deposited in the Josephine Basin. The rocks formed in the island arc itself are mostly confined to the Oregon part of the Western Klamath terrane.

During the Nevadan Orogeny, which took place in the Klamath Mountains around 157–150 Ma (see 6.4: Mesozoic Era (250 – 66 Ma)), the events of the Siskiyou orogeny in the Klamath province repeated, and the Western Klamath Terrane was accreted to North America. The pattern of accretion continues to the west of the Klamath Mountains, and into the later part of Mesozoic, with the accretion of the mélange of the Coast Range Franciscan Formation (see 11.2: Lithology of the Coast Ranges).

Sedimentary Evidence for Home-Grown Terranes

While fossil evidence suggests that the older, Eastern Klamath Terrane may be exotic in origin, evidence seems to be mounting in favor of a home-grown explanation for the younger, Mesozoic, terranes. One source of evidence comes from the ages of sediment grains found in the sedimentary rocks within these terranes. Because sedimentary depositional processes do not reset the radiometric dating clock (see 5.4: Absolute Dating of Geologic Materials), radiometric dating isn't very helpful for determining the age of deposition of a sedimentary rock. Instead, it gives the age of the source rock, but this can also be very useful information. In this case, these ages can help distinguish between exotic and home-grown scenarios.

Imagine a grain of sand on the beach of an ocean island located far from a continent. This grain of sand must have been eroded from the rocks on the island, transported by rivers and deposited on the beach. Its age would therefore have to match the age of

the volcanic rocks on the island. This would hold true for the detrital sedimentary rocks in deeper marine environments near this island arc as well. Since there are no other sources for detrital sediment, the grains would have to come from the arc itself. By contrast, sand found in a sea between a home-grown island arc and the main continent would contain some grains from the island arc and some grains from the continent. Since the continent contains rocks that were much older, even at the time, the ages of sedimentary grains in this environment would be highly variable and contain some very old grains, older than the island arc. This later scenario is what geologists have found for the Galice Formation and other sedimentary rocks of the Mesozoic Klamath terranes. The Mesozoic terranes of the Klamath Mountains, therefore, may not represent island arcs brought in from afar, but rather, tell the story of a long-lived subduction zone, which alternates between different styles of behavior. These subduction styles are sometimes referred to as Mariana type (after the Mariana islands) and Chilean or Andean type (after the Andes mountains in Chile). Mariana type subduction includes back arc spreading behind an ocean island arc and is also sometimes referred to as ocean-ocean subduction. Andean style subduction is associated with a shallower angle of subduction and a volcanic arc mountain range located on the main continent. The modern Cascade Range is an example of Andean type volcanic arc mountain range (see 7.1: The Cascadia Subduction Zone and the Cascade Continental Volcanic Arc).

Query 10.1.2

This interactive element is not available in this format. Visit the link or scan the QR code to access it online.

View this Interactive Content online

Connection to the Sierra Nevada

Geologists have noticed similarities between the geology of the terranes in the Klamath Mountains and the geology of other accreted terranes in western North America, most notably those found in the Sierra Nevada to the southeast and Oregon's Blue Mountains to the northeast (figure 10.1.3). This correlation implies that the changes between Andean and Mariana type subduction that drove the creation and accretion of these terranes occurred across continental scales. The same terrane sequence likely underlies much of western North America, but in most places the terranes have been covered by younger geology. These terranes are exposed in places where younger uplift events have returned these rocks to the surface, as discussed in 10.5: Uplifting a Mountain Range.

A quick glance at a map of the Sierra Nevada, Klamath and Blue Mountains, shows that the Klamath Mountains lie considerably west of the both adjacent ranges. This is due to two factors. The first is the shape of the coastline during accretion; the Klamath province was probably a cape or promontory along the coast at the time. However, this only explains part of the separation. The Klamath mountains were also moved further west by tectonic events that occurred after accretion.

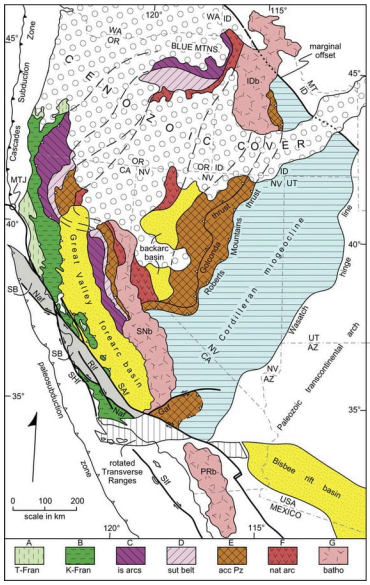


Figure 10.1.3: Map illustrating the correlation between terranes of the Sierra Nevada, Klamath and Blue Mountains. The geology of the Klamath Mountains can be traced to matching geology of the Sierra Nevada and Blue Mountains. Dark purple and pale purple striped areas (C and D in the legend) represent Mesozoic accreted terranes. Brown with cross hatching represents Paleozoic accreted terranes and red with "v" marks represents rocks equivalent to the oldest rocks of the Eastern Klamath Block. Dotted lines project the probable locations of the accreted terrane sequence beneath Cenozoic Cover. Accretionary Expansion by William R. Dickinson was originally published in *Geosphere*, which is published under the terms of the CC-BY-NC license. Access a detailed description.

References

1. Chapman, A. D., Grischuk, J., Klapper, M., Schmidt, W., & LaMaskin, T. (2024). Middle Jurassic to Early Cretaceous orogenesis in the Klamath Mountains Province (Northern California–southern Oregon, USA) occurred by tectonic switching: Insights from detrital zircon U-Pb geochronology of the Condrey Mountain schist. *Geosphere*, *20*(3), 749–777. https://doi.org/10.1130/GES02709.1
2. Hamilton, W. (1969). Mesozoic California and the underflow of Pacific mantle. *Geological Society of America Bulletin*, *80*(12), 2409–2430.
3. Harden, D. (2003). *California Geology* (2nd edition). Pearson.
4. Irwin, W. P. (2003). Correlation of the Klamath Mountains and Sierra Nevada. In *Open-File Report* (2002–490). U.S. Geological Survey. https://doi.org/10.3133/ofr02490
5. Kauffmann, M. E., & Garwood, J. (2022). *The Klamath Mountains: A Natural History*. Backcountry Press.
6. LaMaskin, T. A., Rivas, J. A., Barbeau, D. L., , Jr., Schwartz, J. J., Russell, J. A., & Chapman, A. D. (2021). A crucial geologic test of Late Jurassic exotic collision versus endemic re-accretion in the Klamath Mountains Province, western United States, with implications for the assembly of western North America. *GSA Bulletin*, *134*(3–4), 965–988. https://doi.org/10.1130/B35981.1
7. Snoke, A. W., & Barnes, C. G. (2006). *The development of tectonic concepts for the Klamath Mountains province, California and Oregon*. https://pubs.geoscienceworld.org/gsa/books/book/574/chapter/3803324/The-development-of-tectonic-concepts-for-the
8. Surpless, K. D., Alford, R. W., Barnes, C., Yoshinobu, A., & Weis, N. E. (2023). Late Jurassic paleogeography of the U.S. Cordillera from detrital zircon age and hafnium analysis of the Galice Formation, Klamath Mountains, Oregon and California, USA. *GSA Bulletin*, *136*(3–4), 1488–1510. https://doi.org/10.1130/B36810.1

This page titled 10.1: Assembling a Continent is shared under a CC BY-NC 4.0 license and was authored, remixed, and/or curated by Emily Wright.

10.2: The McCloud Limestone- An Ancient Coral Reef

Coral Reefs Around Volcanic Islands

During the Permian Period, somewhere in the vast expanse of the Panthalassa Ocean, there was a balmy tropical island arc. Like many tropical islands today, these islands were ringed with coral reefs. Today, fringing reefs form around volcanic islands and grow into barrier reefs, and atolls in response to a combination of island subsidence and sea level fluctuations (Figures 10.2.1 and 10.2.2).

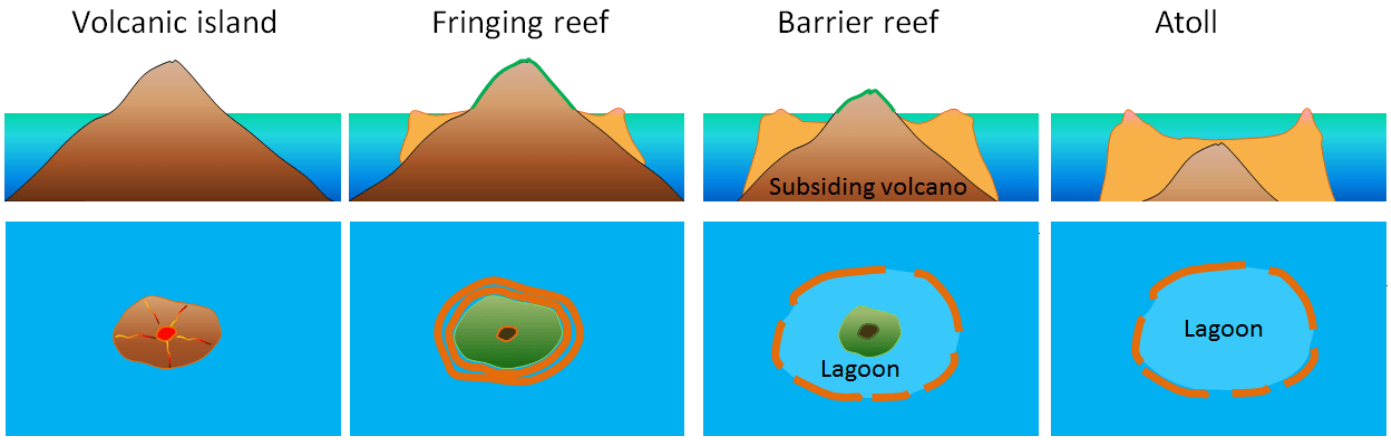


Figure 10.2.1:"Steps in the development of coral reefs" by Steven Earl is licensed under CC BY 4.0. Access a detailed description.



Figure 10.2.2: Moorea Island in French Polynesia can be thought of as a modern analog for the environment of formation for the McCloud Limestone. Photograph by dany13 is licensed under CC BY 2.0.

The McCloud Fauna

From a distance, Permian coral reefs might have looked similar to modern coral reefs (Figure 10.2.2), but up close, Permian reef communities looked rather different than those present today (Figure 10.2.3). The end-Permian mass extinction, sometimes called the “Great Dying” was the largest mass extinction in earth history and it hit coral reefs hard. The leading interpretation for the cause of the extinction is an increase in greenhouse gasses globally related to large volcanic eruptions in Siberia. The increase in greenhouse gasses is thought to have corresponded with rapid warming, ocean acidification and decrease in oxygen (see 17.2: The Past). More than eighty percent of marine species went extinct. When coral reefs returned, the species that evolved

to fill the open niches were very different.



Figure 10.2.3: This diorama of a Permian seafloor at the Museum of Natural History in Pittsburgh, Pennsylvania features orange, horn-shaped rugose corals, which are a common fossil in the McCloud Limestone. This photograph by James St. John is licensed under CC BY 2.0. Access a detailed description.



Figure 10.2.4: Fossils in McCloud Limestone collected near Shasta Lake, CA. Fossils include bryozoans (near the dime in the top photo) and rugose corals (right of the dime in the bottom photo). Dime for scale. "McCloud Bryozoan" and "McCloud Rugose Coral" by Emily Wright are licensed under CC BY-NC 2.0.

The fossils of the McCloud Limestone have helped geologists piece together the history of the Eastern Klamath Terrane. Paleontologists have observed that coral and fusulinid species of the McCloud Limestone are distinctly different from the species found in rocks that were part of mainland Pangea at the time, such those found in the Basin and Range Province (see 8.6: The Oldest Rocks in the Basin and Range). This has been used as evidence to argue that the Eastern Klamath Terrane was of exotic origin, and must have been several thousand kilometers offshore during the Permian to prevent mixing of species with the Pangean coast. Review your knowledge of exotic terranes in Query 10.2.1.

Query 10.2.1

This interactive element is not available in this format. Visit the link or scan the QR code to access it online.

View this Interactive Content online

Box 10.2.1: Lake Shasta Caverns

Near Lake Shasta, a network of caverns has formed in the McCloud Limestone. Caverns form in limestone because it is soluble in acidic water. Natural rainwater is slightly acidic and therefore, water percolating through the ground can dissolve limestone. Groundwater can eat away large cavities of limestone. If the water table is then lowered, due to uplift or stream base level change, these cavities become caves or caverns. Continued flow of water through these caverns dissolves and reprecipitates the limestone creating features called speleothems. Stalactites and stalagmites are examples of speleothems.

There are many other limestone and marble caverns in the Klamath Mountains. Since coral reefs and other carbonate rocks often occur in island arcs, many of the Klamath terranes contain limestone and marble. Many of the caves in the Klamath Mountains are remote and only accessible to experienced spelunkers, but others have manufactured tunnel entrances and other infrastructure, which make them accessible to the general public. Oregon Caves (in Oregon) is a national monument (shown on map in Figure 10.2.2 and may be accessed by guided tour. Lake Shasta Caverns are privately owned and also shown to visitors by tour.



Figure Box 10.2.1: Speleothems in the Lake Shasta Caverns. "Lake Shasta Caverns National Natural Landmark" by Vy Vu is licensed under CC BY-NC-ND 4.0.

Video Box 10.2.1: Karst

If you would like to learn more about how limestone caverns form, watch this video, “Karst”, which explains the process in greater detail.

This interactive element is not available in this format. Visit the link or scan the QR code to access it online.

View this YouTube Video online

References

1. Belasky, P., Stevens, C., & Hanger, R. (2002). Early Permian location of western North American terranes based on brachiopod, fusulinid, and coral biogeography. *Palaeogeography, Palaeoclimatology, Palaeoecology*, *179*, 245–266. https://doi.org/10.1016/S0031-0182(01)00437-0
2. Harden, D. (2003). *California Geology* (2nd edition). Pearson.
3. Hickey, H. (2018, December 6). *What caused Earth's biggest mass extinction?* Stanford Doerr School of Sustainability. https://sustainability.stanford.edu/news/what-caused-earths-biggest-mass-extinction
4. King, E. (2015, April 18). *Ocean acidification triggered mass extinctions 252 million years ago*. Climate Home News. https://www.climatechangenews.com/2015/04/18/ocean-acidification-triggered-mass-extinctions-252-million-years-ago/
5. *Lake Shasta Caverns National Natural Landmark*. (n.d.). Sierra Nevada Geotourism Developed in Associattion with National Geographic. Retrieved July 17, 2024, from https://sierranevadageotourism.org/entries/lake-shasta-caverns-national-natural-landmark/969cc90d-b65b-40e4-bd7c-46d3f3bd1c97
6. Stevens, C. H., Yancey, T. E., & Hanger, R. A. (1990). Significance of the provincial signature of Early Permian faunas of the eastern Klamath terrane. In D. S. Harwood & M. M. Miller (Eds.), *Paleozoic and Early Mesozoic Paleogeographic Relations; Sierra Nevada, Klamath Mountains, and Related Terranes* (Vol. 255, p. 0). Geological Society of America. https://doi.org/10.1130/SPE255-p201
7. Wignall, P. B., & Bond, D. P. G. (2024). The great catastrophe: Causes of the Permo-Triassic marine mass extinction. *National Science Review*, *11*(1), nwad273. https://doi.org/10.1093/nsr/nwad273
8. Zubin-Stathopoulos, K. D., Beauchamp, B., Davydov, V. I., & Henderson, C. M. (2013). Variability of Pennsylvanian–Permian Carbonate Associations and implications for NW Pangea Palaeogeography, east-central British Columbia, Canada. *Geological Society, London, Special Publications*, *376*(1), 47–72. https://doi.org/10.1144/SP376.1

This page titled 10.2: The McCloud Limestone- An Ancient Coral Reef is shared under a CC BY-NC 4.0 license and was authored, remixed, and/or curated by Emily Wright.

10.3: The Josephine Ophiolite- A Little Slice of the Mantle

Obduction: A Rare but Important Event

When students first learn to classify plate boundaries, they learn that when oceanic lithosphere and continental lithosphere converge, it must always be the oceanic lithosphere that subducts. This is generally true, of course, but tectonic plates have been moving and converging for billions of years on Earth, and in such a great expanse of time, even unlikely and unusual events must sometimes occur. One such rare event is the process called obduction. The root “sub-” in “subduction” means “beneath” or below; “ob-”, by contrast means “toward,” “to,” “on,” “over,” or “against." Thus, in obduction, the oceanic lithosphere is pushed onto the continental lithosphere, rather than the usual subduction, in which it is pushed below. The resulting fragment of oceanic lithosphere, when eventually exposed at the surface, is known as an ophiolite.

California has had a long history of being a convergent plate boundary and so perhaps it should be no surprise that there are many ophiolites in California, including in the Coast Ranges (see 11.2: Lithology of the Coast Ranges), Sierra Nevada (see 9.2: Ancient Seas Form the Oldest Rocks) and the Klamath Mountains. There are multiple ophiolites in the Klamath Province, including the Trinity Ophiolite, Preston Peak Ophiolite and Josephine Ophiolite. This last is one of the most complete and best exposed ophiolites in North America, making a great case study for any student of plate tectonics. The Josephine Ophiolite is named for Josephine County, Oregon, but like many things in geology, ophiolites have no concern for arbitrary state boundaries. A large portion of the Josephine Ophiolite can also be found in Del Norte County, California (Figure 10.3.1.



Figure 10.3.1: Location of the Josephine Ophiolite, after Shellnutt et al., 2021. "Josephine Ophiolite Location Map" by Emily Wright is licensed under CC BY-SA 4.0.

To understand the geologic history of the Josephine Ophiolite, you will need to be familiar with the geography of a subduction zone. Review your knowledge of important seduction zone terminology in Query 10.3.1.

Query 10.3.1

This interactive element is not available in this format. Visit the link or scan the QR code to access it online.

View this Interactive Content online

Although there are many ways in which obduction can occur, the obduction of the Josephine Ophiolite is thought to be the result of the collapse of a back-arc basin. Prior to obduction, during the late Triassic Period into the Jurassic, the subduction zone exhibited Mariana type subduction. An oceanic island arc was separated from the mainland continent by a thin strip of oceanic lithosphere produced at a small spreading ridge resulting from back-arc extension (Figure 10.3.2). This might have looked like a mirror image of the east coast of modern Asia. In this analogy, the Josephine Ophiolite would be forming in the Sea of Japan (Figure 10.3.3). Later, Mariana type subduction transitioned to Andean type subduction and back-arc extension ceased. The greater compressive stress associated with Andean type subduction caused buckling and collapse of the former back-arc basin. As the Japan-like island arc (the Rogue-Chetco arc) was accreted onto the mainland, the Josephine Ophiolite was caught up in the mix.

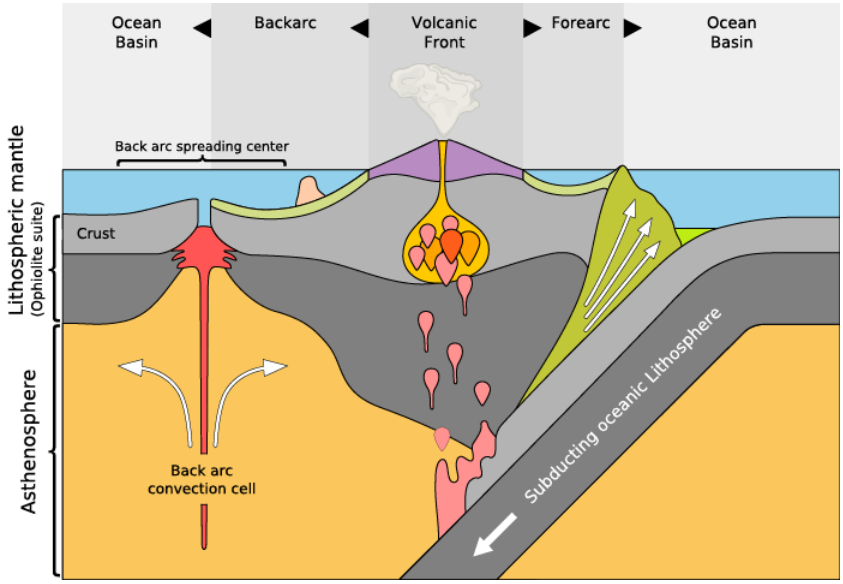


Figure 10.3.2: An island arc with a back arc spreading center. The Josephine Ophiolite is thought to have formed in a back arc spreading center. "Back Arc Spreading" by Emily Wright is licensed under CC BY-SA 4.0 / A derivative from the original work. Access a detailed description.

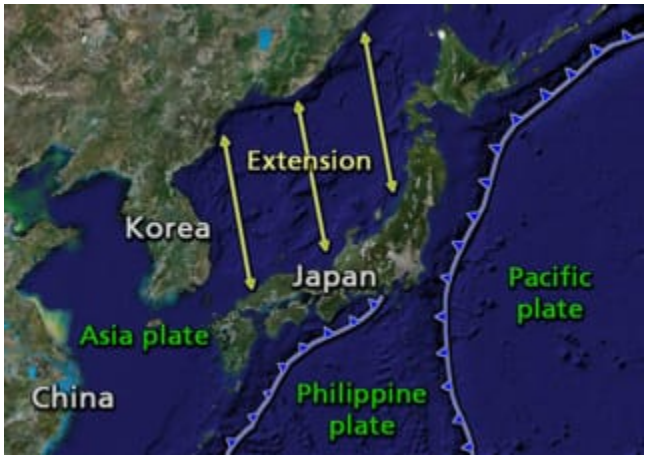


Figure 10.3.3: Japan is separated from mainland Asia by extension due to back arc spreading; a modern analogy to the formation of the Josephine Ophiolite. This map shows how extension separates Japan from China and Korea as the Pacific and Philippine plates subduct beneath the Asia plate. "Japan separation" by Oghmoir is licensed under CC BY-SA 3.0.

Mid Ocean Ridges and the Ophiolite Sequence

Most of the earth is covered by oceanic lithosphere and even that makes up only a tiny fraction of the oceanic lithosphere that has ever existed on Earth. Unlike continental lithosphere, oceanic lithosphere is constantly being created and destroyed. Only very occasionally do small bits of this very common earth material get obducted to another plate. This fact makes ophiolites incredibly valuable to geologists. Not only do they help tell the story of terrane accretion, but they also provide a rare glimpse into the inner workings of a far more common process, the creation of oceanic crust at mid ocean ridges (Figure 10.3.4). There is a

specific stratigraphy or sequence of layers present in all complete ophiolites. The Smith River cuts through all of these layers of the Josephine Ophiolite, just east of Crescent City, California (Figure 10.3.5).

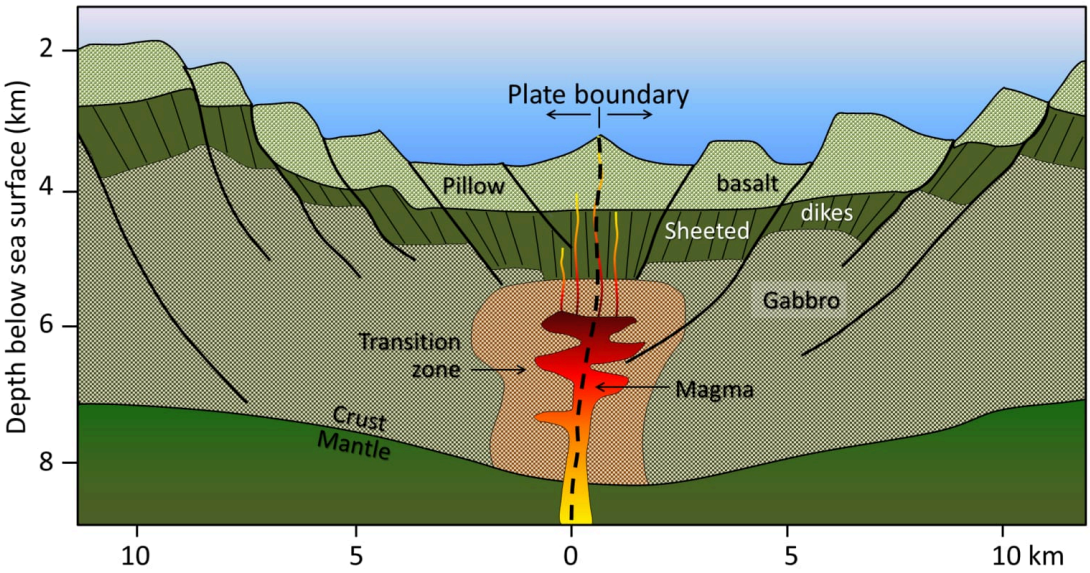


Figure 10.3.4: Sea floor spreading at a mid-ocean ridge produces the layers of the ophiolite sequence. This work by Steven Earle is licensed under CC BY 4.0. Access a detailed description.



Figure 10.3.5: The middle fork of the wild and scenic Smith River tumbles through the basalt of the Josephine Ophiolite. "Basalt Outcrop Smith River" by David Bazard is licensed under CC BY-NC-SA 2.0.

Query 10.3.2

This interactive element is not available in this format. Visit the link or scan the QR code to access it online.

View this Interactive Content online

Peridotite

The lowest layer in the ophiolite sequence is a layer of peridotite. Peridotite is the rock of the mantle. The brittle lithosphere that makes up tectonic plates includes a little bit of the top of the mantle. Therefore, when a piece of a plate is obducted, a little of the mantle comes along. An excellent place to see this mantle rock exposed is at the confluence of the South Fork Smith River with the main Smith River. At first glance the rock appears a light orange color, but when a fresh surface is exposed with a rock hammer, the inside is a dark shade of green. Because peridotite is so rich in iron, the surface of the rock is easily oxidized once exposed, leaving a rust colored weathering rind (Figure 10.3.6).



Figure 10.3.6: Peridotite outcrop at the confluence of the middle and south forks of the Smith River, northern California. The weathered surface of the rock appears orange due to the oxidation of iron, but a closer view shows freshly exposed dark green rock near the tip of the knife.
"Peridotite Outcrop" and "Peridotite Serpentinized Outrcrop" by David Bazard are licensed under CC BY-NC-SA 2.0.

Layered Gabbro

The lava that erupts at mid ocean ridges is fed by a magma chamber near the base of the crust. Not all of the magma in this chamber ultimately erupts at the surface though; some cools and solidifies at the edges of the chamber as it moves with the tectonic plate away from the mid ocean ridge. Partial melting of this mantle produces mafic magma, which forms gabbro when cooled intrusively. In the Josephine Ophiolite, the gabbro has a layer structure, which is thought to have formed as a result of episodes of fractionation occurring within the chamber and producing layers of settled early formed crystals (Figure 10.3.7). For further explanation of fractionation see 7.1: The Cascadia Subduction Zone and the Cascade Continental Volcanic Arc.



Figure 10.3.7: Crystal settling at the base of the magma chamber creates layering in the resulting intrusive igneous rock. This layering was originally horizontal, but has been titled in the process of obduction. "Layered Gabbro" and "Layered Gabbro Close Up" by David Bazard are licensed under CC BY-NC-SA 2.0.

Sheeted Dikes

At a mid ocean ridge, magma moves upward from the magma chamber to erupt at the surface through cracks in the rock that overly the magma chamber. The magma that cools within these cracks forms basalt dikes. Although technically intrusive, this magma cools quickly enough to form an aphanitic texture and is therefore called basalt, rather than gabbro. Both the layered gabbro and the sheeted dikes can be seen along the main fork of the Smith River (Figure 10.3.8).



Figure 10.3.8: Fine-grained mafic (basaltic) dikes intrude into the lighter-colored, coarse-grained gabbro. The contact between the basaltic (mafic) dike and the gabbro is at the tip of the knife blade. "Sheeted Mafic Dikes" and "Mafic Dike Margin" by David Bazard are licensed under CC BY-NC-SA 2.0.

Pillow Basalt

When lava erupts underwater, it cools very quickly forming a glassy outer shell, as more lava forces its way into this shell, the shell cracks and a new shell forms around the expanding lava. The result is a blobby or pillowy structure that forms as these basalt “pillows” successively pile on top of each other. You can see video footage of this process in the video “Pillow Lava”. The pillow basalt layer can be seen further upstream, along the middle fork of the Smith River (Figure 10.3.9).



Figure 10.3.9: Pillow basalt in the Josephine Ophiolite. In some places the matrix rock between the pillows has been weathered away. In others, the matrix forms light-colored, resistant rock surrounding the dark pillows. "Pillow Basalt Detail" and "Pillow 'Breccia'" by David Bazard are licensed under CC BY-NC-SA 2.0.

Marine Sedimentary Rocks

As the oceanic crust moves away from the mid ocean ridge, marine sediments settle on top of the pillow basalts. In a large ocean basin, these sediments would be mostly biochemical sedimentary rocks such as limestone and chert, which form from the accumulation of the mineralized hard exterior parts of dead plankton. But since the Josephine Ophiolite formed in a back arc basin, close to a continental volcanic arc, there was a large input of sediment eroded from the continent. The Galice Formation, which overlies the Josephine Ophiolite, consists of detrital sedimentary rocks, with sediment sourced in the Klamath Mountains and the active Sierra Nevada volcanic arc. Figure 10.3.10 shows the contact between the basalt and the Galice Formation. The contact represents the Jurassic ocean floor where sediments accumulated at about 160 Ma. The contact has now been tilted to near vertical during the process of obduction.



Figure 10.3.10: Contact of the oceanic basalt (greenish rock to the right) and the overlying pelagic sediments (layered rock on the left). "Contact Pillow Basalt and Pelagic Seds" by David Bazard is licensed under CC BY-NC-SA 2.0.

Query 10.3.3

This interactive element is not available in this format. Visit the link or scan the QR code to access it online.

View this Interactive Content online

You may find a review of Chapter 10: Klamath Mountains (Introduction section) helpful in completing this activity.

Turquoise Waters, Ultramafic Soils and Carnivorous Plants

In the whole earth, ultramafic rock is the most common type of rock there is, because it makes up Earth's mantle, which is the largest of Earth's layers by volume (84%). However, the density of ultramafic rock usually prevents it from rising into the crust, thus, this iron and magnesium rich chemistry is relatively rare in rocks exposed at the surface. The result is a soil chemistry unique to regions with ophiolites, known as ultramafic soil, or sometimes serpentine soil. Serpentine minerals are the result of metamorphism of ultramafic rock. Because the parent material for the soil is rich in heavy metals, the soil is also relatively poor in lighter elements that are essential nutrients for plant life. In the region of the Josephine Ophiolite, the effect of the soil chemistry on the ecology is striking. Just outside the bounds of the ophiolite itself, the plant kingdom thrives. Healthy redwood stands, like those found in Jedediah Smith Redwoods State Park (part of the Redwood National and State Park system) rank among the highest known biomass of standing vegetation on earth, but the forest within the Josephine Ophiolite is very different in character. Although this is the wettest part of California, the forest in some ways resembles that of a much drier climate, although growth is limited by nutrients, not by water. Some plants that do take root in the inhospitable ultramafic soil have unique adaptations to deal with the shortage of nutrients. The California pitcher plant (*Darlingtonia californica*), receives some of its nutrients from insects that it traps within its "pitcher" Figure 10.3.10. Other carnivorous plants found on serpentine soils are Horned butterwort (*Pinguicula macroceras*) and Round-leaved sundew (*Drosera rotundifolia*).



Figure 10.3.11: The California pitcher plant (Darlingtonia californica) has adapted to the low-nutrient ultramafic soils of the Josephine Ophiolite by luring and trapping insects for nutrients. "Darlingtonia californica" by Noah Elhardt is licensed under CC BY-SA 3.0.

The unique geology of the Josephine Ophiolite, also gives an inviting appearance to the rivers that run through it. The Smith River is one of the cleanest rivers in the contiguous United States. On sunny days the sunlight penetrates the clear water and reflects off the serpentinite below, giving the water a picturesque hue of turquoise (Figure 10.3.12).



Figure 10.3.12: An X post by Redwood National and State Parks celebrating the turquoise color of the Smith River. View Detailed Description. "Post" by Redwood National and State Parks is in the Public Domain. Access a detailed description.

Box 10.3.1: Mantle Magma Chambers Fuel the War Machine

The two main minerals in peridotite are olivine and pyroxene and the ultramafic chemistry is usually described as being rich in iron and magnesium. However, the mantle is also relatively rich in other heavy metals when compared with the crust. One such element is chromium, which can be found in the mineral Chromite (Fe_2CrO_4). California's ultramafic rocks, including those of the Josephine Ophiolite, contain pods and slivers of chromite. These small pockets are not concentrated enough to make chromite mining economically viable in today's global economy. Since 1961, the United States has imported all of its chromite. But chromite is considered a strategic mineral, meaning that it is necessary for military or industrial use during periods of national emergency. During World War II, when the global supply of chromite was cut off and it was needed for production of steel for the war effort, chromite mines operated throughout the Klamath Mountains, Coast Ranges and the Sierra Nevada foothills. The search for chromite motivated geological mapping of the ultramafic rocks in the Klamath Mountains during and after the war. This mapping effort in turn helped lead geologists to important conclusions about terrane accretion and plate tectonics.

Acknowledgements

For this section, I'd like to give a special thanks to Dr. David Bazard, who has kindly shared his photos in a public platform for the benefit of this project. If you are interested in taking your own journey into the mantle, you will appreciate Dave Bazard's Josephine Ophiolite map.

References

1. California Division of Mines and Geology. (1957). *Mineral commodities of California: Geologic occurrence, economic development, and utilization of the state's mineral resources* (Lauren A. Wright, Ed.).
2. Casteran, R. (2022, September 22). *Chromite mining*. Oregon Encyclopedia. https://www.oregonencyclopedia.org/articles/chromite_mining/
3. Dengler, L. (2023, June 18). Exploring the Josephine Ophiolite which shows mantle. *Eureka Times Standard*. https://www.times-standard.com/2023/06/18/lori-dengler-exploring-the-josephine-ophiolite-which-shows-mantle/
4. Harden, D. (2003). *California Geology* (2nd edition). Pearson.
5. Harper, G. (1984). The Josephine Ophiolite, northwestern California. *Geological Society of America Bulletin - GEOL SOC AMER BULL*, *95*. https://doi.org/10.1130/0016-7606(1984)95<1009:TJONC>2.0.CO;2
6. Serpentine soil. (2024). In *Wikipedia*. https://en.Wikipedia.org/w/index.php?title=Serpentine_soil&oldid=1225226416
7. Shellnutt, J. G., Dostal, J., & Lee, T.-Y. (2021). Linking the Wrangellia flood basalts to the Galápagos hotspot. *Scientific*

Reports, *11*(1), 8579. https://doi.org/10.1038/s41598-021-88098-7
8. *Smith River*. (n.d.). National Wild and Scenic River System. Retrieved July 1, 2024, from https://www.rivers.gov/river/smith
9. Strickler, M. D. (n.d.). *Josephine Ophiolite*. Retrieved July 1, 2024, from http://homework.uoregon.edu/mstrick/GeoTours/Josephine%20Ophiolite/JoOphiolite.html
10. Surpless, K. D., Alford, R. W., Barnes, C., Yoshinobu, A., & Weis, N. E. (2023). Late Jurassic paleogeography of the U.S. Cordillera from detrital zircon age and hafnium analysis of the Galice Formation, Klamath Mountains, Oregon and California, USA. *GSA Bulletin*, *136*(3–4), 1488–1510. https://doi.org/10.1130/B36810.1
11. U.S. Forest Service. (n.d.). *Serpentine Soils and Plant Adaptations*. Retrieved July 1, 2024, from https://www.fs.usda.gov/wildflowers/beauty/serpentines/adaptations.shtml

This page titled 10.3: The Josephine Ophiolite- A Little Slice of the Mantle is shared under a CC BY-NC 4.0 license and was authored, remixed, and/or curated by Emily Wright.

10.4: Plutons of the Klamath Mountains

The Stitching in the Quilt

Drivers along Interstate-5 between the Oregon border and the Great Valley have the pleasure of excellent views on both sides of the highway. The freeway here passes right through the intersection of the Klamath Mountains and the Cascade Range. To the east, Mount Shasta presents an imposing view of an active volcano, and to the west, the 160 Ma granite mountain of Castle Crags provides a view of a volcano long gone. The Castle Crags Pluton is one of many such plutons in the Klamath Mountains province, but it is the most famous plutonic outcropping on account of its visibility to travelers. Today, most travelers merely glimpse the crags as they speed by at 70 miles per hour, but Castle Crags has been an important cultural landmark since prehistoric times. The ancient Siskiyou Trail, which was the main route between the Great Valley and the Willamette Valley, passed near Castle Crags. Today Castle Crags is designated as a state park.



Figure 10.4.1: "Castle Crags, California" by Thomas Shahan is licensed under CC BY-NC 2.0.

Plutonic rocks in the Klamath Mountains do not necessarily follow the same pattern of younging to the west that is seen in other rock types. For example, in the eastern part of the province, within the Redding subterrane, two plutons can be found in close proximity, with widely varying ages. The Mule Mountain Pluton is approximately 400 Ma, consistent with the age of the terrane, but the nearby Shasta Bally Batholith is a mere 136 Ma, younger than any of the Klamath terranes. The Mule Mountain Pluton formed within the island arc prior to accretion, whereas the Shasta Bally Batholith represents a much younger episode of volcanism that cross cuts the geology of the older terrane. During episodes of Andean type subduction, arc volcanism occurs within the continent and the earlier accreted terranes become the basement onto which volcanoes are erupted and into which plutons are intruded. Though the volcanoes have been eroded, the plutons remain as evidence that a volcanic range once existed. Shasta Bally is part of the youngest of these episodes preserved in the Klamath Mountains. Castle Crags formed during an earlier episode that corresponds to the formation of the accretionary wedge mélange that would eventually become the Rattlesnake Creek terrane. Because igneous intrusions can be easily radiometrically dated (see 5.4: Absolute Dating of Geologic Materials), the plutons in the Klamath Range have helped geologists determine the timing of faulting associated with accretion. You can practice a simplified version of the relative dating required in Query 10.4.1.

Query 10.4.1

This interactive element is not available in this format. Visit the link or scan the QR code to access it online.

View this Interactive Content online

You may find review of 5.1: Relative Dating helpful in completing this activity.

Castle Crags, like many plutons in the Klamath Mountains, is a zoned pluton. As the magma initially intruded into the ultramafic country rock, the outside of the chamber cooled more quickly, producing a finer-grained texture, though still coarse enough to be considered phaneritic. This forms a solidified but still warm layer at the edge of the pluton, which insulates the interior and allows it to cool more slowly, producing granitic rock with large mineral crystals near the interior. There are also compositional differences between the various zones of the pluton as the magma composition changed over time (see 7.1: The Cascadia Subduction Zone and the Cascade Continental Volcanic Arc).

Like the plutonic rocks of the Sierra Nevada (see 9.3: The Sierra Nevada Batholith), Castle has gone from being a magma chamber deep within the crust to a prominent, craggy outcrop due to differential erosion. The granitic rock of the pluton is more resistant to weathering and erosion than the surrounding ultramafic rocks of the Eastern Klamath terrane. Also much like the Sierra Nevada, the pluton was carved into spires by glacial erosion during the Pleistocene Epoch (see 9.6: Ice Shapes the Landscape).

References

1. Irwin, W. P., & Wooden, J. L. (1999). *Plutons and accretionary episodes of the Klamath Mountains, California and Oregon*. US Geological Survey. https://pubs.usgs.gov/publication/ofr99374
2. Michael Wopat. (2015). Castle Crags State Park, Geological Gems of California State Parks, GeoGem Note 23. In Syd Brown, Mike Fuller, Bill Short, & Chris Wills (Eds.), *California Geological Survey Special Report 230 under Interagency Agreement C01718011 with California State Parks*. https://www.parks.ca.gov/pages/734/files/GeoGem%20Note%2023%20Castle%20Crags%20State%20Park.pdf

This page titled 10.4: Plutons of the Klamath Mountains is shared under a CC BY-NC 4.0 license and was authored, remixed, and/or curated by Emily Wright.

10.5: Uplifting a Mountain Range

From Continental Shelf to Alpine Peaks

When first learning about the idea of terrane accretion, it is easy to imagine that as a terrane gets accreted to a continent, it is thrust up into a mountain range and has remained a high mountain range until the present day. Indeed, this is roughly what is shown in Figure 10.1.1. As is often the case in geology, however, reality is a bit more complicated. In hundreds of millions of years time, mountain ranges tend to come and go. For example, there is evidence that, by the Late Cretaceous, after all the Klamath Terranes had been accreted, the Klamath province was part of the forearc basin of the Sierra Nevada arc, along with the Great Valley to the south (see 12.2: Geology of the Great Valley). What is now a high mountain range was, at that time, below sea level and accumulating marine sediment. In the intervening time, both the Klamath Range and the Great Valley have been uplifted above sea level, but while the Great Valley remains relatively low and flat, the Klamath Range has become mountainous.

Exactly when, why and how the Klamath province went from being a low, flat continental shelf, to high mountain peaks is a question of great interest to geologists. The challenge with understanding mountain uplifts is that uplifting mountains are erosional environments. Not only does the process of erosion leave nothing in the rock record, but erosion can also erase the rock record of earlier events as sediments are stripped away. Very little of the once thick Cretaceous sediments remain anywhere in the Klamath Province, and younger Tertiary sediments are not common either.

Extensional Faulting

Although Cenozoic faulting is not common in the Klamath Mountains province, there are a few extensional faults in the southern part of the Klamath Mountains. These extensional faults cut across the older thrust faults that formed during Mesozoic accretion, and therefore, according to the Principle of Cross Cutting (see 5.1: Relative Dating), must represent a younger period of tectonic evolution. One major extensional structure in the southern Klamath Mountains is the La Grange Fault, a large low angle normal fault, called a detachment fault. This fault was first discovered at the LaGrange Mine (see Box 10.5.1: La Grange Mine), when miners stripped away the gravels of the Weaverville Formation and uncovered the fault surface. The fault surface is composed of cataclasite, a type of rock that is formed as a result of the sliding and grinding that occurs during fault motion and has distinct slickenlines (Figure 10.5.1) indicating the direction of fault motion. The strike of the La Grange Fault is Northeast and the slickensides indicate a south to south eastward motion for the hanging wall. Based on the displacement of specific rock units, geologists estimate that total displacement was about 60 km (roughly 40 miles). This normal fault motion also uplifted the footwall block on the northern side of the fault, bringing deeper sections of basement rock to the surface. Although younger than the more common Mesozoic compressional faults in the Klamath Mountains, the La Grange fault is no longer active. Since it is a low angle fault that fault has also been eroded in places, leaving a rather circuitous trace on a map (Figure 10.5.2).



Figure 10.5.1: Surface of the La Grange Fault near the La Grange Mine. "LaGrange Fault Surface" was taken by Susan Cashman in 2014 and used here with permission.

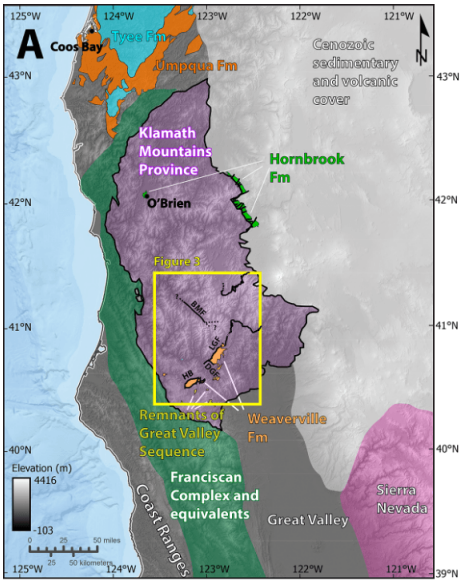


Figure 10.5.2: Simplified lithologic map showing select provinces and Cretaceous–Neogene geologic formations overlain on a hillshade digital elevation model BMF—Browns Meadow fault, LGF—La Grange fault, HB—Hayfork basin, DGF—Democrat Gulch fault. Yellow box shows location of Figure 3 in Michalak et al. (2023). The yellow box and the letter A are not relevant to this publication. This figure by Michalak et al. was originally published in *Geosphere*, which is published under the terms of the CC-BY-NC license. Access a detailed description.

South of the La Grange fault, there are several other normal faults of similar age and similar strike. Some of these faults form grabens (see 8.2: Rifting in the Basin and Range), which form one of the few depositional environments where sediment could accumulate during the uplift of the Klamath Mountains.

Insights from the Weaverville Formation

As the Klamath Mountains uplifted, very little of the eroded material stayed in the area and accumulated as sediment. The most notable exception is the Weaverville Formation (Figure 10.5.2, which accumulated in small grabens and basins formed by extensional faulting. The lower Weaverville Formation is composed of sandstone, mudstone, and claystone with minor interbedded coal and tuff, which are interpreted to have formed in lake environments. These transition to pebble and cobble conglomerate in the upper Weaverville formation, suggesting a transition from the lake environment to one with rivers or streams. Deposition of the Weaverville Formation began in the early to middle Miocene and possibly continued into the late Miocene.

The source rocks for the Weaverville Formation are the rocks of the Terranes and Plutons of the Klamath province. Some of these rocks are gold bearing, much like those of the Sierra Nevada (see 9.4: Gold of the Sierra Nevada), making the Weaverville Formation a productive Placer deposit (see container box). Importantly, the Weaverville Formation seems to be sourced entirely within the Klamath Province. This is significant because it implies that by the time the Weaverville Formation was being deposited, there was already enough elevation in the Klamath Mountains to isolate the grabens and basins from rivers draining more distant sources. The older Cretaceous Hornbrook Formation and Eocene Tyee Formation of the Oregon Coast Ranges (Figure 10.5.2 contain grains that have been identified as coming from sources as far away as the Sierra Nevada and the Idaho Batholith (in Idaho). This would imply that, up until at least Eocene time, the area that is now the Klamath Mountains was flat enough to host a river system fed by distant tributaries, but that by the Miocene this was no longer the case. Based on studies of the Weaverville Formation, combined with other geologic evidence, geologists have identified a major pulse of mountain uplift during the Miocene Epoch.

Box 10.5.1: La Grange Mine

The Klamath Mountains province ranks second in gold abundance of all the California geomorphic provinces. Not long after the California gold rush began, prospectors realized that the Klamath Mountains bore similarities to the northern Sierra Nevada. In 1848 Major Pearson B. Reading discovered gold in the Trinity River and people came from all over the world to make their fortune in the Klamath Mountains. The La Grange Mine was among the largest and most successful mines in the Klamath Mountains. Between 1893 to 1915, the La Grange mine was the largest hydraulic mine in California. The La Grange Mine owed its success in part to the Sawyer Decision of 1884, which significantly restricted mining of placer deposits in the Sierra Nevada because hydraulic mining was affecting agriculture downstream in the Central Valley (see 9.4: Gold of the Sierra Nevada). The Sawyer Decision did not affect hydraulicing in the Trinity River, however, because the Trinity River, a tributary of the Klamath River, flows directly from the mountainous terrain of the Klamath Mountains into the Pacific Ocean without passing through agricultural lands. The La Grange Mine continued to operate until 1918, when economic issues surrounding World War I made the cost of mining too high to be profitable. Today the mine is recognized as a historical landmark with a roadside marker along Highway 299.

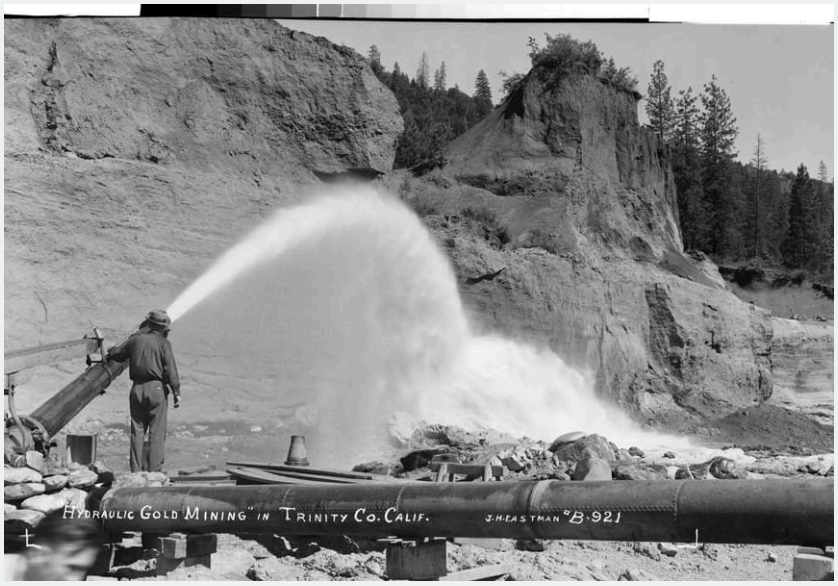


Figure Box 10.5.1: "Hydraulic gold mining in Trinity County, Calif." by Jervie Henry Eastman is In Copyright - Non-Commercial Use Permitted.

The Klamath Mountains in the Quaternary

Though the Klamath Mountains were likely already a topographically elevated region in the Neogene, they were not fully shaped into their current configuration until more recently. Like the Cascade Range (see 7.8: Glaciers in the Cascades) and the Sierra Nevada (see 9.6: Ice Shapes the Landscape), the Klamath Mountains have been heavily shaped by glaciers during the Pleistocene Epoch. One effect of this glacial erosion is the formation of high alpine lakes, which make places like the Trinity Alps popular backpacking destinations.



Figure 10.5.3: Sapphire Lake in the Trinity Alps is an example of an alpine lake in glacially carved terrain. "Sapphire Lake -- Suicide Ridge -- Trinity Alps" by Gary Robertson is licensed under CC BY-NC 2.0.

Until quite recently, the Trinity Alps also hosted the lowest elevation glaciers in California: Salmon Glacier and Grizzly Glacier. These glaciers sat at around 2500 meters (8200 feet), about 520 meters (1,700 feet) below other California Glaciers. Their low elevation is made possible by high rates of precipitation. However, these glaciers experienced significant retreat in recent decades. Salmon Glacier disappeared in 2015 and by 2021, Grizzly Glacier, the last remaining glacier in the Klamath Mountains, had retreated and broken apart to the point that it is no longer classified as a glacier.

In this chapter, you have learned about several geologic events that shaped the Klamath Mountains. Query 10.5.1 will help you place these events into the context of geologic time.

Query 10.5.1

This interactive element is not available in this format. Visit the link or scan the QR code to access it online.

View this Interactive Content online

Acknowledgements:

Special thanks to Dr. Melanie Michalak for her help with the research and editing of this chapter.

References:

1. Cashman, S. M., & Cashman, K. V. (2006). Cataclastic textures in La Grange fault rocks, Klamath Mountains, California. In A. W. Snoke & C. G. Barnes (Eds.), *Geological Studies in the Klamath Mountains Province, California and Oregon: A volume in honor of William P. Irwin* (Vol. 410, p. 0). Geological Society of America. https://doi.org/10.1130/2006.2410(21)
2. Christensen, D. (2021). Evidence for middle Miocene elevated topography isolating the southern Klamath mountains province: A u-pb & lu-hf detrital zircon study of the Weaverville formation. *Cal Poly Humboldt Theses and Projects*. https://digitalcommons.humboldt.edu/etd/529
3. Garwood, J. M., Fountain, A. G., Lindke, K. T., Hattem, M. G. van, & Basagic, H. J. (2020). 20th Century Retreat and Recent Drought Accelerated Extinction of Mountain Glaciers and Perennial Snowfields in the Trinity Alps, California. *Northwest Science*, *94*(1), 44–61. https://doi.org/10.3955/046.094.0104

4. Hamusek, B. (2004, December). *The La Grange Mine: Changing the Landscape in the Quest for Gold*. California Department of Transportation. https://dot.ca.gov/-/media/dot-media/programs/environmental-analysis/documents/ser/lagrange-historical-site-lesson-plan-grade7-a11y.pdf
5. Kauffmann, M. (2020, April 24). *The Last Glacier in the Klamath Mountains*. Michael Kauffmann. https://www.michaelkauffmann.net/2020/04/the-last-glacier-in-the-klamath-mountains/
6. *Klamath Mountains Province*. (n.d.). Western Mining History. Retrieved July 3, 2024, from https://westernmininghistory.com/library/415/page1/
7. La Grange Mine. (2013, August 10). *Visit Trinity*. https://visittrinity.com/history/mining/la-grange-mine/
8. Michalak, M. J., Cashman, S. M., Langenheim, V. E., Team, T. C., & Christensen, D. J. (2023). Neogene faulting, basin development, and relief generation in the southern Klamath Mountains (USA). *Geosphere*, *20*(1), 237–266. https://doi.org/10.1130/GES02612.1
9. Monserrat, L. (2022, May 24). *Glacier change* [Text]. OEHHA. https://oehha.ca.gov/climate-change/epic-2022/impacts-physical-systems/glacier-change
10. Schweickert, R. A., & Irwin, W. P. (1989). Extensional faulting in southern Klamath Mountains, California. *Tectonics*, *8*(1), 135–149. https://doi.org/10.1029/TC008i001p00135
11. Snoke, A. W., & Barnes, C. G. (2006). *The development of tectonic concepts for the Klamath Mountains province, California and Oregon*. https://pubs.geoscienceworld.org/gsa/books/book/574/chapter/3803324/The-development-of-tectonic-concepts-for-the
12. *Weaverville District*. (n.d.). Western Mining History. Retrieved July 3, 2024, from https://westernmininghistory.com/library/449/page1/

This page titled 10.5: Uplifting a Mountain Range is shared under a CC BY-NC 4.0 license and was authored, remixed, and/or curated by Emily Wright.

10.6: Chapter Summary

10.1 Assembling a Continent

- The Klamath Mountains have historical significance in the development of the idea of terrane accretion.
- Terranes are composed of ancient island arcs.
- Melange forms through the accretion of sediments and other oceanic crustal rocks in an accretionary wedge.
- The Klamath Mountains are composed of several accreted terranes, with a general pattern of alternation between terrane and mélange.
- Large east-dipping thrust faults separate terranes.
- The sequence of terranes in the Klamath Mountains is similar to the sequence of terranes in the Sierra Nevada.

10.2 The McCloud Limestone: An Ancient Coral Reef

- The McCloud Limestone formed in a coral reef during the Permian Period.
- Permian coral reef communities were composed of many species that went extinct in the end-Permian mass extinction.
- Comparison of fossil species found in different geologic units can help geologists understand the paleoenvironment.

10.3 The Josephine Ophiolite: A Little Slice of the Mantle

- Obduction is the uplift of oceanic lithosphere onto continental lithosphere and it is less common by far than subduction.
- The Josephine Ophiolite formed in a back-arc basin and was obducted when a tectonic change resulted in the collapse of the back-arc basin and accretion of the island arc.
- Ophiolites themselves are rare, but the ophiolite sequence makes up most of the crust on earth (the oceanic crust).
- The ophiolite sequence forms as magma cools within a magma chamber and lava erupts on the ocean floor at mid ocean ridges (or back-arc spreading ridges).
- The ultramafic chemistry of ophiolites produce unique soils and correspondingly unique ecosystems.

10.4 Plutons of the Klamath Mountains

- The story of the Klamath mountains involves alternation of island arc volcanism and continental arc volcanism.
- Continental arc volcanism resulted in emplacement of plutons that cross-cut older accreted terranes.
- Dating of plutons in combination with cross cutting relationships allows for the dating of accretion events.
- Zoned plutons result from the slow cooling of magma chambers from outside inwards.

10.5 Uplifting a Mountain Range

- During the Cretaceous Period, when the Sierra Nevada volcanic arc was forming, the Klamath province was part of the forearc basin, much like the Great Valley.
- The topographic difference between the Klamath Mountains and the Great Valley is the result of Neogene uplift.
- The uplift of the current mountain range is a much younger event than the events involving the accretion of the bedrock.
- Normal faults in the southern Klamath, such as the La Grange Fault contributed to mountain uplift.
- The Weaverville Formation is composed of sedimentary fill formed in Neogene grabens and basins.
- Glacial erosional features formed during the Pleistocene Epoch.
- Small glaciers were still present in the Klamath Mountains at the start of the 21st century.

This page titled 10.6: Chapter Summary is shared under a CC BY-NC 4.0 license and was authored, remixed, and/or curated by Emily Wright.

10.7: Detailed Figure Descriptions

Figure 10.1 Province Map

The Klamath Mountains province is a mountainous province near the northwest corner of California. The province continues into Oregon though this is not shown on this California map. The Province is bounded by the Cascade Range to the east and the Coast Range to the west. It also shares a small border with the Great Valley to the southeast.

Figure 10.1.1 The process of accretion at a subduction zone

This diagram illustrates the accretion of an island arc. The relative motion between the continental crust and oceanic crust is convergent.

At time 1 (A) in the diagram, an island arc sits offshore of a continent and two subduction zones are present. These are labeled "subducting slabs" in the diagram. Oceanic crust between the island arc and the continent subducts beneath the continent, while crust on the other side of the island arc subducts beneath the island arc. This process forms two parallel subduction zones. Ocean sediments have accumulated on top of the oceanic crust.

At time 2 (B), the island arc has moved closer to the continent and an accretionary wedge composed of oceanic sediments has developed along the edge of the continent.

At time 3 (C), the island arc has reached the continent and accreted to it. The two subduction zones have merged into one and the former accretionary wedge sits between the main continent and the accreted arc, both of which are now part of the continent.

Figure 10.1.2 Terrane map of the Klamath mountains

The geology of the Klamath Mountains and the Coast Ranges in Oregon and northern California. Geology of the surrounding area is simply labeled as “Mesozoic and Tertiary sedimentary rock, postdates accretion of Klamath Terranes," which is included for geographic context. From west to east, the terranes of the Klamath mountains are:

- F, Mesozoic rock of Coast Ranges; mostly Franciscan Fm.
- Wk, Western Klamath Terrane, mostly Jurassic
- WPz, Western Paleozoic and Triassic Terrane
- CM, Central Metamorphic Terrane (Devonian)
- EK, Eastern Klamath Terrane (Early Paleozoic to Jurassic)

Other rocks on this map include

- C, Condrey Mountain Schist (Mesozoic) which is surrounded by WPz and is located near the Oregon/California border
- Jp, Jurassic Plutons which are scattered throughout all terranes except F and
- Kh, Cretaceous Hornbrook Formation which exists along the eastern edge of the Klamath Mountains, near the Oregon/California border.

Reference areas identified

- Redwoods National and State Parks; located in the F region
- Oregon Caves National Monument located at the junction of a Jp region within the WPz region
- Eureka in an MzT region
- Crescent City in the F region
- Hiouchi at the border of the F and Wk regions
- Yreka in the EK region
- Redding in the MZT region
- Roseburg, Oregon in the MzT region
- Medford, Oregon in the MzT region

Query 10.1.2 Mariana and Andean Style Subduction

This activity requires the identification of images and therefore the full activity may not be appropriate for all learners. To receive feedback for the text-based portion of the activity only, press the “check” button after sorting the first two items.

The Geological Tactile Image Repository contains a diagram illustrating Andean type subduction, called, “Continental Subduction Zone”. The “Oceanic Subduction Zone” graphic may also be helpful in explaining Mariana type subduction, although it does not include a back-arc spreading ridge.

Figure 10.1.3 Map illustrating the correlation between terranes of the Sierra Nevada, Klamath and Blue Mountains

This Figure is included for the purpose of showing the correlation between the geology of the Klamath Mountains with the Sierra Nevada and the Blue Mountains. Although the Klamath mountains are west of both the Sierra Nevada and the Blue Mountains (in northeast Oregon), the sequence of rocks occurs roughly in the same order, with a general westward younging trend. Due to the western location of the Klamath Range, a significant curve is required in the dotted lines that connect the geologic units.

Within each of the three provinces, there are distinct blocks representing major rock packages (terranes) arranged vertically according to their age or relative sequence of formation. These blocks typically:

- Span from older rock formations at the bottom to younger ones near the top.
- Are labeled with text indicating terrane names or broad rock group names (e.g., “Eastern Klamath Terrane,” “Central Metamorphic Terrane,” etc.).
- Sometimes include smaller subdivisions labeled with specific sub-terranes or rock groups

Figure 10.2.1 Steps in the development of coral reefs

Development of a Coral Reef, in four stages:

1. A volcanic island with no coral reef.
2. A fringing reef develops.
3. After the volcano continues to subside, the fringing reef grows to a barrier reef and a lagoon separates the main island from the reef.
4. The original volcanic island has subsided below sea level, but the barrier reef continues to grow upwards, forming a ring that surrounds a lagoon.

Figure 10.2.3 Diorama of a Permian seafloor

The Permian community of organisms shown in the diorama occupy similar niches to modern seafloor organisms, but the individual species are quite different from those in the same niches today. Shown here are rugose corals, algae, gastropods, richthofenid brachiopods, and spiriferid brachiopods. The rugose corals featured in the center of the photograph are most relevant to this text. Large, radial, bright orange coral polyps emerge from a horn-shaped skeleton. Unlike modern corals, each individual skeleton is isolated and the polyps are much larger, like a small anemone.

Figure 10.3.2 Island arc with a back arc spreading center

The volcanic arc is divided into five zones. The subducting oceanic lithosphere dives beneath the continental lithosphere at the boundary between the ocean basin and the forearc. Inland from the forearc, the volcanic front sits above the zone where flux melting occurs as a result of subduction. Inland from here is the backarc, where a back arc convection cell in the asthenosphere produces a back arc spreading center in the lithosphere. This area is characterized by rising magma pushing upward through a parting in the crust. The oceanic lithosphere produced by this back arc spreading center is the ophiolite suite, which forms the back arc ocean basin.

Figure 10.3.4 Sea floor spreading at a mid-ocean ridge

This geologic cross-section illustrates how new oceanic crust forms at a mid-ocean ridge. It depicts the layers of crust and mantle beneath the seafloor, the upward movement of magma, and the structure of the oceanic lithosphere. The image shows depth from the seafloor down to about 9 kilometers and a horizontal distance of about 20 kilometers across the ridge axis. (A tactile graphic, Mid Ocean Ridge, is available from the Geological Tactile Image Repository.)

Key Features (Top to Bottom)

- Seafloor Topography
  - A rift valley sits at the center, labeled “Plate boundary,” where the seafloor is pulled apart.
  - On either side of the rift, layers of oceanic crust are shown, dipping away from the ridge axis.
- Oceanic Crust Layers
  - Pillow basalts: Green, lumpy structures near the seafloor, representing lava erupted underwater.
  - Sheeted dikes: Vertical dark bands that ferd lava to the surface.
  - Gabbro: Coarse-grained intrusive rock at deeper levels of the crust, crystallized from slowly cooling magma.
- Transition Zone between the crust and the underlying mantle
- Magma Chamber
  - Magma sits beneath the rift, feeding material into the crust above.
  - Wavy lines indicate the upward flow of magma toward the surface.
- Mantle
  - Beneath the crust and transition zone lies the mantle, which serves as the source of magma.

Scale and Orientation

- The vertical axis is labeled “Depth below sea surface (km)” and ranges from 0 to 9 km.
- The horizontal axis is labeled in kilometers, spanning from -10 to +10 km, centered on the ridge axis.
- The central black dashed line marks the plate boundary, with diverging arrows at the plate boundary indicating seafloor spreading.

Figure 10.3.12 Smith River X Post

A post by Redwood National and State Parks (@RedwoodNPS). The post reads, “‘I woke up like this #nofilter’ - the Smith River; The Smith River is the only undammed river in California, boasting an impressive title of one of the cleanest rivers in the lower 48. The spectacular turquoise color comes from the serpentinite rocks at the bottom.”

Figure 10.5.2 LaGrange Fault Map

The La Grange Fault is located along the south of the Klamath Mountains Province. The trace of the La Grange Fault is long and circuitous, running from southwest to northeast and closely following the topography on account of the low angle of dip. A large pocket of Weaverville Formation lies adjacent to the La Grange Fault along its southwest stretch. The Weaverville Formation is bounded on the south by the Democrat Gulch Fault, which extends southeast from the La Grange Fault. The Hayfork Basin lies to the southwest. Remnants of the Great Valley Sequence are scattered throughout this area. Due north of the La Grange Fault lies the Browns Meadow Fault, which extends in a line oriented northwest to southeast.

This page titled 10.7: Detailed Figure Descriptions is shared under a CC BY-NC 4.0 license and was authored, remixed, and/or curated by Emily Wright.

11: COAST RANGES

Introduction to the Coast Ranges

The Coast Ranges are a series of mountains and valleys trending northwest-southeast along the western edge of North America. The California Coast Ranges begin near Santa Barbara and extend northward to the Oregon border, following the coastline of California. The Coast Ranges are a major division of the physiographic provinces of California, and abut the Klamath province and Great Valley to the east, and the Transverse province to the south. Although the Coast Ranges are not immediately adjacent to the Sierra Nevada, in some places they are geologically similar, as portions of the former Sierra Nevada have been amalgamated into the Coast Ranges through tectonic violence.

We can look across California from west to east and see the Coast Ranges descending into the plains of the Central Valley, then rising again into the Sierra Nevada, as shown in (Figure 11.1):

Almost every major event in California's geologically brief lifespan has left indelible imprints in the rocks of the Coast Ranges. Magma that cooled as the supercontinent of Pangaea began to break up? Check. Agonized seafloor rocks being forced underneath continents, even as a daring few escaped onto the continent? Yep. Bizarrely transformed metamorphic rocks thoroughly altered at temperatures less than your kitchen's oven? Uh huh. The San Andreas ripping apart western California and implanting magma bodies which to this day feed hot springs and geysers? You bet.

In the 1994 Boomer nostalgia film *Forrest Gump*, the titular character, played by Bay Area native (and former community college student) Tom Hanks unwittingly intersects with major historical events such as the Vietnam War and Watergate, along the way meeting figures such as Elvis Presley, John Lennon, JFK, LBJ, and Nixon. The Coast Ranges are like Forrest Gump. They've unintentionally been in the right place to witness a lot of the important geologic events in California.

In this chapter we will divide the complexity of the Coast Ranges into broad geographic categories. We will talk about two regions:

- the Northern Coast Ranges and
- the Southern Coast ranges

The Northern Coast Ranges are primarily composed of sedimentary rocks that were deposited during the Mesozoic and Cenozoic Eras. The Southern Coast Ranges are generally younger, and are composed of sedimentary rocks that were deposited during the Cenozoic Era. For time ranges of these time periods it may be useful to review the timeline from the chapter Geologic Time.

We will also parse the major rock units in the Coast Ranges, including:

- The Coast Range Ophiolite
- The Franciscan Complex
- The Great Valley Sequence
- Quaternary rocks, including volcanics

For fun we will examine some of the most interesting features of the Coast Ranges, including:

- Geothermal fields of hot bubbling mud fed by the wake of the San Andreas fault
- A coal mining region, right here in California
- Metamorphic rocks so altered they could be described as Seussian



Figure 11.1: Location of the Coast Ranges Province of California. “The Coast Ranges Province of California” by Emily Wright, a derivative of the original work, is licensed under CC-BY-NC. Access a detailed description.

Learning Objectives

By the end of this chapter, you should be able to:

- Describe how plate tectonics influences the geology of the Coast Ranges.
- Explain our current understanding of the origins of the Coast Range Ophiolite, Great Valley Sequence, and Franciscan Complex.
- Explain the origins and organization of ophiolite sequences generally.
- Explain Coast Range geomorphic features associated with transpression and transtension.
- Describe San Francisco Bay during the last glacial maximum.

11.1: A Complicated Land
11.2: The Coast Range Ophiolite
11.3: The Great Valley Sequence
11.4: The Franciscan Complex
11.5: Cenozoic Events
11.6: Quaternary Events
11.7: Representative Coast Range Rocks
11.8: Chapter Summary
11.9: Detailed Figure Descriptions

This page titled 11: Coast Ranges is shared under a CC BY-NC 4.0 license and was authored, remixed, and/or curated by Allison Jones & Steven Newton.

11.1: A Complicated Land

A Complex Geological Story

There's more complexity in the Coast Ranges than can be described in one book, much less this one brief chapter, but one place to start is to understand that, along most of their length, the Coast Ranges are the place where the North American plate and the Pacific plate meet. This one seemingly-simple statement explains a lot about the Coast Ranges. But fully understanding what this means takes some unpacking.

The Coast Ranges were first formally mapped in 1895 by Professor Andrew Cowper Lawson of UC Berkeley, a distinguished mineralogist known today to geology students as the guy with the beard of unusual and splendid magnificence. The hirsute Lawson understood the importance of field work–indeed, he founded the first systematic field geology course in the west–and during his explorations of the Coast Ranges he accidentally discovered the San Andreas fault in a linear valley south of San Francisco. At the time Lawson had no idea that the San Andreas's offsets were anything more than a local disruption. That changed in 1906, and Lawson headed a massive research effort to examine this fault that had ruptured such a great distance and so catastrophically tore the state apart. However, Lawson came from a time before plate tectonic theory; in 1906 he could describe *what* happened geologically, but not *why*.

Box 11.1.1: A mineral's namesake

The mineral Lawsonite is named after Professor Andrew Lawson by two of his graduate students. The mineral is typical of blueschist facies metamorphic rocks and was first described in 1895 for occurrences on Ring Mountain on the tiburon peninsula, Marin County, California.



Box Figure 11.1.1: Sample of the pastel pink mineral lawsonite surrounded by mica schist. This specimen is 6.1 cm long. "Lawsonite" by Rob Lavinsky via Wikimedia Commons is licensed under CC BY-SA 3.0.

Plate Tectonics: Unlocking the Mystery

Though Lawson would not live to see the advent and acceptance of plate tectonic theory in the late 1960s, today we know that comprehending the California Coast Ranges is impossible without plate tectonic theory. Just as biology prior to Darwin's theory of evolution has been described as mere butterfly collecting–assembling organisms without understanding how they came to be–geology before plate tectonics was conceptually hobbled and unable to explain regions such as the Coast Ranges.

Why do we find pillow basalts–lava that can only form underwater–in contact with metamorphic rocks such as eclogites that have been subjected to brutal extremes of heat and pressure, and both of these right next to unaltered sandstones? If all this formed in place, when these eclogites were metamorphosed, why weren't the pillow basalts and the sandstones also metamorphosed? These sorts of Coast Range juxtapositions make no sense–until one understands that tectonics has brought all these disparate pieces together from far away.

There are also complications of time and order.

In certain places in the world–Grand Canyon, for example–rock formations obediently accede with geologist's wishes by forming one atop the other, with the occasional fault or fold distorting otherwise relatively flat sedimentary units. It is possible to stand on the South Rim of Grand Canyon and look down to the river and see the Tapeats Sandstone neatly lying atop even older Vishnu Schist, and the Bright Angel Shale atop the Tapeats, and the Muav Limestone atop the Bright Angel, on and on and on, right up to the younger Kaibab Limestone on which visitors stand. In such situations, we can easily understand that the layers are in order, with the oldest at the bottom and the youngest at the top.

California just isn't like that.

How do you explain how old a rock assemblage is when most of it formed far from California, then was brought in by tectonics to collide with and stick onto California, a process that altered and metamorphosed the rocks? What's the proper age of the assemblage? When it first formed in its original state? When it moved and accreted onto California? When metamorphism so transformed the original rocks that they are unrecognizable? There is not an easy answer here.

Further complicating the age of rock groupings, several of the major groups date *from the same time range*. Geology uses a fancy word for this: "coeval," meaning forming at the same time. Because of the devilish difficulties coeval rocks pose for interpretation, we might as well just relabel them as "evil."

Distinguishing the Northern and Southern Coast Ranges

To understand the distinctions between the northern and southern Coast Ranges, closely examine Figure 11.1.1:

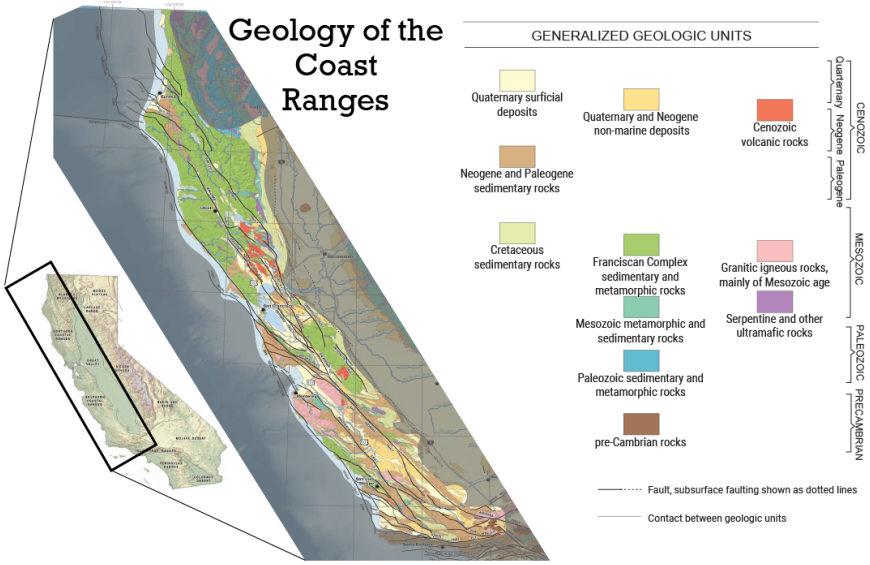


Figure 11.1.1: The California Coast Ranges are a series of mountains that lie to the west of the Central (Great) Valley near the coast. The Coast Ranges are primarily composed of Franciscan Complex rocks, with minor serpentinite, granitic igneous rocks, and pre-Cambrian rocks. It is cut by the San Andreas and associated faults. "Geologic Map of the Coast Ranges" by Emily Wright, a derivative of the original, is licensed under CC BY-NC. Access a detailed description.

While there is not a sharp demarcation in this map, we can roughly say the San Francisco Bay Area divides the north from the south. Furthermore, the geologic character of the northern region is quite distinct from the south, as indicated by the generalized geologic units legend.

Northern Coast Ranges

In Figure 11.1.1, the dominant color of the northern Coast Ranges is green, which the legend identifies as “Franciscan complex sedimentary and metamorphic rocks.” This isn’t quite true nor complete; for example, there are also significant igneous rocks, as well as a host of younger igneous and sedimentary rocks interspersed within the Franciscan in pockets too small to be mapped separately on a map of this scale. Moreover, one should not imagine that the northern regions are monolithically and uniformly one type of rock; when you see a map such as this, with broad swaths of single color, the discerning student should understand that this indicates not uniformity, but rather an overgeneralization of areas lacking detailed mapping.

When you actually go to the Franciscan and observe the outcrops, you find not blank uniformity, but fantastic variety, with rock exposures whose ages swing wildly from time period to time period, and whose rock types change abruptly from igneous to metamorphic to sedimentary and back again, in some places all changing radically within a few meters of each other. It’s a jumble, but could with sufficient research be parsed into more detail than shown on this map. Part of the lack of detail for this region is the result of the map scale; it’s a big zone and if all details were included, the map would be unreadable. But even if you were to find the most detailed geologic maps of this area, you’d still find huge swaths of green dismissed as “Franciscan”. By contrast, much more detail has been mapped in the southern Coast Ranges, and even in the sparsely populated Eel River Valley, one of the few non-Franciscan regions of the northern Coast Ranges. One reason for this is that there isn’t much petroleum in the Franciscan, and hence there has been less economic incentive for intense exploration and mapping.

Southern Coast Ranges

The Southern California Coast Ranges contain petroleum deposits, and a lot of other things. A close examination of Figure 11.1.2 shows that the Franciscan is plentiful in the south as well as the north. Moreover, we find significant areas of light brown “Neogene and Paleogene sedimentary rocks” (this is where oil is found).

There is also a lot more dramatic faulting in the south compared to the north. The San Andreas fault falls right in the middle of southern region, but it is accompanied by a myriad of accomplices, fracturing and slicing rock and creating serious headaches for any geologist trying to envision these pieces back when they were together (the word for this kind of tectonic reconstruction is palinspastic, a term that doesn’t help matters much).

One very unusual thing going on in the south is the pink areas of the generalized geologic map, which the legend calls “Granitic igneous rocks mainly of Mesozoic age.” That’s very strange–we normally associate granitic rocks as having formed very deep in the crust, cooling slowly, and unlikely to be seen at the surface. It would take great upheavals to bring granitic rock from the depths of its formation to the surface where geology students can pick at it with rock hammers.

Yet there are multiple places in California where there is abundant granitic rock, most notably the Sierra Nevada [link]. Are these pieces in the southern Coast Ranges chunks of the Sierra Nevada? It seems crazy, but there is a plausible hypothesis for bringing Sierran rocks all along the coast as far as Marin, as will be detailed later when discussing the Salinian Block.

First, let’s start with the oldest of the major rock units in these ranges: the Coast Range Ophiolite.

This page titled 11.1: A Complicated Land is shared under a CC BY-NC 4.0 license and was authored, remixed, and/or curated by Allison Jones & Steven Newton.

11.2: The Coast Range Ophiolite

Where to Find the Coast Range Ophiolite

We find California's Coast Range Ophiolite (CRO) in a relatively narrow sliver of rocks to the eastern side of the Coast Ranges, concentrated west of the Sacramento Valley, the Diablo Range, and in Lake and Sonoma counties. The Coast Range Ophiolite abuts the Great Valley Sequence to the east and the Franciscan Complex to the west, as shown in Figures 11.2.1 and 11.2.2:

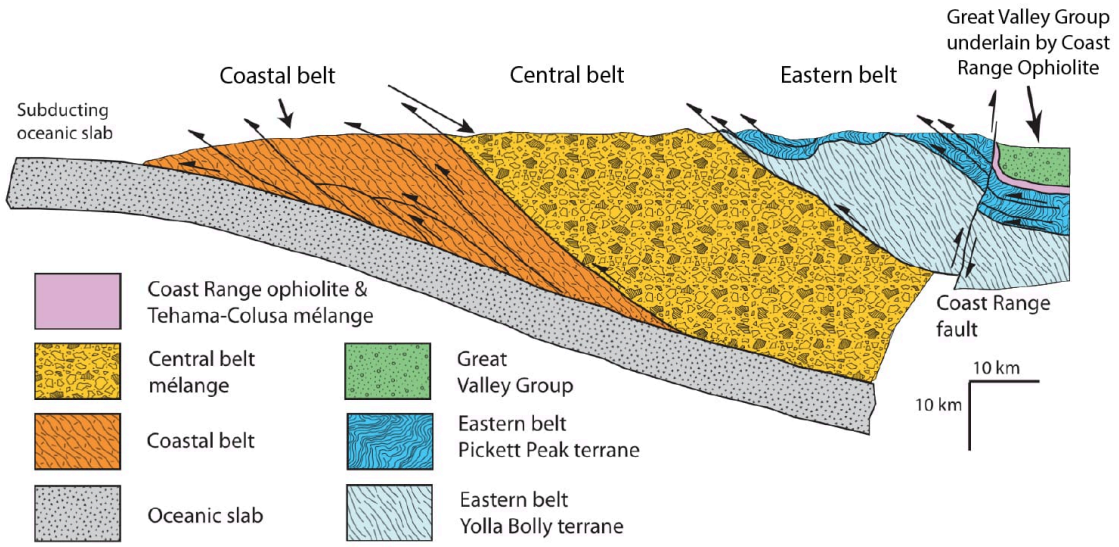


Figure 11.2.1: Cross section of the Mesozoic active margin of California. Metamorphic ages generally become younger to the west; metamorphic grade becomes generally lower from west to east. "Mesozoic Cross-Section of the Coast Range Ophiolite and Franciscan Complex" by Allison Jones, a derivative of the original by Shervais et. al, is licensed under CC BY 4.0. Access a detailed description.

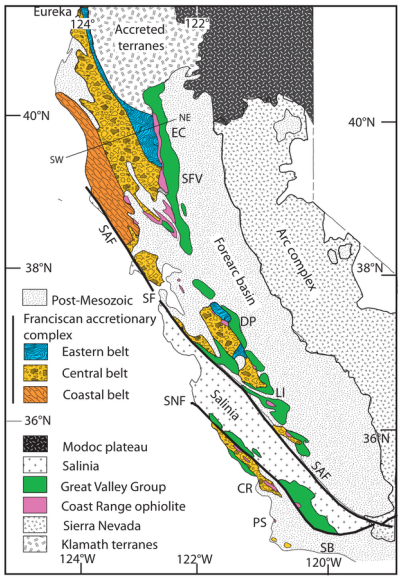


Figure 11.2.2: Geologic map of California showing main elements of the Coast Range geology. Eastern belt (blue), Central belt (yellow), and Coastal/Western belt (orange). The Great Valley Group (green) and Coast Range ophiolite (pink) are also shown. SF—San Francisco, SB—Santa Barbara, SAF—San Andreas fault, SNF—Sur-Nacimiento fault. Major Coast Range ophiolite localities (N-S): EC—Elder Creek, SFV— Stonyford (Black Diamond Ridge), DP—Del Puerto Canyon, Ll—Llanada, CR—Cuesta Ridge, PS—Point Sal. "Map of the Franciscan Complex and Coast Range Ophiolite" by Shervais et. al is licensed under CC BY. Access a detailed description.

The Coast Range Ophiolite is often left out of larger-scale maps, due to its small areal extent. Though Hopson et al. identify 23 separate Coast Range Ophiolite exposures spread over 700 km across the state, most of the exposures are relatively small compared to other groups, such as the Franciscan.

However, the Coast Range Ophiolite is important in two respects. First, it is the oldest rock unit in the Coast Ranges, the foundation of this story. Second, its very existence here speaks to the intense tectonic violence that shaped western California into the twisted, mangled, shattered wreckage that it is today.

What's an Ophiolite?

An ophiolite such as the Coast Range Ophiolite is a suite of rocks, a set of three distinct rock types that form together as part of a single process. The three rock types are pillow basalts, sheeted dikes, and gabbro. See also chapters on the Klamath Mountains and the Sierra Nevada for other examples of ophiolites in California.

Basalt is an iron-rich, silica-poor volcanic rock very familiar to visitors to the Hawaiian islands, because each island is composed of basalt and little else. This dark, volcanic rock begins life as lava, but in an ophiolite sequence there's another twist: it forms under water, making distinct bulbous shapes that look like clusters of grapes. These clusters are strangely termed "pillow basalts," though nothing about them is shaped like a pillow and they are certainly not something you'd want to rest your head on to sleep (see Figure 11.2.3).

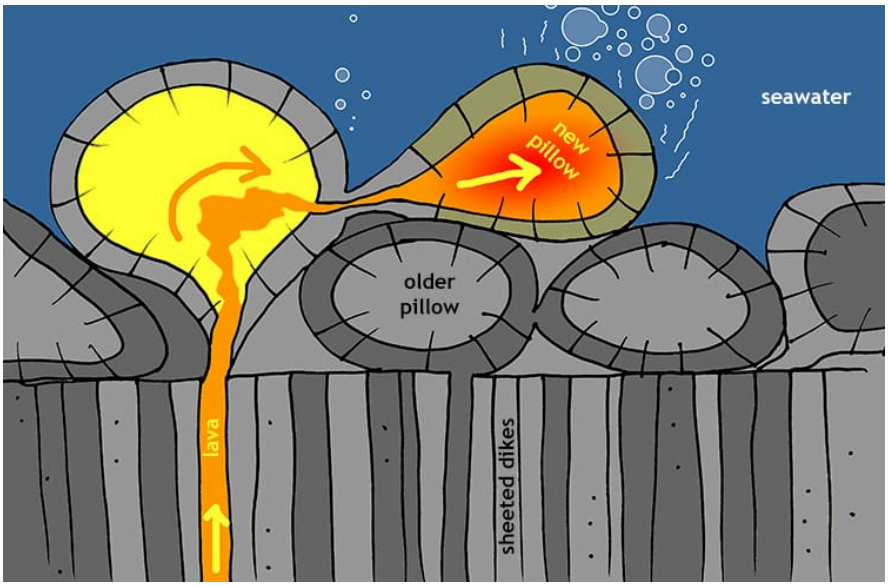


Figure 11.2.3: An illustration of pillow basalt formation. Lava erupts underwater, cooling into bulbous shapes called pillows as it hits the seawater. New pillows form on top of older ones. pillow lava water by Callan Bentley is licensed under CC BY 4.0.

Beneath the pillow basalt, we find sheeted dikes. These tend to be a little harder to recognize, but often look like thin lines all roughly going in the same direction. One way to think about these linear features is that they are pipes or conduits bringing molten rock up to the surface. The rock that makes up these cooled conduits is dark like basalt, but often a little coarser grained; it gets the name diabase, which is intermediate in crystal size between basalt and gabbro. One way to distinguish diabase from basalt is that while basalt often has crystals so small that none are visible to the naked eye, diabase can display well-formed rectangular crystals of plagioclase feldspar.

Going further down in the ophiolite sequence, we find gabbro, is a phaneritic, dark, dense rock (see Minerals and Rocks: Igneous Rocks). Gabbro forms large crystals because it has plentiful time to cool; in this sense, it follows the same long formation time as granitic rocks, though they are chemically on opposite ends of the spectrum.

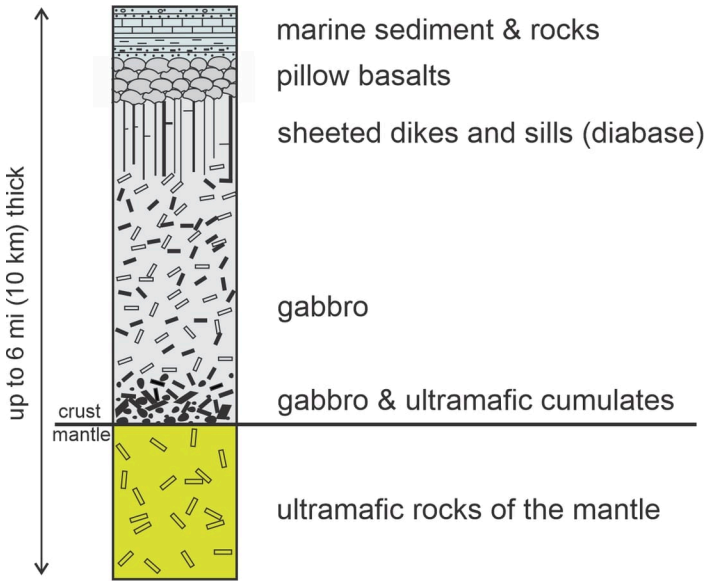


Figure 11.2.4: Ophiolite sequence, with marine sediment underlain by pillow basalts, sheeted dikes, and gabbro. Such sequences are typically around 10 km (6 mi) thick. "Ophiolite cross section" by Dexter Perkins, Open Petrology is licensed under CC BY-NC-SA 4.0. Access a detailed description.

The ophiolite suite is pillow basalt, sheeted dikes, gabbro. Okay... So what?

Let's do a little thought experiment. Off the top of your head, think of the most common type of rock on the planet. Some might say granite. Others will think sandstone. Some may suspect it's a trick question and say clay. Wrong, all wrong.

If you take a research drilling vessel (such as the recently retired JOIDES *Resolution* or the *Chikyu*) anywhere in the ocean and start drilling, you will hit some sort of mud and unconsolidated "ooze" made of radiolaria, or foraminifera, or diatoms. But that's just a relatively thin veneer of sediment on the ocean floor. Drilling deeper, and you hit–insert drum roll! – pillow basalts. Then sheeted dikes. Then gabbro. Everywhere in the ocean. Everywhere you drill. Always in this order. The entire ocean crust is an ophiolite suite.

Because the oceans constitute almost exactly 70% of the Earth's surface, if you randomly start drilling on Earth, you have a 7/10 chance of immediately hitting an ophiolite sequence. Although we humans have a bias toward thinking of our cities and forests and deserts and such to be very important and consequential, the humbling truth is that the Earth could shrug off its mountains and grass plains and continents and keep going along without even noticing. We don't count for much; ophiolites do.

If you've been reading carefully, a puzzling thought should have formed by now. Ophiolites are seafloor crust. And they're really common around the world. But what business does seafloor crust have being part of the California Coast Ranges? How could this deep oceanic rock have ended up so far from the ocean?

Query 11.2.1

This interactive element is not available in this format. Visit the link or scan the QR code to access it online.

View this Interactive Content online

How might the Coast Range Ophiolite have formed?

We know a few things, but the complete picture will require much more research. One thing we know: because the Coast Range Ophiolite is igneous, its rocks are amenable to radiometric dating techniques, which have established dates of mid to late-

Jurassic, from about 166 to 153 Ma, making it roughly coeval with the Smartville Ophiolite in the Sierra Nevada, the Josephine Ophiolite in the Klamath Mountains and other ophiolites in southern Oregon.

Another thing we know: at the time the Coast Range Ophiolite was moving toward California, there existed a giant subduction trench all along the coast of western North America. Much further to the east we had the Sierran magmatic arc, which at this time involved a series of volcanoes similar to the modern Cascades; flux melting from this subduction zone would eventually generate the granitic material that would one day become the Sierra Nevada.

In the most rudimentary sense, what happened to form the Coast Range Ophiolite was some oceanic lithosphere was coughed up–for reasons we don't fully understand–rather than being pushed down into the mantle, the far more common fate of oceanic lithosphere. Geologists have a fancy term for this: obduction (see also Klamaths chapter - Josephine ophiolite section). This obduction process would have involved dismembering whatever coherence these rocks had, and they were separated and twisted. These obducted ocean crust fragments then became sutured on the western edge of North America.

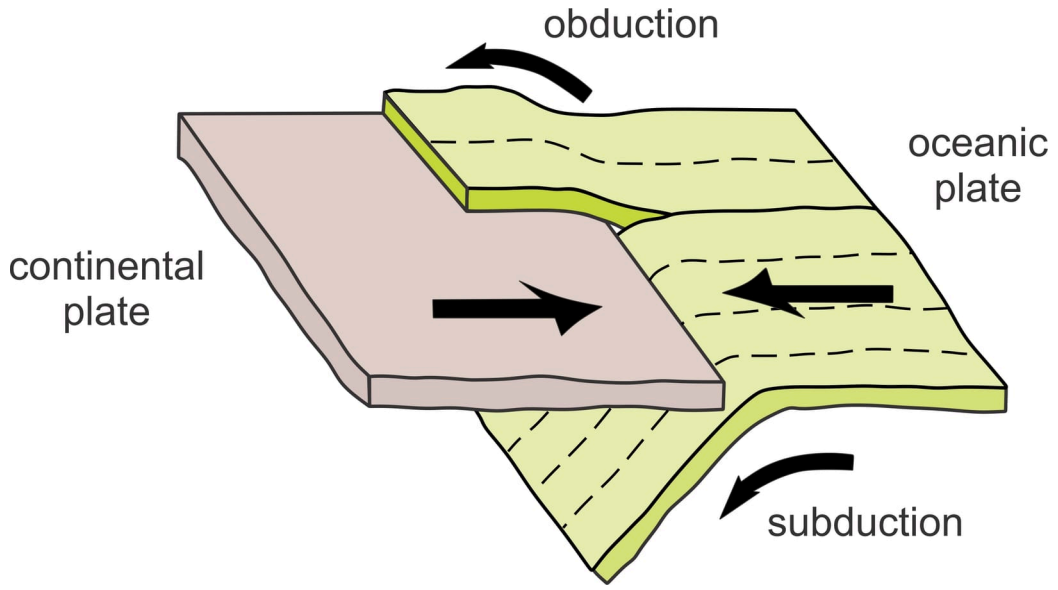


Figure 11.2.5: Obduction and subduction, which occur as plates converge. In subduction, the oceanic plate decends below the continental plate. In obduction, portions detach from the subducting oceanic plate and overlie the continental plate. "Obduction and subduction" by Dexter Perkins et. al, A derivative from the original, is licensed under CC BY-SA 4.0.

Now that we have established the basement in this region, we're going to add more on top of it.

References

1. Dickinson, William R., Clifford A. Hopson, and Jason Saleeby. 1996. "Alternate Origins of the Coast Range Ophiolite (California); Introduction and Implications". GSA Today 6 (2): 1–10.
2. Hopson, C., Mattinson, J, Pessango, E, 1981. "Coast Range Ophiolite, Western California," in Ernst, W.G. (ed.), *The Geotectonic Development of California*. Prentice-Hall, Englewood Cliffs, NJ.

This page titled 11.2: The Coast Range Ophiolite is shared under a CC BY-NC 4.0 license and was authored, remixed, and/or curated by Allison Jones & Steven Newton.

11.3: The Great Valley Sequence

Forarc Basin Sediments

When you drive along I-5 in central California, you encounter landscapes so flat that you could mistake them for the endless agricultural fields of the Midwest. But underneath the rectangular plots there exists an incredible story: buried as deeply as 12 km, there are the shattered fragments of a chain of giant volcanoes. Their eroded clasts, plucked apart by oxidizing amphibole and feldspars disintegrating into clay, washed down streams and out into the ocean. But because the Coast Range Ophiolite hindered movement of these clasts to the west, they settled in deep offshore basins, grain piled upon grain, filling what would become the Central Valley with the debris of a California that no longer exists. We call this configuration a forearc basin (Figure 11.3.1) .

Gravity and water, over many millions of years, transferred the husk of dead volcanoes from their high loft in the east down into the Central Valley, piling thick sediment layers that would, in time, consolidate to become mudstones, sandstones, conglomerates. This is the Great Valley Sequence.

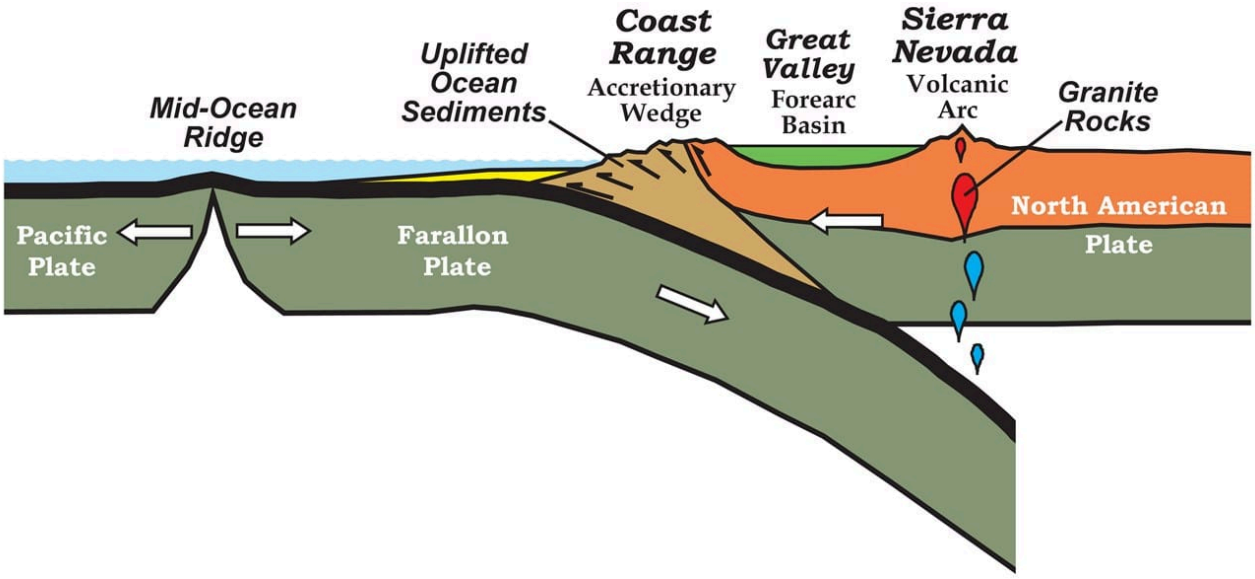


Figure 11.3.1: The Great Valley Sequence formed in the forearc basin between the volcanic arc of the Sierra Nevada and the Coast Range accretionary wedge. "Ancient Subduction Zone" by the National Park Service is in the public domain. Access a detailed description.

For most of the Central Valley, you cannot see these sedimentary rocks because you drive only on the most recent layer of compacted dirt. But as you approach the Coast Ranges's eastern edge, the rocks of the Great Valley Sequence burst from the ground like breaching whales, turning upwards until they are near vertical. Of course, according to the principle of original horizontality, (see Geologic Time), these rocks too were once horizontal, and have since been tilted during the later uplift of the Coast Ranges (see Formation of the San Andreas Fault). In places such as the Monticello Dam near Lake Berryessa, these alternating layers of Great Valley Sequence sediment are stacked for hundreds of meters at an angle so near vertical that the strata might as well be trees in a forest.



Figure 11.3.2: An impressive rock outcrop of turbidites in the Venado Sandstone, located near Lake Berryessa in California. It highlights the classic alternating light and dark bands of sandstone and shale typical of deep-sea turbidity current deposits. The rock layers are steeply tilted, nearly vertical, due to tectonic deformation. "Lake Berryessa turbidites" by Mikesclark via Wikimedia Commons is licensed under CC BY-SA 3.0.

Forming at the same time as the Great Valley Sequence, but to the west, a vast complex now scraped off the descending Farallon Plate and crumpled, twisting and torquing, unsettled in its new home. This is the time of the Franciscan.

Query 11.3.1

This interactive element is not available in this format. Visit the link or scan the QR code to access it online.

View this Interactive Content online

This page titled 11.3: The Great Valley Sequence is shared under a CC BY-NC 4.0 license and was authored, remixed, and/or curated by Allison Jones & Steven Newton.

11.4: The Franciscan Complex

What the Franciscan Is

If you look at older textbooks or journal papers, you can find the Franciscan Formation. Or the Franciscan Group. Or the Franciscan terrane. Or the Franciscan Assemblage. Today, perhaps due to general exhaustion over the issue, geologists have settled on calling this vast part of western California the Franciscan Complex. In the future it may yet be rebranded as something else.

In any event, the name is inconsequential compared to what the Franciscan Complex is and the story it tells about California's geologic development.

The rocks of the Franciscan are, as you might imagine, varied and quite complicated. Sedimentary, metamorphic, and igneous rocks are all represented within the formation and it is not uncommon to glimpse 4-5 different rock types of the Franciscan Complex within the span of a single photograph (Figure 11.4.1).

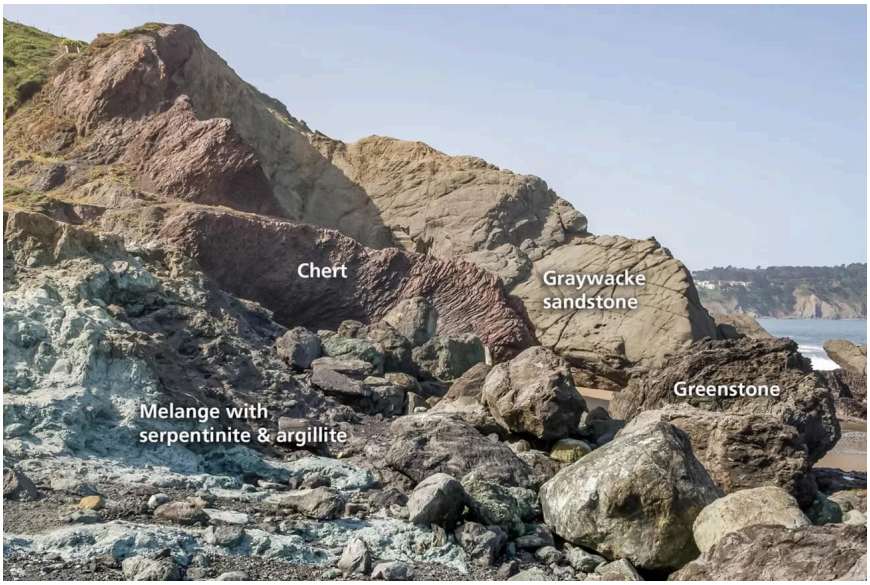


Figure 11.4.1: An outcrop of representative Franciscan rocks at Baker Beach, San Francisco. Green-blue rocks in the foreground are melánge with serpentinite and argillite. Behind them, red radiolarian chert outcrops. Behind the chert is greenstone and graywacke sandstone. Outcrop by the National Park Service is in the public domain.

The Franciscan contains a lot of ocean sediment and a lot of oceanic volcanic rocks. But most everything has been metamorphosed to some degree. And some of the Franciscan rocks have been greatly metamorphosed, altered beyond all recognition so thoroughly that it is hard to imagine the immensity of heat and pressure that have shaped them.

The Franciscan contains sedimentary rocks: greywackes, a dark, dirty-looking sandstone filled with fragments of other rocks, suggesting sediment raining down from eroding surfaces. Research suggests that the source of lithic fragments in Franciscan greywacke derived from the same source as the Great Valley Sequence, in other words, from the now missing volcanoes that once sat above the Sierra Nevada Batholith.

Franciscan chert is a glassy burgundy rock consisting almost entirely of the microscopic glassy shells of single-celled organisms called radiolaria, now stacked in fine layers hundred of meters thick.

The Franciscan has igneous rocks: pillow basalts, rounded remnants of volcanic eruptions underwater. Much of this basalt has been metamorphosed to greenstone, but the pillow structures are still visible.

The Franciscan also has metamorphics, such as serpentinite, California's state rock, with its elegant, slippery, brilliant green surfaces. There is also blueschist, a very rare and highly altered metamorphic rock that comes to us by the strange combination of incredible pressure and cool temperatures. The Franciscan Complex has all of these and more.

Query 11.4.1

This interactive element is not available in this format. Visit the link or scan the QR code to access it online.

View this Interactive Content online

Query 11.4.2

This interactive element is not available in this format. Visit the link or scan the QR code to access it online.

View this Interactive Content online

Forming the Franciscan

The story begins with the breakup of the supercontinent Pangaea, about 200 million years ago. As the separating continents moved apart, giant subduction trenches formed along their advancing edges. Along the west coast of North America, this was one in a series of such subduction events which, through terrane accretion, assembled what is now California (see A Brief Geologic History of California) Because Earth's size is virtually unchanging, if you create new crust–for example, where the expanding proto-Atlantic grew–you have to remove old crust at the same rate. Subduction zones accomplish this by having denser, colder crustal material slide down into the deep mantle, where ancient gigantic slabs surround the Earth's core, phantoms of a lost world. These subduction zones also feed water-rich rock into the trenches, whereupon this aqueous bounty aids the distribution of heat as the slabs descend, allowing magma to form in a process called flux melting (see Cascades).

Meanwhile, as the seafloor of the proto-Pacific advanced toward the bleeding edge of North America, the Farallon trench awaited to consume it. Had this process proceeded smoothly, we would not have the Franciscan Complex, but rather a deep offshore trench, not unlike what currently exists off of modern day Chile and Peru. But a significant portion of this seafloor crust would jam in the trench, scrape off, become part of North America - repeatedly. That's the Franciscan Complex.

The Franciscan, much like the Sierra Nevada metamorphic belts, can be divided into at least three accreted terranes, but all three formed through dominantly mélange style accretion (see Klamath Chapter, section 10.2) For the sake of this text, we'll refer to the Franciscan as a whole.

When did this happen? Wakabayashi (2015) finds evidence for subduction beginning at 165 Ma, and lasting until 25 Ma. Mulcahy et al. (2018) estimate that Franciscan subduction was occurring no later than 180 Ma, a date significantly older than much previous research. In any event, this began in the Jurassic and continued emplacing material until quite recently, about 25 Ma.

Discerning students might frown about these dates, remembering that the previous section had given a Coast Range Ophiolite date of 166 Ma–not much different than the Wakabayashi date, and earlier than the Mulcahy date. Part of the reasoning for putting the Coast Range Ophiolite as the foundation is that the Franciscan kept going for over a hundred million years, while the Coast Range Ophiolite had a briefer span. Another reason is that the structural arrangement in the eastern Coast Ranges suggests the Coast Range Ophiolite lies underneath the Great Valley Sequence, which is contemporaneous with the Franciscan. So because the Coast Range Ophiolite is beneath the Great Valley Sequence, and the Franciscan and Great Valley Sequence were coeval, then it reasons that the Coast Range Ophiolite is older than the Franciscan, except in those places where it's about the same age. Remember earlier when we said this story was complicated?

The phrase you encounter when reading about the Franciscan is "accretionary wedge," which is not particularly useful unless you have a diagram of what this means. To wit, Figure 11.4.2:

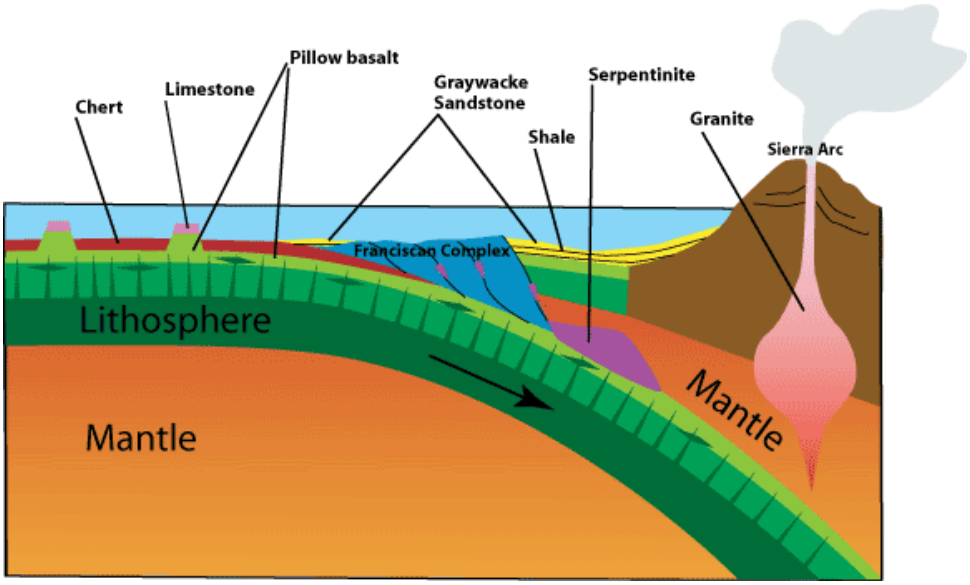


Figure 11.4.2: Cross section of the West Coast of North America at about 100 Ma, when the Franciscan complex was forming. Subduction by the National Park Service is in the public domain. Access a detailed description and accessibility guidance.

In this diagram we find the area indicated as the Franciscan Complex wedged in between mighty tectonic forces–to the west, the relentless movement of the Farallon plate crashing into North America, while to the east, the immovable North American continent acting as a doorstop. This wedge of Franciscan is accreted, or stuck onto, North America–hence the name *accretionary wedge*.

The rocks of the Franciscan are caught in the middle and transferred from the Farallon plate to the North American plate. They are also crushed, squeezed, torqued, and shattered to a degree difficult to imagine. This is why Franciscan rocks are so hard to map or describe–they are a jumbled mess of different rocks all swirled together, as if someone put a petrology book in a blender.

One important thing to notice in Figure 11.4.2 is the location of sea level. Both the Franciscan Complex and the Great Valley Sequence were forming offshore in the Mesozoic. The tectonic environment of the Coast Ranges is quite different today; a transform boundary has replaced subduction. However, even north of the Mendocino Triple Junction, where subduction continues to this day, the outcrops of the Franciscan Complex are very far from the modern accretionary wedge. In both cases, the rocks have been moved to their current location by later events of the Cenozoic.

Query 11.4.3

This interactive element is not available in this format. Visit the link or scan the QR code to access it online.

View this Interactive Content online

References

1. Berkland, J.O., Raymond, L.A., Kramer, J.C., Moores, E.M., O'day, M.; What is Franciscan?. AAPG Bulletin 1972;; 56 (12): 2295a–2302. doi: https://doi.org/10.1306/819A421A-16C5-11D7-8645000102C1865D
2. Blake, M.C., Jr., and D.L. Jones, 1981, The Franciscan assemblage and related rocks in northern California: a reinterpretation, pp. 306-329, in Ernst, W.G. (ed.), The Geotectonic Development of California. Prentice-Hall, Englewood Cliffs, NJ.
3. Dickinson, W.R., Ingersoll, R.V., Cowan, D.S., Helmold, K.P., Suczek, C.A., 1982, Provenance of Franciscan graywackes in coastal California. GSA Bulletin (1982) 93 (2): 95–107. https://doi.org/10.1130/0016-7606(1982)93<95:POFGIC>2.0.CO;2
4. Goodstein, David L. States of Matter. Dover Publications, 2014. ISBN 0-486-49506-X (p. 1). https://www.amazon.com/States-Matter-Dover-Books-Physics-ebook/dp/B00LV86COS/
5. Mulcahy, S. R., Starnes, J. K., Day, H. W., Coble, M. A., & Vervoort, J. D. (2018). Early onset of Franciscan subduction. Tectonics,

37, 1194–1209. https://doi. org/10.1029/2017TC004753
6. Wakabayashi, J. Anatomy of a subduction complex: architecture of the Franciscan Complex, California, at multiple length and time scales. International Geology Review, 2015. Vol. 57, Nos. 5–8, 669–746, http://dx.doi.org/10.1080/00206814.2014.998728

This page titled 11.4: The Franciscan Complex is shared under a CC BY-NC 4.0 license and was authored, remixed, and/or curated by Allison Jones & Steven Newton.

11.5: Cenozoic Events

Formation of the San Andreas Fault

Whew. We emplaced the Coast Range Ophiolite. Then the Great Valley Sequence and the Franciscan Complex came along, both added at about the same time. Can we take a breather? Not yet. There's still a lot that happens in the story of how the Coast Ranges came to be.

When we last left the situation, the breakup of Pangaea had created subduction trenches on the edge of what would become North America, and major parts of California at last formed: the Sierra Nevada, the Coast Ranges, the Great Valley Sequence.

Subduction continued at the proto-North American edge as the continent continued its migration to the northwest, rotating as it did so. Magma formation ceased, the Sierran volcanoes died out and eroded into the Great Valley, and for a time, California experienced a rare time of calm.

But things were about to get interesting. About 30 Ma, aimed straight at the giant subduction trench that formed western edge of the continent, was something that would not submit and compliantly dive into oblivion. A spreading center–a location where new ocean crust is formed–headed toward California (Figure 11.5.1). And unlike the old, cold, dense ophiolitic crust that normally would descend into the trench, never to be heard from again, the spreading center was youthful and hot, meaning that its rocks were less dense and relatively buoyant.

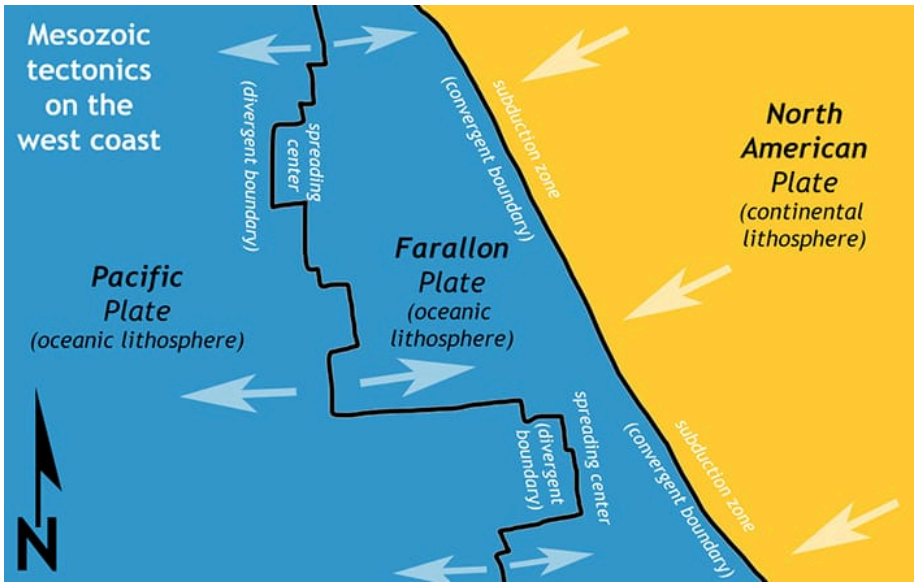


Figure 11.5.1: The tectonic setting of the west coast of North America in the Mesozoic was quite different than today, as shown in this interpretive map view. Mesozoic map by Callan Bentley is licensed under CC BY-NC 4.0. Access a detailed description.

When the subduction trench encountered this warm, buoyant spreading center, things got messy. Try holding a basketball underwater in a swimming pool and you'll get the idea. The spreading center and the trench collided, wrestled, argued irreconcilably–but it was an impossible situation. The trench couldn't stop what it was doing–the spreading center couldn't be subducted. It's not unreasonable to imagine giant earthquakes as the two plates fought. In terms of geologic violence and drama, thirty million years ago off the coast approximately where Los Angeles is today would have been a very interesting thing to witness.

In time, these two contending parts of the world agreed to disagree and go their separate ways, and in that moment–maybe by 28 Ma–the San Andreas fault was born. The San Andreas fault is the solution to the inability of the spreading center to subduct. The San Andreas split the old Farallon plate, creating two "triple junctions," places where three plates come together. Today we call these the Mendocino Triple Junction and the Rivera Triple Junction. The Mendocino Triple Junction is, unsurprisingly, near Cape Mendocino, while the Rivera Triple Junction is off the tip of Baja California. These are the two tectonic ends of the San Andreas system.

But they used to be much closer together. Over time, the Mendocino Triple Junction and Rivera Triple Junction migrated away from each other in a northwest-southeast trend, growing and lengthening the San Andreas fault between them. One place that yields good information on this process, and how fast it all happened, is one of the newest National Parks in the U.S.

Pinnacles National Park

If you head to Pinnacles National Park from the east, you drive down a long, linear valley to get to the park entrance. The valley is unremarkable to non-geologists, but to those who know what to look for, this straight-line indentation in the surface of the Earth is the San Andreas fault.

Pinnacles is home to a steep and remarkable assemblage of cliffs and boulders and talus caves, all of which make for exciting, if somewhat grueling, hiking and climbing. Visitors often seek out the famous California condors, whose recovery from near extinction has been helped greatly by efforts at Pinnacles.

But what's really interesting here is the rocks. This rhyolitic volcanic area erupted about 23.5 Ma, and it happened to do so right on the newborn San Andreas. Since that time, the ground has shifted–both sides of the fault moving to the northwest, but the east side moving slower to the northwest. This fault action has ripped apart the volcanic complex so that today we find the original edifice in two halves–one half, the Pinnacles. Another half, called the Neenach Volcano, exists 314 km (195 miles) to the south (Figure 11.5.2).

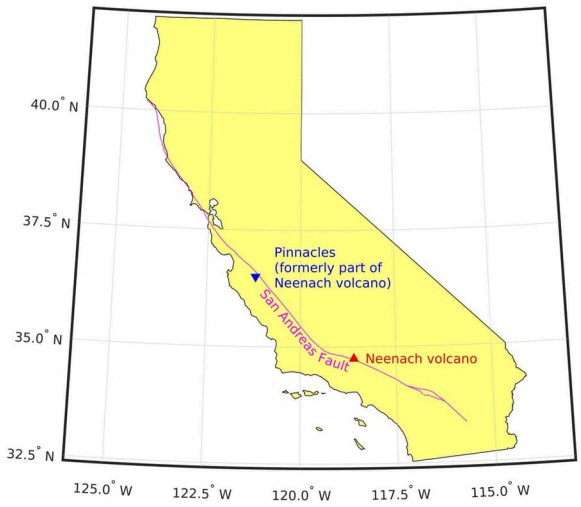


Figure 11.5.2: Pinnacles, California offset by the San Andreas Fault. The Pinnacles was formerly part of the Neenach volcano. Its present-day location is 314 km (195 mi) northwest from the volcano that the San Andreas sliced it from. "Pinnacles, California Offset by San Andreas Fault" by the USGS is in the public domain.

Query 11.5.1

This interactive element is not available in this format. Visit the link or scan the QR code to access it online.

View this Interactive Content online

At Pinnacles National Park you'll find the northern half of a once whole volcano which was split in two and ended up 314 km (195 mi) north of its other half. This occurred at the Neenach Volcano which is long extinct, and whose other half can be found 25 miles west of the city of Lancaster. This video discusses this oddity and how it involves the San Andreas fault.

Video 11.5.2: The California Volcano That Split in Two

At Pinnacles National Park you'll find the northern half of a once-whole volcano that was split in two and ended up 195 miles north of its other half. This occurred at the Neenach Volcano, which is long extinct, and whose other half can be found 25 miles west of the city of Lancaster. This video discusses this oddity and how it involves the San Andreas fault.

This interactive element is not available in this format. Visit the link or scan the QR code to access it online.

View this YouTube Video online

Where Things Get "Creepy"

The San Andreas Fault system today experiences a variety of slip behavior. South of the town of Parkfield, large earthquakes have occurred and it appears that this segment of the San Andreas Fault is locked (Figure 11.5.3). North of San Juan Bautista, the fault has produced large earthquakes like the M7.9 San Francisco earthquake in 1906, and the M6.9 Loma Prieta earthquake in 1989. This northern section of the fault is also currently locked. Between the two locked segments, from San Juan Bautista to the town of Parkfield, the fault experiences both seismic slip, producing small earthquakes of M5 or smaller, and aseismic slip, or "creep." Aseismic slip does not generate seismic waves and can only be detected from geodetic observations (GPS). While creeping faults may not always generate sizable earthquakes, they do slowly deform anything constructed above them.

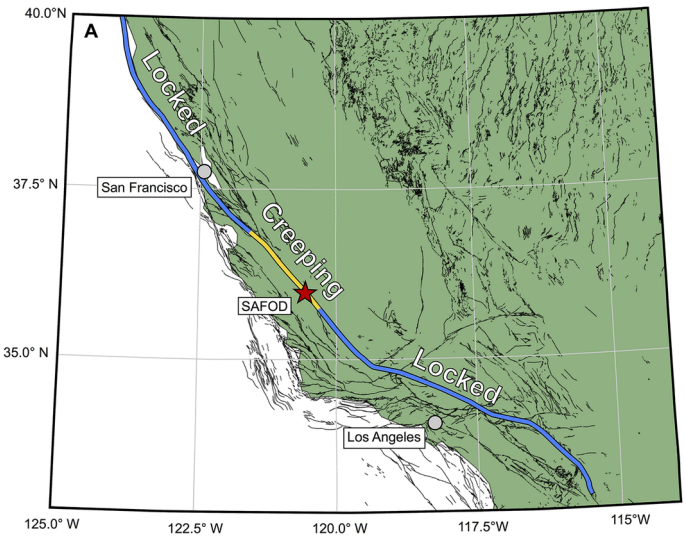


Figure 11.5.3: Map of the San Andreas Fault showing locked (blue) and creeping (yellow) sections. Black lines are other active faults. Fault map by Coffey et. al is licensed under CC BY. Access a detailed description.

In addition to the San Andreas Fault, a number of faults within the strike-slip system also experience creep. Take the Hayward Fault, which underlies one of the most populous regions of the San Francisco Bay Area and experiences aseismic creep in certain locations at a rate of ~5 mm/year. Constructed in 1923, University of California Berkeley's Memorial Stadium sits right atop one of such creeping locations (Figure 11.5.4). From 2010-2012 the stadium underwent a $321 million renovation to increase its seismic safety after receiving a "poor" rating in 1998. Aseismic creep continues to displace the historic football stadium.

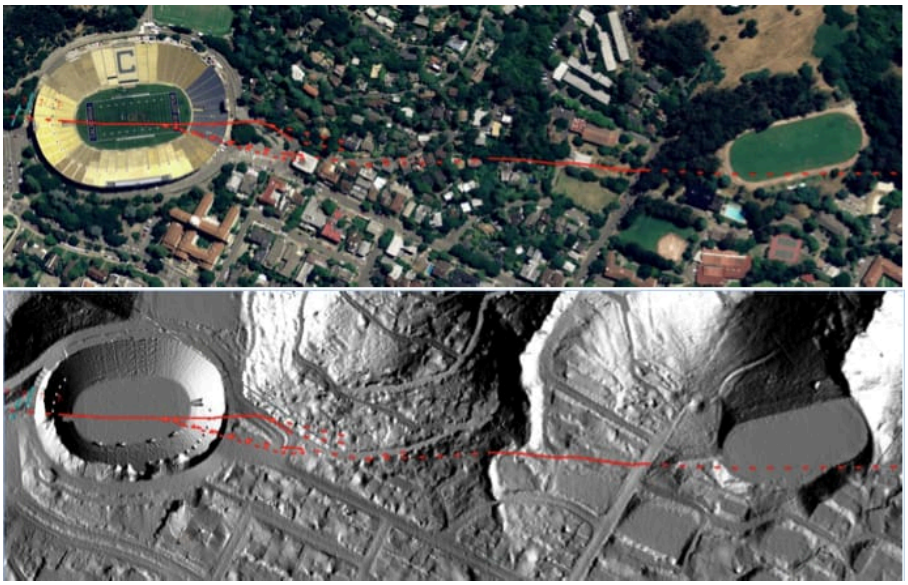


Figure 11.5.4: Aerial view (top) and LiDAR image (bottom) of UC Berkeley Memorial Stadium and surrounding area. The trace of the Hayward fault is indicated by red solid (known) and dashed (inferred) lines. Berkeley Memorial Stadium by Horst Rademacher is licensed under CC BY-NC 4.0. Access a detailed description.

Another major branch of the San Andreas Fault system, the Calaveras Fault, which extends 123 km (76 mi) from Danville to Hollister, is also creeping aseismically. It has slowly shifted sidewalks, retaining walls, and even the foundations of homes creating some interesting architectural features (Figure 11.5.5.



Figure 11.5.5: The creeping Calaveras fault has shifted this home such that the columns on the front porch now tilt to the left. This work by Allison Jones is licensed under CC BY.

The Salinian Block

If you drive past filming locations for Alfred Hitchcock's movie *The Birds*, past the abandoned site of a canceled nuclear reactor sitting nearly right on top of the San Andreas fault, and go west until the road ends at the Bodega Head parking lot, you will find granitic rock.

This is a weird place to find that. Usually in California we think of plutonic rock as Sierran, associated with emplacement tens of kilometers deep, where the poor heat conduction allows large crystals to slowly assemble out of the magma. Major uplift has exposed these rocks in the Sierra Nevada (link)... but what's with Bodega Head?

Travel a bit further south from Bodega Head and you find the high ridge that is the backbone of the Point Reyes National Seashore. Granitic rock, again. The San Andreas close and to the east, again. Point Lobos? Granitic rock again. Further south, and we find the same pattern again and again, pockets of granitic rock proximal to the San Andreas, usually to the west side of the fault. What's going on?

The Salinian Block encompasses much of the coastline of California, from near Santa Barbara to as far north as Bodega Head. It has many rocks that are not granitic, of course, but while we can form a sandstone just about anywhere, is it an unusual thing to come across granitic exposures so far from a place where they might have formed. The Mesozoic volcanic arc and the magma chambers that fed it were much further to the east, forming the batholiths that now make up the Sierra Nevada and Peninsular Ranges. What could bring granitic rocks so far from where granitic rocks form?

One theory involves the Garlock fault, which is a left-lateral fault slicing the southern terminus of the Sierra Nevada. Movements along the Garlock could tend to move southern Sierran rocks to the west. The Garlock intersects with the San Andreas, which is a right-lateral strike slip fault. One can imagine periodic exchanges, like passengers changing trains, where the Garlock pushes portions of granite to the west, across the San Andreas, where these blocks could now board the Pacific Plate and head northwest, in the direction of Alaska. It wouldn't be all of the southern Sierra Nevada, just episodic blocks sent cruising northward. And we do find Salinian granite as discrete, relatively small blocks: Bodega Head, the ridge of Point Reyes, Point Lobos (Figure 11.5.6).



Figure 11.5.6: Decomposing Salinian block granite on the coast just south of Point Lobos. This work by Allison Jones is licensed under CC BY 4.0.

It's a neat story. But many researchers have taken issue with this idea to explain the Salinian Block. They point to greater similarities in the rock to the Mojave region, and even further south to the granitic emplacements of Baja California, an idea especially supported by paleomagnetic data. At this point, we need to conclude there is not enough data on this Salinian Block issue to pronounce a conclusion. Sometimes in science we must step back to allow for clarifying research, rather than rushing to a convenient and hasty, but erroneous, conclusion.

San Andreas-Related Volcanics

A series of Cenozoic volcanic fields exist within the Coast Ranges of California. They get progressively younger to the northwest and have been diced up by right lateral faults of the San Andreas Fault system, making their history somewhat difficult to unravel. From south to north and oldest to youngest they are the: Quien Sabe/Mt Burdell, Berkeley/Tolay, Sonoma, and Clear Lake volcanic fields (Figure 11.5.5). These volcanic fields also, not coincidentally, get generally younger to the north. The Quien Sabe and Burdell Mountain volcanic fields have been dated to ~11 Ma, both emplaced around the same time, but they have been separated by ~175 km of right lateral slip of the East Bay fault system. Similarly, the slightly younger Berkeley and Tolay volcanic fields formed at ~10-8 Ma and have been offset by . The Sonoma Volcanics were formed between 8-2.5 Ma and have been displaced at least 28 km along the Rodgers Creek fault.

These volcanic fields are temporally and spatially associated with the northwestward migration of the Mendocino Triple Junction

suggesting that, rather than the product of subduction related flux melting (like the Cascades) they are the result of mantle upwelling into an opening in the subducting Farallon plate.

Figure 11.5.7 indicates the locations of these young volcanic fields as well as the locations of the Mendocino Triple Junction over the last 12 million years.

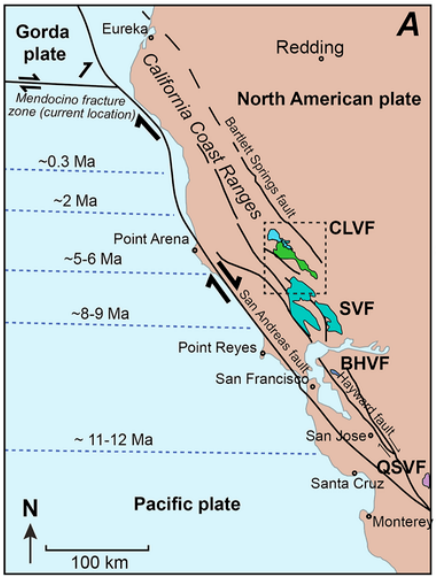


Figure 11.5.7: Schematic map of northern California, showing the Coast Range volcanic centers, major regional faults, and approximate position of the Mendocino triple junction over the past 12 million years. CLVF = Clear Lake Volcanic Field (green), SVF = Sonoma Volcanic Field (teal), BHVF = Berkeley Hills Volcanic Field (blue), QSVF = Quien Sabe Volcanic Field (purple). Modified from McLaughlin and Ohlin (1984); Stanley and Rodriguez (1995). This work by Allison Jones, a derivative of the original, is licensed under CC BY. Access a detailed description.

The Berkeley Hills volcanic field is yet another slightly older volcanic field. This one is Late Miocene-Pliocene in age and is located in the Berkeley Hills in Alameda and Contra Costa Counties. Some of its best exposures can be found in the Robert Sibley Volcanic Regional Preserve and near the Caldecott Tunnel. The primary volcanic unit here is the Moraga Formation which hosts basaltic lava flows, shallow intrusions, volcanic breccias and volcaniclastic sediments. It is underlain by the Orinda formation, interpreted to be 12-14 Ma river deposits, which lies unconformably over the Great Valley Group. The Moraga formation is overlain by younger sedimentary units. These units are all folded into a syncline - the Siesta Valley Syncline - and thus are repeated from west to east.

Eighty miles south of the Berkeley volcanics and on the opposite side of the Hayward/Calaveras Fault system is the Quien Sabe volcanic field. Some research suggests that these two fields are of the same origin. Mount Burdell north of Novato in Marin County is also home to similar volcanic rocks suggesting that it may also be similarly displaced Quien Sabe volcanics.

The Sonoma/Napa volcanics are mostly Pliocene age. They are highly variable in their composition containing andesite, basalt, rhyolite flows, pyroclastic tuff, and breccia, diatomaceous mud, silt, and sand. There is also some obsidian and perlitic glass. Notably, the Sonoma/Napa volcanics supply the Sonoma and Napa valleys with rich soils that contribute to the region's world-renowned viticulture. Older parts of the Sonoma Volcanics have been displaced 28 or more km along the Rodgers Creek fault in the last 7 million years.

The Clear Lake volcanic field is the youngest and the northernmost of the young volcanic fields in the Coast Ranges of California. It has been active through the Pleistocene, with the most recent eruptions occurring about 11,000 years ago. The Clear Lake Volcanic Field is now home to the world's most productive geothermal energy power plants, which supply enough electricity for about 850,000 homes in the region.The Geysers geothermal field south of Clear Lake along Geyser Creek is currently the world's largest complex of geothermal power plants, containing 22 plants that generate an average of 955 MW (Figure 11.5.8). Here, groundwater percolates down through fractures in the permeable Franciscan Complex greywacke where it is heated by shallow magma. The greywacke here is overlain by a relatively impermeable layer which traps steam. Wells have been drilled down to extract the steam which is in turn converted to electricity by turbines. The Geysers Geothermal field has been used for electric power since 1960.



Figure 11.5.8: Sonoma Calpine 3 plant at The Geysers geothermal power complex, Sonoma County, California. Sonoma plant geysers by Stepheng3 via Wikimedia Commons is licensed under CC0 1.0.

Transpression and Transtension

Another symptom of San Andreas faulting in the Coast Ranges is their elevation. Approximately 3.5 million years ago, the Pacific and North American Plates went from sliding alongside each other in true strike-slip fashion, to moving at a slight angle to one another. This small shift had huge consequences for the topography of the Coast Ranges.

While most of the plate motion of the San Andreas fault today is strike slip (about 90% of it) the remaining 10% is actually compressional. It was only about 1-2 million years ago that uplift of the Coast Ranges really began in earnest. They continue to rise today by about 1-2 mm (1/16 of an inch) per year. This combination of strike slip motion and compression is known as transpression. It can thicken the crust in two ways: by faulting it or by folding it. Both deformation styles are present in the Coast Ranges.

This crustal deformation is even more dramatic where a fault bends. In a right-lateral fault like the San Andreas and its ancillary faults, a bend to the left will result in an even more locally shortened and thickened area. This is known as a restraining bend (Figure 11.5.9). Should the same right-lateral fault instead take a bend to the right, it will instead experience stretching and thinning forming down-dropped features like sag ponds. This is known as transtension and the resulting feature is called a releasing bend. Both releasing and restraining bends are common all along the SAF. The aforementioned Clear Lake Volcanic Field is a transtensional basin.

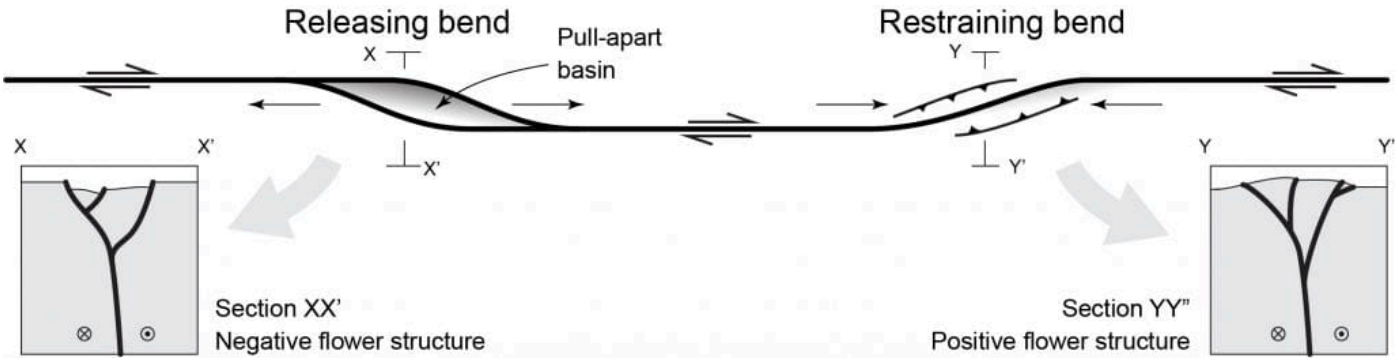
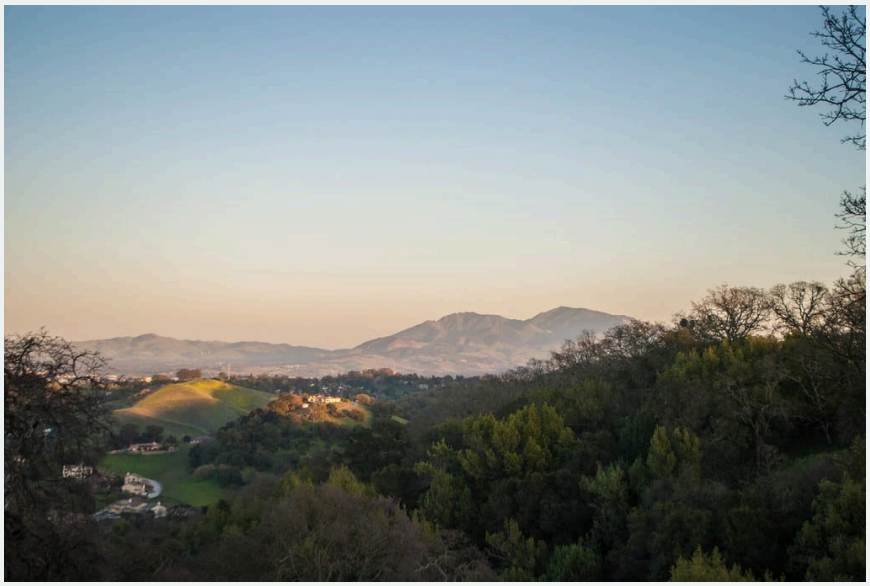


Figure 11.5.9: Releasing and restraining bends. Left: A releasing bend forms when a fault bends, creating localized areas of extension with a negative flower structure beneath it. This can form locally down-dropped blocks and features like pull-apart basins and sag ponds. Right: A restraining bend forms when a fault bends, creating an area of localized compression with a positive flower structure beneath it. This can form locally uplifted blocks and features like mountains, reverse faults, thrust faults, and anticlines. Strike-slip fault by John Waldron & Morgan Snyder, Open Education Alberta, is licensed under CC BY-NC.

Box: Mount Diablo

One of the most notable areas of recent uplift in the Coast Ranges is Mount Diablo, the highest peak in the Diablo Range (Box Figure 11.5.1). Rising 1,173 meters (3,849 feet) above sea level, Mount Diablo's south peak was selected as the initial point (where the Mount Diablo Base and Mount Diablo Meridian lines intersect) for cadastral surveys. It has since been used as the reference point for much of California and all of Nevada.



Box Figure 11.5.1: View of Mount Diablo in Contra Costa County looking south. "Mount Diablo" by Wayne Hsieh via Flickr is licensed under CC BY-NC.

Mount Diablo consists of typical Coast Range rocks: Franciscan Complex, Coast Range Ophiolite, and Great Valley Sequence rocks are all present. While these rocks initially formed below the surface of the ocean, today they form Mount Diablo's two peaks.

The actual uplift of Mount Diablo is geologically very recent, occurring only in the last 2 million years. Right lateral strike slip motion on the Calaveras and Clayton-Marsh Creek-Greenville faults on either side of the mountain contributed to the formation of a thrust fault beneath the mountain that continues to raise the mountain ever higher. The so-called Mount Diablo Thrust Fault also folded the layers above it into a large anticline.

Also unique to the vicinity of Mount Diablo is a very rare-in-California appearance of the organic sedimentary rock coal, which is found on the northern flanks of the mountain and was deposited between the Paleocene and Miocene (Box Figure 11.5.2). During this time, multiple changes in sea level occurred. During the third of these cycles, tectonic uplift caused the continental shelf to rise, forming shallow marshes. These marshes, in addition to the hot and humid climate of the time, led to the growth of marsh flora that would eventually be buried to form coal. This coal was discovered in 1859 and coal mining operations quickly began to supply coal to nearby San Francisco. These coal mines operated until the early 1900s until the small coal seams were depleted. The Black Diamond mines, named after the "black diamond" coal, were to this day the largest producer of coal in the state of California producing more than 400 million short tons of coal.



Box Figure 11.5.2: A dark seam of coal cutting through a mining shaft at the Hazel-Atlas mine. This work by Allison Jones is licensed under CC BY 4.0.

The coal here is interbedded with silica-rich sandstone. In the 1920s, a silica mine was started and sold to the Hazel-Atlas Glass Company which produced glass jars, bottles, and other glass items in Oakland. 1.8x 10^6 short tons of sand was recovered between the 1920s and the 1940s. Today, the Hazel-Atlas mine is maintained by East Bay Area Parks staff and can be visited on guided tours.

Not all of the Coast Ranges are so heavily influenced by the transform boundary. On its northward migration the Mendocino Triple Junction has yet to reach the Oregon border, leaving about 170 km of California Coast Ranges that have yet to be twisted and mangled by the San Andreas. The furthest northern Coast Ranges are part of the forearc of the Cascadia Subduction Zone, and as such have experienced somewhat different uplift processes, discussed in more detail in the chapter on the Klamath Mountains. But the grasp of the San Andreas is far reaching; in geologic time, the fight between ridge and trench is still ongoing, and the front seats to watch the action are now in Humboldt County.

Northern Coast Range Folding and Faulting

Near the Mendocino Junction, the Coast Range has been shaped by both convergent and transform plate motions. As the Juan de Fuca Plate (and the Gorda Plate) subducts beneath the North American Plate, it pushes against it, creating east-west compressional stress. Meanwhile, further south, the Pacific Plate slides against the North American Plate along the San Andreas fault. As it does so, it drags the edge of the North American Plate with it. This northward motion of southern and central California pushes against the northern part of the state, creating north-south compression. These two sources of compression combine, resulting in net northeast-southwest compression. This stress has caused the crust to crumple in a combination of folding and thrust faulting (see Geologic Structures and Seismology). The northwest-southeast striking thrust faults can be seen on the geologic map. The crest of the anticlines frequently form ridges and the synclines form valleys. On the coast, the uplifting anticlines are associated with features like sea cliffs, typical of an uplifting coastline, whereas the subsiding synclines are host to estuaries, lagoons and bays (see California's Coastline). These include the several Lagoons near Redwood National Park and the second largest bay in California, Humboldt Bay. Because it is one of the few parts of California that is tectonically subsiding (even as the surrounding region uplifts), Humboldt Bay is experiencing the fastest rate of sea level rise in the state.

Faulting in this region has not only contributed to the uplift of the anticlines and shaped the topography of the landscape, but also poses earthquake hazards. Although the biggest earthquake threat in this region lies offshore, crustal thrust faults within the North American Plate pose their own set of issues. The College of the Redwoods Eureka Campus was built in 1968, right along the Little Salmon Fault (before the fault was mapped by geologists). Many of the original buildings have now been demolished and new ones built in locations that comply with state laws regarding active faults (see California's Earthquakes).

References

1. *2006 Humboldt | Friends of the Pleistocene*. (n.d.). Retrieved September 13, 2024, from https://www.fop.cascadiageo.org/field-trips/pacific-cell-field-trips/2006-humboldt/
2. Ball, J. L. (2022). Stratigraphy and eruption history of maars in the Clear Lake Volcanic Field, California. *Frontiers in Earth Science*, *10*, 911129. https://doi.org/10.3389/feart.2022.911129
3. Coffey, G. L., Savage, H. M., Polissar, P. J., Cox, S. E., Hemming, S. R., Winckler, G., & Bradbury, K. K. (2022). History of earthquakes along the creeping section of the San Andreas fault, California, USA. *Geology*, *50*(4), 516–521. https://doi.org/10.1130/G49451.1
4. Patton, J., Williams, T., Anderson, J., & Leroy, T. (n.d.). *Tectonic land level changes and their contribution to sea-level rise, Humboldt Bay region, Northern California*.

This page titled 11.5: Cenozoic Events is shared under a CC BY-NC 4.0 license and was authored, remixed, and/or curated by Allison Jones & Steven Newton.

11.6: Quaternary Events

Recent Times

The Quaternary refers to rocks 2.58 Ma to today. Almost all of the Quaternary consists of the Pleistocene Epoch, with the exception of the last 11.7 ka, which is termed the Holocene Epoch. The Holocene can be understood in human terms as the time after the last Ice Age, corresponding to when agriculture, cities, laws, warfare, and reality TV shows developed. A proposed new division, the "Anthropocene," would demarcate human influence on the globe; however, there is to date no official agreement about how to delineate the Anthropocene from the Holocene.

The last part of our story of the development of the Coast Ranges involves something very cool and something not quite so good.

Formation of San Francisco Bay

At the beginning of this chapter, we talked about dividing the northern and southern sections of the Coast Ranges by San Francisco Bay, which is one of the few deep-water ports in the western US, and became the launching point for most of the gold prospectors who flooded into California after the gold discovery in 1848.

Today on weekdays hundreds of thousands of commuters cross numerous bridges over the waters of San Francisco Bay, perhaps looking wistfully across its undulating surface as they sit frozen in universal gridlocked traffic. The vast bay looks as if it's always been there. The reality is that San Francisco Bay only recently assumed its current shape, and the earliest peoples in the region saw a landscape completely unrecognizable today.

During the last Ice Age, vast quantities of evaporated water stayed stuck on land in the form of glacial ice. Tremendous ice sheets covered most of what is today Canada, and in a few places crept south as far as Olympia, Washington and New York City, which is why Central Park has such distinct glaciated features (but that's a story for another book). Because so much water was locked up in glacial ice but evaporation continued, sea level dropped precipitously during the last Ice Age: over 100 meters lower than its present level.

About eighteen thousand years ago, the climate began to come out of the Ice Age and all this land-based ice began to melt, surging back into the oceans steadily through streams and rivers, and on occasion, as in the Great Missoula Floods, bursting downhill towards the oceans in titanic surges of water. By about eight thousand years ago, sea level was close to where it is today (or at least, where it was a few decades ago).

What does this mean for San Francisco Bay? As astounding as it is to contemplate, for all except the last few thousand years, you could have walked across a broad, relatively flat valley festooned with redwood trees and ferns, from San Francisco to Berkeley to San Jose to Marin. *There simply was no San Francisco Bay*. At the lowest points, a significant river drained toward the ocean, and had you followed it, you could have walked several days on landscapes today underwater until you reached the Farallon Islands (Figure 11.6.1), now far out to sea and barely visible on a clear day.

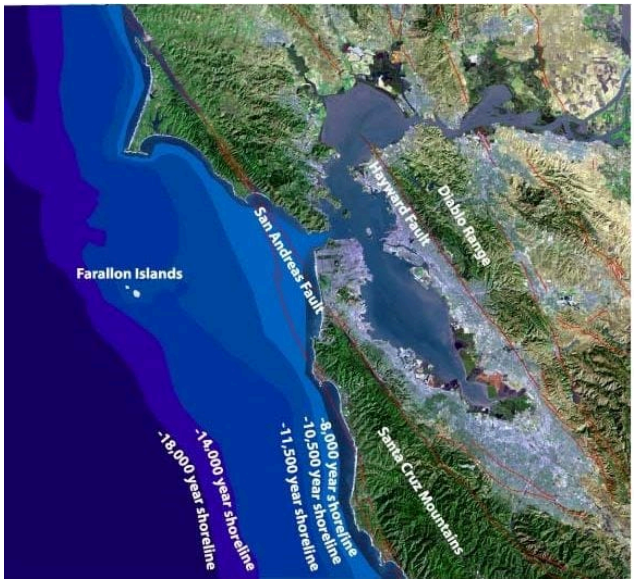


Figure 11.6.1: Satellite image of San Francisco Bay Area showing major faults (red lines), geographic features, and shoreline positions after the last glacial maximum. From 18,000-11,500 years ago, you could have walked to the Farallon Islands. "Shoreline Change Since the Last Glacial Maximum" by the USGS is in the public domain. Access a detailed description.

When humans first came into North America and the San Francisco region, at least by fourteen thousand years ago (though there are credible recent claims for dates thousands of years earlier), they experienced a landscape that would today be utterly unrecognizable. They no doubt left vestiges of their lives–shell mounds, discarded worked stones, burial sites. We don't find any of these today from fourteen thousand years ago; most of the archeological sites on land within the current San Francisco Bay date from a mere two thousand years ago. But there was a California we can hardly even imagine–bursting with all manner of life. And that's where the tragedy comes in.

A Menagerie of Extinction

An old ad campaign for the dairy company Berkeley Farms played on the seeming contradiction of farming within the densely urbanized environment near UC Berkeley by asking, "Cows in Berkeley? Mooo!" For those peoples who first explored this ancient California–from the damp forests of the north to the salty, wave-kissed coasts to the parched deserts of the south–the question might have been, "Saber-toothed cats in Berkeley? Run for your lives!"

Smilodon fatalis, the saber-toothed cat, and our official state fossil, existed in California at the same time as the earliest human migrants, forming a rather disconcerting welcoming committee. (It should be noted that *Smilodon* was not a tiger, as they are sometimes mistakenly named, and not closely related to modern big cats.) Though there is no direct evidence of *Smilodon* predation on humans, and humans range on the smaller side of typical *Smilodon* prey, it is reasonable to think that these fierce carnivores greeted the arrival of groups of vulnerable two-legged meat as an agreeable variation on their usual fare.



Figure 11.6.1: Painting of the Saber-toothed cat (*Smilodon fatalis*), which lived in North America until 13,000 years ago. *Smilodon fatalis* derives from the Greek word "blade" "chisel" or "tooth." "Smilodon" by Charles R. Knight is in the public domain.

Saber-toothed cats were not the only large predator encountered by early humans. The short-faced bear (*Arctodus simus*) would have been a uniquely terrifying animal to encounter, standing at over 3 meters and weighing in over 600 kg. An averaged sized human would have looked directly at their eye level as the bears approached.

Many other species flourished in Pleistocene California: dire wolves, camels, bison, horses, sloths. Fossils of all these were excavated and are currently displayed at the La Brea Tar Pits museum in Los Angeles.

Perhaps most magnificently of all, the Columbian mammoth (*Mammuthus columbi*) strolled the plains of the Golden State. These massive proboscideans clocked in at over 4 meters at the shoulder, far larger than modern elephants, and they exhibited elaborately curved tusks much longer than any living relative. While many people have heard of Wooly mammoths, we didn't have them here, as they existed at much higher latitudes than California. In our state, Columbian mammoths roamed in great herds, perhaps led in a matriarchal group, as today's elephants exist. They used to be quite common; a Columbian mammoth fossil has even been discovered on the campus grounds of a California community college, Las Positas College in Livermore.

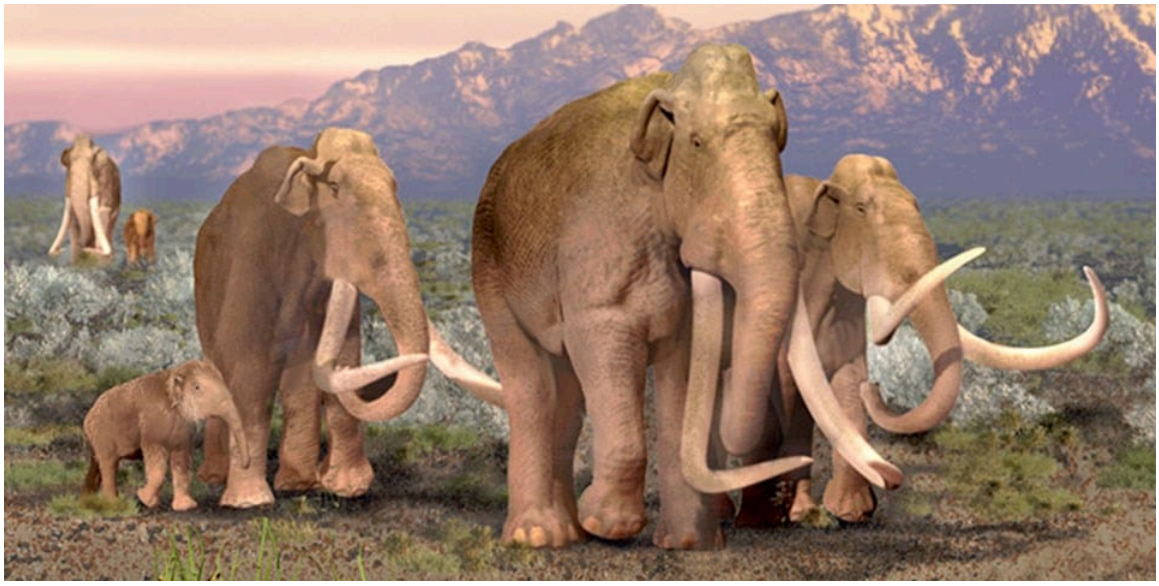


Figure 11.6.1: Digital illustration of the Columbian mammoth (*Mammuthus columbi*), which roamed California during the Pleistocene. "Mammoth" by the National Park Service is in the public domain.

So why don't we have elephants and camels and bison and giant elephant-like animals in California today? When one examines

the end dates for most of the animals described above, the number 12,000 years ago keeps coming up. That seemed to be an abrupt break in the type of species living in California.

This decline can certainly be attributed to climatic changes. If conditions change an animal's food source, they tend to go extinct. But because of the overlapping timing of human settlement in this continent, there is another factor possible here: we killed them. Elsewhere in the United States, there exists clear evidence of human butchering of mammoths. It is not unreasonable to think that clever, motivated humans found ways to hunt the animals listed above. Would that have been enough to drive all these California species extinct in such a short time? Perhaps we should ask the passenger pigeon (*Ectopistes migratorius*), which used to darken American skies in the billions in the nineteenth century, now remembered only by a few stuffed museum specimens.

A Note

At this point, we must acknowledge that the sections above have been brief and by necessity have left out a great deal of detail. Especially missing from the above sections is a full sense of the scope of unsettled issues and controversial questions. Much is unknown, or poorly known, and this provides fertile ground for geologic researchers to investigate further, and to disagree with each other using evolving evidence. Certainly a great deal of what is conjectured above will, in time, be shown to not be aligned with new evidence and will be revised.

Introductory science students might see such large gaps in knowledge as a sign of scientific weakness, but such a view profoundly misunderstands what science is. Science is not a list of facts to be memorized. Rather, science is better understood as a series of critical questions about issues not yet resolved. To recall Plutarch, a mind should be seen not as a vessel to be filled, but as a fire to be kindled.

In science nothing is ever *proven*. Rather, incorrect ideas can be shown to be incompatible with evidence; in other words, science is a systematic process to falsify what does not fit existing data. With new and evolving instruments and techniques, data can change, and therefore so can the conclusions. Having significant parts of the story of California geology unknown or not yet resolved is a sign of strength, not a failing. If we already knew all the answers, it would be boring.

This page titled 11.6: Quaternary Events is shared under a CC BY-NC 4.0 license and was authored, remixed, and/or curated by Allison Jones & Steven Newton.

11.7: Representative Coast Range Rocks

Serpentinite

California's state rock, serpentinite, is composed of minerals belonging to the serpentine group and is commonly found in the Coast Ranges. Forming from the metamorphism of mafic and ultramafic igneous rocks, serpentinite often appears green and scaly like a serpent for which it is named.

In some parts of the Coast Ranges, serpentinite outcomes come in a block-in-matrix form. In these locations, coherent blocks of metamorphosed mafic rocks are surrounded by serpentinite that appears to have accommodated slip around the blocks. This is visible in places like Ring Mountain in Marin County. Ring Mountain is also home to the only Mariposa Lily Population (see Minerals and Rocks).



Figure 11.7.1: Turtle rock on Ring Mountain in Marin County is a block of blueschist suspended in a matrix of serpentinite, here covered in grass. "Turtle Rock blueschist block on Ring Mountain" by Christierowe via Wikimedia Commons is licensed under CC BY-SA 4.0.

Eclogite

Eclogite is a unique and rare metamorphic rock that represents the highest set of temperatures and pressures (Figure 11.7.2). For eclogite to form, the atomic ingredients in the protolith basalt reorganize to form distinctive red- and green-colored minerals: the rich green of omphacite (a kind of pyroxene, see Minerals and Rocks), and the cranberry-red of garnet (the variety called pyrope). Eclogites are astonishingly dense, which is perhaps not surprising considering they form to be stable at pressures corresponding to depths of at least 50 km. Eclogite can be found in the Francsican complex in places like Ring Mountain in Marin County and along the coast near the town of Jenner.

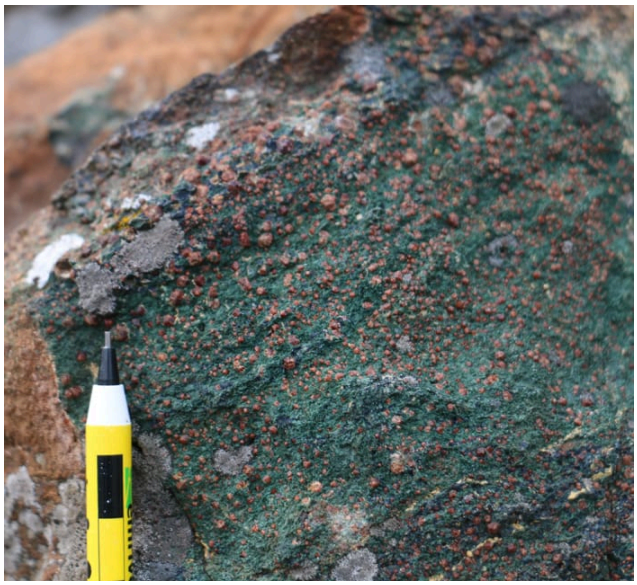


Figure 11.7.2: Eclogite consists of the green mineral omphacite (a variety of pyroxene) and prominent red pyrope (a variety of garnet). This outcrop appears on Ring Mountain, near Tiburon, California. "Eclogite" by Callan Bentley is licensed under CC BY-NC 4.0.

Blueschist

Blueschist is the rock that results when basaltic protoliths are driven deeper into the subduction zone, to ~35 to 50 km depth (Figure 11.7.3). The rate of subduction is greater than the rate of thermal equilibration; as a result, the subducted basalt soon finds itself at conditions where the pressure is quite high, but the temperature is still relatively cold. These are the conditions at which the minerals lawsonite and glaucophane form. Metabasalts in the Angel Island Terrane, one of the terranes of Franciscan, have seen these conditions, and where basalt was present, it has been recrystallized to make blueschist. Outcrops of these unique blueschists can be found on Angel Island in San Francisco Bay.

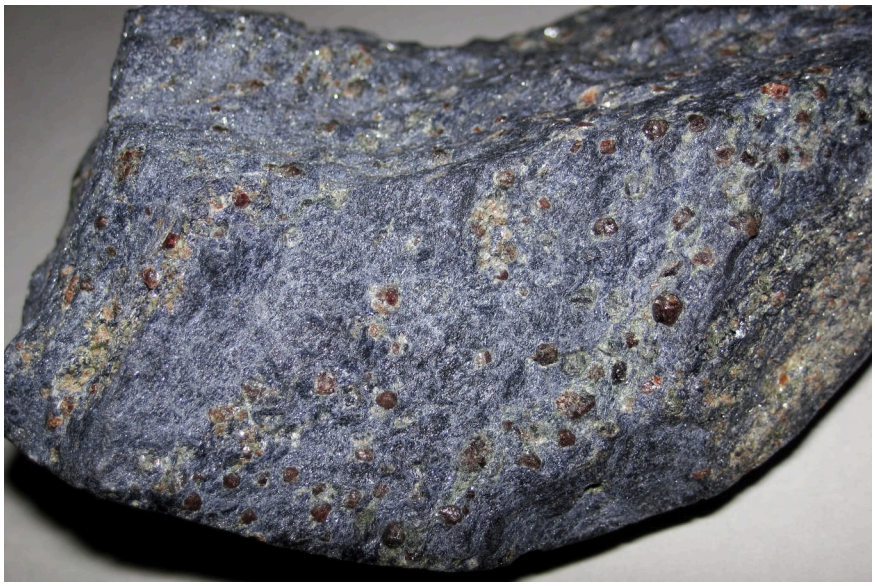


Figure 11.7.3: Blueschist with garnets from Ward Creek, western Sonoma County, California, USA likely derived from Mesozoic-aged Franciscan Complex. Approximately 8 cm across. "Garnetiferous blueschist (Ward Creek, Sonoma County, California, USA) 2" by James St. John via Flickr is licensed under CC BY.

Radiolarian Chert

Chert is a dense, fine-grained chemical sedimentary rock that is composed of silica. While chert can be formed by a few different

processes, radiolarian chert specifically is formed from an accumulation of tiny (0.5-1 mm) silica shells or “tests” of marine plankton called Radiolaria on the ocean floor (Figure 11.7.4). Franciscan chert contains some tropical and subtropical forms of Radiolaria suggesting that the sediments formed much further south than their present day location. The Franciscan chert is often called ribbon chert, named for its hard silica-rich chert beds separated by soft, clay-rich shale beds. Franciscan chert is best viewed at the Marin Headlands in San Francisco, but it can also be found in other parts of the Coast Ranges such as on Mount Diablo in the East Bay Area (Figure 11.7.5) and along the coastline in Redwood National Park.

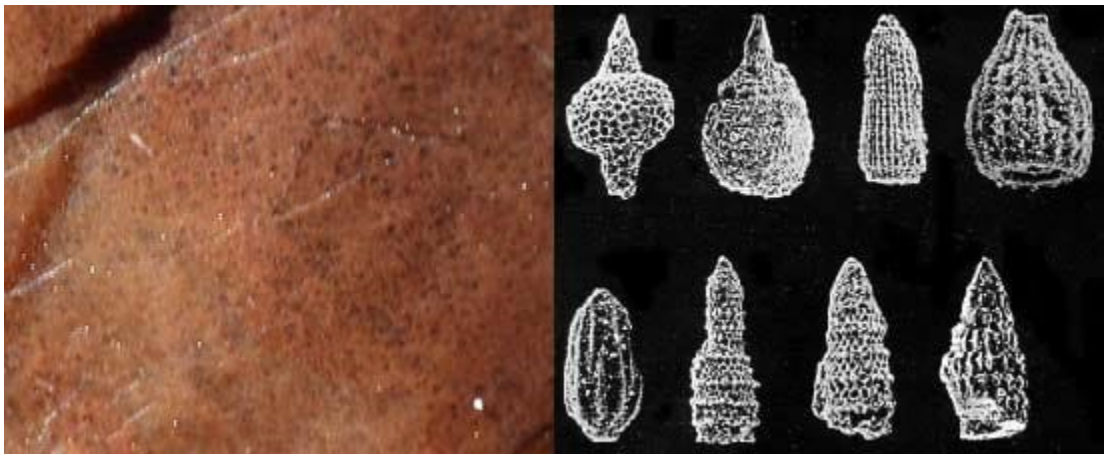


Figure 11.7.4: A magnified piece of chert shows radiolaria as small dark spheres about the size of a pencil point (left), and a scanning electron microscope image of extracted radiolaria (right). "Radiolarian chert" by the National Park Service Public Domain.

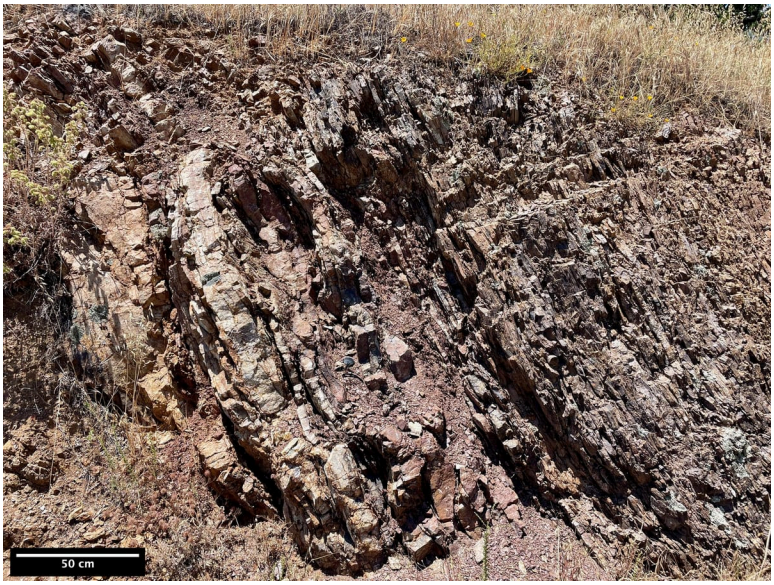


Figure 11.7.5: Steeply dipping beds of radiolarian red chert of the Franciscan Complex on Mount Diablo. This is one of many locations in the Coast Ranges where Franciscan Complex cherts outcrop. "Franciscan Complex Chert on Mount Diablo (with scale bar)" by Allison Jones is licensed under CC BY-NC 4.0

Greywacke Sandstone

Approximately 90% of the Franciscan Complex is composed of greywacke, an immature, poorly sorted sandstone containing grains of angular rock fragments. It is often called a "dirty sandstone" and typically forms as a result of turbid, mud- and sand-laden underwater landslides, called turbidity flows, which occur along steep continental slopes associated with subduction zones (Figure 11.7.6). These flows often result in marine sediments that grade from coarse in size at the bottom to fine at the top. Once lithified, these rocks are known as turbidites.

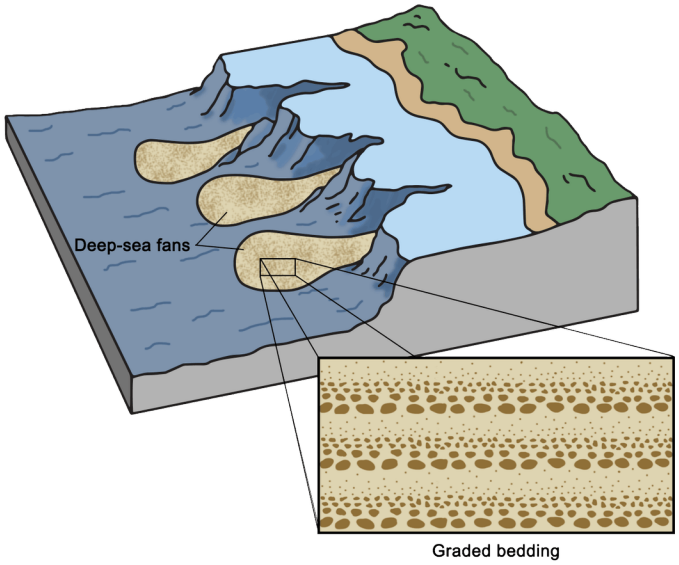


Figure 11.7.6: Sediment-laden turbidity currents flow from a continental slope into the deep ocean, forming deep-sea fans. These fans deposit graded beds, which are characterized by a decrease in grain size from bottom to top. "Turbidity Current" by Elizabeth J. Hermsen and Jonathan R. Hendricks, a derivative from the original, is licensed under CC BY-NC-SA 4.0.

Greywacke sandstones of the Franciscan sometimes contain clam and ammonites from the Jurassic and Cretaceous, providing ages for the Franciscan. Outcrops of Francsican graywacke are common at Baker Beach at the southern end of the Golden Gate Bridge (Figure 11.7.7), the Cliff House in San Francisco, and Salt Point State Park.



Figure 11.7.7: Graywacke sandstone exposed at Baker Beach in the Presidio of San Francisco displays small holes, a type of weathering called tafoni, which is typical for this type of rock. "Baker Beach Graywacke" by the National Park Service is in the public domain.

Graywacke in the Coast Ranges is not exclusive to the Franciscan: Greywacke also occurs in the older Great Valley Group. Graded greywacke of the Great Valley Group can be seen at Lake Berryessa (see Great Valley Sequence).

This page titled 11.7: Representative Coast Range Rocks is shared under a CC BY-NC 4.0 license and was authored, remixed, and/or curated by Allison Jones & Steven Newton.

11.8: Chapter Summary

11.1: A Complicated Land

- The Coast Ranges are defined by tectonic complexity. They lie along the boundary between the North American and Pacific plates, shaping their dynamic geology.
- Plate tectonic theory is essential to understanding the Coast Ranges. Before the theory was developed, geologists could describe the region's features but not explain why different rock types were juxtaposed.
- The Coast Ranges contain diverse and seemingly contradictory rock formations. Rocks such as pillow basalts, eclogites, and unaltered sedimentary rocks are found together due to tectonic accretion.
- Dating rock assemblages in the Coast Ranges is challenging. Many rocks did not originally form in California but were transported and altered by tectonic forces, making it difficult to assign a single "age" to an assemblage.
- The Coast Ranges lack simple, layered rock sequences. Unlike the Grand Canyon, where sedimentary layers are neatly stacked, Coast Range rocks are faulted, folded, and jumbled together.

11.2: The Coast Range Ophiolite

- The Coast Range Ophiolite is a relic of an ancient ocean floor. It's a mix of mantle rock, oceanic crust, and deep-sea sediments, all jammed together and stranded on land by tectonic forces.
- Most ophiolites come from mid-ocean ridges, but the Coast Range Ophiolite is likely from a forearc setting, meaning it formed near a subduction zone, where one plate was diving under another.
- Subduction gave it a one-way ticket to California. As oceanic crust was being shoved down into the mantle, bits of it were scraped off and plastered onto the growing edge of North America, creating the Coast Range Ophiolite.
- Over millions of years, this once-deep-sea rock got fractured, metamorphosed, and chemically altered, transforming parts of it into serpentinite, California's state rock.
- The Coast Range Ophiolite is old, but figuring out exactly how old is tricky. The best estimates place it at around 165 to 175 million years old, making it Jurassic in age.

11.3: The Great Valley Sequence

- The Great Valley Sequence consists of marine sedimentary rocks deposited in a forearc basin.
- These sediments were eroded from the Sierra Nevada volcanic arc and transported westward.
- Much of the sediment was deposited by turbidity currents, forming turbidites.
- The sequence records deep marine environments including submarine fans and channels.
- It lies structurally between the Sierra Nevada batholith and the Franciscan Complex.
- The rocks are now exposed along the western edge of the Great Valley, where they have been uplifted and folded.

11.4: The Franciscan Complex

- The Franciscan Complex formed in a subduction zone at California's ancient continental margin.
- It includes a mix of oceanic crust, seafloor sediments, and rocks scraped from the subducting plate.
- Rocks were subjected to intense pressure and low temperatures, producing metamorphic rocks like blueschist.
- Chert, greenstone, greywacke, and serpentinite are common rock types in the Franciscan.
- Tectonic forces created a chaotic mixture of rock types, sometimes called a mélange.
- Fossils of deep-sea organisms, like radiolaria, are found in chert layers.

11.5: Cenozoic Events

- The subduction of the Farallon Plate ended during the Cenozoic as the Pacific-Farallon Ridge was consumed.
- A transform boundary developed between the Pacific and North American Plates, creating the San Andreas Fault system.
- New faults formed inland from the plate boundary, including the Hayward and Calaveras Faults.

- The Coast Ranges experienced significant uplift beginning in the Miocene and continuing into the present.
- Volcanic activity shifted inland and northward as subduction ended.
- Ongoing plate movement continues to cause earthquakes and shape the landscape of the Coast Ranges.

11.6: Quaternary Events

- The Quaternary period includes the Pleistocene, Holocene, and potentially the Anthropocene epochs.
- Ice Age climate fluctuations influenced sea level, erosion, and ecosystems in the Coast Ranges.
- The region hosted large Ice Age mammals like Columbian mammoths and saber-toothed cats. Many of these species went extinct at the end of the Pleistocene, possibly due to climate change and human activity.
- The Holocene epoch saw the development of modern climates and ecosystems.
- Some scientists propose the Anthropocene to mark significant human impact on Earth's systems.

11.7: Representative Coast Range Rocks

- The California Coast Ranges are an exceptional place to view a myriad of rock types including: Serpentinite, radiolarian chert, greywacke, blueschist, and eclogite.
- Serpentinite is California’s state rock and forms through metamorphism of mantle rocks at subduction zones.
- Radiolarian chert forms from the accumulation of silica-based microfossils on the deep ocean floor.
- Greywacke sandstone is a poorly sorted sedimentary rock common in the Franciscan Complex.
- Greenstone is metamorphosed basalt, often altered by low-grade metamorphism in subduction settings.
- Blueschist forms under high-pressure, low-temperature conditions and contains blue minerals like glaucophane.
- Eclogite is a high-pressure metamorphic rock formed deeper in subduction zones, less common at the surface.

This page titled 11.8: Chapter Summary is shared under a CC BY-NC 4.0 license and was authored, remixed, and/or curated by Allison Jones & Steven Newton.

11.9: Detailed Figure Descriptions

Figure 11.1 Location of the Coast Ranges Province of California

The Coast Ranges province spans 400 miles, from Humboldt south to Santa Barbara. The province has two distinct regions. The Northern Coast Ranges run parallel to the coast from the Oregon border south to the northern San Francisco Bay Area. The Southern Coast Ranges run parallel along the coast from the eastern San Francisco Bay Area south to Santa Barbara.

Figure 11.1.1 Geology of the Coast Ranges

This geologic map of the California Coast Ranges depicts various rock units, faults, and geologic time periods. A legend on the right explains the different colors representing distinct rock types and ages. A small inset map in the bottom left shows California with a black rectangle highlighting the Coast Ranges region.

- The main map displays the Coast Ranges with different colors scattered throughout, corresponding to geologic units, indicating rock types and ages.
- Fault lines occur throughout the region and are represented by dashed lines for subsurface faults and solid lines for surface faults.
- The map extends from northern to southern California, showing major geological features and formations.

The legend categorizes the geologic units by age and rock type:

Cenozoic (youngest rocks)

- Quaternary surficial deposits
  - Along the immediate coastline of California
  - In river valleys and floodplains, including:
    - Salinas Valley
    - Russian River valley
    - Santa Clara Valley
  - In coastal lowlands and alluvial basins
  - Especially common near San Francisco Bay, Monterey Bay, and southern coastal plains
- Quaternary and Neogene non-marine deposits
  - Interior valleys of the Coast Ranges
  - Foothills east of major coastal mountains
  - Parts of:
    - Salinas Valley margins
    - Southern Coast Ranges near Santa Barbara and Ventura
- Cenozoic volcanic rocks
  - Northern Coast Ranges, especially:
    - Clear Lake volcanic field
    - North of San Francisco Bay
  - Small, scattered patches elsewhere in the northern map area
- Neogene and Paleogene sedimentary rocks
  - Widespread throughout the central and southern Coast Ranges
  - Large belts:
    - West of the San Andreas Fault
    - Between coastal areas and interior valleys
  - Prominent in:
    - Santa Cruz Mountains
    - Central Coast near Big Sur
    - Southern Coast Ranges north of Los Angeles Basin

Mesozoic

- Cretaceous sedimentary rocks
  - Scattered belts mainly in the central Coast Ranges
  - Often adjacent to Franciscan Complex rocks
  - Common in fault-bounded slivers near major faults
- Franciscan Complex (sedimentary and metamorphic rocks)
  - Extensive belt along the western side of the Coast Ranges
  - Dominant unit in:
    - Northern Coast Ranges
    - West of the San Andreas Fault
  - Continues discontinuously from northern California southward
- Granitic igneous rocks (mainly Mesozoic age)
  - Limited and isolated bodies within the Coast Ranges
  - Most visible in:
    - Southern Coast Ranges
    - Near Santa Barbara and Ventura areas
  - Much less extensive than in the Sierra Nevada (shown only in inset context)
- Serpentinite and other ultramafic rocks
  - Narrow, linear bodies scattered throughout the Coast Ranges
  - Commonly:
    - Along major fault zones
    - Near the San Andreas Fault system
  - Especially visible in central California
- Mesozoic metamorphic and sedimentary rocks
  - Smaller belts interspersed among Franciscan and Cretaceous units
  - Mostly in the central and southern Coast Ranges
  - Often fault-bounded

Paleozoic

- Paleozoic sedimentary and metamorphic rocks
  - Very limited exposures
  - Mostly in the southern Coast Ranges
  - Appear as small, isolated patches

Precambian (oldest rocks)

- Pre-Cambrian rocks
  - Extremely rare and very small exposures
  - Isolated locations in the southernmost Coast Ranges

Figure 11.2.1 Cross section of the Mesozoic active margin of California

This diagram illustrates a cross-section of the Coast Range Ophiolite and Franciscan Complex during the Mesozoic, highlighting major geologic features, faulting, and the relationship between tectonic units. It shows the subducting oceanic slab, various belts of the Franciscan Complex, and the overlying Great Valley Group.

Key Features:

- Subducting Oceanic Slab: Located at the base of the diagram, this region represents the oceanic plate sinking beneath North America.
- Franciscan Complex Belts (just above the Oceanic Slab):
  - Coastal Belt (lowest layer): A highly deformed zone above the subducting slab, consisting of mélange (a chaotic mix of rock types).
  - Central Belt Mélange (next layer): Another deformed rock unit, distinguished by its blocky, jumbled texture.

    - Eastern Belt (highest layer in this complex): Subdivided into the Pickett Peak and Yolla Bolly terranes, these rocks were deeply buried and metamorphosed before being uplifted.
- Coast Range Ophiolite & Tehama-Colusa Mélange (next layer): A section of ancient oceanic crust that was scraped off the subducting slab and now forms part of the Coast Ranges.
- Great Valley Group (highest layerr): Overlies the Coast Range Ophiolite and represents sediments deposited in the ancient forearc basin.
- Coast Range Fault: A significant fault separating the Great Valley Group from the Franciscan Complex, marking a major tectonic boundary.

This cross-section helps illustrate how subduction and accretion have shaped the Coast Ranges over millions of years, with different belts representing materials scraped from the oceanic plate and stacked onto North America.

Figure 11.2.2 Location of the Coast Range Ophiolite

This figure shows the location of the Coast Range ophiolite. The Coast Range ophiolite is located in a narrow north-south trending band along the eastern edge of the northern Coast Ranges, where the Coast Ranges meet the Central Valley (it is not present where the Coast Ranges directly abut the Klamath Mountains). The Great Valley Group parallels this band to the east. There are fragments of Coast Range Ophiolite in some areas west of the main band, as well as fragments in both the eastern and western portions of the southern Coast Ranges.

The map divides California into different geologic or tectonic origins.

- Accreted terranes (western and northwestern California)
    - In the northwestern corner, large areas are labeled “Accreted terranes.”
    - These represent crustal fragments that formed elsewhere and were later attached to North America.
    - The Klamath terranes appear in the far north, shown with a distinct line pattern.
    - These units dominate the geology near the Oregon border and the far northern Coast Ranges.
- Franciscan accretionary complex
    - This complex forms a long, narrow belt along much of coastal California and is subdivided into three belts: Eastern belt, Central belt, and Coastal belt
    - These belts run roughly northwest–southeast, parallel to the coastline, and represent rocks scraped off a subducting oceanic plate during long-term subduction along the continental margin.
- Coast Range ophiolite
    - The Coast Range ophiolite occurs in narrow, discontinuous slices.
    - These rocks represent ancient oceanic crust and upper mantle that were emplaced onto the continent.
    - They commonly lie between the Franciscan Complex and the Great Valley Group.
- Great Valley Group
    - The Great Valley Group forms a long, continuous band through central California.
    - This unit represents thick marine sedimentary rocks deposited in a forearc basin.
    - The map explicitly labels this region as the “Forearc basin.”
    - It lies between the Franciscan rocks to the west and the Sierra Nevada to the east.
- Sierra Nevada
    - The Sierra Nevada is shown on the eastern side of the map with a light, patterned fill.
    - This region represents a large continental magmatic arc, formed by long-lived subduction-related volcanism and plutonism.
    - It forms the eastern boundary of the Great Valley basin.
- Salinia block
    - The Salinia terrane appears as a long, narrow block along the central California coast, shown with a cross pattern.
    - It is offset from the Sierra Nevada and interpreted as a displaced fragment of continental crust.
    - The block is bounded by major faults and contrasts sharply with surrounding accretionary rocks.
- Modoc Plateau
    - In the northeastern corner, the Modoc Plateau is shown with a dark patterned fill.
    - This region represents volcanic and extensional geology, distinct from the accretionary and subduction-related rocks to the west.
- Fault systems
    - The San Andreas Fault (SAF) is prominently marked as a thick black line running northwest–southeast through coastal and central California.
    - It separates the Pacific Plate (to the west) from the North American Plate (to the east).

- Other fault-related labels appear, including SF (San Francisco area) and additional structural abbreviations marking fault-bounded regions.

Figure 11.2.4 Ophiolite sequence

Marine sediment and rocks are underlain by pillow basalts in relatively narrow bands. Below, sheeted dikes and sills (diabase) are underlain by a deep layer of gabbro. Just below this, we reach the earth's crust, with gabbro and ultramafic cumulates. Below this lie the ultramafic rocks of the mantle. This entire sequence can reach up to 6 miles in depth.

Figure 11.3.1 The Great Valley Sequence

The Farallon Plate subducts beneath the North American Plate, forming key geologic features of California: the Coast Range, Great Valley, and Sierra Nevada.

Key Features and Processes

- Mid-Ocean Ridge: Located on the left, where new oceanic crust forms as the Pacific Plate and Farallon Plate move apart.
- Subduction Zone: The Farallon Plate descends beneath the North American Plate. As it sinks, water is released, causing melting in the mantle.
- Geologic Provinces:
  - Coast Range: Formed from uplifted ocean sediments scraped off the subducting plate in an accretionary wedge.
  - Great Valley: A low-lying region, the forearc basin, filled with sediments eroded from nearby mountains.
  - Sierra Nevada: A chain of volcanoes, or volcanic arc, formed from rising magma produced by melting of the subducting plate. Cooled magma beneath the volcanic arc form granite rocks, which later uplift to form the Sierra Nevada batholith.

Tectonic Motion

- The Pacific Plate and Farallon Plate move apart at the Mid-Ocean Ridge.
- The Farallon Plate subducts beneath North America, driving volcanic activity and mountain-building processes.

Figure 11.4.2 Cross section of the West Coast of North America at about 100 Ma

As the ocean crust and lithosphere thrust under the North American plate, pillow basalts, chert, and limestone-capped seamounts were scraped off and mixed with graywacke sandstone and shale shed from the continent, to create the Franciscan. In addition, as the lithosphere continued to move beneath the North American plate, serpentinite formed at the upper mantle. All of these elements pushed up against the Sierra Arc, which has a core of granite.

Accessibility Guidance

The process illustrated in this diagram is described within the text. However, the process is difficult to understand without a diagram. Some users may therefore benefit from the tactile image, Continental Subduction Zone, which includes an accretionary wedge.

Figure 11.5.1 The tectonic setting of the west coast of North America in the Mesozoic

The Farallon plate sat between the continental North American plate to the east, and the Pacific plate to the west. The Farallon and Pacific plates are labeled "oceanic lithosphere" on the map, while the North American plate is labeled "continental lithosphere." The boundary between the Pacific and Farallon plates was divergent (a spreading center). The boundary between the Farallon and the North American place was convergent (a subduction zone).

Figure 11.5.3 Map of the San Andreas Fault showing locked and creeping sections

The San Andreas Fault runs along the coastline north of San Francisco and moves inland just north of Monterey Bay. It then proceeds in a southeast direction, terminating at the Salton Sea. As discussed in the text, the northern and southern sections of the fault are locked. Between the locked segments, from San Juan Bautista to Parkfield, the fault is creeping. Key landmarks shown along the fault are San Francisco in the northern segment and Los Angeles in the southern segment. The San Andreas Fault Observatory at Depth (SAFOD), a USGS project, is located in the creeping zone, near Parkfield.

Figure 11.5.4 UC Berkeley Memorial Stadium and the Hayward Fault (Aerial and LiDAR Views)

- This figure shows two views of the UC Berkeley Memorial Stadium and the surrounding neighborhood. One view is an aerial photograph, and the other is a LiDAR image that highlights differences in ground elevation. In both images, the path of the Hayward Fault is indicated, with a solid line marking the portion of the fault whose position is well-established and a dashed line marking where the fault trace is inferred.

The stadium was constructed directly across the Hayward Fault. The fault runs lengthwise through the seating bowl and divides the stadium into two structural halves, with each half located on opposite sides of the fault. Because the Hayward Fault here experiences primarily aseismic creep, the two sides of the ground slowly slide past one another over time. As a result, the eastern and western halves of the stadium are gradually shifted out of alignment. This ongoing movement causes cracks, foundation separation, and deformation in stadium walls and seating sections.

In the surrounding neighborhood, the same slow fault movement also displaces streets, retaining walls, and building foundations. The LiDAR image highlights subtle offset landforms that are not easily visible in regular photographs.

Figure 11.5.7 Schematic map of Northern California

This schematic map of northern California illustrates several volcanic fields, major faults, and the changing position of the Mendocino Triple Junction over the past 12 million years.

The volcanic fields are shown as separate geographic clusters, each labeled with its name and its approximate age range. From southeast to northwest, the volcanic fields shown are:

- Quien Sabe Volcanic Field (~12 Ma),
- Berkeley Hills Volcanic Field (~10 Ma)
- Sonoma Volcanic Field (~7-10 Ma)
- Clear Lake Volcanic Field (4-8 Ma)

The map also shows several major right-lateral strike-slip faults that are part of the San Andreas Fault system. The volcanic fields get progressively younger in the direction of the migrating Mendocino Triple Junction, which is marked at several past positions spaced along the coastline.

The displacement of volcanic units along the fault system indicates that parts of these volcanic fields have been offset by tens to hundreds of kilometers over time. The figure illustrates the link between plate boundary evolution, fault motion, and volcanic activity in the Coast Ranges during the Cenozoic.

Figure 11.6.1 Satellite image of San Francisco Bay Area

This satellite image of the San Francisco Bay Area highlights the region's major faults, mountain ranges, and paleoshorelines—past positions of the coastline after the Last Glacial Maximum (LGM). The image shows how significantly sea level has risen over the past 18,000 years and contextualizes California's dynamic coastline and tectonic setting.

Geographic Features

- The San Francisco Bay Area is shown in high-resolution satellite imagery, including the cities around the San Francisco Bay, Diablo Range to the northeast, and Santa Cruz Mountains to the southwest.
- The Pacific Ocean lies to the west, and the San Francisco Bay is central in the image.
- Farallon Islands are labeled offshore to the west, and were accessible on foot between 11,500 and 14,000 years ago
- The San Andreas Fault runs offshore parallel to the coast.
- The Hayward Fault runs through the East Bay hills near Oakland and Berkeley.

Paleoshorelines

- The map includes labeled shoreline positions representing times when sea levels were lower due to glacial ice storage:
  - ~18,000 years ago (farthest west)
  - ~14,000 years ago
  - ~11,500 years ago
  - ~10,500 years ago
  - ~8,000 years ago (closest to the modern shoreline)
- These zones are represented as nested, semi-transparent colored bands extending progressively farther offshore with increasing age.

This page titled 11.9: Detailed Figure Descriptions is shared under a CC BY-NC 4.0 license and was authored, remixed, and/or curated by Allison Jones & Steven Newton.

12: GREAT VALLEY

Introduction to the Great Valley

The geologic history of the Great Valley of California (Figure 12.1) is a fascinating story that spans millions of years. The valley's formation can be traced back to the tectonic forces that shaped the region. It all began with the subduction of the Farallon Plate beneath the North American Plate, which initiated the uplift of the Coast Ranges and the creation of a deep basin, known as the Great Valley. Over time, sedimentary rocks, eroded from the surrounding mountains, accumulated in the basin.

Around 20 million years ago, volcanic activity associated with the Cascades Range started to deposit ash and lava flows in the region. These volcanic materials, along with the continued sedimentation, contributed to the filling of the Great Valley. Subsequent tectonic activity, including faulting and folding, further shaped the valley's landscape.

Approximately 2.5 million years ago, the first of several glacial episodes occurred, affecting the region. The advancing and retreating glaciers modified the topography, carving out valleys and leaving behind moraines and other glacial deposits.

As the last Glacial Maximum ended 18,000 years ago, the valley experienced a period of increased volcanic activity, which resulted in the formation of volcanic cones and lava domes, and volcanic lava flows that came into the valley, oftentimes following existing riverbeds formed by glacial melt and tectonic uplift. This made for a true dance of fire and ice.

More recently, in the past several thousand years, the Great Valley has been shaped by the meandering of major rivers, such as the Sacramento and San Joaquin Rivers, which have deposited vast amounts of sediment and created fertile floodplain soils. Human activities, including agriculture and water management, have significantly influenced the landscape in the modern era.

Today, the Great Valley stands as a testament to the complex interplay of tectonic forces, volcanic activity, glaciation, and river processes. Its geologic history has played a crucial role in shaping the diverse ecosystems and agricultural productivity of this vast and dynamic region.



Figure 12.1: Location of the Great Valley Province of California. "The Great Valley Province of California" by Emily Wright, is licensed under CC-BY-NC / a derivative from the original work. Access a detailed description.

Learning Objectives

By the end of this chapter, you should be able to:

- Describe the Great Valley in terms of its rock types, age, and tectonic development.
- Assess the geologic hazards and risks associated with the Great Valley.
- Recall the major geologic units in this province as presented on a simplified map of California.
- Analyze the development and economic potential of natural resources within the Great Valley.
- Define how petroleum was formed and migrated to make the Great Valley's oil and gas fields.

12.1: Geomorphology and General Overview of the Great Valley Province
12.2: Geology of the Great Valley
12.3: Soil, Streams and Agriculture
12.4: Natural Hazards of the Great Valley Province
12.5: Natural Resources of the Great Valley
12.6: Chapter Summary
12.7: Detailed Figure Descriptions

This page titled 12: Great Valley is shared under a CC BY-NC 4.0 license and was authored, remixed, and/or curated by Cole Heap.

12.1: Geomorphology and General Overview of the Great Valley Province

Physiographic Properties and Characteristics of the Great Valley

California's Great Valley, often referred to as the Central Valley, is a 644 kilometer-long (400 mile) structural depression that stretches from the Transverse Range just south of Bakersfield northward to the Cascade Range (Figure 11.1). The Valley averages a width of 80 km (50 miles), that when combined with its length, makes for an area that is approximately 52,000 km^2 (20,000 square miles). This area has very little relief, making most of the Valley sit close to sea level.

Physiographically, the Great Valley can be divided into two large parts: the northern one-third is known as the Sacramento Valley and the southern two-thirds is known as the San Joaquin Valley. The San Joaquin Valley can be split further into the San Joaquin Basin and the Tulare Basin. The San Joaquin and Sacramento Valleys meet in the Delta area where the combined discharge of the Sacramento and San Joaquin Rivers flows through the Great Valley's one natural outlet, the Carquinez Strait, on its way to San Francisco Bay and the Pacific Ocean. Just east of the Delta, several streams issue from the Sierra Nevada into the valley and flow to the Delta in an area referred to as the Eastside Streams.

The San Joaquin Valley is a Mediterranean environment with long, hot, and dry summers and wet winters. It lies north of the Transverse Range and south of the Sacramento Valley. The San Joaquin Valley produces close to 13% of the United States' agricultural products which include grapes, raisins, cotton, almonds, citrus, and a plethora of vegetables. Each of these crops are water intensive, so pumping groundwater in the Great Valley for crop production is not uncommon.

The Great Valley is a large structural trough filled with sediments of Jurassic to Holocene age, as much as 20 km (12 miles) deep in the San Joaquin Valley, and as much as 9.6 km (6 miles) deep in the Sacramento Valley.

Sedimentary deposits filling the Valley vary somewhat depending on location. For example, the valley fill in the Sacramento Valley is predominantly fine-grained volcanic-derived sediments, although relatively coarse-grained deposits do occur along the river channels and the alluvial fans emanating from the Cascade Range and the northern Sierra Nevada.

In the San Joaquin valley, coarse grained sediments are more widespread, especially on the eastern side, and also occur along the major rivers; fine-grained sediments are associated with the largest amount of subsidence attributed to groundwater withdrawals recorded in the valley. Throughout this region, valley fill is capped by surface sediments are Pleistocene alluvium that are derived from the Sierra Nevada and the Temblor Range. These sediments were deposited on floodplains and low topography associated with river runoff and periodic flooding.

As is outlined in Chapter 17, three major watersheds exist within the Great Valley: the Sacramento River Basin, the San Joaquin River Basin, and the Tulare Lake Basin. The only drainage from the province is into the San Francisco Bay.

References

1. California Department of Food and Agriculture (2010). California Agriculture Statistical Report 2008-2009.
2. California Department of Conservation & Division of Oil, Gas, and Geothermal Resources. (1983). *California Oil & Gas Fields: Northern California* (TR10 ed., Vol. 3).
3. California Department of Conservation & Division of Oil, Gas, and Geothermal Resources. (1991). *California Oil & Gas Fields: Southern, Central coastal, and Offshore Californi* (TR12 ed., Vol. 2).

This page titled 12.1: Geomorphology and General Overview of the Great Valley Province is shared under a CC BY-NC 4.0 license and was authored, remixed, and/or curated by Cole Heap.

12.2: Geology of the Great Valley

Geology of the Great Valley

The Great Valley is underlain by a thick sequence of sedimentary units often referred to as the Great Valley Sequence. This up to 20,000 meter (~66,000 feet) thick stratigraphic interval is Jurassic age or younger and is bound within an asymmetrical synclinal trough with a more gently dipping eastern limb. The push and pull of the tectonic plates, combined with a shallow interior seaway, caused much of California to be covered by ocean water—it's crazy to think that ocean water came all the way up to the foot of the newborn Sierra Nevada as shown in Figure 12.2.1. This figure displays the paleogeography of the Great Valley during the Middle Miocene (~20-15 million years ago).The solid yellow line indicates subduction, while the dashed red line shows the strike-slip motion of the newly formed San Andreas Fault.

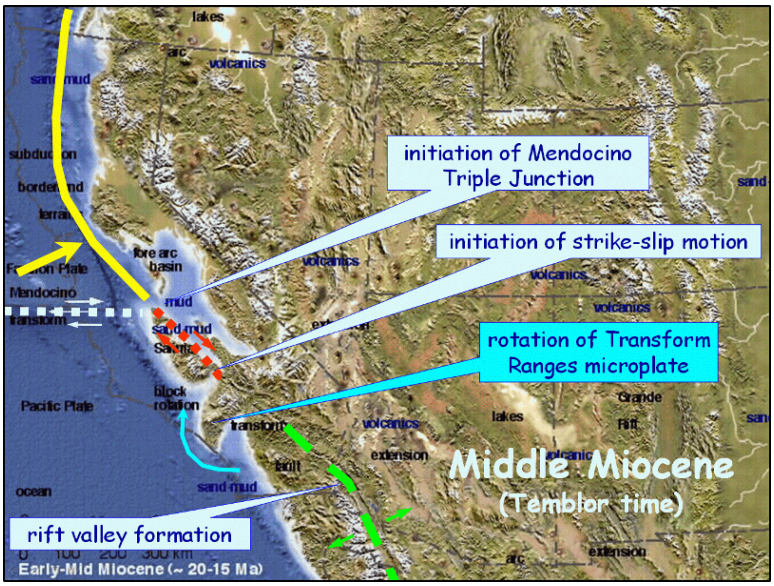


Figure 12.2.1: Paleogeography of the Great Valley during the Middle Miocene (~20-15 million years ago). "Paleogeography of the San Joaquin Valley Over Geologic Time" by Bartow and Nilsen is licensed under CC BY-NC 4.0. Access a detailed description.

As the seas withdrew in the early Eocene, terrestrial sediment deposition from the Sierra Nevada to the east increased. During the Eocene, there was tectonic uplift occurring at the boundaries of the valley which further caused the sea to recede, reducing deposition.

Sacramento Valley

The Sacramento Valley, located in Northern California, has a complex geologic history spanning millions of years. Its formation can be traced back to various tectonic activities, including the subduction of the Farallon Plate beneath the North American Plate, the uplifting of the Sierra Nevada Mountains, and the creation of the California Coast Ranges. Figure 13.2.2 is a simplified cross section of the Sacramento Valley that complements the geologic history outlined below. The left side of the figure is the westside of the valley and is punctuated by the presence of the Kirby Hills Fault. The right side of the figure shows the granitic basement of the Sierra Nevada. The yellow color represents major sandstone units, while the grey color represents fine-grained sediments, such as shale.

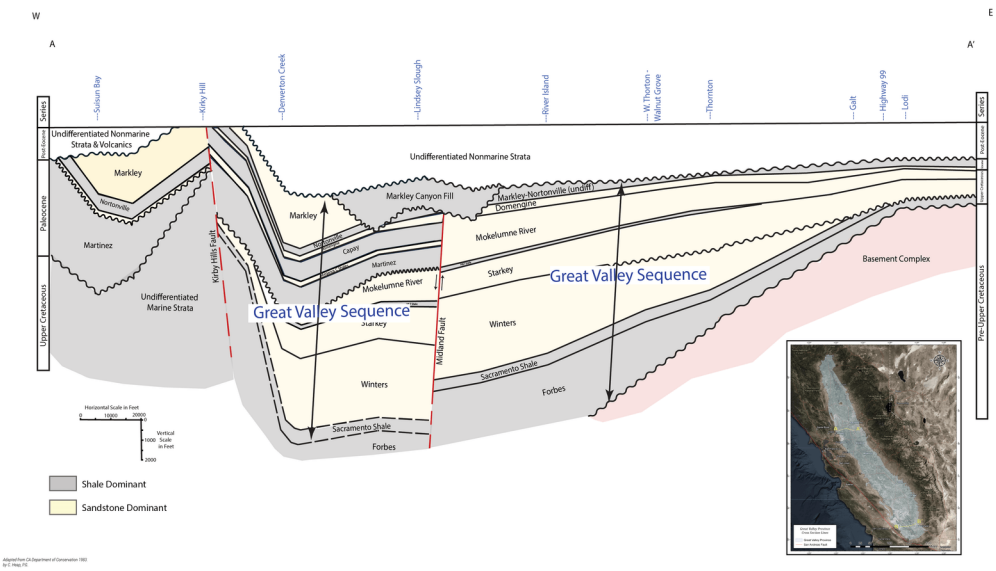


Figure 12.2.2: Cross section through the southern Sacramento Valley. "Simplified Cross Section though Sacramento Valley" by Cole Heap, P.G. and adapted from California Department of Conservation is in the public domain. Access a detailed description.

Precambrian Era

During the Precambrian era (approximately 4.6 billion to 541 million years ago), the Sacramento Valley did not exist as a distinct geographical feature. It was part of a larger landmass that underwent extensive geological changes due to tectonic activity, volcanic eruptions, and the gradual formation of sedimentary rocks.

Paleozoic Era

During the Paleozoic era (541 million to 252 million years ago), the Sacramento Valley region was submerged under a shallow sea. Sedimentary rocks, such as sandstone and shale, were deposited as the sea advanced and retreated. These sedimentary rocks are now found in the western part of the valley, forming a significant portion of the deeply buried strata that overlie the granitic basement.

Mesozoic Era

During the Mesozoic era (252 million to 66 million years ago), the Farallon Plate began to subduct beneath the North American Plate. This subduction resulted in intense tectonic activity and the uplift of the ancestral Sierra Nevada Mountains to the east of the Sacramento Valley. The deposition of sedimentary rocks continued in the valley as rivers carried eroded material from the rising mountains, forming sandstones, shales, and conglomerates.

Cenozoic Era

Around 66 million years ago, the Cenozoic era began with the Paleogene period. The tectonic forces continued to uplift the Sierra Nevada Mountains, and the Sacramento Valley underwent subsidence, resulting in the formation of a large basin. The valley was initially filled with marine and non-marine sediments, including sand, silt, and clay. Fossils of marine creatures, such as clams and gastropods, are found in these sediments, indicating the presence of a shallow sea.

During the Neogene period (23 million to 2.6 million years ago), the Sacramento Valley experienced significant volcanic activity as a result of the subduction of the Farallon Plate. Numerous volcanic eruptions occurred, depositing volcanic ash and lava flows across the region. These volcanic materials contributed to the fertile soils of the Sacramento Valley, making it an agriculturally productive region today.

Quaternary Period

The Quaternary period (2.6 million years ago to the present) brought further changes to the Sacramento Valley. Glaciations occurred in the Sierra Nevada Mountains, resulting in the formation of large glaciers and the erosion of the mountain slopes. The eroded material, including sand, gravel, and boulders, was carried by rivers and deposited in the valley, forming alluvial fans and floodplains.

The Sacramento River and its tributaries played a crucial role in shaping the valley's landscape during this period. The river system transported sediments from the mountains and deposited them in the valley, creating fertile soils for agriculture. Human settlement and agriculture in the Sacramento Valley have been heavily influenced by these geological processes.

The geologic history of the Sacramento Valley involves the formation of sedimentary rocks during the Paleozoic and Mesozoic eras, the uplift of the Sierra Nevada Mountains, volcanic activity during the Neogene period, and the deposition of alluvial sediments during the Quaternary period. These seemingly simple, yet disparate geological processes have shaped the landscape, soils, and agricultural productivity of the Sacramento Valley.

Inset Box 12a: Sutter Buttes

The Sutter Buttes, located in Northern California, stand as a captivating geological wonder and hold significant historical and cultural importance. Rising abruptly from the surrounding flatlands of the Sacramento Valley, these majestic volcanic domes form the world's smallest mountain range. Revered as a sacred site by Native American tribes such as the Maidu and Yuba, the Sutter Buttes have been a focal point of indigenous myths and spiritual practices for centuries. Beyond their cultural significance, these Buttes are a haven for biodiversity, hosting a diverse array of plant and animal species amidst their rugged terrain. Hiking enthusiasts and nature lovers are drawn to the region, eager to explore the unique flora and fauna that thrive in this distinctive landscape. Preserving the Sutter Buttes not only conserves an ecological gem but also pays homage to the rich heritage of the Native American communities deeply intertwined with the land.

The scattered hills of Sutter Buttes rise ~2,000 feet (610 m) above the dead flat floor of the southern Sacramento Valley about 55 miles (~89 km) northwest of Sacramento. The Buttes are the defunct remains of a volcano that was active during Pleistocene time (~1.6 million years ago). The Buttes were created through a combination of volcanic eruptions and subsequent erosion processes. The core of the Buttes consists of volcanic and plutonic rocks, including andesite, dacite, and basalt, which solidified from lava flows and magma intrusions. As these volcanic materials accumulated, they gradually shaped the iconic dome-like structures that now define the landscape. Surrounding the core is an apron of fragmental material that was created by eruptions of the lava domes. This apron extends roughly 11 miles (18 km) east-to-west and 10 miles (16 km) north-to-south. Between the core and the debris apron are what appear as small valleys, referred to as the “moat.” This region of the Buttes was formed by erosion of older, exposed sedimentary rocks that underlie the volcanic rocks. Figure 12.2.3 was taken by the Expedition 32 crew. It has been cropped and enhanced to improve contrast, and lens artifacts have been removed. Additional images taken by astronauts and cosmonauts can be viewed at the NASA/JSC Gateway to Astronaut Photography of Earth.



Figure 12.2.3: Astronaut photograph ISS032-E-10482 was acquired on July 29, 2012, with a Nikon D2Xs digital camera using a 180 mm lens, and is provided by the ISS Crew Earth Observations experiment and Image Science & Analysis Laboratory, Johnson Space Center. Caption by William L. Stefanov, Jacobs/ESCG at NASA-JSC. "Sutter Buttes, California" by NASA Earth Observatory is in the public domain. Access a detailed description.

What is a dead volcano doing out in the middle the Sacramento Valley floor? While not all geologists agree, many would say that the volcano is the southern extension of the High Cascades. One can in fact draw a line from the Cascades and connect directly to the Sutter Buttes. The problem is that there is no indication as to why the Buttes exist so far away from volcanoes like Lassen, where swarms of andesite and rhyolite domes exist just like those that make up Sutter Buttes. Additionally, why are the Buttes so far south of the modern oceanic trench, which ends off of Cape Mendocino. Such a trench could not have extended so far south as the Buttes within the last 2 million years.

However, some geologists theorize that the Sutter Buttes are more closely related to volcanoes that formed the Coast Range and erupted as the Mendocino triple junction passed from onshore to offshore as it traveled northward. And why would just one volcano be left along a 177-mile (255 km) stretch? Such questions are not uncommon to the science of geology and lead to continued areas of active research.

Over the millennia, extensive erosion from wind, water, and other natural forces sculpted the once larger volcanic complex into the distinct set of buttes seen today. The surrounding flatlands of the Sacramento Valley were once part of the larger volcanic terrain, but the Sutter Buttes now stand as solitary sentinels amid the vast plains. Their unique geologic history and relative isolation have contributed to their exceptional biodiversity, fostering the growth of diverse plant communities, and supporting a variety of animal species that have adapted to this distinct environment. Exploring the geology of the Sutter Buttes offers not only a glimpse into the dynamic geological past of California but also provides valuable insights into the processes that have helped to shape the Great Valley.

San Joaquin Valley

The San Joaquin Valley, located in central California, has a rich and complex geologic history that spans millions of years. This region has been shaped by various geological processes, including tectonic activity, sedimentation, and erosion. Similar to the Sacramento Valley, the San Joaquin Valley contains old sediments beneath Cenozoic aged sediments. Figure 12.2.4 exhibits a simplified cross section through the San Joaquin Valley. The left side of the figure is the westside of the valley and is punctuated by the presence of the San Andreas Fault. The right side of the figure shows the granitic basement of the Sierra Nevada. The yellow color represents major sandstone units, while the blue color represents fine-grained sediments, such as shales. The non-shaded portion labeled “Tulare” represents fluvial-deltaic sandstones and shales where the majority of the San Joaquin Valley’s groundwater is extracted from. The cross section extends from Paso Robles to the west of the valley, to the Round Mountain area, east of Bakersfield. The colors represent sedimentary strata thar dominantly comprised of silts and shales in grey and sandstones, in yellow. The pink color represents the Jurassic age granitic and pre-Cretaceous meta-sediments that formed through intrusive

igneous and regional metamorphic processes. As noted in Figure 12.3.4, the westside of this sedimentary basin is deeper and contains close to 20,000 meters (66,000 ft) of sedimentary rock. Major formations are also labeled on the cross section. These formations have significance to the valley as they help to tell the history of the southern portion of the Great Valley. Much of which has been pieced together through oil and gas exploration efforts; in fact, many of these formations contain petroleum.

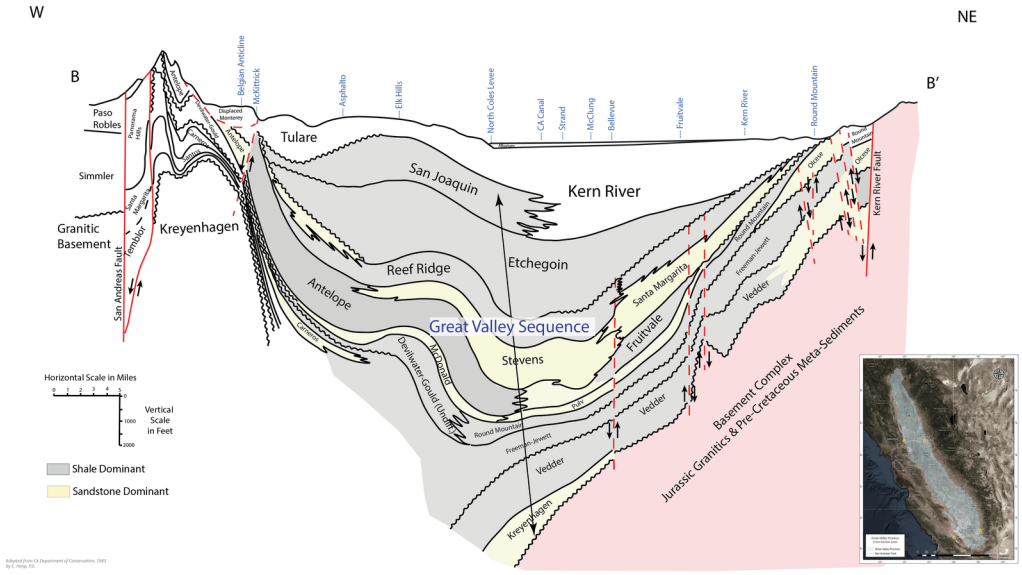


Figure 12.2.4: Cross section through the southern San Joaquin Valley. "Simplified Cross Section though San Joaquin Valley" by Cole Heap, P.G. and adapted from California Department of Conservation is in the public domain. Access a detailed description.

Tied to thick sedimentary stratigraphy is the geologic history of the San Joaquin Valley. The following is a high-level geologic history of the San Joaquin Valley that complements the simplified cross section displayed in Figure 12.2.4.

Paleozoic Era

During the Paleozoic Era (540-250 million years ago), the San Joaquin Valley area was covered by a shallow sea. Sediments, primarily composed of sand, silt, and clay, accumulated on the seafloor. Over time, these sediments were compacted and lithified, forming dominant sedimentary rock sequences of sandstone and shale.

Mesozoic Era

During the Mesozoic Era (250-65 million years ago), the San Joaquin Valley region experienced significant tectonic activity. The area was part of a large subduction zone, where an oceanic plate was being forced beneath the North American Plate. This subduction resulted in the formation of a volcanic arc along the western edge of the valley.

Volcanic activity in the region led to the emplacement of intrusive rocks, such as granites, as well as the extrusion of volcanic flows and ash deposits. These volcanic rocks can be found in the western foothills of the valley.

Cenozoic Era

Starting with the Paleogene Period (65-23 million years ago), the early part of the Cenozoic Era, the San Joaquin Valley area was uplifted and subjected to intense tectonic forces. This uplift led to the erosion of the existing rocks and the deposition of sediments in the valley.

In a combination of tectonic uplift and down drop, the San Joaquin Valley became a basin accumulating thick layers of sediment derived from the surrounding mountains. The sediments consisted of sand, silt, and clay, which were deposited by rivers and streams flowing from the adjacent Sierra Nevada and Coast Ranges. These sediments eventually compacted and formed the geologic formations known as the Great Valley Sequence.

During the Neogene Period (23-2.6 million years ago), the San Joaquin Valley underwent further tectonic activity, resulting in the formation of the San Andreas Fault system. This fault system is a major right-lateral strike-slip fault, with the main trace located along the western edge of the valley. The San Andreas Fault has played a significant role in shaping the valley's geology. It has accommodated the horizontal displacement of the Pacific Plate relative to the North American Plate, resulting in the formation of the Transverse Ranges and the uplift of the Coast Ranges. During this time, movement of large granitic blocks in the Temblor Range along the San Andreas Fault caused large, periodic loads of sediment to be deposited on the west side of the valley. When combined with movement along the San Andreas Fault, one particularly large granitic block, called the Salinian Block, accounted for large pulses of sediment to be deposited from the south to the north as shown in Figure 12.2.5. There are numerous sand bodies shown in this diagram that filled the basin to form portions of the Great Valley Sequence. Note how this diagram represents active deposition west of Buena Vista Hills during Late Miocene time. The yellow color in the figure exhibits sediment transport off of the Salinian highlands (i.e. the Temblor Range) on the westside of the valley and deposition into the Central Valley.

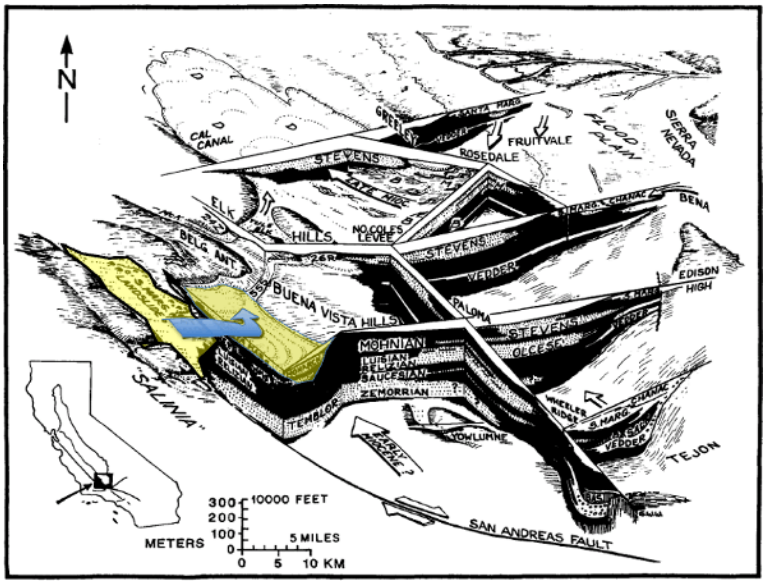


Figure 12.2.5: Diorama of deposition from the moving Salinian Grantic Block. "Spill and Fill" by Web and California Department of Conservation is in the public domain. Access a detailed description.

These deposits were sorted by energy and grain size resulting in rhythmic deposits of sandstone-shale-sandstone, called turbidites (Figure 12.2.6). This figure is a great example of a turbidite deposit that resulted from pulses of sand being transported by gravity from a high elevation into water. The shale-sandstone layering not only shows times of high-energy, but also times of low-energy, which allow silts and clays, that once compacted and lithified, form the sedimentary rock known as shale. These turbidite deposits account for a large portion of petroleum reserves on the westside.



Figure 12.2.6: Rhythmic layering of shale, sandstone, gypsum, shale, sandstone, and shale (shown from the bottom of the image to the top). "Panoche Hills Turbidites" by Cole Heap, P.G. is licensed under CC BY-NC 4.0. Access a detailed description.

As the shallow inland sea remained at this time, diatoms and other plankton thrived in it, and when these organisms died, they accumulated on the basin floor to create organic-rich shales that include the Eocene Kreyenhagen, and Miocene Monterey Formations. Figure 12.2.7 is an image of compacted diatom frustules (the hard and porous cell wall or external layer of diatoms) capture with a scanning electron microscope. Diatomite forms in marine environments, as well as some lake environments. Note how the average thickness of the diatoms are 100 microns. The average thickness of human hair is 70 microns. The integrated effects of heat and time then acted on the buried organic matter within these shales to create oil, and the detritus eroded from the Coast Ranges and the Sierra Nevada provided reservoir rocks where the oil could accumulate.

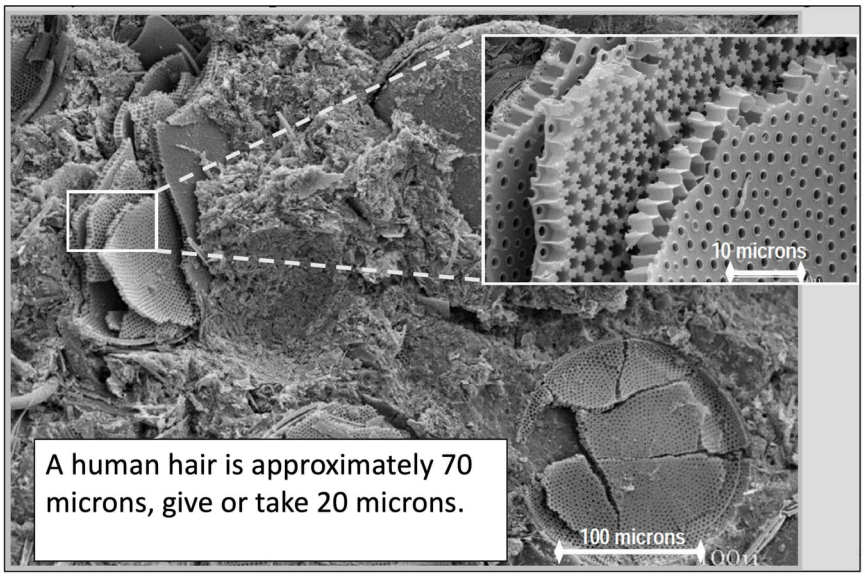


Figure 12.2.7: Scanning electron microscope image of diatomite, a bioclastic sedimentary rock made of opaline frustules of diatoms. "SEM Diatomite" by California Geologic Energy Management Division and is in the public domain. Access a detailed description.

Evidence of the shallow inland sea is shown in Figure 12.2.8 the Santa Margarita Formation near the Coalinga Oil Field. The light-colored beds contain *arcida*, or oysters, that once dwelled in a nearshore environment of the shallow inland sea that filled the southern portion of the San Joaquin Valley. Figure 12.2.9 shows an oyster from the same strata shown in Figure 12.2.8.



Figure 12.2.8: Oyster beds in the Santa Margarita Formation near Coalinga Oil Field. "Sandy Oysters" by Cole Heap, P.G. is licensed under CC BY-NC 4.0. Access a detailed description.

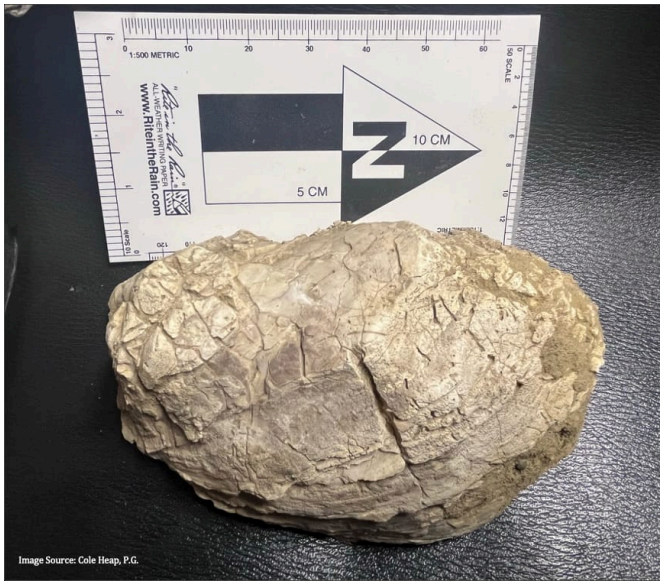


Figure 12.2.9: *Arcida* (oyster) from the Santa Margarita Formation near Coalinga Oil Field. "Santa Margarita Oyster" by Cole Heap, P.G. is licensed under CC BY-NC 4.0. Access a detailed description.

Further evidence of this paleo inland sea may be found in rock samples collected, as drill core, hundreds to thousands of feet below ground surface. Drill core is very much like taking a straw and sticking it into layered cake. When the straw is removed, the cake layers may be observed. This is a great example of how drill core is collected and interpreted, allowing geologists to understand when sea levels were high, when they were low, and when the Great Valley was an inland sea.

When geologists observe sequences of rock in drill core that consist of limestone, and shale that is capped with sandstone, they interpret a decrease in sea level. The sandstone makes for near shore, or beach-like, environment. It is near and in the water line that oysters tend to make their homes. Thus, the presence of oyster beds and this sea level decrease noted in the rock record help geologists to understand when an inland sea was present and when it began to disappear (this is referred to as sea regression). The opposite is also true. When drill core shows a sequence of sandstone and shale that is capped with limestone, sea level rise may be inferred (this is referred to as sea transgression).

Query 12.2.1

This interactive element is not available in this format. Visit the link or scan the QR code to access it online.

View this Interactive Content online

Quaternary Period

In the Quaternary Period (2.6 million years ago - present), the San Joaquin Valley experienced continued tectonic activity and climate fluctuations. The San Andreas Fault remained active, producing numerous earthquakes throughout the region.

Climate changes during this period resulted in cycles of erosion and deposition. During wetter periods, rivers and streams flowing from the mountains transported large amounts of sediment into the valley. In drier periods, these waterways cut down into their own deposits, creating terraces and alluvial fans.

In modern times, human activities, such as agriculture and water extraction, have also significantly impacted the San Joaquin Valley's geology and hydrology.

Overall, the geologic history of the San Joaquin Valley is a testament to the dynamic nature of Earth's processes, including tectonic forces, erosion, sedimentation, and climate fluctuations. It has resulted in the formation of diverse rock formations and landscapes that contribute to the unique character of the region both on the surface and in the subsurface.

Inset Box 12b: Sharklook Hill - More Evidence of a Shallow Interior Seaway

Sharktooth Hill, located in Kern County, California, is a renowned geological site that has captured the interest of paleontologists and fossil enthusiasts alike. The area is famous for its rich and diverse fossil deposits, dating back to the Miocene epoch, approximately 15 to 16 million years ago. The region was once a shallow marine environment, part of an ancient oceanic system known as the Pacific Coast Seaway.

The geological formations at Sharktooth Hill consist primarily of sedimentary rocks, such as sandstone and shale, which have perfectly preserved a plethora of marine fossils. Among the most notable findings are the abundant fossilized shark teeth, giving the site its name. These teeth belong to various species of prehistoric sharks, including the fearsome Megalodon, an ancient giant shark that ruled the oceans millions of years ago. Figure 12.2.10 shows an upper tooth from an extinct white shark speices (middle Miocene in age). In addition to shark teeth, researchers have unearthed numerous other marine fossils, including bony fish, marine mammals, rays, and invertebrates, offering valuable insights into the paleoenvironment and the ancient marine ecosystem that once thrived in this area. Today, Sharktooth Hill remains an important site for scientific research and a popular destination for fossil collectors and tourists eager to explore the geological wonders of California's ancient past.

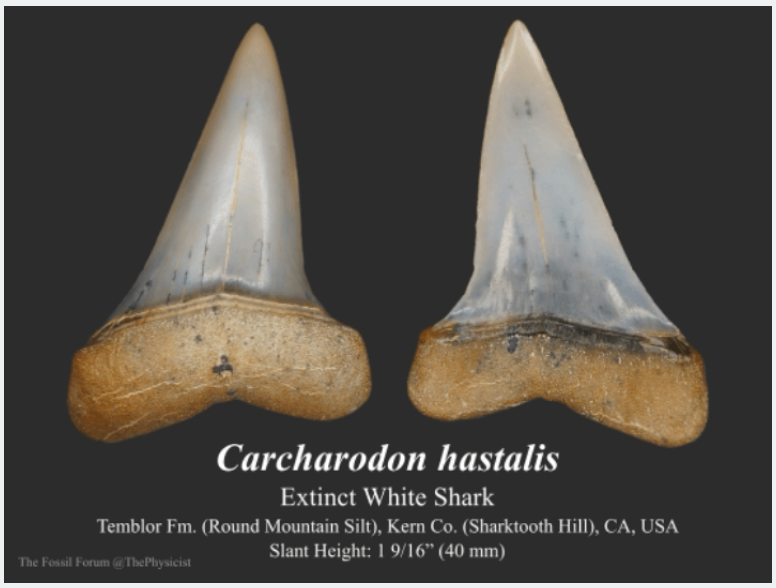


Figure 12.2.10: Carcharodon hastalis (shark) tooth found at Sharktooth Hill, CA. by N. Pearson (2022) is licensed under CC BY-NC 4.0. Access a detailed description.

References

1. California Department of Conservation & Division of Oil, Gas, and Geothermal Resources. (1983). *California Oil & Gas Fields: Northern California* (TR10 ed., Vol. 3).
2. California Department of Conservation & Division of Oil, Gas, and Geothermal Resources. (1991). *California Oil & Gas Fields: Southern, Central coastal, and Offshore California* (TR12 ed., Vol. 2).
3. McPherson, J. G., & Miller, D. D. (1990). Depositional Settings and Reservoir Characteristics of the Plio-Pleistocene Tulare Formation, South Belridge Field, San Joaquin Valley, California. *Structure, Stratigraphy and Hydrocarbon Occurrences of the San Joaquin Basin, California*, *The Pacific Section American Association of Petroleum Geologists*.doi: 10.32375/1990-GB65.17
4. Page, B. M. (1966). Geology of the Coast Range of California. *Geology of Northern California*, *California Division of Mines* (Bulletin 190), 255-276.
5. Page, R. W. (1983). Data on Depths to the Upper Mya Zone of the San Joaquin Formation in the Kettleman City Area, San Joaquin Valley, California. *US Geological Survey*.doi:10.3133/ofr81699
6. *Tulare Basin | USGS California Water Science Center*. (n.d.). California Water Science Center. Retrieved July 10, 2023, from https://ca.water.usgs.gov/projects/c...are-basin.html
7. Webb, G. W. (1983). Stevens and earlier Miocene turbidite sandstones, southern San Joaquin Valley, California. *American Association Petroleum of Geologists*, *Bulletin 65*, 438-465.

This page titled 12.2: Geology of the Great Valley is shared under a CC BY-NC 4.0 license and was authored, remixed, and/or curated by Cole Heap.

12.3: Soil, Streams and Agriculture

Soil, Streams, and Agriculture

Most of the surface of the Great Valley is covered by recent and Pleistocene-age alluvium that has been shed off the Sierra Nevada on the west side of the valley, as well as smaller volumes of sediment eroded from the Coastal and Temblor Ranges. Streams serve as pathways for sediment transportation from the mountains to the valley floor, where they are deposited. As a stream loses energy, it becomes less capable of carrying sediment and deposits it onto the broad, flat floodplains of the Great Valley. These sediments, characterized by distinct clay-rich mineralogy, contribute to the fertility of the agricultural land. The fine-grained alluvium is periodically replenished by spring runoff, making it one of California's most valuable natural resources.

This model of deposition follows the concept of the three zones of a river (Figure 12.4.1). Each zone is based on the dominant process that is operating in that part of the river system and include source, transport and sink. Source indicates erosion from steep slopes and migrating river channels that mechanically weather existing rock. The sediment that is transported includes sand, mud and pebbles that have been abraded, or mechanical weathered through physical forces of rock rubbing and pounding against rock within the river. Transport involves the movement of the weathered materials down slope. Sink is where the transportation energy runs out due to lack of slope, energy in the river system, and/or density of the sediment being transported. Sediments are deposited river deltas and floodplains, very much like those that exist within the Great Valley.

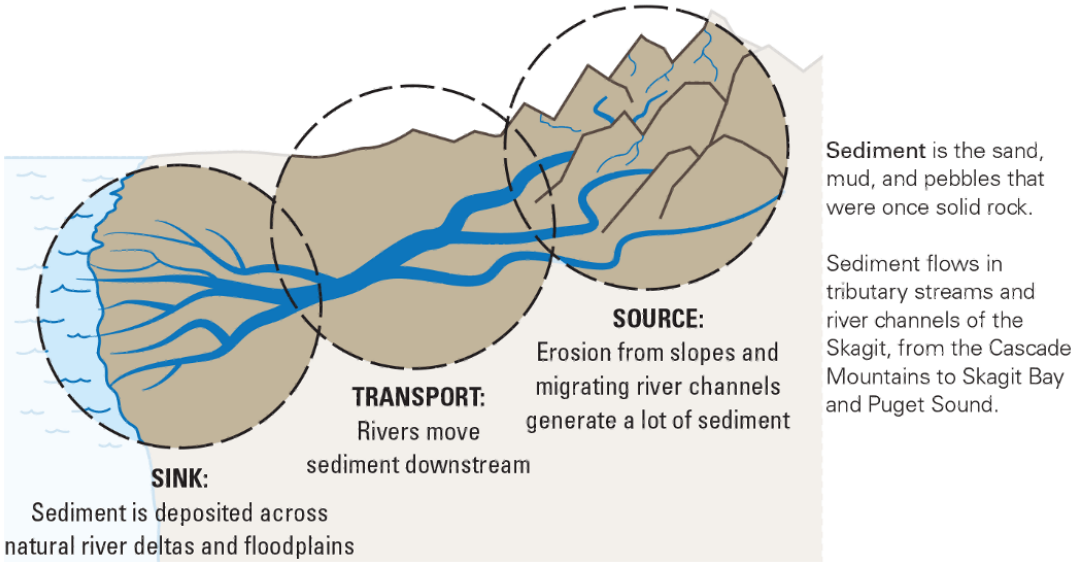


Figure 12.3.1: Based on the dominant processes operating within a river system, three zones may be identified: source, transport, and sink . "Sediment Transport in Streams: Source to Sink" by Pacific Coast and Marine Science Center and the USGS is in the public domain. Access a detailed description.

Periodic glaciation of the Sierra Nevada has had significant impacts on the landscape as well. The effects of global climate change have also strongly influenced the rivers within the Great Valley. During glaciation periods, large amounts of sediment accumulated in moraines at the edges of alpine glaciers. Sierra Nevada rivers, fueled by abundant glacial meltwater and a considerably wetter climate during those times, transported most of this sediment downstream to the Sierra foothills and into the Great Valley. Geologists refer to these episodic alluvial deposits as glacial outwash. Over the past 2 million years, at least four major pulses of deposition occurred as sediment washed out from the Sierra Nevada during glacial episodes.

In the central to lower parts of the Great Valley, younger alluvium has buried older deposits, which geologists have identified through drill cores obtained from beneath the valley floor. Much of the understanding of sediment characteristics stems from early and recent petroleum exploration efforts. Currently, the floodplains of the Sacramento and San Joaquin Rivers and their tributaries receive sediment during times of river overflow, further burying the older layers of sediment and soils. However, along the Sierra foothills, the older alluvium can be observed at the surface. Due to the ongoing uplift of the Sierra Nevada relative to

the Great Valley, rivers continuously cut downward into the landscape (Figure 12.4.2). Blue traces in Figure 12.4.2 represent some but not all of the major rivers found flowing within the Great Valley. The transparent blue is an outline of the Great Valley from Redding in the north to Bakersfield in the south.This cutting action leads to the formation of stream terraces, with remnants of older floodplain surfaces know as stream terraces (Figure 12.4.3). Note that each T marks a different time with T1 standing higher than existing younger terraces (T3). In this example, the present floodplain (T4) will evolve to form a new terrace as tectonic uplift and river incision continues. Stream terraces can be identified by their flat surfaces (Figure 12.4.4). The Merced River comes out of the foothills and onto the Great Valley floor approximately 48 km (30 miles) east of Turlock, CA in Figure 12.4.4. This particular butte the exhibits sandstone and kaolinitic clay is a great example of a river terrace in the Great Valley. Along the edges of the main river valleys, multiple terrace levels have been preserved at various elevations above the modern rivers. These terrace levels provide a record of the sequential downcutting of the rivers over time. As the elevation above the modern rivers increases, older valleys and deposits can be found.



Figure 12.3.2: Major rivers of the Great Valley Province. “Great Valley Province Major Rivers” by Cole Heap, P.G. is licensed under CC BY-NC 4.0. Constructed in a GIS using data from California Open Data Portal. Access a detailed description.

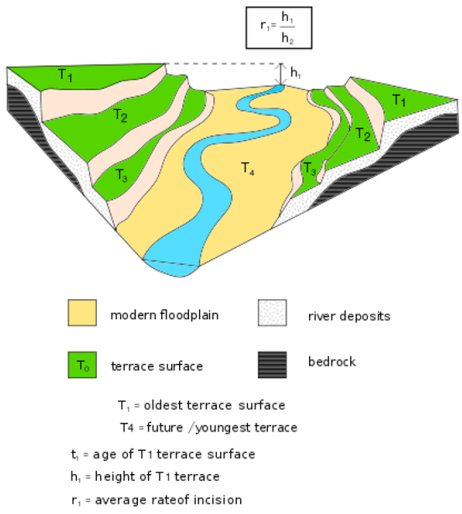


Figure 12.3.3: A series of terraces along a river. By Sushant Savla CC BY-NC 4.0. Access a detailed description.



Figure 12.3.4: Ione formation river terrace near Merced Falls in the Sierra Nevada foothills. "Ione Formation" by California Division of Mines and Geology licensed under public domain. Access a detailed description.

Query 12.3.1

This interactive element is not available in this format. Visit the link or scan the QR code to access it online.

View this Interactive Content online

References

1. Arkley, R. J. (1954). Soils of eastern Merced County, California: California Division of Mines and Geology Bulletin. 182
2. Bertoldi, G. L., Johnston, R. H., & Evenson, K. D. (1991). Ground Water in the Great Valley, California - A Summary Report. *U.S. Geological Survey Professional Paper*, *1401-A*.
3. California Department of Food and Agriculture (2010). California Agriculture Statistical Report 2008-2009.
4. Davis, G. H., Logren, B. E., & Mack, S. (1964). Use of ground-water reservoirs for storage of surface water in the San Joaquin Valley, California. *U.S. Geological Survey Water-Supply*, *Paper 1618*.
5. USGS. https://www.usgs.gov/media/images/sediment-diagram-source-sink. Accessed July 30, 2023

This page titled 12.3: Soil, Streams and Agriculture is shared under a CC BY-NC 4.0 license and was authored, remixed, and/or curated by Cole Heap.

12.4: Natural Hazards of the Great Valley Province

Natural Hazards of the Great Valley Province

Amidst its scenic landscapes and agricultural abundance, the Great Valley is also prone to various natural hazards that pose significant challenges to its residents and infrastructure. From earthquakes and floods to droughts and wildfires, the region experiences a wide range of hazards that demand careful planning, preparedness, and response.

One of the primary natural hazards that the Great Valley faces is seismic activity. Located within the seismically active Pacific Ring of Fire, the valley is susceptible to earthquakes due to its proximity to major fault lines, including the San Andreas Fault. These seismic events have the potential to cause widespread damage to buildings, roads, and other critical infrastructure, disrupting daily life and posing a significant threat to public safety.

In addition to earthquakes, the Great Valley is also vulnerable to flooding. With its extensive network of rivers and waterways, including the Sacramento and San Joaquin Rivers, the region experiences periodic flooding, especially during the rainy season. The combination of heavy rainfall, snowmelt from the nearby Sierra Nevada Mountains, and inadequate flood control measures can result in overflowing rivers, inundated farmlands, and potential damage to homes and businesses.

Furthermore, the Great Valley grapples with the challenges of drought. Despite being a major agricultural hub, the region relies heavily on limited water resources, including groundwater and surface water from rivers and reservoirs. Prolonged periods of drought, exacerbated by climate change, can lead to water shortages, impacting agricultural productivity, wildlife habitats, and the overall economic well-being of the region.

Another natural hazard, as secondary hazard of drought, that affects the Great Valley is the threat of wildfires. With its vast stretches of grasslands, forests, and agricultural lands, the region is susceptible to wildfires, particularly during the dry season when vegetation becomes highly flammable. These fires can spread rapidly, destroying crops, endangering wildlife, and posing risks to human lives and properties.

Given the magnitude and diversity of natural hazards faced by the Great Valley, it becomes crucial for residents, policymakers, and emergency management agencies to be well-prepared and proactive in mitigating risks and managing potential disasters. Through effective land-use planning, infrastructure development, early warning systems, and community engagement, the region can enhance its resilience and minimize the impact of these hazards on its communities.

In this context, understanding and studying the natural hazards specific to the Great Valley is of paramount importance. By delving into the characteristics, historical occurrences, and potential future trends of earthquakes, floods, droughts, and wildfires, we can foster a comprehensive approach to hazard mitigation, emergency response, and long-term sustainability in this vital region of California.

Water in a Sinking Valley – Land Subsidence

Completion of California's State and Federal water projects that bring water from California's wet north to its dry south allowed some groundwater aquifers to recover, and subsidence decreased in these areas. Subsidence, particularly in the San Joaquin Valley, continues today at nearly historically high rates of more than 1 ft/yr.

Land subsidence is a significant problem in California's Great Valley, characterized by the gradual sinking of the Earth's surface. This issue primarily stems from extensive groundwater extraction, agricultural practices, and geological factors. The Great Valley is an important agricultural region and one of the most productive in the United States, but the excessive pumping of groundwater has led to severe consequences. In California, large areas of land subsidence are well documented in the first half of the 20th century, as exhibited in Figure 12.4.1.



Figure 12.4.1: *Left Image:* Land subsidence near Hanford, CA between 1955 and 1977. *Right Image*: An illustration of subsidence from 1988 to 2016. "Measurement of land subsidence in the San Joaquin Valley" by USGS is in the public domain. Access a detailed description.

The Great Valley relies heavily on groundwater to sustain its agricultural activities due to limited surface water availability. Over the years, extensive pumping of groundwater has caused the subsurface aquifers to deplete rapidly. As groundwater is extracted, the pore spaces in the underground rock layers collapse, causing the land above to sink and resulting in land subsidence.

The consequences of land subsidence are far-reaching and detrimental. Infrastructure such as roads, bridges, and canals are damaged as the ground sinks, leading to increased maintenance costs and reduced functionality. Furthermore, subsidence increases the risk of flooding as the capacity of canals and drainage systems diminishes. This poses a significant threat to the agricultural industry, as excess water cannot be efficiently managed, potentially causing crop damage and water contamination.

The rate of land subsidence in the Great Valley has been alarming. In some areas, the land has sunk several feet over the past decades. Figure 12.4.2 exhibits land subsidence as recorded by synthetic aperture radar (SAR) in 2017 within the San Joaquin Valley. Note that negative values, complemented by the purples and blues, imply areas of recharge where water may even be seeping to the surface. Positive values associated with yellows and reds imply areas of greater subsidence or lowering of ground elevation relative to sea level. The highest rates of subsidence occur in regions with extensive agricultural activities and heavy groundwater pumping.

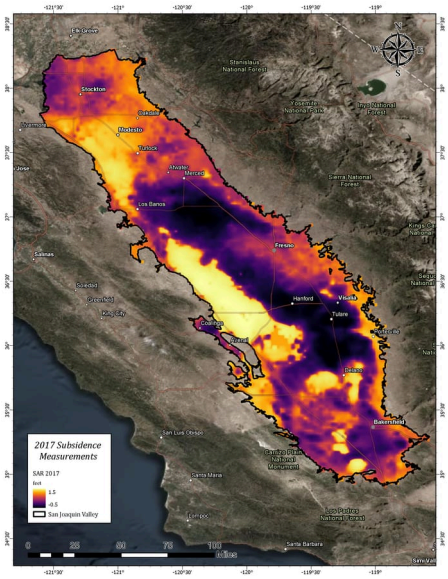


Figure 12.4.2: 2017 map of the San Joaquin Valley showing the measured subsidence from synthetic aperture radar (SAR) attributed to groundwater extraction.*"2017 Subsidence Measurements"* by Cole Heap, P.G. is licensed under CC BY-NC 4.0. Constructed in a GIS using data from California Open Data Portal. Access a detailed description.

To address this issue, California has implemented various measures to manage groundwater use more sustainably. In 2014, the Sustainable Groundwater Management Act (SGMA) was enacted, which requires local groundwater sustainability agencies to develop and implement plans to achieve groundwater sustainability within 20 years. These plans aim to balance groundwater extraction with replenishment, ensuring long-term water availability while mitigating land subsidence.

In addition, work is ongoing to predict land subsidence throughout the valley. In 2009, the USGS produced the Great Valley Hydrogeologic Model (CVHM). The aim of this model was to introduce subbasin water managers to how water moves in a hydrogeologic system. This concept would then be complemented by water modelers to make predictions on water moving into and out of the basin. The CVHM has a large list of parameters for managers and modelers alike that must be set before any predictions may be made. The list of data input requirements is related to geology, topography, remote sensing, climate, land use, soils, and chemistry, to name a few. These may come in the form of measured porosity and permeability from a drill core, or the total dissolved solids measured in a water sample taken from the subsurface. Other data inputs may include annual precipitation, or even predictions of future precipitation wherein a second layer of error may be introduced into the resulting predictions. Due to how quickly each of these inputs can change, coupled with the amount of time it takes to run the model from data input to prediction output, the CVHM has not been updated since 2014. Coincidentally, this is also when SGMA was signed into California law.

Recent efforts to predict land subsidence have integrated geospatial methods with statistical modeling of geographically weighted regression with geologic and engineering variables. Such efforts have resulted in an 87% accuracy of land subsidence prediction.

However, the road to mitigating land subsidence in the Great Valley remains challenging. Reversing the effects of subsidence is a slow and costly process, and the region continues to face significant groundwater challenges. Effective water management practices, increased surface water storage, and innovative technologies are crucial in combating land subsidence and ensuring the long-term sustainability of the Great Valley's agricultural industry.

Flooding

Paradoxically, while this region is one in which subsidence due to over-extraction of groundwater is a serious challenge, this region is also under threat of flooding! Because the Great Valley is such a large, low-lying region of minimal relief with occasion gentle slopes. In fact, the whole valley averages an elevation of ~90 m (300 ft) above sea level. The valley is susceptible to the hazard of flooding by the large rivers that flow across it. The combination of heavy rainfall, snowmelt from the nearby Sierra Nevada Mountains, and inadequate drainage systems can lead to significant flooding events. Additionally. The extensive network of irrigation canals, constructed to facilitate farming, can exacerbate the flooding risk if they become overwhelmed or

experience structural failures during intense rainfall or river surges. When these factors converge, the Great Valley becomes prone to overflowing rivers, breached levees, and widespread inundation, causing substantial damage to infrastructure, agriculture, and residential areas.

In addition to the natural factors, human activities in the Great Valley can intensify the flood hazard. Urbanization and development have altered the landscape, replacing permeable surfaces with impermeable ones like roads, parking lots, and buildings. This change disrupts the natural water infiltration process, increasing surface runoff and reducing the area's ability to absorb excess water (see Chapter 17 for more info on natural runoff processes). Furthermore, the construction of levees and flood control channels, while intended to protect populated areas, can create a false sense of security. If these infrastructure systems are not properly maintained or fail to withstand the forces of a severe flood event, the consequences can be devastating, leading to widespread flooding and loss of life and property.

Tulare Lake Basin

The Tulare Lake Basin is in the southern San Joaquin Valley and covers parts of Fresno, Kings, Kern, and Tulare counties. The Tulare Lake Basin includes input from the Kings, Kaweah, and Tule Rivers, as well as the Pine Flat Reservoir, Lake Kaweah, and Success Reservoir, which all drain to the historic Tulare Lake. Kern River flows into the southernmost portion of Tulare Lake. Tulare Lake was once the largest freshwater lake in California. Historically, Tulare Lake would flood during the winter months due to heavy rain and snowfall in the Sierra Nevada. The excess water would flow into Tulare Lake, causing it to expand and overflow its banks, creating a natural floodplain that was beneficial for agriculture and wildlife. Figure 12.5.3 exhibits the approximate boundary of what was once considered to be the largest freshwater lake west of the Mississippi River.

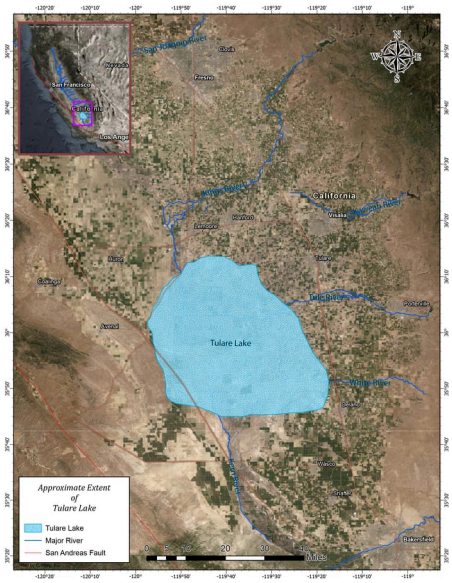


Figure 12.4.3: Approximate extent of Tulare Lake in the southern portion of the Great Valley (San Joaquin Valley). "Approximate Extent of Tulare Lake" by Cole Heap, P.G. is licensed under CC BY-NC 4.0. Constructed in a GIS using data from California Open Data Portal and Esri aerial imagery. Access a detailed description.

Over the years, Tulare Lake has gradually disappeared due to a combination of factors, including, damming of rivers, diversions for irrigation, increase water demand for agriculture, and climate change—a great example being the drought that has stricken most of the Great Valley. Today, most of Tulare Lake is a dry lakebed and is predominantly used for agriculture, with the surrounding areas being some of the most productive agricultural regions in the world. However, these rich soils do not come without risk. During the winter of 2022, the Tulare Lake Basin experienced an unprecedented amount of precipitation, with much of the Sierra Nevada snowpack melting in the higher April temperatures, leading to large volumes of runoff and a rapid resurgence of Tulare Lake (Figure 12.4.4). A March 2023 pineapple express storm, brought a resurgence of Tulare Lake where floodwaters covered 6th Avenue south of Corcoran, Kings County, CA. Heavy precipitation and runoff is shown having flooded communities and agricultural fields in former Tulare Lake. Before 2023, Tulare Lake emerged in 1997, 1983, and 1969, with 1969 and 1983 holding the records for the wettest years until being broken by the 2023 events. American settlers drained the lake, dammed key rivers that provided recharged to the lake, and then planted crops on the dried lakebed. Figure 12.4.5 is what many citizens of the San Joaquin Valley are accustomed to seeing.



Figure 12.4.4: A March 2023 pineapple express storm, brought a resurgence of Tulare Lake where floodwaters covered 6th Avenue south of Corcoran, Kings County, CA by California Department of Water Resources is in the public domain. Access a detailed description.

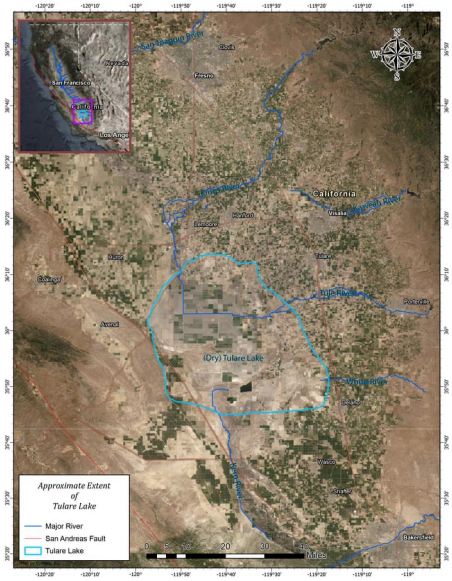


Figure 12.4.5: Dry Tulare Lake south of Lemoore, CA. "Approximate Extent of (Dry) Tulare Lake" by Cole Heap, P.G. is licensed under CC BY-NC 4.0. Constructed in a GIS using data from California Open Data Portal and Esri aerial imagery. Access a detailed description.

Overall, the Great Valley in California faces a significant hazard of flooding due to a combination of natural factors, such as heavy rainfall, snowmelt, and inadequate drainage, as well as human modifications to the landscape. As previously stated, due to the low-lying relief in the Great Valley makes it difficult for excess water to flow away quickly. Many of the streams throughout the valley can be a flood hazard during a wet season. For this reason, it is crucial for the region to implement comprehensive flood management strategies, including improved infrastructure maintenance, land-use planning, and effective emergency response systems, to mitigate the risks and protect the communities and resources within the Great Valley.

Query 12.4.1

This interactive element is not available in this format. Visit the link or scan the QR code to access it online.

View this Interactive Content online

Seismicity

The Great Valley is relatively seismically stable compared to the surrounding regions, but seismicity still poses as a hazard. This stability is primarily due to the Valley's location away from major active faults. However, it is still influenced by seismic hazards originating from nearby faults. One of the significant faults near the eastern edge of the Great Valley is the Sierra Nevada frontal fault system. This fault system includes the Owens Valley Fault and the Garlock Fault, which pose a potential seismic hazard to the eastern parts of the Great Valley. However, in recent years the USGS has made an effort to better define what is known as the Great Valley fault system.

The Great Valley fault system defines a tectonic boundary between the Coast Ranges and the Great Valley in California, as the rock types go from hard igneous and metamorphic rocks to softer sedimentary rocks. This fault has been active throughout the Quaternary, and has been the source of several significant (greater than magnitude 6) historic earthquakes, including the 1983 M 6.5 Coalinga earthquake and the 1892 Vacaville–Winters earthquake sequence. However, the locations and geometries of individual faults in the Great Valley fault system are poorly constrained, and fault slip rates and paleoearthquake chronology are largely unknown. Figure 12.4.6 shows ground shaking potential throughout California. Notably, the Great Valley has a low shaking potential.

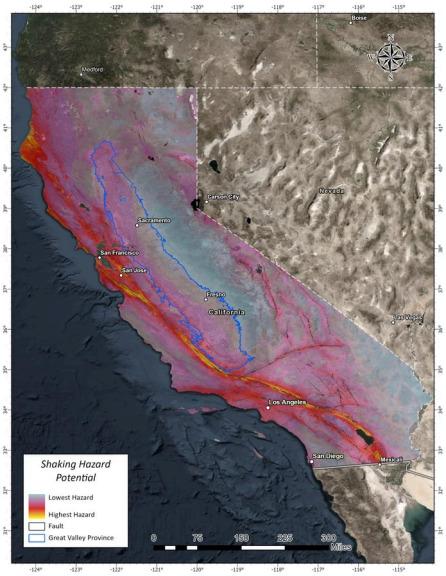


Figure 12.4.6: "Shaking Hazard Potential". Brighter colors indicate a higher shaking and ground motion hazard. "Shaking Hazard Potential" by Cole Heap, P.G. is licensed under CC BY-NC 4.0. Constructed in a GIS using data from California Open Data Portal and Esri aerial imagery.
Access a detailed description.

In terms of faults within the Great Valley itself, the most prominent one is the Concord-Green Valley Fault. It runs through the western part of the valley, southwest of Sacramento, and is an active fault with an estimated age of several million years. The Green Valley Fault has the potential to generate moderate earthquakes and is a significant consideration for seismic hazard assessment within the Great Valley. The probability for one or more magnitude 6.7 or greater earthquakes between 2003 to 2032 is 4%

Additionally, the Winters Fault is another fault system located within the Great Valley. It runs along the western side of the valley

near the town of Winters. While it is considered a minor fault, it can still contribute to seismic hazards in the region.

It is important to note that the Great Valley is predominantly characterized by tectonic forces related to the Pacific-North American plate boundary, rather than major fault activity within the valley itself. The Buena Vista fault, the Plieto fault, the Wheeler Ridge fault, and of course the San Andreas fault are all great examples of active faults that exist due to plate interaction and form the boundary between the Central Valley and the Coast Ranges. The primary seismic hazards in the Great Valley come from the transmission of seismic energies from surrounding fault systems and the amplification of ground shaking due to the valley's sedimentary basin. All the more reason to understand how faults propagate energy through brittle and ductile failure.

While faults on the fringes of the Great Valley province have been zoned by the Alquist-Priolo Earthquake Fault Zoning Act (AP Act), most faults are concealed by younger rocks and are not zoned as an active seismic hazard. This does not mean that larger, dormant faults are not present in the valley. Understanding the seismic hazards associated with these faults within and near the Great Valley is crucial for implementing effective mitigation measures and ensuring the safety and resilience of the communities in the region.

Query 12.4.1

This interactive element is not available in this format. Visit the link or scan the QR code to access it online.

View this Interactive Content online

Query 12.4.1

This interactive element is not available in this format. Visit the link or scan the QR code to access it online.

View this Interactive Content online

Inset Box 12.4.1: 1983 Coalinga-Naschmarkt Earthquake

The 1983 Coalinga earthquake, also known as the Coalinga-Naschmarkt earthquake, struck central California on May 2, 1983. It was a magnitude 6.5 earthquake that originated near the city of Coalinga. The earthquake caused significant damage to the region, with the epicenter located in a sparsely populated area, reducing the impact on human life. However, the effects were felt over a wide area, and the earthquake caused several injuries and one fatality. The damage was mainly concentrated in Coalinga, where buildings suffered structural failures, roads were cracked, and water and gas lines were disrupted. Figure 12.5.7 displays the Nunez fault being located northwest of the city of Coalinga (pink shape represents the city limits of Coalinga). The San Andreas fault is in the lower left corner of the map (to the southwest of Coalinga).

The Coalinga earthquake was notable for its unique fault behavior. It occurred on a previously unrecognized fault known as the Elkhorn Scarp, which is a branch of the active San Andreas Fault system. The fault ruptured the ground surface along a 24-kilometer-long (15 miles) segment, causing a prominent surface rupture. This surface rupture was well-documented and studied by geologists, providing valuable insights into earthquake mechanisms. The earthquake also triggered numerous aftershocks in the following weeks, which further contributed to the seismic activity in the region.

Despite the significant damage caused by the Coalinga earthquake, the response and recovery efforts were relatively efficient. Emergency services were promptly deployed, and local authorities quickly assessed the damage and aided affected residents. The earthquake served as a wake-up call for seismic awareness in the region, leading to increased efforts in

earthquake preparedness and building code revisions. The Coalinga earthquake highlighted the ongoing seismic risk in California and underscored the importance of implementing measures to mitigate future damage and protect the population from the potential devastation of larger earthquakes.

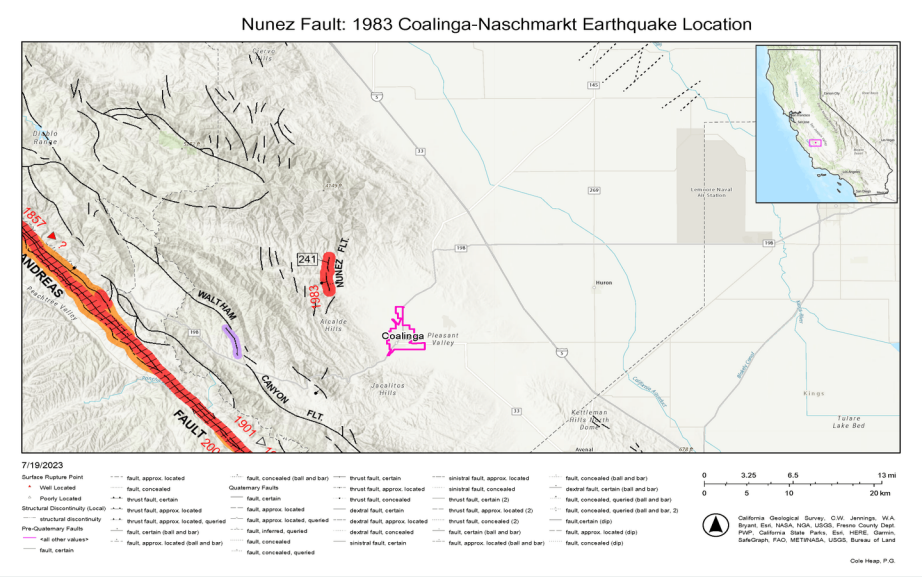


Figure Inset Box 12.4.1: "Nunez Fault: 1983 Coalinga-Naschmarkt Earthquake Location" by Cole Heap, P.G. is licensed under CC BY-NC 4.0. Constructed in a GIS using data from California Open Data Portal. Access a detailed description.



Figure Inset Box12.4.2: Building at 187 South 6th Street, Coalinga, CA, severely damaged by the May 1983 Coalinga-Nunez earthquake by USGS and is in the public domain. Access a detailed description.

References

1. Bawden, G. W., Sneed, M., Stork, S. V., & Galloway, D. L. (n.d.). Measuring human-induced land subsidence from space. *U.S. Geological Survey Fact Sheet*, 069–03, 4. http://water.usgs.gov/pubs/fs/fs06903/*New Data Shows Subsidence Continued in Water Year 2021, But Pace Slower than Seen in Previous Droughts*. (2022, February 16). California Department of Water Resources. Retrieved July 10, 2023, from https://water.ca.gov/News/News-Releases/2022/Feb-22/New-Data-Shows-Subsidence-Continued-in-Water-Year-2021-Pace-Slower-than-Previous-Droughts

2. *CGS Map Sheet 48: Earthquake Shaking Potential for California (revised 2016)*. (1999, May 11). Retrieved July 10, 2023, from https://data.ca.gov/dataset/cgs-map-sheet-48-earthquake-%20shaking-potential-for-california-revised-20161
3. Faunt, C. C., Sneed, M., Traum, J., & Brandt, J. T. (2016). Water availability and land subsidence in the Great Valley, California, USA. *Journal of Hydrogeology*, *24*, 675-678.
4. Garone, P. (2011). *The Fall and Rise of the Wetlands of California's Great Great Valley* (1st ed.). University of California Press.
5. Muarry, K. D., & Lohman, R. B. (n.d.). Short-Lived Pause in Central California Subsidence after Heavy Winter Precipitation of 2017. *Science Advances*, *4*(8). doi:10.1126/sciadv.aar8144
6. Pond, J. F. (1972). Land subsidence in the western states due to ground-water overdraft. *Water Resources*, *Bulletin 8*, 113-118.
7. Shakal, A. F., & Ragsdale, J. T. (1983). Strong Motion Data From the Coalinga, California Earthquakes and Aftershocks. *The 1983 Coalinga, California Earthquakes*, *CDMG Special Publication 66*(OSMS 83-04).
8. *SGMA Data Viewer*. (n.d.). SGMA Portal. Retrieved May 5, 2023, from https://sgma.water.ca.gov/webgis/?appid=SGMADataViewer#currentconditions
9. *Subsiding Areas in California | USGS California*. (n.d.). California Water Science Center. Retrieved March 5, 2023, from https://ca.water.usgs.gov/land_subsidence/california-subsidence-areas.html

This page titled 12.4: Natural Hazards of the Great Valley Province is shared under a CC BY-NC 4.0 license and was authored, remixed, and/or curated by Cole Heap.

12.5: Natural Resources of the Great Valley

Natural Resources of the Great Valley

The Great Valley, CA, is known for its abundant geologic-based natural resources, with some of the main resources consisting of oil and natural gas, groundwater, and mineral deposits, including metallic ores.

The valley is home to significant reserves of oil and natural gas. Oil exploration and extraction have been a vital industry in the region for many years, contributing to California's overall energy production. The underground sedimentary formations within the valley hold substantial reserves of these valuable fossil fuels.

Petroleum: Oil and Natural Gas

Petroleum, also known as crude oil, forms over millions of years through the decomposition of organic materials such as diatoms and plankton that settle at the bottom of ancient oceans. In fact, the Great Valley was once the home of a shallow inland sea where algae, such as plankton and diatoms, once thrived. Figure 12.6.1 is a map of the San Joaquin basin during the late Miocene (10.4-5 Ma). This map reflects the source and deposition of principle sediments and source rocks that make up the Great Valley Sequence in the San Joaquin Valley. Thus, once living oceanic microorganisms are the ultimate source of petroleum found in the Great Valley. Furthermore, in California, the process of petroleum formation is similar to other regions on the globe where petroleum may be found. The elements of a petroleum system include formation, source rocks, migration, and trapping.

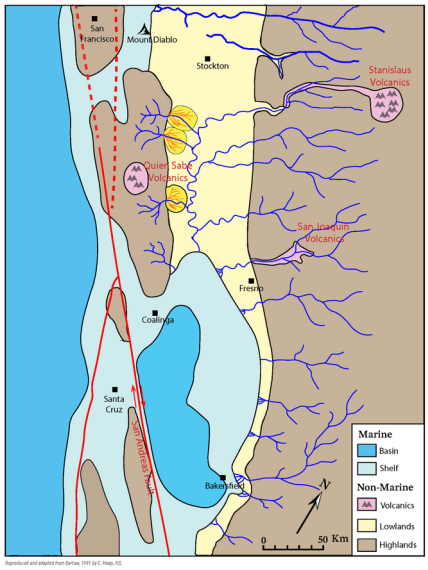


Figure 12.5.1: Map of the San Joaquin basin during the late Miocene. "Late Miocene Paleogeography of the San Joaquin Valley" by Cole Heap, P.G. and adapted from Barrow is licensed under CC BY-NC 4.0. Access a detailed description.

The petroleum formation process begins with the deposition of organic materials in ancient marine environments, such as ancient seabeds, deltas, some river systems, and carbonate reefs. Over time, these organic remains accumulate and are buried under layers of sediment. As more sediment accumulates, heat and pressure increase, transforming the organic matter into kerogen—a wax-like substance.

The rocks containing the kerogen are known as source rocks. In the Great Valley, significant petroleum deposits are found in source rocks from the Eocene Kreyenhagen and Miocene Monterey Formations (45 Ma and 22 Ma, respectively). These rocks have suitable conditions for the conversion of kerogen into petroleum due to the right combination of heat, pressure, and organic material.

Once petroleum forms, it migrates upward through porous and permeable rocks, such as sandstones, until it reaches a trapping

mechanism. Traps can be formed by various geological structures, including anticlines (folded rock formations), fault traps (resulting from movement along faults), and stratigraphic traps (changes in rock layers). These traps prevent the petroleum from further migration and trap it. Where the petroleum is trapped, this is known as a reservoir (often referred to as “reservoir rock”). Figure 12.5.2 exhibits a typical petroleum system as may be found in the Great Valley. Figure 12.5.3 provides a closer look at the types of oil and gas traps that may exist globally. Additionally, Video 15.5.1, "How Oil and Gas Reservoirs Form" further complement the cycle of petroleum formation, migration, and trapping.

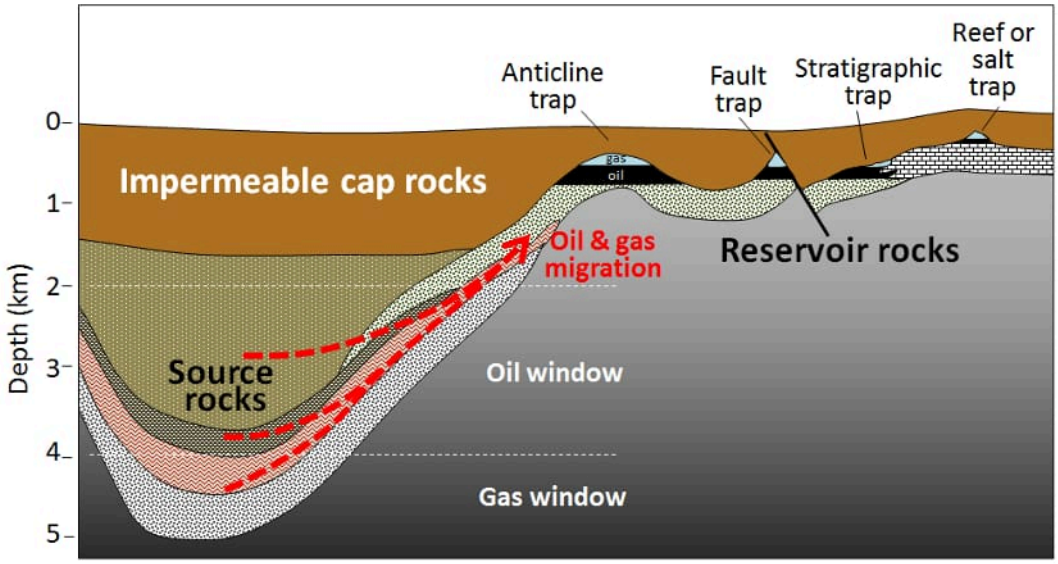


Figure 12.5.2: "Migration of oil and gas from source rocks into traps in reservoir rocks" by Steven Earle (2015) is licensed under CC BY 4.0. Access a detailed description.

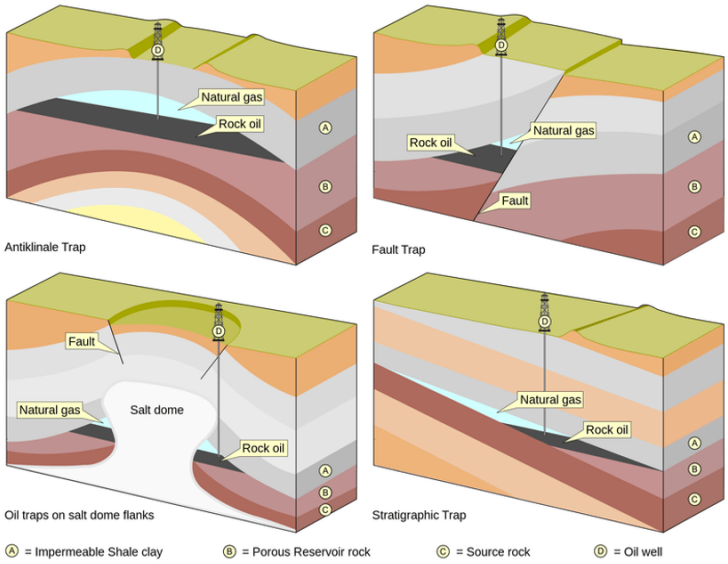


Figure 12.5.3: Diagram showing the structure of several different types of oil and gas traps by Magenta Green is licensed under CC BY 4.0. Access a detailed description.

Video 12.5.1: How Oil and Gas Reservoirs Form

This video explains how fossil fuels like coal, oil, and gas are formed. There are no captions, but a transcript is available.

This interactive element is not available in this format. Visit the link or scan the QR code to access it online.

View this YouTube Video online

Video 12.5.1: "Oil and Gas Formation" by EarthScience Western Australia is in the public domain.

Query 12.5.1

This interactive element is not available in this format. Visit the link or scan the QR code to access it online.

View this Interactive Content online

The concept of wildcatting, or the risky practice of drilling for petroleum in an area where no oil has been discovered, was practiced in the early part of the 20th century. Rural California was no different. Figure 12.5.4 shows an oil discovery at McKittrick Oil Field, southwest of Bakersfield, where enormous deposits of oil were discovered, and working-class rig hands became multimillionaires. Back then, drilling for oil was more luck than it was science as geology was coming of age in the oil boom.



Figure 12.5.4: Wildcatters pushing their luck at drilling oil wells in regions that, at the time, were not well explored. Geology was coming of age in the oil boom. "Wildcatters" by California Energy Management Division, is in the public domain. Access a detailed description.

Geologists used a whole toolbox when it comes to understanding what is going on in the subsurface. Petroleum geologists, as with many other geologists, use their skills to map the subsurface to identify oil reservoirs, water in the pore space, faults, and more. Subsurface mapping is a crucial geophysical technique used to visualize and understand the structures and properties of the Earth's subsurface layers. The primary objective of subsurface mapping is to create detailed, 2D and 3D representations of the geological features and formations beneath the Earth's surface.

To achieve this, subsurface mapping employs a range of advanced tools and technologies. Among the most commonly used are magnetic surveys, seismic reflection, electrical resistivity tomography (ERT), the collection of drill core, borehole logging, and exploratory drilling. Magnetic surveys used to detect variations in the Earth's magnetic field caused by subsurface rock formations,

and usually help identify steep discontinuities such as faults. Magnetic surveys survey are usually conducted alongside seismic reflection, which utilizes controlled energy sources and receivers to analyze the reflected energy waves to create a subsurface image.

Electrical resistivity tomography measures the electrical resistivity of subsurface materials, helping identify variations in composition, and borehole logging involves analyzing rock samples retrieved from drilled boreholes to provide detailed information about the lithology and physical properties of the subsurface.

Gravity surveys measure variations in Earth's gravitational fields to identify subsurface structures. Collecting drill core is a process by which cylindrical rock samples are obtained from the subsurface, providing a continuous record of the geological formations and structures encountered (Figure 12.5.5). Cores like this may be found throughout the Great Valley, but many are held by private companies, such as energy companies, to be used in subsurface mapping and to confirm the presence of hydrocarbons. Subsurface mapping is very similar to surface mapping of a region's geology but brings together many physics-based tools and techniques to put together a view into the geology hundreds and even thousands of feet below the Earth's surface. Figure 12.5.6 is a subsurface map showing the overall thickness of what is known as the Corcoran Clay. This subsurface map exhibits a dominant clay layer found in the San Joaquin Valley. The colored portions of the map indicate where the clay is found, based on well logs and drill core. The contour lines define the thickness (in feet) along the lines. Thicknesses are inferred between contour lines. Where no color or contours are shown, the clay will not found in the subsurface. The Corcoran Clay is discussed in detail in Chapter 18. This map was generated using information observed in drill core and from well logs consisting of measurements of resistivity, gamma ray, density and porosity. Of note, clays give off natural gamma ray, something that is also recorded on well logs and subsequently interpreted to identify clay-rich intervals in the subsurface.

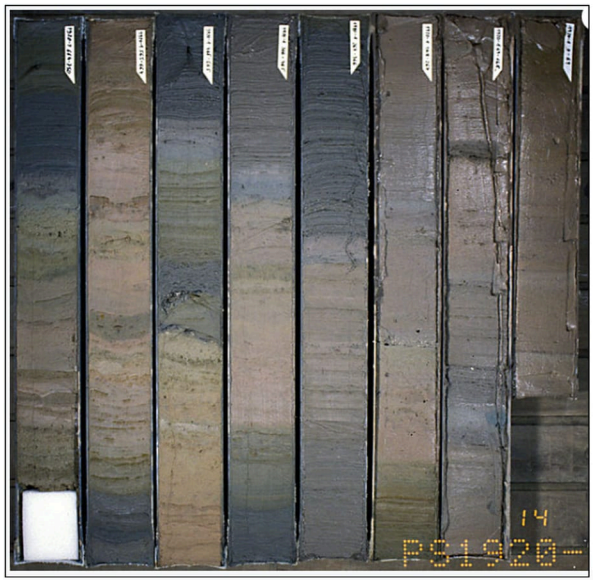


Figure 12.5.5: Sediment core taken with a gravity corer at the Greenland continental slope by Hannes Grobe (2008) is licensed under CC BY-NC 4.0. Access a detailed description.

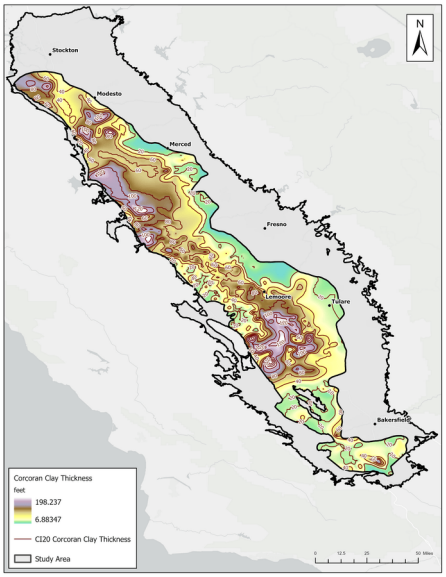


Figure 12.5.6: “Corcoran Clay Thickness”. A subsurface map of a dominant clay layer found in the San Joaquin Valley. “Corcoran Clay Thickness” by Cole Heap, P.G. is licensed under CC BY-NC 4.0. Constructed in a GIS using data from California Open Data Portal. Access a detailed description.

By combining these tools, scientists and engineers can gain valuable insights into the Earth's subsurface, such as locating natural resources and assessing geological hazards. Once a promising location is identified, wells are drilled to access the reservoirs and extract petroleum.

Figure 12.5.7 is a map displaying the Great Valley Province and its oil and gas fields, all which have been well defined through subsurface mapping and historical oil production. A notable pattern can be observed on the western side of the Valley, particularly in the Kern County area, where the fields are arranged *en echelon* relative to the San Andreas Fault. By examining the geological history of the Valley, which involves subduction and subsequent strike-slip movement, it becomes evident that the geological formations and their structures, including anticlines and synclines, where oil and gas are trapped, align with the northwest-to-southeast direction of the San Andreas Fault's motion.

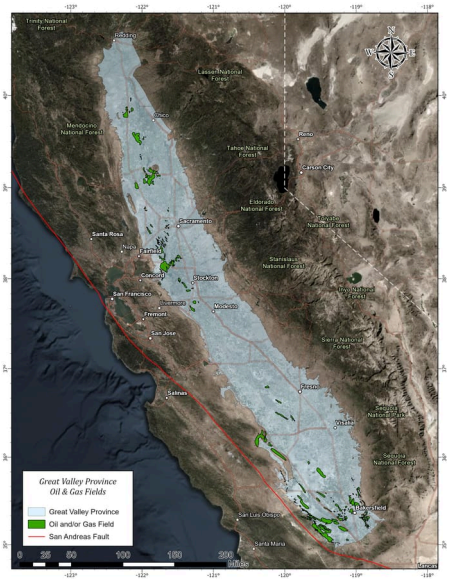


Figure 12.5.7: “Great Valley Province oil and gas fields” by Cole Heap, P.G. is licensed under CC BY-NC 4.0. Constructed in a GIS using data from California Open Data Portal. Access a detailed description.

In California, petroleum extraction involves both conventional and unconventional methods. Conventional extraction typically involves drilling vertical wells into reservoirs and utilizing natural reservoir pressure to bring the petroleum to the surface.

Unconventional methods, such as hydraulic fracturing (fracing) and steam injection are also used in specific areas to access petroleum trapped in tight rocks or in sands where there is high-viscosity oil. Interest in steam-assisted production was limited before the 1973 oil embargo and the ensuing jump in petroleum prices. In 1979 most of the United States proved the potential for heavy oil reserves in California and the concept has been present in the Valley ever since. This is an important fact associated with California's petroleum production history, as the vast majority of California's oil fields are comprised of heavy oil.

Query 12.5.1

This interactive element is not available in this format. Visit the link or scan the QR code to access it online.

View this Interactive Content online

Most of California's heavy oil is in the San Joaquin Valley. The Bakersfield area (i.e Kern County), alone, counts for about 72% of the proved heavy-oil reserves in the state. In 1983, Kern County accounted for about 404,000 barrels of oil per day of the 669,000 produced in California (roughly 60%). In 2023 that number was down to 326,000 barrels of oil per day of the 463,000 produced in California (roughly 70%). Video 12.5.2 is from the Kern River Oil Field and exhibits the large number of wells that cover a large geographic area on the west side of Bakersfield. These wells are extracting oil from the late Miocene to Pliocene Kern River Formation comprised of sandstones and mudstones deposited in a braided fluvial environment. The Kern River Formation reaches a maximum thickness of 800 m (2600 ft)!

Video 12.5.2: Flyover of the Kern River Oil Field, Bakersfield, CA

This video flyover shows oil fields in a flat, arid region. It has no narration, but a text description is available.

This interactive element is not available in this format. Visit the link or scan the QR code to access it online.

View this YouTube Video online

Video 12.5.2: "Oil Fields - Kern County" by The Drone Guy. Used with permission.

It's important to note that environmental considerations and regulations play a crucial role in petroleum extraction in California, especially given the state's focus on sustainability and minimizing environmental impacts. This is one reason why a new geologically related industry known as carbon capture and sequestration (CCS) is on the rise.

Carbon capture and sequestration in California's Great Valley involves capturing carbon dioxide (CO_2) emissions from the air, known as direct capture, or from industrial sources, such as power plants and refineries. The captured CO_2 is then injected deep underground into suitable geological formations to prevent its release into the atmosphere, thus helping to mitigate climate change impacts. In partnership with the Federal and State government, petroleum geologists are using their knowledge of deep geologic formations, the mapping of pore space, and geologic trapping mechanisms of faults, stratigraphic pinch-outs, and structural traps (e.g. anticlines and synclines) to identify candidate formations for CCS. In 2023 there were approximately three CCS projects that have been federally approved and are waiting on state approval to start injection and storage.

Geothermal Energy

The Great Valley is situated within a region of active tectonic activity and volcanic hotspots. This geothermal energy potential has been harnessed, making the valley an ideal location for geothermal power plants. The heat from underground sources is tapped to generate electricity, providing a renewable and sustainable energy source.

The Great Valley does not have significant geothermal plays. While the region does have some geothermal potential, it is not as prominent as in other areas of the state. The primary geothermal resources in California are concentrated in the northern part of the state, particularly in the areas around The Geysers, located in the Mayacamas Mountains of Sonoma and Lake Counties, and the Imperial Valley in the southern part of the state. Each of these active geothermal plays, and those geographical areas within California that are currently being explored, are found within highly faulted and tectonically active areas. As already noted, tectonic activity in the Great Valley is minimal. However, trapped and existing heat from steam injection operations are being considered for geothermal potential, but oil and gas reservoirs would either need to be depleted, or operations stopped to allow access to the injected steam. At this time, the economics of geothermal energy do not look as good as the economics behind existing oil and gas operations. It should be noted that several hot springs exist within the Great Valley on the westside of the San Joaquin Valley near Firebaugh, but as of 2023, there are no geothermal plays that hold economic viability.

Groundwater

The valley's geology plays a crucial role in storing and supplying groundwater. Underground aquifers and permeable formations provide ample water resources for agricultural irrigation and drinking water supplies. Groundwater pumping from the valley supports the region's extensive agricultural activities.

The Great Valley is renowned for its fertile soil and extensive agricultural activities, making it one of the most productive agricultural regions in the United States. Groundwater, through wells and irrigation systems, provides a reliable and sustainable water source for irrigation, allowing farmers to cultivate a wide range of crops throughout the year. The availability of groundwater enables the agriculture sector to flourish, contributing significantly to the local and regional economy through job creation, export revenue, and food production.

In addition to agriculture, groundwater plays a crucial role in supporting the industrial sector in the Great Valley. Many industries, including food processing, manufacturing, and beverage production, rely on a steady and accessible water supply for their operations. Groundwater sources provide a reliable and cost-effective solution for meeting industrial water demands, contributing to the growth and development of various industrial activities in the region. The availability of groundwater resources attracts investment, facilitates business expansion, and enhances the overall economic competitiveness of the Great Valley.

Furthermore, groundwater serves as a crucial resource for domestic water supply in the Great Valley. Many communities and households in the region depend on groundwater wells for their daily water needs. The accessibility and quality of groundwater sources provide a reliable and safe drinking water supply, reducing reliance on external water sources and associated costs. The availability of groundwater for domestic use promotes residential growth, facilitates population stability, and contributes to the overall quality of life in the Great Valley.

Many of the confined and unconfined aquifers would not exist if not for the Great Valley Sequence. Thus, the Great Valley's geology drives the success of agricultural productivity, industrial growth, and economic productivity.

Mineral Deposits

The Great Valley is known for its diverse mineral resources. The region has significant deposits of minerals such as chromite, copper, gold, mercury, and tungsten. Other minerals used in construction or industrial applications include asbestos, high-grade clay, diatomite, granite, gypsum, and limestone. These minerals are essential for construction materials, cement production, glass manufacturing, and various industrial processes.

The valley is also recognized for its deposits of metallic ores. Copper, zinc, gold, silver, and manganese are among the minerals that have been extracted from the region's mines. These metals have economic importance and are used in various industries, including electronics, construction, and manufacturing.

The geologic-based natural resources in the Great Valley have shaped its economy, providing valuable energy sources, raw materials for industry, and supporting agricultural productivity.

References

1. Bartow, J. A. (1987). *The cenozoic evolution of the San Joaquin valley, California* US Geological Survey. doi:10.3133/ofr87581
2. California Department of Conservation & Division of Oil, Gas, and Geothermal Resources. (1983). *California Oil & Gas Fields:*

Northern California (TR10 ed., Vol. 3).
3. California Department of Conservation & Division of Oil, Gas, and Geothermal Resources. (1991). *California Oil & Gas Fields: Southern, Central coastal, and Offshore California* (TR12 ed., Vol. 2).
4. *Geothermal Resources*. (n.d.). California Department of Conservation. Retrieved July 1, 2023, from https://www.conservation.ca.gov/calgem/geothermal
5. Faunt, C. C., Sneed, M., Traum, J., & Brandt, J. T. (2016). Water availability and land subsidence in the Great Valley, California, USA. *Journal of Hydrogeology*, *24*, 675-678.
6. Guerard Jr., W. F. (1998). Heavy Oil in California. *California Department of Oil and Gas, Publication No. TR28*.
7. Hill, F. L. (1964). Harvester gas field: California Department of Conservation, Division of Oil and Gas, Summary of Operations, California Oil Fields, 50, 1, 11-15.
8. McPherson, J. G., & Miller, D. D. (1990). Depositional Settings and Reservoir Characteristics of the Plio-Pleistocene Tulare Formation, South Belridge Field, San Joaquin Valley, California. *Structure, Stratigraphy and Hydrocarbon Occurrences of the San Joaquin Basin, California*, *The Pacific Section American Association of Petroleum Geologists*. doi: 10.32375/1990-GB65.17
9. Webb, G. W. (1983). Stevens and earlier Miocene turbidite sandstones, southern San Joaquin Valley, California. *American Association Petroleum of Geologists*, *Bulletin 65*, 438-465.

This page titled 12.5: Natural Resources of the Great Valley is shared under a CC BY-NC 4.0 license and was authored, remixed, and/or curated by Cole Heap.

12.6: Chapter Summary

12.1 Physiographic Properties and Characteristics of the Great Valley

- The Great Valley in California is a large, flat region that stretches over 644 kilometers (400 miles) with a width of 80 kilometers (50 miles). It is divided into the Sacramento Valley in the north and the San Joaquin Valley in the south.
- The Great Valley is a geographically diverse region with distinct parts, the Sacramento Valley and the San Joaquin Valley, known for its agricultural productivity.
- The San Joaquin Valley is a Mediterranean environment with hot, dry summers and wet winters. It is a major agricultural region, producing a significant portion of the United States' agricultural products, including grapes, raisins, cotton, almonds, citrus, and vegetables.
- The San Joaquin Valley plays a significant role in supplying a wide range of agricultural products for the United States.
- The Great Valley is filled with sediment deposits that are several kilometers deep, with the San Joaquin Valley reaching up to 4.8 kilometers (3 miles) and the Sacramento Valley up to 9.6 kilometers (6 miles). Groundwater pumping for agriculture has caused subsidence, particularly in areas with fine-grained sediments.
- Groundwater pumping for agriculture has led to subsidence in certain areas of the Great Valley, highlighting the importance of sustainable water management practices.

12.2 Geology of the Great Valley

- The Great Valley is a sedimentary basin with a thick sequence of sedimentary units called the Great Valley Sequence. It was formed through tectonic activities and the Western Interior Seaway, which covered much of California with ocean water.
- The Great Valley, including the Sacramento Valley and the San Joaquin Valley, has a diverse and dynamic geologic history influenced by tectonic forces, sedimentation, and climate changes.
- The Sacramento Valley in Northern California has a complex geologic history shaped by tectonic activities, including subduction, uplift of the Sierra Nevada Mountains, and the creation of the California Coast Ranges.
- The formation of the valley involved a series of events ranging from ancient oceans, tectonic uplift, and deposition of sediment from nearby mountains and key fluvial systems such as the Sacramento and Feather Rivers.
- The San Joaquin Valley in central California has a rich geologic history influenced by tectonic activity, sedimentation, and erosion. The region has been shaped by the movement along the San Andreas Fault and the deposition of sediment from granitic blocks, contributing to the formation of turbidite deposits and petroleum reserves.
- The formation of the valley involved a series of events ranging from ancient oceans, tectonic uplift, and deposition of sediment from nearby mountains, with dominant influence from the San Andreas Fault system to the west and fluvial systems to the east.

12.3 Soil, Streams and Agriculture

- The Great Valley's surface is predominantly covered by recent and Pleistocene-age alluvium, deposited by streams carrying sediment from the Sierra Nevada and nearby ranges. The clay-rich sediments contribute to the fertility of the agricultural land and are periodically replenished by spring runoff.
- The Great Valley's fertile agricultural land is primarily composed of clay-rich alluvium deposited by streams originating from the Sierra Nevada and nearby ranges.
- Periodic glaciation of the Sierra Nevada has resulted in the accumulation of sediment in moraines, which rivers transported downstream during wetter climate periods. These episodic alluvial deposits, known as glacial outwash, have contributed to the sedimentation in the Great Valley over the past 2 million years.
- Glacial outwash from the Sierra Nevada during periods of glaciation has significantly influenced the sedimentation in the Great Valley.
- In the central to lower parts of the Great Valley, younger alluvium has buried older sediment deposits. However, along the Sierra foothills, older alluvium can still be observed at the surface. Ongoing uplift of the Sierra Nevada has led to river downcutting and the formation of stream terraces, providing a record of the valley's sequential geological history.
- Ongoing uplift of the Sierra Nevada has resulted in river downcutting and the formation of stream terraces, revealing the valley's geological history and the burial of older sediment layers.

12.4 Natural Hazards

- The Great Valley of California faces a range of natural hazards, including seismic activity, flooding, drought, and wildfires. These hazards demand careful planning and preparedness to mitigate risks and protect residents and infrastructure.
- The Great Valley faces a diverse range of natural hazards, including earthquakes, floods, droughts, and wildfires, which require proactive planning and response measures.
- Land subsidence is a significant problem in the Great Valley, primarily caused by extensive groundwater extraction for agriculture. This sinking of the land has detrimental effects on infrastructure, increases flood risk, and poses challenges to water management.
- Land subsidence caused by excessive groundwater extraction poses risks to infrastructure and water management.
- The Great Valley is susceptible to seismic hazards, primarily from nearby faults such as the Sierra Nevada frontal fault system and the Concord-Green Valley Fault. While the Great Valley itself is relatively seismically stable, the transmission of earthquakes from surrounding fault systems can pose risks.
- Understanding the seismic hazards from nearby faults and their potential impacts is crucial for ensuring the safety and resilience of the Great Valley's communities.
- The Great Valley in California, stretching from the Sacramento Valley to the San Joaquin Valley, is susceptible to significant flooding due to its low-lying nature and the presence of major rivers like the Sacramento and San Joaquin. Heavy rainfall, snowmelt, and inadequate drainage systems can lead to overflowing rivers, breached levees, and widespread inundation.
- The Great Valley in California faces a significant flood hazard due to its geographical characteristics, major rivers, and inadequate drainage systems.
- The flat and fertile nature of the valley, along with an extensive irrigation network, contribute to the challenge of excess water removal during intense rainfall or river surges.
- The Tulare Lake Basin experiences a complex relationship between water availability, agriculture, and climate change, highlighting the need for sustainable water management practices in the region.

12.5 Natural Resources of the Great Valley

- The Great Valley in California is rich in natural resources, including oil and natural gas, groundwater, and mineral deposits such as metallic ores. These resources play a significant role in the region's energy production, agricultural activities, and industrial development.
- The Great Valley's natural resources, such as oil and natural gas, groundwater, and mineral deposits, are essential for energy production, agricultural productivity, industrial growth, and economic development.
- Petroleum extraction is a vital industry in the Great Valley, with substantial reserves of oil and natural gas found in the underground sedimentary formations. The geological process of petroleum formation, migration, and trapping contributes to the presence of these valuable fossil fuels.
- The same key concepts used in petroleum reservoir identification are being used today to identify subsurface carbon capture and sequestration project potential.
- Groundwater is a crucial resource in the Great Valley, supporting agricultural irrigation, industrial activities, and domestic water supply. The availability and accessibility of groundwater sustain the region's extensive agricultural sector and promote economic growth.
- Proper management and sustainable use of these resources are crucial for ensuring long-term economic viability and environmental stewardship in the region.
- The Great Valley is known for its diverse mineral resources, including metallic ores and minerals used in construction and industry. Copper, gold, silver, and other metals are extracted from the region's mines and play a vital role in various industries.
- The geological characteristics and processes that have created these resources highlight the importance of understanding and protecting the Great Valley's geology for future generations.

This page titled 12.6: Chapter Summary is shared under a CC BY-NC 4.0 license and was authored, remixed, and/or curated by Cole Heap.

12.7: Detailed Figure Descriptions

Figure 12.1 Location of the Great Valley of California

The Great Valley represents the central portion of California and runs up and down the state (truly north and south), covering approximately 11% of California's land mass. The Great Valley Province is bounded by the Klamath Mountains on the north and the Cascade range on the northeast. It abuts the Sierra Nevada along its eastern and southern flanks. Along its western flank it abuts the Northern Coastal Ranges and the Southern Coastal Ranges (which meet the Sierra Nevada in the south).

Figure 12.2.1: Paleogeography of the Great Valley during the Middle Miocene

This image is a geological map highlighting tectonic activities during the Middle Miocene period, approximately 20 to 15 million years ago (Temblor time). The map shows the western coast of North America, including parts of present-day California and Baja California, with various geological features and tectonic movements identified. Key elements and annotations on the map include the initiation of the Mendocino Triple Junction located off the northern coast of California, indicated by an arrow pointing to a line representing the plate boundary; the initiation of strike-slip motion, indicated by an arrow pointing towards the southern part of California where the San Andreas Fault is located; the rotation of the Transform Ranges Microplate, shown with an arrow pointing to the southeastern region indicating the microplate's rotation; and the rift valley formation, indicated with an arrow pointing towards the beginning of a rift valley formation along the Baja California region. The map also shows volcanic arcs and basins throughout the region.

The overall image presents a detailed view of the tectonic activities and geological changes during the Middle Miocene, with significant emphasis on the movements and interactions of different tectonic plates and microplates in the region.

Figure 12.2.2 Cross section through the southern Sacramento Valley

This image is a geological cross-section depicting the stratigraphy and fault structures of the Great Valley Sequence in California in the Sacramento Valley. The cross-section runs from west (W) to east (E) and includes detailed labels of various geological formations and features.

The west side of the cross-section shows undifferentiated nonmarine strata and volcanics, with specific layers labeled as Markley and Nortonville. Below these layers are undifferentiated marine strata, depicted in gray to indicate shale dominance, and a section labeled Martinez. The Kirby Hills Fault, marked by a red dashed line, separates these layers from the main Great Valley Sequence.

The Great Valley Sequence, predominantly sandstone-dominant and shown in light yellow, is divided into several formations including Mokelumne River, Starkey, Winters, Sacramento Shale, and Forbes. The Midland Fault, another significant fault, is also marked and separates different sections within the Great Valley Sequence.

Towards the east side of the cross-section, undifferentiated nonmarine strata are depicted again, along with the Basement Complex shown in pink, indicating older, pre-Upper Cretaceous rocks.

The top of the cross-section features labels indicating various geographic locations such as Suisun Bay, Kirkly Hill, Denverton Creek, Lindsey Slough, River Island, Walnut Grove, Thornton, Highway 99, Galt, and Lodi. The lower right corner includes an inset map of California, highlighting the area covered by the Great Valley Sequence with a shaded region.

Overall, this geological cross-section illustrates the complex stratigraphy and fault structures within the Great Valley Sequence, showing the relationships between different geological layers and the significant fault lines that affect them.

Additional Details

Stratigraphic Layers

The cross section displays a stack of sedimentary rock layers representing the Great Valley Sequence, which is the thick package of sedimentary rocks deposited in the valley basin over geologic time. These rocks are mostly sedimentary strata formed from materials eroded from surrounding highlands and deposited in a marine to nonmarine trough.

- Undifferentiated non-marine strata and volcanic rocks are shown toward the western side.
- Beneath these, there are undifferentiated marine strata dominated by shale (gray shading) and specific labeled units such as Martinez.
- The central part of the section is dominated by the Great Valley Sequence, shown with a lighter color (often yellow for sandstone-dominant units). Within this section are several formations labeled, such as:
  - Mokelumne River
  - Starkey
  - Winters
  - Sacramento Shale
  - Forbes
  - These represent different depositional sequences and sediment types (e.g., sandstone vs shale) that accumulated through time.
  - Geosciences LibreTexts

Fault Structures

The cross section highlights major faults that cut through these rocks:

- Kirby Hills Fault - Marked with a dashed red line on the left side, this fault separates the marine and non-marine strata from the main Great Valley Sequence. It offsets the older units and indicates tectonic activity in the region.
- Midland Fault - Another structural break in the rocks within the sequence, showing displacement of rock layers and local structural complexity.

These faults illustrate how the Sacramento Valley's basin was affected by tectonic forces, folding, and faulting as sediments were deposited and later deformed.

Geographic and Map Context

Across the top of the cross section, names of modern geographic locations lie above the corresponding rock layers. These include places like:

- Suisun Bay
- Kirby Hill
- Denverton Creek
- Lindsey Slough
- River Island
- Walnut Grove
- Thornton
- Highway 99
- Galt
- Lodi

Figure 12.2.3: Astronaut photograph of Sutter Buttes

This aerial view of a landscape shows a central mountainous area surrounded by agricultural land and urban development. The central feature is labeled as the "central core," which appears as a rugged, elevated area with radial patterns of erosion. Surrounding the central core is a region labeled "moat," which appears to be a lower-lying area encircling the central core.

Further out from the central core and moat is a larger area labeled "debris apron," which consists of material that has spread out from the central core, forming a fan-like pattern. This debris apron is a mix of rough terrain and flatter areas used for agriculture.

To the right of the central core and debris apron, the landscape transitions into a grid of fields and agricultural plots. The fields are green and brown, indicating different stages of crop growth or types of land use. On the far-right side of the image is Yuba City, an urban area with a denser network of streets and buildings.

The overall image captures the geological and human-modified features of the landscape, highlighting the relationship between the natural mountainous region and the surrounding agricultural and urban areas.

Figure 12.2.4: Cross section through the southern San Joaquin Valley

This image is a geological cross-section depicting the stratigraphy and fault structures of the Great Valley Sequence in California, in the San Joaquin Valley, specifically focusing on the area from west (W) to northeast (NE). The cross-section includes detailed labels of various geological formations and fault lines, illustrating the complex subsurface geology of the region.

On the left side of the cross-section the stratigraphy includes formations such as Paso Robles, Simmler, and Kreyenhagen. These layers are separated by the prominent San Andreas Fault, marked by a red line with arrows indicating relative motion. To the right of the San Andreas Fault is the Granitic Basement, indicating older, more stable rock formations.

Moving eastward, the Great Valley Sequence is depicted as a series of alternating shale-dominant (gray) and sandstone-dominant (light yellow) layers. Key formations within this sequence include the San Joaquin, Reef Ridge, Etchegoin, Antelope, Stevens, and Fruitvale. Several fault lines cut through these layers, indicating significant geological activity.

Further to the northeast, the Kern River and the Kern River Fault are prominent features. The Kern River Fault is marked by a red line and indicates a significant geological boundary. The formations in this area include Santa Margarita, Vedder, and the Basement Complex, consisting of Jurassic granitic and pre-Cretaceous meta-sediments, shown in pink.

The top of the cross-section features labels indicating various geographic locations such as Elk Hills, North Cross Levee, CA Canal, Strand, McClung, Bellevue, Frendale, and Round Mountain. The lower right corner includes an inset map of California, highlighting the area covered by the Great Valley Sequence with a shaded region.

Overall, this geological cross-section illustrates the complex stratigraphy and fault structures within the Great Valley Sequence, showing the relationships between different geological layers and the significant fault lines that affect them. The cross-section provides a detailed view of the subsurface geology, highlighting the interaction between different formations and fault systems in this region.

Figure 12.2.5: Diorama of deposition from the moving Salinian Granitic Block

This 3D geological cross-section diagram depicts the complex fault structures and stratigraphy of a region in California. The diagram is oriented with north (N) at the top and includes a map inset of California in the lower left corner, showing the location of the cross-section. The cross-section illustrates a series of faulted and folded geological layers, with labels indicating various formations and geographic locations.

Key features include the San Andreas Fault, which runs diagonally from the lower left to the upper right, marked prominently as a major fault line. The Buena Vista Hills are located centrally, with various geological layers shown folded and faulted around this area. To the left side of the diagram are the Elk Hills and Buena Vista Hills, with the Elk Hills showing a complex structure of faulted layers. Towards the upper right, the areas of Fruitvale and Rosedale are indicated, showing regions affected by the geological structures. Various geological layers are labeled with names such as Stevens, Vedder, Paloma, Chanac, and others, shown in different colors and patterns to indicate their composition and geological age.

The diagram also includes features like the CAL Canal, Bakersfield area, Edison High, and the Sierra Nevada to provide geographic context. The vertical scale on the lower left shows measurements in meters and feet, while the horizontal scale indicates distances in miles and kilometers. Overall, this 3D cross-section provides a detailed view of the geological structures in the region, highlighting the interaction between different formations and the impact of major fault lines like the San Andreas Fault. The diagram effectively conveys the complexity of the subsurface geology, showing how various layers have been deformed

and displaced over time.

Figure 12.2.6: From the bottom of the image to the top: Rhythmic layering of shale and sandstone

This close-up view of a rock outcrop shows distinct stratification, featuring layers of different rock types. A pen is placed horizontally across the outcrop, providing a sense of scale and highlighting a specific layer. The rock layers exhibit variations in color and texture, with darker and lighter bands alternating. The darker layers appear to be shale or mudstone, characterized by fine-grained material and a more weathered surface. The lighter layers are likely composed of more resistant materials such as sandstone.

The pen, positioned near the center of the image, serves as a reference point for the thickness and orientation of the layers, which are horizontal. The presence of the pen also emphasizes a particular feature within the rock, possibly a vein of quartz or calcite, which stands out due to its lighter color and crystalline appearance. This vein is roughly the width of the pen and runs parallel to the stratification of the rock, indicating a secondary geological process that occurred after the initial deposition of the sedimentary layers.

Overall, the image provides a detailed view of the rock's stratigraphy and highlights the different compositions and textures present in the outcrop. The inclusion of the pen for scale helps to contextualize the size and features of the rock layers, offering insights into the geological history and processes that formed them.

Figure 12.2.7: Scanning electron microscope image of diatomite

This scanning electron microscope (SEM) photograph shows a highly magnified view of microstructures. The main part of the image reveals a complex arrangement of tiny, intricate structures with various textures and patterns. The magnification scale indicates that the image includes features at a microscopic level, with a scale bar showing 100 microns for reference.

In the lower right corner of the main image, there is a broken, circular structure with a pattern of holes, resembling a diatom, which is a type of microscopic algae. This circular structure is labeled with a scale bar indicating 100 microns, helping to provide a sense of scale for the other features in the image.

In the upper right corner, there is a zoomed-in inset showing a close-up of a specific area from the main image. This inset focuses on a detailed section with a perforated, lattice-like pattern, similar to the structure of diatom frustules. The scale bar in this inset shows 10 microns, illustrating the fine details of the microstructure.

A label at the bottom of the image states, "A human hair is approximately 70 microns, give or take 20 microns." This provides a point of reference for understanding the size of the structures in the image, emphasizing how small these microscopic features are in comparison to something familiar like the diameter of a human hair.

Overall, this SEM image provides a detailed view of microscopic structures, showcasing the intricate and delicate patterns that are not visible to the naked eye. The included scale bars and comparison to the size of a human hair help contextualize the extreme magnification and the tiny scale of the observed features.

Figure 12.2.8: Oyster beds in the Santa Margarita Formation

This image shows an exposed geological outcrop in a semi-arid landscape. The outcrop consists of several distinct layers of rock and sediment, visible as horizontal bands of varying color and texture. The upper part of the outcrop is capped with a dark, coarse-grained layer, likely composed of basalt or another volcanic rock, which is more resistant to erosion compared to the layers below it.

Below this dark cap, there are several lighter-colored layers of sedimentary rock, which may include sandstone, siltstone, or mudstone. These layers appear to be more easily eroded, as evidenced by the more rounded and weathered appearance of the slope. The outcrop is situated on a hillside covered with sparse vegetation, including dry grasses and small shrubs, typical of a semi-arid environment.

In the foreground, there are more dense bushes and grasses growing along the base of the outcrop. The presence of these plants

suggests some accumulation of moisture and soil at the lower levels of the slope. The overall scene depicts a clear example of sedimentary layering, weathering processes, and the impact of vegetation on the landscape in a dry environment.

Figure 12.2.9: *Arcida* (oyster) from the Santa Margarita Formation

This image shows a close-up view of a fossil specimen, specifically a fossilized oyster, placed on a dark background. The fossil has a rough, irregular surface with a light beige to tan coloration and appears to have a weathered, cracked texture. Next to the fossil is a white measuring card with metric and imperial units, providing a scale for the specimen. The measuring card has a large black arrow pointing to the right, marked with "Z" at the arrowhead and labeled with increments in centimeters along the top and left edges, and inches along the right edge.

The fossil is roughly oval in shape and measures approximately 10 centimeters in length, as indicated by the measuring card. The surface of the fossil shows various cracks and fractures, suggesting that it may have been subjected to weathering or pressure over time. The fossil's texture and appearance indicate it is a fossilized oyster, showcasing the preserved details of its ancient shell.

The overall image provides a clear view of the fossil's size, shape, and texture, with the measuring card serving as a useful reference for scale and orientation. The close-up nature of the photograph allows for detailed examination of the fossil's surface features and composition.

Figure 12.2.10: *Carcharodon hastalis* (shark) tooth

This image shows two fossilized shark teeth from the extinct white shark species *Carcharodon hastalis*. The teeth are displayed against a dark background, highlighting their distinct features. Both teeth have a triangular shape with sharp, smooth edges and a broad, robust base.

The teeth are labeled with their origin: "Temblor Fm. (Round Mountain Silt), Kern Co. (Sharktooth Hill), CA, USA," indicating that they were found in the Temblor Formation in Kern County, California, specifically at Sharktooth Hill, a well-known fossil site. The slant height of the teeth is noted as "1 9/16" (40 mm)," providing a measurement for the size of the fossils.

Below the image, the scientific name *Carcharodon hastalis* is prominently displayed, along with the common name "Extinct White Shark." The detailed labels and clear presentation emphasize the significance of these fossils as valuable specimens from an extinct species of shark.

Overall, the image provides a detailed and informative view of the fossilized teeth, showcasing their size, shape, and origin, and offering insights into the paleontological significance of these remains.

Figure 12.3.1: Based on the dominant processes operating within a river system

This illustration shows the process of sediment transport in a river system, from its source to its deposition in a sink. The diagram is divided into three main sections: source, transport, and sink, each depicted with corresponding landscapes and processes.

On the right side, labeled "Source," the illustration shows mountains with streams and rivers originating from slopes and migrating river channels. This section highlights that erosion from slopes and river channels generates a lot of sediment. The rivers are shown as blue lines running down the mountains, carrying sediment with them.

In the middle section, labeled "Transport," the diagram illustrates how rivers move sediment downstream. The rivers are depicted flowing through a more leveled landscape, continuing to carry sediment towards lower elevations.

On the left side, labeled "Sink," the illustration shows the sediment being deposited across natural river deltas and floodplains as the rivers reach their mouths. The rivers are shown spreading out into multiple channels, depositing sediment into a body of water, likely a bay or sound.

To the right of the diagram, there is explanatory text that reads: "Sediment is the sand, mud, and pebbles that were once solid rock. Sediment flows in tributary streams and river channels of the Skagit, from the Cascade Mountains to Skagit Bay and Puget

Sound."

Overall, the illustration provides a clear and simplified view of the sediment transport process in a river system, from its initial erosion in the mountains, through transport by rivers, to its final deposition in deltas and floodplains. The accompanying text helps contextualize the illustration by explaining what sediment is and describing the specific example of the Skagit River system.

Figure 12.3.2: Major rivers of the Great Valley Province

This detailed map of California focuses on the Great Valley Province and its major rivers. The map shows a shaded area in the central part of the state, representing the Great Valley Province, which stretches from the northern to the southern parts of the state. The Great Valley Province is bordered by various national forests and parks, including Trinity National Forest, Lassen National Forest, Mendocino National Forest, Tahoe National Forest, Eldorado National Forest, Stanislaus National Forest, Inyo National Forest, and Sequoia National Forest.

The map highlights major rivers within the Great Valley Province in blue. Some of these rivers include the Sacramento River, Feather River, American River, Cosumnes River, Mokelumne River, Calaveras River, Stanislaus River, Tuolumne River, Merced River, Chowchilla River, Fresno River, San Joaquin River, Kings River, Tule River, Kaweah River, White River, and Kern River. These rivers are shown flowing through the valley and contributing to the region's hydrology.

The San Andreas Fault is marked with a red line, running parallel to the California coast from the northern part of the state down through the central region, highlighting a significant geological feature.

Several cities and towns are labeled, including Redding, Chico, Sacramento, Fairfield, Santa Rosa, Napa, Concord, San Francisco, Livermore, Fremont, San Jose, Salinas, Modesto, Stockton, Fresno, Bakersfield, and San Luis Obispo. Additionally, nearby states and regions are indicated, with Reno and Carson City in Nevada marked to the east of California.

Overall, this map provides a comprehensive view of the Great Valley Province in California, emphasizing its major rivers, the San Andreas Fault, and the surrounding geographic and political features.

Figure 12.3.3: A series of terraces along a river

This diagram illustrates the formation and structure of river terraces in a valley. The key elements of the diagram include the modern floodplain, labeled T4, representing the youngest and most recent sediment deposition area. River deposits are represented by dotted areas within the floodplain, indicating zones of active sediment deposition by the river. Terrace surfaces are labeled T1, T2, T3, and T4, with T1 being the oldest terrace surface and T4 being the youngest or future terrace. These terraces are depicted in green. Beneath the terraces and floodplain is bedrock, shown in a striped pattern, indicating the solid rock foundation of the valley.

The diagram includes additional annotations and a formula: $r1 = h1 / h2$, indicating the average rate of incision, where h1 is the height of the T1 terrace, and h2 is another height measurement related to the terrace surfaces. The term t1 represents the age of the T1 terrace surface, while h1 denotes the height of the T1 terrace.

Overall, the diagram provides a visual explanation of how river terraces are formed over time through processes of erosion and deposition. The terraces represent different periods of river activity, where the river has cut down into its bed, leaving behind elevated surfaces that mark previous levels of the floodplain. The inclusion of labels and the formula helps to contextualize the diagram, offering insights into the geological processes that shape river valleys and their terraces.

Figure 12.3.4: Ione formation river terrace near Merced Falls

This black-and-white photograph depicts a pastoral scene with a grassy field in the foreground and a hill in the background. The field is dotted with a few scattered trees, one of which stands prominently in the center of the image. The trees appear to be deciduous, as they are without leaves, suggesting the photo might have been taken in the late fall or winter.

In the background, atop the hill, there is a structure or collection of structures, partially obscured by trees and the hill's slope. These structures appear to be ruins or possibly an old fortification, as indicated by their rough, stone-like appearance and irregular outlines. The hill itself is sparsely vegetated, with patches of grass and some small shrubs.

The overall scene is tranquil and seems to be set in a rural or semi-rural area, characterized by open spaces and natural elements. The photograph captures a moment of stillness, highlighting the contrast between the open, grassy field and the more rugged, structured hill in the background. The lack of leaves on the trees and the presence of the ruins give the image a somewhat desolate yet serene atmosphere.

Figure 12.4.1: Land subsidence near Hanford, CA

This figure shows two photographs that illustrate land subsidence in the San Joaquin Valley, California, over several decades. Each image highlights a specific time period and amount of subsidence.

The left image, taken in 1977, shows a man standing next to a utility pole with a sign reading "San Joaquin Valley, California, BM 5861, Subsidence 9M, 1925-1977." The sign indicates the amount of land subsidence that has occurred between 1925 and 1977. The pole is marked with the year 1955 near the top, showing the level of the ground in 1955, and the man stands next to a marker indicating the ground level in 1977. The background features a field of crops, illustrating the agricultural setting of the area.

The right image, taken in 2016, shows a woman standing next to a measuring rod with signs indicating subsidence levels for the years 1988, 2004-2008, and 2016. The woman holds a sign reading "San Joaquin Valley, California, Subsidence 6.2 ft, 1988-2016, USGS 2016." This part of the image also highlights the amount of land subsidence that has occurred over the specified period. The background shows a concrete barrier and an open field, emphasizing the ongoing nature of the subsidence issue.

Together, these photographs provide a visual representation of the significant land subsidence in the San Joaquin Valley over multiple decades. The images effectively illustrate the dramatic changes in ground level and highlight the impact of subsidence on the region. The presence of the individuals and markers for different years offers a clear and tangible sense of the extent of subsidence over time.

Figure 12.4.2: 2017 map of the San Joaquin Valley showing the measured subsidence from synthetic aperture radar (SAR)

This map depicts the measurements of land subsidence in the San Joaquin Valley, California, for the year 2017. The map uses a color gradient to illustrate varying levels of subsidence, with dark purple representing less subsidence and bright yellow to orange indicating greater subsidence. The color scale on the map ranges from -0.5 feet to 1.5 feet, showing the depth of subsidence across the region.

The San Joaquin Valley is outlined in black, encompassing a large central portion of California. Major cities and towns within and around the valley are marked, including Stockton, Modesto, Turlock, Merced, Atwater, Los Banos, Fresno, Hanford, Tulare, Visalia, Delano, Porterville, Bakersfield, and more.

The map shows significant subsidence areas particularly in the central and southern parts of the valley, with noticeable concentrations around Merced, Atwater, Los Banos, and Fresno, where the colors shift towards bright yellow and orange, indicating higher subsidence levels. Northern and peripheral areas of the valley show less subsidence, represented by darker purple shades.

Surrounding geographical features and landmarks such as the Sierra National Forest, Yosemite National Park, Kings Canyon National Park, and Los Padres National Forest are also labeled, providing context for the valley's location within the broader landscape of California.

The map includes a compass rose in the upper right corner for orientation and a scale bar at the bottom indicating distances in miles, helping to understand the spatial extent of the subsidence. The title "2017 Subsidence Measurements" along with "SAR 2017" indicates that the data was collected using Synthetic Aperture Radar (SAR) technology.

Overall, this map provides a clear visualization of the areas within the San Joaquin Valley that experienced varying degrees of land subsidence in 2017, highlighting the regions most affected by this geological process.

Figure 12.4.3: Approximate extent of Tulare Lake

This map illustrates the approximate historical extent of Tulare Lake in California. The main map shows a detailed satellite view of the region with Tulare Lake labeled, indicating its former size and location.

Major rivers that feed into the lake, such as the San Joaquin River, Kings River, Tule River, and Kaweah River, are highlighted in blue. These rivers are significant in the region's hydrology and their connections to the lake are clearly depicted. The San Andreas Fault is marked with a red line, running through the southwestern part of the map, indicating its geological significance in the area.

The map labels various towns and cities within and around the former lakebed, including Fresno, Clovis, Hanford, Lemoore, Visalia, Tulare, Delano, Wasco, Shafter, and Bakersfield. The agricultural and urban landscape surrounding the former lake is visible, with numerous fields and grid-like patterns indicating extensive farming activities.

There is also an inset map providing a broader view of California, showing the location of the main map area in relation to the entire state. The inset map includes major cities such as San Francisco, Los Angeles, and other landmarks to provide geographic context.

Overall, this map effectively visualizes the historical extent of Tulare Lake, highlighting its size and the major rivers that contributed to it, along with the current geographic and urban features of the region.

Figure 12.4.4: A March 2023 pineapple express storm brought the resurgence of Tulare Lake

This image shows a road that is partially submerged in water, with a clear "Road Closed" sign prominently displayed in the foreground. The road extends straight ahead into the distance, bordered by water on both sides, suggesting that it is either a causeway or a road through a flood-prone area.

In the foreground, the "Road Closed" sign is accompanied by orange traffic cones, sandbags, and barriers to prevent vehicles from proceeding further. The sign is mounted on a barricade with two orange warning lights on top, which are likely to be flashing to alert drivers of the hazard. Additionally, there is another smaller sign behind the main barricade that reads "Water Over Road"

The scene is set under a blue sky with scattered clouds, and the water level appears calm but high enough to have submerged part of the road. Power lines run parallel to the road, stretching into the distance, and the surrounding landscape appears flat and expansive.

The image effectively captures a moment of road closure due to flooding, illustrating the impact of high water levels on infrastructure and the measures taken to ensure safety by closing the road and warning drivers of the hazard. The peacefulness of the scene contrasts with the underlying issue of flooding and the potential disruption it causes.

Figure 12.4.5: Dry Tulare Lake south of Lemoore, CA

This map is titled "Approximate Extent of Tulare Lake" and shows the approximate extent of the historical Tulare Lake, which is now dry. The main map features a detailed satellite view of the region with the outline of Tulare Lake identified, indicating where the lake once existed. Major rivers, including the San Joaquin River, Kings River, Tule River, Kaweah River, and White River, are shown with their pathways and connections to the lake area.

The San Andreas Fault run through the southwest edge of the lake. The map includes several towns and cities, such as Fresno, Clovis, Visalia, Tulare, Hanford, Lemoore, Delano, Wasco, Shafter, Bakersfield, Huron, Avenal, and Coalinga, providing context for the surrounding human geography.

An inset map shows the broader geographical context of California, highlighting the location of the main map area within the state. This inset includes major cities such as San Francisco and Los Angeles for reference.

Overall, this map provides a visual representation of the historical extent of Tulare Lake, emphasizing the major rivers that contributed to it and the current geographical and urban features in the region.

Figure 12.4.6: “Shaking Hazard Potential”

This map depicts the shaking hazard potential in California and parts of neighboring states. The map uses a color gradient to represent different levels of seismic hazard, ranging from blue for the lowest hazard to red for the highest hazard. This gradient

shows areas at risk for seismic activity and potential ground shaking.

The San Andreas Fault, a major geological feature known for its seismic activity, is prominently marked on the map. Other faults are also indicated, contributing to the overall understanding of seismic risk in the region. The map highlights the Great Valley Province with a blue outline, encompassing the central valley of California.

Major cities and towns are labeled, including Sacramento, San Francisco, San Jose, Fresno, Los Angeles, San Diego, and more. The map also extends to neighboring regions, showing parts of Nevada, with cities like Carson City and Las Vegas marked. Medford in Oregon and Boise in Idaho are also labeled, providing a broader geographic context.

The highest hazard areas are concentrated along the San Andreas Fault, particularly around the Los Angeles and San Francisco regions, where the color shifts to red. Lower hazard areas are indicated by blue and purple shades, found in the central and eastern parts of California and extending into Nevada.

The map includes a compass rose in the upper right corner for orientation and a scale bar at the bottom, indicating distances in miles. The legend titled "Shaking Hazard Potential" explains the color gradient used to represent different levels of seismic risk, along with markings for faults and the Great Valley Province.

Overall, this map provides a comprehensive visualization of seismic hazard potential in California, highlighting areas most at risk for significant ground shaking due to earthquakes. It emphasizes the importance of understanding seismic risks for urban planning and safety in these regions.

Figure Inset Box 12.4.1: “Nunez Fault: 1983 Coalinga-Naschmarkt Earthquake Location”

This detailed map illustrates the location of the 1983 Coalinga-Naschkmarkt Earthquake along the Nunez Fault. The map covers a region in California near the city of Coalinga.

The Nunez Fault, where the earthquake occurred, is identified as a short span in the center of the map. The San Andreas Fault runs along the western side of the map, illustrating its major impact on the region's geology. Significant historical rupture points along the San Andreas occurred in 1857 and 1901.

The map includes several labels for geographic locations and features, such as the Diablo Range, Alcalde Hills, and Pleasant Valley. The town of Coalinga is marked with a magenta outline, showing its proximity to the Nunez Fault. Other notable locations include the Lemoore Naval Air Station and various hills and valleys in the area.

Various fault types are indicated with different line styles, explained in the legend at the bottom of the map. The legend details the symbols used for surface rupture points, fault certainty, structural discontinuities, pre-Quaternary faults, and Quaternary faults. This comprehensive legend helps interpret the geological features and fault lines displayed on the map.

In the top right corner, an inset map provides a broader geographic context, showing the location of the main map area within California. Major cities such as San Francisco, Los Angeles, and San Diego are marked, helping to situate the earthquake location within the state.

The map includes a compass rose for orientation and a scale bar indicating distances in miles and kilometers. The title "Nunez Fault: 1983 Coalinga-Naschkmarkt Earthquake Location" clearly defines the map's focus, and the date "7/19/2023" indicates the publication or update date of the map.

Overall, this map provides a detailed and informative view of the geological features and fault lines in the Coalinga region, emphasizing the location and context of the 1983 earthquake along the Nunez Fault.

Figure Inset Box 12.4.2: Building at 187 South 6th Street, Coalinga, CA

This image is a black-and-white photograph showing the aftermath of an earthquake, likely from the 1983 Coalinga earthquake, given the previous context. The scene depicts significant structural damage to buildings and scattered debris.

In the foreground, there is a car covered in debris, suggesting that parts of the nearby structures collapsed onto it. Behind the

car, a person is walking through the rubble, which covers the ground extensively, indicating a considerable amount of destruction. The person appears to be either a rescue worker or a bystander assessing the damage.

The background shows a building that has partially collapsed. The structure's upper floor has fallen, causing the lower part of the building to crumble and disintegrate. Walls and ceilings are visibly damaged, with interiors of rooms exposed due to the collapse. The remains of the building are surrounded by a large amount of debris, including bricks, concrete, and other construction materials.

Overall, the photograph captures the severe impact of the earthquake, highlighting the destruction of infrastructure and the chaotic scene in the aftermath. The presence of the person in the image adds a human element, emphasizing the scale of the disaster and the immediate response to assess and address the damage.

Figure 12.5.1: Map of the San Joaquin basin during the late Miocene

This geological map illustrates the distribution of various geological formations and features in the San Joaquin Valley, California during the late Miocene. The map highlights both marine and non-marine environments, with a focus on volcanic formations and major fault lines.

The San Andreas Fault runs along the western side, diagonally from the bottom center of the map near Santa Cruz, continuing up past Coalinga, and into the region near San Francisco. This fault line is a major geological feature in California known for its seismic activity.

Marine environments are primarily located along the western edge of the map, adjacent to the Pacific Ocean. A marine basin (where deeper marine sediments are found) is shown in a region between Bakersfield and Coaling. Around the basin and extending northward and southward along the coast is a marine shelf (a shallower marine area).

Three volcanic areas are identified. The "Quien Sabe Volcanics" is on the coast halfway between San Francisco and Coalinga. The "Stanislaus Volcanics" are to the northeast of the Quien Sabe Volcanics. The "San Joaquin Volcanics" are to the southest of the Quien Sabe Volcanics, near Fresno.

Lowland areas run north-south in the center of the map. Highland areas run north-south on the eastern and western sides of the lowlands.

Several cities and geographical features are labeled on the map. These include San Francisco, Santa Cruz, Coalinga, Stockton, Fresno, Bakersfield, and Mount Diablo. Rivers and water bodies are depicted in blue lines, showing the drainage patterns and hydrology of the region.

Overall, this geological map provides a comprehensive overview of the diverse geological formations and environments in the region, highlighting key features such as volcanic areas, marine basins, and the San Andreas Fault.

Video 12.5.1: Oil and Gas Formation

What drives our cars, buses and planes, powers our electricity and allows us to cook our food and heat our water? Most of today's energy needs are met by fossil fuels like coal, oil and gas. These unique high energy fuels are non-renewable resources that took millions of years to form. About two billion years ago, marine organisms like algae and microscopic animals and plants died and settled on the ocean floor.

Beneath other sediments in the ocean and in the absence of oxygen, these fossils changed into a substance called kerogen. Under heat and pressure, kerogen gradually changes into oil or gas. The whole process usually takes at least a million years.

At the molecular level, oil and gas are hydrocarbons made up of hydrogen and carbon atoms. The constant pressure and movement of the Earth's crust squeezes oil and gas through the pores or spaces within rocks. Some oil and gas reaches the Earth's surface and seeps out naturally into land or water.

Often it is trapped beneath the surface by impermeable layers or rock structures like faults and folds. Within the crust, oil or gas deposits build up and form reservoirs. Reservoirs are like vast sponges filled with oil and gas.

They can be as large as a city. To find oil and gas deposits, geologists use a number of different survey techniques, including

seismic surveys, gravitational surveys and geological mapping. Seismic surveys use reflected sound waves to produce a 3D view of the Earth's interior.

New technologies, such as four dimensional projections and sophisticated graphic renderings of rock structures, are improving the way we find conventional oil and gas deposits. Energy resources that are currently difficult or expensive to extract are called unconventional oil and gas. In a world with limited energy resources, people are looking at more efficient ways of tapping into unconventional oil and gas or at alternative and renewable sources of energy from biofuels or the sun.

What do you think will be the energy sources of the future?

Video 12.5.2 Oil Fields - Kern County

This video shows an aerial flyover of oil fields in Kern County, California, in the southern San Joaquin Valley, where hundreds of wells extend across a flat, arid landscape in dense, repeating patterns connected by access roads. There is no narration. Background audio consists of generic music.

The most visible equipment is pump jacks, each with a counterweighted arm moving up and down in a steady rhythm to bring oil to the surface. These are evenly spaced across the landscape, creating a repeating pattern that extends for miles. Also visible are storage tanks, which appear as large cylindrical structures grouped near clusters of wells, where extracted oil is temporarily held.

Kern County is one of California's most productive oil regions because the San Joaquin Valley is a major sedimentary basin, formed as sediments eroded from surrounding mountains accumulated over millions of years. These sediments created layered rocks with pore spaces that can store petroleum. The dense spacing of pump jacks reflects how oil is distributed within these rocks—not as large underground pools, but within porous layers that vary in thickness and permeability. In Kern County, these conditions, along with thick, heavy oil, require many closely spaced wells to extract the resource.

This video supports learning by connecting the surface pattern of wells and storage tanks to the geologic history of California's sedimentary basins, helping explain why this region, especially Kern County, has such extensive and concentrated oil field development.

Figure 12.5.2: "Migration of oil and gas"

This cross-sectional diagram illustrates the geological processes involved in the formation and migration of oil and gas. The diagram shows different layers of rock and the conditions under which oil and gas are trapped and stored.

The top layer of the diagram is labeled "Impermeable cap rocks," and is shown in brown. These rocks act as a seal, preventing the upward movement of oil and gas. Below this layer are "Reservoir rocks," depicted in a lighter color, which are porous and capable of storing hydrocarbons.

Beneath the reservoir rocks are the "Source rocks," highlighted in shades of green and red. These rocks contain organic material that, under heat and pressure, transforms into oil and gas. The depth of these layers is marked on the left side of the diagram, ranging from 0 to 5 kilometers.

The diagram also shows different types of traps where oil and gas can accumulate. An "Anticline trap" is formed by the upward arching of rock layers, creating a pocket where oil and gas can collect. A "Fault trap" is created by the movement of rock along a fault line, which can trap hydrocarbons in the displaced rocks. A "Stratigraphic trap" is formed by variations in rock layers, such as changes in rock type or thickness, which can trap hydrocarbons. A "Reef or salt trap" is formed by the presence of a reef or salt dome, creating a barrier that traps oil and gas.

The diagram highlights the migration of oil and gas with red dashed arrows, showing the movement from the source rocks to the reservoir rocks. The "Oil window" and "Gas window" are also indicated, representing the depth ranges where temperatures and pressures are sufficient to convert organic material into oil and gas, respectively.

Overall, this diagram provides a detailed overview of the geological conditions and processes involved in the formation, migration, and trapping of oil and gas, illustrating the complexities of hydrocarbon accumulation in the Earth's subsurface.

Figure 12.5.3: Diagram showing the structure of several different types of oil and gas traps

This series of four cross-sectional diagrams illustrates different types of geological traps for oil and natural gas. Each diagram shows how hydrocarbons are trapped in the Earth's subsurface and how they are accessed by drilling.

The first diagram, labeled "Anticline Trap," shows a fold in rock layers forming an arch, with oil and natural gas accumulating at the crest of the fold. The layers include impermeable shale clay (A), porous reservoir rock (B), and source rock (C). An oil well (D) is depicted drilling into the reservoir rock, extracting the trapped hydrocarbons.

The second diagram, labeled "Fault Trap," depicts a geological fault where rock layers are displaced. The fault creates a barrier, trapping oil and natural gas in the reservoir rock against the impermeable shale clay. The oil well (D) drills into the reservoir rock to access the hydrocarbons.

The third diagram, labeled "Oil Traps on Salt Dome Flanks," illustrates how a salt dome can create traps for hydrocarbons. The salt dome pushes upward, deforming the surrounding rock layers. Oil and natural gas accumulate on the flanks of the dome, trapped by the impermeable shale clay and fault structures. An oil well (D) is shown drilling into the reservoir rock on the flank of the salt dome.

The fourth diagram, labeled "Stratigraphic Trap," shows how variations in rock layers can create traps for hydrocarbons. Changes in rock type or thickness can isolate pockets of oil and natural gas in the reservoir rock, with impermeable shale clay forming a seal. The oil well (D) drills into the reservoir rock to extract the trapped hydrocarbons.

In all diagrams, the key elements are labeled: A represents impermeable shale clay, B represents porous reservoir rock, C represents source rock, and D represents the oil well. These diagrams provide a clear visual explanation of the different mechanisms by which oil and natural gas can be trapped and accessed in the Earth's subsurface.

Figure 12.5.4: Wildcatters pushing their luck at drilling oil wells

This black-and-white photograph depicts a group of oil workers posing in front of an oil drilling rig. The scene appears to be from an earlier era of oil exploration, likely in the early to mid-20th century, judging by the attire and equipment.

The workers, about twenty in number, are dressed in work overalls and hats, many of them covered in oil and grime, indicating they have been working hard in the field. They are standing and crouching in rows, looking directly at the camera with expressions ranging from serious to slightly smiling. The group is positioned in front of the oil rig, which towers above them and dominates the background.

The drilling rig itself is a tall, lattice-like structure made of metal, typical of the oil rigs used during that period. There is a significant amount of equipment and machinery at the base of the rig, with piles of earth and materials scattered around. In the background, there are some industrial buildings and storage tanks, likely used for processing and storing the oil extracted from the well.

The landscape around the rig is barren, with sparse vegetation and signs of heavy industrial activity. Utility poles with wires stretch across the scene, suggesting the presence of necessary infrastructure to support the drilling operations.

Overall, this photograph captures a moment in the daily life of oil workers during the early days of oil exploration and drilling, highlighting the physical demands of the job and the industrial nature of the work environment. The image serves as a historical snapshot of the oil industry's development and the people who worked in it.

Figure 12.5.5: Sediment core

This image shows a collection of sediment cores taken from the ocean, displayed in vertical sections. Each core is housed in a long, narrow box, allowing for a clear view of the different layers of sediment that have accumulated over time. The cores are aligned side by side, with labels at the top indicating specific depths or sections.

The sediment cores display a variety of colors and textures, ranging from lighter shades of beige and brown to darker tones of

gray and black. These variations represent different types of sediment and geological periods, providing valuable information about the ocean's history and environmental changes.

The layers within each core are distinct, showing horizontal stratification that indicates different depositional events. Some layers appear more homogeneous, while others show more variation and complexity, such as changes in grain size or the presence of distinct sedimentary structures.

The cores are meticulously labeled, with small tags at the top of each section to ensure accurate identification and reference. At the bottom right corner of the image, a notation "14 PS1920–" is visible, likely serving as an identifier for the specific core or collection of cores.

Overall, this image captures the detailed and informative nature of ocean sediment cores, showcasing their importance in understanding the geological and environmental history of the Earth's oceans.

Figure 12.5.6: “Corcoran Clay Thickness”

This map depicts the thickness of the Corcoran Clay layer in California's Central Valley. The map shows variations in the thickness of the clay layer using a color gradient, with darker colors representing greater thickness and lighter colors indicating thinner layers. The gradient ranges from light yellow to dark brown, and the legend at the bottom left indicates that the thickness varies from 6.88 feet to 198.24 feet.

Contour lines are overlaid on the color gradient to provide precise measurements of the clay thickness. These lines are labeled with numerical values indicating the thickness in feet, offering detailed information about the distribution of the clay layer. The study area is outlined in black, encompassing a significant portion of the Central Valley, providing a clear boundary for the analyzed region.

Major cities within the study area are labeled, including Stockton, Modesto, Merced, Fresno, Tulare, Lemoore, and Bakersfield. These labels help provide geographic context for the clay thickness data, making it easier to understand the implications for different parts of the valley. Additionally, a compass rose is located at the top right corner of the map, indicating north for orientation, and a scale bar at the bottom right corner provides a reference for distance, indicating 0, 12.5, 25, and 50 miles.

Spatial patterns shown on the map:

- The Corcoran Clay is not uniformly thick across the valley.
  - In several large zones near the middle of the valley, especially in the central and south-central regions, the clay layer is very thick, commonly 100 to 200 feet.
  - These thick zones form elongated areas, meaning they stretch for long distances north–south rather than forming isolated spots.
  - Moving away from these central zones, the clay layer becomes gradually thinner.
  - Along the eastern edge of the valley and near the southern end, thickness commonly drops to 20 to 40 feet, and in some places becomes even thinner.
- Thickest deposits (shown in dark reds and purples with tightly spaced contours) occur in several elongated, basin-centered zones, particularly:
  - In the central to southern Central Valley, near and west of Fresno, Lemoore, and Tulare.
  - In parts of the northern Central Valley, southwest of Stockton and Modesto.
- Thinner areas (greens and light yellows) tend to occur:
  - Along the eastern margins of the valley near the Sierra Nevada.
  - Toward the southernmost end of the valley near Bakersfield, where thickness values decrease and contours spread out.
- The contour patterns suggest broad structural or depositional basins, with thickness increasing toward basin centers and decreasing toward valley margins.

The map highlights that the thickest areas of the Corcoran Clay layer are located primarily in the western and central parts of the valley, with thinner layers towards the eastern edges. This distribution is critical for understanding groundwater flow, subsidence, and agricultural practices in the region, as the Corcoran Clay acts as a significant confining layer affecting these factors. Overall, this map provides a detailed and informative visualization of the Corcoran Clay thickness across the Central Valley, helping to understand its geological and hydrological implications.

Figure 12.5.7: “Great Valley Province oil and gas fields”

This detailed map shows the Great Valley Province in California, highlighting oil and gas fields, the San Andreas Fault, and surrounding geographical features. The Great Valley Province is shaded in light blue, encompassing a large portion of central California, known for its significant agricultural and industrial activities.

The map marks oil and gas fields within the Great Valley Province in green. These fields are distributed throughout the region, with notable concentrations near Bakersfield, Fresno, and Stockton. The presence of these fields indicates areas of active or potential hydrocarbon extraction, which is crucial for understanding the region's economic and industrial landscape.

The San Andreas Fault, a major geological feature known for its seismic activity, is prominently marked with a red line running diagonally from the northwest to the southeast, passing near cities such as San Francisco, San Jose, and Bakersfield. This fault line is a key factor in the geological stability and earthquake risk of the area.

The map also labels major cities and towns, including Redding, Chico, Sacramento, Stockton, Modesto, Fresno, Visalia, Bakersfield, Santa Rosa, Napa, Fairfield, Concord, Livermore, Fremont, San Jose, Salinas, San Luis Obispo, and Santa Maria. These labels provide context for the human geography of the region, showing the proximity of urban centers to the oil and gas fields.

Surrounding natural features and national forests, such as the Trinity National Forest, Mendocino National Forest, Lassen National Forest, Tahoe National Forest, Eldorado National Forest, Stanislaus National Forest, Sierra National Forest, Sequoia National Park, and Sequoia National Forest, are also marked, highlighting the diverse landscapes that make up California.

The map includes a compass rose in the upper right corner for orientation and a scale bar at the bottom indicating distances in miles, providing a reference for the scale of the area depicted. The title "Great Valley Province Oil & Gas Fields" along with the legend helps to interpret the map's focus on hydrocarbon resources within the broader geographical context of the region.

Overall, this map provides a comprehensive visualization of the Great Valley Province, emphasizing the distribution of oil and gas fields, the significance of the San Andreas Fault, and the region's major urban and natural features.

This page titled 12.7: Detailed Figure Descriptions is shared under a CC BY-NC 4.0 license and was authored, remixed, and/or curated by Cole Heap.

13: MOJAVE AND COLORADO DESERTS

Introduction to the Mojave and Colorado Deserts

Most of the southeastern portion of the state of California is a desert environment. In fact, the USGS estimates that approximately 30% of the state of California is a desert environment! In this chapter, you will learn about geologic processes and features that are associated with desert environments, with a special focus on the highlights of the Mojave and Colorado Desert Provinces.

The Mojave and Colorado Desert Provinces are situated in the southeastern portion of the state of California. They share a geographic border with the Basin and Range Province to the north, as well as many geologic qualities, so the reader is encouraged to review the Chapter on the Basin and Range along with their reading of this chapter (Figure 13.1). In addition to offering unique landscapes and an opportunity to explore vast remote desert environments, these desert provinces are a source of mineral wealth and are the weekend playgrounds of many residents of southern California.



Figure 13.1: The Mojave and Colorado Desert Provinces of California. The highlighted area includes both the Mojave and the Colorado Desert areas, which are discussed as one province in the text. "The Mojave and Colorado Desert Provinces of California" by E. Wright, is licensed under CC BY-NC 4.0 / derivative from the original work. Access a detailed description of this map.

Learning Objectives

By the end of this chapter, you should be able to:

- Locate the Mojave and Colorado Desert provinces of California on a map of the state.
- Explain how the Mojave and the Colorado Deserts are created by geographic features, latitude, and atmospheric circulation.
- Describe the primary bedrock geologic characteristics of the Mojave and Colorado Desert Provinces.
- Recall the general geologic evolution of the Mojave and Colorado Desert Provinces.
- Describe the dominant desert weathering and erosion processes and their products in the Mojave and Colorado Desert Provinces.
- Describe evidence for climate changes impacting the Mojave and Colorado Desert Provinces.
- Describe the mineral resources in California's desert provinces.
- Assess the geologic hazards and risks associated with the Mojave and Colorado Desert Provinces.

13.1: Physiographic Features of the Mojave and Colorado Desert Provinces

13.2: Geologic Overview and Evolution of the Mojave and Colorado Desert Provinces
13.3: Creating the Desert Environment
13.4: Wind Driven Sediment Transport
13.5: Sand Dunes and Dune Fields
13.6: Erosional Desert Land Forms
13.7: Water in the Desert
13.8: Geological Resources of the Desert Provinces
13.9: Geologic Hazards of the Mojave and Colorado Desert Provinces
13.10: Chapter Summary
13.11: Detailed Figure Descriptions

This page titled 13: Mojave and Colorado Deserts is shared under a CC BY-NC 4.0 license and was authored, remixed, and/or curated by Martha House.

13.1: Physiographic Features of the Mojave and Colorado Desert Provinces

Location and Geomorphology of California's Desert Geomorphic Provinces

Together, the Mojave and Colorado Desert Provinces form a triangular wedge of desert terrain in southeast California, which shares many of the general physiographic and geologic features found to the north in the Basin and Range Province. Two distinct deserts underlie this region: the Mojave Desert and the Colorado Desert. Both regions exhibit basin and range style topography, although it is more muted than that of the Basin and Range Province. While the geology of these two regions records a long portion of Earth's history, climatic changes during the last million years are largely responsible for most landscape features present today. For that reason, these two deserts make an excellent study ground for desert processes.

The Mojave Desert is bounded by the Garlock fault to the north (Figure 13.1.1). Lying in the rain shadow of the southern Sierra Nevada mountains and the Transverse Ranges, the overall range in elevation of this high desert region is between 610-1220 meters (2000-4000 ft) above sea level. The I-15 highway travels northeast across this region.

The Colorado Desert lies to the south of the Mojave and extends to the southeastern border of California. It is part of the larger Sonoran Desert region, which extends into northern Mexico and western Arizona. The average elevation of this low desert region is approximately 305 m (1000 ft) above sea level; the lowest point is -82m (-269 ft) below sea level at the Salton Sea and the highest peaks are no more than 914 m (3000 ft) above sea level. Because of its overall low average elevation, it is sometimes referred to as the "Salton Trough". Although this region is arid, lying in the rain shadow of the Peninsular Ranges to the west, large portions are heavily irrigated for agriculture (the Imperial and Coachella Valleys that are north and south respectively of the Salton Sea).

Important and well known geographical landmarks in these regions include Red Rocks State Park, the Kelso Dunes, Mitchell Caverns, the Mojave National Monument, Joshua Tree National Park, Anza-Borrego Desert State Park, Sonny Bono Salton Sea National Wildlife Refuge, and the Coachella Valley.



Figure 13.1.1: Map of the Mojave and Colorado Desert Provinces from space. US highways, San Andreas and Garlock faults are labeled for reference. Salton Sea is in the southeast corner of the image. "Map of the Mojave and Colorado Desert Provinces from space" by Martha House, is licensed under CC BY-NC 4.0 / a derivative from the Map of Mojave. Access a detailed description of this map.

Mountains and Valleys

The simplified geological relationships in this region can be described as North-South trending exposures of uplifted basement rocks in the footwalls of Northwest-Southeast trending normal faults. Rocks exposed in these ranges include Late Proterozoic igneous and metamorphic rocks, Paleozoic sedimentary units, and Mesozoic igneous and metamorphic rocks (Figure 13.1.2). Ranges containing these older units are separated by basins filled with unlithified or weakly lithified sedimentary deposits that include alluvial fans and extensive seasonal (dry) lake beds, as well as sand dune fields and features, and the tracks of ephemeral river systems. Throughout this province, outcrops of younger (Late Cenozoic) volcanic rocks (cones, domes, flows, and tuff) overlap and are cut by the normal faults.

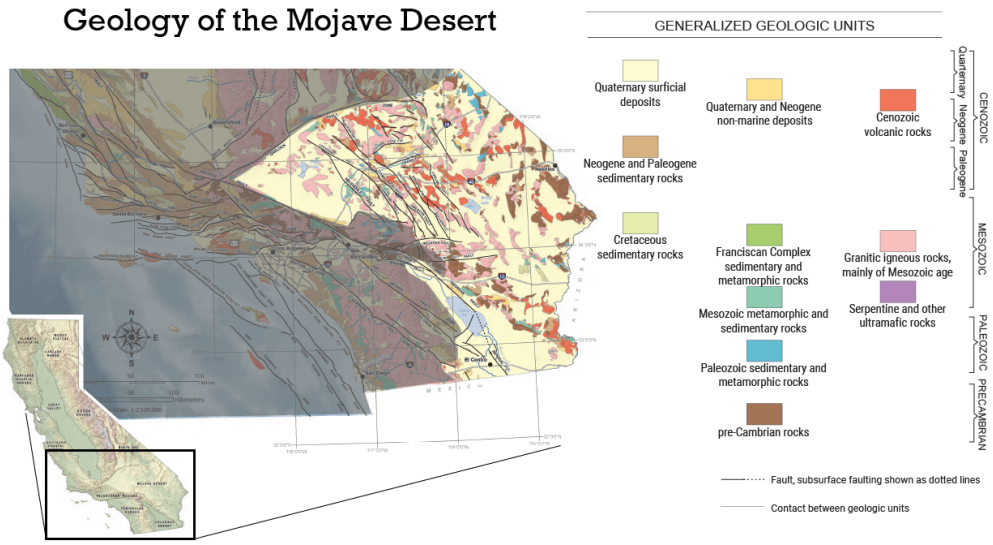


Figure 13.1.2: Excerpt from the Geologic Map of California with the Mojave and Colorado Desert Provinces highlighted. “Excerpt from the Geologic Map of California” by E. Wright, is licensed under CC BY-NC 4.0 / a derivative from the Geology of California. Access a detailed description of this map.

The southern portion of the Colorado Desert Province marks a transition from continental rift-related fault features to those associated with seafloor spreading in the northern Gulf of California to the south. The geologic features of this region are discussed in more detail in the following sections.

Box13.1.1: Mojave and Colorado Deserts Biosphere Reserve

The Mojave and Colorado Desert regions that lie within California were included into the World Network of Biosphere Reserves by the United Nations Educational, Scientific, and Cultural Organization (UNESCO) in 1984. Biosphere reserves are learning areas for sustainable development under diverse ecological, social and economic contexts, touching the lives of more than 250 million people. There are currently 727 biosphere reserves in 131 countries, including 22 transboundary sites.

Biosphere Reserves involve local communities and all interested stakeholders in planning and management. They integrate three main "functions":

- Conservation of biodiversity and cultural diversity
- Economic development that is socio-culturally and environmentally sustainable
- Logistic support, underpinning development through research, monitoring, education and training

These three functions are pursued through the Biosphere Reserves' three main zones:

- Core Areas comprise a strictly protected zone that contributes to the conservation of landscapes, ecosystems, species and genetic variation
- Buffer Zones surround or adjoin the core area(s), and are used for activities compatible with sound ecological practices that can reinforce scientific research, monitoring, training and education.

- Transition Area where communities foster socio-culturally and ecologically sustainable economic and human activities.

The Mojave and Colorado Deserts Biosphere Reserve includes a cluster of 3 core areas (Death Valley National Park, Joshua Tree National Park, and Anza-Borrego Desert State Park and Santa Rosa and San Jacinto National Monument) and a substantial percentage of the northern Mojave and Colorado Deserts surrounding these areas, the Mojave and Colorado Deserts Biosphere Reserve is one of only 46 ecosystems in the United States with this special designation.

References

1. *Mojave Desert Geomorphic Province. (n.d.). Digital-Desert. Retrieved September 4, 2023, from http://digital-desert.com / geomorphic-provinces/mojave-desert.html*
2. *What are Biosphere Reserves?* (n.d.). UNESCO. Retrieved August 31, 2023, from https://en.unesco.org/biosphere/about
3. Wick, B., & Hansen, K. (2016, March 12). *A Monumental Addition in California*. NASA Earth Observatory. Retrieved August 31, 2023, from https://earthobservatory.nasa.gov/images/87668/a-monumental-addition-in-california

This page titled 13.1: Physiographic Features of the Mojave and Colorado Desert Provinces is shared under a CC BY-NC 4.0 license and was authored, remixed, and/or curated by Martha House.

13.2: Geologic Overview and Evolution of the Mojave and Colorado Desert Provinces

Introduction to a Geologic Overview

The bedrock geology of this region is virtually identical to that of the Basin and Range Province, encompassing a broad range of geologic time and environments. The sequence of events that impacted this region is similar to that of most of the Western US and is described in more detail in A Brief Geologic History of California. Readers are encouraged to refer to Basin and Range to review the geologic similarities of these areas.

The Oldest Rocks of the Mojave Region

Basement and overlying sedimentary rocks of the Mojave and Colorado Desert Provinces are similar in ages and characteristics. As in the Basin and Range Province to the north, the oldest rocks exposed in the Mojave and Colorado Desert regions have ages of 1.7-2.5 billion years ago (early Proterozoic in age). They consist of metamorphic rocks derived from pre-existing sedimentary, volcanic, and igneous intrusive rocks (Figure 13.2.1). Some of these rocks contain high-grade metamorphic minerals and textures consistent with having experienced pressures and temperatures typical of the lower crust between 20 and 40 km (12 and 25 miles) below the Earth's surface. About 1.4 billion years ago, magmas intruded these older rocks (including the magmas that created the mineral deposits at Mountain Pass). Rocks similar to these form a basement complex throughout the eastern Mojave region and throughout the Great Basin and beyond. They formed in association with a long period of mountain building as smaller land masses were gradually assembling to form the core of the modern continental landmasses.



Figure 13.2.1: A typical outcrop of ancient metamorphic rocks consisting of poorly foliated amphibolite schist and gneiss with granitic dikes and intrusions exposed in the Providence Mountains of California. The rock hammer in front of the outcrop is about 30 cm for scale. "Gneiss" by USGS, is in the public domain.

Passive Margin Sedimentary Rocks & Fossiliferous Limestones

After about 1.4 billion years, erosion gradually wore down the landscape of this region to a nearly level plain, similar in character to the modern continental core of Australia or the Canadian Shield region. The large "supercontinent," Rodinia, that had assembled earlier in time began to break apart, and a proto-Pacific basin began to develop. The edge of the North America continent gradually sank beneath the ocean surface, and a thick sequence of sedimentary rocks began to accumulate on the continental margin. This passive continental margin setting persisted for nearly 800 million years, starting in the late Proterozoic and lasting

through all of Paleozoic time (570-245 million years ago).

Rocks containing sediments laid down in this passive margin environment are preserved throughout the Mojave and Colorado Province today in uplifted fault-block ranges. The oldest of these sedimentary deposits formed from sand, mud, and limey sediments deposited in shallow marine conditions, similar to the modern continental shelf around the Gulf of Mexico. In these environments, limey (Ca-rich) sediments consisting of the calcareous skeletal remains of algae and invertebrate shell material or precipitates directly from agitated, warm seawater. Extensive precipitation produced a thick sequence of carbonates (limestone and dolostone) that contain abundant fossils. Ancient carbonate rocks like those in the Mojave region tend to be enriched in the mineral dolomite ($CaMg(CO_3)_2$). Dolomite is typically a secondary mineral replacement of original calcite ($CaCO_3$) material. For more information, refer to Rocks and Minerals.

While the older carbonates in southeastern California formed from planktonic algae, several of the ranges within the Mojave Desert contain outcrops of Cambrian fossiliferous carbonates with abundant and varied fossils. These units include the lower through middle Cambrian Latham Shale, Chambless Formation, and Cadiz formation, which are correlated to the Carrera Formation of the Great Basin region, as well as the Tapeats Sandstone and Bright Angel Shale of the Grand Canyon region. These units contain a range of marine organisms including Cambrian trilobites (Figure 13.2.2) and algal structures (Figure 13.2.3), and Devonian sponges (stromatoperoids) and corals. In late Paleozoic time, coralline reefs became significant producers of carbonate sediments in this area.



Figure 13.2.2: An *Olenellus gilberti* trilobite, Order Redlichiida, Family Olenellidae, 15 mm along the axis, collected from the Pioche Shale, California, USA, from the late Lower Cambrian (Toyonian). "Olenellus gilberti lowlight CRF" by Dwergenpaartje, is licensed under CC BY-SA 3.0.



Figure 13.2.3: Oblate oncolites, a type of stromatolite, the size of a quarter in a carbonate matrix of the Chambless formation. These rounded structures are defined by concentric rings surrounding a core of rock or shell material and are preserved in a homogeneous grey limestone and dolomite matrix "Pisolites" by USGS, is in the public domain.

Mesozoic Deformation and Igneous Rocks

As with other regions throughout North America, Mesozoic units in the Mojave and Colorado Desert Provinces record evidence of a changing geologic environment. Beginning around 250 million years ago, the western margin of North America went from being a passive to an active continental margin (Figure 13.2.4). As depicted in this image, the western margin of the continent began to override and subduct the adjacent oceanic crust beneath the Pacific Ocean. Along with subduction of oceanic crust, uplift of the continental margin began, and erosion began to strip away the exposed rocks and sediments. Magma generated by subduction processes began to intrude upward, some of which reached the surface and erupted to form volcanoes. Beginning in the Jurassic Period, an extensive volcanic arc developed across the greater Mojave region. Deep below the surface, a series of great igneous intrusions (called batholiths) were gradually intruded throughout the region. These igneous rocks (consisting mostly of granite) form the cores of many of the ranges throughout the Mojave region. Great granitic intrusions formed in the Jurassic (170-140 million years ago) and again in mid-Cretaceous time (about 100 million years ago).

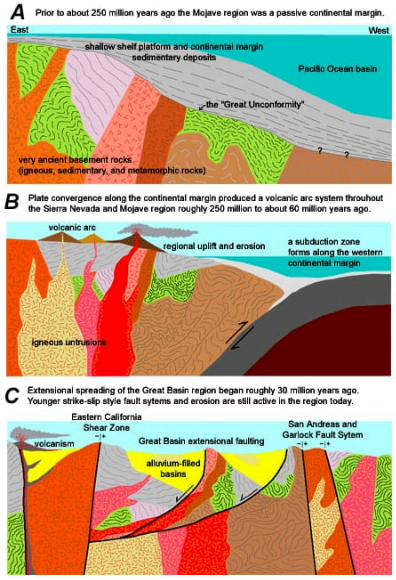


Figure 13.2.4: Simplified geologic history of the Mojave region in three panels: A) Prior to 250 million years ago, the Mojave was a passive continental margin with sediment deposits. B) From 250 to 60 million years ago, volcanic arcs formed due to plate convergence. C) Starting 30 million years ago, extensional faulting created alluvium-filled basins, with strike-slip faults and erosion active today. "Generalized geologic history of the Mojave Desert region" by USGS, is in the public domain. Access a detailed description of this image.

Late Cenozoic Volcanism, Faulting, and a Wetter Climate

The history of late Tertiary and Quaternary faulting and tectonism in the Mojave and Colorado Desert Provinces is unlike any other geologic province in California. The tectonic framework is most similar to the basin and range style structures to the north and east. While crustal extension was important here, this region is lacking deep basinal deposits and large normal faults like the Basin and Range Province to the north. Rather than basin and range style faulting, fault systems active in the region today are associated with regional right-lateral shearing forces associated with the San Andreas Fault System, the Garlock Fault, and the Eastern California Shear Zone all of these fault systems display measurable right-lateral displacements in the range of hundreds of kilometers, along with a component of normal faulting.

Throughout the Late Tertiary and Quaternary periods, large volcanic eruptions occurred fairly frequently in association with extension of the crust (for more information, see Basin and Range. Volcanic ash blanketed the landscape, and many of these ash beds are preserved in the alluvial deposits that accumulated in the basins. Eruptions associated with cinder cones and lava beds within the Mojave National Preserve began in the Late Tertiary (around 7 Ma) and have continued episodically through late Quaternary time (in the past one million years). The last volcanic episode in this area occurred roughly 8,000 years ago.

Late Cenozoic Basins

Sedimentary rocks that fill the basins of the Mojave, like those of the Basin and Range province to the north, document the age of crustal extension and the erosional responses to uplifting ranges. Across the region, sediments seem to begin accumulating

between 22-16 Ma, at the same time as early volcanic activity.

Rainbow Basin, near Barstow is a good place to practice field mapping and is therefore visited by many geology programs. The Barstow Beds, which are found in this area, are examples of fossiliferous units that provide insight into past climate in the region. The Barstow Beds are a 650 meter thick section of sedimentary units of Miocene age that are folded and faulted by subsequent tectonic activity. Mudstone, sandstone and conglomerate are interbedded with ash layers, which allow these units to be dated (16-13 Ma). Layers contain a range of mammal fossils including dogs, bears, cats, mammoths, horses, and camels. To the north, similar units are found at Red Rock Canyon State Park, indicating that these fauna were widespread at this time.

The Salton Trough in the southern region of this province is home of the Salton Sea. This transtensional basin (see the Basin and Range chapter) formed because of crustal stretching and subsidence caused by the meeting of the right lateral San Andreas Fault with the northern limit of the East Pacific Rise. This geologic interaction produced a large "graben" or rift valley that filled with sediments deposited by the Colorado River over millions of years. The Salton Sea was created in 1905 when the Colorado River breached an irrigation canal and flooded the low-lying region.

References

1. Dohrenwend, J. C. (2007). Tertiary and Quaternary Deposits. In *Geology and Mineral Resources of the East Mojave National Scenic Area, San Bernardino County, California* (pp. 73-75). USGS.
2. *Geology of Joshua Tree National Park | U.S. Geological Survey*. (n.d.). USGS.gov. Retrieved September 3, 2023, from https://www.usgs.gov/geology-and-ecology-of-national-parks/geology-joshua-tree-national-park
3. Glazner, A. F., Walker, J. D., Bartley, J. M., & Fletcher, J. M. (2002). Cenozoic evolution of the Mojave block of southern California. In *Geologic Evolution of the Mojave Desert and Southwestern Basin and Range* (Vol. 195, pp. 19-41). Geological Society of America
4. Harden, D. R. (2004). *California Geology*. Pearson Prentice Hall.
5. Haxel, G. B. (2007). Latest Proterozoic and Paleozoic strata. In *Geology and Mineral Resources of the East Mojave National Scenic Area, San Bernardino County, California* (pp. 56-58). USGS.
6. Haxel, G. B. (2007). Ultrapotassic rocks, carbonatite, and rare earth element deposit, Mountain Pass, southern California. In *Geology and Mineral Resources of the East Mojave National Scenic Area, San Bernardino County, California* (pp. 17-55). USGS.
7. Haxel, G. B., & Miller, D. M. (2007). Mesozoic Rocks. In *Geology and Mineral Resources of the East Mojave National Scenic Area, San Bernardino County, California* (pp. 59-68). USGS.
8. Hodges, C. A., & Theodore, T. G. (2007). Introduction. In *Geology and Mineral Resources of the East Mojave National Scenic Area, San Bernardino County, California* (pp. 4-8). USGS.
9. *Joshua Tree National Park (U.S.* (n.d.). National Park Service. Retrieved August 31, 2023, from https://www.nps.gov/jotr/index.htm
10. Miller, D. M., Wooden, J. L., & Conway, C. M. (2007). Proterozoic rocks and their mineralization. In *Geology and Mineral Resources of the East Mojave National Scenic Area, San Bernardino County, California* (pp. 12-16). USGS.
11. Miller, R. J., & Rytuba, J. J. (2007). Tertiary Rocks. In *Geology and Mineral Resources of the East Mojave National Scenic Area, San Bernardino County, California* (pp. 67-72). USGS.
12. *Natural History of the Granite Mountains*. (n.d.). Sweeney Granite Mountains. Retrieved September 2, 2023, from https://granite.ucnrs.org /natural-history-of-the-granite-mountains/
13. *Our Dynamic Desert*. (2009, December 18). Our Dynamic Desert. Retrieved August 31, 2023, from https://pubs.usgs.gov/of/2004/1007/intro.html
14. Palmer, A. R., & Halley, R. B. (n.d.). Physical stratigraphy and trilobite biostratigraphy of the Carrara Formation (Lower and Middle Cambrian) in the southern Great Basin. *USGS Professional Paper*, *1047*, 139. 10.3133 / pp1047
15. Stone, P., Stevens, C. H., & Orchard, M. J. (n.d.). *Fossils At Red Rock Canyon State Park, California*. My Stream. Retrieved September 4, 2023, from https://inyo.coffeecup.com/site/redrock/redrockfossils.html
16. Theodore, T. G. (2007). *Geology and Mineral Resources of the East Mojave National Scenic Area, San Bernardino County, California*. USGS.
17. Voiland, A. (2019, August 2). *Dreaming in the Mojave Desert*. NASA Earth Observatory. Retrieved August 31, 2023, from https://earthobservatory.nasa.gov/images/145400/dreaming-in-the-mojave-desert
18. Walker, A. S. (1996). *Deserts: Geology and Resources*. USGS.

This page titled 13.2: Geologic Overview and Evolution of the Mojave and Colorado Desert Provinces is shared under a CC BY-NC 4.0 license and was authored, remixed, and/or curated by Martha House.

13.3: Creating the Desert Environment

How Deserts Form

The Mojave and Colorado Desert Provinces are desert environments. Deserts are defined as locations of low precipitation; they exhibit extreme temperatures because of the lack of moisture in the atmosphere, including low humidity and scarce cloud cover. Without cloud cover, the Earth's surface absorbs more of the Sun's energy during the day and emits more heat at night, meaning that even though the days can be extremely hot, the nights can still be quite cold.

Deserts are not randomly located on the Earth's surface. The Mojave and Colorado Desert Provinces, like many of the world's deserts, are located at latitudes between 15° and 30°. These deserts occur at the interfaces of major wind belts and are regions where the rate of evaporation exceeds that of precipitation (**Figure** 13.3.1).

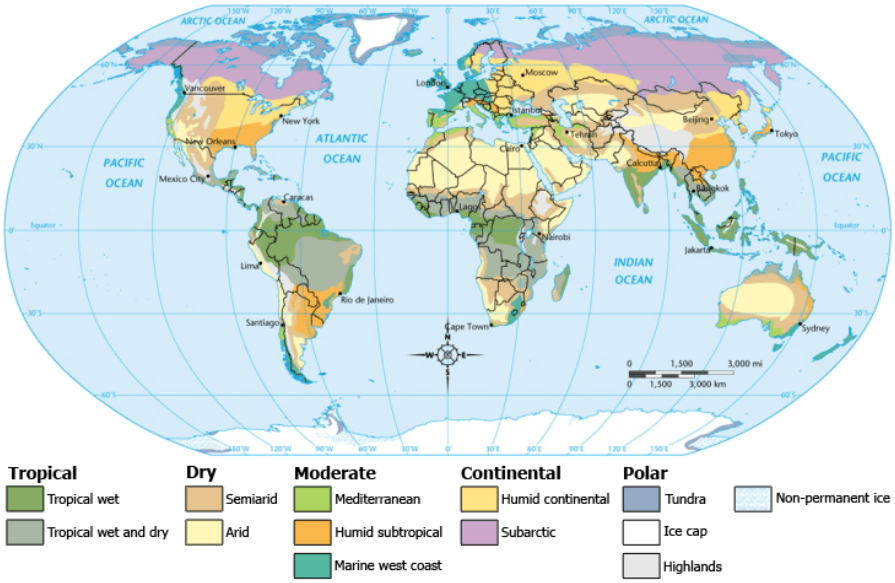


Figure 13.3.1: Major global climatic regions in relation to atmospheric convection cells and the Earth's continents. Rising air and low pressure creates rain and wet environments at 0° and 60° latitudes, while high pressure, sinking air creates drier conditions at 30° and 90° latitudes. As a result, regions in arid and semi-arid latitude zones have little or no vegetation "Climate map" by Paul Webb, is licensed under CC BY-SA 3.0. Access a detailed description of this map.

In these regions, prevailing wind circulation in the atmosphere causes sinking, dry air currents that create deserts like the African Sahara and Australian Outback. These deserts can readily be observed from space based on their notable lack of vegetation (Figure 13.3.2). Similar effects are found in polar regions, as cool dry air falls to the Earth, although polar regions are cold and dry, rather than hot and dry.



Figure 13.3.2: Earth from NASA's DSCOVR satellite shows arid desert regions of the African Sahara and the deserts of the Arabian Peninsula as tan regions."Earth image" by Raziel Abulafia, is licensed under CC0.

The Mojave and Colorado Desert Provinces are also impacted by their locations in the rain shadows of nearby mountain ranges. Rain shadow deserts form in the leeward side of mountain ranges (Figure 13.3.3). As the wind drives air up and over mountains, atmospheric moisture is released as snow or rain. Atmospheric pressure is lower at higher elevations, causing the moisture-laden air to cool. Cool air holds less moisture than hot air, and precipitation occurs as the wind rises up the mountain. After releasing its moisture on the windward side of the mountains, the dry air descends on the leeward or downwind side of the mountains to create an arid region with little precipitation called a rain shadow.

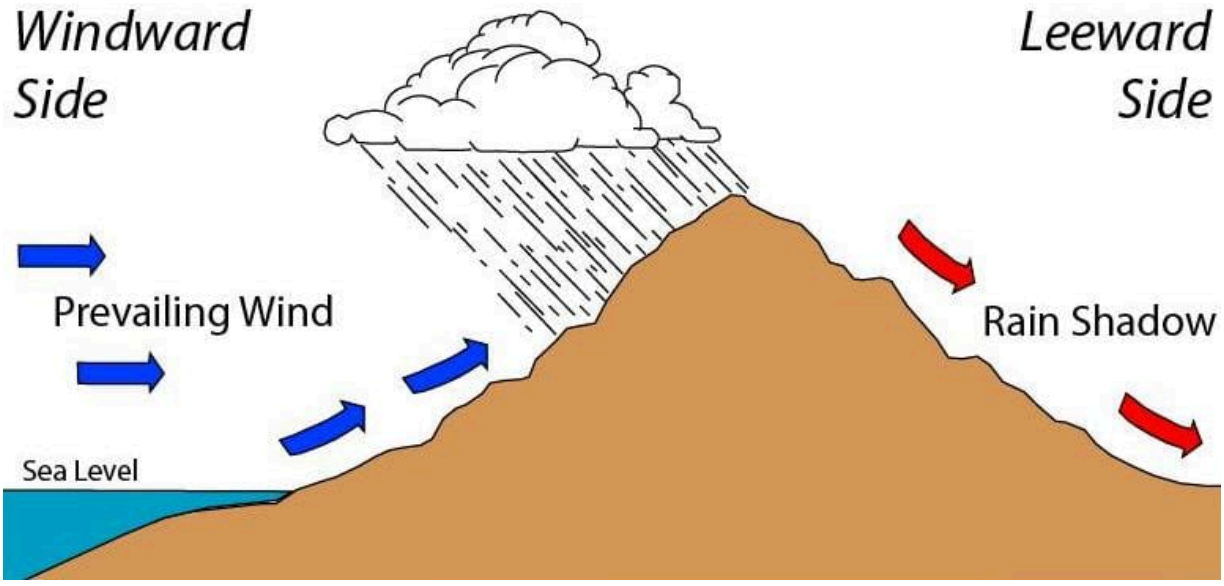


Figure 13.3.3: Diagram of a rain shadow and its effects. “Rain shadow effect” by Meg Stewart, is licensed under CC BY-SA 2.0. Access a detailed description.

Video: Rain Shadow

This brief video explains the formation of rain shadows in response to topographic barriers.

This interactive element is not available in this format. Visit the link or scan the QR code to access it online.

View this YouTube Video online

California's desert regions in the eastern part of the state are created by the rain shadow effect superimposed on regional belts of high atmospheric pressure that are established by interactions between the Trade Winds and the Prevailing Westerlies. Throughout the state, as westerly moist air from the Pacific rises over the Sierra Nevada and Cascades Mountains and the Transverse Ranges, it cools and loses moisture as condensation and precipitation on the upwind or rainy side of the mountains. This rain shadow effect also controls the climate conditions in the Basin and Range and Modoc Plateau Provinces to the north, and the Mojave and Colorado Desert provinces to the south.

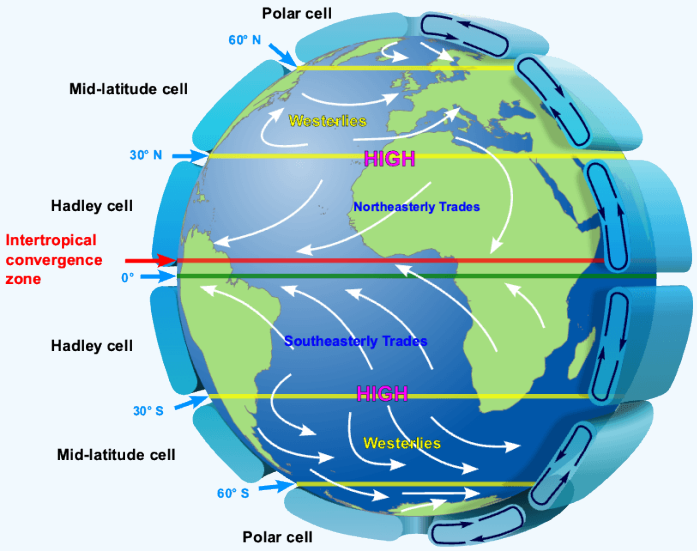
Desert Weathering

Weathering takes place in desert climates by the same means as other climates, only at a slower rate. Without abundant water in the arid environment, the chemical breakdown of rocks proceeds extremely slowly relative to equivalent rocks in humid climates. However, the mechanical breakdown of rock proceeds relatively quickly in the arid climate. In wet regions, the ground remains partially or fully saturated; as a result, plants covering the landscape bind the soil, and hence, prevent erosion. In dry climates, soil forms very slowly, and much of the bedrock remains exposed to erosion.

Box 13.3.1 Atmospheric Circulation and Deserts

Adapted from Introduction to Oceanography by Paul Webb.

Geographic location, atmospheric circulation, and the Earth's rotation are the primary causal factors of deserts. Solar energy converted to heat is the engine that drives the circulation of air in the atmosphere and water in the oceans. The strength of the circulation is determined by how much energy is absorbed by the Earth's surface, which in turn is dependent on the average position of the Sun relative to the Earth. In other words, the Earth is heated unevenly depending on latitude and angle of incidence. Latitude is a line circling the Earth parallel to the equator and is measured in degrees. The equator is 0° and the North and South Poles are 90° N and 90° S respectively (see the diagram of generalized atmospheric circulation on Earth). Angle of incidence is the angle made by a ray of sunlight shining on the Earth's surface. Tropical zones are located near the equator, where the latitude and angle of incidence are close to 0°, and receive high amounts of solar energy. The poles, which have latitudes and angles of incidence approaching 90°, receive little or almost no energy.



Inset Box Figure 13.3.1: Major global climatic regions in relation to atmospheric convection cells. Rising air and low pressure creates rain and wet environments at 0° and 60° latitudes, while high pressure, sinking air creates drier conditions at 30° and 90° latitudes. "Earth Global Circulation - en" by Kaidor, is licensed under CC BY-SA 3.0. Access a detailed description of this figure.

Generalized air circulation within the Earth's atmosphere consists of three cells of circulating air that span the space between the equator and poles in both hemispheres: the Hadley Cell, the Ferrel or Mid-latitude Cell, and the Polar Cell (Inset Box Figure 13.3.1). In the Hadley Cell, located over the tropics and closest to the equatorial belt, the sun heats the air, causing it to rise. The rising air cools and releases its contained moisture as tropical rain. The rising dried air spreads away from the equator and toward the north and south poles, where it collides with dry air in the Ferrel Cell. The combined dry air sinks back to the Earth at 30° latitude. This sinking drier air creates belts of predominantly high pressure at approximately 30° north and south of the equator, called the horse latitudes. Arid zones between 15° and 30° north and south of the equator thus exist within which desert conditions predominate. The descending air flowing north and south in the Hadley and Ferrel cells also creates prevailing winds called trade winds near the equator, and westerlies in the temperate zone.

Physical forces in the desert that break down rocks include the daily heating and cooling of rocks on the surface, expansion of plant roots in cracks, the freezing and melting of ice in cracks, and exposure to wind and precipitation (particularly during storms). When rainfall occurs, particularly long-slow drenching rain, the mountain slopes become saturated. The added weight induces rock falls, landslides, and other forms of mass movement of material down slope. Even though rain falls infrequently in the desert, when it does rain, large quantities of sediment move down slope and into canyons entrained in flash-flood waters or as debris flows (Figure 13.3.4). A debris flow is a moving mass of rock fragments, mud, soil, and enough water to keep the mass fluid. They typically travel at great speeds down steep canyons, but may move slowly across a gentle surface of an alluvial fan. They can flow for great distances until the water they contain dissipates or separates from the alluvial material.



Figure 13.3.4: Poorly sorted debris flow sediments. "Debris flow channel, Ladakh, NW Indian Himalaya" by DanHobley, is licensed under CC BY-SA 3.0.

The churning action of flood waters or sediment-choked debris flows pulverize rocks into fragments (gravel, sand, silt, and clay). As rocks break into smaller and smaller fragments, the surface area of the resulting sediment volume increases. This increase in surface area accelerates the chemical changes that convert feldspar and other minerals in granite into clays. Soluble components in the rock dissolve and are carried away. With increasing distance away from mountain sediment source areas, the average size of rock fragments steadily diminishes and particles become increasingly round in shape.

One unique weathering product in deserts is desert varnish. Also known as desert patina or rock rust, it is made of thin dark brown layers of clay minerals and iron and manganese oxides that form on very stable surfaces within arid environments (Figure 13.3.5). The exact way this material forms is still unknown, though biologic mechanisms have been proposed.



Figure 13.3.5: Petroglyphs carved into dark desert varnish. This work by Bob Cates, is licensed under CC-BY-NC-ND 2.0.

References

1. *Harden, D. R. (2004). California Geology. Pearson Prentice Hall.*
2. *Johnson, C., Affolter, M. D., Inkenbrandt, P., & Mosher, C. (2023). An Introduction to Geology. Salt Lake Community College.https://slcc.pressbooks.pub/introgeology/*

3. *Our Dynamic Desert*. (2009, December 18). Our Dynamic Desert. Retrieved August 31, 2023, from https://pubs.usgs.gov/of/2004/1007/intro.html
4. Palmer, A. R., & Halley, R. B. (n.d.). Physical stratigraphy and trilobite biostratigraphy of the Carrara Formation (Lower and Middle Cambrian) in the southern Great Basin. *USGS Professional Paper*, *1047*, 139. 10.3133 / pp1047
5. Stoffer, P. (2004). *Desert Landforms and Surface Processes in the Mojave National Preserve and Vicinity* [Open-File Report 2004-1007]. USGS.
6. Walker, A. S. (1996). *Deserts: Geology and Resources*. USGS.

This page titled 13.3: Creating the Desert Environment is shared under a CC BY-NC 4.0 license and was authored, remixed, and/or curated by Martha House.

13.4: Wind Driven Sediment Transport

Sediment Transported by Wind

While water is still the dominant agent of erosion in most desert environments, wind is also a notable agent of weathering and erosion. Possessing lower energy than water, wind transport nevertheless moves sand, silt, and dust. When wind blows, it carries sediment, called the sediment "load" (Figure 13.4.1). In much the same way that water carries sediment, wind does likewise, and the sediment is distributed between the bedload and suspended load. As with water, in wind these components depend on wind velocity.



Figure 13.4.1: Dust blows across a playa in the arid Mojave Desert. "Searles Lake duststorm" by Bobak Ha'Eri, is licensed under CC BY-SA 2.5.

Sand size material moves by a process called saltation in which sand grains are lifted into the moving air and carried a short distance where they drop and splash into the surface (Figure 13.4.2). This movement knocks and dislodges other sand grains which are then carried a short distance and splash dislodging still others.

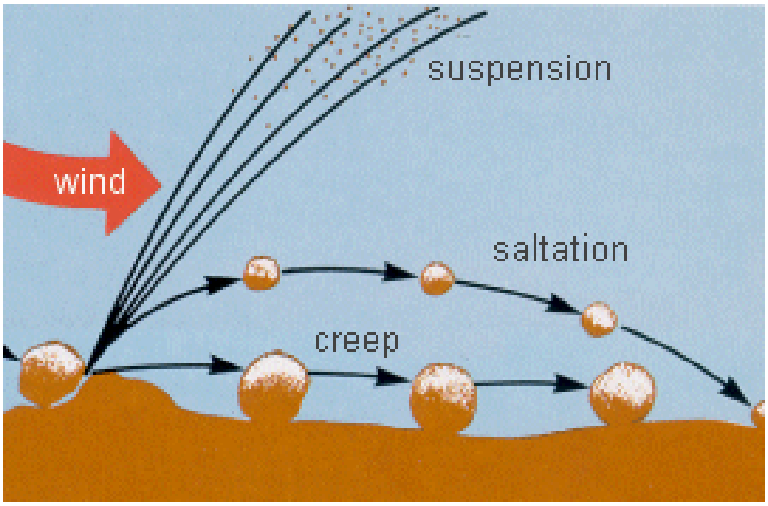


Figure 13.4.2: Three modes of wind-driven sediment movement. Wind moves sediment by suspension in the air, saltation (bouncing at the surface of the Earth) and creep (essentially incrementally being pushed from behind). "Diagram showing mechanics of saltation" by NASA, is in the public domain.

The zone of saltating sand is an effective agent of erosion through sand abrasion. Rocks and boulders lying on the surface may be blasted and polished by saltating sand (Figure 13.4.3). When predominant wind directions shift, multiple sandblasted and polished faces may appear. Such wind abraded desert rocks are called ventifacts (Figure 13.4.4).



Figure 13.4.3: Windblown quartz grains eroded from outcrops of the nearby Navajo Sandstone with a color that has been caused by iron staining. They are relatively even in size or well-sorted, and are rounded and frosted due to abrasion. "Hematite stain sand" by Mark A. Wilson, is in the public domain.



Figure 13.4.4: Wind-abraded ventifact. A black cobble on the desert floor is surrounded by smaller gravel and sand sized sedimentary fragments. The ventifact contains a distinctive faceted ridge formed by wind abrasion on the windward side of the cobble. The windward and leeward sides of this rock are smooth due to abrasion. "Ventifact Mojav eDesert" by Wilson4469, is licensed under CC0.

Query 13.4.1

This interactive element is not available in this format. Visit the link or scan the QR code to access it online.

View this Interactive Content online

Deflation and Desert Pavement

Desert pavement is a layer of interlocking pebbles that protect smaller sediments below (Figure 13.4.5). When a rock is removed a layer of sand can be found below. Wind easily removes the sand, leaving only the larger pebbles behind. Deflation, the lowering of the land surface by the removal of sand, silt and clay by wind erosion, has been long supposed responsible for the formation of desert pavement (Figure 13.4.6).



Figure 13.4.5: Gravel and cobble sized sedimentary rock fragments are closely juxtaposed in an exposed in desert pavement. There is very little space between these particles; sand sized and smaller particles have been removed by wind transport "Desert pavement" by Michael C. Rygel, is licensed under CC BY-SA 3.0.

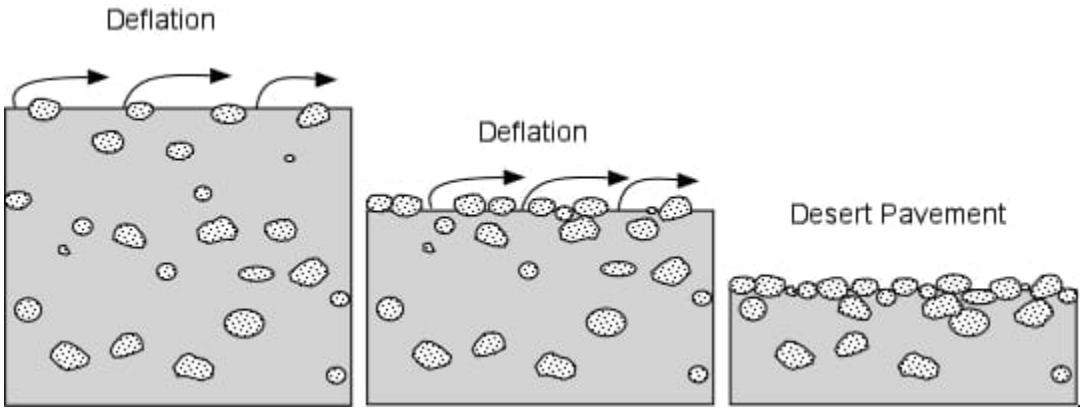


Figure 13.4.6:

In the process of deflation, the wind continually removes the smallest sized sediment until only the larger sizes are left, deflating the surface and creating desert pavement. "Deflation" by Noonat, is licensed under CC BY-SA 3.0.

There is evidence that other factors may be at work, as well. One theory states that the rocks are lifted to the surface by shrinking and swelling of clay layers below, while other studies suggest that pebbles started at the surface and smaller sediments were deposited around them. Regardless of how it forms, once desert pavement is in place, it helps shield any underlying sediments from eroding away.

Hazards of Blowing Sediment

For every bucket of sand that migrates into the Kelso Dunes, an undetermined volume of dust is generated that disappears into the wind. Dust storms in the Mojave region can be quite intense, and a hazard when dust concentrations are high enough to cause

white-out conditions. Windblown dust can be harmful to people breathing it. Dust may contain toxic compounds and it can carry pathogens such as the virus that causes Valley Fever; it also carries away valuable topsoil. On the other hand, dust that settles into stony soils of the desert provides improved retention of moisture and adds nutrients. Thus, dust can be both beneficial and destructive.

References

1. Harden, D. R. (2004). *California Geology*. Pearson Prentice Hall.
2. Johnson, C., Affolter, M. D., Inkenbrandt, P., & Mosher, C. (2023). *An Introduction to Geology*. Salt Lake Community College. https://slcc.pressbooks.pub/introgeology/
3. *Our Dynamic Desert*. (2009, December 18). Our Dynamic Desert. Retrieved August 31, 2023, from https://pubs.usgs.gov/of/2004/1007/intro.html

This page titled 13.4: Wind Driven Sediment Transport is shared under a CC BY-NC 4.0 license and was authored, remixed, and/or curated by Martha House.

13.5: Sand Dunes and Dune Fields

Forming Sand Dunes

Sand dunes are accumulations of sand; when they coalesce in large areas, these are called "dune fields". Such features often come to mind when people envision a desert environment.

An internal cross section of a sand dune shows a feature called cross bedding. As wind blows up the windward side of the dune, it carries sand to the dune crest depositing layers of sand parallel to the windward side (Figure 13.5.1). The sand builds up the crest of the dune and pours over the top until the leeward (downwind or slip) face of the dune reaches the angle of repose, the maximum angle which will support the slip face. Dunes are unstable features and move as the sand erodes from the stoss side and continues to drop down the leeward side covering previous stoss and slip-face layers and creating the cross beds. Mostly, these are reworked over and over again, but occasionally, the features are preserved in a depression, then lithified.

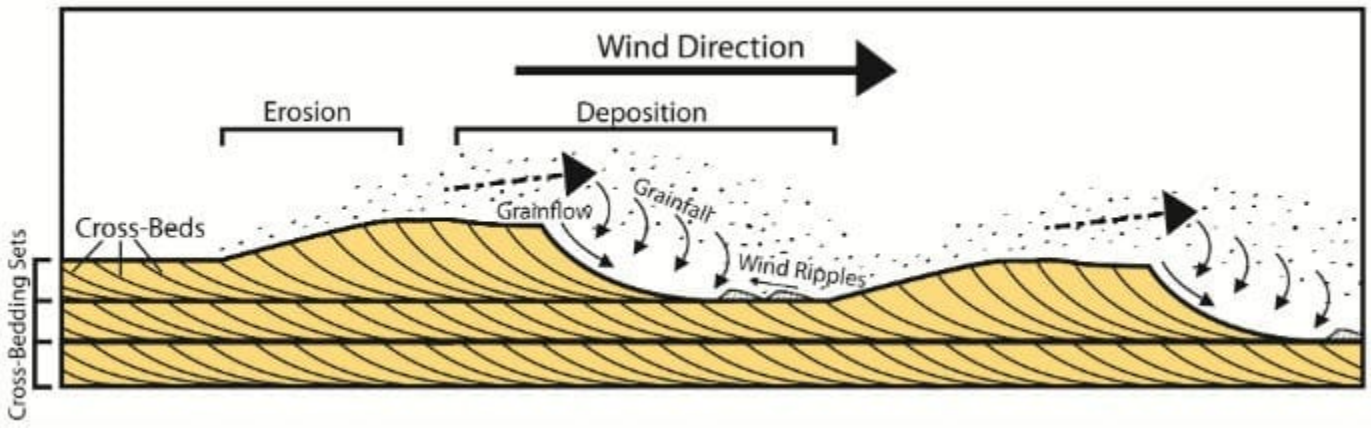


Figure 13.5.1: An illustrated cross section of a sand dune shows internal sediment layers that form cross bedding. As the wind blows from right to left, sand grains are pushed up the gentle slope of the dune. They then fall down the leeward face, forming tilted layers called "cross beds". "Formation of cross-bedding" by NPS, is in the public domain. Access a detailed description.

Types of Sand Dunes

The size, character, and extent of dune fields depend on many variables that determine the supply and mobility of eolian sediments. Factors include source materials, wind direction and magnitude, precipitation patterns, and landscape configurations relating to sediment supply, migration paths, and depositional setting. During wet periods, vegetation cover stabilizes dunes, leads to soil formation, and limits eolian sediment supply from source regions (playas, washes, fans, etc.). Conversely, during arid periods these source regions are re-activated.

The linkage between climate and dune reactivation is not clearly resolved. When dry periods persist, the supply of sediment provided by streams may cease, and the readily wind-transportable material may diminish. As a result, sand dunes may erode away due to lack of the supply of new sand, and desert pavements may form. The probable most effective climate for sand dune field formation is a balance of episodic, intense storms (to generate and move sediments to eolian source areas) with intervening windy, long, hot, dry periods (to hinder soil development and plant growth).

The Algodones Dune field, also known as the Imperial Dunes, is located southeast of the Salton Sea. This dune field is located at the junction of Arizona, California, and Baja California del Norte in Mexico) and displays a variety of different dune types. It is approximately 72 kilometers long by 10 kilometers wide (45 miles by 6 miles) and extends along a northwest-southeast line that correlates to the prevailing northerly and westerly wind directions.

Distinctive dune forms are visible in a photo of the Algodones Dune field taken from space (Figure 13.5.2). They include transverse megadunes and linear dunes. The transverse dunes, appearing much like a large tank tread along the long axis of the dune field, are the largest features. They were formed by strong and constant northwesterly winds. A fine pattern of smaller dunes has formed

along the crests and windward (northwestern) sides of these large dunes and point to continuing sediment transport activity. Networks of small dunes along the western side of the dune field suggest that wind direction here is more variable, and perhaps influenced by the large transverse dunes themselves. Long, linear dunes extending northwest-southeast are visible along the western edge of the dune field.

The oldest of the dunes in Figure 13.5.2 are the large, compound crescent dunes in the middle of the field. Compound crescent dunes are crescent-shaped and have other dunes on top of them. The crests run diagonally, southwest to northeast. This orientation is an indication that the dunes formed earlier than others in the field, at a time when wind conditions were different. The compound crescent dunes in this dune field are between 15,000 and 18,000 years old and slowly creeping southeast.

The rest of the dunes in Figure 13.5.2 are younger. Most are simple crescent dunes (the most common type in the world) that get their crescent shape when winds blow consistently in the same direction. These dunes are migrating toward the east-southeast.

The last type of formation in Figure 13.5.2 are linear dunes that run in long lines down the western edge of the field.

The source of sediment in this dune field is Lake Cahuilla, a large freshwater lake that occasionally forms in southern California. The lake fills when the Colorado River Delta clogs with silt, diverting the river to the north into the Imperial Valley. It slowly disappears when the river returns to its former course. Waves on the shores of the lake deposit the sand that feeds this dune field.

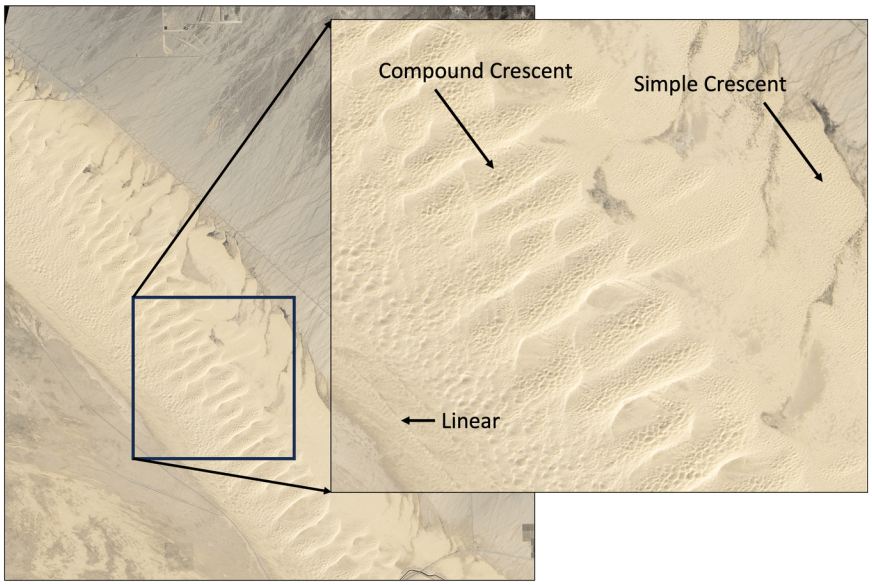


Figure 13.5.2: A portion of the Algodones dune field, which is situated between alluvial fans shed from adjacent mountain ranges. Compound crescent, simple crescent, and linear dunes are indicated. "Algodones Dune Field" by M. House after work by NASA, is in the public domain / a derivative of the original work. Access a detailed description of this map.

Kelso Dunes and Devils Playground

The Kelso Dunes and Devils Playground is a large area of eolian (wind blown) sand deposits within the Mojave National Preserve, east of Barstow, California. The dune field is also the largest in the Mojave Desert region and is notable because of its “booming” sands. A booming sound is created when people run down these dunes, probably due to the rounded shape of the sand grains in these dunes (Figure 13.5.3).



Figure 13.5.3: The Kelso dune field contains a high dune that stands out from the surrounding low-lying desert region. "Star Dune in the Kelso Dune Field" by USGS, is in the public domain.

Depositional features that can be found here include dunes (both actively-forming / migrating dunes and plant-stabilized dunes), sand sheets (sandy flats areas transitional between the source areas and the dunes), and sand ramps (sand build-ups on the flanks of the mountains). This dune field is located in the southeastern end of the greater Soda Lake-Kelso basin where the Granite Mountains and southern Providence Mountains form a barrier to prevailing winds. Wind entraining a flux of sand derived mostly from the Mojave River area at the western end of the basin is deposited near the rising mountain front of the Granite and Providence Mountains, causing the coarser fractions to accumulate.

During the Quaternary, the climate has changed. Wet regions have become drier and drier regions have become wetter. This change in climate has influenced the formation, stabilization, destruction, and re-activation of dune field systems through time in this region. The Kelso Dunes probably looked much different during the wetter periods of the Quaternary than they do today. In fact, field evidence suggests they may have been mostly or entirely stabilized by plant cover in the past.

Lake sediments constitute one of the major sources for eolian sediment, along with sediments derived from lower (distal) alluvial fans and ephemeral washes (such as Mojave River for the Kelso Dunes field). Investigations have demonstrated that at least two major pulses of dune emplacement occurred between 35,000 to 25,000 and 15,000 to 10,000 years before present, and a period of active dune reworking and construction has been ongoing for most of the past 4,000 years. These are times of dramatic increase in sediment supply from drying lakes and river input.

References

1. Dohrenwend, J. C. (2007). Development of pediment domes. In *Geology and Mineral Resources of the East Mojave National Scenic Area, San Bernardino County, California* (pp. 76-80). USGS.
2. *Geology of Joshua Tree National Park | U.S. Geological Survey*. (n.d.). USGS.gov. Retrieved September 3, 2023, from https://www.usgs.gov/geology-and-ecology-of-national-parks/geology-joshua-tree-national-park
3. Harden, D. R. (2004). *California Geology*. Pearson Prentice Hall.
4. *Johnson, C., Affolter, M. D., Inkenbrandt, P., & Mosher, C. (2023). An Introduction to Geology. Salt Lake Community College. https://slcc.pressbooks.pub/introgeology/*
5. *Our Dynamic Desert*. (2009, December 18). Our Dynamic Desert. Retrieved August 31, 2023, from https://pubs.usgs.gov/of/2004/1007/intro.html

This page titled 13.5: Sand Dunes and Dune Fields is shared under a CC BY-NC 4.0 license and was authored, remixed, and/or curated by Martha House.

13.6: Erosional Desert Land Forms

Alluvial Fans and Bajadas

Erosional processes are powerful forces that shape the land in the desert. These features can be considered as depositional (composed of sediment accumulations) or erosional (remnants of bedrock). Many of the desert landforms in this region were formed by processes active today, but many are remnants of the past.

As streams emerge into the valleys from the adjacent mountains, they create desert landforms called alluvial fans. When the stream emerges from the narrow canyon, the flow is no longer constrained by the canyon walls and spreads out. At the lower slope angle, the water slows down and drops its coarser load. As the channel fills with this conglomeratic material, the stream is deflected around it. This deposited material deflects the stream into a system of radial distributary channels in a process similar to how a delta is made by a river entering a body of water. This process develops a system of radial distributaries and constructs a fan shaped feature called an alluvial fan. Alluvial fans continue to grow and may eventually coalesce with neighboring fans to form an apron of alluvium along the mountain front called a bajada (Figure 13.6.1).



Figure 13.6.1: A large bajada developed at the base of the Hexie Mountains in the southern Mojave Desert, Southern California. The bajada forms a continuous sloping alluvial fan blanket that marks the transition between the mountains and the adjacent basin. "Bajadas coming down from the Providence Mountains. Seen from Joshua Tree, California" by G31©MEAGHAN, is licensed under CC BY-SA 3.0.

Query 13.6.1

This interactive element is not available in this format. Visit the link or scan the QR code to access it online.

View this Interactive Content online

Pediments and Inselbergs

As the mountains erode away and their sediment accumulates first in alluvial fans, then bajadas, the mountains eventually are buried in their own erosional debris. Such buried mountain remnants are called inselbergs, "island mountains," as first described by the German geologist Wilhelm Bornhardt (1864–1946). These features are quite common in these desert provinces, and are

found throughout the Mojave and Colorado Desert Provinces (Figure 13.6.2).



Figure 13.6.2: Inselbergs in Joshua Tree National Park. Inselbergs of granitic rock stand as higher hills and pillars among the low lying desert that surrounds them. "Lost Horse Valley from top of Ryan Mountain" by USGS, is licensed under public domain.

The "ocean" that these islands rise from is made up of pediments. A pediment is a gently sloping erosion surface or plain of low relief formed by running water in an arid or semiarid region at the base of a receding mountain front. As the front of the mountains is eroded by physical and chemical weathering, it retreats or is worn backward; a pediment is left on the land that the mountain front once occupied.

Large areas within the Mojave Desert are pediment surfaces. These pediments reflect both the antiquity of some mountain structures in the region and the persistent arid climatic conditions in the region. Perhaps the most notable pediment in the region is Cima Dome, a very broad, shield-shaped upland area within the Mojave National Preserve (Figure 13.6.3). This great, gently-sloped upland area represents a region where desert-style weathering and erosion has stripped away most of the relief to the point that the erosion keeps pace with surface weathering. The surface gradient is gentle enough to prevent gully-style down cutting.



Figure 13.6.3: The broad, gently sloped Cima Dome is an example of a pediment surface. The Cima Dome can be seen on the skyline behind the relatively flat desert surface in the foreground. The flat plain in the foreground is also a pediment with a thin veneer of alluvium. "Cimadome" by LCGS Russ, is licensed under CC BY 3.0.

In the Mojave Desert, many of the pediment surfaces are developed in granitic rocks, possibly due to the more-or-less uniform weathering and erosion characteristics of these large, homogeneous granitic intrusions.

Spheroidal Weathering

Some of the granitic bedrock exposed as inselbergs or elsewhere in this desert environment exhibits rounded shapes that are typical of spheroidal weathering. Spheroidal weathering is a type of exfoliation that produces rounded features and is caused when chemical weathering moves along joints in the bedrock. Imagine a trickle of rainwater or groundwater slowly moving along fractures within granite. As the water comes into contact with a potassium feldspar, a common mineral which is known for the ease with which it reacts with water and hydrogen, a new, soft clay mineral (kaolinite) replaces the feldspar. Kaolinite tends to build up around edges of the granite. There is an abundance of surface area for the clay to build up in because of the abundant joints, or cracks, in the rock. Because the clay is soft, the clay-rich edges of the granite erode and become softer and rounded (Figure 13.6.4). Eventually, this process can round out large amounts of rock in strange and picturesque ways (Figure 13.6.5) . Thin, rounded concentric sheets of rock also have a tendency to peel off in spheroidal masses.

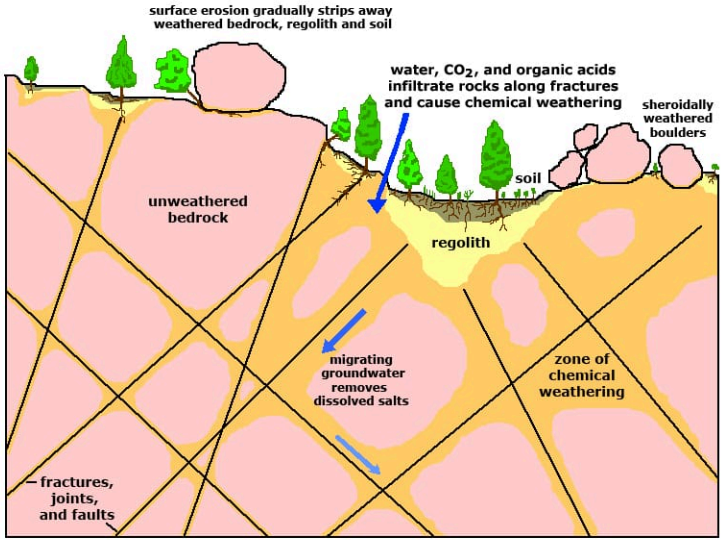


Figure 13.6.4: The process of spheroidal weathering. Fractures in bedrock are infiltrated by water, CO_2, and organic acids causing chemical weathering. Weathering by Phil Stoffer is in the public domain. Access a detailed description.

In humid regions, spheroidal weathering of granite typically occurs in the subsurface, as the bedrock breaks down into soil. In contrast, in arid regions the rate of chemical weathering is slow relative to the rate of surface erosion. As a result, in granitic terrains knob-shaped outcrops and spheroidal blocks accumulate on the surface. In the Mojave region, granite typically breaks down to form fairly uniform quartz and feldspar-rich, coarse-sandy sediments.



Figure 13.6.5: Spheroidally weathering granitic rocks in Joshua Tree National Park. Joshua trees in the foreground are ~3 meters tall. This work by Allison Jones is licensed under CC BY 4.0.

References

1. Dohrenwend, J. C. (2007). Tertiary and Quaternary Deposits. In *Geology and Mineral Resources of the East Mojave National Scenic Area, San Bernardino County, California* (pp. 73-75). USGS.
2. *Geology of Joshua Tree National Park | U.S. Geological Survey*. (n.d.). USGS.gov. Retrieved September 3, 2023, from https://www.usgs.gov/geology-and-ecology-of-national-parks/geology-joshua-tree-national-park
3. Harden, D. R. (2004). *California Geology*. Pearson Prentice Hall.
4. *Johnson, C., Affolter, M. D., Inkenbrandt, P., & Mosher, C. (2023). An Introduction to Geology. Salt Lake Community College. https://slcc.pressbooks.pub/introgeology/*
5. *Natural History of the Granite Mountains*. (n.d.). Sweeney Granite Mountains. Retrieved September 2, 2023, from https://granite.ucnrs.org/natural-history-of-the-granite-mountains/
6. *Our Dynamic Desert*. (2009, December 18). Our Dynamic Desert. Retrieved August 31, 2023, from https://pubs.usgs.gov/of/2004/1007/intro.html

This page titled 13.6: Erosional Desert Land Forms is shared under a CC BY-NC 4.0 license and was authored, remixed, and/or curated by Martha House.

13.7: Water in the Desert

Water Shapes the Landscape

While deserts are defined as arid regions, there is still abundant evidence of water in the landscape. Although rain does not fall often, rains can be quite heavy when they do fall, causing intense flash flooding. Thus, water is an important element in shaping the landscape. To read more about water in California, see California's Water. Another chapter, California's Climate, contains helpful information about past climate since it can impact the amount of available water in a particular region.

Playas and Ephemeral Rivers

There are areas within deserts that form enclosed basins, zones where streams enter, but none drain out. The water in these enclosed basins is removed by evaporation and a dry lake bed is formed called a playa.

Playas are among the flattest of all landforms. Such a dry lake bed may cover a large area and be filled after a heavy thunderstorm to only a few inches deep. They may preserve evidence of seasonal water by way of mud cracks (Figure 13.7.1) or salt deposits.



Figure 13.7.1: Typical playa in the Mojave Desert. The dessicated playa surface is covered with a mosaic of mud cracks. "Mudcracked playa, Mojave Desert, California" by Marli Miller with permission.

Playa lakes and desert streams that contain water only after rainstorms are called intermittent or ephemeral. Because of intense thunderstorms, the volume of water transported by ephemeral drainage in arid environments can be substantial during a short period of time. Desert soil structures lack organic matter that promotes infiltration by absorbing water. Instead of percolating into the soil, the runoff compacts the ground surface, making the soil hydrophobic or water-repellant. Because of this hardpan surface, ephemeral streams may gather water across large areas, suddenly filling with water from storms many miles away.

High-volume ephemeral flows, called flash floods, may move as sheet flows or sheet wash, as well as be channeled through normally dry arroyos or canyons. Flash floods are similar to debris flows in that they are a major factor in desert deposition. Dry channels can fill quickly with ephemeral drainage, creating a mass of water and debris that charges down the arroyo, and even overflowing the banks (Figure 13.7.2). Flash floods pose a serious hazard for desert travelers because the storm activity feeding the runoff may be miles away. People hiking or camping in arroyos that have been bone dry for months, or years, have been swept away by sudden flash floods.



Figure 13.7.2: Alluvial fan deposits cut by a dry stream. Alluvial fan deposits consisting of angular boulders and smaller cobbles, gravel, and sand deposits cover the desert landscape. A clearly developed channel where water recently flowed is apparent due to the finer sediment sizes and channels carved in them. "Wash 3" by USGS, is in the public domain.

The Mojave River

The Mojave River is the largest drainage system in the Mojave Desert. Its modern extent and capacity is only a fraction compared to its extent during the Last Glacial Maximum. At its peak during this last ice age, the Mojave River drainage basin extended from the San Bernardino Mountains in the west; it flowed east and north ultimately merging with the Amargosa River before draining into Lake Manley in Death Valley. At this peak period, waters of the Mojave River drainage system flowed through, or contributed water to, several great Pleistocene Lakes: Lake Manix (which incorporated modern dry lake basins Afton, Troy, Coyote, Harper, and Cronese basins), and Lake Mojave (including dry Soda Lake and dry Silver Lake basins). Today Soda Lake is the current terminal point of the Mojave River (although it has flowed into Silver Lake in historic times) (Figure 13.7.3).

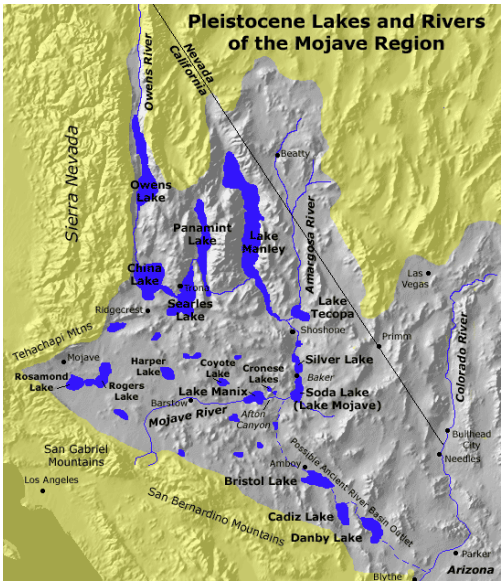


Figure 13.7.3: Map of the interconnected Pleistocene lake system of California. "Pleistocene Lakes and Rivers of Mojave" by Philip Stoffer, USGS, is in the public domain. Access a detailed description of this map.

The Mojave River: a 3D Journey

This silent video tracks the path of the Mojave River using remote sensing data that is draped over a digital elevation model. It is described below.

This interactive element is not available in this format. Visit the link or scan the QR code to access it online.

View this YouTube Video online

The animation opens with an aerial view of western San Bernardino County, California. The map displays county boundaries, cities, seven dry lakes, and intermittent and perennial streams. The map then zooms into the length of the Mojave River channel. The Mojave River is the largest of the streams and rivers that flow through the area and extends more than 100 miles east from its source in the San Bernardino Mountains to the end east of Afton Canyon (Thompson, 1929; Lines, 1996). Next, locations of points of interest appear on the map, including Mojave Forks Dam, Mojave Water Agency, Upper Narrows, Lower Narrows, and Afton Canyon. The floodplain aquifer boundary is then displayed, as is the surface water and groundwater monitoring sites in the area. The cities, dry lakes, points of interest, the river channel, and the monitoring sites remain visible for the duration of the river tour. The fly-through tour then begins, providing a 3D topographic view of the entire river channel length, which is dry for the entire length. The animation begins at the junction of Deep Creek and West Fork Mojave River at Mojave River Forks Reservoir located at the northern foot of the San Bernardino Mountains at an elevation of about 3,000 feet above sea level. From the reservoir, the river generally flows northward through the city of Victorville. The animation slows down as it approaches and travels through the Upper and Lower Narrows (small canyons). The tour continues generally north and northeastward through the city of Barstow and, eventually through Afton Canyon. After emerging from Afton Canyon, the river splits into separate channels leading to East Cronise Lake and Soda Lake.

Videographer: Sally House USGS California Water Science Center shouse@usgs.gov

This drainage system evolved along with the changing landscape beginning in late Tertiary time when tectonic uplift of mountain ranges around the Mojave region and changes in regional climatic conditions were occurring at the same time. The modern river system began developing as westward-flowing stream drainages were blocked by the uplift of the Transverse Ranges along the greater San Andreas Fault System. The combination of blocked drainage systems and increased precipitation with the onset of cooler or ice age conditions at the close of the Tertiary resulted in the filling of basins with water (and sediments). Progressively through the latest Tertiary and into the Quaternary periods, lakes filled and streams overflowed through low divides between ranges and flooded adjacent basins. In this manner, the Mojave River evolved from the spilling over of lakes in the western Mojave Desert region. These large lakes do not exist today. Two large lakes that played a significant role in the development of the landscape in the Mojave National Preserve area were Lake Manix and Lake Mojave. Sediments associated with these ancient lake deposits (and others in the region) record a story of climate change in the region (Figure 13.7.4).



Figure 13.7.4: Pleistocene Lake Manix sediments. Easily eroded, horizontal ancient lake sediments are exposed in this arid desert landscape. These horizontal layers have been cut and exposed by modern stream systems. "LakeManixSediments" by Wilson44691, is licensed under public domain.

Lake Manix (Figure 13.7.3) was a large inland lake that was located in the Barstow, CA region and Lake Mojave was in the Baker, CA region; there are many remnants of these larger features that persist today. The development of these lakes and other lakes

in the region was progressive with time, with Manix Lake filling first, and Lake Mojave forming later when the Lake Manix filled to capacity and spilled westward, ultimately carving Afton Canyon during the last glacial maximum about 18,000 years ago.

The Salton Sea

The Salton Sea is California's largest lake (Figure 13.7.5). It was formed by accident in the early 1900s, when water diverted from the Colorado River broke through canal gates and filled the low-lying basin—continuing a long history of drying and filling. Today, the lake is fed primarily by the runoff from farm irrigation, and to a lesser extent from urban runoff, groundwater and rainfall. This lake has no natural outlet, so water must evaporate to leave the system; this makes it saltier than the ocean.

The sea occupies a transtensional rift valley called the Salton Trough. Home to important agricultural areas, this rift valley graben reflects the combined effects of the San Andreas fault and the northern limits of the East Pacific Rise.



Figure 13.7.5: The Salton sea. In this aerial image, the Salton Sea is surrounded by a desert landscape of uplifted mountains and surrounding sedimentary basins. To the northwest and southeast of the Salton Sea, agricultural areas appear as a patchwork of green squares. The Imperial Valley lies to the south. "Imperial Valley and Salton Sea, California" by NASA, is in the public domain.

This area has become an environmental problem, with periodic episodes of fish-die offs and an ongoing odor of decay. On the other hand, brines derived from this sea may ultimately be a valuable source of lithium.

Query 13.7.1

This interactive element is not available in this format. Visit the link or scan the QR code to access it online.

View this Interactive Content online

References

1. Dohrenwend, J. C. (2007). Tertiary and Quaternary Deposits. In Geology and Mineral Resources of the East Mojave National Scenic Area, San Bernardino County, California (pp. 73-75). USGS.
2. Geology of Joshua Tree National Park | U.S. Geological Survey. (n.d.). USGS.gov. Retrieved September 3, 2023, from https://www.usgs.gov/geology-and-ecology-of-national-parks/geology-joshua-tree-national-park
3. Harden, D. R. (2004). California Geology. Pearson Prentice Hall.
4. Lines, G.C., 1996, Ground-water and surface-water relations along the Mojave River, Southern California: U.S. Geological

Survey Water-Resources Investigations Report 95-4189, 43 p., https://doi.org/10.3133/wri954189.
5. Natural History of the Granite Mountains. (n.d.). Sweeney Granite Mountains. Retrieved September 2, 2023, from https://granite.ucnrs.org/natural-history-of-the-granite-mountains/
6. Our Dynamic Desert. (2009, December 18). Our Dynamic Desert. Retrieved August 31, 2023, from https://pubs.usgs.gov/of/2004/1007/intro.html
7. Reheis, M. C., Miller, D. M., Paces, J. B., Oviatt, C. G., Redwine, J. R., Kaufman, D., Bright, J., & Wan, E. (2021). Geomorphic history of Lake Manix, Mojave Desert, California: Evolution of a complex terminal lake basin. Elsevier. https://doi.org/10.1016/j.geomorph.2021.107901
8. Thompson, D. (1929). The Mojave Desert Region, California. a Geographic, Geologic, and Hydrologic Reconnaissance. Department of the Interior.
9. Walker, A. S. (1996). Deserts: Geology and Resources. USGS.

This page titled 13.7: Water in the Desert is shared under a CC BY-NC 4.0 license and was authored, remixed, and/or curated by Martha House.

13.8: Geological Resources of the Desert Provinces

Evaporite Deposits

The Mojave and Colorado Desert Provinces are the home to extensive evaporite deposits, as well as an important rare earth element mine. This section will discuss these resources. Gold and copper mines are also found throughout the region, generally associated with Mesozoic and Cenozoic igneous rocks; refer to Sierra Nevada for more about these types of resources.

A by-product of the development of playa lakes is the accumulation of evaporite deposits which can be mined. Evaporites are minerals that form by precipitation directly from water. They are typically water soluble, so when lakes refill, the minerals dissolve. The catalyst for their formation is the high salinity levels that develop as the lakes evaporate. Evaporite minerals are often referred to as “salts”, and indeed, table salt (halite) is an example of one such evaporite mineral (Figure 13.8.1), as is sylvite (KCl). Other well-known evaporite minerals include gypsum and calcite.



Figure 13.8.1: Halite from Searles Lake is an example of an evaporite mineral from this region. In this image of a specimen collected by someone, clusters of pink Halite cubes grown on a finer substrate. “Halite Nahcolite” by Rob Lavinsky, is licensed under CC BY-SA 3.0.

Halite is mined as a food additive, chemical agent, water softener, or road de-icer. Gypsum is used as a building material; it is the main component in dry wall and is also used as a fertilizer. Other evaporites include sylvite-potassium chloride-which is used in agriculture, medicine, food processing, and other applications.

The mineral hanksite is another evaporite mineral found in this area (Figure 13.8.2). It was first identified at Searles Lake in 1888 and named for an American geologist (Henry Garber Hanks). It is a sulfate mineral ($Na_{22}K(SO_4)_9(CO_3)_2Cl$) that can be found in dry lakes, typically buried in mud.



Figure 13.8.2: A cluster of dark colored doubly terminated hexagonal hanksite crystals collected from Searles Dry Lake. "Hanksite crystal step from Searles Dry Lake, California" by Alisha Vargas, is licensed under CC BY 2.0.

Sodium borates are another type of salt which accumulate in the California dry lakes. Borates are hydrous minerals built on the Borate anion (BO_4). These include ulexite (Figure 13.8.3), borax, colemanite, and kernite. These minerals were the basis for the borax industry that developed initially in the Death Valley region. Over time, borate mining moved away from the Death Valley region, and focused on the Searles Lake region in the Mojave where mining continues at present (Figure 13.8.4). The origin of the boron (B) in these minerals is thought to be nearby volcanic materials. As hot water associated with young volcanic centers leached these rocks, it carried boron into the playa lakes, where it precipitated as borate minerals.



Figure 13.8.3: Ulexite specimen of "TV rock" collected from near Boron, CA. Elongate fibrous Ulexite crystals in this specimen occur as columnar masses on a calcite base and are roughly 6 cm long. "Ulexite Calcite" by Rob Lavinsky, is licensed under CC-BY-SA-3.0



Figure 13.8.4: Trona, CA, which abuts Searles Lake, is the location of borate mining. In this desert landscape, the large flat white playa is the source of borate minerals mined here. "Trona CA on Searles Lake" by Bobak Ha'Eri, is licensed under CC BY-SA 2.5.

Box 13.8.1: Searles Lake Borate Mining

Searles Lake is known for the abundance of rare elements and evaporate minerals, such as trona, hanksite, and halite formed within its sediments. Evaporites are minerals that are left behind when saltwater evaporates. During the Pleistocene Epoch (beginning approximately 2 million years ago), Searles Lake was one of a chain of lakes fed by stream flow from the Sierra Nevada to the west. Lake levels rose and fell depending on glacial outwash from the Sierra Nevada as climate shifted. Successive layers of sediment were deposited as lake levels fluctuated, preserving an important record of regional climate change. The lakes gradually dried up completely as climatic conditions became hotter and drier (as today), forming a string of playas—enclosed basins with no outlets.

Borates that are mined at Searles Lake are chemical compounds that include the element boron (B) and are important as providers of an essential plant micronutrient, for metallurgical applications, and as components of specialized types of glass, anticorrosive coatings, fire retardants, and detergents.

The Rio Tinto mine is one of Earth's richest borate deposits (Inset Figure X.2). Together with mines in Argentina, they produce almost 40 percent of the world's supply of industrial borate minerals. The mining complex in Searles Lake playa includes tailings piles, open pit, processing facilities and settling ponds spread across approximately 54 square kilometers (21 square miles).These mining operations extract sodium and potassium-rich minerals (primarily borax and salt) for industrial use.

This mine is the largest open-pit mine in California and is among the largest borate mines in the world (Inset Box Figure 13.8.1). Concentric benches along the pit wall are accentuated by shadows and mark successive levels of material extraction. Mine tailings are visible as stacked terraces along the northern boundary of the mine. Ore processing facilities occupy a relatively small percentage of the area, and are located directly to the west of the open pit.



Inset Box Figure 13.8.1: One of Earth's richest borate deposits is at the center of the largest open-pit mine in California. This aerial image of an open pit mine reveals the large pits surrounded by mining infrastructure in the desert landscape. Settling ponds can be seen along with the terraced levels of the open pit. "Rio Tinto Borax Mine" by NASA, is licensed under public domain.

Borate minerals such as borax, kernite, and ulexite are found in the deposits at the Rio Tinto mine. The first mining claim in the area was filed in 1913 following the discovery of boron-bearing nodules during well drilling. Much of the mine workings were underground until 1957, when U.S. Borax changed to open-pit mining.

Query 13.8.1

This interactive element is not available in this format. Visit the link or scan the QR code to access it online.

View this Interactive Content online

Lithium Mining

A massive underground brine pool known as The Salton Sea Geothermal Reserve, located about 90 miles south of Palm Springs has been identified as a potentially important source of the element lithium. This region, which is now referred to as Lithium Valley, has one of the worlds largest deposits of lithium. Lithium (Li) is used in many modern batteries, such as those used in electric cars, smart phones and grid energy storage. This very light weight metal allows batteries to hold their charge for a long time. This type of energy storage is critical to reducing the use of fossil fuels.

Lithium is widely occurring, but does not tend to occur in its elemental form; rather, it occurs as ions in fluids, or as a minor element in granitic rocks or pegmatites. High concentrations of this element are relatively rare, but large deposits can be found in dry lakes where years of evaporation have concentrated lithium and other elements found in briney waters on the dry lake beds. In most places on earth, Lithium is mined by flooding these dry lakes or by pumping brines rich in lithium to the surface and allowing brine pools to evaporite. However, the Salton Sea deposit is contained in brines that are already pumped through geothermal systems that generate power for southern California. The Li-rich brines were considered to be waste products until recently, but with growing dependence on this element, companies are looking at technology that can be used to extract Lithium from the brines without relying on evaporative processes.

Video How the troubled Salton Sea could become the worlds largest Lithium supplier

This video discusses the production of lithium at the Salton Sea and its potential value.

This interactive element is not available in this format. Visit the link or scan the QR code to access it online.

View this YouTube Video online

Rare Earth Mining

In the eastern edge of the Mojave Province, the largest concentration of rare earth elements in the western hemisphere is currently mined. The Mountain Pass Mine (Figure 13.8.5, Figure 13.8.6), located on the border of California and Nevada is a strategically important source of the rare earth elements Lanthanum, Cerium, Neodymium, Samarium, Europium, and Gadolinium. These materials are used as catalysts for metallurgy and for manufacturing of glass and ceramics, as well as magnets.

The large, high grade reserves of rare earth elements here (REE's) are hosted in carbonatite which intrudes 1.7 Ga gneisses. Carbonatite is an unusual Ca-rich igneous intrusive rock. The most important rare earth elements, Cerium and Lanthanum, are concentrated in a rare carbonate mineral called bastnasite $(Ce,La)CO_3F$.



Figure 13.8.5: The Mountain Pass Mine, imaged by the Advanced Land Imager (ALI) on NASA's Earth Observing-1 (EO-1) satellite on May 28, 2011. In this image, the Mountain Pass mine, adjacent to US15, appears as a light colored disturbance to the desert landscape. "Mountain Pass 2011" by NASA, is licensed under public domain.



Figure 13.8.6: The Mountain Pass Rare Earth Mine and Processing Facility is the only active and scaled rare earth mining and processing facility in the United States. The facility is owned by MP Materials. The mine contains a large terraced pit, large tailings piles and numerous buildings associated with the processing of material that has been extracted. "Mountain Pass Rare Earth Mine and Processing Facility" by Tmy350, is licensed under CC BY-SA 4.0.

Video ({13{.}8{.}\eatSpaces{1} \endSpaces}\): Rare earths crunch? Why we need them and who has them

This short video discusses the value of geologic deposits that contain high concentrations of rare earth metals.

This interactive element is not available in this format. Visit the link or scan the QR code to access it online.

View this YouTube Video online

Query 13.8.2

This interactive element is not available in this format. Visit the link or scan the QR code to access it online.

View this Interactive Content online

References

1. Dohrenwend, J. C. (2007). Tertiary and Quaternary Deposits. In Geology and Mineral Resources of the East Mojave National Scenic Area, San Bernardino County, California (pp. 73-75). USGS.
2. Fuller, M. (n.d.). Anza-Borrego Desert SPm California State Parks. Retrieved August 31, 2023, https://www.parks.ca.gov/?page_id=638
3. General Geologic Setting. (2007). In Geology and Mineral Resources of the East Mojave National Scenic Area, San Bernardino County, California (pp. 10-11). USGS.
4. Geology of Joshua Tree National Park | U.S. Geological Survey. (n.d.). USGS.gov. Retrieved September 3, 2023, from

https://www.usgs.gov/geology-and-ecology-of-national-parks/geology-joshua-tree-national-park
5. Governor Newsom Visits Lithium Valley to Highlight Momentum on Becoming Global Source for Battery Production | California Governor. (2023, March 20). California Governor. Retrieved September 4, 2023, from https://www.gov.ca.gov/2023/03/20/governor-newsom-visits-lithium-valley-to-highlight-momentum-on-becoming-global-source-for-battery-production/
6. Hansen, K. (2015, October 8). Shrinking Shoreline of the Salton Sea. NASA Earth Observatory. Retrieved August 31, 2023, from https://earthobservatory.nasa.gov/images/86746/shrinking-shoreline-of-the-salton-sea
7. Harden, D. R. (2004). California Geology. Pearson Prentice Hall Shrinking Shoreline of the Salton Sea.
8. Haxel, G. B. (2007). Ultrapotassic rocks, carbonatite, and rare earth element deposit, Mountain Pass, southern California. In Geology and Mineral Resources of the East Mojave National Scenic Area, San Bernardino County, California (pp. 17-55). USGS.
9. Haxel, G. B., & Miller, D. M. (2007). Mesozoic Rocks. In Geology and Mineral Resources of the East Mojave National Scenic Area, San Bernardino County, California (pp. 59-68). USGS.
10. Hodges, C. A., & Theodore, T. G. (2007). Introduction. In Geology and Mineral Resources of the East Mojave National Scenic Area, San Bernardino County, California (pp. 4-8). USGS.
11. Lithium Valley: A look at the major players near the Salton Sea seeking billions in funding. (2022, May 13). The Desert Sun. https://www.desertsun.com/story/news/2022/05/13/lithium-valley-look-major-players-near-salton-sea-seeking-billions-funding/9665978002/
12. Miller, D. M., Wooden, J. L., & Conway, C. M. (2007). Proterozoic rocks and their mineralization. In Geology and Mineral Resources of the East Mojave National Scenic Area, San Bernardino County, California (pp. 12-16). USGS.
13. Miller, R. J., & Rytuba, J. J. (2007). Tertiary Rocks. In Geology and Mineral Resources of the East Mojave National Scenic Area, San Bernardino County, California (pp. 67-72). USGS.
14. Our Dynamic Desert. (2009, December 18). Our Dynamic Desert. Retrieved August 31, 2023, from https://pubs.usgs.gov/of/2004/1007/intro.html
15. Searles Lake, California. (2005, July 10). NASA Earth Observatory. Retrieved August 31, 2023, from https://earthobservatory.nasa.gov/images/5662/searles-lake-california
16. Theodore, T. G. (2007). Geology and Mineral Resources of the East Mojave National Scenic Area, San Bernardino County, California. USGS.
17. Walker, A. S. (1996). Deserts: Geology and Resources. USGS.
18. YouTube. Retrieved September 4, 2023, from https://www.forbes.com/sites/alanohnsman/2022/08/31/californias-lithium-rush-electric-vehicles-salton-sea/?sh=519ed1d4f631

This page titled 13.8: Geological Resources of the Desert Provinces is shared under a CC BY-NC 4.0 license and was authored, remixed, and/or curated by Martha House.

13.9: Geologic Hazards of the Mojave and Colorado Desert Provinces

Seismic Hazard

Like other provinces in California, earthquakes are a primary geologic hazard in the Mojave and Colorado Desert Provinces; you can learn more about earthquakes in California in California's Earthquake Hazards. Other hazards are the result of the desert environment. In particular, dust storms (discussed in Basin and Range), debris flows and flash floods are matters of concern.

The Mojave and Colorado Desert Provinces include a continuation of the Eastern California Shear Zone (Walker Lane) described in the chapter on the Basin and Range, and are bounded by the San Andreas Fault itself (Figure 13.9.1). As such, it's a region of seismic risk.

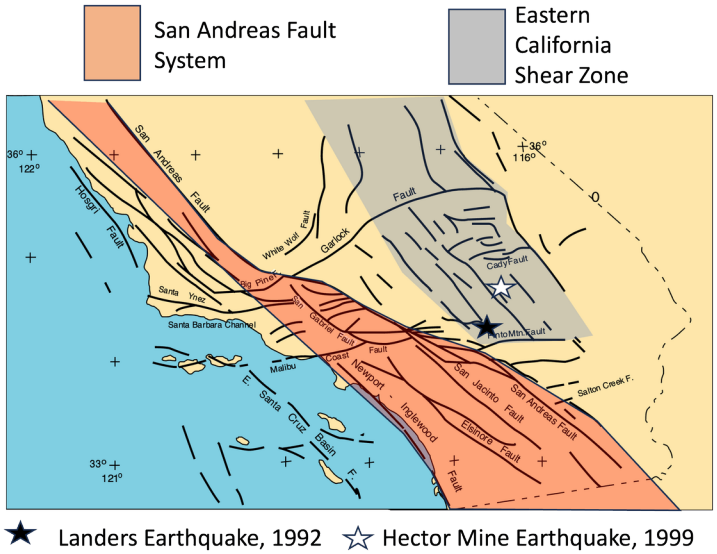


Figure 13.9.1: A map of southern California faults highlighting the Eastern California Shear zone in the eastern part of the state, along the Nevada border, and the San Andreas Fault System, which trends northwest and, with the exception of the western Transverse Ranges, is generally adjacent to the California Coast. The approximate locations of the epicenters for the Hector Mine and Landers earthquakes in the Mojave Desert are shown with stars. This work by M. House, a derivative of the original, is licensed under CC BY-SA 4.0. Access a detailed description.

Two notable earthquakes have occurred in this region since 1990: The Landers Earthquake of 1992 and the Hector Mine Earthquake of 1999 (Figure 13.9.2). Both of these earthquakes ruptured areas in the Mojave Desert and had relatively large magnitudes (7.3 for the Landers quake and 7.1 for the Hector Mine quake) but were relatively low in damage due to their remote locations. The system of faults ruptured in these events were within the Eastern California shear zone.

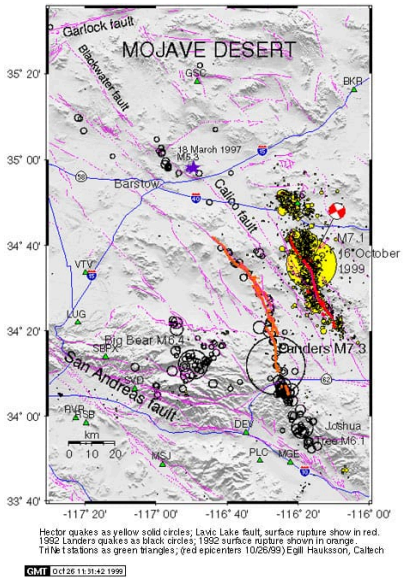


Figure 13.9.2: Map showing the relative location of the 1999 Hector Mine. "Hector Mine Earthquake Map" by SCEDC, is licensed under CC BY-SA 4.0. Access a detailed description of this map.

In the case of the Landers earthquake, five separate faults ruptured: Johnson Valley, Landers, Homestead Valley, Emerson, and Camp Rock faults. The total rupture length was ~85 km (53 miles), and the faults slipped from 2 meters (~6 ft) to a maximum of 6 meters (~18 ft). Nearby faults also experienced triggered slip and minor surface rupture. The Hector Mine earthquake was located relatively near, and ruptured a set of faults that were similarly oriented.

Other notable seismic hazards are found in the Brawley region in the Imperial Valley, south of the Salton Sea (Figure 13.9.3). The Brawley Seismic Zone (BSZ) extends from the northern end of the Imperial fault to the southern end of the San Andreas fault. The BSZ represents the northernmost extension of the spreading center axis associated with the East Pacific Rise which runs up the axis of the Gulf of California and is in the process of rifting the Baja California Peninsula away from the mainland of Mexico.

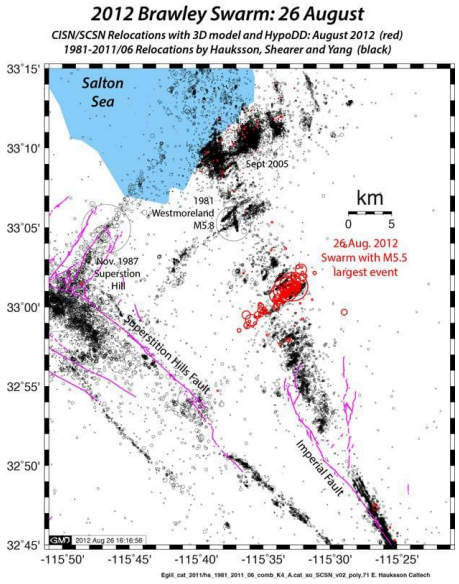


Figure 13.9.3: Map of CISN / SCSN Relocations for Brawley seismic zone events. "Map of CISN / SCSN Relocations for Brawley seismic zone events" by USGS, is licensed under public domain. Access a detailed description of this map.

In the 1960's and 1970's, the southern part of the BSZ was very active. Several swarms included many thousands of events, but with a largest magnitude of only M5.0 or less; most occurred along Northeast striking faults. From 1981 to 2000, the Brawley Seismic Zone was quiet, although an event in 2005 occurred along the south shore of the Salton Sea, with a magnitude of M5.1.

Flooding

Although these desert provinces are generally dry, periodic storms have a profound impact. For example, strong summer monsoonal storms in 2022 washed out roads throughout the Mojave National Preserve and demonstrated the process of landscape modification in action (Figure 13.9.4). The impact of flash floods and debris flows that result are discussed in 13.7: Water in the Desert.



Figure 13.9.4: Extensive road damage following summer monsoons. A road surface is broken and undermined by a flood that is now over. Sediment channels indicate the path of the floodwaters across the road surface "Extensive road damage following summer monsoon" by NPS, is licensed under public domain.

References

1. Carlowicz, M. (2019, July 24). *Measuring Movement from the Ridgecrest Quake*. NASA Earth Observatory. Retrieved August 31, 2023, from https://earthobservatory.nasa.gov/images/145318/measuring-movement-from-the-ridgecrest-quake
2. General Geologic Setting. (2007). In *Geology and Mineral Resources of the East Mojave National Scenic Area, San Bernardino County, California* (pp. 10-11). USGS.
3. *Geology of Joshua Tree National Park | U.S. Geological Survey*. (n.d.). USGS.gov. Retrieved September 3, 2023, from https://www.usgs.gov/geology-and-ecology-of-national-parks/geology-joshua-tree-national-park
4. Harden, D. R. (2004). *California Geology*. Pearson Prentice Hall.
5. *Our Dynamic Desert*. (2009, December 18). Our Dynamic Desert. Retrieved August 31, 2023, https://pubs.usgs.gov/of/2004/1007/intro.html
6. Walker, A. S. (1996). *Deserts: Geology and Resources*. USGS.

This page titled 13.9: Geologic Hazards of the Mojave and Colorado Desert Provinces is shared under a CC BY-NC 4.0 license and was authored, remixed, and/or curated by Martha House.

13.10: Chapter Summary

13.2: Physiographic Features of the Mojave & Colorado Desert Provinces

- The Mojave and Colorado Desert provinces are arid environments in the southeastern part of California.
- The relief in this area is more subdued than that of the Basin and Range province to the north, but geologic features are similar.

13.3: Geologic Overview and Evolution of the Mojave and Colorado Desert Provinces

- Rocks range in age from Late Proterozoic to Late Cenozoic in age are exposed in uplifted mountain ranges are as old as 2.5 Ga.
- Paleozoic rocks exposed in uplifted ranges consist of sediments deposited in a passive margin setting and have many marine fossils.
- Mesozoic rocks in the region are mostly granitic and metamorphic, associated with changing plate boundaries.
- Cenozoic units are typically found in down-dropped basins and contain evidence of dramatic changes in climate and tectonic setting over the past 30 million years.

13.4: Creating the Desert Environment

- The Mojave and Colorado Desert provinces are arid due to their position in the high pressure atmospheric belt associated with the meeting of the Prevailing Westerlies and the Northeast trade winds.
- These regions also occupy the rain shadow of the Sierra Nevada, Transverse ranges and Peninsular ranges.
- Weathering is dominated by physical processes here.

13.5: Wind Driven Sediment Transport

- Wind and water are the dominant modes of sediment transport in this region.
- Dune fields are established when wind is blocked and sediment is dropped.
- Blowing sand is abrasive and can sculpt ventifacts.

13.6: Sand Dunes and Dune Fields

- There are several large dune areas in the Mojave and Colorado Desert region. Such sand dunes and dune fields develop when there is adequate sediment supply and a way for sediment that is deposited to be stabilized.

13.7: Erosional Desert Landforms

- Inselbergs are remnants of old mountains that are surrounded by their own erosional debris.
- Pediments are flattened or low angle surfaces of bedrock with very little alluvium.
- Bedrock often exhibits spheroidal weathering as a result of chemical weathering.
- Desert pavement develops as light, small sediment is blown away from larger particles.

13.8: Water in the Desert

- Although deserts are dry environments, water in the form of flash floods can be an effective modifier of the landscape.
- The Mojave River is today an ephemeral stream which flows underwater for part of its stretch.
- Many dry lakes in this region were once connected in a larger system of lakes.

- The Salton Sea is a remnant of a flood event in which the Colorado river spilled its banks.

13.9: Geologic Resources in the Desert Provinces

- Evaporites are important resources in this region, forming in dry lakes.
- Strategically important resources, such as lithium, form in these environments associated with the Salton Sea Brine pools.
- Rare Earth elements are mined at Mountain Pass in eastern California.

13.10: Geologic Hazards

- Seismic hazard in this area is present due to the proximity of the San Andreas fault and the transition to the spreading center in the Gulf of Mexico.
- Flooding is a seasonal hazard here due to monsoonal storms.

This page titled 13.10: Chapter Summary is shared under a CC BY-NC 4.0 license and was authored, remixed, and/or curated by Martha House.

13.11: Detailed Figure Descriptions

Figure 13.1: Geologic Province Map

A map of California highlights the area that corresponds to the Mojave and Colorado Desert Geomorphic Provinces. The larger Mojave Desert Province is northeast of the Colorado Desert Province; they are separated by northwest trending San Andreas Fault. Together, these geomorphic provinces define a triangular region in the southeastern edge of the state. The western boundary of this larger geomorphic province is formed by the states of Nevada and Arizona. The northern boundary is the east-northeast trending Garlock fault, which separates the Mojave and Colorado Desert Provinces to the south from the (from east to west) Basin and Range, Sierra Nevada and Great Valley Province. Along their southwestern boundary, these provinces are bounded by the Transverse Range Province and the Peninsular Ranges Province. The southern boundary is truncated by the Mexican border.

Figure 13.1.1 Map of the Mojave and Colorado Desert Provinces from space

The map shows the intersection of the east-northeast trending Garlock fault with the northwest trending San Andreas fault. These faults meet at a point that defines the western limit of the combined Mojave and Colorado Desert Provinces. To the north of the Garlock Fault is the southern edge of the Basin and Range, Sierra Nevada, and Great Valley Provinces. To the southwest of the San Andreas Fault is the Los Angeles Basin, which lies at the junction of the Transverse Ranges Province to the west, and the Peninsular Ranges Province to the south. The region encompassed by the Mojave and Colorado Desert Provinces is arid and contains numerous mountain ranges separated by valleys, some of which are very light in color, indicating the presence of seasonal lakes. Major highways cross this region, including US 10, which travels east from Los Angeles; US 15 travels northeast through the center of this province; and US 40 travels east-west across this region. Joshua Tree National Park is situated along the southwest edge of this province, north of US 10 where it meets the San Andreas Fault. The Salton Sea is west of the San Andreas Fault, in the adjacent Peninsular Ranges Province.

Figure 13.1.2 Excerpt from the Geologic Map of California with the Mojave and Colorado Desert Provinces

An excerpt of the larger state map focuses on the combined provinces of the Mojave and Colorado Desert. This map highlights map units according to large ranges of geologic age and lithology. Most of the bedrock geology of this region has been mapped as Quaternary surficial deposits, which generally correspond to basin regions. Areas of older rocks are found in uplifted mountains. Isolated regions of pre-Cambrian rocks are located along the boundary between the Mojave and Colorado Desert Provinces, where they form a northwestern linear belt corresponding to and along the eastern edge of the provinces. Smaller occurrences are found throughout the central part of the province. Mesozoic granitic igneous rocks occur throughout the region, as do Cenozoic rocks of volcanic origin. Paleozoic sedimentary and metamorphic rocks are scattered throughout the northeastern portions of the province, as in the central western region. Major fault systems are oriented northwest as well as east-west. The northwest trending faults occur in the western part of the province and truncate parallel east-west trending faults in the northern central part of the province.

Figure 13.2.4 Simplified geologic history of the Mojave region in three panels

Three panels describe the simplified geologic and tectonic history of the Mojave region.

Panel A depicts geologic events prior to 250 million years ago when the Mojave region was a passive continental margin. At this time, the ancient Pacific Ocean Basin was situated to the west. A blanket of passive margin marine sedimentary deposits covered the shallow shelf platform and continental margin on top of very ancient basement rocks (igneous, sedimentary, and metamorphic rocks). The border between the shallow shelf platform and the basement rocks is labeled "the Great Unconformity." The basement rock is made of igneous, sedimentary, and metamorphic rocks that are labeled very ancient.

Panel B depicts plate convergence along the continental margin that produced a volcanic arc system throughout the Sierra Nevada and Mojave regions roughly 250 million to about 60 million years ago. The volcanic arc system developed to the west of the active east-directed subduction zone, along the western continental margin. Between these two is a region of uplift and erosion. Igneous intrusions are found below the volcanic arc.

Panel C depicts extensional spreading of the Great Basin region, which began roughly 30 million years ago. Your strike-slip style fault systems and erosions are still active in the region today. The San Andreas and Garlock Fault System is on the west side of the image and volcanism is found on the east side. Between these is the Great Basin extensional faulting with alluvium-filled basins.

Figure 13.3.1 Major global climatic regions in relation to atmospheric convection cells and the Earth's continents

A map of the world with continents and oceans. The continents are color-coded by climate type. The climate types are divided into categories and then sub-categories. Tropical climates are divided into tropical wet and tropical wet and dry.

Tropical wet climate areas are found in much of central America, the western and northern Amazon Basin in South America, equatorial Africa, coastal India, coastal southeast Asia, the Indonesian Archipelago, and equatorial Pacific Islands. Tropical wet and dry areas include southern Mexico; northern South America; the central, southern, and western Amazon Basin in South America; south of equatorial Africa except along the west coast; inland southeast Asia; northern Australia; the Philippines; and southernmost Japan.

Dry climates include semiarid and arid conditions. Semiarid areas are western, non-coastal North America from central Mexico to southern Canada, except for the highest mountains in the Rockies; the highlands of Venezuela; the Chilean highlands; onshore areas of Morocco and Tunisia; areas of Africa on the northern and southern borders; the equatorial regions; much of Madagascar: the highland regions of southeast Asia; Australia between the coastal areas and the central area; Mongolia; inland China; much of the Middle East; and Turkey. Arid regions include the Mojave and Sonoran deserts of the US and Mexico; coastal south America from Ecuador, Peru, and Chile; north Africa and the western coast of southern Africa; Ethiopia; the Saudi Arabian peninsul; inland Iran; western Pakistan; central Australia; and inland China north of the Himalayas.

Moderate climates include Mediterranean, humid subtropical, and marine west coast types. Mediterranean climates include coastal southern California and northernmost Mexico, Spain and the Mediterranean, eastern South Africa, and southern coastal Australia. Humid subtropical includes the southeast US, as well as southern Brazil, Uruguay, mainland China, northern India, and central Japan. Marine west coast conditions are found on the west coasts of central and northern California, Canada, and coastal southern Alaska and the Aleutian Islands, and coastal southern Chile, as well as the west coasts of the British Isles and northern Europe, western Scandinavia, southeast coastal Australia and New Zealand, and parts of the eastern Philippines.

Continental climates are humid continental and subarctic conditions. Humid continental climate examples include north and central US and southern Canada, as well as central, non-coastal Scandinavia, northern Europe, and northeast China. Subarctic climates are found in most of Canada and Alaska, northern Scandinavia, northern Russia and Siberia, and coastal Greenland.

Polar climates include tundra, ice cap, and highlands conditions. Tundra areas include northernmost Alaska and Canada, and Greenland coastal areas, as well as northernmost Siberia. Icecap regions are Antarctica and inland Greenland. Highlands areas include the highest Rocky Mountains, the highest of the Andes Mountains, and the Himalayas.

Non-permanent ice is the last category, and it includes near coastal Antarctica, and the area around the islands of northern Canada and offshore of Siberia.

Figure 13.3.3 Diagram of a rain shadow and its effects

The rain shadow effect is illustrated by a cross-section of a mountain with the sea on one side and an area labeled “rain shadow” on the other. The side facing the sea is the windward side and arrows labeled prevailing wind point towards the mountains. When the arrows reach the mountains, they move upwards along the mountain face. Near the top of the mountains, clouds form and rain falls on the side of the mountains facing the sea.

The side of the mountains facing away from the sea is the leeward side. Here the arrows portraying air movement move down the mountain. There is no rainfall on this leeward side.

Inset Box Figure 13.3.3 Atmospheric Circulation and Deserts

The pattern of global circulation of the atmosphere is based on where on the globe cooler air sinks and where warmer air rises, and on the interaction of this air movement as the Earth rotates beneath. Earth's surface is divided into three major areas - warmer areas near the equator called the tropics, colder areas near the poles called the polar regions, and areas in between the tropics and the poles called the temperate zones. The atmosphere above, can similarly be divided into zones or cells based on, but not identical to, these same areas. The atmospheric cells are the Hadley cells associated with the tropics, the polar cells associated with the polar regions, and the mid-latitude cells (also called the Ferrel cells) associated with the temperate zones.

The cells are three dimensional motion of the atmosphere which is determined by whether the air in a cell is warm, cold, or interacting between warm and cold areas.

Starting with the tropics, this is where the Earth's surface receives the maximum amount of solar heating because the rays of the sun, no matter what season of the year, strike the surface at the highest angle (angle of incidence of the sun's rays). Because this is the area of maximum solar heating, the atmosphere above is an area of warm air and warm air rises. As the air rises, and as the globe spins beneath the atmosphere a wind pattern is set up to the north and south of the equator, near Earth's surface.

These winds are easterly - they come from the east and move towards the west. However, they do not move straight east to west; the Earth's rotation sets up a pattern of northeast winds, north of the equator and southeast winds, south of the equator as indicated by the arrows in the diagram. This is the most consistent wind pattern on Earth. They are the trade winds, because in the days of sailing ships, they were the winds used to power the trade fleets sailing the oceans between the continents. These winds meet or converge, near the equator, and establish the meteorological equivalent of the equator - the intertropical convergence zone, sometimes abbreviated ITCZ.

The ITCZ is the boundary between the atmospheric Hadley cells and as these winds of relatively warm air converge, they rise and cannot fall back to Earth because the air below them is also warm. This warm air continues to move in the upper atmosphere, now away from the ITCZ, until the air beneath is no longer the warm rising air of the tropics. Just beyond the tropics at approximately 30° north and south of the equator, this air, now cooler because of its time in the upper atmosphere, and because warm air is no longer rising beneath it, can finally sink to the surface of Earth.

Next consider the polar regions. This is the coldest air in the atmosphere. The polar regions receive the least amount of solar surface heating of any area on Earth. Two things combine to make this situation. First the angle of incidence of the sun's rays is lowest in the polar regions. When these areas receive sunlight, they get much less solar energy for the sunlight than does the Earth's surface in the tropics. Secondly, each polar region has a time of no sunlight (their respective winter seasons) when they get no solar energy. Even with the opposite occurring in their respective summers, it's not enough to effectively heat Earth's surface by much. Cold air sinks and moves over the surface of Earth away from the poles as indicated by the arrows moving outwards from the north and south poles.

As the air moves over Earth's surface and away from the poles, it gets comparatively warmer and by the time it gets just beyond the polar regions, to approximately 60° north and south of the equator, it starts to rise.

Now consider the temperate zones of the mid-latitude or Ferrel cells in between. They are between a colder polar cell from 90° to 60° and a warmer Hadley cell from 0° to 30° of latitude north and south of the equator. At 60° is warmer air rising, and at 30° air is cooler air falling. This sets up a 3-dimensional pattern with the surface winds moving from west to east, or westerly winds, as indicated by the arrows on the figure.

The pattern is cool air (and generally dry air) falling at 30° and 90° north and south of the equator; and warm air (and generally moist air) rising at 0° and 60° north and south of the equator. The warm, dry air at 30° north of the equator, is a major contributor to the formation of both the Mojave and the Colorado deserts of California.

Figure 13.5.1 Illustrated cross-section of a sand dune

The wind direction in the image is from left to right, with three cross-bedding sets at the bottom of the image. As grainflow moves with the wind, it creates an area of erosion to the left and an area of grainfall to the right. This creates an area of deposition and a depression where wind ripples travel in reverse (from right to left). This pattern is repeated twice on the image to depict this as a process that happens in multiple areas.

Figure 13.5.2 A portion of the Algodones dune field

The Algonones dune field includes both crescent and linear dunes. In the aerial overview, the dune field appears as a broad band of light tan sand trending northwest-southeast, within which we see a series of parallel dunes that trend southwest-northeast, almost like rungs of a ladder. A section of the area is enlarged to show a zone of arcuate simple crescent dunes that is adjacent to a zone of complex crescent dunes with a more chaotic shape. Long narrow linear dunes that trend northwest-southeast (transverse to the trend of the other dunes in the image) are in the southwest portion of the dune field.

Figure 13.6.4 The process of spheroidal weathering

A cross-section showing fractures, joints and faults within the unweathered bedrock. Groundwater migrates along the fractures, joints, and faults which causes the removal of dissolved salts. These regions are zones of chemical weathering. At the surface water, CO2, and organic acids infiltrate rocks along fractures and cause chemical weathering. Also at the surface are sheroidal wethered boulders and areas of erosion which gradually strip away weathered bedrock, regolith and soil.

Figure 13.7.3 A map of the interconnected Pleistocene Lake system of California

A digital elevation model focuses on the region of the Mojave Desert to the south of the Sierra Nevada and Tehachapi Mountains, and to the north of the San Gabriel and San Bernardino Mountains, and extending to the Colorado River on the east. A network of ancient lakes developed throughout this region. A central part of this system is the Mojave river, which flows northeastward from the San Gabriel mountains, and connects a number of these lakes including the ancient Lake Manix, Cronese Lakes, and Soda Lake (also known as Lake Mojave). Flow from this system continued northward to Lake Tecopa (near Shoshone, CA), and then into Lake Manley (in the modern Death Valley region). This lake drained into a series of large lakes to the west: Panamint Lake, China Lake. and Owens Lake.

Figure 13.9.1 A map of southern California faults highlighting the Eastern California Shear zone

Please add a detailed description of this diagram, with all embedded text labels included.

Figure 13.9.2 Map showing the relative location of the 1999 Hector Mine

The epicenters of a range of earthquakes in the Mojave Desert Province are plotted atop a digital elevation model. The region depicted is northeast of the San Andreas Fault and includes Joshua Tree National Park in the southeast and the Garlock Fault in the north. It is centered on Barstow, CA. Earthquake epicenters form distinctive clusters. A linear belt of epicenters includes the 1999 Hector Mine Earthquake; this belt trends north-northwest and is located to the east and slightly south of Barstow. A second cluster forms a linear belt that includes the Landers Earthquake epicenter. This belt is parallel to that of the Hector Mine cluster but located slightly west of it. Another large cluster of epicenters is plotted around Big Bear Mountain. The epicenter of the 1999 Hector Mine Earthquake is southeast of Barstow. The epicenter of the Landers Earthquake is south-southeast of Barstow and slightly southwest of the Hector Mine earthquake. Zones of aftershocks are also shown. These form linear belts that trend north-northwest through the Hector Mine epicenter and a second linear belt through the Landers epicenter is parallel to that of the Hector Mine trend but located to the west of it.

The San Andreas Fault System runs along the western side of the state begining at the coast in the lower part of the image and moving inward twoards the top. A list of all the labeled faults in the San Andreas Fault System (from north to south and east to west): Big Oine, San Gabriel, Malibu Coast, Newport-Inglewood, Elsinor, San Jacinto, San Andreas, and Salton Creek.

The Eastern California Sheer Zone is found in the north-eastern region of the image. It has many fault lines. The Landers Earthquae (1992) and the Hector Mine Earthquake (1999) are found on the sourther edge of this Zone.

Figure 13.9.3 Map of CISN / SCSN Relocations for Brawley seismic zone events

Clusters of epicenters in this map occur in two distinct linear belts. One belt is west-southwest of the Salton Sea, where a cluster of epicenters is aligned with the northwest trending Superstition Hills fault. The northern edge of this zone is a broad region of epicenters with a northeast trending sense. The second zone falls along the north-northwest trending Imperial Fault to the south and extends northward to the southeastern shores of the Salton Sea, where it merges with a broad northeast trending zone of epicenters and some events offshore in the Salton Sea itself. In this second zone, a recent cluster of events is associated with the northeast trending 2012 Brawley swarm. A map label notes "26 Aug. 2012 swarm with M5.5 largest event."

This page titled 13.11: Detailed Figure Descriptions is shared under a CC BY-NC 4.0 license and was authored, remixed, and/or curated by Martha House.

14: TRANSVERSE RANGES

Introduction to the Transverse Ranges

The Transverse Ranges Province is a geologically diverse region with a complex geologic history. Much of the early geologic evolution of this region can be correlated to that of other geomorphic provinces in California. However, this province is also somewhat of an anomaly when compared to others across the state of California: as the name suggests, the mountains, valleys, and faults within the Transverse Ranges Province are oriented east-west, *transverse* to the dominant north-south trends seen elsewhere in California and western North America overall. How did this region come to be oriented in such a different way compared to surrounding regions? How have the dramatic changes to the California plate boundary over the late Cenozoic impacted this region?

This chapter will present a general overview of the region that will allow for comparison to other provinces and will direct you to the relevant chapters for more information. Our focus here will be on the Late Cenozoic geology of the region impacted by the emerging San Andreas fault system. We'll see that this period produced dramatic structural rotation and translation of large crustal blocks along with the development of deep structural basins that are a major source of oil and gas. Modern transpression across this region that is accommodated by reverse and strike-slip faults continues to shape the landscape, producing unusually steep relief that is subject to landslides, as well as active seismic risk that impacts millions of Californians.

Note that the evolution of this region is closely related to the northern Peninsular Ranges Province (including the offshore Borderlands Region). This is particularly notable in the case of the Los Angeles Basin, which is located to the south of the Transverse Ranges Province. Because of the similarities, we'll be discussing the Los Angeles basin and the offshore northern borderlands region in this chapter even though they aren't strictly part of this province.



Figure 14.1: Location of the Transverse Ranges Province of California. This east-west trending province is situated south of the Coast Ranges Province, southwest of the Mojave Province, and to the north of the Peninsular Ranges Province. The province includes the offshore Channel Islands of San Miguel, Santa Barbara, Santa Cruz, Santa Rosa and Anacapa. Access a detailed description of this image. "The Transverse Ranges Province of California" by Emily Wright, is licensed under CC BY-NC / a derivative from the original work.

Learning Objectives

By the end of this chapter, you should be able to:

- Locate the Transverse Ranges Province and its major elements (mountain ranges, faults and key geologic features) on a geologic map of the state.

- Explain how the modern physiographic features found within the Transverse Ranges are produced by Late Cenozoic tectonism.
- Describe the primary bedrock geologic characteristics of the Transverse Ranges province.
- Recall the general geologic evolution of the Transverse Ranges Province in the context of the evolution of California.
- Explain the origin and current location of petroleum reserves within the Transverse Ranges Province.
- Assess the geologic hazards and risks associated with the Transverse Ranges Province.

14.1: Physiographic Overview of the Transverse Ranges Province
14.2: Bedrock Geology of the Transverse Ranges Province
14.3: Cenozoic Sedimentation and Basin Development
14.4: Tectonic and Structural Evolution of the Transverse Ranges
14.5: Geologic Hazards of the Transverse Ranges Province
14.6: Mineral and Petroleum Resources of the Transverse Ranges Province
14.7: Chapter Summary
14.8: Detailed Figure Descriptions

This page titled 14: Transverse Ranges is shared under a CC BY-NC 4.0 license and was authored, remixed, and/or curated by Martha House.

14.1: Physiographic Overview of the Transverse Ranges Province

Location of the Transverse Ranges

The Transverse Ranges Province is an east-west trending region in California that is adjacent to the San Andreas Fault System. This region is bounded by the Coast Ranges Province to the north, the Mojave Province to the east, and the Peninsular Ranges Province to the south; the San Andreas System runs through this region. To the west, this province extends offshore to include the northern Channel Islands, along with the submarine basins that separate them.

Physiographic Features

Fault-bounded east-west trending ranges are a distinctive feature of this region (Figure 14.1.1). Pronounced and well-known ranges such as the San Bernardino, San Gabriel, Santa Monica, and Santa Ynez Mountains, as well as the northern Channel Islands are recreational destinations for many of those in southern California. Smaller east-west trending ranges create a visually stunning landscape and provide additional opportunities to study geologic exposures.

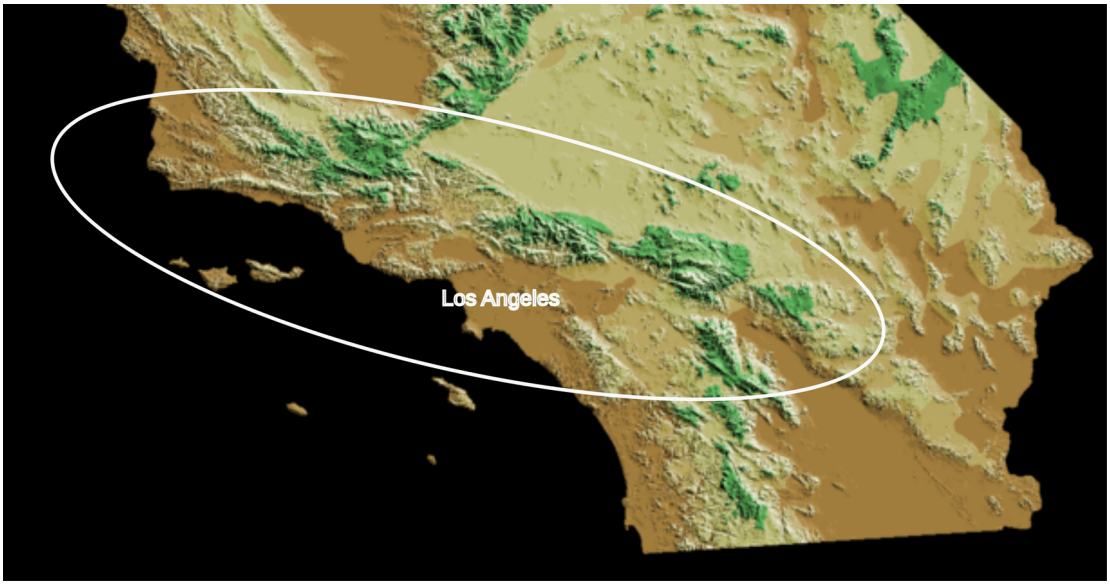


Figure 14.1.1: Digital elevation model of the Transverse Ranges Province highlighting mountains and valleys of Southern California. The Transverse Ranges Province is encircled; Los Angeles is on the boundary between this province and the Peninsular Ranges Province to the south. "Southern California digital elevation map" by USGS is in the public domain. Access a detailed description.

The east-west trending ranges in this province are separated by modern sedimentary basins, the larger of which are the Santa Barbara-Ventura-Soledad Basins and the Los Angeles Basin. Cenozoic sediments within these large subsurface basins are deformed and locally uplifted by recent (Pleistocene and younger) faulting such that their strata can be observed in outcrop as well as in drill cores. Sedimentary deposits within these basins preserve the history of basin development, erosion of adjacent ranges, and changes in sea level that impacted this region since the Mesozoic. Most of these basins host oil-bearing units, as seen by the abundance of oil drilling infrastructure throughout the region.

Query 14.1.1

This interactive element is not available in this format. Visit the link or scan the QR code to access it online.

View this Interactive Content online

References

1. Harden, D. R. (2004). *California Geology*. Pearson Prentice Hall.
2. Norris, R. M., & Webb, R. W. (1976). *Geology of California*. Wiley.
3. Wallace, R. E. (1990). *The San Andreas Fault System, California US Geological Survey Professional Paper 1515*. USGS.

This page titled 14.1: Physiographic Overview of the Transverse Ranges Province is shared under a CC BY-NC 4.0 license and was authored, remixed, and/or curated by Martha House.

14.2: Bedrock Geology of the Transverse Ranges Province

A Review of the Geologic Map of this Region

The excerpt of the state geologic map shown in Figure 14.2.1 highlights major geologic features in the Transverse Ranges. The San Andreas fault is a prominent feature, trending northwest and forming the southern boundary of the western portion of this province, including the lozenge-shaped San Bernadino Mountains. As the San Andreas Fault trends northwestward, it crosses to the northern boundary of the San Gabriel Mountains. The southern boundary of the San Gabriel Mountains is the San Gabriel Fault. Other major fault systems in this region include a number of east-west striking faults which are truncated by the southern San Gabriel Fault on the east. These faults extend offshore to the west.

Precambrian and Mesozoic metamorphic and igneous intrusive rocks occur in the eastern region, corresponding to the San Bernadino and San Gabriel Mountains. Patches of Paleozoic sedimentary rocks occur in the north-central San Bernardino Mountains, and patches of Paleozoic sedimentary rocks are found in the western San Gabriel Mountains. The western portion of the Transverse Ranges Province, including the Channel Islands, is dominated by younger (Neogene and Paleogene) sedimentary rocks and volcanics. The southern edges of the province and patches within the western part of the province include Quaternary surficial deposits.

Proterozoic Metamorphic and Igneous Basement Rocks

The geologic map of the region helpful for understanding the distribution of bedrock geology. Elongate east-west mountainous regions generally demarcate the location of the oldest rocks, which have been brought to the surface via faulting Figure 14.2.1.

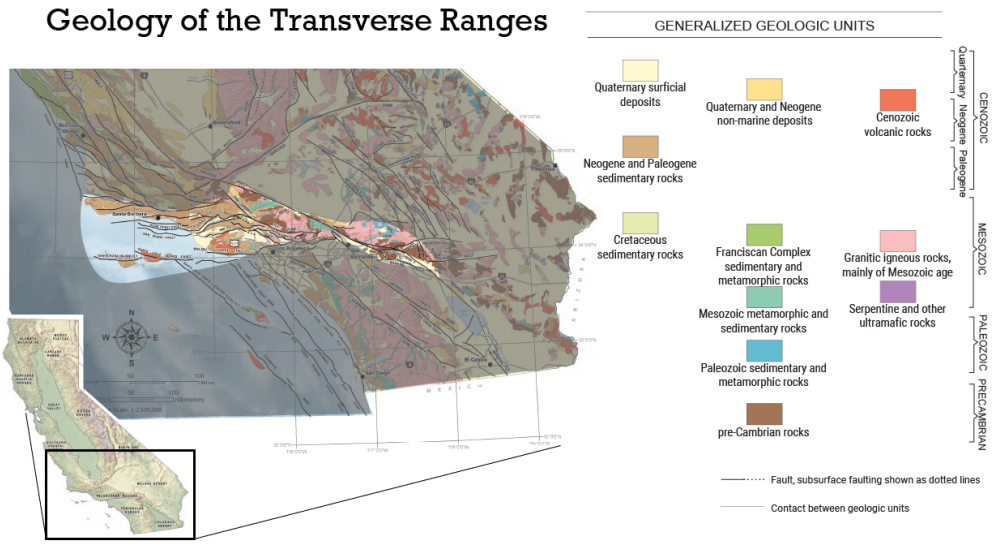


Figure 14.2.1: Geology of the Transverse Ranges Province of California. Excerpt from the Geologic Map of California with the Transverse Ranges Province highlighted. "Excerpt from the Geologic Map of California" by E. Wright, is licensed under CC BY-NC / a derivative of the original work. Access a detailed description of this image

The oldest rocks in this region are the Proterozoic metamorphic and igneous rocks exposed throughout the San Gabriel Mountains and the extreme eastern and western San Bernardino Mountains (Figure 14.2.2). These rocks are complexly deformed metasedimentary rocks that include pelitic schists, calcareous gneisses, amphibolites, and igneous gneisses of various protolith compositions that range in age from 1.71 to 1.6 Ga.



Figure 14.2.2: Foliated Mendenhall Gneiss. Boulder of alternating black and white foliated layers is approximately 33 cm (13 in) in length. "Mendenhall Gneiss' by M.A. House, is licensed under CC BY-NC-SA. Access a detailed description.

A suite of younger plutonic rocks dated at approximately 1.3 Ga intrudes the older units. An interesting component of this phase of plutonism is an anorthosite complex. Unlike the other units, this complex of plagioclase-rich crystalline rocks (Figure 14.2.3) is less highly deformed and some of the original cumulate textures are preserved.



Figure 14.2.3: The San Gabriel Anorthosite outcrops adjacent to CA 2 in the central San Gabriel Mountains. The white rocks of the anorthosite are distinctive, as are associated mafic dikes, which are the diagonal bands of rock seen in the left portion of this image. "Anorthosite Road Cut" by M.A. House, is licensed under CC BY-NC-SA.

Late Proterozoic-Early Paleozoic rocks are also found in the San Bernardino Mountains. These rocks include meta-sedimentary rocks that are thought to represent ancient passive margin facies that can be correlated to those in the Death Valley and White Mountains regions (see Basin and Range).

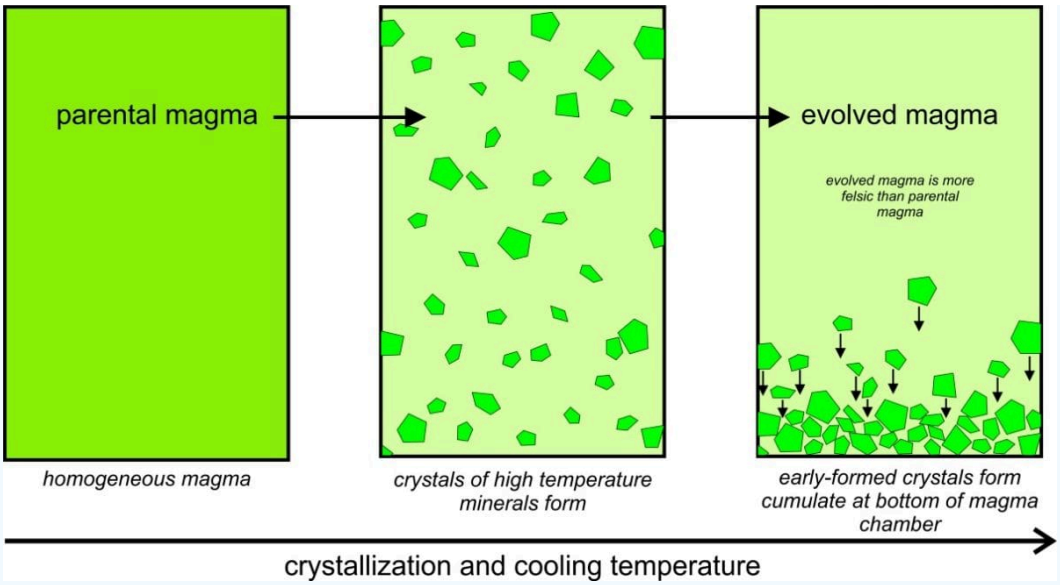
Box 14.2.1: More About Anorthosites

Anorthosites are interesting and relatively unusual plutonic rocks that are more than 90% Ca-plagioclase (Inset Figure 14.2.1). They also have some Fe- or Mg-bearing minerals such as pyroxenes and olivines, and Fe/Ti oxides. Anorthosites make up much of the highlands of our moon, but they are relatively rare on Earth.



Inset Figure 14.2.4: A sample of San Gabriel Anorthosite from Soledad Canyon, Los Angeles County. It is composed almost entirely of Ca-plagioclase. "San Gabriel Anorthosite (Mesoproterozoic, ~1.2 Ga; Soledad Canyon, Los Angeles County, California, USA) 1" by James St. John via Flickr is licensed under CC BY.

The formation of anorthosites has been enigmatic for petrologists for several reasons. The main problem is that in many areas where these large igneous bodies have been described, it's difficult to explain the massive accumulations of concentrated Ca-rich plagioclase crystals in these massifs. Fractional crystallization is a mechanism that has been proposed for the formation of these plutons. In this process, low-density plagioclase crystals are buoyantly separated from denser Fe-bearing minerals within a cooling magma chamber (Inset Figure 14.2.2). As shown in this image, as denser materials sink within the parental chamber, cumulate layers form within the magma chamber as it cools. These layers concentrate denser minerals within distinct layers at the base, and less dense minerals like Ca-Plagioclase, concentrate at upper levels in the chamber. These denser layers are effectively separated from the remaining magma, which evolves to a more felsic composition than that with which it began.



Inset Figure 14.2.5: Formation of a cumulate during partial crystallization. "Evolved Magma" by D. Perkins, is licensed under CC BY-NC-SA. Access a detailed description.

When such layers are well-developed, these geologic structures are called layered mafic intrusions. The concentrated mafic and ultramafic layers in these structures may include economically valuable concentrations of platinum, palladium, nickel, titanium, and chromium. These features have been exploited by mining operations in the Bushveld Anorthosite Complex in South Africa and the Stillwater Complex in Montana, USA.

Geologic evidence for fractional crystallization and density stratification is preserved in the San Gabriel Mountains anorthosite complex, although there are no economically distinct layers like those in larger layered intrusions. Instead, the anorthosite is associated with low-quartz rock types such as syenite, and mafic rocks such as gabbros.

Despite this seemingly simple explanation for the formation of many of these plutonic complexes, clear evidence for fractional crystallization is sometimes missing, leaving petrologists stumped as to their origin. This is because our understanding of the formation of such Ca-Plagioclase rich rocks requires the accumulation of very mafic components as well, and they are sometimes absent. Further, many of the massif-style anorthosites like that in the San Gabriel Mountains range in age from 1.9-1.2 Ga. As a result, the scientific community continues to debate the composition of the original magma that leads to the formation of these structures. One possibility is that conditions of the crust and mantle at that time of their formation were different in such a way that anorthositic complexes could form via fractional crystallization and allow for the rapid and complete removal of any cumulate layers that might have formed. An interesting petrologic problem for sure!

The Mesozoic Pelona Schist and the Vincent Thrust

A prominent basement unit within the Transverse Ranges is the Pelona Schist. This well-foliated unit is mostly found as a gray schist, but contains distinctive lenses of greenschist facies metabasalts, meta-sandstones and calcareous units. This unit, which may represent a metamorphosed turbidite sequence, is thought to underlie the entire Transverse Ranges region since it appears as clasts within younger sedimentary units. Similar rocks have been found in eastern California and into Arizona, where this unit is variably called the Rand or Orocopia schist, and to the north in the Coast ranges, where it is thought to be equivalent to the Franciscan complex (see Coast Ranges).

Mesozoic Plutonism

Like much of California, Mesozoic plutonism associated with arc volcanism impacted the Transverse Ranges. Within the San Gabriel and San Bernardino Mountains, granitic and dioritic plutonic bodies were emplaced in three stages at 207-241 Ma, at 165-150 Ma and at 85-120 Ma. The compositions of these units are comparable to those in the Sierra Nevada Range (see Sierra Nevada) and indicate that the ancient Mesozoic arc extended to this region at that time.

Query 14.2.1

This interactive element is not available in this format. Visit the link or scan the QR code to access it online.

View this Interactive Content online

References

1. Carter, B. A. (1980). *Geology of the anorthosite-syenite terrain, San Gabriel Mountains, Los Angeles County, California: Supplement 1 from "Structure and petrology of the San Gabriel anorthosite-syenite body, Los Angeles County, California" (Thesis)* [Thesis]. https://doi.org/10.22002/D1.1039
2. Carter, B. A. (1987). The San Gabriel anorthosite-syenite-gabbro body, San Gabriel Mountains, California. In *Cordilleran Section of the Geological Society of America Centennial Field Guide* (pp. 203-206). Geological Society of America.
3. Ehlig, P. L. (1981). Origin and tectonic history of the basement terrane of the San Gabriel Mountains, Central Transverse Ranges. In *The Geotectonic Development of California* (Vol. 1, pp. 253-283). Prentice-Hall.
4. Evan, J. G. (1982). *The Vincent thrust, eastern San Gabriel Mountains, California. USGS Bulletin 1507*. USGS. https://doi.org/10.3133/b1507.
5. Evans, J. G. (1978). *Postcrystalline deformation of the Pelona Schist bordering Leona Valley, southern California* (Professional Paper 1039 ed.). USGS. https://doi.org/10.3133/pp1039.
6. *Geologic Formations - Channel Islands National Park (U.S.* (2016, June 21). National Park Service. Retrieved January 19, 2024, from https://www.nps.gov/chis/learn/natur...formations.htm
7. *Geology of the San Gabriel Mountains*. (n.d.). CSUN. Retrieved February 15, 2024, from https://www.csun.edu/science/geoscience/fieldtrips/san-gabriel-mts/geology-san-gabriels.html
8. Hall, C. A. (1981). Evolution of the western Transverse Ranges microplate: Late Cenozoic faulting and basinal development. In *The Geotectonic Development of California* (pp. 559-582). Prentice-Hall.
9. Harden, D. R. (2004). *California Geology*. Pearson Prentice Hall.
10. Ingersoll, R. V., & Ernst, W. G. (1987). *Cenozoic Basin Development of Coastal California* (R. V. Ingersoll & W. G. Ernst, Eds.). Prentice-Hall.
11. KellerLynn, K. (2016). *Santa Monica Mountains National Recreation Area Geologic Resources Inventory Report*. US Department of the Interior.
12. Morton, D. M., & Miller, F. K. (2006). *Geologic Map of the San Bernardino and Santa Ana 30' x 60' quadrangles, California* [Map]. USGS.
13. Norris, R. M., & Webb, R. W. (1976). *Geology of California*. Wiley.

This page titled 14.2: Bedrock Geology of the Transverse Ranges Province is shared under a CC BY-NC 4.0 license and was authored, remixed, and/or curated by Martha House.

14.3: Cenozoic Sedimentation and Basin Development

Basin Formation Across the Transverse Ranges Province

The Cenozoic geology of this region is dominated by basin formation, deposition, and deformation. Beginning in the Late Cretaceous, the changing nature of the North American and Pacific plate boundary led to dramatic changes across the region that would become the modern Transverse Ranges Province. Initially situated in a fore-arc basin that is suggested to be related to that of the Great Valley at this time, this region then experienced significant crustal extension and rotation that led to the formation of numerous deep basins, including the Ventura Basin, the Los Angeles Basin, and those separating the offshore Channel Islands from one another (Figure 14.3.1). These basins preserve a record of deep to shallow marine environments, along with periodic uplift and erosion.

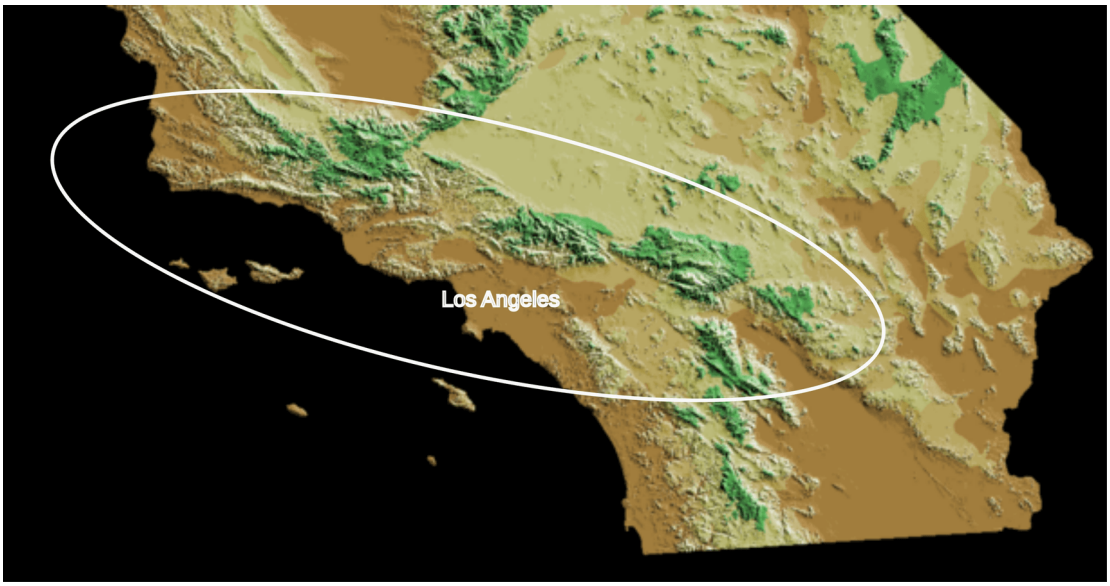


Figure 14.3.1: Digital elevation model of the Transverse Ranges Province highlighting mountains and valleys of Southern California. The Transverse Ranges Province is encircled; Los Angeles is on the boundary between this province and the Peninsular Ranges Province to the south. "Southern California digital elevation map" by USGS is in the public domain. Access a detailed description.

As the modern San Andreas fault system organized beginning at approximately 5 Ma, transpressional deformation inverted and deformed many of these basins and led to pronounced uplift of the adjacent ranges that continues today. While much of the sedimentary history of these deep (and in some cases, still underwater) basins is known from drill cores, the sedimentary record of basin formation in some areas can be directly accessed in fault-bounded hills and ranges within and adjacent to the modern basins. Indeed, geomorphic features across the modern landscape, along with historical earthquakes demonstrate that the forces responsible for this deformation continue today.

Ventura Basin

An example of the dramatic changes experienced by this region is found in the confines of the Ventura Basin in the Western Transverse Ranges (Figure 14.3.2). The Ventura Basin occupies the region to the north of the Santa Monica Mountains and generally south of the Santa Ynez Mountains. The basin is named for the City of San Buenaventura located in its central region. Extending east-west, this synclinal basin is continuous with the offshore Santa Barbara Basin to the west and the Soledad Basin to the east.

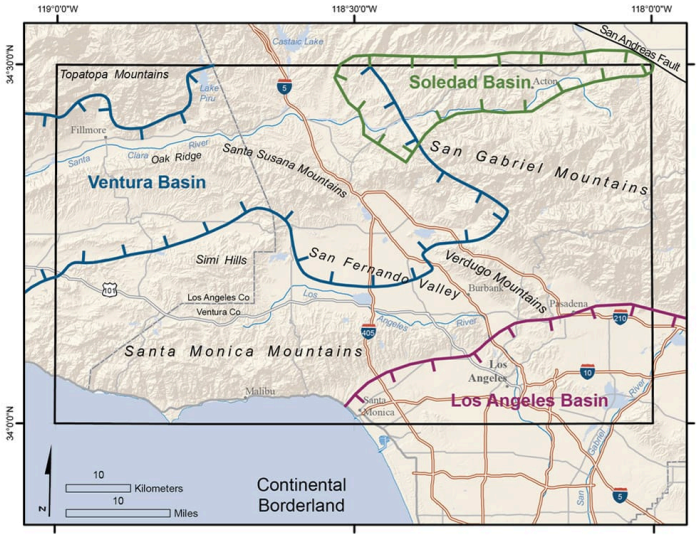


Figure 14.3.2: Principal late Tertiary to Quaternary depositional basins and upland areas where bedrock units are exposed within the Los Angeles 30' x 60' quadrangle. The Soledad basin is represented by Miocene strata, which are truncated to the southwest by the San Gabriel Fault and subsequently overlapped by Pleistocene deposits of the Ventura basin; the Ventura and Los Angeles basin boundaries represent the limits of associated Pliocene and Pleistocene formations. "Preliminary RGM Los Angeles" by the USGS, is in the public domain.

The central part of the Ventura Basin is unusually deep, containing approximately 17,700 m of mostly marine sediment that is as old as Late Cretaceous in age. Marine basin deposits here are like those found in the Great Valley to the north and other basins across southern California. Based on the sedimentary rocks within this basin, workers have inferred that this region occupied a position offshore of a volcanic arc early in its history; this arc was likely the southern extent of the ancient Sierra Nevada arc. Sometime during the Late Eocene, regional uplift and erosion of this region led to an influx of shallow marine and non-marine sediments that continued through the Early Miocene. Sedimentary units of this period are arkosic sandstones, conglomerates, and siltstones, some of which are fossiliferous. These units record a gradual, but widespread regional uplift as sedimentary facies seem to shift from shallow water to non-marine in character. These deposits are comparable to ancient fore-arc units found in the Great Valley Sequence at this time.

Within the basin, sedimentary units are folded into a broad syncline, with anticlinal structures along the northern and southern flanks, where important oil fields are located (Figure 14.3.3). These anticlinal structures are associated with Pleistocene reverse faults which push ranges to the north and south over the intervening basin area.

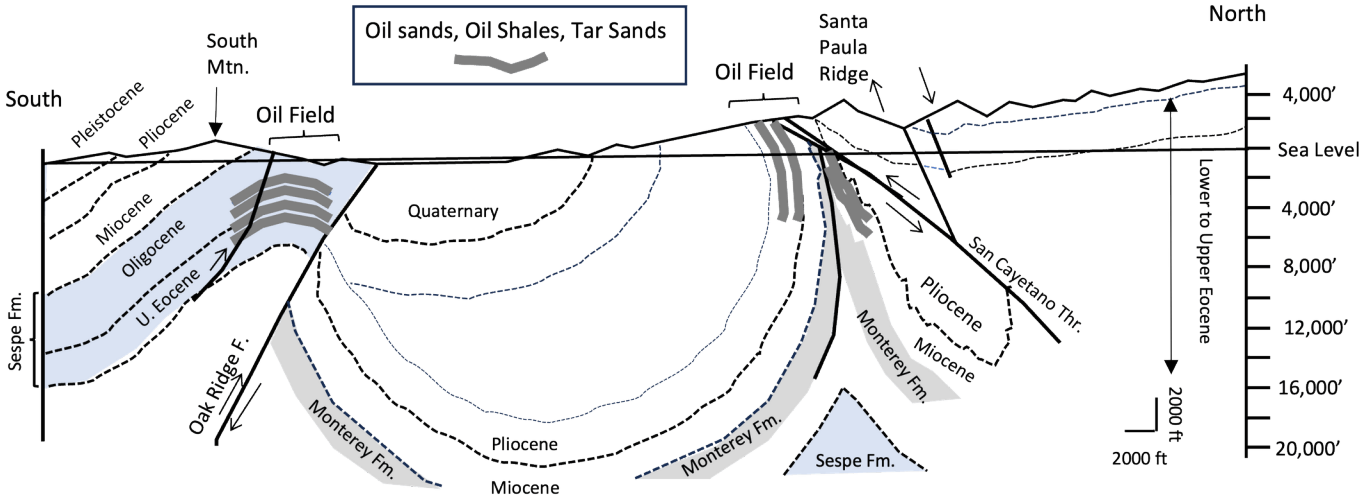


Figure \(\PageIndex{3}\): Simplified cross-section through the central Ventura Basin. Units are folded into an anticline/syncline pair and then offset by north and south dipping reverse faults. The Miocene Monterey Formation and the Oligocene/Upper Eocene Sespe Formation are highlighted. Areas of oil production are near the top of the southern anticline, in the Sespe Formation, and also near the Santa Paula Ridge in the north, where the Monterey Formation comes close to the surface. "Simplified cross-section through the central Ventura Bssin", by M. A. House is licensed under CC BY-NC /a derivative of the original by the California Division of Mines and Geology (now the California Department of Conservation). Access a detailed description of this image.

The Late Eocene-Early Miocene Sespe formation is a distinctive unit deposited during this period. This collection of non-marine conglomerates, sandstones and siltstones weathers a distinctive red and green color (Figure 14.3.4); the distinctive red appearance in some areas is comparable to that of Permian Red Beds (Figure 14.3.5). The Sespe formation is found in other basins throughout the western Transverse Ranges Province, indicating that the uplift and erosion that led to its formation impacted much of this region. Overall, these rocks are generally very resistant to erosion. Where subsequent faulting has uplifted them, they are ridge forming. For example, the ~40 Ma shallow marine Coldwater Sandstone, which precedes the deposition of the Sespe Formation, forms much of the mountainous Santa Ynez Range on the north side of Santa Barbara.



Figure 14.3.4: Lower Sespe formation outcrop is a weathered, poorly-sorted conglomerate (with all sediment sizes from boulders on to silt); Santa Ynez Mountains, CA. "Sespe Conglomerate" by Antandrus is licensed under CC BY-SA 3.0.



Figure 14.3.5: Typical outcrop of the Sespe Formation, north of Santa Barbara, California. The red rocks in the center are Sespe; lighter-colored rocks on the mountainside in the background are the Coldwater Formation. "Sespe Formation Outcrop, SB" by Antandrus is licensed under CC BY-SA 3.0.

The lithology of clasts within the Sespe Formation have been used to study the pattern of uplift and the paleogeography at the time of its deposition. Clasts within the lower Sespe Formation are granites and volcanic rocks that appear to be derived from source rocks found in the modern Mojave region, indicating that this basin was located further to the east and south at the time of deposition of this part of the formation. Higher in the section, blocks of metamorphic Franciscan basement rocks appear, indicating that the basement rocks of the western San Gabriel Mountains were exposed and eroding at this time.

As the plate boundary continued to evolve, renewed basin subsidence led to a return of deep marine conditions in the central and western Ventura Basin at approximately 17 Ma. Along with the deposition of deep marine units, rhyolitic and basalt volcanic debris, which is quite extensive in some areas, appears in the basin. In areas to the south, these units (called the Conejo Volcanics) can be quite substantial.

The shift to deep marine basin conditions led to deposition of the deep-water Rincon Formation (shales) and the Monterey Formation (marine shales and siltstones, and abundant diatomaceous oozes; Figure 14.3.6). These units are key elements of oil reserves in central and southern California: the Monterey Formation and its equivalents is the source rock for oil and gas reserves throughout the Transverse Ranges and the Peninsular Ranges Provinces, as well as the Great Valley Province. To learn more, see Great Valley.



Figure 14.3.6: Monterey Formation, Gaviota State Park, California, USA. Fine grained, well laminated shales tilt to the left. "Monterey Formation Outcrop, SB Area" by Antandrus is licensed under CC BY-SA 3.0.

Soledad Basin

The complexity of basin geometries and histories in this region can be appreciated by comparing the history of the central Ventura Basin to that of its eastern equivalent: the Soledad Basin. This collection of shallow marine and non-marine sediments occupies much of the western San Gabriel Mountains today (Figure 14.3.2).

While deep marine conditions prevailed in the central and western Ventura Basin in the Miocene, the depositional setting of the area that would become the Soledad Basin was shallow marine to non-marine in nature. Take, for example, the Vasquez Formation, a non-marine alluvial fan deposit which is broadly contemporaneous with deposition of the Monterey Formation (Figure 14.3.7). While siliceous oozes were actively deposited in the Ventura basin to the west, non-marine alluvial fan deposits of the Vasquez Formation were shed off the surrounding ranges and deposited in the Soledad basin. These very different depositional settings co-existed along a structural trend and attest to the complexity of reconstructing the history of the region.



Figure 14.3.7: Tilted outcrops of the Vasquez formation at Vasquez Rocks County Park. Bedded sandstones and conglomerates of fluvial and lacustrine origin were deposited in Late Oligocene-Early Miocene and tilted by motion on the developing San Andreas Fault System. These units are part of the Soledad Basin. "Vasquez Rocks County Park" by Thomas, is licensed under CC BY 2.0.

As is the case with other non-marine units of the Transverse Ranges, the ridge-forming conglomerates and sandstones of the Vasquez Formation are resistant to erosion. This unit can be observed at Vasquez Rocks Natural Area, where layers of conglomerate and sandstone have been uplifted and tilted due to interactions with the San Andreas fault system. Subsequent erosion has created interesting landforms that have been the backdrop for numerous films and TV shows over the years.

Los Angeles Basin

The Los Angeles Basin and coastal plain region lies at the junction of the Transverse Ranges and the Peninsular Ranges Provinces (Figure 14.3.8). The Santa Monica Mountains and the Puente, Repetto, and Elysian Hills mark the northern limits of the modern basin; these anticlinal, fault bounded uplifts expose much of the basin stratigraphy. Smaller basins to the north of these uplifts (such as those beneath the modern San Gabriel and San Fernando Valleys) contain units like those in the central part of the basin, and so are an extension of the modern Los Angeles basin.

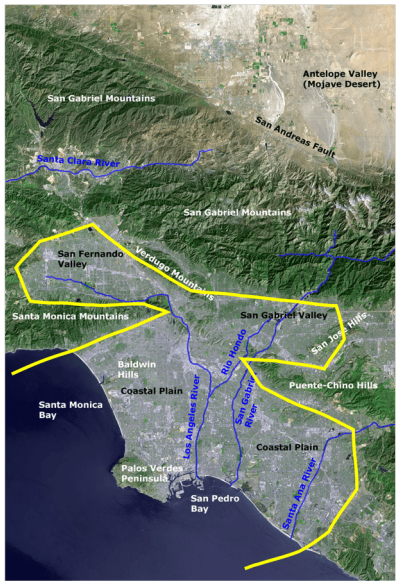


Figure 14.3.8: Approximate extent of the Los Angeles Basin (outlined in yellow). Details of the extent of the basin are described in the text. Major mountains and hills are labeled as described in the text. The major rivers that run across the basin are marked in blue. These include, from west to east, the Los Angeles River, the Rio Hondo River, the San Gabriel River, and the Santa Ana River. These units are part of the Soledad Basin. "LA Overhead" by NASA is in the public domain.

To the southwest, the basin continues to the base of the Palos Verdes hills, an anticlinal uplift in which basin units are uplifted across the north verging Palos Verdes Fault. Units then plunge southward of this anticline to the offshore termination of the basin.

The general structure within the basin is a northwest trending syncline (Figure 14.3.9). This structure, along with the anticlinal uplifts, anticlines like the Wilmington Anticline, and associated reverse faults are the product of transpressional deformation beginning at approximately 5 Ma. In addition to these compressional structures, the Los Angeles basin is sliced into four distinct blocks. These blocks are separated from one another by the northwest trending right-lateral Newport-Inglewood and Whittier-Elsinore Faults and the Santa Monica Mountain-Raymond Hill fault system (Figure 14.3.9). While the Newport-Inglewood and Whittier-Elsinore faults, which are truncated by the Santa Monica Mountain fault, have an older history (see Peninsular Ranges Chapter), they are also responsible for vertically shuffling basin blocks such that they have distinctive depths and depositional histories. These histories result in different sediment thicknesses, but across the region, key units such as the Sespe Formation, Miocene Volcanic units, and equivalents of the Monterey Formation (which are locally called the Puente Formation and the Modelo Formation) are preserved.

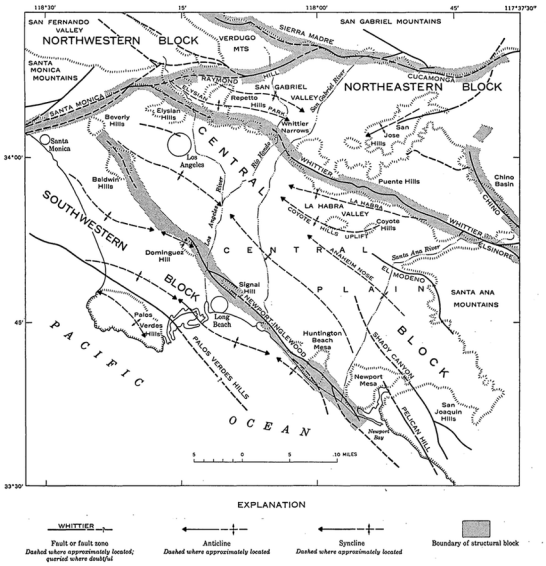


Figure 14.3.9: Major structural blocks of the Los Angeles Basin. Details of this image are discussed in the text. "Major Structural Blocks of the Los Angeles Basin" by USGS/R. F. Yerkes, T. H. McCulloh, J. E. Schoellhamer and J. G. Vedder is in the public domain. Access a detailed description of this image.

Query 14.3.1

This interactive element is not available in this format. Visit the link or scan the QR code to access it online.

View this Interactive Content online

References

1. (n.d.). YouTube: Home. Retrieved February 15, 2024, from https://www.geophile.net/FieldTrips/Geol150_PVtrip/PV_fieldtrip03.htm
2. *Geologic Formations - Channel Islands National Park (U.S.*. (2016, June 21). National Park Service. Retrieved February 15, 2024, from https://www.nps.gov/chis/learn/nature/geologicformations.htm
3. *Geology of the San Gabriel Mountains*. (n.d.). CSUN. Retrieved February 15, 2024, from https://www.csun.edu/science/geoscience/fieldtrips/san-gabriel-mts/geology-san-gabriels.html
4. Hall, C. A. (1981). Evolution of the western Transverse Ranges microplate: Late Cenozoic faulting and basinal development. In *The Geotectonic Development of California* (pp. 559-582). Prentice-Hall.
5. Harden, D. R. (2004). *California Geology*. Pearson Prentice Hall.
6. Ingersoll, R. V., & Ernst, W. G. (1987). *Cenozoic Basin Development of Coastal California* (R. V. Ingersoll & W. G. Ernst, Eds.). Prentice-Hall.
7. KellerLynn, K. (2016). *Santa Monica Mountains National Recreation Area Geologic Resources Inventory Report*. US Department of the Interior.
8. Meisling, K. E., & Weldon, R. J. (1989). Late Cenozoic tectonics of the northwestern San Bernardino Mountains, Southern California. *Geological Society of America Bulletin*, *101*(1), 106-128.
9. Morton, D. M., & Miller, F. K. (2006). *Geologic Map of the San Bernardino and Santa Ana 30' x 60' quadrangles, California* [Map]. USGS.
10. Norris, R. M., & Webb, R. W. (1976). *Geology of California*. Wiley.
11. Wallace, R. E. (1990). *The San Andreas Fault System, California US Geological Survey Professional Paper 1515*. USGS.
12. Weldon, R. J. (1986). *Simplified geologic map of the Western San Bernardino Mountains: Supplement 12 from "The late Cenozoic geology of Cajon Pass : implications for tectonics and sedimentation along the San Andreas fault " (Thesis)* [Map]. https://doi.org/10.22002/D1.1038

13. Yeats, R. S., & Grigsby, R. B. (1987). Ventura Avenue anticline: Amphitheater locality, California. In *Cordilleran Section of the Geological Society of America Centennial Field Guide* (Vol. 1, pp. 219-224). Geological Society of America.
14. Yerkes, R. F., McCulloh, T. H., Schoellhamer, J. E., & Vedder, J. G. (1965). *Geology of the Los Angeles Basin, California-an Introduction*. USGS.

This page titled 14.3: Cenozoic Sedimentation and Basin Development is shared under a CC BY-NC 4.0 license and was authored, remixed, and/or curated by Martha House.

14.4: Tectonic and Structural Evolution of the Transverse Ranges

A Changing Plate Boundary

The Transverse Ranges Province has evolved over time from an active Mesozoic subduction zone to Early-Middle Cenozoic transtension produced by simultaneous extension, shearing and rotation, and finally to a modern transpressional (compression and shear) setting beginning approximately 5 Ma. These dramatic changes can be linked to specific stages of the development of the San Andreas system and its fault system precursors beginning at approximately 20 Ma (Figure 14.4.1).

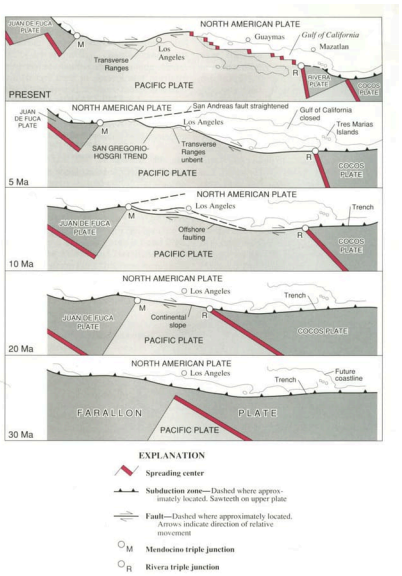


Figure 14.4.1: Sequential diagrams showing plate-tectonic evolution of the San Andreas transform fault system. "Formation of the San Andreas" by USGS/W.P. Irwin, is in the public domain. Access a detailed description of this image.

Geologic relationships described in the previous section indicate that the future Transverse Ranges region was offshore or adjacent to an active subduction zone and volcanic arc through the Early Cenozoic. This convergent plate boundary separated the Farallon and North American Plates and, as shown in Figure 14.4.1, persisted until approximately 30 Ma. However, as the Pacific Plate approached this plate boundary, a triple junction developed that launched the development of the ancestor to our modern transform boundary. As the single triple junction evolved into the current two separate triple junctions (the Mendocino and Rivera Triple Junctions) that migrated away from one another, a transform boundary evolved in between them as shown in Figure 14.4.1 in the panel labeled "20 Ma".

This initial boundary was not the San Andreas Fault System that we think of today. Rather, it was located farther to the west and offset was accommodated by different faults. The diagrams in Figure 14.4.1 illustrate the change in position of the transform boundary at 10 Ma, 5 Ma and today. Over this time, the boundary migrated inland. For a broader review of these changes, see A Brief Geologic History of California.

Query 14.4.1

This interactive element is not available in this format. Visit the link or scan the QR code to access it online.

View this Interactive Content online

Rotation of the Western Transverse Ranges

At about 20 Ma, large portions of the Transverse Ranges Province were farther south than today. Over time, they migrated northward and began to rotate clockwise relative to North America and one another as shown in Figure 14.4.2. In this image, the Mendocino Triple Junction is north of the future location of San Francisco, and separates a transform boundary, a convergent boundary to the north, and a developing transform boundary to the southeast. At the same time, the Rivera Triple Junction is located offshore (west) of what will become Santa Barbara, and both are almost directly west of the future San Diego.

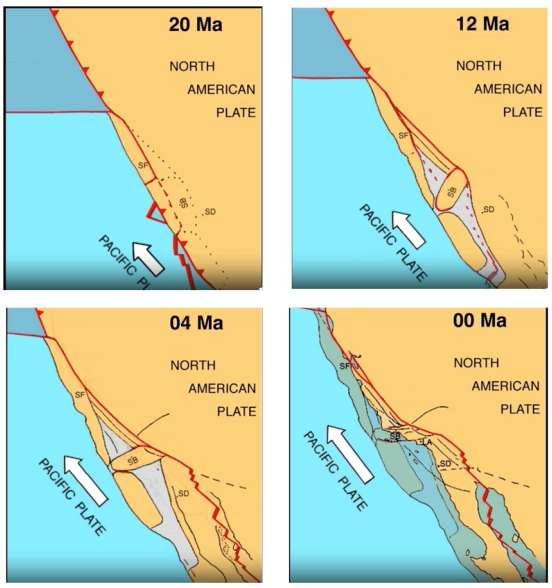


Figure 14.4.2: Sequential diagrams showing the rotation of the Western Transverse Ranges. Time panels are shown for 20, 12, and 4 Ma, and today. Labels are Santa Barbara (SB), San Francisco (SF), and San Diego (SD). The white arrow aims northwest, indicating the relative motion of the Pacific Plate relative to the North American Plate. The red lines are the plate boundaries at different times. Dashed lines indicate future crustal blocks that will be rotated via plate interactions. "Rotation of the Western Transverse Ranges" by M. A. House, a derivative of the original, is in the public domain. Access a detailed description of this image.

This rotation was accompanied by crustal thinning and renewed basin subsidence as indicated in the portions of Figure 14.4.2 labeled 12 and 4 Ma. Areas that were particularly impacted in the western Transverse Ranges Province include the Santa Monica Mountains, the Santa Ynez Range, and the northern Channel Islands (Santa Rosa, Santa Cruz, Santa Barbara, San Miguel, and Anacapa Island). Paleomagnetic data and stratigraphic studies suggest that the sedimentary units preserved in these regions were deposited offshore of modern-day San Diego and were carried northward into their current position. They have also been significantly reoriented through more than 75 degrees of clockwise rotation beginning in Miocene times.

Along with clockwise rotation, local extension produced deep pull-apart basins that evolved into the major depocenters (such as the Ventura Basin) across the Western Transverse Ranges (see the chapter on the Basin and Range Province for a discussion of pull-apart basins). Normal faulting also produced non-marine basins (such as the Soledad Basin) found in the western San Gabriel Mountains, and the interaction of these normal faults with the evolving transform boundary produced additional transtensional pull-apart basins such as the Ridge Basin, which provide important information about the history of faulting in this region.

The influx of Miocene volcanic units discussed in the section on basin stratigraphy accompanied this rotation, presumably as

volcanic eruptions produced magma that was created via decompression melting in response to crustal thinning (see the Chapter on the Basin and Range).

As rotation progressed and the developing San Andreas Fault System continued to interact with the North American Plate, the future plate boundary adjacent to the Transverse Ranges region was no longer parallel to the relative plate motion between the Pacific and North American plates. This so-called “Big Bend” in the San Andreas system caused the transtensional setting to evolve into one of transpression across the region beginning at approximately 5 Ma.

This can be seen in the panel labeled 4 Ma in Figure 14.4.2, in which the elongated Santa Barbara Block is oriented almost east-west, and the triangular basin that had opened south of it is larger. The elongate crustal block to the south has continued to migrate northward and the area that will become San Diego is now separated from the rest of North America by a transform boundary that extends northward from the proto-Gulf of California.

Transpression

Transpression results when the forces of compression and shear are distributed across this zone due to the geometry of the plate boundary here (Figure 14.4.3).

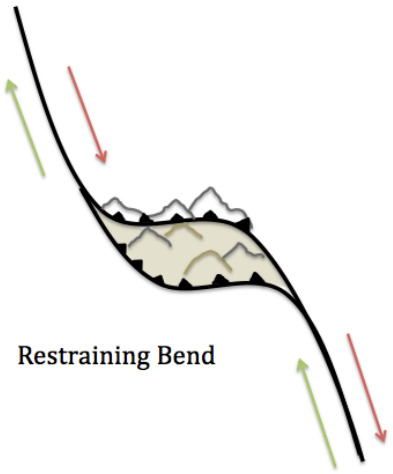


Figure 14.4.3: Diagram of a restraining bend geometry similar to that of the Transverse Ranges Province. A northwest striking right-lateral strike-slip is offset from a similar fault by a zone of reverse faulting such that there is a left step in the plate boundary from south to north. The restraining bend is bounded by two north-dipping reverse faults that cause mountains to form in this region. "Restraining Bend" by GeoAsh is licensed under CC BY-SA 4.0. Access a detailed description of this image.

Consider that we typically discuss the San Andreas fault as a “right-lateral strike-slip fault”. This is true along much of its length where it is oriented parallel to the overall relative plate motion between the North American and Pacific Plates that it separates. However, the situation is somewhat more complex in this region where the San Andreas fault system strikes roughly northwest-southeast. Here, the plate motion has a component that is perpendicular to the orientation of the boundary, creating a situation of compression along with shear that is reflected in the geologic structures that form. While the San Andreas Fault System itself is certainly dominated by right-lateral shear motion, many of the faults across the Transverse Ranges Province are reverse faults or even left-lateral!

Transpression has dramatically modified this region over a relatively brief period and continues to be active today. Across the Transverse Ranges Province today, the Earth’s crust is compressed and shortens by about 10–15 mm/yr (0.4-0.6 in/yr). Figure 14.4.4 shows GPS (Global Positioning System) vectors for sites across this region. The length of the vectors reflects the rate of movement; the angle reflects the direction. The figure shows that throughout the Transverse Ranges Province, motion is to the northwest, but regions east of the San Andreas Fault System have little or no motion. In the area where the San Andreas Fault System bends eastward through the Transverse Ranges Province, vectors are no longer parallel to the fault boundary, which is the cause of transpression here.

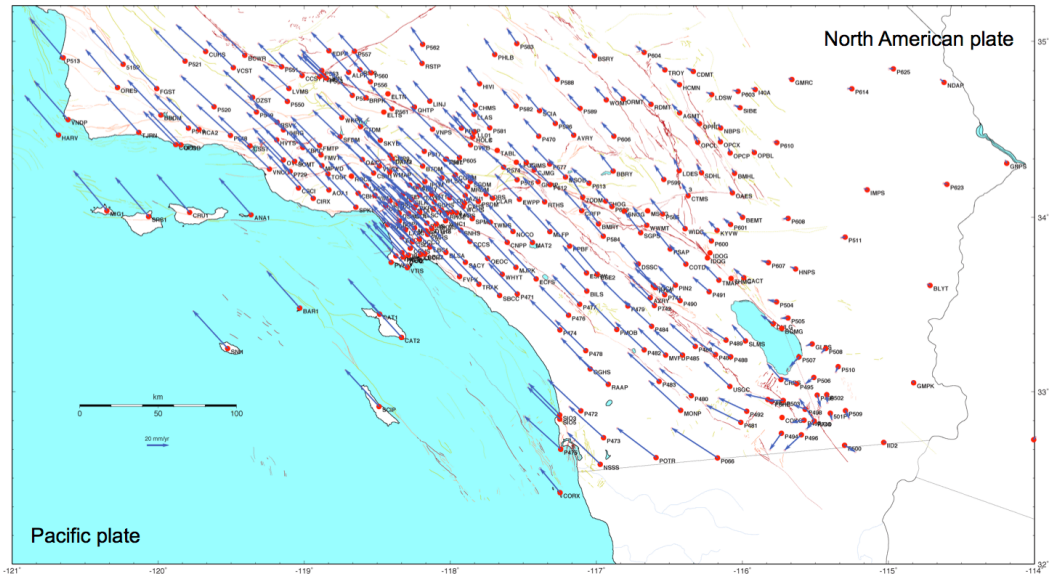


Figure 14.4.4: Current GPS (global positioning system) permanent station network in Southern California, showing movement of locations throughout the region because of the large-scale movement of the Pacific Plate relative to the North American Plate. Vectors generally indicate the region is moving to the north west. Vector lengths indicate a range of rates that are approximately 40 mm/yr. To the east of the San Andreas fault, the vectors are much shorter. "SCIGN map vectors" by the Southern California Earthquake Center, USC is in the public domain. Access a detailed description of this image.

This compression also results in the uplift of the western Transverse Ranges Province; ranges here have been uplifted rapidly during the Quaternary, with rates of uplift estimated at 4—8 mm/yr (0.16-0.32 in/yr). These rapid rates of uplift are averages; uplift associated with individual earthquakes can be quite significant. For example, one event in 1971 (the San Fernando Earthquake) produced 2 m (6.6 ft) of uplift in the nearby mountains!

Additional evidence of uplift is seen along coastal regions and in the northern Channel Islands. In these coastal areas, numerous marine terraces can be used to track the rate and timing of uplift (Figure 14.4.5). A marine terrace is formed by an uplifted wave-cut platform (see Chapter 16) that often contains ancient beach deposits and shells. These deposits were actively formed when the surface was at sea level; waves erode the bedrock to a flat surface. Over time, some of these surfaces are tectonically uplifted (they can also be stranded above sea level if sea level drops, but the situation in the Transverse Ranges is one of tectonic uplift due to transpression). These uplifted shorelines have been used to constrain rates and episodes of coastal uplift over thousands of years that date to hundreds of thousands of years.



Figure 14.4.5: "Stair-step" landscape of uplifted marine terraces on western San Clemente Island are similar to those found throughout the Transverse Ranges Province coastal region. The lowest terrace, where the road near the shore is visible, has been dated to 120,000 years by U-series analysis of corals (Muhs and others, 2002). "Marine terraces" by Daniel Muhs/USGS is in the public domain.

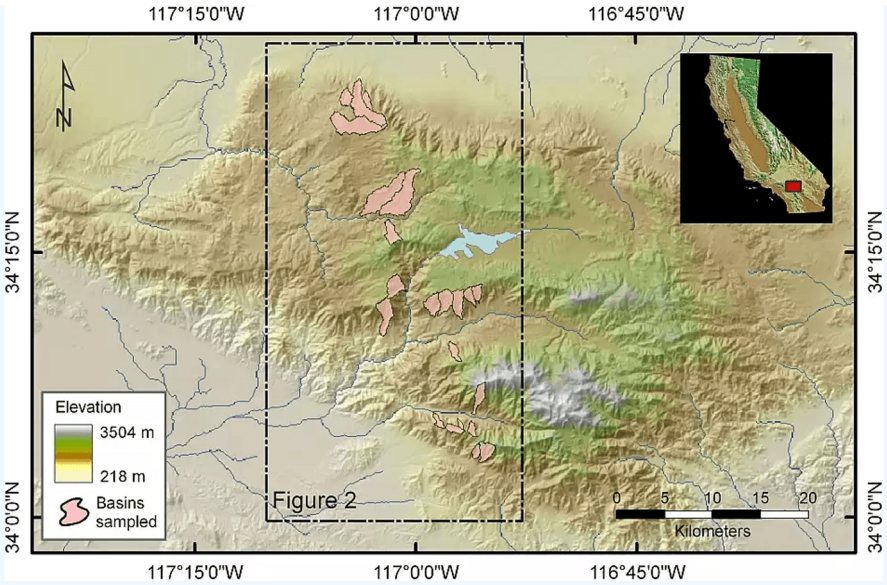
Box 14.4.1: Denudation Rates and Topography

The following text is adapted from "Denudation rate chronologies and the topographic development of the San Bernardino Mountains, California". This work, by Steve Binnie and William M. Phillips is licensed under CC BY-NC-SA 3.0 / a derivative from the original work.

How does the topography of mountains develop? What roles do crustal processes such as faulting and surface processes such as erosion play? These questions have long been a focus of geomorphic research. In the past decade, improved techniques for measuring rates of denudation (removal of material leading to a reduction in the relief and elevation of a landscape) have sparked new insights into these topics. The following is a case study for a landscape astride the San Andreas fault zone that uses denudation rates measured over different time scales to track topographic development.

The following study constructs a denudation rate chronology that compares rates averaged over millions of years with rates averaged over thousands to hundreds of thousands to years.

The San Bernardino Mountains in southern California (Inset Figure 14.4.1) is an ideal location for examining how topography develops. This range retains remnants of topography formed prior to the beginning of mountain building in the late Miocene, about 6 Ma. The relict topography consists of a gently undulating plateau in the north and central portions of the mountains. Much of this low-relief landscape is mantled by deeply weathered granite originally contiguous with a similar granitic weathering mantle found in the lower lying Mojave Desert to the north. The weathering of the granite formed under a more humid climate prior to uplift of the San Bernardino Mountains. The southern third of the range comprises a series of east-west–trending ridges of high, rugged topography separated by major faults located in the intervening valleys. Here the relic landscape has been erased by vigorous erosion. These characteristics make it possible to track topographic development from early block uplift to later slicing up of the landscape by faulting.

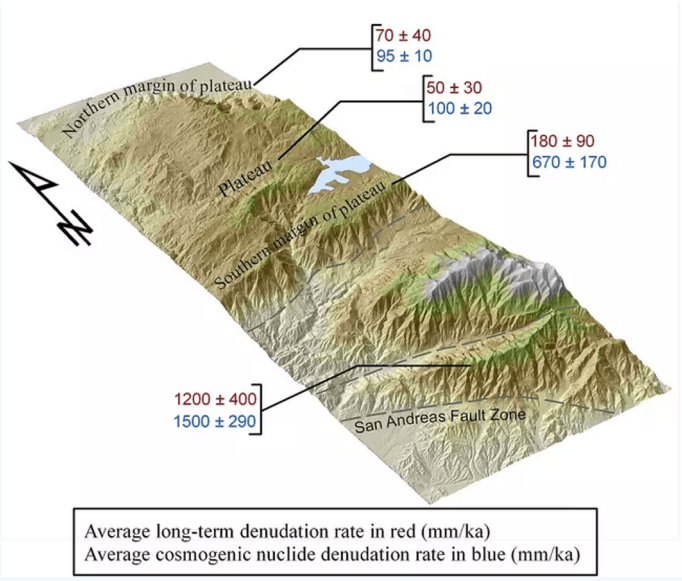


Inset Figure 14.4.1: Location map of the San Bernardino Mountains. The north and central portions of the mountains exhibit a broad, gently undulating plateau that contrasts sharply with the steep narrow ridges in the south. Pink shaded areas are the basins sampled for cosmogenic nuclide analysis (modified from Binnie et al., 2008). "Location map of the San Bernardino Mountains" by Steve Binnie and William M. Phillips is licensed under CC BY-NC-SA 3.0. Access a detailed description.

Denudation rates (reported in units of millimeters per thousand years or mm/ka) were measured in three different ways and over three different timescales in the San Bernardino Mountains. First, by dating and reconstructing the pre-uplift topography, rates of denudation since uplift began can be determined. These rates are computed by dividing the amount of incision of the relic topography by the age of uplift initiation. Second, in the southern part of the mountains, thermochronology was used.

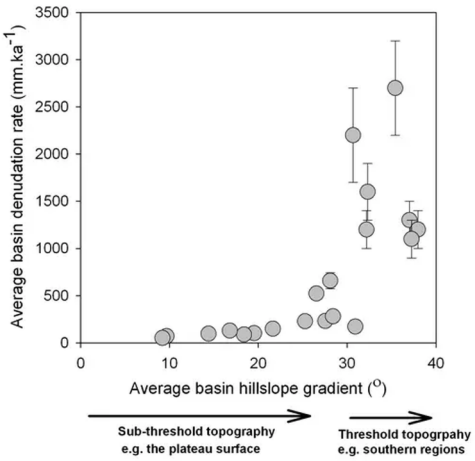
Thermochronology uses radiometric dating of minerals in rocks together with information about the thermal structure of the earth's crust. Each type of mineral has a closure temperature corresponding to the temperature at which the mineral begins to retain the products of radioactive decay. The depth below the earth's surface at which closure begins can be determined from geothermal gradients (rate at which temperature increases with depth). Dividing the closure depth by the radiometric age gives a denudation rate (some geologists term this rate "exhumation" rather than denudation). Thermochronologic denudation rates in the San Bernardino Mountains are also averaged over millions of years. The third method uses terrestrial cosmogenic nuclides. Terrestrial cosmogenic nuclides are generated by cosmic rays penetrating the top few meters of the Earth's surface. The concentration of these nuclides reflects a balance between the rate of production and the rate at which they are lost due to denudation and radioactive decay. By measuring the concentration of nuclides in surface rocks, calculating a value for the nuclide production rate at the sampling site, and using known values for radioactive decay, a denudation rate can be determined. As this denudation rate is averaged over the length of time the nuclides have resided in the near-surface, the period over which the rate is applicable is itself a function of the denudation rate, but will typically be on the order of thousands to hundreds of thousands of years. These principles also apply to spatially averaged denudation rates for whole river basins determined by sampling alluvial (stream) sediments; this is the procedure used in this study.

Results (Inset Figure 14.4.2) show that denudation rates measured with all techniques are much lower in the northern part of the San Bernardino Mountains (70-100 mm/ka) where relic topography is preserved than in the southern part (180-1500 mm/ka). For example, in the northern margin of the plateau, average long term denudation rates are 70 mm/yr and cosmogenic rates are 95 mm/yr, with errors of 40 and 10 mm/yr, respectively. To the south, at the plateau, average long term denudation rates are 50 mm/yr and cosmogenic rates are 100 mm/yr, with errors of 30 and 20 mm/yr, respectively. At the southern maring of the plateau, average long term denudation rates are 180 mm/yr and cosmogenic rates are 670 mm/yr, with errors of 90 and 170 mm/yr, respectively. Immediately north of the San Adnreas fault, the highest rates are found: average long term denudation rates are 1200 mm/yr and cosmogenic rates are 1500 mm/yr, with errors of 400 and 290 mm/yr, respectively. When incision and thermochronologic rates averaged over million year timescales are compared with cosmogenic rates averaged over thousands to hundreds of thousands of years, we see that rates in the south are similar despite the very different averaging periods. This suggests that denudation rates of the narrow, rapidly uplifting ridges in the south have been relatively consistent over the last million years or so.



Inset Figure 14.4.2: A north-south transect through the San Bernardino Mountains giving mean denudation rates for the plateau, its northern and southern margins, and one of the steep southern ridges. Denudation rates (in mm/ka) derived over million year timescales using incision and thermochronology techniques are shown in red; rates measured over millennial timescales by cosmogenic nuclide analysis are shown in blue. Dashed gray lines indicate major faults. Rates in the south are similar over different timescales; rates on the plateau and its southern margin vary over different timescales (modified from Binnie et al., 2008). "A north-south transect through the San Bernardino Mountains" by Steve Binnie and William M. Phillips is licensed under CC BY-NC-SA 3.0. Access a detailed description.

Denudation rates in the north and central parts, on and around the edges of the plateau, are more rapid over shorter timescales, with the increase being more pronounced around the southern margin of the plateau than on the top. One explanation for this faster, more recent denudation is that the topography of the plateau is evolving, and doing so by the headward retreat of the steep drainage basins around the southern plateau periphery cutting back and gradually removing the plateau and the pre-uplift topography. Comparing the cosmogenic nuclide-derived denudation rates with average hillslope gradients (measured in angles of the steepness of slopes) of the San Bernardino Mountains illustrates another important result (Inset Figure 14.4.3). Here, average hill-slope gradients of 10-30° corresponds to low denudation rates (less than 100 mm/ka), while denudation rates increase linearly at hill slopes of more than 30° . A broadly linear relationship exists between denudation rates and hillslope gradients; that is, denudation increases as hillslopes steepen. This relationship decouples when hillslopes are steeper than around 30°, whereupon denudation rates no longer correspond to hillslope angles. This approximately 30° value delineates a change in how slopes erode.



Inset Figure 14.4.3: Denudation rates for the basins plotted against their respective average hillslope gradients. A broadly linear trend between the two is apparent where hillslope gradients are low (on the plateau). This trend breaks down for hillslopes of approximately 30° (found mostly in the southern regions of the mountains). Using space-for-time substitution, the left to right trajectory of this plot represents the progressive development of threshold hillslopes during mountain building. "Denudation rates for the basins" by Steve Binnie and William M. Phillips is licensed under CC BY-NC-SA 3.0. Access a text version of this chart.

The survival of pre-uplift topography on the plateau, coupled with the denudation rate chronologies, suggests a sequence for the landscape evolution of the San Bernardino Mountains. The left hand side of the denudation rate-hillslope gradient plot (Inset Figure 14.4.3) shows data mostly from the top of the plateau, where pre-uplift surfaces indicate that topography has been relatively unaffected by orogenesis. The right hand side of the plot contains data mostly from the southern parts of the mountains, where hillslopes are at threshold. Different parts of the San Bernardino Mountains are, therefore, experiencing different stages of the topographic response to orogenesis. As mountains begin to develop, their slopes steepen, denudation rates increase and, if crustal uplift is rapid enough, topography achieves threshold hillslopes. This notion of how threshold topography develops may be applicable to other ranges similar to the San Bernardino Mountains.

Query 14.4.1

This interactive element is not available in this format. Visit the link or scan the QR code to access it online.

View this Interactive Content online

References

1. Bierman, P., & Steig, E. J. (1996). Estimating rates of denudation using cosmogenic isotope abundances in sediment. *Earth Surface Processes and Landforms*, *21*(2), 125-140.
2. Binnie, S. A., Phillip, W. M., Summerfield, M. A., Fifield, L. K., & Spotila, J. A. (2008). Patterns of denudation through time in the San Bernardino Mountains, California: Implications for early-stage orogenesis. *Earth and Planetary Science Letters*, *276*(1-2), 62-72.
3. Binnie, S. A., Phillips, W. M., Summerfield, M. A., & Fifield, L. K. (2007). Tectonic uplift, threshold hillslopes, and denudation rates in a developing mountain range. *Geology*, *35*(8), 743-746.
4. Burbank, D. W. (1996). Bedrock incision, rock uplift and threshold hillslopes in the northwestern Himalayas. *Nature*, *279* (6565), 505-510.
5. Ehlig, P. L. (1981). Origin and tectonic history of the basement terrane of the San Gabriel Mountains, Central Transverse Ranges. In *The Geotectonic Development of California* (Vol. 1, pp. 253-283). Prentice-Hall.

6. Granger, D. E., Kirchner, J. W., & Finkel, R. (1996). Spatially Averaged Long-Term Erosion Rates Measured from In Situ-Produced Cosmogenic Nuclides in Alluvial Sediment. *Journal of Geology*, *104* (3), 249-258.
7. Hall, C. A. (1981). Evolution of the western Transverse Ranges microplate: Late Cenozoic faulting and basinal development. In *The Geotectonic Development of California* (pp. 559-582). Prentice-Hall.
8. Harden, D. R. (2004). *California Geology*. Pearson Prentice Hall.
9. Ingersoll, R. V., & Ernst, W. G. (1987). *Cenozoic Basin Development of Coastal California* (R. V. Ingersoll & W. G. Ernst, Eds.). Prentice-Hall.
10. Lal, D. (1991). Cosmic ray labeling of erosion surfaces; in situ nuclide production rates and erosion models. *Earth and Planetary Science Letters*, *104*(2-4), 424-439.
11. Meisling, K. E., & Weldon, R. J. (1989). Late Cenozoic tectonics of the northwestern San Bernardino Mountains, Southern California. *Geological Society of America Bulletin*, *101*(1), 106-128.
12. Montgomery, D. R., & Brandon, M. T. (2002). Topographic controls on erosion rates in tectonically active mountain ranges. *Earth and Planetary Science Letters*, *201*(3-4), 481-489.
13. Muhs, D. R. (2022). MIS 5e sea-level history along the Pacific coast of North America. *Earth System Science Data*, *14*(3), 1271-1330. https://doi.org/10.5194/essd-14-1271-2022
14. Muhs, D. R., Simmons, K. R., Kennedy, G. L., & Rockwell, T. K. (2002). The last interglacial period on the Pacific Coast of North America: Timing and paleoclimate. *GSA Bulletin*, *114*(5), 569–592. https://doi.org/10.1130/0016-7606(2002)114<0569:TLIPOT>2.0.CO;2
15. Norris, R. M., & Webb, R. W. (1976). *Geology of California*. Wiley.
16. Oberlander, T. M. (1972). Morphogenesis of granitic boulder slopes in the Mojave Desert, California. *Journal of Geology*, *80*(1), 1-20.
17. Proctor, R. J., & Crook, Jr., R. (1987). Sierra Madre thrust fault, Arcadia, California. In *Cordilleran Section of the Geological Society of America Centennial Field Guide* (218th ed., Vol. 1, p. 217). Geological Society of America.
18. Sidder, A. (2020, 10 9). Southern California's Crustal Motion Tells of Earthquake Hazards. *EOS*, *101*. https://doi.org/10.1029/2020EO150199.
19. Spotila, J. A., Farley, K. A., Douglas, Y. J., & Reiners, P. W. (2001). Near-field transpressive deformation along the San Andreas fault zone in Southern California, based on exhumation constrained by (U-Th)/He dating. *Journal of Geophysical Research*, *106*(B12), 30,909-30,922.
20. Spotila, J. A., House, M. A., Blythe, A. E., Niemi, N. A., & Bank, G. C. (2002). Controls on the erosion and geomorphic evolution of the San Bernardino and San Gabriel Mountains, Southern California. *Contributions to crustal evolution of the Southwestern United States. Special Paper - Geological Society of America*, *365*, 205-230.
21. Wallace, R. E. (1990). *The San Andreas Fault System, California" US Geological Survey Professional Paper 1515*. USGS.
22. Yerkes, R. F., McCulloh, T. H., Schoellhamer, J. E., & Vedder, J. G. (1965). *Geology of the Los Angeles Basin, California-an Introduction*. USGS.

This page titled 14.4: Tectonic and Structural Evolution of the Transverse Ranges is shared under a CC BY-NC 4.0 license and was authored, remixed, and/or curated by Martha House.

14.5: Geologic Hazards of the Transverse Ranges Province

Earthquakes in the Transverse Ranges

Like much of California, the Transverse Ranges Province is a zone of considerable seismic hazard. The region is crisscrossed by numerous active faults with considerable potential for damage. Two important examples are the 1971 San Fernando Earthquake and the 1994 Northridge Earthquake. These events occurred on reverse faults typical of this region and they exemplify the impact of such structures on the region's communities.

The 1971 M 6.7 San Fernando earthquake ruptured the Sierra Madre fault. This fault is part of a reverse fault system at the foot of the San Gabriel Mountains. Studies of this fault system indicate it has ruptured at least two times in the past 15,000 years, with likely magnitudes as high as 7.5 or 7.6 Mw. In addition to the uplift caused by the San Fernando quake, severe damage occurred in the surrounding areas in response to shaking (reaching XI, or extreme) on the Modified Mercalli Intensity Scale; Figure 14.5.1). Damage to a large dam in the area caused the evacuation of approximately 80,000 downstream residents for four days and major transportation corridors were obstructed. Of particular concern was the partial collapse of two medical facilities (Olive View Medical Center and Veterans Administration Hospital). Both facilities were situated near the fault: some of the Medical Center buildings were within 300 m of the fault, and the VA Hospital buildings were within 5 km (3.1 mi) of the rupture. Of the 65 fatalities associated with this event, more than half occurred due to the failure of these medical facilities.

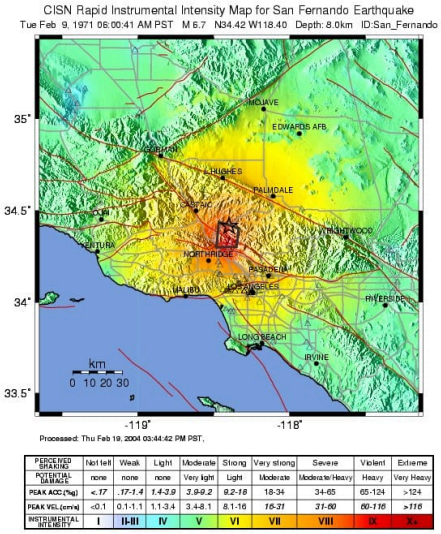


Figure 14.5.1: The 1971 San Fernando earthquake, also known as the Sylmar earthquake — Los Angeles County, Southern California. Shake map of the magnitude 6.7 earthquake occurring in the San Fernando Valley on February 9, 1971. Epicenter is marked at the star. Shaking maximum is Intensity IX northeast of the epicenter. "San Fernando earthquake" by USGS is in the public domain. Access a detailed description of this image.

The 1994 Northridge earthquake occurred on a previously unknown, buried reverse fault that did not break the surface (now known as a "blind thrust" after the fact that it did not break the surface). This 6.7 Mw earthquake killed 57 people and caused massive devastation across much of the LA basin due to seismic amplification within basin sediments; shaking was felt as far as 137 km (85 mi) away (Figure 14.5.2). Damage was particularly pronounced in basin areas of Santa Monica, Simi Valley, and Santa Clarita and as far away as the city of Anaheim located 80 km (50 mi) away. The shaking caused highway collapse and rail line ruptures, as well as pancaking of apartment buildings with weak first floor levels or garages, and ruptured gas and water lines among other challenges (see Chapter on earthquake hazards). As if it weren't bad enough, shaking stirred up clouds of fine dust that contained spores of a fungus (coccidioidomycosis) that led to an outbreak of Valley Fever. This fungal infection of the lungs is very difficult to eradicate and can cause severe long-term health impacts.

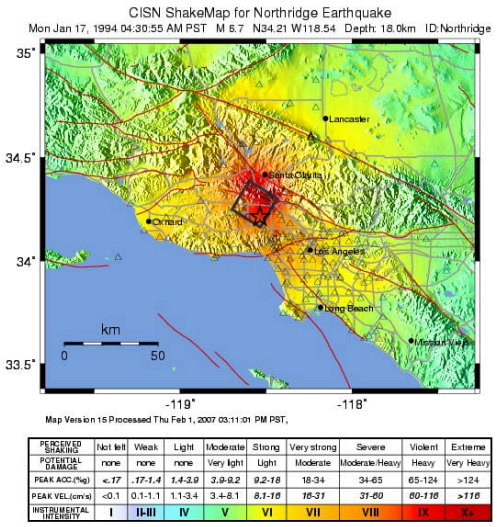


Figure 14.5.2: ShakeMap computed for the 1994 Northridge earthquake (see trinet for this and other archived events); the square indicates the estimated location and surface projection of the fault in this case. Maximum shaking was north of the epicenter. Intensity levels were as high as X+. "Shake Map for Northridge" by USGS is in the public domain. Access a detailed description of this image.

Video 14.5.1: A geologist talks about the Northridge earthquake

This video is an interview with a professional U.S.G.S. geologist concerning the Northridge earthquake.

This interactive element is not available in this format. Visit the link or scan the QR code to access it online.

View this YouTube Video online

Following the Northridge event, scientists revisited geophysical data from across the region and identified additional "blind thrusts" like the one that ruptured in the Northridge event (Figure 14.5.3). In the case of the Northridge earthquake, scientists realized that the structure that ruptured in 1994 might be related to an earlier rupture in 1987 (the M6 Whittier Narrows Earthquake). Continued work revealed other potentially hazardous structures buried beneath the Los Angeles Basin that could be associated with earthquakes of M6.2-6.7 and as high as Mw7.1. This potential, along with the possibility of seismic amplification in the many basin areas of the Transverse Ranges Province presents considerable risk for the residents.

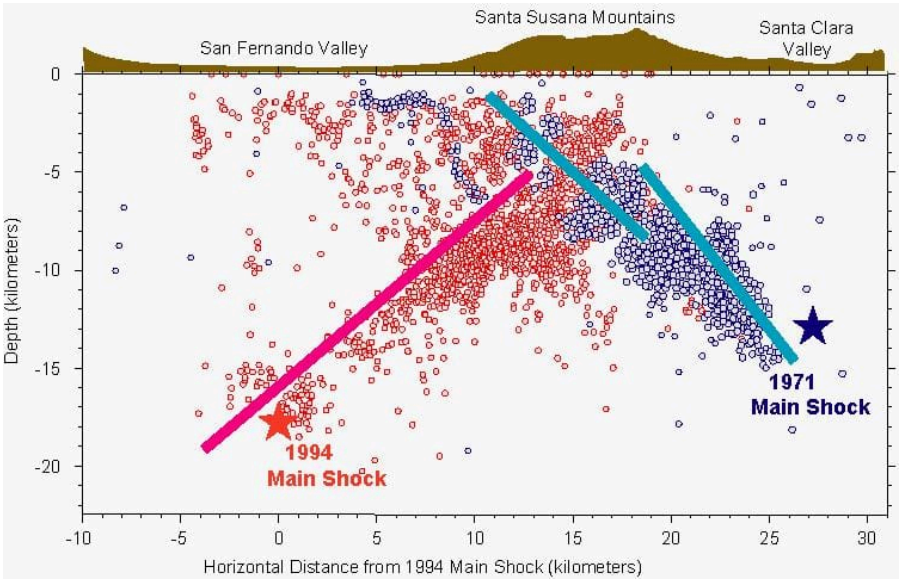


Figure 14.5.3: This cross-section beneath the San Fernando Valley shows models designed to trace rupture areas using seismic data from the Northridge Earthquake and the San Fernando Earthquake. This cross section is oriented with north to the right. Models of the fault planes of the 1994 Northridge dip to the south and do not reach the surface. Model results from the 1971 San Fernando earthquakes dip to the north and suggest that movement on the buried thrust fault responsible for the Northridge earthquake terminated about 5 kilometers beneath the surface. This movement may have terminated against one of the faults that moved in 1971. The hypocenters of the two shocks are at the lower limits of each of the fault models, and the arrays of dots indicate locations of aftershocks. "San Fernando cross section of fault models" by USGS is in the public domain. Access a detailed description.

Inset Box 14.5.1 State Responses to Major Earthquakes

Each time a major seismic event impacts California, we learn more about our risk and exposure to the hazard. In the case of earthquakes, enhanced instrumentation tells us more about the type of shaking we can expect. This information guides building design and code development that keeps us safe. The San Fernando and Northridge earthquakes led to the development and expansion of several important programs that keep Californians safer.

Following the San Fernando event, the Alquist-Priolo Special Studies Act was enacted. This act restricts construction of buildings designed for human occupancy across potentially active faults. It relies on maps of Alquist-Priolo Earthquake Fault Zones, which are created based on mapping information provided by the California Department of Conservation (CDC). In addition to the enhanced focus on residential buildings, the state created the The Hospital Safety Act of 1972 to ensure that new or retrofitted hospital buildings are sited, designed, and constructed so that they are able to remain operable following earthquakes. This event also highlighted the need for better communication among scientists, engineers, and emergency responders, leading to the creation of the first Earthquake Clearinghouse established by the CDC to promote better communication between.

The state also sought to better describe and understand the potential shaking damage to buildings via implementation of the California Strong Motion Instrumentation Program. This program's goal is to maximize the volume of data by furnishing and maintaining instruments at selected lifeline structures, buildings, and ground response stations. Information learned from this network informs development of building design to withstand potential shaking. To date, The program has installed more than 900 stations, including 650 ground-response stations, 170 buildings, 20 dams and 60 bridges.

Following the Northridge event, the California Legislature created the California Earthquake Authority (CEA), which is a publicly managed but privately funded organization that offers minimal earthquake damage coverage. In addition, a substantial effort was also made to reinforce freeway bridges against seismic shaking, and a law requiring water heaters to be properly strapped was passed in 1995. In addition, the Federal Emergency Management Agency (now under the U.S. Department of Homeland Security) awarded the California Geological Survey nearly $20 million to accelerate the zoning of earthquake hazards under the Seismic Hazards Mapping Act of 1990. These Seismic Hazard Zones, or Zones of Required Investigation, delineate where there is a high likelihood of these hazards occurring in future earthquake events. Local city and county permitting agencies are required to request "special geological and engineering studies" be performed within these zones prior to land development and construction.

Flooding in the Transverse Ranges

We typically think of California as the land of earthquakes. However, residents know that flooding is a periodic hazard for many of our communities. You can learn more about this hazard in our chapter on California Water. In the case of the Transverse Ranges Province, flooding is a major concern in low lying regions. This is because our steep ranges collect a lot of moisture from storms arriving from the Pacific Ocean to the west. When rainfall is very high, the water cannot infiltrate the ground and instead runs off into our heavily inhabited basin regions. Such dramatic episodes lead to the debris flows that we've seen in the Santa Barbara area, and coastal flooding observed throughout the state.

Historical flooding in the Los Angeles basin led to dramatic decisions to ensure the safety of area residents: the paving and channelization of major rivers and the construction of range front debris basins. (Figure 14.5.4) This action, taken by the US Army Corps of Engineers, was largely in response to serious flooding in 1938. This 50-year flood event was caused by the confluence of 2 major storms that deposited more than 1 year of precipitation in a few days. Flooding killed more than 100 people in the Transverse Range region (Figure 14.5.5). The event was so severe that the Los Angeles river's course was actually changed!



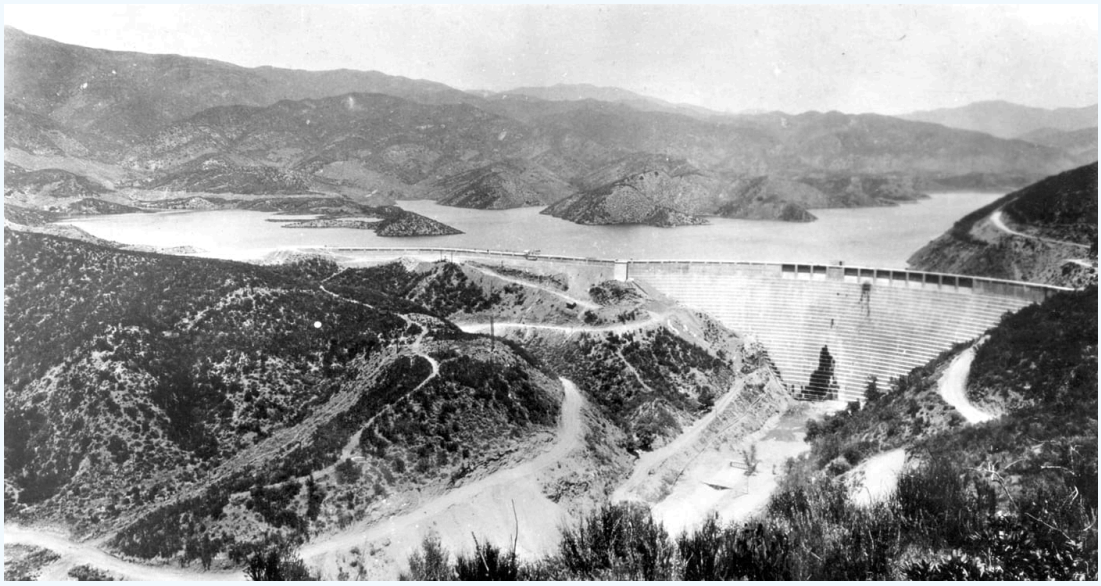
Figure 14.5.4: The concrete channel of a portion of the Los Angeles River. Water flows through the central part of the channel. Sloped banks prevent flooding and erosion. "MTA Los Angeles River" by anarchosyn, is licensed under CC BY-SA 2.0.



Figure 14.5.5: Los Angeles River. View upstream from above Victory Blvd. showing breaches in paved levees in and below a sharp curve in channel alignment. River mile 32.0. This image is from the Report on Engineering Aspects, Flood of March 1938 by the U.S. Engineer Office in Los Angeles and compiled in August 1938. The Los Angeles River and the river's tributaries flooded after a very wet rainy season and one particularly bad storm on March 1-3, 1938. After this flood, the Army Corps of Engineers set about ensuring extensive flooding would not cause such extreme damage in the future. "Los Angeles River Flood" by the United States Army Corps of Engineers is in the public domain.

Inset Box 14.5.2: The Saint Francis Dam Disaster

The epic 1938 flooding of Los Angeles was not the first major event impacting this region. In 1928, a man-made flood killed more than 350 residents of the western Transverse Ranges when the Saint Francis Dam broke. This dam was built by the Bureau of Water Works and Supply (now Los Angeles Department of Water and Power) under the leadership of William Mulholland in response to growing water needs in Los Angeles and was in San Francisquito Canyon of the Western Transverse Ranges (Inset Figure 14.5.1).



Inset Figure 14.5.1: View of the St. Francis dam looking to the north, with water in its reservoir, in February 1927, before it failed.

"St. Francis Dam" by H.T. Stearns/USGS is in the public domain.

The dam was placed above a reddish conglomerate/sandstone unit that contained gypsum and rested in fault-contact with a foliated mica schist interspersed with talc. The fault separating these units was the San Francisquito Fault, which was determined to be inactive. Throughout the period of filling and use, areas of seepage beneath and adjacent to the dam were observed, along with cracks within the dam (which were sealed upon inspection). None of these issues were deemed to be of significant concern. However, the dam catastrophically failed just before midnight on March 12, 1928. While there are no surviving witnesses to what followed, reconstructions of the event indicate that a 37 m (120 ft) high flood wave had traveled 1.6 - 2.4 km (1-1.5 mi) at an average speed of 29 km/hr (18 mi/hr). A large piece of the dam itself, weighing approximately 9,000 metric tons was found about three-quarters of 1.6 km (1 mi) below the dam site. The devastation was complete (Inset Figure 14.5.2).



Inset Figure 14.5.2: Damage from the St. Francis Dam Flood March 12-13, 1928, Los Angeles County, California. Taken from the same location as Inset Figure 5.1 showing the remains of the dam and reservoir floor. The dam failed at 11:58:30 p.m. Monday March 12, 1928. The left (west) abutment of the dam was entirely swept away and the inactive San Francisquito Fault is clearly visible, being located along the contact zone of schist and conglomerate. Adventurous hikers should note that this dam remnant no longer stands, as it was deemed an “attractive nuisance,” and unfortunately removed. "St. Francis Dam after the 1928 failure" by H.T. Stearns/USGS is in the public domain.

Flooding damaged the towns of Fillmore and Santa Paula and ultimately washed out to the Pacific Ocean south of the town of Ventura 87 km (54 mi) downstream. Subsequent investigations suggested that dam failure was in part due the fact that its unstable foundations were built on unsuitable bedrock. Superintendent and chief engineer of the Los Angeles Water Department William Mulholland was in the habit of personally intervening in dam designs, and he in fact inspected the St. Francis Dam hours before its deadly destruction. It should be noted that Mulholland had no formal degrees or expertise in engineering and was, for want of a better term, a self-taught engineer. An inquest considered, but did not advocate for, criminal charges against Mulholland.

As a result of this failure, enhanced dam safety legislation was enacted, and civil engineers were required to be licensed by the state.

Inset Box Video 14.5.1: The Story of the St. Francis Dam

This short video reviews the story of this dam and the ultimate disaster that unfolded.

This interactive element is not available in this format. Visit the link or scan the QR code to access it online.

View this YouTube Video online

Landslides

Due to the steep relief of the ranges within the Transverse Ranges Province, and the relatively unconsolidated or foliated nature of the rocks in these ranges, landslides are an additional hazard of this region. Some of these landslides are dramatic, forceful events and others are long-term creeping events. The two examples discussed here demonstrate that these processes are ongoing in this region. There are many other examples, however; one only needs to monitor the news!

The Blackhawk Landslide is a prehistoric landslide that can be observed to the north of the San Gabriel Mountains. The debris and trail of this mass of material can be readily viewed using aerial imagery (Figure 14.5.6). It appears as a long "river" of sediment that meets a fan deposit at its foot. The structure is approximately 8 km (5 mi) long and 9-30 m (30-100 ft) thick. Fossils preserved in ponds on its surface indicate the slide is no younger than 17,000 years old.



Figure 14.5.6: The Blackhawk Slide was a mammoth landslide that came off of Blackhawk Mountain, on the north side of the San Bernardino Mountains, an estimated 17,000 years ago, which is recent in geologic time. It is spread across the Lucerne Valley in Southern California. "Blackhawk Slide" by Doc Searls is licensed under CC BY 2.0.

The story of this slide is incredible: it's thought that roughly 17,000 years ago, Pennsylvanian limestone in the headwall of the slide (now situated to the south, in Blackhawk Canyon) collapsed as weathered metamorphic rock beneath it gave way. Once loose, this rock avalanche moved down-canyon at high speeds that reached 270 km/hr (170 mi/hr). Once the slide reached the flat areas to the north, it hit a small hill that acted as a ramp that launched the mass of debris as much as 120 m (400 ft) above the ground. Once airborne, the debris then traveled along a cushion of air at speeds as high as 385 km/hr (270 mi/hr) before collapsing. All told, the mass of rock fell more than 1200 m and traveled approximately 8 km (5 mi) in approximately 80 seconds!

Another example of an important mass wasting event in the Transverse Ranges Province is the Portuguese Bend Landslide Complex on the south side of the Palos Verdes Peninsula (Figure 14.5.7) This large area of slope failure includes multiple slide areas that have been more or less continually moving since 1956, but initiated as early as 600,000 years ago. The site is situated on ancient landslides that appear to have been active as early as 400,000 to 600,000 years ago. The cause of the slide is related to the orientation of the main geologic unit here (the Monterey Formation, a series of shales, diatomites and tuffs that contain a type of clay called bentonite, which swells when wet). These mass movements are a combination of earth flow, and translational and rotational slides that are driven by gravity sliding along bedding planes. The sliding is amplified by the addition of moisture

via irrigation and natural rainfall.



Figure 14.5.7: A photo of the Portuguese Bend Reserve on March 12, 2016. In the foreground is the Portuguese Bend landslide area. In the background are Inspiration Point, Portuguese Point, Long Point, and the Terranea Resort. "Portuguese Bend Reserve" by Pricetveyron is licensed under CC BY-SA 4.0.

Modern sliding in the Portuguese Bend region was first noticed when the area was under development in 1956. Despite this movement, large numbers of homes were built in the area. These homes were subsequently destroyed by sliding that occurred throughout the last part of the 20th century and into the 21st century at rates of approximately 0.2-11 m/yr (1 in/yr up to 35 ft/yr). As a result, the area of active sliding has been converted to a natural area with trails. However, the effects of ongoing sliding are apparent in the continued buckling of roads that cross the area and the hummocky nature of the region (Figure 14.5.8). In addition, active slides in similar lithologies along the northern limb of the Palos Verdes anticline formed in 2023 in response to heavy winter rains. These slides have destroyed houses and roads in this heavily populated and desirable area.



Figure 14.5.8: Upset earth with small cracks and offsets less than 1 meter in the Portuguese Bend Landslide, March 12, 2016. "Portuguese Bend Landslide" by Pricetveyron is licensed under CC BY-SA 4.0.

References

1. (n.d.). YouTube: Home. Retrieved February 15, 2024, from https://www.geophile.net/FieldTrips/...ieldtrip03.htm

2. (n.d.). Studying the Setting and Consequences of the Earthquake. Retrieved February 15, 2024, from https://pubs.usgs.gov/of/1996/ofr-96-0263/mainshk.htm
3. *The 1971 San Fernando Earthquake*. (n.d.). California Department of Conservation. Retrieved February 15, 2024, from https://www.conservation.ca.gov/cgs/...s/san-fernando
4. *About – California Earthquake Clearinghouse*. (n.d.). California Earthquake Clearinghouse. Retrieved February 15, 2024, from https://californiaeqclearinghouse.org/about/
5. *Alquist-Priolo Earthquake Fault Zones*. (n.d.). California Department of Conservation. Retrieved February 15, 2024, from https://www.conservation.ca.gov/cgs/alquist-priolo
6. *California Strong Motion Instrumentation Program*. (n.d.). California Department of Conservation. Retrieved February 15, 2024, from https://www.conservation.ca.gov/cgs/smi/program
7. Coleman, W. (n.d.). *1994 Northridge earthquake*. Wikipedia. Retrieved February 15, 2024, from https://en.Wikipedia.org/wiki/1994_N...dge_earthquake
8. Ehlig, P. L. (1987). Portuguese Bend landslide complex, southern California. In *Cordilleran Section of the Geological Society of America Centennial Field Guide* (pp. 179-184). Geological Society of America.
9. *FS 2005-3107: Southern California Landslides—An Overview*. (n.d.). USGS Publications Warehouse. Retrieved February 15, 2024, from https://pubs.usgs.gov/fs/2005/3107/
10. *Geology of the San Gabriel Mountains*. (n.d.). CSUN. Retrieved February 15, 2024, from https://www.csun.edu/science/geoscie...-gabriels.html
11. Harden, D. R. (2004). *California Geology*. Pearson Prentice Hall.
12. Ingersoll, R. V., & Ernst, W. G. (1987). *Cenozoic Basin Development of Coastal California* (R. V. Ingersoll & W. G. Ernst, Eds.). Prentice-Hall.
13. Norris, R. M., & Webb, R. W. (1976). *Geology of California*. Wiley.
14. *Portuguese Bend Landslide | Rancho Palos Verdes, CA - Official Website*. (n.d.). City of Rancho Palos Verdes. Retrieved February 15, 2024, from https://www.rpvca.gov/719/Landslide-...gement-Program
15. Proctor, R. J., & Crook, Jr., R. (1987). Sierra Madre thrust fault, Arcadia, California. In *Cordilleran Section of the Geological Society of America Centennial Field Guide* (218th ed., Vol. 1, p. 217). Geological Society of America.
16. Shaw, J., Plesch, A., Dolan, J. F., Pratt, T. L., & Fiore, P. (2002). Puente Hills Blind-Thrust System, Los Angeles, California. *Bulletin of the Seismological Society of America*, *92*(8), 2946–2960.
17. Shreve, R. L. (1987). Blackhawk Landslide, southwestern San Bernadino County, California. In *Cordilleran Section of the Geological Society of America Centennial Field Guide* (Vol. 1, pp. 109-114). Geological Society of America.
18. Sidder, A. (2020, 10 9). Southern California's Crustal Motion Tells of Earthquake Hazards. *EOS*, *101*. https://doi.org/10.1029/2020EO150199.
19. *St. Francis Dam*. (n.d.). Wikipedia. Retrieved February 15, 2024, from https://en.Wikipedia.org/wiki/St._Francis_Dam
20. Wolfe, F. D., Shaw, J. H., Plesch, A., Ponti, D. J., Dolan, J. F., & Legg, M. R. (2019). The Wilmington Blind-Thrust Fault: An Active Concealed Earthquake Source beneath Los Angeles, California. *Bulletin of the Seismological Society of America*, *109*(5), 1890–1906. https://doi.org/10.1785/0120180335

This page titled 14.5: Geologic Hazards of the Transverse Ranges Province is shared under a CC BY-NC 4.0 license and was authored, remixed, and/or curated by Martha House.

14.6: Mineral and Petroleum Resources of the Transverse Ranges Province

Petroleum, Natural Asphalt Seeps and the La Brea Tar Pits

Courtesy of the extensive basin deposits throughout the Transverse Ranges Province, oil and gas production is widespread. To learn more about the geologic origin and processes behind the formation of oil and gas, see Great Valley.

Due to deformation of basin sediments throughout the Transverse Ranges Provinces, circumstances are just right for the preservation of valuable oil and gas reserves. The widespread oil source rock here (the Monterey Formation and its equivalents) is found in virtually every basin. Transpressional folding and faulting of basin units have created structural traps for oil, and lithologies are present to not only store the oil (for example the Sespe formation), but also cap it and prevent additional migration (for example, the Rincon Formation).

Major oil fields are found throughout this region (Figure 14.6.1). In the LA Basin, oil fields lie along two northwest striking trends. The southernmost of these extends from the region north of Huntington Beach through the northeast edge of the Palos Verdes Peninsula and northward to the area of Santa Monica. The northern trend extends from north of Anaheim through downtown Los Angeles and slightly where it meets the southern trend. In the Ventura Basin, oil fields generally lie along an east west striking trend that extends offshore to the area south of Santa Barbara and inland as far as the area around Santa Clarita.

These trends generally parallel major fault systems and fold structures in the region (see Cenozoic Sedimentation and Basin Development).

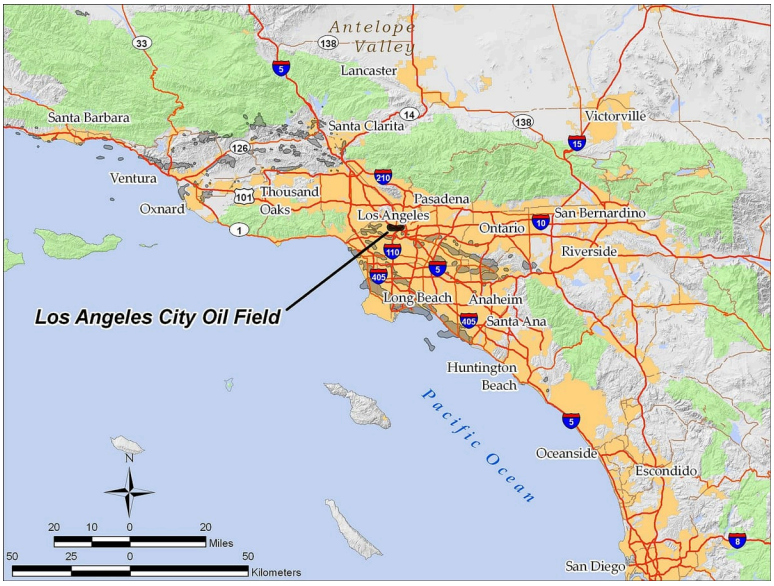


Figure 14.6.1:Map of oil fields in the Transverse Ranges Province. Areas of oil production are shown in gray shaded zones (locations are described in the text). "Los Angeles Field Locations" by Antandrus is licensed under CC BY-SA 3.0

The Wilmington Field, which trends northwest and is located to the northeast of the Palos Verdes Peninsula (Figure 14.6.2), beginning the Torrance area and continuing southeast to the region of Belmont, roughly 16 km (10 miles) in length and 8 km (5 miles) at its widest point. This field is an important element of the oil production in this region and has been in operation since 1932 and is the third largest oil field in the US in terms of total oil production. Once oil production initiated in this region in the late 1800's, oil infrastructure expanded everywhere. Oil derricks sprouted across the region (Figure 14.6.3).

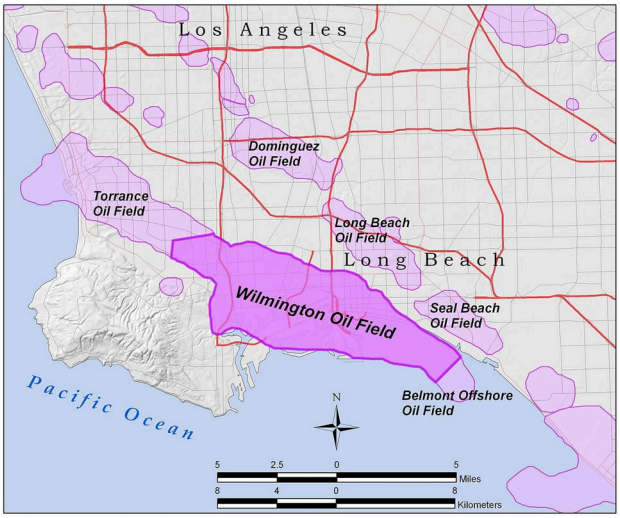


Figure 14.6.2: Wilmington Oil Field within the Los Angeles Basin. This field is northeast of the Palos Verdes Peninsula and is continuous with the Torrance Oil Field to the northwest. "Wilmington Oil Field" by Antandrus is licensed under CC BY-SA 3.0. Access a detailed description.



Figure 14.6.3: Two men standing near a wooden shed in the midst of dozens of oil derricks in a Los Angeles oil field. Court Street and Toluca Street, 1904. A large wooden vat is at left. These wells had been producing for over 40 years when this image was taken (1904). "Two men standing near a wooden shed" is licensed under public domain.

Oil infrastructure is not needed to find signs of oil in this region, however. For example, the La Brea Tar Pits is a by-product of this abundant resource in the Transverse Ranges. The tar pits are a natural asphalt (or "la brea" in Spanish) seep. This pond of fluid asphalt has trapped and preserved an incredible number of animal fossils dating back 38,000 years (Figure 14.6.4).



Figure 14.6.4: Bubbles of gas emerge from the surface of the fluid asphalt deposits at the La Brea Tar Pits. "Tar bubble, La Brea CA" by Daniel Schwen is licensed under CC BY-SA 2.5.

Natural petroleum seeps occur in basins throughout the Transverse Ranges Province and offshore. In fact, it's not uncommon for visitors to beaches in this region to get tar on their feet or clothing. This is because of submarine seeps that wash ashore and the occasional outcrops of reservoir rocks along the coastal cliffs (Figure 14.6.5).



Figure 14.6.5: Tar sandstone from the Monterey Formation of Miocene age (10 to 12 million years old), of southern California, USA. "Tar Sandstone California" by James St. John (jsj1771) is licensed under CC BY 2.0.

The local Chumash and Tongva people, Indigenous inhabitants across this region exploited this resource, using it to seal boats.

Inset Box 14.6.1 Camouflaging Oil Production in the City

While large oil derricks no longer exist, there is still abundant evidence of active oil and gas production across this region. However, in order to reduce community objections, many of these areas are camouflaged.

For example, the THUMS facility offshore of Long Beach consists of four artificial islands that were designed to camouflage the work that goes on there. Also called “Astronaut Islands” in honor of NASA astronauts who lost their lives, these islands hide drilling rigs and other oil production infrastructure (Inset Figure 14.6.1).



Inset Figure 14.6.1: One of the four THUMS artificial islands near Long Beach Harbor. These islands contain generic buildings designed to hide oil production infrastructure. The name, THUMS, is an acronym based on the first letter of the companies that constructed them: Texaco, Humble, Unocal, Mobile, and Shell. "THUMS Oil Island" by donielle, is licensed under, CC BY-SA 2.0.

Another example of a camouflage oil facility is found in west Los Angeles (Inset Figure 14.6.2). This facility is creatively built to look like a building with a tower - possibly a church? But it hides equipment that taps the underlying Beverly Hills Oil Field!



Inset Figure 14.6.2: The Brietburn Drilling Rig in Beverly Hills. This camouflage rig looks like a tower; it actually hides oil production equipment that taps the Beverly Hills Field. "Breitburn Drilling Rig" by Pi3.124, is licensed under CC BY-SA 3.0.

Mining in the Transverse Ranges Province

In addition to oil and gas, other natural geologic resources include precious metals (Gold and Silver), barite and gypsum, and sand and gravel quarrying. While precious metals are not widespread, they do occur in the crystalline basement rocks of the San

Gabriel and San Bernardino Mountains, and aficionados spend time panning for gold in the rivers of these ranges today. In the case of barite, gypsum and sand and gravel, these are all resources derived from the extensive sedimentary basins in this area. Sand and gravel mines can be found in the alluvial fans that flank the larger ranges.

References

1. Harden, D. R. (2004). *California Geology*. Pearson Prentice Hall.
2. Ingersoll, R. V., & Ernst, W. G. (1987). *Cenozoic Basin Development of Coastal California* (R. V. Ingersoll & W. G. Ernst, Eds.). Prentice-Hall.
3. *La Brea Tar Pits*. (n.d.). UCMP Berkeley. Retrieved February 15, 2024, from https://ucmp.berkeley.edu/quaternary/labrea.html
4. Malinconico, M. L. (2015). *Carbonacea*. NA. https://carbonacea.blogspot.com/2015/08/los-angeles-basin-most-prolific-and.html
5. Norris, R. M., & Webb, R. W. (1976). *Geology of California*. Wiley.
6. *Wilmington Oil Field*. (n.d.). Wikipedia. Retrieved February 15, 2024, from https://en.Wikipedia.org/wiki/Wilmington_Oil_Field
7. Yeats, R. S., & Grigsby, R. B. (1987). Ventura Avenue anticline: Amphitheater locality, California. In *Cordilleran Section of the Geological Society of America Centennial Field Guide* (Vol. 1, pp. 219-224). Geological Society of America.
8. Yerkes, R. F., McCulloh, T. H., Schoellhamer, J. E., & Vedder, J. G. (1965). *Geology of the Los Angeles Basin, California-an Introduction*. USGS.

This page titled 14.6: Mineral and Petroleum Resources of the Transverse Ranges Province is shared under a CC BY-NC 4.0 license and was authored, remixed, and/or curated by Martha House.

14.7: Chapter Summary

14.1 Physiographic Overview of the Transverse Ranges Province

- The Transverse Ranges Province is an east-west oriented region in southern California.
- This region consists of east-west trending basins and uplifted ranges.

14.2 Bedrock Geology of the Transverse Ranges Province

- Igneous and metamorphic rocks as old as Proterozoic-Late Mesozoic are uplifted in ranges of in this region.
- An unusual anorthosite complex is included in the Proterozoic rocks.
- Mesozoic meta-sediments preserved in uplifted ranges are similar to the Franciscan Assemblage found along the Coast Ranges.
- Mesozoic plutonic rocks are similar to those found elsewhere in California, in regions where the ancient arc magma chamber is preserved.

14.3 Cenozoic Sedimentation and Basin Development

- Numerous deep basins throughout the region preserve sediments that date back to Late Cretaceous ages and are deformed by reverse faulting and folding.
- Important basins are the Ventura-Soledad Basin in the Western Transverse Ranges and the extensive Los Angeles Basin, which is on the boundary of the Peninsular Ranges Province.
- Basin sediments are mostly marine, but include periodic deposits of non-marine units.
- The Sespe Fm. (Oligocene) is a collection of non-marine sands and conglomerates which records regional uplift.
- The Miocene Monterey Formation (and its equivalents) is found in most basins and is the origin of petroleum deposits in this region.

14.4 Tectonic and Structural Evolution

- This portion of California's plate boundary changed from one of subduction to one of transform activity in the Middle to Late Cenozoic.
- Large portions of the Transverse Ranges originated southward and have been carried into their current positions along with significant rotation in the Late Cenozoic.
- The development of the Big Bend along the emerging San Andreas Fault system created a restraining bend in this region which produced transpressional deformation that resulted in uplifted ranges, deformed basins and crustal thickening.
- The Transverse Ranges continue to be compressed in a north-south sense by reverse faulting and left-lateral shearing.

14.5 Geologic Hazards of the Transverse Ranges Province

- This region has significant earthquake hazards from both strike-slip and reverse faults.
- Earthquakes in this region prompted new legislation and have prompted the creation of collaborative studies of the seismic risk.
- Flooding is a seasonal hazard in this region due to extreme weather events; these events are both natural and man-made.
- Past flood events greatly impacted the region and led to measures to control river responses.
- Landslides are widespread due to steep terrain and many areas of frictionally weak rock and continue to be a concern for residents.

14.6 Mineral and Petroleum Resources of the Transverse Ranges Province

- The basin deposits of this area contain large reserves of oil and gas derived from Miocene sedimentary rocks.

- Oil production has been going on for more than 100 years in this region.
- Mining activities centered on resources derived from sedimentary rocks occur in this region.

This page titled 14.7: Chapter Summary is shared under a CC BY-NC 4.0 license and was authored, remixed, and/or curated by Martha House.

14.8: Detailed Figure Descriptions

Figure 14.1 Location of the Transverse Ranges Province of California

This province is situated south of the Coast Ranges Province, southwest of the Mojave Province, and to the north of the Peninsular Ranges Province. Province is oriented east-west and includes the offshore Channel Islands of San Miguel, Santa Barbara, Santa Cruz, Santa Rosa and Anacapa. The shaded relief base map reveals an east west ridge of mountains that is continuous across this province. South of this ridge of mountains is a flatter geologic basin with isolated uplifted mountain ranges.

Figure 14.1.1 Digital elevation model of the Transverse Ranges Province

This image shows a shaded relief map of Southern California highlighting the Los Angeles region, illustrating how basins and surrounding mountain ranges reflect active tectonics and faulting, with a white oval marking the area of focus. The label “Los Angeles” appears near the center. The Pacific Ocean is shown to the left, clearly separating land and water. Within the outlined area, low, smooth regions represent sediment-filled basins, while raised, textured areas represent mountain ranges, including the Transverse and Peninsular Ranges, which trend in different directions. The contrast between flat basins and uplifted mountains reflects ongoing crustal movement, where deformation along faults creates both elevation and space for sediment accumulation.

Figure 14.2.1 Geology of the Transverse Ranges Province of California

This map highlights map units found within the Transverse Ranges Province according to large ranges of geologic age and lithology. The San Andreas fault is a prominent feature, trending northwest and forming the southern boundary of the western portion of this province, including the lozenge-shaped San Bernardino Mountains. As the San Andreas Fault trends northwestward, it crosses to the northern boundary of the San Gabriel Mountains. The southern boundary of the San Gabriel Mountains is the San Gabriel Fault. Other major fault systems in this region include a number of east-west striking faults which are truncated by the southern San Gabriel Fault on the east. These faults extend offshore to the west.

Precambrian and Mesozoic metamorphic and igneous intrusive rocks occur in the eastern region, corresponding to the San Bernardino and San Gabriel Mountains. Patches of Paleozoic sedimentary rocks occur in the north-central San Bernardino Mountains, and patches of Paleozoic sedimentary rocks are found in the western San Gabriel Mountains. The western portion of the Transverse Ranges Province, including the Channel Islands, is dominated by younger (Neogene and Paleogene) sedimentary rocks and volcanics. The southern edges of the province and patches within the western part of the province include Quaternary surficial deposits.

Figure 14.2.2: Foliated Mendenhall Gneiss

This image shows a boulder of foliated Mendenhall gneiss, about 33 cm (13 inches) long, resting on soil with small rocks and nearby vegetation, illustrating how foliation and folded mineral layers record metamorphic processes and tectonic deformation deep within the Earth. The rock displays alternating black and white mineral layers arranged in wavy, parallel bands that curve across the surface and wrap around the edges. This layered pattern, called foliation, is part of the rock’s internal structure. The banding and folding indicate the rock formed under high heat and pressure and was later deformed by tectonic forces, such as compression during mountain building.

Figure 14.2.5: Evolved Magma

This image shows how magma evolves during cooling through fractional crystallization, where crystal formation and settling change composition and produce more felsic, evolved magma over time. Arrows indicate progression from left to right, and a bottom label reads “crystallization and cooling temperature.” In the left panel, the magma is labeled “parental magma” and described as “homogeneous magma,” with no visible crystals. In the middle panel, “crystals of high temperature minerals form,” shown as small shapes distributed throughout the magma. In the right panel, labeled “evolved magma,” text states “evolved magma is more felsic than parental magma.” Crystals are concentrated at the bottom, with arrows pointing downward, and a

caption reads “early-formed crystals form cumulate at bottom of magma chamber.” Across the diagram, crystal position, arrows, and labels show that as magma cools, early-formed minerals crystallize and settle out, leaving the remaining melt more silica-rich.

Figure 14.3.2 Principal late Tertiary to Quaternary depositional basins and upland areas

The map labels three basins: Ventura Basin (to the east), Soledad Basin (to the west), and Los Angeles Basin (to the south). Mountain ranges labeled include the Topatopa Mountains (far northwest), Santa Susana Mountains (northwest), San Gabriel Mountains (northeast), Verdugo Mountains (west), Santa Monica Mountains (southwest), and the Simi Hills (between the Santa Susana and Santa Monica mountains). Additional labeled features include Oak Ridge (between the Topatopa, Santa Susana and Santa Monica mountains), and the San Fernando Valley (middle of the map).

A labeled fault, the San Andreas Fault, appears near the upper right edge. Rivers and water bodies shown include the Santa Clara River, the Los Angeles River, Lake Piru, and Castaic Lake.

Cities and towns labeled on the map include Fillmore, Acton, Burbank, Pasadena, Los Angeles, Santa Monica, and Malibu. County labels include Los Angeles Co and Ventura Co. Major highways shown include Interstate 5, Interstate 405, Interstate 210, Interstate 10, and U.S. Route 101.

The coastline is shown along the lower edge of the map, with the offshore area labeled Continental Borderland. Map reference elements include a north arrow, scale bars for kilometers and miles, and latitude and longitude labels along the border.

Figure 14.3.3. Simplified cross-section through the central Ventura Basin

A cross section from north to south across the Ventura basin reveals a series of folds and faults that are typical of this region and that include oil sands, oil shales, and tar sands. In this example, a large syncline made of Miocene through Quaternary aged sedimentary rocks underlies the Ventura Basin. The Monterey Formation is the base layer in this synclinal structure. To the north, the San Cayetano Thrust fault pushes older rocks in the Santa Paula Range southward over this subsurface synclinal formation, causing oil bearing units in the footwall to be slightly overturned toward the south, beneath an oil field directly to the south of the Santa Paula Ridge.

To the south, the south-dipping Oak Ridge reverse fault pushes Upper Eocene through Pleistocene rocks northward over the syncline. Upper Eocene through Oligocene oil-bearing layers in the in the hanging wall of the Oak Ridge fault are anticlinally folded beneath an oil field to the north of South Mountain.

Figure 14.3.9 Major structural blocks of the Los Angeles Basin

A map of the Los Angeles area southward from the San Gabriel Mountains shows major structural blocks. At the north is the northwestern block, which includes the San Fernando Valley, the Santa Monica Mountains and the Verdugo mountains and is bounded on the south by the east-west striking Santa Monica and Raymond Hill fault system. The northeastern block is located south of the San Gabriel Mountains and includes the San Jose Hills, and the San Gabriel Valley. It includes the northwest-trending Elysian Park anticline and the Repetto Hills and is bounded to the south by the northwest striking Whittier Fault. The Central Block is located to the southwest. Bounded to the northeast by the Whittier fault, this block includes most of Los Angeles and involves several northwest trending anticlines. Its southwestern edge is the northwest striking Newport-Inglewood Fault and related faults. Across this system to the southwest is the Southwestern Block. This area is bounded on the north by the Santa Monica Fault, and includes Santa Monica, The Baldwin and Dominguez Hills areas, Long Beach, and the Palos Verdes Peninsula. Notable anticlinal and synclinal structures trend northwest-southeast in this region.

Figure 14.4.1 Evolution of the San Andreas Fault system

A time series shows steps in the evolution of the San Andreas fault system.

1. At 30 Ma, the Farallon Plate is being subducted beneath the North American Plate. The Pacific Plate is offshore and is separated from the Farallon Plate via a divergent plate boundary.
2. At 20 Ma, the Farallon Plate has been subducted and broken into two smaller plates (the Juan de Fuca Plate to the north and

the Cocos plate to the south) which continue to be subducted beneath North America. These plates are separated by a right lateral transform boundary which has developed between the Pacific Plate and the North American Plate. The northern triple junction between the Juan de Fuca Plate, the Pacific Plate and the North American pPate is called the Mendocino Triple Junction. The southern triple junction between the Cocos Plate, the Pacific Plate and the North American Plate is called the Rivera Triple Junction

3. At 10 Ma, the distance between the Mendocino and Rivera Triple Junctions has increased as the right lateral transform boundary between the Pacific and North American Plates has lengthened. Subduction continues to the north of the Mendocino Triple Junction and to the South of the Rivera Triple junction.
4. At 5 Ma, the distance between the Mendocino and Rivera Triple junctions has continued to increase as the right lateral transform boundary between the Pacific and North American Plates has lengthened. Subduction continues to the north of the Mendocino Triple Junction and to the South of the Rivera Triple junction.
5. At Present, the modern San Andreas fault system has developed between the Mendocino and Rivera Triple Junctions. Subduction of the Juan de Fuca Plate occurs north of the Mendocino Triple Junction, while sea floor spreading has developed to the south of the Rivera Triple Junction, in the Gulf of California.

Figure 14.4.2 Sequential diagrams showing the rotation of the Western Transverse Ranges

Four panels outline the gradual changes in the configuration of the Transverse Ranges from 20 Ma to present.

At 20 Ma, the western margin of North America consists of three different types of plate boundaries. In the north, the Juan de Fuca Plate is subducted beneath North America. At the Mendocino Triple Junction, the boundary becomes a transform style where the Pacific Plate slides northwestward along the North American Plate. This boundary changes to one of divergence at the Rivera Triple Junction where the Pacific Plate and Cocos Plate diverge. To the South, the Cocos Plate is subducted beneath North America. From the Mendocino Triple Junction southward along this boundary, the crustal blocks which will become the area (block) around San Francisco, Santa Barbara area (block) and the Channel Islands block are aligned parallel to the coastline. The future Santa Barbara area and San Diego area are at roughly the same latitude, inland from the Rivera Triple Junction, and the block that will become the future Channel Islands is south of this.

By 12 Ma, the area is now mostly the transform boundary between the North American Plate and the Pacific Plate. The elongate San Francisco block is separated from the North American Plate by several large faults that parallel plate motion. To the south, the Santa Barbara block has begun to rotate in a clockwise fashion and is approximately 45 degrees from its original position. Basins have opened to the north and south of this rotated block. The Channel Islands block remains parallel to the coast and is now bounded by a basin on its east and southern edges. The San Diego block remains inland.

At 4 Ma, the Pacific Plate continues to move to the northwest relative to North American Plate. A transform boundary that is parallel to this motion has developed inland from the San Francisco, Santa Barbara blocks, and meets a divergent boundary just north of the San Diego block. This divergent boundary is under the future Gulf of California, separating the future Baja Peninsula from the rest of North American Plate. This San Francisco block and Channel Islands blocks remain roughly parallel to the plate motion, but the Santa Barbara block has rotated almost 90 degrees clockwise relative to its initial position. A triangular basin has developed north of this block, and a large linear basin has developed south of it, separating the Channel Islands block from the San Diego block.

0 Ma shows the present configuration of the southern California Plate boundary. The modern San Andreas fault system is developed, taking a large bend to the east in the vicinity of Los Angeles, after which it meets that rifting associated with the submerged East Pacific Rise, which continues under the Gulf of California. The San Francisco block has moved to it's present location, and the Santa Barbara block has fully rotated into it's east-west orientation. The offshore Channel Islands block is completely submerged and remains parallel to the plate motion. Basins that opened to the north of the Santa Barbara block are now partially submerged, and those to the south are completely submerged offshore of San Diego and the modern Baja Peninsula.

Figure 14.4.3 Diagram of a restraining bend geometry similar to that of the Transverse Ranges Province

A restraining bend is formed when a right lateral transform boundary bends to the right. In this example, which is a simplification of the "Big Bend" that the San Andreas system takes in the Transverse Ranges area, a right lateral strike-slip fault is oriented roughly north-south. The fault bends to the right and then returns to its original orientation. In the region where it has bent to

the right (east), the boundary is now no longer parallel to the plate motion. Because it is almost perpendicular, the plate motion is resolved into a compressional vector and a shear vector. Most of the motion is compressional however, so a series of reverse faults form in this section. These faults lead to the formation of mountain ranges that are oriented in an east-west sense, like the strike of the faults.

Figure 14.4.4 Current GPS (global positioning system) permanent station network in Southern California

A map of the Transverse Ranges including the offshore Channel Islands and the Salton Sea shows the locations of hundreds of GPS stations across this region with vectors representing the rate of movement relative to North America. The movement detected by the stations to the west of the San Andreas boundary indicates that they are uniformly moving to the northwest (with the Pacific Plate) at rates of approximately 40 mm/yr. Stations located inland from the San Andreas boundary show no movement; the abrupt transition is consistent with the location of the San Andreas fault system.

Inset Figure 14.4.1 Location map of the San Bernardino Mountains

This is a topographic map showing the San Bernardino Mountains which range in elevation from 218 m to 3504 m. Basins sampled include 7 near the central basin, 7 further south, and 4 further northeast.

Inset Figure 14.4.2 A north-south transect through the San Bernardino Mountains

This is a topographic map showing the long term denudation and cosmogenic nuclide denudation. The table below lists these from north to south.

Denudation rates

Feature	Average long-term denudation rate (mm/ka)	Average cosmogenic nuclide denudation rate (mm/ka)
Northern margin of plateau	70 ± 40	95 ± 10
Plateau	50 ± 30	100 ± 20
Southern margin of plateau	180 ± 90	670 ± 170
Ridge near San Andreas Fault Zone	1200 ± 400	1500 ± 290

Inset Figure 14.4.3 Denudation rates for the basins

The graph is a scatter plot showing average basin denudation rate (mm·ka^{-1}) versus average basin hillslope gradient (degrees). At low gradients (about 8–22°), denudation rates are low, generally below 200 mm·ka^{-1}. As hillslope gradients increase above ~25–30°, denudation rates rise sharply to values between about 1000 and 3000 mm·ka^{-1}, with larger uncertainty. The x-axis is divided into sub-threshold topography at lower gradients and threshold topography at higher gradients. The table below is of the data on the graph.

Denudation Rates

Avg. basin hillslope gradient (°)	Avg. basin denudation rate (mm·ka^{-1})	Approx. uncertainty (± mm·ka^{-1})
9	50	30
10	70	40
14	90	40
16	120	40

Avg. basin hillslope gradient (°)	Avg. basin denudation rate (mm·ka⁻¹)	Approx. uncertainty (± mm·ka⁻¹)
18	110	40
19	100	30
21	150	40
24	230	50
26	520	70
27	230	50
28	650	80
29	300	60
30	150	40
31	1200	200
31	1600	300
31	2200	500
36	2700	500
37	1100	200
37	1250	200
38	1200	200

Figure 14.5.1 The 1971 San Fernando earthquake, also known as the Sylmar earthquake — Los Angeles County, Southern California

Instrumental intensity information surrounding the epicenter of the Sylmar earthquake is mapped. Intensity generally decreases with distance from the quake. Maximum intensity levels of XI or extreme in the area between Northridge and the San Gabriel Mountains were measured. South of Northridge, intensity levels of VII (very strong) were reached. Beyond this, almost the entire Los Angeles region, including Palmdale, Malibu and the areas just north of Long Beach, experienced intensity levels of VI (strong).

The Instrumental Intensity scale that is included relates Instrumental Intensity to Peak Velocity, Peak Acceleration, Potential Damage, and Perceived Shaking. This scale is listed tabulated here.

Instrumental Intensity Scale

Perceived Shaking	Not Felt	Weak	Light	Moderate	Strong	Very Strong	Severe	Violent	Extreme
Potential Damage	none	none	none	Very Light	Light	Moderate	Moderate/ Heavy	Heavy	Very Heavy
Peak Acceleration (% g)	<0.17	0.17-1.4	1.4-3.9	3.9-9.2	9.2-18	18-34	34-65	66-124	>124
Peak Velocity (cm/s)	<0.1	0.1-1.1	1.1-3.4	3.4-8.1	8.1-16	16-31	31-60	60-116	>116
Instrumental Intensity	1	II-III	IV	V	VI	VII	VIII	IX	X+

Figure 14.5.2 The ShakeMap computed for the 1994 Northridge earthquake

Instrumental intensity information surrounding the epicenter of the Northridge earthquake is mapped. Intensity generally decreases with distance from the quake. Maximum intensity levels of XI or extreme in the area between Santa Clarita and

Northridge were measured. South of Northridge, intensity levels of VII (very strong) were reached as far south as south Los Angeles and into Oxnard. Beyond this, almost the entire Los Angeles region, including Palmdale, Malibu and the areas just north of Long Beach, experienced intensity levels of VI (strong).

he Instrumental Intensity scale that is included relates Instrumental Intensity to Peak Velocity, Peak Acceleration, Potential Damage, and Perceived Shaking. This scale is listed tabulated here.

Instrumental Intensity Scale

Perceived Shaking	Not Felt	Weak	Light	Moderate	Strong	Very Strong	Severe	Violent	Extreme
Potential Damage	none	none	none	Very Light	Light	Moderate	Moderate/ Heavy	Heavy	Very Heavy
Peak Acceleration (% g)	<0.17	0.17-1.4	1.4-3.9	3.9-9.2	9.2-18	18-34	34-65	66-124	>124
Peak Velocity (cm/s)	<0.1	0.1-1.1	1.1-3.4	3.4-8.1	8.1-16	16-31	31-60	60-116	>116
Instrumental Intensity	1	II-III	IV	V	VI	VII	VIII	IX	X+

Figure 14.5.3: Northridge Event

This image is a cross-section beneath the San Fernando Valley comparing the 1971 San Fernando and 1994 Northridge earthquakes, illustrating how fault geometry, main shock locations, and aftershock distributions are used to map buried thrust faults and understand where rupture begins and stops at depth. This diagram showcases how main shock locations and aftershock patterns provide critical evidence for mapping hidden faults, helping explain how large earthquakes occur on buried thrust systems beneath the Los Angeles region.

The profile is oriented with north to the right, and surface labels include San Fernando Valley, Santa Susana Mountains, and Santa Clara Valley. The horizontal axis is labeled “Horizontal Distance from 1994 Main Shock (kilometers)”, and the vertical axis is labeled “Depth (kilometers)”, increasing downward from near 0 at the surface to about 20 kilometers depth. Two main earthquakes are marked with star symbols:

- A red star labeled “1994 Main Shock” located deeper on the left side, near the base of the pink fault plane
- A blue star labeled “1971 Main Shock” located on the right side at a slightly shallower depth, near the base of the teal fault plane

Colored lines represent modeled fault planes:

- A pink line shows the 1994 Northridge fault, dipping downward toward the south and not reaching the surface
- A teal line shows the 1971 San Fernando fault, dipping in the opposite direction toward the north

Hundreds of small plotted points represent aftershocks:

- Red circles cluster around the pink fault plane, marking aftershocks associated with the 1994 Northridge earthquake
- Blue circles cluster around the teal fault plane, marking aftershocks associated with the 1971 San Fernando earthquake

These aftershock clusters form elongated patterns that trace the shape and extent of each fault surface at depth. The two fault planes approach each other but remain separate. The geometry and distribution of aftershocks suggest that the Northridge rupture terminated about 5 kilometers below the surface, likely where it encountered structural barriers related to the 1971 fault system. The placement of the star symbols at the lower ends of each fault plane indicates the likely starting points, or hypocenters, of rupture, while the spread of dots shows how energy propagated along the faults.

Figure 14.6.2 Wilmington Oil Field within the Los Angeles Basin

The image is a map of the Los Angeles–Long Beach coastal region showing the locations of several oil fields in relation to cities, the coastline, and offshore areas. The Torrance Oil Field is located near the coast west of Long Beach, inland from the Pacific Ocean and south of central Los Angeles. The Dominguez Oil Field lies north of Long Beach, inland and south of Los Angeles. The

Long Beach Oil Field is situated within and just north of the city of Long Beach. The Wilmington Oil Field occupies a large area south of Long Beach, extending from inland areas near the city southward to the coastline and continuing offshore. Southeast of Long Beach, near the coast, is the Seal Beach Oil Field. Farther offshore to the southeast, beyond the coastline, is the Belmont Offshore Oil Field, located entirely in ocean waters.

This page titled 14.8: Detailed Figure Descriptions is shared under a CC BY-NC 4.0 license and was authored, remixed, and/or curated by Martha House.

15: PENINSULAR RANGES

Introduction to the Peninsular Ranges

The Peninsular Ranges province of California, which includes the coasts of Orange and San Diego counties, is known throughout the world as the home of beautiful beaches, surfing, usually fantastic weather, and many theme parks. It's also just south of the Transverse Ranges, which makes for an easy drive north to the winter ski resorts of the San Gabriel and San Bernardino Mountains. This is how the challenge known as "California Double" began, to both surf and ski between sunup and sundown of the same day. Life here can be downright delightful, but geologically, things are complicated.

The province is named after a series of northwest-southeast trending mountain ranges starting south of the Transverse Ranges and extending into Mexico, where the mountains form the spine of the Baja California Peninsula. These mountains are underlain by a batholith. The California portion of this batholith has historically been referred to as the Southern California batholith, ignoring the reality that most of the batholith and the mountains are actually in Mexico and only the small, northernmost tip is in California. In an effort to help correct this misconception, more recent publications have started to refer to the batholith as the Peninsular Ranges batholith instead.

These ranges formed as part of the Mesozoic volcanic arc that dominated what is now the western coast of California (see Geologic History Mesozoic Era (250 – 66 Ma)) and are therefore similar, but not identical, in rock type and timing to the Sierra Nevada. While there are small exposures of pre-Mesozoic rock in the mountains, most of the rock exposed in the Peninsula Ranges and on the coastal plain is Mesozoic and younger.

The coastal plain to the west of the mountains, along with its beaches, is dominated by marine terraces, headlands, sea cliffs, wave-cut platforms, pocket beaches, and other landforms common on erosional coasts where earthquakes are common (see California Coastline Anatomy). While the province is named after the mountains, most of the population, and the resources in use today are concentrated on the coastal plain. Generally, when people think of this part of California, they think beaches, not mountains. For most people, the mountains form a picturesque background that enhances living near or vacationing on the beach (Figure 15.1).



Figure 15.1: Aerial view of Newport Beach, California, with the mountains of the Peninsular Ranges in the background. "Newport Beach, 2013" by D Ramey Logan via Wikimedia Commons is licensed under CC BY-SA 3.0.

Learning Objectives

By the end of this chapter, you should be able to:

- Describe the Peninsular Ranges province in terms of its key geographic and geologic features.
- Explain how the Peninsular Ranges fit into the broader context of the tectonics and geologic history of California.
- Describe the timing of the formation and characteristics of the rocks of the Peninsular Ranges, including their similarities and differences with the Sierra Nevada.
- Assess the geologic hazards and risks associated with the Peninsular Ranges province.
- Describe the natural resources within the Peninsular Ranges province.

15.1: Geomorphology of the Peninsular Ranges

15.2: Tectonics and Geologic History of the Peninsular Ranges Province

15.3: Rocks of the Peninsular Ranges

15.4: Geologic Hazards of the Peninsular Ranges

15.5: Natural Resources of the Peninsular Ranges

15.6: Chapter Summary

15.7: Detailed Figure and Video Descriptions

This page titled 15: Peninsular Ranges is shared under a CC BY-NC 4.0 license and was authored, remixed, and/or curated by Debra Brooks.

15.1: Geomorphology of the Peninsular Ranges

Welcome to the Peninsular Ranges!

The California Peninsular Ranges begin south of the Sierra Nevada and Transverse Ranges at the Jurupa Mountains northwest of Riverside, California (Figure 15.1.1). They extend south approximately 200 km (125 miles) to the US-Mexican border; they then continue further south another 1250 km (775 miles) into Mexico forming the Baja California Peninsula. They are bounded by the Pacific Ocean to the west, the Transverse Ranges to the north, the Salton Trough and Gulf of California to the east, and extend south into Mexico ending in the Pacific Ocean at the southern tip of the Mexican state of Baja California Sur. The peninsula of Baja California is a major global geographic feature, only the Malay Peninsula of southeast Asia is longer.



Figure 15.1.1: The relationship of the Baja California Peninsula to California and Mexico, as described in the text. “Baja California” by Emily Wright a derivative from "Relief Map" is licensed under CC BY-NC 4.0.

The Peninsular Ranges province within California is south of the Transverse Ranges province and west of the Colorado Desert province (Figure 15.1.2). It includes all of Orange and San Diego counties, and western Riverside county. While the Peninsular Ranges are the southernmost mountain ranges on the California coast, they have more in common with the Sierra Nevada than they do with the Coast Ranges north of the Transverse Ranges.



Figure 15.1.2: Location of the Peninsular Ranges province within California. “Peninsular Ranges Province of California” by Emily Wright, a derivative from "California Geomorphic Provinces" is licensed under CC BY-NC 4.0. Access a detailed description.

The Mountains of the Peninsular Ranges Province

The mountains of the Peninsular Ranges are generally taller to the north and east than to the south and west with San Jacinto Peak at 3,304 m (10,839 ft.) as the tallest mountain within the many ranges (Figure 15.1.3).



Figure 15.1.3: The north face of San Jacinto Peak, Riverside County, California. "Mt. San Jacinto from North" by Wattewyl via Wikimedia Commons is licensed under CC BY 3.0.

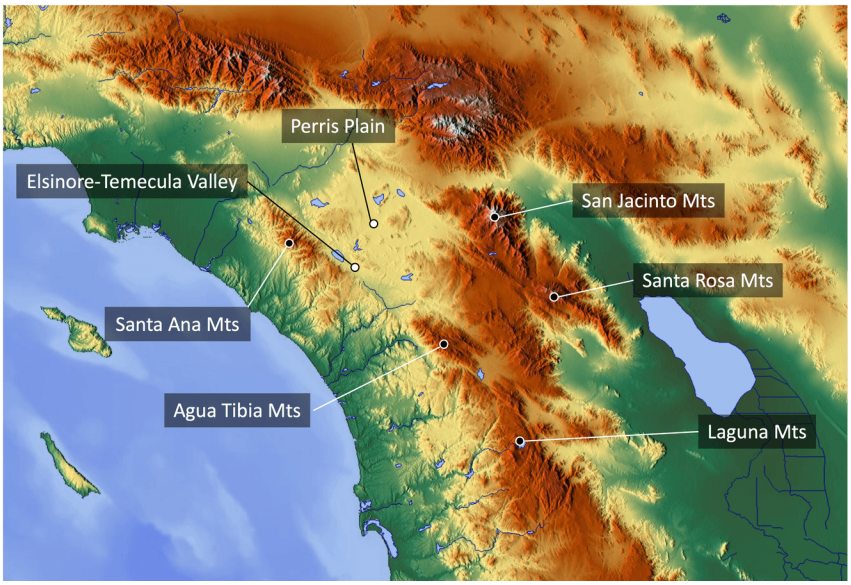


Figure 15.1.4: Mountain ranges and other geomorphic features of the Peninsular Ranges. “Peninsular Ranges Geomorphology” by Emily Wright, a derivative from "Relief Map" is licensed under CC BY-NC 4.0. Access a detailed description.

The California Peninsular Ranges include the Santa Ana, Agua Tibia, San Jacinto, Santa Rosa, and Laguna Mountains, as well as numerous smaller ranges (Figure 15.1.4). Confusion sometimes occurs because many of the mountain ranges are locally subdivided and referred to as smaller mountain ranges. For example, a location within the Laguna Mountains of San Diego county, might also be considered to be within the Sawtooth Mountains, the Laguna Mountains, the In-Ko-Pah Mountains, or the Cuyamaca Mountains depending upon your exact location. Also, individual mountain peaks, such as Palomar Mountain, may be referred to as if they are an entire mountain range in and of themselves rather than being a single mountain. Many of these smaller mountain ranges in the southern part of the province are fault bounded or partly fault bounded. Most of the smaller mountain ranges in the northern part of the province are instead very large monadnocks, or erosional exposures of the plutonic igneous rock of the batholith below (Figure 15.1.5).



Figure 15.1.5: Mount Rubidoux in Riverside, California. An example of a large monadnock formed by the uplift and erosion of the Peninsular Ranges batholith. "Mount Rubidoux" by Takwish via Wikimedia Commons is licensed under CC BY-SA 2.5.

Similar to the mountains of the Sierra Nevada (see The Sierra Nevada Today), the eastern slopes of the larger ranges generally dip more steeply than the western slopes. They may be, but not always are, fault bounded. The orientation of faulting in the Peninsular Ranges mirrors the plate boundary as expressed in the San Andreas fault system and is almost always right-lateral strike-slip (see Jointing and Faulting), but many of the individual faults within the local fault zones may also have a large dip-slip component. For example, the Elsinore-Temecula Valley, or Elsinore trough, is an area of transtension in the northern Peninsula Ranges and is

also referred to as the Elsinore graben, even though the faults bounding it are strike-slip faults rather than normal faults. For the Elsinore fault, the motion is primarily strike-slip (up to 40 km possible offset), but there is also a large dip-slip component (up to 200 m) present in the accumulated offset. The actual San Andreas fault zone is not part of the province, but two of the major fault zones in the Peninsula Ranges – the San Jacinto, and the Elsinore, are considered to be part of the greater San Andreas fault system. The third major fault zone in the province, the Newport-Inglewood fault zone, while not considered an actual part of the greater San Andreas system, is also a right-lateral strike-slip fault zone with a northwest-southeast orientation (Figure 15.1.6).

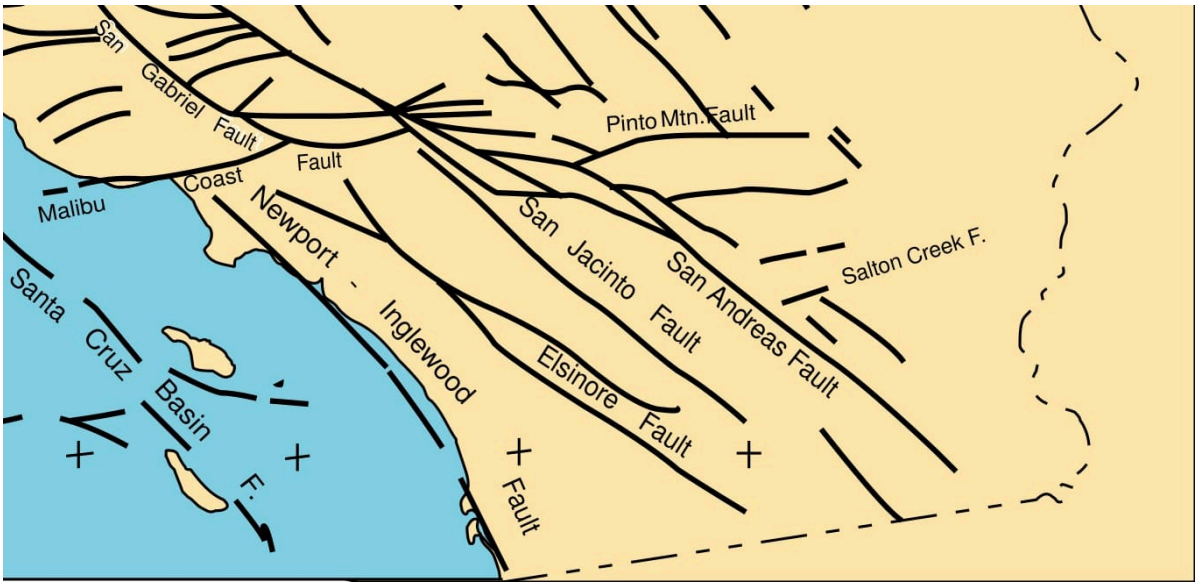


Figure 15.1.6: Simplified fault map of southernmost California, which includes the locations of the San Andreas fault zone and the three major fault zones in the Peninsular Ranges province. "Faults of Southernmost California" by Debra Brooks is a derivative of "SoCal Faults" via Wikimedia Commons is licensed under CC BY-NC 4.0. Access a detailed description.

These fault zones also separate the northern Peninsular Ranges province into three major blocks. Starting along the coast with the Newport-Inglewood fault zone and its southern extension the Rose Canyon fault zone (mapped, but not labeled in Figure 15.1.6) and moving eastwards to the Elsinore fault zone is the Santa Ana block, which includes the coastal plain and the Santa Ana Mountains. These are the oldest plutons in the Peninsular Ranges.

Between the Elsinore and the San Jacinto fault zones is the Perris Block, which includes most of the Perris Plain and the Elsinore-Temecula Valley. Within the Perris Block, the Peninsular Ranges are divided into eastern and western ranges based upon differences in age, changes in the geochemistry and mineralogy of the rocks, and changes in their geophysical properties. Also starting in the southern part of the Perris Block and extending south into Mexico, is the Cuyamaca-Laguna Mountains shear zone, a major fault boundary related to terranes accreting onto what was then the plate boundary during the early Cretaceous.

The San Jacinto Block is the easternmost block of the Peninsular Ranges and includes the San Jacinto and Santa Rosa Mountains and is to the east of the San Jacinto fault zone. These are the youngest plutons in the Peninsular Ranges and the highest mountains in the province.

The mountains also form a drainage divide, with most of the streams in the Peninsular Ranges flowing west into the Pacific Ocean rather than east into the Salton Trough. The western, Pacific-facing slopes experience more rainfall than the eastern facing slopes. The mountains also form a barrier to the onshore flow of moisture from the ocean which creates a rain shadow (see Regional Extent and Overview of the Basin and Range) that is largely responsible for the arid conditions in the Colorado Desert province.

Between the larger mountain ranges are a series of fault-bounded, or partially fault-bounded valleys and plains. Of particular note at the north of the province are the Perris Plain and the Elsinore-Temecula Valley. The Perris Plain in western Riverside county extends northeast from the Santa Ana Mountains and the Elsinore fault zone, is cross-cut by the San Jacinto fault zone and ends near the northernmost San Jacinto Mountains. It is not a flat plain as implied by its name, but rather a distinctive erosional surface of monadnocks both large and small of exposed plutonic rock. Some of the monadnocks are large enough to be referred to as mountains or even mountain ranges (Figures 15.1.5 and 15.2.2). In contrast, the Elsinore-Temecula Valley to the south is a fault bounded valley between the San Ana and the San Jacinto Mountains, bounded by the Elsinore fault zone on the west and the San Jacinto fault zone on the east. In San Diego county, the inland valleys are usually erosional surfaces similar to the Perris Plain but are more likely to be fault-bounded or partly fault bounded.

The Coastal Plain of the Peninsular Ranges Province

The westernmost part of the Peninsular Ranges province is the coastal plain. This part of the province is dominated by marine terraces (see California Coastline Anatomy) that stairstep their way down and west to the ocean (Video 15.1.1).

Video 15.1.1: Marine Terrace Formation

An illustration of the multistep process that creates marine terraces. This video has no sound. Access a detailed description.

This interactive element is not available in this format. Visit the link or scan the QR code to access it online.

View this YouTube Video online

Multiple marine terraces step down towards the Pacific Ocean along the coast, a legacy of both the earthquake activity in southern California and the global fall and then rise in sea level associated with Pleistocene glaciations. There is no evidence of Pleistocene glaciation in the mountains of the Peninsular Ranges of California. The only evidence of the Pleistocene glaciations is preserved in the marine terraces on the coast. Terracing starts in Orange county north of Newport Beach and continues south along CA Hwy 101, locally referred to as Pacific Coast Highway or PCH (Figure 15.1.7) all the way to the US-Mexican border and then continues into Mexico.



Figure 15.1.7: CA Hwy 101, or Pacific Coast Highway, crossing marine terraces above the beaches in Crystal Coast State Park, Orange County, California. "Crystal Cove State Park" by D Ramey Logan via Wikimedia Commons is licensed under CC BY-SA 3.0.

Depending upon the location along the coast, the number of marine terraces varies from nine to sixteen, becoming broader and more numerous to the south in San Diego county. The city of San Diego is actually built upon an extremely broad marine terrace. Along with the terraces, the coastline is a classic example of an erosional coast with numerous sea cliffs, sea arches, sea caves, sea stacks, wave-cut platforms, and pocket beaches (Figure 15.1.8). Second only to marine terraces, are the number of pocket beaches along the coast. Unlike many areas of the world where beaches are very sandy and extend for miles, many of the beaches on the coastal plain of the Peninsular Ranges are rocky pocket beaches in coves between headlands where the beaches are at the base of the sea cliffs or bluffs formed by the marine terraces. Video 15.1.2 shows how rugged and rocky the coast can be.



Figure 15.1.8: Goff Cove, Laguna Beach, California, an example of erosional coastal landforms in the Peninsular Ranges province. "Laguna beach" by karlfonza via Wikimedia Commons is licensed under CC BY-SA 4.0.

Video 15.1.2: Corona Del Mar Arch Rock

An example of just how rugged the beach can be on an erosional coast is illustrated in this drone video. This video has music and no narration. Access a detailed description.

This interactive element is not available in this format. Visit the link or scan the QR code to access it online.

View this YouTube Video online

Another significant feature of the Peninsular Ranges is the propensity for mass wasting especially on the western slopes facing the ocean. Just as in the Transverse Ranges to the north, landslides, debris flows, slumps, and other forms of mass wasting are common on the relatively better watered, ocean-facing slopes of the mountains. The numerous sea cliffs formed by the marine terraces frequently fail during winter storms much to the dismay of the homeowners of the large homes built on top of the cliffs. Not only homes may be lost; mass wasting has also become a continuing problem with the railroad right-of-way. Between 2019 and 2024, the coastal rail corridor between San Luis Obispo and San Diego has been severed by landslides near San Clemente multiple times (Video 15.1.3) and it is estimated that it will take millions of dollars to either remediate the slope or move the rail lines away from the coast.

Video 15.1.3: Landslide Halts Rail Service

A news report of a landslide taking out a hiking/bike path and the rail line in San Clemente, Orange County, California on January 25, 2024.

This interactive element is not available in this format. Visit the link or scan the QR code to access it online.

View this YouTube Video online

There are also major water features along the coast. San Diego has the largest natural harbor and deepwater port in southern California. It is home to one of the largest Navy installations in the country (Figure 15.1.9) and was formed by the Point Loma Peninsula in the north extending south and protecting the local coast from west and northwest waves. In this protected environment, a sand spit from the mouth of the Tijuana River to the south grew northwards and eventually connected with two small islands to form another protective barrier to the south.

The other major coastal water features in the Peninsular Ranges province are the estuaries and lagoons that are aligned along the entire coast down to the United States-Mexico border. All are important breeding, feeding, and nesting habitats for both native and migratory birds. Most have open channels to the Pacific, but they vary in the amount of freshwater discharge, therefore some are salt marshes, others are wetlands, tidal wetlands, and/or lagoons. Most are now designated as either marine conservation areas, ecological reserves, or nature preserves.



Figure 15.1.9: Satellite image of San Diego Bay and the greater San Diego-Tijuana metropolitan area. San Diego Bay is the third largest natural bay in California at 19 km (12 miles) long and 1.6 to 4.8 km (1 to 3 miles) wide; a detailed description is present in the text. NASA photo San Deigo Bay via Wikimedia Commons is in the public domain.

References 15.1

1. Abbott, P. L. (1999). *The Rise and Fall of San Diego*. Sunbelt Publications.
2. *Baja California State (Mexico) size comparison*. (n.d.). MapFight. https://mapfight.xyz/map/baja.california.state/
3. Baird, A.K., & Miesch, A. T. (1984). USGS Professional Paper 1284: *Batholithic Rocks of Southern California – A Model of the Petrochemical Nature of their Source Materials*. U.S. Geological Survey.
4. Barrie, D. S., Tatnall, T. S., & Gath, E. M. (1992). Neotectonic Uplift and Ages of Pleistocene Marine Terraces, San Joaquin Hills, Orange County, California. In E. G. Heath & W. L. Lewis (Eds.), *The Regressive Pleistocene Shoreline Southern California: Coastal Southern California 1992 Annual Field Trip Guidebook No. 20*. (pp. 115-121). South Coast Geological Society, Inc.
5. Campa, A. J. (2024, January 25). Landslide in San Clemente halts train service indefinitely. *LA Times*. https://www.latimes.com/california/story/2024-01-25/metrolink-amtrak-san-clemente-landslide-train-service-halted
6. Carney, K. (2024, June 20) *California Counties by Population*. California Demographics by Cubit. https://www.california-demographics.com/counties_by_population
7. Clarke, Chris (2021, January 19). Rain Shadow Desert: Why the Rain Often Skips The Desert. *SoCal Focus PBS SoCal*. https://www.pbssocal.org/socal-focus/rain-shadow-desert-why-the-rain-often-skips-the-desert
8. Harden, D. R. (2004). *California Geology* (2nd ed.). Pearson Prentice Hall.
9. Irwin, W. P. (1990). Geology and Plate-Tectonic Development. In R. E. Wallace (Ed.), USGS Professional Paper 1515: *The San Andreas Fault System, California*. (pp. 61-80). U.S. Geological Survey. https://pubs.usgs.gov/pp/1990/1515/
10. Jahns, R. H. (1954). Chapter I: Geology of the Peninsular Range Province, Southern California and Baja California. In R. H. Jahns (Ed.), CDMG Bulletin 170: *Geology of Southern California*. (pp. 29-52). California Division of Mines and Geology.
11. Kern, J. P. (1977). Origin and history of upper Pleistocene marine terraces, San Diego, California. *Geological Society of America Bulletin,* 88(11), 1553-1566. https://doi.org/10.1130/0016-7606(1977)88<1553:OAHOUP>2.0.CO;2
12. Kern, J. P., & Rockwell, T. K. (1992). Chronology and Deformation of Quaternary Marine Shorelines, San Diego County,

California. In E. G. Heath & W. L. Lewis (Eds.), *The Regressive Pleistocene Shoreline Southern California: South Coast Geological Society Annual Field Trip Guidebook 20*. (p. 1-7). South Coast Geological Society, Inc.
13. Morton, D. M., Miller, F. K., Kistler, R. W., Premo, W. R., Lee, C-T. A., Langenheim, V. E., Wooden, J. L., Snee, L. W., Clausen, B. L., & Cossette, P. (2014). Framework and petrogenesis of the northern Peninsular Ranges batholith, southern California. In D. M. Morton & F. K. Miller (Eds.), GSA Memoir 211: *Peninsular Ranges Batholith, Baja California and Southern California*. (pp. 61-143). Geological Society of America. https://doi.org/10.1130/2014.1211(03)
14. Norris, R. M., & Webb, R. W. (1990). *Geology of California* (2nd ed.). John Wiley and Sons.
15. Paterson, S., Clausen, B., Memeti, V., & Schwartz, J. J. (2017). Arc magmatism, tectonism, and tempos in Mesozoic arc crustal sections of the Peninsular and Transverse Ranges, southern California, USA. In B. Kraatz, J. S. Lackey, & J. E. Fryxell (Eds.), GSA Field Guide 45: *Field Excursions in Southern California: Field Guide to the 2016 GSA Cordilleran Section Meeting*. (pp. 81-186). Geological Society of America. https://doi.org/10.1130/2017.0045(04)
16. Schulz, M., Lawrence, C., Muhs, D., Prentice, C., & Flanagan, S. (2018, March 8). *Landscapes from the waves – marine terraces of California*. USGS Fact Sheet 2018-3002. https://doi.org/10.3133/fs20183002
17. Treiman, J. A. (compiler). (1998). *Quaternary Fault and Fold Database of the United States*. [Data set] U.S. Geological Survey. https://earthquake.usgs.gov/cfusion/qfault/show_report_AB_archive.cfm?fault_id=126&section_id=c
18. Walawender, M. J. (2012). *Roadside Geology along Sunrise Highway*. Sunbelt Publications.

This page titled 15.1: Geomorphology of the Peninsular Ranges is shared under a CC BY-NC 4.0 license and was authored, remixed, and/or curated by Debra Brooks.

15.2: Tectonics and Geologic History of the Peninsular Ranges Province

Given a Few 100 Million Years, What Could Possibly Happen?

In some parts of the world, the rocks of today reveal a history of continuous change occurring in an area as plate tectonic forces slowly move that location over Earth's surface. That is not the geologic history of California (see A Brief Geologic History of California) nor of the Peninsular Ranges. The rocks and landforms seen in the Peninsular Ranges of today have a long history with three distinct phases. First, the region was a passive margin far removed from a plate boundary, then part of a subduction complex at a convergent plate boundary, where terranes were accreted from areas to the west. Finally it became a transform plate boundary, which also brought in terranes, but now from locations to the south. Each phase overprinted the earlier ones, and was then also overprinted by ongoing erosion, deposition, and changes in sea level.

Before the Late Paleozoic/Mesozoic - A Passive Margin

Before and during much of the Paleozoic, the west coast of North America and what would become California was a passive margin or an area offshore of a passive margin. The supercontinent prior to Pangea, Rodinia, had started to break up during the Precambrian, and as part of that break-up, a Proto-Pacific Oceanic basin formed as the Laurentia plate (most of today's North America) and Antarctica split apart (Figure 15.2.1).

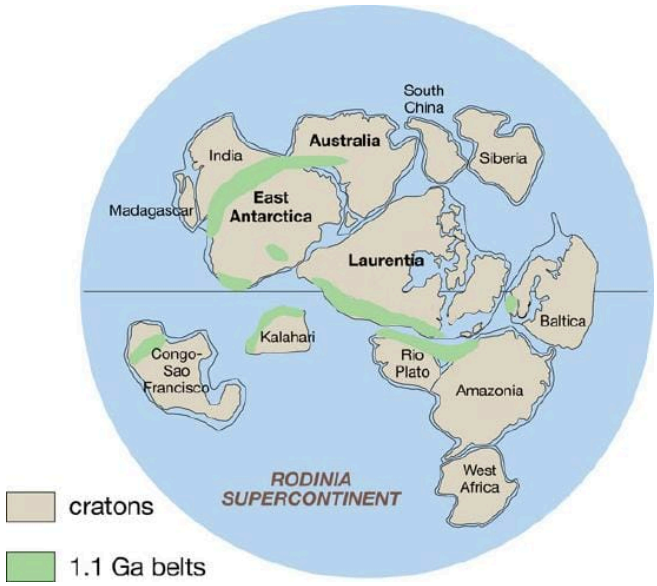


Figure 15.2.1: Possible reconstruction of the supercontinent of Rodinia starting to break apart at 1.1 Ga or 1100 Ma. The 1.1 Ga belts are fold mountain belts created by the continental collisions that built Rodinia. Laurentia will eventually become most of what is now North America. East Antarctica is starting to separate from it and the proto-Pacific Ocean basin is starting to form. "Rodinia Breakup" by Steven Newton, a derivative of "Rodinia Reconstruction", is licensed under CC BY-NC 4.0. Access a detailed description.

A modern example of a passive margin is the current east coast of the United States, with the nearest plate boundary, the Mid-Atlantic ridge, half an ocean away. Along such a passive margin, the dominant geologic processes are erosion and deposition in coastal, nearshore, and continuingly deeper water environments. Each depositional environment leaves its signature in the rock and these signatures are found in the Paleozoic rock of southern California.

While evidence of these depositional environments remains in the rocks in other parts of southern California, little evidence remains in the Peninsular Ranges province. Most of the evidence for this passive margin is found northeast of the Peninsular Ranges in Death Valley in the Mojave province (see Geologic Overview and Evolution of the Mojave and Colorado Desert Provinces) and in Nevada. The Paleozoic rocks of these areas are interpreted as a nearshore, carbonate platform with water

depths increasing to the west.

Remnants of the presumed equivalent of these carbonate rocks are found in the eastern and northern parts of the Peninsular Ranges as metamorphic rock. They are presumed equivalent, because the intrusion of the batholithic rocks from below metamorphosed and essentially destroyed the fossils in them that could have been used to definitively correlate them. What remains are roof pendants, septa, and inclusions of the now-metamorphosed rock. Roof pendants are rock that has not yet eroded off the top of the batholith. Septa occur when the plutons making up the batholith while rising sometimes leave part of the metamorphosed rock trapped between; septa therefore separate different plutons or different parts of the same pluton. Inclusions are pieces of rock that were torn away as the pluton was rising, fell into the magma, but didn't melt.

Most of these rocks were subsequently eroded away as the Peninsular Ranges uplifted and the batholith was exposed. However, some of these rocks can still be found today in the San Jacinto and the Santa Rosa Mountains, and near the city of Riverside. The marble quarries in and near the Jurupa Mountains near Riverside (Figure 15.2.2) are a major source for the carbonate rock used to make cement and concrete throughout southern California since the 1890s.

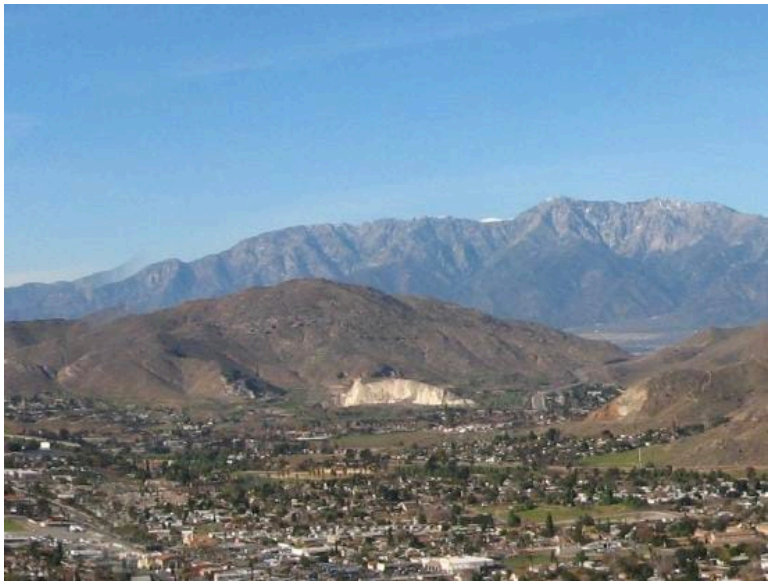


Figure 15.2.2: The white rock of Jensen's Quarry at the base of the hills in the middle distance is part of a roof pendant and is also an abandoned marble quarry in the Jurupa Mountains, northwest of Riverside, California. The San Gabriel Mountains of the Transverse Ranges are in the background. "Jensen's Quarry in the Distance" by Debra Brooks is a derivative of "Riverside Panorama" by Staticfish via Wikimedia Commoms and is licensed under CC BY-NC 4.0.

Mesozoic and Early Cenozoic - Subduction, Batholiths, and Volcanism

Early in the Mesozoic, the west coast of North America began to change dramatically as the existing passive margin became an active margin. A subduction zone formed as the North American plate began to override the oceanic, Farallon plate to the west; this correlates with the break-up of Pangea and the eventual opening of the Proto-Atlantic Ocean. From Canada to Mexico a convergent plate boundary formed, with subduction (see Tectonic Plates, Plate Motions, and Plate Boundaries) and uplift occurring near the coast, batholiths forming at depth, and eventually volcanic island chains forming along the eastern shore of the Pacific Ocean. A modern example of California-then would be the Indonesian archipelago of today (Figure 15.2.3). While the volcanoes have long since eroded away completely, the magma chambers that fed the volcanoes have become batholiths (see The Sierra Nevada Batholith).



Figure 15.2.3: Satellite image of the Indonesian Archipelago. Astronaut Photo by NASA is in the public domain.

Subduction began during the Permian-Triassic and continues through to today in northernmost California, whereas it ended in southern California approximately 30 to 25 million years ago. Subduction can be relatively simple and uniform, with oceanic lithosphere being overridden by continental lithosphere, or it can be quite complex, which is what happened in the Peninsular Ranges province. One major complication is that the subducting oceanic lithosphere is not always uniform and may include oceanic plateaus, island arcs, or even small microplates of continental lithosphere. When such irregularities are part of the subducting plate either they may be accreted to the overriding plate (see Assembling a Continent), or they may change the angle of the subducting plate, which influences whether or not molten rock forms at depth. Also, if molten rock is forming at depth, it may melt at a different depth than it did previously. If the depth at which rock melts changes, the chemistry of the magma changes because it moves upward through either a greater or lesser amount of upper mantle and/or crustal rock as it rises (see The Cascadia Subduction Zone and the Cascade Continental Volcanic Arc).

During the mid-Jurassic, approximately 170 to 160 million years ago, the oldest rocks of the batholith formed under an offshore island arc. Batholiths usually are an amalgamation of many smaller intrusions, or plutons, that intrude near each other or into each other, forming the larger structure. Later in the Cretaceous, approximately 120 million years ago, part of an island arc system accreted to the North American plate forming the Cuyamaca-Laguna Mountain shear zone. It is one of the features, along with age, chemistry, mineralogy, and geophysical properties that define the separation between the eastern and western parts of today's batholith. Subduction continued through this collision and magma production was concentrated in what is now the western areas of today's batholith.

Query 15.2.1

This interactive element is not available in this format. Visit the link or scan the QR code to access it online.

View this Interactive Content online

The earliest deposits of sedimentary rock in the Peninsular Ranges province are dated by marine fossils to be Jurassic. This is a time of uplift and therefore erosion, but little sediment accumulated in the province except along the western seacoast, and then unconformably on metasedimentary rock of marine origin. The inference is that the pre-existing sedimentary rock was metamorphosed by the intrusion of the plutons below and that the continuing uplift made for steeper slopes and fewer onshore depressions in which sediment could accumulate, so much, if not most of the sediment being eroded was washed out to sea. Also, much of the sediment that was deposited is of volcanic origin with deposition more extensive to the north and less extensive to the south. The protolith for much of the metamorphic rock found in the interior of the mountains is also inferred to be sedimentary rock of this age.

At approximately 105 million years ago, the angle of the subducting plate became shallower, and magma generation moved east farther from the location of the trench, concentrating under what is now the eastern part of today's batholith. The geological conditions changed and therefore magma generation changed, becoming more voluminous, chemically homogenous, and felsic. The resulting plutons and their rise towards the surface helped uplift the eastern parts of the batholith, which is why today's mountains are taller in the east than in the west. The magmatic stoping through preexisting plutons helped create the dike complexes that lead to both the development of gold and other metal deposits in what would become the mining districts of northern San Diego and southern Riverside counties.

Around 85 million years ago, subduction shallowed even further, and magma generation moved even further east and out of the Peninsular Ranges province altogether. With the subsequent uplift of the Peninsular Ranges, the volcanoes that formed in those island arcs and onshore areas have long since died and been eroded away. What remains of them in the rock record is some of their lava flows preserved within the stratigraphy of the western Peninsular Ranges, their eroded clasts in the sedimentary rocks of the coastal plain and offshore, and the plutons of the Peninsular Ranges batholith that were the magma scources for their lava flows.

Sediment deposition during the Cretaceous varies from north to south. To the north, sediment deposition is dominated by a sequence of forearc basin sediments unconformably overlying volcanic rock, while to the south, there is also conglomeritic sediment deposited unconformably on both volcanic rock and the exposed rocks of the batholith. The movement of magma generation to the east, meant that while erosion continued, uplift in this area slowed, as cooling and contraction of the plutons accelerated because of the lack of new magma rising from below. The Cretaceous is also a time of globally high sea level and the rise of sea level meant marine sediment was deposited on the older non-marine sedimentary rock.

Query 15.2.2

This interactive element is not available in this format. Visit the link or scan the QR code to access it online.

View this Interactive Content online

Query 15.2.3

This interactive element is not available in this format. Visit the link or scan the QR code to access it online.

View this Interactive Content online

Query 15.2.4

This interactive element is not available in this format. Visit the link or scan the QR code to access it online.

View this Interactive Content online

Late Cenozoic - From Subduction to Transform Faulting

Subduction of the Farallon plate under the North American plate continued through the Mesozoic and into the Cenozoic. For the earliest Cenozoic, one of the largest differences that occurred is the absence of igneous activity. No new igneous intrusions, and

no new volcanic activity but lots of erosion. Especially to the south in San Diego county, erosion there continued all the way down to the plutonic rocks of the batholith. This continued through the early and middle Paleogene with relatively few sedimentary rocks deposited during the Paleocene, but sedimentation increasing during the Eocene. This is also a time of globally high sea level, so while the older rock is non-marine, most of the later rock is marine.

Everything changed dramatically during the late Paleogene (Figure 15.2.4 – 30 Ma). In southern California, somewhere between 30-25 million years ago part of the mid-ocean ridge system in the Pacific Ocean intersected with the subduction zone and two triple-junctions formed. This would start the evolution of the plate boundary into the transform plate boundary of today.

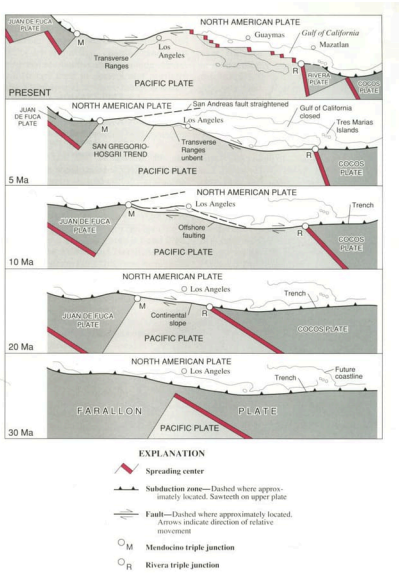


Figure 15.2.4: A sequence of maps showing the evolution of the plate boundary in California over the last 30 million years from a subduction zone to a transform plate boundary. This series of maps are all oriented with east at the top rather than the convention of north at the top. "San Andreas Fault Sequential Diagrams" by W.P. Irwin in USGS Professional Paper 1515 is in the public domain. Access a detailed description.

Prior to 30 million years ago, the entire coast of California and Mexico was a subduction zone, with the Farallon plate subducting beneath North America. The Pacific plate was separated from the Farallon plate by a mid-ocean ridge or spreading center. Around 30 million years ago, a corner of the Pacific plate began to approach the subduction zone. As the Pacific plate intersected with the subduction zone, the plate boundary reconfigured as two triple junctions separated by a transform fault (Figure 15.2.4 – 20 Ma).This new transform fault divided the Farallon plate into two plates. The Juan de Fuca plate (the northern remnant of the Farallon plate) continued subducting under California north of the Mendocino triple junction, while the Cocos plate (the southern remnant of the Farallon plate) continued subducting under Mexico. An offshore transform fault (the proto-San Andreas fault) began to form between the Mendocino and the Rivera triple junctions. The Baja California Peninsula did not yet exist and what would become the Peninsular Ranges of today were on the North American plate.

Extension began and greatly affected the areas both east and west of the Peninsular Ranges about 20 million years ago. To the west it would form the offshore, southern California Borderlands and to the east it would form the Salton Trough. The extension in the offshore borderlands is dominated by a series of east-dipping normal faults and the upper corners of the fault blocks form offshore islands with deep basins between (Figure 15.2.5 and also Rift-Related Faulting in Eastern California). The islands form a sediment source area to the west, and sedimentation on the western side of the ranges is sourced from both the islands to the west and the mountains to the east.

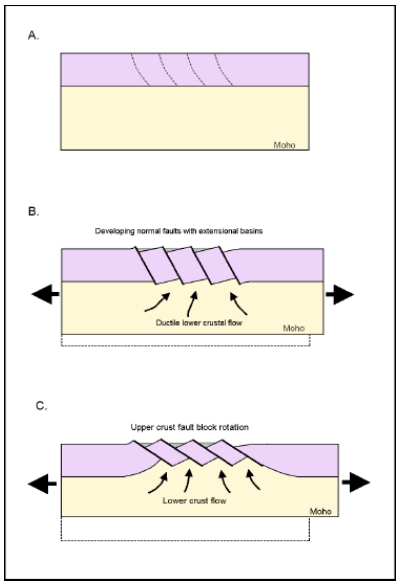


Figure 15.2.5: Formation of tilted fault blocks. "Tilted blocks" by Aturn4000 via Wikimedia Commons is licensed under CC BY-SA 3.0. Access a detailed description.

Complications have increased over the last 20 million years as the plate boundary for California and Mexico transitioned from a pattern of subduction and transform faulting to today's configuration of subduction, transform faulting, and divergence. Video 15.2.1 shows the movement that occurred as faulted blocks moved north over time.

Video 15.2.1: Development of the Plate Boundary of southern California and northern Mexico over the last 20 Ma

It may be helpful to preview the rest of the discussion in the text as a short video. This video has no narration, but is described, step-by-step, in the text. Details on the rotation of the Transverse Ranges to the north of the Peninsular Ranges are covered in the chapter on the Transverse Ranges (see Tectonic and Structural Evolution of the Transverse Ranges).

This interactive element is not available in this format. Visit the link or scan the QR code to access it online.

View this YouTube Video online

By 10 million years ago (Figure 15.2.4 – 10 Ma), the transform fault that forms the plate boundary had grown longer, as the triple junctions further separated. The Peninsular Ranges were still on the North American plate.

Moving forward to about 5 million years ago (Figure 15.2.4 – 5 Ma), the active trace of the transform fault in the north jumped to the shoreline and included the San Gregorio-Hosgri fault system of central California, while the active trace of the transform fault system to the south was still offshore. However, the region that would become the Gulf of California is starting to slowly extend. The Peninsular Ranges were not yet part of a peninsula at this time but would be soon; estimates of the opening of the Gulf of California range from approximately 7 to 4 million years ago.

During the last 5 million years (Figure 15.2.4 - present), the Gulf of California has continued to open, as the extension that was occurring in the proto-Gulf of California shifts to transform faults connecting small spreading centers, and the plate boundary has shifted or jumped to the east and has become a divergent plate boundary. With the opening of the Gulf of California and the start of a divergent plate boundary, the Peninsular Ranges are now on the Pacific plate. Approximately 2 million years ago, the active transform boundary jumped to its current location as the San Andreas fault zone.

The plate boundary of today is convergent in the north, a transform fault for most of the rest of California, and divergent in the

south-easternmost part of California. Volcanism has resumed in the divergent Salton Trough to the east and tectonic activity continues as the Gulf of California opens. In the northern coastal plain of the Peninsular Ranges, broad, shallow anticlines and synclines have formed because of the resulting transpression. The earthquake activity along with global sea level changes caused by the Pleistocene glaciations created multiple episodes of marine terracing on the coastal plain.

References

1. Abbott, P. L. (1999). *The Rise and Fall of San Diego*. Sunbelt Publications.
2. Baird, A.K., & Miesch, A. T. (1984). USGS Professional Paper 1284: *Batholithic Rocks of Southern California – A Model of the Petrochemical Nature of their Source Materials*. U.S. Geological Survey.
3. Bentley, C., Layou, K., Kohrs, R., Jaye S., Affolter, M., & Ricketts, B. (2020). *Historical Geology*. WordPress. https://opengeology.org/historicalgeology/
4. Ferrell, D. (2002, May 9). Mountain Shifts Slowly From Stone to Cement. *LA Times*. https://www.latimes.com/archives/la-xpm-2002-may-09-surround-09-story.html
5. Goodge, J. W., Vervoort, J. D., Fanning, C. M., Brecke, D. M., Farmer, G. L., Williams, I. S., Myrow, O. M., & Depaolo, D. J. (2008). A positive test of East Antarctica-Laurentia Juxtaposition Within the Rodinia Supercontinent. *Science* 321(5886), 235-240. DOI: 10.1126/science.1159189
6. Harden, D. R. (2004). *California Geology* (2nd ed.). Pearson Prentice Hall.
7. Herzig, C. T., & Kimbrough, D. L. (2014). Santiago peak volcanics: Early Cretaceous arc volcanism of the western Peninsular Ranges batholith, southern California. In D. M. Morton & F. K. Miller (Eds.), GSA Memoir 211: *Peninsular Ranges Batholith, Baja California and Southern California*. (pp. 345-364). Geological Society of America. DOI: https://doi.org/10.1130/2014.1211(09)
8. Irwin, W. P. (1990) Geology and Plate-Tectonic Development. In R. E. Wallace (Ed.), USGS Professional Paper 1515: *The San Andreas Fault System, California*. (pp. 61-80). U.S. Geological Survey. https://pubs.usgs.gov/pp/1990/1515/
9. Jahns, R. H. (1954). Chapter I: Geology of the Peninsular Range Province, Southern California and Baja California. In R. H. Jahns (Ed.), CDMG Bulletin 170: *Geology of Southern California*. (pp. 29-52). California Division of Mines and Geology.
10. Kern, J. P. (1977). Origin and history of upper Pleistocene marine terraces, San Diego, California. *Geological Society of America Bulletin,* 88(11), 1553-1566. DOI: https://doi.org/10.1130/0016-7606(1977)88<1553:OAHOUP>2.0.CO;2
11. Langenheim, V. E., Jachens, R. C., & Aiken, C. (2014). Geophysical framework of the Peninsular Ranges batholith – Implications for tectonic evolution and neotectonics. In D. M. Morton & F. K. Miller (Eds.), GSA Memoir 211: *Peninsular Ranges Batholith, Baja California and Southern California*. (pp. 1-20). Geological Society of America. DOI: https://doi.org/10.1130/2014.1211(01)
12. Levin, H. (2013). *The Earth Through Time* (10th ed.). Wiley.
13. Lipps, J. H., Lozinsky, R. L., Pedersen-Guzman, J., Scott, E., & Babilonia, L. (2017). Geology, Stratigraphy, and Paleontology of the Santa Ana Mountains, California, USA. In B. Kraatz, J. S. Lackey, & J. E. Fryxell (Eds.), GSA Field Guide 45: *Field Excursions in Southern California: Field Guide to the 2016 GSA Cordilleran Section Meeting*. (pp. 31-47). Geological Society of America. DOI: https://doi.org/10.1130/2017.0045(02)
14. Liu, L., Gurnis, M., Seton, M., Saleeby, J., Müller, D., & Jackson, J. M. (2009). Oceanic plateau subduction beneath North America and its geological and geophysical implications. *Eos*, 90(52) D121A-1643. https://authors.library.caltech.edu/records/6dezj-rwn46
15. Morton, D. M., Miller, F. K., Kistler, R. W., Premo, W. R., Lee, C-T. A., Langenheim, V. E., Wooden, J. L., Snee, L. W., Clausen, B. L., & Cossette, P. (2014). Framework and petrogenesis of the northern Peninsular Ranges batholith, southern California. In D. M. Morton & F. K. Miller (Eds.), GSA Memoir 211: *Peninsular Ranges Batholith, Baja California and Southern California*. (pp. 61-143). Geological Society of America. DOI: https://doi.org/10.1130/2014.1211(03)
16. Norris, R. M., & Webb, R. W. (1990). *Geology of California* (2nd ed). John Wiley and Sons.
17. Paterson, S., Clausen, B., Memeti, V., & Schwartz, J. J. (2017). Arc magmatism, tectonism, and tempos in Mesozoic arc crustal sections of the Peninsular and Transverse Ranges, southern California, USA. In B. Kraatz, J. S. Lackey, & J. E. Fryxell (Eds.), GSA Field Guide 45: *Field Excursions in Southern California: Field Guide to the 2016 GSA Cordilleran Section Meeting*. (pp. 81-186). Geological Society of America. DOI: https://doi.org/10.1130/2017.0045(04)
18. Prothero, D. R. (2017). *California's Amazing Geology*. CRC Press.
19. Saleeby, J., & Dunne, G. (2015). Temporal and tectonic relations of early Mesozoic arc magmatism, southern Sierra Nevada, California. In T. H. Anderson, A. N. Didenko, C. L. Johnson, A. I. Khanchuk, & J. H. MacDonald, Jr. (Eds.), GSA Special Paper 513: *Late Jurassic Margin of Laurasia - A Record of Faulting Accommodating Plate Rotation*. (pp. 223-268). Geological Society of America. DOI: https://doi.org/10.1130/2015.2513(05)
20. Schoellhamer, J. E., Vedder, J. G., Yerkes, R. F., & Kinney, D. M. (1981). USGS Professional Paper 420-D: *Geology of the Northern Santa Ana Mountains, California*. U.S. Geological Survey.
21. Walawender, M. J. (2012). *Roadside Geology along Sunrise Highway*, Sunbelt Publications.
22. Wetmore, P. H., Herzig, C., Alsleben, H., Sutherland, M., Schmidt, K. L., Schultz, P. W., & Paterson, S. R. (2003). Mesozoic

tectonic evolution of the Peninsular Ranges of southern and Baja California. In S. E. Johnson, S. R. Paterson, J. M. Fletcher, G. H. Girty, D. L. Kimbrough, & A. Martín-Barajas (Eds.), GSA Special Paper 374: *Tectonic evolution of northwestern México and the southwestern USA*. (pp. 93-116). Geological Society of America. DOI: https://doi.org/10.1130/0-8137-2374-4.93

This page titled 15.2: Tectonics and Geologic History of the Peninsular Ranges Province is shared under a CC BY-NC 4.0 license and was authored, remixed, and/or curated by Debra Brooks.

15.3: Rocks of the Peninsular Ranges

It's All About the Rocks

Plutonic igneous rock is the most common rock in the Peninsular Ranges province. Even a quick glance at the geologic map of the province (Figure 15.3.1) shows that the majority of the outcrops are "granitic igneous rocks, mainly of Mesozoic age." By comparison, outcrops of "Cenozoic volcanic rocks" are so small they do not appear on a map at this scale. However, they do exist. They occur within the roof pendants or as Cenozoic flows on the westernmost slopes of the Ranges. "Mesozoic metamorphic and sedimentary rocks" are also rare, occurring mostly on the northern or western parts of the mountains as roof pendants or in the central part of the province as shear zones. Sedimentary rock and sediment ("Quaternary surficial deposits", "Neogene and Paleogene sedimentary rocks", "Cretaceous sedimentary rocks" and "Quaternary and Neogene non-marine deposits") do occur in the intermontane valleys, but most sedimentary rock is found west of the mountains on either the coastal plain or in the northern valleys and plains where the Peninsular Ranges province abuts the Transverse Ranges province.

Although Paleozoic and Precambrian rock designations are present in the legend of the geologic map, there are no outcrops of these rocks indicated on the map of the Peninsular Ranges. The "Paleozoic sedimentary and metamorphic rocks" outcrops are too small to appear at this map scale, but are present as roof pendants. "Pre-Cambrian rocks" are found elsewhere in California, but not here. Also, two types of Mesozoic rock, famously associated with California, do not occur in the Peninsular Ranges province. Neither "Mesozoic serpentine and other ultramafic rocks", nor the Mesozoic "Franciscan Complex sedimentary and metamorphic rocks" occur here.

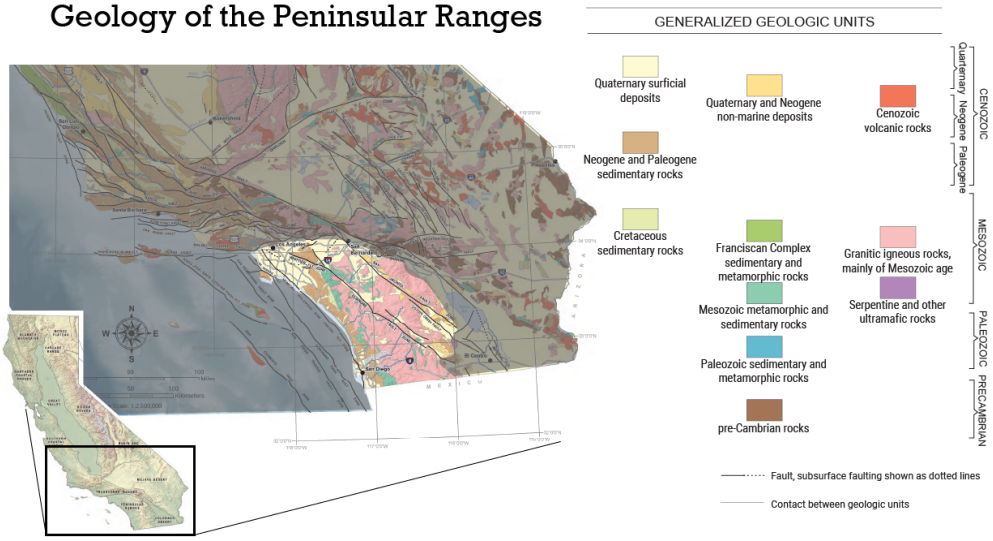


Figure 15.3.1: Geologic map of the Peninsular Ranges Province of California. A detailed description of the rock units is included within the text. "Geology of the Peninsular Ranges" by Emily Wright, a derivative from the "Geology of California" is licensed under CC BY-NC 4.0.

Metamorphic Rock of the Peninsula Ranges

The metamorphic rock in the Peninsular Ranges is mostly metasedimentary rock that was originally part of the passive margin that existed before subduction began and the batholith intruded. The schists and gneisses of today are related to either collisions as terranes were accreted, or as younger plutons metamorphosed rock in the older existing plutons or the sedimentary rock they were intruding.

Emplacement of the plutons during the Mesozoic metamorphosed the existing, mostly marine sedimentary rock of the passive margin. These rocks are the oldest rock in the Peninsular Ranges and are concentrated as roof pendants in the northeastern ranges or along the western slopes of the western ranges (Figure 15.3.1). To the north and east these rocks are primarily a mix of gneiss, schist, quartzite, and marble. The marble has been extensively quarried in the greater Riverside, California area (see

Tectonics and Geologic History of the Peninsular Ranges Province). The Peninsular Ranges province is also the location of one of the major North American mineral type localities for calc-silicate minerals (Box 15.3.1).

Box 15.3.1: Crestmore Quarry, Riverside County, California

Crestmore Quarry in Riverside County, California is known globally for its rare minerals. It is the type locality, or place of original discovery, for minerals, such as jennite, merwinite, wrightmanite and others. Some of these minerals have not been found anywhere in the world other than Crestmore.

The rare minerals, and the not so rare minerals, at Crestmore occurred during metamorphism, but at Crestmore, there were multiple episodes of metamorphism and metasomatism also occurred. Metasomatism is when the minerals are metamorphosed in an extremely wet environment and the generous amount of fluid in the system allows ions to exchange with abandon and grow new minerals totally different from the original minerals. Most of the time, when rock is metamorphosed, metasomatism does not occur because there is usually not enough fluid. Also, most of the time, when magma is involved, it is a silicate magma intruding into a silicate rock. At Crestmore silicate magma intruded into carbonate rock.

When metasomatism does occur, the new minerals are usually not especially rare minerals, rather they are metallic ore minerals. The heat, pressure, and abundant fluid allows the metallic ions to form oxide and sulfide minerals. This is how many gold, copper, tin, lead, zinc, and other metallic ores occur. At Crestmore however the multiple episodes of metamorphism and the wide range in chemistry made the situation complex and created situations where different types of minerals, calc-silicate minerals, grew instead of metallic ore minerals.

The protoliths at Crestmore were marine sedimentary rock, of possible Mississippian age, that were metamorphosed by the intrusion of the Peninsular Ranges batholith and became roof pendants of schists, quartzite, and marble (Box Figure 15.3.1).



Box Figure 15.3.1: Sky Blue Limestone (actually a marble), Crestmore Quarry, Riverside County, California. This sample is approximately 15 cm by 8 cm (6 inches by 3 inches). "Crestmore Sky Blue" by Debra Brooks is licensed under CC BY-NC 4.0.

The original intrusion was described as a quartz diorite. The conventions for naming igneous rock were standardized in the 1960s and today it would be called a tonalite, which is the most common composition of the rocks in the batholith. Contact metamorphic aureoles formed from 5 to 60 cm (2 inches to 2 feet) wide.

Subsequently, a new magma with a different composition intruded into the quartz diorite (tonalite), a quartz monzonite, a rock with less plagioclase feldspar and quartz and more potassium feldspar. This second intrusion, of a rock with yet another different chemistry, started a separate phase of metamorphism. Then pegmatite dikes intruded. The composition of the minerals in the pegmatite dikes changes from north to south, most have quartz and feldspars, but the northern dikes also

include minerals such as epidote, prehnite, and zircon, while the southern dikes are more likely to have andradite garnets instead. With three different episodes of intrusion, each one with a different silicate chemistry, into predominantly carbonate rock there was ample opportunity to create new and varied minerals.

As of 2022, 162 different, verified and validated mineral types have been found at Crestmore, and it's the type locality of 9 minerals.

Similar rocks are found as roof pendants and inclusions in the northern San Jacinto and Santa Rosa Mountains. In the Santa Ana Mountains of the northwest, the metamorphic rocks are only slightly metamorphosed and the original protoliths are still discernible. This is the Bedford Canyon formation, it dips to the west, and its base is not exposed. It includes slatey siltstones, meta-graywacke, metaconglomerate, and some marble. In places it has been intruded by the batholith. The rare fossils in the marble have been provisionally dated to the middle Jurassic. Farther south in San Diego county, the rocks of the Peñasquitos Formation are probably equivalent.

Within the batholith, the Julian Schist and its probable equivalents are the most common metamorphic rock. The protolith for the Julian Schist are metasedimentary rocks deposited in a deep-water environment and metavolcanic rock, which were then metamorphosed, deformed, and then intruded by batholithic rocks.

Plutonic Igneous Rock of the Peninsular Ranges

The most common rocks in the province are the plutonic igneous rocks that form the mountains of the Peninsular Ranges (Figure 15.3.2). These mountains are a result of Mesozoic subduction on the west coast of California as described previously (see Tectonics and Geologic History of the Peninsular Ranges Province). The Peninsular Ranges batholith is complex. Most batholiths are more uniform, but the Peninsular Ranges batholiths is divided into eastern and western parts based upon the changes that occurred in subduction over time and the resulting differences in the chemistry and mineralogy of the rock, which also leads to differences in the geophysical properties of the rock. The plutonic igneous rock of the batholith as a whole encompasses a range of chemistry.

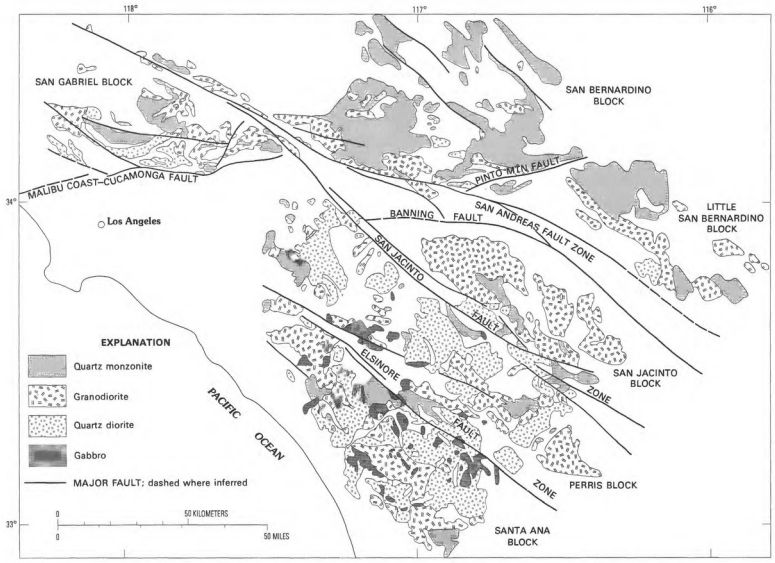


Figure 15.3.2: Simplified geologic map of the Peninsular Ranges and the Transverse Ranges with only plutonic igneous rock and major fault zones mapped. The plutonic rocks south of the Banning fault zone are in the Peninsular Ranges province. Rocks north of that fault are in the Transverse Ranges province and not part of the Peninsular Ranges batholith. "Generalized Geology" by A. K. Baird and A. T. Miesch is in the public domain. Access a detailed description.

The three major types of plutonic igneous rock: gabbro, diorite, and granite (see Igneous Rocks and see also The Sierra Nevada Batholith), are all present in the Peninsular Ranges batholith. However, plutonic rocks can have a large variety of compositions, and each composition has its own name. The most common composition of plutonic igneous rock throughout the Peninsular Ranges batholith is tonalite. Tonalites are a type of granitic rock where the feldspars are more likely to be plagioclase than potassium feldspar (Figure 15.3.3). Tonalite is a relatively new designation and when the map in Figure 15.3.2 was originally created the name

tonalite was not used. Much of what is mapped as either quartz diorite or granodiorite on the map would instead be mapped as tonalite today.



Figure 15.3.3: A sample of tonalite, composed predominantly of feldspars and quartz with some hornblende and possible biotite. "Rocks - Tonalite" by Khruner via Wikipedia is licensed under CC BY-SA 4.0.

The western part of the batholith formed as part of an island arc system offshore of North America during the Jurassic. During the Cretaceous, part of another island arc moving obliquely up from the south accreted onto the existing island arc system (see Assembling a Continent to review the concept of terrane accretion). The collision of the two produced the oldest deformation in the Cuyamaca-Laguna Mountain shear zone, one of the many transitions that divide the Peninsular Ranges batholith into western and eastern parts. The western part of the Peninsular Ranges batholith includes the remains of this accreted island arc.

In the western Peninsular Ranges, the plutonic rocks are generally older than 105 million years; have more compositional variation and include rocks that are mafic through felsic. They have a slightly different chemical signature with higher concentrations of magnesium and also isotopic values that indicate that the magma formed in the asthenosphere and migrated up through mostly oceanic lithosphere. The rocks of the western batholith have compositions from gabbro to diorite to tonalite but are mostly tonalite. Notice in Figure 15.3.2, that the outcrops of gabbro are in the western half of the batholith. These rocks also have different geophysical properties and are more dense, more magnetic, and have a higher seismic velocity than the rocks of the eastern Peninsular Ranges.

In the eastern Peninsular Ranges, the plutonic rocks are 105 to 80 million years old and formed after changes occurred in the subduction process. The angle of the plate became shallower, and the production of magma moved inland, further from the trench, and to the east of the Cuyamaca-Laguna Mountain shear zone. Instead of forming beneath oceanic lithosphere, the plutons were now forming under continental lithosphere. The magma was now rising through both more rock, and more felsic rock, and therefore the rocks of the eastern ranges are less varied in composition and are primarily tonalite with some granite. They contain less magnesium and also have different isotopic signatures because of interacting with a different lithospheric composition as the magma rises towards the surface. Because of their different chemistry and mineralogy, they are also less dense, less magnetic, and have a lower seismic velocity.

The rocks of the eastern Peninsular Ranges batholith are also extremely similar in timing, chemistry, and mineralogy to the rocks of the Sierra Nevada batholith. They both formed during the Cretaceous from 105 to 80 million years ago. The chemistry and mineralogy of these batholiths is similar – the eastern Peninsular Ranges rocks are mostly tonalite with some granite, while the rocks of the Sierra Nevada are mostly granodiorite (a rock intermediate in composition between granite and tonalite) with some tonalite and granite. Their isotopic signatures are similar as are the trace elements present in both.

Query 15.3.1

This interactive element is not available in this format. Visit the link or scan the QR code to access it online.

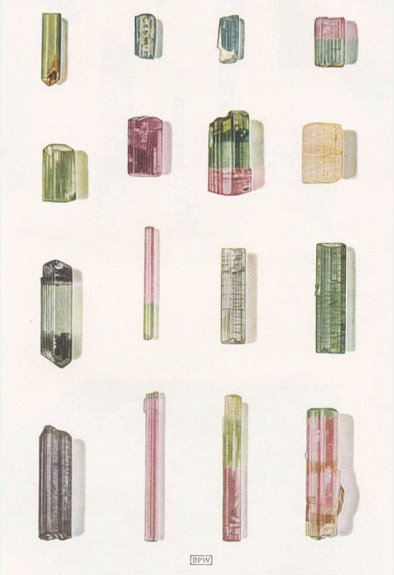
View this Interactive Content online

Some of the individual plutons in the Peninsular Ranges are associated with complex dike systems related to successive intrusions. In the western batholith, this includes ring dike complexes related to emplacement of plutons. Also there are pegmatitic dikes that formed during the latest stages of the intrusion, many of which include gemstones and rare minerals (Box 15.3.2). Dikes form when magma cools in cracks in the rock; pegmatitic is the texture formed when unusually large crystals form (see Igneous Rocks).

Box 15.3.2: Pegmatites of the Pala District of San Diego County

Northeast San Diego county and southwest Riverside county are the location of 14 pegmatite districts. Pegmatite dikes are known for their large, well-formed crystals which are frequently prized by museums and private collectors. Occasionally, pegmatites may have uncommon chemical compositions and both rare minerals and gem quality minerals are found. The Pala District which is mostly on the Pala Indian Reservation in the San Luis Rey River Valley of northeast San Diego County is known for gemstones and spectacular crystals of lithium, bismuth, and phosphate minerals, but especially lithium minerals.

Formal mining of the Pala District began in the 1870s but mining was most active from 1900 to 1922. Even though it is commonly referred to as a mining district, it was never formally organized as one, such as what happens when mining precious metals. There are six mines in the district and the most commonly mined minerals are lepidolite (lithium mica), tourmaline (pink varieties include both lithium and manganese), and spodumene (a lithium bearing pyroxene mineral). Other minerals mined include amblygonite, beryl (aquamarine and morganite), feldspar, and quartz. Morganite, the pink variety of beryl, was originally discovered at Pala in 1902. In this same year, commercial qualities of kunzite, the gemstone variety of spodumene, was also discovered and Pala is still a major producer of kunzite. Tourmaline, however, is the gem mineral that made Pala famous. Variegated or color-zoned tourmaline in shades of pink and green are especially prized, in particular “watermelon tourmaline” where instead of the more common elongate crystals with color changes from pink to green (Box Figure 15.3.2), the center of the crystal is pink and the outer zone of the crystal is green, which reminds people of watermelons.



Box Figure 15.3.2: Color-zoned, gem tourmaline from the Pala and Mesa Grande Districts, San Diego County, California. From the Don M. George, Jr. Mineral Collection, California Institute of Technology. "Color zoned crystals of gem tourmaline" by David P. Willoughby, in CDMG Special Report 7-A Gem- and Lithium-Bearing Pegmatites of the Pala District, San Diego County, California is in the public domain.

One of the reasons the mining was so intense during the early 1900s was Dowager Empress of China Cixi adored pink tourmaline, which increased its appeal and demand skyrocketed during her lifetime. Between 1902 and 1910, 120 tons of gem-quality pink tourmaline was shipped to China from mines in San Diego county. Demand later fell, but never entirely, and pink tourmaline is still prized today by many collectors.

The pegmatites are usually granitic, frequently with graphic granite as an outer or border zone and finer-grained granitic rock within. The gem-bearing pegmatites are granitic but occur in fractures in gabbro. They vary in size from centimeters to meters thick, and the gem bearing pegmatites almost always occur in the “pocket” pegmatites where the pegmatitic dikes bulge outward and the inner core has large quantities of mostly euhedral crystals ranging in size from fine- to very coarse-grained. There is little to no open space in the pockets or bulges, and what might have been “open” is generally filled with clay minerals. The Pala pegmatites are believed to have formed during the final stages of crystallization within the pluton by internal segregation of magmatic fluids, not from outside fluids moving into the pluton.

Mining continues to this day, the sixth mine in the district was only patented in 1979. While lithium is a strategic mineral, most of the mines concentrate on mining gemstones and large collectable crystals of common minerals such as feldspar and quartz. Also, the mines frequently augment their income by allowing people to pay a fee and search through the tailings for minerals.

Volcanic Igneous Rock of the Peninsular Ranges

Volcanic igneous rock is comparatively rare in the Peninsular Ranges. Most of the volcanic rock from the Cretaceous island arcs eroded away long ago, along with the volcanoes. The rocks that remain most commonly outcrop in the western part of the Peninsular Ranges and their composition is generally basaltic or andesitic with a chemistry that corresponds to the gabbro and diorite plutons also found in this part of the ranges. Their existence is also inferred from volcanic clasts found in much of the sediment and sedimentary rock on the coastal plain. The two most common volcanic rock formations are the Santiago Peak Volcanics and the El Modena Volcanics.

Santiago Peak Volcanics outcrop in the western Peninsular Ranges discontinuously from Orange county through San Diego county and into Mexico ending at the Aqua Blanca fault zone in Baja California (Figure 15.3.4).

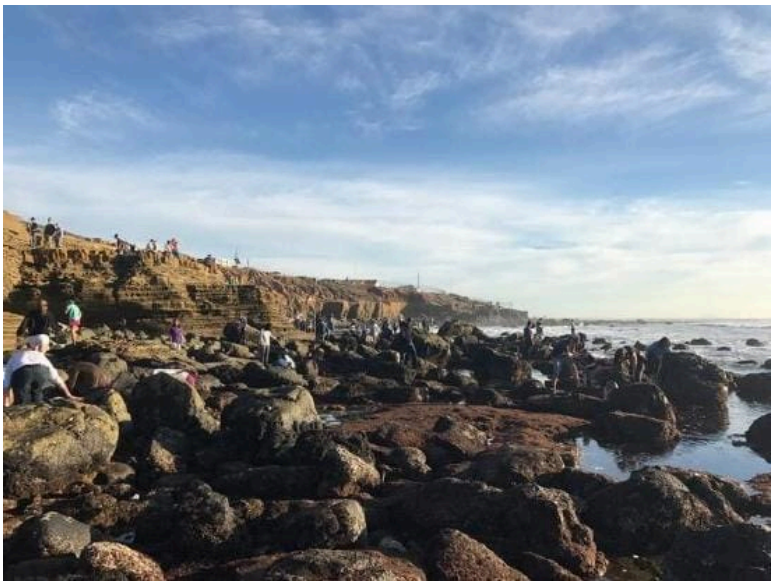


Figure 15.3.4: Wave eroded boulders of the Santiago Peak Volcanics on a wave-cut platform at Cabrillo National Monument, San Diego County, California. "Santiago Peak Volcanics Boulders" by the National Park Service is in the public domain.

They extruded onto the metamorphic Bedford Canyon Formation and both the Bedford Canyon Formation and the Santiago Peak Volcanics were subsequently intruded by rocks of the Peninsular Ranges batholith, therefore in many locales the Santiago Peak Volcanics have been slightly metamorphosed. They include flows, volcaniclastic breccia, welded tuff, and dikes. Composition varies but is mostly andesitic. Radioactive age dating places them as Early Cretaceous (oldest date 128.3 ± 2.5 million years ago) and their age is used to date the beginning of island arc volcanism.

The El Modena Volcanics represent a much younger episode of volcanism. They are interbedded with marine, fossiliferous sedimentary rock, which establishes their age as Miocene. They also vary in composition from basalt to andesite and include palagonite tuffs and in some locations pillow structures indicating that they had at times erupted underwater (see The Josephine Ophiolite- A Little Slice of the Mantle). This timing also corresponds with after the plate boundary in southern California had transitioned from a subduction zone to a transform fault and during a period of extension. Outcrops are in the northwest part of the province in the foothills of the Santa Ana Mountains or in the coastal San Joaquin Hills to the immediate west.

Sedimentary Rock and Sediment of the Coastal Plain

West of the mountains, sedimentary rock and sediment reign. The coastal plain of the Peninsular Ranges is dominated by sedimentation, mostly from the mountains with marine terraces and beaches as the major landforms. Sedimentary rock formations are seldom continuous along the coast. Near the Orange-San Diego county line the mountains extend west almost to the sea (Figure 15.3.5). It is therefore convenient to discuss the sedimentary rocks as the northern or Orange county formations and the southern or San Diego county formations. Even though the formations are not continuous, almost always the depositional environments are similar, or are environments that would reasonably coexist.



Figure 15.3.5: Satellite image of the western Peninsular Ranges and the coastal plain. Note that the southern Santa Ana Mountains swing to the west and almost extend to the coast providing a north-south barrier to the movement of sediment. Astronaut Photo by NASA via Wikimedia Commons is in the public domain. Access a detailed description.

Mesozoic Sedimentary Rock and Sedimentation

The history of Mesozoic sedimentation and sedimentary rock in the Peninsular Ranges province actually begins in the Jurassic metasedimentary rock, previously discussed under metamorphic rock. The sedimentary protoliths for much of this rock are easy to ascertain. The Bedford Canyon Formation in the north and the Peñasquitos Formation to the south both record a history of west-dipping conglomerates and sandstones with abundant volcaniclastic material. In places they are then overlain by volcanic flows followed by erosion.

Jurassic to Cretaceous deposition begins on this erosional surface with alluvial fan deposits along the mountain front that are thicker, more continuous, and start earlier to the north (Jurassic Trabuco Formation) and get thinner, less continuous, and start later to the south (Cretaceous Lusardi Formation). These deposits are then overlapped by marine sediment as sea level rises. As the Cretaceous continues, deposition of shallow marine sediments and turbidite deposits follow (north - Ladd and Williams Formations; south - Point Loma and Cabrillo Formations). Turbidites are underwater landslide deposits (Video 15.3.1) with recognizable patterns of graded bedding and they are usually indicative of earthquake activity (Figure 15.3.6). The Late Cretaceous formations start as marine, but gradually become non-marine over time.



Figure 15.3.6: Point Loma Formation in San Diego County, California. "Turbidite-3" by Zimbres via Wikimedia Commons is licensed under CC BY-SA 3.0.

Video 15.3.1: Turbidites

A more detailed description of how turbidites form and what they geologically represent.

This interactive element is not available in this format. Visit the link or scan the QR code to access it online.

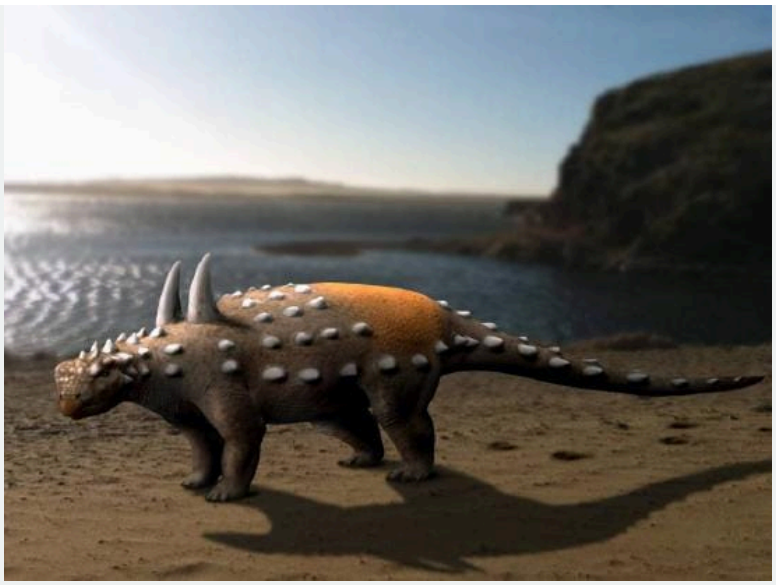
View this YouTube Video online

This repeating depositional pattern of the sea comes in (it onlaps) and the sea appears to move out (either it offlaps or uplift occurs), only to repeat again, is the story of the coastal plain throughout the Mesozoic and the Cenozoic. This pattern continues into present time with formation names changing and timing tracked by the usually abundant fossils that occur in the marine deposits.

The Point Loma Formation of San Diego county and the Williams Formation of Orange county, are also among the few stratigraphic units in California where dinosaur fossils have been found (Box 15.3.3).

Box 15.3.3: Southern California's Dinosaurs

Incomplete hadrosaur fossils have been found in both the Point Loma Formation and the Williams Formation. In the Point Loma Formation, these consist of incomplete back and tail vertebra, a femur, and a partial lower jaw. In the Williams Formation, it is foot bones, a couple of back vertebrae, and a toe. In both locations it is not possible to determine the exact species of hadrosaur from the fossils that have been found.



Box Figure 15.3.3.1: Conception of how *Aletopelta coombsi* might have looked. "Life Restoration" by Nobu Tamura via Wikimedia Commons is licensed under CC BY-SA 4.0.

The best dinosaur find in California is that of an incomplete skeleton of an ankylosaur, *Aletopelta coombsi* or "wandering shield" in the Point Loma Formation which is now on display in the San Diego Natural History Museum (Box Figure 15.3.3.1). While it may be incomplete, it is the most complete dinosaur fossil ever found in California (Box Figure 15.3.3.2). It was found by the museum's field paleontologist, Brad Riney, in 1987 in Carlsbad, California, during a project to extend a road. The complete hindquarters of the animal were recovered, including its back legs still attached to its pelvic bones, along with armor plates, spikes, and eight teeth. Unfortunately, even though much of the skeleton was found, neither its skull nor tail bones were found.

The Point Loma Formation is marine. Therefore, the fossils are believed to have been washed out to sea and buried and preserved in marine sediment. Some of the ankylosaur's bones had been encrusted with oyster fossils and a shark tooth was also found mixed in with the remains.

Even though it is the most complete dinosaur fossil ever found in California, it's not California's State Dinosaur. That honor goes to *Augustynolophus morrisi*, whose skull was found in 1936 in the Panoche Hills in central California, and two other skulls were subsequently found in the same hills in 1939 and 1941.



Box Figure 15.3.3.2: The ankylosaur, *Aletopelta coombsi*, on display in the San Diego Natural History Museum. "Aletopelta" by ケラトプス ユウタ (2019) via Wikimedia Commons is licensed under CC BY-SA 4.0.

To summarize the geological story of the Mesozoic, it starts with an arid climate and alluvial fan deposits along the mountain front that are thicker and more continuous in Orange county and thinner and less continuous in San Diego county. These deposits are then overlapped by marine sediment as sea level rose, and then deposition of turbidite and shallow marine sediments occurred, followed by either uplift or a fall in sea level, or both, because an unconformity separates Mesozoic from Cenozoic sedimentary rock. This also means that any evidence of the Cretaceous-Paleogene boundary no longer exists in the coastal Peninsular Ranges province, so there is no evidence here of how the dinosaurs became extinct.

Cenozoic Sedimentary Rock and Sedimentation

The Cenozoic begins in both the northern and southern parts of the coastal plain with an unconformity. In the southern part of the coastal plain, there is no record of early Paleogene sedimentary rock, any deposition from this time has been eroded away. In the northern part of the coastal plain the Silverado Formation is deposited on the unconformity and repeats the story of ongoing changes in sea level. The lower three members of the formation are non-marine, while the uppermost member is marine indicating rising sea level. This rise in sea level continues into the mid-Paleogene with rocks of this age abundant on both the northern and southern parts of the coastal plain.

On the southern coastal plain, the mid-Paleogene sedimentary rock is the La Jolla Group. The members of the La Jolla Group record a history of non-marine to coastal to marine to non-marine environments. This pattern continues on the northern coastal plain with the Santiago Formation unconformably deposited on the Silverado Formation and also recording a history of a marine environment transitioning into a non-marine environment. The Santiago Formation is conformably overlaid by the non-marine Sespe and then the marine Vaqueros Formations; the La Jolla Group to the south is unconformably overlaid by the Poway Group.

The Poway Group, formerly referred to as the Poway Conglomerate, includes some of the most interesting rocks of southern California. The cobbles in the conglomerates are large, well-rounded, and include a distinctive rhyolitic composition. The depositional environments are non-marine to marine and include stream channels to submarine fan deposits, the question becomes, where was their source rock? No suitable source rock for these cobbles has been found anywhere in southern California. The second question raised by these cobbles is how did they get so widely distributed? While they are mostly found in San Diego county, they are also found on islands in the California borderlands to the north and west, far from San Diego county.

To find the source required looking at the geography of the Paleogene and at that time, the plate boundary was a subduction zone, the Gulf of California had not opened, and the Peninsular Ranges were part of the North American plate (Video 15.3.2). Matching the geochemistry and mineralogy of the cobbles locates the source as a mountain range in Sonora, Mexico.

Video 15.3.2: History of the Poway Group Cobbles

The formation and subsequent dispersal of the cobbles in the Poway Group is illustrated in the following animation. This video has no sound. Access a detailed description.

This interactive element is not available in this format. Visit the link or scan the QR code to access it online.

View this YouTube Video online

The mid-Paleogene was a time of warm climates, and high sea level, the late Paleogene was a time of a cooling climate and drop in sea level as ice ages began in the polar regions. Sea level fell and erosion increased in the Peninsular Ranges. Late Paleogene rocks are missing in the northern coastal plain and while present on the southern coastal plain their deposits are thicker to the south and get progressively thinner and eventually disappear to the north. These rocks are part of the non-marine Otay Formation and known for the high levels of bentonite, a clay formed by the alteration of volcanic ash and are also a source of vertebrate fossils. The large variety and number of fossils found paint a picture of rolling hills, grasslands, herds of grazing animals: oreodonts, small rhinoceros and camels, with small burrowing mammals, such as mice, shrews, hedgehogs, gophers, and rabbits, along with fox-like dogs, short-faced dogs, and saber-toothed carnivores. Many of the fossils are of creatures that still exist today, but some, like oreodonts, have no living analogs.

The fall in sea level and the increasing erosion also mean that there is a regional unconformity between the rocks of the late

Paleogene and the Neogene. The Neogene begins a time of massive tectonic change as the plate boundary transitions from a subduction zone to a transform boundary (Figure 15.2.4). In the northern coastal plain, much of the sediment came from sources to the north in addition to the Peninsular Ranges to the east. Here, the Neogene sequence begins with the deposition of the Topanga Formation, which interfingers with the El Modena Volcanics, indicating that extension and volcanism occurred together. The extension created a series of tilted fault blocks in the Borderlands to the west forming a now submerged topography of ridges and basins (Figure 15.2.5). As the ridges grew, they also became a sediment source for the rocks on the coastal plain, an example is the San Onofre Breccia.

The San Onofre Breccia outcrops discontinuously along the coast from Laguna Beach to Oceanside, with the best exposures near Dana Point. It has blueschist clasts that are large and angular, therefore their source must be close (see Sedimentary Rocks) and is inferred to be a now-submerged ridge to the west. Santa Catalina Island and the Palos Verde Peninsula in the Los Angeles basin are believed to be exposed remains of this ridge because the Catalina Schist outcrops in these locations today.

In the northern coastal plain both the Monterey and the Puente Formations are then deposited during the mid to late Neogene. The Puente Formation is of economic importance because it is a common source rock for the oil fields of northern Orange county. Further south is the marine Capistrano Formation. It is mostly marine sandstones and siltstones, but in the cliffs of Dana Point it includes a submarine fan deposit, which is well exposed and includes conglomeritic lenses (Figure 15.3.7).



Figure 15.3.7: Geology students examining a large boulder eroded from a conglomeritic lens of the Capistrano Formation, Dana Point, Orange County, California. "Conglomeritic Boulder at Dana Point" by Debra Brooks is licensed under CC BY-NC 4.0.

Continuing south, the San Diego Formation unconformably overlies the San Onofre Breccia. It ranges in age from late Neogene to Pliocene and begins as a shallow marine sandstone, but gradually the environment changes to non-marine and the size of the clasts increases.

The lower marine section has abundant microfossils that have been used to analyze water temperature. At the base of the formation, the fossils indicate water temperatures were warmer, about 20° C (68° F) and they then decreased to approximately 15° C (59° F) at the top of the marine sequence. This correlates with the cooling temperatures and falling sea levels that occurred going into the Pliocene and the beginnings of the Ice Ages. This pattern of transitioning from marine to non-marine is repeated in the Niguel Formation of southern Orange county and the Fernando Formation of northern Orange county.

The Pliocene and Pleistocene also record the formation of marine terraces with increasing terrace formation into the Pleistocene. An estimated rise and fall of sea level of approximately 190 m (625 feet) has been documented in the greater San Diego region. During the Pleistocene, the earthquake activity along with the changes in sea level created most of the marine terraces seen today. The youngest sedimentation is from the failure of marine terraces along the coast, leaving deposits of landslide debris, and the Quaternary alluvial deposits being washed down and out from the slopes of the Peninsular Ranges mountains.

Tectonic activity was also increasing during this time as the Gulf of California continued to open. The resulting transpression caused deformation of the sedimentary rock units of the northern coastal plain forming broad, shallow anticlines and synclines. This broad and shallow folding will help set up some of the traps, or structures within rock that can contain fluids, which make up

the oil fields in the greater Los Angeles basin of the Transverse Ranges and the northernmost Peninsular Ranges provinces.

Query 15.3.2

This interactive element is not available in this format. Visit the link or scan the QR code to access it online.

View this Interactive Content online

References

1. Abbott, P. L. (1999). *The Rise and Fall of San Diego*. Sunbelt Publications.
2. Baird, A.K., & Miesch, A. T. (1984). USGS Professional Paper 1284: *Batholithic Rocks of Southern California – A Model of the Petrochemical Nature of their Source Materials*. U.S. Geological Survey.
3. Germinario, M. (1993). The Early Mesozoic Julian Schist, Julian, California. In R. G. Gastil & R. H. Miller (Eds.), GSA Special Paper 279: *The Prebatholithic Stratigraphy of Peninsular California*. (pp. 107-118). Geological Society of America. DOI: https://doi.org/10.1130/SPE279-p107
4. Harden, D. R. (2004). *California Geology* (2nd ed.). Pearson Prentice Hall.
5. Herzig, C. T., & Kimbrough, D. L. (2014). Santiago Peak volcanics: Early Cretaceous arc volcanism of the western Peninsular Ranges batholith, southern California In D. M. Morton & F. K. Miller (Eds.), GSA Memoir 211: *Peninsular Ranges Batholith, Baja California and Southern California*. (pp. 61-143). Geological Society of America. DOI: https://doi.org/10.1130/2014.1211(09)
6. Hildebrand, R. S. (2013). GSA Special Paper 495: *Mesozoic Assembly of the North America Cordillera*. Geological Society of America. DOI: https://doi.org/10.1130/SPE495
7. Jahns, R. H. (1954a). Chapter I: Geology of the Peninsular Range Province, Southern California and Baja California. In R. H. Jahns (Ed.), CDMG Bulletin 170: *Geology of Southern California*. (pp. 29-52). California Division of Mines and Geology.
8. Jahns, R. H. (1954b). Chapter VII: Pegmatites of Southern California. In R. H. Jahns (Ed.), CDMG Bulletin 170: *Geology of Southern California*. (pp. 37-50). California Division of Mines and Geology.
9. Le Bas, M. J., & Streckeisen, A. L. (1991). The IUGS systematics of igneous rocks. *Journal of the Geological Society, London*. 148 825-833. https://edisciplinas.usp.br/pluginfile.php/7940993/mod_resource/content/1/rockclassification.pdf
10. MacKevett, E. M. (1951) Special Report 5: *Geology of the Jurupa Mountains, San Bernardino and Riverside Counties, California*. California Division of Mines and Geology.
11. Nilsen, T. H., & Abbott, P. L. (1981). Paleography and Sedimentology of Upper Cretaceous Turbidites, San Diego, California. *American Association of Petroleum Geologist Bulletin*, 65 (7) 1256-1284.
12. Nordstrom, C. E. (1970). Lusardi Formation: A Post-Batholithic Cretaceous Conglomerate North of San Diego, California. *Geological Society of America Bulletin*, 81(2) 601-606. DOI https://doi.org/10.1130/0016-7606(1970)81[601:LFAPCC]2.0.CO;2
13. Norris, R. M., & Webb, R. W. (1990). *Geology of California* (2nd ed). John Wiley and Sons.
14. Perkins, D. (2022). *Petrology: An Introduction to Igneous and Metamorphic Rocks and Processes*. WordPress. https://opengeology.org/petrology/
15. Prothero, D. R. (2017). *California's Amazing Geology*. CRC Press.
16. Rivero, C., & Shaw, J. W. (2011) Active folding and blind thrust faulting induced by basin inversion processes, inner California borderlands. In J. Shaw & J. Suppe, (Eds.) AAPG Memoir 94: *Thrust fault-related folding*. (pp. 187-214). American Association of Petroleum Geologists. DOI:10.1306/13251338M943432
17. Schoellhamer, J. E., Vedder, J. G., Yerkes, R. F., & Kinney, D. M. (1981). USGS Professional Paper 420-D: *Geology of the Northern Santa Ana Mountains, California*. U.S. Geological Survey.
18. Shaw, S. E., Todd, V. R., Kimbrough, D. L., & Pearson, N. J. (2014). A west-to-east geologic transect across the Peninsular Ranges batholith, San Diego County, California: Zircon $^{176}Hf/^{177}Hf$ evidence for the mixing of crustal- and mantle-derived magmas, and comparisons with the Sierra Nevada batholith. In D. M. Morton & F. K. Miller (Eds.), GSA Memoir 211: *Peninsular Ranges Batholith, Baja California and Southern California*. (pp. 61-143). Geological Society of America. DOI: https://doi.org/10.1130/2014.1211(03)
19. Silver, L. T., & Chappell, B. W. (1988). The Peninsular Ranges Batholith: an insight into the evolution of the Cordilleran batholiths of southwestern North America. *Earth and Environmental Transactions of the Royal Society of Edinburgh*, 79(2-3), 105-121. DOI: https://doi.org/10.1017/S0263593300014152

20. Wetmore, P. H., Herzig, C., Alsleben, H., Sutherland, M., Schmidt, K. L., Schultz, P. W., & Paterson, S. R. (2003). Mesozoic tectonic evolution of the Peninsular Ranges of southern and Baja California. In S. E. Johnson, S. R. Paterson, J. M. Fletcher, G. H. Girty, D. L. Kimbrough, & A. Martín-Barajas (Eds.), GSA Special Paper 374: *Tectonic evolution of northwestern México and the Southwestern USA*. (pp 93-116). Geological Society of America. DOI:https://doi.org/10.1130/0-8137-2374-4.93
21. Wetmore, P. H., Schmidt, K. L., Paterson, S. R., & Herzig, C. (2002). Tectonic implications for the along-strike variation of the Peninsular Ranges batholith, southern and Baja California. *Geology*, 30(3) 247-250.
22. Williams Formation. (n.d.). DBpedia. Retrieved Juky 22, 2024, from https://dbpedia.org/page/Williams_Formation
23. Yerkes, R. F. (1957). USGS Professional Paper 274-L: *Volcanic Rocks of the El Modeno Area, Orange County, California*. U.S. Geological Survey.

References for Box 15.3.1: Crestmore Quarry, Riverside County, California

1. Burnham, C. W. (1951). Chapter VII: Contact metamorphism at Crestmore, California. In R. H. Jahns (Ed.), CDMG Bulletin 170: *Geology of Southern California*. (pp. 61-70). California Division of Mines and Geology.
2. Devito, F., Parcel, R. T. & Jefferson, G. T. (1971). Field Trip No. 5: Contact metamorphic minerals at Crestmore Quarry, Riverside, California. In W. A. Elders (Ed.), *Geological Excursions in Southern California*. UCR Campus Museum.
3. Eakle, A. S. (1927). Famous Mineral Localities: Crestmore Quarry, Riverside County, California. *American Mineralogist*, 12 319-321. http://minsocam.org/MSA/collectors_corner/arc/crestmoreca1.htm
4. Glazner, A. F., Bartley, J. M. & Coleman, D. S. (2019). A more informative way to name plutonic rocks. *GSA Today*, 29(2) 4-10. DOI: https://rock.geosociety.org/net/gsatoday/science/G384A/article.htm
5. Mindat.org (n.d.). *Crestmore quarries, Crestmore, Jurupa Valley, Riverside County, California, USA*. [Data set]. https://www.mindat.org/loc-3449.html
6. Woodford, A. O., Crippen, R. A. & Garner, K. B. (1941) Section across Commercial Quarry, Crestmore, California. *American Mineralogist*, 26 351-381. http://www.minsocam.org/msa/collectors_corner/arc/crestmoreca2.htm

References for Box 15.3.2: Pegmatites of the Pala District of San Diego County

1. Herberling, L. (n.d.). *History of Mining in Southern California*. San Diego Natural History Museum. https://www.sdnhm.org/exhibitions/all-that-glitters/history/history-of-mining-in-southern-california/
2. Jahns, R. H., & Wright, L. A. (1951). CDMG Special Report 7-A: *Gem- and Lithium-Bearing Pegmatites of the Pala District*. California Division of Mines and Geology.
3. Mindat.org (n.d.). *Pala Mining District, San Diego County, California, USA*. [Data set]. https://www.mindat.org/loc-3560.html
4. Morton, D. M., Sheppard, J. B., Miller, F. K., & Lee, C-T. A., (2018). Petrogenesis of the cogenetic Stewart pegmatite-aplite, Pala, California: Regional implications. *Lithosphere* 11(1) 91-128. https://doi.org/10.1130/L1026.1
5. Pala, California. (2024, July 22). In *Wikipedia*. https://en.Wikipedia.org/wiki/Pala,_California

References for Box 15.3.3: Southern California's Dinosaurs

1. Abbott, P. L. (1999). *The Rise and Fall of San Diego*. Sunbelt Publications.
2. Ford, T. L., & Kirkland, J. I. (2001). Carlsbad Ankylosaur (Ornithischia, Ankylosauria): An Ankylosaur and Not a Nodosaurid. In K. Carpenter (Ed.), *The Armored Dinosaurs* (pp. 239-260). Indiana University Press.
3. Hayes, G. (2017, September 24). Say Hello to California's New State Dinosaur: Augustynolophus morrisi. *Geotripper*. https://geotripper.blogspot.com/2017/09/say-hello-to-californias-new-state.html
4. Katz, B. (2017, September 27). Meet California's new State Dinosaur. *Smithsonian Magazine*. https://www.smithsonianmag.com/smart-news/meet-augustynolophus-morrisi-californias-new-state-dinosaur-180965038/
5. San Diego Natural History Museum (n.d.) *Ankylosaur*. https://www.sdnhm.org/exhibitions/fossil-mysteries/fossil-field-guide-a-z/ankylosaur/

This page titled 15.3: Rocks of the Peninsular Ranges is shared under a CC BY-NC 4.0 license and was authored, remixed, and/or curated by Debra Brooks.

15.4: Geologic Hazards of the Peninsular Ranges

In a place so lovely, what could possibly go wrong?

Geologic hazards occur everywhere. Every area has its potential geologic hazard be it earthquakes, volcanoes, tsunamis, mass wasting, subsidence, floods, swelling clays, quicksand, beach erosion, sea level rising, saltwater intrusion, or groundwater contamination, just to name a few. In the Peninsular Ranges province, the rock types might not be that varied compared to many parts of California, but the landscape and the topography are varied, which leads to a host of potential hazards. Therefore, while there are no active volcanoes here (anymore), and tsunamis generally arrive with plenty of warning and much smaller amplitudes, making them much less of a problem than in northern California, everything else on that list can and does happen here. Many of these problems, while important – especially if they are affecting your home or your business – are fortunately mostly local and not wide-ranging within the province. This chapter will focus on the challenges that can and eventually may affect many people or large areas of the province.

Earthquakes

Earthquakes are generally number one on the list of California hazards. Earthquakes occur when tectonic stress builds up and the rock snaps, breaks, and moves with the best place for this to happen being at or near a plate boundary (see Earthquakes). The local plate boundary, the San Andreas fault zone (SAFZ), is not in the Peninsular Ranges province but is just outside it as is indicated in Figure 15.1.6. Two of the three major fault zones within the Peninsular Ranges are considered to be part of the greater San Andreas fault system – the San Jacinto and the Elsinore. The third major fault zone, the Newport-Inglewood-Rose Canyon fault zone, while not part of the greater San Andreas, parallels it, to the west, just onshore in some places, and just offshore in others. While the SAFZ represents a significant hazard, the local fault zones are closer and therefore present a greater local hazard. Especially since they all have a history of moderate to large earthquakes in recent times.

Query 15.4.1

This interactive element is not available in this format. Visit the link or scan the QR code to access it online.

View this Interactive Content online

The San Jacinto fault zone (SJFZ) is one of the most seismically active fault zones in all of southern California. Estimates are that up to 80% of the slip rate between the North American and Pacific plates in southern California is occurring because of earthquakes in the SJFZ. Estimates of the largest possible earthquake on the SJFZ is M_W7.5. It splays off the SAFZ in Lytle Creek in the San Gabriel Mountains of the Transverse Ranges province and crosses into the Peninsular Ranges province near Loma Linda, California, and then crosses into the Colorado Desert province south of the Santa Rosa Mountains and can be traced on the Interactive Fault Activity Map of California.

There is a long history of moderate to large earthquakes in the SJFZ. The most famous historic earthquake in the Peninsular Ranges, the 1812 San Juan Capistrano earthquake, was originally believed to have been on the Newport-Inglewood fault zone, then on the SJFZ, but now recent studies on interactions between fault zones indicates it occurred as a joint rupture of the SJFZ and the SAFZ. Seismologists now believe that the rupture most likely began on the SAFZ, then jumped between the two fault zones in Cajon Pass to the SJFZ, which increased the amount of fault rupture and magnitude. It has an estimated magnitude of M_W7.5 and is now being referred to as the 1812 Wrightwood earthquake, even though most of the damage occurred at the Missions along the coast, especially San Juan Capistrano (Figure 15.4.1). In all, at least 6 earthquakes with M6 or higher have occurred on the SJFZ since 1899. The largest being the 1918 M_L6.8 near the town of San Jacinto.



Figure 15.4.1: The remains of the Great Stone Church at Mission San Juan Capistrano, destroyed in a large earthquake on December 8, 1812. Extensive damage occurred throughout Alta California and 40 people died in the collapse of the church. "Great Stone Church 02" by Bernard Gagnon via Wikimedia Commons is licensed under CC BY-SA 3.0.

The next major fault zone to the west, the Elsinore fault zone (EFZ), is much less seismically active. It is one of the quieter fault zones in southern California in historic times but has the potential for earthquakes as large as M_W7.5. The last major earthquake to occur was a M_L6.0 in 1910. There were however two larger earthquakes in the 1890s, estimated M_W6.8 and M_W6.5 that may have occurred on either the EFZ or the SJFZ. This is before California had many seismometers and the epicentral locations calculated from those older more distant seismometers are not as precise as they are today. Since the 1890s, earthquakes as large as M7 have also occurred in Mexico on the southern extension of the EFZ, the Laguna Salada fault zone.

The third major fault zone in the Peninsular Ranges province is the Newport-Inglewood – Rose Canyon fault zone. Frequently it is referred to by either its northern name, the Newport-Inglewood fault zone (NIFZ), or its southern name, the Rose Canyon fault zone (RCFZ). This fault zone hugs the coast and passes from just onshore to just offshore, as seen in the Interactive Fault Activity Map of California. Potential largest magnitude estimates are M_W7.5 for the NIFZ, which is particularly scary because its northern end is in the heavily populated greater Los Angeles area, which includes Orange county. The RCFZ is a southern extension of the NIFZ and is mostly offshore and not as well studied, which is also scary because San Diego is another heavily populated area.

The NIFZ, however, is the location of one of the most important historical earthquakes in California, the 1933, M_W6.4 Long Beach earthquake. It is the second deadliest earthquake in California, 120 people died and it destroyed among other things 70 schools and damaged another 50. Luckily school was out for the day, or it is estimated that thousands of children would have died or been injured. This led to the passage of the Field Act, which requires state approval for all public-school buildings with respect to earthquake safety (see The Hazard of Place). The epicenter for this quake was not in Los Angeles county near the Inglewood end of the fault, but rather south of Huntington Beach. It's called the Long Beach earthquake because that is where maximum death and destruction occurred, even though the epicenter was not near Long Beach.

Evidence of a new potential increase to earthquake hazards in the Peninsular Ranges province comes from an unlikely location; Oklahoma. In the early 2000s, Oklahoma experienced an alarming increase in earthquake activity with their epicenters closely aligned with producing oil fields. Water was being injected into oil fields where fracking had occurred to help with the recovery of the remaining oil and in the process was lubricating long dormant fault zones. The Los Angeles Basin is also a major oil producing area and seismologists studying the earthquake history of the region noted a similar alignment of some earthquakes prior to 1935 with oil fields. Further investigation of the production practices pre-1940s indicate that several historic earthquakes, including the 1933 Long Beach earthquake may have been related to oil production. There is no indication that this is continuing to occur today, the geology of the Los Angeles basin and the Oklahoma oil fields is different and modern oil production practices are not the same as they were in the 1930s.

Because earthquakes are a major potential hazard in the Peninsular Ranges province, in order to estimate what could happen, the Southern California Earthquake Center (SCEC) in 2014 made a series of videos. These videos estimate fatalities and damage following a moderate earthquake on local faults in highly populated areas of the state. The following videos (Videos - 15.4.1, 15.4.2, 15.4.3, 15.4.4, 15.4.5) for the highly populated areas within the Peninsular Ranges are from that series.

Video 15.4.1: Magnitude 6.8 Earthquake on the Newport-Inglewood Fault

What if? What would happen to Torrance, Long Beach, Huntington Beach, if an earthquake approximately the size of the 1994 Northridge earthquake were to happen on the northern, onshore part of the Newport-Inglewood fault near the Los Angeles-Orange County line? This area which was sparsely populated when the 1933 Long Beach earthquake occurred is now densely populated and the story is no longer the same. This video has no sound. Access a detailed description.

This interactive element is not available in this format. Visit the link or scan the QR code to access it online.

View this YouTube Video online

Video 15.4.2: Magnitude 6.9 Earthquake on the San Joaquin Fault

What if? What would happen to Huntington Beach, Costa Mesa and Santa Ana, California, if an earthquake approximately the size of the 1994 Northridge earthquake were to happen on the San Joaquin fault? The San Joaquin or San Joaquin Hills thrust fault is a blind thrust fault onshore of the Newport-Inglewood fault in central Orange County, California. This video has no sound. Access a detailed description.

This interactive element is not available in this format. Visit the link or scan the QR code to access it online.

View this YouTube Video online

Video 15.4.3: Magnitude 6.5 Earthquake on the Palos Verdes Fault

What if? What would happen to Compton, Long Beach, and Huntington Beach, if an earthquake approximately the size of the 1994 Northridge earthquake were to happen on the Palos Verde fault? The Palo Verde fault is offshore between Santa Catalina Island and the Orange county coastline. This video has no sound. Access a detailed description.

This interactive element is not available in this format. Visit the link or scan the QR code to access it online.

View this YouTube Video online

Video 15.4.4: Magnitude 6.5 Earthquake on the Rose Canyon Fault

What if? What would happen to San Diego and Chula Vista, California, and Tijuana, Mexico, if an earthquake approximately the size of the 1994 Northridge earthquake were to happen on the Rose Canyon fault? This video has no sound. Access a detailed description.

This interactive element is not available in this format. Visit the link or scan the QR code to access it online.

View this YouTube Video online

Video 15.4.5: Magnitude 6.5 Earthquake on the Elsinore Fault

What if? What would happen to Corona, Yorba Linda, and Santa Ana, if an earthquake approximately the size of the 1994 Northridge earthquake was to happen on the northern Elsinore fault? This video has no sound. Access a detailed description.

This interactive element is not available in this format. Visit the link or scan the QR code to access it online.

View this YouTube Video online

The situation has changed since 1933, notice that if any of these earthquakes were to happen, it would immediately move to at least second place on the death and destruction list of California earthquakes. All of these models indicate that such an earthquake happening today will potentially kill or injure more people than did the 1933 Long Beach earthquake.

Query 15.4.1

This interactive element is not available in this format. Visit the link or scan the QR code to access it online.

View this Interactive Content online

Floods

Usually when people think of flooding in California they think of the Great Valley or the Delta, not southern California. With a Mediterranean climate along the coast and relatively dry climates within the mountains, flooding would not seem to be much of an issue in southern California, and usually, it isn't. Flash floods occur in the mountains after rainstorms, but usually they are local events and not wide ranging. However, some of the largest and most damaging floods in the history of California have occurred, at least partly, in southern California.

There is a long history of mostly coastal flooding in the Peninsular Ranges province. Since California became a state, significant flood events have occurred in one part or all of the Peninsular Ranges in 1862, 1891, 1916, 1938, 1969, 1980, and 2005. Of particular note are the Great Flood of 1862 (Box 15.4.1) and the flood of 1938.

Box 15.4.1: California's Great Flood of 1862 – in southern California

In 1862, the western front of the Civil War came to a standstill during what is one of the largest flood events ever experienced on the west coast of the United States. Now known as the Great Flood of 1862, continuous rain fell for anywhere from 28 to 42 days on the west coast and major flooding occurred from British Columbia to Mexico and was especially bad in the

states of California, Oregon, and Nevada. In California, much of the Central Valley flooded and Sacramento was under 4 feet of water. On January 10, 1862, the newly elected Governor of California, Leland Stanford, arrived at his inauguration at the State Capital in a rowboat.

Within two more weeks the flooding in Sacramento was so bad that the State Legislature temporarily moved to San Francisco. The rain and flash flooding that occurred in the mountainous areas of the state, including the Peninsular Ranges, destroyed many of the mining camps, most of which were never rebuilt. Statewide, an estimated 4000 people are believed to have died, over 200,000 cattle, most of the bridges in the state were destroyed, as was approximately one-third of all property, and the state went bankrupt.

In southern California, approximately 35 inches of rain fell over 28 consecutive days starting on December 24, 1861. The Santa Ana River, the major river system in the northern Peninsular Ranges, flowed wall-to-wall in Santa Ana Canyon and when the canyon opened onto the coastal plain near Anaheim, it flooded Anaheim and destroyed it along with its vineyards and farms.

By February the flood waters of the Santa Ana River had merged on the coastal plain with those of the San Gabriel and Los Angeles Rivers to create a temporary inland sea from Signal Hill to Huntington Beach that was over 29 km (18 miles) long and with standing water over 1.2m (4 feet) deep. The water did not recede for over 3 months. In San Diego, high tides and the storm surge from an offshore storm backed up the San Diego River and it cut a new channel to the harbor. The hills and marine terraces were heavily eroded, and many were cut by gullies and channels. A 15.25 m (50 foot) arroyo was eroded at San Luis Rey and like Sacramento to the north, Mission Valley was underwater.

While the Great Flood of 1862 did not start the California citrus industry, it helped set the stage for the citrus industry to flourish in the 1870s. Prior to the Great Flood, much of southern California was cattle ranches and over 10,000 cattle are estimated to have died in the flood in southern California. Many of the ranchers became farmers because they could not afford to replace the cattle they had lost. And the climate in many of the destroyed areas of southern California, such as Riverside, Anaheim, and San Diego was perfect for citrus.

In southern California this flood still stands as the worst flood to have occurred in modern times. Sedimentological studies indicate that large flood events may happen as frequently as every 100-200 years. Also, while it took the floodwaters until summer to recede in many areas, once the flood was over, California went into a period of drought that lasted until 1864.

The flood of 1938 (Figure 15.4.2) is what finally mobilized the state into taking action to prevent massive flooding and started an era of dam building for both flood prevention and water storage with Prado Dam on the lower Santa Ana River completed in 1941.

During the 1938 flood, it rained for 5 days, 87 people died and damage was $78 million ($1.69 billion in today's dollars). The Santa Ana River broke its levee near Santa Ana Canyon and the cities of Anaheim, Buena Park, and Santa Ana flooded. Flood waters in Anaheim and Santa Ana were almost 2m (6 feet) deep. Almost every bridge and railroad crossing over the river was destroyed.



Figure 15.4.2: The mouth of the Santa Ana River near Huntington Beach, California, during the flood of 1938. The Pacific Ocean and Santa Catalina Island are in the background. Major breaks in the levee system are visible. US Hwy 101 along the coast and major streets are submerged by the flood waters. "Santa Ana River during the flood of 1938" is copied courtesy of the Orange County Archives and is licensed under CC BY 2.0. Access a detailed description.

Why this history of massive flooding? It's partly because of ARkStorms, for Atmospheric River 1000 Storms, storms that occur every 500-1000 years when atmospheric rivers bring days of extreme weather that overwhelm existing water control systems (Video 15.4.6). While not every flood event is an ARkStorm, the 1862 flood was. With global warming, it's possible that storms of this magnitude will occur even more frequently than every 500 to 1000 years in the future.

Video 15.4.6: ARkStorm

This film depicts the realistic outcome of a hypothetical, but plausible massive storm hitting the state of California. It presents an overview by the U.S. Geological Survey of the danger an ARkStorm could bring.

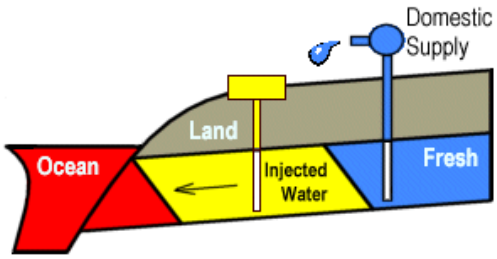
This interactive element is not available in this format. Visit the link or scan the QR code to access it online.

View this YouTube Video online

Saltwater Intrusion

Saltwater or seawater intrusion is a coastal problem. It occurs when the local groundwater aquifer is open to seawater and there is a possibility that saltwater will advance inland (see Threats to California's Water). Problems occur when the balance between saltwater and freshwater is disturbed, which generally happens when fresh water is pumped out faster than it can be replenished, or as sea level rises. As sea level rises, there is more water exerting pressure on the seafloor sediments and this can help drive more saltwater into the aquifers near shore.

In Orange and San Diego counties the most common method used to try and prevent this from happening is the use of injection wells close to the coast (Figure 15.4.3). Rather than try to build a solid barrier, freshwater, frequently recycled water (yellow in the figure), is pumped or injected into the ground closer to the coast to form a fluid barrier between the saltwater (red) and the freshwater (blue). Freshwater wells are then sited inland further from the coast.



Confined Aquifer with Freshwater Injection

Figure 15.4.3: Cross-section of a confined coastal aquifer with freshwater injection wells. Fresh water (yellow) is being pumped or injected into the ground between saltwater (red) and freshwater (blue). "Freshwater Injection" by Los Angeles County Public Works is in the public domain.

In coastal Orange county, there are two groundwater barriers created by injection wells, the northernmost is the Alamitos Barrier Project, a joint project near the Los Angeles and Orange county line and the Talbert Barrier near Huntington Beach and Fountain Valley, California. The Alamitos Barrier is a joint project between Los Angeles and Orange counties and maintains a system of 59 injection wells near Seal Beach and Long Beach, California. The Talbert Barrier by the Orange County Water District is a series of 102 injection wells over three miles. The injection wells vary from 100 to 685 feet deep and are located to form a fluid barrier.

The area between these two barriers is known as the Sunset Gap and is currently being monitored because in 2015 a water well 3 miles inland in Huntington Beach had to be taken offline because of saltwater intrusion. Currently the monitoring of salt levels by both geophysical and chemical methods shows that saltwater is slowly moving onshore and approaching the production wells. New monitoring wells were drilled and data from them is being used to design a new injection well barrier.

There are other techniques that can be used to monitor the movement of saltwater onshore. The most common ones are geophysical methods based on changes in the electrical resistivity of the water. Geophysical techniques such as this are generally much cheaper than drilling monitoring wells and can cover larger areas of interest, but do not provide the detailed water quality information gathered by a monitoring well.

Two factors will lead to this becoming an even more important problem to mitigate in the future – population growth and rising sea level. Both will contribute to an increased risk and preventing saltwater intrusion will become even more important.

Mass Wasting

Mass wasting is the technical term used to describe what are commonly called landslides. Mass wasting can occur anywhere but is most likely to occur in areas with high relief and steep slopes, or steep slopes and weak rock. In fact, coastal California, including the Peninsular Ranges province has some of the best conditions in the world for mass wasting. Most of the mass wasting that occurs in the Peninsular Ranges province occurs along the coast in the marine terraces. While the slopes in the mountains are steep and have high relief, most of the rock in the mountains is very strong, competent plutonic igneous rock that seldom hosts landslides. Where they do occur in the mountains is in shear zones or other areas where the rock has been highly fractured and while they do occasionally occur, they are relatively uncommon.

The marine terraces are another story. They are frequently oversteepened and with slopes well above the angle of repose (Figure 15.4.4). The rock is almost always sedimentary, relatively young, and extremely well-watered. All that is needed is a trigger for mass wasting to occur and in most of southern California dozens, if not hundreds, of small earthquakes occur daily. Most of these earthquakes are so small that humans cannot feel them, but they are still large enough to trigger mass wasting. Most of the time, mass wasting will be some type of slide, with slumps being the most common. Slumps occur when material moves downslope as a unit on a curved plane.



Figure 15.4.4: Oversteepened cliffs of Torrey Sandstone at Torrey Pines State Beach, San Diego County, California. Notice the piles of sediment at the base of the cliff. As sediment weathers from the cliff, wave action at high tide removes the finer-grained sediment, leaving only the larger pebbles and cobbles behind. "Torrey Pines 2024-06" by Allison Jones is licensed under CC BY-NC 2.0

An example of what can happen is illustrated in this video (Video 15.4.7) of Black's Beach in San Diego county. In January 2023, a slump occurred that brought much of the bluff down onto the beach.

Video 15.4.7: Black's Beach Bluff Collapse

TV report of a slump occurring at Black's Beach, San Diego County, California.

This interactive element is not available in this format. Visit the link or scan the QR code to access it online.

View this YouTube Video online

Much of the time slumps bringing down beach cliffs is only a hazard to the people on the beach below, and unfortunately people are sometimes injured or even die. Sometimes however there is development at the top of the cliff and houses or businesses may be lost. In southern Orange county the railroad right-of-way is at the base of the cliffs and during stormy, wet winter weather, mass wasting takes out the train tracks on a fairly regular basis. The opposite situation occurs in San Diego county, where the railroad right-of-way is on the marine terrace at the top of the cliffs and so far, there has not been a problem, but the potential for one exists.

Query 15.4.3

This interactive element is not available in this format. Visit the link or scan the QR code to access it online.

View this Interactive Content online

Climate Change

As the world's climate warms, the effects on coastal communities will be huge. Most of what is likely to occur however is that the hazards already existing, floods caused by storms, saltwater intrusion, mass wasting, will become more frequent and exacerbated over time. Added to this will be flooding from rising sea level and the possibility for beaches to disappear. Most coastal communities are dependent upon their beaches and tourism for much of their economy, which means that even if ways are found to help the residents stay in their homes, if the beaches are gone, the communities may die anyway.

References

1. Barrows, A. G. (1974). CDMG Special Report 114: *A Review of the Geology and Earthquake History of the Newport-Inglewood Structural Zone, Southern California*. California Division of Mines and Geology.
2. Bryant, W. A., compiler (2017). *Quaternary Fault and Fold Database of the United States*. [Data set]. U.S. Geological Survey. https://earthquake.usgs.gov/cfusion/qfault/show_report_AB_archive.cfm?fault_id=186&section_id=
3. Burger, H. R., Sheehan, A. F., & Jones, C. H. (2006). *Introduction to Applied Geophysics*. Cambridge University Press.
4. California Geological Survey (2015). *Fault Activity Map of California*. [Data set]. State of California. https://maps.conservation.ca.gov/cgs/fam/
5. Campa, A. J. (2024, January 25). Landslide in San Clemente halts train service indefinitely. *LA Times*. https://www.latimes.com/california/story/2024-01-25/metrolink-amtrak-san-clemente-landslide-train-service-halted
6. Carney, K. (2024, June 20) *California Counties by Population*. California Demographics by Cubit. https://www.california-demographics.com/counties_by_population
7. County of Orange & Orange County Operational Area. (2019, May). *Flood, Dam, and Reservoir Failure Annex Emergency Operations Plan*. 67p. Orange County Emergency Management Organization. https://ochealthinfo.com/sites/hca/files/import/data/files/96194.pdf
8. Earthquake Hazards Program. (n.d.). *M6.4 March 10, 1933 Long Beach, California Earthquake*. U.S. Geological Survey. https://www.usgs.gov/programs/earthquake-hazards/science/m64-march-10-1933-long-beach-california-earthquake
9. Edwards, B. D., & Evans, K. R. (2005, May 17) *Saltwater Intrusion in Los Angeles Area Coastal Aquifers – the Marine Connection*. USGS Fact Sheet 030-02 https://pubs.usgs.gov/fs/old.2002/fs030-02/
10. Ellsworth, W. L. (1990). Earthquake history, 1769-1989. In R. E. Wallace (Ed.), USGS Professional Paper 1515: *The San Andreas Fault System, California*. (pp. 153-181). U.S. Geological Survey. https://pubs.usgs.gov/pp/1990/1515/
11. Field, E. H., Biasi, G. P., Bird, P., Dawson, T. E., Felzer, K. R., Jackson, D. D., Johnson, K. M., Jordan, T. H., Madden, C., Michael, A. J., Milner, K. R., Page, M. T., Parsons, T., Powers, P. M., Shaw, B. E., Thatcher, W. R., Weldon, R. J. II, & Zeng, Y. (2015, March). *UCERF3: A New Earthquake Forecast of California's Complex Fault System*. USGS Fact Sheet 2015-3009 https://pubs.usgs.gov/fs/2015/3009/pdf/fs2015-3009.pdf
12. Harden, D. R. (2004). *California Geology* (2nd ed.). Pearson Prentice Hall.
13. Hart, M. W. (1991). Landslides in the Peninsular Ranges, Southern California. In M. J. Walawender & B. B. Hanan (Eds.), *Geological Excursions in Southern California and Mexico: Guidebook for the 1991 Annual Meeting Geological Society of America San Diego, California*. (pp. 349-371). Department of Geological Sciences, San Diego State University.
14. Hough, S. E., & Graves, R. W. (2020). The 1933 Long Beach Earthquake (California, USA): Ground Motions and Rupture Scenario. *Scientific Reports*. 10(10017). https://doi.org/10.1038/s41598-020-66299-w
15. Hough, S. E., & Page, M. (2016). Potentially Induced Earthquakes during the Early Twentieth Century in the Los Angeles Basin. *Bulletin of the Seismological Society of America*, 106(6) 2419-2435. https://doi.org/10.1785/0120160157
16. Los Angeles County Department of Public Works. (2024). *Seawater Barrier – Alamitos Barrier Project*. https://pw.lacounty.gov/core-service-areas/water-resources/seawater-barrier/
17. Masters, N. (2012, November 29). The Santa Ana River: How It Shaped Orange County. *Lost LA PBS SoCal*. https://www.pbssocal.org/shows/lost-la/the-santa-ana-river-how-it-shaped-orange-county
18. Masters, N. (2017, March 3). The Southern California Deluge of 1938. *Lost LA PBS SoCal*. https://www.pbssocal.org/shows/lost-la/the-southern-california-deluge-of-1938
19. Plummer, C. C., Carlson, D. H. & Hammersley, L. (2016). *Physical Geology* (15th Ed.). McGraw-Hill Education.
20. Porter, K., Wein, A., Alpers, C., Baez, A., Barnard, P., Carter, J., Corsi, A., Costner, J., Cox, D., Das, T., Dettinger, M., Done, J., Eadie, C., Eymann, M., Ferris, J., Gunturi, P., Hughes, M., Jarrett, R., ... Jones, L., Chief Scientist, Cox, D., Project Manager. (2011). USGS Open-File Report 2010-1312: *Overview of the ARkStorm scenario*. U.S. Geological Survey. https://pubs.usgs.gov/of/2010/1312/
21. Riverside County Flood Control and Water Conservation District. (2024). *District History*. https://rcflood.org/district-history
22. Rodriguez Padilla, A. M., Oskin, M. E., Rockwell, T. K., Delusina, I., & Singleton, D. M. (2021). Joint earthquake ruptures of the San Andreas and San Jacinto faults, California, USA. *Geology*, 50(4) 387-391.
23. Sarmiento, V. (2020, August). President's Message – Keeping Seawater Out of Drinking Water. *OC Water News*

Hydrospectives. Orange County Water District. https://www.ocwd.com/news-events/newsletter/2020/august-2020/president-s-message-keeping-seawater-out-of-drinking-water/
24. Southern California Earthquake Data Center (2013). *Earthquake Information*. [Data set]. Caltech. DOI:10.7909/C3WD3xH1
25. The Bowers Museum. (2023, January 12). Swept Under: Historic Flooding in Orange County. *The Bowers BLOG*. https://www.bowers.org/index.php/collection/collection-blog/swept-under-historic-flooding-in-orange-county
26. Troxell, H. C., & Others. (1942). USGS Water-Supply Paper 844: *Floods of March 1938 in southern California*. U.S. Geological Survey
27. U.S. Army Corps of Engineers. (n.d.). *Prado Dam*. https://www.spl.usace.army.mil/Missions/Asset-Management/Prado-Dam/
28. USGS California Water Science Center. (n.d.). *Seawater Intrusion*. U.S. Geological Survey. https://ca.water.usgs.gov/sustainable-groundwater-management/seawater-intrusion-california.html

References for Box 15.4.1: California's Great Flood of 1862 – in southern California

1. Dettinger, M. D., & Ingram, B. L. (2013). The Coming Megafloods. *Scientific American*, *308*(1), 64–71. http://www.jstor.org/stable/26017895
2. Dowd, K. (2022, January 11). The deadly 1862 California flood that wiped out and reshaped the state. *SFGate*. https://www.sfgate.com/weather/article/deadly-1862-flood-wiped-out-california-16761390.php
3. Moore, A. (2024, March 1). The Great Flood of 1862. *California Historical Society*. https://californiahistoricalsociety.org/blog/the-great-flood-of-1862/
4. Philpott, T. (2020, August 26). The Biblical Flood That Will Drown California. *Mother Jones*. *https://www.motherjones.com/environment/2020/08/california-flood-arkstorm-farmland-climate-change/*
5. Smith, J. (2003, June 26). San Diego's five worst floods. *San Diego Reader*. https://www.sandiegoreader.com/news/2003/jun/26/unforgettable-san-diegos-five-worst-floods/
6. Taylor W. L., & Taylor, R. W. (2007). The Great California Flood of 1862. *The Fortnightly Club of Redlands, California*. https://www.redlandsfortnightly.org/papers/Taylor06.htm

This page titled 15.4: Geologic Hazards of the Peninsular Ranges is shared under a CC BY-NC 4.0 license and was authored, remixed, and/or curated by Debra Brooks.

15.5: Natural Resources of the Peninsular Ranges

A Rich Land

Any area as varied as the Peninsular Ranges must have multiple natural resources. Some such as water and precious metals are in relatively short supply, but others such as building materials are abundant. Much of the development of urban centers in the Peninsular Ranges is not only related to the presence of a major harbor and seaport along its coast, but also because the materials necessary to build an urban infrastructure: sand, gravel, and limestone (concrete and cement), oil and gas (energy), sand and asphalt (road building), specialized sand – glass sand (windows), clay (sewer pipe), and gypsum (plaster and drywall) are abundant and many of these commodities are still mined today.

California has a history of prospecting and mining precious metals, and the Peninsular Ranges were actively prospected. While precious metals have been discovered and mined here (gold, silver, nickel, mercury, and tin are examples), most mines have long since played out and the mining of precious metals is mostly just a memory. Gemstones and rare or collectible minerals are still mined. For much of the world, the Peninsular Ranges are still a prime location for tourmaline, kunzite, and other collectible rare minerals and gems.

Water (or Rather the Lack of Potable Water)

One of the key resources necessary for life is water. In the Peninsular Ranges province, as in many areas of southern California, this is the resource that frequently presents the biggest challenges. Drought has been a major influence throughout California's history; 2011-2017 was the longest drought recorded so far, with 2012-2014 as the driest three consecutive years on record. All the counties in the Peninsular Ranges started importing water to meet local needs decades ago – Orange in the 1920s, San Diego in the 1940s, and Riverside in the 1950s. In any given year, San Diego county imports approximately 70% to 90% of its potable water, Orange county imports approximately 50%, and estimates of how much water Riverside county imports vary greatly but are less than either Orange or San Diego counties.

Most of the local water districts are part of the greater Metropolitan Water District of Southern California (MWD) which acts as a regional water wholesaler, managing the sale and disbursement of water from the Colorado River and northern California. Without the purchase of outside water, most of the water districts in Peninsular Ranges would not be able to meet the needs of their resident populations. Depending upon imported water is not the only way local water districts are trying to improve the availability of water. Water conservation is strongly encouraged by all the water districts within the province, but the coastal areas are in a more precarious situation than the inland areas.

The water supply situation, and water rates, for coastal areas are high because of the large amount of imported water needed. Northern Orange county uses a combination of approximately 75% local groundwater and 25% imported water to supply the county's water needs, augmented by recycling. Southern Orange county imports over 80% of its water. San Diego county has even less water and more people. Because it purchases almost all of its water; its water rates are astronomical compared to most of the country and it has developed a very sophisticated water purchasing system (Video15.5.1).

Video 15.5.1: Where San Diego County Gets Its Water

A detailed overview of the different sources of water in San Diego county and how it manages its purchasing of so much of its water supply.

This interactive element is not available in this format. Visit the link or scan the QR code to access it online.

View this YouTube Video online

Therefore these counties have considered options that other areas would consider prohibitively expensive. In Orange county, this is a massive recycling effort, the Groundwater Replenishment System (GWRS), which recycles the water that goes through sewage treatment plants and then uses this recycled water to replenish the groundwater basin and for injection wells to maintain the fluid barrier protecting the aquifer from saltwater intrusion. San Diego county has taken a different approach and instead of massive recycling, it has built a desalination plant, which provides approximately 10% of the county's water. Desalination is removing the salts from seawater to make it potable.

Fortunately, for Riverside county, there is more available groundwater there than is available in either Orange or San Diego counties. Also, one of the MWD's newest and largest reservoirs is in Riverside county outside Hemet, CA. Diamond Valley Lake (Figure 15.5.1), is an off-stream reservoir used to store water from both the Colorado River and the California State Water Project (see Water Infrastructure and Management) in a roughly central location between Los Angeles and San Diego for use during times of drought or other emergencies.



Figure 15.5.1: Diamond Valley Lake, a reservoir in the Metropolitan Water District's water storage system, with the San Jacinto Mountains in the background. "Diamond Valley Lake View San Jacinto" by Zindor via Wikimedia Commons is licensed under CC BY-SA 4.0.

The Diamond Valley Lake reservoir also has the advantage of being on the Pacific plate. One of the major concerns of the MWD is that all of its outside water sources have either canals or pipelines that cross the San Andreas fault system; having the water storage on this side of the plate boundary helps ameliorate the potential problem of not being able to get water into southern California in the event of a large earthquake. Work on the project started in 1995 and was completed in 2003 and it was one of the largest construction projects in the nation during the 1990s. Full, it provides a 6-month water supply for the MWD and at over 260 billion gallons, holds more water than Lake Havasu on the Colorado River and almost as much water as all of the other reservoirs in southern California combined.

One of the misconceptions about water use in southern California and in the Peninsular Ranges province in particular is that much of the water use is for agriculture. While this is true in eastern Riverside county in areas that are part of the Colorado Desert province, it is not true in western Riverside County or in Orange and San Diego counties. While some farming does still exist, the increasing population and pressure for land for homes and businesses means that agriculture is becoming a smaller and smaller part of the economy. By 2007-2008, only 12 of 31 the water agencies in Orange county reported any agricultural water use. In 2015, agricultural water use was down to only 8% of the county's water in San Diego county and it is expected to continue to decline. Therefore, more and more of the water supply is now supporting urban populations rather than agriculture.

Precious Metals, Not So Precious Metals, and Oil

California is the Golden State, our state mineral is gold, and gold mining has a long history in the Peninsular Ranges province. Gold has never, however, been as important of a commodity in the Peninsular Ranges as it was and is in the Sierra Nevada or other parts of the state (see Gold of the Sierra Nevada). While gold has been discovered in many parts of the Peninsular Ranges, only two major gold mining districts were in the province – the Julian District in San Diego county and the Pinacate District in Riverside county.

Julian is the more famous and was the more productive of the two. Gold was discovered in 1870, and the mining district was formed that year. A gold rush occurred, with miners flocking to the area to stake claims. Most of the gold mining is within or adjacent to the Julian Schist associated with the Cuyamaca-Laguna Mountains shear zone. Of the nine significant mines in the district, the most productive was the Stonewall Jackson or Stonewall Mine. Approximately 220,000 ounces of gold total was mined in the Julian District, and of that about 45% was from the Stonewall Mine, which produced over $2 million in gold between its discovery in 1870 and closure in 1926. Production in the Julian district as a whole was from 1870 to 1926, with peak production in 1870 to 1880 and 1888 to 1896. The mines are now closed, and Julian today is better known for its annual Apple Days Festival every autumn.

The Pinacate Mining District in Riverside county has a different history; placer gold (see Gold of the Sierra Nevada) was discovered there in 1850, and hard-rock mining did not begin there until 1874 when the Good Hope Mine was developed. The hard-rock mining was mostly native gold in quartz veins in quartz monzonite and quartz diorite/tonalite. Of the seven significant gold mines in the district, approximately 104,000 ounces of gold total was mined, with the Good Hope Mine as the largest producer. The Good Hope was active from 1874 to 1936, and most active and productive from 1889-1894 (Figure 15.5.2). Today this area of Riverside county is mostly housing developments.

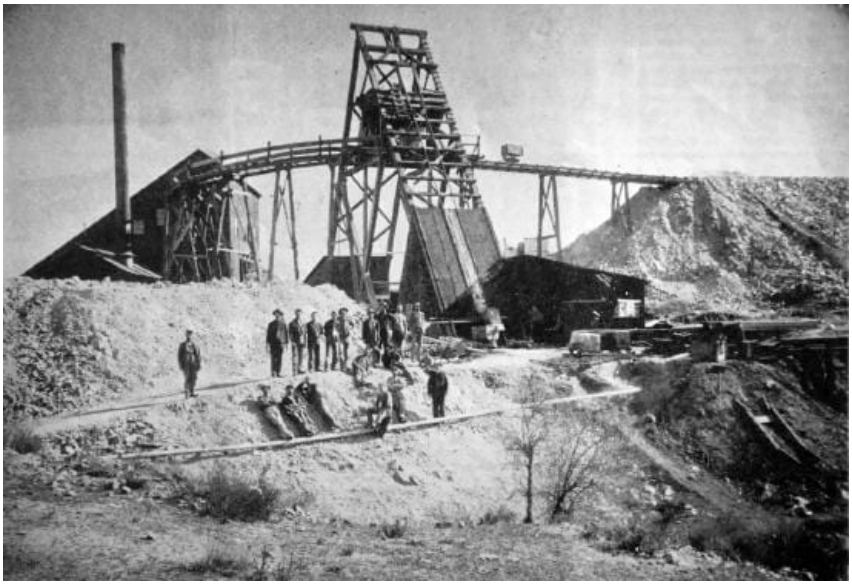


Figure 15.5.2: The main shaft of the Good Hope Mine in 1907, Riverside County, California, with the head frame, tramway to the mill, and the waste dump. Good Hope Mine 1907 from the collection Rob Skinner via Wikimedia Commons is in the public domain.

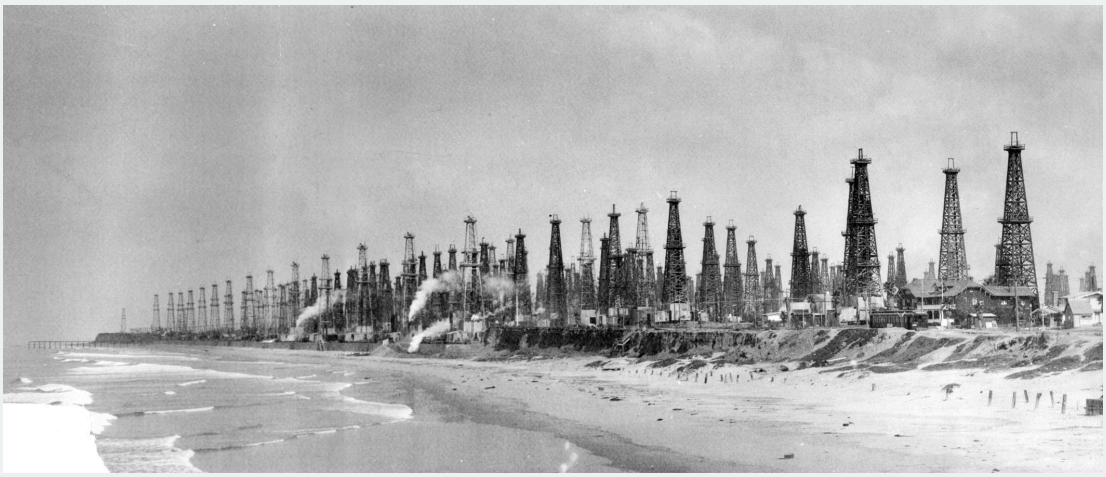
If gold is number one on the list of sought after precious metals, its sister, silver, is not far behind. San Diego county and the western part of Riverside county within the Peninsular Ranges are not known for silver mining. Orange county however was the home of the Silverado Mining District, and which created quite a stir between 1878 to 1881 but produced very little silver, along with some lead and zinc. Other precious metals and metals mined in the Peninsular Ranges province include mercury, tungsten, tin, and minor amounts of copper and molybdenum. However, most of these ventures were relatively short-lived and frequently were associated with shortages that occurred during either WWI or WWII, and once the war was over, prices dropped, and those mines were no longer economic.

"Black Gold" however is another story. Oil production from the coastal plain of both the Peninsular Ranges and Transverse Ranges provinces began in the late 1800s and continues through to today (Box 15.5.1).

Box 15.5.1: Oil and Gas in the Peninsular Ranges Province

Most of the Peninsular Ranges province has no history of oil discovery or production. Oil fields are not usually found in plutonic igneous rock, which is the major rock type in the province. Oil is usually associated with sedimentary rock, which means the best possibility of finding oil in the province is on the coastal plain.

Just like Riverside county is split between two provinces, the Peninsular Ranges in the west and the Colorado Desert in the east, Orange county is also split between two provinces. The very northernmost part of Orange county is in the Los Angeles Basin of the Transverse Ranges province and that is where almost all of the oil production occurs. So, while Orange county is a major oil producing county in California, most of the oil production is not from the Peninsular Ranges province. The exceptions are Orange county's southernmost oil fields in Huntington Beach and Newport Beach which extend south of the basin along the marine terraces, the beach, and the Newport-Inglewood fault zone (Box Figure 15.5.1).



Box Figure 15.5.1: Huntington Beach in 1926 – a sea of oil derricks with the old Huntington Inn and the Red Car, the electric train from Los Angeles. "Huntington Beach, 1926" is copied courtesy of the Orange County Archives and is licensed under CC BY 2.0.

The Huntington Beach oil field was discovered in 1920 and is still in production today. Peak production was achieved in 1923 with 156 producing wells. It is a "supergiant" oil field having produced over a billion barrels of oil from 1920 to 2000 and is the fifth largest oil field in California. One of the interesting historical facts about this oil field is that it is one of the earliest oil fields discovered on the recommendation of geologists. Most oil wells drilled at the time were by "wildcatters" men with much drilling experience and little formal geology training. The first well was drilled by Standard Oil of California (today's Chevron Corporation) and they were planning on drilling in Newport Beach, but a company geologist sent to evaluate the recommended prospect in Newport Beach strongly suggested that instead the company drill the first well in Huntington Beach.

Drilling began in a barley field in December of 1919 and oil was discovered at a depth of 725 m (2379 feet). It went into production at a rate of 70 barrels of oil a day in May of 1920 and altered the history of the city of Huntington Beach by increasing the interest in drilling in the area. The second well drilled, Bolsa Chica #1, would change the history of Huntington Beach. It was completed at 777 m (2549 feet) as an uncontrolled gusher. It blew out and started an environmental disaster with 1742 gallons a day flowing into the lowlands, but the oil boom was on. Gold rush, oil boom; the pattern was the same, people flocked to the area in search of potential opportunities and riches.

Lease prices on the land within and around Huntington Beach skyrocketed from $25-$50 an acre to over $1000 an acre. By the end of 1920 all the land for 4 miles around the discovery well, Huntington A-1, was leased. Population exploded as oil well after oil well was drilled and began producing. It took a crew of 15 men to maintain an individual oil well on a weekly basis, and within months the population of Huntington Beach had jumped from about 1500 to over 6000. Everything was in demand, housing, food, clothing, recreation. Among other businesses, five pool halls were built, and they became unofficial hiring halls for oil field workers. Scams, graft, and illicit business flourished. And many made fortunes and employment was high.

One scheme that was not a scam is worth noting. In 1916, before the oil field was discovered, an encyclopedia company had been offering a deal – buy a set of encyclopedia and get a small lot for free. Land was cheap enough then that the encyclopedia company could afford to buy a set of lots, subdivide them, and give them away as a promotion for buying encyclopedias. The lots were very well placed and the people who had bought encyclopedias made small fortunes from oil leases.

For decades Huntington Beach had a boom and a not-quite-as-bad-as-bust economy, with good years and bad, depending upon the variations in the price of oil, regulation, and the national economy. In the 1950s the city started on a program to have the oil companies clean-up and remove the old wooden derricks and replace them with steel pumping units. By 1964, Huntington Beach had 1776 active oil wells producing just over 16 million barrels of oil. By the 1970s land was becoming more valuable for housing and oil production declined as wells were capped.

In 1991, Huntington A-1 was permanently sealed by filing it with cement, a process known as "abandonment", which ensures the well is safely closed off. It had been inactive and non-operational since 1968. By 2000, over a billion barrels of oil had been produced along with 845cf of natural gas. The Huntington Beach oil field however is still producing and in 2013 the US Geological Survey estimated that there are still probably 3500 million barrels of oil left to produce.

Building Commodities

As with most of the world, the most common commodities mined in the Peninsular Ranges province are those needed to maintain the infrastructure and to build towns and cities – gravel and sand and fill dirt (concrete, roadbeds, fill), limestone and marble (concrete, cement, and steel production), building stone and dimension stone (riprap, buildings and ornamental stone features), clay (sewer pipe, tile, and pottery), gypsum (plaster and drywall), silica and specialty sand (glassmaking, ceramics, abrasives, electronics, computer chips, steel production), and gemstones (adornment, lasers, abrasives, and cutting tools).

Sand and gravel are the most commonly mined building materials. Commonly called aggregate, these materials are used in making concrete, back top, plaster and stucco for buildings. Also, it is used as road base, railroad ballast, and fill. The economic complication that arises with aggregate is that it is bulky, heavy, and has a comparatively low-unit cost as a commodity. Therefore, it needs to be mined close to where it will be used, or the transportation costs can dramatically increase the fuel consumption driving up building costs; and the fuel consumption and gas emissions can dramatically increase air pollution.

What this means geologically is that in most urban areas, there is always a need for a nearby source of aggregate. The Peninsular Ranges are no exception and almost any stream coming out of the mountains or their foothills, dumps sand and gravel when the slope gets gentler at their base and the streamflow slows (Figure 15.5.3). Therefore, there is an extensive history of ongoing, open pit aggregate mining at the base of the Peninsular Ranges and their foothills. The mountain front is where gravel pits are mined and abandoned, and reopened, as needed depending upon local building projects. Predictions by the California Geological Survey in 2018 are that there is approximately 41 to 50 years worth of reserves in Orange and Riverside counties and 11 to 20 years of reserves for San Diego county.



Figure 15.5.3: Abandoned, and now flooded, gravel pit in Santiago Creek, Orange, California. "Flooded Gravel Pit in Santiago Creek" by Debra Brooks is licensed under CC BY-NC 4.0.

Limestone and marble for cement making is still actively quarried in the northern Peninsular Ranges mostly in the area around Riverside, California, and areas in the northern Perris Block. While marble and limestone have been mined in both San Diego and

Orange counties in the past, their deposits are relatively small and today mining is concentrated in Riverside county. Quarrying limestone and marble for cement started in the 1890s. During WWII it was extensively quarried for use in the former steel mills of Fontana, California. While the steel mills may be closed, building still continues in southern California, and therefore, so does quarrying marble to make cement.

Quarrying dimension stone and building stone also has a history throughout the Peninsular Ranges. Nationally most of the dimension stone used is marble, and while some marble is mined for building use in the Peninsular Ranges, most of the dimension stone mined is plutonic igneous rock, mostly granite and other felsic igneous rock, but also some gabbro.

Most of the granite in the Transverse Ranges is highly fractured and cannot be used for dimension stone, therefore the Peninsular Ranges have become the major source for most of the dimension stone used in southern California. Granite and other plutonic igneous rock have been used for riprap in breakwaters and jetties, as well as for building facings, flooring, monuments, and even kitchen countertops. Most of today's quarries are in Riverside or in San Diego counties. Of special importance for monuments and building facing is the "black granite" or gabbro, quarried in San Diego county. It has been highly prized since the 1920s and is not only used locally in California, but also in the rest of the nation and internationally.

Clay has been mined throughout the Peninsular Ranges province since the 1880s, but most of the clay mined today is in either Riverside or Orange Counties. Of special interest is kaolin, or kaolinite, the clay used to make porcelain and fine china which is found in the Silverado Formation and mined in the Alberhill district in the Temescal Valley of the Perris Block in Riverside county. The other common use for kaolinite is in cement production and this is how most of the kaolinite mined in Riverside county is used. Common clay, which is the most commonly mined clay, is mostly used for sewer pipe, tile, bricks, pottery, and as a liner for solid waste dumps. It is found in the Ladd Formation and also mined in the Alberhill district of Riverside county as well as many other locales, including El Toro and San Juan Capistrano in Orange county.

Gypsum and silica, two other building commodities, were historically mined in the Peninsular Ranges province. Gypsum, along with sand, gravel, and clay was once mined in Gypsum Canyon in Orange county, but those mines are long closed. The sand and gravel pits were the last to close and they closed in 2004. Plans are to use the site for a veteran's cemetery and as open space. Silica was also mined in both Riverside and Orange counties. The primary use was for glass making and again the silica sand mines are closed. In Orange county the silica mine was an open pit mine in Mission Viejo that closed in the 1990s and is now an industrial-business complex. In Riverside county the silica was once mined in Temescal Canyon, Corona, and near Hemet.

Other Commodities – Still Mined or Once Mined

The other commodity still mined in the Peninsular Ranges province are gemstones (see Rocks of the Peninsular Ranges). Pala and the other pegmatite districts in northern San Diego county and southern Riverside county still have open mines, but they are mostly aimed at providing minerals for collectors and museums, and not engaged in any large-scale mining operations.

There are two other commodities that have been mined in the past – coal and salt. Low quality, lignite coal has been mined in Riverside county at Alberhill and in Orange county in Black Star Canyon in the late 1800s. These mines were relatively small operations and are long closed. Although the coal mine in Black Star Canyon was temporarily reopened during WWII. Salt was also mined by the Irvine Company for use in water softening systems in upper Newport Back Bay of Orange County from the 1930s until 1969. The Salt Works were closed because of extensive damage from the flood of 1969 (Figure 15.5.4).



Figure 15.5.4: The Salt Works in Newport Back Bay, Orange County California. "Salt Works, Upper Newport Bay" is courtesy of the Orange County Archives and is licensed under CC BY 2.0.

The history of resources in the Peninsular Ranges province, as in most of California, is one of change. In the popular accounts of American history, California began with a gold rush. Comparatively few people, however, profited from the 1849 Gold Rush. Far more extensive, and ultimately more useful, has been the mining of mineral commodities necessary to build the cities, towns, railroads, roads, freeways, and airports of today. Without these resources, it would be very difficult to accommodate the large population that now lives in southern California.

Query 15.5.1

This interactive element is not available in this format. Visit the link or scan the QR code to access it online.

View this Interactive Content online

References

1. Almanza, R. (2024, June 24). Anaheim Approves Orange County's First Veterans Cemetery in Gypsum Canyon. *The Department of California of the American Legion*. https://calegion.org/anaheim-approves-orange-countys-first-veterans-cemetery-in-gypsum-canyon/
2. Brigandi, P. (2019). The Silverado Mining Boom of 1878. OC Historyland. https://www.ochistoryland.com/silverado
3. Clinkenbeard, J. P., & Gius, F. W. (2018). CGS Map Sheet 52: *Aggregate Sustainability in California*. California Geological Survey.
4. Currier, L. W. (1960). USGS Bulletin 1109: *Geologic Appraisal of Dimension-Stone Deposits*. U.S. Geological Survey.
5. Daviess, S. N., & Bramlette, M. N. (1953). USGS Open-File Report: *The Alberhill and other clay deposits of Temescal Canyon, Riverside County, California*. U.S. Geological Survey. https://doi.org/10.3133/ofr5352
6. Ferrell, D. (2002, May 9). Mountain Shifts Slowly From Stone to Cement. *LA Times*. https://www.latimes.com/archives/la-xpm-2002-may-09-surround-09-story.html
7. Gale, H. S. (1934). Geology of Huntington Beach Oil Field, California. *Bulletin of the American Association of Petroleum Geologists* 18(3) 327-343.
8. Jacobi, L., & Martin, S. (2009, March), Water Usage in Orange County: 2007-2008. *Orange County Profiles*. 14 (1) 1-4. CSUF Center for Demographic Research. https://www.fullerton.edu/cdr/_resources/pdf/profiles/profilesv14n1.pdf
9. Marquis, G. D. (2023). *California Non-Fuel Mineral production 2020*. California Geological Survey.
10. Metropolitan Water District of Southern California. (2024, April). Safeguarding Southern California's Water Reliability. Fact

Sheet: *Diamond Valley Lake_ A Reservoir of Resilience*. Metropolitan Water District of Southern California. https://www.mwdh2o.com/media/2iloidmg/2024_dvl-fact-sheet_final-for-web.pdf
11. Metropolitan Water District of Southern California. (n.d.). *How We Get Out Water: Infrastructure Serving Our Communities*. Metropolitan Water District of Southern California. https://www.mwdh2o.com/your-water/how-we-get-our-water/
12. Miller, R. V., Shumway, D. O., & Hill, R. L. (1991). CDMG Special Report 165: *Mineral land Classification of the Temescal Valley Area, Riverside County, California*. California Division of Mines and Geology. https://www.conservation.ca.gov/cgs/Documents/Publications/Special-Reports/SR_165-MLC-Report.pdf
13. Mindat.org (n.d.). *Blue Light Mine, Silvarado, Orange County, California, USA*. [Data set]. https://www.mindat.org/loc-28559.html
14. Mindat.org (n.d.). *Julian Mining District, San Diego County, California, USA*. [Data set]. https://www.mindat.org/loc-3558.html
15. Mindat.org (n.d.). *Pinacate Mining District, Riverside County, California, USA*. [Data set]. https://www.mindat.org/loc-295044.html
16. Mindat.org (n.d.). *Temescal Valley, Riverside County, California, USA*. [Data set]. https://www.mindat.org/loc-293875.html
17. Mount, J., Hanak, E. & Peterson, C. (2023, April). Fact Sheet: *Water Use in California*. Public Policy Institute of California. https://www.ppic.org/publication/water-use-in-california/
18. Municipal Water District of Orange County. (2023, July). *Water Reliability Study*. Municipal Water District of Orange County. https://www.mwdoc.com/wp-content/uploads/2023/08/MWDOC_2023-OC-Water-Reliability-Study-Final.pdf
19. Naishadham, S. (2022, May 29) How San Diego secured its water supply, at a cost. *Associated Press*. https://apnews.com/article/california-droughts-environment-san-diego-81ab84fafe94a0c5c298ede24fd2f7f1#
20. Odell, A., Bower, S., Funk, A., & Cleveland, L. (2021, December). Final Report: *San Diego Basin Study*. Bureau of Reclamation and the City of San Diego Public Utilities Department. https://www.sandiego.gov/sites/default/files/2023-11/Copy%20of%20SDBS%20Final%20Report%20Dec%202021%20%28April%202022%29.pdf
21. Perazzo, P. B., & Perazzo, G. P. (2024). *San Diego County Stone Industry*. Stone Quarries and Beyond. https://quarriesandbeyond.org/states/ca/quarry_photo/ca-san_diego_indus_2.html
22. Robbins, J. (2019, June 11) As Water Scarcity Increases, Desalination Plants Are on the Rise. *Yale Environment 360*. Yale School of the Environment https://e360.yale.edu/features/as-water-scarcity-increases-desalination-plants-are-on-the-rise
23. Silva, A. (2000, March 19). Diamond Valley Lake Reservoir Dedicated Project Doubles Region's Storage Capacity. *Los Angeles Daily News* https://web.archive.org/web/20140113195844/http://www.thefreelibrary.com/DIAMOND+VALLEY+LAKE+RESERVOIR+DEDICATED+PROJECT+DOUBLES+REGION%27S...-a083421758
24. Todd, V. R. (2015). USGS Open-File Report 94-16: *Geologic map of the Julian 7.5" quadrangle, San Diego County, California*. U.S. Geological Survey. https://doi.org/10.3133/ofr9416
25. Water Systems Consulting, Inc. (2021, July 1). *City of Riverside 2020 Urban Water Management Plan*. City of Riverside Public Utilities. https://riversideca.gov/utilities/sites/riversideca.gov.utilities/files/pdf/residents/RPU%20Final%202020%20UWMP%20%282%29.pdf
26. Weber, F. H. Jr., (1963). CDMG County Report 3: *Geology and Mineral Resources of San Diego County, California*. California Division of Mines and Geology.
27. Whittle, S. (Ed.). (2022, February 2). The Salt Works. *The Historical Marker Database*. https://www.hmdb.org/m.asp?m=148658
28. Williams, J. (n.d.). *Dimension Stone Statistics and Information*. National Minerals Information. U.S. Geological Survey. https://www.usgs.gov/centers/national-minerals-information-center/dimension-stone-statistics-and-information

References for Box 15.5.1: Oil and Gas in the Peninsular Ranges Province

1. Gautier, D. L., Tennyson, M. E., Cook, T. A., Charpentier, R. R., & Klett, T. R. (2013, February). *Remaining Recoverable Petroleum in Ten Giant Oil Fields of the Los Angeles Basin, Southern California*. U.S. Geological Survey Fact Sheet 2012-3120. https://pubs.usgs.gov/fs/2012/3120/fs2012-3120.pdf
2. Higgins, D. G. (City Historian). (1976). *Oil Fields – A Brief History of the Oil Fields at Huntington Beach, California*. City of Huntington Beach Public Library. https://cms3.revize.com/revize/huntingtonbeachca/Documents/Departments/Library/Contact%20Us%20About/Historical%20Files/Historical%20Files%20Oil/070920-6.pdf
3. Pepper, A. (1991, January 24). City's first oil well to be preserved. *Orange County Register*. https://cms3.revize.com/revize/huntingtonbeachca/Documents/Departments/Library/Contact%20Us%20About/Historical%20Files/Historical%20Files%20Oil/090518-22.pdf
4. Testa, S. M. (2007). History of Oil Along the Newport-Inglewood Structural Zone – Los Angeles County, California. *Oil-Industry History* 8(1) 9-35. Petroleum History Institute. https://aegsc.org/chapters/inlandempire/pdf/Oil-Industry%20History%20Volume%208%20Nov%201%202007.pdf
5. Yerkes, R. F., McCulloh, T. H., Schoellhamer, J. E., & Vedder, J. G. (1965). USGS Professional Paper 420-A: *Geology of the Los Angeles Basin, California – an Introduction*. U.S. Geological Survey.

This page titled 15.5: Natural Resources of the Peninsular Ranges is shared under a CC BY-NC 4.0 license and was authored, remixed, and/or curated by Debra Brooks.

15.6: Chapter Summary

15.1 Geomorphology of the Peninsular Ranges

- The Peninsular Ranges extend from southern California into Mexico and in Mexico form the spine of the Baja California Peninsula.
- The Peninsular Ranges are the remains of part of the batholith that was beneath the volcanic arc that dominated the geology of western North America during the Mesozoic.
- The uplift and subsequent erosion of the Mesozoic volcanic arc exposed the batholith and created monadnocks, some of which are large enough to be small mountain ranges.
- The Peninsular Ranges form a drainage divide and create the rain shadow effect for the Colorado Desert province.
- The eastern two of the three major fault zones within the Peninsular Ranges are considered part of the larger San Andreas fault system, even though the San Andreas fault zone is outside the Peninsular Ranges province.
- All of the major fault zones within the Peninsular Ranges are right-lateral strike-slip fault zones and align with the orientation of the San Andreas fault zone.
- The coastal plain is an erosional coast dominated by marine terraces.
- Estuaries and lagoons are common along the coast, as well as mass wasting.

15.2 Tectonics and Geologic History of the Peninsular Ranges

- Before or during the early Paleozoic what will become California is offshore of a passive margin.
- During the Permian-Triassic subduction begins offshore of the passive margin and an island arc forms as a batholith is created below.
- During the early Cretaceous another island arc accretes to form the Cuyamaca-Laguna Mountain shear zone, part of the boundary between the western and eastern batholiths of today. Pluton formation and volcanism are in what is the western part of today's batholith.
- Near the end of the early Cretaceous, at about 105 million years ago, the angle of subduction became shallower and pluton formation and volcanism moves further from the trench and from what is now the western part of today's batholith to the eastern part.
- During the late Cretaceous, at about 85 million years ago, the angle of subduction changes again and becomes even more shallow; pluton formation and volcanism move even further from the trench and completely out of the Peninsular Ranges province. Subduction continues offshore, but in the Peninsular Ranges there is no volcanism, uplift slows and erosion becomes the dominant surface process.
- During the Paleogene, 30-25 million years ago, the plate boundary changes from subduction to transform as part of the mid-ocean ridge system reaches the subduction zone.
- During the early Neogene, 20 million years ago, extension begins. East of the Peninsular Ranges the Salton Trough develops; west of the Peninsular ranges in the California borderlands, a valley and ridge topography forms. The coastal areas now have sediment sources from both the Peninsular Ranges to the east and the borderlands to the west.
- During the late Neogene, about 7 to 5 million years ago, the extension to the east in the Salton Trough develops into a divergent plate boundary and the Gulf of California opens. The plate boundary is transferred and the Peninsular Ranges are now part of the Pacific plate.
- During the early Pleistocene, approximately 2 million years ago, the transform part of the plate boundary jumps to the San Andreas fault zone.

15.3 Rocks of the Peninsular Ranges

- Most of the rock in the Peninsular Ranges formed as plutonic igneous rock in a large Mesozoic batholith. The igneous rock of the Peninsular Ranges batholith includes all three major types of plutonic igneous rock – felsic (granitic), intermediate (dioritic), and mafic (gabbroic); with the most common rock being tonalite, a felsic rock related to granite.
- The oldest rock in the Peninsular Ranges province is the metamorphic rock of the roof pendants above the batholith.
- The Peninsular Ranges batholith is divided into a western and an eastern part based upon changes in chemistry, mineralogy, and geophysical properties of the rock. The rocks of the western batholith are older and more varied than are the rocks of the eastern batholith. The rocks in the eastern batholith are also more likely to be felsic.

- The rocks in the eastern Peninsular Ranges batholith are similar to the rocks of the Sierra Nevada batholith in age, chemistry, and mineralogy.
- The Peninsular Ranges are famous for pegmatitic minerals and gemstones.
- The volcanoes of the Peninsular Ranges eroded away long ago and the volcanic rocks remaining are mostly basalts and andesites on the western slopes of the mountains and clasts in sedimentary rock of the coastal plain.
- Most of the sedimentary rock of the Peninsular Ranges is on the coastal plain. Before the Neogene, sediment sources were to the east in the mountains. During the Miocene, sediment also came from the north and the west.
- The distinctive Poway Group cobbles were used to help reconstruct the geography of the Paleogene in southern California.
- The sedimentary rock of the coastal plain records a long history of repeating cycles of the rise and fall of sea level.
- Dinosaur fossils have been found in the Cretaceous sedimentary rocks of the coastal plain.

15.4 Geologic Hazards of the Peninsular Ranges

- The major geologic hazard faced by the residents of the Peninsular Ranges province is a large earthquake on one the major fault zones within the province or on the San Andreas fault zone, just outside the province.
- The three major fault zones within the Peninsular Ranges province are the San Jacinto, the Elsinore, and the Newport-Inglewood-Rose Canyon fault zones. All of these fault zones have a history of moderate to large earthquakes in historic times.
- The Peninsular Ranges province has a history of major floods. After the flood of 1938, dams were built to help with both flood control and water storage.
- Saltwater intrusion of the coastal aquifers is a major challenge to having potable groundwater.
- Injection wells and fluid barriers are the most common method used to try and combat saltwater intrusion.
- Mass wasting is a common problem on the sea cliffs and bluffs of the marine terraces along the coast.
- Climate change will exacerbate the current geologic hazards in the Peninsular Ranges and probably make them occur more frequently as it also floods coastal areas.

15.5 Natural Resources of the Peninsular Ranges

- Potable water is a major resource that is lacking in the Peninsular Ranges province.
- Most of the potable water in the Peninsular Ranges is purchased and imported from either the Colorado River or the rivers of northern California and must be transported across the San Andreas fault zone.
- Efforts to help with the water challenges in the Peninsular Ranges include conservation, recycling, and desalination.
- While gold mining occurred and was successful in the Peninsular Ranges batholith in the past; the gold deposits were never as plentiful and as rich as in the Sierra Nevada batholith.
- Gemstone mining still occurs in the Peninsular Ranges.
- Most mining for precious metals ended in the Peninsular Ranges after WWII.
- Oil and gas production occurs in the northernmost part of the Peninsular Ranges province in the southern part of the Los Angeles basin.
- Most of what has been mined in the Peninsular Ranges and is still mined today are building commodities such as sand and gravel, limestone and marble, building stone, clay, and specialty sand.
- Previously both coal and salt have been mined in the Peninsular Ranges.

This page titled 15.6: Chapter Summary is shared under a CC BY-NC 4.0 license and was authored, remixed, and/or curated by Debra Brooks.

15.7: Detailed Figure and Video Descriptions

Figure 15.1.2 Location of the Peninsular Ranges province

The Peninsular Ranges province borders the Pacific Ocean. It is south of the Transverse Ranges province and North of Mexico, between the Pacific Ocean to the west and the Colorado Desert province to the east.

Figure 15.1.4 Mountain ranges and other geomorphic features of the Peninsular Ranges

Although the Elsinore and San Jacinto faults are not labeled in the figure, they are clearly visible in the topography as strikingly linear features that bound mountain ranges. West of the Elsinore fault are the Santa Ana Mountains, which are also the northernmost range, and the Laguna Mountains which are further south. The Elsinore-Temecula Valley and the Agua Tibia Mountains parallel the Elsinore fault. The Perris Plain sits between the two faults. The San Jacinto Mountains and the Santa Rosa Mountains, just to their southeast, are both east of the San Jacinto fault.

Figure 15.1.6 Simplified fault map of southernmost California

Simplified fault map of southern California which locates the San Andreas fault zone and the major fault zones in the Peninsular Ranges provinces. In order, moving west and away from the San Andreas fault zone, are the San Jacinto fault zone, the Elsinore fault zone and the Newport-Inglewood fault zone. The other labeled fault zones on the map are not part of the Peninsular Ranges and can be ignored for this discussion.

Figure 15.2.1 Possible reconstruction of the supercontinent of Rodinia

At 1.1 Ga or 1100 Ma, Rodinia is equatorial and what will become Madagascar, India, East Antarctica, Australia, South China, and Siberia are in the northern hemisphere. Laurentia and Baltica straddle the equator, with Rio Plato, Amazonia, and West Africa extending from them into the southern hemisphere. Congo-Sao Francisco and Kalahari are larger islands to the south and west of the main landmass.

Fold mountain belts related to building Rodinia, or remains from a pre-Rodinia supercontinent, connect Madagascar, India, and Australia to East Antarctica; and also connect Laurentia to Rio Plato and Amazonia. The island of Congo-Sao Francisco is segmented by another, and the island of Kalahari has one on its northern border.

There is no fold mountain belt connecting East Antarctica and Laurentia and they are starting to separat. The area between becomes the proto-Pacific ocean basin.

Figure 15.2.4 A sequence of maps showing the evolution of the plate boundary in California

This figure tries to capture 30 million years of tectonic history in southern California in a sequence of maps. The important relationships change with each successive map and therefore they are labeled by their timing expressed as millions of years ago, abbreviated as “Ma” on each map. What is important is how the tectonics change with time, and that is described in detail in the text.

To delineate the tectonic changes, the plates are labeled - Farallon, Juan de Fuca, Cocos, Pacific, and North American. There relative locations are described in the text. The types of plate boundaries are indicated by variations in line width, color, and the addition of “teeth” symbols and arrows as indicated in the legend. In the text, these are named and described without using the symbolism of the visual descriptors. Triple junctions, where three plates meet, are also indicated by symbols and labels and their motion - moving apart through time is tracked be descriptions in the text. To help connect each map with the geology of today,

some major cities and geomorphic features are labeled and notes attached. Most of these are nice additional labels, but are not relevant to the context in which the figure is used in this part of this chapter.

Figure 15.2.5 Formation of tilted fault blocks

This is a series of three block diagrams.

The uppermost block diagram, labeled A, is of the non-extended crust with dashed lines on the top of the block indicating where faulting will occur.

The middle block diagram, labeled B and titled “Developing normal faults with extensional basins”, shows the area under extension as indicated by the arrows pulling the block in opposite directions. The block has also become thinner and longer if you compare its current outline to its older outline as indicated by the dashed former block boundary. The top of the block is cut by normal faults that dip to the right (east) and also form tilted east-dipping fault blocks, like leaning dominos. The upper right or eastern side of each fault block is elevated to form a ridge, while the lower, left or western side is now at the bottom of a valley. Arrows within the block show ductile, lower crust is rising under the tilted fault blocks helping them uplift.

The lower block diagram, labeled C, is the same physical situation as in the B or middle block diagram, except that the extension and thinning of the crust has become more extreme and the tilt of the faults has increased while the dip of the faults has lessened. This block diagram is titled “Upper crust fault block rotation”, which can be seen because the dip of the faults is now less than it was in block diagram B. Or, if you consider the fault blocks as dominos, the dominos are now more tilted in block diagram C than they were in block diagram B.

Figure 15.3.2 Simplified geologic map of the Peninsular Ranges and the Transverse Ranges

This image is a geologic map of Southern California showing major fault zones, rock units, and crustal blocks, illustrating how fault systems segment the region and control the distribution of rock types and tectonic movement. Labels, patterns, and line styles convey information rather than color alone. Major labeled fault systems include:

- San Andreas Fault Zone, running diagonally across the map
- San Jacinto Fault Zone
- Elsinore Fault Zone
- Malibu Coast–Cucamonga Fault
- Pinto Mountain Fault
- Banning Fault

These faults are shown as lines, with some segments dashed to indicate inferred locations. Several crustal blocks are labeled, including:

- San Gabriel Block
- San Bernardino Block
- Little San Bernardino Block
- San Jacinto Block
- Perris Block
- Santa Ana Block

The city Los Angeles is marked near the coast, and the Pacific Ocean is labeled to the southwest. Rock types are shown using patterns and listed in the legend under “Explanation”:

- Quartz monzonite
- Granodiorite
- Quartz diorite
- Gabbro

A note in the legend states, “MAJOR FAULT: dashed where inferred.” A scale bar shows distances in both kilometers and miles. The arrangement of fault lines cuts across and separates the crustal blocks, while the patterned rock units are distributed unevenly

across these blocks.

This map shows how major fault systems divide Southern California into moving blocks and influence the distribution of igneous rock types, helping explain regional tectonics and seismic activity.

Figure 15.3.5 Satellite image of the western Peninsular Ranges and the coastal plane

This satellite view of Southern California, centered on the Los Angeles region, shows how coastlines, mountain ranges, and fault-controlled valleys reflect active tectonics and landscape evolution. Labels and landforms provide multiple ways to interpret the scene. The Pacific Ocean appears on the left as a deep blue area, with the coastline forming a smooth boundary. Along the coast are labeled urban areas, including Los Angeles, Long Beach, and Los Angeles Harbor.

Inland, the landscape transitions from densely developed, lighter-toned areas to more rugged, brown and tan terrain. Several mountain ranges are labeled, including the Santa Ana Mountains, San Jacinto Mountains, Palomar Mountains, and Laguna Mountains. A prominent linear feature labeled “Elsinore Fault” runs through the inland region, forming a long, narrow valley that aligns with the fault trace. This straight, elongated feature contrasts with the surrounding irregular terrain and reflects tectonic movement along the fault.

Scattered darker patches inland represent lakes or reservoirs, while variations in texture and elevation distinguish valleys from elevated terrain. The contrast between coastal plains, fault-aligned valleys, and uplifted mountain ranges shows how crustal movement shapes the region’s topography.

This image, by connecting satellite-observed landforms—coastlines, mountains, and linear valleys—to underlying fault systems, helps explain how tectonic processes shape the landscape of Southern California.

Figure 15.4.2

An aerial photo of the mouth of the Santa Ana River at the Pacific Ocean with Santa Catalina Island on the horizon. The main river channel is indicated on the photo with multiple levee breaks and flood waters rushing out. Also labeled are US Hwy 101 and major streets, all flooded.

Video 15.1.1

This video is a cartoon with no narrative. It’s a cross-section of a slope facing the ocean. Sea level falls and eventually stabilizes and becomes constant. The image pans in and sea level is at the bottom corner of the image. The wave action then cuts into and erodes the slope forming a wave-cut platform. Sea level rises again, and the wave-cut platform is submerged. Sea level stabilizes and the waves erode a new wave-cut platform on the slope above the submerged one.

The image pans in again and the first or lower, submerged wave-cut platform is no longer in the image. The second wave-cut platform is now at the top of the image, not submerged and has become a marine terrace. The land now starts to rise, and sea level now appears to fall until it is no longer visible. The land continues to uplift.

Sea level now rises again, but the land continues to rise also, so sea level does not submerge the marine terrace; instead, the waves start to erode another wave-cut platform below the marine terrace. The land continues to rise, and sea level appears to fall. The second wave-cut platform becomes a second marine terrace, below the upper one. The land continues to rise and eventually sea level also rises to a point below the lower marine terrace and the waves start to erode yet another wave-cut platform. The land continues to rise, and sea level falls again. There are now three marine terraces on the slope in the image, looking like a series of stair steps on the slope.

The land stops rising, and development occurs on the three marine terraces. They are covered with buildings and trees. Sea level now rises again to a level below the bottom of the third or lowest marine terrace. The waves begin to erode a new wave-cut platform, but they also undercut the slope of the lowest marine terrace, and a landslide occurs. The buildings at the edge of the slope are destroyed as they fall onto the wave-cut platform below.

Video 15.1.2

This video is of a drone flight at Corona Del Mar State Beach. There is no narration, but music plays throughout the flight.

The drone approaches the coast from the sea and heads toward sea stacks supporting an arch. It dives into and through the arch and over a wave-cut platform towards the cliff face of a marine terrace heading straight for the drone operator. The cliff face is approximately four to five times the height of the drone operator.

It banks to the right and another arch along the cliff face comes into view and the drone dives and heads through it, coming out the other side to fly parallel to the coast over more wave-cut platforms towards a large sea stack.

As the sea stack approaches, the drone rises and flies over it and turns right towards the coast and makes a U-turn and flies back parallel to the coast over the wave-cut platforms again then banks left towards the original sea stack and arch and flies back through it in the opposite direction, heading out to sea.

It then banks again as it rises up and the immediate coastline is revealed to be a series of small pocket beaches with wave-cut platforms and tidepools off each headland separating the small beaches. The drone then dives and for the third time travels through the sea arch, but this time, it banks to the left rather than the right.

It heads across the wave-cut platform and continues to bank left out to sea making another U-turn. As if flies past the sea stack, a flock of sea birds are visible perched on the seaward side of the sea stack.

It circles around and once again flies through the arch. It then banks left as it approaches the cliff face of the marine terrace and again flies past the sea stack with the perching sea birds and then flies around and through the arch a fifth and last time.

Video 15.3.2

During the Jurassic, subduction of the Farallon plate was occurring off the coast of the North American plate and volcanoes formed in what is now Sonora, Mexico.

By the Eocene, the volcanoes had eroded, and their sediment was being transported by rivers and streams to the Pacific Ocean and was washed out to sea and deposited in a submarine fan.

In the late Cenozoic, the plate boundary in southern California transitions from a subduction zone to a transform fault boundary and northward movement on strike-slip faulting begins. An area being moved by the fault northwards starts to slowly rotate clockwise and it includes the lower part of the submarine fan deposits of the Poway Group Cobbles. Movement on the strike-slip faults also displaces the upper part of the submarine fan deposits and the river and stream channels to the northwest.

The upper part of the submarine fan and river and stream channels will end up in today's San Diego county as part of the Poway Group. The lower part of the submarine fan becomes part of the Transverse Ranges province as it is moved northwest and rotated into its current position.

The submarine fan deposits are found today as outcrops in the northern Channel Islands.

Video 15.4.1

The video begins with a fault map/fault model of the state of California. Faults are represented in three dimensions as planes dangling down into the Earth. Suddenly, the locations of scattered cities also appear on the map and the video zooms in to display the local area of the Newport-Inglewood fault. The fault segment that is going to break is highlighted in yellow on Earth's surface and the other faults in the area are represented by white mesh planes. The surrounding local faults then disappear from the map while the Newport-Inglewood fault remains. The major freeways are now added to the map.

Suddenly the world changes perspective and tips up on end so that the view is a cross-section into the Earth with the Newport-Inglewood fault highlighted as a yellow mesh plane extending down. The picture then rotates 180° displaying the fault plane in three-dimensions. The model then dips and swings back to map-view. As it swings to map view, color starts to appear on the surface representing the damage done by the imaginary earthquake. The map comes to a stop, and a colored legend for damage according to the Mercalli Intensity scale is displayed. The scale ranges through, weak, light, moderate, strong, very strong, and

finally severe. The terms weak, strong and severe are shown on the scale, others are implied by the color transitions.

Damage is as follows: An oval shaped 'bull's eye" has appeared with severe shaking at the center, gradationally changing to weak shaking with distance from the fault. Damage is only indicated on land, areas underwater are not color coded for damage.

Areas of severe shaking surround the fault and extend across greater metropolitan Los Angeles from the Santa Monica Mountains south to the Los Angeles-Orange county line and from the coast inland to I-5.

Very strong shaking surrounds the severe shaking, starting at the coast near Malibu, up and across the Santa Monica Mountains, to the Santa Susanna Mountains, the San Fernando Valley, over the Verdugo Hills, around through Pasadena, the western Chino hills and northern Santa Ana Mountains, down and across the Santa Ana River plain including the cities of Santa Ana and Anaheim, to the north of the San Joaquin Hills on the coast near Newport Beach.

Strong shaking extends from Malibu to Point Dume and swings up through the Santa Monica Mountains and the Westlake Village area to the Susana Mountains, the Simi Valley and the Santa Clarita Valley. Then down the western San Gabriel Mountains over as far as Sierra Madre and down past the eastern Chino Hills near Prado Dam, into the northern Santa Ana Mountains again and down including Irvine and the San Joaquin Hills and offshore near Laguna Beach.

Light to moderate shaking extends over past Oxnard to near Ventura, up and around and through the Santa Susana Mountains, over the northwestern San Gabriel Mountains towards Lancaster in the High Desert and down through the San Gabriel Mountains to Rancho Cucamonga and south along the I-15 and into the Santa Ana Mountains just west of Corona-east of Riverside, south through the mountains to come out near the coast south of San Clemente near the San Diego county line. Santa Catalina island is also colored for light to moderate shaking.

Weak shaking covers the rest of the image, west towards Santa Barbara, north into the High Desert, east toward San Bernardino, and South towards San Diego. All of these cities are just off the image.

Then the numbers appear for total fatalities, injuries, and damage.

If the earthquake occurred at 2 am local time, fatalities and injuries estimated at 9,589, concentrated in the area of severe shaking.

If the earthquake occurred at 2 pm local time, fatalities and injuries estimated at 15,430, concentrated in the areas of severe to very strong shaking.

If the earthquake occurred at 5 pm local time, fatalities and injuries estimated at 12,158, concentrated in the areas of severe, very strong, or strong shaking to the south.

Damage is estimated at $44.2 billion and includes the entire greater Los Angeles-Orange county metropolitan area as far west as Ventura, north to the Santa Clarita Valley, east to Corona, and south to Laguna Beach.

Video 15.4.2

The video begins with a fault map/fault model of the state of California. Faults are represented in three dimensions as planes dangling down into the Earth. Suddenly, the locations of scattered cities also appear on the map and the video zooms in to display the local area of the San Joaquin fault. The fault segment that is going to break is highlighted in yellow on Earth's surface and the other faults in the area are represented by white mesh planes. The surrounding local faults then disappear from the map while the San Joaquin fault remains. The major freeways are now added to the map.

Suddenly the world changes perspective and tips up on end so that the view is a cross-section into the Earth with the San Joaquin fault highlighted as a yellow mesh plane extending down. The picture then rotates 180° displaying the fault plane in three-dimensions. The model then dips and swings back to map-view. As it swings to map view, color starts to appear on the surface representing the damage done by the imaginary earthquake. The map comes to a stop, and a colored legend for damage according to the Mercalli Intensity scale is displayed. The scale ranges through, weak, light, moderate, strong, very strong, and finally severe. The terms weak, strong and severe are shown on the scale, others are implied by the color transitions.

Damage is as follows: An oval shaped 'bull's eye" has appeared with severe shaking at the center, gradationally changing to weak shaking with distance from the fault. Damage is only indicated on land, areas underwater are not color coded for damage.

Areas of severe shaking surround the fault and extend up the coast to approximately the Bolsa Chica State Beach, inland to Santa Ana and extend to the foothills of the Santa Ana Mountains. Then continue south along the mountain front to Rancho Santa Margarita, and around and to the coast at San Clemente.

Very strong shaking surrounds the severe shaking, starting at the coast near Seal Beach, inland to Norwalk, then Brea, curves through Chino Hills State Park, south along the spine of the Santa Ana Mountains, and to the coast near Camp Pendleton.

Strong shaking extends from the coast near the Ocean Trails Reserve on the Palos Verde Peninsula, to downtown Los Angeles, along the I-10 eastward to the I-15 in Rancho Cucamonga, curves south, east of Norco, and down through Lake Elsinore. It continues south along the I-15 corridor to Murrieta, and then south to Oceanside. The eastern half of Santa Catalina Island also experiences strong shaking.

Light to moderate shaking extends inland from the coast at Santa Monica and north across the Santa Monica Mountains into the San Fernando Valley, curves over the Verdugo Hills and along the mountain front of the San Gabriel Mountains past Cajon Pass and the City of San Bernardino to Beaumont. From there light to moderate shaking continues south along the San Jacinto Mountain foothills to Warner Springs, and then down to just north of San Diego.

Weak shaking covers the rest of the image; therefore it extends beyond Thousand Oaks, north into the High Desert Region, beyond Palm Springs, and south of the US-Mexican border, and all of these areas are just off the image.

Then the numbers appear for total fatalities, injuries, and damage.

If the earthquake occurred at 2 am local time, fatalities and injuries estimated at 4,104 concentrated in the innermost area of severe shaking.

If the earthquake occurred at 2 pm local time, fatalities and injuries estimated at 8,008, concentrated in the area of severe shaking.

If the earthquake occurred at 5 pm local time, fatalities and injuries estimated at 6,057, concentrated in the areas of severe, very strong, to strong shaking.

Damage is estimated at $24.1 billion and includes all of Orange county and north and east into Los Angeles and Riverside counties.

Video 15.4.3

The video begins with a fault map/fault model of the state of California. Faults are represented in three dimensions as planes dangling down into the Earth. Suddenly, the locations of scattered cities also appear on the map and the video zooms in to display the local area of the Palos Verde fault offshore between Santa Catalina Island and Orange county, paralleling the Newport-Inglewood fault. The fault segment that is going to break is highlighted in yellow on Earth's surface and the other faults in the area are represented by white mesh planes. The surrounding local faults then disappear from the map while the Palo Verde fault remains. The major freeways are now added to the map.

Suddenly the world changes perspective and tips up on end so that the view is a cross-section into the Earth with the Palos Verde fault highlighted as a yellow mesh plane extending down. The picture then rotates 180° displaying the fault plane in three-dimensions. The model then dips and swings back to map-view. As it swings to map view, color starts to appear on the surface representing the damage done by the imaginary earthquake. The map comes to a stop, and a colored legend for damage according to the Mercalli Intensity scale is displayed. The scale ranges through, weak, light, moderate, strong, very strong, and finally severe. The terms weak, strong and severe are shown on the scale, others are implied by the color transitions.

Damage is as follows: The Palos Verdes fault is offshore and a line of severe shaking has appeared along the coast, gradationally changing to weak shaking with distance from the coast. Damage is only indicated on land, areas underwater are not color coded for damage.

A line of severe shaking appears along the coast from Seal Beach to Newport Beach.

Very strong shaking surrounds the severe shaking, starting at the coast near Long Beach, extending up and over towards Compton, curving eastwards across I-5 to Brea, down to Anaheim and over to the mountain front of the Santa Ana Mountains. It extends past Irvine and then down to Laguna Beach. Very strong shaking is also experienced in the area around Avalon on Santa Catalina

Island.

Strong shaking extends inward from the coast near LAX, curving around and up the image to downtown Los Angeles, across and around to Whittier, down to Brea and into Anaheim Hills. Then south along the mount front of the Santa Ana Mountains to Trabuco Canyon, along the spine of the Santa Ana Mountains, curving south and offshore south of Oceanside. Most of the rest of San Catalina Island also experiences strong shaking.

Light to moderate shaking extends inland north of Santa Monica and over the Santa Monica Mountains into the San Fernando Valley and north off the image. It reappears on the image in the San Gabriel Mountains past the Verdugo Hills and then along the San Gabriel Mountain from almost to Rancho Cucamonga. It then follows the I-15 corridor south and off the image.

Weak shaking covers the rest of the image, west and north from Malibu, and east of the I-15 corridor.

Then the numbers appear for total fatalities, injuries, and damage.

If the earthquake occurred at 2 am local time, fatalities and injuries estimated at 367, concentrated in the severe shaking area, right on the coast.

If the earthquake occurred at 2 pm local time, fatalities and injuries estimated at 397, concentrated in the areas of severe to strong shaking closer to the coast.

If the earthquake occurred at 5 pm local time, fatalities and injuries estimated at 338, concentrated in the areas of severe to strong shaking closer to the coast.

Damage is estimated at $3.14 billion and includes the entire greater Los Angeles-Orange-San Diego county metropolitan area from Torrance and Compton in Los Angeles county south to Oceanside in San Diego county. Maximum damage is in Orange county from Seal Beach to Newport Beach.

Video 15.4.4

The video begins with a fault map/fault model of the state of California. Faults are represented in three dimensions as planes dangling down into the Earth. Suddenly, the locations of scattered cities also appear on the map and the video zooms in to display the local area of the Rose Canyon fault. The fault segment that is going to break is highlighted in yellow on Earth's surface and the other faults in the area are represented by white mesh planes. The surrounding local faults then disappear from the map while the Rose Canyon fault remains. The major freeways are now added to the map.

Suddenly the world changes perspective and tips up on end so that the view is a cross-section into the Earth with the Newport-Inglewood fault highlighted as a yellow mesh plane extending down. The picture then rotates 180° displaying the fault plane in three-dimensions. The model then dips and swings back to map-view. As it swings to map view, color starts to appear on the surface representing the damage done by the imaginary earthquake. The map comes to a stop, and a colored legend for damage according to the Mercalli Intensity scale is displayed. The scale ranges through, weak, light, moderate, strong, very strong, and finally severe. The terms weak, strong and severe are shown on the scale, others are implied by the color transitions.

Damage is as follows: An oval shaped 'bull's eye" has appeared with severe shaking at the center, gradationally changing to weak shaking with distance from the fault. Damage is only indicated on land, areas underwater are not color coded for damage.

Areas of severe shaking surround the fault and extend north to Encinitas and across to the I-15 corridor, then south just past the I-15 and I-8 corridor into Mexico.

Very strong shaking surrounds the severe shaking, starting at the coast near Oceanside, curving north and inland to Fallbrook, over towards Pala and then south into Mexico.

Strong shaking extends from north of Camp Pendleton, over to the spine of the mountains, south through Otay lake into Mexico.

Light to moderate shaking extends north and off the image and south on a line through Mt. Palomar and Alpine into Mexico.

Weak shaking covers the rest of the image east of a line through Borrego Springs and Campo.

Then the numbers appear for total fatalities, injuries, and damage.

If the earthquake occurred at 2 am local time, fatalities and injuries estimated at 366, concentrated in the area of severe shaking around Mission Bay and Imperial Beach.

If the earthquake occurred at 2 pm local time, fatalities and injuries estimated at 345, concentrated in the areas of severe shaking around Mission Bay, Old Town, and Kearny Mesa.

If the earthquake occurred at 5 pm local time, fatalities and injuries estimated at 308, concentrated in the areas of severe shaking around Mission Bay, Old Town, and Kearny Mesa.

Damage is estimated at $4.22 billion and includes the entire greater San Diego area south from Torrey Pines to the US-Mexican border and inland to eastern extent of the I-15 / I-805 corridor.

Video 15.4.5

The video begins with a fault map/fault model of the state of California. Faults are represented in three dimensions as planes dangling down into the Earth. Suddenly, the locations of scattered cities also appear on the map and the video zooms in to display the local area of the Elsinore fault. The fault segment that is going to break is highlighted in yellow on Earth's surface and the other faults in the area are represented by white mesh planes. The surrounding local faults then disappear from the map while the Elsinore fault remains. The major freeways are now added to the map.

Suddenly the world changes perspective and tips up on end so that the view is a cross-section into the Earth with the Elsinore fault highlighted as a yellow mesh plane extending down. The picture then rotates 180° displaying the fault plane in three-dimensions. The model then dips and swings back to map-view. As it swings to map view, color starts to appear on the surface representing the damage done by the imaginary earthquake. The map comes to a stop, and a colored legend for damage according to the Mercalli Intensity scale is displayed. The scale ranges through, weak, light, moderate, strong, very strong, and finally severe. The terms weak, strong and severe are shown on the scale, others are implied by the color transitions.

Damage is as follows: An oval shaped 'bull's eye" has appeared with severe shaking at the center, gradationally changing to weak shaking with distance from the fault. Damage is only indicated on land, areas underwater are not color coded for damage.

Areas of severe shaking surround the fault and extend from Corona towards Riverside curving down to Perris and over to Wildomar. Then across the Santa Ana Mountains to Mission Viejo, up the Santa Ana Mountain front through villa Park and Anaheim Hills over to Corona.

Very strong shaking surrounds the severe shaking, coming onshore near Huntington Beach, curving up to Montebello and over to near the I-10 and I-15 interchange, along the I-10 to Loma Linda, and then through the San Timoteo Badlands swings down and around to Murrieta, across the San Ana Mountains, and offshore near Dana Point.

Strong shaking comes onshore near Long Beach, then up to the downtown Los Angeles area, swings east along the San Gabriel Mountain front and into the mountains near Claremont. Over the mountains towards Wrightwood and then curves east toward Cajon Pass and along the San Bernardino Mountain front to Mentone. From there it is south to Anza and around to Palomar Mountain, and offshore near Oceanside.

Light to moderate shaking comes onshore near Santa Monica and north across the Santa Monica Mountains into the San Fernando Valley, across the San Gabriel Mountains to near Pear Blossom and the off the image. Light to moderate shaking then reappears on a line down through Lucerne, around to the San Jacinto Pass, and down the eastern mountain front of the San Jacinto Mountains into Mexico.

Weak shaking covers the rest of the image, west of Malibu and east of Palm Springs to Borrego Springs down into Mexico. Then the numbers appear for total fatalities, injuries, and damage.

If the earthquake occurred at 2 am local time, fatalities and injuries estimated at 236, concentrated in the area of severe shaking. If the earthquake occurred at 2 pm local time, fatalities and injuries estimated at 220, concentrated in the area of severe damage in the Santa Ana River Canyon or in the area of very strong shaking along the Santa Ana River southwest of Santa Ana. If the earthquake occurred at 5 pm local time, fatalities and injuries estimated at 1,207, concentrated in the area of severe shaking in the Santa Ana River Canyon or in the area of very strong shaking along the Santa Ana River southwest of Santa Ana.

Damage is estimated at $2.21 billion and includes the Corona-Norco-Riverside corridor along the I-15, the Santa Ana River Canyon, greater Santa Ana area and the Dana Point-San Clemente area.

This page titled 15.7: Detailed Figure and Video Descriptions is shared under a CC BY-NC 4.0 license and was authored, remixed, and/or curated by Debra Brooks.

16: CALIFORNIA COASTLINE

Introduction to California Coastlines

Think of the idea of California, and amid palm trees and movie stars and Yosemite, you probably will picture the iconic image of shirtless surfers plying Pacific waters. The coastline of California is fundamentally part of the California experience. Whether through surfing or sunbathing or walking, or enjoying one of the many dog-friendly off-leash areas, where sloppy-tongued hounds frolic in the sun and air of a mongrel beach, the coasts are part of what it means to live in California. About 80% of California residents live within an hour's drive of a beach.

And yet, few California residents appreciate the complex geologic processes that sculpt and create our rugged occidental boundary. Nor do many residents or visitors know the major hazard lurking just offshore–not sharks, which very rarely interact with the humans with whom they share the waters, but rip currents, which are fast movements of water that can quickly drag hapless beach swimmers far from shore. Rip currents cause the majority of beach rescues and contribute to an annual rate of 1.1 drowning deaths per 100,000 California residents.

With California's majestic Pacific sunsets, people yearn to own a home with an ocean-view, as close to the coastline as possible. However, many of these homes have simply been built too close to the shore, with little consideration for how quickly an eroding coast can retreat. El Niño Southern Oscillation (ENSO) warm events, known as El Niño, can collapse meters of shoreline in a single storm. Efforts to mitigate losses of homes by reinforcing shorelines with concrete, boulders, or other structures succeed primarily as vain demonstrations of hubris, often exacerbating the problem they attempt to solve. Climate change and rising ocean levels further contribute to the loss of shoreline; a 2023 USGS study estimated that by the year 2100, some areas of California will lose as much as 70% of the existing shoreline. Moreover, evidence suggests that climate change is creating ever larger waves along the California coast, contributing to accelerated erosion.

The California Constitution (Article 10, § 4) guarantees public access to beaches, and while many enjoy California's sandy beaches and the recreational opportunities, public access to the shoreline has eroded like shifting sands. A seemingly strong piece of legislation, the 1976 California Coastal Act is today routinely violated without serious consequence by those who carve out private areas on public beaches and prevent would-be beach visitors from accessing shorelines.

This chapter explores these connections between geologic processes, such as plate tectonics and erosion, with humans and our interactions with the vast interface of the California coast.



Figure 16.1: The endemic California surfer. "Surf's up" by Steven Newton is licensed under CC BY-NC 4.0. Access a detailed description.

Learning Objectives

At the end of this chapter, you should be able to:

- Describe the typical features and processes observed along the California coastline.
- Assess hazards associated with California's coastline, including rip currents, erosion, and tsunamis.
- Analyze how shoreline structures, such as breakwaters and seawalls, affect the coast.
- Know the legal issues affecting access to the coast, as part of the California Coastal Act of 1976, and frequent efforts to subvert and ignore this legislation.

16.1: Coastal Processes

16.2: California Coastline Anatomy

16.3: California Coastal Hazards

16.4: Human Alteration and Mitigation

16.5: Coastal Access

16.6: The Edge of California

16.7: Chapter Summary

16.8: Detailed Figure Descriptions

References

1. Shyong, F. (2021, July 9). The beach is there for all of us — We just have to get there. Los Angeles Times. https://www.latimes.com/california/story/2021-07-09/beach-restrictions-race
2. Centers for Disease Control (2023, June 12). Drowning Data. Retrieved October 3, 2023, from https://www.cdc.gov/drowning/data/index.html
3. Gammon, K. (2023, May 27). Up to 70% of California beaches could disappear by end of the century. The Guardian. https://www.theguardian.com/us-news/2023/may/27/california-beaches-erosion-2100-study
4. Rott, N. (2023, August 1). Surf's up! Wave heights increase on California's coast as the climate warms. Retrieved October 5, 2023, from https://www.npr.org/2023/08/01/1191216362/surfs-up-wave-heights-increase-on-californias-coasts-as-climate-warms

This page titled 16: California Coastline is shared under a CC BY-NC 4.0 license and was authored, remixed, and/or curated by Steven Newton.

16.1: Coastal Processes

Changing Shores

The first thing to understand about shoreline processes is that the coastlines move. Not only the water, but also the sand and rock fragments as they are carried along the shoreline; not only the wind, but also the California cliffs themselves, pushed upward out of the cold sea by tectonic motion and uncountable earthquakes. In an emergent shoreline, the land is pushed up faster than it can be brought down by the erosive force of crashing waves. Although not every part of the coast is rising at the same rate, overall California's emergent shorelines put bare rock directly into waves, with pockets of sand in between, which is a very different situation than the beaches elsewhere in the country, such as the sandy arc of the Gulf of Mexico and the long barrier islands along the East Coast.

How fast is the coast rising? Estimates for the San Diego region for the last million years put the rate at 14 cm/1000 years, with an acceleration in the last 80 ka to 30 cm/1000 years, with one area as much as 45 cm/1000 years. Other areas of the state experience different rates. Because of this tectonic uplift, California's coast is raw and rocky (Figure 16.1.1).



Figure 16.1.1: Dynamic, uplifting, highly-eroded, rocky California coastline, north of Bodega, CA. Note Aspen the dog for scale. "Beach" by Steven Newton is licensed under CC BY-NC 4.0. Access a detailed description.

Query 16.1.1

This interactive element is not available in this format. Visit the link or scan the QR code to access it online.

View this Interactive Content online

Ocean Waves

Waves are a powerful erosive force that incessantly attacks coastlines. The time period between waves is called the wave period. The wave period is measured in seconds, and varies depending on the source of the waves, but is usually within the range of 6 to 16 seconds. If we take as an example a period of one wave every 10 seconds, then a coastline is hit with 6 waves every minute, every day 8,640 waves, and every year 3 million waves. That is an immense, repeated force applied to rocks facing the ocean

(see Figure 16.1.2). The fact that rocky shorelines exist in California at all is a testament to the geologic speed of tectonic uplift relative to the speed of erosion.



Figure 16.1.2: Energetic waves pummeling a rocky coast, Point Lobos, CA. "Waves" by Steven Newton is licensed under CC BY-NC 4.0. Access a detailed description.

Almost all waves are generated by wind, though not in the way most people assume. Wind does not push waves along; rather, the laminar flow of wind over a slightly curved surface creates areas of low pressure (see Figure 16.1.3). Ocean waves form when low pressure areas lift the ocean upward by the pressure differential, in the same way a curved airplane wing experiencing a fast laminar flow of air creates the lift that allows airplanes to fly. This lifting effect is also what drives sailboats forward, their curved sails creating the lower pressure in front of them that pulls sailboats forward nearly 45° into the direction of the wind.

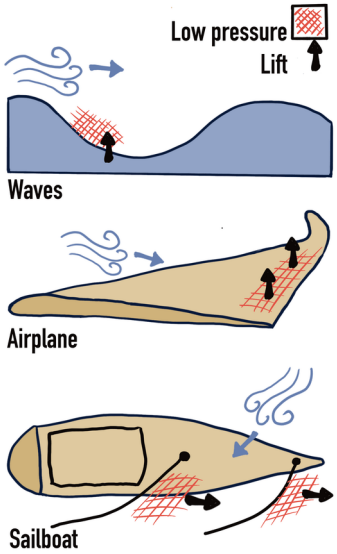


Figure 16.1.3: The phenomenon of lift illustrated in three circumstances: ocean waves, an airplane wing allowing a plane to fly, a sailboat. "Phenomenon of lift" by Steven Newton is licensed under CC BY-NC 4.0. Access a detailed description.

Wind-created waves can form far offshore, in storms across oceans, producing ocean swells that rapidly approach coastlines. But once these waves reach shallow water, something strange begins to happen: In the deep ocean, waves are relatively fast and flat. As they approach coasts, they slow down and rise up (see Figure 16.1.4). This happens because in shallow water the wave base, or the bottom of the wave where the wave energy dissipates, begins to interact with the ocean floor creating drag; the term of art is that waves “feel bottom.”

The point at which waves feel bottom is when the water depth decreases to one half of the wavelength of the wave. The wavelength is the distance between two wave crests. If, for example, waves just offshore were 100 meters apart, then one half of this wavelength would be 50 meters. When such incoming waves reach a depth of 50 meters, the waves begin to change.

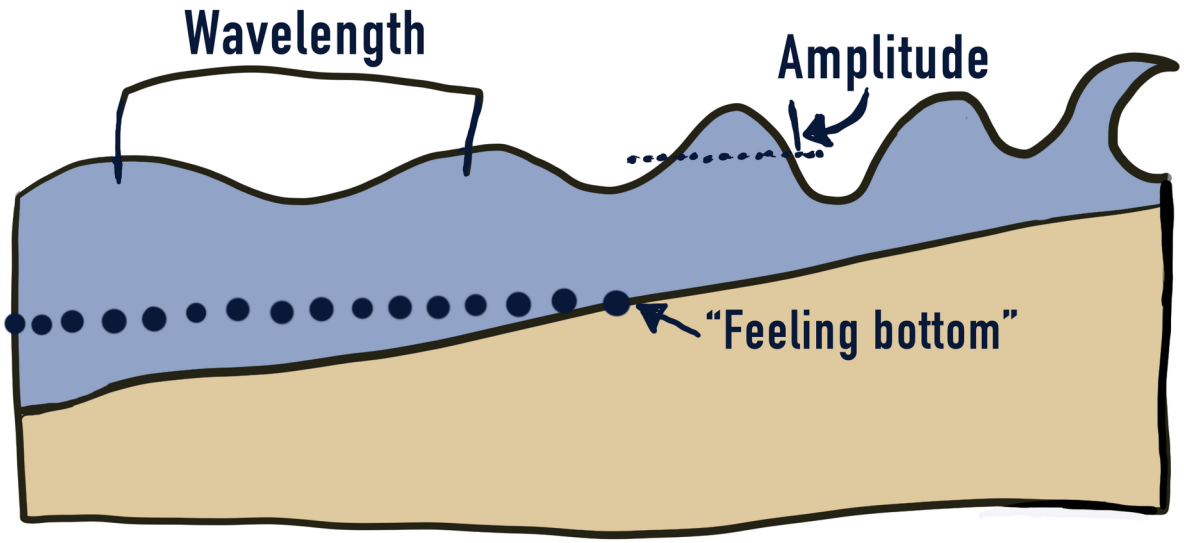


Figure 16.1.4: Wavelength, amplitude, and the phenomenon of "feeling bottom." "Wavelength and amplitude" by Steven Newton is licensed under CC BY-NC 4.0. Access a detailed description.

One change is that the wavelength decreases. The wave velocity also slows. The height of the wave, also called the amplitude, rises up. And when we reach the critical depth of just 1/7th of the original wavelength, the wave crests and spills over in the familiar breakers that beach visitors see and that surfers seek out.

Next time you're at the beach, look far out to sea. You'll see mild swells, pulses of water coming in fast. Then as they near the shore, you'll see distinct waves, slower than they initially were, start to rise up.

Incoming waves rarely approach the shoreline at exactly 90°, but rather approach it at some smaller angle. As waves approach the coast and begin to feel bottom, the edge of the wave closest to shore, which is in the shallowest water, slows down. The line of the wave warps. As a consequence of this warping, the angle of wave approach crashes into beaches diagonally, thrusting masses of water up onto the sand and rock (called the swash), whereupon this water recedes back into the sea (called the backwash). The motion creates a kind of zig-zag, with waves pushing up, and retreating waters pulling back.

This zig-zag results in water moving parallel along the coast, a phenomenon termed longshore current (see Figure 16.1.5). The longshore current sets sediment in motion, and the movement of sediment by a longshore current is termed longshore drift (sometimes also called littoral drift). Both the longshore current and the longshore drift tend to move parallel to the beach.

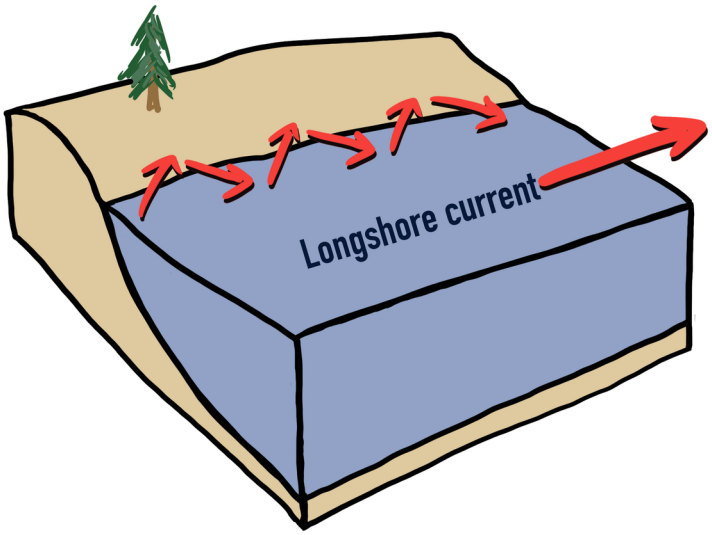


Figure 16.1.5: Longshore current moving parallel to the coastline. "Longshore current" by Steven Newton is licensed under CC BY-NC 4.0. Access a detailed description.

But what if the shoreline is not a straight line? What if some part of the shore juts out away from the rest of the coast, a promontory that meets the incoming waves first?

In such instances, the waves warp around the promontory. A headland, which is the proper name for a promontory, meets the waves before the normal coastline, and hence the waves slow down around the headland. The waves bend. This phenomenon is called wave refraction (see Figure 16.1.6).

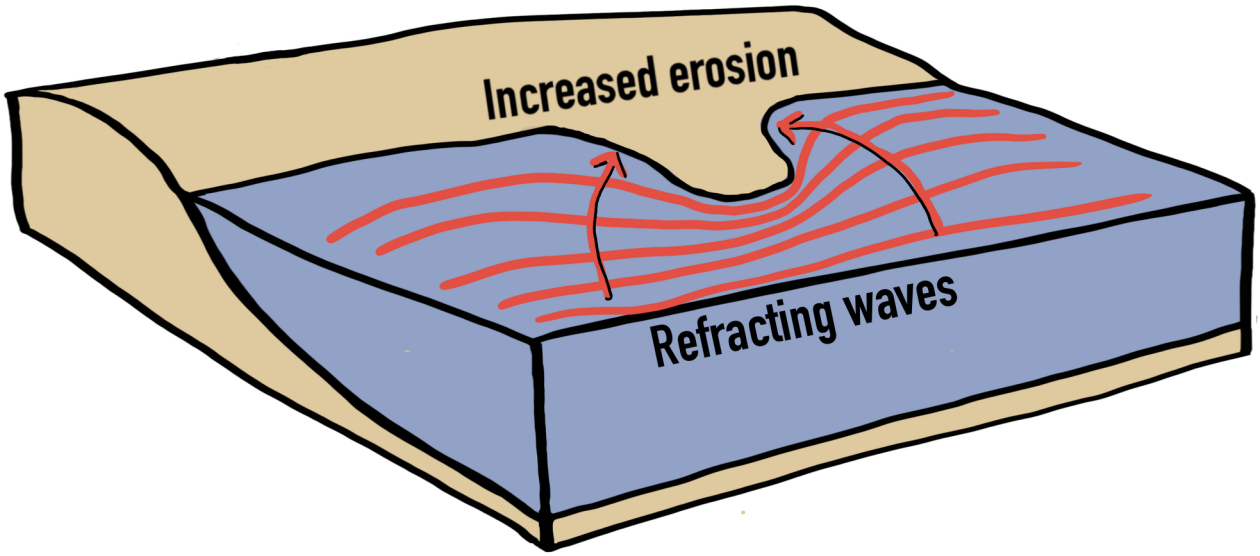


Figure 16.1.6: A headland causing wave refraction, with the waves warping around the headland and increasing erosion along the headland sides. "Diagram of Headland and Wave Refraction" by Steven Newton is licensed under CC-BY-NC 4.0. Access a detailed description.

Wave refraction changes where waves focus their erosive energy; the waves concentrate on the sides of headlands. The sides of a headland therefore erode faster than other areas, such as beaches, or even the tip of the headland. This means that the headland will, in time, be cut off from the shore.

Wave refraction accounts for many of the shoreline features–bays, headland, arches, sea stacks–on display all along the California coast. It is no exaggeration to say that the major reason our California coast looks the way it does is because of the phenomenon

of wave refraction.

Query 16.1.2

This interactive element is not available in this format. Visit the link or scan the QR code to access it online.

View this Interactive Content online

Larger Forces Influencing Waves

Another major process along California coasts is less visible. As winds kick up waves, as waves move water, all of these movements are affected by the rotation of the Earth. From the perspective of looking from space at the north pole, Earth rotates in a counter-clockwise fashion. This rotation means that winds and water flows are not moving on a stable platform, but rather on a shifting base. A good analogy would be trying to walk a straight line on a merry-go-round; no matter how one tries, one's straight path would appear curved because the merry-go-round itself is rotating.

This curving is called the Coriolis effect. Wind seems to be blowing in a straight line, directly from areas of high pressure to areas of low pressure. But in fact the wind bends because of the Coriolis effect, which is a result of the rotation of the Earth.

For the purposes of this book, we do not need to go into this somewhat confusing phenomenon further than to say that in the Northern Hemisphere, the Coriolis effect creates deflections to the right. Oceanography textbooks often make an odd analogy of a pirate's cannon firing a cannon ball, so following this tradition, if you were a pirate (and really, who doesn't at some point envy the corsair lifestyle?) and you fired a cannon ball anywhere in the vicinity of California, its path would deflect to the right. It doesn't matter which direction the cannon is pointing.

Here's where this fits with our story: oceanic wind directions off the coast of California tend to move from the northwest to the southeast, roughly following the edge of California from north to south. As a consequence of the Coriolis effect, and a by-product called Ekman transport, surface water tends to pull away from the California coast. And as nature abhors a vacuum, colder, deeper, nutrient-rich water rushes in to replace the displaced surface water. This phenomenon is called upwelling (Figure 16.1.7 and Figure 16.1.8).

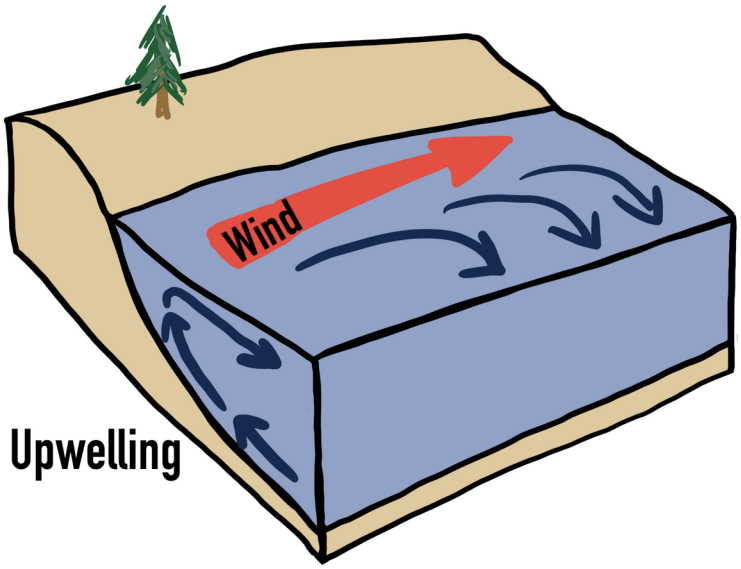


Figure 16.1.7: Wind and the Coriolis effect creating the phenomenon of upwelling along the California coast, allowing deeper, colder, nutrient-rich water to rise to the surface. "Diagram of Upwelling" by Steven Newton is licensed under CC-BY-NC 4.0. Access a detailed description.

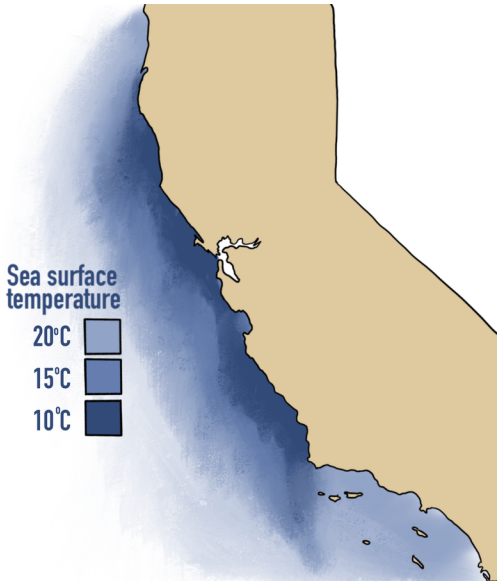


Figure 16.1.8: Typical sea surface temperatures along the California coast, showing the strong cooling effect of coastal upwelling. "Diagram of Sea Surface Temperature from NOAA data" by Steven Newton is licensed under CC-BY-NC 4.0. Access a detailed description.

Upwelling brings to the surface cold, deep water teeming with nutrients, which are vital to the ecosystem off California's coastline. These nutrients feed phytoplankton, who then feed zooplankton, who then feed little fish, then bass and salmon, then seals and sea lions, then white sharks. This complex trophic chain hinges upon upwelling and the nutrients upwelling delivers.

Small changes to upwelling can produce big effects on California marine life. Climate change is thought to influence the amount of upwelling. ENSO warm events (El Niño) reduce the amount of upwelling. In recent years, deficits of upwelling combined with inland drought have prompted regulatory authorities to curtail ocean fishing; in 2023, the entire commercial and recreational salmon season was canceled.

Swimmers in Santa Monica generally do not require wetsuits, but if one enters the water north of Santa Barbara without neoprene protection, the water is so cold that hypothermia can set in within minutes. The reason so much of California's coastal waters is so cold, and why surfers, small craft sailors, and swimmers require wetsuits, is directly because of the phenomenon of frigid, upwelling waters.

Query 16.1.3

This interactive element is not available in this format. Visit the link or scan the QR code to access it online.

View this Interactive Content online

References

1. Abbott, P. L. (1999). The Rise and Fall of San Diego (p. 195). Sunbelt Publications.
2. Einhorn, C. (2023, April 3). California Salmon Stocks Are Crashing. A Fishing Ban Looks Certain. The New York Times. https://www.nytimes.com/2023/04/03/c...alifornia.html
3. Jacox, M.G., J Fiechter, A.M. Moore, and C.A. Edwards (2015). ENSO and the California Current coastal upwelling response. Journal of Geophysical Research: Oceans, 120, doi:10.1002/2014JC010650
4. National Oceanographic and Atmospheric Administration (2023, January 5). Oceanography of the Northern California Current Study Area. NOAA.gov. Retrieved October 5, 2023, from https://www.fisheries.noaa.gov/west-...ent-study-area

This page titled 16.1: Coastal Processes is shared under a CC BY-NC 4.0 license and was authored, remixed, and/or curated by Steven Newton.

16.2: California Coastline Anatomy

Overview of the California Shoreline

The shoreline anatomy of California follows patterns found elsewhere around the world, wherever tectonic uplift exceeds erosion and sea level rise.

Headlands, as mentioned in the previous section, are rock promontories that stick out into the ocean relative to the rest of the coast (see Figure 16.2.1). The dynamics of wave refraction cause incoming waves to warp, or bend, around headland, concentrating the erosive power of the crashing waves on the sides of headlands. The headland flanks erode quicker than the point of the headland, and much quicker than the embayments further back.

This phenomenon of uneven erosion is known as differential erosion, and this accounts for much of the shape of California's coastline.

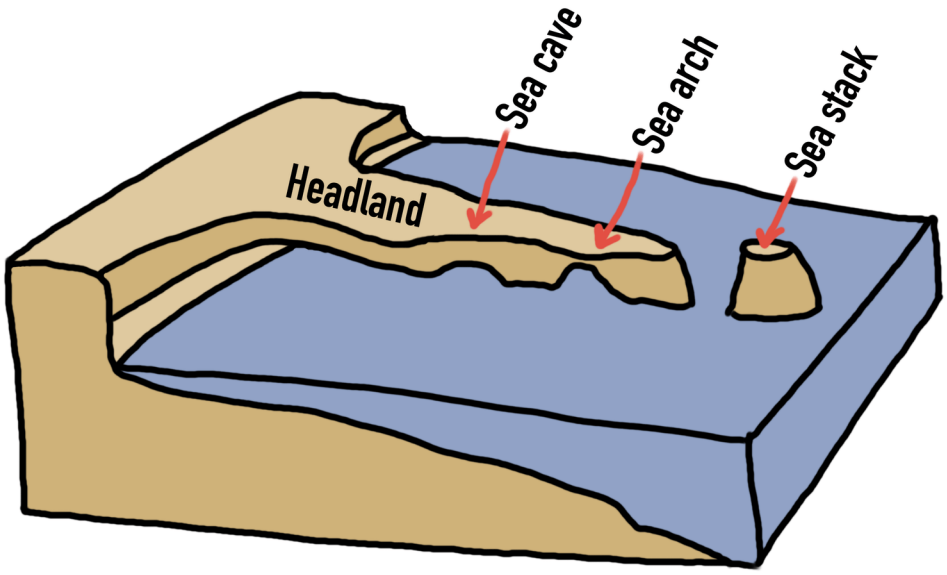


Figure 16.2.1: Typical coastal features resulting from differential erosion, including headlands, sea caves, sea arches, and sea stacks. "Coastal features" by Steven Newton, is licensed under CC BY-NC 4.0. Access a detailed description.

Because of the "pincer" focus of refracting waves, headlands inevitably erode along their sides first, forming sea caves (Figure 16.2.2). Sea cave indentations may grow until they break through to the other side and meet in the middle, forming a thoroughgoing sea arch (Figure 16.2.3).



Figure 16.2.2: A well-developed sea cave along the coast north of Santa Cruz, CA. "Sea cave" by Steven Newton, is licensed under CC BY-NC 4.0. Access a detailed description.



Figure 16.2.3: A sea arch south of Jenner, CA, formed by wave refraction and differential erosion. "Sea arch" by Steven Newton, is licensed under CC BY-NC 4.0. Access a detailed description.

Arches are vulnerable to collapse, and in geologic time, we should think of these dramatic structures as temporary. Indeed, changes are visible even in human time frames; one may go to Santa Cruz and visit the Natural Bridges Park and wonder why there seems to be only one “bridge,” only one remaining arch; the other two fell down, in 1905 and 1980.

When an eroded headland, undercut by sea caves which merge to become a sea arch, reaches its end stage, the last arch collapses and leaves the point of the headland as an island out to sea. This island is then called a sea stack (see Figure 16.2.4).



Figure 16.2.4: Distant sea stacks, remnants of a former headland, at the confluence of the Russian River and the Pacific Ocean, Jenner, CA. "Sea stacks" by Steven Newton, is licensed under CC BY-NC 4.0. Access a detailed description.

Sometimes sea stacks then act as a barrier that creates an area of low wave energy in the longshore drift, which allows sand to build up between the sea stack and the coast. This is called a tombolo (see Figure 16.2.5).



Figure 16.2.5: A tombolo created from a former sea stack that has accumulated enough sand behind it to reattach to shore. Marine terraces are also shown. Near Jenner, CA. "Tombolo" by Steven Newton, is licensed under CC BY-NC 4.0. Access a detailed description.

Recognizing sea stacks, and mentally tracing them back to the existing shore, can give one a breathtaking view of how the coast used to look before wave refraction sculpted the complex features we see today.

Wave refraction is not the only erosive work of waves. As waves crash ashore, several times per minute, 24/7, they carry with them sand, pebbles and even small boulders during particularly energetic waves. This incessant “sand blasting” of the rocks under the waves creates flattened, wave-cut platforms. Most of the time, you don’t see wave-cut platforms because they are under water. However, in a tectonically active emergent coastline, these wave-cut platforms get raised up out of the water by successive quakes.

When these wave-cut platforms are above sea level, they stand out as flat zones along the coast, punctuated by narrow steep cliffs, with further plateaus inland. This pattern is called marine terraces. Many developed places along the California coast are built on marine terraces, because of the desirability of flat land. The city of San Diego, in particular, is built on staggered marine

terraces (Figure 16.2.6).

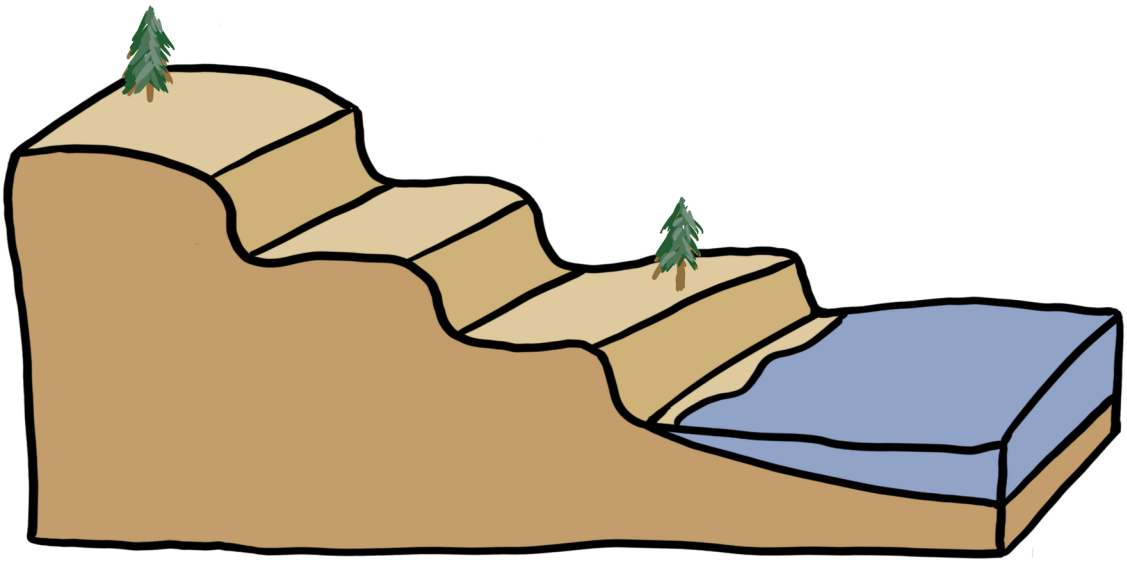


Figure 16.2.6: Three marine terraces, with the oldest to the left and the youngest to the right, with a newly forming terrace under the water. A similar configuration exists in San Diego, which is settled on three marine terraces. "Marine terraces" by Steven Newton, is licensed under CC BY-NC 4.0. Access a detailed description.

If the wave-cut platforms have hosted headlands which eroded into sea stacks, then the marine terraces may also preserve “fossil” sea stacks, now completely on dry land, as in Figure 16.2.7.



Figure 16.2.7: A marine terrace with “fossil” sea stacks, rubbed smooth by now-extinct Columbian mammoths (*Mammuthus columbi*). Note Aspen the dog for scale. Goat Rock, Jenner, CA. "Mammoth rocks" by Steven Newton, is licensed under CC BY-NC 4.0. Access a detailed description.

References

1. Abbott, P. L. (1999). *The Rise and Fall of San Diego*. Sunbelt Publications.

This page titled 16.2: California Coastline Anatomy is shared under a CC BY-NC 4.0 license and was authored, remixed, and/or curated by Steven Newton.

16.3: California Coastal Hazards

Sharks Aren't the Problem

Many people mistakenly think that a prime hazard in California coastal waters is shark attacks, so let's take a bite out of this misconception.

The waters of northern California are indeed a major feeding ground for white sharks (*Carcharodon carcharias*), who enjoy tasty pinnipeds well-fed from the food chain created by upwelling. But the real incidence of shark attacks is much lower than most people realize. According to the International Shark Attack file, in 2022 only five human fatalities occurred worldwide. Only one person died of a shark attack in the entire United States in all of 2022. In the same time period, hippopotamuses are estimated to have killed 500 people worldwide, or one-hundred times the number of fatal shark attacks. So if you must insist upon fearing a wild animal, judge the real dangers and be afraid of hippos.

If you still find yourself skeptical of this information, check out the Instagram account of @scott_fairchild, which hosts scores of drone videos of white sharks approaching unaware California swimmers, surfers, and paddle boarders, getting within a few meters of the humans, and then leaving them alone. Sharks are ubiquitous in California waters, but they are not a major hazard.

Rip Currents

Perhaps the greatest hazard along California coasts, responsible for about 80% of beach rescues, is the phenomenon of rip currents. (They are sometimes mistakenly confused with "rip tides," but the currents have nothing to do with tidal fluxes.) Rip currents form as temporary, fast-moving, narrow streams of water that move perpendicular to the coast, out to sea. They can quickly drag swimmers away from shore and induce panic in the swimmers, who struggle in vain to swim back to shore directly. This panic, and the potential for leg cramps, can lead to drowning.

Rip currents can form on any beach, but they are particularly likely during periods of vigorous waves, in areas where an underwater sand bar may have a breach that allows water to exit in one spot with speed. There are often only subtle signs, from the perspective of a swimmer, that rip currents have formed at a beach.



Figure 16.3.1: Aerial photograph of a green dye exposing a rip current; note waves break less in region of rip current. "Rip current" by NOAA is in the public domain/ A derivative from the original work. Access a detailed description.

A typical scenario for a rip current situation is this: a person wades into shallow water, into an area where a rip current has formed. While the person is standing on sand, all is fine. However, one big wave and suddenly the person is in water too deep to stand.

Then the person discovers that the water is surging away from the beach, away from shore, into ever deeper water. A normal instinct is to swim against this flow, directly back to the beach; after all, dry land is right there.

Rip currents are capable of flows exceeding 2.4 meters/second. Michael Phelps is the most decorated Olympic swimmer of all time, winning 28 medals. Phelp's record for the 100 meter is 47.57 seconds, a rate of 2.1 meters/second. So even the fastest swimmers in the world can't make progress against a rip current, and such bursts cannot be long sustained, especially for non-Olympic class swimmers. Rip currents simply flow faster than any person can swim, and unlike swimmers, rip currents don't get tired.

A person in a rip current might look up and gauge that despite vigorous swimming, no progress had been made; in fact, the shoreline is now further away. This is where panic sets in. The swimmer may try to swim full blast. And here tragedy begins; leg muscles under such use easily cramp. Experiencing a hamstring cramp (a "charlie horse") causes intense pain, akin to a bone break, disabling not only efforts to swim, but even to tread water.

There is a simple solution, and encouragingly, more and more public beaches now display signs informing swimmers of what to do when caught in a rip current. The simple solution is to avoid swimming directly against the flow, but rather to swim parallel to the beach. Rip currents are narrow, a few tens of meters in width. A short swim sideways and one is out of the rip current, and then able to return normally to the dry beach.

Video 16.3.1: Rip Current Science

Watch the following video to learn more about the dangers of rip currents and how to spot them.

This interactive element is not available in this format. Visit the link or scan the QR code to access it online.

View this YouTube Video online

Tsunamis

Not every shoreline hazard is so easily avoided. Any beach exposed to the unrestricted ocean faces the risk of tsunamis. Tsunamis are waves generated not by wind, but by geologic forces, such as earthquakes, submarine landslides, or meteorite impacts. Tsunamis are orders of magnitude larger than wind-generated waves, and can inundate coastal areas with devastating and deadly effects.

In 2004, the Boxing Day earthquake near Indonesia launched a tsunami estimated to have killed a quarter of a million people on both sides of the Indian Ocean. In 2011, the Tōhoku tsunami in Japan killed about twenty thousand people, despite a robust warning system and extensive defensive preparations.

Tsunami casualties could occur along the California coast, even if the source of the waves was on the other side of the Pacific Ocean. We know this because of an earthquake and tsunami in the year 1700. The giant quake occurred on the Cascadia subduction zone and launched a tsunami across the Pacific, where it hit eastern Japan in what became known as the "orphan tsunami." This tsunami was an "orphan" because no obvious "parent" quake was felt in Japan prior to the tsunami's arrival. We do not know if the 1700 event created similar tsunamis in the Pacific Northwest or California because there are no written records from that time.

But we do know of other tsunamis that have affected the California coast. The 1964 Alaskan quake spawned a tsunami that killed 12 people in Crescent City, California. Crescent City was also affected by the 2011 Tōhoku tsunami, killing one and sinking over a dozen boats in harbor.

How future tsunamis will affect the California coast is hard to predict. A major quake far away can send waves, moving at the speed of a jet, across the Pacific. It is also possible that more local fault activity can generate waves, with less warning.

Warnings about the approaching 2011 tsunami provided enough time for panicked, fleeing residents in coastal areas, such as

Watsonville and Santa Cruz, to clog roads with so much traffic that roads ground to “a standstill." This does not bode well for future evacuations.

Query 16.3.1

This interactive element is not available in this format. Visit the link or scan the QR code to access it online.

View this Interactive Content online

Coastal Erosion

No one drowns from coastal erosion, but people do lose their homes.

The major problem with coastal erosion is that homes have simply been built too close to the shoreline. Often homes are built on cliffs of weak rock, or even mounds of compacted sand. The metastasizing, haphazard building spree of mid-20th century California held little concern for whether or not it was geologically safe to build in unstable areas. Now California faces the consequences of these reckless development decisions.

One case study is the coastal town of Pacifica, just south of San Francisco. The bluffs underlying the northern part of Pacifica are not part of a formal geologic formation, but are described by the USGS as sand sometimes “firm in a few places.” That might be too generous.

The problem of the development of Pacifica can be illustrated by comparing two USGS topographic maps (Figure 16.3.2). In the first map, from 1950, there is no development on the ocean side of Edgemar, as noted by the 100 foot contour interval. Nineteen-fifty was on the cusp of a postwar building boom and soon everything would change. Everything–except the sandy, weak cliffs rapidly returning to the sea. This second map is from 1980 and shows extensive development on the ocean side of Edgemar. There are several rectangular blocks right at the edge along a road called Esplanade Ave. These pink blocks indicate large apartment buildings.

Query 16.3.1

This interactive element is not available in this format. Visit the link or scan the QR code to access it online.

View this Interactive Content online

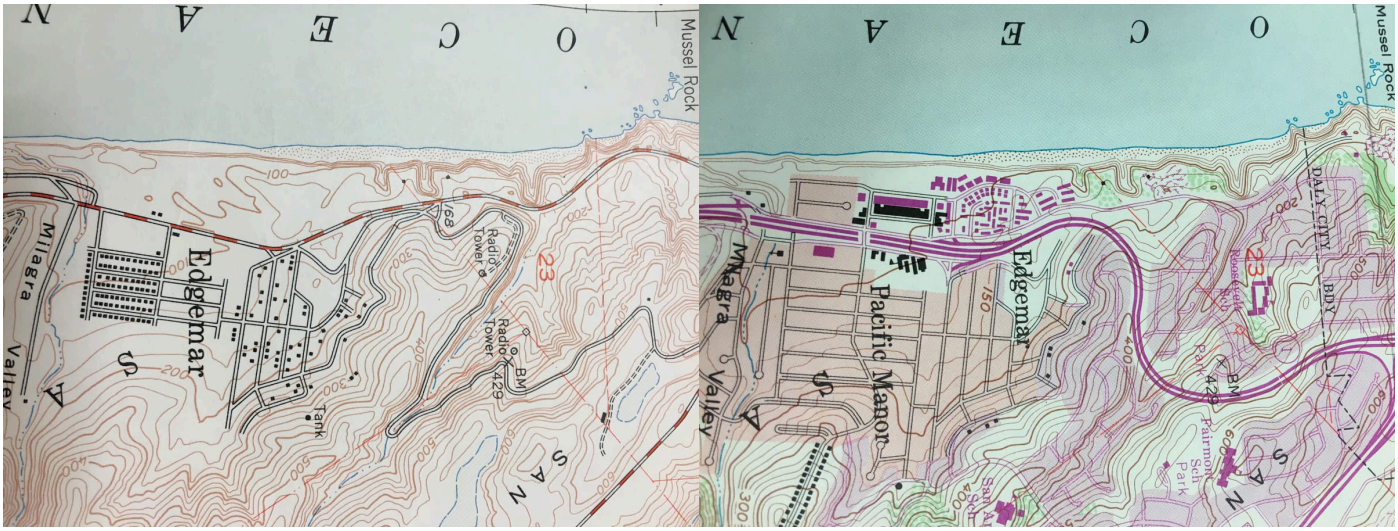


Figure 16.3.2: Comparison of two topographic maps of Esplanade Avenue, Pacifica (left: 1950, right: 1980). Sources: USGS (Cartographer). (1950, 1980). S. San Francisco quadrangle, 7.5-minute series [map]; 1:24,000. Washington, DC: U.S. Geological Survey. "Topo maps" by USGS is in the public domain/ A derivative from the original work. Access a detailed description.

Of note in both maps is the presence of Mussel Rock, a granitic Salinian Block remnant pushed out away from the coast by right-lateral strike-slip motion along the San Andreas fault. Even in the 1950 map, the location of the San Andreas and its 1906 trace of surface disruption were well-known. Note the presence in the 1980 map of a new public elementary school, the Franklin D. Roosevelt School, built virtually on top of the San Andreas fault trace. That this area was developed at all shows disregard for the obvious geologic hazards, and irresponsibility by public officials that can only be characterized as reckless disregard for human life.

Slightly to the south of the fault, along Esplanade Ave, a dozen single-family homes were built in 1949, near the edge, about 30 meters away, of the steep sandy cliff. Residents could hear the soothing crashing of waves 70 feet below. It was truly a beautiful place to live, with sunsets over the Pacific Ocean, whale watching from one's living room, and calming views of sailboats plowing the waves. It was the perfect neighborhood–except for where it was built.

This stretch of homes was condemned following the El Niño storms of 1997/1998, which dramatically moved the cliff face back. In some cases, the erosion was so severe that the foundations of these Esplanade Ave. homes were exposed as they projected into open air. The southernmost ten homes were demolished immediately, while two others lingered, uninhabited, until the 2010s.

This loss of homes was hardly a surprise. As Snell et al. 2000 estimated, this area has experienced between 0.5 - 0.6 meters/year of cliff retreat over the last 146 years. So the initial ~30 meter buffer was never expected to last longer than about 60 years. It lasted 49 years.

Slightly northward of the location of these lost homes, a series of large apartment buildings were constructed, on the same weak cliff material, the base of which would be reached on a regular basis by waves. Efforts to delay the impending collapse of the sandy cliffs are shown in Figure 16.3.3.



Figure 16.3.3: Dubious attempts to “armor” the coastline against wave erosion, Esplanade Ave., Pacifica, CA. "Esplanade Ave" by Steven Newton, is licensed under CC BY-NC 4.0. Access a detailed description.



Figure 16.3.4: A closer look at attempts to “armor” the coastline, Esplanade Ave., Pacifica, CA. "Rip rap" by Steven Newton, is licensed under CC BY-NC 4.0. Access a detailed description.

Just north of the buildings shown above, a series of large apartment buildings were constructed in 1962. These are the five pink rectangles visible in the 1980 topographic map (Figure 16.3.2). Initially, there were tens of meters of flat ground on the ocean side of these apartments; however, the 20 meter sand cliff between them and the ocean is of such weak material that one can easily carve into the sand with one’s finger. It was just a matter of time and physics before wave erosion pulled back the cliff to the point where it endangered these buildings and the residents within, as illustrated in Figure 16.3.5.



Figure 16.3.5: Coastal erosion threatening an apartment complex on Esplanade Ave., Pacifica, CA. When this building was constructed in 1962, 10-20 meters of land separated the cliff edge from the building, but rapid erosion pulled back the cliff over five decades. This building was later demolished. "Esplanade Ave #2" by Steven Newton, is licensed under CC BY-NC 4.0. Access a detailed description.

The City of Pacifica began "red-tagging" (forcing evictions) and demolishing these buildings in 2016-2017 after the owner declined to pay for their removal (seeFigure 16.3.6). This demolition displaced a large number of low-income residents in Pacifica, many of whom lived there using Section 8 housing vouchers, which are frequently not accepted by other Bay Area landlords, leaving few local options for former residents. However, the red-tagging and the removal of these buildings was manifestly necessary given the geologic dangers.



Figure 16.3.6: Cliff erosion resulted in the dreaded “red tag” informing tenants that they may no longer legally live at their home. These notices were placed at 320 Esplanade Ave, Pacifica, prior to the building’s demolition. "Esplanade Ave #3" by Steven Newton, is licensed under CC BY-NC 4.0. Access a detailed description.

In 2022, a study by the Coastal Process Group at UC San Diego Scripps Institute of Oceanography analyzed rates of coastal cliff erosion along 866 kilometers (538 miles) of California Coastline. Their findings can be seen in the California Coastal Cliff Erosion Viewer. If you zoom in on Pacifica, you will see that indeed rates of cliff retreat in the area surrounding Pacifica are high; some 1 km sections had average erosion rates as high as 1.2 meters per year during an interval in the 2010s, but Pacifica certainly isn’t the only stretch of coastline with erosion rates this high. In fact, when you first open this map, zoomed out to the whole state, a different region pops out. At this scale, the rates shown are averaged over 50 km sections and one section near Cape Mendocino appears to eclipse the rest of California. The average erosion rate for the whole 50 km section is 0.85 meters per year, with some

individual 1 km sections reaching rates of nearly one and half meters per year.

This remote region of the California Coast is sometimes called “the Lost Coast.” Much of the “rock” (if it can even be called that) in this region is part of the “Wildcat Formation,” a geologic unit composed of little more than mud. Earlier in this chapter, you learned that sea cliffs result when tectonic uplift outpaces erosion. Even the strongest, most erosion resistant bedrock will eventually be leveled to a beach if there is no driving force to lift it upwards. Conversely, where bedrock is soft, unstable, and easily eroded, tectonic uplift must be extremely rapid to keep pace and maintain a cliff. Perhaps it is no surprise then that the 50 kilometers of coastline with the highest average erosion rate in the state aligns precisely with the Mendocino Triple Junction, an area of significant tectonic activity.

Clifftop erosion along the Lost Coast doesn’t make news for destroying homes the way it does in Pacifica; that’s because there aren’t any homes there to be destroyed, of course. The combination of uplift and erosion makes maintaining even roads in this area a significant challenge, let alone towns or cities. It is the remote nature of this region that makes it a popular destination for backpackers and cyclists.



Figure 16.3.7: A photo taken just south of Centerville Beach in 2023 following a winter of heavy precipitation and a nearby M6.4 earthquake on Dec 20, 2022. A fence constructed to keep visitors away from the cliff edge is no longer adequately performing its function. "Hanging Fence" by Emily Wright, licensed under CC BY 4.0. Access a detailed description.

Query 16.3.2

This interactive element is not available in this format. Visit the link or scan the QR code to access it online.

View this Interactive Content online

References

1. Bay Area News Group (2011, March 11). Live blog: Tsunami waves hit Bay Area. The Mercury News. https://www.mercurynews.com/2011/03/11/live-blog-tsunami-waves-hit-bay-area/
2. International Shark Attack File (n.d.). The ISAF 2022 shark attack report. Florida Museum. Retrieved October 7, 2023, from https://www.floridamuseum.ufl.edu/shark-attacks/yearly-worldwide-summary/
3. J. McKinley. (2011, March 16). Sleepy California Town, and a Tsunami Magnet. The New York Times. https://www.nytimes.com/2011/03/17/us/17crescent.html
4. National Oceanographic and Atmospheric Administration (2023, July 28). Rip Currents. NOAA. Retrieved October 7, 2023, from https://www.noaa.gov/jetstream/ocean/rip-currents

5. Snell, C. B., Lajoie, K. R., & Medley, E. W. (2000). "Sea Cliff Erosion at Pacifica, Ca, Caused by 1997/1998 El Niño Storms, in Proceedings of sessions of Geo-Denver 2000 - Slope stability 2000 (pp. 294-308). https://doi.org/10.1061/40512(289)22

This page titled 16.3: California Coastal Hazards is shared under a CC BY-NC 4.0 license and was authored, remixed, and/or curated by Steven Newton.

16.4: Human Alteration and Mitigation

Protecting an Eroding Coastline

With all of the potential loss of homes and land along the California coastline, it stands to reason that efforts would be made to protect the shore, to build structures to protect and preserve people's property. Unfortunately, such structures, like the mythological Hydra, which regrew two heads for every head Hercules severed, often create new secondary problems without solving the original issue.

One obvious way to protect an eroding coastline is to "armor" it using large rocks. The term for such rocks is rip-rap. A related structure is a seawall (see Figure 16.4.1), where a concrete wall is erected to absorb the energy of incoming waves and protect areas behind it. A problem with both of these protections, however, is what happens to the fierce energy of incoming waves.

On an unaltered beach, powerful waves roll up, carrying with them sand and debris, until the point where the waves lose enough energy that they pull back, leaving some of the sand behind. That's nature's way of preserving a beach.

If there is rip-rap or a seawall, however, then the incoming waves hit these structures before the waves have dissipated all their energy. The waves reflect back off these rigid surfaces. And as the outgoing waves reflect, they carry away sand on the beach. The unintended net effect of this hardening of the shoreline is not to preserve the beach, but rather to destroy it by reducing the very sand which made the beach desirable in the first place. In some cases, sand loss is so deep that the seawall itself is undermined and collapses.

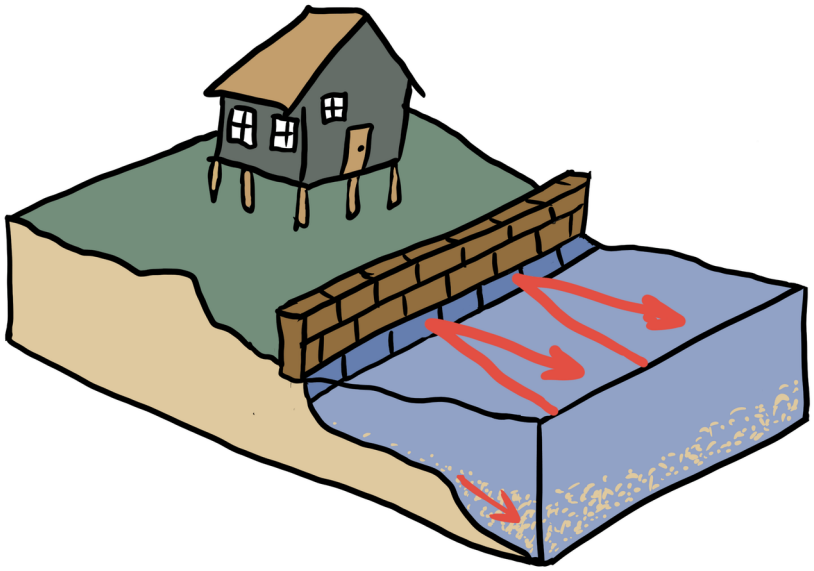


Figure 16.4.1: A seawall protecting the house behind the wall, but reflecting wave energy in a way that removes beach sand. "Seawall" by Steven Newton is licensed under CC-BY-NC 4.0. Access a detailed description.

While seawalls are built parallel to the beach, another common human alteration is to construct a wall perpendicular to the beach, jutting out into the water. A single wall constructed out into the water perpendicular to the beach is called by the unfortunate term groin. When such walls protect the entrance to a harbor or a river, they are termed jetties; they are often found in pairs. These structures are composed of a variety of materials, including rock, concrete, metal, and wood.

Groins can be a useful means of docking a boat when there is no nearby harbor. But the primary use of groins/jetties involves altering the longshore drift of sand that continuously moves along a coast, driven by the longshore current. In a normal, unaltered coastline, this sand can move freely; however, in an altered situation, the sand piles up on the "upstream" side of a groin/jetty (Figure 16.4.2).

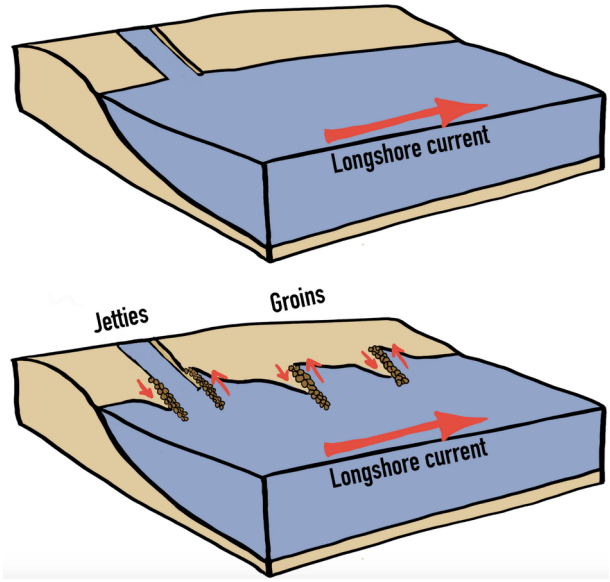


Figure 16.4.2: Before and after human alteration to the shoreline. The top diagram shows the “before” case. The bottom diagram shows the “after” scenario, with considerable erosion/deposition created by jetties and groins interacting with the longshore drift. "Levee and groins" by Steven Newton is licensed under CC-BY-NC 4.0. Access a detailed description.

This accumulation of sand may be desirable for a homeowner who wishes to increase the size of that property’s beach. However, it comes at a cost. There is no way to change the net amount of sand flowing in a longshore drift. If you accumulate sand in front of your beach by installing a groin, this will remove sand from your neighbor’s beach. Your neighbor may then install a groin too, spreading the problem further down the coast, in a littoral arms race. The end result is a defacement of the shape of the beach, into a series of step-like shapes, without any actual change in the amount of sand on that beach. While California has few instances of this mutilation of the coastline, other areas of the country, in particular the East Coast barrier islands, are pock-marked with these ugly, and ultimately futile, attempts to seize a little more beach in front of one’s property. Worse still, the beach areas depleted of sand now have less protection from wave erosion during storms.

Another way to interact with longshore drift is a breakwater. A breakwater is a structure built in the water parallel to the beach, but some distance away from the beach. Figure 16.4.3 the before/after effects of the installation of a breakwater.

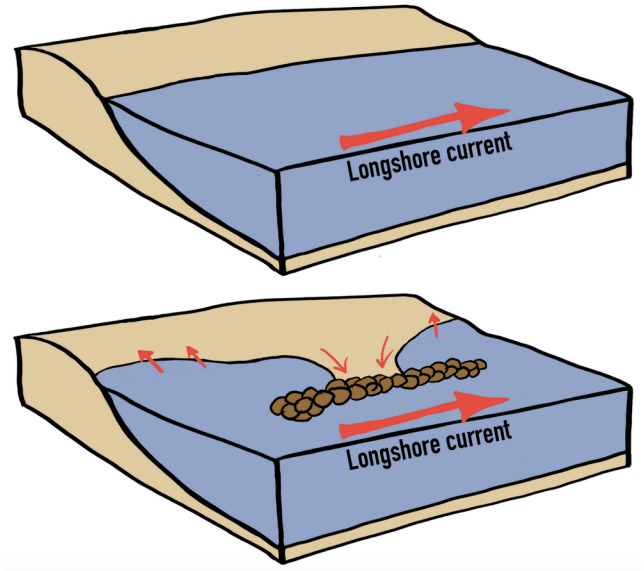


Figure 16.4.3: Before and after the installation of a breakwater. The top diagram shows the “before” case, without any human alteration to the shoreline. The bottom diagram shows the “after” scenario, with considerable erosion/deposition created by a breakwater interacting with the longshore drift. "Breakwater" by Steven Newton is licensed under CC-BY-NC 4.0. Access a detailed description.

The bottom line is this: human intervention at the shoreline always has consequences. The natural forces of waves, longshore

current, and longshore drift do not yield to negotiation or bargaining. What brings sand to one place steals it from another, with mutilation of the shoreline the only lasting effect.

Query 16.4.1

This interactive element is not available in this format. Visit the link or scan the QR code to access it online.

View this Interactive Content online

This page titled 16.4: Human Alteration and Mitigation is shared under a CC BY-NC 4.0 license and was authored, remixed, and/or curated by Steven Newton.

16.5: Coastal Access

The Battle over Martins Beach

California's public beaches are a spectacle of natural beauty and a bounty for recreation. But what if you can't get to them?

For a century, surfers and beach-goers enjoyed Martins Beach, just south of Half Moon Bay, Given the protections of access enshrined in the 1976 California Coastal Act, they had every reason to expect to continue enjoying Martins Beach. The only way to get to this beach, isolated on each side by steep cliffs, is by a road leading from Highway 1. Because public use had long been established, the law required this road to remain open.

But in 2008, billionaire venture capitalist Vinod Khosla purchased the property. Prior to the purchase, the San Mateo County Planning and Building Department informed him of the requirement for continued access. In a demonstration of the phrase that money can't buy class, Khosla promptly locked the gate to the access road anyway. The Surfrider Foundation sued. A group called Friends of Martins Beach sued. A state senate bill, SB968, to restore access was passed and signed by the governor. The California State Lands Commission tried to buy an easement. The California Court of Appeal for the First Appellate District ruled against Khosla. Khosla appealed to the Supreme Court, but SCOTUS declined to take the case. None of these setbacks mattered; the Martins Beach gate remained closed. Seemingly no governmental entity, even under the imposition of fines, can compel someone with unlimited funds, infinite spite, and a phalanx of lawyers, to obey the law. Or, as the *New York Times* put it: "Aggressive, shameless, obsessive and optimistic, the tech billionaire Vinod Khosla is willing to litigate the California coast for the rest of his life." In 2020, the State of California sued Khosla and the case remains ongoing.

Public Use

Public use of public shorelines has long been a bitterly acrimonious and contentious issue in ocean-bordering states, just as common entry to "public" swimming pools has sparked racially-motivated violence throughout the last century, and some municipalities have restricted "public" parks to local residents. In the absence of national governing legislation, laws regarding public beach access vary widely from state to state, and have often involved overt exclusion of certain racial and ethnic groups. Though today many of these "resident-only" restrictions have not survived legal challenge, the practical problem of actually getting to public beaches now acts as a proxy for formerly openly-racist exclusions.

One legal concept here is called the "public trust doctrine," which posits that natural features–the sky, the oceans, the beaches–are public property belonging to the citizens of the nation rather than any one individual. A related concept is the "right to roam" doctrine, which is widespread outside of the United States though unknown here; this is a legal permission for the public to access private farmlands, lakes, rivers, and mountains for non-disruptive, non-commercial recreational purposes such as hiking.

California legislates against private usurpation of the public coastline, but it is not alone. Surprisingly, Texas has a generous allowance in its 1959 Texas Open Beaches Act, which states: "[I]t is declared and affirmed to be the public policy of this state that the public, individually and collectively, shall have the free and unrestricted right of ingress and egress to and from the state-owned beaches."

On the other side of this issue stand states such as Connecticut, which offers very limited rights to public coastlines, a fact brilliantly mocked by documentarian Michael Moore in his show *TV Nation*. In an episode segment called "The 'Public' Beaches of Greenwich, CT," the filmmaker arranges for a diverse group of New York residents to be bused to a beach in Greenwich, where the bus is summarily turned away at the gate due to the lack of a "permit." The would-be beach-goers are then transferred to a ship, but as they approach the shore, they are stopped by police boats. Undeterred, the lifejacket-clad citizens then leap into the water and swim to shore, where they are subjected to a barrage of harassment from local beach goers and are escorted off the beach under the view of police. One helpful gentleman suggests that if they really want to swim at the beach, they should first buy a local house. Keep in mind, this stunt happens on a *public* shoreline. (Subsequent court decisions ruled against Connecticut's resident-only beach policies.)

California's population dramatically increased in the 1960s and 1970s, leading to rising housing values, and new development along coastlines. In response to this increasing pressure on natural areas, in 1972 voters passed Proposition 20, which began the process leading to the 1976 California Coastal Act. This legislation established a Coastal Commission and enacted protections

for public access. To wit, the Act reads: "[M]aximum access, which shall be conspicuously posted, and recreational opportunities shall be provided for all the people consistent with public safety needs and the need to protect public rights, rights of private property owners, and natural resource areas from overuse."

The caveats of this language–exclusions for private property, safety, and natural resources–undermine its protections and place it somewhat below Texas' stronger affirmation of public rights. The protection of private property is particularly problematic, because as discussed above, installations such as seawalls armoring one stretch of beach (in front of a house, for example) come at the expense of neighboring areas. Another problem is its definition of the private/public demarcation of the beach. Nonetheless, the Act has provided a strong tool for regulators (often when prompted by activists) to restrict and fine private parties who steal this public resource.

Defining "Beach"

The definition of a beach can be ambiguous. Where does the beach begin and end and what can be owned in the stretch of sand approaching the waves? Is the beach seaward of the line where vegetation ends and the sand begins? That's how the demarcation is drawn in Oregon and Washington, which have very generous laws similar to the one in Texas.

But in California, the distinction is the mean high tide mark. For practical purposes this is often distinguished as "wet sand vs. dry sand." Dry sand, that's potentially someone's property. Wet sand, which must have been inundated by the daily tide, is public. This line isn't always clear and is certainly not marked. Further confusing this definition, specific tidal height varies as tides cycle twice a month between spring and neap tides, with no indication of what the mean tide should be. Moreover, many shore side homeowners have had to make easements to allow public access, so some stretches of "dry sand" are public while others are not. An additional problem is how the dry/wet dividing line will change from historical precedent with future rising sea level.

In 2015, a CNN reporter and an employee of the California Coastal Commission tested this issue at Escondido Beach, in Malibu, where they were confronted within minutes by a security guard threatening a $1500 fine and a lifetime ban from the beach. They declined to move and the security guard summoned police. When the employee of the California Coastal Commission produced a map and explained the law, the responding officers ascertained that the beach-goers were there legally and left them to enjoy their afternoon.

But having to produce a map upon demand, much less endure a law enforcement confrontation, each time one wants to go to a beach is a high bar for "public access." This is particularly a deterrent to communities unaccustomed to the expectation of polite and respectful interactions with police. Something to keep in mind in such situations is that private security guards are not law enforcement and can act only as far as verbal intimidation and aggressive threats allow. Still, no one wants to spend a relaxing day at the beach having to assert one's rights to be there, and that's the point; if private homeowners are able to chase away legal visitors through menace and bullying, then they've stolen the beach from the public.

Getting There

Even in areas where beach access is clear, there remains the problem of getting there. In California, it's hard to go anywhere except via car. So local areas wishing to discourage beach visitors can legally do so by restricting or time-limiting parking areas, or by imposing draconian parking payments. Connecticut, previously mentioned as a particularly difficult beach access state, has beaches where non-residents can only enter by purchasing single-entry passes–but the only places to buy such passes are far from the beach and not open on weekends. At Compo Beach in Westport, CT, nonresidents are charged $30/day for parking during the week and $50/day on weekends. Most Los Angeles area parking fees are much lower, though this one-fee-fits-all system still imposes a significant burden on less affluent beach visitors, and may contribute to the fact that one-third of Californian African-Americans visit the beach less than once per year.

Malibu beach houses are notorious for erecting unauthorized "no parking" signs, for painting legal curbside parking red, and in one case, erecting a fake Potemkin-village four-car garage facing in order to trick would-be beach-goers into thinking there was no access. The City of Malibu has even removed official signs aiding beach access, in the name of safety.

What about public transportation options? Not in Palos Verdes, where in the 1980s residents succeeded in restricting public transit buses from servicing the area. Even if a beach were serviced by a bus line, how does one carry a surfboard on a crowded bus? Not to mention wrangling children, beach towels, and a cooler? Though public transit seems a possible alternative, the lack of service and practical realities mean that for most beach-goers, cars are the only way to access the public beach.

In the United States, just as public swimming pools have a difficult history of racial segregation, beaches have faced similar racial issues. In 1912, a black family, Charles and Willa Bruce, purchased a stretch of beach in Los Angeles with the intent of developing a beach recreation area open to African Americans, who were excluded from most other nearby beaches. Soon the KKK began a campaign of harassment, including posting “No Trespassing” signs reminiscent of modern Malibu signs. After years of arson and violence, the city of Manhattan Beach seized the property through eminent domain in 1924. Nearly a century later, the State of California recognized the injustice and returned the land to the Bruce’s descendants. The land is estimated to be worth as much as $75 million.

References

1. Armborst, T., D'Oca, D., Theodore, G., & Gold, R. (2017, August 27). Six “Weapons” Cities Use to Keep You off (or on) the Beach. Next City. Retrieved October 19, 2023, from https://nextcity.org/features/arsenal-of-exclusion-keep-public-off-free-beaches
2. Chamings, A. (2023, July 10). Affluent California city accused of tearing down public beach access signs. Retrieved October 21, 2023, from https://www.sfgate.com/bayarea/article/malibu-public-beach-access-sign-feud-18193172.php?IPID=SFGate-HP-Editors-Picks
3. Bowles, N. (2018, August 30). Every Generation Gets the Beach Villain It Deserves. The New York Times. Retrieved October 21, 2023, from https://www.nytimes.com/2018/08/30/technology/vinod-khosla-beach.html
4. Kahrl, A. (2018, May 21). Free the Beach. Boston Review. Retrieved October 19, 2023, from https://www.bostonreview.net/articles/andrew-w-kahrl-free-beach/
5. Kaur, H. (2020, January 8). California is suing a Silicon Valley billionaire for blocking public access to a beach. Retrieved October 21, 2023, from https://www.cnn.com/2020/01/07/us/california-lawsuit-vinod-khosla-beach-trnd/index.html
6. Michael Moore, TV Nation. (1995, July 21). The "Public" Beaches of Greenwich, CT. (Season 2, Episode 1: We're #1). https://www.youtube.com/watch?v=lMS-EfcWrSw
7. National Agricultural Law Center (n.d.). The Public Domain: Basics of the Public Trust Doctrine. Retrieved October 20, 2023, from https://nationalaglawcenter.org/the-public-domain-basics-of-the-public-trust-doctrine/
8. Mossburg, C. (2022, June 30). Multimillion-dollar beach property taken from Black owners in Jim Crow era is cleared to be returned. Retrieved October 21, 2023, from https://www.cnn.com/2021/10/01/us/bruces-beach-los-angeles-property-return/index.html
9. O'Neill, A. (2015, September 5). Drawing a line in the sand in Malibu. Retrieved October 21, 2023, from https://www.cnn.com/2015/09/05/us/malibu-day-at-the-beach/index.html
10. Ross, R. (2022, July 21). California beachfront land taken from Black family returned in ceremony. Retrieved October 20, 2023, from https://www.reuters.com/world/us/california-beachfront-land-taken-black-family-returned-ceremony-2022-07-20/
11. Shultz, D. (2021, August 26). A Dilemma for California Legislators: Preserve Public Beaches or Protect Coastal Homes. Retrieved October 21, 2023, from https://www.pbs.org/wnet/peril-and-promise/2021/08/dilemma-california-legislators-preserve-public-beaches-or-protect-coastal-homes/
12. Shyong, F. (2021, July 9). The beach is there for all of us — We just have to get there. Los Angeles Times. https://www.latimes.com/california/story/2021-07-09/beach-restrictions-race

This page titled 16.5: Coastal Access is shared under a CC BY-NC 4.0 license and was authored, remixed, and/or curated by Steven Newton.

16.6: The Edge of California

Living on the Edge

The coastline of California is indelibly part of the California mindset. However, not all is well along our lengthy interface with the Pacific. Access to the coast, though stipulated by law, is routinely restricted. Too many homes have been built absurdly close to this active shoreline, and efforts to protect these homes through structures such as seawalls and groins either fail to offer protection or shift the problem to adjacent areas.

The coastline of California is not Disneyland. The dangers are real. Shoreline erosion will in the future destroy many more homes. And many unwary and uninformed swimmers will fall victim to rip currents.

But there is also great beauty in the sculpted landforms made possible through wave refraction along this dynamic, emergent coastline. And there is satisfaction in understanding how the shore has evolved over geologic time and continues to evolve today.

This page titled 16.6: The Edge of California is shared under a CC BY-NC 4.0 license and was authored, remixed, and/or curated by Steven Newton.

16.7: Chapter Summary

16.1: Coastal Processes

- This chapter looks at how the combination of wave refraction and tectonic uplift shape our coast.
- Wave refraction is a major factor in sculpting the dynamic California coastline.
- The dynamic California coast is unlike many other coasts in the US.

16.2: California Coastline Anatomy

- This chapter details major features of coastal anatomy.
- The evolution of headlands into sea caves, sea arches, and sea stacks is detailed.
- The processes create this anatomy is well understood.

16.3: California Coastal Hazards

- Should you fear sharks more than water currents? It turns out sharks are not much of a hazard
- Shark interactions are common but rarely involve bites; nonetheless, du dum. Du dum. Dudumdudumduhum.
- Rip currents are responsible for most drownings.

16.4: Human Alteration and Mitigation

- If you wanted to protect your property on the coast, should you install a sea wall, a groin, or a breakwater?
- Trick question: they're all detrimental to the coastline, and unstoppable natural processes will win in the end.
- The bottom line is that too many people build too close to the shore.

16.5: Coastal Access

- Beaches are beautiful, but what if you can't get to them?
- Confusing, contradictory laws both guarantee Californians access to the shoreline, and do not guarantee Californians access to the coastline.
- Know your rights--and learn them in this section.

16.6: The Edge of California

- Our coastline is one of the things that define Californian living.
- But too many people have built in precarious places.
- Too many places have restricted beach access to the public, in violation of legislation guaranteeing access.

This page titled 16.7: Chapter Summary is shared under a CC BY-NC 4.0 license and was authored, remixed, and/or curated by Steven Newton.

16.8: Detailed Figure Descriptions

16.1 The endemic California surfer

A wave being plowed by a surfboard, capturing the phenomenon of surface tension in water droplets. This image is decorative in nature, but displays some of the beauty surfers experience.

16.1.1 Dynamic, uplifting, highly-eroded, rocky California coastline

A rocky, highly-eroded beach just north of Bodega, CA, with a large Golden-Bernese dog named Aspen for scale. Clear, foamy water rushes up on a sandy beach, hitting jagged, sculpted rocks, to emphasize how water and waves erode and sculpt coastlines, and how unless those coastline are actively uplifting through tectonics, the coastlines rapidly are flattened. California's coasts tend to have exposed rocky faces and mountains coming right into the surf, while those on the east coast tend to be much flatter. What this emphasizes is the difference with California's coastline being pushed out of the waves by tectonics faster than wave erosion can erode the coast down.

16.1.2 Energetic waves pummeling a rocky coast

Waves crashing on a rocky coastline at Point Lobos, CA. This picture emphasizes the great energy involved with these masses of water striking the rocks 24/7.

16.1.3 The phenomenon of lift illustrated in three circumstances

Three related processes: wave creation in the ocean, the generation of lift on an airplane wing, and the pulling force which moves sailboats forward. The commonality between the three is emphasizes with dark arrows showing the direction of movement generated by hashed areas identifying zones of lower pressure. For waves in the ocean, the hashed area on the face of a swell indicates a zone of uplift created when a smooth, laminar air flow moves over a curved ocean surface. Likewise, in an airplane wing, lift is dependent on laminar air flow moving a greater distance over the top of a wing than below it, creating a difference in pressure that allows airplanes to fly. The hashed area, indicating low pressure and uplift, appears on the back edge of the wing. For sailboats, the combination of curved sails (in the case here, a sloop configuration) creates zones of low pressure on the bow-side of sails, as indicated by the hashed areas. This allows boats to be pulled 45 degrees into the direction of the wind, rather than only being able to sail downwind.

16.1.4 Wavelength, amplitude, and the phenomenon of “feeling bottom.”

A wave cross-section, showing to normal, deep-water wavelength between two crests, and the corresponding wave base at one half of the wavelength. When this wave base intersects with the ocean bottom, we say the wave "feels bottom," and begins to change in the following ways: the waves slow, the amplitude increases, the wavelength shortens, and at 1/7 of the original wavelength, we get a crashing wave. The crashing, spilling waves at the most common type of wave that beach goers are accustomed to seeing, but they actually represent a small fraction of ocean waves because they occur only in water very shallow relative to wavelength.

16.1.5 Longshore current moving parallel to the coastline

Longshore current, showing wave swash and backwash going up the beach, then retreating from the beach, in a zig-zag fashion. The longshore current is the net sum of the movement of the smaller swash/backwash.

16.1.6 A headland causing wave refraction

A headland creating wave refraction, where the waves are initially straight and parallel to each other far from the shore. However,

as they approach the shore, the headland creates an area of shallow water relative to the adjacent areas, meaning that the wave base "feels bottom" there first, and consequently slows down. This bends and warps the wave shapes toward the sides of the headland, where there is increased erosion relative to the adjacent areas. The erosional areas are perpendicular to the direction of the waves, and as the wave form warps around the headland, that perpendicular shape makes the erosion seem to move toward the sides of the headland.

16.1.7 Wind and the Coriolis effect

Upwelling occurs where the combination of wind movement parallel to the coast (shown by the large red arrow) over the ocean and the Coriolis effect create under some conditions a "pulling away" from the coastline, moving parallel to the coast and then moving away from it (shown by the curved arrows on the ocean surface) of the upper regions of the sea. This creates a zone along the coast where deeper, colder, nutrient-rich water can rise to the surface, as indicated by the direction of arrows in the cross-section, showing movement pushing toward the coastline, then circling around and moving back to sea.

16.1.8 Typical sea surface temperatures along the California coast

A simple map of the California coast, showing the effects of the phenomenon of upwelling as it produces cold sea surface temperature regions (10°C) near the Central and Northern California coastline, with a gradation of warmer surface waters (15°C, 20°C) further from land, and also in areas of Southern California waters where upwelling does not occur.

16.2.1 Typical coastal features resulting from differential erosion

Coastal features created by differential erosion. Shown here are a sea stack, a sea arch, a sea cave, and a headland surrounded by beaches. Each of these features is created by wave erosion. Because headlands jut out away from the coast, they are subject to greater erosion, as explained in the previous section, and this erosion progresses first aa sea caves, which then form to meet as a sea arch. When enough erosion has occurred that the arch collapses, then a sea stack is created.

16.2.2 A well-developed sea cave

A sea cave in a cliff just north of Santa Cruz, CA. The deep indentation in the cliff was created by wave action.

16.2.3 A sea arch south of Jenner, CA

A sea arch at Jenner, CA, which has formed from a former headland being eroded in such a way that sea caves on either side meet and create a hole in the rock. This sea arch is less stable and will collapse in time, forming an island called a sea stack.

16.2.4 Distant sea stacks, remnants of a former headland

The coastline at Jenner, CA, showing numerous sea stacks both on the beach and in the water. In time these sea stacks will also be eroded into nothingness, as everything along coastlines should be considered as temporary and ephemeral as the latest meme.

16.2.5 A tombolo created from a former sea stack

Another view of the coastline at Jenner, CA, showing a rugged coastline with numerous sea stacks and a tombolo. This is a former sea stack that has created a calm area on the coastal side, allowing accumulation of drifting sand. In this case is so pronounced that it actually reconnects the former sea stack to land, forming a tombolo.

16.2.6 Three marine terraces

The phenomenon of marine terraces. The area under water is currently flattening the land through wave action, but if tectonics

lifts it up out of the water, this flat area then forms a terrace. There are three dry terraces to the left of the active erosional zone, indicating long periods of tectonics uplift interrupting wave erosion.

16.2.7 A marine terrace with “fossil” sea stacks

"Fossil" sea stacks on a flat marine terrace. The flat land is pocked with these large rocky outcrops, which represent former sea stacks that have been lifted out of the ocean by tectonic movement. Of note is the fact that the San Andreas resides shortly out of frame to the left; because of this proximity, quake here may be quite violent and capable of several meters of uplift in one major quake. These rocks now form a popular bouldering site. Also of note are smooth rubbings 4-5 meters off the ground; the prevailing theory is that Columbian mammoths (*Mammuthus columbi*) used these rocks to groom their long tusks, and it is not a stretch of the imagination to see this scene twelve thousand years ago as these giant proboscideans roamed this marine terrace in family groups, waiting their turn for clean their tusks. (Wooly mammoths may be more familiar to readers, but they did not live at these latitudes.)

16.3.1 Aerial photograph of a green dye exposing a rip current

Rip current on a beach exposed by releasing dye into the ocean. The dye is drawn out in the rip current perpendicular to the shore, in tight flow; this illustrates how narrow rip currents are, and emphasizes that the best way to escape them is to swim parallel to the beach a few tens of meters. Once out of the rip current, swimmers may easily return to shore, though it is impossible to swim directly against the fast flow of a rip current.

16.3.2 Comparison of two topographic maps of Esplanade Avenue, Pacifica

Two topographic maps showing the same area of Esplanade Avenue, Pacifica, CA, as it developed from 1950 to 1980. In that thirty year period, a huge development was built very closet to the Pacifica cliffs, which are highly unstable. Many of these structures have since been condemned and removed.

Left picture: Detail of the 1950 South San Francisco USGS 7.5 minute topographic map. Note that there is no development on the ocean side of the Edgemar neighborhood. Also of note: a sea stack known as Mussel Rock lies at the ocean entry point of the San Andreas fault. In 1950 this area was not developed.

Right picture: Detail of 1980 South San Francisco USGS 7.5 minute topographic map. Note that there is now extensive development along the coast side of the Edgemar neighborhood. In addition, a Daly City neighborhood has been developed near Mussel Rock.

Also of note the position of the San Andreas fault, which cuts across this heavily populated area. All of these postwar developments were put in without regard to either the hazard of eroding cliffs or the seismic violence of the future.

16.3.3 Dubious attempts to “armor” the coastline against wave erosion

Esplanade Ave, Pacifica, detailing the construction mentioned in 16.3.2. In the surf zone is the placement of numerous large boulders ("rip rap") which are intended to absorb wave energy and slow cliff erosion. However, given the nature of these cliffs as unconsolidated sand, such efforts at armoring the coast may only delay the inevitable wave erosion.

16.3.4 A closer look at attempts to “armor” the coastline

The beach below the armoring attempts from 16.3.3. Note the large chunks of concrete that have fallen down the cliff, suggesting the cliff is not successfully stabilized by this artificial hardware. Also of note are the layers of sand in the cliff; if one walks up to these layers, the sand comes apart easily in one's hand. There is no bedrock here; this is all perched on a pillar of loose sand.

16.3.5 Coastal erosion threatening an apartment complex

The cliff-side edge of a large apartment building on Esplanade Ave, Pacifica, now demolished and removed. When this building was constructed, there was a considerable amount of land, but the high rates of erosion have pulled the cliff toward the building with alarming speed. When this photograph was taken, residents were protected from the cliff edge by a wooden fence and netting. Only a few yard separates the building from the sea.

16.3.6 Cliff erosion resulted in the dreaded “red tag”

Official notices affixed to a residential door indicating that occupants may not longer legally live in this residence. One notice reads, "This building is deemed unsafe for human occupancy." The other emphasizes the danger: "Danger! This building is deemed unsafe for human occupancy. It is unlawful for any person to occupy or reside in this building." It gives the address as 329 Esplanade, number 46, and is dated July 13, 2015. Both notices were issued by the City of Pacifica Building Inspection Department.

16.3.7 A photo taken just south of Centerville Beach in 2023

A collapsed section of beach along the Lost Coast at Centerville Beach. This photograph shows a sign, at the headscarp of a recent landslide, warning hikers, "Hazardous Cliff, Stay Away." Now that the sign has nearly fallen that seems to be a bit redundant.

16.4.1 A seawall protecting the house behind the wall

The effects of a sea wall. Incoming waves are reflected by the sea wall with almost full energy, meaning that the waves carry away beach sand (the particles moving away from the wall). In the best case scenario, this eliminates the sand that made the beach enjoyable, and in the worst case, undermines the sea wall itself, causing possible collapse and endangerment of the house behind the sea wall.

16.4.2 Before and after human alteration to the shoreline

The unaltered example shows a waterway entering the ocean, with a smooth coastline and a longshore current parallel to the coast.

After jetties and groins were built the coastline, the pre-existing longshore current began eroding/depositing sand and altering the shoreline. This current is shown moving from left to right in the diagram.The waterway entering the ocean is now protected by rocky jetties that push out into the water. Water is pulled offshore as the current pushes against the first jetty, depositing more sand. Just beyond the second jetty the sand erodes away as water pushes onshore. Similar forces are at play where groins are built out into the water.

16.4.3 Before and after the installation of a breakwater

The unaltered example shows a smooth coastline with a longshore current parallel to the coast.

installation of a breakwater creates sand accumulation behind the breakwater. This alters the shoreline so that the sand eventually reaches the breakwater. In addition, water moves toward the coast on either side of the breakwater, eroding away the sand in those areas.

This page titled 16.8: Detailed Figure Descriptions is shared under a CC BY-NC 4.0 license and was authored, remixed, and/or curated by Steven Newton.

17: CALIFORNIA'S CLIMATE

Introduction to California's Climate

It was a warm Sunday morning on 15 August 2021 as the four members of the Gerrish-Chung family set out on a moderate hike near their home. Covid pandemic remote work allowed the family to relocate from the Bay Area to the bucolic foothills of the Sierra Nevada, in the town of Mariposa, close enough to Yosemite that the El Capitan monolith was visible from their house. This active family familiarized themselves with their new home by completing numerous local hikes, and were so well prepared for these sojourns that in addition to a generous 85-ounce water supply, they even carried a snakebite kit.

Two days later, authorities discovered four bodies exposed on a trail. Jonathan Gerrish, 45, Ellen Chung, 30, their one-year-old daughter Miju, and Oski, the family dog, were found just a mile and half from the top of a trail leading down to the Merced River.

Authorities were perplexed. There were no obvious signs of foul play or animal attack or suicide. They did not appear to have been struck by lightning. Toxicology discovered no signs of drug overdose. In the absence of an explanation of four seemingly-healthy individuals suddenly dying all at once, strange speculations abounded: perhaps they succumbed to toxic algae from the Merced River, perhaps a cloud of carbon dioxide released from an unknown Gold Rush-era mine and asphyxiated them. With no plausible explanation, authorities closed the area as a potential hazmat situation.

Police investigations stalled because of passcode-protected cell phones; however, once the FBI gained access to Jonathan Gerrish's cell, a clearer picture emerged. On that Sunday, the family awoke early and started their hike by 7:30 am, when the outside temperature was just 24°C (76°F). Gerrish's AllTrails app revealed a plan to descend to the Merced River, then return via another trail by 1 pm, before afternoon temperatures rose. They took the first selfie at 7:44 am. They reached the river and took a selfie at 9:05 am. By 10:29 am, they were ascending the trail toward home.

We will never know the full details of what happened next. But one stark fact remains: though the day's hike began with moderate temperatures, by late afternoon the exposed trail would have reached 42°C (109°F). Radiant heat from rocks and soil would have made it even worse. Moreover, this trail had been denuded of vegetation by a massive wildfire three years earlier. Fires of this kind are more common in California because of climate change-induced drought. Because of this earlier conflagration, the family had virtually no shade or relief from the increasingly sweltering sun. The unlocked cell phone revealed desperate attempts to call and text for help, none of which went through because of the lack of cell service.

Heatstroke can kill anyone–the young, the fit, the well-hydrated. For example, one would imagine that teenage athletes would be able to cope with exercising in high temperatures. But at least 50 high school football players are known to have died of heatstroke brought on by games and practices. Fans of the Harry Potter movie franchise may remember the character of Fenrir Greyback, the cannibalistic werewolf aligned with He Who Must Not Be Named. What such fans might not realize is that in 2014, the actor who played the werewolf–David Legano, a fit 50-year old professional martial artist and athlete–went on a solo day hike near Zabriskie Point in Death Valley and died of heatstroke. A month before the Gerrish-Chung family's deadly hike, a 37-year-old ultramarathon runner named Philip Kreycik died in Pleasanton, CA, while on an easy nine-mile loop he expected to complete in under an hour; the estimated outside temperature during his run was as high as 41°C (106°F).

It was not foolishness that doomed the Gerrish-Chung family. In a normal world, they would have no reason to expect that a moderate hike begun with moderate temperatures would transform into a life and death struggle. But this is the new reality for California's new climate. Our experience of playing outdoor sports, of leaving a pet in a car for a few minutes to run into a store, of a family taking a mild hike on a sunny day, all of these expectations are now wildly out of calibration with the lethal climate change our state faces.

This chapter investigates the phenomenon of California's climate in three ways. First, we examine the past climate history of California, which reveals that extremism is the norm rather than the exception. Second, we focus on what is currently happening, especially in regards to the rising temperatures threatening the fragile liveability of this parched state (see Figure 17.1). Lastly, we explore projections for our grim future in a warmer, deadlier California.



Figure 17.1: Polygonal dried mud cracks in the basin of the drought-drained Nicasio Reservoir, Marin County, CA, 2021. "Nicasio" by Steven Newton, is licensed under CC BY-NC 4.0. Access a detailed description.

Learning Objectives

- Describe the key concepts and terminology related to climate.
- Assess how past information informs us about current climate conditions.
- Analyze the potential of future climate changes on the environment and liveability of California.

17.1: Note on Usage

17.2: The Past

17.3: The Present

17.4: The Future

17.5: Hotter, Drier, Tougher

17.6: Chapter Summary

17.7: Detailed Figure Descriptions

References

1. Adams, A. (2021, December 5). New Information Emerges in Report Detailing Deaths of Calif. Family of 3 Who Died on Hiking Trip. People. https://people.com/human-interest/john-gerrish-ellen-chung-family-hiking-deaths-miju-dog-oski-update
2. Anguiano, D. (2021, October 21). California family found dead on hike killed by extreme heat, sheriff says. The Guardian. https://www.theguardian.com/us-news/2021/oct/21/california-family-hike-cause-of-death
3. PBS Newshour (2022, July 20). How extreme heat affects young athletes. Retrieved October 4, 2023, from https://www.pbs.org/newshour/science/how-extreme-heat-affects-young-athletes
4. Gander, K. (2014, July 14). Dave Legeno dead: Harry Potter actor found in Death Valley. The Independent. https://www.independent.co.uk/news/people/dave-legeno-dead-harry-potter-actor-found-in-death-valley-9601652.html
5. Larson, A. (2021, August 27). Pleasanton runner Philip Kreycik likely died from heatstroke in 106-degree weather, investigators say. Retrieved October 4, 2023, from https://www.kron4.com/news/bay-area/pleasanton-runner-philip-kreycik-likely-died-from-heatstroke-in-106-degree-weather-investigators-say/

This page titled 17: California's Climate is shared under a CC BY-NC 4.0 license and was authored, remixed, and/or curated by Steven Newton.

17.1: Note on Usage

Weather vs. Climate

Climate is not weather, and weather is not climate. However, you may have heard these related terms used interchangeably, so parsing their precise meanings is a good place to begin this story.

Following the definitions used by the National Oceanographic and Atmospheric Administration (NOAA), we should think of weather as short-term atmospheric conditions in a particular place, at a particular time. Climate, by contrast, can be best understood as a statistical pattern describing much longer time periods over larger regions, and involving a greater number of factors, including the variations of Earth's orbit and resulting fluctuations in ice ages and interglacial periods.

A single hurricane is *weather*. A pattern of hurricanes over many decades is *climate*.

As you have probably experienced, the weather forecast for an individual day can turn out to be quite inaccurate; in the morning you were assured there was no need for an umbrella, by the afternoon you are soaking wet from rain. Weather forecasts beyond one day become increasingly uncertain; the outer range of published forecasts is usually about ten days. This inability to predict weather, despite excellent data about real-time conditions and powerful computer models, is a function of the branch of science known as chaos theory, which mathematically describes limitations in systems in which very small changes in initial conditions produce very different results. Under the limitations of chaos theory, if there is an almost-unmeasurably small change in humidity or wind speed then that day's weather forecast becomes inaccurate. What chaos theory informs us is that we are simply never going to be able to predict long-term weather, not because of a lack of information or problems with computer models, but because of the laws of nature.

Those who deny the reality of climate change frequently cite this inability to predict short-term weather as an indicator that long-term climate predictions must also be suspect. This claim is without scientific merit, but it reinforces the importance of correctly distinguishing weather and climate. A related intentional misrepresentation of the difference between weather and climate posits that cold winters refute the idea of a warming world.

Climate, in contrast to weather, is highly predictable. We know that through statistical analysis over years of data, summers will tend to be hotter than winters, and winters cooler than summers, and we can moreover discern trends in the lengths and timings and intensities of these patterns. We know that hurricanes and tornadoes tend to be concentrated in certain months, but are virtually unknown in other months. We know that the changes in the concentrations of certain gases in the atmosphere, such as CO_2 (carbon dioxide) and CH_4 (methane), can exert a powerful forcing on the temperature of the atmosphere.

Forcings/Responses

Climate forcing is an important concept to understand. Forcings push climate in complicated directions and create responses. Many things can act as a forcing, including greenhouse gases and particles released from volcanoes; for example, the 1991 eruption of Mt. Pinatubo in the Philippines released so much sulfur dioxide that worldwide temperatures responded with lowered temperatures for two years. Another forcing is the orbital variations known as Milankovitch Cycles, which are linked to ice ages and interglacial periods. Changes in solar radiation–the intensity of sunlight–can also be a climate forcing. And, of course, in the current world the most important forcing of all is the prodigious amount of anthropogenic greenhouse gases, such as CO_2 and CH_4. (Anthropogenic means human-caused.) Of these anthropogenic greenhouse gases, carbon dioxide is currently responsible for the greatest forcing, though the influence of methane is rising.

Radiative Forcing

Radiative forcing refers to the difference between incoming and outgoing energy (see Figure 17.1.1). If the Earth were in balance–not getting hotter or colder–then the radiative forcing would be zero. If radiative forcing is positive, this indicates a warming world, and if negative, a cooling world. We are currently in the situation where more radiation accumulates on Earth than leaves Earth.

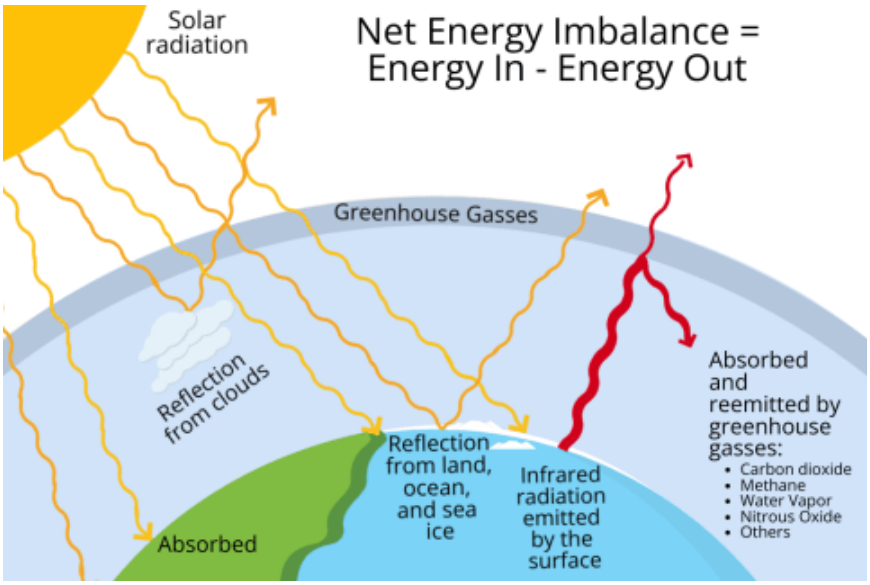


Figure 17.1.1: A diagram of solar radiation and energy inputs and outputs, titled "Net energy imbalance = energy in - energy out." This diagram shows the imbalance in sources heating from radiation versus infrared radiation responsible for cooling the planet. "Net energy imbalance" by Janelle Christensen, USDA is in the public domain. Access a detailed description.

If we choose the year 1750 (before the onset of the Industrial Revolution) as a baseline of 0.0 radiative forcing, then by 1950 the radiative forcing rose to 0.57 watts per square meter. (To understand the units of watts per square meter, think of a solar panel–how much electricity does a square meter solar panel produce?) By 1980, this radiative forcing rose to 1.25 W/m^2. By 2011, 2.29 W/m^2. And by 2019, 2.72 W/m^2. This rise in this radiative forcing speaks to an accelerating heating imbalance for our warming planet; anthropogenic greenhouse gases create this imbalance.

The understanding of climate forcings/responses is superior to simple cause/effect models. In a naive cause/effect model, one change in one place produces a proportional change elsewhere. Complicated, dynamic climate systems require a more informed approach. For example, we might posit that as CO_2 levels rise, all ocean temperatures will also rise in lockstep; however, in reality due to increased ice melting, some oceanic areas near Greenland are actually cooling as this frigid water–recently glacial ice–surges into the surrounding seas. We might imagine that as humans pump CH_4 into the atmosphere, the resulting rising temperatures will produce droughts; however, higher temperatures also exponentially increase the ability of the atmosphere to hold evaporated water, so some intense storms will actually be wetter, causing increased flooding events. This leads to the seeming contradiction that climate change enhances both droughts and floods. How can it be both? This is the reality of complicated forcing/response systems. Climate is inherently multifaceted, requiring more than a naive model of cause and effect. Climate forcing/response is the way to think about these factors.

Climate Change vs. Global Warming

On a final usage note, this book uses the term climate change rather than global warming. One problem with the older term global warming is that while the majority of the planet suffers from increasing heat due to anthropogenic forcings, some areas may experience cooling (recall the aforementioned cold waters near Greenland). Such exceptions will be pounced upon by well-funded, well-organized anti-scientific campaigns to deny the reality of climate change. The term climate change, by contrast, implies a weirding of climate–strange conditions, potentially both warmer and colder, drier and wetter. It is this stochastic destabilization of climate that so concerns scientists.

Query 17.1.1

This interactive element is not available in this format. Visit the link or scan the QR code to access it online.

View this Interactive Content online

Query 17.1.2

This interactive element is not available in this format. Visit the link or scan the QR code to access it online.

View this Interactive Content online

Query 17.1.3

This interactive element is not available in this format. Visit the link or scan the QR code to access it online.

View this Interactive Content online

References

1. Satterfield, D. (2011, January 24). Rebuttal to 'Scientist's Can't Even Predict The Weather Right'. Retrieved September 29, 2023, from https://skepticalscience.com/global-warming-cold-weather.htm
2. Mason, J. (2023, September 3). Does cold weather disprove global warming? Retrieved September 29, 2023, from https://skepticalscience.com/global-warming-cold-weather.htm
3. IPCC, 2021: Chapter 7, Figure 7.6. In: Climate Change 2021: The Physical Science Basis. Contribution of Working Group I to the Sixth Assessment Report of the Intergovernmental Panel on Climate Change [Forster, P., T. Storelvmo, K. Armour, W. Collins, J.-L. Dufresne, D. Frame, D.J. Lunt, T. Mauritsen, M.D. Palmer, M. Watanabe, M. Wild, and H. Zhang, 2021: The Earth's Energy Budget, Climate Feedbacks, and Climate Sensitivity. In Climate Change 2021: The Physical Science Basis. Contribution of Working Group I to the Sixth Assessment Report of the Intergovernmental Panel on Climate Change [Masson-Delmotte, V., P. Zhai, A. Pirani, S.L. Connors, C. Péan, S. Berger, N. Caud, Y. Chen, L. Goldfarb, M.I. Gomis, M. Huang, K. Leitzell, E. Lonnoy, J.B.R. Matthews, T.K. Maycock, T. Waterfield, O. Yelekçi, R. Yu, and B. Zhou (eds.)]. Cambridge University Press, Cambridge, United Kingdom and New York, NY, USA, pp. 923–1054, doi: 10.1017/9781009157896.009 .] https://www.ipcc.ch/report/ar6/wg1/figures/chapter-7/figure-7-6

This page titled 17.1: Note on Usage is shared under a CC BY-NC 4.0 license and was authored, remixed, and/or curated by Steven Newton.

17.2: The Past

Deep Time

Time itself seems frozen across the silent, icy expanses of the White Mountains, which form the eastern California border with Nevada. Rosy-fingered dawn blankets the frigid early morning in sparkling-ice vermillion light, witnessed by herds of wild horses as they watch dawn shadows cast into the broad defile of Owen's Valley, two miles below. Owen's Valley cleaves the White Mountains from the Sierra Nevada with a rift twice as deep as Grand Canyon. On the western side of Owen's Valley, the dizzyingly steep eastern front of the juvenile Sierra Nevada bursts abruptly out of ochre alluvial fans, its jagged granitic peaks challenging the indifferent sky.



Figure 17.2.1: A stand of Bristlecone pines growing on pale-white Reed Dolomite in the White Mountains, CA. "Reed Dolomite" by Steven Newton, is licensed under CC BY-NC 4.0. Access a detailed description.

On the other side of Owen's Valley lie the ancient rocks of the White Mountains, among the oldest in California. One of these antique units is the Reed Dolomite, a white, sugary mixture of calcium and magnesium whose formula is $CaMg(CO_3)_2$. (Students who have completed a Physical Geology lab course will recall that while limestone reacts readily to hydrochloric acid, the similar-looking dolomite must be powdered before it will fizz.) Dolomite cannot form in substantial quantities in today's world, but the dolomites of the White Mountains are hundreds of meters thick. From a distance, the Reed Dolomite hills look covered with snow, as the ground often is, but even in summer the bleached dolomite imparts a pallid color.



Figure 17.2.2: Snow-covered carbonate soil hosting a number of Bristlecone pines (Pinus longaeva) in the high-elevation White Mountains near the eastern border of California/Nevada. "Bristlecone pine" by Rick Goldwaser is licensed under CC BY-NC 4.0. Access a detailed description.

The Reed Dolomite is the preferred home of the Bristlecone pine (*Pinus longaeva*), whose weathered trunks twist out of the pale soil like crenulated corkscrews. They are the oldest individual multicellular organisms on planet Earth. This claim is sometimes heatedly disputed; there is a creosote shrub in the Mojave, the *Larrea tridentata*, that dates to 11.7 ka, however what is being dated are generations of colonial offshoots from a central plant that died long ago, so saying this is the oldest organism is a bit like calculating your age by including your great-great grandparents. There is also evidence for long-survival of bacterial spores in a dormant state, but in terms of continuously active, multicellular, single organisms, nothing is longer in the tooth than Bristlecone pines. The oldest Bristlecone, a particularly gnarled specimen called the Methuselah Tree, was dated in 1957 at 4,789 years, meaning its nascent sprouts saw first light about 2833 b.c. To put that in perspective, Stonehenge was newly begun, construction of the pyramids of Giza was hundreds of years away, and the Trojan War was fifteen hundred years in the future. The Methuselah Tree is an old, old tree. And across the Reed Dolomite slopes of the White Mountains, there are thousands upon thousands of these ancient Bristlecones.

Trees are an excellent tool to assess past climate. Annual tree rings, which can be cored in a non-destructive way, show direct information about conditions. All else being equal, wetter periods produce more tree ring growth and wider rings, while drier or colder conditions stunt tree ring width. Analysis of trends in tree rings can thus establish data about climate.

Dendrochronology

This study and dating of tree rings is called dendrochronology, and it offers powerful windows into past climates (see Figure 17.2.3). The White Mountain Bristlecone dendrochronology yields data for California climate for over 8,000 years. Other tree species also provide information for shorter time periods. Whether using ancient Bristlecone pines, or fast growing sycamores, there is an ancient story embedded in the trees themselves. What do the trees whisper to us?

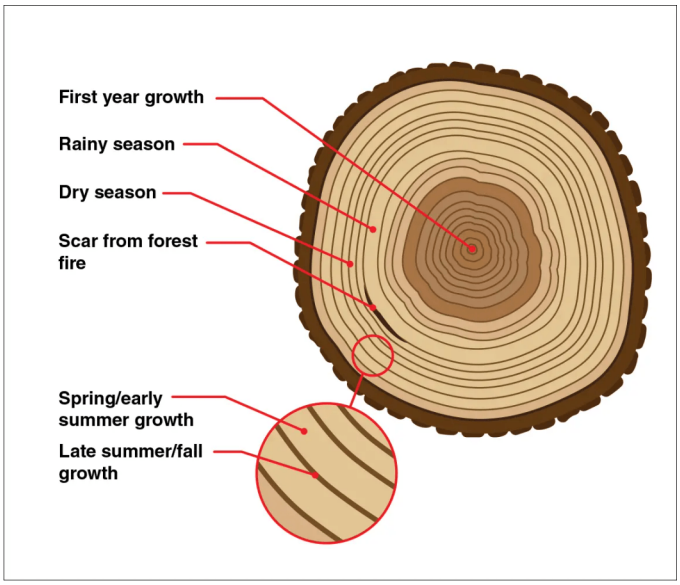


Figure 17.2.3: The dendrochronology principle of differential annual tree ring growth. "Tree rings" by NASA is in the public domain. Access a detailed description.

In the video below, Video 17.2.1, a NOAA paleoclimatologist explains the science behind tree rings and how they provide a record of tree growth under different climate regimes:

Video 17.2.1: Dendrochronology

A video about dendrochronology

This interactive element is not available in this format. Visit the link or scan the QR code to access it online.

View this YouTube Video online

Dendrochronology informs us that California's climate is characterized by *extremes*. California experiences so much climate variation that positing "normal" conditions is almost meaningless. California has been much warmer and much colder than today. California has experienced much wetter periods than today. California has experienced much drier periods than today; in fact, dendrochronology reveals extended "megadroughts" lasting many decades. While there is not a strict definition of the term megadrought, they can be understood as lasting many decades; in other words, shorter duration climate events, such as the Dust Bowl (1932-1939), are not megadroughts.

Megadroughts

According to dendrochronological data, megadroughts gripped California between 892 A.D. and 1112 A.D., and between 1209 A.D. to 1350 A.D. So as William the Conqueror secured his reign in England after 1066, and as the Black Death claimed its first victims in 1346, California suffered profound, deep droughts that parched the land and challenged its inhabitants.

Figure 17.2.4 shows the severity of California droughts over the previous thousand years using a scale called the Palmer Drought Severity Index:

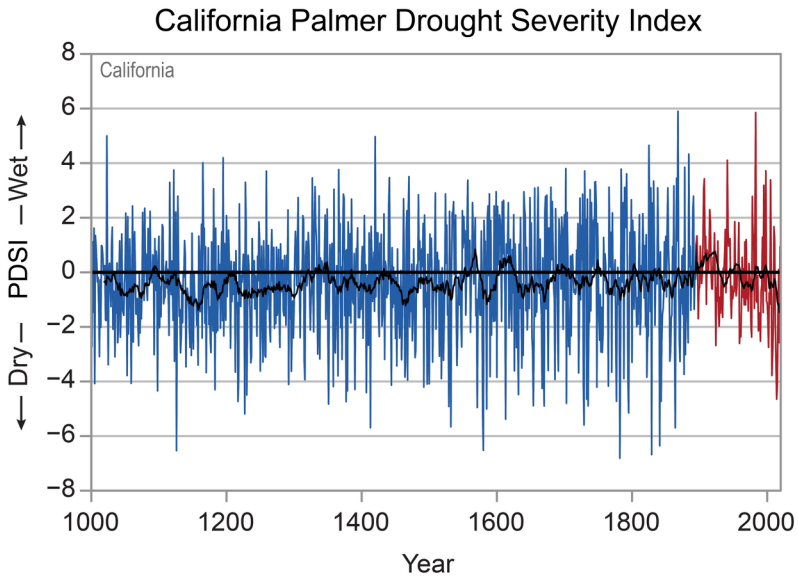


Figure 17.2.4: California Palmer Drought Severity Index Scale, by Frankson, R., L.E. Stevens, K.E. Kunkel, S.M. Champion, D.R. Easterling, W.. "Drought index" by NOAA is in the public domain. Access a detailed description.

This extremism is not limited to the last millennium. Looking further back in time, a 2015 study of pollen collected at Lake Elsinore in Southern California, east of Santa Ana, reveals a period of severe megadroughts between 27.5 - 25.5 ka. These intense, long-lasting droughts changed local vegetation patterns significantly enough to be recorded as pollen changes in lake sediments.

Were such events to repeat today, such prolonged megadroughts would reshape everything about how we live in California. Many argue we are currently entering just such a megadrought.

A cognitive bias for Californians is that the 20th century was actually an unusually wet period. Twentieth century expectations of rainfall, snow melt, and river flows, used in planning for public water projects, are all based on erroneously high assumptions about precipitation. We Californians still talk about drought as if it were a temporary situation, to be addressed by virtuously watering the lawn less; the reality is that this state usually is far drier than can sustain the current inefficient agricultural practices and bloating population growth.

In addition to drought, tremendous precipitation also happens in California. Remember that dendrochronology tells us that California's climate oscillates between extremes. Sometimes outliers involve more precipitation than usual.

During the winter of 1861-1862, a series of storms flooded California so extensively that the Central Valley became an inland sea for months. Downtown Sacramento became impassable; the newly elected governor, Leland Stanford (who would later found the eponymous Stanford University), had to arrive at his own inauguration via boat. The capitol was temporarily relocated from Sacramento to San Francisco. This event involved atmospheric rivers of precipitation that direct one Pacific storm after another toward the West Coast.

ARkstorms

Could this happen again? The United States Geological Survey (USGS) has researched the possibility of a recurrence of the 1861-1862 event, which they term an ARkstorm event. (This rather awkward acronym means "atmospheric river 1000.") The upper estimation of damages to California from a repeat of the 1861-1862 scenario could reach $750 billion, on the order of the entire national GDP of the country of Taiwan.

Just as Frost described the end of the world as either by fire or by ice, California's berserk past climate is a story of apocalypse–severe parching droughts punctuated by catastrophic deluges, oscillating wildly between arid cracked ground swept with wildfires and soaked hillsides collapsing after receiving a year's worth of rain in a day.

Query 17.2.1

This interactive element is not available in this format. Visit the link or scan the QR code to access it online.

View this Interactive Content online

References

1. Ferguson, C. W. (1979). Dendrochronology of Bristlecone Pine, Pinus Iongaeva. Environment International, 2, 209-214. https://doi.org/10.1016/0160-4120(79)90003-5
2. Gupta, R.S., Steinschneider, S., & Ree, P.M. (2023). Understanding the contributions of paleo-informed natural variability and climate change to hydroclimate extremes in the San Joaquin Valley of California. Earth's Future, 11, e2023EF003909. https://doi.org/10.1029/2023EF003909
3. Nutt, D. (2023, November 30). California's Hidden Climate History: A Remarkable 600-Year Tree Ring Analysis. SciTech Daily. Retrieved December 2, 2023, from https://scitechdaily.com/californias...ring-analysis/
4. Cook, B. I., et al., (2016). North American megadroughts in the Common Era: Reconstructions and simulations. Wiley Interdisciplinary Reviews: Climate Change. https://doi.org/ 10.1002/wcc.394
5. Stine, S. (1994) Extreme and persistent drought in California and Patagonia during mediaeval time. Nature 369, 546–549. https://doi.org/10.1038/369546a0
6. Heusser, L. E., Kirby, M. E., & Nichols, J. E. (2015). Pollen-based evidence of extreme drought during the last Glacial (32.6–9.0 ka) in coastal southern California. Quaternary Science Review, 126, 242-253. https://doi.org/doi.org/10.1016/j.quascirev.2015.08.029
7. Columbia Climate School (2022, February 14). Megadrought in Southwest Is Now the Worst in at Least 1,200 Years, Study Confirms. Retrieved November 4, 2023, from https://news.climate.columbia.edu/2022/02/14/megadrought-in-southwest-is-now-the-worst-in-at-least-1200-years-study-confirms/
8. Porter, Keith, et al., (2011). Overview of the ARkStorm scenario: U.S. Geological Survey Open-File Report 2010-1312, 183 p. and appendixes. http://pubs.usgs.gov/of/2010/1312/

This page titled 17.2: The Past is shared under a CC BY-NC 4.0 license and was authored, remixed, and/or curated by Steven Newton.

17.3: The Present

A Mediterranean Climate

The most common way to describe California's climate is "Mediterranean." This is true but too simplistic.

A Mediterranean climate means warm, dry summers with wetter, temperate winters. It is not unusual for rains to cease in spring and not return in any appreciable amount until fall (see Figure 17.3.1:). While this description matches climate patterns for much of California, this state has much elevation variation, numerous differences between coastal and inland areas arising from the buffering effects of ocean proximity, and spans many degrees of latitude–from latitude 32 near the Mexican border to latitude 42 near Oregon.

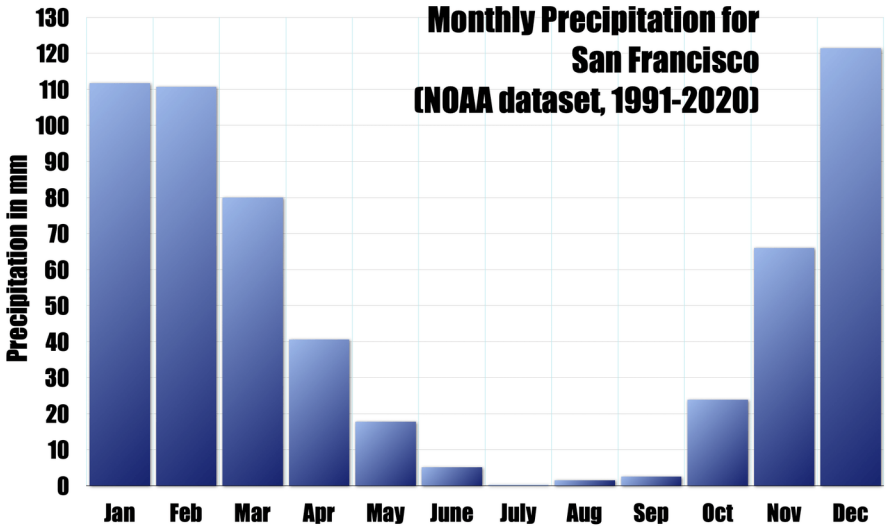


Figure 17.3.1: San Francisco's annual precipitation profile, with months compared to millimeters of precipitation, using a NOAA dataset from 1991-2020. "SF monthly precipitation" by Steven Newton, is licensed under CC BY-NC 4.0. Access a detailed description.

California's climate experiences significant variations on a year-by-year basis. In 2013, average statewide rainfall totals were only 20 cm, while in 1983 that number was 108 cm. When even a straight-forward question such as "How much rain does California get?" is answered by 400% variations, that makes broad characterizations suspect.

California's climate variation is highly local. For example, rainfall in Death Valley averages only 5 cm/year, while Eureka typically receives over 100 cm/year. One reason for Death Valley's peculiar aridity is its position in an exceptional "rain shadow," meaning that surrounding mountain ranges squeeze moisture from clouds before they can reach Death Valley. There's precipitation nearby, but it just doesn't reach Death Valley.

Rain Shadows

The first step in understanding Death Valley's local rain shadow is to know that the dominant flow of wind is from the west to the east, with moisture laden clouds first rising up over the Sierra Nevada foothills. This rising creates orographic precipitation, which is to say that as moisture-rich clouds are forced to higher altitudes, they cool, condense, and drop their moisture. In Death Valley, this orographic precipitation first occurs as clouds move over the Sierra Nevada from west to east, then descend into Owen's Valley, then are driven up over the White-Inyo Mountains, then descend into the Panamint Valley, then rise up over the Panamint Range, and only then does any remaining moisture have a chance of reaching Death Valley. That's why Death Valley is so arid, while the nearby Sierran peaks have frequent snowfall and glaciers.

A profile of the Death Valley rain shadow may be found in Figure 17.3.2.

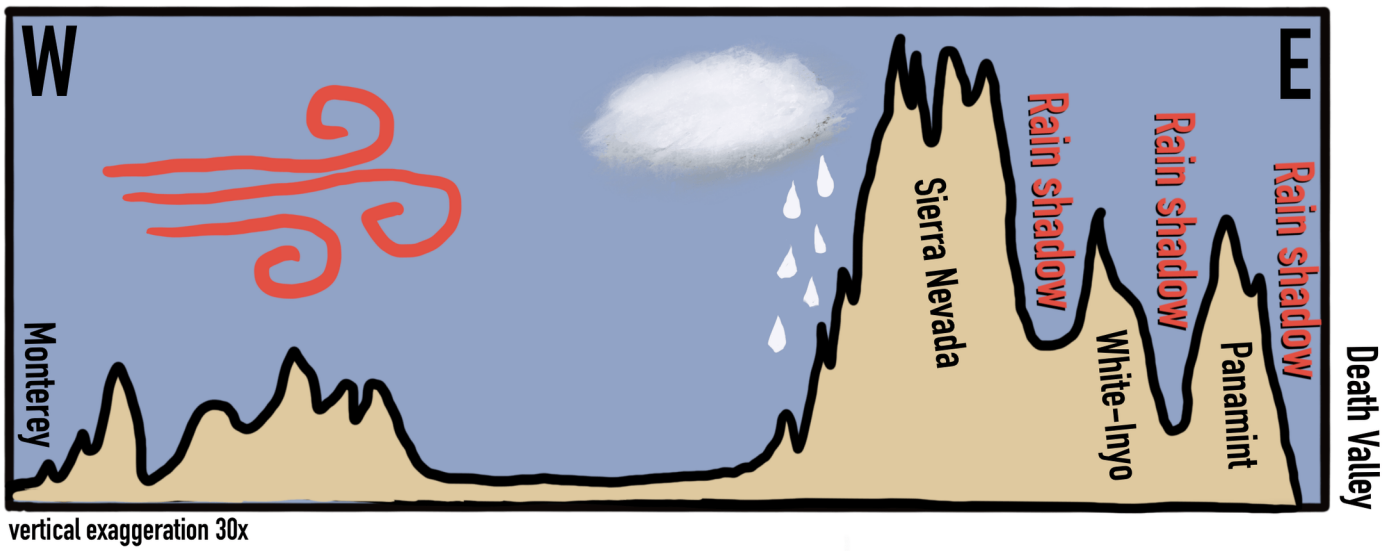


Figure 17.3.2: The rain shadow effect across California from Monterey to Death Valley. As winds trend from west to east, oceanic moisture is blown over the Coast Ranges toward the Sierra Nevada, where it is pushed to higher elevation, triggering precipitation. This pattern repeats eastward in the Owens Valley and Panamint Valley before reaching Death Valley, which experiences very low precipitation due to this phenomenon. "Rain shadow" by Steven Newton, is licensed under CC BY-NC 4.0. Access a detailed description.

Death Valley lies within a region of extremes. The lowest point in the contiguous United States is Badwater in Death Valley, 86 meters below sea level, while the base of the highest point, Mt. Whitney (4221 meters), is just a two-hour drive away. Death Valley is also the site of the hottest recorded temperature on Earth: 56.7°C (134°F), July 1913 (though some dispute this claim). By contrast, the town of Truckee, north of Lake Tahoe, is so cold that it regularly experiences winter days below -30°C.

Trying to squeeze so many diverse conditions into one label–“Mediterranean”–is a fool’s errand. To mangle Tolstoy, in California all climates are alike, but each is extreme in its own way.

Köppen Climate Classification

The “Mediterranean” term derives from a taxonomy known as the Köppen climate classification. This figure shows the Köppen system applied to California.

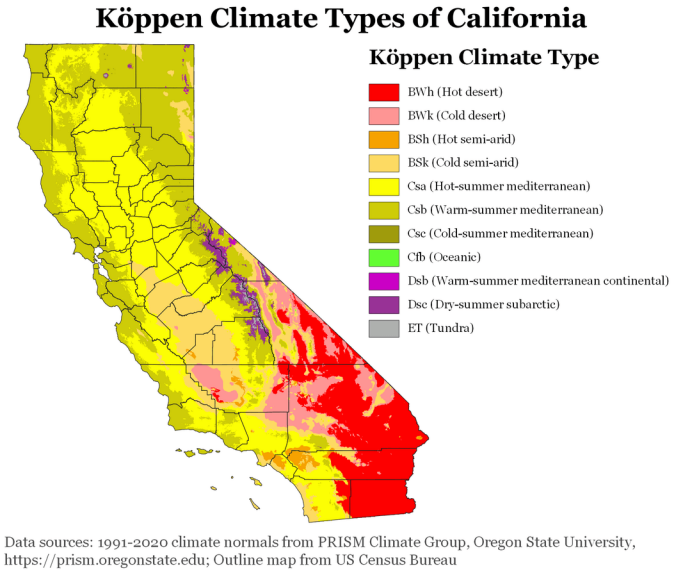


Figure 17.3.3: The Köppen climate classifications for California showing the distribution of 11 different climate zones. "Koppen climate classification" by Adam Peterson is licensed under CC BY-NC 4.0. Access a detailed description.

As Figure 17.3.3: above shows, four out of eleven Köppen zones are described as Mediterranean, with their areas accounting for a plurality of the entire state. However, a closer examination will reveal many other zones: the Mojave is described as “hot desert,” while the High Sierra is called “dry-summer subarctic,” and Mt. Shasta and the high White Mountains are a “tundra.” The variation in Köppen zones–tundra to hot desert–reinforces the idea that representing the whole of California by any one category makes little sense, and we should approach describing California’s climate in highly local terms.

Trends

Rising anthropogenic CO_2 causes many climate forcings and responses. Elevated carbon dioxide affects many climate systems in a multitude of ways. A good analogy for the role of carbon dioxide in climate is the role of elevated blood sugar in diabetes. Chronically high blood sugar hurts nearly every organ in the human body: kidneys, eyes, nerves, skin, the heart. Likewise, chronically high carbon dioxide affects nearly every aspect of the climate: temperature, precipitation, hurricanes, oceanic circulation.

Higher temperatures are a major effect, and these temperatures exacerbate long term drought trends. These droughts have led to reductions in a major way California sustains its water, the vital snow pack. Concomitant with drought is wildfire, and hardly a summer now goes by without major wildfires burning through California’s tinder-dry dead vegetation, some of which dies because of invasive insects previously suppressed by colder winters. One study found after the 2012-2015 drought a 30% rise in ponderosa pine (*Pinus ponderosa*) deaths due to the warmth-induced accelerations of the life cycle of western bark beetles.

But even in a warmer, drier climate, the extremes may present in the opposite way, with atmospheric rivers dousing California with intense storms, leading to flooding, landslides, problems with reservoirs, or even land subsidence.

The bottom line: most of these changes are for the worse. We’ll begin with temperature.

Trends: Higher Temperatures

People could hardly believe the forecasted heat.

It was 29 June 2021, and swaths of the west coast baked under relentlessly sweltering temperatures as a ridge of high pressure trapped air masses. The heat hit worst in Canada, with Lytton, B.C., clocking in at 49.6^{o}C (121.3^{o}F), hotter than Abu Dhabi on the same day, and nearly as hot as a medium-rare steak should be cooked. The following day 90% of the town of Lytton was destroyed in a wildfire, with two fatalities. Over 500 fellow Canadians died from heatstroke. In Seattle, portions of interstate highway 5 closed when its pavement itself buckled due to thermal expansion. Portland, OR, reached 47°C (116°F), shutting down its light rail

system, and spiking sidewalk temperatures at over 82°C (180°F). Redding, CA, achieved 46°C (114°F). Just as electrical demand surged, three separate power plants in California shut down because of the excessive heat. California Governor Newsom declared a state of emergency.

While these scorching temperatures would not be unknown in Phoenix, AZ, the big difference is that air conditioning is much rarer in these cities than in Phoenix, where A/C is fundamental for life support. Relatively mild California temperatures, both in winter and summer, mean that many older homes were built without insulation, double-paned windows, or central air conditioning. One study found that only 54% of California homes used central air conditioning. In temperate locales such as the Bay Area, that number drops to 47%. California has the highest percentage of any mainland state of homes without air conditioning.

This lack of home temperature control in California is becoming unsustainable. As Figure 17.3.4 details, since 2010 there has been a surge of high temperatures, compared to the previous century.

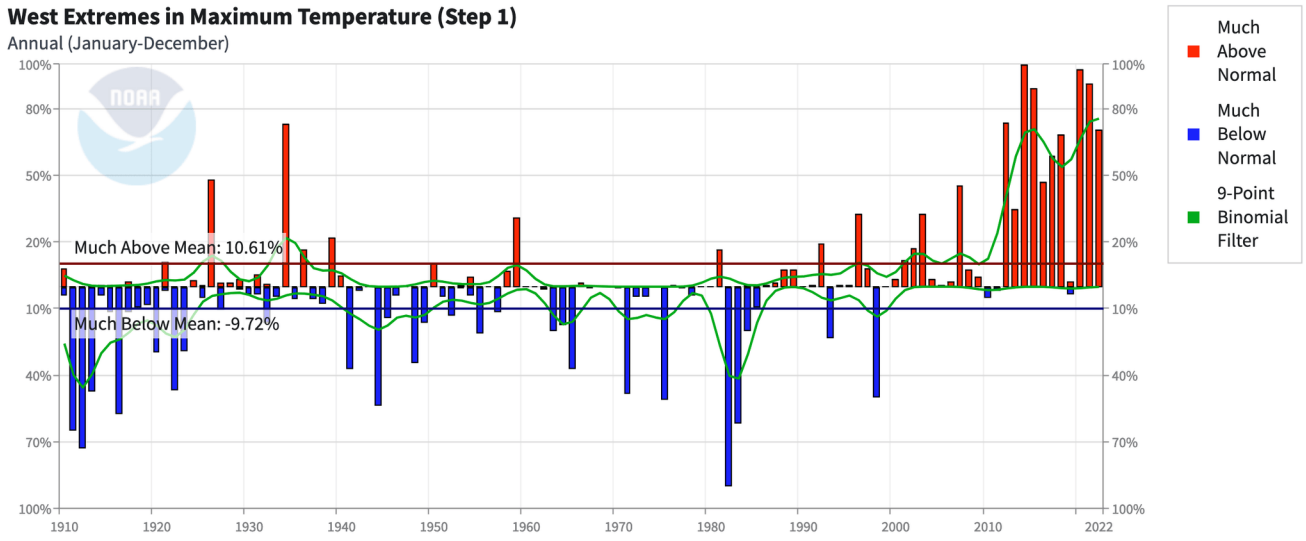


Figure 17.3.4: Extremes in maximum temperature, 1910-2022, with trend lines shows the degree of variation. "US West Extremes" by NOAA licensed under public domain. Access a detailed description.

Trends: High Pressure Ridges

California's climate is characterized by long, dry summers, contrasted with brief, mild winters in which most of the annual precipitation falls in a series of storms. The mountain snow pack created by such storms then gradually melts, supplying some flow to rivers throughout the long dry spell.

At least, that's the way things are supposed to happen.

In recent years, California's precipitation patterns have been disrupted by the presence of the North Pacific High, an area of high pressure that is parked, semi-permanently, off the coast of California. This high pressure area interacts with the jet stream to deflect incoming Pacific moisture, and is a primary reason why California experiences such prolonged periods without significant precipitation (typically May to September). A related phenomenon appeared between 2011-2017, a ridge of high pressure exacerbated by warm ocean temperatures; because of its longevity and effective blockage of incoming storms, it was termed the Ridiculously Resilient Ridge. The Ridiculously Resilient Ridge is thought to be a prime reason for the dramatic droughts in the 2010s.

When west-to-east wind flow encounters the North Pacific High, the winds, and their moisture, is often deflected to the north. Seattle typically receives 100 cm/year of precipitation, while Los Angeles receives about 36 cm/year.

The typical climate pattern is for the North Pacific High to migrate southward in winter, allowing a series of storms to reach California. The winter period, and in particular the months of December, January, and February, is when the majority of moisture reaches parched California.

Trends: Drought

Concomitant with higher temperatures is drought. Four periods of major drought have afflicted California in the new millennium: 2000-2003, 2007-2009, 2012-2016, and 2020-2022. The overall period from 2000 to now constitutes the driest regime in the last 1,200 years.

These periodic droughts are frequently broken by relatively short periods of torrential rainfall. For example, the 2020-2022 drought ended due to winter 2022 rains, with many areas of the state exceeding 200% of normal precipitation.

Trends: Snow pack

At higher elevations, much of California's winter precipitation falls as snow. The California snow pack is a crucial component to the state's water supply because much of the rainfall is not captured and flows directly back toward the sea. (It is somewhat surprising given our periodic droughts that California allows so much of its precipitation to go uncollected, but because of the nature of so much water falling all at once, cities go to great lengths to allow the water to exit, thus avoiding flooding.) The snow pack therefore acts as California's water reserve, and its gradual melting keeps rivers flowing in warmer months; the snow pack is responsible for about 30% of the state's water. This flow is important not only for preserving life in streams, but for holding back saltwater encroachment in the Delta region (see the chapter on California's Water for information about saltwater intrusion).

By custom, snowfall is assessed annually at a station near Donner Summit, and the snow water equivalent (SWE) is determined. One cannot simply measure the inches of existing snow because there is so much variation–loose fluffy snow mixed with compacted snow. SWE is what would result if all the snow in a column melted instantaneously. During the deep drought year of 2015, the Donner snow measurement, performed on 1 April 2015, showed only 5% of the long-term average SWE (see Figure 17.3.5).

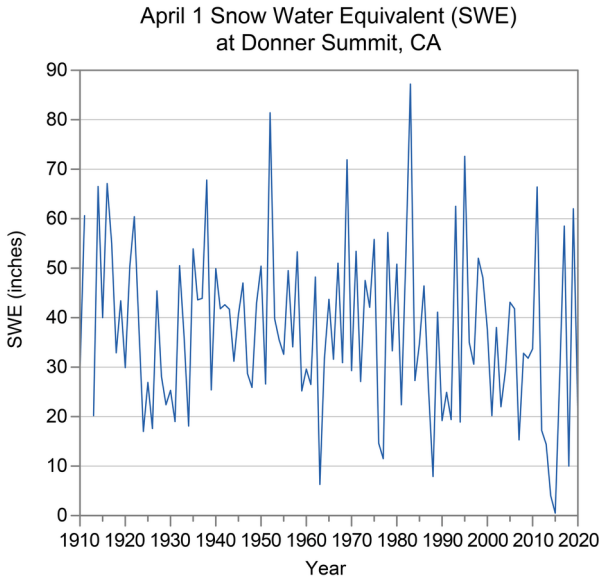


Figure 17.3.5: Snow Water Equivalent at Donner Summit, CA by Frankson, R., L.E. Stevens, K.E. Kunkel, S.M. Champion, D.R. Easterling, W. "Snow water equivalent" by NOAA is in the public domain. Access a detailed description.

Another issue is *where* snow falls. With the warmer temperatures of climate change, the snow line–the elevation at which precipitation drops as snow–rises, but it can't elevate indefinitely. So future increases in the snow line can produce reductions in the snow pack, and hence, in California's water system.

Trends: Atmospheric Rivers

Each of the four recent drought periods mentioned above (2000-2003, 2007-2009, 2012-2016, and 2020-2022) ended with periods of unusually high precipitation, due to the phenomenon of atmospheric rivers. Atmospheric rivers involve a series of Pacific storms, one after another, moving straight toward California in a shape that from the satellite view resembles a river (see

Figure 17.3.6 and Figure 17.3.7).

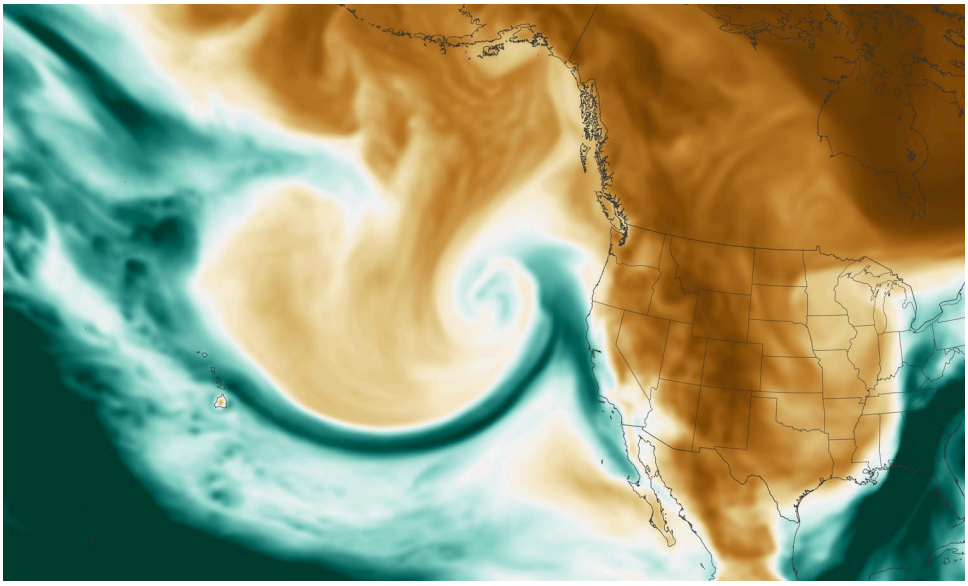


Figure 17.3.6: Illustration of an atmospheric river. "Atmospheric river" by NASA is in the public domain. Access a detailed description.

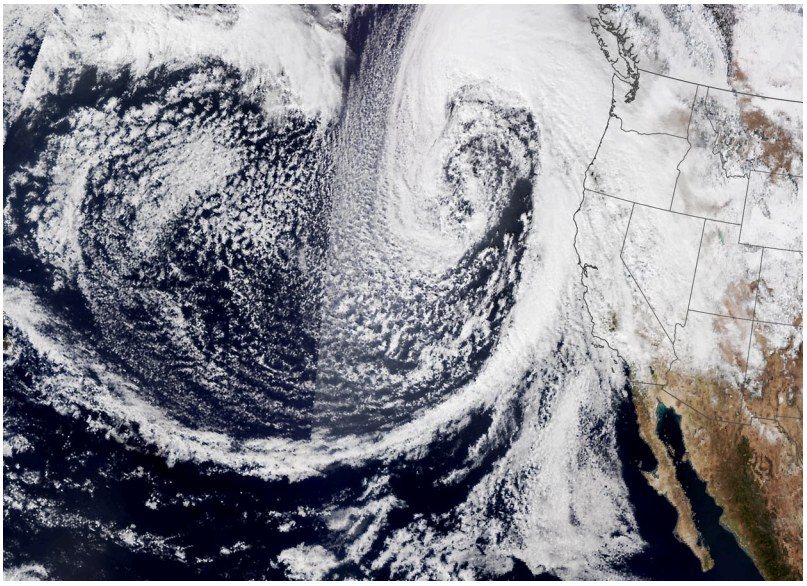


Figure 17.3.7: A 4 January 2023 satellite picture of an atmospheric river. This is the reference that was used to create Figure 17.3.6. "Atmospheric river" by NASA is in the public domain.

In this soundless video below, Video 17.3.1, we see North America enveloped in rotating precipitation patterns as they migrate from west to east across the Pacific Ocean toward California. The circulation patterns seem to take aim directly at California compared to other western states; this is the "atmospheric river" regularly soaking California.

Video 17.3.1: Atmospheric Rivers

A video showing the movement of an atmospheric river, as described in the text.

This interactive element is not available in this format. Visit the link or scan the QR code to access it online.

View this YouTube Video online

Atmospheric rivers reflect the fact that California not only tends to get most of its precipitation during a few months, but even within those wet months, almost all of that precipitation falls during very brief storms, often lasting only a few days. These atmospheric river events account for roughly half of the water in the western U.S.

One might imagine that drought-stricken California would wish to capture this bounty of water, but drainage is actually a more critical concern, and much of this inundation is encouraged through flood infrastructure to return freely to the ocean; the sudden downpouring of atmospheric rivers create severe issues with flooding and landslides. Nonetheless, there have been recent investigations into capturing more of this precipitation via increased dams to ease California's persistent droughts.

All such efforts, though, pale in comparison to the comically-absurd audacity of what has become known as the "Reber Plan." This fantastical proposal set out to capture all the drainage of the Sacramento River, California's largest river, by installing dams across San Francisco Bay (see Figure 17.3.8). While this postwar lark would have stored immense quantities of fresh water, its hydrologic plausibility was always suspect; nonetheless, to test this idea, a giant working scale model of the San Francisco Bay was constructed in Sausalito by the U.S. Army Corps of Engineers, and can be seen today at the Bay Model Visitor Center.

Intriguingly, if the Reber Plan had ever been constructed, and a dam from Marin to Richmond controlled the flow of the Sacramento River, this dam would have offered unanticipated protection for inland California from the problem of climate change–induced sea level rise.

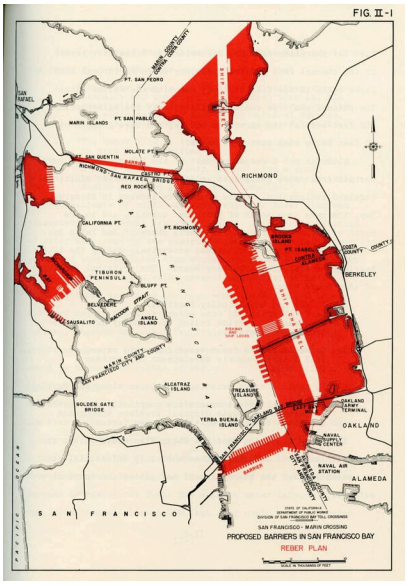


Figure 17.3.8: An illustration of the Reber Plan, showing areas in red where dams would have been constructed in the waters of the San Francisco Bay. "Reber plan" by State of California, Department of Public Works is in the public domain. Access a detailed description.

Query 17.3.1

This interactive element is not available in this format. Visit the link or scan the QR code to access it online.

View this Interactive Content online

References

1. U.S. Energy Information Administration (March 2023). Highlights for air conditioning in U.S. Homes by state, 2020. Retrieved December 6, 2023, from https://www.eia.gov/consumption/residential/data/2020/state/pdf/State%20Air%20Conditioning.pdf
2. Bump, P. (2022, September 7). Californians may no longer be able to avoid air conditioning. The Washington Post. https://www.washingtonpost.com/politics/2022/09/07/californians-may-no-longer-be-able-avoid-air-conditioning/
3. Williams, A.P., Cook, B.I., and Smerdon, J.E. (2022). Rapid intensification of the emerging southwestern North American megadrought in 2020-2021. Nature Climate Change, 12(3), 232-234. https://doi.org/10.1038/s41558-022-01290-z
4. National Public Radio (2023, January 9). California is getting drenched. So why can't it save water for the drought? NPR.org. Retrieved November 9, 2023, from https://www.npr.org/2023/01/07/1147494521/california-weather-storm-water
5. Shao, E., Rojanasakul , M., & Popovich, N. (2023, March 17). A Very Wet Winter Has Eased California's Drought, but Water Woes Remain. The New York Times. https://www.nytimes.com/interactive/2023/climate/california-drought.html
6. Cassidy, E. (January 2023). Atmospheric River Lashes California. NASA Earth Observatory. Retrieved December 8, 2023, from https://earthobservatory.nasa.gov/images/150804/atmospheric-river-lashes-california
7. Vartabedian, R. (2023, January 13). In a Drought, California Is Watching Water Wash Out to Sea. The New York Times. https://www.nytimes.com/2023/01/13/us/california-drought-storms-water-storage.html

This page titled 17.3: The Present is shared under a CC BY-NC 4.0 license and was authored, remixed, and/or curated by Steven Newton.

17.4: The Future

The Climate Future of California

Tides rarely attract a crowd.

But in California, under just the right positions and orbits of the moon and the sun, unusually high tides appear, offering an ominous glimpse of what rising sea levels will look like in the future. These “King Tides” are of interest to earth scientists and the California Coastal Commission, which runs the California King Tides Project, tasked with distributing information about upcoming King Tides and collecting citizen photographs as a way to visualize future sea levels. Their motto: “Snap the shore, see the future.”

And the problematic future looks like Figure 17.4.1:



Figure 17.4.1: In a harbinger of future sea level rise, a King Tide splashes onto the streets of the Embarcadero at the San Francisco waterfront. "King tide" by Steven Newton, is licensed under CC BY-NC 4.0. Access a detailed description.

In this picture, a King Tide puts the ocean nearly level with the Embarcadero, the major traffic artery forming San Francisco’s eastern waterfront. In our current time, King Tides in San Francisco spill only the larger waves onto the streets. Some day, normal high tides will periodically flood the entire road, forcing intermittent traffic closures. As sea level continues to rise, this flooding will happen even under low tide conditions, necessitating the closure of the Embarcadero and the abandonment of San Francisco’s coastline to the swelling brine.

The climate future of California can be assessed in a number ways. We will examine sea level rise and increased heat. These are far from the only effects California can expect from climate change, but understanding them is a place to start.

Sea Level Rise

By 2050, we can expect sea level to rise 0.3 meters. While this might not seem so much, 0.3 meters is more than the entire last century. And the oceans are just getting started with us.

A couple of factors affect sea level. Thermal expansion is one factor rooted in basic physics: objects expand when heated, and contract when cooled. Water is no exception. The vast majority of climate change heat is being absorbed by the world’s oceans, with the consequence that sea level rise will happen from thermal expansion alone.

There is the additional factor of the melting of land-based ice. As glaciers on land liquefy, their water transfers from land into the

oceans–imagine ice-water fire hoses in Greenland and Antarctica aimed directly into the seas. (The distinction of land-based ice from floating sea ice is important, because floating sea ice, which forms seasonally in the Arctic and Antarctica, has no net effect on sea level because it already displaces its volume.)

The best source for information on climate topics comes from the Intergovernmental Panel on Climate Change (IPCC), which periodically releases assessment reports, the most current of which is called AR6 (assessment report number six; released between 2021 and 2023). According to the IPCC AR6, we can attribute 38% of sea level rise to thermal expansion, and 41% from glacial melt (Fox-Kemper et al., 2021). Both of these factors contribute to worldwide sea level rise, but California experiences additional phenomena. The El Niño Southern Oscillation (ENSO) affects ocean temperature on short time scales, and the Pacific Decadal Oscillation (PDO) on longer time scales, each altering the temperature of oceanic waters off California's coast.

How bad will California sea level rise become? There are many different estimates, each based on assumptions about the future we cannot fully know right now.

The IPCC AR6 details a range of projections for sea level rise; the projections differ based on the degree to which future governments do or do not control greenhouse emissions. Figure 17.4.2 shows a middle ground for these scenarios:

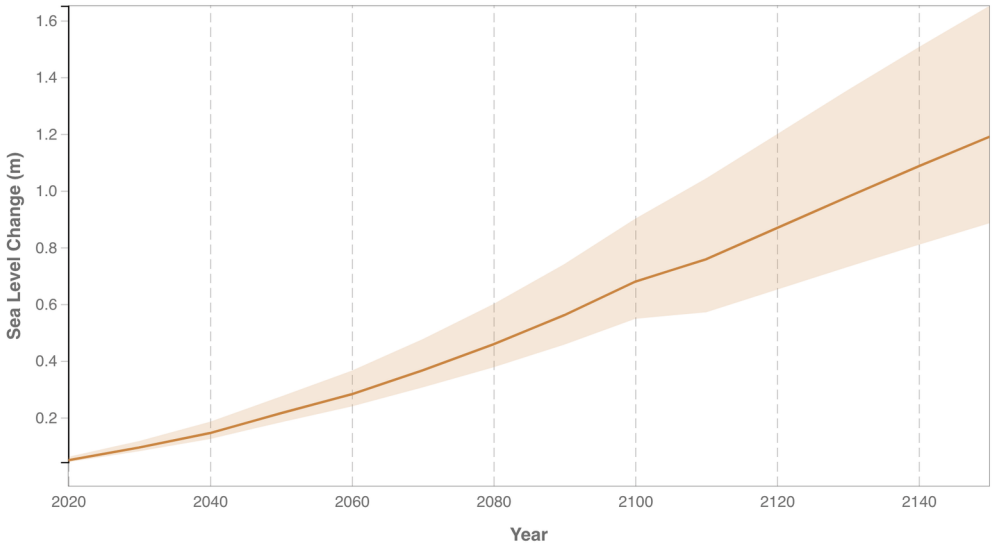


Figure 17.4.2: A graph showing the IPCC AR6 global sea level change projection under the most likely scenario (SSP3-7.0), with the peach color indicating a range of uncertainty. "IPCC projection" by NASA, licensed under public domain. Access a detailed description.

While this projection goes out to the year 2140, visible sea level changes are expected much sooner. According to NOAA, "Sea level along the U.S. coastline is projected to rise, on average, 10-12 inches (0.25 - 0.30 meters) in the next 30 years (2020-2050)."

Even a small amount of sea level rise will have disastrous effects. Higher salt water levels will increase the risk of saline encroachment into freshwater reservoirs. Higher seas will magnify erosional issues along coasts. And because so much of our infrastructure is built so close to the existing sea level, a minor rise can have major effects.

A report by the California Legislative Analyst's Office determined that by 2050, sea level rise will cost California between $8-10 billion of existing property. Slightly more than a meter of sea level rise will displace 28,000 residents of the San Francisco Bay Area. And in the 2 meter range of sea level rise, about two-thirds of Southern California beaches will disappear by 2100.

Increased Heat

The extent of California's future heating depends on a number of variables. IPCC projections typically employ a wide range of projections–high carbon emissions, medium carbon emissions, low carbon emissions–to sweep in the possibilities. However, the worldwide inability of governments to effect meaningful carbon reductions puts us squarely in the "high emissions" zone; when actual observations are compared to projections, the observations almost always meet or exceed the modeled projections for the

highest emissions scenarios.

Figure 17.4.3, a chart of projections for California, is produced by NOAA:

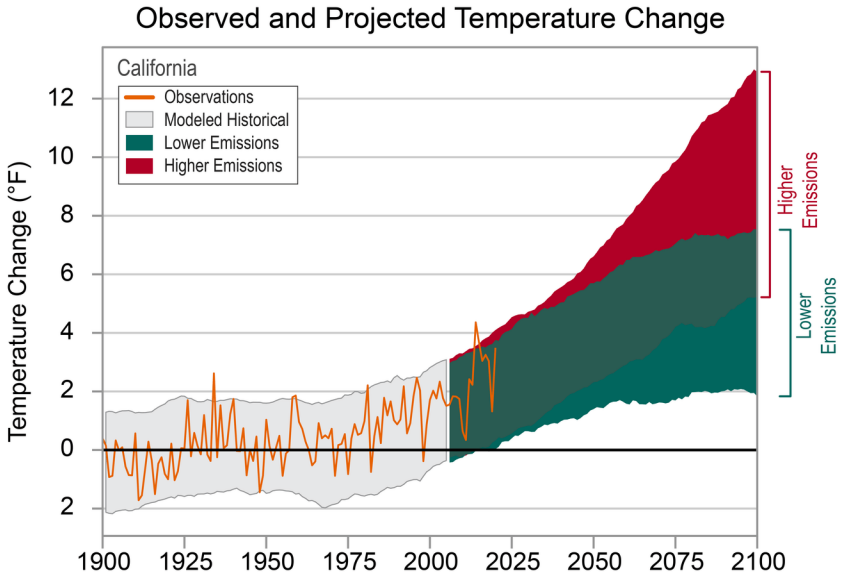


Figure 17.4.3: Observed and Projected Temperature Change in California. "Temperature change" by NOAA is in the public domain. Access a detailed description.

The world is not in the lower emissions scenario, but if we were, then the mildest amount of temperature increases in California would range between 2-8°F; these are temperatures added to the normal average.

Our carbon emissions more closely follow the higher emissions scenario. What this means is that by the year 2100, at the extreme end we can project California temperatures to soar above 12°F from the norm. While this heat will be unevenly distributed, it is not hard to imagine the July daily mean temperature for Los Angeles rising from its present 73°F to 85°F. And for areas of higher elevation, where the vital annual snow pack forms, it is not hard to imagine temperatures rising to the point where very little snow forms and winter precipitation happens primarily as ephemeral rains.

Query 17.4.1

This interactive element is not available in this format. Visit the link or scan the QR code to access it online.

View this Interactive Content online

Query 17.4.1

This interactive element is not available in this format. Visit the link or scan the QR code to access it online.

View this Interactive Content online

References

1. U.S. Energy Information Administration (March 2023). Highlights for air conditioning in U.S. Homes by state, 2020. Retrieved December 6, 2023, from https://www.eia.gov/consumption/residential/data/2020/state/pdf/State%20Air%20Conditioning.pdf
2. Bump, P. (2022, September 7). Californians may no longer be able to avoid air conditioning. The Washington Post. https://www.washingtonpost.com/politics/2022/09/07/californians-may-no-longer-be-able-avoid-air-conditioning/
3. Williams, A.P., Cook, B.I., and Smerdon, J.E. (2022). Rapid intensification of the emerging southwestern North American megadrought in 2020-2021. Nature Climate Change, 12(3), 232-234. https://doi.org/10.1038/s41558-022-01290-z
4. National Public Radio (2023, January 9). California is getting drenched. So why can't it save water for the drought? NPR.org. Retrieved November 9, 2023, from https://www.npr.org/2023/01/07/1147494521/california-weather-storm-water
5. Shao, E., Rojanasakul , M., & Popovich, N. (2023, March 17). A Very Wet Winter Has Eased California's Drought, but Water Woes Remain. The New York Times. https://www.nytimes.com/interactive/2023/climate/california-drought.html
6. Cassidy, E. (January 2023). Atmospheric River Lashes California. NASA Earth Observatory. Retrieved December 8, 2023, from https://earthobservatory.nasa.gov/images/150804/atmospheric-river-lashes-california
7. Vartabedian, R. (2023, January 13). In a Drought, California Is Watching Water Wash Out to Sea. The New York Times. https://www.nytimes.com/2023/01/13/us/california-drought-storms-water-storage.html

This page titled 17.4: The Future is shared under a CC BY-NC 4.0 license and was authored, remixed, and/or curated by Steven Newton.

17.5: Hotter, Drier, Tougher

Swelling Sea Levels and Rising Temperatures

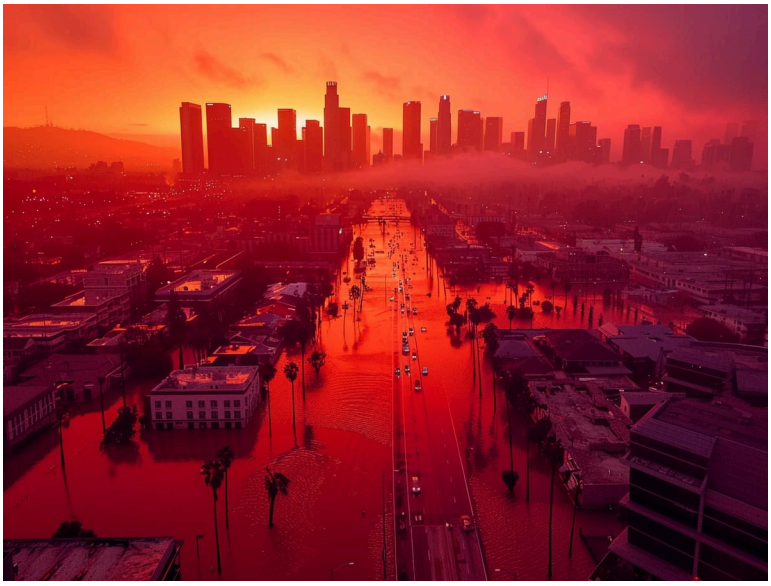


Figure 17.5.1: A dark vision of a future affected by climate change disasters, with a flooded urban landscape reflecting wildfire-smoke skies. "Future LA" by Steven Newton/Midjourney is licensed under CC BY-NC 4.0. Access a detailed description.

At this point in the course, you should have come to a somber understanding not only about the urgent danger of climate change, but also about the nature of California itself.

This is a beautiful state with incredibly diverse geology--the vertiginous cliffs of Yosemite, the baking oven of Death Valley, the stark loneliness of Joshua Tree. But underlying it all–literally–is something terrible. The fearsome San Andreas fault system, and all of its scions, such as the Hollywood and Hayward faults, threatens to without warning collapse our comfortable complacency. As Natalie Merchant sang about California in her song “San Andreas Fault”: “What a wicked ground/ Build a dream, watch it all fall down.”

We have created a fragile, frail civilization here that hangs by the thinnest of threads. An unremarkable eruption at Mt. Shasta, and whole areas of Northern California become unlivable, buried in ash and smothered in lahars. An inevitable, long-overdue shift in California’s major faults, and our most basic life-sustaining infrastructures–housing, roads, electricity, fuel, sewage, gas, dams, drinking water–are ruined.

In addition to these risks, climate change is hammering every imaginable factor–all at once. A small change in snow pack formation and we no longer have enough water to sustain our swelling population. A delicate shift in fog-generating coastal currents, and California’s grand redwood trees go extinct. An inevitable rise in sea level–seemingly no worse than a very high tide except that the high tide is now permanent–and hundreds of thousands of Californians will have to abandon their now-worthless low-lying homes. For most Californians, homes represent their single largest lifetime financial investment. Some may assume that “the government” will construct sea walls to save their homes from rising oceans, when in fact local governments decline to raise taxes to fund schools adequately or to maintain even existing roads.

We obviously can’t prevent a volcano such as Mt. Shasta from erupting, but is there anything we can do about the effects of climate change on California?

California has undertaken some steps to counteract climate change. There have been a few token actions, such as laws tightening motor vehicle emission standards and phasing out sales of new gasoline cars by 2035. The California Climate Commitment pledges $54 billion to reduce fossil fuel and air pollution. Legislation has been signed requiring large businesses to disclose their

carbon footprints. These are all positive steps. The problem is how few other states, and how few other countries, are following California's lead. Without federal action, and without a worldwide program to reduce carbon dioxide emissions drastically–for example, by rapidly ceasing all use of coal for energy production–then California's climate steps are akin to calibrating the clocks on the *Titanic* as it sinks. We can reduce our carbon usage, but if the PRC and India do not follow, then California alone won't be enough.

In K-12 education there is a common trope that climate change lessons should include practical steps young students can take. The thinking is that if children are frightened by climate change information, they may resist accepting the conclusions. But if these lessons are leavened with practical actions–switching light bulbs to LEDs, air-drying clothes, recycling–students may have a sense of agency and control that will make them more likely to accept the science.

But this is a college-level text, and here we have an obligation to tell the truth without condescension. And the truth is that such minor steps are not nearly enough.

One study found that in the United States changing standard light bulbs to LEDs saves an average of 0.17 equivalent tonnes of CO_2 annually, compared to a savings of 117.7 equivalent tonnes of CO_2 annually if a family decides to have one less child. Put another way, a family with one additional child incurs a carbon cost equivalent to 684 teenagers abstaining from recycling for the entirety of their lives.

The truth is that the accelerations of swelling sea levels, rising temperatures, and parching droughts are colossal, existential threats. These threats require changes of equally great magnitude to our economic, legal, and political systems. Switching to more efficient light bulbs does no harm but should not be seen as a substitute for the real work.

If humanity somehow lingers long enough for historians to compose histories of our time period, perhaps these writings will say that good people appreciative of natural beauty and the natural world–such as the lucky residents of the amazing state of California–fought successfully to effect the fundamental structural changes required to deal with climate change.

Query 17.5.1

This interactive element is not available in this format. Visit the link or scan the QR code to access it online.

View this Interactive Content online

References

1. Wynes, S., & Nicholas, K. A. (2017). The climate mitigation gap: Education and government recommendations miss the most effective individual actions. Environmental Research Letters, 12(7). https://doi.org/10.1088/1748-9326/aa7541

This page titled 17.5: Hotter, Drier, Tougher is shared under a CC BY-NC 4.0 license and was authored, remixed, and/or curated by Steven Newton.

17.6: Chapter Summary

17.1: Note on Usage

- An exploration of proper language for discussions about climate.
- This includes the meaning of climate-specific terms such as forcing and response.
- Particular attention is given to how terms of such as "global warming" has been misused by anti-science climate denialists.

17.2: The Past

- Geology brings to the story of climate change not only what is happening today, but also especially the evidence revealed from the distant past.
- One major subject for past climate is the numerous "megadroughts" California has suffered.
- One of the most profitable avenues of research is dendrochronology, the examination of trees rings for climate data.

17.3: The Present

- Does California have a Mediterranean climate? In some ways, yes, but this section examines how this is too simplistic.
- This chapter looks at contemporary trends, such as high pressure ridges, drought, snow pack measurements, and atmospheric rivers.
- The present conditions highlight the fragility and vulnerability of California's climate system, especially in terms of water humans need.

17.4: The Future

- King Tides show us what the future of rising sea levels will look like.
- This section details projections for sea level rise.
- The future involves truly frightening projections of how California might change for the worse.

17.5: Hotter, Drier, Tougher

- Much of the coming changes is already "baked into the cake" is is going to happen without regard to future actions.
- There is not much hope for California's climate remaining as it has been--things are going to change for the worse.
- We need to come to terms with this existential crisis while realizing that our political systems are failing to address the magnitude of the issue.

This page titled 17.6: Chapter Summary is shared under a CC BY-NC 4.0 license and was authored, remixed, and/or curated by Steven Newton.

17.7: Detailed Figure Descriptions

Detailed Figure Descriptions

17.1 Polygonal dried mud cracks

Low water levels at Nicasio Reservoir in Marin County during 2021 during severe drought conditions. Baked-dry polygonal mudcracks lie in land that should be under significant water. This period reflected part of recent drought cycles, and though such reservoirs recover, they will also inevitably drain again as California water demand, and out of control population growth, far exceeds the ability of precipitation to provide for the state in the way it has in the past.

17.1.1 A diagram of solar radiation and energy inputs and outputs

Solar energy imbalance created when greenhouse gases act to trap a portion of solar radiation that would otherwise escape to space and cool Earth. Includes incoming solar radiation, some of which is reflected immediately by high clouds, some of which reaches the ground and is absorbed, and some of which is reflected by ice on land and sea. The flux of energy returns to space, and in normal conditions, the incoming and outgoing energies would be more or less in balance. Today, however, greenhouse gases are stimulated by the infrared radiation emitting from the warmed Earth, and these greenhouse gases therefore return some of that energy back toward Earth, leading to an imbalance.

Solar radiation inputs include absorbed radiation on continents and oceans, minus reflected radiation from clouds and sea ice. Energy absorbed on Earth is then dissipated via "infrared radiation emitted by the surface," which then may interact with anthropogenic gases and be "absorbed and reemitted by greenhouses gases: carbon dioxide, methane, water vapor, nitrous oxide, and others."

17.2.1 A stand of Bristlecone pines growing on pale-white Reed Dolomite

A stand of long-lived Bristlecone pines growing on Reed Dolomite in the White Mountains, CA. The stand of trees grows almost entirely on the white Reed Dolomite, and very sparsely on any other formations visible (probably the early Cambrian Deep Springs or Campito Mountain formations). The soil has a variety of healthy brush growing on it, most plants do not thrive on dolomitic soils; however, Bristlecones have evolved to exploit the opportunity of this less-used substrate, perhaps because of the lessened competition with other faster-growing plans. Many of these Bristlecones are over four thousand years old.

17.2.2 Snow-covered carbonate soil hosting a number of Bristlecone pines

A Bristlecone pine (*Pinus longaeva*) from the White Mountains, CA, with the characteristic barren, twisting corkscrew shape of the trunk, adorned with sparse green leaves. Little of the tree has foliage; nonetheless, these trees are still alive and, in fact, provide a record of growth that proves very useful for paleoclimatology, though they will not provide the clear tree rings found in faster-growing trees at lower elevations.

There is plentiful residual snow on the ground, which is an important source of the plant's water supply, but also reinforces the high altitude, typically above 10,000 feet, at which Bristlecones thrive. Part of their ecological niche is to live on soils and in places where few other plants are able to make a living.

17.2.3 The dendrochronology principle of differential annual tree ring growth

This diagram illustrates the dendrochronology principle of differential annual tree ring growth. All else being equal, wider rings indicate periods of wetter climate and greater growth, while narrower rings indicate a drier and less productive year. Note that these rings may be sampled by a hollow core that does not kill the tree; not every dendrochronologic sample involves cutting

down the tree. If the tree is cut down, then the slice of the trunk used to establish dendrochronology is referred to as a "cookie." These cookies and cores allow for examination of growth differentials and extraction of material for isotopic analysis.

The main image in the diagram is a cross-section of a tree trunk, with specific features identified. At the very center of the trunk is a small circle labeled "first-year growth." Moving outward, a wide tree ring indicates a rainy season, which a narrow tree ring indicates a dry season. Between two rings we see a thick black area that is labeled "scar from a forest fire." A close-up of one area shows the light and darker bands of the tree rings. Thicker light areas indicate spring/early summer growth, while the thinner and darker bands indicate late summer/fall growth.

17.2.4 California Palmer Drought Severity Index Scale

The Palmer Drought Index Scale from the year 1000 to the year 2000. Lower numbers (-8, -6, -4, etc.) indicate drier climate conditions, while higher numbers (2, 4, 6, etc.) indicate wetter years. This thousand-year record shows showing dry periods/wet periods in California from the years 1000 to 2000, as shown from a baseline of 0, with variation upwards indicating wetter periods, and variations downward drier periods.

The period of 1900-2000 show some wet spikes and dry spikes; the fear of climate change-induced drought is that future iterations of this graph will show primarily dry numbers. Of particular note are the low (dry) pulses that occur after the year 1100 and again, in several pulses, throughout the 1200s, 1300s, 1400s, 1500s, 1600s, 1700s, 1800s, and 2000s.

17.3.1 San Francisco's annual precipitation profile

Monthly precipitation profile for San Francisco using NOAA data from 1991 to 2020. The twelve steps on the bottom each correspond to a month (Jan to Dec), while the axis to the left shows precipitation in mm, from 0 to 130. January and December clock in between 110 and 120 mm, respectively, while July-August-September report zero to a few mm.

What this pattern shows is the "Mediterranean" climate noted by long, dry summers with virtually no precipitation from June-Sep, punctuated by wetter winters with rainfall concentrated Nov/Dec/Jan/Feb. Even these rainfall concentrations are something of a misnomer, because precipitation does not fall steadily, as it would in, say, Seattle, but rather comes from just 1-2 major storms that inundate and overwhelm city water systems.

Monthly precipitation for San Francisco (NOAA dataset, 1991 - 2020)

Month	Precipitation in mm
January	112
February	111
March	80
April	41
May	18
June	5
July	1
August	2
September	3
October	24
November	66
December	121

17.3.2 The rain shadow effect across California from Monterey to Death Valley

A elevation cross-section of California from Monterey to Death Valley, with a vertical exaggeration of 30x. Starting in the west near Monterey, we move past the coastal ranges into the flatness of the Central Valley, then begin a long climb up the west face of the Sierra Nevada. At this point the diagram shows rainclouds with drops of rain descending on the Sierran foothills, indicating the process of moisture being precipitated as it rises in elevation (orographic precipitation). The steep east side of the Sierra Nevada therefore creates a rain shadow in the Owens Valley. The White-Inyo mountains create another rain shadow for the Panamint Valley, and the Panamint Hills likewise form another rain shadow for Death Valley.

What this shows is that while precipitation flows from the west (left) to the east (right), when it encounters the Sierra Nevada, much of that moisture is removed by orographic precipitation, and indicated by the cloud and rain drops. Additional rain shadows remove even more moisture before whatever is left arrives in Death Valley, which is one of many factors why Death Valley is one of the driest spots on the planet.

The profile is exaggerated in order to display the height differences in a way greater than would actually be encountered if one were, for example, seeing this profile in a plane traversing the same course.

17.3.3 The Köppen climate classifications for California

California with different regions parsed into various Köppen climate classifications. The Köppen climate classifications are a way of parsing climate zones such as "Dsc (Dry-summer subarctic)" and "BSh (hot semi-arid)." Note that only four of the categories indicate "Mediterranean" conditions, though "Mediterranean" is the most common way to describe California's climate. Problems with this oversimplification are detailed in the chapter section.

This diagram divides California into 11 such categories

- Desert climates dominate the southeastern part of the state:
  - BWh (hot desert), shown in bright red, covers much of southeastern California, including areas near the Mojave and Colorado Deserts.
  - BWk (cold desert) appears in lighter pink in some inland and higher-elevation desert regions.
- Semi-arid climates appear in transition zones:
  - BSh (hot semi-arid) and BSk (cold semi-arid), shown in orange and light tan, occur around desert margins and interior valleys.
- Mediterranean climates cover much of the populated coastal and inland regions:
  - Csa (hot-summer Mediterranean), shown in bright yellow, dominates the Central Valley and large portions of Southern California.
  - Csb (warm-summer Mediterranean), in olive green, is common along the northern and central coast and foothill regions.
  - Csc (cold-summer Mediterranean) appears in limited high-elevation coastal or mountainous areas.
- Mountain and cooler climates are concentrated in higher elevations:
  - Cfb (oceanic) occurs in small coastal and northern areas.
  - Dsb (warm-summer continental Mediterranean) and Dsc (dry-summer subarctic) appear mainly along the Sierra Nevada range, shown in purple tones.
  - ET (tundra), shown in gray, is limited to the highest mountain peaks.

The diagram discusses its sources as "Data sources: 1991-2020 climate normals from PRISM Climate Group, Oregon State University; outline map from US Census Bureau."

17.3.4 Extremes in maximum temperature, 1910-2022

Extremes in maximum temperature from 1910 to 2022, with percentages above or below a baseline. Above-average temperatures begin to become much more common after 1980, and after 2010 are all classified as "much above normal." This reflects the warming trends worldwide during these time periods.

The title is "West extremes in maximum temperature (Step 1) annual (January - December)." Lines indicate "much above normal," "much below normal," and a "9-point binomial filter."

Particular note should be given to the low extremes associated with the 1982-1983 and 1997-1998 El Nino events. Also of note is the trend that after the year 2000, virtually every temperature reading is listed as "much above normal."

The trend from 1910-1980 begins with a small range; however, this range grows greatly in the 1982-1983 period and then expands dramatically after 2010.

17.3.5 Snow Water Equivalent at Donner Summit, CA

Snow Water Equivalent (SWE) at Donner Summit from the years from 1910 to 2020. SWE is in inches, ranging from 0 to 90. What there is significant variation, both high and low, across the time period, the lowest measurements occur within the last few decades, including a reading in 2015 near zero. The table below extracts an estimate for each decade

Estimated April 1 SWE by Decade

Decade	Estimated Avg SWE (inches)
1910–1919	45
1920–1929	30
1930–1939	44
1940–1949	39
1950–1959	40
1960–1969	38
1970–1979	41
1980–1989	36
1990–1999	42
2000–2009	34
2010–2019	20

17.3.6 Illustration of an atmospheric river

A January 2023 atmospheric river forming in the Pacific and heading directly toward California, with a narrow counter-clockwise rotation of moisture moving from the west to the east, hitting California and spreading out along the California coastline. This is typical of the way we receive the majority of our rainfall.

17.3.8 An illustration of the Reber Plan

The quixotic Reber Plan, which was never enacted, but which would have catastrophically altered California water by building a dam across San Francisco Bay, capturing the largest freshwater drainage in the state. The main barrier in the Reber Plan would have been a dam from Pt. San Quentin to Richmond, west to east, roughly following the course of the Richmond-San Rafael bridge. Other inlets and bays would have been paved over. To the north, a shipping channel and lock system would have been constructed right through the current city of Richmond, allowing shipping to each the upper Sacramento river.

This plan was never fulfilled, but one can imagine the environmental devastation this would have wrought had it been constructed.

17.4.1 In a harbinger of future sea level rise, a King Tide splashes onto the streets

King Tide conditions at the San Francisco Embarcadero, where sea level is even with sidewalks and small waves splash salt water onto San Francisco streets. These King Tides give us an indication of what future sea level rise will look like, when the ocean level is this high at the normal high tide.

17.4.2 A graph showing the IPCC AR6 global sea level change projection

Projected sea level rises, with a range of uncertainty indicated on either side of the middle line. One axis tracks from the years 2020 to 2140, while another shows sea level change in meters from 0.2 to 1.6. The middle scenario shows over a meter of sea level rise by 2140. The trend line begins at 0.05 for 2020 with an uncertainty range of 0.03-0.07 meters. The trend lines moves steadily upward steadily ending at roughly 1.2 in 2150 with an uncertainy range of 0.9 - 1.65 meters.

17.4.3 Observed and Projected Temperature Change in California

Historical, current, and project temperature changes in California. One axis shows years from 1900 to 2100, while another shows temperature changes in ^{o}F from -2 to 12. Projected changes are split between "high emissions" and "low emissions" scenarios. The lower emissions track puts us somewhere between 2 to 7°F by 2100. However, we are firmly on the higher emission pathway right now, and if we follow that to its worst conclusions, then we could be looking at increases in overall temperatures on the order of 12°F by 2100.

Estimated Temperature Change by Time Range

Time Range	Observation	Modeled Historical	Lower Emmissions	Higher Emissions
1900–1920	–1.5 to +0.5	–2.0 to +1.5	N/A	N/A
1920–1940	–1.0 to +2.5	–1.8 to +1.8	N/A	N/A
1940–1960	–1.5 to +1.5	–2.0 to +1.7	N/A	N/A
1960–1980	–1.0 to +2.0	–1.5 to +2.2	N/A	N/A
1980–2000	0.0 to +2.5	–1.0 to +3.0	N/A	N/A
2000–2020	+0.5 to +4.0	–0.5 to +3.5	–0.5 to +1.5	–0.5 to +2.0
2020–2040	N/A	N/A	+0.5 to +2.5	+1.0 to +4.0
2040–2060	N/A	N/A	+1.5 to +4.0	+3.0 to +6.5
2060–2080	N/A	N/A	+2.0 to +5.0	+5.0 to +10.0
2080–2100	N/A	N/A	+2.0 to +5.5	+6.0 to +13.0

17.5.1 A dark vision of a future affected by climate change disasters

An AI imagining of the future Los Angeles skyline under severe climate change. Note the flooded roads lined with palm trees, on which cars gingerly make their way through standing water, while the sky is reminiscent of the actual sky conditions on 9 September 2020, which involved an orange-red sky created by an inversion of particles created by out-of-control wildfires. It is interesting to contemplate that all of our infrastructure--skyscrapers, bridges, roads--will remain abandoned for a while, even if future climate change makes conditions on Earth unlivable for humans.

This page titled 17.7: Detailed Figure Descriptions is shared under a CC BY-NC 4.0 license and was authored, remixed, and/or curated by Steven Newton.

18: CALIFORNIA'S WATER

Introduction to California's Water

California's water landscape is a dynamic mosaic shaped by the intricate interplay of geological processes, hydrological dynamics, and human interventions. From the towering peaks of the Sierra Nevada to the fertile valleys of the Central Valley and the dynamic coastline along the Pacific Ocean, the state's diverse geology influences the distribution, availability, and quality of surface water and groundwater resources.

In this chapter, we embark on a journey to explore the geological underpinnings of California's water landscape, delving into the intricate relationships between geology and surface water dynamics. We will examine how geological formations, topographic features, and climatic variability interact to shape the state's hydrological patterns, from the snow-capped mountains that serve as reservoirs of freshwater to the alluvial plains that support vibrant agricultural activities.

In this chapter, we explore the geological underpinnings of California's water landscape, delving into the intricate relationships between geology and surface water dynamics. We will examine how geological formations, topographic features, and climatic variability interact to shape the state's hydrological patterns, from the snow-capped mountains that serve as reservoirs of freshwater to the alluvial plains that support vibrant agricultural activities.

Through exploration of California's geological diversity, we will uncover the myriad ways in which geology influences surface water resources, including river systems, estuarine environments, and coastal zones. We will examine the geological factors that contribute to the state's susceptibility to drought, floods, and climate change, as well as the challenges posed by aging infrastructure, urbanization, and land development.

As we navigate the complexities of California's water landscape, we will also highlight the importance of embracing sustainable water management practices, innovative solutions, and collaborative efforts to address the challenges and opportunities presented by the state's varying geology and water resources. By understanding the geological influences on surface water dynamics and integrating this knowledge into water management strategies and land use planning, we can work towards ensuring the resilience, sustainability, and equitable management of California's precious water resources for generations to come.

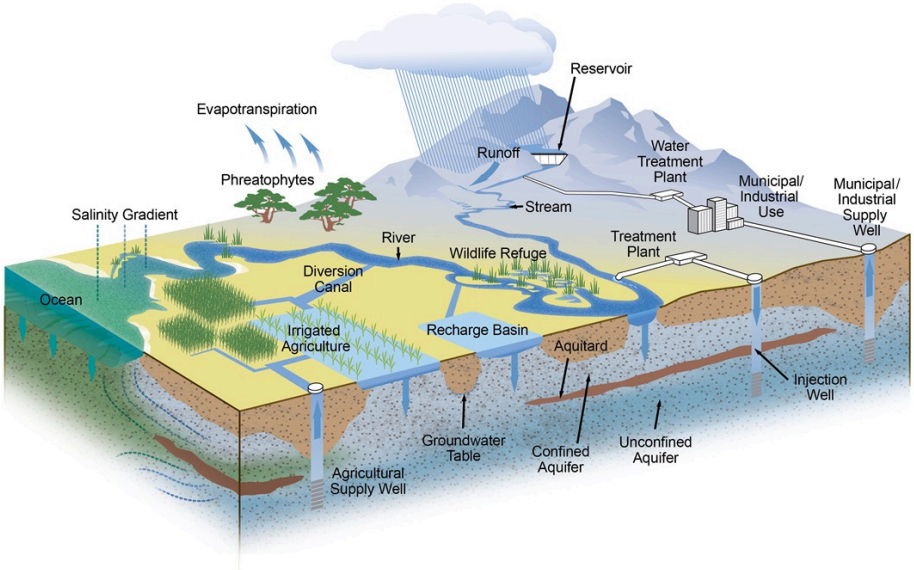


Figure 18.1: Conceptual Model of Water Flow. ("Groundwater basics on Napa County, California" is in the public domain. Access a detailed description of this image.)

Learning Objectives

By the end of this chapter, you should be able to:

- Diagram the hydrologic cycle and explain the roles of pools and fluxes.
- Explain the role of drainage basins in the collection and transport of water in the state of California.
- Describe the locations and characteristics of California's major aquifer systems.
- Explain the role of groundwater in meeting California's water needs and identify issues that results from overuse.
- List examples of California's water infrastructure and explain how and why this infrastructure alters the distribution and availability of water.
- Describe the effects of human impacts, including climate change, agricultural irrigation, and urbanization on water availability in California.
- Identify several key water quality issues in California and their causes.

18.1: The Hydrologic Cycle
18.2: Running Water
18.3: Groundwater
18.4: Water Infrastructure and Management
18.5: Threats to California’s Water
18.6: Understanding California's Water Landscape
18.7: Chapter Summary
18.8: Detailed Figure Descriptions

This page titled 18: California's Water is shared under a CC BY-NC 4.0 license and was authored, remixed, and/or curated by Cole Heap.

18.1: The Hydrologic Cycle

The Hydrosphere and Hydrologic Cycle

While geology is primarily focused on the lithosphere, the rocky layers of Earth from the lithosphere to the core, the lithosphere is profoundly influenced by interactions with Earth's other spheres. One of the most significant is the hydrosphere, which encompasses all the water on Earth, including oceans, rivers, lakes, and groundwater. The hydrosphere plays a fundamental role in shaping California's diverse geology and ecosystems. From its towering mountain ranges to its arid deserts and sprawling coastlines, California's geology, and subsequently it's topography, is intricately intertwined with the movement and distribution of water.

At the heart of California's hydrology lies the hydrologic cycle, a continuous process through which water moves between the Earth's surface, atmosphere, and underground reservoirs. Understanding this cycle is crucial for grasping the complex dynamics of water availability, distribution, and management across the state.

The Hydrologic Cycle: A Primer

The hydrologic cycle, also known as the water cycle, consists of several interconnected processes that recycle Earth's water. It begins with evaporation, where the sun's energy heats surface water bodies, causing liquid water to transform into water vapor and rise into the atmosphere. As this water vapor cools, it undergoes condensation to form clouds. Eventually, the clouds release precipitation—rain, snow, sleet, or hail—which returns water to the Earth's surface.

Once on the surface, precipitation either infiltrates into the ground, replenishing groundwater reservoirs, or flows over the land as runoff, forming streams, rivers, and eventually flowing into larger water bodies such as lakes or the ocean. Meanwhile, plants absorb water through their roots and release it into the atmosphere as water vapor during transpiration. This continuous cycle of evaporation, condensation, precipitation, infiltration, runoff, and transpiration sustains the movement and distribution of water across Earth's surface, shaping landscapes and ecosystems. Figure 18.1.1 illustrates these interconnected processes within California's diverse geology.

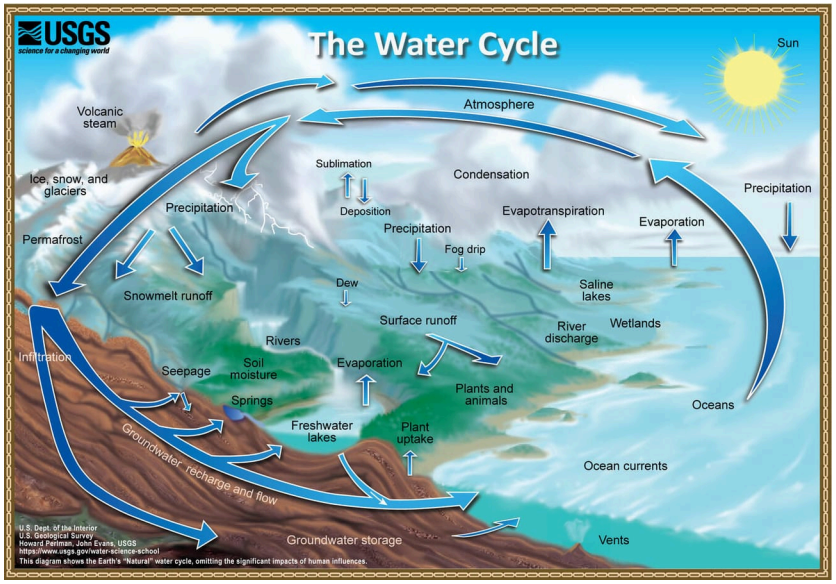


Figure 18.1.1: The Natural Water Cycle by the United States Geological Survey is in the public domain. Access a detailed description of this image.

Video 18.1.1 - The Water Cycle

This video illustrates the path a single water molecule might take along the hydrologic cycle. Heat from the sun causes the molecule to evaporate from the ocean's surface. Once it evaporates, it is transported high in the atmosphere and condenses to form clouds. Clouds can move great distances and eventually the water molecule will fall as rain or snow. Ultimately, the water molecule arrives back where it started...at the ocean.

This interactive element is not available in this format. Visit the link or scan the QR code to access it online.

View this YouTube Video online

The Water Cycle by NASA Goddard Media Studios is in the public domain.

Pools and Fluxes in the Water Cycle

In understanding the hydrologic cycle, it is essential to recognize the roles of pools (reservoirs of water such as lakes, oceans, and aquifers) and fluxes (the processes that move water between these pools). Pools represent the storage of water in different states—liquid, solid (ice), or vapor—while fluxes account for the movement between them. The interactions of pools and fluxes govern the availability and quality of water, both on a natural level and as influenced by human activities, as shown in Figure 18.1.2. Human water use modifies these pools and fluxes, altering how water is stored, moved, and distributed across landscapes.

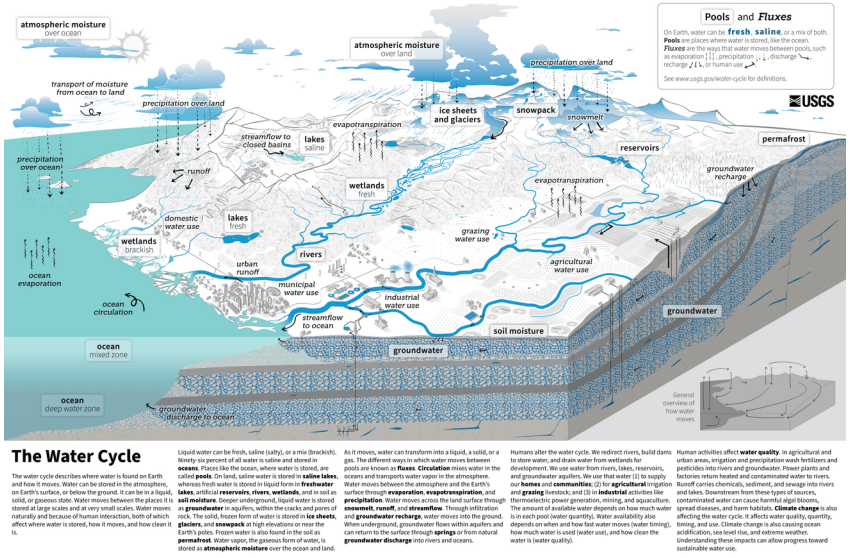


Figure 18.1.2: Water Cycle Diagram - Text Body by the United States Geological Survey is in the public domain. Access a detailed description.

California's Hydrology: A Mosaic of Complexity

California's diverse geography results in an equally complex hydrology, with each region experiencing unique water-related challenges and dynamics. For instance, the Sierra Nevada Mountains serve as a crucial source of freshwater, where snowpack accumulation during the winter melts in the spring, providing a vital water supply for the entire state. In contrast, the Central Valley relies heavily on intricate river networks and aquifers to sustain its agriculture. Coastal areas, desert regions, and fault-controlled basins also exhibit distinct hydrological patterns shaped by their underlying geology.

Precipitation, groundwater recharge, and runoff processes vary significantly across California's hydrological regions, influenced

by the state's diverse topography and climate. Understanding how these processes interact with the geological framework helps to explain the distribution of water resources and their management challenges throughout California.

This page titled 18.1: The Hydrologic Cycle is shared under a CC BY-NC 4.0 license and was authored, remixed, and/or curated by Cole Heap.

18.2: Running Water

Introduction to California's Hydrology: Running Water and Landscape Dynamics

Running water plays a pivotal role in shaping landscapes across California. Streams and rivers not only erode and shape mountains but also deposit sediment in valleys, creating dynamic, ever-changing terrains. Simultaneously, geology significantly influences how water flows across the landscape. This section delves into the interplay between running water and the physical landscape, examining how precipitation, streams, drainage basins, and hydrologic regions define California's hydrology.

Precipitation

Precipitation is a key driver of California's hydrological cycle, affecting the state's water resources and shaping both ecosystems and human activities. Precipitation refers to any form of water—rain, snow, sleet, or hail—that falls from the atmosphere to the Earth's surface. In California, the timing, amount, and distribution of precipitation are critical factors that influence water availability and management.

California's Mediterranean climate results in highly variable precipitation patterns, both spatially and temporally. The state experiences distinct wet winters and dry summers, with most precipitation occurring between November and March. During these months, storms from the Pacific Ocean bring rain and snow, often carried by atmospheric rivers-long, moisture-laden air currents that can result in intense rainfall and snowfall.

The state's diverse geography—coastal plains, mountain ranges, deserts, and valleys—also plays a key role in determining how much precipitation different regions receive. Coastal areas generally experience more rainfall than inland areas, while mountain ranges, such as the Sierra Nevada, receive enhanced orographic precipitation due to the lifting of moist air over elevated terrain. Figure 18.2.1 illustrates the spatial distribution of average annual precipitation across California from 1900 to 1960.

Precipitation in California plays a crucial role in replenishing surface water reservoirs, groundwater aquifers, rivers, and streams—the primary sources of freshwater for the state's residents, agriculture, and industry. Snowpack, in particular, is a critical component of California's water supply, serving as a natural reservoir that gradually releases water during the spring and summer months as it melts. The Sierra Nevada mountain range, with its extensive snowpack, serves as a major source of water for the state's rivers and reservoirs.

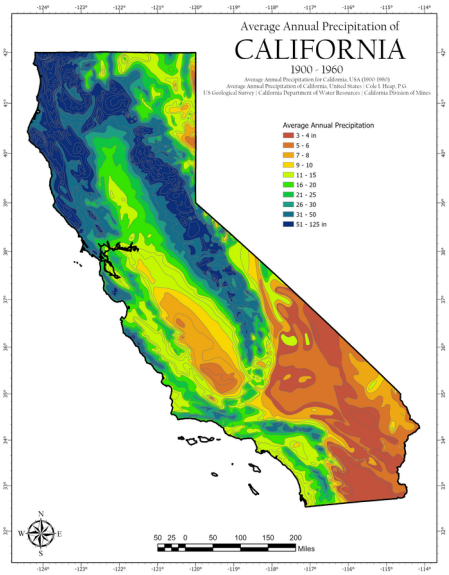


Figure 18.2.1: "Average Annual Precipitation of California (1900-1960)" by Cole Heap form data in the California Open Data Portal is licensed under CC BY-NC 4.0 Constructed in a GIS. Access a detailed description.

However, California's precipitation is highly variable and unpredictable, affected by climate change, natural climate cycles like El Niño and La Niña, and human activities. Droughts, floods, and extreme weather events create significant challenges for water management. Graph 18.2.1 provides an interactive look at California's annual precipitation from 1895 to 2021, demonstrating the extent of this variability.

Statewide Annual Precipitation (1895-2021)

The following interactive graph illustrates California's annual precipitation between 1895 and 2021:

This interactive element is not available in this format. Visit the link or scan the QR code to access it online.

View this Interactive Content online

Statewide Annual Precipitation (1895-2021) by the California Office of Environmental Health Hazard Assessment is in the public domain. Access the data.

Drainage and Runoff

Precipitation in California plays a crucial role in replenishing surface water reservoirs, groundwater aquifers, rivers, and streams—the primary sources of freshwater for the state's residents, agriculture, and industry. A critical element in the movement of water is the concept of drainage basins, or watersheds, which are defined by the geographical areas that drain water to specific rivers and bodies of water. Figure 18.2.2 provides a visual example of how drainage basins are physically organized.

Drainage basins are essential for understanding how water flows across landscapes and their interconnectedness. They function as natural reservoirs, collecting rainwater and snowmelt, regulating streamflow, and contributing to groundwater recharge. Basin boundaries, known as watershed divides, are formed by topographical features like ridgelines and hills that dictate the direction of water flow. The complex interaction of runoff and infiltration within a basin influences both the timing and magnitude of streamflow. Is it any wonder as to how the underlying geology influences waterflow?

California's landscapes exhibit a variety of drainage basin types due to its diverse topography. Mountainous areas like the Sierra Nevada contain elongated drainage basins that follow valleys, while flatter regions such as the Central Valley feature broad, interconnected basins. Coastal areas often exhibit dendritic patterns, while volcanic regions like the Cascades have radial basins that extend outward from central peaks.

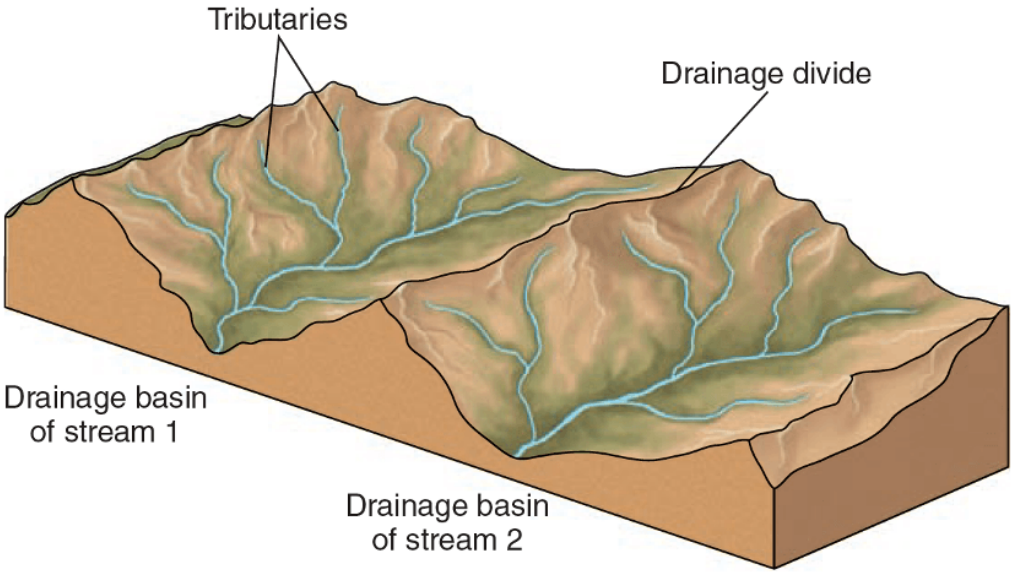


Figure 18.2.2: Basic anatomy of drainage basins by edukemy from "Stream Basins" is licensed under CC BY-NC 4.0. Access a detailed description.

Drainage basins vary in size, shape, and complexity, ranging from small, localized watersheds to vast, interconnected river systems spanning multiple states or countries. The size of a drainage basin is often described in terms of its drainage area, measured in square kilometers or square miles. Larger drainage basins, such as those of major rivers like the Mississippi or Amazon, can encompass millions of square kilometers and drain vast portions of continents.

The shape of a drainage basin is also influenced by the topography of the surrounding landscape, with basins typically conforming to the natural contours of the land. Basins in mountainous regions may be elongated and narrow, following the course of valleys and ridgelines, while basins in flat or gently sloping terrain may be more rounded or irregular in shape. In California, a state marked by diverse landscapes, a variety of drainage basin types can be found. The Sierra Nevada range features elongated deranged basins tracing the contours of valleys and mountain ranges. In the Great Valley, rectangular basins meander through the relatively flat expanse of agricultural lands. Along the rugged coastline of the Pacific Ocean, dendritic basins emerge amidst the coastal cliffs and hillsides, resembling branching tree patterns. In volcanic regions like the Cascades, radial basins emanate from central peaks, mirroring the spokes of a wheel. In regions with alternating bands of resistant and easily eroded rock, trellis basins form parallel valleys and ridges, creating a distinctive pattern across the landscape.

Activity - Types of Drainage Basins 18.2.1

This interactive element is not available in this format. Visit the link or scan the QR code to access it online.

View this Interactive Content online

Streams and Sediment Dynamics

Fluvial environments, where water flows through channels, are another critical component of California's hydrology. Streams transport water across the state, creating and reshaping landscapes as they erode mountains and deposit sediment in valleys. The nature of these streams varies widely, from the sinuous meandering streams to braided streams and straight channels.

Meandering Streams

Meandering streams are common in California's lowland areas, where they form winding paths through the landscape. The

Sacramento River, the longest river in California, is an excellent example of a meandering stream. Meandering streams are characterized by the continuous erosion of outer banks and sediment deposition along inner banks, forming point bars. This dynamic interplay between erosion and deposition helps shape the river's course, creating a constantly changing landscape that provides diverse habitats for various plant and animal species. Figure 18.2.3 shows the river's course through the Central Valley, where its meanders have shifted over time, creating oxbow lakes and fertile floodplains.



Figure 18.2.3: Sacramento River, in the Great Valley, CA, by the University of Oregon is in the public domain. Access a detailed description.

An oxbow lake is a U-shaped body of water formed when a wide meander from a river is cut off, creating a separate, isolated lake. This process occurs when the meander becomes extremely curved and the neck of the meander narrows, eventually causing the river to break through and take a more direct path. The abandoned meander loop, now cut off from the main flow of the river, forms an oxbow lake. Over time, these lakes can become rich in nutrients, supporting diverse aquatic habitats, but they may also dry up if they are not replenished by water from the river or precipitation.

Braided Streams

Braided streams are typified by their complex, intertwined channels, separated by sediment bars. These streams are common in areas with high sediment loads and variable flows. The Santa Clara River, shown in Figure 18.2.4, exemplifies this type of stream. Braided streams often present challenges for flood management and land use, as their shifting courses can alter channel locations over short timescales.



Figure 18.2.4: "Santa Clara River", CA from the air by Shannon1 is licensed under CC BY-SA 2.0. Access a detailed description.

In braided streams, sediment dynamics are characterized by the continuous deposition and reworking of sediment bars and islands. Sediment generally is coarse, forming obstacles for water to attempt to flow around. Flows divide and recombine as they encounter such obstacles, leading to lateral and vertical accretion, which can rapidly alter channel morphology. The shifting nature of braided streams presents challenges for land management and flood control, requiring adaptive strategies to mitigate risks while preserving ecological integrity.

Straight Channels

While less common, straight channels do exist in California's rugged terrain, especially in steep mountainous regions or areas affected by recent glaciation. In the alpine reaches of the Sierra Nevada, for instance, streams cascade down steep slopes, carving straight channels as they descend. These channels, though relatively short-lived in geological terms, showcase the erosive power of water in shaping mountain landscapes.

Activity - Streams in the Hydrologic Cycle 18.2.1

This interactive element is not available in this format. Visit the link or scan the QR code to access it online.

View this Interactive Content online

California's Hydrologic Regions

California is divided into ten hydrologic regions, each with unique geographic, climatic, and hydrological characteristics that influence water availability, quality, and management. These regions provide a framework for understanding California's diverse water resources and the challenges posed by varying landscapes, from coastal zones to desert basins. Figure 18.2.5 provides a visual overview of the state's hydrologic regions.



Figure 18.2.5: "California Hydrologic Regions" by the California Department of Conservation is in the public domain. Access a detailed description.

70% of the groundwater used in the state comes from the Great Valley, 20% comes from the South Coast and Central Coast Hydrologic Regions, and the rest from the remaining hydrologic regions. It is estimated that agriculture uses 34 million acre-feet out of the total 43 million acre-feet available from surface and groundwater. To put that in perspective, one acre-foot is the amount of water needed to cover an acre of land (about the size of a football field) with one foot of water—enough to supply about two average households for a year. That means agriculture uses close to 79% of all available water in the state! The largest source of surface water comes from the Sierra Nevada snowpack melt, which provides an average of 15 million acre-feet of water. The state's infrastructure is designed to capture this runoff and deliver it through the federal Central Valley Project and the Delta State Water Project.

Notably, many of California's drainage basins have steadily declining groundwater levels. Overdraft, which occurs when water is pumped out of an aquifer faster than it can be naturally replenished through rainfall or snowmelt infiltration, is estimated to be between 1-2 million acre-feet per year. This over-extraction can lead to a drop in the water table, dry wells, reduced groundwater storage capacity, and even land subsidence. Although a comprehensive study has not been conducted since 1980, the introduction of the Sustainable Groundwater Management Act (SGMA) in 2014 has made local water agencies responsible for monitoring groundwater levels and managing the volumes being extracted.

Other significant issues that may be found in each hydrologic region concern water quality, lack of data for decision making, poor management of surface and groundwater, and poor agency coordination. Video 18.2.1 shows examples and lends further insight to the complexity of water management in California.

Each of California's hydrologic regions presents unique opportunities and challenges in water resources management, reflecting the state's diverse geography, climate, and socio-economic dynamics. From the snow-capped peaks of the Sierra Nevada to the arid deserts of the Mojave, these regions exemplify the intricate interplay between natural processes, human activities, and water management practices.

North Coast Region

Located along the rugged northern California coastline, this region encompasses the Klamath River drainage and extends into northeastern California. Characterized by dense forests, steep terrain, and some of the highest rainfall levels in the state, the North Coast Region supports diverse ecosystems and important fisheries. Major rivers, such as the Eel River and the Russian River, are critical to local agriculture, fisheries, and municipal water supplies. This region's abundant water resources also support redwood forests and salmon habitats.

San Francisco Bay Region

Encompassing the iconic San Francisco Bay and its surrounding watershed, this highly urbanized region faces unique water

challenges. The San Francisco Bay Region is home to a dense population and extensive urban infrastructure, which contribute to problems such as urban runoff, saltwater intrusion, and habitat degradation. The San Francisco Estuary, where freshwater from the Sacramento and San Joaquin Rivers meets the Pacific Ocean, is crucial for both ecological health and water supply conveyance, making this region vital for statewide water management.

Central Coast Region

Stretching from the San Francisco Peninsula to Santa Barbara County, the Central Coast Region features diverse landscapes, including dramatic coastal cliffs, fertile agricultural valleys, and rich marine ecosystems. Major rivers, such as the Salinas River and the Santa Maria River, are central to supporting the region's agriculture, which is heavily dependent on both surface water and groundwater resources. Groundwater depletion and saltwater intrusion are ongoing concerns in this region due to agricultural demands and limited precipitation.

Sacramento River Region

Centered around the Sacramento River, California's largest river, this region forms the backbone of the state's water supply system. The Sacramento River and its tributaries, including the Feather, Yuba, and American Rivers, drain the northern Central Valley and are crucial to the Sacramento-San Joaquin Delta, a key hub for both water conveyance and ecological health. The region supports extensive agriculture and urban areas while being vital for fisheries and flood control. Figure 18.2.6 illustrates the geographic extent of the Sacramento River Basin and its tributaries.



Figure 18.2.6: "The Sacramento River Basin" by the California Department of Conservation is in the public domain. Access a detailed description.

San Joaquin River Region

The San Joaquin River Basin covers roughly 16,000 square miles (~4, 100 square kilometers) and has been heavily managed through infrastructure projects such as the Central Valley Project. This region plays a critical role in California's agricultural production, though water use has significantly altered natural river flows. Efforts such as the San Joaquin River Restoration Program aim to restore river flows and fisheries. The basin is fed by snowmelt from the Sierra Nevada, with the eastside tributaries, including the Tuolumne, Stanislaus, and Merced Rivers, being dominated by snowmelt runoff. Figures 18.2.7 and 18.2.8 provide detailed maps of the San Joaquin River Basin and its hydrologic features.

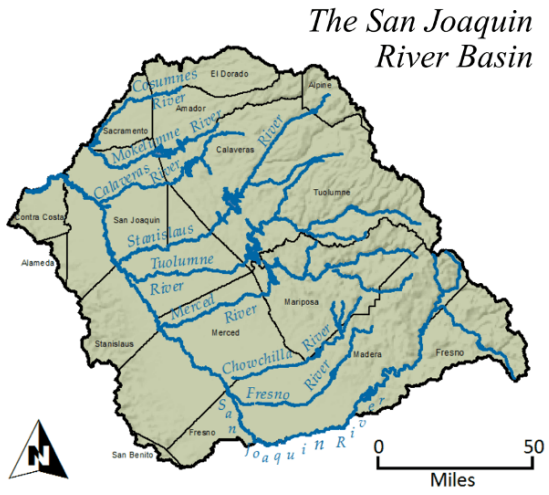


Figure 18.2.7: "The San Joaquin River Basin" by the California Department of Conservation is in the public domain. Access a detailed description.

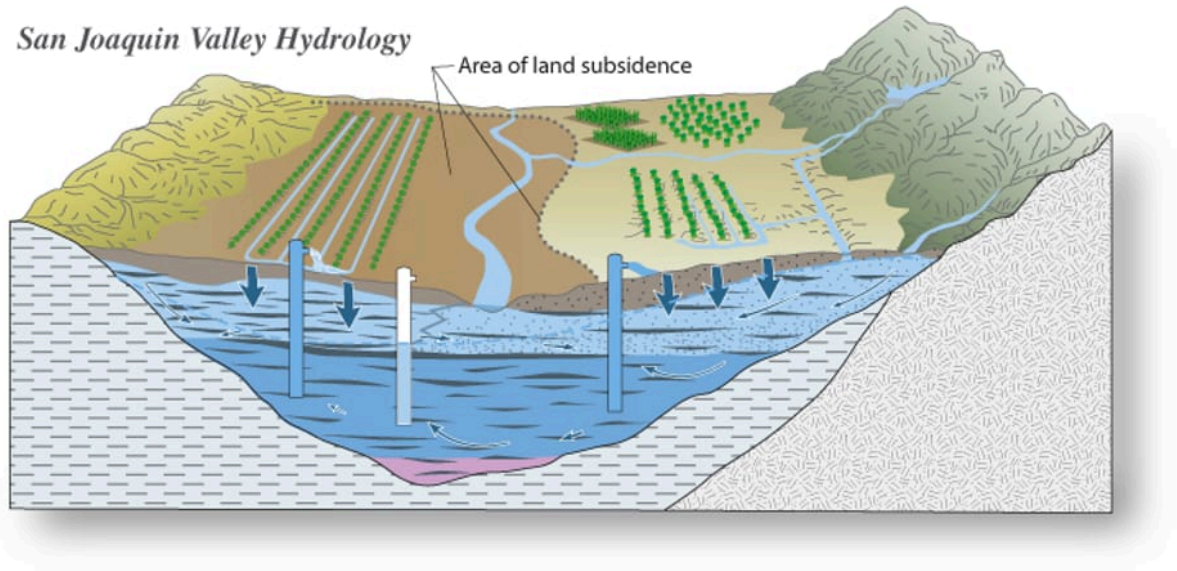


Figure 18.2.8: "The San Joaquin Valley hydrology conceptual model" by the United States Geological Survey is in the public domain. Access a detailed description.

Tulare Lake Region

Historically home to Tulare Lake, once one of the largest freshwater lakes in the United States, the Tulare Lake Basin is now predominantly agricultural and faces challenges related to groundwater depletion and land subsidence. The region's rivers, including the Kings, Kaweah, Tule, and Kern, drain into what was once the Tulare Lakebed, a natural depression in the Central Valley. This closed basin only overflows into the San Joaquin River during extremely wet years. Figure 18.2.9 shows the geographic extent of the Tulare Lake Basin and its main rivers.



Figure 18.2.9: "The Tulare Lake River Basin" by the California Department of Conservation is licensed under public domain. Access a detailed description.

North Lahontan Region

Covering the northeastern corner of California, the North Lahontan Region is part of the Great Basin Desert. This sparsely populated region is characterized by alkaline lakes, sagebrush scrublands, and limited surface water resources. The region's rivers, such as the Susan River, are small and do not contribute to outflows beyond the Great Basin, making water management focused primarily on local use.

South Lahontan Region

Encompassing parts of the eastern Sierra Nevada and the Mojave Desert, the South Lahontan Region features rugged landscapes and iconic desert ecosystems. High-elevation lakes and rivers, such as the Owens River and Truckee River, are central to the region’s hydrology. However, the region is also known for its history of water conflicts, particularly involving the diversion of water from the Owens Valley to supply the city of Los Angeles.

South Coast Region

The South Coast Region is one of California's most densely populated areas, including major metropolitan centers such as Los Angeles, San Diego, and Orange County. This region relies heavily on imported water from the Colorado River, the Sacramento-San Joaquin Delta, and local groundwater supplies to meet the demands of its urban populations, agriculture, and industry. Water management challenges in this region include limited natural water resources, groundwater overdraft, and saltwater intrusion into coastal aquifers. Extensive water infrastructure, including reservoirs, aqueducts, and desalination plants, plays a crucial role in maintaining the region's water supply. Despite the arid climate, the South Coast Region supports diverse ecosystems, including coastal wetlands and chaparral, though many natural water systems have been significantly altered by urban development.

Colorado River Region

Located in southeastern California, the Colorado River Region is defined by its hot, arid desert landscape and its reliance on the Colorado River for water supply. This region includes the Imperial and Coachella Valleys, which are vital agricultural areas dependent on irrigation from the Colorado River. The region faces numerous water management challenges, including salinity issues, overal location of the Colorado River's water, and environmental concerns such as the shrinking of the Salton Sea. Innovative water conservation programs, such as the lining of canals to reduce water loss, are critical to sustaining both agriculture and urban water needs in this region. The Colorado River’s flow into California is tightly controlled through a series of dams and agreements with neighboring states and Mexico, making the region's water management intricately connected to interstate and international agreements.

Connecting Water Basins, Regions, and Groundwater Resources

Throughout the rest of this chapter, we will continue to explore the hydrological and geological features of each region, focusing on how the distinct basins within California's hydrologic regions shape water availability, distribution, and management. These surface water basins not only define the flow and collection of water but also serve as gateways to the state's vital groundwater reserves. As we transition to the next section, we will examine how these same basins influence groundwater recharge, storage, and extraction. By understanding the interplay between surface and groundwater systems and adopting integrated water management approaches, we can work towards ensuring sustainable water resources for future generations and promoting resilience in the face of changing environmental conditions.

References

1. California Department of Water Resources. (1987). *California water: Looking to the future* (Bulletin 160-87, p. 122). Sacramento, CA.
2. California Department of Water Resources. (2020). *California*'s *Groundwater* (Bulletin 118). Sacramento, CA.
3. California Department of Water Resources. (2009). *California Water Plan Update 2009, Volume 1: The Strategic Plan, Chapter 3: Companion State Plans*. Retrieved April 11, 2024 from https://water.ca.gov/-/media/DWR-Website/Web-Pages/Programs/California-Water-Plan/Docs/Update2009/Volume_1_Strategic_Plan/Vol1_Ch03_Companion_State_Plans.pdf
4. California Department of Water Resources. (n.d.). *Home*. Retrieved April 11, 2024, from https://water.ca.gov/
5. California Water Boards: Central Valley R5. (n.d.). *Tulare Lake Basin* (SWAMP). Retrieved April 11, 2024, from https://www.waterboards.ca.gov/centralvalley/water_issues/swamp/tulare_lake_basin/#pastefforts
6. California Water Boards: Central Valley R5. (n.d.). *San Joaquin River Basin* (SWAMP). Retrieved April 11, 2024, from https://www.waterboards.ca.gov/centralvalley/water_issues/swamp/sanjoaquin_river_basin/
7. California Water Boards: Central Valley R5. (n.d.). *Sacramento River Basin* (SWAMP). Retrieved April 11, 2024, from https://www.waterboards.ca.gov/centralvalley/water_issues/swamp/sacramento_river_basin/

This page titled 18.2: Running Water is shared under a CC BY-NC 4.0 license and was authored, remixed, and/or curated by Cole Heap.

18.3: Groundwater

Water Beneath the Surface

California's hydrogeology, the study of how water interacts with geological formations, plays a vital role in sustaining its diverse ecosystems and human activities. Groundwater, the water stored beneath the Earth's surface, is essential for agriculture, industry, and municipal water supplies, especially in a state where surface water resources are highly variable. This section explores the origins, movement, and significance of groundwater within California's complex geological framework.

Aquifers

Groundwater forms as precipitation infiltrates into the ground, filling the spaces within sediments and rocks—spaces known as porosity. While groundwater is sometimes found in large underground caverns, particularly in karst systems, it is far more commonly stored in small, connected pore spaces between grains of sediment. Groundwater must be extracted carefully based on an understanding of both the porosity and permeability of the materials it resides in. Video 18.3.1 demonstrates how porosity and permeability define the characteristics of subsurface water reservoirs, known as aquifers.

Video 18.3.1 - What is an Aquifer?

The following video illustrates what an underground aquifer is and how they form:

This interactive element is not available in this format. Visit the link or scan the QR code to access it online.

View this YouTube Video online

"What is an Aquifer?" by Geoscience Videos licensed under CC BY-NC 4.0.

As water seeps into the ground, some of it is held in the unsaturated zone, near the surface, while the rest moves downward into the saturated zone, where all pore spaces are filled with water. The boundary between these two zones is known as the water table. The depth of the water table varies significantly across California, from a few feet below the surface in river valleys to hundreds of feet underground. Seasonal changes and droughts can cause substantial fluctuations in the water table, with droughts sometimes causing it to drop tens of feet.

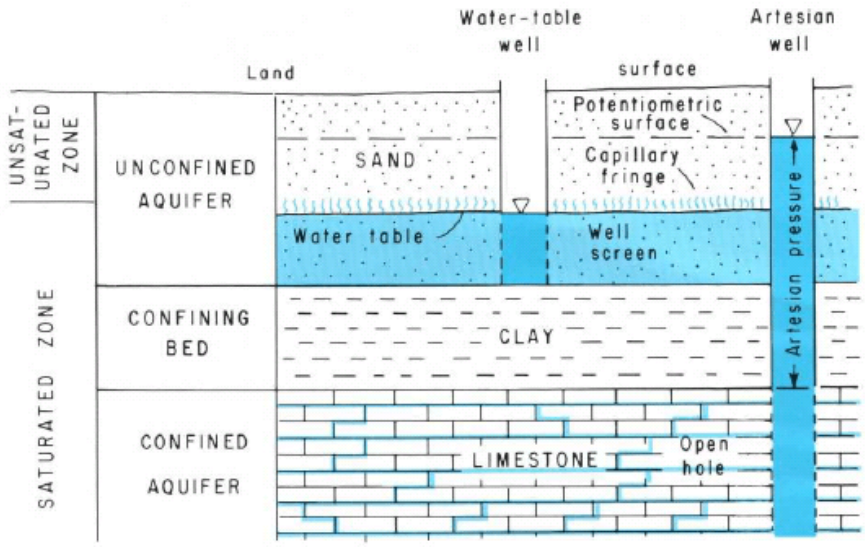


Figure 18.3.1: "Types of aquifers" by Ralph C. Heath is licensed under public domain. Access a detailed description.

Activity - Material Porosity 18.3.1

This interactive element is not available in this format. Visit the link or scan the QR code to access it online.

View this Interactive Content online

Groundwater moves slowly, migrating from areas of high pressure to lower pressure, typically from higher to lower elevations. The rate of movement can vary significantly, ranging from more than 1 foot per day to as little as 1 foot per year. In California, much of the state's groundwater is stored in unconsolidated, young alluvial deposits beneath valleys and basins, particularly in regions like the Central Valley. Figure 18.3.2 illustrates the different types of aquifers found throughout the state, including confined and unconfined aquifers.

Modern groundwater extraction primarily relies on aquifers at relatively shallow depths, typically ranging from a few feet to just over a hundred feet. Confined aquifers, situated between layers of impermeable rock or sediment, store water under pressure. When tapped by a well, this pressure can cause water to rise to the surface without pumping, a phenomenon known as an artesian well (Figure 18.3.3). In contrast, unconfined aquifers are open to the atmosphere through permeable materials, making them easier to recharge through surface water infiltration but also more susceptible to surface contamination. Figure 18.3.2 illustrates the characteristics of both confined and unconfined aquifers, emphasizing the importance of their permeability and pressure dynamics in groundwater management. Groundwater extraction involves drilling wells into the saturated zone of these aquifers.

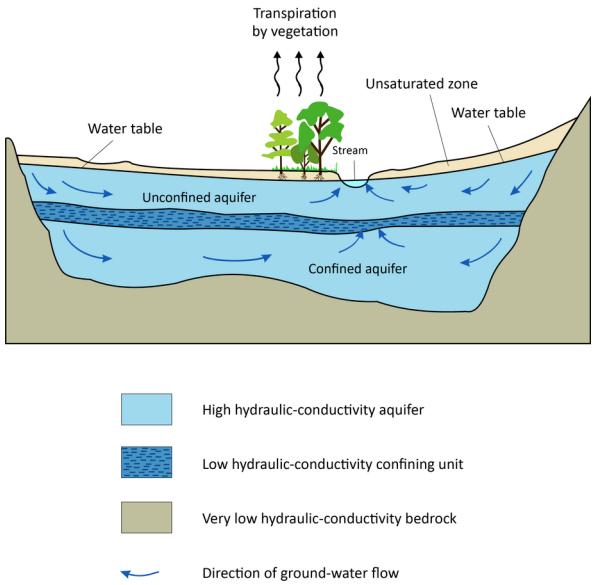


Figure 18.3.2: "Aquifer conditions and water flow" by Hans Hillwaert is licensed under CC BY-NC 4.0 ; view original. Access a detailed description.

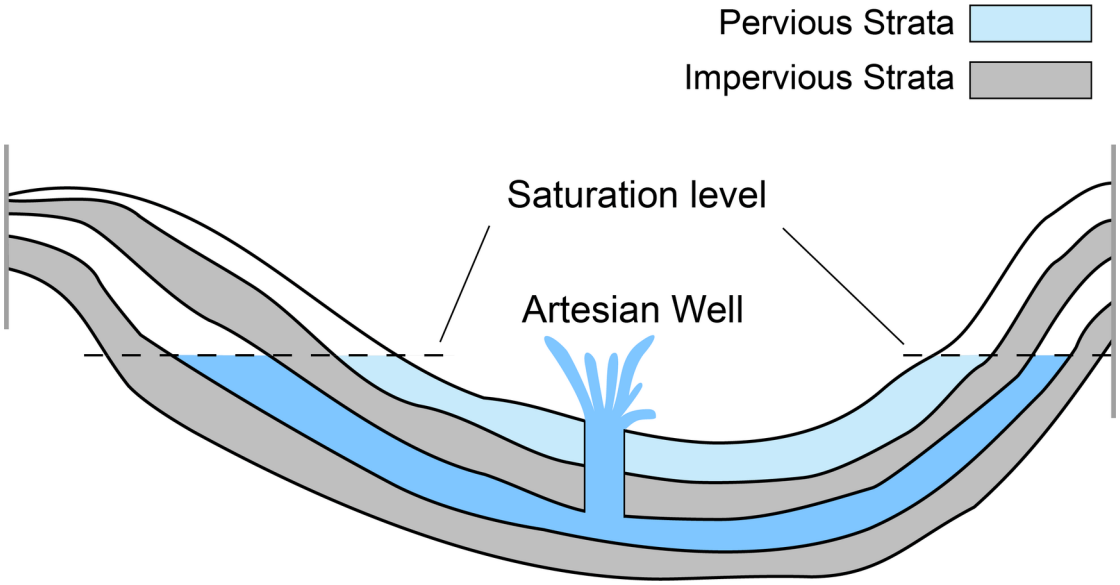


Figure 18.3.3: "Artesian aquifer conditions and well flow" by Andrew Dunn CC BY-NC 4.0. A derivative from the original work, view original. Access a detailed description.

However, continuous extraction of groundwater, especially during prolonged drought periods, causes the water table to drop. In confined aquifers, this reduction in pressure can eliminate artesian conditions, necessitating the use of mechanical pumps to bring water to the surface. The declining water table is a growing concern across California, particularly in agricultural regions where groundwater serves as a critical water supply.

As the water table decreases, the artesian conditions diminish, necessitating the use of mechanical pumps to lift water to the surface. With continuous declines in the water table and a lack of recharge due to drought, wells can eventually run dry.

Quality Aquifers 18.3.2

This interactive element is not available in this format. Visit the link or scan the QR code to access it online.

View this Interactive Content online

California Aquifer Systems

California is home to a variety of aquifer systems, each shaped by the state's diverse geology and playing a critical role in meeting the water needs of agriculture, municipalities, and industry. However, these aquifer systems face significant challenges, including over-extraction and prolonged drought. Table 18.3.1 provides an overview of California's primary aquifer systems, highlighting total water use and the sectors that consume the most water from each system, measured in billion gallons per day.

Table 18.3.1: California Aquifer Systems and Total Water Use

Aquifer System	Total Water Use (bgd)	Principal Consumptive Water Use
Great Valley Aquifer System (Sacramento Valley, Delta, San Joaquin Valley, and Tulare)	9.81	Irrigation (9.91 bgd)
Basin and Range Carbonate and Basin Fill Aquifers	5.70	Irrigation (4.55 bgd); Public Supply (1.08 bgd)
Coastal Basin Aquifers (Santa Clara Valley and Southern CA Coastal)	3.45	Irrigation (1.76 bgd); Public Supply (1.58 bgd)
Pacific Northwest Basaltic Rock and Basin Fill Aquifers	1.34	Irrigation (1.21 bgd)

Figure 18.3.4 complements Table 18.3.1 as it shows the approximate locations and spatial distribution of California's major aquifer systems.

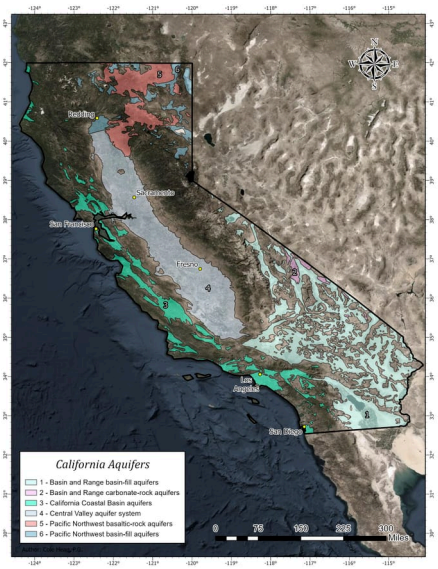


Figure 18.3.4: California Aquifers by geographic location. “California’s Aquifers” by Cole Heap from the California Open Data Portal is licensed under CC BY-NC 4.0. Constructed in a GIS. Access a detailed description.

California's aquifers play a crucial role in supplying water for agricultural, municipal, industrial, and environmental needs across the state. These underground reservoirs of water, stored within porous rock formations and sedimentary deposits, vary in size, depth, and geological characteristics, reflecting the diverse hydrogeological conditions present in different regions of the state. This section provides an overview of California's aquifers, including their locations, associated hydrologic regions, and geological attributes.

Basin and Range Basin-Fill Aquifers

The Basin and Range Basin-Fill Aquifers are found primarily in eastern California, stretching from the eastside of the Modoc Plateau, in Nevada, to the Mojave Desert in the southeast of California. These aquifers are composed of unconsolidated to semi-consolidated alluvial deposits, including gravel, sand, silt, and clay, which have accumulated over millions of years from weathering and erosion of adjacent mountains. The permeability and hydraulic conductivity vary widely due to the heterogeneous nature of the deposits, with coarse-grained materials forming high-permeability zones and finer-grained materials creating low-permeability layers. The aquifers are recharged primarily by precipitation and runoff from surrounding mountains and by infiltration from rivers and streams, with discharge occurring through springs, seeps, and pumping. Faulting and tectonic activity influence groundwater movement, while the arid to semi-arid climate results in limited natural recharge. Over-extraction in some areas has led to declining water levels and land subsidence, necessitating careful groundwater management t

Basin and Range Carbonate-Rock Aquifers

The Basin and Range carbonate aquifers of California, predominantly located in the eastern part of the state, north of the Mojave Desert. These aquifers consist of extensive limestone and dolomite formations, which have developed significant secondary porosity and permeability through the processes of dissolution and fracturing. The carbonate rocks form highly productive aquifers with zones of enhanced permeability along faults and fractures, facilitating substantial groundwater flow. Recharge primarily occurs from precipitation and runoff in the surrounding mountainous areas, with infiltration through sinkholes and karst features. Discharge happens through springs, seeps, and wells. The hydrogeology is heavily influenced by faulting and tectonic activity, which create conduits for groundwater movement and storage. The arid to semi-arid climate limits natural recharge, making sustainable management of these aquifers crucial to prevent over- extraction, declining water levels, and land subsidence. Effective groundwater management is essential to balance use with recharge rates, ensuring the long-term viability of these critical water resources.

California Coastal Basin Aquifers

The California Coastal Basin aquifers are located along the state’s coastal regions, including areas from the San Francisco Bay in the north to the Los Angeles and San Diego basins in the south. These aquifers are primarily composed of unconsolidated

to semi-consolidated alluvial deposits, including sand, gravel, silt, and clay, which allow for varying degrees of permeability and water storage. In some areas, these aquifers are bounded by impermeable bedrock, creating confined aquifers with significant water storage potential.

Recharge primarily occurs through precipitation, stream infiltration, and artificial recharge methods, though the arid to semi-arid climate in many coastal regions limits natural recharge. Over-extraction of groundwater in these aquifers, driven by urban, industrial, and agricultural demands, has resulted in declining water levels and the associated threat of saltwater intrusion, where seawater encroaches into freshwater aquifers. This issue is particularly prevalent in densely populated areas like the Los Angeles Basin.

The hydrogeology of these aquifers is heavily influenced by tectonic activity, with faults and fractures providing pathways for both water flow and potential contamination. Groundwater management strategies in the Coastal Basin aquifers focus on mitigating over-extraction, addressing saltwater intrusion, and ensuring sustainable use. Techniques such as managed aquifer recharge, desalination, and the use of “guardian wells” to create freshwater barriers have become essential tools for maintaining the viability of these critical water resources in California’s coastal regions.

Central Valley Aquifer System

The Central Valley Aquifer System spans over 450 miles (724 km) from the Cascade Mountains in the north to the Tehachapi Mountains in the south, encompassing the Sacramento River Region, San Joaquin River Region, and Tulare Lake Region. This aquifer system, one of the most important in the United States, is composed of unconsolidated sedimentary deposits, including gravel, sand, silt, and clay, deposited by ancient rivers. These sediments create layers with varying permeability and hydraulic conductivity.

Groundwater extraction from the Central Valley Aquifer System exceeds natural recharge rates, leading to a steady decline in water levels, with some areas seeing drops of over 40 feet. Recharge is primarily dependent on precipitation and overland flow, which varies widely across the state. For example, the arid southern half of the Central Valley receives little recharge, while the northern region benefits from greater precipitation and snowmelt. Despite this, groundwater extraction continues to outpace recharge, raising concerns about sustainability.

Pacific Northwest Basaltic-Rock Aquifers

The Pacific Northwest basaltic-rock aquifers in California are primarily found in the northern part of the state, extending from the Klamath Mountains to the Modoc Plateau. These aquifers are composed of layered basalt flows, which have developed secondary porosity and permeability through fracturing and weathering. The basaltic-rock formations create aquifers with varying degrees of permeability, where joints, fractures, and interflow zones facilitate significant groundwater movement. Recharge occurs mainly from precipitation and runoff in the higher elevations, with infiltration enhanced by the porous and fractured nature of the basalt. Groundwater discharge takes place through springs, streams, and wells. The hydrogeology is influenced by the region's volcanic history and tectonic activity, which shape the distribution and flow of groundwater. Due to the region's climate, natural recharge can be substantial, but localized variations in permeability and groundwater flow paths necessitate careful management. Sustainable management practices are crucial to maintain water levels and prevent over-extraction, ensuring the long-term viability of these important groundwater resources.

Pacific Northwest Basin-Fill Aquifers

The Pacific Northwest basin-fill aquifers in California, located primarily in the northern part of the state, extend from the Klamath Mountains to the Modoc Plateau. These aquifers consist of unconsolidated to semi-consolidated alluvial deposits, including gravel, sand, silt, and clay, accumulated over millions of years from weathering and erosion of the surrounding mountains. The permeability and hydraulic conductivity of these aquifers vary widely, with coarse-grained materials forming high-permeability zones and finer-grained materials creating low-permeability layers. Recharge primarily occurs from precipitation and runoff in the surrounding highlands, with additional infiltration from rivers and streams. Groundwater discharge happens through springs, seeps, and wells. The hydrogeology is influenced by the region's complex depositional history and tectonic activity, which affect groundwater flow and storage. The relatively wetter climate of the Pacific Northwest allows for substantial natural recharge, but localized variations in aquifer properties and groundwater flow paths require careful management.

Groundwater Resources to Water Infrastructure

California's diverse aquifer systems are essential for meeting the state's water needs, but ensuring their sustainability requires an integrated approach to water management. As we have explored, the hydrogeological characteristics of these aquifers dictate their recharge rates, storage capacities, and vulnerabilities, especially in the context of over-extraction and changing climate conditions. To maintain a balanced water supply, California relies not only on its aquifers but also on an extensive water infrastructure system that manages surface water resources. In the next section, we will delve into the state's water infrastructure, including dams, reservoirs, aqueducts, and levees, which work in concert with groundwater management to transport and store water across the state. These systems are vital for supporting agriculture, urban areas, and ecosystems, and their management involves the collaboration of federal, state, and private entities.

References

1. California Department of Public Health, 2009, https://www.epa.gov/wqs-tech/water-quality-standards-regulations-california
2. California Department of Water Resources, 2003, California's Groundwater, Bulletin 118, https://water.ca.gov/programs/groundwater-management/bulletin-118
3. United States Office of Ground Water and Drinking Water, December 2023, https://www.epa.gov/ground-water-and-drinking-water/national-primary-drinking-water-regulations
4. U.S. Geological Survey. (n.d.). *General facts and concepts about ground water*. In Sustainability of Ground-Water Resources: Circular 1186. Retrieved April 12, 2024 from https://pubs.usgs.gov/circ/circ1186/html/gen_facts.html

This page titled 18.3: Groundwater is shared under a CC BY-NC 4.0 license and was authored, remixed, and/or curated by Cole Heap.

18.4: Water Infrastructure and Management

Managing and Moving Water Across California

The movement and storage of water in California are part of a complex and interconnected system that directly ties into the hydrologic cycle's pools and fluxes (Figure 18.4.1). These systems, which store and transport water across diverse landscapes, are crucial for managing the state's limited water resources. Without this extensive water infrastructure—including dams, reservoirs, aqueducts, and levees—California would not be able to support its current population or sustain its agricultural economy. This section examines the key components of California's water management systems, including the major projects that distribute water across the state, the challenges they face, and the efforts to maintain and improve these systems in the context of increasing climate variability and population growth. Video 18.4.1 further demonstrates the importance and size of some of California's water infrastructure projects.



Figure 18.4.1: "California water system" by Shannon1 via Wikimedia Commons is licensed under CC BY-SA 3.0. Access a detailed description.

Video 18.4.1 - California State Water Project

This video provides an aerial tour of California's state water project:

This interactive element is not available in this format. Visit the link or scan the QR code to access it online.

View this YouTube Video online

"California State Water Project" by The California Department of Water Resources is in the public domain. Access a transcript for this video.

Dams: Storing Water for the Future

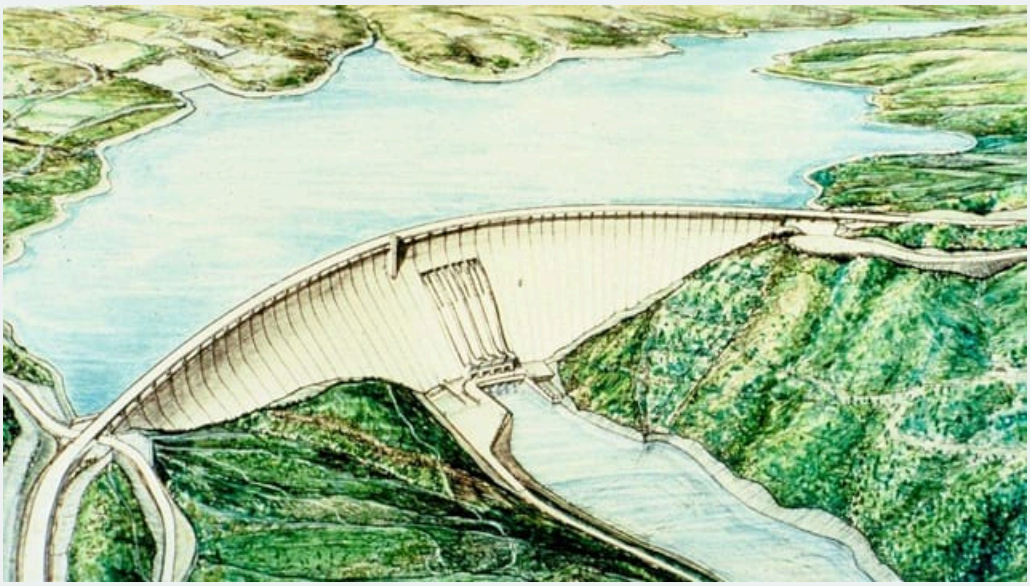
Dams play an essential role in California's water management by storing water, controlling floods, generating hydroelectric power,

and offering recreation. Major structures such as Oroville Dam on the Feather River, Shasta Dam on the Sacramento River, and Folsom Dam on the American River (Figure 18.4.2) are vital for supporting the state's agricultural, urban, and environmental needs. These structures ensure a stable water supply for millions of people, even during extended droughts, while also controlling flooding and generating renewable energy that reduces greenhouse gas emissions. However, they face significant challenges related to seismic hazards, sediment accumulation, and environmental impacts.

The construction of dams in California, particularly in a seismically active region, involves overcoming numerous geologic challenges (Figure 18.4.3). Dams must be designed to handle the potential for earthquakes, foundation instability, and long-term sediment accumulation. The potential flood risk due to dam failure is a stark reminder of the balance between water storage and safety. The case of the Auburn Dam, for example, which faced significant seismic risk concerns, highlights the difficulty of constructing dams in such geologically complex areas. Failure to address seismic concerns could result in catastrophic flooding, emphasizing the need for advanced engineering and design.

Box 18.4.1: The Dam that Would Never Die

The proposed Auburn Dam, situated on the American River in California's Sierra Nevada foothills, has been a subject of controversy and debate since its inception in the mid-20th century (Figure 18.4.1). Initially conceived as a multipurpose project for flood control, water supply, and hydroelectric power generation, the dam's construction faced numerous challenges and opposition from environmental groups and local communities. Advocates argued that the dam would provide essential water storage capacity, particularly during periods of drought, while opponents raised concerns about the potential environmental impacts, including habitat destruction, sedimentation, and threats to endangered species such as the Chinook salmon. Despite decades of planning and intermittent construction efforts, the Auburn Dam project was ultimately halted in the 1980s due to safety concerns related to seismic activity and the potential for catastrophic failure in the event of an earthquake. Today, the remains of the partially constructed dam stand as a testament to the complexities of balancing water resource development with environmental conservation and public safety in California's dynamic landscape.



Box Figure 18.4.1: "A concept drawing of the Auburn Dam" by the U.S Army Corps of Engineers is in the public domain. Access a detailed description.

Another major issue surrounding dams is their impact on sediment transport and aquatic ecosystems. Dams trap sediment that would naturally flow downstream, leading to sediment deficits, erosion, and loss of habitat diversity in riverine environments. This has led to degraded aquatic ecosystems, especially in rivers historically important for species like salmon. The ongoing Klamath Dam removal project, the largest dam removal in U.S. history, is a significant effort to restore fish habitats by removing barriers that have altered natural flow and sediment processes. Scheduled for completion in 2024, the removal of four dams on the Klamath River aims to restore critical salmon habitats that are culturally and economically important to Indigenous peoples such as the Yurok.

In addition to environmental challenges, dams face ongoing concerns about their economic viability and social impacts. The thick sediment accumulated behind dams poses one of the greatest challenges in dam removal projects like Klamath, where the

management of sediment post-removal is crucial for ecosystem restoration. Dams are also criticized for displacing communities, altering land use, and affecting cultural heritage sites. Despite these controversies, the role of dams in California's water management is crucial for meeting the state's current demands. Addressing these issues requires a balance between maintaining infrastructure, managing sediment, and minimizing ecological disruptions.

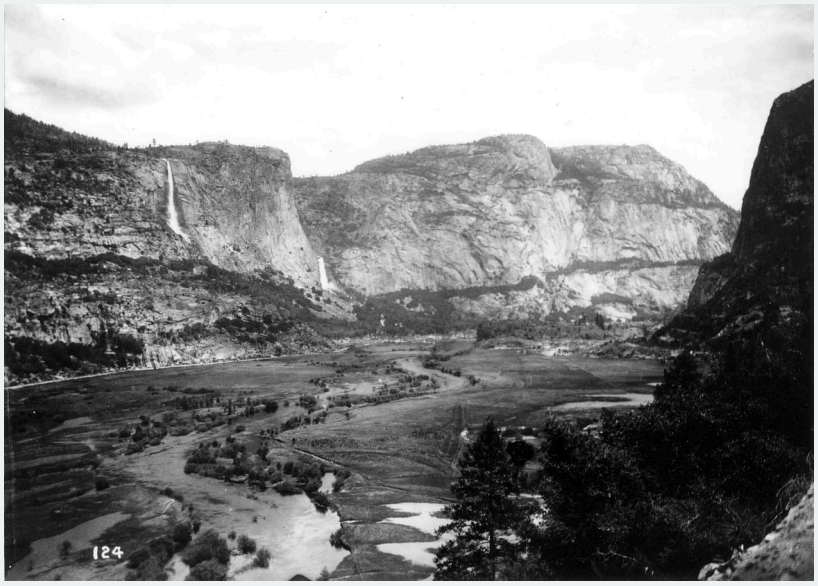
Box 18.4.2: Hetch Hetchy Reservoir

The Hetch Hetchy Reservoir, located in Yosemite National Park, is a significant water storage facility in California, serving as a critical water source for the city of San Francisco and its surrounding areas. Constructed in the early 20th century, the reservoir inundated the once-pristine Hetch Hetchy Valley, sparking controversy and debates over the trade-offs between water supply needs and environmental conservation. Figure 18.4.2is a view across Hetch Hetchy Valley before the dam was built.

The Hetch Hetchy Reservoir was built between 1913 and 1923 as part of the Hetch Hetchy Project, which aimed to provide a reliable water supply to San Francisco and the surrounding Bay Area. The reservoir, formed by the O'Shaughnessy Dam on the Tuolumne River, has a capacity of over 360,000 acre-feet and provides drinking water to over 2.6 million people.

The construction of the Hetch Hetchy Reservoir and the inundation of the Hetch Hetchy Valley sparked controversy and opposition from conservationists, led by John Muir and the Sierra Club. The valley, renowned for its natural beauty and ecological significance, was considered by Muir as the "second Yosemite" and was seen as a natural treasure worth preserving. Box Figure 18.4.3 exhibits what Hetch Hetchy looks like in the modern day.

The decision to dam the Tuolumne River and flood the Hetch Hetchy Valley raised concerns about the loss of habitat, biodiversity, and scenic beauty. Conservationists argued that the valley should be preserved in its natural state for future generations to enjoy and appreciate.



Box Figure 18.4.2: View of Hetch Hetchy Valley in the early 1900s from the southwestern end showing the Tuolumne River flowing through the lower portion of the valley prior to damming. "View across Hetch Hetchy Valley" by the National Park Service is in the public domain. Access a detailed description.



Box Figure 18.4.3: "Hetch Hetchy Panorama – Yosemite National Park" in 2019 by Vulpinus2 is licensed under CC BY-4.0 DEED. Access a detailed description.

Despite the controversy, the Hetch Hetchy Reservoir has provided significant benefits in terms of water supply reliability and municipal water quality for San Francisco and the Bay Area. The reservoir's stored water supports domestic, industrial, and agricultural needs, contributing to the region's economic prosperity and population growth.

In recent years, efforts have been made to balance water supply needs with environmental conservation and restoration in the Hetch Hetchy area. The San Francisco Public Utilities Commission, which manages the Hetch Hetchy Reservoir, has implemented measures to enhance habitat restoration, water quality monitoring, and public access to the surrounding lands.

The Hetch Hetchy Reservoir remains a symbol of the complex trade-offs between water supply demands and environmental conservation in California. While the reservoir provides critical water resources for urban populations, its construction and the flooding of the Hetch Hetchy Valley continue to evoke debates and discussions about the values of natural landscapes and the importance of sustainable water management practices.

Aqueducts: Moving Water Across the State

Aqueducts are the lifeblood of California's water infrastructure, transporting water from areas of surplus, such as Northern California and the Sierra Nevada, to the water-scarce regions of the Central Valley and Southern California. These engineering marvels span hundreds of miles across diverse landscapes, including mountains, valleys, and deserts, overcoming significant geological and logistical challenges. The California Aqueduct (Figure 18.4.2), which carries water over 700 miles from the Sacramento-San Joaquin Delta to Southern California, is one of the largest water conveyance systems in the world. Without such infrastructure, much of California's agriculture and urban water supply would be unsustainable.



Figure 18.4.2: "Aerial photo of the California Aqueduct at the Interstate 205 crossing," just east of Interstate 580 junction by Ikluft is licensed under CC BY-SA 3.0. Access a detailed description.

Aqueducts face significant geologic and engineering challenges, including seismic risks, terrain variability, and the need to cross fault zones. These challenges require robust designs to ensure stability and functionality, even in the face of California's tectonic activity. Aqueducts like the Los Angeles Aqueduct must traverse mountain ranges and deserts, with extensive tunnels, pipelines, and pumping stations ensuring that water flows continuously despite changes in elevation and geography. For example, a single water molecule might fall as rain in the upper Trinity basin, only to be pumped through tunnels, aqueducts, and across the Central Valley before it reaches Southern California.

Maintaining aqueducts is essential for ensuring continuous water delivery. Aging infrastructure, sedimentation, and vegetation encroachment pose challenges that require ongoing maintenance efforts. Sediment accumulation in aqueducts, caused by natural processes in rivers and reservoirs, reduces water flow and requires regular dredging. Water quality is another concern, as contaminants like algae and biofouling can reduce water purity. Addressing these challenges involves collaboration between federal, state, and local agencies to ensure aqueducts remain functional and resilient in the face of changing climate conditions.

Levees: Protecting Against Flooding

Levees are critical for flood protection in California, especially in regions like the Sacramento-San Joaquin Delta and the Central Valley. These engineered barriers prevent flooding by confining river or coastal waters within designated areas, safeguarding communities, agricultural lands, and infrastructure from inundation. Levees are particularly vital in low-lying areas such as the Delta, where they protect against both riverine flooding and sea-level rise (Figure 18.4.3).



Figure 18.4.3: "A levee around a Sacramento suburb" by US Army Corps of Engineers is in the public domain. Access a detailed description

Sacramento-San Joaquin Delta Levees

The Sacramento-San Joaquin Delta, situated in the Sacramento River Region and San Joaquin River Region, is a critical hub for water conveyance and ecosystem support in California. Levees in the Delta region form an extensive network of flood protection infrastructure, designed to safeguard agricultural lands, urban areas, and water supply facilities from inundation. These levees are located along the banks of the Sacramento River, San Joaquin River, and various sloughs and channels within the Delta.

In recent years, concerns have arisen regarding the aging infrastructure of the levee system along the Sacramento River and its surrounding areas. Many of these levees were originally constructed in the early to mid-20th century and were designed to withstand certain flood events based on historical data and engineering practices at the time. However, as time has passed, the effectiveness and reliability of these levees have come into question due to several factors.

Firstly, the aging infrastructure of the levees has raised concerns about their structural integrity and ability to withstand modern flood events, especially in the face of climate change and the potential for more frequent and severe flooding. The original design standards may no longer be sufficient to address the increased risks associated with changing hydrological conditions and rising sea levels.

Secondly, ongoing maintenance and repair efforts are required to address deterioration and erosion of levee structures over time. The Sacramento region's levees are subjected to various forms of wear and tear, including erosion from river currents, seepage, vegetation growth, and burrowing animals. Failure to adequately maintain and reinforce these levees could increase the risk of breaches and inundation during flood events, posing threats to public safety and property.

Furthermore, the aging infrastructure of the Sacramento levees highlights the need for comprehensive risk assessments, long-term planning, and investment in levee rehabilitation and modernization projects. Upgrading and retrofitting levee systems with advanced engineering techniques, materials, and technologies can improve their resilience to flooding and enhance their performance in safeguarding communities and critical infrastructure.

Addressing the concerns surrounding the age of the Sacramento levees requires proactive measures, including robust maintenance programs, infrastructure upgrades, and investments in flood risk management strategies. By prioritizing levee safety and resilience, the Sacramento region can better protect against the threat of flooding and ensure the long-term sustainability of its levee infrastructure.

Central Valley Levees

In addition to the Sacramento-San Joaquin Delta, levees are also prevalent along the rivers and waterways of the Central Valley, encompassing the Sacramento River Region, San Joaquin River Region, and Tulare Lake Region. These levees protect agricultural lands, rural communities, and critical infrastructure from flooding during periods of high water levels. Major rivers in the Central Valley, including the Sacramento River, San Joaquin River, and Kings River, are lined with levees to mitigate flood risks.

Coastal Levees

Along the California coastline, levees are constructed to protect coastal communities, infrastructure, and low-lying areas from storm surges, high tides, and coastal erosion. Coastal levees are located in various hydrologic regions, including the North Coast Region, San Francisco Bay Region, Central Coast Region, and South Coast Region. They are particularly prevalent in densely populated urban areas such as the San Francisco Bay Area, Los Angeles Basin, and San Diego metropolitan area.

Riverine Levees

Riverine levees are constructed along rivers and waterways throughout California to prevent riverine flooding and to channelize flow patterns. These levees are found in multiple hydrologic regions, including the Sacramento River Region, San Joaquin River Region, Santa Ana River Region, and Colorado River Region. They protect agricultural lands, residential areas, and critical infrastructure from inundation during periods of high water levels and heavy rainfall events.

Challenges and Maintenance

Levees are also prominent throughout the Central Valley, where they line the major rivers and provide flood protection to

agricultural lands and rural communities. In coastal regions, such as the San Francisco Bay Area and the Los Angeles Basin, levees protect urban areas from storm surges and high tides. However, like their inland counterparts, these coastal levees face challenges related to aging infrastructure and the increasing threat of sea-level rise.

Despite their importance, levees require ongoing maintenance and modernization. The state is exploring alternative flood control strategies, such as wetland restoration, which could provide natural flood protection by absorbing excess water during flood events. Projects like the Napa River Flood Protection Project demonstrate the potential of using natural systems to enhance flood resilience. These efforts aim to balance human needs with ecological preservation, creating flood management solutions that are sustainable and adaptive to future climate challenges.

A Future of Collaborative Water Management

California's water infrastructure, from dams and aqueducts to levees, is essential for managing the state's water resources in a rapidly changing environment. As the state faces increasing droughts, floods, and population growth, maintaining and modernizing this infrastructure is more important than ever. Collaborative efforts between government agencies, water districts, and communities will be key to ensuring the long-term sustainability of California's water systems, supporting both human needs and environmental health, all being dependent on the surrounding geology.

References

1. California Department of Water Resources. (2020). *California*'s *Groundwater* (Bulletin 118). Sacramento, CA.
2. California State Water Resources Control Board, https://www.waterboards.ca.gov
3. California Regulations, 2008, www.calregs.com
4. National Park Service, Yosemite, Hetch Hetchy Reservoir, https://www.nps.gov/yose/planyourvisit/hh.htm
5. United States Geological Survey, 2008, National Handbook of Recommended Methods for Water-Data Acquisition, Chapter 11, https://pubs.usgs.gov/chapter11/

This page titled 18.4: Water Infrastructure and Management is shared under a CC BY-NC 4.0 license and was authored, remixed, and/or curated by Cole Heap.

18.5: Threats to California's Water

Managing Water Quality and Addressing Environmental Challenges

Water quality in California is a complex topic, shaped by both natural processes and human activities. Understanding the interactions between geology, weathering, human land use, and water chemistry is crucial for managing the state's surface and groundwater resources. Both surface water and groundwater contain a variety of dissolved and solid materials, derived from rainfall, chemical weathering of rocks, and organic contributions from vegetation and animals. However, when undesirable or toxic substances are introduced, either naturally or through human activities, water quality can be compromised, as seen in the Kesterson Reservoir case (Table 18.5.1).

The Kesterson Effect: From Rock to Duck

The Kesterson Reservoir in the San Joaquin Valley became infamous in the 1980s due to the release of toxic substances into its waters, primarily selenium, a naturally occurring element found in the Moreno Formation, which consists of shale and sedimentary rocks. When water percolated through these selenium-rich rocks, agricultural runoff exacerbated the problem by mobilizing this element. Irrigation practices in nearby farmland increased the water flow through the drainage basin, leading to greater dissolution and transportation of selenium into the reservoir. Over time, selenium built up in the ecosystem, eventually reaching toxic levels that harmed local wildlife, particularly waterfowl. This pathway of selenium contamination was described by USGS scientists as the "Kesterson effect," defining the biogeochemical process from "rock to duck." The incident highlights the complex interplay between geology, human agricultural practices, and environmental health, underscoring the need for comprehensive management strategies to mitigate such contamination risks.

Water Contamination and Pollution

While weathering can release both essential and potentially harmful materials into water systems, it's important to recognize that not all substances derived from weathering are toxic. Organic compounds from plants and animals in a drainage basin contribute beneficial materials to water. In groundwater systems, solid particles are filtered through the sediment, which can help purify water as it moves through aquifers. However, water pollution occurs when toxic substances—whether from natural sources like volcanic gases and dissolved metals, or human-induced contaminants such as pesticides—are introduced at harmful concentrations.

Contaminants commonly found in California's waters include arsenic, nitrate, perfluoroalkyl and polyfluoroalkyl substances (PFAS), chromium-6, pesticides, lead, copper, and microorganisms like Escherichia coli and Cryptosporidium (Table 18.5.1). PFAS, often called "forever chemicals" because of their resistance to breaking down in the environment, are a group of synthetic substances widely used in products like non-stick cookware, water-repellent fabrics, firefighting foams, and food packaging. These chemicals have been found in water supplies across the U.S., including California, and can accumulate over time in both the environment and the human body. Exposure to PFAS has been linked to a range of adverse health effects, including liver damage, developmental problems, cancer, and immune system disruption. The persistent nature of PFAS makes them a significant challenge for water management and environmental health.

Table 18.5.1: Common contaminants to California's water supply, their occurrences, and associated risks.

Contaminant	Occurrences and Risks
Arsenic	Arsenic (As) contamination is a significant concern in many parts of California, particularly in areas where naturally occurring geological formations contain elevated levels of this toxic element. Groundwater is particularly susceptible to arsenic contamination. Long-term exposure to arsenic has been linked to various health issues, including cancer and cardiovascular disease.

Contaminant	Occurrences and Risks
Nitrates	Nitrate contamination, primarily stemming from agricultural activities and wastewater discharges, is widespread in California's groundwater and surface water sources. High levels of nitrate pose risks to human health, particularly for infants and pregnant women, as excessive nitrate intake can interfere with the blood's ability to carry oxygen, leading to methemoglobinemia or "blue baby syndrome." This has been common near Kerman and Kettleman City on the westside of the San Joaquin Valley.
Perfluoroalkyl and Polyfluoroalkyl Substances (PFAS)	Perfluoroalkyl and Polyfluoroalkyl Substances (PFAS) compounds, commonly found in firefighting foam, industrial processes, and consumer products. These persistent chemicals can accumulate in the environment and bioaccumulate in organisms, posing potential risks to human health. California has taken proactive measures to regulate PFAS compounds in drinking water, setting MCLs that exceed federal guidelines to ensure greater protection.
Chromium-6	Chromium-6, also known as hexavalent chromium, is a highly toxic form of chromium associated with industrial processes and natural geological occurrences. Elevated levels of chromium-6 in drinking water have been linked to adverse health effects, including cancer. California has established a stringent MCL for chromium-6, reflecting the state's commitment to protecting public health from this hazardous contaminant.
Pesticides and Herbicides	Pesticides and herbicides from agricultural activities in California, known as the nation's leading agricultural producer, contribute to water contamination. Runoff from farmlands and orchards can transport these chemicals into surface water and groundwater, posing risks to aquatic ecosystems and human health. Monitoring and managing pesticide contamination are essential for protecting California's water resources and agricultural sustainability.
Lead and Copper	Lead and copper contamination, although primarily occurring in drinking water distribution systems rather than natural sources, remain significant concerns for water quality in California. Aging infrastructure, particularly in older urban areas, can contribute to the leaching of lead and copper into drinking water, posing risks to public health, especially for vulnerable populations such as children and pregnant women.
Microorganisms	Microorganisms, including bacterial and viral pathogens such as Escherichia coli (E. coli) and Cryptosporidium, can contaminate California's water sources, particularly during heavy rainfall events or sewage system overflows. These microorganisms can cause waterborne diseases and pose serious health risks if ingested through contaminated drinking water or recreational activities.

Many of these pollutants, including nitrate from agricultural runoff, pose serious risks to human health. For instance, high nitrate levels in drinking water are particularly dangerous for infants, potentially causing a condition known as methemoglobinemia, or "blue baby syndrome," which affects oxygen transport in the bloodstream.

Table 18.5.2 highlights some of the differences between federal and California Maximum Contaminant Levels (MCLs), showcasing how California often sets stricter standards to safeguard public health. California's stricter MCLs for certain substances, including chemicals listed under Proposition 65, demonstrate the state's precautionary approach in regulating drinking water. Proposition 65 requires California to publish a list of chemicals known to cause cancer or reproductive harm, which influences the state's MCL standards to reflect heightened protection for public health. Differences between federal and state MCLs often stem from California's need to address unique geological conditions, such as natural arsenic leaching from rock formations, and a focus on cumulative exposure risks.

Table 18.5.2: U.S. EPA MCLs versus California MCLs.

Contaminant	Maximum Contaminant Level (US EPA) mg/L	Maximum Contaminant Level (California) mg/L	Heath Effects
Arsenic (As)	0.010	0.010	Circulation, skin damage, cancer
Cadmium (Cd)	0.005	0.005	Kidney damage
Fluoride (F)	4.0	2	Bone disease
Lead (Pb)	0.015	0.015	Developmental delays, attention disorders, kidney problems
Mercury (Hg)	0.002	0.002	Kidney damage
Nitrate	10	45	Methemoglobinemia (blue-baby syndrome)
Nitrite	1.0	1.0	Methemoglobinemia (blue-baby syndrome)
Perchlorate	--	0.006	Thyroid damage, cancer
Selenium (Se)	0.05	0.05	Hair and/or fingernail loss, circulatory problems
Thallium	0.002	0.002	Hair loss, blood, kidney, intestine and/or liver problems

Addressing the challenges posed by these common contaminants requires a comprehensive approach that integrates monitoring, regulation, infrastructure upgrades, and pollution prevention measures. By prioritizing water quality management and adopting proactive strategies, California can continue to safeguard its water resources and protect public health.

Saltwater Intrusion: A Coastal Threat

Saltwater intrusion, the process by which saline water encroaches into freshwater aquifers, is a significant hazard in California's coastal regions (Figure 18.5.1). This phenomenon is exacerbated by groundwater overdraft, sea-level rise, and coastal development. As freshwater is withdrawn from coastal aquifers, the reduced pressure allows seawater to move inland, contaminating freshwater supplies.

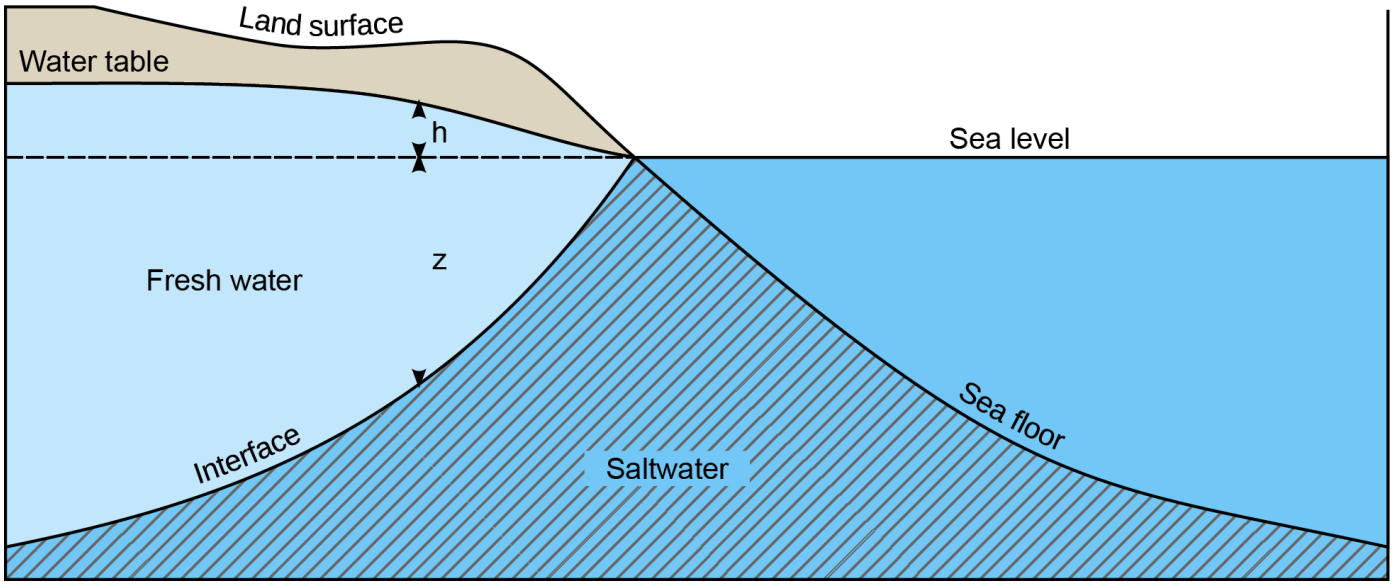


Figure 18.5.1: "Saltwater-freshwater interface along the coast" by Jooja is licensed under CC BY-NC 4.0. Access a detailed description.

California's coastal regions are commonly affected by saltwater intrusion, where freshwater aquifers interface with the Pacific Ocean. Coastal aquifers, particularly those situated in low-lying areas or areas with high groundwater extraction rates, are particularly vulnerable to saltwater intrusion. In regions such as the Central Coast, Southern California, and the San Francisco Bay Area, over-pumping of groundwater for agricultural, industrial, and municipal purposes has led to groundwater depletion, exacerbating the risk of saltwater intrusion.

Sea-level rise, driven by climate change, exacerbates the threat of saltwater intrusion along California's coastline. As sea levels rise, the pressure of saline water against coastal aquifers increases, facilitating the intrusion of seawater into freshwater sources. Low-lying coastal areas, such as the Sacramento-San Joaquin Delta and the Los Angeles Basin, are particularly susceptible to saltwater intrusion as rising seas encroach upon freshwater aquifers and surface water bodies.

Coastal development and urbanization further exacerbate saltwater intrusion hazards by altering natural hydrological patterns and increasing groundwater extraction rates. Urban areas along the coast, including Los Angeles, San Diego, and San Francisco, face increasing challenges in managing saltwater intrusion as population growth and development intensify water demand and groundwater extraction. Figure 18.5.2 illustrates the concentrations of chloride (salt) from offshore. USGS studies show that the geology of the Los Angeles Basin is highly complex, as shown by this modeled figure of Los Angeles seawater intrusion into the Dominguez Gap area stratigraphy. Understanding this geology helps determine where and how fast water moves within the various beds of sediment both onshore and offshore to inform more effective management strategies pertaining to saltwater intrusion.

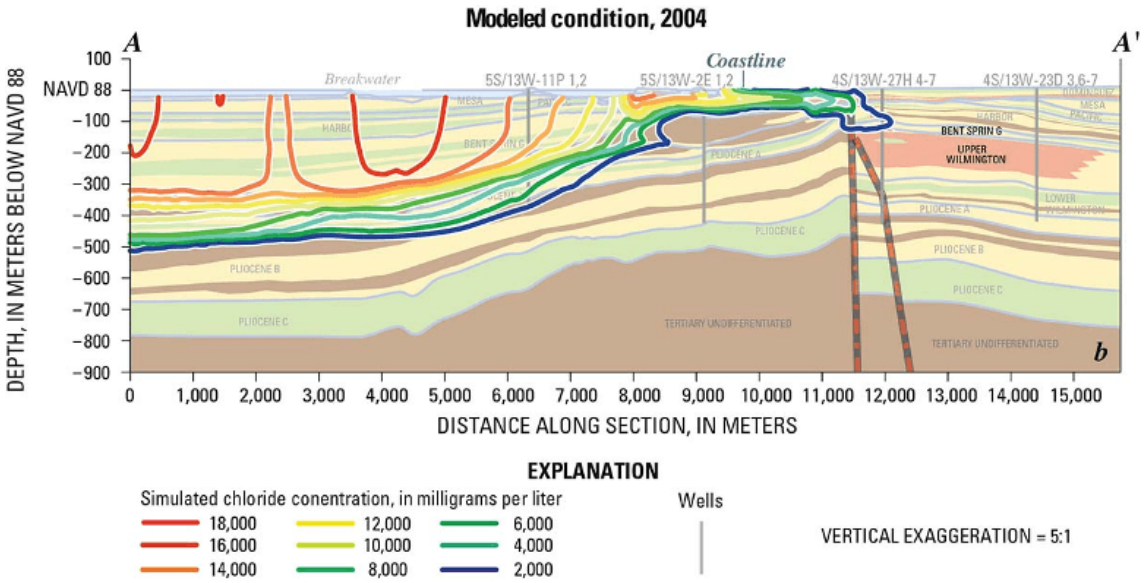


Figure 18.5.2: "Modeled chloride (salt water intrusion) form offshore" by the United States Geological Survey is in the public domain. Access a detailed description.

The Salinas Valley is one of the most severely affected regions, where decades of groundwater extraction have allowed seawater to intrude inland by several miles (18.5.3). Groundwater elevation data from the Salinas Valley in 2019 (Figure 18.5.4) shows concerning trends of decreasing groundwater levels, exacerbating saltwater intrusion risks. In response, California has employed various mitigation strategies, such as "guardian wells" in Los Angeles (Figure 18.5.5), which pump seawater away from freshwater sources or inject freshwater into the aquifer to form a protective barrier.

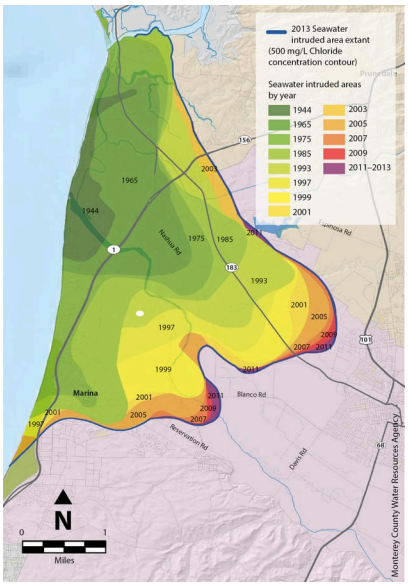


Figure 18.5.3: "Saltwater intrusion" by Brown and Caldwell, released to Monterey County Water Resources Agency is in the public domain. Access a detailed description.

Figure 18.5.4 exhibits groundwater elevation in the Salinas Valley shallow aquifer in 2019. The contours show the groundwater elevation below ground surface (bgs), there are large concerns around saltwater intrusion being so close to the surface and at the same time, the inward gradient, or downslope subsurface flow towards the lower (ie deeper) freshwater table.

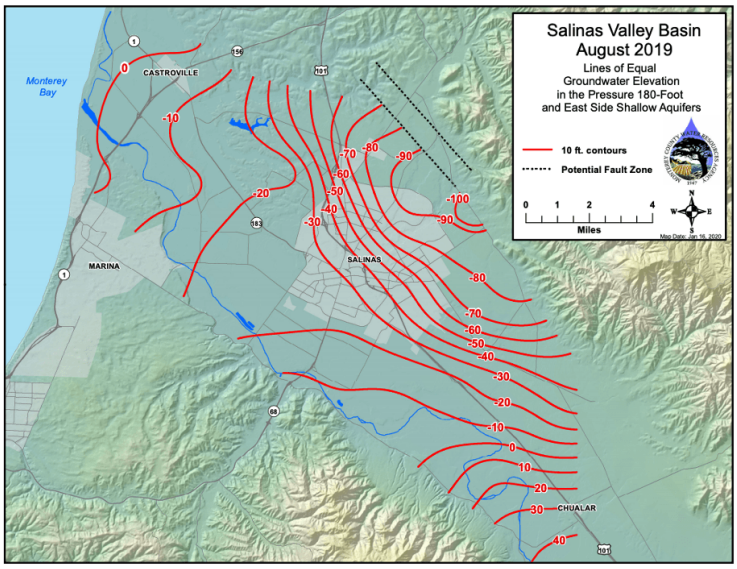


Figure 18.5.4: "Salinas Valley Basin groundwater elevation" by Monterey County Water Resources Agency is in the public domain. Access a detailed description.

In response to the threat of saltwater intrusion, California has implemented various strategies to manage and mitigate its impacts. These include groundwater management practices, such as groundwater recharge and conjunctive use, to replenish depleted aquifers and reduce reliance on groundwater extraction. Coastal protection measures, such as seawater barriers and managed aquifer recharge projects, aim to prevent or minimize the intrusion of saline water into freshwater sources. In some cases, like in Los Angeles, “guardian wells” have been drilled to pump the saltwater out and then transport it via pipelines back out to sea, thus trying to stop saltwater from intruding before it even has a chance to progress further inland. Figure 18.5.5 shows a barrier well pumping saltwater away to be put back into the sea. Meanwhile, a freshwater well continues to operate without interference from intruding saltwater. In other cases, like in Santa Barbara, freshwater has also been pumped into guardian wells to maintain a “barrier” of freshwater that holds back the intruding saltwater.

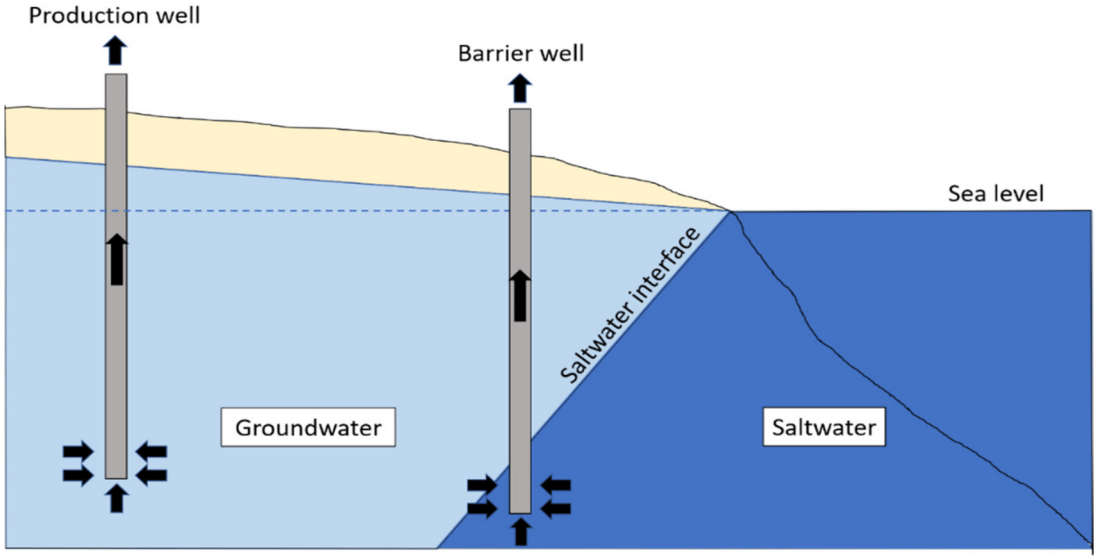


Figure 18.5.5: "Conceptual diagram of saltwater pumping by a barrier well" by Shinichi Ozaki, Christel Abi Akl, Tatsuya Nagino, and Yshinari Hiroshiro is licensed under CC BY-NC 4.0. Access a detailed description.

Figure 18.5.6 exhibits conceptual figures of Los Angeles seawater intrusion: A. In Los Angeles in the 1800s, the potentiometric surface of groundwater (the levels to which pressure in the aquifer would make water rise in cased wells) was above sea level causing net seaward freshwater discharge from the aquifer. B. Potentiometric surface drops below sea level due to pumping as early as the 1920s causing landward seawater intrusion into the aquifer. C. In the 1950s sets of closely spaced wells were installed to inject high-quality fresh water into aquifers – ideally to stem the flow of seawater into coastal aquifers.

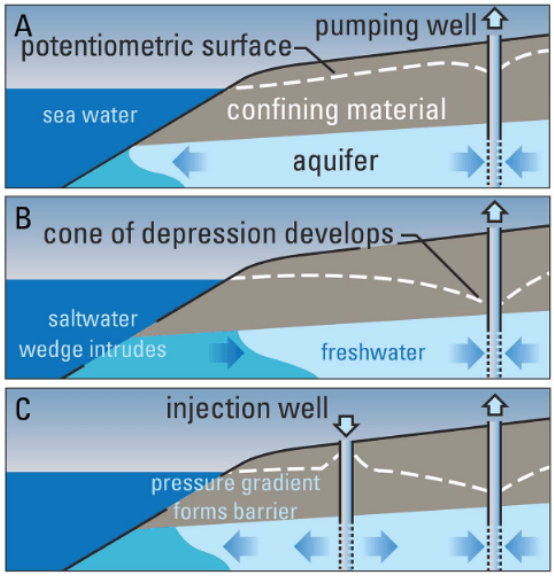


Figure 18.5.6: Seawater intrusion in Los Angeles. "Conceptual diagram of saltwater pumping by a barrier well" by the United States Geological Survey is in the public domain. Access a detailed description.

Furthermore, land-use planning and zoning regulations play a critical role in minimizing the risks associated with saltwater intrusion by guiding development away from vulnerable coastal areas and promoting sustainable water management practices. Collaboration between government agencies, water districts, stakeholders, and the public is essential to effectively address saltwater intrusion hazards and ensure the long-term sustainability of California's coastal and groundwater resources.

Saltwater intrusion poses significant hazards to California's coastal regions and groundwater resources, particularly in areas where freshwater aquifers interface with the Pacific Ocean. Addressing this challenge requires a comprehensive approach that integrates groundwater management, coastal protection measures, land-use planning, and stakeholder collaboration. By implementing proactive strategies and sustainable water management practices, California can mitigate the impacts of saltwater intrusion and safeguard its valuable water resources.

Activity - Assessing Saltwater Contamination 18.5.1

This interactive element is not available in this format. Visit the link or scan the QR code to access it online.

View this Interactive Content online

Land Subsidence: Sinking Ground, Rise Problems

Land subsidence, the gradual sinking of the Earth's surface, occurs when groundwater extraction compacts unconsolidated sediments, especially in regions like the Great Valley Province, where extensive groundwater pumping supports agriculture. As water is withdrawn from aquifers, the loss of pore pressure causes sediment layers to compress, leading to a decline in surface elevation. The effects of subsidence are most visible in the San Joaquin Valley, where parts of the valley floor have sunk by several feet over the past century (Figure 18.5.7).

This phenomenon not only damages infrastructure, such as roads and canals, but also reduces the storage capacity of aquifers, making it harder to replenish water supplies. Subsidence can also worsen saltwater intrusion by lowering the land surface and altering natural water flow patterns, particularly in coastal areas. While tectonic activity also causes subsidence in some parts of California, such as Humboldt Bay, groundwater-induced subsidence in regions like the Central Valley remains a major concern due to its scale and long-term impacts on water management and infrastructure.

One of the primary geological causes of land subsidence in California is the over-extraction of groundwater from underlying aquifers. As groundwater is pumped from aquifers to meet agricultural, municipal, and industrial water demands, the reduction in pore pressure within the aquifer leads to the compaction of overlying sedimentary layers. This compaction results in the gradual sinking of the land surface, a phenomenon known as "subsidence."

In regions with extensive groundwater pumping, such as the Central Valley and parts of Southern California, land subsidence has become a significant concern. The Central Valley, one of the most productive agricultural regions in the United States, relies heavily on groundwater for irrigation. As a result, prolonged and intensive groundwater extraction has led to significant land subsidence in parts of the Central Valley, particularly in the San Joaquin Valley, where subsidence rates have exceeded several inches per year in some areas.

The geological processes underlying land subsidence in California are also influenced by the composition and structure of underlying sedimentary deposits. In areas with unconsolidated sediments, such as alluvial plains and coastal regions, groundwater extraction can lead to rapid compaction and subsidence, most often attributed to stratigraphic intervals of fine grained sediments, such as silts and clays. Additionally, natural processes such as tectonic activity and seismic events can induce localized subsidence, particularly in regions with active faulting and seismicity. However, these often pale in comparison to induced subsidence due to groundwater extraction.

The impacts of land subsidence in California are diverse and can have far-reaching consequences for infrastructure, water management, and environmental sustainability. Subsidence-related infrastructure damage includes the cracking and deformation of roads, bridges, buildings, and other structures, posing risks to public safety and increasing maintenance costs.

Furthermore, land subsidence exacerbates challenges related to water management and sustainability by reducing the storage capacity of aquifers, altering surface water drainage patterns, and exacerbating flooding risks. Subsidence-induced changes in land elevation can also exacerbate seawater intrusion in coastal aquifers, leading to saltwater contamination of freshwater resources.

In response to the challenges posed by land subsidence, California has implemented various strategies and initiatives aimed at managing groundwater resources, reducing groundwater overdraft, and mitigating subsidence-related impacts. These include the implementation of groundwater management plans, regulation of groundwater extraction, promotion of water conservation and efficiency measures, and investment in alternative water sources such as recycled water and stormwater capture. Figure 18.5.7 shows basin prioritization based on the California Sustainable Management Act (SGMA) of 2014.

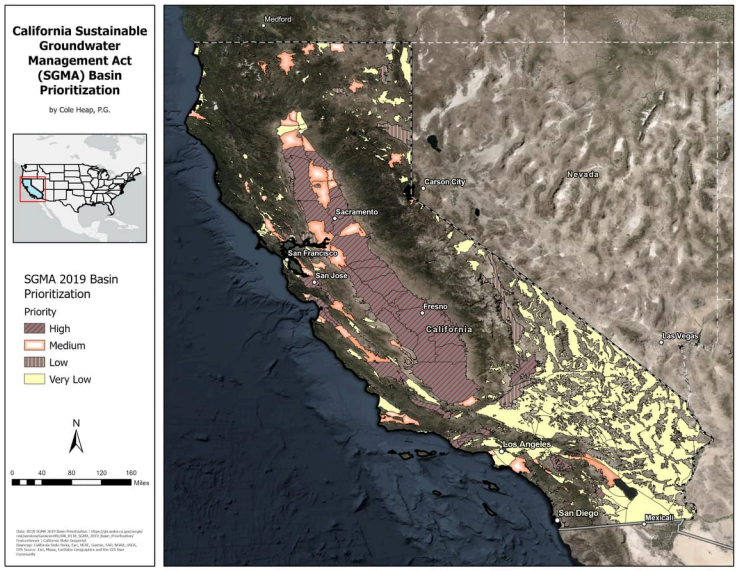


Figure 18.5.7: Basin Prioritization of 2019. “California Sustainable Groundwater Management Act (SGMA) Basin Prioritization” by Cole Heap from data in California Open Data Portal is licensed under CC BY-NC 4.0. Constructed in a GIS. Access a detailed description.

Collaborative efforts among government agencies, water districts, stakeholders, and the public are essential for effectively addressing the complex challenges of land subsidence in California. By implementing proactive measures, promoting sustainable groundwater management practices, and fostering innovation, California can mitigate the impacts of land subsidence while ensuring the long-term resilience of its infrastructure, water resources, and communities.

Surface Water Depletion and Drought: A Worsening Challenge

Surface water depletion, the reduction in the availability of surface water resources due to various factors such as over-extraction, climate change, and land-use practices, presents significant challenges to water management and sustainability in California. As one of the most populous and agriculturally productive states in the United States, California relies heavily on surface water sources for irrigation, municipal supply, and environmental needs. However, increased demand, coupled with changing environmental conditions, has led to the depletion of surface water supplies in various regions across the state.

One of the most common areas affected by surface water depletion in California is the Sacramento-San Joaquin Delta, a critical hub for water conveyance and ecosystem support. The delta serves as a primary source of water for agriculture, urban areas, and environmental conservation in California. However, decades of intensive water diversions for agricultural irrigation and municipal supply have significantly reduced freshwater flows into the delta, leading to habitat degradation, saltwater intrusion, and ecosystem decline.

In addition to the Sacramento-San Joaquin Delta, surface water depletion is also prevalent in other regions of California, particularly in the Central Valley and Southern California. The Central Valley, often referred to as the "breadbasket of the world," relies heavily on surface water for irrigating vast agricultural lands just as well as groundwater aquifers as previously stated. However, groundwater overdraft and competing water demands have strained surface water resources as denizens have fallen back to surface water use to compensation for the lack in groundwater in some areas.

Southern California, including metropolitan areas such as Los Angeles, San Diego, and Orange County, faces challenges related to surface water depletion due to high population density and water demand. The region relies on imported water from distant sources, including the Colorado River and Northern California, to meet its water needs. However, prolonged droughts, regulatory constraints, and competing interests for water allocation have exacerbated the strain on surface water supplies in Southern California.

Climate change further exacerbates surface water depletion in California by altering precipitation patterns, reducing snowpack levels, and increasing the frequency and severity of droughts. Decreased snowpack in the Sierra Nevada Mountains, a vital source of surface water replenishment during the dry season, reduces runoff into rivers and reservoirs, leading to decreased water availability for downstream users.

To address the challenges of surface water depletion, California has implemented various water management strategies and policies aimed at enhancing water conservation, improving water efficiency, and promoting sustainable water use practices. These include investments in water recycling and reuse, implementation of water conservation measures, development of regional water management plans, and enhancement of groundwater recharge and storage projects.

Furthermore, collaborative efforts among stakeholders, including water agencies, agricultural producers, environmental organizations, and local communities, are essential for effectively managing surface water resources and ensuring the long-term sustainability of California's water supply.

Surface water depletion poses significant challenges to water management and sustainability in California. However, by implementing proactive water management strategies, investing in water infrastructure, and fostering collaboration among stakeholders, California can address the impacts of surface water depletion and ensure the resilience of its water resources in the face of changing environmental conditions.

Drought and Climate Change

Drought, a recurrent phenomenon characterized by prolonged periods of below-average precipitation and water scarcity, poses significant challenges to water resources, agriculture, ecosystems, and communities in California. The state's Mediterranean climate, characterized by wet winters and dry summers, makes it inherently susceptible to drought conditions. However, the increasing frequency, intensity, and duration of drought events in California are exacerbated by climate change, leading to heightened concerns about water availability, ecosystem health, and socioeconomic impacts (Figure 18.5.8).

Climate change plays a pivotal role in exacerbating drought conditions in California by altering precipitation patterns, increasing temperatures, and influencing atmospheric circulation patterns. Rising temperatures contribute to increased evaporation rates, leading to greater water loss from soil and vegetation. Additionally, changes in atmospheric circulation patterns, such as the weakening of the Pacific storm track and the expansion of subtropical high-pressure systems, can result in reduced winter precipitation and snowpack levels, further exacerbating drought conditions.



Figure 18.5.8: "Dry lakebed in California" by National Oceanic and Atmospheric Administration is in the public domain. Access a detailed description.

The impacts of drought and climate change in California are multifaceted and far-reaching, affecting various sectors of the economy, environment, and society. Agriculture, which accounts for 40% of California's water consumption, is particularly vulnerable to drought-induced water shortages. Reduced water availability for irrigation can lead to crop failures, decreased agricultural productivity, and economic losses for farmers and rural communities.

Ecosystems and natural habitats in California also face severe challenges during drought events, as diminished water availability disrupts aquatic ecosystems, reduces habitat quality, and threatens the survival of native species. Wetlands, rivers, and streams experience reduced flows, leading to habitat fragmentation and alterations in water temperature and quality, which can negatively impact fish populations and other aquatic organisms. As shown in Figure 18.5.9, the difference between a wet year versus a dry year near Lake Oroville.



Figure 18.5.9: Satellite images of Lake Oroville by the United States Geological Survey is in the public domain. Access a detailed description.

Furthermore, drought conditions exacerbate wildfire risk and intensity in California, as dry vegetation becomes more susceptible to ignition and rapid fire spread. Wildfires not only pose direct threats to human life and property but also have long-term ecological consequences, including habitat destruction, soil erosion, and loss of biodiversity.

Figure 18.6.10 is an animated map of the progression of the historic drought from 2012 to 2014. These maps span December

31, 2013, to July 29, 2014. This animation highlights the rapid spread of extreme and exceptional drought conditions across over 75% of California in this timeframe. This drought has been classified as the worst drought California has experienced in 1,200 years!

Figure 18.6.10 is an animated map of the progression of the historic drought from 2012 to 2014. These maps span December 31, 2013, to July 29, 2014. This animation highlights the rapid spread of extreme and exceptional drought conditions across over 75% of California in this timeframe. This drought has been classified as the worst drought California has experienced in 1,200 years!

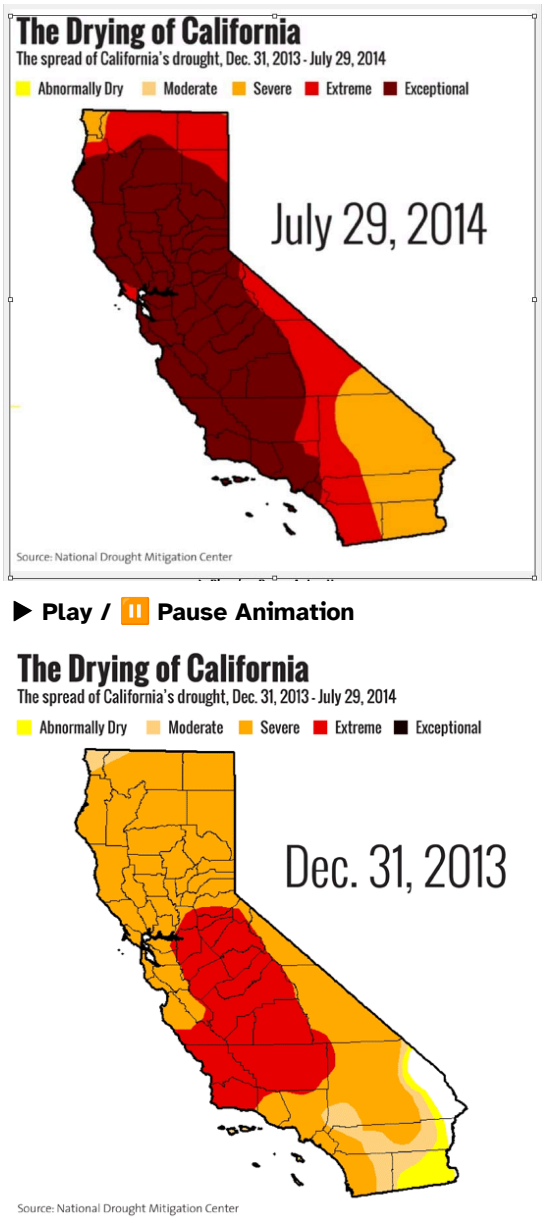


Figure 18.5.10: "Progression of the 2012-2014 historic California drought" by the National Drought Mitigation Center is in the public domain. Access a detailed description .

In response to the escalating challenges posed by drought and climate change, California has implemented various strategies and initiatives aimed at enhancing drought preparedness, water conservation, and climate resilience. These include investments in water infrastructure, such as water recycling and desalination plants, implementation of water conservation measures, development of drought contingency plans, and promotion of sustainable land and water management practices.

Additionally, California has adopted ambitious climate mitigation and adaptation goals, including the reduction of greenhouse gas emissions and the promotion of renewable energy sources, to address the underlying drivers of climate change and build

resilience to its impacts.

Collaborative efforts among government agencies, stakeholders, and communities are essential for effectively addressing the complex challenges of drought and climate change in California. By implementing adaptive strategies, fostering innovation, and promoting sustainable water and land management practices, California can enhance its resilience to drought and climate variability while safeguarding the long-term sustainability of its water resources, ecosystems, and communities.

Activity - Water in the Atmosphere 18.5.1

This interactive element is not available in this format. Visit the link or scan the QR code to access it online.

View this Interactive Content online

Flooding: Natural Hazards and Infrastructure Challenges

Flooding, the overflow of water onto normally dry land, is a recurrent natural hazard in California, influenced by various geologic factors and exacerbated by human activities and climate change. Understanding the geological factors that influence flooding and identifying vulnerable regions are essential for effective flood risk management and resilience building efforts in the state.

Geological factors that contribute to flooding in California include topography, soil characteristics, land use patterns, and proximity to water bodies. California's diverse topography, characterized by mountains, valleys, and coastal plains, plays a significant role in modulating the distribution and intensity of rainfall-runoff processes, influencing flood patterns across the state. Areas located in low-lying coastal plains, river valleys, and floodplains are particularly susceptible to flooding due to their proximity to water bodies and their relatively flat terrain, which facilitates the accumulation of water during heavy rainfall events.

Figure 18.5.11 shows flooding in the Sacramento Valley after weeks of storms. Clear skies on Jan 17, 2023, allowed NASA's Terra satellite to capture flooding in California's Sacramento Valley using Moderate Resolution Imagery Spectroradiometer (MODIS). This satellite imagery shows flooding near Sacramento and the Sutter Buttes in dark blue. The Sutter Buttes look like an island in the north central portion of the satellite image. Flooding intensified with wider rivers and increased snowpack in the mountains. Another storm struck after a brief sunny period, worsening flooding.

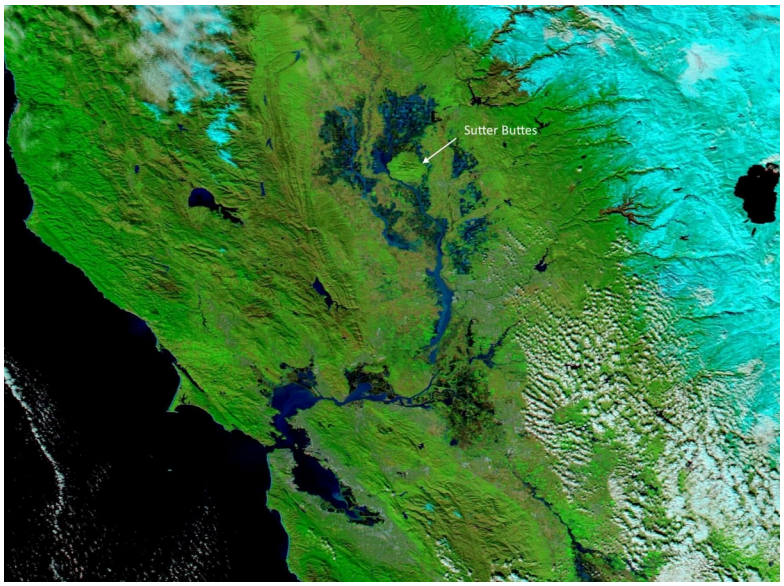


Figure 18.5.11: "Flooding in California's Sacramento Valley (MODIS)" by the National Aeronautics and Space Administration is in the public domain. Access a detailed description.

Soil characteristics also play a crucial role in determining flood susceptibility, with factors such as soil permeability, compaction, and saturation capacity influencing the rate of infiltration and surface runoff. Impermeable soils, such as clay-rich or heavily compacted soils, inhibit water infiltration and promote surface runoff, increasing the risk of flash flooding and urban flooding in developed areas with extensive impervious surfaces.

Land use patterns and human activities further exacerbate flooding risks in California. Urbanization, deforestation, and alteration of natural drainage patterns disrupt the natural hydrological cycle, increasing surface runoff and reducing infiltration rates, leading to higher flood frequencies and intensities. Additionally, the construction of levees, dams, and other flood control infrastructure can alter riverine and coastal ecosystems, exacerbating downstream flooding risks and increasing vulnerability to flood hazards.

Climate change, characterized by rising temperatures, altered precipitation patterns, and increased frequency of extreme weather events, is amplifying the impacts of flooding in California. Changing climate conditions contribute to more frequent and intense rainfall events, leading to increased runoff and higher flood risks, particularly in urbanized areas with limited natural drainage capacity.

Several regions in California are particularly prone to flooding due to a combination of geological, hydrological, and anthropogenic factors. Coastal areas, including low-lying coastal plains and estuarine environments, are vulnerable to flooding from storm surges, high tides, and sea-level rise, which can inundate coastal communities and infrastructure (see California's Coastline).

Riverine floodplains, such as those along the Sacramento and San Joaquin Rivers in the Central Valley, are also susceptible to flooding, especially during periods of heavy rainfall and snowmelt. These floodplains serve as vital agricultural areas but are prone to inundation, posing risks to crops, livestock, and rural communities. A great example of this is in the activity below where one can use the slider to compare a dry Tulare Lake bed against a refilled Tulare Lake bed southwest of Corcoran, CA in the Central Valley. The resurgence of Tulare Lake flooded much of the farm operations outside of Corcoran.

Activity - The Return of Lake Tulare 18.5.1

This interactive element is not available in this format. Visit the link or scan the QR code to access it online.

View this Interactive Content online

Urbanized areas, particularly in densely populated regions such as the San Francisco Bay Area, Los Angeles Basin, and San Diego metropolitan area, face significant flood risks due to extensive impervious surfaces, altered drainage patterns, and proximity to water bodies. Flash flooding, urban flooding, and riverine flooding are common in these urban areas during intense rainfall events.

In response to these challenges, California has implemented various flood risk management strategies, including levee systems and wetland restoration projects, such as the Napa River Flood Protection Project. One particularly innovative solution involves the use of permeable pavement, which is designed to reduce urban runoff by allowing rainwater to infiltrate the ground rather than flowing over impermeable surfaces into storm drains.

In Figure 18.5.12, the sign reads,

> "You are standing on N. School Street which was paved with permeable pavement. Rain that falls on normal pavement rushes downhill through drains, carrying pollutants from the street straight into Wolf Creek where it leaves the community within hours. The permeable pavement on N. School Street allows rainfall to penetrate down to the soil. It is then filtered through the soil and slowly released into the groundwater where it can be used by people and plants downslope."

The technical process of permeable pavement works by allowing water to permeate through minuscule gaps in the concrete, initiating a process of natural filtration. As water seeps through the pavement into the underlying soil, it undergoes purification, removing contaminants and contributing to the recharge of groundwater reservoirs. This replenishment is vital for sustaining aquifers that nourish local flora and fauna, including Wolf Creek during the dry summer and fall seasons, ensuring a consistent water supply for ecosystems and communities.

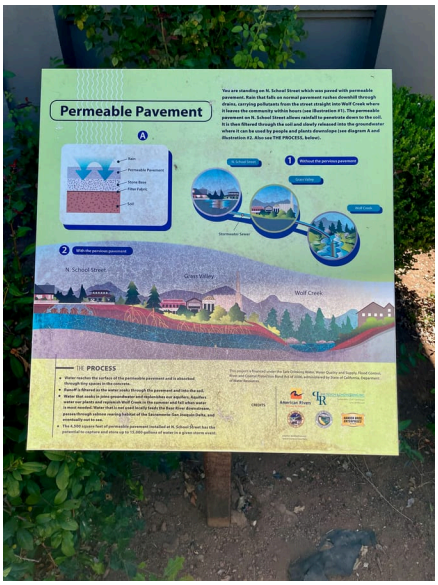


Figure 18.5.12: "Permeable Pavement sign in Grass Valley, California" by Allison Jones is licensed under CC BY-NC 4.0. Access a detailed description.

Furthermore, any excess water not absorbed locally flows downstream, eventually reaching larger water bodies such as the Bear River, and ultimately contributing to the Sacramento-San Joaquin Delta. This flow supports critical ecosystems, including salmon rearing habitats within the delta, before the water finally reaches the Pacific Ocean. The installation of 4,500 square feet of permeable pavement at N. School Street demonstrates the potential of this technology to capture and store up to 15,000 gallons of water during a single storm event, showcasing its practical benefits in urban water management.

Permeable pavement, therefore, represents a sustainable water management practice that not only reduces urban flooding but also enhances groundwater recharge and supports local ecosystems. By integrating permeable pavement and other flood resilience strategies, California can mitigate the risks associated with increased urban runoff while promoting sustainable development in flood-prone areas.

Protecting California's Water Resources

Maintaining the quality of California's water is a complex and ongoing challenge, influenced by both natural geological processes and human activities. From the selenium contamination in Kesterson Reservoir to the persistent threat of PFAS, nitrate, and other pollutants, the state's water systems are continually at risk of degradation. Addressing these issues requires a multi-faceted approach that integrates careful regulation, modern infrastructure, and sustainable water management practices. With the increasing pressure from agricultural runoff, urbanization, and climate change, California must remain vigilant in monitoring and mitigating water quality threats. By prioritizing both surface water and groundwater protection and implementing strategies like stricter Maximum Contaminant Levels (MCLs) and innovative technologies, the state can continue to safeguard public health and the environment for future generations. Collaborative efforts among scientists, policymakers, and local communities will be critical to ensuring that California's water resources remain resilient and sustainable amidst these ongoing challenges.

References

1. 2021 California Code Water Code – WAT, DIVISION 6 - CONSERVATION, DEVELOPMENT, AND UTILIZATION OF STATE WATER RESOURCES. PART 2.74 - Sustainable Groundwater Management CHAPTER 1 - General Provisions Section 10720.
2. California Department of Public Health. (2009). https://www.epa.gov/wqs-tech/water-quality-standards-regulations-california
3. California Department of Water Resources. (2020). *California*'s *Groundwater* (Bulletin 118). Sacramento, CA.
4. California Department of Water Resources. (2003). *California's Groundwater* (Bulletin 118). Retrieved on April 21, 2024 from https://water.ca.gov/programs/groundwater-management/bulletin-118
5. Galloway, D.L., and Burbey, T.J. (2011). Review: regional land subsidence accompanying groundwater extraction. Hydrogeol. J. 19, 1459–1486.
6. Murray, K.D., and Lohman, R.B. (2018). "Short-Lived Pause in Central California Subsidence after Heavy Winter Precipitation of 2017," Science Advances 4, 4 (8). United States: American Association for the Advancement of Science: eaar8144.

doi:10.1126/sciadv.aar8144.
7. Page, B. M. (1966). Geology of the Coast Range of California, chapter 6 in Geology of Northern California: California Division of Mines Bulletin 190, p. 255-276.
8. Page, R. W. (1973). Base of fresh ground water (approximately 3,000 micromhos) in the San Joaquin Valley, California: U.S. Geological Survey Hydrologic Investigations Atlas HA-489.
9. United States Office of Ground Water and Drinking Water, December 2023, https://www.epa.gov/ground-water-and-drinking-water/national-primary-drinking-water-regulations

This page titled 18.5: Threats to California's Water is shared under a CC BY-NC 4.0 license and was authored, remixed, and/or curated by Cole Heap.

18.6: Understanding California's Water Landscape

A Challenging, Complex Landscape

California's water landscape is a complex tapestry woven from the intricate interplay of geological forces, hydrological processes, and human activities. From the towering peaks of the Sierra Nevada to the fertile valleys of the Central Valley and the dynamic coastline along the Pacific Ocean, the state's diverse geology shapes the distribution, availability, and quality of surface water resources.

Throughout this chapter, we have explored the myriad ways in which geology influences California's water dynamics. The mountainous terrain of the Sierra Nevada and Coast Ranges serves as a primary source of surface water, capturing precipitation in the form of snowpack and feeding rivers and streams through snowmelt. The alluvial plains of the Central Valley, deposited over millennia by rivers, support extensive agricultural activities and provide vital groundwater recharge areas. Coastal zones, including estuaries and tidal marshes, serve as transitional zones where freshwater mixes with saltwater, supporting diverse ecosystems and providing critical habitat for wildlife.

However, California's water landscape is not without its challenges. The state's susceptibility to drought, floods, and climate change exacerbates existing water management issues, placing strain on surface water resources and highlighting the need for sustainable water management practices. Aging infrastructure, such as levees and dams, raises concerns about reliability and safety, while increasing urbanization and land development alter natural runoff patterns and degrade water quality.

Moving forward, addressing the complexities of California's water landscape requires a holistic approach that integrates geological knowledge with water management strategies, land use planning, and environmental conservation efforts. By understanding the geological influences on surface water dynamics and embracing innovative solutions, such as green infrastructure, watershed management, and climate-resilient infrastructure, California can navigate the challenges of its water landscape while safeguarding its precious water resources into the future.

This page titled 18.6: Understanding California's Water Landscape is shared under a CC BY-NC 4.0 license and was authored, remixed, and/or curated by Cole Heap.

18.7: Chapter Summary

18.1 The Hydrologic Cycle

- The hydrosphere, encompassing all water on Earth, is vital to California's diverse geology.
- The hydrologic cycle involves evaporation, condensation, precipitation, runoff, infiltration, and transpiration.
- Pools (e.g., lakes, aquifers) and fluxes (e.g., evaporation, precipitation) govern water availability and movement.
- California's geography shapes distinct hydrological regions, influencing water distribution and management.

18.2 Running Water

- Running water shapes California's landscapes through erosion and sediment deposition.
- Precipitation patterns are influenced by California's Mediterranean climate, with most occurring in winter.
- Drainage basins manage water flow across landscapes, with types varying by geography.
- Streams can be meandering, braided, or straight, influencing sediment dynamics and landscape formation.

18.3 Groundwater

- Groundwater, stored in aquifers, is critical for agriculture, industry, and urban use in California.
- Aquifers vary between confined and unconfined, influencing recharge rates and vulnerability to contamination.
- The Central Valley Aquifer system is a major water source but is overdrawn, leading to declining water levels.
- Coastal and Basin and Range aquifers face challenges such as saltwater intrusion and land subsidence.

18.4 Water Infrastructure and Management

- Dams store water, control floods, and generate power but face challenges like sediment buildup and seismic risks.
- Aqueducts transport water across California, overcoming geographical and geological barriers.
- Levees protect against flooding but require maintenance and are vulnerable to aging and environmental changes.
- Collaborative water management is essential for maintaining California’s extensive infrastructure amidst climate change.

18.5 Threats to California’s Water

- Water quality is compromised by both natural and human-induced contamination (e.g., selenium, PFAS).
- Saltwater intrusion threatens coastal aquifers, especially in regions like the Salinas Valley.
- Land subsidence due to groundwater overuse is prevalent in agricultural areas like the Central Valley.
- Surface water depletion and drought exacerbate water shortages, with infrastructure like levees and dams under stress.

18.6 Understanding California’s Water Landscape

- California's diverse geology shapes its water distribution, from snowpack in the Sierra Nevada to coastal estuaries.
- Challenges include droughts, floods, and aging infrastructure, which strain water resources.
- Sustainable management integrating geology, land use, and environmental conservation is critical to navigating these issues.

This page titled 18.7: Chapter Summary is shared under a CC BY-NC 4.0 license and was authored, remixed, and/or curated by Cole Heap.

18.8: Detailed Figure Descriptions

Chapter Cover Image: Conceptual Model of Water Flow

This conceptual model illustrating the interactions between various components of the water management system. In the foreground, we see a cross-section of the land showing different layers of soil and rock. The top layer includes areas of irrigated agriculture, a recharge basin, and a wildlife refuge. A diversion canal redirects river water towards these agricultural fields and recharge areas.

Below the surface, the groundwater table is depicted, showing how water infiltrates through the soil to replenish both confined and unconfined aquifers. The confined aquifer is separated by an aquitard, a lesspermeable layer that restricts water flow.

On the right side of the model, municipal and industrial supply wells draw water from these aquifers for human use. Injection wells are used to recharge the aquifer artificially.

In the background, mountains receive precipitation, which contributes to runoff flowing into streams and reservoirs. This water is directed through treatment plants before being supplied for municipal and industrial uses.

The left side of the model shows the river flowing towards the ocean, passing through various ecosystems, including areas with phreatophytes, plants that draw water from the water table. There is also a depiction of the salinity gradient as the river water meets the ocean.

Overall, the image captures the complex interactions and flow of water through natural and managed systems, highlighting the importance of each component in maintaining the water cycle and supporting various uses.

Figure 18.1.1 The Natural Water Cycle

The water cycle describes where water is found on Earth and how it moves. Water can be stored in the atmosphere, on Earth's surface, or below the ground. It can be in a liquid, solid, or gaseous state. Water moves between the places it is stored at large scales and at very small scales. Water moves naturally and because of human interaction, both of which affect where water is stored, how it moves, and how clean it is.

At the top of the image, the Sun provides energy that drives the cycle. Water evaporates from oceans, lakes, rivers, wetlands, and soil, and also enters the atmosphere through evapotranspiration from plants. Water vapor rises into the atmosphere, where it cools and undergoes condensation to form clouds. In colder regions, water can also change directly between ice and vapor through sublimation and deposition.

Clouds release water back to Earth as precipitation (rain, snow, or hail). In mountainous areas, precipitation contributes to ice, snow, glaciers, and permafrost, with snowmelt runoff flowing downhill into streams and rivers. Some precipitation becomes surface runoff, flowing into rivers, freshwater lakes, wetlands, and eventually the oceans. Smaller processes such as dew and fog drip are also shown.

Part of the water infiltrates the ground through infiltration and seepage, becoming soil moisture or groundwater. Groundwater is stored underground, slowly moving through groundwater recharge and flow, feeding springs, lakes, and rivers, and ultimately discharging into the ocean. Plants absorb water through plant uptake, returning some of it to the atmosphere.

The diagram also shows saline lakes, ocean currents, underwater vents, and volcanic steam, emphasizing that water moves through many interconnected pathways. Overall, the image highlights the continuous, cyclical nature of water movement on Earth and notes that it represents the "natural" water cycle, without emphasizing human impacts.

Figure 18.1.2: Water Cycle Diagram

The diagram presents a visualization of information that is provided as text within the image.

Text Provided within the Diagram

Pools and fluxes: On Earth, water can be fresh, saline, or a mix of both. Pools are places where water is stored, like the ocean. Fluxes are the way that water moves between pools, such as evaporation, precipitation, discharge, recharge, or human use. Visit the Water Cycle page on the USGS website for definitions.

Liquid water can be fresh, saline (salty), or a mix (brackish). Ninety-six percent of all water is saline and stored in oceans. Places like the ocean, where water is stored, are called pools. On land, saline water is stored in saline lakes, whereas fresh water is stored in liquid form in freshwater lakes, artificial reservoirs, rivers, wetlands, and in soil as soil moisture. Deeper underground, liquid water is stored as groundwater in aquifers, within the cracks and pores of rock. The solid, frozen form of water is stored in ice sheets, glaciers, and snowpack at high elevations or near the Earth's poles. Frozen water is also found in the soil as permafrost. Water vapor, the gaseous form of water, is stored as atmospheric moisture over the ocean and land.

As it moves, water can transform into a liquid, a solid, or a gas. The different ways in which water moves between pools are known as fluxes. Circulation mixes water in the oceans and transports water vapor in the atmosphere. Water moves between the atmosphere and the Earth's surface through evaporation, evapotranspiration, and precipitation. Water moves across the land surface through snowmelt, runoff, and streamflow. Through infiltration and groundwater recharge, water moves into the ground. When underground, groundwater flows within aquifers and can return to the surface through springs or from natural groundwater discharge into rivers and oceans.

Humans alter the water cycle. We redirect rivers, build dams to store water, and drain water from wetlands for development. We use water from rivers, lakes, reservoirs, and groundwater aquifers. We use that water (1) to supply our homes and communities; (2) for agricultural irrigation and grazing livestock; and (3) in industrial activities like thermoelectric power generation, mining, and aquaculture. The amount of available water depends on how much water is in each pool (water quantity). Water availability also depends on when and how fast water moves (water timing), how much water is used (water use), and how clean the water is (water quality).

Human activities affect water quality. In agricultural and urban areas, irrigation and precipitation wash fertilizers and pesticides into rivers and groundwater. Power plants and factories return heated and contaminated water to rivers. Runoff carries chemicals, sediment, and sewage into rivers and lakes. Downstream from these types of sources, contaminated water can cause harmful algal blooms, spread diseases, and harm habitats. Climate change is also affecting the water cycle. It affects water quality, quantity, timing, and use. Climate change is also causing ocean acidification, sea level rise, and extreme weather. Understanding these impacts can allow progress toward sustainable water use.

Description of the Diagram

This image is a comprehensive diagram illustrating the water cycle, provided by the U.S. Geological Survey (USGS). The diagram details the various processes and pathways through which water moves on, above, and below the Earth's surface.

At the top left, the Sun is depicted, showing its role in driving evaporation from the ocean's surface. This process is labeled "ocean evaporation," and the water vapor rises into the atmosphere, forming "atmospheric moisture over the ocean." The diagram also illustrates the "transport of moisture from ocean to land," showing how water vapor moves over land where it precipitates as rain or snow, labeled "precipitation over land."

The land area includes various features where water is stored and flows. Snowpack and ice sheets at higher elevations store water as ice, which melts to contribute to rivers and streams, a process called "snowmelt." Rivers and streams transport water, some of which infiltrates the ground to recharge groundwater, depicted as "groundwater recharge." Surface runoff from precipitation flows into rivers, lakes, and wetlands, labeled as "runoff."

Several types of water bodies are shown, including freshwater lakes, saline lakes, rivers, and wetlands (both fresh and brackish). The diagram also shows human influences on the water cycle, such as "domestic water use," "municipal water use," "industrial water use," "agricultural water use," and "grazing water use." Urban runoff and streamflow to oceans illustrate how water returns to the ocean, completing the cycle.

The interaction between surface water and groundwater is highlighted with "groundwater storage," "soil moisture," and "groundwater discharge to ocean." The subsurface section of the diagram shows detailed layers of groundwater flow, indicating how water moves through aquifers and returns to the surface through springs or wells.

The diagram emphasizes various processes like "evapotranspiration," where water is transferred from land and plants back into the atmosphere, and "precipitation over land," contributing to rivers and groundwater. Other processes include "ocean circulation," which distributes water globally, and "groundwater discharge to rivers and oceans."

The diagram includes a legend explaining the different pools and fluxes involved in the water cycle, noting that pools are places where water is stored (such as lakes, rivers, and aquifers), and fluxes are ways water moves between pools (such as evaporation, precipitation, and runoff). A detailed description at the bottom provides additional context about how the water cycle functions and its importance to Earth's systems.

This diagram provides a detailed and informative overview of the water cycle, highlighting the complex interactions between different components of the Earth's hydrological system and the impact of human activities on water movement and storage.

Figure 18.2.1: Average Annual Precipitation for California 1900-1960

This color-coded map of California displays the average annual precipitation from 1900 to 1960. The title of the map is "Average Annual Precipitation of California 1900-1960." The data sources include the US Geological Survey, California Department of Water Resources, and California Division of Mines.

The map uses a gradient color scale to represent different precipitation levels. Dark blue indicates the highest precipitation levels, ranging from 51 to 125 inches annually. Light blue represents moderately high precipitation levels, ranging from 31 to 50 inches. Green signifies mid-range precipitation levels, from 21 to 30 inches. Yellow shows lower precipitation levels, ranging from 11 to 20 inches. Orange and red indicate the lowest precipitation levels, ranging from 3 to 10 inches.

The map shows that the northwestern coastal region of California experiences the highest precipitation levels. Central and southern inland areas, particularly the southeastern part, have much lower precipitation levels, indicated by red. The Sierra Nevada mountain range displays a gradient from high to moderate precipitation levels, transitioning from dark blue to green as it moves eastward. This map visually communicates the variation in precipitation across different regions of California during the first half of the 20th century.

Figure 18.2.2: Basic anatomy of drainage basins

This three-dimensional diagram illustrates the concept of drainage basins and drainage divides. It depicts a landscape with two distinct drainage basins, each collecting water from its respective area.

The left side of the diagram represents the "Drainage basin of stream 1." This area is a network of tributaries, which are smaller streams that feed into a main stream. These tributaries collect precipitation runoff from the surrounding land and funnel it into the main stream, which flows towards a common outlet.

Similarly, the right side of the diagram shows the "Drainage basin of stream 2." Like the first basin, this area consists of tributaries that channel water into a main stream. The tributaries are interconnected, forming a branching pattern that effectively drains the surrounding landscape.

The "Drainage divide" is a ridge or elevated area that separates the two drainage basins. This divide determines the direction of water flow, ensuring that precipitation on one side flows into stream 1 and precipitation on the other side flows into stream 2. The divide prevents water from crossing over into the adjacent drainage basin.

This diagram illustrates how drainage basins and divides function in a landscape, highlighting the role of tributaries in collecting and channeling water and the importance of divides in directing the flow of water into separate basins.

Figure 18.2.3: Sacramento River

The Sacramento River displays classic meandering river patterns. The river winds sinuously through the landscape, forming a series of pronounced loops and bends known as meanders. The surrounding terrain is a mix of agricultural fields and patches of woodland.

The meanders are well-defined, with some sections of the river nearly doubling back on themselves. This natural process occurs as the river erodes its outer banks and deposits sediment on the inner banks, gradually shifting its course over time. The varied

colors and textures of the land, from the dark green of the forested areas to the lighter tones of the fields, highlight the contrast between the cultivated land and the natural river meanders.

The image provides a clear example of fluvial geomorphology, showcasing how rivers dynamically shape the landscape through erosion and deposition, creating the distinctive looping patterns characteristic of meandering rivers.

Figure 18.2.4: Santa Clara River, CA from the Air

The Santa Clara River has a characteristic braided stream formation. The river flows through a valley with multiple interconnected channels separated by wide sediment bars, which appear light-colored in contrast to the surrounding landscape. On both sides of the river, there are patches of agricultural fields and scattered urban development, indicating the river's proximity to human activity. The riverbed itself is wide, with several dry, sandy channels branching and rejoining, reflecting the river's dynamic and shifting nature. The surrounding terrain is a mix of rolling hills and mountainous areas, providing a backdrop to the river's braided pathways. The image captures the river's role in the local geography, demonstrating the interplay between natural river processes and land use in the region.

Figure 18.2.5: California Hydrologic Regions

This detailed map of California shows the state's various hydrologic regions along with county boundaries. This map serves as a comprehensive representation of California's ten hydrologic regions. It illustrates how water resources are managed across different parts of the state and highlights the diversity of water resource management areas. The importance of regional planning in addressing water-related issues is emphasized, as different regions have unique challenges and resources that require tailored management strategies.

The counties found in each hydrological region

Hydrological Region	Counties found in the region
Central Coast	Monterey, San Luis Obispo, Santa Barbara; parts of San Benito, Santa Cruz
Colorado River	Imperial; parts of San Diego, Riverside, San Bernardino, Los Angeles, Kern
North Coast	Del Norte, Humboldt, Trinity, Mendocino, Sonoma; parts of Siskiyou, Modoc, Lake
North Lahontan	Eastern side of Modoc, Lassen, Sierra, Nevada, Placer, El Dorado, Alpine, Mono
Sacramento River	Shasta, Tahema, Glenn, Butte, Plumas, Colusa, Yuba, Sutter, Yolo; parts of Modoc, Lassen, Sierra, Nevada, Placer, El Dorado, Sacramento, Solano, Napa, Lake
San Francisco Bay	Marin, San Francisco, San Mateo; parts of Napa, Solano, Contra Costa, Alameda, Santa Clara
San Joaquin River	Calaveras, Tuolomne, Mariposa, Madera, Merced, Stanislaus, San Juaquin, Amandor; parts of Contra Costa, Sacramento, El Dorado, Alpine, Fresno, San Benito
South Coast	Orange; parts of Ventura, Los Angeles, San Bernardino, Riverside, San Diego
South Lahontan	Inyo; parts of Mono, San Bernardino, Kern, Los Angeles
Tulare Lake	Tulare, Kings; parts of Kern, Fresno

The map is color-coded to differentiate between the hydrologic regions, each of which represents a distinct area based on water resources and watershed management. The Central Coast region is marked in red, the Colorado River region in orange, the North Coast region in light blue, and the North Lahontan region in yellow. The Sacramento River region is depicted in dark blue, the San Francisco Bay region in purple, and the San Joaquin River region in green. The South Coast region is shown in light orange, the South Lahontan region in light green, and the Tulare Lake region in beige. These colors help to visually distinguish the different hydrologic areas within the state.

County boundaries are outlined with thin black lines, helping to distinguish the political boundaries within the state. The map labels major cities and counties, providing geographic context. Notable counties include Los Angeles, San Diego, Fresno, Sacramento, and San Francisco, among others, allowing viewers to easily identify key areas within each hydrologic region.

Additionally, the map marks the South Coast Regional Water Board boundaries with a red dashed line. This indicates the jurisdiction of the South Coast Regional Water Board, which oversees water quality in the South Coast region. This specific boundary helps to delineate areas of regulatory oversight, which is important for managing water quality and resources effectively.

Geographical features such as coastal areas, mountain ranges, and desert regions are also depicted on the map. These features are integral to understanding the state's water resources and hydrologic regions, as they influence the distribution and availability of water across California.

Figure 18.2.6: The Sacramento River Basin

This map of the Sacramento River Basin highlights the extensive network of rivers and tributaries within the basin. The basin spans multiple counties in Northern California.

At the top of the map, the Sacramento River originates in Siskiyou County, flowing southward through Shasta, Tehama, Butte, Glenn, Colusa, Sutter, Yolo, and Sacramento counties. The map shows several major tributaries feeding into the Sacramento River, including the Pit River in Modoc and Lassen counties, the Feather River running through Plumas, Sierra, and Yuba counties, and the American River originating in El Dorado and Placer counties.

Other significant waterways are also depicted, such as Stony Creek in Glenn and Tehama counties, Cache Creek in Lake and Yolo counties, and Putah Creek which flows through Napa and Solano counties. The rivers and creeks are marked with blue lines, providing a clear visual representation of the hydrology within the basin.

This map provides a detailed view of the Sacramento River Basin, showcasing the interconnected waterways that contribute to the river system. It highlights the importance of the basin in Northern California's water management and emphasizes the extensive network of rivers and tributaries that support the region's ecology and hydrology.

Figure 18.2.7: The San Joaquin River Basin

This image is a map of the San Joaquin River Basin, which highlights the intricate network of rivers and tributaries within the basin. The map spans multiple counties in central California, each outlined and labeled for easy identification.

The San Joaquin River Basin is depicted with the main San Joaquin River running prominently through the central part of the basin. The river flows from its headwaters in the Sierra Nevada through various counties including Fresno, Madera, Merced, Stanislaus, and San Joaquin before continuing to its confluence with the Sacramento River.

Several major tributaries feed into the San Joaquin River. To the north, the Calaveras River and the Mokelumne River flow through Calaveras and San Joaquin counties, while the Cosumnes River enters the basin from Sacramento County. To the east, the Tuolumne River runs through Tuolumne and Stanislaus counties, and the Merced River flows through Mariposa and Merced counties. Further south, the Chowchilla River and Fresno River contribute to the basin's network, flowing through Madera and Fresno counties.

The map also features numerous smaller tributaries and streams, providing a detailed view of the hydrological complexity within the basin. These waterways are marked with blue lines, illustrating the extensive water system that supports the region's ecology and water management needs.

The counties within the basin are clearly labeled, including Contra Costa, Alameda, Sacramento, San Joaquin, Calaveras, Amador, Tuolumne, Mariposa, Merced, Madera, and Fresno. This labeling helps to understand the geographical context and the political boundaries within the basin.

A scale bar at the bottom right corner of the map indicates distances of up to 50 miles, providing a reference for the size of the basin. Additionally, a compass rose in the bottom left corner indicates north, aiding in map orientation.

This map provides a comprehensive overview of the San Joaquin River Basin, highlighting its significant rivers and tributaries and the counties it spans. It emphasizes the importance of the basin in central California's water management and ecological health.

Figure 18.2.8: The San Joaquin Valley hydrology conceptual model

This cross-sectional diagram depicts the hydrology of the San Joaquin Valley. It illustrates various hydrological processes and land uses within the valley, emphasizing the interactions between surface water, groundwater, and land subsidence.

The landscape is divided into several zones. On the left side of the diagram, there are agricultural fields and orchards, indicating the extensive farming activities in the valley. Irrigation canals and rivers are shown supplying water to these fields. The agricultural activities are crucial for the region's economy but also significantly impact the valley's water resources.

The central part of the diagram highlights the "Area of land subsidence." This area shows the ground surface sinking due to the excessive extraction of groundwater. Wells are depicted extracting water from the underground aquifers, causing the land above to compress and subside. Arrows pointing downwards illustrate the movement of water from the surface into the subsurface, indicating recharge zones where water infiltrates the ground to replenish the aquifers.

The subsurface layers show the groundwater system, with water stored in porous rock and soil layers. Arrows within these layers indicate the flow of groundwater, moving towards areas of extraction and natural discharge points like springs and rivers. The diagram also shows the interaction between surface water and groundwater, with arrows depicting the movement of water between these two systems.

On the right side of the diagram, there is a mountainous region, representing the Sierra Nevada, which is a significant source of water for the valley through snowmelt and runoff. Streams and rivers originating from the mountains contribute to the valley's surface water supply.

This diagram provides a clear and informative visualization of the hydrological processes in the San Joaquin Valley. It highlights the critical issues of groundwater extraction and land subsidence, showing how agricultural activities and water management practices impact the region's hydrology. The diagram emphasizes the need for sustainable water use and management to address the challenges of land subsidence and water scarcity in the valley.

Figure 18.2.9: The Tulare Lake River Basin

This map of the Tulare Lake River Basin showcases the intricate network of rivers and their tributaries within the basin. The map outlines the basin, which spans several counties in central California.

The Tulare Lake River Basin includes prominent rivers such as the Kings River, the Kaweah River, the Tule River, and the Kern River. These rivers are marked in blue, highlighting their course through the basin. The Kings River flows from the Sierra Nevada mountains through Fresno County, while the Kaweah River and Tule River flow through Tulare County. The Kern River flows south through Kern County, contributing significantly to the water supply in the region.

The map indicates the county boundaries within the basin, with major counties including Fresno, Kings, Tulare, and Kern. These boundaries help to identify the areas affected by the basin's hydrology.

Additionally, the map provides geographical context by including neighboring counties and cities. Counties such as San Benito, San Luis Obispo, Ventura, and Los Angeles are marked, though they are outside the basin boundaries. This helps to understand the broader regional setting of the Tulare Lake River Basin.

This map provides a clear and detailed view of the Tulare Lake River Basin, emphasizing the major rivers and their flow through the region. It highlights the importance of these watercourses for the counties within the basin and underscores the need for effective water management to support the area's agricultural and ecological needs.

Figure 18.3.1: Types of aquifers

This image is a cross-sectional diagram illustrating different types of groundwater wells and the geological layers they penetrate. The diagram is divided into two main zones: the unsaturated zone and the saturated zone.

The uppermost layer is labeled "Land," which covers the ground surface. Beneath this is the unsaturated zone, where the soil and rock contain air and water in their pores but are not fully saturated with water.

Below the unsaturated zone is the saturated zone, which contains two main types of aquifers: the unconfined aquifer and the confined aquifer.

The unconfined aquifer is the uppermost water-bearing layer, consisting of sand. This aquifer is directly influenced by surface conditions and is separated from the atmosphere only by the unsaturated zone. The water table marks the upper surface of the unconfined aquifer, indicating the level at which the ground is fully saturated with water.

Within the unconfined aquifer, there is a "Water-table well," which extends from the land surface down to the water table. This well is designed to draw water directly from the unconfined aquifer. The well screen at the bottom of the well allows water to enter while filtering out sediments.

Beneath the unconfined aquifer is a "Confining Bed" composed of clay, which acts as an impermeable layer preventing water from moving freely between the unconfined aquifer and the underlying confined aquifer.

The confined aquifer lies below the confining bed and is typically made up of permeable materials such as limestone. This aquifer is under pressure because it is trapped between two impermeable layers.

The diagram also shows an "Artesian well" that penetrates through the confining bed into the confined aquifer. Artesian wells tap into pressurized groundwater, which can rise up the well without the need for pumping, often reaching the surface naturally. The "Potentiometric surface" in the diagram indicates the level to which water will rise in tightly cased wells.

This diagram provides a detailed understanding of groundwater systems, illustrating the different types of wells, their construction, and the geological layers they interact with. It highlights the dynamics of groundwater movement and the importance of aquifer and confining layers in groundwater management.

Figure 18.3.2: Aquifer conditions and water flow

This cross-sectional diagram depicts groundwater flow and aquifer systems, focusing on the interactions between unconfined and confined aquifers, the unsaturated zone, and surface features such as streams and vegetation.

The diagram is divided into several layers, each representing different components of the groundwater system. At the top, the land surface is shown with trees and a stream, indicating the presence of surface water and vegetation.

Below the land surface is the unsaturated zone, where the soil and rock contain both air and water in their pores but are not fully saturated. The water table marks the boundary between the unsaturated zone and the saturated zone below it. The water table can be seen intersecting with the stream, illustrating how surface water and groundwater are connected.

The saturated zone contains two main types of aquifers: the unconfined aquifer and the confined aquifer. The unconfined aquifer is the uppermost water-bearing layer, depicted with a high hydraulic-conductivity aquifer material (colored light blue). This aquifer is directly influenced by surface conditions and extends down to the confining layer below it.

The confining layer, marked by low hydraulic-conductivity material (colored with a dashed pattern), separates the unconfined aquifer from the confined aquifer beneath it. The confined aquifer lies below this confining layer and is depicted with high hydraulic-conductivity material, similar to the unconfined aquifer. This confined aquifer is under pressure due to the overlying confining layer and surrounding geological formations.

Groundwater flow is indicated by arrows within the aquifers, showing the movement of water from areas of recharge (where water enters the aquifer) to areas of discharge (where water exits the aquifer, such as into the stream or through wells). The direction of groundwater flow is influenced by the hydraulic gradient and the permeability of the geological materials.

The diagram also shows the processes of transpiration by vegetation, where water is taken up by plant roots and released into the atmosphere through leaves. This process affects the groundwater levels and the overall hydrology of the area.

This diagram provides a comprehensive view of the groundwater system, illustrating the interactions between different aquifer types, surface water, and the processes that influence groundwater movement. It emphasizes the importance of understanding these interactions for effective water management and conservation.

Figure 18.3.3: Artesian aquifer conditions and well flow

This cross-sectional diagram illustrates the concept of an artesian well within a groundwater system. The diagram shows the different geological strata, including pervious (permeable) and impervious (impermeable) layers, and how they interact to create conditions for an artesian well.

The diagram shows a curved structure of geological layers, with the pervious strata forming an aquifer confined between impervious strata. This configuration creates a confined aquifer system, where water is trapped under pressure between the impermeable layers.

The pervious strata are layers of rock or sediment that allow water to pass through them easily. These layers are typically made of materials such as sand, gravel, or fractured rock. The impervious strataare layers that do not allow water to pass through easily. These are usually composed of dense materials like clay or unfractured rock.

The saturation level is indicated, showing the highest level to which water can rise in the aquifer under natural pressure conditions. When a well is drilled into the confined aquifer, the pressure forces the water to rise above the level of the aquifer, often reaching the surface without the need for pumping. This type of well is called an artesian well, illustrated in the diagram by the upward flow of water from the well.

The artesian well is shown tapping into the confined aquifer, with water flowing upwards due to the pressure created by the surrounding impervious layers. This pressure can cause the water to rise significantly above the aquifer, sometimes even resulting in a free-flowing well.

The diagram highlights the importance of geological formations in creating artesian conditions, where natural pressure can be utilized to access groundwater. It also emphasizes the role of pervious and impervious strata in determining the movement and availability of groundwater in an aquifer system.

Figure 18.3.4: California aquifers by geographic location

This map illustrates the various aquifer systems across the state of California, highlighting the geographic distribution and types of aquifers with color-coding for easy identification. The map includes California's major cities, such as San Francisco, Sacramento, Fresno, Los Angeles, and San Diego, as well as important geographic features, including the coastline and major mountain ranges.

The six different types of aquifers highlighted on the map include Basin and Range basin-fill aquifers, Basin and Range carbonate-rock aquifers, California Coastal Basin aquifers, Central Valley aquifer system, Pacific Northwest basaltic-rock aquifers, and Pacific Northwest basin-fill aquifers.

Basin and Range basin-fill aquifers, shown in light green, are found primarily in the eastern part of the state and extend into parts of the central and southern regions. Basin and Range carbonate-rock aquifers, depicted in purple, are scattered in smaller patches, particularly in the eastern areas. California Coastal Basin aquifers, marked in teal, are concentrated along the coastal regions, extending from the north near San Francisco down to the south near San Diego. The Central Valley aquifer system, shown in gray, dominates the central part of California, encompassing the extensive agricultural regions of the Central Valley. Pacific Northwest basaltic-rock aquifers, indicated in red, are located in the northern part of the state. Pacific Northwest basin-fill aquifers, marked in blue, are also found in the northern regions, overlapping slightly with the basaltic-rock aquifers.

Figure 18.4.1: California water system

The is a map of California’s water storage and distribution infrastructure illustrating how water is collected, stored, and moved across the state to serve people, farms, and ecosystems. Major reservoirs are marked with colored symbols or squares whose sizes often reflect their storage capacity (for example, larger squares for reservoirs holding over 2 million acre-feet) and are spread throughout the state — many clustered in the northern and central regions where most precipitation and runoff occur.

Some key reservoirs on the map include Trinity and Shasta in the north, Oroville and Folsom in the central region, and San Luis and New Melones in the south. Major canals and aqueducts, such as the California Aqueduct and the Colorado River Aqueduct, are prominently marked, highlighting the extensive infrastructure required to transport water across California's diverse landscape. This map provides a comprehensive view of California's water storage and distribution system, emphasizing the importance of

managing water resources in a state with varied climate and geographic conditions.

From these reservoirs, an extensive network of canals, aqueducts, and pipelines extends across California. Prominent among these are:

- The California Aqueduct (part of the State Water Project), which carries water southward from the Sacramento-San Joaquin Delta through the Central Valley toward Southern California.
- The Central Valley Project (CVP) infrastructure, a federal system that includes major dams and canals mainly serving agricultural users in the Central Valley.
- Other federal and state conveyance systems that work together to move water across diverse terrain and long distances.

The map also displays rivers and natural waterways, providing geographic context for the engineered infrastructure that taps into these sources. Natural rivers like the Sacramento and San Joaquin feed into this system and serve as the starting points for many major storage facilities and pumping operations.

Labels likely identify key facilities (such as Shasta, Oroville, Folsom, San Luis, and New Melones reservoirs) and major canals/aqueducts, demonstrating how California captures and redistributes water from wetter regions in the north and east toward population centers and agricultural regions in the central and southern parts of the state.

Overall, this demonstrates the scale and complexity of California's water infrastructure — a mix of natural and engineered systems that work together to address the state's very uneven rainfall patterns and geographical water demand.

Video 18.4.1: State Water Project: An Aerial Tour

The California State Water Project starts its journey in the peaks of the Sierra Nevada Mountains in Northern California, where most of California's rain and snow fall each year. The three Upper Feather River lakes, Antelope, Frenchman, and Davis, sit at the top of the State Water Project. Antelope Lake, which is the smallest of the Upper Feather River lakes, is located on Indian Creek, a tributary of the east branch of the North Fork Feather River.

To the southeast is Frenchman Lake, the first lake created for the SWP in 1961, which consists of 21 miles of shoreline and a 139-foot-tall earthen dam. Lake Davis is located on Big Grizzly Creek, a tributary of the Middle Fork Feather River. It is the largest of the three lakes with a capacity of more than 84,000 acre-feet.

The Upper Feather River lakes feed into the North and Middle Forks of the Feather River, which wind their way through Plumas County, providing local water supply along the way. Along the Middle Fork of the Feather River, the freshwater cascades over Feather Falls, a picturesque recreation destination. The Forks of the Feather River feed into Lake Oroville, which is contained by Oroville Dam, the tallest dam in the United States at 770 feet.

Constructed in the 1960s, Lake Oroville is the second-largest reservoir in California and can store more than 3.5 million acre-feet of water. In addition to Oroville Dam, the Oroville Thermolito Complex includes three power plants, Hyatt, Thermolito Diversion Dam, and Thermolito Pumping Generating Power Plant, which together can produce 835 megawatts of electricity, enough clean hydropower to power 1.6 million homes for a year. While its primary purposes are water supply, hydroelectricity generation, and flood control, Lake Oroville also offers a variety of recreation opportunities.

Water continues from Lake Oroville down the Feather River until it meets up with the Sacramento River in southern Sutter County, just north of Sacramento. From there, the water heads south along the Sacramento River, winding its way through the farmlands of the northern Sacramento Valley, through downtown Sacramento, and into California's Sacramento-San Joaquin Delta. Once in the Delta, water is diverted to different parts of the state.

The Cordelia Pumping Plant in Solano County is part of the North Bay Aqueduct System, which provides water to cities in Napa and Solano counties. Water is pumped from the Delta at Barker Slough Pumping Plant and travels over 27 miles in an underground pipeline to its storage terminus in the city of Napa. Further south, water from the Delta is moved to the Clifton Court Forebay in Contra Costa County.

This shallow reservoir sits at the southern end of the Delta and provides storage and flow regulation into the Banks Pumping Plant. At Banks Pumping Plant, water is pumped up a hillside 244 feet to start its journey south, along the 444-mile-long California Aqueduct. The plant includes 11 pumps to move water into the canal and divert water during wet months to off-stream storage reservoirs and groundwater basins south of the Delta to improve water supply reliability.

Just a mile downstream from the Banks Pumping Plant, Bethany Reservoir marks the beginning of the South Bay Aqueduct. Here, the South Bay Pumping Plant moves water to the west to serve communities in Alameda and Santa Clara counties. Along the way, Lake DelVal in Alameda County provides storage and flood control for the South Bay Aqueduct.

Back in the Central Valley, the California Aqueduct stretches south through hundreds of miles of farmland and towns. The aqueduct is the most recognized facility in the State Water Project. It is the primary method for transporting water from northern California to southern California.

The concrete-lined canal winds its way through the valley and travelers along Interstate 5 can see the glistening waters of the canal. The California Aqueduct moves water by gravity with a little help from pumping plants along the way. Along the western side of the Central Valley in Merced County, the California Aqueduct enters O'Neill Forebay.

This body of water is part of the larger San Luis Reservoir Joint Use Complex that serves both the State Water Project and the Federal Central Valley Project. San Luis Reservoir is the nation's largest off-stream reservoir. The reservoir stores water diverted from the Sacramento-San Joaquin Delta for later deliveries to the South Bay Area, Central Valley, Central Coast, and Southern California.

Overlooking San Luis Reservoir is the Romero Visitor Center. Romero offers exhibits and videos that highlight California's world-renowned water delivery system and the importance of water in our lives, along with impressive views of the reservoir. With no watershed to support San Luis, the Gianelli Pumping Generating Plant moves water from the O'Neill Bay into San Luis Reservoir.

The plant generates electricity when water flows are reversed. To the south of San Luis, the Dos Amigos Pumping Plant gives water a 113-foot lift as it continues along the California Aqueduct. Further south is another important branch of the California Aqueduct.

The Coastal Branch Aqueduct provides water for San Luis Obispo and Santa Barbara counties. Water travels through the Coastal Branch Aqueduct to several pumping plants and ends near Vandenberg Air Force Base. Back on the main aqueduct, Buena Vista Pumping Plant, located south of Bakersfield in Kern County, sends the water on the next leg of its journey.

The plant is the first in a series of lifts known as the Valley String Pumping Plants. Here, water is sent up 205 feet. Just a few miles down the aqueduct is T-Rink Pumping Plant.

This facility provides the second lift, moving water up another 233 feet. Just a little further downstream, Chrisman Pumping Plant provides another lift. Here, State Water Project Water is lifted 518 feet for its journey over the Tehachapi Mountains, courtesy of the Edmonston Pumping Plant.

Now it's time for the big lift. Considered one of California's engineering marvels, Edmonston Pumping Plant uses 14 80,000 horsepower pumps to lift water 1,926 feet over the Tehachapi Mountains. The plant is the highest single-lift pumping plant in the world.

From there, water flows through a series of tunnels into the Tehachapi Afterbay, where the aqueduct divides into the West Branch and East Branch of the California Aqueduct. The West Branch of the State Water Project moves water to millions of Californians in Los Angeles and other cities in Southern California. Oso Pumping Plant is the first major structure on the West Branch of the California Aqueduct.

It lifts water 231 feet from Tehachapi Afterbay to Quail Canal, which leads into Quail Lake. From Quail Lake, State Water Project Water travels to Pyramid Lake in Los Angeles County. Visible from Interstate 5, Pyramid Lake provides storage for deliveries from the West Branch and recreational opportunities.

The lake is contained by the 400-foot-tall Pyramid Dam at the southern end of the lake. Pyramid Lake is also home to the Vista del Lago Visitor Center, which offers exhibits on the State Water Project and stunning views of the lake. Further south, Castaic Lake serves as the terminus of the West Branch.

The lake provides storage for the State Water Project as well as recreation opportunities in the Southern California area. The lake is contained by the 425-foot-tall Castaic Dam. Back at the junction, the East Branch of the State Water Project moves water through the Antelope Valley to communities like Riverside and San Bernardino.

The water is used by residents as well as groundwater recharge. Pear Blossom Pumping Plant is located along the East Branch of the California Aqueduct, about 12 miles east of the town of Palmdale. The plant lifts water about 540 feet to continue its journey southeast by gravity to Silverwood Lake.

The newest State Water Project power plant, the Mojave Siphon Power Plant, completed in 1996, generates electricity from the water flowing back downhill on its way to Silverwood Lake. Cedar Springs Dam, a 249-foot-tall earthen dam, creates Silverwood Lake. Located about 30 miles north of the city of San Bernardino, the lake provides regulatory and emergency storage, ensuring deliveries to users along the East Branch, and provides recreation for local communities.

Silverwood Lake also serves to ensure continuity of discharges through the Devil Canyon Power Plant. Devil Canyon Power Plant is situated at the southern base of the San Bernardino Mountains, about 5 miles north of San Bernardino. The power plant generates electricity from water traveling through the plant from Silverwood Lake.

From Devil Canyon, water is moved along the East Branch extension to Crafton Hills Reservoir. This reservoir provides additional storage and water supply for the east side of San Bernardino County. Back on the main segment of the East Branch Aqueduct, Lake Paris in Riverside County marks the end of the lawn.

It is the southernmost State Water Project reservoir and provides water supply and recreation. It's one of the most popular recreational lakes in the State Water Project system. From the headwaters of the Feather River Watershed to the reservoirs of Southern California, DWR's State Water Project provides critical water supply to millions of Californians, thanks to world-class engineering and some help from Mother Nature.

DWR is committed to ensuring the system continues to operate safely and efficiently for generations to come.

Box Figure 18.4.1: A Concept Drawing of the Auburn Dam

This illustration of a large dam, the Auburn Dam, showcases its structure and the reservoir it creates. The dam appears to be an arch dam, a type of dam curved upstream and designed to transfer the weight of the water it holds back into the surrounding rock walls. The illustration highlights the massive scale of the dam, with the reservoir extending into the background, indicating a substantial water storage capacity. This kind of infrastructure is essential for water management, providing water for irrigation, flood control, hydroelectric power generation, and recreational purposes. The surrounding landscape, depicted with lush greenery and hilly terrain, suggests that the dam is situated in a region with significant topographical variation, which is typical for such large-scale dam projects. The engineering and construction of such dams are crucial for sustainable water resource management, particularly in regions with variable water availability.

Box Figure 18.4.2: View of Hetch Hetchy Valley in the early 1900s

The black and white photograph showcases a vast valley flanked by towering cliffs, with two prominent waterfalls cascading down the rock faces. The valley floor is a mosaic of meandering streams, lush vegetation, and open meadows, suggesting a fertile and dynamic landscape shaped by natural water flows. The surrounding cliffs exhibit rugged, exposed rock formations, hinting at the geological history and forces that have sculpted this terrain over millennia. The overall scene conveys a sense of untouched natural beauty, highlighting the interplay between water, rock, and vegetation in this dramatic landscape. This image is a testament to the awe-inspiring power of nature and the intricate processes that continue to shape our planet's surface.

Box Figure 18.4.3: Hetch Hetchy Panorama – Yosemite National Park in 2019

The color photograph displays a serene lake framed by majestic cliffs, under a clear blue sky with a few scattered clouds. The water is calm, reflecting the surrounding landscape. The cliffs rise dramatically from the lake, showcasing their rugged, rocky textures. In the distance, the remnants of waterfalls can be seen, hinting at the geological processes that have shaped this region. The lush greenery along the cliffs contrasts with the barren rock, indicating the presence of vegetation adapted to this environment. This modern-day image, compared to the previous black and white photo, illustrates the enduring natural beauty of this landscape, capturing its timeless essence while highlighting the subtle changes that have occurred over time.

Figure 18.4.2: Aerial photo of the California Aqueduct

The California Aqueduct is a large man-made waterway winding through a vast, dry landscape. The aqueduct appears as a dark blue or black channel that snakes through the arid terrain, which is predominantly light brown and sparsely vegetated, indicating a desert or semi-arid region.

The aqueduct is lined with concrete and follows a curving path, with several sharp bends and turns. There are multiple parallel channels and branches visible, suggesting a complex network of waterways designed to distribute water across the region. The surrounding land includes a mix of agricultural fields, patches of barren land, and scattered buildings or structures, likely farms or small settlements.

In the background, there is a larger, more densely built-up area, possibly a town or industrial complex, indicating human habitation and activity in the region. The sky is clear, with no visible clouds, suggesting a sunny day. The image highlights the contrast between the engineered waterway and the natural, arid landscape it traverses, showcasing the critical role of the aqueduct in providing water to this dry region of California.

Figure 18.4.3: Levee Around a Sacramento Suburb

This aerial view of a suburban area in Sacramento, California, shows numerous houses and tree-lined streets. The houses are primarily single-family homes, and the area appears to be densely populated with a mix of evergreen and deciduous trees providing significant greenery. A river runs alongside the suburb, bordered by the levee, which is a raised embankment designed to prevent flooding. The levee is covered with grass and follows the curve of the river, creating a natural barrier between the water and the residential area. Beyond the suburb and river, the landscape transitions into flat, expansive farmland with large, open fields stretching towards the horizon. The sky is mostly clear, suggesting a calm and pleasant day. The image captures the integration of urban development, natural vegetation, and agricultural land in this region of Sacramento.

Figure 18.5.1: Saltwater-freshwater interface along the coast

The cross-section diagram illustrates the interaction between fresh water and saltwater in a coastal aquifer system. The land surface, composed of sand, lies above the water table, which is the upper surface of the zone where the soil or rocks are permanently saturated with water. Freshwater floats above the denser saltwater, which intrudes from the sea. The interface between the fresh water and saltwater slopes downward beneath the land surface, maintaining a dynamic equilibrium. The thickness of the freshwater lens is denoted by 'h', while 'z' indicates the depth to the interface below sea level. The sea level serves as the reference point for both the water table and the position of the interface. The diagram highlights the importance of managing groundwater resources to prevent saltwater intrusion, which can compromise the quality of freshwater supplies. This understanding is crucial for sustainable water management in coastal regions.

Figure 18.5.2: Modeled chloride (salt water intrusion)

The diagram presents a modeled condition of a coastal aquifer system from the year 2004, showcasing the distribution of chloride concentrations along a cross-sectional view from point A on the far left to A' on the far right. The vertical axis represents depth in meters below the North American Vertical Datum of 1988 (NAVD 88), while the horizontal axis indicates distance along the section in meters. The cross-section includes various geological layers, with depths ranging from the surface to over 800 meters below.

The coastline is marked at around the 10,000-meter mark on the horizontal axis, and several wells are indicated along the section. The explanation box in the diagram provides a color-coded key for simulated chloride concentrations in milligrams per liter, ranging from 2,000 mg/L (blue) to 18,000 mg/L (red). Higher chloride concentrations, depicted in red and orange, are found closer to the coastline, signifying areas of significant saltwater intrusion.

Geological formations such as Pliocene B and C, and Tertiary undifferentiated units are labeled in the cross-section, showing the variation in sediment layers and their influence on groundwater flow and chloride distribution. Wells, such as 5S/13W-11P 1.2 and 5S/13W-2E 1.2, are positioned at different points along the section to monitor and analyze the chloride concentrations and groundwater conditions.

This detailed illustration underscores the complexity of coastal aquifer systems and the importance of monitoring chloride levels to manage and mitigate saltwater intrusion, which can impact freshwater resources. The vertical exaggeration of 5:1 enhances the visualization of the geological formations and the distribution of chloride concentrations.

Figure 18.5.3: Saltwater intrusion

This map illustrates the progression of seawater intrusion into an aquifer system over several decades, specifically focusing on the area around Marina, California. The different colors on the map represent the extent of seawater intrusion in various years, with each color corresponding to a different period.

In 1944, seawater intrusion was limited to a small area along the coast. By 1965, the intrusion had spread inland, encompassing a larger area. This trend continued over the years, with significant expansion noted in 1975, 1985, and 1993. By 1997 and 1999, seawater had intruded further into the aquifer system, indicating a persistent and growing problem.

The map also marks the extent of seawater intrusion for specific years, including 2001, 2003, 2005, 2007, 2009, and 2011, highlighting the continued advance of seawater into the aquifer. The blue line indicates the 2013 seawater intrusion extent, defined by a 500 mg/L chloride concentration contour.

Key infrastructure and landmarks such as Nashua Road, Blanco Road, and Reservation Road are shown on the map, providing geographical context. The map underscores the significant and ongoing challenge of managing seawater intrusion in coastal aquifers, necessitating effective groundwater management strategies to protect freshwater resources.

Figure 18.5.4: Salinas Valley Basin groundwater elevation

This map depicts the groundwater elevation in the Salinas Valley Basin as of August 2019, focusing on the Pressure 180-Foot and East Side Shallow Aquifers. The contour lines represent lines of equal groundwater elevation, with each line indicating a 10-foot change in elevation.

The groundwater elevations range from -100 feet (in the northeaster region) to +40 feet (in the southeastern region), showing significant variation across the basin. The map highlights a potential fault zone with a dotted line running through the central part of the basin, potentially influencing groundwater movement and distribution.

Key locations are marked, including Castroville to the north, Salinas at the center, Marina to the west, and Chualar to the south. The Monterey Bay is shown to the west, providing context for the basin's proximity to the coast.

The contour lines illustrate the groundwater flow direction, which generally moves from higher elevations in the east towards lower elevations near the coast and the Monterey Bay. This flow pattern is crucial for understanding groundwater management and addressing issues such as seawater intrusion, which can affect the quality and availability of groundwater in the basin.

The map provides a detailed snapshot of groundwater conditions in the Salinas Valley Basin, serving as a valuable tool for water resource management and planning in the region.

Figure 18.5.5 Conceptual diagram of saltwater pumping by a barrier well

This diagram illustrates the interaction between production wells and barrier wells in managing the saltwater interface.

On the left side, on land, a production well is depicted. This well extracts groundwater from the subsurface. The arrows pointing towards the well indicate the direction of groundwater flow towards the well as it is pumped out. The production well taps into the groundwater reservoir, drawing freshwater up to the surface for use.

On the right side lies the sea.

In the middle, near the shoreline, a barrier well is shown. This is designed to prevent saltwater intrusion into freshwater aquifers. The arrows around the barrier well illustrate the direction of water movement, with water being injected into the aquifer to create a pressure barrier. This barrier well pushes the saltwater interface back towards the sea, maintaining the separation between freshwater and saltwater.

The saltwater interface is the boundary where freshwater meets saltwater. In coastal areas, over-pumping of groundwater can lead to saltwater moving inland, contaminating freshwater supplies. The diagram shows the sea level and the position of the saltwater interface under natural conditions. Note that the saltwater interface is shown slanting inland from the shoreline, ending near the barrier well.

Overall, this setup helps manage the balance between freshwater and saltwater, ensuring sustainable groundwater extraction while preventing saltwater intrusion.

Figure 18.5.6: Seawater intrusion in Los Angeles

The diagram consists of three parts (A, B, and C), which illustrate the process of saltwater intrusion and the use of injection wells to create a barrier against it.

In part A, we see a pumping well extracting freshwater from an aquifer. The potentiometric surface, which is the level to which water will rise in tightly cased wells, is shown above the aquifer. The aquifer is confined by a layer of impermeable material, preventing water from moving freely upwards. Under normal conditions, the freshwater in the aquifer keeps the saltwater at bay, maintaining a stable interface between the two.

In part B, continued pumping from the well creates a cone of depression in the potentiometric surface around the well. This lowers the water level in the aquifer, reducing the pressure that holds back the saltwater. As a result, a saltwater wedge begins to intrude into the freshwater zone. This intrusion can compromise the quality of the extracted water, as the well starts to draw in saltwater.

In part C, an injection well is used to address the issue of saltwater intrusion. Water is injected into the aquifer through this well, creating a pressure gradient that forms a barrier against the advancing saltwater wedge. This injected water raises the potentiometric surface and helps to push the saltwater back towards the sea, protecting the freshwater resources in the aquifer from contamination.

This process demonstrates how managing groundwater extraction and using injection wells can help maintain the balance between freshwater and saltwater, ensuring a sustainable supply of clean groundwater.

Figure 18.5.7: Basin Prioritization of 2019

This map, titled "California Sustainable Groundwater Management Act (SGMA) Basin Prioritization," categorizes various groundwater basins in California based on their priority levels for sustainable management as mandated by SGMA. The map delineates four priority levels: high, medium, low, and very low. High-priority basins are marked with dense diagonal stripes, medium-priority basins with lighter diagonal stripes, low-priority basins with a pale shade, and very low-priority basins with a very light shade.

The high-priority basins, which are crucial for groundwater management due to their significant role in California's water supply and potential challenges, are concentrated in regions with intensive agricultural activities, high population densities, or both. These areas include parts of the Central Valley, particularly around Fresno and Sacramento, and extend to other regions like San Francisco and San Jose.

Medium-priority basins, which also play an important role but with slightly less urgency, are scattered throughout the state, including areas near Los Angeles and parts of the Central Coast.

Low-priority and very low-priority basins, which have less immediate management needs, cover large portions of the state, particularly in regions with less intensive water use or lower population densities. These areas include much of Northern California outside the Central Valley and extensive parts of Southern California.

The map also includes a small inset showing California's location within the United States, providing a broader geographical context. Additionally, it highlights significant urban centers like Los Angeles, San Diego, and San Francisco, emphasizing the relationship between population centers and groundwater basin prioritization.

The map was created by Cole Heap, P.G., and uses data from the USGS, SGMA 2019 Basin Prioritization report, and various other geographical and environmental sources. It provides a visual guide for understanding the areas where sustainable groundwater management efforts are most needed in California.

Figure 18.5.8: Dry lakebed in California

This lake is almost completely dry, a consequence of severe drought, characterized by a significantly low water level and cracked,

dry ground. The remaining water in the background forms a small, narrow body, indicating that this area was once fully submerged. The trees lining the sides of the water body suggest a natural environment, possibly a lake or reservoir, now drastically reduced in size due to the lack of rainfall or overuse of water resources. The dry, parched soil in the foreground highlights the extent of the drought's impact, with deep fissures and cracks illustrating the severity of the arid conditions.

Figure 18.5.9: Satellite images of Lake Oroville

This image side-by-side comparison of Lake Oroville on June 4, 2019, and June 9, 2021 highlights the impact of drought conditions over two years. The 2019 image depicts Lake Oroville with high water levels, covering a vast area with dense greenery surrounding the lake. The water appears deep and expansive, indicating a period of ample rainfall or water supply.

In contrast, the 2021 image shows a significantly reduced lake size, with much of the lakebed exposed and the water levels drastically lower. The exposed lakebed is a lighter color, indicating dryness and the absence of water. The surrounding areas also appear less green, suggesting vegetation stress or die-off due to prolonged dry conditions. The reduction in water levels over the two-year period is stark, illustrating the severe impact of drought on Lake Oroville and its ecosystem. The visual difference between the two images serves as a powerful illustration of the changing environmental conditions and the challenges posed by water scarcity.

Figure 18.5.10: Progression of the 2012-2014 historic California drought

This animated image shows the progression of drought conditions across California from December 31, 2013, to July 29, 2014, as reported by the National Drought Mitigation Center. The animation highlights different levels of drought severity, marked by color codes: yellow for abnormally dry, orange for moderate drought, light red for severe drought, dark red for extreme drought, and brown for exceptional drought.

At the beginning of the animation on December 31, 2013, the central and southern parts of California are already experiencing severe to extreme drought, while the northern regions are mostly abnormally dry or under moderate drought. As the animation progresses through the months, the drought conditions intensify and spread. By July 29, 2014, the entire state is engulfed in drought, with large areas under extreme or exceptional drought conditions, particularly in the Central Valley and parts of Southern California. This stark visual progression underscores the worsening water scarcity and the environmental stress facing the state over this period.

Figure 18.5.11: Flooding in California’s Sacramento Valley (MODIS)

This satellite image, taken from a broad perspective, showcases the northern California region with a specific emphasis on the Sutter Buttes, a small circular range of volcanic hills in the Central Valley of California, often referred to as the "smallest mountain range in the world."

In the image, different shades of green (covering most of the western region) indicate various types of vegetation and land cover, while the blue and cyan tones (in the eastern region beyond the Sutter Buttes) suggest the presence of water bodies and snow. The dark areas represent bodies of water, including rivers, lakes, and reservoirs. The Sutter Buttes stand out as a distinct feature in the otherwise flat landscape of the Central Valley.

The surrounding landscape includes fertile agricultural fields, evident by the patchwork pattern, as well as natural vegetation in the hills and mountains. To the west, the Pacific Ocean is visible, and the coastal areas appear dark due to the dense forest cover. The urban areas, such as the San Francisco Bay, show a mix of colors indicating the complex land use in these regions. This image provides a detailed view of the diverse geography and land use in northern California, highlighting both natural and human-modified landscapes.

Figure 18.5.12: Permeable Pavement sign in Grass Valley, California

The informative sign titled "Permeable Pavement" explains the concept and process of using permeable pavement to manage stormwater. It provides a comprehensive overview of how permeable pavement works, its benefits, and the specific implementation in the surrounding area. The top section illustrates the structure of permeable pavement. It includes a surface layer of permeable material that allows water to pass through. Beneath this layer, there are additional layers designed to filter and

store water, eventually allowing it to seep into the ground below. This process reduces runoff and helps recharge groundwater.

The main process involves rainwater that falls on the permeable pavement. Instead of running off into storm drains, the water infiltrates through the pavement and the underlying layers of gravel and sand. This filtered water then recharges the groundwater system. The sign also highlights the journey of water from the permeable pavement into nearby creeks and rivers, emphasizing the environmental benefits such as reduced erosion and improved water quality.

The bottom part of the sign details the local implementation of permeable pavement in the area. It describes how the permeable pavement on N. School Street contributes to the health of local water bodies, such as Grass Valley and Wolf Creek. The sign also provides visual aids, including a map and illustrations, to help viewers understand the connection between the permeable pavement and the local watershed. This sign serves as an educational tool for the public, promoting awareness of sustainable stormwater management practices and their positive impact on the environment. It encourages the use of permeable pavement as a practical solution for reducing urban runoff and enhancing groundwater recharge.

Data for Graph 18.2.1: Annual Statewide Precipitation

Table: Annual statewide precipitation in California (1895-2021)

Year	Precipitation (inches)
1895	
1896	26.42
1897	27.07
1898	17.29
1899	20.19
1900	24.48
1901	27.26
1902	23.38
1903	24.92
1904	32.84
1905	24.8
1906	30.09
1907	32.49
1908	19.56
1909	30.95
1910	22.38
1911	27.3
1912	19.14
1913	18.66
1914	30.27
1915	27.86
1916	27.07
1917	20.43
1918	19.1
1919	21.41

Year	Precipitation (inches)
1920	17.87
1921	26.89
1922	24.23
1923	21.07
1924	10.74
1925	25.63
1926	19.24
1927	28.86
1928	20.35
1929	16.25
1930	19.45
1931	15.09
1932	23.11
1933	17.84
1934	16.62
1935	25.77
1936	24.45
1937	24
1938	34.65
1939	17.96
1940	26.74
1941	34.99
1942	27.17
1943	26.28
1944	19.22
1945	23.38
1946	22.46
1947	17.84
1948	20.91
1949	17.45
1950	19.13
1951	24.95
1952	31.75
1953	23.29
1954	22.66
1955	17.61
1956	30.21

Year	Precipitation (inches)
1957	20.78
1958	34.69
1959	17.27
1960	17.7
1961	18.85
1962	21.55
1963	26.83
1964	17.18
1965	27.44
1966	19.68
1967	29.71
1968	18.64
1969	32.88
1970	23.94
1971	25.09
1972	17.59
1973	26.25
1974	30.38
1975	23.32
1976	16.76
1977	11.94
1978	35.25
1979	20.94
1980	29.54
1981	17.98
1982	35.19
1983	42.81
1984	24.75
1985	19.48
1986	30.65
1987	15.01
1988	19.07
1989	20.69
1990	16.46
1991	17.48
1992	19.51
1993	32.56

Year	Precipitation (inches)
1994	15.74
1995	37.7
1996	26.59
1997	29.02
1998	38.67
1999	22.77
2000	22.49
2001	17.08
2002	18.92
2003	25.88
2004	20.14
2005	30.7
2006	30.8
2007	15.3
2008	18.24
2009	18.7
2010	25.11
2011	31.27
2012	17.82
2013	18.58
2014	13.13
2015	17.55
2016	24.17
2017	37.73
2018	17.16
2019	30.11
2020	16.33
2021	11.84

This page titled 18.8: Detailed Figure Descriptions is shared under a CC BY-NC 4.0 license and was authored, remixed, and/or curated by Cole Heap.

19: CALIFORNIA'S EARTHQUAKE HISTORY AND HAZARDS

Introduction: A Noble Quake

The high desert is cold at night. At half past two in the morning, the fierce daylight winds have settled, and the coarse desert sands take their rest, along with dreamers snoring in their beds. Far, far above them all, the Milky Way galaxy–bright and sharp in the clear night–slowly plows across the dark expanse of sky. The universe itself seems quiet.

And then the sound. Rocks grind and crack. Tin water pails clang to the floor and splash. Adobe brick walls grind and teeter and fall, thumping to the ground. A deep grumble, like the yawn of an awakening dragon, fills the air, startling jackrabbits who sprint from an unseen enemy, panicked birds clapping their wings as they escape to the sky. But on the ground, the pain has just begun.

Two hundred kilometers away, naturalist John Muir springs from his cabin with joy as he hears boulders cascade down the vertiginous cliffs of Yosemite. One can learn that a volcano is erupting and consciously decide to visit it, but to experience an earthquake–a noble earthquake!--one must be in just the right confluence of time and place when a temblor occurs. John Muir has never felt an earthquake before and he is excited.

Back in the tiny mining camp of Lone Pine, his enthusiasm was not shared. Of the 59 houses in Lone Pine, 52 collapsed. Of the 250-300 residents of Lone Pine, 27 died in this quake.

Let's consider these numbers. San Francisco currently has over 400,000 housing units, ranging from single family homes to large apartment complexes. In the 1872 Lone Pine quake, 52 of the 59 homes were destroyed–a loss rate of 88%. If a comparable quake today destroyed 88% of San Francisco's housing units, that would be over 350,000 homes lost.

Lone Pine had somewhere between 250 to 300 residents and 27 were killed. If we round the population to 270, then the loss of 27 is a 10% death rate. San Francisco currently has about 815,000 residents. If the 1872 Lone Pine death rate applied to a San Francisco quake, about 81,500 people would be killed. This would far exceed the combined death tolls from all the worst natural disasters in the United States (Galveston, 1900: 8,000 killed; San Francisco, 1906: 3,000 killed; New Orleans, 2005: 1,800 killed).

We don't expect such losses in a future San Francisco quake because we've changed many things since 1872. The main reason Lone Pine experienced such devastation is that so many of its buildings were constructed from adobe bricks. Adobe bricks are basically blocks of dried mud, sometimes mixed with straw. Lone Pine's buildings could not be made from timber because structural wood was scarce in the region, but mud is always plentiful. However, brick buildings are inherently unstable and dangerous because little holds these blocks in place when an earthquake shifts them, sending heavy walls tumbling down on the delicate bodies of those living in such precarious houses. Making a house out of small, shiftable pieces of masonry is a very bad idea in earthquake country.

Put another way: earthquakes don't kill people, buildings do.

A second reason Lone Pine suffered so greatly was its proximity to the fault that generated the quake. Today, just a short distance west of the town, one can still see dramatic fault offsets from 1872; a century and a half of erosion has done little to erase the scars created by this giant quake (see Figure 19.1). Lone Pine was simply too close to the fault and absorbed the full energy of the quake.



Figure 19.1: Fault displacement from the 1872 Lone Pine earthquake. "Lone Pine" by Steven Newton, is licensed under CC BY-NC 4.0. Access a detailed description.

Lessons from Lone Pine

What happened in the 1872 Lone Pine quake has a lot to teach us about California's earthquake hazards.

First, like our 1872 predecessors, far too many modern Californians live in seismically vulnerable buildings. Though we no longer build with weak adobe bricks, many California buildings are unreinforced masonry which can collapse in even moderate quakes. And while many residents assume that "the government" will somehow protect Californians from quake hazards through building codes, in some cases the opposite is true. "Soft first story" buildings have foundation levels relatively open and unreinforced. One reason modern buildings are constructed with a soft first story is to accommodate parking underneath buildings. Many municipalities actually require new multi-family buildings to have such parking, meaning that by code California buildings are designed more vulnerable to earthquakes than they need to be.

Second, like the Lone Pine residents unwittingly living right next to a major fault, the majority of Californians live in just a few urban regions that are the among most seismically dangerous regions in the entire state. There are more seismically stable areas of California, but in those regions fewer people reside. We live in the wrong places in the wrong types of houses.

We could have done better. We could have chosen to build this state in a more rational way. We could have learned lessons from California's rich inventory of historic earthquakes–not just 1872, but also 1700, 1906, 1933, 1971, 1989, 1994, and many more. The history of these quakes could have influenced decisions about development occurred, both in terms of location and also in terms of types of buildings. But California chose instead to grow with little regard to seismic hazard.

Query 19.1

This interactive element is not available in this format. Visit the link or scan the QR code to access it online.

View this Interactive Content online

Query 19.2

This interactive element is not available in this format. Visit the link or scan the QR code to access it online.

View this Interactive Content online

Learning Objectives

By the end of this chapter, you should be able to:

- Describe the ways in which California is vulnerable to earthquake hazards, including California's history of major seismic events.
- Understand the ways in which certain building types add risk from earthquakes, and how some mitigation is possible.
- Analyze how the proximity of populations to known faults increases danger to life.
- Know ways to prepare oneself for the inevitability of devastating future quakes.

00: Front Matter

Table of Contents

19.1: Front Matter

19.1.1: Table of Contents

19.2: The Hazard of Buildings

19.3: The Hazard of Place

19.4: Liquefaction and the Role of Soil Type

19.5: What's Coming

19.6: Beyond the San Andreas - Earthquakes of the North Coast

19.7: Preparing for the Worst

19.8: A State of Danger

19.9: Chapter Summary

19.10: Detailed Figure Descriptions

This page titled 19: California's Earthquake History and Hazards is shared under a CC BY-NC 4.0 license and was authored, remixed, and/or curated by Steven Newton.

19.2: The Hazard of Buildings

Earthquakes Don't Kill People; Buildings Do

Imagine you are walking your dog in an open field, enjoying the ubiquitous California sunshine. At that moment, you feel violent earthquake waves. Are you in danger? Outside of losing your balance, you are not likely to encounter any health hazard in the middle of a field. Seismic waves don't directly hurt the human body. In the open, you can experience the biggest shaking the Earth can offer and nothing will happen to your body other than a few cavity fillings loosening.

If you are inside a building, however, the story can be quite different. Much depends on the type of building.

If an exact repeat of the 1872 Lone Pine quake occurred today, we would not lose 88% of buildings, as we did in Lone Pine; in fact, it is safe to posit that no place in California would lose such a high percentage. Over 60% of Californians live in free-standing, wood-framed single family homes; because of the flexibility of such structures, it is expected that they will perform much better in shaking than older, multi-story masonry structures.

Masonry (bricks or larger blocks) is spectacularly unsuited to earthquake country (see Figure 19.2.1). While masonry has a lot of strength in the up-down direction of compression from gravity, individual blocks can easily shift side-to-side and shear in seismic events. Masonry bears load effectively only in the up-down orientation; when bricks shift position even slightly, they lose the ability to hold up buildings. Some municipalities require retrofitting of masonry buildings–attaching anchors, or cross-bars–but these efforts should be understood as a band-aid rather than a fix. The only comprehensive solution would be to tear down and rebuild vulnerable structures to a higher standard, but given the economic impracticality of such a cure, most municipalities seem to hope that the preventable loss of life will not be too great when the quake comes, and then post-quake reconstruction will occur to those higher engineering standards.



Figure 19.2.1: Unreinforced brick wall in downtown Oakland, 19th and Webster streets. "19th & Webster, Oakland," by Steven Newton, is licensed under CC BY-NC 4.0. Access a detailed description.

Newer buildings, constructed according to scientifically-informed engineering standards, are much more resilient than older buildings. For example, the new City Hall of Hayward, CA, was finished in 1998 and replaced an earlier structure that was, quite literally, being slowly ripped apart by movement of the Hayward fault. The new City Hall sits less than 200 meters from the fault. In order to isolate this building from the inevitable shaking, the base of the structure sits on dozens of giant ball bearings. These isolation bearings mean that as the ground moves, the ball bearings dampen the movement and allow the building to stay in place, with limited transfers of movement from the quake to the building.

The problems, then, comes down to the dangerous antiquity of many older buildings, and especially the construction style known

as soft story buildings.

Soft Story Buildings

A soft story building has an open, poorly-braced ground level. This design performs very poorly in earthquakes, where seismic motion transfers to the building through the ground level. This weakened first story then becomes a risk for the collapse of the entire building.

In the 1989 Loma Prieta and the 1994 Northridge quakes, many of the damaged and collapsed buildings were soft story structures. Figure 19.2.2 shows the heavily damaged Marina District in San Francisco and how motion from the 1989 quake tilted the building laterally due to the collapsed street-level soft story parking garages.



Figure 19.2.2: A building destroyed during the 1989 Loma Prieta quake, with a collapsed soft story. In the Marina District of San Francisco, ad the corner of Beach and Divisadero Streets. "Soft story" by J.K. Nakata, USGS is in the public domain. Access a detailed description.

In Figure 19.2.3:, we see an existing soft-story building and can examine the problematic masonry supports holding up the structure. Even a slight side-to-side motion has the potential of shifting masonry, weakening these load-bearing columns.



Figure 19.2.3: A soft-story apartment building with masonry supports in Oakland, CA. (Image modified for privacy and lighting exposure.) "Soft story" by Steven Newton, is licensed under CC BY-NC 4.0. Access a detailed description.

What Figure 19.2.3: shows is an apartment building with the entire lower level opened to accommodate parking. The effect of this is to weaken the most critical level for seismic building survival. If cross-bracing were installed across the parking spots, then the building would have greater flexibility; as it stands now, a few narrow posts are all that keeps the living areas standing above the parking spots.

Why build this way? Why build a weak soft story in earthquake country? Some soft story buildings have retail shops on the foot-traffic level, necessitating open spaces for displays. But there is a far more common reason for this problematic architecture: parking.

Many cities require new apartments to provide on-site parking. This is an ill-considered response to local overpopulation and consequent street parking shortages. The thinking is, rather than pushing more cars onto already crowded streets, when multi-family apartment buildings are constructed, parking should be accommodated cars on-site. This could be accomplished with a secondary garage or an adjacent lot, but rather than these expensive options, developers often choose to put resident cars underneath the apartments.

Science has developed a wealth of information about the prevention of death and injury from earthquake; however, rather than adopting these scientific findings, many municipalities fail to take the science into account, and in the case of allowing and even requiring soft story parking architecture, actively ignore well-established dangers.

According to the Association of Bay Area Governments, San Francisco has approximately 6,700 soft story buildings. In 2013, San Francisco implemented regulations requiring soft story building owners to retrofit. Many building owners have complied, despite the extraordinary cost, which can run into hundreds of thousands of dollars. However, in the case of noncompliant property owners, the only actions taken to date have been posting "shame notices" of code violation outside the affected buildings.

Query 19.2.1

This interactive element is not available in this format. Visit the link or scan the QR code to access it online.

View this Interactive Content online

References

1. Dal Pino, J. (2019, March 1). The San Francisco Soft-Story Ordinance. Structure Magazine. https://www.structuremag.org/?p=14310
2. Gutierrez, H. (2023, July 6). Hundreds of San Francisco buildings are behind on earthquake retrofits, putting lives at risk. Retrieved June 27, 2024, from https://www.nbcbayarea.com/investigations/soft-story-retrofits-in-san-francisco/3267556/

This page titled 19.2: The Hazard of Buildings is shared under a CC BY-NC 4.0 license and was authored, remixed, and/or curated by Emily Wright.

19.3: The Hazard of Place

Highway to the Danger Zone

There has always been an oddity about where populations developed in California. In this mostly arid state where one would imagine water accessibility would influence urbanization. But today where there is plentiful water–the northern regions–very few people reside, while in the parched deserts of the south, endless ranch house clones, festooned with backyard chlorinated swimming pools, stretch to the arid horizon.

California has an exquisitely beautiful coastline, but few people live within sight of the ocean. Some areas of California have exceptional air quality, but population growth is more concentrated in the Central Valley, which the American Lung Association has described as “the most dangerous place in the United States to breathe."

It’s almost as if California developed with no coherent, rational plan. That’s because California developed with no coherent, rational plan. No one is actually in charge. No single authority is empowered to declare, “Enough!” and veto development in inappropriate, unaesthetic, or hazardous places. So growth has been unmanaged, unplanned--and unsustainable.

This aspect of California is not new. California went from under a hundred thousand residents at the Gold Rush to almost four times as many just a decade later. By 1900, California had almost a million and a half residents; the subsequent two decades added two million more. The prewar population doubled by 1960, then doubled again by the 2010s. You would imagine that such a population explosion corresponded with necessary growth in transportation systems, public utility systems, increased numbers of schools and hospitals, and you would be wrong.

You might imagine that a regulatory agency is tasked with protecting residents by considering if growth should be allowed in seismically dangerous areas, and again you would be wrong.

Let’s examine this feature of California from the intersection of population and seismicity, and how it came to be that Californian urban centers tend to be in such dangerous locations.

Other states experience regular earthquakes. Alaska is very seismically active, but has a population of only 733,000. (San Francisco's population is 815,000.) Most of California’s 38 million residents are not found in the open deserts of the Mojave, or the barren lava flows of the Modoc, but rather are concentrated in three major clusters: the Sacramento-San Joaquin Valley area, the greater Los Angeles area, and the San Francisco Bay region (see Figure 19.2.1).

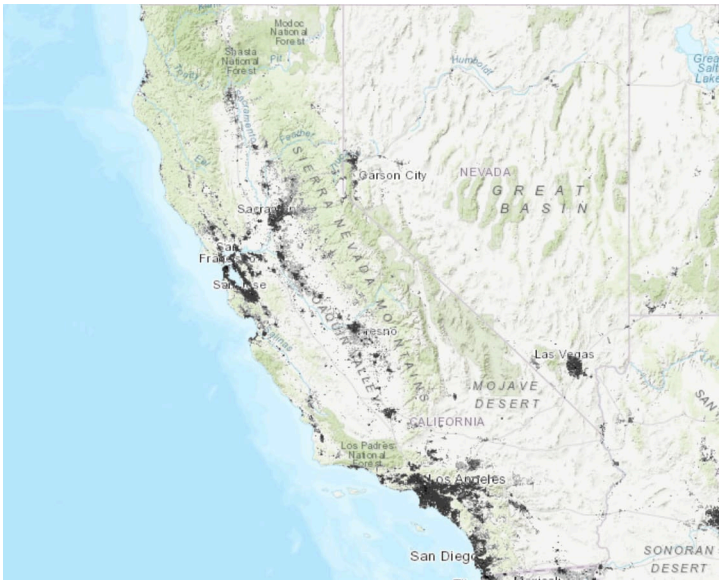


Figure 19.3.1: California population density map, from the USGS Interactive Map. "Population map" by USGS is in the public domain. Access a detailed description.

While Sacramento-San Joaquin Valley is relatively untouched by quakes, the greater Los Angeles area and the San Francisco Bay region sit directly on major earthquake clusters (see Figure 19.3.2).

Quite simply, most Californians live in the most dangerous locations for earthquakes; moreover, many live in the most vulnerable types of buildings.

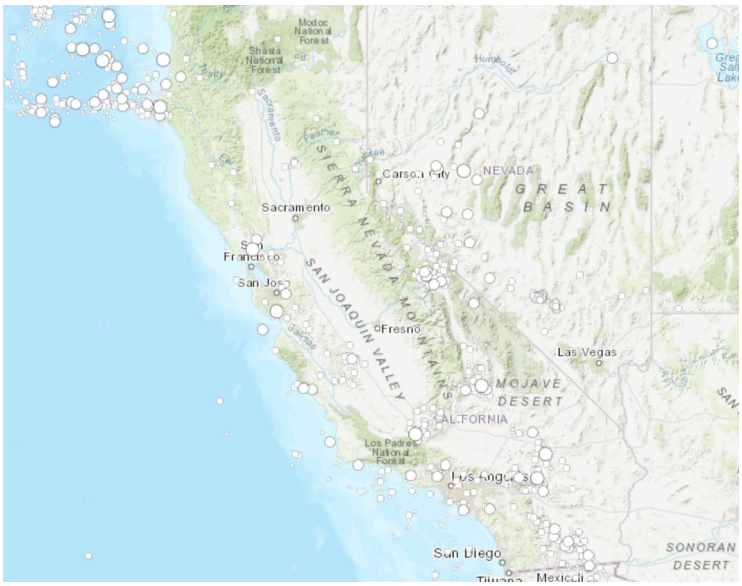


Figure 19.3.2: Seismicity of California, from the USGS Interactive Map. "Seismic map" by USGS is in the public domain. Access a detailed description

One place where the intersection of faults and urban population is particularly acute is the San Francisco Bay Area. The most worrisome fault in this region is the Hayward fault, as explained in this video:

Video 19.3.1: Video about the Hayward fault

Watch this video to learn more about the Hayward fault.

This interactive element is not available in this format. Visit the link or scan the QR code to access it online.

View this YouTube Video online

Proximity to Faults

Earthquake energy decreases rapidly with distance. In other words, if you are 1 km from an earthquake epicenter, your seismic experience will be markedly different from a person 10 km away, and much different still from someone 100 km away. When an earthquake pops, concentric shells of energy spread out at depth at about the speed of sound. One may envision this like a pebble being dropped into a pond, albeit a rather solid one when it comes to the lithosphere. Many factors can lessen, or attenuate, the quake energy, such as fracturing, friction heating, and comminution (pulverizing rock into smaller particles). While the mathematics of this are beyond the scope of this introductory book, suffice it to say that all else being equal, you want to be as far away from faults as possible, and that ground shaking increases exponentially the closer you are.

This phenomenon can be illustrated in shake maps which plot quake intensity. In 2019, a series of earthquakes occurred near Ridgecrest, a small town neither on a ridge nor on a crest, but rather in the middle of a wide basin in the far southern Owen's Valley. The intensity of the largest quake (M_W 7.1, 1 death) is mapped in Figure 19.3.3. The color coding is that the light blue and light green show very little motion and are probably undetectable for most people; conversely, the red and orange zones show

intense shaking. As this diagram shows, the area very close to the epicenter (indicated by a star) has bad shaking which very quickly diminishes even a few kilometers away. At 200 kilometers away, the shaking is mostly unfelt.

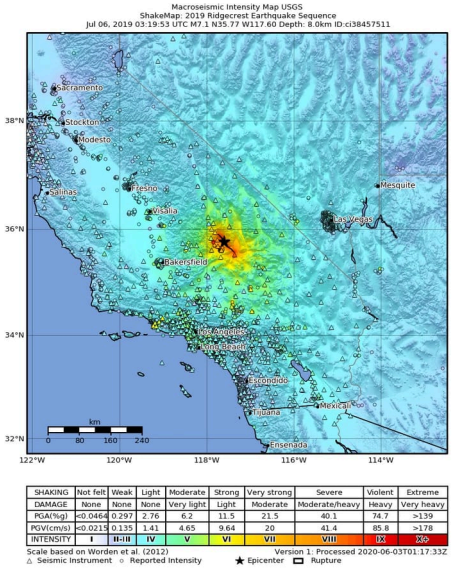


Figure 19.3.3. A shake map showing the intensity of the 2019 Ridgecrest quake. "Population map" by USGS is in the public domain. Access a detailed description.

Most major California cities have developed far too close to major faults. Let's look at a few examples of the intersection of metropolitan areas and faulting.

In Figure Figure 19.3.4, we see the complex fault systems of Southern California. Faults are indicated with red lines. The San Andreas is shown diagonally, moving from the Salton Sea. Note also the great number of recognized faults that branch off the San Andreas.



Figure 19.3.4. Major fault map of Southern California, from the USGS Interactive Map. "Fault map" by USGS is in the public domain. Access a detailed description.

Now in Figure 19.3.5, we take that same fault base map and superimpose the population centers of Southern California. San Diego's cluster of faults is now obscured by the dense housing. The LA region, from Palos Verdes to the San Gabriel Hills, is dense sprawl sitting atop numerous faults.

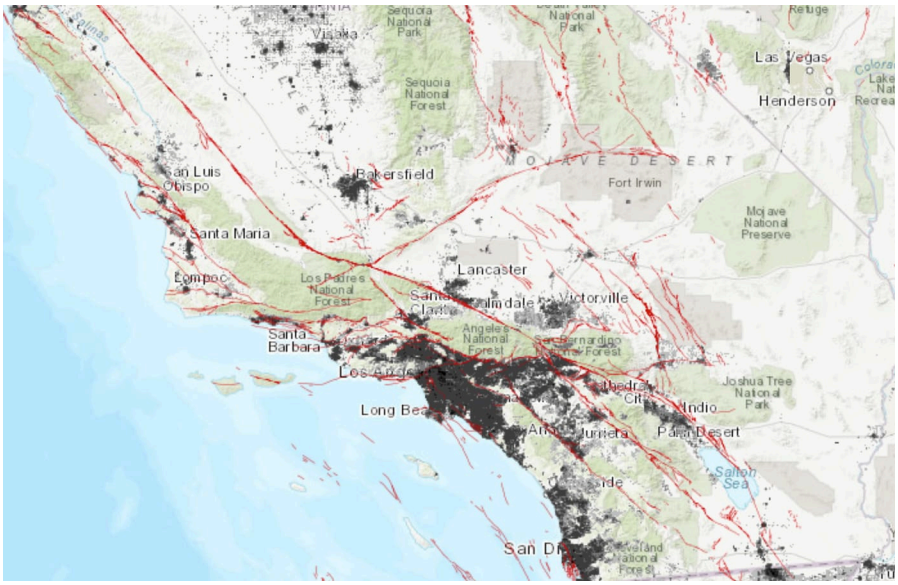


Figure 19.3.5. Major population concentrations superimposed on Southern California fault system. "Fault and population map" by USGS is in the public domain. Access a detailed description.

The Hidden Danger of Thrust Faults

Everyone has heard of the San Andreas fault, but how many are familiar with the Whittier Narrows fault? Charismatic, brand-name strike-slip faults get a lot of media attention. But we should also be concerned about lesser-known reverse faults that branch off from the major tectonic ruptures.

Many faults in California are thrust faults, a type of reverse fault where the angle of the fault plane is very low. Because of this low angle, the surface trace may be covered by the fault movement itself, creating a blind thrust fault. These are illustrated in Figures 19.3.6 and Figure 19.3.7.

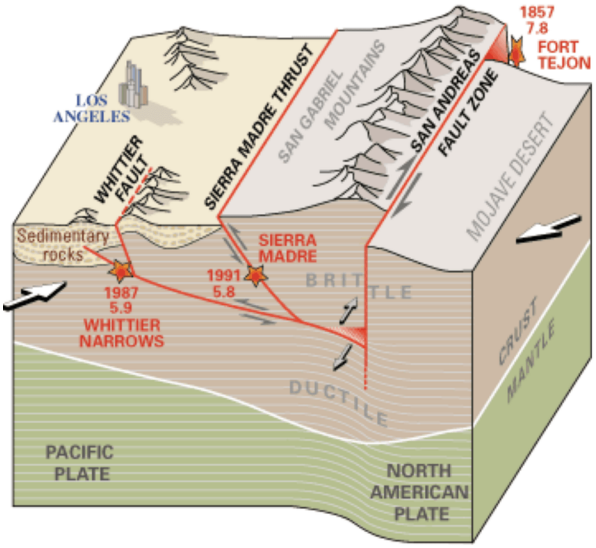


Figure 19.3.6. A diagram illustrating the San Andreas and associated thrust faults. "San Andreas thrust faults 1" by USGS is in the public domain. Access a detailed description.

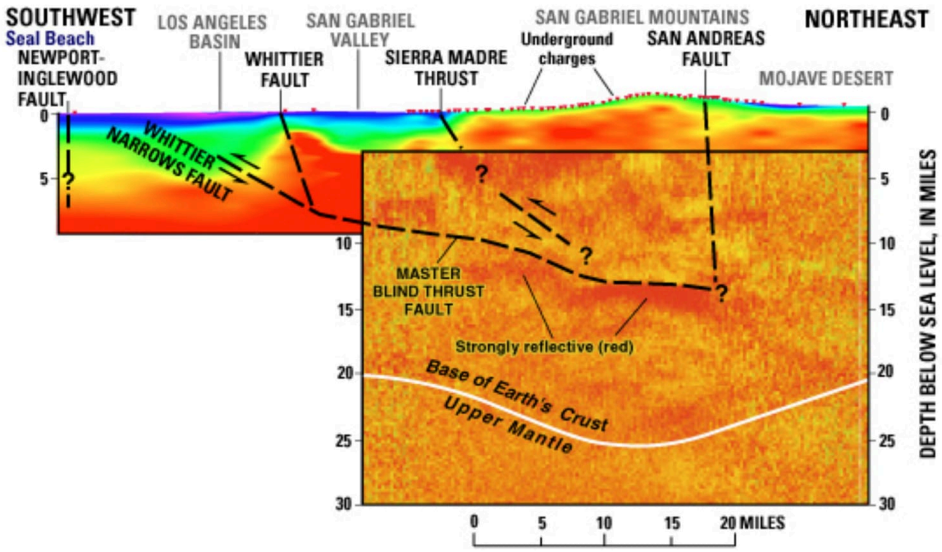


Figure 19.3.7 A scale illustration of the San Andreas fault and associated thrust faults. "San Andreas thrust faults 2" by USGS is in the public domain. Access a detailed description.

Though thrust faults and blind thrust faults are less well known, that does not mean they are less dangerous. In fact, the proximity of such faults to large population centers means that they are more likely to cause damage locally than distant celebrity faults such as the San Andreas. Yet California legislation–most notably the Alquist-Priolo Act–does little to address their dangers.

Failures of the Alquist-Priolo Act

Pop quiz: Does the State of California legally protect residents from buying or living in buildings constructed in seismically dangerous areas?

If you answered, “Yes,” you might want to recalibrate your assumptions about whose interests governments serve. And you might want to read this section carefully.

The M_w6.6 1971 San Fernando earthquake (sometimes referred to as the Sylmar quake) killed 64 people and caused half a billion dollars in damage, including to hospitals and schools. It was the first substantial postwar quake in the modern greater Los Angeles area, where reckless and unplanned expansion grew virulently in the early twentieth century. The 1971 quake became a stress test of modern Southern California infrastructure–fragile highway overpasses, water mains, unstable dams–and the vulnerabilities exposed by this temblor were unsettling.

In response to the 1971 quake, the following year the state of California passed the Alquist-Priolo Earthquake Fault Zoning Act. (The official name has been unnecessarily rebranded numerous times since, so for clarity we will refer to this as the “AP Act.”). There is precedent to California enacting legislation only after a major disaster, rather than preventatively; the 1933 Long Beach quake severely damaged over two hundred schools (see Figure 19.3.8).



Figure 19.3.8: The collapsed John Muir School in Long Beach, destroyed in the 1933 Long Beach Quake. "1933 Long Beach" by W.L. Huber, USGS is in the public domain. Access a detailed description.

The fortuitous thing about the 1933 quake was its timing: it occurred at Beer O'Clock (late on a Friday afternoon) but had it happened just a few hours earlier, then possibly thousands of school children would have died or been injured in the collapsed schools. The 1933 quake led to the swift passage of the Field Act, which proscribed school building construction with unreinforced masonry.

The 1972 AP Act went much further than the 1933 Field Act. The AP Act mandated the creation of official regulatory maps detailing the locations of active faults, with restrictions on building within recognized Earthquake Fault Zones (EFZs). In theory, if real estate developers wanted to build within these restricted areas, they would have to establish the location of the fault (as certified by a licensed Professional Geologist, or P.G.) and allow for a setback, a safety buffer.

The AP Act focuses on ground surface rupture, and this fundamental limitation is the biggest failure of the AP Act. Big quakes don't always rupture the ground. The AP does not consider the degree of ground shaking in its mapping, though one would naively imagine this would be the most important thing to consider. Surface rupture, if it occurs at all, can be a very different thing than shaking intensity.

The AP Act also involves proximity to known faults. Common sense would suggest the benefit of being as far away as possible from active faults. However, the AP language reads: "the area within fifty (50) feet of such faults shall be presumed to be underlain by active branches of the fault unless proven otherwise."

This means that local jurisdictions can mandate as little as a 50 foot setback from an identified surface rupture and comply with the AP. But a major fault system such as the San Andreas is more than just a single crack exposed at the surface, but rather a network of multiple fractures across wide swaths. The AP Act is based on convenient magical thinking that the surface trace is all that matters.

The AP Act is concerned with "active" faults, which it defines as having movement during the Holocene (11.7 ka to today). However, this cutoff is completely arbitrary, ignores the potential of new faults emerging, and assumes that past Holocene activity will be indicative of future movement. Nothing at all prevents an older fracture from reactivating under changing stress conditions.

Because the AP Act involves officially recognized faults, it may ignore unknown or poorly-described faults. For example, the 1994 Northridge Quake (M_w6.7, 57 people killed, with many casualties occurring in soft-first story apartments) did significant damage in the San Fernando Valley from the movement of a poorly-understood blind thrust fault (see Figure 19.3.9). The AP Act's focus on surface rupture does not provide any regulatory protections for residents facing such calamities.



Figure 19.3.9: Damage to a highway from the 1994 Northridge Quake. "1994 Northridge" by USGS is in the public domain. Access a detailed description.

The AP Act focuses on surface exposures of faults, but quakes don't happen right at the surface, but rather many kilometers deep. Often faults curve in the crust, so that the surface exposure is not where the majority of the fault plane resides. Moreover, not every quake even disrupts the surface and offsets the ground. The AP Act's limited focus on the surface is a conceptual blindness that leaves Californians without the protection that a full consideration of the science would bring.

Even more unsettling, the regulations of the AP Act include an incredible exemption: *single-family homes*. The type of home in which most everyone lives is not covered by the AP Act. The original AP Act language did cover single-family homes; however, within two years, an exemption was created at the behest of real estate lobbyists. Potential buyers of homes within an AP Earthquake Fault Zone will be notified of this status, but in the context of the blizzard of disclosures one signs when buying a home, this will hardly raise an eyebrow for eager purchasers who may naively assume that "the government" would not let them buy into a hazardous place.

In this multitude of ways, the California legislation intended to protect residents fails its job. Most Californians live in single-family homes, which aren't restricted by the AP Act. Most Californians live uncomfortably near fault traces, and they are allowed to live and work in buildings that are close to known fault traces. Those are just the faults we know about, and history suggests that our knowledge is incomplete. The AP Act is limited to known faults with surface traces, rather than more salient question of unseen, lurking seismic dangers.

In answer to the pop quiz that began this section, the state of California fails in its responsibility to protect residents from living in dangerous buildings in dangerous areas. Though many resident assume that "the government" will protect them, the AP Act is inadequate for a state with such seismic hazards. Some local jurisdictions have more restrictive laws, but having a piecemeal approach to public safety guarantees that many people will be left less protected than they could be.

In a state as riven with tectonic dangers as California, if we were to adopt reasonable safety measures, such as expanding the no-build zone to several kilometers on either side of fault traces, and taking into consideration not just active fault traces but also suspected faults and also low-angle thrust faults, then there would be very few places where Californians could build at all. Given California's chronic affordable housing shortage, it seems unlikely that this situation will change any time soon.

Query 19.3.1

This interactive element is not available in this format. Visit the link or scan the QR code to access it online.

View this Interactive Content online



Query 19.3.1

This interactive element is not available in this format. Visit the link or scan the QR code to access it online.

View this Interactive Content online



Query 19.3.1

This interactive element is not available in this format. Visit the link or scan the QR code to access it online.

View this Interactive Content online



References

1. Rodriquez-Delgao, C. (2020, July 16). California has some of the worst air quality in the country. The problem is rooted in the San Joaquin Valley. Retrieved June 18, 2024, from https://www.pbs.org/newshour/nation/california-has-some-of-the-worst-air-quality-in-the-country-the-problem-is-rooted-in-the-san-joaquin-valley#:~:text=Today%2C%20the%20direct%20and%20second,pollution%20in%20the%20Fresno%20area
2. Bryant, W. A. (2010). History of the Alquist-Priolo Earthquake Fault Zoning Act, California, USA. Environmental & Engineering Geoscience, XVI(1). https://doi.org/10.2113/gseegeosci.16.1.7

This page titled 19.3: The Hazard of Place is shared under a CC BY-NC 4.0 license and was authored, remixed, and/or curated by Emily Wright.

19.4: Liquefaction and the Role of Soil Type

Liquefaction

A major hazard in earthquakes is a phenomenon termed liquefaction. Liquefaction involves the intersection of three factors: loose soil, wet soil (near water table), and seismic shaking. When unconsolidated saturated soil is subjected to earthquake movement, an unfortunate behavior is that the water creates pressure between loose soil particles, which then "float" in such a way that the ground loses its ability to hold heavy objects, which then proceed to sink into the newly-mobile ground.

Basically, earthquakes take seemingly firm soil and temporarily turn it into a mud slurpee.

If people built only on bedrock, then liquefaction would not be a concern. However, many inhabited areas are constructed on flat land near water, which is the perfect recipe for liquefaction. The California Geological Survey maintains a digital database of some areas of California susceptible to liquefaction.

Even if the ground is not saturated with water, and thus not likely to experience liquefaction, earthquake shaking can still produce a number of undesired effects. All else being equal, bedrock–actual consolidated rock–behaves the best in earthquakes. The accelerations of the quake transmit through bedrock to buildings, but at least the bedrock jolts and then returns to normal. Bedrock does not keep moving and settling long after the quake has passed.

If the soil is natural but unconsolidated–say, soil deposited in a valley or by an alluvial fan–then the soil will boost the apparent earthquake shaking by continuing to move after the quake has passed. Having your house on consolidated soil will make the earthquake appear bigger and last longer than the quake actually is.

Another possibility is soil that is artificial, and this is by far the worst. Natural soil at least has been around for a while and experienced many quakes to help it settle, but artificial fill may be only a few decades old. When earthquake waves hit this very poor soil, substantial settling may occur, and the shaking of the quake appears augmented compared to what it would be on bedrock.

Lessons from Loma Prieta

In the 1989 Loma Prieta earthquake, one of the most heavily damaged areas was the region near Oakland and Alameda, including the Bay Bridge, which partially collapsed, and the I-880 freeway, which completely collapsed, killing 42 people. Despite the lives lost, there was one valuable lesson: the different soils there were recorded by seismographs and provide a textbook example of the role of soil in earthquake damage.

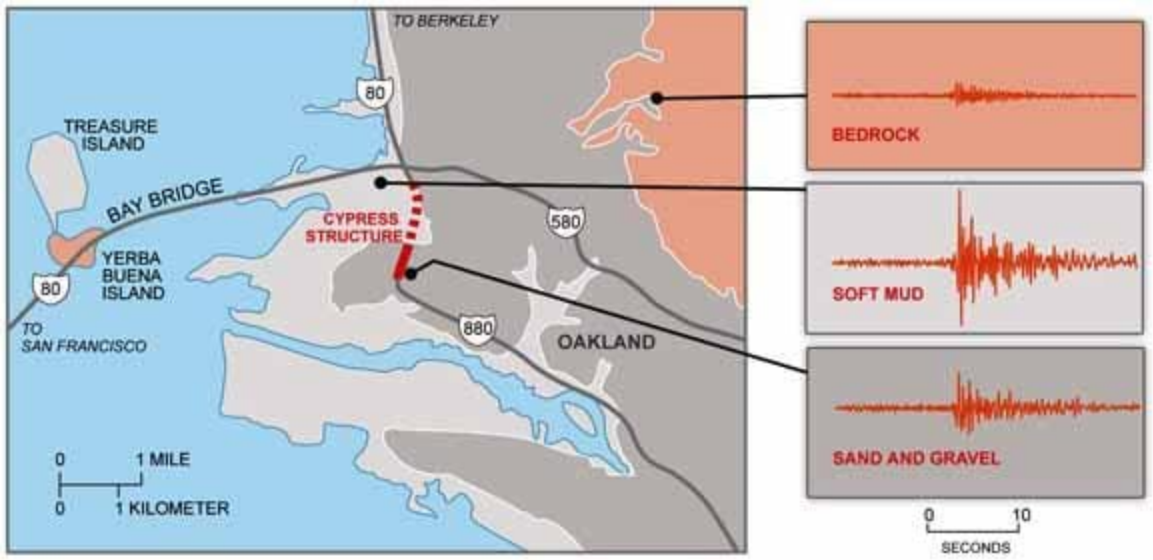


Figure 19.4.1: Shaking in the Oakland-Alameda area in the 1989 Loma Prieta quake, by soil type. "1989 Loma Prieta" by USGS is in the public domain. Access a detailed description.

In Figure 19.4.1:, we find three distinct soil types: bedrock, sand and gravel, and soft mud. The sand and gravel is largely natural, while much of the soft mud is, in fact, artificial fill. The associate seismograms show startling differences between regions only a few kilometers from each other.

If one were on the Oakland hills bedrock, the 1989 Loma Prieta quake would have felt much less than other parts of the Bay Area. In fact, many people doing activities such as driving were unaware a quake had even happened.

If one were on the sand and gravel areas, the shaking was much more intense, and seemed to last longer than the 15 seconds of ground movement the bedrock areas experienced (note how the seismogram from bedrock quickly returns to normal compared to sand and gravel).

Worse still, in the soft mud (artificial) areas, the seismographic record shows even greater intensity and duration. The differences in the apparent shaking are so stark it is as if three completely different earthquakes happened.

This page titled 19.4: Liquefaction and the Role of Soil Type is shared under a CC BY-NC 4.0 license and was authored, remixed, and/or curated by Emily Wright.

19.5: What's Coming

The Risk

How bad is California's earthquake risk, really? Figure 19.5.1: should offer some insight:

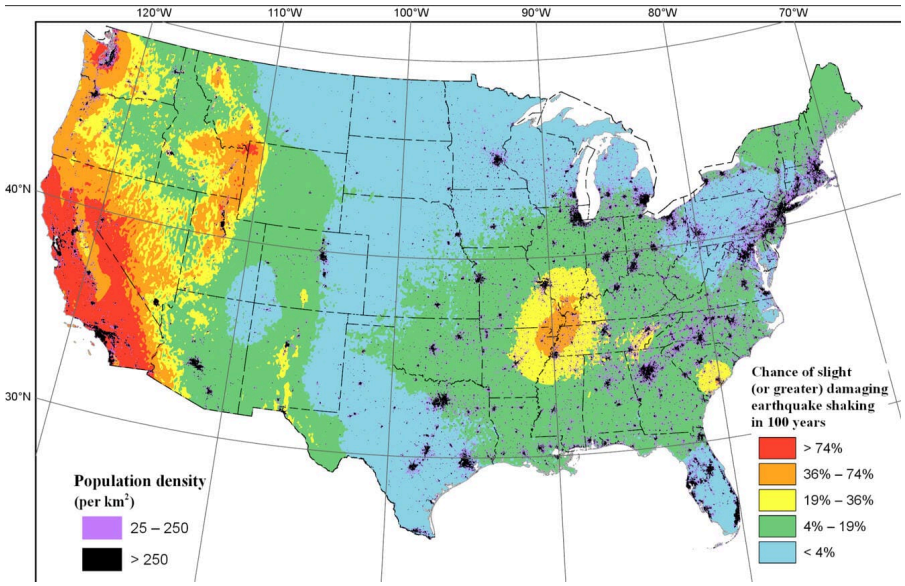


Figure 19.5.1: A map showing national earthquake hazards. "National EQ hazard" by USGS is in the public domain. Access a detailed description.

As this USGS map shows, the nation's earthquake risk is heavily concentrated in California. Alaska also has a similar risk to California, but far fewer people. Though the region is far from plate boundaries, eastern Missouri experienced major quakes in the early 1800s.

We cannot say with any specificity when a particular quake will occur, where it will occur, or how big it will be. However, we can statistically show that there are regions where, on a long time scale, big earthquakes are inevitable. And given the history revealed by trench studies and calculations of recurrence intervals, as well as estimations of stress patterns, we can produce a reasonable idea of which major faults are most likley to rupture, as shown in Figure 19.5.2. This is illustrated in Figure 19.4.2, which displays the percent probability of six major faults in the Bay Area producing a M_w6.7 earthquake before 2043.

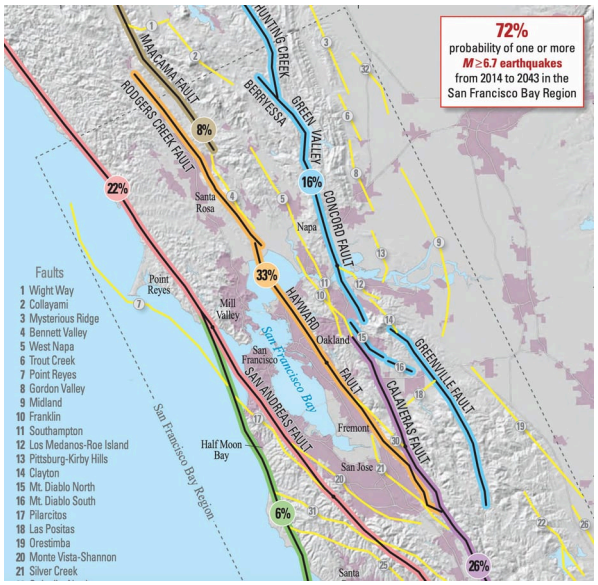


Figure 19.5.2: A map showing Bay Area faults and associated major quake probabilities. "SF Bay fault probabilities" by USGS is in the public domain. Access a detailed description.

While states such as Alaska, Hawaii, and Missouri experience some risk from quakes, only in California do we have the intersection of so many people and so much seismic risk. A major quake on the San Andreas in the Los Angeles or San Francisco Bay region would be catastrophic, potentially killing thousands and disrupting infrastructure of years or decades.

However, there is a another terrifying scenario that surpasses the danger even of quakes generated by the San Andreas fault system. This scenario led one *New Yorker* writer to term it The Really Big One. And the most frightening thing about it is that it actually occurred three centuries ago.

Query 19.5.1

This interactive element is not available in this format. Visit the link or scan the QR code to access it online.

View this Interactive Content online

This page titled 19.5: What's Coming is shared under a CC BY-NC 4.0 license and was authored, remixed, and/or curated by Emily Wright.

19.6: Beyond the San Andreas - Earthquakes of the North Coast

Jan 26, 1700

The evening of Jan 26 felt like any other evening as the Yurok people settled down for the night in what is now northern California, but in the darkness of the night, they were roused with violent shaking. Living in earthquake country, the Yurok were familiar with the sensation of the earth shifting beneath them, but this was different; it was much stronger and lasted much longer. “The earth would quake and quake again and quake again,” they said in the stories they passed on to their grandchildren. The people went to the top of a hill to dance a dance they believed would send the earthquake away. Though their dancing did not end the earthquake, the tradition did save the dancers from what came next. Below, waters rushed in, flooding the coast and devastating the village they’d left behind. It was the strongest earthquake any of these people had felt in their lives or would ever feel again, but there were stories of this kind of earthquake and tsunami from many generations past. The Tolowa people, just north of the Yurok, tell a story of a boy and a girl who were the only ones to make it to high ground. On their return to their coastal village, they found not a single living person.

People all along the coast of the Pacific Northwest, from the Yurok and Tolowa to the people of what is now British Columbia, Canada, told stories of how they survived a megathrust earthquake and tsunami (see Earthquake Mechanics). However, in the next few centuries, many of these oral histories were lost, and the rest nearly forgotten until they were recovered in the 1980s.

Oral History as Geological Evidence

By the 1980s, geologists were well aware that the Pacific Northwest was home to a subduction zone (Figure 19.6.1), but they were somewhat perplexed by the lack of historical earthquakes. Other subduction zones, like those of Japan and Sumatra had a well-documented history of earthquakes. The two largest earthquakes in history, in Chile in 1960 and Alaska in 1964 respectively, had occurred on subduction zones, yet the Cacadia subduction zone remained quiet. Some geologists figured that the Juan de Fuca plate must slide smoothly past the overriding North American plate without locking, much like the creeping sections of the San Andreas Fault in the San Francisco Bay Area, but when the government wanted to put new nuclear power plants in Oregon and Washington, the geologists consulted decided it would be wise to take a deeper look into the earthquake hazards of the Cascadia subduction zone. Perhaps Cascadia was not aseismically creeping; perhaps instead, it had been locked for all of recorded history. If that were true, it would mean that Cascadia was capable of very large earthquakes. The first step to find this out was to ask the people who have been here the longest. An interdisciplinary effort, led by geologist Ruth Ludwin, turned up many oral histories that told of great earthquakes accompanied by flooding waters. The geologists decided to treat the stories they uncovered, not as myths, but as historical evidence.



Figure 19.6.1: Map of the Cascadia subduction zone. "Cascadia Map" by the Federal Emergency Management Agency is in the public domain. Access a detailed description.

The Three Layer Cake

Though the oral histories provided compelling evidence, geologists wanted other evidence to support their case as well. One form of evidence is found in the stratigraphic record found in tidal marshes. A distinctive sequence that geologists affectionately refer to as the “three layer cake” is a clear indicator of an earthquake and tsunami. When a subduction zone is locked, strain accumulates, pushing the coastal land upwards. Muddy tidal flats become marshes as they are lifted higher in the intertidal zone. The soil or marsh peat developed in this ecosystem becomes the first layer of the “cake” (Figure 19.6.2).

During an earthquake, the strain is released and the land drops suddenly back down to the lower part of the intertidal zone, where the marsh plants won’t survive. Within minutes, the first tsunami wave rolls in, followed by others for several hours. The tsunami waves bring in sand from nearby beaches and dunes, depositing the second layer, as shown in the second panel of figure 19.6.2 . Even after the tsunami has retreated, the land is still lower than it was before the earthquake. The marsh has now returned to mud flat, and the third layer, a layer of tidal silt (mud), finishes out the three layer sequence, as shown in the final panel of figure 19.6.2. Gradually, as the land lifts again, the marsh returns and the sequence repeats.

The “three layer cake” has been found throughout the Pacific Northwest coast, including several sites in northern California, and has also been found at other subduction zones around the world. In some places along the Cascadia subduction zone, the three layer sequence repeats itself multiple times, suggesting that the 1700 earthquake was only the most recent of many such events.

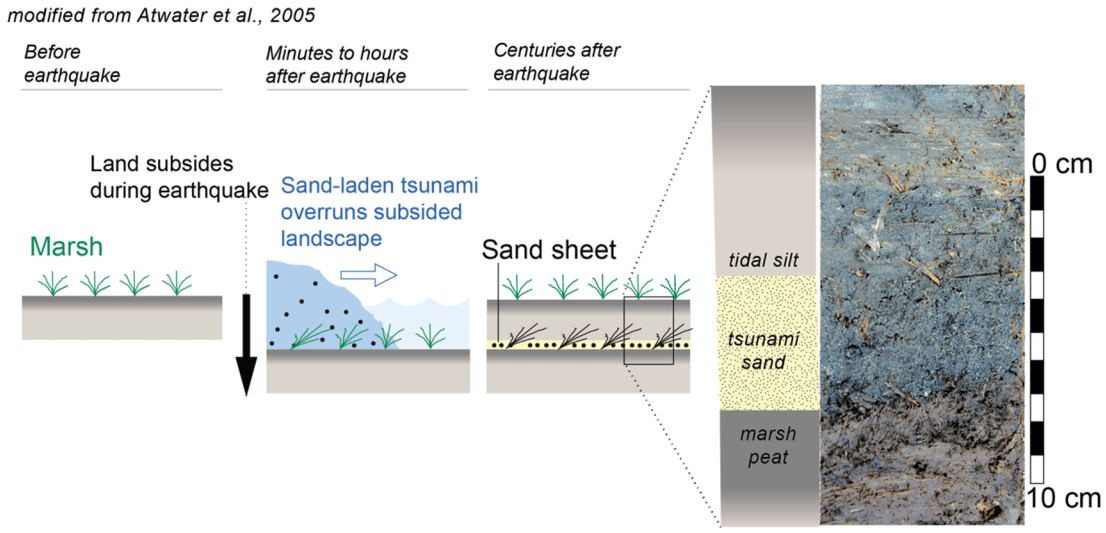


Figure 19.6.2: Diagram showing the three layer sequence that indicates that an earthquake and tsunami has occurred. "Diagram showing land subsidence and sand deposit following tsunami" by Coastal and Marine Hazards and Resources Program is in the public domain / A derivative from the original work by Atwater et. al, 2005. Access a detailed description.

Ghost Forests

When a forest suddenly drops below the high-tide line and becomes a salt marsh, the trees living there can no longer survive. Eventually only the stumps remain, in some places fully buried in the salt marsh and in others exposed at low tide (Figure 19.6.3). These are called ghost forests and they are another piece of evidence in the Cascadia earthquake story.



Figure 19.6.3: Neskowin Ghost Forest in Oregon. "Neskowin Ghost Forest" by RocketSams is licensed under CC BY-SA 4.0.

The Orphan Tsunami

Radiocarbon dating of the ghost forests helped geologists get an idea of when the most recent earthquake along the Cascadia Subduction Zone occurred, but radiocarbon dating is not precise enough to narrow down to a particular year or even a particular decade, and that posed a potential problem because geologist were not yet sure whether the oral histories and geologic evidence came from one single huge earthquake or multiple smaller earthquakes within a few years of one another. Understanding that, of course, is key to understanding the potential future hazard; when Cascadia goes again, will it be in one big one, or two smaller

ones? To help solve this mystery, geologists once again needed some interdisciplinary help; this time from Japanese earthquake historians.

In fact, the Japanese historians were facing a mystery of their own. Japan has a well documented history of both earthquakes and tsunamis. Even the accepted international term, tsunami, is Japanese. Usually, a historical record of a tsunami is accompanied by a record of an earthquake preceding it, but on Jan 27 and 28, 1700, a series of tsunamis hit harbors along the Japanese coast with no known earthquake preceding it. It was called an “orphan tsunami” because it had no parent earthquake.

While even the largest earthquakes are not usually felt outside the region where they occur, tsunamis can be felt all around the world (or all around one ocean basin anyway). For example, the 2011 Tohoku, Japan earthquake produced a tsunami that reached California, though it was relatively small by the time it got here. In 1700, this scenario played in reverse, with the earthquake occurring in North America and the tsunami reaching Japan.

By carefully piecing together many historical records, the historians and geologists together were able to put together a picture of what the 1700 tsunami looked like when it arrived in Japan. The records precisely matched what would be expected for a tsunami generated in Cascadia, and the timeframe fit within the range expected based on the radiocarbon dating. But the Japanese records didn’t just confirm what geologists already knew, they added a new level of detail. By calculating the time it would take the tsunami to arrive in Japan, the team could now establish an exact time for the earthquake, which we now know occurred on Jan 26 at 9:00 pm. They could also determine the size of earthquake that would be required to produce the tsunami that reached Japan. The scientists determined that the earthquake must have been one single, large earthquake that ruptured the entire length of the Cascadia Subduction Zone from Cape Mendocino to British Columbia, causing an M9 earthquake.

Video 19.6.1: Tsunami Forecast Model Animation: Cascadia 1700

This animation shows a model of how the 1700 Cascadia tsunami propagated across the Pacific Ocean and reached Japan. The video contains no audio. Access a detailed description.

This interactive element is not available in this format. Visit the link or scan the QR code to access it online.

View this YouTube Video online

Query 19.6.1

This interactive element is not available in this format. Visit the link or scan the QR code to access it online.

View this Interactive Content online

The Future of Cascadia Earthquakes

The 1700 Cascadia earthquake was the most recent Cascadia subduction zone earthquake and ruptured the entire length of the subduction zone from northern California to British Columbia. But the 1700 earthquake was just the most recent of many earthquakes. Though the older earthquakes don’t have detailed tsunami records from japan, they are preserved in the geologic record. In the past 5000 years, there have been 10 subduction zone earthquakes on the northern section of the Cascadia subduction zone. Geologists estimate the average recurrence interval for full rupture of the 1,100 km (700 mile) subduction zone is 500 to 530 years. If recurrence intervals could be relied on like bus schedules, we would expect an earthquake of near M9 and tsunami to hit the North American coast sometime between 2200 and 2230; plenty of time still to prepare. But earthquakes don’t operate on a schedule. Some of the individual intervals between earthquakes have been as short as a few decades, while others have been as long as a millennium. The next megathrust earthquake could happen tomorrow or it might not happen until

the Space Needle is an archaeological relic.

The issue is further complicated by the fact that the Cascadia subduction zone doesn't always rupture along the full length. Geologists have found that there are three common modes of rupture: (1) full-ruptures along the entire length or nearly the entire length of the subduction zone, producing an earthquake of around M9, as happened in 1700; (2) ruptures of only the southern half or so of the subduction zone, producing an earthquake in the M8 range; and (3) ruptures of only the southern margin (the part in California), producing smaller earthquakes and smaller tsunamis. The average recurrence interval for the third, smallest type of earthquake is estimated at only 240 years, making northern California "overdue" for a subduction zone earthquake.

The Worst Natural Disaster in U.S. History?

If a full rupture were to occur tomorrow, the earthquake would be felt throughout the Pacific Northwest and shaking would last for four to six minutes. In some places the shaking would be strong enough that it would be difficult to stand. During the earthquake the coast would subside by about 2 meters (6 feet), resulting in a sudden increase in relative sea level. In 15 to 30 minutes after the shaking, the first tsunami would arrive. The height of the tsunami will vary along the coast depending on local bathymetry and topography. It may be as high as 9 to 12 meters (30 to 40 feet) in some places. Flooding and dangerous currents may last for days. Additional hazards, like liquefaction, landslides, fires, dam failures, and hazardous material spills are also likely.

Millions of people would be affected as well as property, infrastructure, and the environment. According to a scenario put together by Cascadia Region Earthquake Workgroup (CREW), the number of deaths could exceed 10,000, more than 30,000 people could be injured, and economic losses could approximate $70 billion for Washington, Oregon, and California alone.

Table 19.6.1: Comparison of select natural disasters and the CREW Cascadia disaster scenario

Name	Fatalities	Year	Type	Location	Notes
Sumatra, Indonesia	227,899	2004	Earthquake and tsunami	Indian Ocean	Deadliest earthquake in 21st century
Tohoku, Japan	19,759	2011	Earthquake and tsunami	Japan	
CREW Cascadia Scenario	10,000	Future Scenario	Earthquake and tsunami	U.S., Canada	
1900 Galveston Hurricane	6,000-12,000	1900	Hurricane	Texas	Deadliest natural disaster in U.S. history
1906 San Francisco Earthquake	3,000+	1906	Earthquake	California	Deadliest earthquake in U.S. history

Of course, it is important to remember that the scenario described above is the worst-case full rupture scenario, which is also the least likely. Although this may not be as reassuring to northern Californians as might be to Washingtonians, it is also important to remember that a smaller rupture produces a smaller earthquake and also a smaller tsunami. Additionally, in the smaller scenario, California cities like Eureka, Arcata and Crescent City will not have to compete with the likes of Portland and Seattle when it comes to disaster relief resources.

Box 19.6.1: Tsunami Hazard Maps Change With Updated Science

As scientists gain a better understanding of past Cascadia earthquakes and tsunamis, they are better able to forecast a future tsunami scenario. In some cases this has required updating tsunami hazard zones to reflect current scientific understanding. In the activity below, you can compare two tsunami hazard maps for Crescent City California. The 2021 hazard map is an update to the prior map, created in 2010. Tsunami inundation is now expected to be more extensive in Crescent City than previously thought. For example, Sutter Coast Hospital was previously located about a half mile from the designated hazard zone, but now sits right at the edge.

Query Box 19.6.1

This interactive element is not available in this format. Visit the link or scan the QR code to access it online.

View this Interactive Content online

Access accessibility guidance for this activity.

Although there is no subduction zone to produce a local tsunami off the coast of southern and central California, a tsunami generated by the Cascadia Subduction Zone or the Aleutian Subduction Zone in Alaska could inundate these coastal regions as well. To view maps of tsunami hazard zones along the entire California Coast see California Geological Survey Information Warehouse: Tsunami Hazard Area Map.

Video 19.6.2: What's the ONE THING You Can Do To Survive A Tsunami?

If you'd like to recap what you've learned in this section and learn more about what is being done to prepare, as well as what you can do to prepare if you live in or travel to the tsunami hazard zone, watch this PBS video.

This interactive element is not available in this format. Visit the link or scan the QR code to access it online.

View this YouTube Video online

The Mendocino Triple Junction: An Earthquake Buffet

While a Cascadia Subduction Zone earthquake is perhaps the most ominous of earthquake scenarios for the north coast of California, it is not the only one. There has not been a subduction zone earthquake in over 300 years, but talk to any resident of Humboldt County, and they're sure to have an earthquake story or two to tell you. Most of these stories don't involve significant damage (though a few do), but earthquakes large enough to be felt are a pretty regular part of life near the Mendocino triple junction (Figure 19.6.4). A triple junction is a place where three plate boundaries meet, and each of these plate boundaries, of course, has the potential to cause earthquakes. The San Andreas fault system and the Cascadia subduction zone, make up two of the three arms of the triple junction and are discussed earlier in this section and elsewhere in this chapter. But it is the third arm of triple junction that most frequently awakens the people of Eureka in the night or throws groceries from shelves in Ferndale; that is the Mendocino fracture zone, the transform plate boundary between the two plates of oceanic lithosphere off the coast of California.

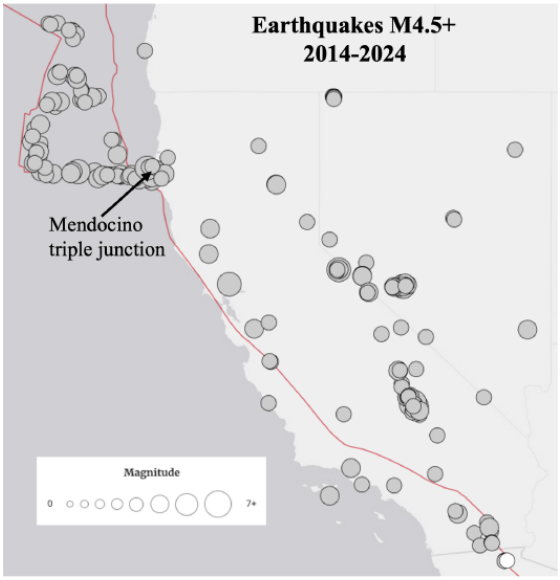


Figure 19.6.4: Earthquakes of Magnitude 4.5 or greater between July 1, 2014 and July 1, 2024 in and near California. "California M4.5 Earthquakes" by Emily Wright was made using the Earthquake Catalog by the USGS, which is in the public domain. An is licensed under CC BY-NC 4.0. Access a detailed description.

In the chapter Cascade Range and Modoc Plateau and elsewhere in this text, we have generally referred to the last remnants of the Farallon plate collectively as the Juan de Fuca plate. This is helpful when discussing broad concepts because the three plates generally move together. Some geologists, however, consider the remnant Farallon plate as three separate plates, the Explorer plate offshore of Vancouver Island, the central Juan de Fuca Plate, and the Gorda plate, a small plate off the coast of northern California (Figure 19.6.5). The Mendocino fracture zone, therefore, is the boundary between the Gorda plate and the Pacific plate (labeled "MFS" for Mendocino Fracture System in figure 19.6.5.

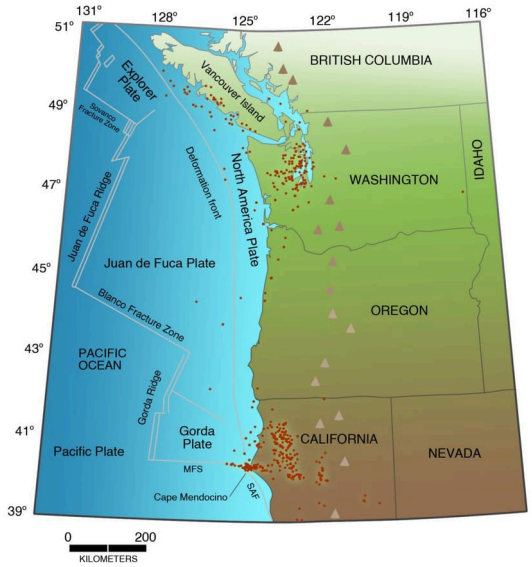


Figure 19.6.5: Plate tectonic map of the Pacific Northwest. MFS, Mendocino Fracture System; SAF, San Andreas Fault; Triangles: Cascade volcanoes; Red dots: earthquakes deeper than 25 km (16 miles). "Earthquakes in the Juan de Fuca Plate" by Robert S. Yeats is licensed under CC BY-NC 4.0. Access a detailed description.

Besides rupture of the three plate boundaries themselves, the triple junction region is also susceptible to intraplate earthquakes within the Gorda plate and the North American plate. There are many crustal faults in the northern coast ranges, which pose challenges to development in the region on account of the Alquist Priolo (AP) Act (see 19.2: The hazard of place). Earthquakes along these faults, however, are relatively rare compared with intraplate earthquakes in the Gorda plate. The Gorda plate could really rather be called a zone of deformation, as it behaves far less like a rigid plate than the main Juan de Fuca plate to the north. As the Pacific Plate presses northward on the Juan de Fuca plate, the little Gorda plate is caught and squeezed between the

two, producing many small faults, and many earthquakes, within the plate. Many of the intraplate earthquakes in the Gorda plate are shallow, offshore earthquakes, but others are deep earthquakes with inland epicenters. The later are generated by intraplate motions in the subducting Gorda slab beneath the North American plate. These are the earthquakes shown in figure 19.6.5.

There have been a few larger earthquakes in this region. The Gorda Plate west of Arcata, California, sustained an earthquake of M7.3-7.6 on January 31, 1922, that was felt in Oregon and Nevada, and as far south as San Jose, California. Another earthquake of M_W 6.9-7.4 thirty miles west of Trinidad, California, on November 8, 1980, destroyed a bridge, liquefied the sand bar at Big Lagoon, and caused six injuries and $1.75 million in damage. Then, on April 25 and 26, 1992, a sequence of earthquakes, beginning with an M_W7.2 mainshock struck Cape Mendocino, injuring 356 people and destroying or damaging 1,108 structures at a cost of $61 million dollars.

Though the Mendocino fracture zone and the Gorda plate do not have the potential to produce the M8 or M9 earthquake that this region anticipates from the Cascadia subduction zone, each smaller quake can serve as a reminder of what could be yet to come. Each time the earth shakes and one takes cover under a desk or buried beneath the pillows in bed, one must wonder, “is this the big one? Will this be the time that the shaking does not stop, but ‘quakes and quakes again and quakes again’?”

Query 19.6.2

This interactive element is not available in this format. Visit the link or scan the QR code to access it online.

View this Interactive Content online

References

1. Atwater, B. F., Musumi-Rokkaku, S., Satake, K., Tsuji, Y., Ueda, K., & Yamaguchi, D. K. (2005). The orphan tsunami of 1700—Japanese clues to a parent earthquake in North America. *Professional Paper*, Article 1707. https://doi.org/10.3133/pp1707
2. *Brochure_crescent_city_2021.pdf*. (n.d.). Retrieved July 2, 2024, from https://rctwg.humboldt.edu/sites/default/files/brochure_crescent_city_2021.pdf
3. *Cape Mendocino Earthquakes 1992 | Redwood Coast Tsunami Work Group*. (n.d.). Retrieved July 3, 2024, from https://rctwg.humboldt.edu/capemendo92
4. Finkbeiner, A. (2015, September 14). The Great Quake and the Great Drowning. *Hakai Magazine*. https://hakaimagazine.com/features/great-quake-and-great-drowning/
5. Goldfinger, C., Nelson, C. H., Morey, A. E., Johnson, J. E., Patton, J. R., Karabanov, E. B., Gutierrez-Pastor, J., Eriksson, A. T., Gracia, E., Dunhill, G., Enkin, R. J., Dallimore, A., & Vallier, T. (2012). Turbidite event history—Methods and implications for Holocene paleoseismicity of the Cascadia subduction zone. In *Professional Paper* (1661-F). U.S. Geological Survey. https://doi.org/10.3133/pp1661F
6. List of disasters in the United States by death toll. (2024). In *Wikipedia*. https://en.Wikipedia.org/w/index.php?title=List_of_disasters_in_the_United_States_by_death_toll&oldid=1227232457
7. Lists of 21st-century earthquakes. (2024). In *Wikipedia*. https://en.Wikipedia.org/w/index.php?title=Lists_of_21st-century_earthquakes&oldid=1229419266
8. *Tsunami_Preparedness_Crescent_City.pdf*. (n.d.). Retrieved July 2, 2024, from https://www.crescentcity.org/media/Emergency%20Preparedness/Tsunami_Preparedness_Crescent_City.pdf
9. Walton, M. A. L., Staisch, L. M., Dura, T., Pearl, J. K., Sherrod, B., Gomberg, J., Engelhart, S., Tréhu, A., Watt, J., Perkins, J., Witter, R. C., Bartlow, N., Goldfinger, C., Kelsey, H., Morey, A. E., Sahakian, V. J., Tobin, H., Wang, K., Wells, R., & Wirth, E. (2021a). Toward an Integrative Geological and Geophysical View of Cascadia Subduction Zone Earthquakes. *Annual Review of Earth and Planetary Sciences*, *49*(Volume 49,

2021), 367–398. https://doi.org/10.1146/annurev-earth-071620-065605
10. Walton, M. A. L., Staisch, L. M., Dura, T., Pearl, J. K., Sherrod, B., Gomberg, J., Engelhart, S., Tréhu, A., Watt, J., Perkins, J., Witter, R. C., Bartlow, N., Goldfinger, C., Kelsey, H., Morey, A. E., Sahakian, V. J., Tobin, H., Wang, K., Wells, R., & Wirth, E. (2021b). Toward an Integrative Geological and Geophysical View of Cascadia Subduction Zone Earthquakes. *Annual Review of Earth and Planetary Sciences*, *49*(Volume 49, 2021), 367–398. https://doi.org/10.1146/annurev-earth-071620-065605
11. Yeats, R. S. (2018). *Earthquakes in the Juan de Fuca Plate*. https://open.oregonstate.education/earthquakes/chapter/earthquakes-in-the-juan-de-fuca-plate/

This page titled 19.6: Beyond the San Andreas - Earthquakes of the North Coast is shared under a CC BY-NC 4.0 license and was authored, remixed, and/or curated by Emily Wright.

19.7: Preparing for the Worst

Is it Possible to Predict Earthquakes?

To quote the USGS, “No.”

Crazed Cats, Earthquake Weather, and Seismic Statistics

When most people think of earthquake prediction, they imagine something like the daily weather forecast they might listen to as they dress for work. Within a reasonable margin of error, meteorologists are able to predict if one is going to need an umbrella that particular day.

Earthquake prediction is not like that. In fact, it’s never going to be like that, though not for lack of trying. Over decades, seismologists have thoroughly researched ideas about ways that the earth might signal a major snap is about to happen. One idea is the measurement of radon gas; if there is a sudden release of radon gas, does this mean it is being liberated by small subterranean fractures forming just before an earthquake? Possibly, but not proven. If groundwater levels abruptly shift, does this mean a quake is imminent? Possibly, but not proven. If local electromagnetic fields fluctuate, could this be a sign? I think you can predict where this is going.

No single or combined set of these kinds of possible indicators has been found to be a reliable barometer for the imminent arrival of a quake. Sometimes radon increases in well water and then a quake happens; other times, no change in radon occurs and then a quake happens. It’s inconsistent.

One common misconception is that animal behavior can indicate a quake’s approach. The idea here is that common household pets possess sensory apparatus unknown to science capable of detecting hitherto undiscovered indicators of the impending arrival of an earthquake. In this way of thinking, when cats run around the house chasing invisible things, this indicates something seismic is about to happen.

The problem with this kind of thinking is that cats are always running around the house chasing invisible things. It’s only after a major quake that a pet owner might remember the feline behavior and think, “Yesterday Mr. Whiskers was acting strange. He must have known the quake was coming!” But there is no connection between a cat’s behavior and a quake; even if one particular cat played with unusual friskiness just before a quake, plenty of other cats slept in the sun, not to mention the legions of tired dogs snoring on the couches of owners who do not allow them on the furniture. None of these events are related to each other. This pareidolia can be considered an error of patternicity, which Michael Shermer defines as imagining a meaningful pattern in meaningless noise.

Another mistaken idea about earthquake prediction is something termed “earthquake weather.” This is usually defined as unseasonably warm and calm days. But there is no pattern of quakes happening more often on warm days, or cold days, or rainy days, or dry days. Understand that in California, most quakes originate many kilometers deep. Surface conditions affect only a few centimeters of the surface rocks and soils, so there is no mechanism for surface weather to have any effect on kilometers-deep rocks.

What we can do instead is talk about earthquake probabilities. For example, we can say that given studies of past quake events, we can make reasonable estimates of the likelihood of repeat (see Video 19.7.1 and Video 19.7.2 below).

Video 19.7.1: Earthquake Prediction 1/2

Watch this first video from the NSF/IRIS, which discusses earthquake prediction and probability.

This interactive element is not available in this format. Visit the link or scan the QR code to access it online.

View this YouTube Video online

Video 19.7.2: Earthquake Prediction 2/2

Watch this second video from the NSF/IRIS, which describes the dangers of rip currents and how to spot them.

This interactive element is not available in this format. Visit the link or scan the QR code to access it online.

View this YouTube Video online

In terms of earthquake probability, geologists have developed techniques in the specialty of paleoseismology that allow detailed dating of when past quakes have happened. When several identified quakes can be dated over a span of time, we can estimate a recurrence interval, or the statistical time between major quakes in a particular location.

One way this works is to dig a deep trench across an active fault, wait for the soil to dry, then scrape a smooth surface on the trench sides. Seismic disruptions in the soil may reveal themselves. Often these disruptions have organic material to be collected and carbon dated, providing detailed timing of the earthquakes. Such trench studies are very valuable for their high resolution of timing and solid evidence for recurrence intervals. One such paleoseismic investigation was led by the USGS's Jim Lienkaemper, who authored a series of papers using trench data collected at Tyson's Lagoon, in Fremont, about the Hayward fault's activity. These studies found evidence for 12 major quakes over the previous 1900 years, with a recurrence interval of 165 ± 65 years. That timing helped quantify our understanding that the Hayward fault is due for a major shake.

Lessons from the Parkfield Experiment

Imagine if one location in Central California had substantial earthquakes on a regular basis–say, every 22 years on average. What if scientists descended upon this place to install arrays of instruments to measure, poke, and prod the ground, its water, its gases, its electrical characteristics–in short, everything you could think of that might be an indicator of a coming quake?

What if you installed all this... and then the quake did not come?

This situation describes the Parkfield experiment, a project begun in the mid 1980s. Magnitude 6 quakes had occurred in this small town in 1857, 1881, 1922, 1934, and 1966. This averages to 22 years between quakes, with a range of 12-32 years apart. This regularity led researchers to conclude that if they installed a diverse array of sensors, they should be able to detect something changing before, during, and after the next quake.

It was calculated with 90-95% confidence that the next Parkfield quake should occur before 1993. But this first year of the Clinton presidency came and went–no quake. Nineteen ninety-four came and went, as did the next year, and the next. The expense of maintaining the equipment and labor to keep this project going became problematic. The dot.com boom and the inevitable dot.com bust happened–still no Parkfield quake. The terrorist attacks of 9/11 occurred and Parkfield remained frustratingly quiet. How long do you keep this going–and how can the project be abandoned, after all the expense of setting it up?

Finally, on 28 September 2004, Parkfield shook with a M_w6.0, as shown below in Video 19.7.3:

Video 19.7.3: Parkfield quake

A video capturing the long-anticipated 2004 Parkfield quake [no audio]. Access a detailed description.

This interactive element is not available in this format. Visit the link or scan the QR code to access it online.

View this YouTube Video online

Scientists eagerly retrieved and analyzed the data from the dense sensor arrays. Now we could see what was going on in the weeks, days, and hours before the quake happened. Was there any clear signal of the impending shake? Something that could then help us recognize similar changes in other faults and advance us closer to the goal of predicting quakes as we predict the weather? Did Parkfield reveal a method to predict earthquakes?

Parkfield did not. Nothing significantly unusual or anomalous was detected. The quake just happened, apparently without a detectable precursor.

The real lesson of the Parkfield experiment, then, is that we should not expect to ever be able to predict a quake the way we predict weather. We probably will never predict the date and time, location, and magnitude of an impending quake. While we cannot, of course, dismiss the possibility that future research may uncover some previously unimagined way to predict earthquakes, the main lesson of the Parkfield experiment is one of limitations.

But this doesn't mean we're helpless. We can determine meaningful earthquake probabilities. We can definitively say, for example, that tomorrow there will be several minor quakes in California, even if we don't know the exact place or magnitude. We can detail where earthquakes have happened in the past, and from that, know that these areas have a higher probability of being future locations. We can perform trench studies to determine recurrence intervals and from that understand future risks.

We can't say the time and date, place, and magnitude of a future quake. But we can give ranges of time in years, approximate areas, and based on past quakes, expected magnitudes. We can say, for example, that there is a high risk along the Hayward Fault, because we know the history of where and how frequently it has snapped. That's different from a weather forecast that tells you if you're going to need an umbrella on a particular day; however, using probabilities we can say that umbrellas are more likely to be needed in December than in July, and that information can be useful too.

Can We Have an Early Warning System?

Though California has long been an international hub of earthquake research, the state did not implement an earthquake early warning system until 2019, nearly three decades after the first early warning system was introduced in Mexico City. Early warning systems in countries like Mexico and Japan are designed to detect large, subduction-created quakes that occur far offshore. Quake waves travel on the order of the speed of sound, so detection of a distant quake could in these situations provide significant time between detection and alert and the arrival of the first seismic waves. This situation is similar to that of the Cascadia Subduction Zone, and indeed ShakeAlert, an early warning system, is likely to be very effective in Del Norte and Humboldt Counties, but most of California's population and critical infrastructure are found along the transform boundary, not the subduction zone.

The idea behind an early warning system is that once a quake is detected, the system sends an alert to cell phones in affected regions. Earthquake waves move about the speed of sound, while electronic signals move at the speed of light. In theory, an early warning system could send signals ahead of an approaching quake, pop up warnings on cell phones, and allow people to move to safer locations prior to the arrival of the quake waves.

To this end, the United States Geological Survey has created a network of seismic stations linked to a phone warning system called ShakeAlert. This is relatively new and is expected to expand into other states. One practical application of ShakeAlert is the connection to the Bay Area Rapid Transit (BART) system allowing automated braking of commuter trains upon detection of a significant quake, replacing a previous system that operated manually.

A few seconds of warning is a good thing. However, a critical examination reveals a few issues. In a very large quake, as the seismic waves spread along a fault, the size may develop rather than be instantaneously recognizable, meaning that early detections may underestimate the size; in other words, because huge quakes displace large areas along faults, the signal for “big quake” may evolve rather than announce itself immediately. By then areas close to the rupture will already be feeling the shaking.

The proximity of faults and people presents another problem with useful earthquake warning systems. California is most likely to have large quakes on the San Andreas, Hayward, or one of the numerous thrust faults branching off the San Andreas. These faults are often right in the midst of urban areas. There will be little time for instruments to detect the quake, for algorithms to process the information, for cell numbers in the affected region to be triggered, and then for people to actually pick up their phone and see the alert. For example, when a major quake happens on the Hayward fault, people in Berkeley and Oakland will experience the full force in mere seconds. In Los Angeles, when the fault that nearly cuts the famous Capitol Records Tower activates, people examining celebrity handprints in the concrete of the nearby Grauman’s Chinese Theatre will feel the quake long before a warning reaches their phones.

Drop and Cover or Triangle of Life?

If you could receive a quake alert on your phone, what would you be able to do?

One long-standing idea about how to survive a quake is to “drop and cover,” meaning to get underneath something such as a table and to cover one’s head. This is what the USGS and the Red Cross recommend, however this protection has limitations. It is possible that if a building is collapsing, and heavy beams are crashing down, these might flatten a table and squish anyone hiding underneath. On the other hand, if one was not under a table that could happen as well. As Conan O'Brien once humorously pointed out when interviewing the USGS's Lucy Jones, even an IKEA table offers more protection than nothing.

A recent idea that needs to be addressed here is the so-called “triangle of life,” the concept that rather than ducking underneath a table, one might have a better chance being on the side of a table. The idea is that a falling beam hitting a table could create a triangular-shaped opening in which one could survive. There is, however, no real scientific support for this concept, which the USGS describes as a “misguided idea” that “doesn’t apply to buildings constructed within the United States." Your best bet is still to drop and cover, to get underneath something sturdy as a shield against falling objects.

The temptation to exit the building one is in might be strong–after all, collapsing buildings are what kill people. Leaving the building seems to make sense, but there is great danger of objects from the sides of the building raining down upon those leaving. For example, if one happens to be near the exit of a skyscraper when a quake happens, and one runs outside to flee the building, one could be heading straight into a curtain of falling glass panes that have detached from the upper levels of the building, shattering on the sidewalk like so many transparent guillotines. Deadly glass panes plummeting from high rises already occur with alarming frequency during large wind storms, and in an earthquake we can expect streets to be hit with heavy glass falling with deadly force.

So staying inside is dangerous, going outside is dangerous–what choice does one have? Even this question rests on a flawed assumption. In reality, when a major earthquake happens, you probably will not be able to move at all. One of the authors (Newton) personally experienced this phenomenon during the 1989 Loma Prieta quake, in which the shaking was so severe that he found himself unable to stay upright when attempting to walk across a living room, and then upon falling to the ground, discovered that the debris of broken glass and brick fragments meant that even crawling was not an option. You may make a plan about what you should do, but in practice you may not be able to move at all and you will ride out the quake in whatever place you happen to find yourself.

Preparation: the Best and Only Option

While there is no way to predict when specific quakes will happen, you can take a number of actions today that can make your life easier afterwards.

Many people may start at a place such as the Red Cross’s earthquake preparation page. However, a critical examination shows that much of this information is problematic.

The Red Cross earthquake preparation list advises that “What you should do before an earthquake” includes “Get a fire extinguisher and learn how to use it safely.” This is about as useful as the demonstration of how a seatbelt works shown to every airline passenger before every flight. The Red Cross notes the importance of “eat[ing] healthy food and get[ting] enough sleep.”

Cheers, thanks for that. The Red Cross also advises, “It’s normal to have a lot of bad feelings, stress, or anxiety”; it’s good to know that the default psychological condition for most people won’t change following a quake. The Red Cross then warns, “Be ready to live without power, gas, or water,” without providing any specifics that would actually help.

With the paucity of good preparation information, people may consider purchasing an “earthquake preparation kit.” Such kits are sold by a number of companies and typically contain similar items, such as emergency food rations, a water bag for collecting water, bandaids, flashlights, a poncho, a survival blanket, and a whistle.

These items are all quite useless. In an actual post-quake environment, emergency food is a low priority; you probably have plenty of non-perishable items around your house, and if not, then humans can go days without food without any ill effect. Water will be the major requirement, but an empty bag for containing water does very little if broken water lines mean that no water comes out from your household tap (and, of course, stores will sell out of bottled water immediately following a quake). You likely already have household bandaids; in any event, they will do nothing for the serious medical issues following a major shake. These kits often emphasize flashlights and glowsticks, but people forced into urban camping may find that bedtimes are far earlier than our current long, light-sustained nights. Ponchos are unnecessary if one has access to one’s normal clothes–which, if you’re able to find your home’s emergency kit, that means you probably still have access to your house. Likewise, survival blankets are unnecessary; even in winter, the majority of California does not experience life-threatening low temperatures. And most useless of all is a whistle. The idea of the whistle’s inclusion in the emergency kit involves you being trapped under a collapsed building; if you can signal by blowing a whistle, then this may guide help to your position (the standard is to make a noise once every minute, so rescuers can work and then stop to listen on a schedule). However, there’s a fatal logic error here. If you have access to the emergency kit with the whistle, then you are not trapped; if you are trapped, you won’t have access to the emergency kit. Outside of the absurdly unlikely circumstance that your home collapses on you in such a way that you are within arm’s reach of this kit, then the whistle will be just as useless as the rest of the items found in such earthquake emergency kits.

Here’s what you really need instead, in order of importance:

- **Water.** Water will be the first thing you need following a devastating quake, but our fragile infrastructure guarantees that many will face household taps that gurgle air rather than provide drinking water. Store bottled water at home, store water in your car, store water at work; you never know where you’re going to be when the quake happens. You really cannot store enough water in preparation for what is about to happen. As a related item, consider a camping water filter or a LifeStraw; these can remove bacteria (and depending on the grade, some viruses) from natural waters, allowing you greater potential water sources. Do not imagine that the government is going to send water trucks into cities to slake the thirst of those affected by a big quake; the freeways and roads will be disrupted and there won’t necessarily be a way for such trucks to reach neighborhoods, nor for you to travel to where the water is located. This is going to be the biggest health concern; people can last about three days without water.
- **Garbage bags.** Lots of garbage bags–think Costco-level. These will not be for throwing out trash, but rather dealing with an issue related to the collapse of the water and sewage system. Within a few hours of a major quake, everyone is going to need to use the toilet. However, not everyone has a sufficiently large or private backyard. A simple solution is this: line the inside of your now non-flushable toilet with a garbage bag. Then seal it up and dispose of it (perhaps remembering how your neighbors let their dog onto your lawn but failed to pick up the waste).
- **Baby wipes.** Every geologist learns, often during the undergraduate capstone course known as Field Camp, what it is like to go many weeks without showering. Geologists also learn that with a sufficient quantity of baby wipes, one can mimic a shower in such a way as to keep oneself somewhat clean. A baby wipe bath is not only hygienic, but good for one’s mental outlook. Dry shampoo is also a pro-tip.
- **Generator.** In many parts of the world unconnected to a power grid, and in seemingly every overcrowded public campground these days, generators are the default way of making electricity. Post-quake, generators may be a good way to make electricity until the reconstruction of our power grid. Many generators include a dual-use option that allows you to use fuel from barbeque propane, which is safer than having loose containers of gasoline around your house. Consider that some areas, post-quake, will be cut off from the electrical system for a very long time. While we are accustomed to thinking that when the power goes off in a storm, it will be restored in a few hours, imagine that instead it’s not just the power lines that have fallen, but the poles themselves that have been uprooted; moreover, the roads to get to the poles may be disrupted and impassable to repair vehicles. Before the electrical lines are reconnected to your house, technicians will have to replace the poles; before they can do that, engineers will have to stabilize the roads and construction workers will have to repave the streets. All this is going to take a very long time. While a generator solution may not be for everyone in every situation, it is worth considering before the quake.
- **Cash.** A group of esteemed philosophers once posited, “Cash rules everything around me, dollar dollar bill y’all.” We should take this admonition to heart. Withdraw and store some money, with the idea that following a quake, when all electricity is out and ATM machines and Venmo and credit cards no longer work, it would be useful to be able to buy some needed items.
- **USB power batteries.** There are a number of relatively inexpensive USB batteries which can power electronics, such as lights

and cell phones. One good thing is that the cell system may have the robustness to survive a quake, unlike the situation with land lines that are very vulnerable. Ad-hoc cell towers are sometimes added at places such as concert venues to increase signal, and it is plausible that such cell towers could restore cell service much quicker than other utilities.

- **Natural gas shutoff wrench.** In the United States, there is no requirement that residential homes have an automatic natural gas shutoff valve, one which when triggered by substantial acceleration turns off gas coming into homes. If the quake breaks the fragile natural gas lines throughout your house, and you start to smell gas, you have a very limited time in which to shut off the gas main. Know where your gas main is, and attach to the main with a string a specialized wrench to allow you to immediately turn off the gas if you smell a leak. Of course, in a big quake, there could be gas main breaks throughout city streets; this happened in the Marina District in San Francisco following the 1989 Loma Prieta quake and sparked the major fires there. You can't do anything about the possibility of city gas mains, but you can try to protect your home with a shutoff wrench.
- **Home modifications.** Everyone can take a few simple measures to improve the safety within a home, including removing glass-framed pictures from areas where you might walk in the night after a quake. Bookshelves can be easily secured to walls. Heavy objects can be placed lower, to reduce the risk of injury if they fall. If you own a home, there are a number of options for long-term strengthening your property, such as the installation of cripple walls and bolting the house to the foundation. In a similar vein, buying earthquake insurance guarantees that you will not receive the unpleasant surprise awaiting virtually every other homeowner--that your home insurance won't cover earthquake damages, and the federal government under FEMA is unlikely to offer much money to rebuild.

You sometimes hear that people should plan to be independent for 72 hours following a major quake. This is optimistic. For some people, the damage following a big quake won't be measured in hours but in weeks and months and years--that's the timeframe to consider for earthquake preparation.

Do not imagine that FEMA or the California Office of Emergency Services or local governments have stockpiled warehouses full of necessary items and stand ready to spring into action. Assume a situation closer to the bungled response to the natural disaster of the 2005 Hurricane Katrina in New Orleans, where tens of thousands of Americans were left ignored and abandoned by their state and federal governments. If history is any guide, you should plan to be on your own. Following a giant quake, there will be no cavalry coming to your rescue–there are only the preparations you make for yourself and your family right now.

References

1. Wald, L., & Scharer, K. (n.d.). Introduction to Paleoseismology. https://www.usgs.gov/programs/earthquake-hazards/introduction-paleoseismology
2. Lienkaemper, J., Williams, P.L., Guilderson, T.P., 2010. "Evidence for a Twelfth Large Earthquake on the Southern Hayward Fault in the Past 1900 Years." Bulletin of the Seismological Society of America, Vol. 100, No. 5A, pp. 2024–2034, October 2010, doi: 10.1785/0120090129
3. Ludwin, R. (n.d.). Earthquake Prediction. https://pnsn.org/outreach/faq/earthquake-prediction
4. Earthquake Hazards Program (2022, March 9). Earthquake Early Warning Around the World. Usgs.gov. Retrieved June 20, 2024, from https://www.usgs.gov/programs/earthquake-hazards/science/earthquake-early-warning-around-world
5. USGS. (n.d.). What is the "Triangle of Life" and is it legitimate? Usgs.gov. https://www.usgs.gov/faqs/what-triangle-life-and-it-legitimate

This page titled 19.7: Preparing for the Worst is shared under a CC BY-NC 4.0 license and was authored, remixed, and/or curated by Emily Wright.

19.8: A State of Danger

No Good News

There is no good news here. Because California's seismic dangers are fueled by inexorable tectonic forces, there is no avoiding future earthquakes. Past earthquakes are very useful for helping us know the extent of future damages and in establishing expected sizes, but in the end, our contemporary infrastructure has never faced the scale of quakes approaching in the future.

If you choose to remain in California, you will be affected by a giant earthquake that could disrupt nearly every aspect of your life, from commuting to your job, to taking a shower, to being able to drink when you are thirsty. And it won't just be you affected–it will be everyone around you, all at once, completely overwhelming police, fire departments, hospitals, and local governments.

Some areas of California have more hazards than others, but every place will be affected to some degree when the fifth largest economy in the world, creating almost four trillion dollars of wealth annually, loses basic functionality and shuts down. Silicon Valley tech giants can't issue the latest app if their workers do not have standing homes, cannot commute to work because of the shattered transportation infrastructure, and won't even be able to zoom in remotely with no electricity or Internet access. The quakes of the future will disrupt our lives in ways that are both predictable and preventable--but no governmental agency in California is addressing this risk with the seriousness it deserves. It would simply cost too much money to do so.

There are options available to you. One simple solution is to choose to live and work elsewhere. The United States contains 49 other states and commonwealths, some of which are quite beautiful, and most of which are less expensive to live than the Golden State. With the exception of Alaska and western Wyoming, all of these other states have a far lower earthquake hazard than California. Not everyone has to live in California.

But if your conscious decision is to bear the risk and remain in this dangerous state, then you have the opportunity to take action. You have the option to prepare in the ways described above. We can't predict the day an earthquake will arrive, but we can assemble today the items needed for the health and comfort of you and your loved ones.

This page titled 19.8: A State of Danger is shared under a CC BY-NC 4.0 license and was authored, remixed, and/or curated by Emily Wright.

19.9: Chapter Summary

19.1: The Hazard of Buildings

- Earthquakes don't kill people--buildings do.
- An exploration of the role of building type in increasing danger from earthquakes, particularly with regard to "soft first story" buildings, which weaken the most important level for structure survival.
- The vulnerability of buildings is well understood, but this geologic information is usually ignored by planners.

19.2: The Hazard of Place

- There once was an earthquake in Nantucket, that shook all the big lobster buckets/ So very fierce was the shaking, with all the Yankees quaking/They said let's move out of here and %&*@ it. Just kidding--places such as Massachusetts do not experience many earthquakes.
- But California does. Every single day. Lots of them, and on occasion, catastrophically big quakes.
- California's place astride major tectonic plates guarantees that we have much more interesting seismic activity than, say, Kansas. But quakes don't fall randomly around the state and we can in fact predict the areas that will be much more susceptible than others. This section is an examination of how proximity to faults, especially hidden faults, changes potential damage from earthquakes.

19.3: Liquefaction and the Role of Soil Type

- An explanation of the phenomenon of liquefaction and how soil type influences the duration and degree of seismic movement.
- Liquefaction is a major hazard, but poorly understood.
- Much of the soil on which people have built in California is vulnerable to liquefaction.

19.4: What's Coming

- Portents and harbingers of doom for the state with the worst intersection of large populations and dangerous seismic hazards.
- Big quakes are inevitable.
- California's earthquake hazards should not be ignored--but often are.

19.5: Beyond the San Andreas - Earthquakes of the North Coast

- The San Andreas is bad--but something even worse lurks off the coast of Northern California, with the potential to devastate a wide swatch of North America.
- The 1700 quake was a catastrophic event.
- A repeat of the 1700 quake would cause tremendous damage to much of western North America.

19.6: Preparing for the Worst

- Is there anything you can do to prepare?
- The Red Cross has thoughts, but they didn't think it through very well, and much of the information is useless.

- This section explains what you *really* need to prepare for the coming shaking.

19.7: A State of Danger

- The seismic danger is probably worse than most people imagine.
- The good news is you can prepare for what's coming and that will make your experience somewhat better.
- If you decide to continue to live in California, you will be affected by the coming quake.

This page titled 19.9: Chapter Summary is shared under a CC BY-NC 4.0 license and was authored, remixed, and/or curated by Emily Wright.

19.10: Detailed Figure Descriptions

19.1 Fault displacement from the 1872 Lone Pine earthquake

An arid landscape, with low hills to the left and areas of rough, rocky ground at their base. Lower down, below the rocky areas, we see a dry valley floor with desert plants. The area of rounded granitic boulders to the left has more-or-less stayed in position, while the area to the right has dropped down along a normal fault (in which the hanging wall moves down as a response to tectonic extension).

Normal faulting is typical for Basin and Range movements, however Basin and Range tectonics also encompass significant side-to-side movements as well. A common misconception is that the basins in Basin and Range are best thought of as grabens, while the ranges are horsts, as in the horst-graben tectonic model; however, this is too simplistic in that the downdropped blocks also rotate and are displaced by strike-slip movements.

19.1.1 Unreinforced brick wall in downtown Oakland

The unreinforced brick wall of a multistory building, in an area noted for its vulnerability to shaking and liquefaction. In other words, this sort of structure is unlikely to survive a major quake. And yet it stands now, unremarked upon except by geology students who recognize the danger, and will continue to be there until the moment when side-to-side shaking moves each brick slightly past the ones above and below, causing the wall to lose its support and crumble to the ground. This is one of thousands of such vulnerable buildings and yet almost nothing is being done to address the hazard.

Anyone below or near this structure when it inevitably collapses will certainly be hurt or killed.

19.1.2 A building destroyed during the 1989 Loma Prieta quake

This is a soft-story apartment building, meaning that the lowest level is the weakest. As you can see in the picture, the lowest level is parking garages (parking being a particularly difficult problem in the Marina District, having a designated parking spot is a practical requirement for living there). The openness of the lowest level significantly weakens the building's ability to respond to earthquakes.

Pictures of this building were so widely circulated following the 1989 quake that it gave the impression of vast, universal damage to the Marina District; however, the reality is that most of these pictures were of this one spectacularly leaning building.

19.1.3 A soft-story apartment building with masonry supports in Oakland, CA

An extant apartment complex in Oakland built with a soft first story, in order to accommodate parking underneath. We see a car parked in one of the carport. Note that the support columns and walls appear to be constructed of masonry bricks rather than solid supports such as a metal poles. This configuration is less than ideal for a region that will experience major earthquake shaking. We can expect that even moderate side-to-side earthquake movement will weaken these supports, up to the point where the entire second level collapses to the street.

19.2.1 California population density map

Some of the state has concentrations of high populations, and most of the state (Modoc, Mojave, north coast, central coast, Owen's Valley) has very low populations. Rather than being evenly distributed, high populations are concentrated in just a few places: the greater Los Angeles region (including San Diego), the Sacramento area, and the San Francisco Bay Area.

19.2.2 Seismicity of California

Historic seismicity in California, shown on the same scale as the population map in 19.2.1. Earthquakes are concentrated in just a few places in California--but that some of these places are major population centers (Los Angeles and the San Francisco Bay Area). There are a few seismically active areas with small populations, such as the north coast near the Mendocino Triple Junction, the Mammoth region, the southern Sierra Nevada-Owen's Valley area.

19.2.3 A shake map showing the intensity of the 2019 Ridgecrest quake

Coding indicating "severe/violent" shaking corresponding to peak ground accelerations between 40-74% of the gravitational acceleration constant. Areas of "strong" and "moderate" shaking surround the vicinity of Ridgecrest. Even a few tens of kilometers from the epicenter, the shaking drops to "very light" and "weak" scales. This emphasizes how quickly shaking diminishes away from the epicenter, and the importance of having population centers as far away from faults as possible; however, in California, we've done exactly the opposite.

19.2.4 Major fault map of Southern California

Major faults in Southern California, indicated in darker red lines over the lighter grey lines of the background. The San Andreas moves diagonally from northwest to southeast. This emphasizes is just how many faults there are in California; there are many darker lines criss-crossing nearly the entire area. However, keep in mind that there are many more than are shown at the scale of this map. There are truly few places in California where one is very far from recognized faults. Those places tend not to be population centers; rather, the areas of great fault concentrations are also among the most heavily populated in California.

19.2.5 Major population concentrations superimposed on Southern California fault system

An intersection of population and faults superimposes the southern population measures from 19.2.1 onto 19.2.4, showing how population centers intersect with recognized faults. Areas of the highest population are Los Angeles and San Diego. Faults run through and around these areas. This intersection of earthquakes and population is a recipe for disaster. If the state had developed with a more even population distribution, then the earthquake risk would also be evenly distributed; however, in this configuration most everyone in the state lives in seismically dangerous area.

19.2.6 A diagram illustrating the San Andreas and associated thrust faults

The San Andreas fault system as it branches underneath the Los Angeles basin with thrust faults. One thrust fault is the Sierra Madre, which runs the full length of Los Angeles just to the east and had a quake of magnitude 5.8 in 1991. Another is the Whittier Narrows, which is south of Los Angeles which runs parallel to the South of Los Angeles, and had a quake of magnitude 5.9 in 1987. There are many other thrust faults, and probably a significant number that we do not know about yet, but which will announce their arrival by creating massive damage in areas far from the actual San Andreas. This problem of thrust faults is one of the most dangerous aspects about where we have built and where the hazards lie.

19.2.7 A scale illustration of the San Andreas fault and associated thrust faults

The thrust faults mentioned in 19.2.6, to scale, showing the depths of the faults and the base of Earth's crust at 20-25 miles below sea level. The San Andreas spans to at least 12 miles below sea level from north to south. The Master Blind Thrust Fault crosses the San Andreas and travels towards the surface as it moves from east to west. The Mast Blind Thrust fault is a strong reflective fault.

The San Andreas fault is far from population centers. But like the trunk of a tree, it has many branches, and these branches are the main danger for people living in Los Angeles. For instance, the Whittier and Sierra Madre Thrust Faults branch off from the

vertical San Andreas and are tens of kilometers away from that main trunk. However, the Whittier and Sierra Madre faults underlie heavily populated regions in the greater Los Angeles basin, meaning that even moderate seismic activity on them will have big consequences for the people living there.

19.2.8 The collapsed John Muir School in Long Beach

This brick building has an extensive amount of damage. In this photograph we see the ornate front entrance, with much of the second-story facade collapsed onto the ground level. We can see into the rooms that were exposed. Had the quake occurred earlier in the day, the school would have been filled with students. So many schools were similarly damaged that it led to the Field Act, one of the first pieces of California legislation meant to reduce the risk from earthquakes.

19.2.9 Damage to a highway from the 1994 Northridge Quake

A section of a freeway overpass that was heavily damaged during the 1994 Northridge quake. The two halves of the elevated section have separated, and one has collapsed to the ground. Strands of rebar spill from the section of the overpass that is still standing and chunks of concrete are piled on the roadbed that has collapsed to the ground. A great deal of the transportation infrastructure in the Los Angeles area was severely damaged by this quake.

19.3.1 Shaking in the Oakland-Alameda area in the 1989 Loma Prieta quake, by soil type

This map shows Oakland and Alameda, including Treasure Island and Yerba Buena Island, and the Bay Bridge. Soil type is indicated on the map, with associated seismograms from the Oakland-Alameda area during the 1989 Loma Prieta quake.

Bedrock shows the least amount of disruption, while natural sand and gravel shows more, and the artificial fill of soft mud shows the greatest amount of movement. This corresponds to the dangers of living on each soil type. These soil types are shown on the map as follows:

- Bedrock appears inland, east of Oakland, and at Yerba Buena Island
- Sand and gravel appear in in broad band of land along the coast and moving into Alameda
- Soft mud appears along the coast in West Oakland and most of Alameda, as well as at Treasure Island. There is also a narrow incursion of soft mud through central Oakland, across Interstates 880, 80, and 580.

At the center of the map, the location of the Cypress Structure is shown in red. This section of Interstate 880 in Oakland collapsed during this quake, killing 42 of the 63 people who died during the event. The Cypress Structure spans an area composed of soft mud and sand-and-gravel; the heaviest damage occurred over the soft soil.

19.4.1 A map showing national earthquake hazards

US mainland earthquake risks, with one significant cluster near New Madrid, MO, and then very little risk outside of California, all of which is listed has having major likelihoods of damaging quakes. This emphasizes that for the contiguous United States, California has an exceptional risk of future seismic danger. Texas, according to this map, has only a 4% change of a damaging earthquake in the next 100 years, while California has a >74% chance.

19.4.2 A map showing Bay Area faults and associated major quake probabilities

Bay Area faults with associated percentage likelihoods of creating M_w6.7 or greater quakes by 2043. The overall probability of one or more earthquake of magnitude greater than 6.7 between 2014 and 2043 in the San Francisco Bay Region is 72%. There are a total of 32 faults shown. The greatest risks come from the Hayward fault (33%), the Calaveras fault (26%) and the San Andreas (22%). Other lesser known faults, such as the San Gregorio fault have only a 6% chance of producing a M_w6.7 or greater quake by 2043.

Bay Area faults and associated major quake probabilities

Faults	Probability of M_w6.7 or greater quake by 2043
Hayward fault - runs through the city of Fremont and connects with the Rogers Creek fault with travels to north of Santa Rosa	33%
Calaveras - runs east of the South Bay region into Oakland	26%
San Andreas - spans the entire region from inland at the bottom of the region towards the coast and runs through Point Reyes.	22%
Concord - connects with multiple other faults which, as a whole, span the entire region to the east (east of Napa)	16%
Maacama - starts at the northern-most edge of the Bay area and travels north	8%
San Gregorio - branches from the San Andreas fault just north of San Francisco and runing along the coast, spanning the souther part of the region	6%

19.5.1 Map of the Cascadia Subduction Zone

The seaward edge of the subduction zone, where the subducting plates begin the descent beneath the North American plate extends from Cape Mendocino, south of Eureka into Canada off the coast of Vancouver Island. The stuck or “locked” part of the interface between North America and the subducting plates, which is the fault that breaks in great earthquakes, extends from nearly the southern extent of the seaward edge of the subduction zone in the south to partway up the coast of Vancouver Island in the north.

19.5.2 Land Subsidence and Sand Deposit Following a Tsunami

The sequence of events shown begins with a marsh that is present before the earthquake event. The land subsides during the earthquake and a sand-laden tsunami overruns the subsided landscape within minutes to hours after the earthquake. This leaves behind a sand sheet. Centuries after the earthquake, the sand sheet becomes buried by tidal silt and eventually the marsh returns. A photograph shows an example of the resulting three layers of sediment: marsh peat, covered by tsunami sand, then tidal silt. The whole sequence is approximately 15 cm (6 inches) thick.

Query Box 19.5.1 Tsunami Hazard Maps Change With Updated Science

The purpose of including this image comparison is to show how tsunami hazard maps can change as scientists refine their understanding of the hazard. Crescent City is intended as an example only and therefore many of the details in these maps, such as street names, etc. are not necessarily relevant to this context. The important information that users should ascertain from the comparison is that more of the area of Crescent City is included in the 2021 tsunami hazard zone than was previously included in the 2010 version. The expanded hazard zone includes areas very near the city's hospital, as well as very near the Elk Valley Rancheria tribal headquarters. There are also some areas that were previously in the hazard zone and are no longer, but this represents a much smaller area overall. Fortunately, the middle school and high school remain safely outside the tsunami hazard zone.

Video 19.5.1 Tsunami Forecast Animation: Cascadia 1700

The video shows a wave propagating across the Pacific Ocean. The wave reaches southern California within 1 to 2 hours, but wave heights there never exceed 3 meters (about 10 feet). The first wave hits Hawaii about 5 hours after the earthquake and tsunami heights in some places in Hawaii are shown as much as 3 meters (about 10 feet). The first tsunami reaches Japan in about 10 hours, but the maximum tsunami height doesn’t arrive until a few hours later, with maximum heights between 1 and 3 meters (about 3 to 10 feet).

19.5.4 California Magnitude 4.5 Earthquakes

Earthquakes of magnitude 4.5 or higher, which have occurred in the decade between July 2014 and July 2024 in California and surrounding areas are shown on a map. A few earthquakes occur individually, and some occur in clusters. One large cluster occurs near the Menocino triple junction and along the Mendocino fracture zone, as well as near the Gorda ridge. Most earthquakes on this map are of magnitude smaller than 5.

19.5.5 Earthquakes in the Juan de Fuca Plate

The tectonics of the Pacific Northwest are described elsewhere in this text (see 3.4: California's Plates and Plate Boundaries and 7.1: The Cascadia Subduction Zone and the Cascade Continental Volcanic Arc). This figure is included here to show the location of the Gorda plate, which is located south of the main part of the Juan de Fuca plate and makes up the portion of plate that is subducting at the Cascadia subduction zone beneath California. This figure also shows the locations of earthquakes deeper than 25 km, which are clustered in northern California, the Olympic Peninsula and Vancouver Island (the ends of the subduction zone), and are largely absent from Oregon (the middle of the subduction zone).

Video 19.6.3 Parkfield quake

The long-awaited Parkfield quake shakes the ground. Large trees on a hill rock back and forth for a few seconds as it passes.

This page titled 19.10: Detailed Figure Descriptions is shared under a CC BY-NC 4.0 license and was authored, remixed, and/or curated by Emily Wright.

INDEX

A

absolute dating
5.4: Absolute Dating of Geologic Materials
5.6: Chapter Summary

accreted terranes
11.8: Chapter Summary

accretion
10.7: Detailed Figure Descriptions

active faults
14.5: Geologic Hazards of the Transverse Ranges Province

aftershocks
4.4: Earthquakes

agricultural economy
18.4: Water Infrastructure and Management

agricultural industry
12.4: Natural Hazards of the Great Valley Province

agricultural land
12.7: Detailed Figure Descriptions

agriculture
12.3: Soil, Streams and Agriculture
12.6: Chapter Summary
15.5: Natural Resources of the Peninsular Ranges
18: California's Water

Alaska
19.5: What's Coming

Alfred Wegener
3: Plate Tectonics

Algodones dune field
13.5: Sand Dunes and Dune Fields

alluvial fans
13.6: Erosional Desert Land Forms
8.4: Sedimentary Products of Rifting in the Basin and Range

ancient subduction zone
11.3: The Great Valley Sequence

anthropocene
11.6: Quaternary Events

anticlines
4.2: Folding

aqueducts
18.4: Water Infrastructure and Management

aquifer
13.7: Water in the Desert

aquifers
18.3: Groundwater
18.8: Detailed Figure Descriptions

arid climate
13.6: Erosional Desert Land Forms

artificial fill
19.4: Liquefaction and the Role of Soil Type

asthenospheric mantle
8.5: Rift-Related Volcanism in Eastern California

atmospheric conditions
17.1: Note on Usage

atmospheric river
17.7: Detailed Figure Descriptions

atmospheric rivers
17.6: Chapter Summary

atolls
10.2: The McCloud Limestone- An Ancient Coral Reef

B

barrier reefs
10.2: The McCloud Limestone- An Ancient Coral Reef

basalt
2.8: Detailed Figure Descriptions

basaltic lava
8.5: Rift-Related Volcanism in Eastern California

Basin and Range
13.2: Geologic Overview and Evolution of the Mojave and Colorado Desert Provinces
8: Basin and Range
8.1: Regional Extent and Overview of the Basin and Range
8.3: Rift-Related Faulting in Eastern California
8.7: Chapter Summary
8.8: Detailed Figure Descriptions

basin formation
14.3: Cenozoic Sedimentation and Basin Development
8.4: Sedimentary Products of Rifting in the Basin and Range

batholith
15: Peninsular Ranges

Bay Area
19.5: What's Coming

beach features
16.8: Detailed Figure Descriptions

beach safety
16.3: California Coastal Hazards

bedrock
19.4: Liquefaction and the Role of Soil Type

bedrock geology
14: Transverse Ranges
14.2: Bedrock Geology of the Transverse Ranges Province

beds
1.2: Geologic Map Symbols

biochemical sedimentary rocks
2.5: Sedimentary Rocks

biodiversity
13: Mojave and Colorado Deserts

blueschist
11.7: Representative Coast Range Rocks

bonding
2.1: Minerals
2.7: Chapter Summary

breakwater
16.4: Human Alteration and Mitigation

brine pools
13.8: Geological Resources of the Desert Provinces

Bristlecone pines
17.7: Detailed Figure Descriptions

brittle deformation
4.3: Jointing and Faulting

building regulations
19.3: The Hazard of Place

buildings
19.2: The Hazard of Buildings
19.9: Chapter Summary

burial
2.3: The Rock Cycle

C

calcite
2.2: Mineral Properties

California
1: Introduction to the Geology of California
10: Klamath Mountains
10.5: Uplifting a Mountain Range
10.6: Chapter Summary
11: Coast Ranges
11.3: The Great Valley Sequence
11.4: The Franciscan Complex
11.5: Cenozoic Events
11.7: Representative Coast Range Rocks
11.9: Detailed Figure Descriptions
12.1: Geomorphology and General Overview of the Great Valley Province
12.5: Natural Resources of the Great Valley
12.7: Detailed Figure Descriptions
13.1: Physiographic Features of the Mojave and Colorado Desert Provinces
13.3: Creating the Desert Environment
13.7: Water in the Desert
14: Transverse Ranges
14.1: Physiographic Overview of the Transverse Ranges Province
14.5: Geologic Hazards of the Transverse Ranges Province
14.8: Detailed Figure Descriptions
15: Peninsular Ranges
15.5: Natural Resources of the Peninsular Ranges
15.7: Detailed Figure and Video Descriptions
16: California Coastline
16.2: California Coastline Anatomy
16.3: California Coastal Hazards
16.5: Coastal Access
16.6: The Edge of California
17: California's Climate
17.2: The Past
17.3: The Present
17.4: The Future
17.5: Hotter, Drier, Tougher
17.6: Chapter Summary
17.7: Detailed Figure Descriptions
18.3: Groundwater
18.4: Water Infrastructure and Management
18.6: Understanding California's Water Landscape
19.10: Detailed Figure Descriptions
19.3: The Hazard of Place
19.5: What's Coming
19.6: Beyond the San Andreas - Earthquakes of the North Coast
19.7: Preparing for the Worst
19.9: Chapter Summary
2: Minerals and Rocks
3.4: California's Plates and Plate Boundaries
3.6: Detailed Figure Descriptions
4: Geologic Structures and Seismology
4.4: Earthquakes
4.6: Chapter Summary
4.7: Detailed Figure Descriptions
5: Geologic Time
5.1: Relative Dating
5.2: Unconformities
6: A Brief Geologic History of California
6.1: Developing a Geologic History
6.3: Paleozoic California (541 – 252 Ma)
6.4: Mesozoic California (250 – 66 Ma)-Subduction and Mountain Building
6.7: Detailed Figure Descriptions
7: Cascade Range and Modoc Plateau
7.1: The Cascadia Subduction Zone and the Cascade Continental Volcanic Arc
7.10: Detailed Figure Descriptions
7.2: Rock Types of the Cascades
7.3: The Variety of Volcanoes in the Cascades and the Modoc Plateau
7.4: Volcanic Hazards
7.5: Mount Shasta
7.6: Lassen Volcanic National Park
7.7: Medicine Lake Volcano
7.8: Glaciers in the Cascades
7.9: Chapter Summary
8.7: Chapter Summary
8.8: Detailed Figure Descriptions
9: Sierra Nevada
9.1: The Sierra Nevada Today
9.7: Natural Hazards of the Sierra Nevada
9.8: Chapter Summary
Geology of California
California coast
16.1: Coastal Processes
California Coastal Act
16: California Coastline
California coastline
16.7: Chapter Summary
California earthquakes
19.8: A State of Danger
California geography
15.1: Geomorphology of the Peninsular Ranges
California geology
11.2: The Coast Range Ophiolite
13.9: Geologic Hazards of the Mojave and Colorado Desert Provinces
14.6: Mineral and Petroleum Resources of the Transverse Ranges Province
15.3: Rocks of the Peninsular Ranges
8.3: Rift-Related Faulting in Eastern California
California Gold Rush
9.4: Gold of the Sierra Nevada
California hazards
15.4: Geologic Hazards of the Peninsular Ranges
Cascade Range
10.4: Plutons of the Klamath Mountains
cascades
7: Cascade Range and Modoc Plateau
Cascadia subductio zone
19.6: Beyond the San Andreas - Earthquakes of the North Coast
Castle Crags
10.4: Plutons of the Klamath Mountains
Cenozoic
10.5: Uplifting a Mountain Range
13.2: Geologic Overview and Evolution of the Mojave and Colorado Desert Provinces
15.2: Tectonics and Geologic History of the Peninsular Ranges Province
6: A Brief Geologic History of California
6.5: Cenozoic California (66 Ma – Present)-Faulting, Uplift, and Basin Formation
Cenozoic Era
11: Coast Ranges
6.6: Chapter Summary
Cenozoic geology
14.3: Cenozoic Sedimentation and Basin Development
Cenozoic volcanic rocks
15.3: Rocks of the Peninsular Ranges
Central Valley
12.1: Geomorphology and General Overview of the Great Valley Province
chapter summary
10.6: Chapter Summary
4.6: Chapter Summary
7.9: Chapter Summary
characteristics
12.1: Geomorphology and General Overview of the Great Valley Province
chemical composition
2.1: Minerals
chemical sedimentary rocks
2.5: Sedimentary Rocks
civil engineering
14.5: Geologic Hazards of the Transverse Ranges Province
clastic
2.5: Sedimentary Rocks
clastic debris
8.4: Sedimentary Products of Rifting in the Basin and Range
clay
2.5: Sedimentary Rocks
cleavage
2.2: Mineral Properties
climate
1: Introduction to the Geology of California
13.1: Physiographic Features of the Mojave and Colorado Desert Provinces
13.10: Chapter Summary
13.11: Detailed Figure Descriptions
13.7: Water in the Desert
17.1: Note on Usage
17.6: Chapter Summary
18: California's Water
8.1: Regional Extent and Overview of the Basin and Range
9: Sierra Nevada
9.1: The Sierra Nevada Today
climate change
12.3: Soil, Streams and Agriculture
12.4: Natural Hazards of the Great Valley Province
13: Mojave and Colorado Deserts
13.8: Geological Resources of the Desert Provinces
16: California Coastline
16.1: Coastal Processes
17: California's Climate
17.1: Note on Usage
17.2: The Past
17.3: The Present
17.4: The Future
17.5: Hotter, Drier, Tougher
17.7: Detailed Figure Descriptions
18.5: Threats to California's Water
18.6: Understanding California's Water Landscape
9.6: Ice Shapes the Landscape
9.9: Detailed Figure Descriptions
climate denial
17.6: Chapter Summary
climate effects
13.5: Sand Dunes and Dune Fields
climate prediction
17.1: Note on Usage
climate variability
18.4: Water Infrastructure and Management
climate_change
11.6: Quaternary Events
coast range
11.3: The Great Valley Sequence
coast range ophiolite
11.2: The Coast Range Ophiolite
Coast Ranges
11: Coast Ranges
11.1: A Complicated Land
11.8: Chapter Summary
coastal access
16.6: The Edge of California
coastal anatomy
16.7: Chapter Summary

coastal erosion
16.3: California Coastal Hazards
16.4: Human Alteration and Mitigation
16.8: Detailed Figure Descriptions
17.4: The Future
coastal features
16.1: Coastal Processes
coastal geology
11.4: The Franciscan Complex
14.3: Cenozoic Sedimentation and Basin Development
15.1: Geomorphology of the Peninsular Ranges
16.1: Coastal Processes
16.8: Detailed Figure Descriptions
coastal hazards
16.3: California Coastal Hazards
16.7: Chapter Summary
coastal management
16.4: Human Alteration and Mitigation
16.8: Detailed Figure Descriptions
coastal processes
16.7: Chapter Summary
coastline
16: California Coastline
16.6: The Edge of California
color
2.2: Mineral Properties
Colorado Desert
13: Mojave and Colorado Deserts
13.1: Physiographic Features of the Mojave and Colorado Desert Provinces
Colorado Plateau
8.8: Detailed Figure Descriptions
columbian_mammoth
11.6: Quaternary Events
community action
17.5: Hotter, Drier, Tougher
compression
4.1: Stress and Strain
condensation
18.1: The Hydrologic Cycle
18.7: Chapter Summary
Connecticut beaches
16.5: Coastal Access
conservation
13: Mojave and Colorado Deserts
construction standards
19.2: The Hazard of Buildings
continental crust
10.7: Detailed Figure Descriptions
continental margin
8.6: The Oldest Rocks in the Basin and Range
continental plates
3.2: Tectonic Plates, Plate Motions, and Plate Boundaries
continental rifting
8: Basin and Range
8.2: Rifting in the Basin and Range
8.4: Sedimentary Products of Rifting in the Basin and Range
continental shelf
10.5: Uplifting a Mountain Range
8.8: Detailed Figure Descriptions
convergent boundaries
3.2: Tectonic Plates, Plate Motions, and Plate Boundaries
3.5: Chapter Summary
cooling process
2.4: Igneous Rocks
coral reefs
10.2: The McCloud Limestone- An Ancient Coral Reef
core
3.1: Earth's Interior
3.5: Chapter Summary
crust
3.1: Earth's Interior
3.5: Chapter Summary
crustal thinning
8.5: Rift-Related Volcanism in Eastern California
crystal structure
2.1: Minerals
crystallization
2.4: Igneous Rocks
9.3: The Sierra Nevada Batholith
cultural landmark
10.4: Plutons of the Klamath Mountains

D

damage
14.5: Geologic Hazards of the Transverse Ranges Province
15.7: Detailed Figure and Video Descriptions
dams
18.4: Water Infrastructure and Management
Death Valley
8: Basin and Range
8.1: Regional Extent and Overview of the Basin and Range
8.8: Detailed Figure Descriptions
deep time
17.2: The Past
definition
2.1: Minerals
deformation
4.1: Stress and Strain
4.2: Folding
dendrochronology
17.2: The Past
17.7: Detailed Figure Descriptions
deposition
2.3: The Rock Cycle
9.6: Ice Shapes the Landscape
desert
13.1: Physiographic Features of the Mojave and Colorado Desert Provinces
13.10: Chapter Summary
13.3: Creating the Desert Environment
13.7: Water in the Desert
desert environment
13: Mojave and Colorado Deserts
13.5: Sand Dunes and Dune Fields
13.9: Geologic Hazards of the Mojave and Colorado Desert Provinces
desert environments
13.4: Wind Driven Sediment Transport
desert features
13.4: Wind Driven Sediment Transport
desert formation
13.11: Detailed Figure Descriptions
desert landforms
13.6: Erosional Desert Land Forms
detailed figure descriptions
11.9: Detailed Figure Descriptions
3.6: Detailed Figure Descriptions
4.7: Detailed Figure Descriptions
6.7: Detailed Figure Descriptions
7.10: Detailed Figure Descriptions
differential erosion
16.2: California Coastline Anatomy
diorite
2.8: Detailed Figure Descriptions
dip
1.2: Geologic Map Symbols
disaster response
19.8: A State of Danger
divergent boundaries
3.2: Tectonic Plates, Plate Motions, and Plate Boundaries
3.5: Chapter Summary
drainage basins
18.2: Running Water
drilling
12.5: Natural Resources of the Great Valley
drinking water
18.5: Threats to California's Water
drought
15.5: Natural Resources of the Peninsular Ranges
17: California's Climate
17.3: The Present
17.6: Chapter Summary
17.7: Detailed Figure Descriptions
18: California's Water
18.3: Groundwater
18.6: Understanding California's Water Landscape
droughts
12.4: Natural Hazards of the Great Valley Province
dune fields
13.5: Sand Dunes and Dune Fields
dune types
13.5: Sand Dunes and Dune Fields
dust storms
13.4: Wind Driven Sediment Transport
dynamic geology
11.8: Chapter Summary

E

Early Paleozoic
8.6: The Oldest Rocks in the Basin and Range
Earth
3.1: Earth's Interior
Earth science
14.7: Chapter Summary
3.3: Mechanisms for Plate Motion
5.4: Absolute Dating of Geologic Materials
6: A Brief Geologic History of California
Earth's history
5.5: The Geologic Time Scale
earth's interior
3.5: Chapter Summary
Earth's structure
3.2: Tectonic Plates, Plate Motions, and Plate Boundaries

earthquake
- 11.5: Cenozoic Events
- 15.6: Chapter Summary
- 15.7: Detailed Figure and Video Descriptions
- 19: California's Earthquake History and Hazards
- 19.10: Detailed Figure Descriptions
- 19.3: The Hazard of Place
- 19.4: Liquefaction and the Role of Soil Type
- 4.4: Earthquakes

earthquake damage
- 19.10: Detailed Figure Descriptions
- 19.4: Liquefaction and the Role of Soil Type

earthquake early warning
- 4.5: Measuring Earthquakes

earthquake geology
- 14.4: Tectonic and Structural Evolution of the Transverse Ranges

earthquake history
- 15.4: Geologic Hazards of the Peninsular Ranges

earthquake magnitude
- 4: Geologic Structures and Seismology

earthquake prediction
- 19.7: Preparing for the Worst

earthquake preparedness
- 19.8: A State of Danger
- 4: Geologic Structures and Seismology

earthquake probabilities
- 19.5: What's Coming

earthquake research
- 4.5: Measuring Earthquakes

earthquake risk
- 13.9: Geologic Hazards of the Mojave and Colorado Desert Provinces
- 19.5: What's Coming
- 3.4: California's Plates and Plate Boundaries

earthquake weather
- 19.7: Preparing for the Worst

earthquakes
- 12.4: Natural Hazards of the Great Valley Province
- 13.9: Geologic Hazards of the Mojave and Colorado Desert Provinces
- 14.5: Geologic Hazards of the Transverse Ranges Province
- 14.7: Chapter Summary
- 15: Peninsular Ranges
- 15.4: Geologic Hazards of the Peninsular Ranges
- 19.2: The Hazard of Buildings
- 19.9: Chapter Summary
- 3: Plate Tectonics
- 4: Geologic Structures and Seismology
- 4.1: Stress and Strain
- 4.3: Jointing and Faulting
- 4.5: Measuring Earthquakes
- 4.6: Chapter Summary
- 8.2: Rifting in the Basin and Range
- 9: Sierra Nevada
- 9.7: Natural Hazards of the Sierra Nevada

eclogite
- 11.7: Representative Coast Range Rocks

ecological systems
- 17.1: Note on Usage

economic impact
- 19.8: A State of Danger

ecosystems
- 13.1: Physiographic Features of the Mojave and Colorado Desert Provinces
- 18.6: Understanding California's Water Landscape
- 18.8: Detailed Figure Descriptions
- 9.1: The Sierra Nevada Today

education
- 1: Introduction to the Geology of California

El Niño
- 16: California Coastline

elevation
- 13.1: Physiographic Features of the Mojave and Colorado Desert Provinces

emergency preparedness
- 12.4: Natural Hazards of the Great Valley Province
- 19.8: A State of Danger

emissions
- 17.4: The Future

energy production
- 12.5: Natural Resources of the Great Valley

engineering
- 19.2: The Hazard of Buildings

environment
- 13.10: Chapter Summary

environmental challenges
- 18.5: Threats to California's Water

environmental conservation
- 15.5: Natural Resources of the Peninsular Ranges

environmental impacts
- 17: California's Climate

Environmental Issues
- 13.7: Water in the Desert

environmental regulations
- 12.5: Natural Resources of the Great Valley

environmental risks
- 17.5: Hotter, Drier, Tougher

environmental science
- 17.3: The Present
- 17.4: The Future
- 8.4: Sedimentary Products of Rifting in the Basin and Range
- 9.7: Natural Hazards of the Sierra Nevada

eolian sediments
- 13.5: Sand Dunes and Dune Fields

erosion
- 10.4: Plutons of the Klamath Mountains
- 12.3: Soil, Streams and Agriculture
- 13.10: Chapter Summary
- 15.2: Tectonics and Geologic History of the Peninsular Ranges Province
- 16: California Coastline
- 16.1: Coastal Processes
- 18.2: Running Water
- 2.3: The Rock Cycle
- 9.6: Ice Shapes the Landscape
- 9.9: Detailed Figure Descriptions

erosion control
- 16.4: Human Alteration and Mitigation

erosion processes
- 13.4: Wind Driven Sediment Transport

erosional processes
- 13.6: Erosional Desert Land Forms

evacuation
- 14.5: Geologic Hazards of the Transverse Ranges Province

evaporation
- 18.1: The Hydrologic Cycle
- 18.7: Chapter Summary

evaporite deposits
- 13.8: Geological Resources of the Desert Provinces

evolution
- 5.3: Dating Rocks Using Fossils

explosive eruptions
- 8.5: Rift-Related Volcanism in Eastern California

extensional tectonics
- 8.3: Rift-Related Faulting in Eastern California

extinct_species
- 11.6: Quaternary Events

extreme heat
- 17: California's Climate

extrusive rock
- 2.8: Detailed Figure Descriptions

F

Farallon Plate
- 6.5: Cenozoic California (66 Ma – Present)-Faulting, Uplift, and Basin Formation

fatalities
- 15.7: Detailed Figure and Video Descriptions

fault
- 1.2: Geologic Map Symbols
- 19.10: Detailed Figure Descriptions
- 8.1: Regional Extent and Overview of the Basin and Range

fault mapping
- 19.3: The Hazard of Place

fault scarps
- 8.3: Rift-Related Faulting in Eastern California

fault systems
- 13.11: Detailed Figure Descriptions
- 13.9: Geologic Hazards of the Mojave and Colorado Desert Provinces
- 14.4: Tectonic and Structural Evolution of the Transverse Ranges

fault zones
- 15.1: Geomorphology of the Peninsular Ranges
- 15.4: Geologic Hazards of the Peninsular Ranges
- 19.3: The Hazard of Place
- 19.5: What's Coming
- 4.4: Earthquakes

faulting
- 4: Geologic Structures and Seismology
- 4.3: Jointing and Faulting
- 8.7: Chapter Summary

faults
- 1: Introduction to the Geology of California
- 1.1: How to Read California's Geologic Map
- 11.5: Cenozoic Events
- 15.7: Detailed Figure and Video Descriptions
- 4.1: Stress and Strain

faunal succession
- 5.6: Chapter Summary

feldspar
- 2.2: Mineral Properties

felsic
- 2.4: Igneous Rocks
- 2.8: Detailed Figure Descriptions

flooding
- 17.3: The Present
- 9.7: Natural Hazards of the Sierra Nevada

floods
12.4: Natural Hazards of the Great Valley Province
18: California's Water
18.6: Understanding California's Water Landscape
fold
1.2: Geologic Map Symbols
folding
4.2: Folding
folds
1.1: How to Read California's Geologic Map
foliation
2.6: Metamorphic Rocks
forarc basin
11.3: The Great Valley Sequence
forces
4.1: Stress and Strain
formation
11.5: Cenozoic Events
formations
1.1: How to Read California's Geologic Map
fossil fuels
12.5: Natural Resources of the Great Valley
fossil preservation
14.6: Mineral and Petroleum Resources of the Transverse Ranges Province
fossil records
12.2: Geology of the Great Valley
fossils
11.6: Quaternary Events
3: Plate Tectonics
5.3: Dating Rocks Using Fossils
5.5: The Geologic Time Scale
8.6: The Oldest Rocks in the Basin and Range
franciscan
11.3: The Great Valley Sequence
11.4: The Franciscan Complex
Franciscan Complex
11: Coast Ranges
11.1: A Complicated Land
11.8: Chapter Summary
fringing reefs
10.2: The McCloud Limestone- An Ancient Coral Reef
future
17.4: The Future

G

gabbro
11.2: The Coast Range Ophiolite
geochronology
5.4: Absolute Dating of Geologic Materials
geohazards
9.7: Natural Hazards of the Sierra Nevada
geologic
1.2: Geologic Map Symbols
geologic age
14.8: Detailed Figure Descriptions
geologic hazards
14: Transverse Ranges
14.7: Chapter Summary
15: Peninsular Ranges
15.4: Geologic Hazards of the Peninsular Ranges
geologic history
10.3: The Josephine Ophiolite- A Little Slice of the Mantle
12: Great Valley
12.2: Geology of the Great Valley
13.11: Detailed Figure Descriptions
13.2: Geologic Overview and Evolution of the Mojave and Colorado Desert Provinces
14.4: Tectonic and Structural Evolution of the Transverse Ranges
15: Peninsular Ranges
6: A Brief Geologic History of California
6.6: Chapter Summary
8: Basin and Range
8.6: The Oldest Rocks in the Basin and Range
geologic map
14.2: Bedrock Geology of the Transverse Ranges Province
2: Minerals and Rocks
geologic processes
16: California Coastline
geologic range
5.3: Dating Rocks Using Fossils
geologic structures
4.6: Chapter Summary
geologic time
5: Geologic Time
5.3: Dating Rocks Using Fossils
geologic time scale
5.6: Chapter Summary
geological
12.1: Geomorphology and General Overview of the Great Valley Province
5.5: The Geologic Time Scale
geological events
5.6: Chapter Summary
geological features
1.1: How to Read California's Geologic Map
11.7: Representative Coast Range Rocks
12.7: Detailed Figure Descriptions
13.6: Erosional Desert Land Forms
14.3: Cenozoic Sedimentation and Basin Development
3: Plate Tectonics
4.3: Jointing and Faulting
9.2: Ancient Seas Form the Oldest Rocks
geological formations
10.5: Uplifting a Mountain Range
11.2: The Coast Range Ophiolite
9.5: Volcanic Features of the Sierra Nevada
geological hazards
13.9: Geologic Hazards of the Mojave and Colorado Desert Provinces
14.5: Geologic Hazards of the Transverse Ranges Province
19.4: Liquefaction and the Role of Soil Type
8.3: Rift-Related Faulting in Eastern California
9.7: Natural Hazards of the Sierra Nevada
geological history
1.1: How to Read California's Geologic Map
10.1: Assembling a Continent
10.4: Plutons of the Klamath Mountains
11.4: The Franciscan Complex
15.2: Tectonics and Geologic History of the Peninsular Ranges Province
15.3: Rocks of the Peninsular Ranges
17.2: The Past
4.1: Stress and Strain
5.5: The Geologic Time Scale
9.9: Detailed Figure Descriptions
geological map
12.7: Detailed Figure Descriptions
2.8: Detailed Figure Descriptions
geological processes
2.3: The Rock Cycle
2.6: Metamorphic Rocks
3.1: Earth's Interior
3.2: Tectonic Plates, Plate Motions, and Plate Boundaries
3.3: Mechanisms for Plate Motion
8.3: Rift-Related Faulting in Eastern California
8.4: Sedimentary Products of Rifting in the Basin and Range
9.3: The Sierra Nevada Batholith
9.4: Gold of the Sierra Nevada
geological relationships
8.2: Rifting in the Basin and Range
geological survey
15.1: Geomorphology of the Peninsular Ranges
geological time
5.5: The Geologic Time Scale
geologichazards
15.6: Chapter Summary

geology
1: Introduction to the Geology of California
1.1: How to Read California's Geologic Map
10: Klamath Mountains
10.1: Assembling a Continent
10.3: The Josephine Ophiolite- A Little Slice of the Mantle
10.5: Uplifting a Mountain Range
10.6: Chapter Summary
10.7: Detailed Figure Descriptions
11: Coast Ranges
11.1: A Complicated Land
11.3: The Great Valley Sequence
11.5: Cenozoic Events
11.8: Chapter Summary
11.9: Detailed Figure Descriptions
12.2: Geology of the Great Valley
12.3: Soil, Streams and Agriculture
12.5: Natural Resources of the Great Valley
12.6: Chapter Summary
12.7: Detailed Figure Descriptions
13: Mojave and Colorado Deserts
13.1: Physiographic Features of the Mojave and Colorado Desert Provinces
13.10: Chapter Summary
13.11: Detailed Figure Descriptions
13.2: Geologic Overview and Evolution of the Mojave and Colorado Desert Provinces
13.3: Creating the Desert Environment
13.4: Wind Driven Sediment Transport
13.7: Water in the Desert
13.8: Geological Resources of the Desert Provinces
14: Transverse Ranges
14.1: Physiographic Overview of the Transverse Ranges Province
14.4: Tectonic and Structural Evolution of the Transverse Ranges
14.7: Chapter Summary
14.8: Detailed Figure Descriptions
15: Peninsular Ranges
15.2: Tectonics and Geologic History of the Peninsular Ranges Province
15.5: Natural Resources of the Peninsular Ranges
15.6: Chapter Summary
15.7: Detailed Figure and Video Descriptions
16.2: California Coastline Anatomy
16.5: Coastal Access
17.5: Hotter, Drier, Tougher
17.6: Chapter Summary
18: California's Water
18.6: Understanding California's Water Landscape
18.7: Chapter Summary
19.6: Beyond the San Andreas - Earthquakes of the North Coast
19.7: Preparing for the Worst
2: Minerals and Rocks
2.1: Minerals
2.2: Mineral Properties
2.7: Chapter Summary
3.1: Earth's Interior
3.6: Detailed Figure Descriptions
4: Geologic Structures and Seismology
4.2: Folding
4.3: Jointing and Faulting
4.4: Earthquakes
4.6: Chapter Summary
4.7: Detailed Figure Descriptions
5: Geologic Time
5.1: Relative Dating
5.2: Unconformities
5.4: Absolute Dating of Geologic Materials
5.5: The Geologic Time Scale
6: A Brief Geologic History of California
6.1: Developing a Geologic History
6.2: Precambrian California (4.6 Ga – 541 Ma)
6.3: Paleozoic California (541 – 252 Ma)
6.4: Mesozoic California (250 – 66 Ma)-Subduction and Mountain Building
6.5: Cenozoic California (66 Ma – Present)-Faulting, Uplift, and Basin Formation
6.7: Detailed Figure Descriptions
7: Cascade Range and Modoc Plateau
7.1: The Cascadia Subduction Zone and the Cascade Continental Volcanic Arc
7.10: Detailed Figure Descriptions
7.2: Rock Types of the Cascades
7.3: The Variety of Volcanoes in the Cascades and the Modoc Plateau
7.4: Volcanic Hazards
7.5: Mount Shasta
7.6: Lassen Volcanic National Park
7.7: Medicine Lake Volcano
7.8: Glaciers in the Cascades
7.9: Chapter Summary
8: Basin and Range
8.1: Regional Extent and Overview of the Basin and Range
8.7: Chapter Summary
9: Sierra Nevada
9.1: The Sierra Nevada Today
9.8: Chapter Summary
9.9: Detailed Figure Descriptions
Geology of California
geomorphic features
8: Basin and Range
geomorphology
12: Great Valley
13.1: Physiographic Features of the Mojave and Colorado Desert Provinces
13.11: Detailed Figure Descriptions
15.1: Geomorphology of the Peninsular Ranges
15.6: Chapter Summary
6: A Brief Geologic History of California
8.1: Regional Extent and Overview of the Basin and Range
9.9: Detailed Figure Descriptions
geophysics
4.5: Measuring Earthquakes
geoscience
Geology of California
geothermal activity
8.5: Rift-Related Volcanism in Eastern California
geothermal energy
12: Great Valley
8.7: Chapter Summary
ghost forest
19.6: Beyond the San Andreas - Earthquakes of the North Coast
GIS
1.1: How to Read California's Geologic Map
glacial erosion
10.5: Uplifting a Mountain Range
glacial formations
9.8: Chapter Summary
glacial melt
17.4: The Future
glacial retreat
6.5: Cenozoic California (66 Ma – Present)-Faulting, Uplift, and Basin Formation
glacier formation
9.6: Ice Shapes the Landscape
glaciers
9.6: Ice Shapes the Landscape
global warming
17.1: Note on Usage
17.6: Chapter Summary
gneiss
2.6: Metamorphic Rocks
gold
9.4: Gold of the Sierra Nevada
gold formation
9.4: Gold of the Sierra Nevada
gold mining
9.8: Chapter Summary
gold recovery
9.4: Gold of the Sierra Nevada
Gorda Plate
3.4: California's Plates and Plate Boundaries
granite
10.4: Plutons of the Klamath Mountains
2.8: Detailed Figure Descriptions
gravitational forces
3.3: Mechanisms for Plate Motion
Great Valley
12: Great Valley
12.1: Geomorphology and General Overview of the Great Valley Province
12.2: Geology of the Great Valley
12.7: Detailed Figure Descriptions
great valley sequence
11: Coast Ranges
11.3: The Great Valley Sequence
greenhouse gases
17.1: Note on Usage
17.7: Detailed Figure Descriptions
greywacke sandstone
11.7: Representative Coast Range Rocks
groin
16.4: Human Alteration and Mitigation
groins
16.6: The Edge of California
ground motion
4.4: Earthquakes
ground shaking
19.3: The Hazard of Place
groundwater
1.1: How to Read California's Geologic Map
12.5: Natural Resources of the Great Valley
12.6: Chapter Summary
15.5: Natural Resources of the Peninsular Ranges
15.6: Chapter Summary
18.1: The Hydrologic Cycle
18.2: Running Water
18.3: Groundwater
18.6: Understanding California's Water Landscape
18.7: Chapter Summary
18.8: Detailed Figure Descriptions
groundwater management
18.3: Groundwater
18.5: Threats to California's Water

H

hardness
2.2: Mineral Properties
2.7: Chapter Summary
hazard mitigation
12.4: Natural Hazards of the Great Valley Province
hazards
13.10: Chapter Summary
19: California's Earthquake History and Hazards
19.9: Chapter Summary
9.7: Natural Hazards of the Sierra Nevada
hazards of blowing sediment
13.4: Wind Driven Sediment Transport

headlands
16.7: Chapter Summary
historical geology
5.3: Dating Rocks Using Fossils
history
19: California's Earthquake History and Hazards
Holocene
11.6: Quaternary Events
Holocene epoch
9.5: Volcanic Features of the Sierra Nevada
horizontal
1.2: Geologic Map Symbols
human alteration
16.4: Human Alteration and Mitigation
human fatalities
16.3: California Coastal Hazards
hurricanes
17.1: Note on Usage
hydrogeology
13: Mojave and Colorado Deserts
18.3: Groundwater
hydrologic cycle
18.1: The Hydrologic Cycle
18.4: Water Infrastructure and Management
18.7: Chapter Summary
hydrology
13.7: Water in the Desert
18: California's Water
18.2: Running Water
18.6: Understanding California's Water Landscape
9.1: The Sierra Nevada Today
hydrosphere
18.1: The Hydrologic Cycle
18.7: Chapter Summary

I

ice age
6.5: Cenozoic California (66 Ma – Present)- Faulting, Uplift, and Basin Formation
identification
2.2: Mineral Properties
igneous
2: Minerals and Rocks
2.3: The Rock Cycle
igneous rock
2.4: Igneous Rocks
igneous rocks
11.4: The Franciscan Complex
14.2: Bedrock Geology of the Transverse Ranges Province
2.7: Chapter Summary
2.8: Detailed Figure Descriptions
6.6: Chapter Summary
Imperial Valley
13.9: Geologic Hazards of the Mojave and Colorado Desert Provinces
inclusions
5.6: Chapter Summary
index fossils
5.3: Dating Rocks Using Fossils
Indigenous peoples
8.1: Regional Extent and Overview of the Basin and Range
infiltration
18.1: The Hydrologic Cycle
18.7: Chapter Summary
injuries
15.7: Detailed Figure and Video Descriptions
Inland Sea
8.8: Detailed Figure Descriptions
inorganic
2.1: Minerals
intermediate
2.4: Igneous Rocks
introduction
18: California's Water
18.2: Running Water
19: California's Earthquake History and Hazards
intrusive igneous rocks
9.3: The Sierra Nevada Batholith
intrusive rock
2.8: Detailed Figure Descriptions
IPCC
17.4: The Future
irrigation
18.8: Detailed Figure Descriptions
isotopic dating
5.4: Absolute Dating of Geologic Materials

J

jetty
16.4: Human Alteration and Mitigation
jointing
4.3: Jointing and Faulting
Juan de Fuca plate
3.4: California's Plates and Plate Boundaries
Jurassic
10.7: Detailed Figure Descriptions
12.2: Geology of the Great Valley

K

Klamath Mountains
10: Klamath Mountains
10.1: Assembling a Continent
10.3: The Josephine Ophiolite- A Little Slice of the Mantle
10.4: Plutons of the Klamath Mountains
10.7: Detailed Figure Descriptions

L

La Brea Tar Pits
14.6: Mineral and Petroleum Resources of the Transverse Ranges Province
Lake Tahoe
9: Sierra Nevada
land use
12.1: Geomorphology and General Overview of the Great Valley Province
landforms
13.10: Chapter Summary
16.6: The Edge of California
3: Plate Tectonics
landscape
12.3: Soil, Streams and Agriculture
13.7: Water in the Desert
landscape evolution
14.4: Tectonic and Structural Evolution of the Transverse Ranges
landscapes
9.9: Detailed Figure Descriptions
landslides
9.7: Natural Hazards of the Sierra Nevada
Late Cenozoic
14: Transverse Ranges
Late Proterozoic
8.6: The Oldest Rocks in the Basin and Range
lateral continuity
5.6: Chapter Summary
Laurentia
6.2: Precambrian California (4.6 Ga – 541 Ma)
layers
3.1: Earth's Interior
levees
18.4: Water Infrastructure and Management
limestone
2.5: Sedimentary Rocks
liquefaction
19.4: Liquefaction and the Role of Soil Type
19.9: Chapter Summary
lithium mining
13.8: Geological Resources of the Desert Provinces
lithology
14.8: Detailed Figure Descriptions
lithosphere
3.3: Mechanisms for Plate Motion
lithospheric plates
3.4: California's Plates and Plate Boundaries
local governments
19.8: A State of Danger
lode deposits
9.4: Gold of the Sierra Nevada
longshore current
16.1: Coastal Processes

M

mafic
2.4: Igneous Rocks
2.8: Detailed Figure Descriptions
magma
2.4: Igneous Rocks
magma cooling
9.3: The Sierra Nevada Batholith
major earthquakes
19.5: What's Coming
management
18: California's Water
mantle
3.1: Earth's Interior
3.5: Chapter Summary
mantle convection
3: Plate Tectonics
3.3: Mechanisms for Plate Motion
map
1.2: Geologic Map Symbols
marble
2.6: Metamorphic Rocks
marine sediments
6.3: Paleozoic California (541 – 252 Ma)
marine species
10.2: The McCloud Limestone- An Ancient Coral Reef
marine terrace
16.2: California Coastline Anatomy
marine terraces
15.1: Geomorphology of the Peninsular Ranges

Martins Beach
16.5: Coastal Access
mass extinction
10.2: The McCloud Limestone- An Ancient Coral Reef
5.5: The Geologic Time Scale
megadrought
17.2: The Past
megadroughts
17.6: Chapter Summary
Mendocino Triple Junction
19.6: Beyond the San Andreas - Earthquakes of the North Coast
Mercalli Intensity
15.7: Detailed Figure and Video Descriptions
Mesozoic
13.2: Geologic Overview and Evolution of the Mojave and Colorado Desert Provinces
15: Peninsular Ranges
15.2: Tectonics and Geologic History of the Peninsular Ranges Province
6: A Brief Geologic History of California
6.4: Mesozoic California (250 – 66 Ma)- Subduction and Mountain Building
9.8: Chapter Summary
Mesozoic age
15.3: Rocks of the Peninsular Ranges
Mesozoic Era
6.6: Chapter Summary
metamorphic
2: Minerals and Rocks
2.3: The Rock Cycle
metamorphic rock
15.3: Rocks of the Peninsular Ranges
9.2: Ancient Seas Form the Oldest Rocks
metamorphic rocks
10.1: Assembling a Continent
11.1: A Complicated Land
11.2: The Coast Range Ophiolite
11.4: The Franciscan Complex
11.7: Representative Coast Range Rocks
13.2: Geologic Overview and Evolution of the Mojave and Colorado Desert Provinces
14.2: Bedrock Geology of the Transverse Ranges Province
2.6: Metamorphic Rocks
2.7: Chapter Summary
6.6: Chapter Summary
metamorphism
2.6: Metamorphic Rocks
6.2: Precambrian California (4.6 Ga – 541 Ma)
9.2: Ancient Seas Form the Oldest Rocks
mineral
2.1: Minerals
mineral composition
2.4: Igneous Rocks
2.8: Detailed Figure Descriptions
mineral deposit
9.4: Gold of the Sierra Nevada
mineral deposits
12.5: Natural Resources of the Great Valley
mineral groups
2.1: Minerals
mineral properties
2: Minerals and Rocks
mineralogy
15.3: Rocks of the Peninsular Ranges
minerals
1: Introduction to the Geology of California
2: Minerals and Rocks
2.2: Mineral Properties
2.6: Metamorphic Rocks
2.7: Chapter Summary
mining
15.5: Natural Resources of the Peninsular Ranges
9.4: Gold of the Sierra Nevada
mining operations
13.8: Geological Resources of the Desert Provinces
Modoc Plateau
7: Cascade Range and Modoc Plateau
Mojave Desert
13: Mojave and Colorado Deserts
13.1: Physiographic Features of the Mojave and Colorado Desert Provinces
13.11: Detailed Figure Descriptions
13.5: Sand Dunes and Dune Fields
Mojave region
13.2: Geologic Overview and Evolution of the Mojave and Colorado Desert Provinces
Mojave River
13.7: Water in the Desert
Monitoring
4.5: Measuring Earthquakes
monoclines
4.2: Folding
Monterey Formation
14.6: Mineral and Petroleum Resources of the Transverse Ranges Province
mountain front
13.6: Erosional Desert Land Forms
mountain ranges
10.5: Uplifting a Mountain Range
15.1: Geomorphology of the Peninsular Ranges
mountains
11: Coast Ranges
9: Sierra Nevada
9.8: Chapter Summary

N

national park
8.1: Regional Extent and Overview of the Basin and Range
natural disaster
19: California's Earthquake History and Hazards
natural disasters
13.9: Geologic Hazards of the Mojave and Colorado Desert Provinces
15.4: Geologic Hazards of the Peninsular Ranges
17: California's Climate
17.5: Hotter, Drier, Tougher
19.5: What's Coming
9.7: Natural Hazards of the Sierra Nevada
natural gas
4.2: Folding
6.4: Mesozoic California (250 – 66 Ma)- Subduction and Mountain Building
natural hazards
12: Great Valley
12.4: Natural Hazards of the Great Valley Province
12.6: Chapter Summary
19.8: A State of Danger
9: Sierra Nevada
naturally occurring
2.1: Minerals
Neogene
14.2: Bedrock Geology of the Transverse Ranges Province
nevada
17.2: The Past
normal faulting
8: Basin and Range
8.5: Rift-Related Volcanism in Eastern California
normal faults
4.3: Jointing and Faulting
8.2: Rifting in the Basin and Range
8.3: Rift-Related Faulting in Eastern California
North America
10.1: Assembling a Continent
6.5: Cenozoic California (66 Ma – Present)- Faulting, Uplift, and Basin Formation
North American Plate
3.4: California's Plates and Plate Boundaries
Northern Coast Ranges
11.1: A Complicated Land
Northridge Earthquake
14.5: Geologic Hazards of the Transverse Ranges Province
nucleation
9.3: The Sierra Nevada Batholith
numerical dating
5.4: Absolute Dating of Geologic Materials
5.6: Chapter Summary

O

obduction
10.3: The Josephine Ophiolite- A Little Slice of the Mantle
ocean dangers
16.3: California Coastal Hazards
ocean waves
16.1: Coastal Processes
16.8: Detailed Figure Descriptions
oceanic crust
10: Klamath Mountains
10.7: Detailed Figure Descriptions
oceanic lithosphere
10.3: The Josephine Ophiolite- A Little Slice of the Mantle
11.2: The Coast Range Ophiolite
oceanic plates
3.2: Tectonic Plates, Plate Motions, and Plate Boundaries
oil
4.2: Folding
oil fields
14.6: Mineral and Petroleum Resources of the Transverse Ranges Province
oil production
14.6: Mineral and Petroleum Resources of the Transverse Ranges Province
oil reserves
14.3: Cenozoic Sedimentation and Basin Development
ophiolite
11.2: The Coast Range Ophiolite
11.8: Chapter Summary
ore deposit
9.4: Gold of the Sierra Nevada

Oregon
10: Klamath Mountains
10.5: Uplifting a Mountain Range
orogeny
6.4: Mesozoic California (250 – 66 Ma)- Subduction and Mountain Building
outdoor activities
17: California's Climate
Owens Valley
8: Basin and Range
8.7: Chapter Summary

P

Pacific
16.6: The Edge of California
Pacific Plate
3.4: California's Plates and Plate Boundaries
6.5: Cenozoic California (66 Ma – Present)- Faulting, Uplift, and Basin Formation
paleoclimate
17.2: The Past
paleogeography
6.4: Mesozoic California (250 – 66 Ma)- Subduction and Mountain Building
8.8: Detailed Figure Descriptions
paleontology
11.4: The Franciscan Complex
11.6: Quaternary Events
14.8: Detailed Figure Descriptions
15.2: Tectonics and Geologic History of the Peninsular Ranges Province
15.3: Rocks of the Peninsular Ranges
5.3: Dating Rocks Using Fossils
5.5: The Geologic Time Scale
paleoseismology
19.7: Preparing for the Worst
Paleozoic
10.7: Detailed Figure Descriptions
13.2: Geologic Overview and Evolution of the Mojave and Colorado Desert Provinces
14.2: Bedrock Geology of the Transverse Ranges Province
6: A Brief Geologic History of California
6.3: Paleozoic California (541 – 252 Ma)
9.2: Ancient Seas Form the Oldest Rocks
9.8: Chapter Summary
Paleozoic era
6.6: Chapter Summary
8.8: Detailed Figure Descriptions
Pangea
8.2: Rifting in the Basin and Range
Panthalassa ocean
10.2: The McCloud Limestone- An Ancient Coral Reef
Parkfield experiment
19.7: Preparing for the Worst
partial melting
8.5: Rift-Related Volcanism in Eastern California
9.3: The Sierra Nevada Batholith
passive margin
6.3: Paleozoic California (541 – 252 Ma)
8.6: The Oldest Rocks in the Basin and Range
Peninsular Ranges
15: Peninsular Ranges
15.1: Geomorphology of the Peninsular Ranges
permeability
18.3: Groundwater
Permian period
10.2: The McCloud Limestone- An Ancient Coral Reef
petroleum
14.6: Mineral and Petroleum Resources of the Transverse Ranges Province
4.2: Folding
petroleum extraction
12.5: Natural Resources of the Great Valley
physiographic
12.1: Geomorphology and General Overview of the Great Valley Province
12.6: Chapter Summary
13.10: Chapter Summary
physiography
9.1: The Sierra Nevada Today
pillow basalts
11.2: The Coast Range Ophiolite
placer deposits
9.4: Gold of the Sierra Nevada
plant ecology
2.6: Metamorphic Rocks
plate boundaries
3: Plate Tectonics
3.2: Tectonic Plates, Plate Motions, and Plate Boundaries
3.4: California's Plates and Plate Boundaries
3.5: Chapter Summary
4.4: Earthquakes
8.2: Rifting in the Basin and Range
plate motion
3.3: Mechanisms for Plate Motion
3.5: Chapter Summary
plate reconstruction
6.1: Developing a Geologic History
plate tectonics
10.1: Assembling a Continent
10.3: The Josephine Ophiolite- A Little Slice of the Mantle
11.1: A Complicated Land
11.5: Cenozoic Events
11.8: Chapter Summary
14.4: Tectonic and Structural Evolution of the Transverse Ranges
14.8: Detailed Figure Descriptions
15.2: Tectonics and Geologic History of the Peninsular Ranges Province
3: Plate Tectonics
3.1: Earth's Interior
3.2: Tectonic Plates, Plate Motions, and Plate Boundaries
3.3: Mechanisms for Plate Motion
3.4: California's Plates and Plate Boundaries
4.1: Stress and Strain
6.1: Developing a Geologic History
6.6: Chapter Summary
Pleistocene
11.6: Quaternary Events
9.6: Ice Shapes the Landscape
Pleistocene Epoch
10.5: Uplifting a Mountain Range
plutonic igneous rock
15.3: Rocks of the Peninsular Ranges
plutonic rocks
9.3: The Sierra Nevada Batholith
plutons
9.3: The Sierra Nevada Batholith
pollution
18.5: Threats to California's Water
porosity
18.3: Groundwater
Precambrian
6.2: Precambrian California (4.6 Ga – 541 Ma)
precipitation
17.3: The Present
17.7: Detailed Figure Descriptions
18.1: The Hydrologic Cycle
18.2: Running Water
18.7: Chapter Summary
18.8: Detailed Figure Descriptions
prediction
19.10: Detailed Figure Descriptions
preparation
19: California's Earthquake History and Hazards
properties
12.1: Geomorphology and General Overview of the Great Valley Province
2.2: Mineral Properties
2.7: Chapter Summary
Proterozoic
13.2: Geologic Overview and Evolution of the Mojave and Colorado Desert Provinces
6.2: Precambrian California (4.6 Ga – 541 Ma)
Proterozoic Eon
6.6: Chapter Summary
public access
16: California Coastline
public health
17: California's Climate
18.5: Threats to California's Water
public safety
16.3: California Coastal Hazards
19.3: The Hazard of Place
4.5: Measuring Earthquakes
public trust doctrine
16.5: Coastal Access
pyroclastic flows
9.5: Volcanic Features of the Sierra Nevada

Q

quartz
2.2: Mineral Properties
2.5: Sedimentary Rocks
quartzite
2.6: Metamorphic Rocks
Quaternary
11.6: Quaternary Events
Quaternary deposits
14.2: Bedrock Geology of the Transverse Ranges Province

R

radioactive decay
5.4: Absolute Dating of Geologic Materials
radiolarian chert
11.7: Representative Coast Range Rocks
radiometric dating
5.4: Absolute Dating of Geologic Materials
rare earth elements
13.8: Geological Resources of the Desert Provinces
recurrence interval
19.7: Preparing for the Worst
regional geology
8.4: Sedimentary Products of Rifting in the Basin and Range

relative dating
5.1: Relative Dating
5.6: Chapter Summary
Relative Dating Methods
5.1: Relative Dating
renewable energy
17.7: Detailed Figure Descriptions
reservoirs
18.4: Water Infrastructure and Management
resilience
19.2: The Hazard of Buildings
retrofitting
19.2: The Hazard of Buildings
reverse faults
4.3: Jointing and Faulting
rhyolitic domes
9.5: Volcanic Features of the Sierra Nevada
ridge push
3.3: Mechanisms for Plate Motion
rift basins
8.4: Sedimentary Products of Rifting in the Basin and Range
rift valley
8.8: Detailed Figure Descriptions
rift valleys
8.2: Rifting in the Basin and Range
rifting
6.2: Precambrian California (4.6 Ga – 541 Ma)
8.3: Rift-Related Faulting in Eastern California
8.6: The Oldest Rocks in the Basin and Range
8.7: Chapter Summary
rip current
16.8: Detailed Figure Descriptions
rip currents
16: California Coastline
16.3: California Coastal Hazards
16.6: The Edge of California
risk
19: California's Earthquake History and Hazards
risk assessment
19.3: The Hazard of Place
risk management
19.2: The Hazard of Buildings
19.8: A State of Danger
risks
19.10: Detailed Figure Descriptions
river processes
12: Great Valley
river system
12.3: Soil, Streams and Agriculture
river systems
9.1: The Sierra Nevada Today
9.9: Detailed Figure Descriptions
rivers
18.2: Running Water
rock cycle
2: Minerals and Rocks
2.3: The Rock Cycle
2.7: Chapter Summary
rock formation
10: Klamath Mountains
rock formations
11.1: A Complicated Land
rock layers
5.5: The Geologic Time Scale
rock record
6: A Brief Geologic History of California
rock units
1.1: How to Read California's Geologic Map
rocks
1: Introduction to the Geology of California
2: Minerals and Rocks
2.3: The Rock Cycle
2.5: Sedimentary Rocks
4.1: Stress and Strain
Rodinia
6.2: Precambrian California (4.6 Ga – 541 Ma)
runoff
18.1: The Hydrologic Cycle
18.7: Chapter Summary
18.8: Detailed Figure Descriptions

S

saber_toothed_cat
11.6: Quaternary Events
Sacramento Valley
12.1: Geomorphology and General Overview of the Great Valley Province
12.6: Chapter Summary
safety
19: California's Earthquake History and Hazards
19.2: The Hazard of Buildings
safety measures
19.3: The Hazard of Place
San Andreas
19.6: Beyond the San Andreas - Earthquakes of the North Coast
San Andreas Fault
11: Coast Ranges
11.1: A Complicated Land
11.8: Chapter Summary
12.7: Detailed Figure Descriptions
13.11: Detailed Figure Descriptions
13.9: Geologic Hazards of the Mojave and Colorado Desert Provinces
14: Transverse Ranges
14.2: Bedrock Geology of the Transverse Ranges Province
14.3: Cenozoic Sedimentation and Basin Development
14.4: Tectonic and Structural Evolution of the Transverse Ranges
14.8: Detailed Figure Descriptions
15.4: Geologic Hazards of the Peninsular Ranges
17.5: Hotter, Drier, Tougher
19.5: What's Coming
3.4: California's Plates and Plate Boundaries
4.4: Earthquakes
San Bernardino Mountains
14.2: Bedrock Geology of the Transverse Ranges Province
San Fernando Earthquake
14.5: Geologic Hazards of the Transverse Ranges Province
San Gabriel Mountains
14.2: Bedrock Geology of the Transverse Ranges Province
San Joaquin Valley
12.1: Geomorphology and General Overview of the Great Valley Province
12.6: Chapter Summary
san_andreas_fault
11.5: Cenozoic Events
sand dunes
13.5: Sand Dunes and Dune Fields
schist
2.6: Metamorphic Rocks
sea arch
16.2: California Coastline Anatomy
sea arches
16.7: Chapter Summary
sea cave
16.2: California Coastline Anatomy
sea caves
16.7: Chapter Summary
sea level rise
17.3: The Present
17.4: The Future
17.5: Hotter, Drier, Tougher
sea stack
16.2: California Coastline Anatomy
sea stacks
16.7: Chapter Summary
Searles Lake
13.8: Geological Resources of the Desert Provinces
seawall
16.4: Human Alteration and Mitigation
seawalls
16.6: The Edge of California
sediment
12.3: Soil, Streams and Agriculture
sediment deposition
12.2: Geology of the Great Valley
sediment movement
13.4: Wind Driven Sediment Transport
sediment sorting
8.4: Sedimentary Products of Rifting in the Basin and Range
sediment supply
13.5: Sand Dunes and Dune Fields
sediment transport
13: Mojave and Colorado Deserts
13.4: Wind Driven Sediment Transport
13.5: Sand Dunes and Dune Fields
13.6: Erosional Desert Land Forms
16.1: Coastal Processes
2.5: Sedimentary Rocks
sedimentary
2: Minerals and Rocks
2.3: The Rock Cycle
2.5: Sedimentary Rocks
sedimentary basin
12.6: Chapter Summary
sedimentary basins
14: Transverse Ranges
14.6: Mineral and Petroleum Resources of the Transverse Ranges Province
sedimentary environments
2.5: Sedimentary Rocks
sedimentary facies
8.8: Detailed Figure Descriptions
sedimentary layers
12.7: Detailed Figure Descriptions
sedimentary record
5.3: Dating Rocks Using Fossils
sedimentary rock
15.2: Tectonics and Geologic History of the Peninsular Ranges Province
15.3: Rocks of the Peninsular Ranges

sedimentary rocks
10.1: Assembling a Continent
11: Coast Ranges
11.1: A Complicated Land
11.3: The Great Valley Sequence
11.4: The Franciscan Complex
11.7: Representative Coast Range Rocks
12: Great Valley
13.2: Geologic Overview and Evolution of the Mojave and Colorado Desert Provinces
14.7: Chapter Summary
14.8: Detailed Figure Descriptions
2.7: Chapter Summary
6.2: Precambrian California (4.6 Ga – 541 Ma)
6.6: Chapter Summary
8.1: Regional Extent and Overview of the Basin and Range
9.2: Ancient Seas Form the Oldest Rocks
sedimentary units
12.2: Geology of the Great Valley
14.4: Tectonic and Structural Evolution of the Transverse Ranges
sedimentaryrock
15.6: Chapter Summary
sedimentation
10.3: The Josephine Ophiolite- A Little Slice of the Mantle
13.6: Erosional Desert Land Forms
15.6: Chapter Summary
6.3: Paleozoic California (541 – 252 Ma)
8.6: The Oldest Rocks in the Basin and Range
8.7: Chapter Summary
sediments
6.4: Mesozoic California (250 – 66 Ma)- Subduction and Mountain Building
8.4: Sedimentary Products of Rifting in the Basin and Range
seismic
19: California's Earthquake History and Hazards
seismic activity
15.7: Detailed Figure and Video Descriptions
19.9: Chapter Summary
4.4: Earthquakes
4.5: Measuring Earthquakes
8.7: Chapter Summary
seismic dangers
19.8: A State of Danger
seismic hazard
13.9: Geologic Hazards of the Mojave and Colorado Desert Provinces
14.5: Geologic Hazards of the Transverse Ranges Province
seismic hazards
19.10: Detailed Figure Descriptions
19.5: What's Coming
8: Basin and Range
seismic safety
19.3: The Hazard of Place
seismic shaking
19.4: Liquefaction and the Role of Soil Type
seismic waves
19.2: The Hazard of Buildings
3.1: Earth's Interior
4: Geologic Structures and Seismology
4.5: Measuring Earthquakes
seismic zone
13.11: Detailed Figure Descriptions
seismically active
15.4: Geologic Hazards of the Peninsular Ranges
seismicity
19.10: Detailed Figure Descriptions
8.3: Rift-Related Faulting in Eastern California
seismology
4: Geologic Structures and Seismology
4.6: Chapter Summary
seismometers
4.5: Measuring Earthquakes
serpentinite
11.7: Representative Coast Range Rocks
11.8: Chapter Summary
ShakeAlert
4.5: Measuring Earthquakes
shaking intensity
19.4: Liquefaction and the Role of Soil Type
shark attacks
16.3: California Coastal Hazards
sheeted dikes
11.2: The Coast Range Ophiolite
shoreline
16.8: Detailed Figure Descriptions
shoreline access
16.5: Coastal Access
shoreline erosion
16.6: The Edge of California
shoreline processes
16.1: Coastal Processes
shoreline protection
16.4: Human Alteration and Mitigation
Sierra Nevada
12.2: Geology of the Great Valley
8.1: Regional Extent and Overview of the Basin and Range
9: Sierra Nevada
9.2: Ancient Seas Form the Oldest Rocks
9.5: Volcanic Features of the Sierra Nevada
9.6: Ice Shapes the Landscape
9.8: Chapter Summary
9.9: Detailed Figure Descriptions
silicate minerals
2.7: Chapter Summary
slab pull
3.3: Mechanisms for Plate Motion
snow accumulation
9.6: Ice Shapes the Landscape
snow pack
17.6: Chapter Summary
soft first story
19.9: Chapter Summary
soft story
19.2: The Hazard of Buildings
soil
12.3: Soil, Streams and Agriculture
12.6: Chapter Summary
19.4: Liquefaction and the Role of Soil Type
soil type
19.9: Chapter Summary
solid state
2.1: Minerals
Southern California
14.7: Chapter Summary
15.1: Geomorphology of the Peninsular Ranges
15.4: Geologic Hazards of the Peninsular Ranges
Southern Coast Ranges
11.1: A Complicated Land
state park
10.4: Plutons of the Klamath Mountains
stratigraphy
12.7: Detailed Figure Descriptions
15.3: Rocks of the Peninsular Ranges
5.3: Dating Rocks Using Fossils
5.5: The Geologic Time Scale
8.6: The Oldest Rocks in the Basin and Range
streams
12.3: Soil, Streams and Agriculture
18.2: Running Water
stress
4.1: Stress and Strain
strike
1.2: Geologic Map Symbols
structural geology
14.3: Cenozoic Sedimentation and Basin Development
14.7: Chapter Summary
9.2: Ancient Seas Form the Oldest Rocks
structures
19.10: Detailed Figure Descriptions
subduction
10.1: Assembling a Continent
10.3: The Josephine Ophiolite- A Little Slice of the Mantle
11.8: Chapter Summary
6.3: Paleozoic California (541 – 252 Ma)
6.4: Mesozoic California (250 – 66 Ma)- Subduction and Mountain Building
9.2: Ancient Seas Form the Oldest Rocks
subduction zone
10: Klamath Mountains
10.4: Plutons of the Klamath Mountains
10.7: Detailed Figure Descriptions
6.5: Cenozoic California (66 Ma – Present)- Faulting, Uplift, and Basin Formation
subduction zones
11.4: The Franciscan Complex
11.7: Representative Coast Range Rocks
9.3: The Sierra Nevada Batholith
Summary
10.6: Chapter Summary
4.6: Chapter Summary
7.9: Chapter Summary
supercontinent
6.2: Precambrian California (4.6 Ga – 541 Ma)
supercontinents
8.2: Rifting in the Basin and Range
superposition
5.6: Chapter Summary
surface water
18.8: Detailed Figure Descriptions
surfboard
16.8: Detailed Figure Descriptions
surfing
16: California Coastline
sustainability
13.8: Geological Resources of the Desert Provinces
sustainable
18: California's Water
sustainable water management
18.5: Threats to California's Water
symbols
1.2: Geologic Map Symbols
synclines
4.2: Folding

T

tectonic
- 4.2: Folding

tectonic activity
- 14.3: Cenozoic Sedimentation and Basin Development
- 8.6: The Oldest Rocks in the Basin and Range
- 9.5: Volcanic Features of the Sierra Nevada

tectonic boundaries
- 10.1: Assembling a Continent

tectonic evolution
- 14: Transverse Ranges
- 14.4: Tectonic and Structural Evolution of the Transverse Ranges
- 14.7: Chapter Summary

tectonic forces
- 11.4: The Franciscan Complex
- 12: Great Valley
- 4: Geologic Structures and Seismology

tectonic history
- 9.2: Ancient Seas Form the Oldest Rocks

tectonic motion
- 3.2: Tectonic Plates, Plate Motions, and Plate Boundaries

tectonic movements
- 14.4: Tectonic and Structural Evolution of the Transverse Ranges

tectonic plates
- 10.3: The Josephine Ophiolite- A Little Slice of the Mantle
- 12.2: Geology of the Great Valley
- 15.2: Tectonics and Geologic History of the Peninsular Ranges Province
- 19.9: Chapter Summary
- 3: Plate Tectonics
- 3.2: Tectonic Plates, Plate Motions, and Plate Boundaries
- 3.3: Mechanisms for Plate Motion
- 3.5: Chapter Summary
- 4.3: Jointing and Faulting
- 8.2: Rifting in the Basin and Range

tectonic stress
- 15.4: Geologic Hazards of the Peninsular Ranges

tectonic uplift
- 16.7: Chapter Summary

tectonics
- 10.5: Uplifting a Mountain Range
- 10.7: Detailed Figure Descriptions
- 11: Coast Ranges
- 11.2: The Coast Range Ophiolite
- 11.5: Cenozoic Events
- 13.11: Detailed Figure Descriptions
- 15: Peninsular Ranges
- 15.6: Chapter Summary
- 19.10: Detailed Figure Descriptions
- 3.1: Earth's Interior
- 4.4: Earthquakes
- 6: A Brief Geologic History of California
- 6.2: Precambrian California (4.6 Ga – 541 Ma)
- 6.3: Paleozoic California (541 – 252 Ma)
- 6.4: Mesozoic California (250 – 66 Ma)- Subduction and Mountain Building
- 6.5: Cenozoic California (66 Ma – Present)- Faulting, Uplift, and Basin Formation
- 9.1: The Sierra Nevada Today
- 9.9: Detailed Figure Descriptions

tectonism
- 8.3: Rift-Related Faulting in Eastern California

temperature extremes
- 17.7: Detailed Figure Descriptions

temperature rise
- 17: California's Climate

tension
- 4.1: Stress and Strain

terrane accretion
- 10: Klamath Mountains
- 10.1: Assembling a Continent

terrane map
- 10.7: Detailed Figure Descriptions

textures
- 2.4: Igneous Rocks

thermal expansion
- 17.4: The Future

three layer cake
- 19.6: Beyond the San Andreas - Earthquakes of the North Coast

thrust system
- 6.3: Paleozoic California (541 – 252 Ma)

tombolo
- 16.2: California Coastline Anatomy

topographic map
- 1.1: How to Read California's Geologic Map

topography
- 13.1: Physiographic Features of the Mojave and Colorado Desert Provinces
- 13.6: Erosional Desert Land Forms
- 9.1: The Sierra Nevada Today

tornadoes
- 17.1: Note on Usage

toxic substances
- 18.5: Threats to California's Water

transform boundaries
- 3.5: Chapter Summary

transport
- 13.10: Chapter Summary

transportation
- 2.3: The Rock Cycle

transportation infrastructure
- 19.8: A State of Danger

transverse ranges
- 14: Transverse Ranges
- 14.7: Chapter Summary
- 14.8: Detailed Figure Descriptions

tree rings
- 17.2: The Past

trench study
- 19.7: Preparing for the Worst

trends
- 17.6: Chapter Summary

triangle of life
- 19.7: Preparing for the Worst

tsunamis
- 16.3: California Coastal Hazards

turbidites
- 11.3: The Great Valley Sequence

U

unconformities
- 5.2: Unconformities

unconsolidated soil
- 19.4: Liquefaction and the Role of Soil Type

underground deformation
- 4: Geologic Structures and Seismology

unique landforms
- 15.1: Geomorphology of the Peninsular Ranges

uplift
- 11.5: Cenozoic Events

urban development
- 12.7: Detailed Figure Descriptions
- 15.5: Natural Resources of the Peninsular Ranges

urban planning
- 15.7: Detailed Figure and Video Descriptions
- 19: California's Earthquake History and Hazards

V

Ventura Basin
- 14.3: Cenozoic Sedimentation and Basin Development

vertical
- 1.2: Geologic Map Symbols

Vinod Khosla
- 16.5: Coastal Access

volcanic
- 9: Sierra Nevada

volcanic activity
- 12: Great Valley
- 12.2: Geology of the Great Valley
- 6.5: Cenozoic California (66 Ma – Present)- Faulting, Uplift, and Basin Formation
- 9.5: Volcanic Features of the Sierra Nevada
- 9.7: Natural Hazards of the Sierra Nevada
- 9.9: Detailed Figure Descriptions

volcanic arc
- 10.3: The Josephine Ophiolite- A Little Slice of the Mantle
- 11.3: The Great Valley Sequence

volcanic features
- 8: Basin and Range
- 8.5: Rift-Related Volcanism in Eastern California
- 9.1: The Sierra Nevada Today
- 9.5: Volcanic Features of the Sierra Nevada
- 9.8: Chapter Summary

volcanic hazards
- 8.5: Rift-Related Volcanism in Eastern California

volcanic islands
- 10.2: The McCloud Limestone- An Ancient Coral Reef

volcanic rock
- 2.4: Igneous Rocks

volcanic rocks
- 10.4: Plutons of the Klamath Mountains
- 14.8: Detailed Figure Descriptions
- 9.2: Ancient Seas Form the Oldest Rocks

volcanic_activity
- 11.5: Cenozoic Events

volcanics
- 6.4: Mesozoic California (250 – 66 Ma)- Subduction and Mountain Building

volcanism
- 10: Klamath Mountains
- 15.2: Tectonics and Geologic History of the Peninsular Ranges Province
- 15.6: Chapter Summary
- 6.6: Chapter Summary
- 8.5: Rift-Related Volcanism in Eastern California
- 8.7: Chapter Summary

volcanoes
- 1: Introduction to the Geology of California
- 3: Plate Tectonics

vulnerability
- 19.9: Chapter Summary

W

water
- 13.7: Water in the Desert
- 18: California's Water
- 18.6: Understanding California's Water Landscape

water contamination
- 18.5: Threats to California's Water

water cycle
- 18.1: The Hydrologic Cycle
- 18.8: Detailed Figure Descriptions

water infrastructure
- 18.4: Water Infrastructure and Management

water management
- 12.4: Natural Hazards of the Great Valley Province
- 17.3: The Present
- 18.2: Running Water
- 18.4: Water Infrastructure and Management
- 18.6: Understanding California's Water Landscape
- 18.8: Detailed Figure Descriptions

water quality
- 18.2: Running Water
- 18.5: Threats to California's Water
- 18.7: Chapter Summary
- 18.8: Detailed Figure Descriptions

water scarcity
- 17.5: Hotter, Drier, Tougher

water supply
- 15.5: Natural Resources of the Peninsular Ranges
- 17.3: The Present
- 18.3: Groundwater

water table
- 18.3: Groundwater

wave
- 16.8: Detailed Figure Descriptions

wave dynamics
- 16.1: Coastal Processes
- 16.8: Detailed Figure Descriptions

wave refraction
- 16.6: The Edge of California
- 16.7: Chapter Summary

weather
- 17.1: Note on Usage

Weather Patterns
- 17.3: The Present

weathering
- 13.4: Wind Driven Sediment Transport
- 13.6: Erosional Desert Land Forms

white mountains
- 17.2: The Past

wilderness areas
- 10: Klamath Mountains

wildfire
- 17: California's Climate

wildfires
- 12.4: Natural Hazards of the Great Valley Province
- 17.5: Hotter, Drier, Tougher

Wilmington Field
- 14.6: Mineral and Petroleum Resources of the Transverse Ranges Province

Wilson Cycle
- 8.2: Rifting in the Basin and Range

wind erosion
- 13.4: Wind Driven Sediment Transport

Y

Yosemite
- 9: Sierra Nevada
- 9.6: Ice Shapes the Landscape
- 9.8: Chapter Summary

young volcanics
- 9.5: Volcanic Features of the Sierra Nevada

This page titled Index is shared under a CC BY-NC 4.0 license and was authored, remixed, and/or curated by Allison Jones.

GLOSSARY

A

abrasion | The grinding and scarping of a rock surface by the friction and impact of rock particles carried by water, wind, and/or ice.

accreted terrane | An island arc or microcontinent that has been accreted to a continent.

accretion | The accumulation of material onto another object. In geology: the accretion of material to the overriding plate during subduction.

accretionary prism | A mass of material accreted from the top of the subducting slab at a suduction zone.

accretionary wedge | A mass of material accreted from the top of the subducting slab at a suduction zone.

active margin | A plate boundary close to a continental margin

age | The smallest geochronologic unit by which the geologic time scale is divided.

alkalinity | The measure of the pH of material. pH = 7 is neutral. Materials with pH>7 are alkaline.

allochthon | A block of rocks that have been transported a great distance from where they formed.

alluvial fan | A triangle-shaped deposit of gravel, sand, and even smaller pieces of sediment. [CC BY-SA 3.0; Mikenorton]

alluvium | A deposit of clay, silt, sand, and gravel left by flowing streams in a river valley or delta, typically producing fertile soil.

Alquist-Priolo Act (AP Act) | California legislation involving restrictions in building near faults; enacted following the 1971 San Fernando Valley quake

amphibolite | A rock composed largely or dominantly of minerals of the amphibole group; can be applied to rocks of either igneous or metamorphic origin

amu | (atomic mass unit); A unit of mass used for expressing atomic and molecular weights.

Andean type subduction | Oceanic lithosphere subducts beneath continental lithosphere producing a continental arc mountain range.

andesite | An intermediate, extrusive igneous rock.

andesitic | Of a composition similar to andesite.

angle of repose | The steepest angle of descent or dip relative to the horizontal plane on which the material can be piled without slumping

angular unconformity | Where horizontally parallel strata of sedimentary rock are deposited on tilted and eroded layers, producing an angular discordance with the overlying horizontal layers.

anthropogenic | Caused by Homo sapiens

anticline | A fold that is generally convex upward, whose core contains the stratigraphically older rocks.

antiform | A fold that is convex upward and for which the ages of the rocks are unknown.

aphanitic | Fine grained igneous texture; the mineral crystals are too small to be seen with the naked eye.

aquifer | A body of permeable rock which can contain or transmit groundwater.

Arctodus simus | The "short-faced bear," an extinct Pleistocene bear much larger than modern grizzly or polar bears

arete | A sharp ridge left by the erosion of glaciers on either side.

ARkstrom | A term used by the USGS to describe giant atmospheric river events, such as the flooding of 1861-1862

arokosic | A sandstone with a considerable amount of feldspar (at least 25%).

artificially induced seismicity | earthquakes created by human activity (e.g., injection of fluids into hot rock in petroleum fracking)

aseismic creep | ground movement along faults without corresponding earthquakes

ash | The smallest size of particle ejected from a volcanic eruption; particles less than 2mm in diameter, composed of rock, mineral and glass particles.

assimilation | In geology: country rock with a different composition is added to magma.

asthenosphere | A layer in Earth's mantle known for its ductility and thought to be a key to the mechanics of plate tectonics

atmospheric river | A weather phenomenon involving multiple successive storms flowing into the West Coast, often resulting in flooding in California

atoll | A ring-shaped island or series of islands, made of coral, surrouding a lagoon.

atomic mass | The total number of protons and neutrons in an atom.

atomic mass unit | (amu); A unit of mass used for expressing atomic and molecular weights.

atomic number | The number of protons in an atom.

axial plane | See axial surface. A planar surface that connects the hinge lines of the strata in a fold

axial surface | See axial plane. A surface that connects the hinge lines of the strata in a fold.

B

back-arc | Located adjacent to a volcanic arc, on the side away from the subduction zone.

bajada | A broad slope of alluvial material at the foot of an escarpment or mountain.

basalt | A mafic, extrusive igneous rock.

basaltic | Of a composition similar to basalt.

batholith | A very large body of intrusive igneous rock, composed of multiple plutons of similar composition and appearance.

bedload | The discharge of sediment particles which are too heavy to be suspended by the turbulent action water or wind flow.

biochemical sedimentary rocks | Sedimentary rocks formed from biologic processes; examples range from pieces of clam shells fused together into a solid mass to microscopic radiolaria fusing into chert

biozone | An interval of geological strata that are defined on the basis of their characteristic fossil taxa.

blind thrust fault | A thrust fault in which the surface exposure is obscured by fault movement

blueschist | A rare metamorphic rock formed in subductionn zones under high pressure but low temperature, allowing the growth of distinctively-blue glaucophane; often called a glaucophane schist; found in metamorphosed former oceanic crust in the Franciscan Complex; notable California exposures include Ring Mountain, Tiburon.

boiling pool | A type of hot spring that exhibits bubbling behavior

boulder | A rock fragment greater than 256 mm in diameter

braided fluvial environment | A river system comprised of multi-threaded channels that branch and merge to create the characteristic braided pattern. Braided channels are highly dynamic with mid-channel bars which are formed, consumed, and re-formed continuously. Such channels form on relatively steep slopes when compared ot meandering rivers, and have a higher capacity to move sediment in the bedload, suspended load, and disolved load of the stream.

breakwater | A structure built parallel to the shore, some distance away from the shore, to effect a wave calming area between it and the beach

breccia | Angular framents of rock.

brittle Failure | Deformation by fracturing (discontinous deformation)

C

caldera | A large hollow basin that forms from the evacuation of a magma chamber during a large volcanic eruption.

cap rock | A layer of hard impervious rock overlying and often sealing in a deposit of oil, gas, or coal.

carbon capture and sequestration | The process of capturing and storing atmospheric carbon dioxide. It is one method of reducing the amount of carbon dioxide in the atmosphere with the goal of reducing global climate change.

carbonate | A mineral with the CO32- anion complex.

carbonate reef | A coral reef is made of thin layers of calcium carbonate and/or magnesium carbonate.

carbonatite | A type of intrusive or extrusive igneous rock defined by mineralogic composition consisting of greater than 50% carbonate minerals.

Cascadia Subduction Zone | The location where the Juan de Fuca Plate suducts beneath the North American Plate; extends from Cape Menocio to Britsh Columbia.

cataclasite | A fine grained, cohesive metamorphic rock, formed due to the local metamorphism in fault zones.

chemical sedimentary rocks | Sedimentary rocks formed abiologically from chemical precipitates, often forming in hot water (e.g., geyserite formed from hot spring containing water saturated with dissolved silica)

chert | A hard sedimentary rock formed from microcrystalline silica; in the California Franciscan context, chert is often biogenic in origin, deriving from the recrystallized remains of silica-shelled radiolaria, a single-celled organism that thrives in equatorial waters

cinder cone | Volcano formed from the accumulation of scoria (cinders) around a single eruptive vent; steep conical hill with a prominent crater.

cirque | A bowl-shaped, amphitheater-like depression that a glacier carves into a mountain or valley sidewall at high elevations.

clast | An individual constituent, grain, or fragment of rock produced by the weathering of a larger rock mass.

clastic | Pertaining to a rock or sediment composed of fragments derived from pre-existing rocksor minerals.

Clear Lake volcanic field | A region north of San Francisco noted for its recent volcanic activity and current geothermal energy production.

climate | A statistical pattern in long-term conditions of precipitation, temperature, etc.

climate change | Long-term variations in climate; in the contemporary world, due to anthropogenic gases.

climate forcing | An external factor exerting an influence on climate, such as orbital variation and changes in greenhouse gases.

climate response | The complex and sometimes nonlinear reaction to climate forcing.

coal | A black or dark brown rock composed of carbonized plant matter, often used as fuel due to it's combustibility.

cobble | A fragment of rock greater than 64 mm and less than 256 mm in diameter.

coeval | Having the same age or date of origin; rocks forming at the same time in different places.

composite cone | An alternate term for composite volcano.

composite volcano | A large volcanic edifice consisting of multiple vents formed over thousands or millions of years and composed of a variety of volcanic materials of a varitey of compositions.

conchoidal fracture | A break along a curved surface which has the properties of a conchoid (a specific mathmatically defined curve), which resembles a scallop shell.

continent-continent convergent boundary | A tectonic environment where two continents collide (e.g., the Indian Plate converging into the Eurasian plate)

continental crust | Thicker, less dense crust which forms earth's continents and continental shelves.

continental drift | A term now supplanted by the theory of plate tectonics describing relative movement of the crust of the Earth; Alfred Wegener first used the term continental drift (*Kontinentalverschiebung*).

continental rift | A region within a continent where continental crust begins to thin and split apart.

continental shelf | A portion of a continent that is submerged under an area of relatively shallow water.

continental volcanic arc | A chain of volcanoes found on continental plate margins that are located along subduction zones.

convergent boundary | A boundary where tectonic plates move toward each other.

coral | A sedentary aquatic invertibrate which secretes a carbonate external skeleton; can also refer to the structure produced by the carbonate secretions, such as a coral reef.

Coriolis effect | The phenomenon of warping/bending due to the rotation of the Earth

country rock | The rock surrounding and igneous intrusion that was in place before the magma intruded.

craton | An old and stable part of the continental lithosphere that is often at the core of a continent.

crescent dune | Mounds of sand that are generally are wider than long and concave on the leeward side.

cross bedding | Layering within a stratum and at an angle to the main bedding plane.

D

dacite | An extrusive igneous rock with composition between feslsic and intermediate.

dacitic | A rock with a composition similar to dacite.

debris flow | Water-laden masses of soil and fragmented rock that are carried down mountainsides and funneled into stream channels.

deflation | Lifting and removal of loose material from the surface by wind turbulence

deformation | General process for folding, faulting, shearing, comrpession, or extension of rocks as a result of various natrual forces (such as confining pressure and temperature)

delta | A landform shaped like a triangle, created by the deposition of sediment that is carried by a river and enters slower-moving or stagnant water. This occurs when a river enters an ocean, sea, estuary, lake, reservoir, or another river that cannot carry away the supplied sediment.

dendrochronology | The study and dating of tree rings; particularly useful for climate studies.

density | Mass per unit volume; a physical property calculated by the division of mass by volume; SI units are kg/m3 but usually expressed as g/cm3

desert pavement | A desert surface covered with closely packed, interlocking angular or rounded rock fragments of pebble and cobble size.

desert varnish | Orange-yellow to black coating found on exposed rock surfaces in arid environments.

detachment fault | Gently dipping normal faults associated with large scale extension; also referred to as “low angle normal faults”

detrital sedimentary rock | see clastic sedimentary rock

detritus | An individual constituent, grain, or fragment of rock produced by the weathering of a larger rock mass.

diabase | a mafic igneous rock with a small but visible crystal size indicating medium cooling rates; diabase's crystal size falls between aphanitic (microscoping) basalt and phaneritic (easily visible) gabbro

diamictite | a general term for a sedimentary rock consisting of nonsorted to poorly sorted terrigenous sediment. Particle sizes may range from clay to boulders, and are suspended within a matrix of mudstone or sandstone.

diapir | a domed formation in which a core of rock or magma has moved upward to pierce the overlying strata.

diatom | A microscopic, single-celled alga of the class Bacillariphyceae (ochrophytes), which lives in freshwater or marine environments. Diatoms secrete walls of silica, called fustules. Although diatoms are known from the Jurassic Perid, they first became abundant in the Cretaceous, ranging to the present.

differential erosion | The unequal erosion occurring at shorelines, primarily due to wave refraction

dike | 1) A sheetlike igneous intrusion that does not follow existing bedding structures; 2) A wall or embankment built to prevent flooding.

dip | The angle that a planar feature makes with the horizontal, measured perpendicualr to the strike and in the vertical plane.

dip-slip fault | A fault on which the movement is parallel to the dip of the fault.

disconformity | A boundary between parallel layers of sedimentary rocks which represents a period of erosion or nondeposition

divergent boundary | A boundary where tectonic plates move away from each other

drainage basin | a region or area occupied by a drainage system, such as a river or stream

drainage divide | a boundary between drainage basins

dropstones | isolated rock fragments that are found within finer layers; often distorts the layers below as if dropped into soft sediment.

ductile Failure | Visable solid-state deformation produces a change in the size and shape of a rock body without fracturing. Usually occurs where temperatures and pressures are high.

E

earthquake | a motion or trembling of the Earth caused by the abrupt release of accumalated strain energy

earthquake weather | An informal term for a phenomenon which does not exist; there is no connection between weather conditions and earthquakes

eclogite | A metamorphic rock consisting of pyroxene omphacite and pyrope-rich garnet.

edifice | A building or structure; in geology: the structure of a volcano; usually a mountain or hill.

effusive | In geology: nonexplosive ourpouring of lava.

emergent shoreline | A shoreline in which processes of tectonic uplift and/or sea level drop exceed the tendency of fierce wave erosion to level shorelines; typical of California coasts

eolian | Wind blown

eon | The largest (formal) geochronologic time unit.

epoch | The smallest geochronologic unit which subdivides Periods.

era | The second largest geochronologic time unit.

erosion | The removal or soil, rock and other material from an area.

erratic | See glacial erratic.

escarpment | a steep slope or long cliff that results from faulting.

evaporite | Water-soluble sedimentary mineral deposit that results from concentration and crystallization by evaporation from an aqueous solution.

exotic | Originating from far away.

explosive | Able or likely to shatter violently or burst apart.

extrusive | Erupted at the surface of the earth and cooled to solid above ground.

F

fault | a boundary between two bodies of rock along which there has been relative motion.

felsic | Low in iron and magnesium and high in silica.

Field Act | California legislation involving restrictions in unreinforced masonry school buildings; enacted following the 1933 Long Beach quake

fire fountain | A jet of lava sprayed into the air by the rapid formation and expansion of gas.

flank | In the context of volcanoes: the slope of side of the volcanic edifice.

flash floods | A rapid flooding of low-lying areas: washes, rivers, dry lakes and depressions.

fluvial environment | A continental environment that is closely connected to the erosive and depositional activity of rivers, streams and are associated with gravity flow processes.

flux melting | Melting that results when a chemical compound is added which lowers the melting temperature of the material.

fold mountain range | Orogenic belt

footwall | The footwall of a fault contains the rocks on the lower side of an inclined/tilted fault plane.

forearc | The location between the suduction zone and the resulting magmatic arc.

fractionation | Minerals crystallize and settle to the bottom of the magma chamber, leaving the remaining melt depleted of those ions.

Franciscan Complex | a complicated, mutli-facted rock unit found in western California, typically made of metamorphosed sea floor rocks accreted onto North America

fumerole | A vent in the surface of the Earth or another rocky planet from which hot volcanic gases and vapors are emitted, without any accompanying liquids or solids.

fusulinid | An extinct order of single-celled organisms, which produced calcareous hard parts.

G

gabbro | Mafic, intrusive igneous rock.

gabbro | a mafic igneous rock with phaneritic (large, visible) crystals, indicating a slow coolilng rate

Geographically Weighted Regression | A spatial analysis technique that takes non-stationary variables into consideration (e.g., climate; demographic factors; physical environment characteristics) and models the local relationships between these predictors and an outcome of interest.

geosphere | The rocky part of planet Earth

geothermal | Related to heat within the earth.

ghost forest | a phenomenon associated with the 1700 Cascadia quake, where land dropped in such a way that living trees were inundated with salt water, killing them

glacial erratic | Rocks that have been transported by ice and deposited elsewhere.

glacial outwash | Sediment transported by the meltwater from a glacier.

glaciation | A episode of relatively cold climate and glacial advance.

glacier | A persistent body of dense ice, formed by the the accumulation and compaction of snow, which is constantly moving under its own weight.

glass | A brittle, transparent or translucent noncystalline solid, usually consisting of silicates.

Global Positioning System (GPS) | A global system of U.S. navigational satellites developed to provide precise positional and velocity data and global time synchronization for travel; it is widely used in earth sciences to measure ground motion.

global warming | a problematic term that implies every place in the world is warming; climate change may, in fact, create some colder areas

graben | Aa fault block, generally elongate, that has been lowered relative to the blocks on either side without major disturbance or pronounced tilting.

graben | An elongate, depressed crustal unit or block bounded by faults on its long sides.

granite | A plutonic rock which contains 10-50% quartz.

granule | A rock fragment having a diameter in the range of 2-4 mm.

greenhouse gasses | Gasses that easily absorb longwave radiation and contribute to the greenhouse effect.

greywacke | a sedimentary rock with sandstone-range clasts often found in the Franciscan Complex, consisting of significant amount of clay and rock fragments, which indicate a relative immaturity of the rock

groin | A structure built perpendicular to the beach, which acts to trap sand on one side and erode sand on the other

groundmass | The majority of smaller mineral crystals that surround the larger phenocrysts in a porphyritic igneous rock.

H

halide | A mineral whose anion is one of the halogen elements: chlorine, fluorine, bromine, etc.

hanging wall | The hanging wall of a fault contains the rocks on the upper side of an inclined/tilted fault plane.

hazard | A geologic process which may present a threat to human civilization.

headland | A shoreline feature jutting out into the ocean

high-grade | High-grade metamorphic rocks are formed by high temperatures and pressures and are characterized by the creation of new minerals.

hinge | The locus of maximum curvature in a fold.

horst | A type of valley and range topography created when the earth's crust is pulled apart.

horst | An elongate, relatively uplifted crustal block that is bounded by faults on its long sides.

hot spring | A location where geothermally heated groundwater emerges at the surface of the earth.

hotspot | A volcanic center that persists for at least a few tens of millions of years that is thought to be the surface expression of a rising mantle plume. They are not associated with volcanic arcs. They may or may not be associated with oceanic ridges.

hummock | A small knoll or mound above ground, typically less than 15 meters in height, which tend to appear in groups or fields.

hummocky | An area with small knolls or mounds which may have been formed along a mass of ice.

hydrocarbons | Compounds of hydrogen and carbon, such as those which are the chief components of petroleum and natural gas.

hydrothermal | Related to hot water.

I

igneous rock | Rock formed from the cooling and solidification of molten magma or lava.

immature (sediment) | Asediment that s not uniform in appearance because the sediment grains are of varied sizes and shapes, and may have a large range of compositions

index-fossil | The fossilized remains or traces of particular plants or animals that are characteristic of a particular span of geologic time or environment, and can be used to identify and date the containing rocks.

inselberg | An isolated rock hill, knob, ridge, or small mountain that rises abruptly from a gently sloping or virtually level surface.

instrusive | Cooled to solid within the earth.

intensity | A measure of the effects of an earthquake at a particular place. It depends on the earthquake magnitude, distance from the epicenter, and local geology.

intraplate | Within a tectonic plate

island arc | A curved chain of islands rising from the deep ocean floor.

isoclinal | denoting a fold of strata so acute that the two limbs are parallel.

J

jetty | A structure built perpendicular to the beach, often in pairs protecting the mouths of rivers or harbors.

joint | a boundary between two bodies of rock along which there has not been relative motion.

Juan de Fuca Plate | A small tectonic plate consisting entirely of oceanic lithosphere formed at the Juan de Fuca Ridge and subducting beneath the North American Plate at the Cascadia Subduction Zone.

K

Kerogen | A complex fossilized organic material, found in oil shale and other sedimentary rock, which is insoluble in common organic solvents and yields petroleum products on distillation.

King Tides | an informal term for tidal phenomenon involving exceptional ranges of highs and lows; involves gravitational influence of moon and sun aligned with their elliptical orbits.

L

lagoon | A body of water seperated from the sea by a sandbank or coral reef.

lahar | An Indonesian term that describes a hot or cold mixture of water, volcanic ash, rock fragments, and other debris that flows down the slopes of a volcano and typically enters a river valley.

land subsidence | a gradual settling or sudden sinking of the Earth's surface owing to subsurface movement of earth materials. Usually occurs due to fluid extraction, such as water or oil, in fine-grained materials.

lava | Molten rock erupted from a volcano or vent above the surface of the earth.

lava dome | See volcanic dome.

lava tube | A natural conduit formed by flowing lava from a volcanic vent that moves beneath the hardened surface of a lava flow.

left-lateral | a description of fault movement, where when one stands on one side of an offset fault and looks to the opposite side, the sense of offset is to one's left; this is a relative definition and does not indicate which side is actually moving.

limb | The area of a fold between adjacent fold hinges.

limestone | A sedimentary rock made chiefly of the mineral calcite.

linear dune | Straight or slightly sinuous sand ridges typically much longer than they are wide.

liquefaction | the phenomenon of loose, wet soil losing its strength when subjected to seismic movement

lithic | Containing abundant fragments of previously formed rocks.

lithosphere | The outermost layer of the solid earth based on mechanical properties, which deforms brittly; includes the crust a small part of the mantle.

loess | Deposits of fine-grained wind-blown dust.

longshore current | The movement of water parallel to a beach, generated by the zig-zag motion of wave swash and wave backwash

longshore drift | The movement of sand parallel to a beach, driven by longshore currents

low grade | Low-grade metamorphic rocks are formed at low temperatures and pressures and are not as altered.

lower mantle | The part of the mantle below about 1,000 km in which the seismic velocity increases slowly with depth.

M

mafic | Rich in iron and magnesium and low in silica.

magma | Molten rock below the surface of the earth.

magmatic differentiation | Separation of molten rock into distinct chemical compositions.

magnitude | measure of the ground motion caused by an earthquake as measured on seismograms

Mammuthus columbi | A columbian mammoth, an extinct animal closely related to modern elephants, prevalent in North America until the end of the last Ice Age; not to be confused with wooly mammoths, which lived at much higher latitudes than California; columbian mammoths had much longer tusks than modern elephants, as well as a distinct prominence the crest of their heads

Mariana type subduction | Oceanic lithosphere subducts beneath oceanic lithosphere with an island arc and a back-arc spreading center.

marine incursion | Flooding of a continent by the ocean. This could be due to sea level rise or tectonic subsidence.

marine terraces | A series of former wave-cut platforms now exposed on land through a combination of tectonic uplift and/or sea level drop

mass extinction | A short period of geologic time in which a large percentage of species become extinct (or die out).

Mc | The minimum magnitude above which all earthquakes within a certain region are reliably recorded.

Mediterranean climate | A climate pattern characterized by wet, temperate winters punctuated by long, dry summers

megadrought | An informal term describing exceptionally dry conditions lasting over a period of many decades

mélange | A mixture of rock types which lacks continuous bedding and contains rock fragments of all sizes; results from tectonic shearing forces, usually at convergent plate boundaries.

Mendocino Triple Junction | the northern tectonic end of the San Andreas fault, where three plates (North American, Pacific, Juan de Fuca) meet in one spot; currently located offshore from Cape Mendocino

Mercalli Intensity Scale | a scale to measure the damage caused by an earthquake from observing its effect on people, the environment, and Earth's surface; reported as a Roman numerial from I to XII

metamorphic core complex | exposures of deep crust exhumed in association with extension via low angle normal faults..

metasediments | A metamorphic rocks of sedimentary origin.

mid-ocean ridge | A continuous mountain range extending through the North and South Atlantic Oceans, the Indian Ocean, and the South Pacific Ocean. It is the source of new crustal material.

Milankovitch cycles | three orbital parameters (eccentricity, obliquity, precession), which in combination can exert climate forcing observable in the geologic record

mineral | A naturally occuring, inorganic, crystalline solid with a defined chemical composition.

miogeocline | Marine sedimentation along a passive margin.

ML | The symbol for local magnitude. Local magnitudes are based on the maximum amplitude of the ground shaking, without distinguishing the different seismic waves.

Moho | Informal name for the Mohorovičič discontinuity

Mohorovičič discontinuity | The boundary between the crust and the mantle; the location within Earth where P-wave velocities abruptly change

from a range of 6.7 to 7.2 km/s to greater than 7.6 to 8.1 km/s

moment magnitude scale | A logarithmic scale to measure of the relative size of an earthquake based on ground motion, area ruptured, fault slip, and properties of the rock; now the standard way to report the magnitude of an earthquake

monocline | A local steepening in an otherwise flat or shallowly dipping area.

moraine | A mass of rocks and sediment carried and deposited by a glacier, typically as ridges at its edges or front.

moraine | An accumulation of till in currently or formerly glaciated regions, typically forming a ridge.

mud pot | A type of acidic hot spring that takes the form of a pool of bubbling mud as a result of the acid and microorganisms decomposing surrounding rock into clay and mud.

mudstone | A sedimentary rock primarily composed of mud-sized clasts. It contains no laminations.

Mw | The symbol for Moment Magnitude, a logarithmic scale to measure of the relative size of an earthquake based on ground motion, area ruptured, fault slip, and properties of the rock; now the standard way to report the magnitude of an earthquake

mylonite | a foliated and often lineated rock with evidence for ductile deformation.

N

native mineral | A mineral with only one element such as gold, copper, sulfur, or carbon.

niche | The specific environmental condtions for which a species is adapted.

nonconformity | A boundary between sedimentary rocks and metamorphic or igneous rocks when the sedimentary rock lies above and was deposited on the pre-existing and eroded metamorphic or igneous rock.

normal fault | a dip-slip fault in which the block above the fault (the hanging wall) has moved downward relative to the block below (the footwall).

normal fault | A fault in which the hanging wall has moved downward relative to the footwall.

North American Plate | The tectonic plate that inlcudes most of North America and part of the Atlantic Ocean.

North Pacific High | an area of long-lasting high atmospheric pressure that develops off the California coast and is responsible for diverting clouds and precipitation

O

obduction | The process by which oceanic lithosphere is thrusted above or into continental lithosphere; not to be consfused with the common word, "abduction".

oblique slip fault | A fault on which the slip is has components of both strike-slip and dip-slip.

obsidian | A rock consisting of volcanic glass.

ocean acidification | Increased carbon dioxide in the atmosphere dissolves in the ocean producing carbonic acid and decreasing ocean pH.

ocean-continent convergent boundary | A convergent plate boundary where an oceanic plate and a continental plate are colliding.

oceanic crust | The crustal rocks that underlie the ocean basins.

oil reserves | An estimate of the amount of crude oil located in a particular economic region with the potential of being extracted. Reserves are calculated based on a proven probable basis and oil pools situated in unattainable depths are not considered part of a nation's reserves.

Olenelloidea | Superfamily of trilobites, a group of extinct marine arthropods.

olistostrome | A sedimentary deposit resulting from a submarine landslide.

oncoids | A coated grain of algal (but not red algal) or microbial origin that is coarser than 2 mm in diameter.

ophiolite | A terrane or part of a terrane that consists of oceanic lithosphere.

orogenic belt | A region subjected to folding and other deformation during an orogenic cycle.

orogeny | a mountain-building event

orographic | Relating to mountains.

orographic precipitation | the phenomenon of precipitation falling as clouds are forced to higher altitudes as they pass over mountains

oxide | A mineral with oxygen as its anion. This excludes minerals with oxygen complexes such as carbonate, sulfate, or silicate.

P

P wave | The type of seismic wave that involves alternating compression and expansion in the direction of propagation.

Pacific plate | the largest of Earth's tectonic plates, spanning Asia to the west and California to the east

paleoearthquake | Old earthquakes that have happened 1000's of years ago.

paleoseismic | The study of past earthquakes using soil and rock records.

palinspastic | a reconstruction of past tectonic movement that recreates the original position of rock units before they were displaced

Pangea | A supercontinent existing from approximately 335 million years ago to 175 million years ago

passive continental margin | The transition from continental crust to oceanic crust within a plate (as opposed to active margins which coincide with the edge of a plate.

passive margin | The edge of a continent that does not experience tectonic activity (e.g. subduction, collision).

pebble | A rock fragment having a diameter in the range of 2-4 mm.

pediment | Very gently sloping inclined bedrock surface.

peridotite | Ultramafic, intrusive igneous rock; the rock that makes up Earth's mantle.

Period | A major rank below an Era and above an epoch.

permeability | The state or quality of a material or membrane that causes it to allow liquids or gases to pass through it.

Petroleum System | Encompasses a pod of active source rock and all genetically related oil and gas accumulations defined by the essential elements (source, reservoir, seal) and processes (generation-migration-accumulation).

Petroleum System | A genetic relationship lining s source rock to all oil and gas it has genrated. It consists of all the geologic elements (carbon) and processes (heat, pressure and time) that re essential for the formation of a petroleum accumulation

Phanerozoic | Phanerozoic means ‘visible life’ and is the current Eon on the geologic time scale having started 541 million years ago.

phenocryst | A mineral crystal in a porphrytic igenous rock wich is larger than a surrounding groundmass of smaller mineral crystals.

phosphate | A mineral with the PO44- anion complex.

plagioclase feldspar | one of the major rock forming silicate minerals, consisting of a range of Na to Ca with a core of aluminium and silicate

plankton | The small and microscopic organisms drifting or floating in the sea or fresh water, consisting chiefly of diatoms, protozoans, small crustaceans, and the eggs and larval stages of larger animals.

plate boundary | Zone of seismic and tectonic activity along the edges of lithospheric plates.

plate tectonics | the theory that the outer layers of Earth move relative to each other

plateau | An region of high, flat topography.

playa | A dry, vegetation-free, flat area at the lowest part of an undrained desert basin.

plug dome | See volcanic dome.

plunging fold | A fold in which the hing line is inclined (not horizontal).

pluton | A body of intrusive igneous rock.

plutonic | Of an intrusive igneous nature.

porosity | The quality or degree of having minute spaces or holes through which liquid or air may pass.

porphyritic | An ingneous texture in which some mineral grains, called phenocrysts, are much larger than the majority of the grains, called the groundmass.

Prevailing Westerlies | Prevailing winds that blow from the west at midlatitudes.

primary wave | The type of seismic wave that involves alternating compression and expansion in the direction of propagation.

Principle of Baked Contacts | The principle stating that the heat of an intrusion will bake (metamorphose) the rocks in close proximity to the intrusion.

Principle of Chilled Margins | A principle that states that the portion of an intrusion that has cooled and crystallized next to cold surrounding rock will form smaller crystals than the portion of the intrusion that cooled more slowly deeper in the intrusion, which will form larger crystals.

Principle of Cross-cutting relationships | A principle of geology that states that the geologic feature which cuts another is the younger of the two features.

Principle of Faunal Succession | A principle of geology that states that fossilized flora and fauna preserved in sedimentary rocks succeed each other vertically in a specific, reliable order that can be identified over wide horizontal distances.

Principle of Inclusion | A geologic principle that states that clasts in a rock are older than the rock itself.

Principle of Lateral Continuity | A principle of geology that states that layers of sediment initially extend laterally in all directions; in other words, they are laterally continuous

Principle of Original Horizontality | A principle of geology that states that layers of sediment are originally deposited horizontally under the action of gravity

Principle of Superposition | A principle of geology that states that in undeformed stratigraphic sequences, the oldest strata will lie at the

bottom of the sequence, while newer material stacks upon the surface to form new deposits over time.

pseudomorph | A mineral whose outward crystal form is that of another mineral; it is described as being "after" the mineral whose outward from it has, e.g. quartz after fluorite.

pull-apart basin | a structural basin where two overlapping (en echelon) strike-slip faults or a fault bend creates an area of crustal extension undergoing tension, which causes the basin to sink down.

pumice | A highly vesicular rock composed of volcanic glass.

pyroclastic | A volcanic texture composed of fragments of a variety of volcanic materials.

pyroclastic flow | A dense, destructive mass of very hot ash, lava fragments, and gases ejected explosively from a volcano and typically flowing downslope at great speed.

Q

quartzite | a hard, non-foliated metamorphic rock which was originally pure quartz sandstone.

R

radiative forcing | the net balance of solar energy entering and exiting Earth; positive radiative forcing means that more energy is coming in than leaving, which is the current condition due to anthropogenic gases

radioisotope | An isotope that has excess nuclear energy, usually due to the number of neutrons in its nucleus, making it unstable.

radiolaria | a singled-celled marine organism which constructs a shell from silica extracted from sea water; radiolaria prefer warm, equatorial waters

radiolarian chert | a silica-rich rock compared of recrystallized fossils of microscopic radiolaria

radiometric dating | The fundamental method of geochronology.

rain shadow | An area of significantly reduced rainfall behind a mountainous region, on the side facing away from prevailing winds, known as its leeward side.

rare earth element | One of 17 metallic elements that include nclude the fifteen lanthanides on the periodic table plus scandium and yttrium

reef | A ridge of jagged rock or coral near the surface of the ocean or other body of water.

relative dating | A process by which the age of one geologic unit is determined relative to that of another.

releasing bend | a curve in a strike-slip fault that creates areas of tension and normal faults; associated with land being lowered, sometimes resulting in sag ponds

reservoir rock | In petroleum geology, any porous or permeable rock that yields oil or gas. Sandstone, limestone, and dolomite are common reservoir rocks, but in California, high-porosity, low permeability diatomite can also be a good reservoir rock.

restraining bend | a curve in a strike-slip fault that creates areas of compression and reverse faults; associated with ridges and mountains being raised

reverse fault | a fault in which the hanging wall moves up relative to the foot wall; this is a relative definition and does not specific which wall is actuall moving

rhyolite | A felsic, extrusive igneous rock.

rhyolitic | Of a composition similar to rhyolite.

Ridiculously Resilient Ridge | a tongue-in-cheek term for exceptionally strong atmospheric pressure formations (see North Pacific High)

rift valley | A lowland region that forms where Earth's tectonic plates move apart, or rift. Rift valleys are found on land and at the bottom of the ocean.

right-lateral | a description of fault movement, where when one stands on one side of an offset fault and looks to the opposite side, the sense of offset is to one's right; this is a relative definition and does not indicate which side is actually moving; many major faults in California, such as the San Andreas, Calaveras, and Hayward, are right-lateral faults

rip current | The phenomenon of water moving swiftly away from the beach, perpendicular to the beach, in a narrow flow; a common cause of drowning

rip-rap | An anti-erosion construction composed of large boulders

Rivera Triple Junction | the southern tectonic end of the San Andreas fault, where three plates (North American, Pacific, Cocos) meet in one spot; currently located offshore south of Baja California

rock gypsum | A chemical sedimentary rock that forms from evaporation. It is composed of many crystals of the mineral gypsum.

rock salt | A chemical sedimentary rock that forms from evaporation. It is composed of many crystals of the mineral halite.

Rodinia | A supercontinent that incorporated almost all the landmasses on Earth for about 450 million years during the Proterozoic Eon (2.5 billion to 541 million years ago).

roof pendant | A mass of country rock that projects downward into and is entirely surrounded by an igneous intrusion such as a batholith or pluton.

roundness | The degree of abrasion of a clastic particle.

runoff | The draining away of water (or substances carried in it) from the surface of an area of land, a building or structure, etc.

S

salinity | concentration of dissolved solids (salts) in a solution.

saltation | A means of particle transport by fluids such as wind or water that occurs when loose materials are removed from a bed and carried by the fluid, before being transported back to the surface.

sand | A clast smaller than a granule (pebble) and larger than a silt grain, with a diameter of 1/16 to 2 mm.

sand ramps | An accumulations of sand sized sediment along the front of mountain ranges.

sand sheets | Flat or gently undulating sandy deposits with only small surface ripples

sandstone | A clastic sedimentary rock composed of grains of sand size.

scoria | A mafic rock with vesicular texture in which more than 50% of the rock is composed of vesicles.

sea arch | A semi-curved cut in the rock of a headland, formed by wave refraction creating differential erosion on the sides of the headland

sea caves | An indentation in a headland or a rocky coast created by wave erosion

sea stack | A remnant of a former headland, now disconnected from the mainland, isolated through differential erosion

sea-floor spreading | The movement of ocean crust away from one another at 1-10 mm per year.

seal rock | A rock whose petrophysical properties, mainly low permeability, make it capable of impeding the upward migration of oil or gas.

seawall | A structure built on land, parallel to the beach, intended to take the impact of waves and forestall wave erosion

secondary wave (S-wave) | a seismic shear wave where the particle motion is perpendicular, or at right angles, to the direction of wave propagation

sedimentary basin | A circular downfolded structure that has been filled with sediment and contains sedimentary rocks.

seismic moment | a measure of the size of an earthquake based upon properties of the rock, the area ruptured when a fault breaks, and the slip or displacement caused by the fault

seismic wave | a general term for energy waves caused by earthquakes, explosions, or machines used to artifically generate energy waves

seismogram | a recording of data from the arrival of earthquake waves or seismic waves

seismograph | a device that records data from the arrival of earthquake waves or seismic waves; seismographs have largely been replaced by computers directly recording data digitally

seismologist | a person who studies earthquakes or the movement of seismic wave energy

seismology | the study of earthquakes or of the movement of seismic wave energy

seismometer | a device to detect data from the arrival of earthquake waves or seismic wave energy; the data detected are now usually recorded on computers, but used to be recorded on seismographs

serpentine soil | Soil that develops where serpentinite or similar rocks are the dominant parent material; rich in heavy-metals relative to other elements.

serpentinite | a metamorphosed ultramafic rock which often presents in a variety of green colors, and has much lower density than its parent rock; serpentinite contains small amounts of chrysotile asbestos, in addition to minerals such as lizardite and antigorite; serpentinite is frequently weakk and easily fractured, making hills underlain by serpentinite particularly vulneralbe to landslides; serpentinite is the rock name, while serpentine is an adjective; California's official state rock

shale | A fine-grained clastic sedimentary rock, formed by the compaction of clay, silt, or mud. It is finly laminated.

shield volcano | A large volcanic edifice consisting of multiple vents formed over thousands or millions of years and composed mainly of basalt and having a broad, flat profile.

silica | A chemical compound of silicon and oxygen.

silicate | A compound whose crystal structure contains SiO_4 tetrahedra.

sill | A sheetlike igneous intrusion that intrudes between existing stratigraphic layers.

siltstone | a clastic sedimentary rock made mostly of silt and fine mud.

slab window | A gap in a subducted plate that forms when a spreading ridge intersects a trench.

slickenfibers | Linear mineral growths on a fault surface, formed during movement of the fault.

slickenlines | Linear striations on a smooth fault surface, formed by the movment of the fault.

slip rate | The average speed of the relative motion between footwall and hanging wall within a specified period

Smilodon californicus | an extinct Pleistocene predatory large cat, found in great numbers in California's La Brea Tar Pits

Smilodon fatalis | an extinct Pleistocene predatory large cat, found in great numbers in California's La Brea Tar Pits

snow water equivalent | the amount of water if a column of snow was melted instantaneously

soft-first story | a seismically vulnerable building design with the street-level floor open and with few supports, commonly designed this way to accommodate parking or retail space

sorting | The process by which particles are naturally separated from dissimilar particles by the agents of transportation.

source rock | Sedimentary rock in which organic material under pressure, heat, and time was transformed into liquid or gaseous hydrocarbons. Source rock is usually shale or limestone.

speleothems | A structure formed in a cave by the precipitation of minerals from water; examples include stalactites and stalagmites.

spheroidal weathering | A form of chemical alteration that affects jointed bedrock and results in the formation of concentric or spherical layers of highly decayed rock.

spreading center | A linear zone in the seafloor, typically found along a mid-ocean ridge, along which magma rises and from which adjacent crustal plates are moving apart.

spreading center | a tectonic area where two plates grow away from each other, with a volcanic line in between; also called a divergent tectonic boundary

Steam Injection (Enhanced Oil Recovery) | technology for producing heavy crude oil and bitumen. High pressure steam is continuously injected into the oil resrvoir to heat the oil and reduce its viscosity, causing the heated oil to mobilize and move to where it is pumped out.

stoss | The side of a dune or rounded feature that faces toward the source of a current

stratigraphic unit | A body of rock of similar rock type and similar charateristics formed within the same time range.

stratovolcano | An alternate term for composite volcano.

strike | The compass direction of a plane as it intersects a horizontal plane.

strike slip fault | Strike-slip faults involve motion which is parallel to the strike of the fault--frequently described as a "side-by-side" motion.

Stromatoperoid | An extinct clade of sea sponges common in the fossil record from the Middle Ordovician to the Late Devonian.[1] They can be characterized by their densely layered calcite skeletons lacking spicules.

subduction | The process of oceanic crust moving beneath another tectonic plate and into the mantle

sufate | A mineral with the SO42- anion.

suflide | A mineral with the S2- anion.

supercontinent | The assembly of most or all of Earth's continental blocks or cratons to form a single large landmass.

suspended load | The portion of sediment carried by a fluid turbulence (water or air) uplifted by the fluid's flow in the process of sediment transportation.Generally consists of smaller particles, like clay, silt, and fine sands.

synclinal Trough | A linear depression or basin that subsides as it receives clastic material, located not far form the source supplying the sediment.

syncline | A fold which the core contains the stratigraphically younger rocks; it is generally concave upward.

syncline | A fold of which the core contains the stratigraphically younger rock. It is generally concave upward.

synform | A fold whose limbs dip inward and for which the ages of the rocks are unknown.

T

tephra | All pieces of all fragments of rock ejected into the air by an erupting volcano.

terrain | An area of land considered in relation to its topography and surface features, especially as they relate to overland travel.

terrane | A fault-bounded area or region with a distinctive stratigraphy, structure, and geological history.

terrigenous | derived from land, as opposed to the ocean (marine).

thermal expansion | the change in size of objects depending on temperature

thin section | A slab of rock ground thin enough for light to pass through it, which is used to study rocks under a microscope.

three layer cake | An informal term to describe the soil disrupted by the 1700 Cascadia quake

thrust fault | a reverse fault (where the hanging wall moves up relative to the foot wall, commonly because of tectonic compression) with a very low angle

till | Glacial sediment.

tombolo | An island or sea stack that has reconnected to land via a sand spit deposited by the wave calming effects of the island or sea stack

Trade Winds | East-to-west prevailing winds that flow in the Earth's equatorial region. T

transform boundary | A plate boundary where plates slide past each other without new lithosphere being created, or old lithosphere being destroyed

transpression | A type of deformation that includes both pure shear (compression) and simple shear (shearing).

transpression | a tectonic condition where side-to-side movement also includes a percentage of compression; a tectonic change favoring transpression in the last few million years is a major reason for the promiment mountains and ridges found in the California Coast Ranges

transtension | A type of deformation that includes both extension and simple shear (shearing).

transtension | a tectonic condition where side-to-side movement also includes a percentage of expansion

transverse dune | A large, strongly asymmetrical, elongated dune lying at right angles to the prevailing wind direction.

trench | a tectonic feature of lowered crust associated with subduction; a California example is the

Trilobite | Extinct marine arthropod

triple junction | The point where three tectonic plates meet.

tsunami | Giant waves produced through tectonic action, volcanic eruption, or meteorite strike into the ocean

tufa | A form of microcrystalline limestone.

tuff | A volcaniclastic igneous rock.

Turbidite | Sediments transported and deposited by density flow generally tends to gradually change from coarse-grained at the base to fine-grained at the top of the sedimentary sequence and that was deposited by turbidity currents.

turbidity flows | a submarine movement of sediment downsope, depositing as a rock known as turbidite, a distinctive sedimentary deposit composed of alternatiing layers of clay and sand-sized clasts, often forming in repeated bands where the lower part of the band has larger grains that fine upwards to smaller grains

U

u-shaped valley | A valley with steep walls that curve into a reltively flat bottom, rembling the letter 'U' in profile; usually the result of glacial erosion.

ultamafic | very rich in iron and magnesium and low in silica.

ultramafic | The chemistry of the mantle; even richer in iron and magnesium (and lower in silica) than mafic rocks.

unconformity | A buried erosional or non-depositional surface separating two rock masses or strata of different ages, indicating that sediment deposition was not continuous.

upwelling | The phenomenon of deep, cold, nutrient-rich water rising to the surface waters because of the effects of wind direction and the Coriolis effect

V

vent | In the context of volcanoes: an opening in a volcanic edifice from which lava or pyroclastic material erupts.

ventifact | A rock that has been abraded, pitted, etched, grooved, or polished by wind-driven sand or ice crystals.

vesicle | A hole produced by a bubble of gas when the lava cools around the bubble.

vesicular | Having many vesicles

viscosity | The state of being thick, sticky, and semifluid in consistency, due to internal friction. In short, the resistance for a fluid to flow.

volcanic arc | A chain of volcanoes formed as a result of subduction, including volcanic island arcs as well as volcanic arc mountain ranges.

volcanic arc mountain range | A chain of volcanoes formed on a continent as a result of oceanic lithosphere subducting beneath contientnal lithosphere.

volcanic butte | An isolated hill or mountain resulting from the differential weathering or erosion and consequent exposure of a volcanic neck, or a of a narrow veritcal igneous instrusion overlying weaker rock

volcanic dome | A steep-sided, rounded accumulation of lava extruded from a volcano to form a dome-shaped or bulbous mass of congealed

laval above and aorund the vent. Commonly parasitic on the flanks of, or within the crater of, larger edifices

volcanic island arc | A chain of volcanic islands formed when one plate of oceanic crust subducts beneath another plate of oceanic crust

volcano | A structure such as a hill or mountain which forms around an individual vent or multiple vents from which lava or pyroclastic material emerges.

W

Walker Lane | A geologic trough roughly aligned with the California/Nevada border southward to where Death Valley intersects the Garlock Fault, a major left lateral, or sinistral, strike-slip fault.

wave amplitude | The height of a wave compared to the theoretical ocean level if no waves were present

wave backwash | The movement of waves down a beach face, back into the ocean

wave period | The time in seconds between successive waves

wave refraction | The warping and bending of waves due to “feeling bottom” in different places along the wavefront

wave swash | The movement of waves up a beach face

wave-cut platform | A flat submerged area subjected to breaking waves, often immediately between sandy beaches and deeper waters

wavelength | The distance in meters between two crests of two waves

waves “feeling bottom” | The phenomenon of waves interacting with the ocean bottom when the oncoming wave reaches depths less than one-half of the wavelength

weather | a short-term atmospheric event at a particular time in a particular place

Western Interior Seaway | The Western Interior Seaway [1] was a huge inland sea. It split North America into two halves for most of the mid- and late-Cretaceous Period. It was up to 2,500 feet (760 m) deep, 600 miles (970 km) wide and over 2,000 miles (3,200 km) long.

wildcatting | Wildcatting is a term used in the oil industry, where companies drill test wells for oil in unexplored or wild areas.

Wilson cycle | The cycle of continental rifting, the formation of a new ocean basin as rifting advances, followed by the closure of the ocean basin as plates collide

X

xenolith | A fragment of rock within a body of igneous rock that is different from the surrounding rock; originating as country rock that became incorporated into a body of magma without melting and assimilating.

This page titled Glossary is shared under a CC BY-NC 4.0 license and was authored, remixed, and/or curated by Allison Jones.

Interactive Geologic Time Scale

This page titled Interactive Geologic Time Scale is shared under a CC BY-NC 4.0 license and was authored, remixed, and/or curated by Allison Jones.

Interactive Geologic Map of California

This page titled Interactive Geologic Map of California is shared under a CC BY-NC 4.0 license and was authored, remixed, and/or curated by Allison Jones.

DETAILED LICENSING

Overview

Title: Geology of California

Webpages: 189

Applicable Restrictions: Noncommercial

All licenses found:

- CC BY-NC 4.0: 95.2% (180 pages)
- Undeclared: 4.8% (9 pages)

By Page

- Geology of California - *CC BY-NC 4.0*
  - Front Matter - *CC BY-NC 4.0*
    - TitlePage - *CC BY-NC 4.0*
    - InfoPage - *CC BY-NC 4.0*
    - Table of Contents - *Undeclared*
    - Licensing - *Undeclared*
    - Program Page - *CC BY-NC 4.0*
    - Preface - *CC BY-NC 4.0*
    - About the Authors - *CC BY-NC 4.0*
    - Acknowledgements - *CC BY-NC 4.0*
    - Land Acknowledgment - *CC BY-NC 4.0*
    - Licensing - *CC BY-NC 4.0*
    - Recommended Citations - *CC BY-NC 4.0*
  - 1: Introduction to the Geology of California - *CC BY-NC 4.0*
    - 1.1: How to Read California's Geologic Map - *CC BY-NC 4.0*
    - 1.2: Geologic Map Symbols - *CC BY-NC 4.0*
    - 1.3: Detailed Figure Descriptions - *Undeclared*
  - 2: Minerals and Rocks - *CC BY-NC 4.0*
    - 2.1: Minerals - *CC BY-NC 4.0*
    - 2.2: Mineral Properties - *CC BY-NC 4.0*
    - 2.3: The Rock Cycle - *CC BY-NC 4.0*
    - 2.4: Igneous Rocks - *CC BY-NC 4.0*
    - 2.5: Sedimentary Rocks - *CC BY-NC 4.0*
    - 2.6: Metamorphic Rocks - *CC BY-NC 4.0*
    - 2.7: Chapter Summary - *CC BY-NC 4.0*
    - 2.8: Detailed Figure Descriptions - *CC BY-NC 4.0*
  - 3: Plate Tectonics - *CC BY-NC 4.0*
    - 3.1: Earth's Interior - *CC BY-NC 4.0*
    - 3.2: Tectonic Plates, Plate Motions, and Plate Boundaries - *CC BY-NC 4.0*
    - 3.3: Mechanisms for Plate Motion - *CC BY-NC 4.0*
    - 3.4: California's Plates and Plate Boundaries - *CC BY-NC 4.0*
    - 3.5: Chapter Summary - *CC BY-NC 4.0*
    - 3.6: Detailed Figure Descriptions - *CC BY-NC 4.0*
  - 4: Geologic Structures and Seismology - *CC BY-NC 4.0*
    - 4.1: Stress and Strain - *CC BY-NC 4.0*
    - 4.2: Folding - *CC BY-NC 4.0*
    - 4.3: Jointing and Faulting - *CC BY-NC 4.0*
    - 4.4: Earthquakes - *CC BY-NC 4.0*
    - 4.5: Measuring Earthquakes - *CC BY-NC 4.0*
    - 4.6: Chapter Summary - *CC BY-NC 4.0*
    - 4.7: Detailed Figure Descriptions - *CC BY-NC 4.0*
  - 5: Geologic Time - *CC BY-NC 4.0*
    - 5.1: Relative Dating - *CC BY-NC 4.0*
    - 5.2: Unconformities - *CC BY-NC 4.0*
    - 5.3: Dating Rocks Using Fossils - *CC BY-NC 4.0*
    - 5.4: Absolute Dating of Geologic Materials - *CC BY-NC 4.0*
    - 5.5: The Geologic Time Scale - *CC BY-NC 4.0*
    - 5.6: Chapter Summary - *CC BY-NC 4.0*
    - 5.7: Detailed Figure Descriptions - *Undeclared*
  - 6: A Brief Geologic History of California - *CC BY-NC 4.0*
    - 6.1: Developing a Geologic History - *CC BY-NC 4.0*
    - 6.2: Precambrian California (4.6 Ga – 541 Ma) - *CC BY-NC 4.0*
    - 6.3: Paleozoic California (541 – 252 Ma) - *CC BY-NC 4.0*
    - 6.4: Mesozoic California (250 – 66 Ma)-Subduction and Mountain Building - *CC BY-NC 4.0*
    - 6.5: Cenozoic California (66 Ma – Present)-Faulting, Uplift, and Basin Formation - *CC BY-NC 4.0*
    - 6.6: Chapter Summary - *CC BY-NC 4.0*
    - 6.7: Detailed Figure Descriptions - *CC BY-NC 4.0*

- 7: Cascade Range and Modoc Plateau - *CC BY-NC 4.0*
  - 7.1: The Cascadia Subduction Zone and the Cascade Continental Volcanic Arc - *CC BY-NC 4.0*
  - 7.2: Rock Types of the Cascades - *CC BY-NC 4.0*
  - 7.3: The Variety of Volcanoes in the Cascades and the Modoc Plateau - *CC BY-NC 4.0*
  - 7.4: Volcanic Hazards - *CC BY-NC 4.0*
  - 7.5: Mount Shasta - *CC BY-NC 4.0*
  - 7.6: Lassen Volcanic National Park - *CC BY-NC 4.0*
  - 7.7: Medicine Lake Volcano - *CC BY-NC 4.0*
  - 7.8: Glaciers in the Cascades - *CC BY-NC 4.0*
  - 7.9: Chapter Summary - *CC BY-NC 4.0*
  - 7.10: Detailed Figure Descriptions - *CC BY-NC 4.0*
- 8: Basin and Range - *CC BY-NC 4.0*
  - 8.1: Regional Extent and Overview of the Basin and Range - *CC BY-NC 4.0*
  - 8.2: Rifting in the Basin and Range - *CC BY-NC 4.0*
  - 8.3: Rift-Related Faulting in Eastern California - *CC BY-NC 4.0*
  - 8.4: Sedimentary Products of Rifting in the Basin and Range - *CC BY-NC 4.0*
  - 8.5: Rift-Related Volcanism in Eastern California - *CC BY-NC 4.0*
  - 8.6: The Oldest Rocks in the Basin and Range - *CC BY-NC 4.0*
  - 8.7: Chapter Summary - *CC BY-NC 4.0*
  - 8.8: Detailed Figure Descriptions - *CC BY-NC 4.0*
- 9: Sierra Nevada - *CC BY-NC 4.0*
  - 9.1: The Sierra Nevada Today - *CC BY-NC 4.0*
  - 9.2: Ancient Seas Form the Oldest Rocks - *CC BY-NC 4.0*
  - 9.3: The Sierra Nevada Batholith - *CC BY-NC 4.0*
  - 9.4: Gold of the Sierra Nevada - *CC BY-NC 4.0*
  - 9.5: Volcanic Features of the Sierra Nevada - *CC BY-NC 4.0*
  - 9.6: Ice Shapes the Landscape - *CC BY-NC 4.0*
  - 9.7: Natural Hazards of the Sierra Nevada - *CC BY-NC 4.0*
  - 9.8: Chapter Summary - *CC BY-NC 4.0*
  - 9.9: Detailed Figure Descriptions - *CC BY-NC 4.0*
- 10: Klamath Mountains - *CC BY-NC 4.0*
  - 10.1: Assembling a Continent - *CC BY-NC 4.0*
  - 10.2: The McCloud Limestone- An Ancient Coral Reef - *CC BY-NC 4.0*
  - 10.3: The Josephine Ophiolite- A Little Slice of the Mantle - *CC BY-NC 4.0*
  - 10.4: Plutons of the Klamath Mountains - *CC BY-NC 4.0*
  - 10.5: Uplifting a Mountain Range - *CC BY-NC 4.0*
  - 10.6: Chapter Summary - *CC BY-NC 4.0*
  - 10.7: Detailed Figure Descriptions - *CC BY-NC 4.0*
- 11: Coast Ranges - *CC BY-NC 4.0*
  - 11.1: A Complicated Land - *CC BY-NC 4.0*
  - 11.2: The Coast Range Ophiolite - *CC BY-NC 4.0*
  - 11.3: The Great Valley Sequence - *CC BY-NC 4.0*
  - 11.4: The Franciscan Complex - *CC BY-NC 4.0*
  - 11.5: Cenozoic Events - *CC BY-NC 4.0*
  - 11.6: Quaternary Events - *CC BY-NC 4.0*
  - 11.7: Representative Coast Range Rocks - *CC BY-NC 4.0*
  - 11.8: Chapter Summary - *CC BY-NC 4.0*
  - 11.9: Detailed Figure Descriptions - *CC BY-NC 4.0*
- 12: Great Valley - *CC BY-NC 4.0*
  - 12.1: Geomorphology and General Overview of the Great Valley Province - *CC BY-NC 4.0*
  - 12.2: Geology of the Great Valley - *CC BY-NC 4.0*
  - 12.3: Soil, Streams and Agriculture - *CC BY-NC 4.0*
  - 12.4: Natural Hazards of the Great Valley Province - *CC BY-NC 4.0*
  - 12.5: Natural Resources of the Great Valley - *CC BY-NC 4.0*
  - 12.6: Chapter Summary - *CC BY-NC 4.0*
  - 12.7: Detailed Figure Descriptions - *CC BY-NC 4.0*
- 13: Mojave and Colorado Deserts - *CC BY-NC 4.0*
  - 13.1: Physiographic Features of the Mojave and Colorado Desert Provinces - *CC BY-NC 4.0*
  - 13.2: Geologic Overview and Evolution of the Mojave and Colorado Desert Provinces - *CC BY-NC 4.0*
  - 13.3: Creating the Desert Environment - *CC BY-NC 4.0*
  - 13.4: Wind Driven Sediment Transport - *CC BY-NC 4.0*
  - 13.5: Sand Dunes and Dune Fields - *CC BY-NC 4.0*
  - 13.6: Erosional Desert Land Forms - *CC BY-NC 4.0*
  - 13.7: Water in the Desert - *CC BY-NC 4.0*
  - 13.8: Geological Resources of the Desert Provinces - *CC BY-NC 4.0*
  - 13.9: Geologic Hazards of the Mojave and Colorado Desert Provinces - *CC BY-NC 4.0*
  - 13.10: Chapter Summary - *CC BY-NC 4.0*
  - 13.11: Detailed Figure Descriptions - *CC BY-NC 4.0*
- 14: Transverse Ranges - *CC BY-NC 4.0*
  - 14.1: Physiographic Overview of the Transverse Ranges Province - *CC BY-NC 4.0*
  - 14.2: Bedrock Geology of the Transverse Ranges Province - *CC BY-NC 4.0*
  - 14.3: Cenozoic Sedimentation and Basin

Development - *CC BY-NC 4.0*
- 14.4: Tectonic and Structural Evolution of the Transverse Ranges - *CC BY-NC 4.0*
- 14.5: Geologic Hazards of the Transverse Ranges Province - *CC BY-NC 4.0*
- 14.6: Mineral and Petroleum Resources of the Transverse Ranges Province - *CC BY-NC 4.0*
- 14.7: Chapter Summary - *CC BY-NC 4.0*
- 14.8: Detailed Figure Descriptions - *CC BY-NC 4.0*

◦ 15: Peninsular Ranges - *CC BY-NC 4.0*
- 15.1: Geomorphology of the Peninsular Ranges - *CC BY-NC 4.0*
- 15.2: Tectonics and Geologic History of the Peninsular Ranges Province - *CC BY-NC 4.0*
- 15.3: Rocks of the Peninsular Ranges - *CC BY-NC 4.0*
- 15.4: Geologic Hazards of the Peninsular Ranges - *CC BY-NC 4.0*
- 15.5: Natural Resources of the Peninsular Ranges - *CC BY-NC 4.0*
- 15.6: Chapter Summary - *CC BY-NC 4.0*
- 15.7: Detailed Figure and Video Descriptions - *CC BY-NC 4.0*

◦ 16: California Coastline - *CC BY-NC 4.0*
- 16.1: Coastal Processes - *CC BY-NC 4.0*
- 16.2: California Coastline Anatomy - *CC BY-NC 4.0*
- 16.3: California Coastal Hazards - *CC BY-NC 4.0*
- 16.4: Human Alteration and Mitigation - *CC BY-NC 4.0*
- 16.5: Coastal Access - *CC BY-NC 4.0*
- 16.6: The Edge of California - *CC BY-NC 4.0*
- 16.7: Chapter Summary - *CC BY-NC 4.0*
- 16.8: Detailed Figure Descriptions - *CC BY-NC 4.0*

◦ 17: California's Climate - *CC BY-NC 4.0*
- 17.1: Note on Usage - *CC BY-NC 4.0*
- 17.2: The Past - *CC BY-NC 4.0*
- 17.3: The Present - *CC BY-NC 4.0*
- 17.4: The Future - *CC BY-NC 4.0*
- 17.5: Hotter, Drier, Tougher - *CC BY-NC 4.0*
- 17.6: Chapter Summary - *CC BY-NC 4.0*
- 17.7: Detailed Figure Descriptions - *CC BY-NC 4.0*

◦ 18: California's Water - *CC BY-NC 4.0*
- 18.1: The Hydrologic Cycle - *CC BY-NC 4.0*
- 18.2: Running Water - *CC BY-NC 4.0*
- 18.3: Groundwater - *CC BY-NC 4.0*
- 18.4: Water Infrastructure and Management - *CC BY-NC 4.0*
- 18.5: Threats to California's Water - *CC BY-NC 4.0*
- 18.6: Understanding California's Water Landscape - *CC BY-NC 4.0*
- 18.7: Chapter Summary - *CC BY-NC 4.0*
- 18.8: Detailed Figure Descriptions - *CC BY-NC 4.0*

◦ 19: California's Earthquake History and Hazards - *CC BY-NC 4.0*
- 00: Front Matter - *Undeclared*
  - Table of Contents - *Undeclared*
- 19.1: Front Matter - *Undeclared*
  - 19.1.1: Table of Contents - *Undeclared*
- 19.2: The Hazard of Buildings - *CC BY-NC 4.0*
- 19.3: The Hazard of Place - *CC BY-NC 4.0*
- 19.4: Liquefaction and the Role of Soil Type - *CC BY-NC 4.0*
- 19.5: What's Coming - *CC BY-NC 4.0*
- 19.6: Beyond the San Andreas - Earthquakes of the North Coast - *CC BY-NC 4.0*
- 19.7: Preparing for the Worst - *CC BY-NC 4.0*
- 19.8: A State of Danger - *CC BY-NC 4.0*
- 19.9: Chapter Summary - *CC BY-NC 4.0*
- 19.10: Detailed Figure Descriptions - *CC BY-NC 4.0*

◦ Back Matter - *CC BY-NC 4.0*
- Index - *CC BY-NC 4.0*
- Glossary - *CC BY-NC 4.0*
- Interactive Geologic Time Scale - *CC BY-NC 4.0*
- Interactive Geologic Map of California - *CC BY-NC 4.0*
- Detailed Licensing - *CC BY-NC 4.0*
- Detailed Licensing - *Undeclared*

This page titled Geology of California is shared under a CC BY-NC 4.0 license and was authored, remixed, and/or curated by Allison Jones, Cole Heap, Debra Brooks, Emily Wright, Martha House, Steven Newton, & Steven Skinner.

DETAILED LICENSING

Overview

Title: Geology of California

Webpages: 189

Applicable Restrictions: Noncommercial

All licenses found:

- CC BY-NC 4.0: 95.2% (180 pages)
- Undeclared: 4.8% (9 pages)

By Page

- Geology of California - *CC BY-NC 4.0*
  - Front Matter - *CC BY-NC 4.0*
    - TitlePage - *CC BY-NC 4.0*
    - InfoPage - *CC BY-NC 4.0*
    - Table of Contents - *Undeclared*
    - Licensing - *Undeclared*
    - Program Page - *CC BY-NC 4.0*
    - Preface - *CC BY-NC 4.0*
    - About the Authors - *CC BY-NC 4.0*
    - Acknowledgements - *CC BY-NC 4.0*
    - Land Acknowledgment - *CC BY-NC 4.0*
    - Licensing - *CC BY-NC 4.0*
    - Recommended Citations - *CC BY-NC 4.0*
  - 1: Introduction to the Geology of California - *CC BY-NC 4.0*
    - 1.1: How to Read California's Geologic Map - *CC BY-NC 4.0*
    - 1.2: Geologic Map Symbols - *CC BY-NC 4.0*
    - 1.3: Detailed Figure Descriptions - *Undeclared*
  - 2: Minerals and Rocks - *CC BY-NC 4.0*
    - 2.1: Minerals - *CC BY-NC 4.0*
    - 2.2: Mineral Properties - *CC BY-NC 4.0*
    - 2.3: The Rock Cycle - *CC BY-NC 4.0*
    - 2.4: Igneous Rocks - *CC BY-NC 4.0*
    - 2.5: Sedimentary Rocks - *CC BY-NC 4.0*
    - 2.6: Metamorphic Rocks - *CC BY-NC 4.0*
    - 2.7: Chapter Summary - *CC BY-NC 4.0*
    - 2.8: Detailed Figure Descriptions - *CC BY-NC 4.0*
  - 3: Plate Tectonics - *CC BY-NC 4.0*
    - 3.1: Earth's Interior - *CC BY-NC 4.0*
    - 3.2: Tectonic Plates, Plate Motions, and Plate Boundaries - *CC BY-NC 4.0*
    - 3.3: Mechanisms for Plate Motion - *CC BY-NC 4.0*
    - 3.4: California's Plates and Plate Boundaries - *CC BY-NC 4.0*
    - 3.5: Chapter Summary - *CC BY-NC 4.0*
    - 3.6: Detailed Figure Descriptions - *CC BY-NC 4.0*
  - 4: Geologic Structures and Seismology - *CC BY-NC 4.0*
    - 4.1: Stress and Strain - *CC BY-NC 4.0*
    - 4.2: Folding - *CC BY-NC 4.0*
    - 4.3: Jointing and Faulting - *CC BY-NC 4.0*
    - 4.4: Earthquakes - *CC BY-NC 4.0*
    - 4.5: Measuring Earthquakes - *CC BY-NC 4.0*
    - 4.6: Chapter Summary - *CC BY-NC 4.0*
    - 4.7: Detailed Figure Descriptions - *CC BY-NC 4.0*
  - 5: Geologic Time - *CC BY-NC 4.0*
    - 5.1: Relative Dating - *CC BY-NC 4.0*
    - 5.2: Unconformities - *CC BY-NC 4.0*
    - 5.3: Dating Rocks Using Fossils - *CC BY-NC 4.0*
    - 5.4: Absolute Dating of Geologic Materials - *CC BY-NC 4.0*
    - 5.5: The Geologic Time Scale - *CC BY-NC 4.0*
    - 5.6: Chapter Summary - *CC BY-NC 4.0*
    - 5.7: Detailed Figure Descriptions - *Undeclared*
  - 6: A Brief Geologic History of California - *CC BY-NC 4.0*
    - 6.1: Developing a Geologic History - *CC BY-NC 4.0*
    - 6.2: Precambrian California (4.6 Ga – 541 Ma) - *CC BY-NC 4.0*
    - 6.3: Paleozoic California (541 – 252 Ma) - *CC BY-NC 4.0*
    - 6.4: Mesozoic California (250 – 66 Ma)-Subduction and Mountain Building - *CC BY-NC 4.0*
    - 6.5: Cenozoic California (66 Ma – Present)-Faulting, Uplift, and Basin Formation - *CC BY-NC 4.0*
    - 6.6: Chapter Summary - *CC BY-NC 4.0*
    - 6.7: Detailed Figure Descriptions - *CC BY-NC 4.0*

- 7: Cascade Range and Modoc Plateau - *CC BY-NC 4.0*
  - 7.1: The Cascadia Subduction Zone and the Cascade Continental Volcanic Arc - *CC BY-NC 4.0*
  - 7.2: Rock Types of the Cascades - *CC BY-NC 4.0*
  - 7.3: The Variety of Volcanoes in the Cascades and the Modoc Plateau - *CC BY-NC 4.0*
  - 7.4: Volcanic Hazards - *CC BY-NC 4.0*
  - 7.5: Mount Shasta - *CC BY-NC 4.0*
  - 7.6: Lassen Volcanic National Park - *CC BY-NC 4.0*
  - 7.7: Medicine Lake Volcano - *CC BY-NC 4.0*
  - 7.8: Glaciers in the Cascades - *CC BY-NC 4.0*
  - 7.9: Chapter Summary - *CC BY-NC 4.0*
  - 7.10: Detailed Figure Descriptions - *CC BY-NC 4.0*
- 8: Basin and Range - *CC BY-NC 4.0*
  - 8.1: Regional Extent and Overview of the Basin and Range - *CC BY-NC 4.0*
  - 8.2: Rifting in the Basin and Range - *CC BY-NC 4.0*
  - 8.3: Rift-Related Faulting in Eastern California - *CC BY-NC 4.0*
  - 8.4: Sedimentary Products of Rifting in the Basin and Range - *CC BY-NC 4.0*
  - 8.5: Rift-Related Volcanism in Eastern California - *CC BY-NC 4.0*
  - 8.6: The Oldest Rocks in the Basin and Range - *CC BY-NC 4.0*
  - 8.7: Chapter Summary - *CC BY-NC 4.0*
  - 8.8: Detailed Figure Descriptions - *CC BY-NC 4.0*
- 9: Sierra Nevada - *CC BY-NC 4.0*
  - 9.1: The Sierra Nevada Today - *CC BY-NC 4.0*
  - 9.2: Ancient Seas Form the Oldest Rocks - *CC BY-NC 4.0*
  - 9.3: The Sierra Nevada Batholith - *CC BY-NC 4.0*
  - 9.4: Gold of the Sierra Nevada - *CC BY-NC 4.0*
  - 9.5: Volcanic Features of the Sierra Nevada - *CC BY-NC 4.0*
  - 9.6: Ice Shapes the Landscape - *CC BY-NC 4.0*
  - 9.7: Natural Hazards of the Sierra Nevada - *CC BY-NC 4.0*
  - 9.8: Chapter Summary - *CC BY-NC 4.0*
  - 9.9: Detailed Figure Descriptions - *CC BY-NC 4.0*
- 10: Klamath Mountains - *CC BY-NC 4.0*
  - 10.1: Assembling a Continent - *CC BY-NC 4.0*
  - 10.2: The McCloud Limestone- An Ancient Coral Reef - *CC BY-NC 4.0*
  - 10.3: The Josephine Ophiolite- A Little Slice of the Mantle - *CC BY-NC 4.0*
  - 10.4: Plutons of the Klamath Mountains - *CC BY-NC 4.0*
  - 10.5: Uplifting a Mountain Range - *CC BY-NC 4.0*
  - 10.6: Chapter Summary - *CC BY-NC 4.0*
  - 10.7: Detailed Figure Descriptions - *CC BY-NC 4.0*
- 11: Coast Ranges - *CC BY-NC 4.0*
  - 11.1: A Complicated Land - *CC BY-NC 4.0*
  - 11.2: The Coast Range Ophiolite - *CC BY-NC 4.0*
  - 11.3: The Great Valley Sequence - *CC BY-NC 4.0*
  - 11.4: The Franciscan Complex - *CC BY-NC 4.0*
  - 11.5: Cenozoic Events - *CC BY-NC 4.0*
  - 11.6: Quaternary Events - *CC BY-NC 4.0*
  - 11.7: Representative Coast Range Rocks - *CC BY-NC 4.0*
  - 11.8: Chapter Summary - *CC BY-NC 4.0*
  - 11.9: Detailed Figure Descriptions - *CC BY-NC 4.0*
- 12: Great Valley - *CC BY-NC 4.0*
  - 12.1: Geomorphology and General Overview of the Great Valley Province - *CC BY-NC 4.0*
  - 12.2: Geology of the Great Valley - *CC BY-NC 4.0*
  - 12.3: Soil, Streams and Agriculture - *CC BY-NC 4.0*
  - 12.4: Natural Hazards of the Great Valley Province - *CC BY-NC 4.0*
  - 12.5: Natural Resources of the Great Valley - *CC BY-NC 4.0*
  - 12.6: Chapter Summary - *CC BY-NC 4.0*
  - 12.7: Detailed Figure Descriptions - *CC BY-NC 4.0*
- 13: Mojave and Colorado Deserts - *CC BY-NC 4.0*
  - 13.1: Physiographic Features of the Mojave and Colorado Desert Provinces - *CC BY-NC 4.0*
  - 13.2: Geologic Overview and Evolution of the Mojave and Colorado Desert Provinces - *CC BY-NC 4.0*
  - 13.3: Creating the Desert Environment - *CC BY-NC 4.0*
  - 13.4: Wind Driven Sediment Transport - *CC BY-NC 4.0*
  - 13.5: Sand Dunes and Dune Fields - *CC BY-NC 4.0*
  - 13.6: Erosional Desert Land Forms - *CC BY-NC 4.0*
  - 13.7: Water in the Desert - *CC BY-NC 4.0*
  - 13.8: Geological Resources of the Desert Provinces - *CC BY-NC 4.0*
  - 13.9: Geologic Hazards of the Mojave and Colorado Desert Provinces - *CC BY-NC 4.0*
  - 13.10: Chapter Summary - *CC BY-NC 4.0*
  - 13.11: Detailed Figure Descriptions - *CC BY-NC 4.0*
- 14: Transverse Ranges - *CC BY-NC 4.0*
  - 14.1: Physiographic Overview of the Transverse Ranges Province - *CC BY-NC 4.0*
  - 14.2: Bedrock Geology of the Transverse Ranges Province - *CC BY-NC 4.0*
  - 14.3: Cenozoic Sedimentation and Basin

Development - *CC BY-NC 4.0*
- 14.4: Tectonic and Structural Evolution of the Transverse Ranges - *CC BY-NC 4.0*
- 14.5: Geologic Hazards of the Transverse Ranges Province - *CC BY-NC 4.0*
- 14.6: Mineral and Petroleum Resources of the Transverse Ranges Province - *CC BY-NC 4.0*
- 14.7: Chapter Summary - *CC BY-NC 4.0*
- 14.8: Detailed Figure Descriptions - *CC BY-NC 4.0*

◦ 15: Peninsular Ranges - *CC BY-NC 4.0*
- 15.1: Geomorphology of the Peninsular Ranges - *CC BY-NC 4.0*
- 15.2: Tectonics and Geologic History of the Peninsular Ranges Province - *CC BY-NC 4.0*
- 15.3: Rocks of the Peninsular Ranges - *CC BY-NC 4.0*
- 15.4: Geologic Hazards of the Peninsular Ranges - *CC BY-NC 4.0*
- 15.5: Natural Resources of the Peninsular Ranges - *CC BY-NC 4.0*
- 15.6: Chapter Summary - *CC BY-NC 4.0*
- 15.7: Detailed Figure and Video Descriptions - *CC BY-NC 4.0*

◦ 16: California Coastline - *CC BY-NC 4.0*
- 16.1: Coastal Processes - *CC BY-NC 4.0*
- 16.2: California Coastline Anatomy - *CC BY-NC 4.0*
- 16.3: California Coastal Hazards - *CC BY-NC 4.0*
- 16.4: Human Alteration and Mitigation - *CC BY-NC 4.0*
- 16.5: Coastal Access - *CC BY-NC 4.0*
- 16.6: The Edge of California - *CC BY-NC 4.0*
- 16.7: Chapter Summary - *CC BY-NC 4.0*
- 16.8: Detailed Figure Descriptions - *CC BY-NC 4.0*

◦ 17: California's Climate - *CC BY-NC 4.0*
- 17.1: Note on Usage - *CC BY-NC 4.0*
- 17.2: The Past - *CC BY-NC 4.0*
- 17.3: The Present - *CC BY-NC 4.0*
- 17.4: The Future - *CC BY-NC 4.0*
- 17.5: Hotter, Drier, Tougher - *CC BY-NC 4.0*
- 17.6: Chapter Summary - *CC BY-NC 4.0*
- 17.7: Detailed Figure Descriptions - *CC BY-NC 4.0*

◦ 18: California's Water - *CC BY-NC 4.0*
- 18.1: The Hydrologic Cycle - *CC BY-NC 4.0*
- 18.2: Running Water - *CC BY-NC 4.0*
- 18.3: Groundwater - *CC BY-NC 4.0*
- 18.4: Water Infrastructure and Management - *CC BY-NC 4.0*
- 18.5: Threats to California's Water - *CC BY-NC 4.0*
- 18.6: Understanding California's Water Landscape - *CC BY-NC 4.0*
- 18.7: Chapter Summary - *CC BY-NC 4.0*
- 18.8: Detailed Figure Descriptions - *CC BY-NC 4.0*

◦ 19: California's Earthquake History and Hazards - *CC BY-NC 4.0*
- 00: Front Matter - *Undeclared*
  - Table of Contents - *Undeclared*
- 19.1: Front Matter - *Undeclared*
  - 19.1.1: Table of Contents - *Undeclared*
- 19.2: The Hazard of Buildings - *CC BY-NC 4.0*
- 19.3: The Hazard of Place - *CC BY-NC 4.0*
- 19.4: Liquefaction and the Role of Soil Type - *CC BY-NC 4.0*
- 19.5: What's Coming - *CC BY-NC 4.0*
- 19.6: Beyond the San Andreas - Earthquakes of the North Coast - *CC BY-NC 4.0*
- 19.7: Preparing for the Worst - *CC BY-NC 4.0*
- 19.8: A State of Danger - *CC BY-NC 4.0*
- 19.9: Chapter Summary - *CC BY-NC 4.0*
- 19.10: Detailed Figure Descriptions - *CC BY-NC 4.0*

◦ Back Matter - *CC BY-NC 4.0*
- Index - *CC BY-NC 4.0*
- Glossary - *CC BY-NC 4.0*
- Interactive Geologic Time Scale - *CC BY-NC 4.0*
- Interactive Geologic Map of California - *CC BY-NC 4.0*
- Detailed Licensing - *CC BY-NC 4.0*
- Detailed Licensing - *Undeclared*

This page titled Geology of California is shared under a CC BY-NC 4.0 license and was authored, remixed, and/or curated by Allison Jones, Cole Heap, Debra Brooks, Emily Wright, Martha House, Steven Newton, & Steven Skinner.